

# **Chemical Syntheses and Evaluations of Novel Anti-Infective Small Molecules**

**By Daniel W. Carney**

**B.Sc. Worcester Polytechnic Institute, 2009**

**A Dissertation**

**Submitted in Partial Fulfillment of the Requirements for the**

**Degree of Doctor of Philosophy**

**in the Department of Chemistry at Brown University**

**Providence, Rhode Island**

**May 2014**

**© Copyright 2014**

**By**

**Daniel W. Carney**

**This dissertation by Daniel W. Carney is accepted in its present form**

**by the Department of Chemistry as satisfying the**

**dissertation requirement for the degree of Doctor of Philosophy.**

**Date**

\_\_\_\_\_

\_\_\_\_\_

**Professor Jason K. Sello, Advisor**

**Recommended to the Graduate Council**

**Date**

\_\_\_\_\_

\_\_\_\_\_

**Professor Christopher T. Seto, Reader**

**Date**

\_\_\_\_\_

\_\_\_\_\_

**Professor Paul G. Williard, Reader**

**Approved by the Graduate Council**

**Date**

\_\_\_\_\_

\_\_\_\_\_

**Professor Peter M. Weber,  
Dean of the Graduate School**

## Curriculum Vitae

Daniel Carney was born in Worcester, MA on May 7, 1987. He received his diploma in 2005 from St. John's High School in Shrewsbury, MA and enrolled at Worcester Polytechnic Institute (WPI) in Worcester, MA for undergraduate studies in chemistry. During his time WPI, Daniel conducted research at the U.S. Army Natick Soldier Research Development and Engineering Center (NSRDEC) under the direction of Dr. Heidi Schreuder-Gibson. In 2008 he initiated a collaborative research project between the NSRDEC and the research lab of Professor Robert E. Connors at WPI. Daniel was a Charles O. Thompson Scholar (2006), received the provost award for outstanding Major Qualification Project in chemistry (2009), and graduated from WPI with high distinction in 2009, receiving a B.Sc. in chemistry.

Daniel enrolled in the graduate school at Brown University in the Fall of 2009 to pursue his doctoral degree in chemistry where he joined the lab of Professor Jason K. Sello. Daniel's research has focused on organic synthesis, medicinal chemistry, drug design, and chemical biology. His research has been presented at the 1<sup>st</sup> International Conference on Frontiers in Pharmaceutical Sciences in 2012 as well as at the Gordon Research Conference on High Throughput Chemistry and Chemical Biology in 2013. While at Brown, Daniel was recognized by the AAAS/Science Program for Excellence in Science (2009), and was awarded a 2013 dissertation fellowship by the Chemistry Department.

### **Publications**

- 5) Carney, D. W.; Schmitz, K. R.; Truong, J. V.; Sauer, R. T.; Sello, J. K.; *Restriction of the Conformational Dynamics of the Cyclic Acyldepsipeptide Antibiotics Improves Their Antibacterial Activity. J. Am. Chem. Soc.* **2014.** 136, 1922-1929. [dx.doi.org/10.1021/ja410385c](https://doi.org/10.1021/ja410385c)

- 4) Nelson, C. S.; Carney, D. W.; Derdowski, A.; Williard, P. G.; Sello, J. K.; Atwood, W. J. *A Retrograde Trafficking Inhibitor of Ricin and Shiga-Like Toxins Inhibits Infection of Cells by Human and Monkey Polyomaviruses.* *Mbio.* **2013**, 4(6), e00729-13. dx.doi.org/10.1128/mBio.00729-13
  
- 3) Changtong, C.; Carney, D.W.; Luo, L.; Zoto, C. A.; Lombardi, J. L.; Connors, R. E. *A porphyrin molecule that generates, traps, stores, and releases singlet oxygen.* *J. Photochem. Photobiol. A.* **2013**, 260, 9-13 dx.doi.org/10.1016/j.jphotochem.2013.03.003
  
- 2) Carney, Daniel W.; Truong; Jonathan V.; Sello, Jason K. *Investigations of the Configurational Stabilities of Chiral Isocyanoacetates in Multicomponent Reactions.* *J. Org. Chem.*, **2011**, 76 (24), 10279–10285. dx.doi.org/10.1021/jo201817k
  
- 1) Schreuder-Gibson, H.; Gibson, P.; Owens, J.; Gill, H. I.; Orlicki, J.; Prugh, A.; Thornberg, C.; Engel, R.; Walker, J.; Yeomans, W.; Stote, R. I.; Carney, D.; Zukas, W. *Self-Detoxifying Materials for Chemically and Biologically Protective Clothing.* **2008**, NATICK/TR-08/008L.

#### **Patents**

- 1) Atwood, W.; Nelson, C.; Sello, J.K.; Carney; D. W. *Compounds for the Treatment and Prevention of Infections.* **2013**, PCT/US2013/050479; WO2014014814 A1

## Preface and Acknowledgements

*To my wife and my family for their constant support and encouragement*

I must also acknowledge Professor Jason K. Sello. I am ever grateful for his constant support, guidance and enthusiasm. I am also grateful to the Brown Chemistry Department, its faculty, and its staff for their support and for providing an exceptional environment for scientific research and higher learning.

## Table of Contents

Curriculum Vitae .....	iv
Preface and Acknowledgements .....	vi
Table of Contents.....	vii
List of Tables .....	x
List of Figures .....	xi
List of Reagent Abbreviations .....	xv
Chapter 1 – Introduction to Anti-Infective Drug Discovery and Research Summary .....	1
References .....	5
Chapter 2 – Dihydroquinazolinone Retrograde Transport Inhibitors.....	9
Introduction .....	9
Results.....	13
Experimental Contributors.....	32
Experimental Procedures.....	32
Chapter 3 – Acyldepsipeptide (ADEP) Antibiotics: A Promising Group of Antibacterial Agents.....	63
Introduction .....	63
Design of conformationally constrained ADEP peptidolactones.....	68
References .....	71
Chapter 4 – Isocyanide Based Multicomponent Reactions and Synthesis of Pipecolate Containing Peptides.....	75
Introduction .....	75
Results.....	79
Experimental Contributions.....	92
Experimental Procedures.....	93
Chapter 5 – Synthesis of ADEPs with Conformationally Constrained Peptidolactones. ....	117
Introduction .....	117
Results.....	118
Experimental Contributions.....	129
Experimental.....	129

References .....	161
Chapter 6 – Evaluation of ADEPs with Conformationally Constrained Peptidolactones.....	163
Introduction .....	164
Measurement of ADEP peptidolactone dynamics via <sup>1</sup> H-NMR Deuterium Exchange.....	166
<i>In vitro</i> Assessment of ClpP Binding and Activation by the Rigidified ADEPs.....	169
Assessment of the Bioactivities of the Conformationally Constrained ADEPs in Antibacterial Assays.....	171
ADEP Activity in mouse models of infection.....	173
Conclusion.....	177
Experimental Contributions .....	181
Experimental Section .....	181
References .....	184
Chapter 7 – Synthesis and Evaluation of ADEPs with Modified side Chains .....	188
Introduction .....	188
ADEPs with peptidomimetic side chains.....	190
Side Chain Medicinal Chemistry .....	195
ADEP binding and activation of <i>M. tuberculosis</i> ClpP.....	200
Experimental Contributions.....	203
Experimental Procedures.....	203
Chapter 8 – The Acyldepsipeptide <i>N</i> -Acylidifluorophenylalanine Moiety is Necessary and Sufficient for ClpP Activation. ....	227
Introduction .....	227
Results.....	228
Conclusions .....	235
Experimental Contributions.....	236
Experimental Methods .....	236
References .....	258
Chapter 9 – <i>N</i> -Acylidifluorophenylalanine Fragment Hit to lead development.....	262
Introduction.....	262
Results.....	262
Discussion.....	270
Experimental Contributions.....	271



Experimental Methods .....	271
References .....	279
Chapter 10 – Fragment based potentiation of ADEP antibacterial activity.....	281
Background .....	281
Results.....	282
Conclusions .....	287
Experimental Contributions .....	288
Experimental Procedures.....	288
References .....	289
Chapter 11 – Antibacterial Phenylcyclohexane Caboxylates (PCHCs).....	292
Introduction .....	292
Conclusions .....	305
Experimental Contributions .....	305
Experimental Procedures.....	305
References .....	310
Appendix of Compound Spectra .....	312
Chapter 2 – Dihydroquinazolinone Retrograde Transport Inhibitors.....	313
Chapter 4 – Isocyanide Based Multicomponent Reactions and Synthesis of Pipecolate Containing Peptides.....	357
NMR and MassSpectra.....	357
Isocyanoacetate Epimerization Chromatograms.....	388
Advanced Marfey Analysis Chromatograms.....	403
LC Chromatograms.....	418
Chapter 5 – Synthesis of ADEPs with Conformationally Constrained Peptidolactones .....	420
Chapter 7 – Synthesis and Evaluation of ADEPs with Modified side Chains .....	457
Chapter 8 – The <i>N</i> -Acyldifluorophenyllanine Moiety is Necessary and Sufficient for ClpP Activation.....	485
Chapter 9 – <i>N</i> -Acyldifluorophenylalanine Fragment Hit to lead development.....	512
Chapter 11 – Antibacterial Phenylcyclohexane Caboxylates (PCHCs) .....	523

## List of Tables

Table 2.1 - Anti-JCPyV Activity of DHQ Inhibitors at 25 $\mu$ M with Varied Heterocycle Moiety .....	21
Table 2.2 - Anti-JCPyV Activity of DHQ Inhibitors at 25 $\mu$ M with Varied Amide Moiety .....	244
Table 2.3 - Anti-JCPyV Activity of DHQ Inhibitors at 25 $\mu$ M with Varied Benzo Moiety.....	25
Table 4.1 - Passerini 3 Component Condensations with a Chiral Isocyanoacetates .....	85
Table 4.2 – The Effect of U-4CR Reactants on the Stereochemical Configuration of a Chiral Isocyanoacetate	86
Table 4.3 – Ugi 4 Component Condensations with Chiral Isocyanoacetates .....	89
Table 4.4 – Effect of Benzylamine-Cyclohexanone Pre-condensation Time on Isocyanoacetate Epimerization .....	90
Table 4.5 – Joullié-Ugi 3 Component Condensations with Isocyanoacetates .....	91
Table 5.1 - Synthesis of pentapeptolides.....	125
Table 5.2 - Synthesis of peptidolactones .....	126
Table 5.3 – Sequential acylation of peptidoactones.....	127
Table 6.1 – Antibacterial activity of ADEPs against <i>B. mycooides</i> .....	172
Table 6.2 – Comparison of <i>in vitro</i> and <i>in vivo</i> ADEP properties .....	173
Table 10.1 - Potentiation of ADEP antibacterial activity in <i>S. coelicolor</i> by N- acyldifluorophenylalanine analog.....	285
Table 10.2 – Potentiation activity of fragment 15 toward various antibacterial agents.....	286
Table 10.3 - Potentiation of ADEP antibacterial activity in Mycobacteria.....	287
Table 11.1 – Antibacterial Activity of CPHCs against <i>B. subtilis</i> .....	302

## List of Figures

Figure 1.1 – The role of Small molecules in the central dogma of life <sup>1</sup> .....	1
Figure 2.1 – Small molecule inhibitors of retrograde trafficking.....	10
Figure 2.2 – Retrograde trafficking of endosome cargo.....	11
Figure 2.3 – Recent developments in Retro-2 research. ....	12
Figure 2.4 – Inhibition of JCPyV infectivity by Retro-2 purchased from Chembridge.. ....	14
Figure 2.5 – Synthesis of Retro-2 and corresponding dihydroquinazolinone.. ....	15
Figure 2.6 – Retro-2 structural studies. ....	16
Figure 2.7 – Inhibitory activities of Retro-2 analogs.....	17
Figure 2.8 - Retro-2 <sup>cycl</sup> prevents infection with three polyomaviruses.....	18
Figure 2.9 – Retro-2 <sup>cycle</sup> diversification strategy A) Retro-2 <sup>cycle</sup> has 3 easily diversifiable moieties.. .....	20
Figure 2.10 – Synthesis and Activity of n-butylamino dihydroquinazolinone .....	26
Figure 2.11 - Synthesis and Activity of quinazolinone and <i>N</i> -methyl-dihydroquinazolinone analog.....	27
Figure 2.12 – Inhibition of JCPyV infectivity in SVG-A Cells. ....	28
Figure 3.1 – Structure and Function of Clp proteolytic complex .....	65
Figure 3.2 - Structures of natural product ADEPs and optimized synthetic analogs thereof.....	66
Figure 3.3 - Effect of ADEP binding on ClpP structure .....	67
Figure 3.4 – Effect of pipercolate methylation on ADEP activity. ....	69
Figure 4.1 – Keenan synthesis of enantiomerically pure substituted pipercolate residues .....	75
Figure 4.2 - Examples of typical isocyanide based multicomponent reactions.....	76
Figure 4.3 – Isocyanide resonance structures and common methods for isocyanide preparation .....	77

Figure 4.4 – Synthesis and common reactions of isocyanoacetates .....	78
Figure 4.5 – Synthesis of pipercolate containing tripeptides using the Joullié-Ugi reaction according to the method reported by Socha et al.....	80
Figure 4.6 – Deconvolution of JU-3CR product mixture .....	82
Figure 4.7 - Hypothetical mechanisms for isocyanoacetate epimerization .....	86
Figure 4.8 – Synthesis and crystal structure of tripiperideine.....	91
Figure 5.1 – Retrosynthetic analysis of ADEPs with conformationally constrained macrocycles	117
Figure 5.2 – Synthesis of N-methylalanine containing tripeptide .....	118
Figure 5.3 – Multicomponent synthesis of pipercolate containing tripeptides.....	119
Figure 5.4 – Rationalization of the diastereoselectivity observed in JU-3CR with 4-substituted dehydropiperidines.....	121
Figure 5.5 - Synthesis of protected allo-threonine .....	122
Figure 5.6 - Synthesis of proline esters and potential product degradation mechanism .....	123
Figure 5.7 – Peptidolactone acylation with fully assembled side chain .....	127
Figure 5.8 – Structures of ADEP molecules containing conformationally constrained amino acids .....	129
Figure 6.1 – Structures of ADEP molecules containing conformationally constrained amino acids .....	163
Figure 6.2 - Trans-annular hydrogen bonding in an ADEP.....	164
Figure 6.3 – Effects of conformationally constrained amino acids on difluorophenylalanine amide deuterium exchange .....	167
Figure 6.4 – Effects of conformationally constrained amino acids on alanine amide deuterium exchange .....	169

Figure 6.5 – Activation of ClpP and competition with ClpX by ADEPs in vitro.....	170
Figure 6.6 – Structures and in vivo activities of Bayer Healthcare AG optimized ADEPs .....	174
Figure 6.7 – Treatment of deep-seated <i>S. aureus</i> infection in mouse thigh .....	175
Figure 6.8 – Effect of optimized ADEPs in mouse model of <i>S. aureus</i> (ATCC 29213) infection...	177
Figure 7.1 – ADEP-ClpP binding Interactions .....	189
Figure 7.2 – ADEP Peptidomimetics.....	190
Figure 7.3 – Synthesis and antibacterial activity of ADEPs with peptide side chains .....	192
Figure 7.4 – Synthesis and evaluation of ADEP with side chain carbon branching .....	194
Figure 7.5 – Activation of ClpP by ADEPs with IGF/LGF mimic side chains.....	195
Figure 7.6 – Synthesis and antibacterial activity of ADEPs with hydroxyl terminating side chains .....	196
Figure 7.7 – $\alpha,\beta$ -unsaturation in ADEP side chain acyl groups .....	198
Figure 7.7 – Structure and biological activity of fully optimized ADEPs .....	199
Figure 7.8 – Activation of MBT ClpP1P2 by Optimized ADEPs.....	201
Figure 7.9 – X-ray crystal structure of ADEP 17c bound to MTB ClpP1P2 .....	202
Figure 8.1 - Deconstruction of an acyldepsipeptide in search of fragments with antibacterial activity against <i>B. subtilis</i> .....	229
Figure 8.2 – Structures and antibacterial activity of <i>N</i> -acyldifluorophenylalanine fragment analogs against <i>B. subtilis</i> .....	231
Figure 8.3 - ClpP Binding of Key <i>N</i> -acyldifluorophenylalanine Fragment Analogs .....	233
Figure 8.4 – Lists of proteins positively identified as specifically bound to N-E-2- heptenoyldifluorophenylalanine affinity matrix.....	234
Figure 9.2 – Structures and antibacterial activity of a Prototypical ADEP and N- heptenoyldifluorophenylalanine fragemtns.....	263

Figure 9.3 – IMCR for the synthesis or combinatorial libraries bearing the N-heptenyldifluorophenylalanine ClpP activation pharmacophore .....	264
Figure 9.4 – IMCR library containing the N-heptenyldifluorophenylalanine ClpP activation pharmacophore .....	266
Figure 9.5 – Analogs of N-heptenyldifluorophenylalanine coupled to carbocyclic amines do not exhibit antibacterial activity against <i>B. mycoides</i> .....	267
Figure 9.6 – Antibacterial activity of ADEP fragments and a circularization strategy to minimize entropic penalties for binding to ClpP .....	268
Figure 9.7 – Diversity oriented synthesis and antibacterial activity of circularized ADEP fragments .....	270
Figure 10.8 – Potentiation of ADEP antibacterial activity in <i>S. coelicolor</i> by various fragments	283
Figure 10.2 - Structures of N-acyldifluorophenylalanine analogs. ....	285
Figure 11.1 – Activators of self-Compartmentalized Proteases (ACPs) identified in HTS .....	2932
Figure 11.2 – Retrosynthesis of phenylcyclohexane carboxylates.....	2954
Figure 11.3 – Synthesis of dichloroacrolein .....	2965
Figure 11.4 – Synthesis of phenylcyclohexyl carboxylates .....	2965
Figure 11.5 – Compound 1a <sup>1</sup> H NMR .....	2987
Figure 11.6 - Compound 1a 2D NOSEY spectrum .....	2987
Figure 11.7 – PCHC relative stereochemistry .....	2998
Figure 11.8 – Stereoselective and chemoselective reduction of 1a .....	3009
Figure 11.9 – Compound 10, <sup>1</sup> H NMR. ....	3009
Figure 11.10 - Compound 1a 2D NOSEY spectrum .....	300
Figure 11.11 – Effects of PCHC dehydration and reduction on antibacterial activity .....	303
Figure 11.12 – Attempts to Validate ClpP as PCHC target. ....	304

## List of Reagent Abbreviations

<b>(Boc)<sub>2</sub>O</b>	Di-tert-butyl dicarbonate
<b>AcOH</b>	Acetic acid
<b>DCC</b>	<i>N,N'</i> -Dicyclohexylcarbodiimide
<b>DCM</b>	Dichloromethane
<b>DIPEA</b>	<i>N,N</i> -Diisopropylethylamine
<b>DMAP</b>	4-Dimethylaminopyridine
<b>DME</b>	Dimethoxyethane
<b>DMF</b>	<i>N,N</i> -Dimethylformamide
<b>EDC</b>	1-Ethyl-3-(3-dimethylaminopropyl)carbodiimide
<b>EtOAc</b>	Ethyl acetate
<b>EtOH</b>	Ethanol
<b>HATU</b>	(1-[Bis(dimethylamino)methylene]-1H-1,2,3-triazolo[4,5-b]pyridinium 3-oxid hexafluorophosphate)
<b>HOBT</b>	Hydroxybenzotriazole
<b>LDA</b>	Lithium diisopropylamide
<b>L-FDAA</b>	1-fluoro-2-(4-dinitrophenyl)-5-L-alanine amide
<b>MeOH</b>	Methanol
<b><i>n</i>-BuLi</b>	<i>n</i> -Butyllithium
<b>NMM</b>	<i>N</i> -Methylmorpholine
<b>PCC</b>	Pyridinium chlorochromate
<b>Pd/C</b>	Palladium on carbon
<b>tBME</b>	tert-Butyl methyl ester

<b>TBSCI</b>	tert-Butyldimethylsilyl chloride
<b>TEA</b>	Triethylamine
<b>TFA</b>	Trifluoroacetic acid
<b>THF</b>	Tetrahydrofuran
<b>TMSCI</b>	trimethylsilyl chloride
<b>TPTU</b>	2-(2-Pyridon-1-yl)-1,1,3,3-tetramethyluronium tetrafluoroborate



## Chapter 1 – Introduction to Anti-Infective Drug Discovery and Research

### Summary

Small molecules are an integral component of the chemistry of life.<sup>1</sup> In biology, small molecules are responsible for mediating essential functions, such as inter- and intra-cellular signaling, regulation of gene expression, and modulation of enzyme activity. The role of small molecules in biology has long been exploited by scientists and physicians in order to study the complex chemical mechanisms of life and also to improve the health and wellbeing of our society.<sup>2</sup>

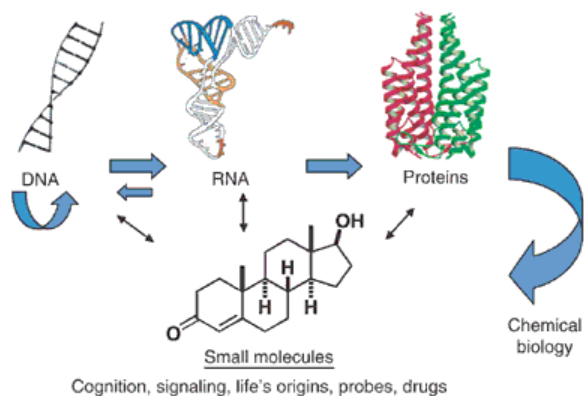


Figure 1.1 – The role of Small molecules in the central dogma of life<sup>1</sup>

One area of medicine in which small molecule therapeutics are used abundantly is the treatment of infectious diseases. Our bodies are inhabited by a multitude of foreign organisms including bacteria, viruses, fungi, and even other eukaryotes. While many of these commensal microorganisms form symbiotic relationships with their host, some are pathogenic; in such cases their growth and replication comes at the expense of the host's health and resources. Small molecules can be used to selectively inhibit the growth and replication of pathogenic organisms allowing our bodies' immune systems to effectively clear the harmful infection. Modern molecular medicine has afforded us with many small molecule therapeutics that are used to

treat a wide variety of infectious diseases.<sup>2</sup> However, there are still many infectious diseases for which adequate treatments are not available. There are some diseases, that for a lack of interest and/or a lack of innovation, for which no small molecule therapeutics have yet been discovered. Added to this shortcoming is the problem of drug resistance. As a result of evolution and genetic variation in pathogenic organisms, the use of an anti-infective small molecule inevitably selects for individual organisms that are resistant.<sup>3-5</sup> Eventually, all anti-infective agents become obsolete because of the evolution of resistance. Anti-infective drug discovery is thus challenging and must be an ongoing endeavor. The primary challenge in modern anti-infective drug discovery is the discovery and validation of new drug targets.<sup>6,7</sup> In many cases, viable drug targets are not obvious, and their discovery is often times serendipitous. Historically, there have been two general approaches to drug target discovery and validation, the classical, molecule-centric approach and the more modern gene-centric approach.<sup>2,8-10</sup>

In a molecule-centric approach, researchers search for small molecules that induce a phenotype of interest in a biological system. Once a small molecule is discovered that induces the desired phenotype, the target of the small molecule must be identified. *In vitro* target based screening can then be used to discover additional classes of potential drug leads. Since the small molecule was discovered on the basis of a phenotypic screen, the target is validated very early in the discovery process. Essentially all small molecule therapeutics that are based on or inspired by natural products were discovered in this manner.<sup>2</sup>

We are currently in a “post-genomic era” wherein there is a wealth of genomic information available from widely available and inexpensive rapid DNA sequencing technologies. Genomic information has led an explosion in the proposal of new drug targets based on genes that are believed to be disease determinants.<sup>8-10</sup> Unfortunately, this gene-centric approach to

target identification has yielded many drug leads that fail in preclinical and clinical development.<sup>6,11,12</sup> High attrition rates are often a result of poor target validation in the early stages of drug development. As a consequence, time and resources are all too often wasted on drug leads that fail in clinical trials where there are ineffective, exhibit unanticipated toxicity, or exhibit unacceptable side-effects.<sup>6,12,13</sup> Given the disappointing outcomes of the gene-centric approach to drug discovery, some researchers are actively trying to salvage it by defining the important criteria for target selection.<sup>14,15</sup>

The challenges faced in genome-guided drug discovery have spurred increased efforts in whole cell based phenotypic screening coupled with chemical genetics in order to identify small molecule drug leads and robustly validated drug targets.<sup>16-19</sup> The molecule-centric approach to target identification has been very successful in anti-infective drug discovery. This is most likely because a lack of growth by a microorganism is a very simple phenotype to assay for. However, in order to assay for the inhibition of growth in a micro-organism, one requires a source of small molecules. Natural products and natural product inspired synthetic compounds are an excellent source of bioactive small molecules.<sup>20-22</sup> An intrinsic advantage of natural products is that they have been selected over millions of years of evolution for the purpose of killing or critically perturbing organismal physiology. An alternative source of potential small molecule therapeutics is purely synthetic compounds produced in the laboratory. Although these molecules do not benefit from the advantages of evolution, large libraries of synthetic small molecules can be constructed and evaluated with remarkable efficiency. In recent years, diversity oriented synthesis<sup>23-25</sup> and high-throughput screening technology has matured to a state wherein identification of synthetic small molecules that modulate the function of nearly any protein is possible.<sup>13,26</sup>

Diversity-oriented synthesis has become a mainstay strategy used to develop highly active drug leads. Diversity-oriented synthesis strategies seek to build collections of compounds with high efficiency.<sup>23,24</sup> Reactions or sequences of reactions that rapidly generate complexity are highly valued. The synthetic planning process for diversity oriented synthesis can be very different than target oriented synthesis. For instance, reactions that have with poor stereo-, regio-, and or chemo-selectivity, which are typically avoided in target oriented synthesis, can be advantageous in diversity oriented synthesis. Furthermore, in diversity oriented synthetic planning, it is important to carefully consider at which points in the synthesis diversification steps take place. Ideally, diversification should occur at mid to late stages in the synthesis in order to minimize the work required to produce a collection of compounds.<sup>23,24</sup>

In the age of high-throughput screening, combinatorial chemistry<sup>27-29</sup>, a form of diversity oriented synthesis, has become a common technique for preparing large libraries of small molecules. This strategy is intrinsically non-rational, therefore the discovery of highly active compounds is serendipitous. In order to have strong odds at discovering analogs with strong activity within combinatorial library, collections on the order of hundreds to thousands of compounds must be prepared and evaluated. This task may seem daunting. However, it is, in fact, routine for labs that specialize in high-throughput chemistry, particularly in the pharmaceutical industry. The ease with which large combinatorial libraries can be constructed has also been facilitated by recent developments of clever strategies such as solid-phase synthesis<sup>30-32</sup>, split-and-pool synthesis<sup>23,33-35</sup> and compound indexing with molecular tags<sup>36-41</sup>.

As an alternative to combinatorial chemistry, diversity oriented synthesis can also be applied in rational design strategies.<sup>42-44</sup> Rational design is hypothesis driven and enables researchers to focus their synthetic and screening efforts on a smaller subset of compounds.

Rational drug design usually relies on the availability of detailed structural information about a small molecule ligand and the biomolecular receptor of its target. Combinatorial synthesis and rational design are distinct strategies for hit to lead drug development, both of which have their merits and weaknesses.

With the broader context of anti-infective drug discovery in mind, I will introduce the central themes of my PhD research. I have pursued molecule-centric approaches to addressing the problem of infectious diseases that are in need of new drug targets. First, I will discuss the discovery of drug leads for the treatment of human polyomavirus and papillomavirus infections, diseases for which there are few good drug targets or small molecule therapeutics. In a new strategy for antiviral drug development, I pose the question: can host physiology be modulated in order to prevent intracellular trafficking of the viruses and inhibit infection? Our data suggests that the answer is yes. I will then discuss the development of new antibacterial drug leads that are active against multi-drug resistant bacterial pathogens. The focus of my work has been natural products that kill bacterial via perturbation of protein turnover. Currently, there are no marketed drugs that utilize this strategy. Here I pose the question: can bacterial proteolysis be targeted for antibacterial therapy? Again, my results indicate that this question can be answered in the affirmative. Throughout the subsequent chapters we will encounter specific examples of many of the topics introduced in this chapter. It is the goal of this dissertation to provide readers with an in depth look at my Ph.D. research and thought process as well as a perspective on relevant topics in modern drug discovery.

## References

1. Schreiber, S. L. Small molecules: the missing link in the central dogma. *Nature chemical biology* **2005**, *1*, 64-66.
2. Drews, J. Drug discovery: a historical perspective. *Science* **2000**, *287*, 1960-1964.

3. Cox, G.; Wright, G. D. Intrinsic antibiotic resistance: Mechanisms, origins, challenges and solutions. *International Journal of Medical Microbiology* **2013**.
4. Bush, K.; Courvalin, P.; Dantas, G.; Davies, J.; Eisenstein, B.; Huovinen, P.; Jacoby, G. A.; Kishony, R.; Kreiswirth, B. N.; Kutter, E. Tackling antibiotic resistance. *Nature Reviews Microbiology* **2011**, *9*, 894-896.
5. Walsh, C. *Antibiotics: actions, origins, resistance*. American Society for Microbiology (ASM): 2003; .
6. Bunnage, M. E. Getting pharmaceutical R&D back on target. *Nature chemical biology* **2011**, *7*, 335.
7. Smith, C. Drug target validation: Hitting the target. *Nature* **2003**, *422*, 341-347.
8. Lenz, G. R.; Nash, H. M.; Jindal, S. Chemical ligands, genomics and drug discovery. *Drug Discov. Today* **2000**, *5*, 145-156.
9. Eisenberg, D.; Marcotte, E. M.; Xenarios, I.; Yeates, T. O. Protein function in the post-genomic era. *Nature* **2000**, *405*, 823-826.
10. Chanda, S. K.; Caldwell, J. S. Fulfilling the promise: drug discovery in the post-genomic era. *Drug Discov. Today* **2003**, *8*, 168-174.
11. Sams-Dodd, F. Target-based drug discovery: is something wrong? *Drug Discov. Today* **2005**, *10*, 139-147.
12. Kola, I.; Landis, J. Can the pharmaceutical industry reduce attrition rates? *Nature reviews Drug discovery* **2004**, *3*, 711-716.
13. Bleicher, K. H.; Böhm, H.; Müller, K.; Alanine, A. I. Hit and lead generation: beyond high-throughput screening. *Nature Reviews Drug Discovery* **2003**, *2*, 369-378.
14. 1000 Genomes Project Consortium A map of human genome variation from population-scale sequencing. *Nature* **2010**, *467*, 1061-1073.
15. 1000 Genomes Project Consortium An integrated map of genetic variation from 1,092 human genomes. *Nature* **2012**, *491*, 56-65.
16. Butcher, E. C. Can cell systems biology rescue drug discovery? *Nature Reviews Drug Discovery* **2005**, *4*, 461-467.
17. Strausberg, R. L.; Schreiber, S. L. From knowing to controlling: a path from genomics to drugs using small molecule probes. *Science* **2003**, *300*, 294-295.
18. Terstappen, G. C.; Schlüpen, C.; Raggiaschi, R.; Gaviraghi, G. Target deconvolution strategies in drug discovery. *Nature Reviews Drug Discovery* **2007**, *6*, 891-903.

19. Zon, L. I.; Peterson, R. T. *In vivo* drug discovery in the zebrafish. *Nature reviews Drug discovery* **2005**, *4*, 35-44.
20. Tyler, V. E. Natural products and medicine: an overview. *Medicinal resources of the tropical forest: Biodiversity and its importance to human health* **1996**, *1*.
21. Newman, D. J.; Cragg, G. M. Natural products as sources of new drugs over the 30 years from 1981 to 2010. *J. Nat. Prod.* **2012**, *75*, 311-335.
22. Mishra, B. B.; Tiwari, V. K. Natural products: an evolving role in future drug discovery. *Eur. J. Med. Chem.* **2011**, *46*, 4769-4807.
23. Schreiber, S. L. Target-oriented and diversity-oriented organic synthesis in drug discovery. *Science* **2000**, *287*, 1964-1969.
24. Burke, M. D.; Schreiber, S. L. A Planning Strategy for Diversity-Oriented Synthesis. *Angewandte Chemie International Edition* **2004**, *43*, 46-58.
25. O'Connor, C. J.; Beckmann, H. S.; Spring, D. R. Diversity-oriented synthesis: producing chemical tools for dissecting biology. *Chem. Soc. Rev.* **2012**, *41*, 4444-4456.
26. Macarron, R.; Banks, M. N.; Bojanic, D.; Burns, D. J.; Cirovic, D. A.; Garyantes, T.; Green, D. V.; Hertzberg, R. P.; Janzen, W. P.; Paslay, J. W. Impact of high-throughput screening in biomedical research. *Nature reviews Drug discovery* **2011**, *10*, 188-195.
27. Balkenhohl, F.; von dem Bussche-Hünnefeld, C.; Lansky, A.; Zechel, C. Combinatorial synthesis of small organic molecules. *Angewandte Chemie International Edition in English* **1996**, *35*, 2288-2337.
28. Terrett, N. K.; Gardner, M.; Gordon, D. W.; Kobylecki, R. J.; Steele, J. Combinatorial synthesis—the design of compound libraries and their application to drug discovery. *Tetrahedron* **1995**, *51*, 8135-8173.
29. Kodadek, T. The rise, fall and reinvention of combinatorial chemistry. *Chem. Commun.* **2011**, *47*, 9757-9763.
30. Bunin, B. A.; Ellman, J. A. A general and expedient method for the solid-phase synthesis of 1, 4-benzodiazepine derivatives. *J. Am. Chem. Soc.* **1992**, *114*, 10997-10998.
31. Simon, R. J.; Kania, R. S.; Zuckermann, R. N.; Huebner, V. D.; Jewell, D. A.; Banville, S.; Ng, S.; Wang, L.; Rosenberg, S.; Marlowe, C. K. Peptoids: a modular approach to drug discovery. *Proc. Natl. Acad. Sci. U. S. A.* **1992**, *89*, 9367-9371.
32. DeWitt, S. H.; Kiely, J. S.; Stankovic, C. J.; Schroeder, M. C.; Cody, D. M.; Pavia, M. R. "Diversomers": an approach to nonpeptide, nonoligomeric chemical diversity. *Proc. Natl. Acad. Sci. U. S. A.* **1993**, *90*, 6909-6913.

33. Houghten, R. A.; Pinilla, C.; Blondelle, S. E.; Appel, J. R.; Dooley, C. T.; Cuervo, J. H. Generation and use of synthetic peptide combinatorial libraries for basic research and drug discovery. *Nature* **1991**, *354*, 84-86.
34. Lam, K. S.; Salmon, S. E.; Hersh, E. M.; Hruby, V. J.; Kazmierski, W. M.; Knapp, R. J. A new type of synthetic peptide library for identifying ligand-binding activity. *Nature* **1991**, *354*, 82-84.
35. Tan, D. S.; Foley, M. A.; Shair, M. D.; Schreiber, S. L. Stereoselective synthesis of over two million compounds having structural features both reminiscent of natural products and compatible with miniaturized cell-based assays. *J. Am. Chem. Soc.* **1998**, *120*, 8565-8566.
36. Ohlmeyer, M. H.; Swanson, R. N.; Dillard, L. W.; Reader, J. C.; Asouline, G.; Kobayashi, R.; Wigler, M.; Still, W. C. Complex synthetic chemical libraries indexed with molecular tags. *Proc. Natl. Acad. Sci. U. S. A.* **1993**, *90*, 10922-10926.
37. Kerr, J. M.; Banville, S. C.; Zuckermann, R. N. Encoded combinatorial peptide libraries containing non-natural amino acids. *J. Am. Chem. Soc.* **1993**, *115*, 2529-2531.
38. Clark, M. A.; Acharya, R. A.; Arico-Muendel, C. C.; Belyanskaya, S. L.; Benjamin, D. R.; Carlson, N. R.; Centrella, P. A.; Chiu, C. H.; Creaser, S. P.; Cuozzo, J. W. Design, synthesis and selection of DNA-encoded small-molecule libraries. *Nature chemical biology* **2009**, *5*, 647-654.
39. Halpin, D. R.; Lee, J. A.; Wrenn, S. J.; Harbury, P. B. DNA display III. Solid-phase organic synthesis on unprotected DNA. *PLoS biology* **2004**, *2*, e175.
40. Wrenn, S. J.; Weisinger, R. M.; Halpin, D. R.; Harbury, P. B. Synthetic ligands discovered by in vitro selection. *J. Am. Chem. Soc.* **2007**, *129*, 13137-13143.
41. Melkko, S.; Scheuermann, J.; Dumelin, C. E.; Neri, D. Encoded self-assembling chemical libraries. *Nat. Biotechnol.* **2004**, *22*, 568-574.
42. Mandal, S.; Moudgil, M.; Mandal, S. K. Rational drug design. *Eur. J. Pharmacol.* **2009**, *625*, 90-100.
43. Gane, P. J.; Dean, P. M. Recent advances in structure-based rational drug design. *Curr. Opin. Struct. Biol.* **2000**, *10*, 401-404.
44. Lybrand, T. P. Ligand—protein docking and rational drug design. *Curr. Opin. Struct. Biol.* **1995**, *5*, 224-228.



## Chapter 2 – Dihydroquinazolinone Retrograde Transport Inhibitors.

**Parts of this work have been published in the following manuscript:** Nelson, C. S.; Carney, D. W.; Derdowski, A.; Williard, P. G.; Sello, J. K.; Atwood, W. J. *A Retrograde Trafficking Inhibitor of Ricin and Shiga-Like Toxins Inhibits Infection of Cells by Human and Monkey Polyomaviruses. Mbio.* **2013**, 4(6), e00729-13. dx.doi.org/10.1128/mBio.00729-13.

### Introduction

High-throughput phenotypic screening recently led to the discovery of small-molecules that protect mice from lethal doses of the plant toxin, ricin as well as the related bacterial Shiga-like toxins (Stx1 and Stx2).<sup>1</sup> Ricin and Stx toxins are both type 2 ribosome inactivating proteins (RIPs) that pose serious human health risks. Ricin, which is isolated from castor beans, is extremely lethal (LD50 22 µg/Kg) and has recently emerged as a potential bio-terrorism agent.<sup>2</sup> Stx toxins are virulence factors produced by *Shigella dysenteriae* and *Escherichia coli* that can cause hemorrhagic colitis, hemolytic-uremic syndrome, and sometimes death. No small molecule therapeutics have been approved for the treatment of Ricin or Stx intoxication. Furthermore, before the discovery by Stechmann *et al.* there were no obvious targets to be exploited in order to treat ricin intoxication.<sup>1</sup>

Stechmann *et al.* developed a whole-cell based assay wherein inactivation of the ribosome by ricin could be monitored based on the incorporation of radiolabeled leucine into newly synthesized proteins. In the high throughput screen, small molecules that could inhibit ricin activity could be identified by their capacity to increase radiolabeled leucine uptake when compared to untreated cells. A library of 16,480 drug-like compounds were screened using the assay and two hits, named Retro-1 and Retro-2, were positively identified (Figure 2.1). These compounds were independently shown to exhibit toxin inoculum-dependent protection of HeLa

cells against ricin, Stx1, and Stx2. Furthermore, Retro-2 was shown to protect mice from a lethal ricin challenge. Finally, Stechmenn *et al.* showed that the compounds did not interact with the toxins themselves, but rather inhibited retrograde transport of the toxins by interacting with a host cellular factor, which has yet to be identified.

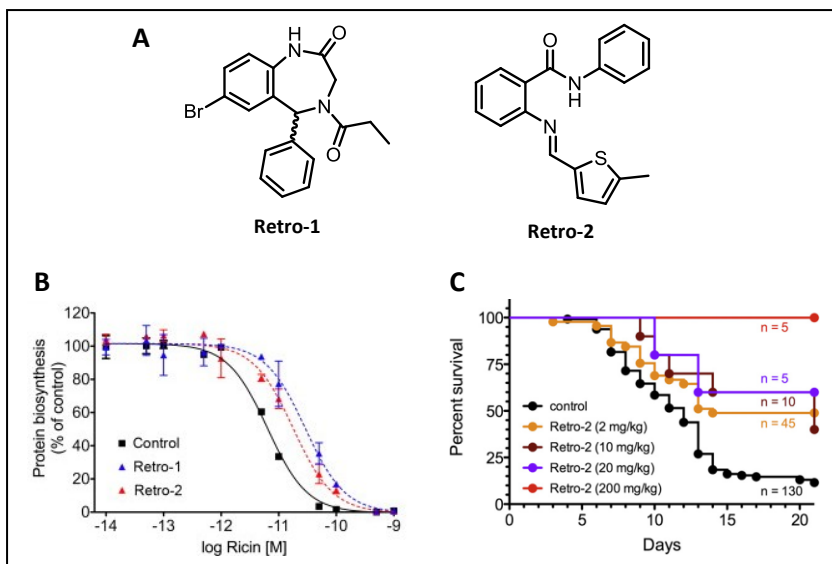


**Figure 2.1 – Small molecule inhibitors of retrograde trafficking A) structures of HTS hits, Retro-1 and Retro-2 B) Effects of Retro-1 and Retro-2 (20  $\mu$ M) on protein biosynthesis in cells treated with varying concentrations of ricin<sup>1</sup> C) Retro-2 protects mice from lethal Ricin challenge. Mice were treated intraperitoneally with a single dose of compound 1 hour prior to animal exposure to ricin (2  $\mu$ g/Kg, nasal instillation).<sup>1</sup>**

Retrograde trafficking is an important intracellular transport phenomenon wherein protein, lipids, and small molecules are chaperoned from endosomes to the trans-Golgi network, Golgi-membranes, and in some cases directly to the endoplasmic reticulum (ER) (Figure 2.2).<sup>3</sup> It is the primary mechanism of recycling chaperones, receptors, and other cargo molecules that are targeted to the cell membrane from the Golgi. This transport route is often times exploited by toxins and viral pathogens for entry into the cytoplasm.<sup>3,4</sup> Retro-1 and Retro-2 apparently block toxin retrograde transport without significantly affecting endogenous trafficking.<sup>1</sup>

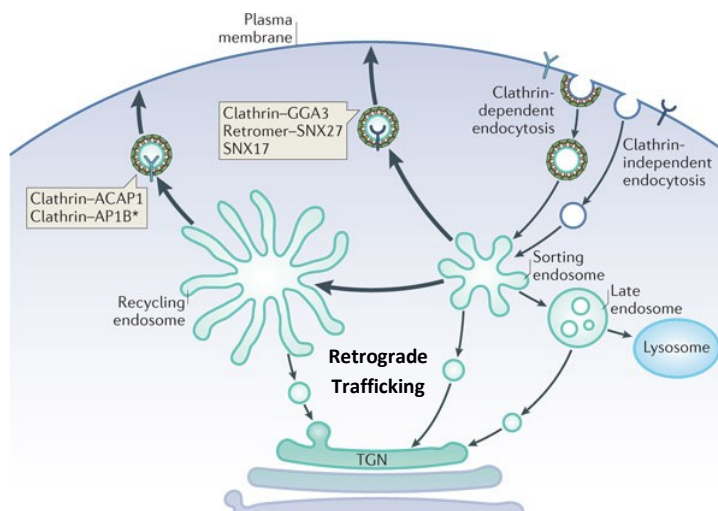
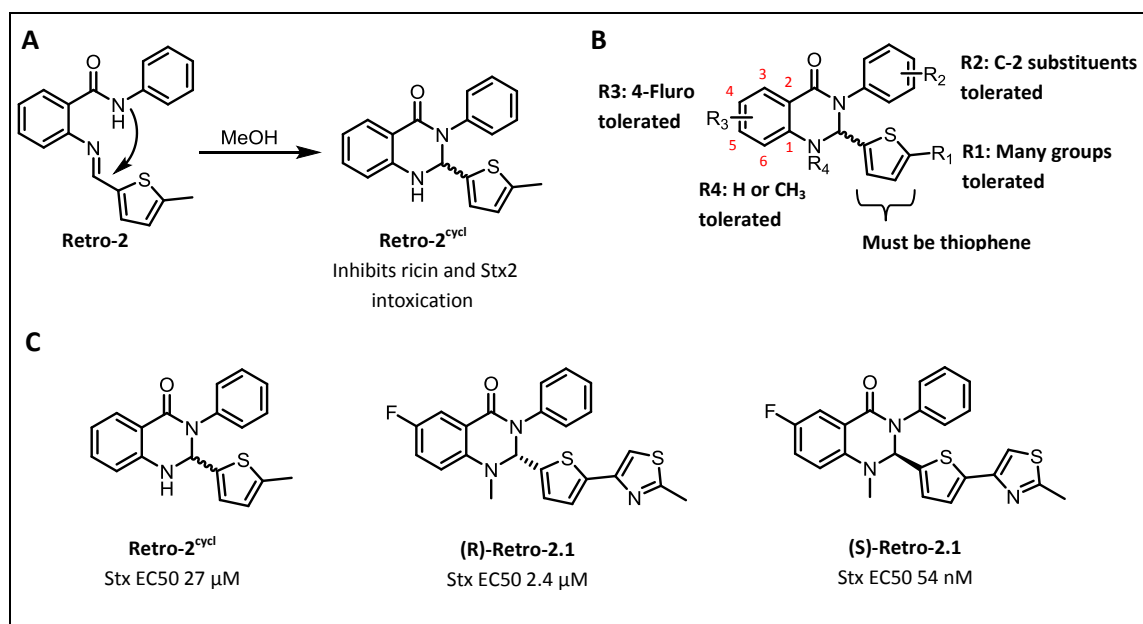


Figure 2.2 – Retrograde trafficking of endosome cargo.<sup>5</sup> Endosomal cargo that is delivered from the cell membrane surface by clathrin-dependent and -independent endocytosis can have several fates. Cargo can be recycled directly back to the cell surface, transported to the lysosome, or transported to the trans-Golgi network (TGN) via retrograde trafficking.

Since its initial disclosure by Stechmann *et al*, Retro-2 has received considerable attention, including several developments published during the course of our own studies. First, the structure of Retro-2 was revised in 2012 when it was shown by Park *et al.* that Retro-2 undergoes a facile ring closure to form a dihydroquinazolinone (DHQ) structure, named Retro-2<sup>cycl</sup>, in protic solvent (Figure 2.3A).<sup>6</sup> Park *et al.* also independently verified that Retro-2<sup>cycle</sup> is able to protect cells from ricin and Stx2. In 2013, two medicinal chemistry reports were published by Cintrat and co-workers concerning Retro-2<sup>cycl</sup>. The first report describes an extensive SAR study and structure optimization (Figure 2.3B).<sup>7</sup> Over 100 analogs were synthesized and evaluated for their ability to protect cells against Stx1. The optimized structure that emerged (Retro-2.1) was an *N*-methyl-dihydroquinazolinone with an elaborated thiophene moiety and a fluorinated benzo moiety. In the second report, the enantiomers of their lead structure were separated, and it was shown that the (*S*)-*N*-methyl-dihydroquinazolinone was significantly more active than the (*R*)-enantiomer and was an overall 500 fold more potent than Retro-2<sup>cycl</sup> (Figure 2.3C).<sup>8</sup>



**Figure 2.3 – Recent developments in Retro-2 research** A) Retro-2 spontaneously cyclizes in protic solvent to form bioactive DHQ Retro-2<sup>cycl</sup>.<sup>6</sup> B) Summary of published SAR for Retro-2<sup>cycl</sup>.<sup>7</sup> C) Activity of Retro-2<sup>cycl</sup> and optimized analogs for inhibition of Stx intoxication.<sup>8</sup>

Our realization of the utility of retrograde transport inhibitors for protecting cells from ricin and Shiga-like toxins led us to hypothesize that the same strategy may be useful for blocking infection by certain viruses. Human polyomaviruses (PyV) and papillomaviruses (HPV) are two families of viruses that exploit the host-retrograde trafficking pathway during cell entry. While there are minor differences in the infectivity pathways of these two viruses, they both pose serious health risks via cell entry via retrograde trafficking.<sup>9,10</sup>

Polyomaviruses have small, non-enveloped, icosahedral virions containing double-stranded DNA.<sup>11</sup> The viruses have established latent infection in the vast majority of the human population.<sup>11,12</sup> It is estimated that as much as 90% of the adult population is seropositive for BK polyomavirus (BKPyV) and as much as 40% of adults are seropositive for JC polyomavirus (JCPyV).<sup>12</sup> Typically, polyomavirus infections persist without symptoms in humans unless an individual becomes immunocompromised, such as in AIDS or immunomodulatory therapy. Increased replication and dissemination of polyomaviruses can lead to the development of

neurodegenerative progressive multifocal leukoencephalopathy (PML) in the case of JCPyV infection, which affects 3-5% of AIDS patients.<sup>13,14</sup> BKPyV is most often problematic during immunosuppressive treatments and can lead to the development of hemorrhagic cystitis and polyomavirus nephropathy (PVN) in as much 10% of transplant patients.<sup>11,15</sup> Papillomaviruses are also nonenveloped, DNA viruses<sup>16</sup> Unlike the PyV, which exhibits broad dissemination, HPV infection and replication is limited to the basal layer of epithelial tissue.<sup>17</sup> These viruses are believed to be associated with as much as 5% of all forms of cancer, most notable of which are cancer of the cervix and uterus.<sup>16,18</sup> Prophylactic vaccination against certain types of HPV has been rather successful. However, HPV related diseases will remain a significant human health problem for at least several decades in individuals who refuse vaccination or who become infected before receiving vaccination. Currently, there are no approved small-molecule therapeutics for the treatment or prevention of PyV and HPV infection.

Here, we demonstrate that interference with retrograde transport by DHQ analogs of Retro-2 is effective for inhibiting successful PyV and HPV infection. The Pyv infectivity assay was used as a benign platform for investigating DHQ retrograde transport inhibitor structure-activity relationships (SARs). Through the course of investigating the DHQ SARs, we discovered analogs with significantly improved potency. Finally, as a means to demonstrate the generality of retrograde transport interference as a strategy for combating a variety of pathogens, we also show that our optimized DHQs exhibit similarly improved efficacy against HPV infection.

## Results

### *Inhibition of JC polyomavirus infection by Retro-2*

The mechanism of infection by polyomaviruses is still an active area research. It has been established that the viruses bind to a cell surface receptor before internalization via the

endocytotic pathway and transport to the endosomes.<sup>19-21</sup> The viron is then trafficked from early or late endosomes to the ER where the capsid is partially disassembled and then retrotranslocated into the cytosol.<sup>22-26</sup> While it is not yet known specifically how the PyV virions are targeted to the ER and which cellular machinery facilitate their transport, it is clear that trafficking proceeds via the retrograde pathway. Our collaborators in the Atwood group from the Brown Molecular Biology, Cell Biology, and Biochemistry department originally purchased Retro-2 from Chembridge and tested its effects on JCPyV infection. Indeed, the compound exhibited a clear inhibitory effect on JCPyV infectivity (Figure 2.4).

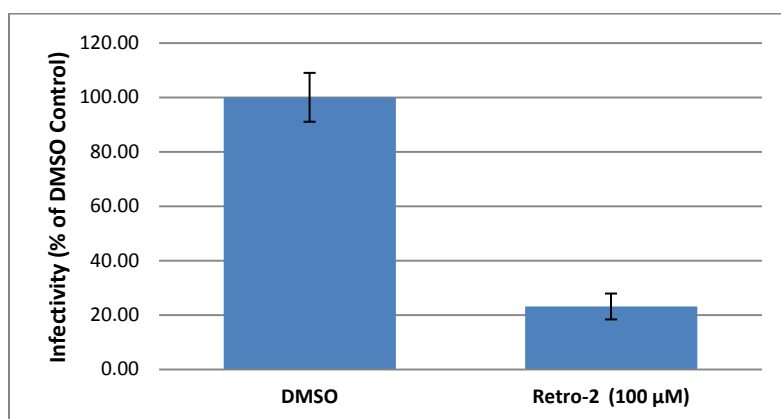
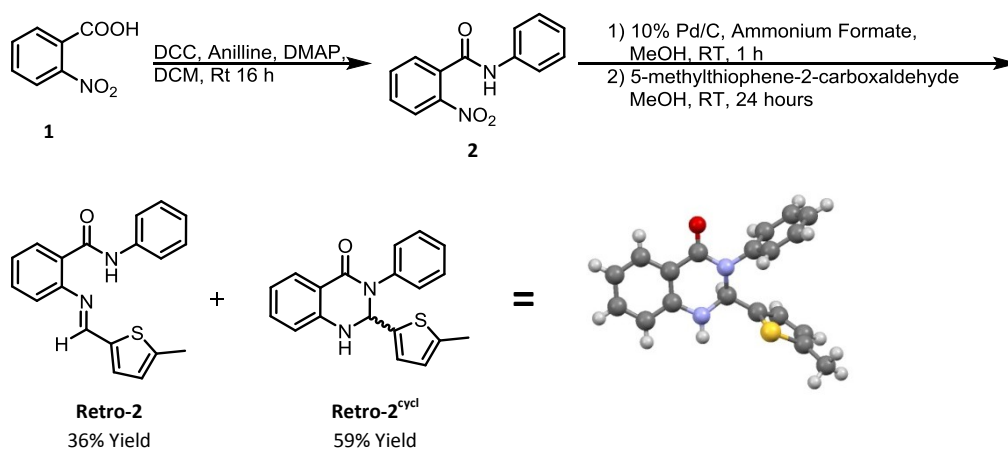


Figure 2.4 – Inhibition of JCPyV infectivity by Retro-2 purchased from Chembridge. Infected cells were scored and normalized to the DMSO-treated control. The data represent the average of triplicate samples. Error bars indicate the standard deviation.

#### *Retro-2 structural studies*

Upon their discovery that Retro-2 inhibited JCPyV infection, our collaborators approached us for assistance with structural validation of the Retro-2 supplied from Chembridge. The subsequent experiments were completed prior to the disclosure by Park *et al.*<sup>6</sup> regarding the cyclization of Retro-2. Our initial analysis of the compound's <sup>1</sup>H-NMR spectrum revealed some peculiarities. Two diagnostic signals that we anticipated for the Retro-2 structure, downfield singlets for the secondary aromatic amide proton ( $\delta = 10-11$  ppm) and the proton bonded to the imine carbon ( $\delta = 8-9$  ppm), were not observed. We therefore attempted

to synthesize Retro-2 according to a procedure described in the patent literature (Figure 2.5).<sup>27</sup> 2-nitrobenzoic acid (**1**) was coupled to aniline using standard carbodiimide chemistry. The resulting 2-nitrobenzanilide (**2**) was converted to the corresponding 2-aminobenzanilide via palladium on carbon catalyzed transfer hydrogenation in methanol and subsequently condensed with 5-methylthiophene-2-carboxaldehyde. The reaction yielded two products, which were separable by flash chromatography on silica gel. The spectroscopic data for one of the products corresponded to what was expected for Retro-2, while the spectroscopic data for the second product matched the bioactive compound obtained from Chembridge. Crystallographic X-ray diffraction revealed the second product to be a dihydroquinazolinone derivative of Retro-2, the same structure that would eventually be referred to as Retro-2<sup>cycl</sup> by Park *et al.*<sup>6</sup>



**Figure 2.5 – Synthesis of Retro-2 and corresponding dihydroquinazolinone. The dihydroquinazolinone structure was confirmed by X-ray diffraction crystallography.**

In further chemical investigations, we found that incubation of Retro-2 in methanol with a Lewis acid catalyst such as scandium (III) triflate resulted in rapid cyclization to the corresponding DHQ (Figure 2.6A). This was unsurprising as imine structures such as Retro-2 are commonly invoked as intermediates to DHQs.<sup>28-31</sup> We also found that Retro-2<sup>cycle</sup> was slowly converted into secondary amine (**2**) upon treatment with sodium cyanoborohydride and acetic

acid in methanol (Figure 2.6B). This observation indicates that in protic solvent, such as methanol or water, DHQ formation is reversible. Therefore, even if administration of Retro-2<sup>cycl</sup> effectively inhibits PyV infectivity, there is the distinct possibility that the active compound may be the ring-opened Retro-2. A regioisomer of Retro-2 was prepared in a similar manner as Retro-2 (Figure 2.6C) and was tested for bioactivity to determine if an imine structure was necessary and sufficient for bioactivity.

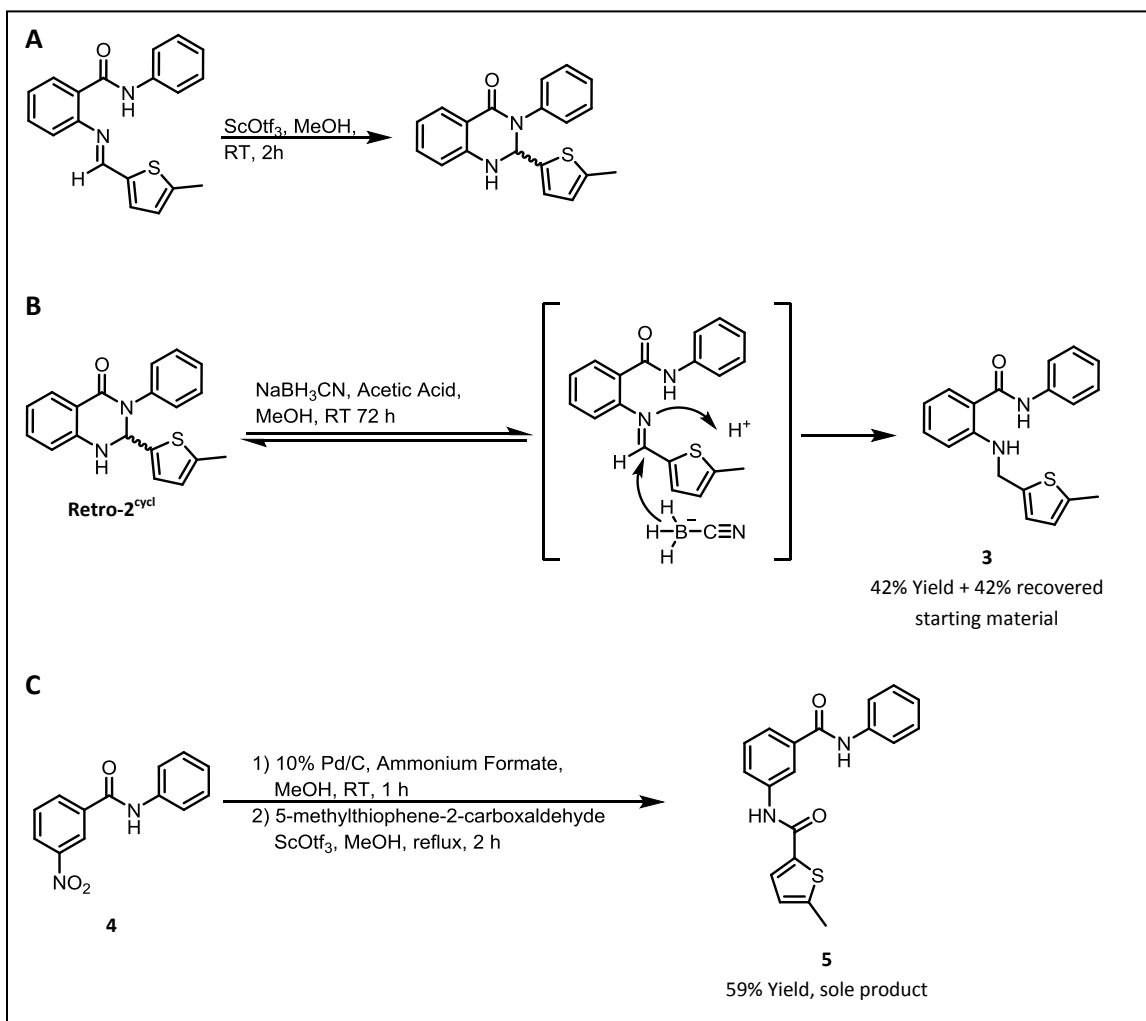


**Figure 2.6 – Retro-2 structural studies** A) Retro-2 rapidly cyclizes to for Retro-2<sup>cycl</sup> in protic solvent with a Lewis acid catalyst B) Treatment of Retro-2cycle with sodium cyanoborohydride and acetic acid in methanol leads to ring opening and imine reduction. C) Synthesis of an uncyclizable Retro-2 regioisomer.



The inhibitory effects of Retro-2, Retro-2<sup>cycl</sup>, reduced species **3**, and regioisomer **5** on JCPyV infection were tested (Figure 2.7). SVG-A cells were incubated with 100 μM of each compound and challenged with JCPyV. Unsurprisingly, both Retro-2 and Retro-2<sup>cycl</sup> inhibited polyomavirus infection with similar efficacies. Compounds **3** and **5** both showed very little activity. These results strongly suggest that Retro-2 spontaneously cyclizes in aqueous media and that Retro-2<sup>cycl</sup> is the bioactive compound.

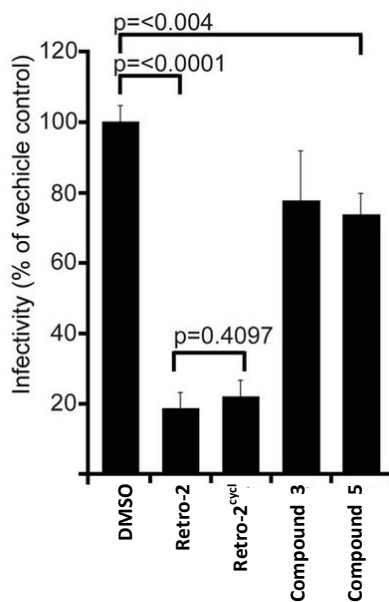
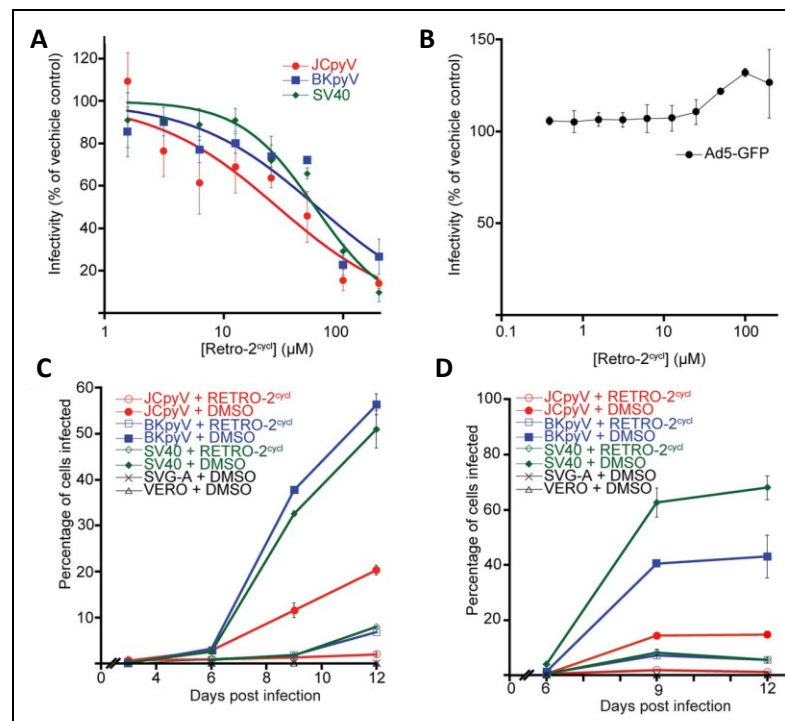


Figure 2.7 – Inhibitory activities of Retro-2 analogs: Cells were pretreated with the Indicated compound or DMSO and inoculated with JCPyV. Infected cells were scored and normalized to the DMSO treated control. The data represent the average of triplicate samples. Error bars indicate the standard deviation.

#### *Inhibition profile of Retro-2<sup>cycle</sup> against monkey and human polyomaviruses*

Retro-2<sup>cycle</sup> that was synthesized in-house was tested against three polyomaviruses and green fluorescent protein (GFP)-expressing adenovirus (Ad5-GFP) as a negative control. Adenoviruses do not exploit retrograde trafficking in their infectivity pathway. When administered prior to viral inoculation, Retro-2<sup>cycle</sup> exhibited a dose dependent reduction in infection of Vero cells by all three polyomaviruses (Figure 2.8A), but had no effect on the infection by Ad5-GFP (Figure 2.8B). As anticipated, Retro-2<sup>cycle</sup> activity is specific to viruses that exploit retrograde trafficking. Most individuals are infected with JCPyV or BkPyV prior to

immunosuppression. We were therefore interested to know if Retro-2<sup>cycl</sup> could prevent viral spreading in established tissue culture infections. Untreated cells were inoculated with three different polyomaviruses. Following one round of productive infection, 100  $\mu$ M retro-2<sup>cycl</sup> was added to these cells and maintained during the course of the experiment. Treatment of cells resulted in a reduction of infected cells compared to the vehicle control (Figure 2.8C). By the conclusion of the experiment (12 days), Retro-2<sup>cycl</sup> had significantly diminished the spreading of SV40 (84% inhibition), BKPyV (89%), and JCPyV (90.5%). To examine whether the treatment of these cultures with retro-2<sup>cycl</sup> inhibited virion production, supernatants from each time point were used to re-infect naive cells that were not Retro-2<sup>cycl</sup> treated. Cultures that were previously treated with Retro-2<sup>cycl</sup> produced significantly less infectious virions (Figure 2.8D). These observations demonstrate that Retro-2<sup>cycl</sup> decreases the cell-to-cell spreading of polyomaviruses in previously infected cultures.



**Figure 2.8 - Retro-2<sup>cycl</sup> prevents infection with three polyomaviruses. (A) Dose-dependent effect of retro-2<sup>cycl</sup> treatment on infection. Cells were preincubated with the indicated concentrations of retro-2<sup>cycl</sup> prior to inoculation with virus. Infections were scored and normalized to a DMSO-treated control. (B) Retro-2<sup>cycl</sup> does not**

block infection by adenovirus. Cells were pretreated with equivalent concentrations of retro-2<sup>cycl</sup> prior to infection with an Ad5-GFP. Cells were scored and normalized to a DMSO-treated sample. (C) Retro-2<sup>cycl</sup> prevents virus spreading in a multicycle growth assay. Cells were inoculated with virus for 72 h. Cells were then maintained in the presence of 100  $\mu$ M retro-2<sup>cycl</sup>. Cells were scored for infection every 3 days. (D) Retro-2<sup>cycl</sup>-treated cultures release less infectious virus into culture medium. Tissue culture medium was harvested every 3 days and used to infect naive cells not treated with retro-2cycl. The data represent the mean of three replicates, and error bars indicate the standard deviation.

### Dihydroquinazolinone Structure-Activity Relationships and Optimization

The remarkable inhibitory activity exhibited by Retro-2<sup>cycl</sup> encouraged us to pursue structure activity relationship (SAR) and compound optimization studies. These studies were in the late stages of completion when the SAR studies by the Cintrat group were reported.<sup>7,8</sup> The Retro-2<sup>cycl</sup> structure can be divided into three distinct moieties (figure 2.9A), a heterocycle moiety, an amide moiety, and a benzo moiety. We therefore carried out compound diversification in consecutive phases wherein one moiety was varied independently of the other two. At the end of each phase, the most active compound served as a new lead structure for the subsequent diversification phase. In addition to characterizing key structure-activity relationships, our strategy also led to the discovery of optimized drug leads with significantly improved anti-viral activity as compared to Retro-2<sup>cycl</sup>.

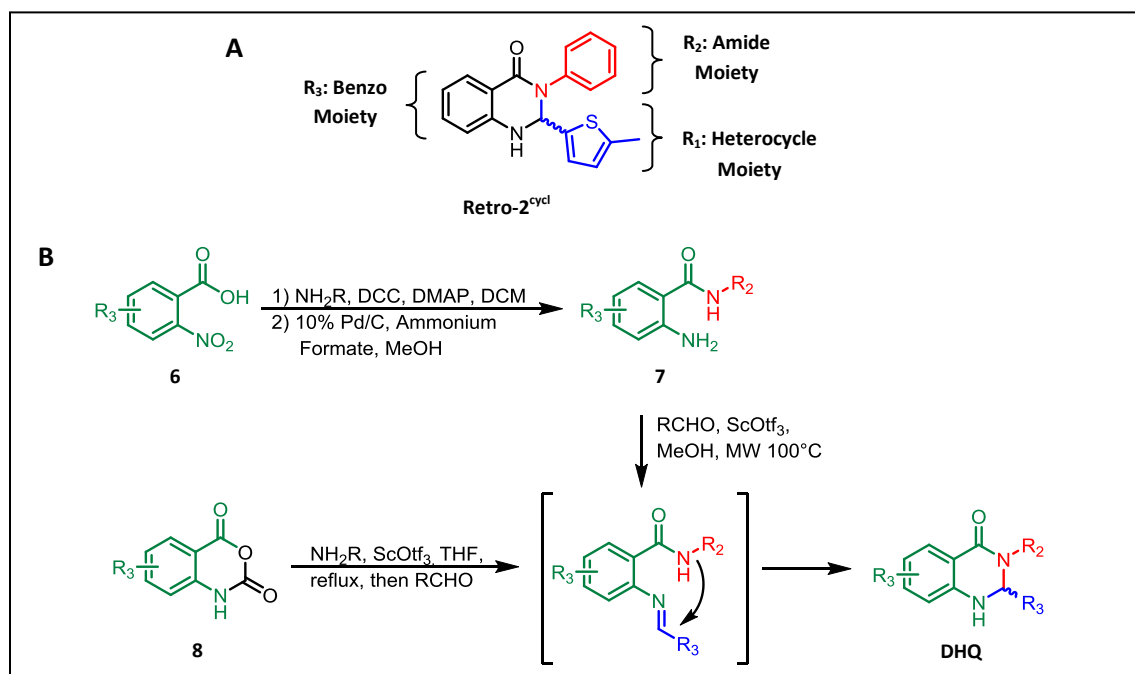


Figure 2.9 – Retro-2<sup>cycl</sup> diversification strategy A) Retro-2<sup>cycl</sup> has 3 easily diversifiable moieties. B) Synthetic schemes for the preparation of Retro-2<sup>cycl</sup> analogs.

Two routes were used for the synthesis of DHQs (Figure 2.9B). In one route, primary amines were condensed with a 2-nitrobenzoic acid (**6**) with dicyclohexylcarbodiimide (DCC) and dimethylaminopyridine (DMAP) then reduced to an amine via transfer hydrogenation with ammonium formate and palladium on carbon in methanol to afford anthranilamides (**7**). The anthranilamide intermediates were condensed with an aromatic aldehyde in the presence of scandium (III) triflate under microwave irradiation to afford the desired DHQ. Alternatively, DHQs were prepared in one pot by reaction of an isatoic anhydride (**8**) with a primary amine in THF followed by addition of an aromatic aldehyde and scandium (III) triflate. Preparation of DHQs from isatoic anhydrides was the preferred route. However in certain instances, the availability of starting materials as well as the poor nucleophilicity of aniline required preparation of DHQ's from the corresponding 2-nitrobenzoic acid (**6**).

The first moiety investigated was the heterocycle bound to the dihydroquinazolinone stereogenic carbon (Table 2.1). In particular, two structural aspects of the heterocycle moiety were investigated: the identity of the heteroatom as well as position and identity of the heterocycle substituent. Compounds **9-11** had unsubstituted heterocycle moieties and all exhibited significantly attenuated activity compared to Retro-2<sup>cycl</sup>. Interestingly, compound **12**, bearing a 5-methylfuran moiety, had similar activity to that of Retro-2<sup>cycl</sup>, which bears a 5-methylthiophene moiety. These data suggest that the identity of the heteroatom has a minor role in the apparent inhibitory activity. Although the thiophene ring provides greater potency, it is apparent that a furan ring can also be tolerated. The effects of position and identity of the thiophene substituent are also noteworthy. Compound **13**, bearing a methyl group at the 4 position, had nearly equal activity compared to Retro-2<sup>cycl</sup>. On the other hand, compound **14**, bearing a methyl group at the 3 position, had similar activity to the DHQs with unsubstituted

heterocycle moieties. Inhibitory activity is significantly enhanced when the heterocycle bears an ethyl group at the 5 position (compound **15**). However, activity is severely attenuated when the heterocycle is a benzothiophene ring (compound **16**). These results partially agree with the Cintrat results. While the observed heterocycle substituent effects are in agreement with those reported by Cintrat *et al*, they did not find that 5-alkyl furan groups could be tolerated. Further extension of the C-5 thiophene substituent as in the case of Retro2.1, or dialkylsubstitution at thiophene C-4 and C-5 positions could lead to further enhancement of activity. We did not pursue further optimization of the heterocycle moiety. Instead, the 5-ethylthiophene moiety was held constant throughout our investigation of the remaining moieties.

**Table 2.1 - Anti-JCPyV Activity of DHQ Inhibitors at 25  $\mu$ M with Varied Heterocycle Moiety**

Compound	R <sub>1</sub>	Infectivity (% DMSO Control)	Compound	R <sub>1</sub>	Infectivity (% DMSO Control)
Retro-2 <sup>cycl</sup>		57.5 $\pm$ 5.9	<b>13</b>		55.6 $\pm$ 14.4
<b>9</b>		81.1 $\pm$ 16.9	<b>14</b>		76.4 $\pm$ 1.1
<b>10</b>		92.4 $\pm$ 4.45	<b>15</b>		47.8 $\pm$ 3.8
<b>11</b>		69.9 $\pm$ 27.8	<b>16</b>		95.3 $\pm$ 14.3
<b>12</b>		64.4 $\pm$ 12.7			

Cells were preincubated with the indicated concentrations of retro-2<sup>cycl</sup> prior to inoculation with virus. Infections were scored and normalized to a DMSO-treated control. The data represent the mean of three replicates with indicated standard error.

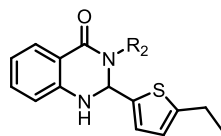
We next turned our attention to the amide moiety (Table 2.2). Most of the amide substituents retained similar activity to that of compound **15**, including compound **17**, which has

only a hydrogen as the amide substituent. Dramatic improvements in activity were observed when the amide moiety was either a benzyl (compound **22**) or methylnaphthyl (compound **24**) group. Realization of the improvement in antiviral activity by the incorporation of a benzyl group into the amide moiety was rather fortunate. Many substituted benzyl amines are commercially available, thus enabling even further investigation into the structure-activity relationships of the amide moiety. We investigated the effects of electron donating methoxy group(s) (compounds **25-28**), a fluorine atom (compounds **29-30**), and an electron withdrawing nitro group (compounds **31-32**) at various positions on the benzene ring. In most cases, the addition of substituents on to the benzyl group was tolerated, aromatic nitro groups being the main exception. The incorporation of a *para*-fluoro substituent (compound **29**) resulted in a significant improvement in activity compared to the unsubstituted benzyl amide analog **22**. In this phase, our SAR results diverge significantly from those reported by Cintrat, which did not explore benzyl substituents. It is conceivable that their Retro-2.1 would benefit significantly by substituting its phenyl amide for a 4-fluorobenzyl group.

In reactions without a chiral substrate, a racemic mixture of two enantiomeric DHQs is produced. In two cases, chiral  $\alpha$ -methylbenzylamines (compounds **33-34**) were used to generate the amide moieties with the hopes of achieving stereochemical induction at the stereocenter that is created in the DHQ forming cyclization reaction.<sup>32</sup> The chiral  $\alpha$ -methylbenzyl groups both attenuated activity compared to the unsubstituted benzyl group. However, attenuation of activity was more severe with the (*R*)- $\alpha$ -methylbenzylamide than with the (*S*)- $\alpha$ -methylbenzylamide. It is worth noting that our DHQ forming reactions with chiral  $\alpha$ -methylbenzylamines as substrates produced the products as single diastereomers and are therefore enantiomerically pure. We have not yet been able to determine the configuration of the DHQ stereocenters in these products to see if they correspond to the stereochemical

preferences reported by Cintrat.<sup>8</sup> Enantioselective dihydroquinazolinone syntheses that are not substrate controlled have been reported,<sup>29,33,34</sup> and their application to the synthesis of Retro-2<sup>cycl</sup> analogs is obviously very enticing. However, these compounds can not be stably prepared due to ring opening and closing under equilibrium conditions.

Table 2.2 - Anti-JCPyV Activity of DHQ Inhibitors at 25 $\mu$ M with Varied Amide Moiety



Compound	R <sub>2</sub>	Infectivity (% DMSO Control)	Compound	R <sub>2</sub>	Infectivity (% DMSO Control)
17	H	41.4 ± 1.39	26		27.5 ± 1.78
18		76.4 ± 1.12	27		13.7 ± 0.455
19		69.9 ± 27.8	28		16.4 ± 3.92
20		42.4 ± 2.58	29		7.62 ± 0.981
21		45.7 ± 10.3	30		14.0 ± 2.64
22		13.3 ± 1.13	31		30.6 ± 3.17
23		50.4 ± 2.32	32		44.5 ± 8.76
24		14.5 ± 0.654	33		32.4 ± 13.7
25		21.2 ± 5.12	34		52.7 ± 1.46

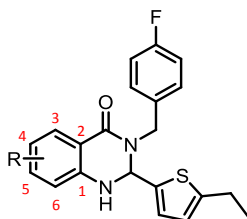
Cells were preincubated with the indicated concentrations of retro-2<sup>cyd</sup> prior to inoculation with virus. Infections were scored and normalized to a DMSO-treated control. The data represent the mean of three replicates with indicated standard error.

In our third phase of SAR investigation, the benzo moiety was varied while the heterocycle and amide moieties were held constant as a 5-ethylthiophene group and a 4-fluorobenzyl group respectively (Table 2.3). We first examined the effect of methylation at each



of the four otherwise unsubstituted aromatic carbons of the Benzo moiety. Methyl groups were tolerated at C-3 (**35**) and C-4 (**36**). However, methyl substituents at C-5 (**37**) and C-6 (**38**) resulted in severe attenuation of activity. Similarly, a chlorine atom was well tolerated at C-4 (**39**) but attenuated activity slightly when present at C-5 (**40**). A fluorine atom at C-4 (**41**) improved activity and was tolerated at C-5 (**42**). These data suggest that C-5 and C-6 make close contact with the target binding pocket. However there is likely to be space for substituents at C-3 and C-4. Overall the SAR results of our third diversification phase are highly consistent with Cintrat's reported SAR.

**Table 2.3 - Anti-JCPyV Activity of DHQ Inhibitors at 25 $\mu$ M with Varied Benzo Moiety**



Compound	Structure	Infectivity (% DMSO Control)	Compound	Structure	Infectivity (% DMSO Control)
<b>35</b>	3-Methyl	10.2 $\pm$ 5.68	<b>39</b>	4-Chloro	13.7 $\pm$ 16.2
<b>36</b>	4-Methyl	8.34 $\pm$ 2.76	<b>40</b>	5-Chloro	21.3 $\pm$ 2.82
<b>37</b>	5-Methyl	67.1 $\pm$ 9.12	<b>41</b>	4-Fluoro	4.45 $\pm$ 0.613
<b>38</b>	6-Methyl	44.5 $\pm$ 2.51	<b>42</b>	5-Fluoro	8.82 $\pm$ 7.52

Cells were preincubated with the indicated concentrations of retro-2<sup>cycl</sup> prior to inoculation with virus. Infections were scored and normalized to a DMSO-treated control. The data represent the mean of three replicates with indicated standard error.

Halogenated species (compounds **39-42**) could enable elaboration of the dihydroquinazolinone substructure via the use of aromatic substitution or cross-coupling reactions. As a proof of principle, *n*-butylamino analog **45** was prepared (Figure 2.10). A SNAr reaction of 4-fluoro-2-nitroamide **43** with *n*-butylamine provided 4-(*n*-butylamino)-2-nitroamide **44**. Reduction of the 2-nitro group followed by condensation/cyclization with 5-ethyl-2-thiophenecarboxaldehyde provided DHQ **45**. Unfortunately, incorporation of the *n*-butylamino group at C-4 resulted in a severe attenuation of activity (Infectivity at 25  $\mu$ M: 71.0  $\pm$  8.28 %

DMSO Control). It is feasible that smaller amino groups might be better tolerated. However, no additional analogs were prepared.

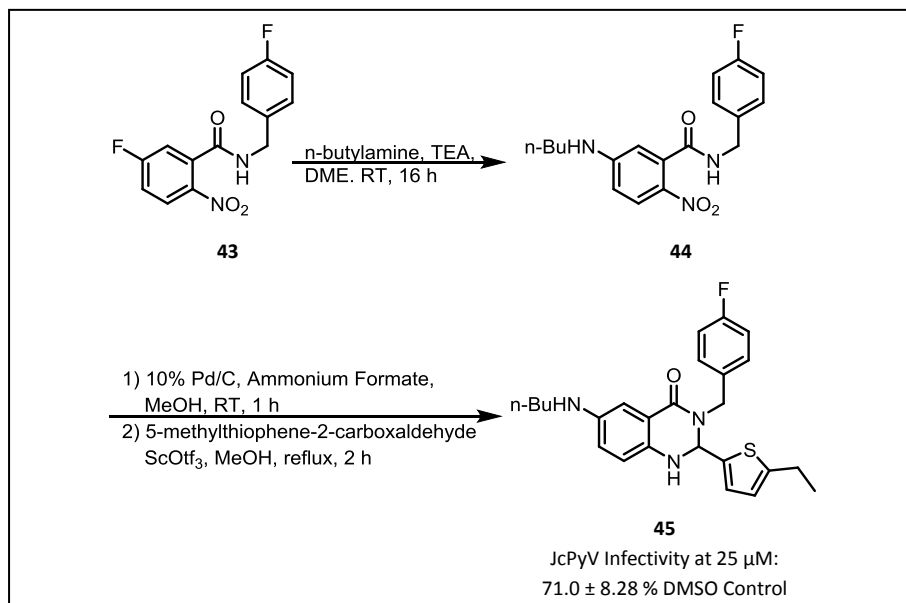
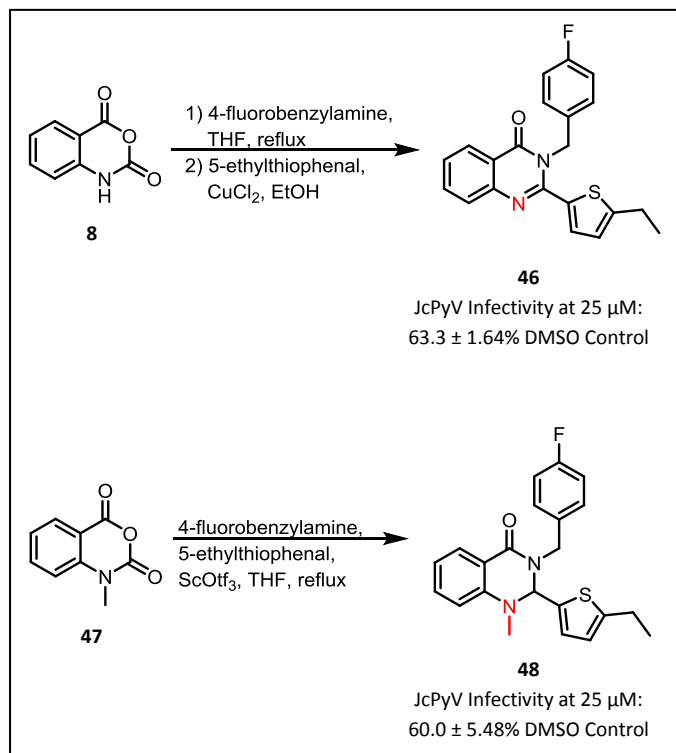


Figure 2.10 – Synthesis and Activity of *n*-butylamino dihydroquinazolinone

Two final analogs were synthesized in order to probe SAR around the DHQ aromatic amine (Figure 2.11). First, we evaluated the significance of DHQ oxidation state by preparing the quinazolinone form of compound **29**. The quinazolinone species (**46**) has a more planar geometry than the corresponding DHQ (**29**). Also, **46** lacks the *N*-1 amino hydrogen, a potentially important hydrogen bond donor. Ultimately, we found quinazolinone **46** to be much less active than DHQ **29**, which is also consistent with the SAR reported by Cintrat. Additionally, we prepared an *N*-methyl-DHQ (**48**) and found that this compound was also much less active than DHQ **29**. These results indicate that the DHQ amino group plays an important role in the substrate-target binding interaction, most likely in the form of a hydrogen bond. This SAR is a major point of contention with the results published by Cintrat. In fact, the optimized compound from Cintrat's medicinal chemistry program is a *N*-methyl-dihydroquinazolinone. Although Cintrat's results are based upon inhibition of Stx intoxication and our results are based upon

inhibition of viral infection, the compounds should be affecting the same host cellular factor.

The differences between Cintrat's and our results are therefore very difficult to reconcile.



**Figure 2.11 - Synthesis and Activity of quinazolinone and *N*-methylidhydroquinazolinone analogs.**

The most potent Retro-2<sup>cycl</sup> analog discovered in this study was DHQ **41**. In order to determine the fold improvement in potency of our optimized compound over Retro-2<sup>cycl</sup>, dose response curves were generated for both compounds and IC<sub>50</sub> values for inhibition of JcPyV Infectivity in SVGA cells were calculated (Figure 2.12). There was an overall 6.7 fold improvement in potency from the original lead Retro-2<sup>cycl</sup> (IC<sub>50</sub> = 51 μM) to our optimized compound, DHQ **41** (IC<sub>50</sub> = 8.1 μM).

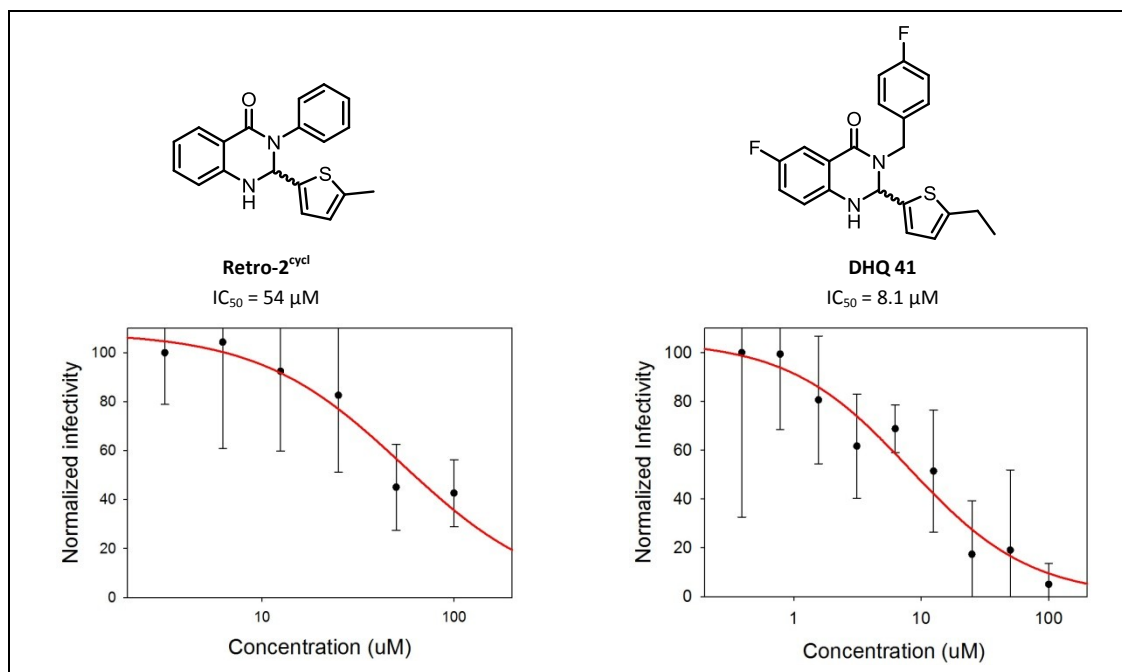


**Figure 2.12 – Inhibition of JCPyV infectivity in SVG-A Cells: dose response for Retro-2<sup>cycl</sup> and optimized analog 38.** Cells were preincubated with the indicated concentrations of retro-2<sup>cycl</sup> prior to inoculation with virus. Infections were scored and normalized to a DMSO-treated control. The data represent the mean of three replicates with indicated standard error.

#### *Inhibition of papylomavirus infection by dihydroquinazolinones*

The infectivity pathway for human papillomaviruses is not as thoroughly understood as for polyomaviruses. What is known, is that HPV is internalized by endocytosis and first trafficked to the endosomal vesicles.<sup>9,35,36</sup> A partially disassembled HPV capsid escapes from the late endosome and is eventually trafficked to the nucleus for replication.<sup>36,37</sup> Elucidation of the details of HPV transit between late endosomes and the nucleus is an ongoing area of research. It was recently shown by the DiMaio group that HPV is trafficked through the retrograde pathway, and is sensitive to inhibition by Retro-2<sup>cycl</sup>.<sup>10</sup> In collaboration with the DiMaio group, we have tested the effects of our optimized DHQ **41** on HPV infectivity relative to Retro-2<sup>cycl</sup>. dose response curves were generated for both compounds and IC<sub>50</sub> values for inhibition of HPV Infectivity in HeLaM cells were calculated (Figure 2.13). There was an overall 6.7 fold

improvement in potency from the original lead Retro-2<sup>cycl</sup> (IC<sub>50</sub> = 160 μM) to our optimized compound, DHQ **41** (IC<sub>50</sub> = 24 μM), which is very similar to the difference in potency of the same compounds for inhibition of polyomavirus infectivity.

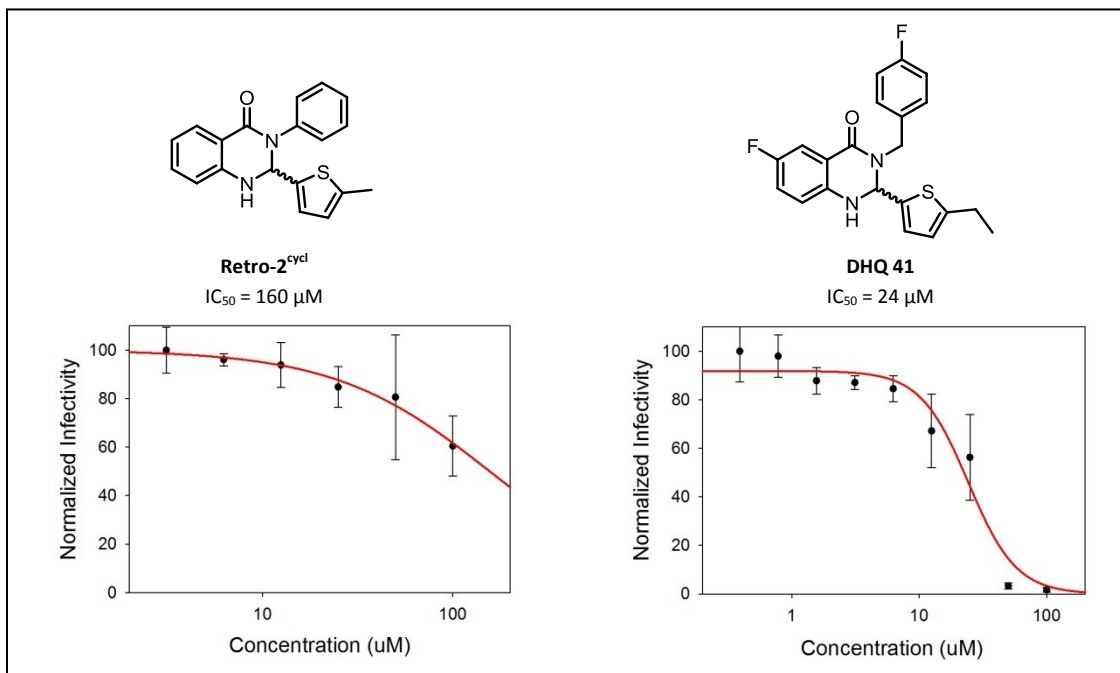


**Figure 2.13 – Inhibition of HPV infectivity in HeLaM Cells: dose response for Retro-2<sup>cycl</sup> and optimized analog 41.** Cells were preincubated with the indicated concentrations of retro-2<sup>cycl</sup> prior to inoculation with virus. Infections were scored and normalized to a DMSO-treated control. The data represent the mean of three replicates with indicated standard error.

*Optimized dihydroquinazolinone inhibitor interferes with retrograde trafficking.*

In order to confirm that the optimized DHQ (**41**) was inhibiting retrograde trafficking, we conducted a proximity ligation assay, which detects co-localization between viral the capsid proteins and localized host cell marker proteins (Figure 2.14). Marker proteins were chosen from sites where the virions are delivered immediately downstream from their trafficking through the retrograde pathway. Against JCPyV, we immunostained for viral capsid protein, VP1, and ER protein, PDI (protein disulfide isomerase) in SVGA cells. Against HPV, we immunostained for viral capsid protein, L1, and Golgi protein, TGN46, in HeLaM cells. In the

assay, colocalization is indicated by a fluorescent signal, which is detected only when the target proteins are within 40 nm of each other. Cells were pretreated with either Retro-2<sup>cycl</sup>, DHQ **41**, or DMSO then inoculated with virus. Cells were fixed and immunostained after an 8 hour period for JCPyV or a 16 hour period for HPV. In DMSO treated cells, there is strong colocalization of target proteins for both JCPyV and HPV. In Retro-2<sup>cycl</sup> and DHQ **41** treated cells there is a clear reduction in colocalization of target proteins for both JCPyV and HPV. Furthermore, in the case JCPyV, DHQ **41** appears to inhibit colocalization more potently than Retro-2<sup>cycl</sup>. This trend is less clear in the case of HPV. In any case, we can conclude that the optimized DHQ **41** inhibits retrograde transport in a similar manner as Retro-2<sup>cycl</sup>.

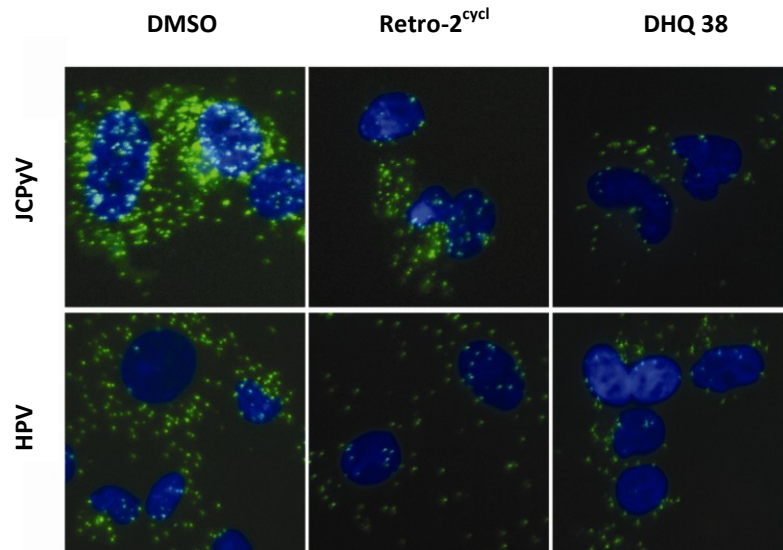


Figure 2.14 – HPV and JCPyV Proximity Ligation Assay: Cell nuclei are indicated by blue fluorescence. Green fluorescence indicates co-localization of target proteins: JCPyV – capsid protein VP1 and ER protein PDI; HPV – capsid protein L1 and Golgi protein TGN 46.

## Discussion

Typical anti-infective therapeutic strategies involve targeting the pathogen itself with a small molecule that perturbs the pathogen's physiology.<sup>40</sup> However, pathogens also rely on nuances in host physiology in order to effectively infect or deliver virulence factors such as toxins to the host. In certain instances, it may be possible to perturb the host's physiology in a non-toxic manner such as to make the host's physiology incompatible with the pathogen,

thereby inhibiting infection and/or virulence factor delivery. As demonstrated by this report, such a strategy can have the fortuitous benefit of having a broad spectrum of efficacy. Polyomaviruses, papylomaviruses, ricin, and Shiga-like toxins all exploit retrograde trafficking in their mechanisms of infection or intoxication. Despite stark differences between these species, one similarity in their intracellular trafficking allows them all to be treated with a single small molecule. We suspect that there are many other pathogens that would be susceptible to treatment by DHQ retrograde trafficking inhibitors as well.

Herein we report a study of the structure-activity relationships associated with DHQ inhibitors of retrograde trafficking. As a result of our investigations, we have also discovered new compounds with significantly improved potency. We used a whole-cell based polyomavirus infectivity model as platform for measuring compound efficacy. This assay avoids the use of potentially dangerous toxins or viruses but the SAR results should be generally applicable. This was demonstrated by showing that an inhibitor optimized to inhibit polyomavirus infection exhibited similarly improved activity against human papillomavirus as compared to Retro-2<sup>cycl</sup>. Our PyV infectivity assay does suffer from large standard errors and is not yet amenable to high-throughput analysis. However, optimization of this assay is currently underway in the Atwood Lab.

The key DHQ structural features that led to improvement in activity were the incorporation of a C-5 ethyl group onto the thiophene moiety, incorporation of a p-fluorobenzyl group as the amide moiety, and addition of a fluorine atom onto C-4 of the Benzo moiety. We have compared our results to similar SAR studies that were reported during the late stages of our investigation.<sup>7,8</sup> Several of our findings are in agreement and the combined data sets suggest structural modifications that could lead to optimized compounds that surpass the potency of

both lead compounds, Retro-2.1 and DHQ **41**. There is also one major point of disagreement between the two studies. While the Cintrat group reported that *N*-methylidihydroquinazolinones exhibit enhanced activity, we observed a severe attenuation of activity resulting from methylation of the DHQ amino nitrogen. It seems unlikely that this inconsistent SAR should be toxin or virus specific if the compounds are targeting a single host cellular factor. Target deconvolution is the next crucial step for developing DHQ retrograde trafficking inhibitors into small-molecule therapeutics. The SAR studies described in this report as well as by Cintrat should guide the design of affinity probes, with which we hope to identify the specific sub-cellular target of the DHQ retrograde trafficking inhibitors.

### Experimental Contributors

Chemical synthesis of all compounds was completed by Daniel Carney with the assistance of Undergraduate students, Bennet Ferris '12 and Julia Stevens '15. All viral infectivity and proximity ligation assays were completed by Dr. Christian Nelson at the Atwood Lab in the Brown University MCB department and the DiMaio Lab in the Yale University Department of Biology. X-ray diffraction crystallography was performed and analyzed by Prof. Paul Williard of the Brown University Chemistry Department.

### Experimental Procedures

#### Cells, Viruses, Plasmids, and Antibodies

SVG-A cells were maintained in MEM complete media (minimal essential media containing 10% fetal bovine serum, 1% penicillin, 1% streptomycin) and have been previously described.<sup>38</sup> HeLaM cells were maintained in DMEM complete media (Dulbecco's modification of minimal essential media containing 10% fetal bovine serum, 1% penicillin, 1% streptomycin, 10mM HEPES pH 7.5). HeLaM cells, a subclone of HeLaS3 cells, were a kind gift from Walther



Mothes (Yale University). The Mad1-SVE $\Delta$  strain of JCPyV used in these experiments has previously been described.<sup>39</sup> The p16sheLL plasmid, which contains HPV L1 and L2, and pCAG-HcRed were obtained from Addgene. The antibodies to PDI, SV40 VP1, and TGN46 were purchased from Abcam. Polyclonal sera to HPV L1 was a kind gift from Patty Day. The PAB597 hybridoma was a kind gift from Ed Harlow.

### **Proximity ligation assays**

Co-localization experiments between virus and ER or Golgi markers was performed using proximity ligation assays, as previously described (Bethyl Labs) (24222489, 23569269). The primary antibodies used for PLA were anti-VP1 and PDI in the case of JCPyV, and L1 and TGN46 in the case of HPV. Cells were pretreated with Retro-2<sup>cycl</sup>, Retro-2C10, or vehicle control for 0.5 h prior to inoculation with virus. SVGA cells (JCPyV) or HeLaM cells (HPV) were then inoculated with virus at an MOI of 100 for 1 h at 37°C. Virus was removed by aspiration and any unbound virus was removed by washing with media. Fresh media was added containing either 0.1 mM Retro-2<sup>cycl</sup> or Retro-2C10, or a vehicle control. Cells were then incubated at 37°C for 8 h (JCPyV) or 16 h (HPV) prior to fixation with 4% PFA. Cells were permeabilized with PBS containing 0.5% Triton X-100 for 0.5 h, washed three times in PBS, then blocked in 5% Donkey Serum for 1 h at 37°C. For JCPyV, cells were then stained for VP1 (1:1000 dilution) and PDI (1:100 dilution) by overnight incubation at 4°C. For HPV, cells were stained with L1 (1:1000 dilution) and TGN46 (1:200 dilution) by incubation for 2h at 37°C. These cells were then immunostained using the proximity ligation assay, following manufacturer's instructions. Cells were washed and the cell nuclei were counterstained using DAPI. Fluorescence micrographs were collected by confocal microscopy and maximal z-projections were displayed.

### **Flow cytometric scoring of viral infection**

JCPyV infected SVG-A cells were detached from 12-well plates by aspirating the growth media, washing once with phosphate buffered saline (PBS), and detaching with Trypsin-EDTA. These cells were then transferred to flow cytometry tubes and pelleted by centrifugation at 600 x g for 5 min, washed with PBS and fixed in 0.5 mL 4% paraformaldehyde (PFA) for 10 min. For JCPyV infected SVGA cells, these samples were pelleted and washed with PBS, and permeabilized with 0.5 mL PBS containing 1% Triton X-100 for 10 min at 21°C. Cells were then pelleted and resuspended in 0.1 mL PBS containing 3% BSA and an Alexa Fluor labeled monoclonal antibody to VP1 (PAB 597-AF488). After incubation for 1 h at 21°C, cells were washed once with PBS and infected cells were scored by flow cytometry (BD FACSCalibur).

HPV infected HeLaM cells were detached from 12-well plates by aspirating the growth media, washing once with phosphate buffered saline (PBS), and detaching with Trypsin-EDTA. These cells were then transferred to flow cytometry tubes and pelleted by centrifugation at 600 x g for 5min, washed with PBS and fixed in 0.5 mL 4% paraformaldehyde (PFA) for 10 min. Infected cells were then scored flow cytometry for HcRed expression.

### **Inhibition of JCPyV infection by Retro-2<sup>cycl</sup> analogs**

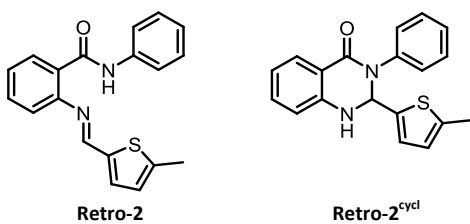
SVG-A cells were seeded in 12 well plates at a density of  $1 \times 10^5$  cells per well and incubated overnight at 37°C. Cells were then pre-incubated for 0.5 h with 25  $\mu$ M of Retro-2<sup>cycl</sup>, the indicated Retro-2<sup>cycl</sup> analog, or the vehicle control. The final DMSO concentration was 0.04%. JCPyV was then added at an MOI of 0.25 and allowed to infect in the presence of the indicated compound for 72 h. Samples were then processed for flow cytometry as indicated above. An infected culture that was not treated with Retro-2<sup>cycl</sup> (~20% total infected cells) was then normalized to 100% and any reduction in infection in the Retro-2<sup>cycl</sup> or Retro-2C10 treated

samples were compared to this untreated control. Three independent experiments were performed and used to calculate standard deviations.

For the IC50 analysis, 1:2 serial dilutions of Retro-2<sup>cycl</sup> or Retro-2C10 were performed in DMSO to generate 2500x stocks. These dilutions were then added to complete media, such that the media contained a 1x concentration of the indicated concentration of compound in a final DMSO concentration of 0.04%. Samples were pretreated with the indicated compound and challenged with JCPyV or HPV as above. Three independent experiments were performed and used to calculate standard deviations.

### Chemical synthesis-general

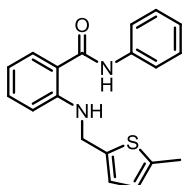
All commercially available reagents were used without further purification. Reactions were carried out in oven dried glassware, with dry solvent, and under ambient atmosphere. All spectra were referenced to residual solvent signals in DMSO<sub>d6</sub> (2.50 ppm for <sup>1</sup>H, 39.51 ppm for <sup>13</sup>C).



### Synthesis of Retro-2 and Retro-2<sup>cycl</sup>

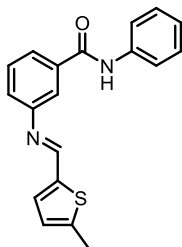
To a stirring solution of 2-aminobenzanilide was added 5-methyl-2-thiophenecarboxaldehyde (86.3  $\mu$ L, .80 mmol). After 24 hours, the reaction was concentrated and then chromatographed on silica gel with 20-40% ethyl acetate in hexanes. Retro-2 and Retro-2<sup>cycl</sup> were cleanly separated and then further purified by recrystallization from ethanol and ethyl acetate respectively. Yields: Retro-2 47.2 mg (36%), Retro-2<sup>cycl</sup> 78.0 mg (59.4%).

Characterization: Retro-2 FAB HRMS:  $C_{19}H_{16}N_2OSNa^+$  Predicted: 343.0881 Found: 343.0870.  $^1H$  NMR (600MHz, DMSO- $d_6$ )  $\delta$  = 11.00 (s, 1 H), 8.79 (s, 1 H), 8.00 (dd,  $J$  = 1.5, 7.7 Hz, 1 H), 7.76 (d,  $J$  = 7.7 Hz, 2 H), 7.65 (d,  $J$  = 3.7 Hz, 1 H), 7.59 (dt,  $J$  = 1.5, 7.7 Hz, 1 H), 7.42 - 7.32 (m, 4 H), 7.10 (s, 1 H), 7.01 (dd,  $J$  = 1.1, 3.7 Hz, 1 H), 2.55 (s, 3 H).  $^{13}C$  NMR (151MHz, DMSO- $d_6$ )  $\delta$  = 164.1, 155.7, 148.4, 147.4, 139.3, 138.6, 136.2, 132.3, 129.9, 128.8, 128.0, 127.5, 126.2, 123.6, 119.8, 119.4, 15.7 Retro-2<sup>cycl</sup> FAB HRMS:  $C_{19}H_{16}N_2OSNa^+$  Predicted: 343.0881 Found: 343.0888  $^1H$  NMR (400MHz, DMSO- $d_6$ )  $\delta$  = 7.73 (d,  $J$  = 8.0 Hz, 1 H), 7.61 (d,  $J$  = 2.8 Hz, 1 H), 7.41 - 7.34 (m, 2 H), 7.34 - 7.28 (m, 3 H), 7.27 - 7.20 (m, 1 H), 6.82 (d,  $J$  = 8.3 Hz, 1 H), 6.77 (t,  $J$  = 7.5 Hz, 1 H), 6.72 (d,  $J$  = 3.5 Hz, 1 H), 6.55 (d,  $J$  = 3.5 Hz, 1 H), 6.40 (d,  $J$  = 3.0 Hz, 1 H), 2.31 (s, 3 H).  $^{13}C$  NMR (151MHz, DMSO- $d_6$ )  $\delta$  = 161.5, 146.3, 142.0, 140.5, 139.2, 133.7, 128.7, 127.9, 126.4, 126.3, 126.2, 124.4, 117.9, 115.5, 115.2, 69.6, 14.9



**2-(((5-methylthiophen-2-yl)methyl)amino)-N-phenylbenzamide (3).** Retro-2<sup>cycl</sup> (143 mg, 0.444 mmol) was dissolved in methanol (4 mL) then treated with sodium cyanoborohydride (83 mg, 1.3 mmol) followed by acetic acid (.4 mL). The slow formation of a new product was observed by tlc (2:1 hexanes:ethyl acetate). After 3 days the reaction was concentrated and then chromatographed on silica gel with a hexanes/ethyl acetate solvent gradient. Both the desired product (62 mg, .187 mmol, 42%) as well as unreacted starting material (64 mg, .200 mmol, 45%) were recovered. FAB HRMS:  $C_{19}H_{18}N_2OSNa^+$  Predicted: 345.1038 Found: 345.1052  $^1H$  NMR (600MHz, DMSO- $d_6$ )  $\delta$  = 10.11 (s, 1 H), 7.78 (t,  $J$  = 5.7 Hz, 1 H), 7.76 - 7.65 (m, 3 H), 7.45 - 7.28 (m, 3 H), 7.16 - 7.06 (m, 1 H), 6.85 (d,  $J$  = 2.9 Hz, 1 H), 6.81 (d,  $J$  = 8.4 Hz, 1 H), 6.68 (t,  $J$  = 7.5 Hz, 1

H), 6.66 - 6.61 (m, 1 H), 2.38 (s, 3 H).  $^{13}\text{C}$  NMR (151MHz, DMSO- $d_6$ )  $\delta$  = 168.0, 148.5, 140.5, 139.0, 138.1, 132.6, 129.0, 128.5, 125.0, 124.9, 123.5, 120.6, 116.1, 114.9, 111.6, 41.6, 14.9.



**(E)-3-(((5-methylthiophen-2-yl)methylene)amino)-N-phenylbenzamide (4).**

Dicyclohexylcarbodiimide (1.03 g, 5.00 mmol) and 3-nitrobenzoic acid (0.987 g, 5.55 mmol) were dissolved in DCM (20 mL) and allowed to stir for 5 minutes before the addition of aniline (0.500 mL, 5.55 mmol) and dimethylaminopyridine (.068 g, .055 mmol). The coupling reaction was allowed to proceed for 16 hours at which point the DCM was evaporated. The solid residue was resuspended in ethyl acetate and filtered through a silica gel plug to remove the dicyclohexylurea byproduct. The filtrate was then concentrated and the desired nitrobenzamide isolated by silica gel chromatography using a hexanes/ethyl acetate solvent gradient. Yield: 1.118 g, 92%. FAB HRMS:  $\text{C}_{13}\text{H}_{10}\text{N}_2\text{O}_3\text{Na}^+$  Predicted: 265.0589 Found: 265.0595.  $^1\text{H}$  NMR (600MHz, DMSO- $d_6$ )  $\delta$  = 10.57 (s, 1 H), 8.79 (t,  $J$  = 1.8 Hz, 1 H), 8.44 (ddd,  $J$  = 0.9, 2.3, 8.2 Hz, 1 H), 8.41 (td,  $J$  = 1.3, 7.7 Hz, 1 H), 7.84 (t,  $J$  = 8.1 Hz, 1 H), 7.79 (d,  $J$  = 7.7 Hz, 2 H), 7.39 (d,  $J$  = 7.7 Hz, 1 H), 7.38 (d,  $J$  = 7.7 Hz, 1 H), 7.14 (tt,  $J$  = 1.1, 7.3 Hz, 1 H)  $^{13}\text{C}$  NMR (151MHz, DMSO- $d_6$ )  $\delta$  = 163.3, 147.7, 138.6, 136.3, 134.1, 130.1, 128.6, 126.1, 124.1, 122.4, 120.6.

The Nitrobenzamide (0.242 g, 1.00 mmol) was dissolved in methanol (3 mL) then treated with 10% Palladium on carbon (72.3 mg) and ammonium formate (350 mg, 5.5 mmol). The reaction was allowed to proceed for 45 minutes before being filtered through celite to remove the palladium on carbon. The filtrate was treated with 5-methyl-2-thiophenecarboxaldehyde (0.128

mL, 1.2 mmol) and scandium (III) triflate (0.076 g, 0.154 mmol) and then heated to reflux for 2 hours. Upon cooling to room temperature, the product precipitated from solution and was isolated by filtration. yield: 0.190 g, 59%. FAB HRMS:  $C_{19}H_{16}N_2OSNa^+$  Predicted: 343.0881 Found: 343.0888.  $^1H$  NMR (600MHz, DMSO- $d_6$ )  $\delta$  = 10.28 (s, 1 H), 8.78 (s, 1 H), 7.82 (t,  $J$  = 1.7 Hz, 1 H), 7.82 - 7.78 (m, 3 H), 7.56 - 7.52 (m, 2 H), 7.45 (ddd,  $J$  = 1.1, 2.0, 7.9 Hz, 1 H), 7.38 - 7.33 (m, 2 H), 7.11 (tt,  $J$  = 1.1, 7.3 Hz, 1 H), 6.97 - 6.94 (m, 1 H), 2.53 (d,  $J$  = 0.7 Hz, 3 H).  $^{13}C$  NMR (151MHz, DMSO- $d_6$ )  $\delta$  = 165.1, 154.7, 150.9, 145.9, 140.1, 139.1, 135.9, 134.6, 129.3, 128.5, 126.9, 125.1, 124.0, 123.6, 120.4, 120.2, 15.6

### **Dihydroquinazolinone synthesis general procedure 1.**

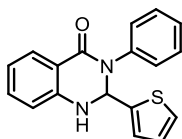
Dicycloheptylcarbodiimide (5.00 mmol) and a nitrobenzoic acid (5.55 mmol) were dissolved in DCM (20 mL) and allowed to stir for 5 minutes before the addition of a primary amine (5.55 mmol) and dimethylaminopyridine (0.055 mmol). The coupling reaction was allowed to proceed for 16 hours, after which the DCM was evaporated. The solid residue was resuspended in ethyl acetate and filtered through a silica gel plug to remove the dicyclohexylurea byproduct. The filtrate was then concentrated and the desired nitrobenzamide isolated by silica gel chromatography using a hexanes/ethyl acetate solvent gradient.

The nitrobenzamide intermediate (0.5 mmol) was dissolved in methanol (2.5 mL). To the solution was added 10% Pd/C (75 mg) and ammonium formate (32 mg, 0.5 mmol). After 1 hour the reaction was filtered. The filtrate was adjusted to a volume 1mL in methanol and then treated with an aldehyde (0.55 mmol) and scandium (III) triflate (0.05) mmol. The reaction was microwave irradiated at 100°C for 1 hour, after which the solvent was removed. The product dihydroquinazolinones were isolated by silica gel chromatography with a hexanes/ethyl acetate

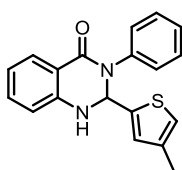
solvent gradient. The chromatographed products were subsequently purified by recrystallization.

### Dihydroquinazolinone synthesis general procedure 2.

An isatoic anhydride (1.20 mmol) was added to THF (6 mL) and heated to 60°C. To the hot solution of isatoic anhydride was added a primary amine or ammonia (1.00 mmol), which was allowed to react for 1-2 hours. Once the amine had been completely consumed, an aldehyde (1.20 mmol) and scandium triflate (0.1 mmol) were added and allowed to react at 60°C for an additional 3-5 hours, after which the solvent was removed. The product dihydroquinazolinones were isolated by silica gel chromatography with a hexanes/ethyl acetate solvent gradient. The chromatographed products were subsequently purified by recrystallization.

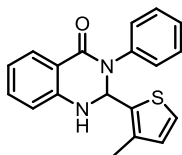


3-phenyl-2-(thiophen-2-yl)-2,3-dihydroquinazolin-4(1H)-one. FAB HRMS:  $C_{18}H_{14}N_2O_2Na^+$   
Predicted: 313.0953 Found: 313.0945.  $^1H$  NMR (400MHz, DMSO- $d_6$ )  $\delta$  = 7.72 (d,  $J$  = 7.3 Hz, 1 H), 7.62 (d,  $J$  = 3.0 Hz, 1 H), 7.58 (dd,  $J$  = 0.8, 1.9 Hz, 1 H), 7.43 - 7.35 (m, 2 H), 7.35 - 7.28 (m, 3 H), 7.28 - 7.23 (m, 1 H), 6.83 (d,  $J$  = 8.0 Hz, 1 H), 6.79 - 6.70 (m,  $J$  = 1.0, 7.5, 7.5 Hz, 1 H), 6.33 (dd,  $J$  = 1.9, 3.4 Hz, 1 H), 6.25 (t,  $J$  = 3.3 Hz, 2 H).  $^{13}C$  NMR (75MHz, DMSO- $d_6$ )  $\delta$  = 161.8, 152.9, 146.5, 143.1, 140.6, 133.7, 128.7, 127.9, 126.3, 117.8, 115.5, 114.9, 110.4, 108.4, 67.3.



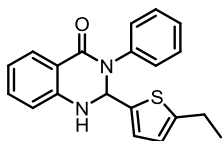
**2-(4-methylthiophen-2-yl)-3-phenyl-2,3-dihydroquinazolin-4(1H)-one.** FAB HRMS:

$C_{19}H_{16}N_2OSNa^+$  Predicted: 343.0881 Found: 343.0872.  $^1H$  NMR (400MHz, DMSO- $d_6$ )  $\delta$  = 7.73 (dd,  $J$  = 1.5, 7.8 Hz, 1 H), 7.62 (d,  $J$  = 2.8 Hz, 1 H), 7.42 - 7.29 (m, 5 H), 7.27 - 7.22 (m, 1 H), 6.94 - 6.90 (m, 1 H), 6.82 (d,  $J$  = 8.0 Hz, 1 H), 6.80 - 6.74 (m, 2 H), 6.44 (d,  $J$  = 2.8 Hz, 1 H), 2.07 (d,  $J$  = 0.8 Hz, 3 H).  $^{13}C$  NMR (101MHz, DMSO- $d_6$ )  $\delta$  = 161.5, 146.3, 144.6, 140.5, 136.2, 133.8, 128.7, 128.3, 128.0, 126.3, 126.3, 120.9, 118.0, 115.6, 115.3, 69.4, 15.3.



**2-(3-methylthiophen-2-yl)-3-phenyl-2,3-dihydroquinazolin-4(1H)-one.** FAB HRMS:

$C_{19}H_{16}N_2OSNa^+$  Predicted: 343.0881 Found: 343.0885.  $^1H$  NMR (400MHz, DMSO- $d_6$ )  $\delta$  = 7.74 (dd,  $J$  = 1.5, 7.8 Hz, 1 H), 7.48 (d,  $J$  = 2.0 Hz, 1 H), 7.37 - 7.29 (m, 3 H), 7.25 - 7.17 (m, 4 H), 6.83 - 6.75 (m, 2 H), 6.67 (d,  $J$  = 5.0 Hz, 1 H), 6.54 (d,  $J$  = 2.0 Hz, 1 H), 1.91 (s, 3 H).  $^{13}C$  NMR (75MHz, DMSO- $d_6$ )  $\delta$  = 161.8, 146.6, 140.2, 137.0, 135.1, 133.8, 129.5, 128.6, 127.9, 127.5, 126.7, 124.2, 117.8, 115.0, 114.9, 67.9, 13.3.

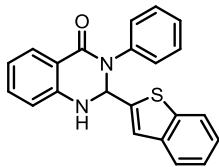


**2-(5-ethylthiophen-2-yl)-3-phenyl-2,3-dihydroquinazolin-4(1H)-one.** FAB HRMS:  $C_{20}H_{18}N_2OSNa^+$

Predicted: 357.1038 Found: 357.1028.  $^1H$  NMR (400MHz, DMSO- $d_6$ )  $\delta$  = 7.74 (dd,  $J$  = 1.5, 7.8 Hz, 1 H), 7.63 (d,  $J$  = 2.8 Hz, 1 H), 7.41 - 7.34 (m, 2 H), 7.34 - 7.29 (m, 3 H), 7.27 - 7.21 (m, 1 H), 6.83 (d,  $J$  = 8.0 Hz, 1 H), 6.80 - 6.76 (m, 1 H), 6.75 (d,  $J$  = 3.5 Hz, 1 H), 6.58 (td,  $J$  = 1.1, 3.3 Hz, 1 H), 6.42 (d,  $J$  = 2.8 Hz, 1 H), 2.67 (q,  $J$  = 7.4 Hz, 2 H), 1.13 (t,  $J$  = 7.4 Hz, 3 H).  $^{13}C$  NMR (75MHz, DMSO- $d_6$ )  $\delta$

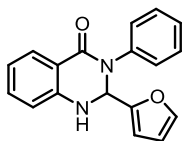


= 161.5, 146.7, 146.3, 141.7, 140.5, 133.8, 128.7, 128.0, 126.4, 126.3, 126.1, 122.7, 118.0, 115.5, 115.2, 69.7, 22.7, 15.6



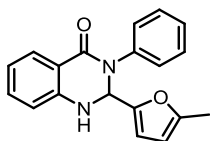
**2-(benzo[b]thiophen-2-yl)-3-phenyl-2,3-dihydroquinazolin-4(1H)-one.** FAB HRMS:

$C_{22}H_{16}N_2OSNa^+$  Predicted: 379.0881 Found: 379.0866.  $^1H$  NMR (400MHz, DMSO- $d_6$ )  $\delta$  = 7.88 - 7.82 (m, 1 H), 7.79 - 7.71 (m, 3 H), 7.42 - 7.37 (m, 4 H), 7.37 - 7.33 (m, 1 H), 7.33 - 7.28 (m, 3 H), 7.28 - 7.22 (m, 1 H), 6.86 (d,  $J$  = 8.0 Hz, 1 H), 6.80 (dt,  $J$  = 1.0, 7.5 Hz, 1 H), 6.64 (d,  $J$  = 3.3 Hz, 1 H).  $^{13}C$  NMR (101MHz, DMSO- $d_6$ )  $\delta$  = 161.4, 146.2, 145.3, 144.8, 140.4, 138.3, 134.0, 128.8, 128.0, 126.5, 124.9, 124.5, 123.8, 123.0, 122.6, 118.2, 115.6, 115.3, 107.6, 69.9.



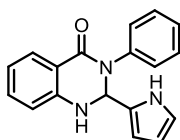
**2-(furan-2-yl)-3-phenyl-2,3-dihydroquinazolin-4(1H)-one.** FAB HRMS:  $C_{18}H_{14}N_2O_2Na^+$  Predicted:

313.0953 Found: 313.0945.  $^1H$  NMR (400MHz, DMSO- $d_6$ )  $\delta$  = 7.72 (d,  $J$  = 7.3 Hz, 1 H), 7.62 (d,  $J$  = 3.0 Hz, 1 H), 7.58 (dd,  $J$  = 0.8, 1.9 Hz, 1 H), 7.43 - 7.35 (m, 2 H), 7.35 - 7.28 (m, 3 H), 7.28 - 7.23 (m, 1 H), 6.83 (d,  $J$  = 8.0 Hz, 1 H), 6.79 - 6.70 (m,  $J$  = 1.0, 7.5, 7.5 Hz, 1 H), 6.33 (dd,  $J$  = 1.9, 3.4 Hz, 1 H), 6.25 (t,  $J$  = 3.3 Hz, 2 H).  $^{13}C$  NMR (75MHz, DMSO- $d_6$ )  $\delta$  = 161.8, 152.9, 146.5, 143.1, 140.6, 133.7, 128.7, 127.9, 126.3, 117.8, 115.5, 114.9, 110.4, 108.4, 67.3



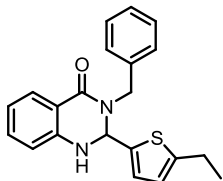
**2-(5-methylfuran-2-yl)-3-phenyl-2,3-dihydroquinazolin-4(1H)-one.** FAB HRMS:  $C_{19}H_{16}N_2O_2Na^+$

Predicted: 327.1109 Found: 327.1125.  $^1H$  NMR (400MHz, DMSO- $d_6$ )  $\delta$  = 7.72 (dd,  $J$  = 1.0, 7.8 Hz, 1 H), 7.62 (d,  $J$  = 3.0 Hz, 1 H), 7.42 - 7.33 (m, 4 H), 7.30 (ddd,  $J$  = 1.8, 7.0, 8.3 Hz, 1 H), 7.24 (tt,  $J$  = 1.8, 7.3 Hz, 1 H), 6.83 (d,  $J$  = 8.0 Hz, 1 H), 6.78 - 6.72 (m, 1 H), 6.17 (d,  $J$  = 3.3 Hz, 1 H), 6.11 (d,  $J$  = 3.0 Hz, 1 H), 5.93 (dd,  $J$  = 1.0, 3.0 Hz, 1 H), 2.16 (s, 3 H).  $^{13}C$  NMR (75MHz, DMSO- $d_6$ )  $\delta$  = 161.8, 151.7, 150.8, 146.4, 140.6, 133.6, 128.7, 127.9, 126.3, 117.7, 115.5, 115.0, 109.4, 106.5, 67.3, 13.3.



**3-phenyl-2-(1H-pyrrol-2-yl)-2,3-dihydroquinazolin-4(1H)-one.** FAB HRMS:  $C_{18}H_{15}N_3ONa^+$

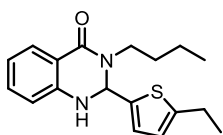
Predicted: 312.1113 Found: 312.1118.  $^1H$  NMR (400MHz, DMSO- $d_6$ )  $\delta$  = 10.72 (br. s., 1 H), 7.72 (dd,  $J$  = 1.5, 7.8 Hz, 1 H), 7.34 - 7.26 (m, 3 H), 7.26 - 7.21 (m, 3 H), 7.21 - 7.15 (m, 1 H), 6.79 (dd,  $J$  = 0.5, 8.3 Hz, 1 H), 6.75 (ddd,  $J$  = 1.0, 7.1, 7.5 Hz, 1 H), 6.63 (dt,  $J$  = 1.5, 2.6 Hz, 1 H), 6.18 (d,  $J$  = 2.3 Hz, 1 H), 5.89 (t,  $J$  = 3.5 Hz, 1 H), 5.81 (q,  $J$  = 2.7 Hz, 1 H).  $^{13}C$  NMR (75MHz, DMSO- $d_6$ )  $\delta$  = 162.4, 146.8, 140.7, 133.4, 130.0, 128.5, 127.9, 126.6, 126.1, 118.2, 117.8, 115.9, 115.1, 107.6, 107.1, 68.1.



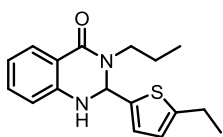
**3-benzyl-2-(5-ethylthiophen-2-yl)-2,3-dihydroquinazolin-4(1H)-one.** FAB HRMS:  $C_{21}H_{20}N_2OSNa^+$

Predicted: 371.1194 Found: 371.1186.  $^1H$  NMR (600MHz, DMSO- $d_6$ )  $\delta$  = 7.70 (dd,  $J$  = 1.8, 7.7 Hz, 1 H), 7.37 (d,  $J$  = 2.6 Hz, 1 H), 7.36 - 7.33 (m, 2 H), 7.32 - 7.30 (m, 2 H), 7.30 - 7.25 (m, 2 H), 6.87

(d,  $J = 3.7$  Hz, 1 H), 6.74 (dt,  $J = 1.1, 7.5$  Hz, 1 H), 6.71 (d,  $J = 8.1$  Hz, 1 H), 6.65 (td,  $J = 1.1, 3.3$  Hz, 1 H), 5.90 (d,  $J = 2.6$  Hz, 1 H), 5.26 (d,  $J = 15.4$  Hz, 1 H), 3.92 (d,  $J = 15.4$  Hz, 1 H), 2.69 (dq,  $J = 1.1, 7.5$  Hz, 2 H), 1.14 (t,  $J = 7.5$  Hz, 3 H).  $^{13}\text{C}$  NMR (151MHz, DMSO- $d_6$ )  $\delta = 161.7, 146.6, 146.1, 141.2, 137.5, 133.4, 128.4, 127.6, 127.4, 127.1, 126.0, 122.6, 117.7, 114.8, 114.7, 66.5, 46.7, 22.7, 15.6$ .

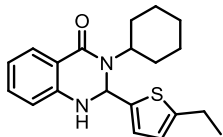


**3-butyl-2-(5-ethylthiophen-2-yl)-2,3-dihydroquinazolin-4(1H)-one.** FAB HRMS:  $\text{C}_{18}\text{H}_{22}\text{N}_2\text{OSNa}^+$   
 Predicted: 337.1351 Found: 337.1366.  $^1\text{H}$  NMR (600MHz, DMSO- $d_6$ )  $\delta = 7.64$  (dd,  $J = 1.5, 8.1$  Hz, 1 H), 7.33 (d,  $J = 2.6$  Hz, 1 H), 7.27 - 7.21 (m, 1 H), 6.88 (d,  $J = 3.7$  Hz, 1 H), 6.73 - 6.67 (m, 2 H), 6.64 (td,  $J = 1.0, 3.6$  Hz, 1 H), 6.00 (d,  $J = 2.6$  Hz, 1 H), 3.86 (ddd,  $J = 6.6, 8.4, 13.6$  Hz, 1 H), 2.83 (ddd,  $J = 5.5, 8.3, 13.7$  Hz, 1 H), 2.68 (dq,  $J = 1.1, 7.5$  Hz, 2 H), 1.59 - 1.51 (m, 1 H), 1.51 - 1.43 (m, 1 H), 1.34 - 1.21 (m, 2 H), 1.13 (t,  $J = 7.5$  Hz, 3 H), 0.87 (t,  $J = 7.3$  Hz, 3 H).  $^{13}\text{C}$  NMR (151MHz, DMSO- $d_6$ )  $\delta = 161.5, 146.4, 146.0, 142.0, 133.1, 127.4, 125.7, 122.5, 117.5, 115.2, 114.6, 66.7, 43.7, 29.5, 22.6, 19.5, 15.6, 13.6$ .



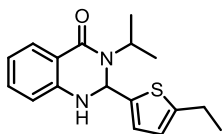
**2-(5-ethylthiophen-2-yl)-3-propyl-2,3-dihydroquinazolin-4(1H)-one.** FAB HRMS:  $\text{C}_{17}\text{H}_{20}\text{N}_2\text{OSNa}^+$   
 Predicted: 323.1194 Found: 323.1188.  $^1\text{H}$  NMR (400MHz, DMSO- $d_6$ )  $\delta = 7.68 - 7.61$  (m, 1 H), 7.36 (br. s., 1 H), 7.24 (dt,  $J = 1.5, 7.7$  Hz, 1 H), 6.88 (d,  $J = 3.5$  Hz, 1 H), 6.74 - 6.67 (m, 2 H), 6.63 (d,  $J = 3.5$  Hz, 1 H), 6.01 (d,  $J = 2.3$  Hz, 1 H), 3.88 - 3.74 (m, 1 H), 2.81 (ddd,  $J = 5.7, 8.1, 13.5$  Hz, 1 H), 2.67 (q,  $J = 7.6$  Hz, 2 H), 1.67 - 1.55 (m, 1 H), 1.55 - 1.42 (m, 1 H), 1.13 (t,  $J = 7.6$  Hz, 3 H), 0.85

(t,  $J = 7.5$  Hz, 3 H).  $^{13}\text{C}$  NMR (101MHz, DMSO- $d_6$ )  $\delta = 161.6, 146.4, 146.1, 142.1, 133.2, 127.4, 125.7, 122.6, 117.5, 115.2, 114.7, 66.8, 45.8, 22.7, 20.8, 15.7, 11.2.$



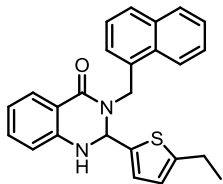
**3-cyclohexyl-2-(5-ethylthiophen-2-yl)-2,3-dihydroquinazolin-4(1H)-one.** FAB HRMS:

$\text{C}_{20}\text{H}_{24}\text{N}_2\text{OSNa}^+$  Predicted: 363.1507 Found: 363.1522.  $^1\text{H}$  NMR (400MHz, DMSO- $d_6$ )  $\delta = 7.65$  (dd,  $J = 1.2, 7.7$  Hz, 1 H), 7.28 (d,  $J = 2.4$  Hz, 1 H), 7.21 (ddd,  $J = 1.5, 6.8, 8.6$  Hz, 1 H), 6.85 (d,  $J = 3.7$  Hz, 1 H), 6.70 (t,  $J = 7.5$  Hz, 1 H), 6.66 (d,  $J = 8.1$  Hz, 163 H), 6.58 (d,  $J = 3.4$  Hz, 1 H), 6.08 (d,  $J = 2.9$  Hz, 1 H), 4.23 (t,  $J = 11.9$  Hz, 1 H), 2.64 (q,  $J = 7.4$  Hz, 2 H), 1.76 (d,  $J = 10.8$  Hz, 2 H), 1.68 (br. s., 1 H), 1.57 (br. s., 3 H), 1.39 - 1.15 (m, 4 H), 1.11 (t,  $J = 7.5$  Hz, 3 H).  $^{13}\text{C}$  NMR (101MHz, DMSO- $d_6$ )  $\delta = 161.2, 145.7, 145.7, 144.0, 133.0, 127.6, 125.2, 122.4, 117.6, 116.4, 114.9, 63.0, 53.4, 30.3, 30.3, 25.7, 25.6, 24.9, 22.6, 15.5.$



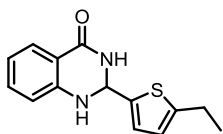
**2-(5-ethylthiophen-2-yl)-3-isopropyl-2,3-dihydroquinazolin-4(1H)-one.** FAB HRMS:

$\text{C}_{17}\text{H}_{20}\text{N}_2\text{OSNa}^+$  Predicted: 323.1194 Found: 323.1180.  $^1\text{H}$  NMR (600MHz, DMSO- $d_6$ )  $\delta = 7.66$  (dd,  $J = 1.1, 7.7$  Hz, 1 H), 7.26 (d,  $J = 2.9$  Hz, 1 H), 7.22 (ddd,  $J = 1.5, 7.3, 8.2$  Hz, 1 H), 6.87 (d,  $J = 3.7$  Hz, 1 H), 6.71 (t,  $J = 7.5$  Hz, 1 H), 6.68 (d,  $J = 8.1$  Hz, 1 H), 6.59 (d,  $J = 3.7$  Hz, 1 H), 6.06 (d,  $J = 2.9$  Hz, 1 H), 4.55 (spt,  $J = 6.8$  Hz, 1 H), 2.64 (q,  $J = 7.5$  Hz, 2 H), 1.23 (d,  $J = 7.0$  Hz, 3 H), 1.11 (t,  $J = 7.5$  Hz, 3 H), 1.04 (d,  $J = 7.0$  Hz, 3 H).  $^{13}\text{C}$  NMR (151MHz, DMSO- $d_6$ )  $\delta = 161.2, 145.8, 145.7, 143.8, 132.9, 127.5, 125.2, 122.3, 117.6, 116.3, 114.8, 63.0, 45.6, 22.6, 20.3, 20.1, 15.5.$



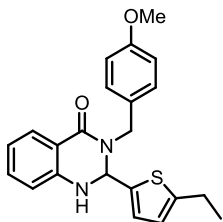
**2-(5-ethylthiophen-2-yl)-3-(naphthalen-1-ylmethyl)-2,3-dihydroquinazolin-4(1H)-one.** FAB

HRMS:  $C_{25}H_{22}N_2OSNa^+$  Predicted: 421.1351 Found: 421.1359.  $^1H$  NMR (400MHz, DMSO- $d_6$ )  $\delta$  = 8.13 - 8.06 (m, 1 H), 8.00 - 7.94 (m, 1 H), 7.91 (d,  $J$  = 7.8 Hz, 1 H), 7.76 (d,  $J$  = 7.8 Hz, 1 H), 7.58 - 7.46 (m, 4 H), 7.34 (d,  $J$  = 2.3 Hz, 1 H), 7.32 - 7.26 (m, 1 H), 6.91 (d,  $J$  = 3.5 Hz, 1 H), 6.80 - 6.74 (m, 1 H), 6.68 (d,  $J$  = 8.3 Hz, 1 H), 6.67 - 6.64 (m, 1 H), 5.89 (d,  $J$  = 15.4 Hz, 1 H), 5.80 (d,  $J$  = 2.5 Hz, 1 H), 4.22 (d,  $J$  = 15.7 Hz, 1 H), 2.69 (q,  $J$  = 7.5 Hz, 2 H), 1.14 (dt,  $J$  = 1.3, 7.4 Hz, 3 H).  $^{13}C$  NMR (101MHz, DMSO- $d_6$ )  $\delta$  = 161.6, 146.6, 146.0, 140.8, 133.7, 133.5, 132.2, 131.1, 128.6, 128.2, 127.8, 126.5, 126.2, 126.0, 125.5, 123.6, 122.7, 117.8, 114.9, 114.7, 65.8, 44.4, 22.7, 15.7.



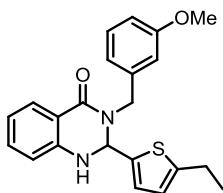
**2-(5-ethylthiophen-2-yl)-2,3-dihydroquinazolin-4(1H)-one.** FAB HRMS:  $C_{14}H_{14}N_2OSNa^+$

Predicted: 281.0725 Found: 287.0730.  $^1H$  NMR (400MHz, DMSO- $d_6$ )  $\delta$  = 8.39 (br. s, 1 H), 7.60 (dd,  $J$  = 1.5, 7.8 Hz, 1 H), 7.28 - 7.22 (m, 1 H), 7.21 (br. s, 1 H), 6.91 (d,  $J$  = 3.3 Hz, 1 H), 6.74 (d,  $J$  = 8.1 Hz, 1 H), 6.72 - 6.66 (m, 2 H), 5.92 (t,  $J$  = 1.8 Hz, 1 H), 2.74 (dq,  $J$  = 0.8, 7.6 Hz, 2 H), 1.18 (t,  $J$  = 7.6 Hz, 3 H).  $^{13}C$  NMR (151MHz, DMSO- $d_6$ )  $\delta$  = 163.0, 147.2, 146.7, 143.4, 133.3, 127.2, 125.3, 122.7, 117.4, 115.0, 114.6, 62.8, 22.8, 15.8.



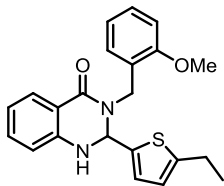
**2-(5-ethylthiophen-2-yl)-3-(4-methoxybenzyl)-2,3-dihydroquinazolin-4(1H)-one.** FAB HRMS:

$C_{22}H_{22}N_2O_2SNa^+$  Predicted: 401.1300 Found: 401.1285.  $^1H$  NMR (400MHz, DMSO- $d_6$ )  $\delta$  = 7.69 (dd,  $J$  = 1.3, 7.6 Hz, 1 H), 7.34 (d,  $J$  = 2.8 Hz, 1 H), 7.32 - 7.19 (m, 3 H), 6.90 (d,  $J$  = 8.6 Hz, 2 H), 6.86 (d,  $J$  = 3.5 Hz, 1 H), 6.73 (t,  $J$  = 7.5 Hz, 1 H), 6.69 (d,  $J$  = 7.8 Hz, 1 H), 6.65 (d,  $J$  = 3.5 Hz, 1 H), 5.84 (d,  $J$  = 2.5 Hz, 1 H), 5.22 (d,  $J$  = 14.9 Hz, 1 H), 3.80 (d,  $J$  = 14.9 Hz, 1 H), 3.73 (s, 3 H), 2.68 (q,  $J$  = 7.5 Hz, 2 H), 1.14 (t,  $J$  = 7.6 Hz, 3 H).  $^{13}C$  NMR (101MHz, DMSO- $d_6$ )  $\delta$  = 161.6, 158.6, 146.6, 146.1, 141.3, 133.5, 129.3, 129.1, 127.6, 126.0, 122.7, 117.7, 114.8, 114.7, 113.9, 66.2, 55.1, 46.0, 22.7, 15.7.



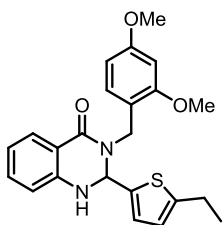
**2-(5-ethylthiophen-2-yl)-3-(3-methoxybenzyl)-2,3-dihydroquinazolin-4(1H)-one.** FAB HRMS:

$C_{22}H_{22}N_2O_2SNa^+$  Predicted: 401.1300 Found: 401.1282.  $^1H$  NMR (400MHz, DMSO- $d_6$ )  $\delta$  = 7.69 (dd,  $J$  = 1.4, 7.7 Hz, 1 H), 7.39 (d,  $J$  = 2.5 Hz, 1 H), 7.32 - 7.22 (m, 2 H), 6.92 - 6.82 (m, 4 H), 6.78 - 6.69 (m, 2 H), 6.64 (d,  $J$  = 3.3 Hz, 1 H), 5.90 (d,  $J$  = 2.8 Hz, 1 H), 5.23 (d,  $J$  = 15.4 Hz, 1 H), 3.90 (d,  $J$  = 15.4 Hz, 1 H), 3.72 (s, 3 H), 2.68 (q,  $J$  = 7.5 Hz, 2 H), 1.14 (t,  $J$  = 7.6 Hz, 3 H).  $^{13}C$  NMR (101MHz, DMSO- $d_6$ )  $\delta$  = 165.2, 159.4, 146.6, 141.3, 139.1, 133.5, 129.6, 127.6, 126.0, 122.6, 119.6, 117.7, 114.8, 113.2, 112.4, 66.6, 55.0, 46.7, 22.7, 15.7.



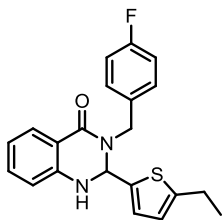
**2-(5-ethylthiophen-2-yl)-3-(2-methoxybenzyl)-2,3-dihydroquinazolin-4(1H)-one.** FAB HRMS:

$C_{22}H_{22}N_2O_2SNa^+$  Predicted: 401.1300 Found: 401.1289.  $^1H$  NMR (400MHz, DMSO- $d_6$ )  $\delta$  = 7.67 (dd,  $J$  = 1.4, 7.7 Hz, 1 H), 7.41 (d,  $J$  = 2.8 Hz, 1 H), 7.32 - 7.24 (m, 2 H), 7.22 (d,  $J$  = 7.3 Hz, 1 H), 7.02 (d,  $J$  = 7.8 Hz, 1 H), 6.93 (t,  $J$  = 7.5 Hz, 1 H), 6.85 (d,  $J$  = 3.5 Hz, 1 H), 6.77 - 6.69 (m, 2 H), 6.67 - 6.63 (m, 1 H), 5.92 (d,  $J$  = 2.3 Hz, 1 H), 5.11 (d,  $J$  = 15.9 Hz, 1 H), 3.96 (d,  $J$  = 15.9 Hz, 1 H), 3.81 (s, 3 H), 2.69 (q,  $J$  = 7.6 Hz, 2 H), 1.14 (t,  $J$  = 7.5 Hz, 3 H).  $^{13}C$  NMR (101MHz, DMSO- $d_6$ )  $\delta$  = 157.0, 146.2, 141.5, 133.5, 128.4, 127.7, 127.6, 125.9, 122.7, 120.4, 117.7, 114.9, 114.8, 110.7, 66.8, 55.4, 42.1, 22.7, 15.7.



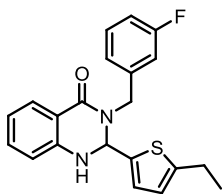
**3-(2,4-dimethoxybenzyl)-2-(5-ethylthiophen-2-yl)-2,3-dihydroquinazolin-4(1H)-one.** FAB

HRMS:  $C_{23}H_{24}N_2O_3SNa^+$  Predicted: 431.1405 Found: 431.1405.  $^1H$  NMR (400MHz, DMSO- $d_6$ )  $\delta$  = 7.69 (dd,  $J$  = 1.4, 7.7 Hz, 1 H), 7.36 (d,  $J$  = 2.8 Hz, 1 H), 7.30 - 7.23 (m, 1 H), 7.14 (d,  $J$  = 8.3 Hz, 1 H), 6.84 (d,  $J$  = 3.5 Hz, 1 H), 6.76 - 6.68 (m, 2 H), 6.65 (d,  $J$  = 3.5 Hz, 1 H), 6.59 (d,  $J$  = 2.5 Hz, 1 H), 6.52 (dd,  $J$  = 2.4, 8.5 Hz, 1 H), 5.87 (d,  $J$  = 2.5 Hz, 1 H), 5.08 (d,  $J$  = 15.4 Hz, 1 H), 3.89 (d,  $J$  = 15.4 Hz, 1 H), 3.79 (s, 3 H), 3.75 (s, 3 H), 2.69 (q,  $J$  = 7.5 Hz, 2 H), 1.14 (t,  $J$  = 7.6 Hz, 3 H).  $^{13}C$  NMR (101MHz, DMSO- $d_6$ )  $\delta$  = 161.6, 160.0, 158.1, 146.5, 146.0, 141.6, 133.4, 129.2, 127.6, 125.7, 122.7, 117.6, 117.0, 115.0, 114.7, 104.7, 98.4, 66.5, 55.5, 55.2, 41.5, 22.7, 15.7.



**2-(5-ethylthiophen-2-yl)-3-(4-fluorobenzyl)-2,3-dihydroquinazolin-4(1H)-one.** FAB HRMS:

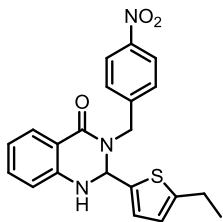
$C_{21}H_{19}FN_2OSNa^+$  Predicted: 389.1100 Found: 389.1109.  $^1H$  NMR (400MHz, DMSO- $d_6$ )  $\delta$  = 7.69 (dd,  $J$  = 1.6, 7.7 Hz, 1 H), 7.40 (d,  $J$  = 2.8 Hz, 1 H), 7.38 - 7.32 (m, 2 H), 7.31 - 7.25 (m, 1 H), 7.19 - 7.12 (m, 2 H), 6.87 (d,  $J$  = 3.5 Hz, 1 H), 6.79 - 6.69 (m, 2 H), 6.64 (td,  $J$  = 1.0, 3.5 Hz, 1 H), 5.94 (d,  $J$  = 2.5 Hz, 1 H), 5.16 (d,  $J$  = 15.4 Hz, 1 H), 3.98 (d,  $J$  = 15.4 Hz, 1 H), 2.68 (dq,  $J$  = 0.9, 7.5 Hz, 2 H), 1.13 (t,  $J$  = 7.5 Hz, 3 H).  $^{13}C$  NMR (101MHz, DMSO- $d_6$ )  $\delta$  = 161.8, 146.7, 146.2, 141.3, 133.8, 133.8, 133.5, 129.6, 129.5, 127.6, 127.4, 126.1, 122.6, 117.7, 115.3, 115.1, 114.8, 114.8, 66.7, 46.3, 22.7, 15.7.



**2-(5-ethylthiophen-2-yl)-3-(3-fluorobenzyl)-2,3-dihydroquinazolin-4(1H)-one.** FAB HRMS:

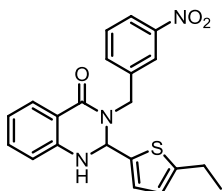
$C_{21}H_{19}FN_2OSNa^+$  Predicted: 389.1100 Found: 389.1082.  $^1H$  NMR (400MHz, Acetone)  $\delta$  = 7.70 (dd,  $J$  = 1.1, 8.0 Hz, 1 H), 7.44 (d,  $J$  = 2.5 Hz, 1 H), 7.41 - 7.33 (m, 1 H), 7.29 (dt,  $J$  = 1.6, 7.6 Hz, 1 H), 7.16 (d,  $J$  = 7.6 Hz, 1 H), 7.14 - 7.05 (m, 2 H), 6.88 (d,  $J$  = 3.3 Hz, 1 H), 6.78 - 6.71 (m, 2 H), 6.67 - 6.62 (m, 1 H), 6.00 (d,  $J$  = 2.5 Hz, 1 H), 5.16 (d,  $J$  = 15.7 Hz, 1 H), 4.06 (d,  $J$  = 15.7 Hz, 1 H), 2.68 (q,  $J$  = 7.5 Hz, 2 H), 1.13 (t,  $J$  = 7.5 Hz, 3 H).  $^{13}C$  NMR (101MHz, Acetone)  $\delta$  = 163.5, 161.9, 161.0, 146.7, 146.3, 141.2, 140.8, 140.7, 133.6, 130.4, 130.3, 127.6, 126.2, 123.4, 123.4, 122.6, 117.8, 114.9, 114.7, 114.2, 114.0, 113.7, 67.0, 46.7, 22.7, 15.7.





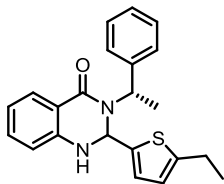
**2-(5-ethylthiophen-2-yl)-3-(4-nitrobenzyl)-2,3-dihydroquinazolin-4(1H)-one:** FAB HRMS:

$C_{21}H_{19}N_3O_3SNa^+$  Predicted: 416.1045 Found: 416.1061.  $^1H$  NMR (400MHz, DMSO- $d_6$ )  $\delta$  = 8.27 - 8.12 (m, 2 H), 7.69 (dd,  $J$  = 1.5, 8.1 Hz, 1 H), 7.55 (d,  $J$  = 8.8 Hz, 2 H), 7.49 (d,  $J$  = 2.3 Hz, 1 H), 7.36 - 7.25 (m, 1 H), 6.89 (d,  $J$  = 3.5 Hz, 1 H), 6.82 - 6.71 (m, 2 H), 6.63 (td,  $J$  = 0.9, 3.5 Hz, 1 H), 6.07 (d,  $J$  = 2.5 Hz, 1 H), 5.15 (d,  $J$  = 16.2 Hz, 1 H), 4.29 (d,  $J$  = 16.2 Hz, 1 H), 2.67 (q,  $J$  = 7.4 Hz, 2 H), 1.12 (t,  $J$  = 7.5 Hz, 3 H).  $^{13}C$  NMR (101MHz, DMSO- $d_6$ )  $\delta$  = 162.1, 146.9, 146.6, 146.4, 146.0, 141.1, 133.7, 128.4, 127.6, 126.4, 123.5, 122.6, 117.8, 114.9, 114.6, 67.4, 47.0, 22.7, 15.8.

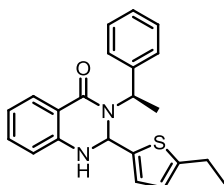


**2-(5-ethylthiophen-2-yl)-3-(3-nitrobenzyl)-2,3-dihydroquinazolin-4(1H)-one.** FAB HRMS:

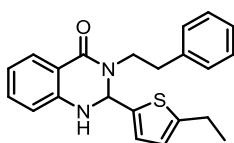
$C_{21}H_{19}N_3O_3SNa^+$  Predicted: 416.1045 Found: 416.1038.  $^1H$  NMR (400MHz, DMSO- $d_6$ )  $\delta$  = 8.17 - 8.04 (m, 2 H), 7.76 (d,  $J$  = 7.8 Hz, 1 H), 7.74 - 7.67 (m, 1 H), 7.67 - 7.56 (m, 1 H), 7.48 (d,  $J$  = 2.3 Hz, 1 H), 7.30 (dt,  $J$  = 1.6, 7.6 Hz, 1 H), 6.88 (d,  $J$  = 3.5 Hz, 1 H), 6.83 - 6.71 (m, 2 H), 6.66 - 6.58 (m, 1 H), 6.13 (d,  $J$  = 2.5 Hz, 1 H), 5.07 (d,  $J$  = 15.4 Hz, 1 H), 4.39 (d,  $J$  = 15.7 Hz, 1 H), 2.65 (q,  $J$  = 7.5 Hz, 2 H), 1.10 (t,  $J$  = 7.6 Hz, 3 H).  $^{13}C$  NMR (101MHz, DMSO- $d_6$ )  $\delta$  = 162.2, 147.7, 146.8, 146.4, 141.3, 140.4, 134.3, 133.7, 129.9, 127.6, 126.4, 122.6, 122.1, 117.8, 114.9, 114.6, 67.4, 46.9, 22.7, 15.7.



2-(5-ethylthiophen-2-yl)-3-((S)-1-phenylethyl)-2,3-dihydroquinazolin-4(1H)-one. FAB HRMS:  $C_{22}H_{22}N_2OSNa^+$  Predicted: 385.1351 Found: 385.1342.  $^1H$  NMR (400MHz, DMSO- $d_6$ )  $\delta$  = 7.71 (d,  $J$  = 7.8 Hz, 1 H), 7.43 - 7.35 (m, 4 H), 7.34 - 7.28 (m, 1 H), 7.28 - 7.20 (m, 2 H), 6.81 (d,  $J$  = 3.3 Hz, 1 H), 6.74 (t,  $J$  = 7.5 Hz, 1 H), 6.65 (d,  $J$  = 8.1 Hz, 1 H), 6.61 (d,  $J$  = 3.3 Hz, 1 H), 5.90 (q,  $J$  = 7.1 Hz, 1 H), 5.78 (d,  $J$  = 3.0 Hz, 1 H), 2.66 (q,  $J$  = 7.7 Hz, 2 H), 1.36 (d,  $J$  = 7.3 Hz, 3 H), 1.12 (t,  $J$  = 7.6 Hz, 3 H).  $^{13}C$  NMR (101MHz, CHLOROFORM- $d$ )  $\delta$  = 161.6, 146.0, 145.8, 143.6, 141.5, 133.3, 128.5, 127.8, 127.3, 126.8, 125.3, 122.5, 117.8, 115.9, 115.0, 63.0, 51.0, 22.6, 17.5, 15.6.

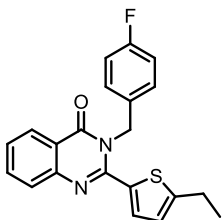


**2-(5-ethylthiophen-2-yl)-3-((R)-1-phenylethyl)-2,3-dihydroquinazolin-4(1H)-one.** FAB HRMS:  $C_{22}H_{22}N_2OSNa^+$  Predicted: 385.1351 Found: 385.1335.  $^1H$  NMR (400MHz, DMSO- $d_6$ )  $\delta$  = 7.71 (dd,  $J$  = 1.5, 7.8 Hz, 1 H), 7.42 - 7.35 (m, 4 H), 7.34 - 7.28 (m, 1 H), 7.28 - 7.22 (m, 2 H), 6.81 (d,  $J$  = 3.5 Hz, 1 H), 6.78 - 6.70 (m, 1 H), 6.65 (d,  $J$  = 8.1 Hz, 1 H), 6.61 (d,  $J$  = 3.5 Hz, 1 H), 5.90 (q,  $J$  = 7.2 Hz, 1 H), 5.78 (d,  $J$  = 3.0 Hz, 1 H), 2.66 (q,  $J$  = 7.5 Hz, 2 H), 1.36 (d,  $J$  = 7.3 Hz, 3 H), 1.12 (t,  $J$  = 7.6 Hz, 3 H).  $^{13}C$  NMR (101MHz, DMSO- $d_6$ )  $\delta$  = 161.5, 146.0, 145.8, 143.6, 141.5, 133.3, 128.5, 127.8, 127.2, 126.8, 125.3, 122.5, 117.8, 115.9, 115.0, 63.0, 51.0, 22.6, 17.5, 15.6



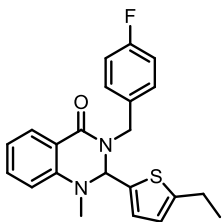
**2-(5-ethylthiophen-2-yl)-3-phenethyl-2,3-dihydroquinazolin-4(1H)-one.** FAB HRMS:

$C_{22}H_{22}N_2OSNa^+$  Predicted: 385.1351 Found: 385.1369.  $^1H$  NMR (400MHz, DMSO- $d_6$ )  $\delta$  = 7.65 (d,  $J$  = 7.8 Hz, 1 H), 7.37 (s, 1 H), 7.33 - 7.25 (m, 3 H), 7.25 - 7.17 (m, 3 H), 6.92 (d,  $J$  = 3.5 Hz, 1 H), 6.77 - 6.68 (m, 2 H), 6.68 - 6.62 (m, 1 H), 6.04 (d,  $J$  = 2.3 Hz, 1 H), 4.09 - 3.93 (m, 1 H), 3.14 - 3.01 (m, 1 H), 2.98 - 2.84 (m, 1 H), 2.81 - 2.71 (m,  $J$  = 5.1, 9.0, 9.0 Hz, 1 H), 2.68 (q,  $J$  = 7.3 Hz, 2 H), 1.13 (t,  $J$  = 7.6 Hz, 3 H).  $^{13}C$  NMR (101MHz, DMSO- $d_6$ )  $\delta$  = 161.7, 146.7, 146.2, 141.8, 139.1, 133.3, 128.6, 128.4, 127.4, 126.2, 125.9, 122.6, 117.5, 114.9, 114.6, 67.0, 45.9, 33.6, 22.7, 15.7.



**2-(5-ethylthiophen-2-yl)-3-(4-fluorobenzyl)quinazolin-4(3H)-one.** FAB HRMS:  $C_{21}H_{17}FN_2OSNa^+$

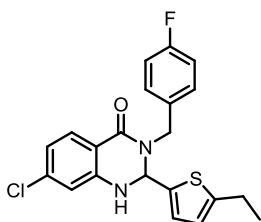
Predicted: 387.0943 Found: 387.0938.  $^1H$  NMR (400MHz, DMSO- $d_6$ )  $\delta$  = 8.14 (dd,  $J$  = 1.3, 8.3 Hz, 1 H), 7.85 (dt,  $J$  = 1.4, 7.6 Hz, 1 H), 7.67 (d,  $J$  = 7.8 Hz, 1 H), 7.59 - 7.50 (m, 1 H), 7.19 - 7.07 (m, 5 H), 6.83 (dd,  $J$  = 0.8, 3.8 Hz, 1 H), 5.45 (s, 2 H), 2.81 (q,  $J$  = 7.5 Hz, 2 H), 1.23 (t,  $J$  = 7.5 Hz, 3 H).  $^{13}C$  NMR (101MHz, DMSO- $d_6$ )  $\delta$  = 162.5, 161.8, 160.1, 152.0, 150.0, 147.0, 135.0, 134.0, 133.1, 133.1, 129.6, 128.1, 128.0, 127.2, 126.6, 124.7, 119.7, 115.8, 115.5, 48.2, 22.8, 15.8.



**2-(5-ethylthiophen-2-yl)-3-(4-fluorobenzyl)-1-methyl-2,3-dihydroquinazolin-4(1H)-one.**

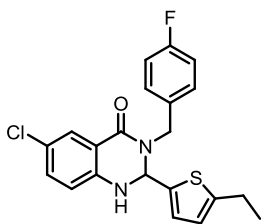
$C_{22}H_{21}FN_2OSNa^+$  Predicted: 403.1256 Found: 403.1266.  $^1H$  NMR (400MHz, DMSO- $d_6$ )  $\delta$  = 7.80

(dd,  $J = 1.5, 7.6$  Hz, 1 H), 7.46 - 7.40 (m, 1 H), 7.40 - 7.33 (m, 2 H), 7.21 - 7.12 (m, 2 H), 6.93 (d,  $J = 3.5$  Hz, 1 H), 6.88 (dt,  $J = 1.0, 7.5$  Hz, 1 H), 6.69 (d,  $J = 8.1$  Hz, 1 H), 6.65 (td,  $J = 1.0, 3.5$  Hz, 1 H), 5.92 (s, 1 H), 5.13 (d,  $J = 15.4$  Hz, 1 H), 3.95 (d,  $J = 15.4$  Hz, 1 H), 2.77 (s, 3 H), 2.68 - 2.60 (m, 2 H), 1.11 (t,  $J = 7.5$  Hz, 3 H).  $^{13}\text{C}$  NMR (101MHz, DMSO- $d_6$ )  $\delta = 161.3, 147.0, 146.4, 134.1, 133.5, 133.5, 129.6, 129.5, 127.8, 127.7, 122.6, 118.3, 115.3, 115.1, 112.9, 73.3, 46.3, 34.9, 22.6, 15.5$ .



**7-chloro-2-(5-ethylthiophen-2-yl)-3-(4-fluorobenzyl)-2,3-dihydroquinazolin-4(1H)-one.**

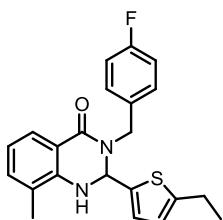
$\text{C}_{21}\text{H}_{18}\text{FN}_2\text{OSNa}^+$  Predicted: 423.0710 Found: 423.0718.  $^1\text{H}$  NMR (400MHz, DMSO- $d_6$ )  $\delta = 7.71 - 7.65$  (m, 2 H), 7.33 (dd,  $J = 5.7, 8.5$  Hz, 2 H), 7.15 (t,  $J = 8.8$  Hz, 2 H), 6.89 (d,  $J = 3.5$  Hz, 1 H), 6.79 - 6.73 (m, 2 H), 6.68 - 6.63 (m, 1 H), 6.02 (d,  $J = 2.5$  Hz, 1 H), 5.12 (d,  $J = 15.4$  Hz, 1 H), 3.99 (d,  $J = 15.4$  Hz, 1 H), 2.69 (q,  $J = 7.5$  Hz, 2 H), 1.14 (t,  $J = 7.5$  Hz, 3 H).  $^{13}\text{C}$  NMR (101MHz, DMSO- $d_6$ )  $\delta = 161.1, 160.2, 147.2, 147.0, 140.9, 138.1, 133.6, 133.6, 129.7, 129.6, 129.5, 126.4, 122.8, 117.8, 115.3, 115.1, 113.9, 113.4, 66.7, 46.3, 22.7, 15.7$ .



**6-chloro-2-(5-ethylthiophen-2-yl)-3-(4-fluorobenzyl)-2,3-dihydroquinazolin-4(1H)-one.**

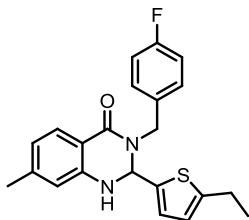
$\text{C}_{21}\text{H}_{18}\text{FN}_2\text{OSNa}^+$  Predicted: 423.0710 Found: 423.0725.  $^1\text{H}$  NMR (400MHz, DMSO- $d_6$ )  $\delta = 7.63$  (dd,  $J = 2.5, 5.3$  Hz, 2 H), 7.42 - 7.29 (m, 3 H), 7.20 - 7.12 (m, 2 H), 6.88 (d,  $J = 3.3$  Hz, 1 H), 6.76 (d,

$J = 8.8$  Hz, 1 H), 6.67 - 6.63 (m, 1 H), 6.01 (d,  $J = 2.5$  Hz, 1 H), 5.13 (d,  $J = 15.2$  Hz, 1 H), 4.01 (d,  $J = 15.2$  Hz, 1 H), 2.68 (q,  $J = 7.4$  Hz, 2 H), 1.14 (t,  $J = 7.6$  Hz, 3 H).  $^{13}\text{C}$  NMR (101MHz, DMSO- $d_6$ )  $\delta = 160.7, 146.9, 145.0, 140.9, 133.4, 129.6, 129.6, 126.6, 126.3, 122.7, 121.4, 116.9, 115.8, 115.3, 115.1, 66.6, 46.4, 22.7, 15.7$ .



**2-(5-ethylthiophen-2-yl)-3-(4-fluorobenzyl)-8-methyl-2,3-dihydroquinazolin-4(1H)-one.**

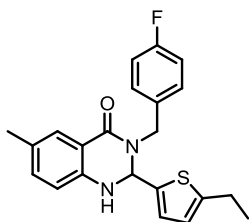
$\text{C}_{22}\text{H}_{21}\text{FN}_2\text{OSNa}^+$  Predicted: 403.1256 Found: 403.1265.  $^1\text{H}$  NMR (400MHz, DMSO- $d_6$ )  $\delta = 7.57$  (d,  $J = 8.1$  Hz, 1 H), 7.45 - 7.32 (m, 2 H), 7.18 (t,  $J = 7.8$  Hz, 3 H), 6.97 (d,  $J = 3.5$  Hz, 1 H), 6.81 (d,  $J = 3.3$  Hz, 1 H), 6.71 - 6.65 (m, 1 H), 6.62 (d,  $J = 3.3$  Hz, 1 H), 5.90 (d,  $J = 3.8$  Hz, 1 H), 5.27 (d,  $J = 15.9$  Hz, 1 H), 4.04 (d,  $J = 14.9$  Hz, 1 H), 2.67 (q,  $J = 7.6$  Hz, 2 H), 2.07 (s, 3 H), 1.13 (t,  $J = 7.6$  Hz, 3 H).  $^{13}\text{C}$  NMR (101MHz, DMSO- $d_6$ )  $\delta = 162.1, 146.4, 142.0, 134.1, 129.7, 129.6, 125.5, 125.5, 122.9, 122.8, 117.6, 115.4, 115.2, 66.1, 46.5, 22.7, 16.8, 15.7$ .



**2-(5-ethylthiophen-2-yl)-3-(4-fluorobenzyl)-7-methyl-2,3-dihydroquinazolin-4(1H)-one.**

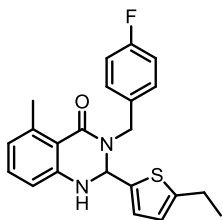
$\text{C}_{22}\text{H}_{21}\text{FN}_2\text{OSNa}^+$  Predicted: 403.1256 Found: 403.1241.  $^1\text{H}$  NMR (400MHz, DMSO- $d_6$ )  $\delta = 7.57$  (d,  $J = 7.8$  Hz, 1 H), 7.37 - 7.29 (m, 3 H), 7.19 - 7.11 (m, 2 H), 6.85 (d,  $J = 3.5$  Hz, 1 H), 6.63 (td,  $J = 0.9, 3.4$  Hz, 1 H), 6.56 (dd,  $J = 1.0, 8.1$  Hz, 1 H), 6.51 (s, 1 H), 5.90 (d,  $J = 2.5$  Hz, 1 H), 5.15 (d,  $J = 15.2$

Hz, 1 H), 3.95 (d,  $J = 15.4$  Hz, 1 H), 2.68 (q,  $J = 7.6$  Hz, 2 H), 1.16 - 1.11 (m, 3 H).  $^{13}\text{C}$  NMR (101MHz ,DMSO- $d_6$ )  $\delta = 162.1, 146.4, 143.9, 142.0, 134.1, 134.0, 133.9, 129.6, 129.6, 125.5, 125.5, 122.9, 122.7, 117.5, 115.4, 115.2, 115.2, 66.1, 46.5, 22.7, 16.8, 15.6$ .



2-(5-ethylthiophen-2-yl)-3-(4-fluorobenzyl)-6-methyl-2,3-dihydroquinazolin-4(1H)-one.

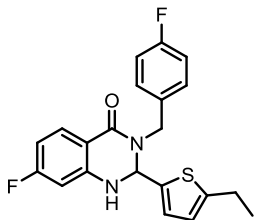
$\text{C}_{22}\text{H}_{21}\text{FN}_2\text{OSNa}^+$  Predicted: 403.1256 Found: 403.1250.  $^1\text{H}$  NMR (400MHz ,Acetone)  $\delta = 7.50$  (s, 1 H), 7.34 (dd,  $J = 5.6, 8.1$  Hz, 2 H), 7.23 - 7.07 (m, 4 H), 6.85 (d,  $J = 3.5$  Hz, 1 H), 6.71 - 6.54 (m, 2 H), 5.90 (d,  $J = 2.3$  Hz, 1 H), 5.16 (d,  $J = 15.4$  Hz, 1 H), 3.97 (d,  $J = 15.4$  Hz, 1 H), 2.67 (q,  $J = 7.4$  Hz, 2 H), 2.21 (s, 3 H), 1.13 (t,  $J = 7.3$  Hz, 3 H).  $^{13}\text{C}$  NMR (101MHz ,DMSO- $d_6$ )  $\delta = 161.9, 146.6, 144.0, 141.4, 134.4, 129.6, 129.5, 127.5, 126.4, 126.1, 122.6, 115.3, 115.1, 115.0, 114.8, 66.8, 46.3, 22.7, 20.1, 15.8$ .



2-(5-ethylthiophen-2-yl)-3-(4-fluorobenzyl)-5-methyl-2,3-dihydroquinazolin-4(1H)-one.

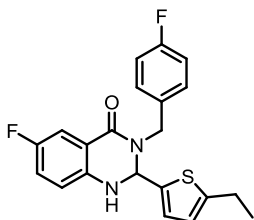
$\text{C}_{22}\text{H}_{21}\text{FN}_2\text{OSNa}^+$  Predicted: 403.1256 Found: 403.1262.  $^1\text{H}$  NMR (400MHz ,DMSO- $d_6$ )  $\delta = 7.50$  (s, 1 H), 7.34 (dd,  $J = 5.6, 8.6$  Hz, 2 H), 7.21 (d,  $J = 2.5$  Hz, 1 H), 7.19 - 7.13 (m, 2 H), 7.11 (dd,  $J = 2.0, 8.1$  Hz, 1 H), 6.85 (d,  $J = 3.5$  Hz, 1 H), 6.67 - 6.60 (m, 2 H), 5.89 (d,  $J = 2.5$  Hz, 1 H), 5.16 (d,  $J = 15.2$  Hz, 1 H), 3.97 (d,  $J = 15.4$  Hz, 1 H), 2.67 (q,  $J = 7.5$  Hz, 2 H), 2.21 (s, 3 H), 1.13 (t,  $J = 7.5$  Hz, 3 H).

$^{13}\text{C}$  NMR (101MHz ,DMSO- $d_6$ )  $\delta$  = 161.9, 146.6, 144.0, 141.4, 134.4, 129.6, 129.5, 127.5, 126.4, 126.1, 122.6, 115.3, 115.1, 115.0, 114.8, 66.8, 46.3, 22.7, 20.2, 15.8.



**2-(5-ethylthiophen-2-yl)-7-fluoro-3-(4-fluorobenzyl)-2,3-dihydroquinazolin-4(1H)-one.**

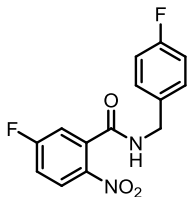
$\text{C}_{21}\text{H}_{18}\text{F}_2\text{N}_2\text{OSNa}^+$  Predicted: 407.1006 Found: 407.1025.  $^1\text{H}$  NMR (600MHz ,DMSO- $d_6$ )  $\delta$  = 7.74 (dd,  $J$  = 6.6, 8.8 Hz, 1 H), 7.66 (d,  $J$  = 2.6 Hz, 1 H), 7.37 - 7.30 (m, 2 H), 7.18 - 7.12 (m, 2 H), 6.89 (d,  $J$  = 3.7 Hz, 1 H), 6.65 (td,  $J$  = 1.0, 3.6 Hz, 1 H), 6.54 (dt,  $J$  = 2.4, 8.7 Hz, 1 H), 6.49 (dd,  $J$  = 2.2, 10.6 Hz, 1 H), 5.99 (d,  $J$  = 2.6 Hz, 1 H), 5.13 (d,  $J$  = 15.4 Hz, 1 H), 3.98 (d,  $J$  = 15.4 Hz, 1 H), 2.69 (q,  $J$  = 7.3 Hz, 2 H), 1.14 (t,  $J$  = 7.5 Hz, 3 H).  $^{13}\text{C}$  NMR (151MHz ,DMSO- $d_6$ )  $\delta$  = 165.4, 162.7, 161.6, 148.7, 147.4, 141.5, 134.1, 134.1, 131.2, 131.1, 130.1, 130.0, 126.7, 123.2, 115.7, 115.6, 111.9, 105.7, 105.6, 101.1, 100.9, 67.2, 46.7, 23.2, 16.2.



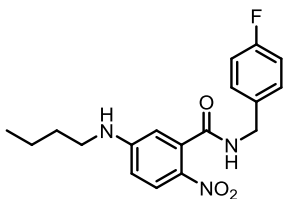
**2-(5-ethylthiophen-2-yl)-6-fluoro-3-(4-fluorobenzyl)-2,3-dihydroquinazolin-4(1H)-one (38).**

$\text{C}_{21}\text{H}_{18}\text{F}_2\text{N}_2\text{OSNa}^+$  Predicted: 407.1006 Found: 407.1018.  $^1\text{H}$  NMR (400MHz ,DMSO- $d_6$ )  $\delta$  = 7.43 - 7.37 (m, 2 H), 7.34 (dd,  $J$  = 5.6, 8.3 Hz, 2 H), 7.23 - 7.12 (m, 3 H), 6.87 (d,  $J$  = 3.5 Hz, 1 H), 6.76 (dd,  $J$  = 4.5, 8.8 Hz, 1 H), 6.66 - 6.62 (m, 1 H), 5.97 (d,  $J$  = 2.5 Hz, 1 H), 5.12 (d,  $J$  = 15.4 Hz, 1 H), 4.02 (d,  $J$  = 15.2 Hz, 1 H), 2.68 (q,  $J$  = 7.6 Hz, 2 H), 1.13 (t,  $J$  = 7.5 Hz, 3 H).  $^{13}\text{C}$  NMR (151MHz ,DMSO-

d<sub>6</sub>)  $\delta$  = 162.2, 161.0, 160.6, 155.8, 154.2, 146.7, 142.8, 140.9, 133.6, 133.6, 129.6, 129.5, 126.2, 122.6, 121.1, 120.9, 116.7, 116.6, 115.5, 115.5, 115.2, 115.1, 112.8, 112.6, 66.8, 46.4, 22.7, 15.6.



**5-fluoro-N-(4-fluorobenzyl)-2-nitrobenzamide.** Dicyclohexylcarbodiimide (412 mg, 2 mmol) and a 5-fluoro-2-nitrobenzoic acid (407 mg, 2.2 mmol) were dissolved in DCM (10 mL) and allowed to stir for 5 minutes before the addition of a p-fluorobenzylamine (0.227 mL, 2 mmol.) and dimethylaminopyridine (24 mg, 0.2 mmol). The coupling reaction was allowed to proceed for 16 hours, after which the DCM was evaporated. The solid residue was resuspended in ethyl acetate and filtered through a silica gel plug to remove the dicyclohexylurea byproduct. The filtrate was then concentrated and the desired nitrobenzamide isolated by silica gel chromatography using a hexanes/ethyl acetate solvent gradient. Yield: 477 mg, 82%. HRMS (FAB) Predicted ( $C_{14}H_{10}F_2N_2O_3 + Na$ )<sup>+</sup>:315.0557, Found: 315.0564. <sup>1</sup>H NMR (400MHz, DMSO-d<sub>6</sub>)  $\delta$  = 9.25 (t,  $J$  = 5.4 Hz, 1 H), 8.18 (dd,  $J$  = 4.8, 8.6 Hz, 1 H), 7.68 - 7.50 (m, 2 H), 7.41 (dd,  $J$  = 5.6, 8.3 Hz, 2 H), 7.29 - 7.08 (m, 2 H), 4.44 (d,  $J$  = 5.8 Hz, 2 H). <sup>13</sup>C NMR (101MHz, DMSO-d<sub>6</sub>)  $\delta$  = 165.2, 164.3, 162.7, 162.6, 160.1, 143.2, 135.5, 135.4, 134.8, 134.8, 129.5, 129.4, 127.6, 127.5, 117.7, 117.4, 116.6, 116.4, 115.2, 115.0, 42.0.

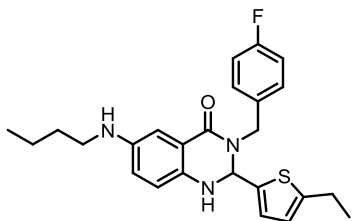




**5-(butylamino)-N-(4-fluorobenzyl)-2-nitrobenzamide.**

5-fluoro-N-(4-fluorobenzyl)-2-

nitrobenzamide (605 mg, 2 mmol) was dissolved in dimethoxy ethane (8 mL) and treated with butylamine (217  $\mu$ L, 2.2 mmol) and triethylamine (278  $\mu$ L, 2 mmol). The reaction was allowed to proceed for 36 hours, after which the solvent was removed *in vacuo* and the product was isolated as a bright yellow solid by flash chromatography. Yield: 440 mg, 64%. HRMS (ESI) Predicted ( $C_{18}H_{20}FN_3O_3 + H$ )<sup>+</sup>:346.1567, Found: 346.1565. <sup>1</sup>H NMR (400MHz, CHLOROFORM-d)  $\delta$  = 7.97 (d, *J* = 9.1 Hz, 1 H), 7.46 - 7.30 (m, 2 H), 7.09 - 6.93 (m, 2 H), 6.54 - 6.37 (m, 2 H), 6.21 (t, *J* = 5.6 Hz, 1 H), 4.94 (t, *J* = 5.2 Hz, 1 H), 4.55 (d, *J* = 5.8 Hz, 2 H), 3.26 - 3.06 (m, 2 H), 1.66 - 1.54 (m, 2 H), 1.40 (qd, *J* = 7.4, 14.9 Hz, 2 H), 0.95 (t, *J* = 7.3 Hz, 3 H). <sup>13</sup>C NMR (101MHz, CHLOROFORM-d)  $\delta$  = 167.9, 163.4, 161.0, 153.0, 135.8, 133.9, 133.4, 133.4, 129.8, 129.7, 127.8, 115.6, 115.4, 111.1, 110.9, 43.4, 43.0, 30.9, 20.1, 13.7.

**6-(butylamino)-2-(5-ethylthiophen-2-yl)-3-(4-fluorobenzyl)-2,3-dihydroquinazolin-4(1H)-one.**

5-(butylamino)-N-(4-fluorobenzyl)-2-nitrobenzamide (368 mg, 1.1 mmol), was dissolved in methanol (5 mL). To the solution was added 10% Pd/C (150 mg) and ammonium formate (64 mg, 1 mmol). After 1 hour the reaction was filtered. The filtrate was adjusted to a volume 2mL in methanol and then treated with 5-ethyl-2-thiophenecarboxaldehyde (138  $\mu$ L, 1.1 mmol) and scandium (III) triflate (49 mg, 0.1) mmol. The reaction was microwave irradiated at 100°C for 1 hour, after which the solvent was removed *in vacuo*. The DHQ (bright yellow solid) product was isolated by silica gel chromatography with a solvent gradient of 30-50 % ethyl acetate in hexanes. The chromatographed product was subsequently purified by recrystallization from

ethyl acetate. Yield 236 mg, 54%. HRMS (ESI) Predicted ( $C_{25}H_{28}FN_3OS + H$ )<sup>+</sup>: 438.2015, Found: 438.2002. <sup>1</sup>H NMR (400MHz, CHLOROFORM-d) δ = 7.34 - 7.26 (m, 4 H), 7.06 - 6.95 (m, 2 H), 6.75 - 6.68 (m, 2 H), 6.58 - 6.52 (m, 2 H), 5.69 (s, 1 H), 5.51 (d, *J* = 14.8 Hz, 1 H), 4.14 (br. s., 1 H), 3.87 (d, *J* = 15.3 Hz, 1 H), 3.17 - 3.09 (m, 2 H), 2.73 (dq, *J* = 1.0, 7.5 Hz, 2 H), 1.67 - 1.56 (m, 2 H), 1.44 (qd, *J* = 7.3, 14.9 Hz, 2 H), 1.23 (t, *J* = 7.5 Hz, 3 H), 0.97 (t, *J* = 7.4 Hz, 3 H). <sup>13</sup>C NMR (101MHz, CHLOROFORM-d) δ = 163.3, 162.9, 160.9, 148.4, 139.8, 137.2, 132.9, 132.8, 129.6, 129.5, 126.0, 122.3, 120.9, 117.8, 117.1, 115.5, 115.3, 112.5, 67.5, 46.4, 45.3, 31.2, 23.4, 20.2, 15.6, 13.8.

### X-ray crystallography

A specimen of  $C_{19}H_{16}N_2OS$ , approximate dimensions 0.150 mm x 0.250 mm x 0.250 mm, was used for the X-ray crystallographic analysis. The X-ray intensity data were measured on a Bruker Apex 1 diffractometer.

The integration of the data using a monoclinic unit cell yielded a total of 5596 reflections to a maximum  $\theta$  angle of 18.43° (1.12 Å resolution), of which 1181 were independent (average redundancy 4.738, completeness = 98.5%,  $R_{int}$  = 6.64%,  $R_{sig}$  = 5.20%) and 899 (76.12%) were greater than  $2\sigma(F^2)$ . The final cell constants of  $a$  = 6.575(6) Å,  $b$  = 13.446(12) Å,  $c$  = 18.616(17) Å,  $\beta$  = 99.161(12)°, volume = 1625.(3) Å<sup>3</sup>, are based upon the refinement of the XYZ-centroids of reflections above  $20\sigma(I)$ . The calculated minimum and maximum transmission coefficients (based on crystal size) are 0.9506 and 0.9699.

The structure was solved and refined using the Bruker SHELXTL Software Package, using the space group  $P 2(1)/c$ , with  $Z = 4$  for the formula unit,  $C_{19}H_{16}N_2OS$ . The final anisotropic full-matrix least-squares refinement on  $F^2$  with 227 variables converged at  $R1 = 5.01\%$ , for the observed data and  $wR2 = 13.47\%$  for all data. The goodness-of-fit was 1.093. The largest peak in

the final difference electron density synthesis was  $0.145 \text{ e}^-/\text{\AA}^3$  and the largest hole was  $-0.194 \text{ e}^-/\text{\AA}^3$  with an RMS deviation of  $0.039 \text{ e}^-/\text{\AA}^3$ . On the basis of the final model, the calculated density was  $1.310 \text{ g/cm}^3$  and  $F(000)$ ,  $672 \text{ e}^-$ . Disorder in this crystal structure was noted for the thiophene ring and the methine carbon atom of the dihydroquinazolinone ring to which it is attached. This disorder was nicely modeled by a nearly  $180^\circ$  rotation about the C-C bond between C(14) and C(15) bond as well as an out of plane displacement of the C(14) relative to the remaining nine atoms of the dihydroquinazolinone ring. Constraints were applied to the fragment C(14) through C(19) and S(1) in the initial stages of the refinement but were released in the final model. The final model refined to a nearly 2:1 ratio of conformers. Only the major conformer is depicted in Figure 5.

#### References

1. Stechmann, B.; Bai, S.; Gobbo, E.; Lopez, R.; Merer, G.; Pinchard, S.; Panigai, L.; Tenza, D.; Raposo, G.; Beaumelle, B.; Sauvaire, D.; Gillet, D.; Johannes, L.; Barbier, J. Inhibition of Retrograde Transport Protects Mice from Lethal Ricin Challenge. *Cell* **2010**, *141*, 231-242.
2. Audi, J.; Belson, M.; Patel, M.; Schier, J.; Osterloh, J. Ricin poisoning: a comprehensive review. *JAMA* **2005**, *294*, 2342-2351.
3. Johannes, L.; Popoff, V. Tracing the retrograde route in protein trafficking. *Cell* **2008**, *135*, 1175-1187.
4. Sandvig, K.; van Deurs, B. Delivery into cells: lessons learned from plant and bacterial toxins. *Gene Ther.* **2005**, *12*, 865-872.
5. Hsu, V. W.; Bai, M.; Li, J. Getting active: protein sorting in endocytic recycling. *Nature Reviews Molecular Cell Biology* **2012**, *13*, 323-328.
6. Park, J. G.; Kahn, J. N.; Tumer, N. E.; Pang, Y. Chemical Structure of Retro-2, a Compound That Protects Cells against Ribosome-Inactivating Proteins. *Sci Rep* **2012**, *2*, 631.
7. Noel, R.; Gupta, N.; Pons, V.; Goudet, A.; Garcia-Castillo, M. D.; Michau, A.; Martinez, J.; Buisson, D.; Johannes, L.; Gillet, D. N-methyldihydroquinazolinone derivatives of Retro-2 with enhanced efficacy against Shiga toxin. *J. Med. Chem.* **2013**, *56*, 3404-3413.

8. Gupta, N.; Pons, V.; Noel, R.; Buisson, D. A.; Michau, A.; Johannes, L.; Gillet, D.; Barbier, J.; Cintrat, J. (S)-N-Methyldihydroquinazolinones are the Active Enantiomers of Retro-2 Derived Compounds against Toxins. *ACS Medicinal Chemistry Letters* **2013**.
9. Laniosz, V.; Dabydeen, S. A.; Havens, M. A.; Meneses, P. I. Human papillomavirus type 16 infection of human keratinocytes requires clathrin and caveolin-1 and is brefeldin a sensitive. *J. Virol.* **2009**, *83*, 8221-8232.
10. Lipovsky, A.; Popa, A.; Pimienta, G.; Wyler, M.; Bhan, A.; Kuruvilla, L.; Guie, M. A.; Poffenberger, A. C.; Nelson, C. D.; Atwood, W. J.; DiMaio, D. Genome-wide siRNA screen identifies the retromer as a cellular entry factor for human papillomavirus. *Proc. Natl. Acad. Sci. U. S. A.* **2013**, *110*, 7452-7457.
11. Jiang, M.; Abend, J. R.; Johnson, S. F.; Imperiale, M. J. The role of polyomaviruses in human disease. *Virology* **2009**, *384*, 266-273.
12. Kean, J. M.; Rao, S.; Wang, M.; Garcea, R. L. Seroepidemiology of human polyomaviruses. *PLoS pathogens* **2009**, *5*, e1000363.
13. Ferenczy, M. W.; Marshall, L. J.; Nelson, C. D.; Atwood, W. J.; Nath, A.; Khalili, K.; Major, E. O. Molecular biology, epidemiology, and pathogenesis of progressive multifocal leukoencephalopathy, the JC virus-induced demyelinating disease of the human brain. *Clin. Microbiol. Rev.* **2012**, *25*, 471-506.
14. Boothpur, R.; Brennan, D. C. Human polyoma viruses and disease with emphasis on clinical BK and JC. *Journal of Clinical Virology* **2010**, *47*, 306-312.
15. Binet, I.; Nickeleit, V.; Hirsch, H. H.; Prince, O.; Dalquen, P.; Gudat, F.; Mihatsch, M. J.; Thiel, G. Polyomavirus disease under new immunosuppressive drugs: a cause of renal graft dysfunction and graft loss. *Transplantation* **1999**, *67*, 918-922.
16. Chaturvedi, A. K.; Engels, E. A.; Pfeiffer, R. M.; Hernandez, B. Y.; Xiao, W.; Kim, E.; Jiang, B.; Goodman, M. T.; Sibug-Saber, M.; Cozen, W.; Liu, L.; Lynch, C. F.; Wentzensen, N.; Jordan, R. C.; Altekruse, S.; Anderson, W. F.; Rosenberg, P. S.; Gillison, M. L. Human papillomavirus and rising oropharyngeal cancer incidence in the United States. *J. Clin. Oncol.* **2011**, *29*, 4294-4301.
17. Schiller, J. T.; Day, P. M.; Kines, R. C. Current understanding of the mechanism of HPV infection. *Gynecol. Oncol.* **2010**, *118*, S12-S17.
18. Parkin, D. M.; Bray, F. The burden of HPV-related cancers. *Vaccine* **2006**, *24*, S11-S25.
19. Querbes, W.; O'Hara, B. A.; Williams, G.; Atwood, W. J. Invasion of host cells by JC virus identifies a novel role for caveolae in endosomal sorting of noncaveolar ligands. *J. Virol.* **2006**, *80*, 9402-9413.

20. Engel, S.; Heger, T.; Mancini, R.; Herzog, F.; Kartenbeck, J.; Hayer, A.; Helenius, A. Role of endosomes in simian virus 40 entry and infection. *J. Virol.* **2011**, *85*, 4198-4211.
21. Qian, M.; Cai, D.; Verhey, K. J.; Tsai, B. A lipid receptor sorts polyomavirus from the endolysosome to the endoplasmic reticulum to cause infection. *PLoS pathogens* **2009**, *5*, e1000465.
22. Schelhaas, M.; Malmström, J.; Pelkmans, L.; Haugstetter, J.; Ellgaard, L.; Grünewald, K.; Helenius, A. Simian Virus 40 depends on ER protein folding and quality control factors for entry into host cells. *Cell* **2007**, *131*, 516-529.
23. Lilley, B. N.; Gilbert, J. M.; Ploegh, H. L.; Benjamin, T. L. Murine polyomavirus requires the endoplasmic reticulum protein Derlin-2 to initiate infection. *J. Virol.* **2006**, *80*, 8739-8744.
24. Magnuson, B.; Rainey, E. K.; Benjamin, T.; Baryshev, M.; Mkrtchian, S.; Tsai, B. ERp29 triggers a conformational change in polyomavirus to stimulate membrane binding. *Mol. Cell* **2005**, *20*, 289-300.
25. Rainey-Barger, E. K.; Magnuson, B.; Tsai, B. A chaperone-activated nonenveloped virus perforates the physiologically relevant endoplasmic reticulum membrane. *J. Virol.* **2007**, *81*, 12996-13004.
26. Goodwin, E. C.; Lipovsky, A.; Inoue, T.; Magaldi, T. G.; Edwards, A. P.; Van Goor, K. E.; Paton, A. W.; Paton, J. C.; Atwood, W. J.; Tsai, B.; DiMaio, D. BiP and multiple DNAJ molecular chaperones in the endoplasmic reticulum are required for efficient simian virus 40 infection. *MBio* **2011**, *2*, e00101-11.
27. Gillet, D.; Barbier, J.; Johnnes, L.; Stechman, B.; Bai, S. World Intellectual Property Organization Patent PTC/IB2009/006334, **2009**.
28. Narasimhulu, M.; Lee, Y. R. Ethylenediamine diacetate-catalyzed three-component reaction for the synthesis of 2,3-dihydroquinazolin-4(1H)-ones and their spirooxindole derivatives. *Tetrahedron* **2011**, *67*, 9627-9634.
29. Prakash, M.; Kesavan, V. Highly Enantioselective Synthesis of 2,3-Dihydroquinazolinones through Intramolecular Amidation of Imines. *Org. Lett.* **2012**, *14*, 1896-1899.
30. Sharma, M.; Pandey, S.; Chauhan, K.; Sharma, D.; Kumar, B.; Chauhan, P. M. S. Cyanuric Chloride Catalyzed Mild Protocol for Synthesis of Biologically Active Dihydro/Spiro Quinazolinones and Quinazolinone-glycoconjugates. *J. Org. Chem.* **2012**, *77*, 929-937.
31. Wang, M.; Zhang, T. T.; Liang, Y.; Gao, J. J. Strontium chloride-catalyzed one-pot synthesis of 2, 3-dihydroquinazolin-4(1H)-ones in protic media. *Chinese Chemical Letters* **2011**, *22*, 1423-1426.

32. Escalante, J.; Ortíz-Nava, C.; Flores, P.; Priego, J. M.; García-Martínez, C. Synthesis, NMR and Crystallographic Studies of 2-Substituted Dihydroquinazolinones Derived from (S)-Phenylethylamine. *Molecules* **2007**, *12*, 173-182.
33. Cheng, D.; Tian, Y.; Tian, S. Catalytic Asymmetric Synthesis of Dihydroquinazolinones from Imines and 2-Aminobenzamides. *Advanced Synthesis & Catalysis* **2012**, *354*, 995-999.
34. Wang, G.; Miao, C.; Kang, H. Benign and Efficient Synthesis of 2-Substituted 4(3H)-Quinazolinones Mediated by Iron(III) Chloride Hexahydrate in Refluxing Water. *Bull. Chem. Soc. Jpn.* **2006**, *79*, 1426-1430.
35. Schelhaas, M.; Ewers, H.; Rajamäki, M.; Day, P. M.; Schiller, J. T.; Helenius, A. Human papillomavirus type 16 entry: retrograde cell surface transport along actin-rich protrusions. *PLoS pathogens* **2008**, *4*, e1000148.
36. Schiller, J. T.; Day, P. M.; Kines, R. C. Current understanding of the mechanism of HPV infection. *Gynecol. Oncol.* **2010**, *118*, S12-S17.
37. Sapp, M.; Bienkowska-Haba, M. Viral entry mechanisms: human papillomavirus and a long journey from extracellular matrix to the nucleus. *FEBS journal* **2009**, *276*, 7206-7216.
38. Major, E. O.; Miller, A. E.; Mourrain, P.; Traub, R. G.; de Widt, E.; Sever, J. Establishment of a line of human fetal glial cells that supports JC virus multiplication. *Proc. Natl. Acad. Sci. U. S. A.* **1985**, *82*, 1257-1261.
39. Vacante, D. A.; Traub, R.; Major, E. O. Extension of JC virus host range to monkey cells by insertion of a simian virus 40 enhancer into the JC virus regulatory region. *Virology* **1989**, *170*, 353-361.
40. De Clercq, E. Antiviral drugs in current clinical use. *Journal of Clinical Virology*, **2004**, *30*(2), 115-133.

## Chapter 3 – Acyldepsipeptide (ADEP) Antibiotics: A Promising Group of Antibacterial Agents

### Introduction

The increasing numbers of infections caused by multi-drug resistant bacteria portends a major public health crisis<sup>1</sup> The fact that no new structural classes of antibacterial drugs were introduced between 1962 and 2000 is evidence of a troubling innovation gap in medicine that exacerbates the drug resistance problem. Unfortunately, most drugs in use today target a relatively small subset of proteins and nucleic acids with essential roles in DNA replication, transcription, translation and cell envelope homeostasis.<sup>2</sup> This is problematic because genetic mutations or genes that confer resistance to one antibacterial drug can also confer resistance to others with the same target or mechanism of action.<sup>2</sup> To circumvent “cross-resistance”, we must identify and validate new antibacterial drug targets.

Proteolysis is an important aspect of bacterial cell physiology that has yet to be exploited by antibacterial drugs. Among the most interesting proteolytic drug targets to emerge in the past decade is the proteolytic complex formed by ClpP (caseinolytic peptidase) and its accessory AAA+ partners (ATPases associated with diverse cellular activities). ClpP is a highly conserved peptidase that serves two known functions in the cell. One of its primary roles is the degradation of misfolded and denatured proteins, which facilitates recycling of peptide and protein building blocks for future biosynthesis. Additionally, ClpP degrades a variety of transcription factors that regulate virulence-factor production and stress responses<sup>3-7</sup>. Genetic studies have established that the *clpP* gene and genes encoding the AAA+ partners are essential for virulence in some pathogenic bacteria (*e.g.*, *Staphylococcus aureus*, *Listeria monocytogenes*, and *Streptococcus pneumoniae*) and for viability in others (*e.g.*, *Mycobacterium tuberculosis*)<sup>8-15</sup>.

These physiological requirements of ClpP make it an attractive target for the development of antibacterial drugs.

The Clp complex belongs to a structural class of proteins known as self-compartmentalized proteases. ClpP monomers self-assemble into heptameric rings that stack face-to-face to form a barrel-shaped tetradecamer (figure 3.1 A).<sup>16-18</sup> The interior solvent-filled chamber of the “barrel” is decorated with fourteen serine protease active sites and, in principle, is large enough to accommodate a 50 kDa protein.<sup>16-18</sup> However, narrow axial pores at each end of the barrel prevent entry of folded proteins into the proteolytic chamber.<sup>16-18</sup> In fact, only peptides smaller than ~10 amino acids may freely diffuse into the ClpP proteolytic chamber and be degraded. Consequently, ClpP proteolytic activity is tightly regulated. In the degradation of folded proteins, ClpP functions in conjunction with accessory ATPase partners (ClpA, ClpB, ClpC, ClpE, ClpL, and ClpX) and occasionally adapter proteins that bind to the accessory ATPases as an additional means of activity modulation (Figure 3.1 B).<sup>19</sup> ATPase monomers assemble into hexameric rings that bind to the two apical faces of the ClpP tetradecamer where they recognize, unfold, and coaxially translocate substrates into the proteolytic chamber of ClpP<sup>20-23</sup>.



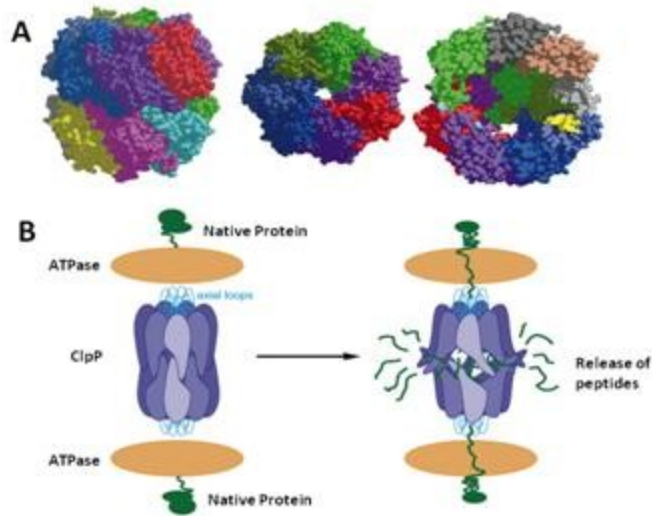
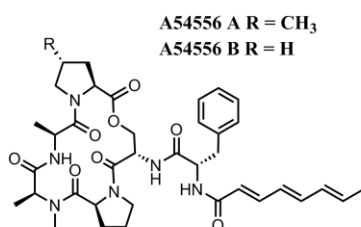


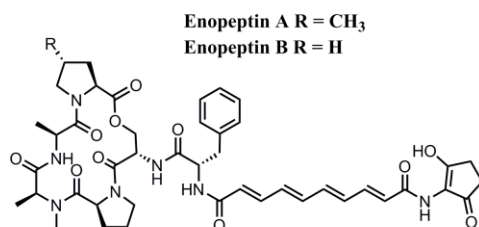
**Figure 3.1 – Structure and Function of Clp proteolytic complex: A) Crystal structure of *E. coli* ClpP: side on view (left), apical face (middle), and cutaway revealing interior proteolytic chamber (right).<sup>16</sup> B) Cartoon illustration of the Clp complex structure and mechanism of proteolysis.<sup>7</sup>**

Several molecules reported to perturb ClpP activity have been discovered in mechanistic investigations of natural products with antibacterial activity or in biased screens for ClpP activators. These compounds are classified as activators or inhibitors of ClpP. Treatment of bacteria with inhibitors of ClpP phenocopies the effects of *clpP* null mutations (*i.e.*, compromised virulence or viability)<sup>24,25</sup>, whereas bacteria are killed upon exposure to ClpP activators.<sup>26</sup> The first ClpP activators to be reported were the acyldepsipeptide antibiotics (ADEPs).<sup>27,28</sup> The prototypical members of this group of antibiotics are “A54556A and B” produced by *Streptomyces hawaiiensis*<sup>27</sup> and enopeptins A and B produced by *Streptomyces sp.* RK-1051<sup>28</sup> (Figure 1.2). Since their initial discovery, ADEPs have been reported to exhibit potent activity against a broad range of Gram-positive bacterial pathogens including *S. aureus*<sup>27-30</sup>, *S. pneumoniae*<sup>27,29</sup>, various *Enterococci*<sup>29</sup>, *M. tuberculosis*<sup>31</sup>, and multi-drug resistant strains of these bacteria.<sup>29,30</sup> Importantly, the ADEPs do not exhibit cross-resistance with any clinically used antibacterial drug classes.<sup>29,32</sup>

### Natural Product ADEPs

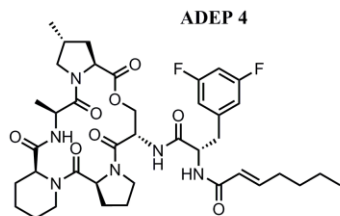


*Michel et al. 1985*

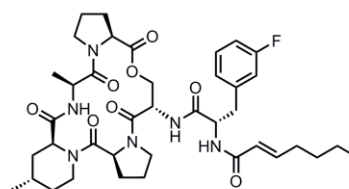


*Osada et al. 1991*

### Synthetic ADEPs



*Hinzen et al. 2006*



*Socha et al. 2010*

**Figure 3.2 - Structures of natural product ADEPs and optimized synthetic analogs thereof.**

The Bayer group was the first to show that ClpP was the sub-cellular target of the ADEPs. Subsequent structural studies indicated that ADEPs bind in pockets at interfaces of ClpP subunits, which also happen to serve as the docking sites for accessory ATPases, and mediate ClpP activation via opening of its axial pores.<sup>33,34 29,34,35</sup> As a result of the axial pore expansion, ADEP-activated ClpP is able to degrade oligopeptides and structurally disordered or nascent proteins in the absence of accessory ATPases (Figure 3.3). The direct cause of ADEP cytotoxicity has been ascribed to degradation of the essential cell-division protein, FtsZ, by ADEP-activated ClpP.<sup>36</sup> In this regard, the ADEPs are unique because most antibiotics inhibit rather than activate their targets.

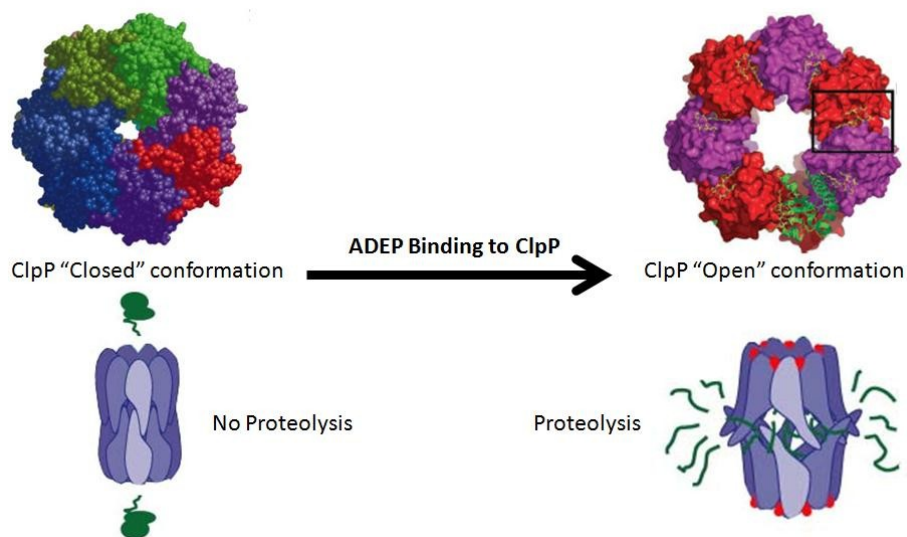


Figure 3.9 - Effect of ADEP binding on ClpP structure (top) and activity (bottom) <sup>7,16,34</sup>

The efficacy of ADEPs at killing pathogenic bacteria and their unique mode of action have prompted efforts to assess their medicinal potential. The natural products were found to be inactive in mouse models of MRSA infections, despite their potent antibacterial activity *in vitro* <sup>32</sup>. Their physicochemical and pharmacokinetic profile was defined by poor water solubility, rapid systemic clearance, and chemical instability. Medicinal chemistry was used to optimize the structures of the ADEPs to enhance their stability and biological activity. The most potent molecule developed by Bayer Healthcare AG, known as ADEP-4, differs from the natural ADEPs in three ways. <sup>32</sup> First, it has a more chemically stable hexenoyl moiety in place of a conjugated polyene. Second, rather than phenylalanine in its appendant side chain, ADEP-4 has a 3,5-difluorophenylalanine, which was credited with improving compound bioavailability and binding to ClpP. Finally, the natural ADEPs have a *N*-methylalanine residue within the core macrocycle, whereas ADEP-4 has a cyclic amino acid, pipecolate (a six-membered ring), at the same position. The last feature was deemed to be particularly important for antibacterial activity, leading to the proposal that the incorporation of this cyclic residue rigidifies the ADEP peptidolactones. This rigidification was predicted to reduce the entropic penalty of ClpP binding. <sup>32</sup> An ADEP

analog bearing a proline in place of the *N*-methylalanine had no antibacterial activity<sup>32</sup>, suggesting that proline, which is even more conformationally constrained than pipecolic acid, fortifies a conformation of the peptidolactone that is incompatible with ClpP binding. Thus, any productive rigidifying structural features must enforce a low-energy conformation that is recognized by ClpP.<sup>37</sup> ADEP-4 has up to 160-fold greater potency than the natural ADEPs against multi-drug resistant isolates of *S. aureus* and *S. pneumoniae*. ADEP-4 also showed impressive activity *in vivo*. In fact, mice with potentially lethal infections of *S. aureus* were cured by intravenous administration of ADEP-4.<sup>29</sup> More recently, ADEP-4 and its analogs have been reported to be toxic to *M. tuberculosis in vitro*, particularly in combination with efflux pump inhibitors.<sup>31</sup> Also, it has been reported to completely eradicate *S. aureus* biofilms *in vitro* and in mouse models of chronic infection when co-administered with the anti-bacterial drug rifampicin.<sup>38</sup>

### Design of conformationally constrained ADEP peptidolactones

Our lab has been interested in the effects of conformational dynamics on ADEP activity. The aforementioned observation that the incorporation of pipecolic acid into the ADEP peptidolactone results in increased potency as a result of conformational restriction prompted further investigation. Socha *et al.* reported the synthesis and biological evaluation of an ADEP analog with a 4-methylpipecolic acid residue in the peptidolactone (compound **2**).<sup>30</sup> The methyl substituent was predicted to further restrict the conformational flexibility of the pipecolate residue by imposing large energetic penalties to certain conformations.(Figure 3.4A). It was hypothesized that the added conformational restriction in the 4-methylpipecolate residue itself would translate into an overall rigidification of the ADEP peptidolactone. Consistent with this hypothesis, compound **2** with 4-methyl pipecolate was 2- and 4-fold more potent than *des*-

methyl analog **1** against clinical isolates of methicillin-resistant *S. aureus* and vancomycin-resistant *E. faecalis*, respectively (Figure 3.4B).<sup>30</sup>

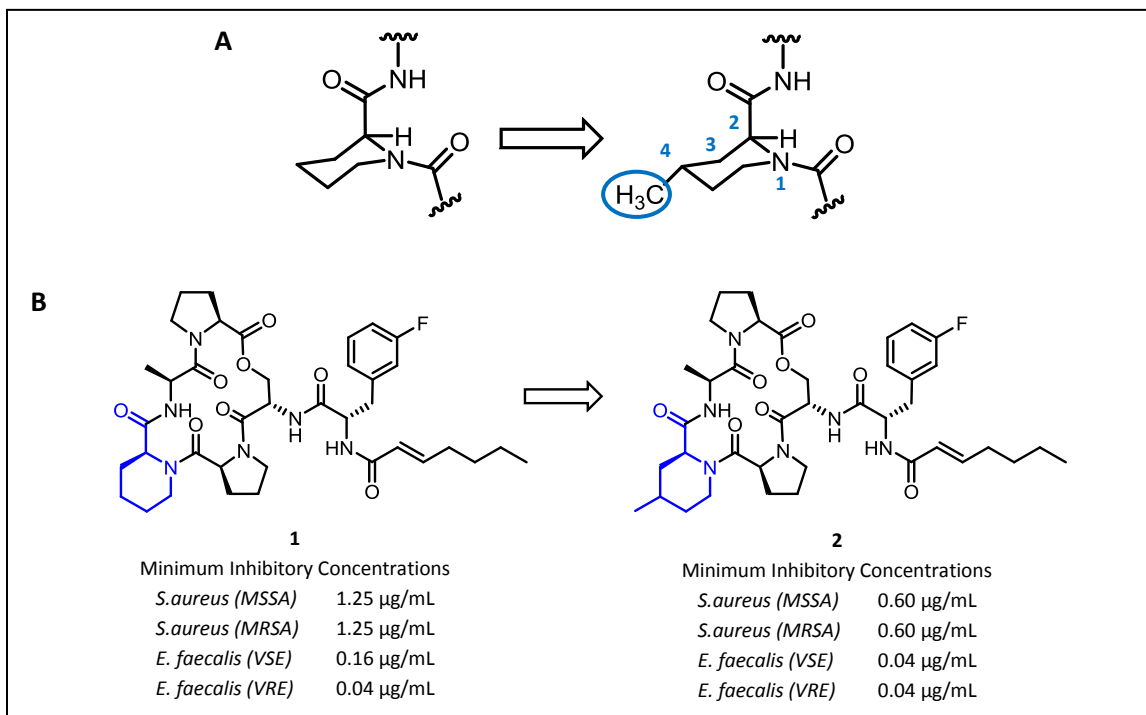


**Figure 3.4 – Effect of pipercolate methylation on ADEP activity.** A) Lowest energy conformation of pipercolate residues: C-2 carbonyl prefers axial orientation to minimize allylic strain, C-4 equatorial methyl group fortifies stable chair conformation by minimizing unfavorable syn-diaxial strain. B) Incorporation of 4-methylpipercolate improves antibacterial activity against laboratory and clinical strains of *S. aureus* and *E. faecalis*: MSSA - Methicillin-susceptible *S. aureus* (ATCC 35556), MRSA - Methicillin-resistant *S. aureus* (clinical isolate from blood), VSE – Vancomycin-susceptible *E. faecalis* (ATCC 29212), Vancomycin-resistant *E. faecalis* (clinical isolate from rectal swab).

Motivated by these initial findings, we sought to study the phenomenon of peptidolactone conformational restriction in greater detail. Specifically we wanted to thoroughly test the hypothesis that incorporation of conformationally constrained amino acid residues into the ADEP peptidolactone was rigidifying the macrocycle as a whole. Additionally, we sought to define the impacts of ADEP conformational dynamics on their binding to and activation of ClpP and on their bioactivity.

To begin, we designed a series of ADEP molecules that we expected would exhibit a range of peptidolactone conformational restriction. The relatively flexible peptidolactone of the natural products would serve as a baseline point of comparison for ADEPs that incorporated various combinations of conformationally constrained amino acids in their peptidolactones. First, we envisioned substituting the *N*-methylalanine residue of natural ADEP peptidolactones with pipercolate residues bearing C-4 substituents of varying size. As discussed already, cyclic amino acids are typically more conformationally constrained compared to their acyclic counterparts, and ring substituents can limit ring conformational dynamics by imposing high energetic penalties to certain conformations (*e.g.*, 1,3- diaxial strain). In a separate approach, we envisioned replacing the serine residue of the peptidolactone with *allo*-threonine, a serine analog with a methyl substituent on the  $\beta$ -carbon. This amino acid is more conformationally constrained because the  $\beta$ -methyl group confers additional torsional strain about both the  $C\alpha$ - $C\beta$  bond and  $C\beta$ -O bond. Importantly, we predicted that the methyl substituent of *allo*-threonine would not sterically clash with ClpP. We had originally envisioned also preparing analogs with a threonine residue in place of the natural serine residue. However, precursors to these ADEP analogs failed to cyclize. Presumably, the stereochemistry of the threonine  $\beta$ -methyl substituent enforces an unfavorable conformation for macrocyclization.

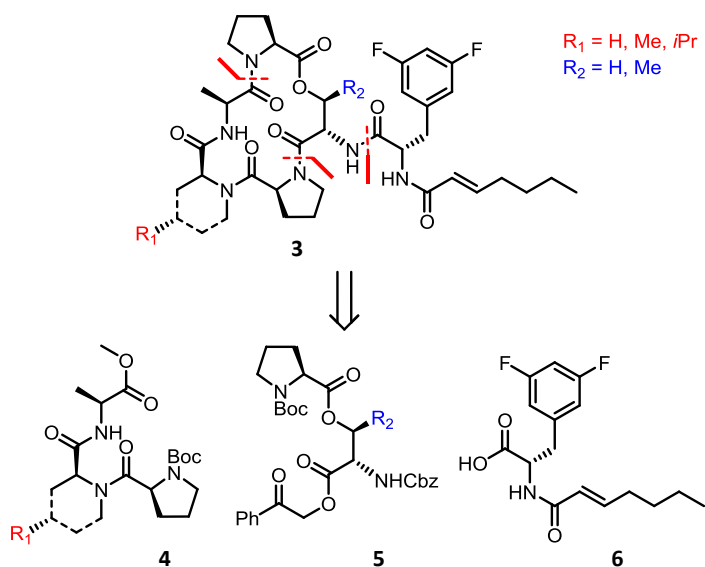


Figure 3.5 - Retrosynthetic analysis of ADEPs with conformationally constrained macrocycles

To access these proposed ADEP analogs, we envisioned using a reported convergent synthetic strategy (Figure 3.5).<sup>32,39,40</sup> The ADEP structure can be retrosynthetically disconnected to yield three fragments of similar size and complexity, specifically a tripeptide (**4**), a proline ester (**5**), and a *N*-heptenoyldifluorophenylalanine side chain (**6**). Tripeptides (**4**) containing *N*-methylalanine, pipecolic acid, 4-methylpipecolic acid, or 4-isopropylpipecolic acid would be coupled to proline esters (**5**) containing serine or allo-threonine then cyclized to generate peptidolactones with various combinations of conformationally flexible and conformationally constrained amino acids. After attachment of the side chain (**6**) the resulting ADEPs would be evaluated to determine the effects of the conformationally constrained amino acids on peptidolactone rigidity and ADEP activity. The following three chapters will describe in detail our chemical synthesis and evaluation the proposed ADEPs.

## References

1. Boucher, H. W.; Talbot, G. H.; Bradley, J. S.; Edwards, J. E.; Gilbert, D.; Rice, L. B.; Scheld, M.; Spellberg, B.; Bartlett, J. Bad Bugs, No Drugs: No ESKAPE! An Update from the Infectious Diseases Society of America. *Clinical Infectious Diseases* **2009**, *48*, 1-12.

2. Walsh, C. *Antibiotics: actions, origins, resistance*. American Society for Microbiology (ASM): 2003; .
3. Maurizi, M. R.; Thompson, M. W.; Singh, S. K.; Kim, S. Endopeptidase Clp: ATP-dependent Clp protease from *Escherichia coli*. *Meth. Enzymol.* **1993**, *244*, 314-331.
4. Gominet, M.; Seghezzi, N.; Mazodier, P. Acyl depsipeptide (ADEP) resistance in *Streptomyces*. *Microbiology* **2011**, *157*, 2226-2234.
5. Gottesman, S.; Wickner, S.; Maurizi, M. R.; Beals, C. R.; Clipstone, N. A.; Ho, S. N.; Crabtree, G. R.; Zamir, I.; Zhang, J.; Lazar, M. A. Protein quality control: triage by chaperones and proteases 815. *Genes Dev.* **1997**.
6. Sauer, R. T.; Baker, T. A. AAA proteases: ATP-fueled machines of protein destruction. *Annu. Rev. Biochem.* **2011**, *80*, 587-612.
7. Yu, A. Y. H.; Houry, W. A. ClpP: a distinctive family of cylindrical energy-dependent serine proteases. *FEBS Lett.* **2007**, *581*, 3749-3757.
8. Raju, R. M.; Goldberg, A. L.; Rubin, E. J. Bacterial proteolytic complexes as therapeutic targets. *Nature Reviews Drug Discovery* **2012**, *11*, 777-789.
9. Roberts, D. M.; Personne, Y.; Ollinger, J.; Parish, T. Proteases in *Mycobacterium tuberculosis* pathogenesis: potential as drug targets. *Future microbiology* **2013**, *8*, 621-631.
10. Frees, D.; Qazi, S. N. A.; Hill, P. J.; Ingmer, H. Alternative roles of ClpX and ClpP in *Staphylococcus aureus* stress tolerance and virulence. *Mol. Microbiol.* **2003**, *48*, 1565-1578.
11. Frees, D.; Sorensen, K.; Ingmer, H. Global Virulence Regulation in *Staphylococcus aureus*: Pinpointing the Roles of ClpP and ClpX in the *sar/agr* Regulatory Network. *Infect. Immun.* **2005**, *73*, 8100-8108.
12. Kwon, H.; Kim, S.; Choi, M.; Ogunniyi, A. D.; Paton, J. C.; Park, S.; Pyo, S.; Rhee, D. Effect of Heat Shock and Mutations in ClpL and ClpP on Virulence Gene Expression in *Streptococcus pneumoniae*. *Infect. Immun.* **2003**, *71*, 3757-3765.
13. Kwon, H.; Ogunniyi, A. D.; Choi, M.; Pyo, S.; Rhee, D.; Paton, J. C. The ClpP Protease of *Streptococcus pneumoniae* Modulates Virulence Gene Expression and Protects against Fatal Pneumococcal Challenge. *Infect. Immun.* **2004**, *72*, 5646-5653.
14. Robertson, G. T.; Ng, W.; Foley, J.; Gilmour, R.; Winkler, M. E. Global transcriptional analysis of *clpP* mutations of type 2 *Streptococcus pneumoniae* and their effects on physiology and virulence. *J. Bacteriol.* **2002**, *184*, 3508-3520.
15. Gaillot, O.; Pellegrini, E.; Bregenholt, S.; Nair, S.; Berche, P. The ClpP serine protease is essential for the intracellular parasitism and virulence of *Listeria monocytogenes*. *Mol. Microbiol.* **2000**, *35*, 1286-1294.



16. Wang, J.; Hartling, J. A.; Flanagan, J. M. The Structure of ClpP at 2.3 Å Resolution Suggests a Model for ATP-Dependent Proteolysis. *Cell* **1997**, *91*, 447-456.
17. Wang, J.; Hartling, J. A.; Flanagan, J. M. Crystal Structure Determination of Escherichia coli ClpP Starting from an EM-Derived Mask, *J. Struct. Biol.* **1998**, *124*, 151-163.
18. Szyk, A.; Maurizi, M. R. Crystal structure at 1.9 Å of *E. coli* ClpP with a peptide covalently bound at the active site. *J. Struct. Biol.* **2006**, *156*, 165-174.
19. Butler, S. M.; Festa, R. A.; Pearce, M. J.; Darwin, K. H. Self-compartmentalized bacterial proteases and pathogenesis. *Mol. Microbiol.* **2006**, *60*, 553-562.
20. Gottesman, S.; Roche, E.; Zhou, Y.; Sauer, R. T. The ClpXP and ClpAP proteases degrade proteins with carboxy-terminal peptide tails added by the SsrA-tagging system. *Genes Dev.* **1998**, *12*, 1338-1347.
21. Singh, S. K.; Grimaud, R.; Hoskins, J. R.; Wickner, S.; Maurizi, M. R. Unfolding and internalization of proteins by the ATP-dependent proteases ClpXP and ClpAP. *Proceedings of the National Academy of Sciences of the United States of America* **2000**, *97*, 8898-8903.
22. Baker, T. A.; Sauer, R. T. ATP-dependent proteases of bacteria: recognition logic and operating principles. *Trends Biochem. Sci.* **2006**, *31*, 647-653.
23. Alexopoulos, J. A.; Guarné, A.; Ortega, J. ClpP: a structurally dynamic protease regulated by AAA proteins. *J. Struct. Biol.* **2012**.
24. Böttcher, T.; Sieber, S. A. β-Lactones as Specific Inhibitors of ClpP Attenuate the Production of Extracellular Virulence Factors of Staphylococcus aureus. *J. Am. Chem. Soc.* **2008**, *130*, 14400-14401.
25. Böttcher, T.; Sieber, S. A. Structurally Refined β-Lactones as Potent Inhibitors of Devastating Bacterial Virulence Factors. *ChemBioChem* **2009**, *10*, 663-666.
26. Leung, E.; Datti, A.; Cossette, M.; Goodreid, J.; McCaw, S. E.; Mah, M.; Nakhamchik, A.; Ogata, K.; El Bakkouri, M.; Cheng, Y. Activators of cylindrical proteases as antimicrobials: identification and development of small molecule activators of ClpP protease. *Chem. Biol.* **2011**, *18*, 1167-1178.
27. Michel, K. H.; Kastner, R. E. *A54556 antibiotics and process for production thereof* **1985**.
28. OSADA, H.; YANO, T.; KOSHINO, H.; ISONO, K. Enopeptin A, a novel depsipeptide antibiotic with anti-bacteriophage activity. *J. Antibiot.* **1991**, *44*, 1463-1466.
29. Brotz-Oesterhelt, H.; Beyer, D.; Kroll, H.; Endermann, R.; Ladel, C.; Schroeder, W.; Hinzen, B.; Raddatz, S.; Paulsen, H.; Henninger, K.; Bandow, J. E.; Sahl, H.; Labischinski, H. Dysregulation of bacterial proteolytic machinery by a new class of antibiotics. *Nat. Med.* **2005**, *11*, 1082-1087.

30. Socha, A. M.; Tan, N. Y.; LaPlante, K. L.; Sello, J. K. Diversity-oriented synthesis of cyclic acyldepsipeptides leads to the discovery of a potent antibacterial agent. *Bioorg. Med. Chem.* **2010**, *18*, 7193-7202.
31. Ollinger, J.; O'Malley, T.; Kesicki, E. A.; Odingo, J.; Parish, T. Validation of the essential ClpP protease in *Mycobacterium tuberculosis* as a novel drug target. *J. Bacteriol.* **2012**, *194*, 663-668.
32. Hinzen, B.; Raddatz, S.; Paulsen, H.; Lampe, T.; Schumacher, A.; Häbich, D.; Hellwig, V.; Benet-Buchholz, J.; Endermann, R.; Labischinski, H.; Brötz-Oesterhelt, H. Medicinal Chemistry Optimization of Acyldepsipeptides of the Enopeptin Class Antibiotics. *ChemMedChem* **2006**, *1*, 689-693.
33. Li, D. H. S.; Chung, Y. S.; Gloyd, M.; Joseph, E.; Ghirlando, R.; Wright, G. D.; Cheng, Y.; Maurizi, M. R.; Guarne, A.; Ortega, J. Acyldepsipeptide antibiotics induce the formation of a structured axial channel in ClpP: a model for the ClpX/ClpA-bound state of ClpP. *Chem. Biol.* **2010**, *17*, 959-969.
34. Lee, B.; Park, E. Y.; Lee, K.; Jeon, H.; Sung, K. H.; Paulsen, H.; Rubsamen-Schaeff, H.; Brötz-Oesterhelt, H.; Song, H. K. Structures of ClpP in complex with acyldepsipeptide antibiotics reveal its activation mechanism. *Nat Struct Mol Biol* **2010**, *17*, 471-478.
35. Kirstein, J.; Hoffmann, A.; Lilie, H.; Schmidt, R.; RübSamen-Waigmann, H.; Brötz-Oesterhelt, H.; Mogk, A.; Turgay, K. The antibiotic ADEP reprogrammes ClpP, switching it from a regulated to an uncontrolled protease. *EMBO Molecular Medicine* **2009**, *1*, 37-49.
36. Sass, P.; Josten, M.; Famulla, K.; Schiffer, G.; Sahl, H.; Hamoen, L.; Brötz-Oesterhelt, H. Antibiotic acyldepsipeptides activate ClpP peptidase to degrade the cell division protein FtsZ. *Proceedings of the National Academy of Sciences* **2011**, *108*, 17474-17479.
37. Mann, A. Conformational restriction and/or steric hindrance in medicinal chemistry. *The Practice of Medicinal Chemistry* **2003**, *2*, 233-250.
38. Conlon, B.; Nakayasu, E.; Fleck, L.; LaFleur, M.; Isabella, V.; Coleman, K.; Leonard, S.; Smith, R.; Adkins, J.; Lewis, K. Activated ClpP kills persisters and eradicates a chronic biofilm infection. *Nature* **2013**, *503*, 365-370.
39. Hinzen, B. Antibacterial macrocycles. **2005**.
40. Schmidt, U.; Neumann, K.; Schumacher, A.; Weinbrenner, S. Synthesis of Enopeptin B from *Streptomyces* sp RK-1051. *Angewandte Chemie International Edition in English* **1997**, *36*, 1110-1112.

## Chapter 4 – Isocyanide Based Multicomponent Reactions and Synthesis of Pipecolate Containing Peptides.

**Contents of this chapter have been published in the following manuscript:** Carney, Daniel W.; Truong, Jonathan V.; Sello, Jason K. *Investigations of the Configurational Stabilities of Chiral Isocyanoacetates in Multicomponent Reactions.* *J. Org. Chem.*, **2011**, 76 (24), 10279–10285. dx.doi.org/10.1021/jo201817k

### Introduction

Although robust synthetic routes to ADEPs had been established before our lab began its investigations in the field,<sup>1-3</sup> the desire to incorporate substituted pipecolate residues into the peptidolactone necessitated the development of some new synthetic methodologies. The building block required for standard peptide synthesis, Boc-pipecolic acid, was considered somewhat cost-prohibitive (~ \$16/gram), and substituted pipecolic acids are not commercially available. Furthermore, synthesis of substituted pipecolic acid substituents requires a multi-step synthesis in and of itself (Figure 4.1).<sup>4</sup> To circumvent these challenges, we turned to isocyanide based multicomponent reactions (IMCR), specifically the Joullié-Ugi 3-component reaction, as an alternative to standard peptide coupling for the preparation of pipecolate containing peptides (Figure 4.2).

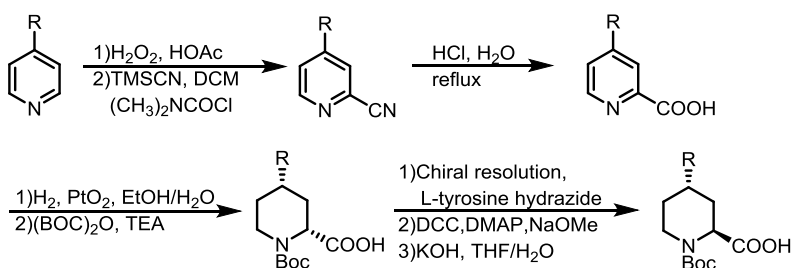


Figure 4.1 – Keenan synthesis of enantiomerically pure substituted pipecolate residues<sup>4</sup>

Multicomponent reactions are those in which three or more reactants are combined to yield a product that contains most of the atoms from the reactants. Two of the most prominent isocyanide based multicomponent reactions are the Passerini 3-component reaction (P-3CR) and

the Ugi 4-component reaction (U-4CR) (figure 4.2). These reactions are particularly useful because their products resemble depsipeptides and peptides. The P-3CR, discovered in 1921, combines an isocyanide with a carboxylic acid and either a ketone or aldehyde to yield an  $\alpha$ -acyloxycarboxamide.<sup>5</sup> The U-4CR, discovered in 1959, combines an isocyanide with an amine, a carboxylic acid, and either a ketone or aldehyde to yield a bis-amide.<sup>6,7</sup> A related reaction, known as the Joullié-Ugi 3-component reaction (JU-3CR), uses as cyclic imine substrate in place of the amine and an aldehyde and is useful for preparing structures that contain cyclic amino acid residues.

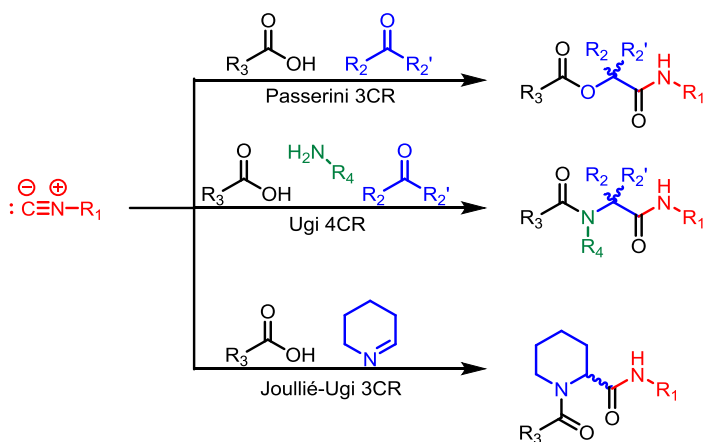


Figure 4.2 - Examples of typical isocyanide based multicomponent reactions.

The versatility of these reactions makes them exceptional tools for diversity-oriented synthesis. Indeed, a small collection of 10 isocyanides, 10 amines, 10 aldehydes/ketones, and 10 carboxylic acids can be combined in all possible combinations to produce 10,000 unique small molecules using the U-4CR. A limitation of these reactions is the fact that two stereoisomers are formed, usually in a 1:1 ratio. Very few instances of substrate directed stereoselectivity have been reported.<sup>8</sup> Furthermore, no asymmetric catalysts have been reported for the U-4CR.

Central to IMCRs is the unique structure and reactivity of the isocyanide substrates. Isocyanides are a class of organic compounds characterized by a functional group with an

unusual electronic structure and unique reactivity. The negatively charged carbon is divalent, allowing it to react with both nucleophiles and electrophiles much like a carbene. Nevertheless, isocyanides are surprisingly stable compounds and have even been isolated from natural sources.<sup>9,10</sup> They are relatively easy compounds to synthesize, with thirteen important preparative methods discovered since 1859,<sup>11</sup> several of which are outlined in figure 4.3. The most commonly employed method for the synthesis of isocyanides is by dehydration of the corresponding formamide.<sup>12</sup> The availability and unique reactivity of isocyanides have led to their extensive utilization in target-oriented and diversity-oriented organic synthesis.<sup>11</sup>

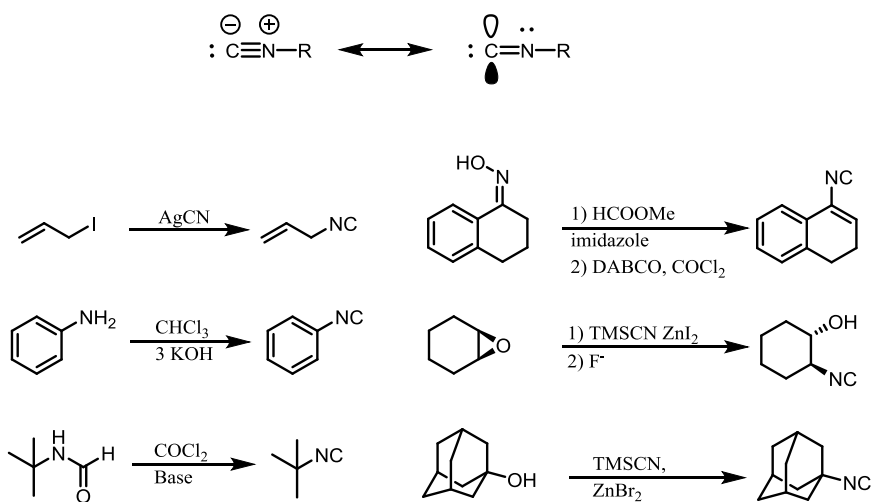


Figure 4.3 – Isocyanide resonance structures and common methods for isocyanide preparation

An interesting class of isocyanides that has received considerable attention recently is the Isocyanoacetates. Isocyanoacetates are particularly useful synthons in the preparation of peptides via IMCRs. These reagents have a secondary site of reactivity in addition to the isocyanide functional group itself. The combination of the two strong electron withdrawing ester and isocyano functional groups lowers the pKa of the  $\alpha$ -protons to  $\sim$ 9-11. Although racemization of chiral isocyanoacetates is a potential liability, they can be prepared in high enantiomeric purity by the formamide dehydration method when the reaction is run at low

temperature and in the presence of a mild tertiary amine base such as *N*-methylmorpholine (Figure 4.4).<sup>13</sup> In addition to the intriguing reactivity of their isocyanide functional group, the  $\alpha$ -carbon of isocyanoacetates can act as a nucleophile upon deprotonation. The isocyanoacetate enolate can be alkylated and also engage in Aldol and Knoevenagel condensations with carbonyl compounds.<sup>14</sup> Isocyanoacetates have also been used as substrates in the synthesis of functionalized heterocycles wherein the nucleophilicity of their  $\alpha$ -carbon is essential.<sup>14,15</sup> More recently, Danishefsky and co-workers used these compounds as chiral substrates in the preparation of *N*-methyl peptides containing  $\alpha$ -amino acids of prescribed configurations.<sup>16,17</sup> The  $\alpha$ -acidity of chiral isocyanoacetates can be problematic in peptide synthesis due to the possibility of their racemization. Nevertheless, it is possible to avoid racemization with careful handling of these compounds as we will discuss in the following sections.

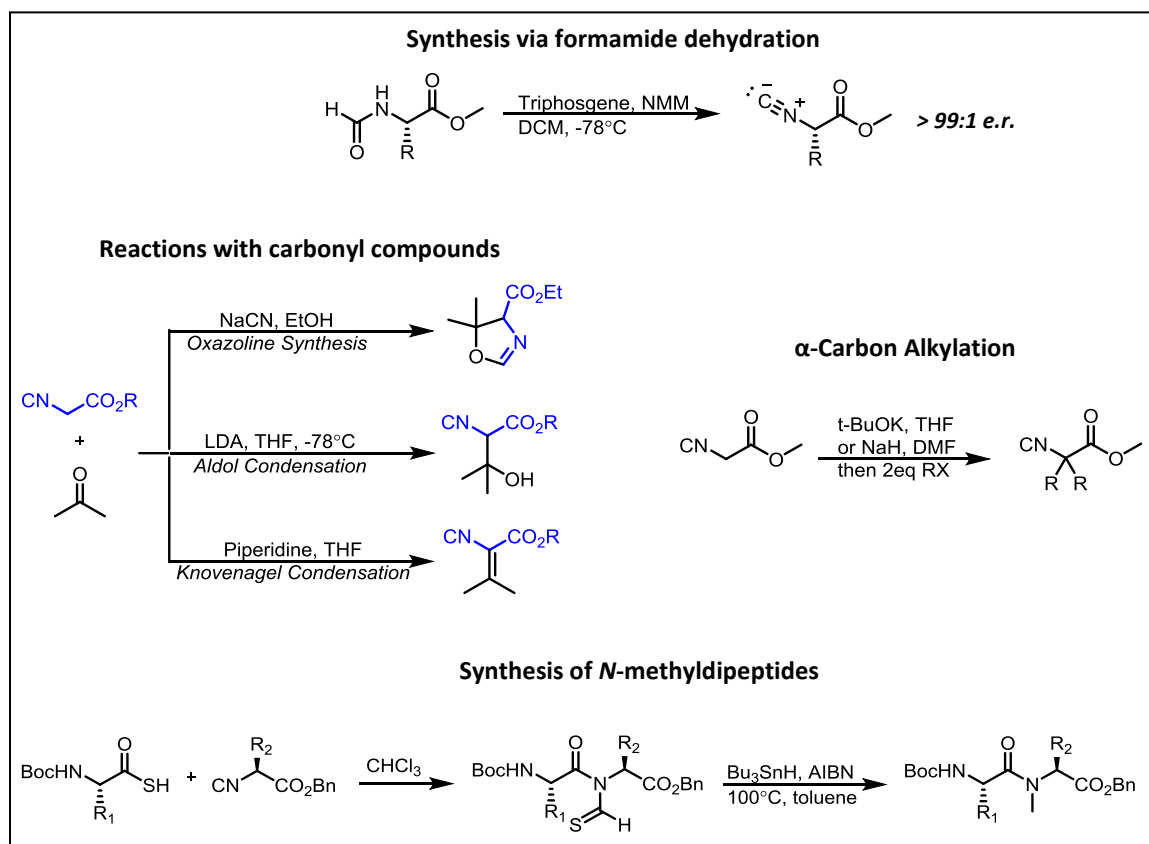


Figure 4.4 – Synthesis and common reactions of isocyanoacetates

## Results

The piperolate containing tripeptides required for ADEP synthesis were prepared using the Joullié-Ugi 3-component reaction (JU-3CR) (Figure 4.5A). Cyclic imines were prepared by *N*-chlorination of piperidine or its 4-substituted analogs, followed by base-promoted dehydrohalogenation. Socha *et al.* reported that treatment of piperidine (**1**) with bleach and acetic acid with a catalytic amount of *t*-butanol yielded *N*-chloropiperidine (**2**) in high yield and purity after aqueous workup. The *N*-chloropiperidine (**2**) was then treated with sodium methoxide in methanol generating  $\Delta^1$ -piperideine (**3**) *in situ*, which was treated directly with Boc-Proline (**4**) and the isocyanoacetate derived from alanine methyl ester (**5**). The corresponding JU-3CR product (**mix-6**) was isolated in good yield, but as a mixture of 4 diastereomers. Socha apparently did not realize this initially and reported that the JU-3CR yielded a 70:30 mixture of only 2 diastereomers. This misinterpretation by Socha was a result of poor resolution of the diastereomeric mixture in an HPLC analysis of the saponified mixture of tripeptides (**mix-7**) (Figure 4.5C). Although the desired Boc-*S*-Pro-*S*-Pip-*S*-Ala-Ome was a minor product, the apparent diastereoselectivity in this JU-3CR was unprecedented and unexpected. We therefore decided to investigate the phenomenon further. However, when the reaction sequence was repeated and the methyl ester JU-3CR product (**mix-6**) was analyzed by HPLC, a more complex mixture of diastereomers was revealed (Figure 4.5B).

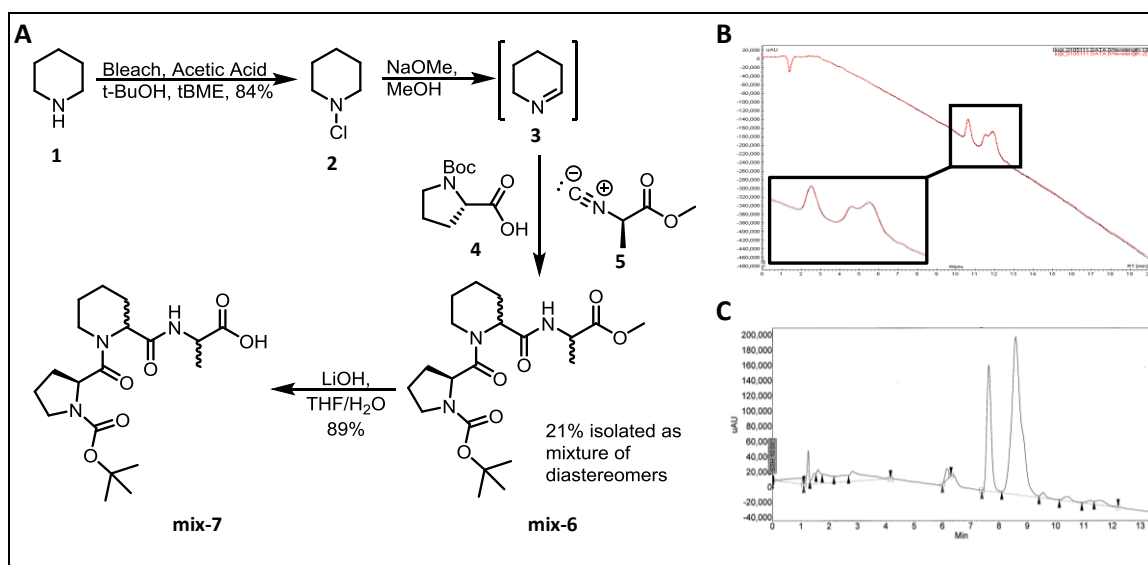


Figure 4.5 – Synthesis of piperolate containing tripeptides using the Joullié-Ugi reaction according to the method reported by Socha *et al.* A) Synthesis of  $\Delta^1$ -piperideine (3a) and subsequent Joullié-Ugi reaction B) HPLC chromatogram of methyl ester Joullié-Ugi product (6a) reveals a complex mixture of diastereomers. C) HPLC chromatogram of saponified Joullié-Ugi product (7a) reveals an apparent 30:70 mixture of only two diastereomers.

It is known that isocyanoacetates are  $\alpha$ -acidic. Thus, an explanation for the observation of a complex mixture of diastereomeric products emerging from the JU-3CR is racemization of the chiral isocyanoacetate. Since the JU-3CR inherently yields a mixture of two diastereomers epimeric at the piperolate  $\alpha$ -carbon, racemization of the isocyanoacetate would cause the reaction to yield a mixture of 4 diastereomers. To test this hypothesis, the 4 diastereomeric peptides (6) that would result from a JU-3CR incorporating a racemic isocyanoacetate were independently synthesized using standard peptide synthesis. Each tripeptide was analyzed by HPLC. An overlay of the pure tripeptide diastereomers' chromatograms with the JU-3CR product (**mix-6**) confirmed our hypothesis (Figure 4.6A). Each pure diastereomer peak had a retention time corresponding to a peak in the **mix-6** chromatogram. Additionally, **mix-6** was separated into two fractions using HPLC, and each fraction was subjected to Advanced Marfey Analysis (Figure 4.6B).<sup>18</sup> The concentrated fractions were hydrolyzed and then the constituent amino acids were derivitized with the chiral Marfey reagent, **L-FDAA**. LC-MS analysis of the derivitized



amino acids indicated that the first fraction contained a tripeptide composed only of the amino acids (*S*)-Proline, (*S*) alanine, and (*S*)-pipecolate, while the second fraction contained a mixture of tripeptides composed of the amino acids (*S*)-Proline, (*S*)-alanine, (*R*)-alanine, (*S*)-pipecolate, and (*R*)-pipecolate. These Marfey Analysis results are also consistent with incorporation of a racemic isocyanoacetate into the JU-3CR.

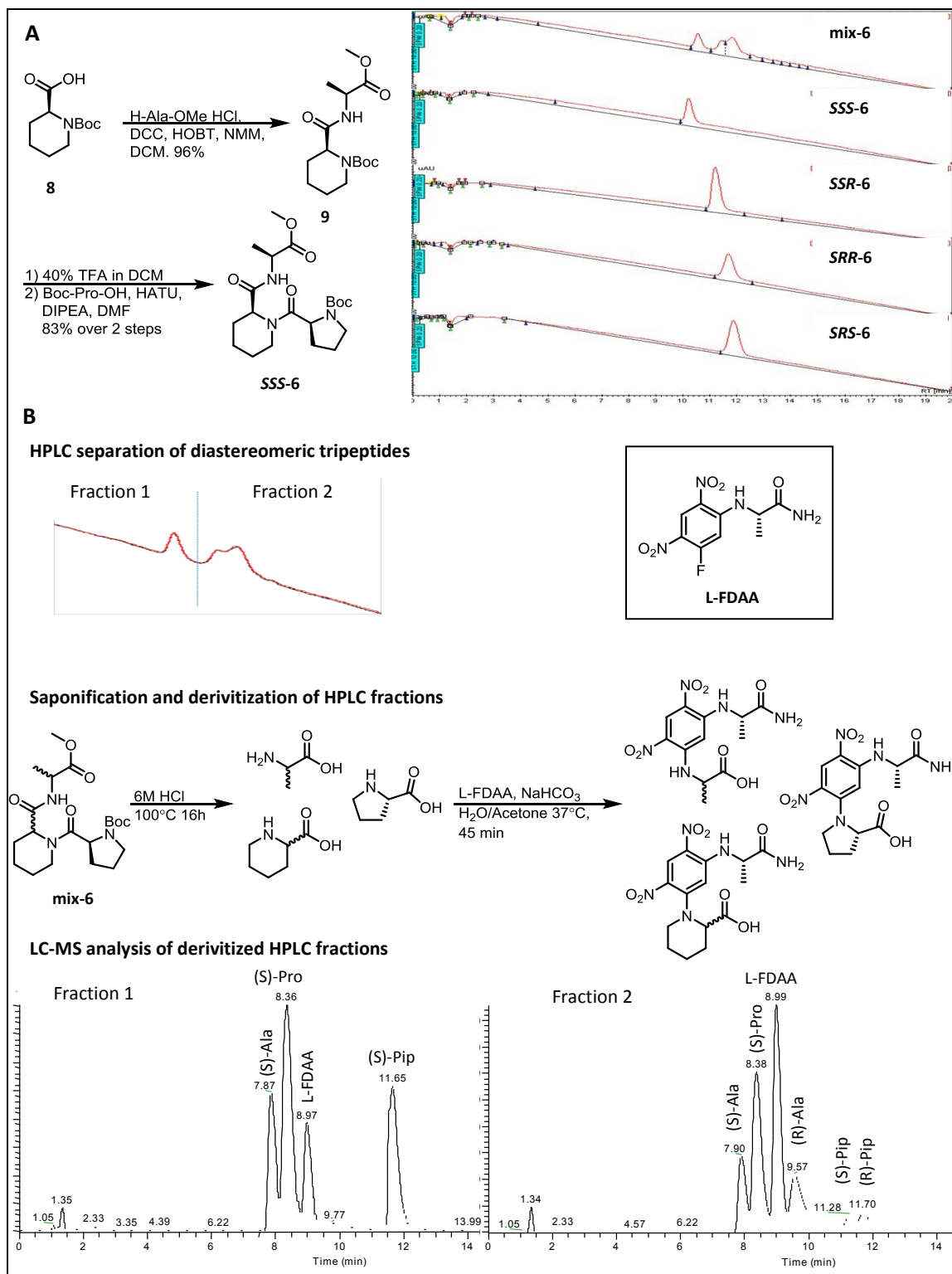


Figure 4.6 – Deconvolution of JU-3CR product mixture: A) Synthesis of selected tripeptide with prescribed residue configurations by standar peptide coupling and HPLC chromatogram overlay of the JU-3CR product with each pure

tripeptide diastereomer that would result from incorporation of a racemic isocyanoacetate. B) HPLC separation of the JU-3CR product mixture and Advanced Marfey Analysis of each fraction.

The revelation that the chiral isocyanoacetate was not configurationally stable in the Joullié-Ugi reaction reported by Socha *et al.* had severe implications for our vision of using multicomponent reactions for peptide synthesis. The inherent lack of stereoselectivity in these multicomponent reactions is often tolerated because of their high yield and simple execution;<sup>19</sup> however, the inclusion of configurationally unstable isocyanoacetate substrates should be avoided because they yield an unacceptably complex mixture of diastereomers. We decided to examine the problem in greater detail and scope. We wanted to know if isocyanoacetate racemization in the Joullié-Ugi reaction was inevitable or a consequence of reaction conditions, which could potentially be optimized to suppress isocyanoacetate epimerization. Furthermore, we wished to study the behavior of chiral isocyanoacetates in other important multicomponent reactions such as the Passerini and Ugi reactions.

Our examination began with a rigorous survey of the literature regarding the reactivity of isocyanoacetates in IMCR. Interestingly, we found that there is some controversy regarding their configurational stability in some of these reactions. It has been reported that chiral isocyanoacetates are configurationally stable under P-3CR.<sup>2021</sup> This is to be expected since the P-3CR does not incorporate a significantly basic substrate. A JU-3CR involving a chiral isocyanoacetate, which lead to an optically active product, has also been reported.<sup>22</sup> On the contrary, in 2008, Banfi *et al.* reported a JU-3CR in which isocyanoacetate racemization did occur.<sup>23</sup> Information in the literature regarding the configurational stability of chiral isocyanoacetates under Ugi reaction conditions is also limited and ambiguous. In 1973, Failli *et al.* reported the preparation of an optically active isocyanide prepared from phenylalanine methyl ester. However, the product obtained by condensation of this isocyanide with

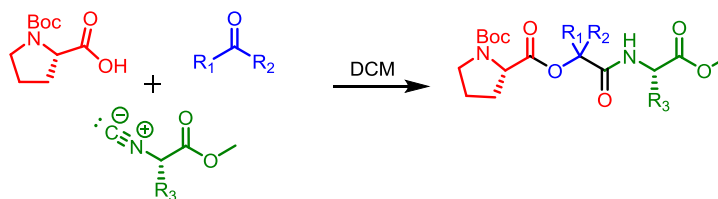
cyclohexanone-dimethylhydrazone and formic acid was not optically active, indicating that the isocyanide had racemized.<sup>24</sup> In 2001, Kessler and co-workers reported engaging chiral isocyanoacetates in the Ugi reaction and obtaining a product mixture of four diastereomers. However, the authors attributed this product mixture to isocyanide racemization during dehydration of the formamides.<sup>25</sup> In 2008, Berłożecki and co-workers reported the only systematic evaluation of chiral isocyanoacetate configurational stability under Ugi conditions that we were able to identify.<sup>26</sup> It was found that at room temperature in DCM, the isocyanides did indeed racemize under U4CR conditions. It was also shown that isocyanide stereochemical integrity was maintained when the reaction was conducted at low temperature and with a BF<sub>3</sub> Lewis acid catalyst. Unfortunately, the reaction yields were very low under these non-racemizing conditions.

Broadly held notions about the configurational instability of chiral isocyanoacetates in IMCRs led to the development of non-racemizable isocyanoacetate surrogates. In 2009 Zhdanko and Nenajdenko reported the development of OBO esters of isocyanoacetates.<sup>27</sup> These compounds were configurationally stable under moderately basic conditions as well as the Ugi reaction and were efficiently saponified using TFA. However, a total of five synthetic operations were required to transform a CBZ protected amino acid into its corresponding isocyanoacetate OBO ester. In 2010 Ostaszewski and co-workers used acetyl protected 2-isocyanoethanols as nonracemizable isocyanoacetate equivalents in the Ugi reaction.<sup>28</sup> The deprotected alcohols were ultimately oxidized to form aldehydes. The configurational stability of isocyanoacetates was most recently addressed in a 2010 review by Gulevich *et al*, in which it was explicitly stated that Ugi reaction conditions racemize chiral isocyanoacetates.<sup>14</sup> Despite evidence reported by Berłożecki *et al*. that non-racemizing Ugi reaction conditions do exist, it has been assumed that these reaction cannot be executed without racemization of chiral isocyanoacetates. It also

seemed that such a small number of examples did not justify a broad generalization about the utility of chiral isocyanoacetates in IMCR.

We initially sought to confirm the configurational stability of isocyanoacetates in P-3CR by reacting the isocyanoacetate derived from (*S*)-*N*-formylalanine methyl ester and Boc-proline in Passerini reactions in dichloromethane with one of three aldehydes or two ketones (Table 4.1). We specifically chose this reaction because it does not include a substrate of sufficient basicity to promote racemization of a chiral isocyanoacetate. The products were analyzed by Advanced Marfey Analysis and in all cases the observation of (*R*)-alanine was negligible indicating that no racemization of the isocyanoacetate had occurred. These results suggest that racemization of the chiral isocyanoacetates in IMCRs must be promoted by a basic substrate. With confidence in our handling of chiral isocyanoacetates as well as in the reliability of our analytical method, we proceeded to study the U-4CR and the JU-3CR.

Table 4.1 - Passerini 3 Component Condensations with a Chiral Isocyanoacetates



Entry	R <sub>1</sub> /R <sub>2</sub>	R <sub>3</sub>	Yield	Isocyanoacetate Epimerization %
1	H/Ph	CH <sub>3</sub>	56	<5.0 <sup>a</sup>
2	H/CH <sub>2</sub> CH <sub>2</sub> Ph	CH <sub>3</sub>	91	<5.0 <sup>a</sup>
3	H/ <i>i</i> Pr	CH <sub>3</sub>	88	<5.0 <sup>a</sup>
4	CH <sub>2</sub> CH <sub>2</sub> CH <sub>2</sub>	CH <sub>3</sub>	50	<5.0 <sup>a</sup>
5	CH <sub>2</sub> (CH <sub>2</sub> ) <sub>3</sub> CH <sub>2</sub>	CH <sub>3</sub>	92	<5.0 <sup>a</sup>

Reported yields are the average of two trials. Isocyanide epimerization was inferred from Marfey Analysis of products in all cases. Reactions were carried out at 2M concentration in dichloromethane. Aldehyde reactions ran for 24 hours and ketone reactions for 48 hours. All components were combined in an equimolar ratio. <sup>a</sup>In reactions with the isocyanoacetate derived from (*S*)-*N*-formylalanine methyl ester, epimerization in quantities less than 5% could not be reliably quantified.

The reported epimerization of chiral isocyanoacetates in U-4CR and JU-3CRs could be explained by two distinct base promoted mechanisms (Figure 4.7). In one mechanism, the reactants and/or intermediates promote epimerization by abstraction of a proton from the isocyanoacetate  $\alpha$ -carbon. Alternatively, epimerization could occur via the reversible formation of an oxazole intermediate.<sup>29-31</sup> Either or both of these mechanisms is feasible, but the complexities of these multicomponent reactions preclude unambiguous elucidation of the operative mechanism(s) for epimerization. Nevertheless, we assessed the influence of reagents and reaction conditions over the configurational stability of chiral isocyanoacetates.

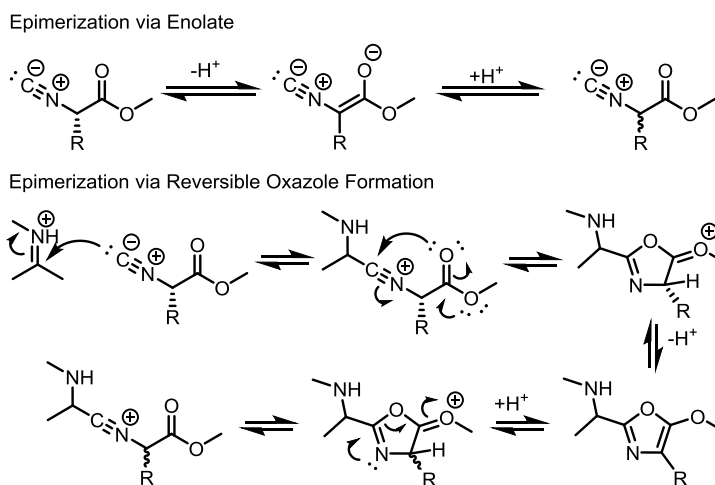


**Figure 4.7 - Hypothetical mechanisms for isocyanoacetate epimerization**

We first conducted a series of epimerization experiments wherein enantiomerically pure isocyanoacetate prepared from (*S*)-*N*-formylalanine methyl ester was incubated with substrates of the U-4CR reaction. After incubation for the indicated time, the enantiomeric purity of the isocyanide was determined by chiral GC/MS analysis (Table 4.2). While the isocyanoacetate was configurationally stable alone and in the presence of Boc-proline, it racemized quickly when incubated with benzylamine, a typical U-4CR reaction substrate. We observed that racemization was nearly instantaneous in methanol but took a few hours in dichloromethane. The relative

rates of racemization in these two solvent, which are commonly used in IMCra, is notably congruent with their polarities. In any case, our data clearly indicate that a typical amine substrate in a U-4CR reaction can promote epimerization of the isocyanoacetate.

**Table 4.2 – The Effect of U-4CR Reactants on the Stereochemical Configuration of a Chiral Isocyanoacetate**

Reactant(s)	Enantiomeric Ratio (S:R) in Methanol / Dichloromethane		
	0 hours	2 hours	20 hours
None	99:1 / 98:2	99:1 / 97:3	99:1 / 97:3
Boc-Proline	99:1 / 98:2	99:1 / 97:3	99:1 / 98:2
Benzylamine	51:49 / 93:7	52:48 / 67:36	racemic / racemic
Isobutyraldehyde + Benzylamine	99:1 / 99:1	52:48 / 99:1	racemic / 66:34
Benzaldehyde + Benzylamine	97:3 / 98:2	90:10 / 98:2	61:39 / 97:3
Cyclohexanone + Benzylamine	73:27 / 99:1	54:46 / 81:19	racemic / racemic
Boc-Proline + Benzylamine	99:1 / 99:1	79:21 / 91:9	racemic / racemic

Enantiomeric ratios were determined by chiral GC-MS. Incubations were conducted at 0.5M concentration. Samples were analyzed at the indicated time points.

We hypothesized that the capacity of the amine to promote epimerization should be attenuated in the presence of the oxo-compound and carboxylic acid substrates of the U-4CR. The oxo-compound undergoes a reversible reaction with the amine forming an imine and thus limits the availability of free amine for epimerization. The Bronstead acidity of the carboxylic acid should also attenuate the basicity of the amine. Both imine formation and protonation were in a series of experiments. First, the enantiomerically pure isocyanoacetate was incubated with benzylamine that had been allowed to react for two hours with benzaldehyde, isobutyraldehyde, or cyclohexanone. Consistent with our hypothesis, the rates of epimerization were suppressed relative to those observed in incubations with benzylamine alone. Additionally, there was a correlation between the reactivity of the oxo-compound and the relative rates of isocyanoacetate epimerization. Specifically, the addition of the ketone had a smaller effect on

the rate of epimerization than did either aldehyde (Table 4.2). Indeed, the condensation equilibria for aldimines generally lie further in favor of products than do those for ketimines.<sup>32</sup>

3225

We suspected that the carboxylic acid component should limit the availability of the basic amine species via proton transfer. Accordingly, when the enantiomerically pure isocyanoacetate was added to a solution of Boc-proline and benzylamine, the rates of epimerization were suppressed relative to those of the incubations with benzylamine alone (Table 4.2).

Since the carbonyl compound and the carboxylic acid reactants individually suppress isocyanoacetate epimerization by the amine, one would expect these reactants to synergistically suppress epimerization in an U-4CR. We assessed epimerization in U-4CRs by reacting Boc-proline, benzylamine, and enantiomerically pure isocyanoacetate derived from (*S*)-*N*-formylalanine methyl ester with five different oxo-compounds, including three aldehydes and two symmetric ketones. Moreover, Boc-proline, benzylamine, and isobutyraldehyde were reacted with three additional isocyanoacetates derived from *N*-formylamino acid esters (Table 4.3). In reactions with aldehydes and cyclobutanone, the enantiomeric ratios of the isocyanoacetate derived amino acids in the reaction products were determined by Advanced Marfey Analysis. Isocyanoacetate epimerization in the reaction with cyclohexanone was assessed by measuring the relative ratios of the two possible diastereomeric products using LC-MS. In reactions with cyclohexanone and all three aldehydes, we deduced that epimerization of all four isocyanoacetates was negligible. Additionally, the U-4CR of Boc-proline, methylamine, isobutyraldehyde and the isocyanoacetate derived from (*S*)-*N*-formylleucine methyl ester yielded the expected product in 68% yield with 4.2% epimerization of the isocyanoacetate. Unexpectedly, in the case of cyclobutanone, an appreciable amount of epimerization was observed. A possible explanation for this observation is that imine formation is not quantitative



with the strained cyclic ketone. A significant amount of free amine would therefore be available to effect isocyanoacetate epimerization.

**Table 4.3 – Ugi 4 Component Condensations with Chiral Isocyanoacetates**

Entry	R <sub>1</sub> /R <sub>2</sub>	R <sub>3</sub>	Yield	Isocyanoacetate Epimerization %
1	H/Ph	CH <sub>3</sub>	86	<5.0 <sup>a</sup>
2	H/CH <sub>2</sub> CH <sub>2</sub> Ph	CH <sub>3</sub>	58	<5.0 <sup>a</sup>
3	H/iPr	CH <sub>3</sub>	96	<5.0 <sup>a</sup>
4	H/iPr		95	2.3
5	H/iPr		98	3.7
6	H/iPr		96	3.6
7	CH <sub>2</sub> CH <sub>2</sub> CH <sub>2</sub>	CH <sub>3</sub>	81	30
8	CH <sub>2</sub> (CH <sub>2</sub> ) <sub>3</sub> CH <sub>2</sub>	CH <sub>3</sub>	90	5.6

Reported yields are the average of two trials. Isocyanide epimerization was inferred from Marfey Analysis of products in all cases except entry 8, for which epimerization was inferred from LC-MS analysis of the reaction product. Reactions were carried out at 2M concentration. Aldehyde reactions ran for 24 hours and ketone reactions for 48 hours after a 2 hour pre-condensation of benzylamine and the indicated oxo-compound. All components were combined in an equimolar ratio. <sup>a</sup>In reactions with the isocyanoacetate derived from (*S*)-*N*-formylalanine methyl ester, epimerization in quantities less than 5% could not be reliably quantified.

Since our preliminary results showed that reaction of the amine and the oxo-compound significantly affected isocyanoacetate epimerization, we systematically analyzed the effect of their pre-condensation time on the reaction outcome. With isobutyraldehyde, isocyanoacetate epimerization was minimal with a pre-condensation time of seconds and undetectable with a pre-condensation time of one hour or longer. In contrast, epimerization was significant in

reactions with cyclohexanone when the pre-condensation time was less than two hours (Table 4.4). These observations are consistent with the relative suppression of amine-promoted isocyanoacetate epimerization by aldehydes and ketones as described above (see Table 4.2). Collectively, these observations indicate in most cases the isocyanoacetates are configurationally stable in U-4CRs.

**Table 4.4 – Effect of Benzylamine-Cyclohexanone Pre-condensation Time on Isocyanoacetate Epimerization.**

Precondensation Time	0min	30min	60min	120min
Isocyanoacetate Epimerization %	9.1	6.5	6.4	5.6

Isocyanoacetate epimerization inferred from LC-MS analysis of the products. Reactions were carried out at 2M concentration for 48 hours after the indicated pre-condensation time.

In light of our studies of U-4CRs (*vide supra*), reports of chiral isocyanoacetate epimerization in the JU-3CR are especially curious as there is no basic amine substrate.<sup>23</sup> In our observations, we suspected that the apparent isocyanoacetate epimerization was a consequence of the manner in which the cyclic imine was prepared. The cyclic imine **3** was prepared by base-promoted dehydrohalogenation of *N*-chloropiperidine (**2**) and used without purification due to its instability. We proposed that residual base from the dehydrohalogenation was promoting racemization of the isocyanoacetate. We found that residual sodium ethoxide could be quenched upon completion of the dehydrohalogenation reaction by the addition of water. The cyclic imine was then extracted with diethylether. As an additional means of purification, **3** was induced to undergo a reversible trimerization yielding crystalline and easily isolated tripiperideine (**10**) (Figure 4.8).<sup>33-35</sup> JU-3CR reactions of four different chiral isocyanoacetates with Boc-proline and a molar excess of **10** (containing 1.5 equivalents of  $\Delta^1$ -piperideine) yielded the expected peptides in moderate to good yields (Table 4.5). Advanced Marfey Analyses of

these products revealed 17-28% epimerization of the isocyanoacetate substrates. In the JU-3CR with the isocyanoacetate derived from (*S*)-*N*-formyl leucine methyl ester, we found that epimerization could be reduced to 3.4% by using 1 equivalent of **3a**, in the form of tripiperideine (**10**). The reaction with this stoichiometry provided the product in only 31% yield, which compares unfavorably to the reaction with an excess of tripiperideine (Table 4.5, entry 2).

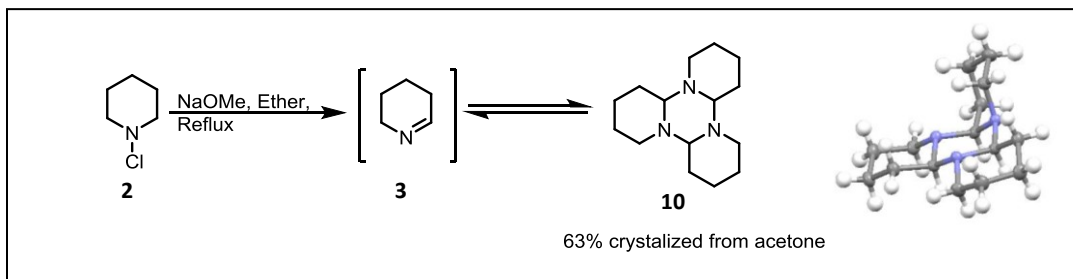


Figure 4.8 – Synthesis and crystal structure of tripiperideine

**Table 4.5 – Joullié-Ugi 3 Component Condensations with Isocyanoacetates**

Entry	R	Yield	Isocyanoacetate Epimerization %
1	CH <sub>3</sub>	70	20.3
4		54 (31)	18.4 (3.4)
5		58	16.8
6		54	28.1

Reported yields are the average of two trials. Isocyanide epimerization was inferred from Marfey Analysis. Reactions were carried out at 1M concentration for 48 hours with a .5 molar excess of  $\Delta$ 1-piperideine. The yields and epimerizations of reactions with equimolar reactants are shown in parentheses.

Discovery of a non-racemizing JU-3CR protocol was a rewarding feat; however, the low yields observed in these reactions were concerning. We pursued multiple strategies in an attempt to

boost the yields of these reactions. Heating of the reaction diminished the overall reaction yield, presumably due to degradation of either the isocyanide or cyclic imine. We also tried adding scandium (III) triflate, a Lewis acid that has been reported to catalyze U-4CR; however, addition of 10 mol % of the catalyst had little effect on the reaction yield. Ultimately we found that extension of the reaction duration to 7 days resulted in dramatically improved yields to ~70% (see chapter 5 for more detail).

Although chiral isocyanoacetates have previously been shown to be configurationally stable in the Passerini three component reactions,<sup>21</sup> they have seldom been used as substrates in U-4CRs and JU-3CRs because of concerns about their potential for racemization in the course of the reaction. Indeed, several groups have used elaborate protecting groups and cumbersome reaction conditions to avoid isocyanoacetate epimerization.<sup>26-28</sup> Our observations suggest that these strategies may only be necessary in select cases. We have shown that isocyanoacetate epimerization does not take place in canonical U-4CR with aldehydes and can be significantly suppressed in those with ketone substrates by increasing the pre-condensation time. Further, we have discovered a procedure for racemization-free JU-3CR with chiral isocyanoacetates and  $\Delta^1$ -piperidine (**3**). These findings should prompt reconsideration of multicomponent reactions for the diversity- and target-oriented synthesis of structurally complex peptides as alternatives to the classical synthetic methods that are labor-intensive and require expensive coupling reagents. Importantly, these studies validate our strategy of using the JU-3CR to construct peptidate containing tripeptides for ADEP synthesis.

### Experimental Contributions

Synthesis and analysis of all compounds was performed by Daniel Carney with the assistance of Brown University undergraduate student, Jonathan Truong '12. X-ray crystallographic analysis was performed by Prof. Paul G. Williard.

## Experimental Procedures

**General:** All commercially available reagents were used without further purification. All reactions were conducted in oven dried glassware, under ambient atmosphere, using dry solvents unless otherwise stated. All spectra were referenced to residual solvent signals in CDCl<sub>3</sub> (7.27 ppm for <sup>1</sup>H, 77.0 ppm for <sup>13</sup>C).

***Direct Measurement of Chiral Isocyanoacetate Epimerization.*** As described in Table 1, the capacity of substrates of the Ugi four component reaction to promote epimerization of a chiral isocyanoacetate was assessed. 100μL aliquots of 1 M stock solutions of the enantiomerically pure isocyanoacetate derived from (*S*)-*N*-formylalanine in either methanol or dichloromethane were treated with substrates of the Ugi four component reaction. Negative control experiments in which the isocyanoacetate solution was not treated with any substrate were carried out in parallel. Epimerization of the isocyanoacetate was assessed by chiral gas chromatography- mass spectrometry analysis. At the indicated time points, 3μL samples were removed from the isocyanoacetate solutions and dissolved in 1 mL of dichloromethane. From the resulting solution, splitless injections of 1 μL were made onto a Varian CP Chirasil-DEX 25 m x 0.32 mm column with an inlet temperature of 150°C and a detector temperature of 220°C. Initial column temperature of 50°C was held for 4 min., followed by a 12°C/min. ramp to 150°C then holding for 2 min. Enantiomeric ratios were determined by integration of the total ion chromatogram.

### ***Indirect Measurement of Chiral Isocyanoacetate Epimerization (Advanced Marfey Analysis)***

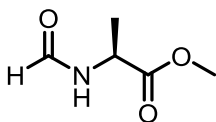
As described in Tables 2-4, epimerization was inferred from either measurement of the enantiomeric ratio of the isocyanoacetate-derived amino acid in the U-4CR product or of the diastereomeric ratios of the products. The enantiomeric ratios of the isocyanoacetate-derived amino acids in the U-4CR products were determined by Advanced Marfey Analysis. According to

the published procedure,<sup>14</sup> the multicomponent reaction products were hydrolyzed under acidic conditions and the resulting amino acids were reacted with 1-fluoro-2,4-dinitrophenyl-5-L-alanine amide (L-FDAA). 5 mg of the product to be analyzed was dissolved in 0.5 ml of 6M HCl in a 2 dram glass vial. The solution was heated on a hot plate and vortexed occasionally until all the material dissolved. It was then transferred to a long-stemmed ampoule, flame-sealed, and heated at 110° C overnight. The hydrolyzed amino acid solution was transferred to a 2 dram glass vial where the water was removed by heating to 40° C and flushing with a stream of nitrogen gas. The MCR product hydrolysate was dissolved in 0.5 ml of H<sub>2</sub>O. 50 µl of this hydrolyzed amino acid solution was transferred to a 1 dram glass vial and charged with 20 µl of 1M NaHCO<sub>3</sub> and 50 µl of 0.03M L-FDAA dissolved in acetone. The vial was placed in a 37°C incubator for 45 min during which time the solution turned orange in color. Finally, 20µl of 1M HCl was added to quench the reaction. The quenched solutions of the derivatized amino acids were diluted four-fold with methanol. 3 µl samples were separated on a Higgins Analytical-Hasil C18 column (100 mmx1.8mm) using a binary mobile phase: A = H<sub>2</sub>O/0.1% formic acid and B = acetonitrile. Solvent gradient: 20-60% B over 20 minutes at .250mL/min, UV Detection: 350nm, negative ion mode used for mass detection. Epimerization was quantified directly by integration of the Marfey Analysis UV chromatograms. As determined in limits of detection experiments, the ratio of derivatized (*R*) and (*S*)- alanine could not be measured in quantities less than 5%.

Alternatively, isocyanoacetate epimerization in reactions with symmetric ketones (*e.g.*, cyclohexanone) was assessed by measuring the relative ratios of the two possible diastereomeric U-4CR products using LC-MS. After flash chromatography, the MCR products were dissolved in methanol to a concentration of 1 mg/mL. 3 µl samples were separated on a Higgins Analytical-Hasil C18 column (100mmx1.8mm). The compounds were separated using a binary mobile phase: A = H<sub>2</sub>O/0.1% formic acid and B = acetonitrile. Solvent gradient: 20-60% B

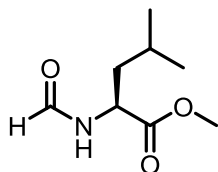
over 20 minutes at .250 mL/min, UV Detection: 214 nm, positive ion mode used for mass detection.

**General Amino Acid Ester Formylation Procedure.** Dicyclohexylcarbodiimide (DCC) (6.5 mmol, 1.34g) was dissolved in dichloromethane (DCM) (20 mL) and cooled to 0°C. To this solution, 98% formic acid (6.5 mmol, 0.25 mL) was added and allowed to stir for 10 minutes, over the course of which a white precipitate formed. The amino acid methyl ester hydrochloride (5 mmol, 0.908 g) and dimethylaminopyridine (DMAP) (1.0 mmol, 123 mg) were added directly to the solution of the *O*-formylisourea. 5 mL of DCM was used to rinse residual reagent from the neck of the flask into the reaction. Finally, *N*-methyl morpholine (NMM) (8 mmol, 0.88 mL) was added and the reaction was allowed to stir for 16 hours. Upon completion, the reaction was concentrated *in vacuo* to near dryness then suspended with cold ethyl acetate and filtered through a short silica gel column (0.5"x1"). The filtrate was concentrated *in vacuo* and the residue was applied directly to a silica gel column (5"x2" column). The *N*-formylamino acid methyl ester product was eluted using a Ethyl acetate:Hexanes mobile phase. Often times, the product was contaminated with dicyclohexyl urea (DCU) after flash chromatography. To remove this impurity, the concentrated residue was dissolved in ethyl acetate (0.5-1 mL) and stored at -20°C overnight during which time the contaminating DCU precipitated. The precipitate was filtered and washed with -20°C ethyl acetate. The filtrate was concentrated to a colorless oil.

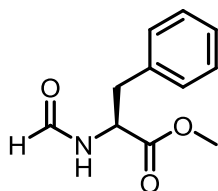


**(S)-*N*-formylalanine methyl ester.** Yield 1.162 g (89%). <sup>1</sup>H-NMR (400 MHz, CDCl<sub>3</sub>) δ 8.20 (1 H, s), 6.20 (1 H, broad s), 4.71 (1H, dt, *J*=7.2 Hz, 7.2 Hz), 3.78 (3H, s), 1.46 (3 H, d, *J*=7.2 Hz); <sup>13</sup>C-NMR

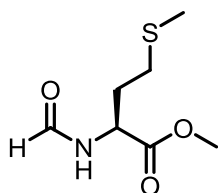
(100 MHz, CDCl<sub>3</sub>) δ 173.1, 160.4, 52.6, 46.8, 18.5. HRMS (FAB) calcd for [C<sub>5</sub>H<sub>9</sub>NO<sub>3</sub>+Na]<sup>+</sup> 154.0480, found 154.0483



**(S)-N-formylleucine methyl ester.** Yield 801 mg (82%). <sup>1</sup>H-NMR (400 MHz, CDCl<sub>3</sub>) δ 8.22 (1 H, s), 6.01 (1 H, Broad s), 4.76 (1 H, td, *J*=8.8, 3.5 Hz), 3.76 (3 H, s), 1.68 (2 H, m), 1.59 (1 H, m), 0.97(3 H, d, *J*=6.1 Hz), 0.95 (3 H, d, *J*=6.1 Hz); <sup>13</sup>C-NMR (100 MHz, CDCl<sub>3</sub>) δ 173.1, 180.6, 52.5, 49.3, 41.7, 24.8, 22.9, 21.9 HRMS (FAB) [M+Na]<sup>+</sup> calcd for [C<sub>8</sub>H<sub>15</sub>NO<sub>3</sub> + Na]<sup>+</sup> 196.0950, found 196.0955



**(S)-N-formylphenylalanine methyl ester.** Yield: 869 mg (84%). <sup>1</sup>H-NMR (400 MHz, CDCl<sub>3</sub>) δ 8.19 (1 H, s), 7.28 (3 H, m), 7.11 (2 H, dd, *J*=7.9 1.0 Hz), 6.05 (1 H, broad s), 4.99 (1 H, dt, *J*=7.9, 6.10 Hz) 3.76 (3 H, s) 3.18 (1 H, d, *J*=5.3 Hz), 3.16 (1H, d, *J*= 5.3Hz); <sup>13</sup>C-NMR (100 MHz, CDCl<sub>3</sub>) δ 171.5, 180.4, 129.3, 128.9, 127.3, 52.5, 51.8, 37.7; HRMS (FAB) calcd for [C<sub>11</sub>H<sub>13</sub>NO<sub>3</sub> + Na]<sup>+</sup> 230.0793, found 230.0785

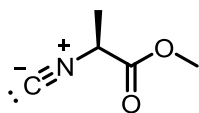


**(S)-N-formylmethionine methyl ester.** Yield 939mg (98%). <sup>1</sup>H-NMR (400 MHz, CDCl<sub>3</sub>) δ 8.25 (1 H, s), 6.35 (1 H d, *J*=5.3 Hz), 4.82 (1 H, td, *J*=7.85.3 Hz), 3.79 (1 H, s) 2.53 (2H, t, *J*=7.10 Hz), 2.21, (1

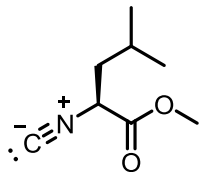


H, m), 2.10 (1 H, s), 2.04 (1 H, m); <sup>13</sup>C-NMR (100 MHz, CDCl<sub>3</sub>) δ 172.0, 160.7, 52.8, 50.2, 31.6, 29.8, 15.5 HRMS (FAB) calcd for [C<sub>7</sub>H<sub>13</sub>NO<sub>3</sub>S + Na]<sup>+</sup> 214.0514, found 214.0508

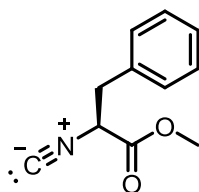
**General Procedure for *N*-formylamino Acid Ester Dehydration.** The *N*-formylamino acid ester was dissolved in dry DCM (20 mL) under nitrogen and cooled to -78°C. Triphosgene (0.35 equivalents) was dissolved separately in dry DCM (5 mL). The triphosgene solution was added dropwise to the cold *N*-formylamino acid ester solution. After stirring for 5 minutes, neat NMM (2 equivalents) was added slowly over the course of 10 minutes. With all reagents added, the reaction was stirred at -78°C for 2 hours and quenched by the addition of water (10 mL). The heterogeneous mixture was allowed to warm until all of the ice had melted and the two phases were partitioned. The aqueous phase was extracted with an additional 20 mL DCM, which was pooled and dried over magnesium sulfate. The dried solution was then filtered through a short silica gel column (1.5"x1") and concentrated *in vacuo*.



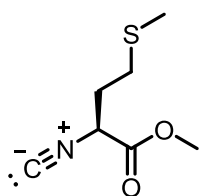
**Isocyanacetate derived from (*S*)-*N*-formylalanine methyl ester.** Yield: 723.9 mg (71.2%). <sup>1</sup>H-NMR (400 MHz, CDCl<sub>3</sub>) δ 4.35 (1 H, quart, *J*=7.3 Hz), 3.84 (3 H, s), 1.67 (3 H, d, *J*=7.3 Hz); <sup>13</sup>C-NMR (100 MHz, CDCl<sub>3</sub>) δ 167.6, 159.5, 53.4, 51.6, 19.4. LRMS (EI) [M]<sup>+</sup> 113, [M-45]<sup>+</sup> 68, [M-54]<sup>+</sup> 59, [M-59]<sup>+</sup> 54.



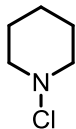
**Isocyanoacetate derived from (S)-N-formylleucine methyl ester.** Yield: 506 mg (80%). <sup>1</sup>H-NMR (400 MHz, CDCl<sub>3</sub>) δ 4.29 (1 H, dd, *J*=10.1, 4.8 Hz), 3.83 (3 H, s), 1.87 (2 H, m), 1.70 (1 H, m), 0.99 (6 H, t, *J*=6.6 Hz); <sup>13</sup>C-NMR (100 MHz, CDCl<sub>3</sub>); δ 167.7, 160.1, 55.1, 53.3, 41.3, 24.8, 22.6, 20.9. LRMS (EI) [M-15]<sup>+</sup>140, [M-43]<sup>+</sup> 112, [M-59]<sup>+</sup> 96, [M-87]<sup>+</sup> 68, [M-100]<sup>+</sup> 55.



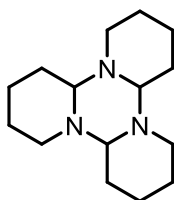
**Isocyanoacetate derived from (S)-N-formylphenylalanine methyl ester.** Yield 596mg (80%). <sup>1</sup>H-NMR(400 MHz, CDCl<sub>3</sub>) δ 7.34 (3 H, m), 7.27 (2H, m), 4.48 (2 H, dd, *J*=8.28, 4.88 Hz), 3.82 (3 H, s), 3.28 (1 H, dd, *J*=14.03, 4.82 Hz) 3.15 (1 H, dd, *J*=13.81, 8.33 Hz); <sup>13</sup>C-NMR (100 MHz, CDCl<sub>3</sub>) δ 166.6, 160.9, 134.3, 129.3, 128.89, 127.9, 58.0, 53.4, 38.9. LRMS (EI) [M-32]<sup>+</sup> 157, [M-59]<sup>+</sup> 130, [M-98]<sup>+</sup> 91



**Isocyanoacetate derived from (S)-N-formylmethionine methyl ester.** Yield: 563 mg (81%). <sup>1</sup>H-NMR(400 MHz, CDCl<sub>3</sub>) δ 4.57 (1 H, dd, *J*=7.89, 6.14 Hz) 3.85 (3 H, s) 2.60 - 2.81 (2 H, m) 2.21 (2 H, dd, *J*=14.03, 7.00 Hz) 2.12 (3 H, s); <sup>13</sup>C-NMR (100 MHz, CDCl<sub>3</sub>) δ 167.0, 160.7, 54.8, 53.5, 31.8, 26.6, 15.4. LRMS (EI) [M]<sup>+</sup> 173, [M-59]<sup>+</sup> 114, [M-86]<sup>+</sup> 87, [M-99]<sup>+</sup> 74, [M-112]<sup>+</sup> 61.

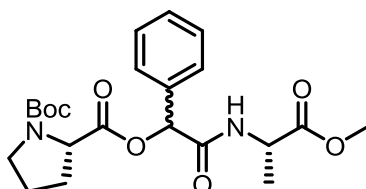


**N-chloropiperidine (2).** Piperidine (5.8 mmol, 1.39 mL), and *tert*-butanol (5.8, 0.55 mL) were added to methyl *tert*-butyl ether (MTBE) (30 mL) and cooled to 0°C. Acetic acid (11.8 mmol, 0.68 mL) and commercial grade cleaning bleach (11.8 mmol, 23.5 mL) were added simultaneously with stirring. The reaction was stirred for 30 minutes after which water (15 mL) was added. The phases were partitioned and the organic phase washed with brine (15 mL). The organic material was dried over magnesium sulfate then concentrated. Yield 1.17 g (84.0%). <sup>1</sup>H-NMR (400 MHz, CDCl<sub>3</sub>) δ 3.14 (4 H, s broad), 1.72 (4 H, quint, *J*=5.7 Hz), 1.46 (2 H, s broad); <sup>13</sup>C-NMR (100 MHz, CDCl<sub>3</sub>) δ 63.9, 27.6, 22.9 LRMS (EI) [M]<sup>+</sup> 119.3

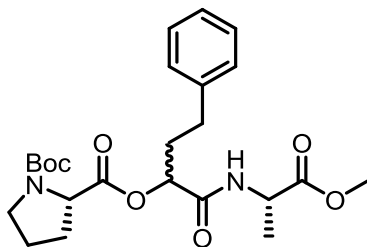


**Tripiperideine (10).** *N*-chloropiperidine (0.915 g, 7.65 mmol) was dissolved in diethylether (5 mL). To this solution, 25% sodium methoxide in methanol (2.28 mL, 9.95 mmol) was added. The reaction was refluxed for 45 minutes, over the course of which a white precipitate formed. The reaction was allowed to cool to room temperature after which water (7 mL) added resulting in solvation of the white precipitate. The phases were partitioned and the aqueous phase was washed with diethylether (4x10 mL). All of the organic phases were pooled and dried over MgSO<sub>4</sub>. The ether layers was then filtered and concentrated yielding a pale, yellow oil. The oil was dissolved in a minimum volume of acetone from which crystals began to form at 0°C. Either a seed crystal or scratching the inside of the flask with a glass stirring rod was required to induce crystallization. Once crystals were visible at 0°C the solution was stored at -20°C for 2-3 days

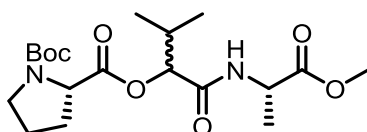
after which the large white tri-piperidine crystals were filtered and washed with -20°C acetone. Yield: 0.4086 g (64%). <sup>1</sup>H-NMR (400 MHz, CDCl<sub>3</sub>) δ 3.13 (3 H dt, *J*=10.64, 5.04 Hz), 2.80 (3 H, dd, *J*=6.8, 1.9 Hz), 2.02 (3 H dt, *J*=11.2, 5.9 Hz) 1.72 (9 H, m), 1.57 (6 H, m), 1.31 (3 H, m); <sup>13</sup>C-NMR (100 MHz, CDCl<sub>3</sub>) δ 81.9, 46.4, 29.2, 25.8, 22.3.



**Passerini product derived from reaction of Boc-proline, isocyanide derived from (S)-N-formylalanine methyl ester, and benzaldehyde (Table 4.1, Entry 1). Mixture of diastereomers and rotamers.** Yield: 130mg(56%). <sup>1</sup>H-NMR (400 MHz, CDCl<sub>3</sub>) δ 8.03, 7.60, 6.79, 6.77, (2 H, 4 doublets, *J*=7.7 Hz), 7.32-7.53 (10 H, m), 6.17, 6.13, 6.08 (2 H, 3 singlets), 4.45-4.68 (3H, m), 4.28-4.42 (1H, m), 3.76, 3.73, 3.72 (6H, 3 singlets), 3.35-3.67 (4H, m), 2.10-2.41 (3H, m), 1.78-2.04 (5H, m), 1.41-1.56 (20 H, m), 1.32 (2H, s), 1.23 (2H, s); <sup>13</sup>C-NMR (100 MHz, CDCl<sub>3</sub>) δ 173.0, 172.8, 172.2, 170.8, 168.7, 168.2, 155.4, 154.6, 135.5, 134.9, 130.1, 128.9, 128.8, 128.8, 128.6, 128.6, 128.1, 127.7, 127.0, 80.4, 80.2, 80.1, 77.3, 76.1, 75.5, 59.2, 59.0, 52.7, 52.3, 48.2, 48.1, 46.9, 46.8, 30.7, 30.0, 29.9, 28.5, 28.4, 28.1, 24.7, 24.4, 17.6, 17.3. HRMS (FAB) calcd for [C<sub>22</sub>H<sub>30</sub>N<sub>2</sub>O<sub>7</sub> + Na]<sup>+</sup> 457.1951, found 457.1930

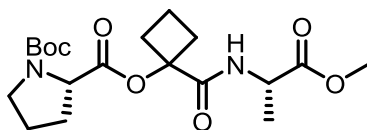


**Passerini product derived from reaction of Boc-proline, isocyanoacetate derived from (*S*)-*N*-formylalanine methyl ester, and hydrocinnamaldehyde (Table 4.1, Entry 2). Mixture of diastereomers and rotamers. Yield: 221mg (91%).<sup>1</sup>H-NMR(400 MHz, CDCl<sub>3</sub>) δ 7.75, 7.43, 6.68 6.56 (2H, 4 doublets, *J*=7.50 Hz), 7.13 - 7.23 (10 H, m), 5.29 (1 H, dd, *J*=7.80, 4.10 Hz), 5.20 (1 H, dd, *J*=7.76, 4.30 Hz), 4.52-4.63 (2 H, m), 4.48, 4.39 (1 H, 2 doublet of doublets, *J*=8.50, 4.10 Hz), 4.28 (1 H, dd, *J*=8.20, 5.70 Hz), 3.77, 3.74, 3.72 (6H, 3 singlets), 3.39 - 3.65 (4 H, m), 2.71 (8 H, m), 2.04 - 2.39 (4 H, m), 1.83 - 2.04 (4 H, m), 1.38- 1.55 (24 H, m);<sup>13</sup>C-NMR (100 MHz, CDCl<sub>3</sub>) δ 173.0, 172.8, 171.3, 169.7, 169.4, 155.3, 140.7, 128.5, 128.4, 128.4, 126.1, 126.0, 80.3, 80.2, 73.9, 73.2, 59.1, 59.0, 52.3, 52.2, 48.1, 48.0, 46.8, 46.8, 33.5, 33.1, 31.1, 31.1, 30.1, 30.0, 28.4, 28.3, 24.9, 24.5, 17.4. HRMS (FAB) calcd for [C<sub>24</sub>H<sub>34</sub>N<sub>2</sub>O<sub>7</sub> + Na]<sup>+</sup> 485.2264, found 485.2288**

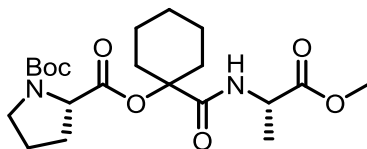


**Passerini product derived from Boc-Proline, isocyanoacetate derived from (*S*)-*N*-formylalanine methyl ester, and isobutyraldehyde (Table 4.1, Entry 3). Mixture of diastereomers and rotamers. Yield 186 mg (88%).<sup>1</sup>H-NMR (400 MHz, CDCl<sub>3</sub>) δ 7.86, 7.31, 6.55, 6.57 (2 H, 4 doublets, *J*=7.02 Hz), 5.16 (1H, d, *J*=3.5 Hz), 5.01, 5.07 (1H, 2 doublets, *J*= 2.6, 4.4 Hz), 4.49-4.64 (2 H, m), 4.34- 4.49 (1 H, m), 4.30 (1 H, dd, *J*=7.8, 5.3 Hz), 3.75, 3.71, 3.70 (6H, 3 singlets), 3.37-3.8 (4H, m), 1.72 - 2.64 (10 H, m) 1.21- 1.47 (24 H, m) 0.80 - 1.01 (12 H, m);<sup>13</sup>C-NMR (100 MHz, CDCl<sub>3</sub>) δ 173.1, 172.7, 171.4, 169.4, 169.3, 80.29, 80.17, 78.4, 77.6, 59.2, 59.0, 52.2, 48.1 48.0 46.8, 46.7,**

30.2, 30.1, 30.0, 28.5, 28.3, 24.9, 24.4, 19.2, 18.9, 17.3, 17.2, 16.3, 16.0. HRMS (FAB) calcd for  $[C_{19}H_{32}N_2O_7 + Na]^+$  423.2107, found 423.2125.

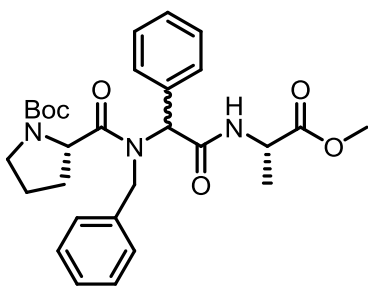


**Passerini product derived from Boc-proline, isocyanoacetate derived from (S)-N-formylalanine methyl ester, and butylamine (Table 4.1, Entry 4). Mixture of rotamers.** Yield: 105mg (50%).  $^1H$ -NMR (400 MHz,  $CDCl_3$ )  $\delta$  7.27, 6.37 (1 H, 2 doublets,  $J=5.6$  Hz), 4.53 (1H, dt,  $J= 7.3$  Hz, 7.3 Hz), 4.28 (1H dd,  $J= 8.3, 4.6$ ), 3.75, 3.72 (3 H, 2 singlets), 3.37-3.61 (2H, m), 2.73-2.85 (1H, m), 2.62-2.73 (1H, m), 2.17-2.43 (3H, m), 1.83-2.13 (5 H, m), 1.44 (9 H, s), 1.42 (3H, d,  $J= 7.3$  Hz);  $^{13}C$ -NMR (100 MHz,  $CDCl_3$ )  $\delta$  173.1, 171.4, 171.3, 155.0, 80.9, 80.2, 59.0, 52.2, 48.2, 46.8, 32.4, 29.9, 28.4, 24.6, 17.3, 14.7 HRMS (FAB) calcd for  $[C_{19}H_{30}N_2O_7 + Na]^+$  421.1951, found 421.1945



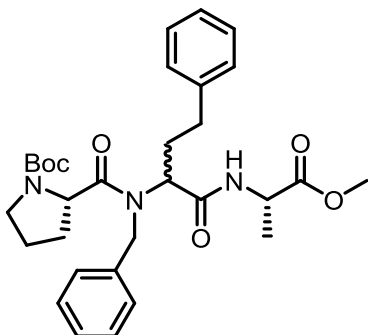
**Passerini product derived from Boc-proline, isocyanoacetate derived from (S)-N-formylalanine methyl ester, and cyclohexanone (Table 4.1, Entry 5). Mixture of rotamers.** Yield: 207mg (92%).  $^1H$ -NMR (400 MHz,  $CDCl_3$ )  $\delta$  7.63, 7.38, 6.30 (1 H, 3d,  $J=7.30$  Hz), 4.51 (1 H, dt,  $J=7.3$  Hz, 7.3 Hz), 4.31, 4.24 (1H, 2 doublets of doublets,  $J=8.30, 4.50$  Hz), 3.72 (3 H, s), 3.38- 3.60 (2 H, m), 2.17 - 2.42 (2 H, m), 1.77- 2.14 (6 H, m), 1.65 (4 H, m), 1.19 - 1.57 (14 H, m);  $^{13}C$ -NMR (100 MHz,  $CDCl_3$ )  $\delta$  174.7, 173.7, 173.3, 154.7, 138.6, 128.8, 127.3, 126.2, 126.1, 125.8, 79.6, 77.2, 66.1, 56.7, 52.1, 49.5, 48.5, 47.3, 30.6, 28.6, 28.5, 28.4, 24.6, 17.5, 15.0. HRMS (FAB) calcd for  $[C_{21}H_{34}N_2O_7 + Na]^+$  449.2264, found 449.2278

**Ugi Reaction General Procedure.** To a 1 dram glass vial containing the prescribed volume of methanol, oxo-compound (.5 mmol) and benzylamine (.5mmol, 54.6 $\mu$ L) were added. After a pre-condensation time of 0-2 hours, Boc-Proline (.5 mmol, 107.6 mg) and the isocyanoacetate (.52mmol) were added. With all reactants added the solution was allowed to stir for either 24 hours in reactions with aldehydes or 48 hours in reactions with ketones. The reactions were concentrated *in vacuo* and subsequently dissolved in 1:1 hexanes:ethyl acetate. The solution was then applied to a silica gel column (4"x.75"). Unreacted isocyanide was eluted with 3:1 hexanes:ethyl acetate and the product with 1:1-1:2hexane:ethyl acetate.



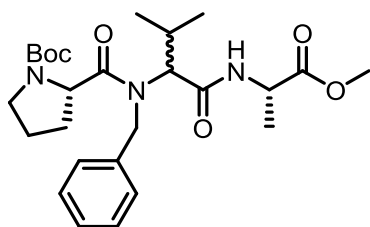
Ugi product derived from Boc-proline, benzylamine, isocyanoacetate derived from (*S*)-*N*-formylalanine methyl ester, and benzaldehyde (Table 4.3, Entry 1). Mixture of diastereomers and rotamers. Yield: 234 mg (86%).  $^1\text{H-NMR}$  (400 MHz,  $\text{CDCl}_3$ )  $\delta$  8.11, 7.69, 6.36, 6.10 (2 H, 4 doublets,  $J=7.0$  Hz) 6.95-7.56 (20 H, m), 6.68 (1H, m), 6.57 (1 H, s), 6.27, 6.16, 5.96, (1 H, 3 singlets), 1.29, 5.24, 5.21, 5.14 (1H, 4xs), 4.35-4.78 (4.5H, m), 4.18-4.30 (1H, m) 3.96-4.10 (.5 H m), 3.80, 3.74, 3.73, 3.69 (6 H, 4 singlets) 3.56-3.67(1 H, m), 3.21-3.56 (3 H, m), 1.99-2.40 (2 H, m), 1.59-1.99 (4 H, m) 1.33-1.58 (23 H, m) 1.25 (1.5 H, 2), 0.95, (1.5 H, d,  $J=7.3$  Hz);  $^{13}\text{C-NMR}$  (100 MHz,  $\text{CDCl}_3$ )  $\delta$  175.1, 174.9, 174.7, 173.6, 173.2, 173.0, 169.2, 167.7, 154.7, 138.0, 137.8, 135.5, 135.3, 130.6, 130.4, 129.8, 129.6, 129.4, 129.0, 128.8, 128.7, 128.6, 128.3, 128.2, 127.9, 127.8, 127.1, 126.9, 126.7, 126.7, 126.6, 126.3, 80.3, 79.9, 77.2, 63.3, 62.3, 56.5, 54.8, 52.4, 52.2, 52.1,

50.1, 48.6, 48.4, 47.4, 47.2, 30.6, 29.8, 28.6, 28.5, 28.4, 28.4, 25.1, 24.8, 17.3. HRMS (FAB) calcd for  $[C_{29}H_{37}N_3O_6+Na]^+$  546.2580, found 546.2588

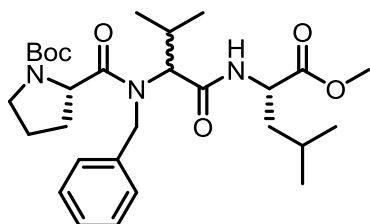


Ugi product derived from Boc-proline, benzylamine, isocyanoacetate derived from (*S*)-*N*-formylalanine methyl ester, and hydrocinnamaldehyde (Table 4.3 Entry 2). Mixture of diastereomers and rotamers. Yield: 167 mg (58%).  $^1H$ -NMR (400 MHz,  $CDCl_3$ )  $\delta$  8.27, 6.70 (1 H, 2 doublets,  $J = 6.1$  Hz), 7.77, 6.80 (1 H 2 doublets,  $J = 7.3$  Hz, 1 H), 7.07-7.40 (20H, m), 7.03 (2H, d,  $J=7.0$  Hz), 5.45 (0.5 H, dd,  $J=7.9, 5.0$  Hz), 5.20, 5.15 (1 H, 2 singlets), 4.74-4.83 (.5 H, m), 4.47-4.73 (3 H, m), 4.46, 4.42, 4.38 (1.5 H, 3 singlets), 4.28 (1 H, t,  $J=7.1$  Hz), 3.95 (.5 H, dd,  $J=7.3, 6.3$  Hz), 3.67 (3 H, s), 3.70 (3 H, s) 3.56-3.64 (1 H, m), 3.34-3.55 (3 H, m), 2.66-2.95 (2 H, m), 2.39-2.64, (3 H, m), 2.11-2.29 (1 H, m), 1.71-2.03, (6 H, m) 1.52-1.71 (2 H, m), 1.49 (2 H, d,  $J=7.4$  Hz), 1.29-1.47 (20 H, m), 1.27 (2 H, s), 1.14 (2H, d,  $J=7.4$  Hz) 1.34, 1.14 (6 H, 3 doublets,  $J=7.3$  Hz);  $^{13}C$ -NMR (100 MHz,  $CDCl_3$ )  $\delta$  175.8, 174.3, 173.5, 173.4, 170.5, 168.9, 154.6, 154.5, 145.7, 141.6, 140.7, 138.3, 138.2, 130.6, 128.7, 128.5, 128.4, 128.4, 128.3, 128.3, 128.0, 127.5, 126.9, 126.5, 126.1, 125.8, 83.6, 80.2, 79.9, 77.2, 62.2, 59.3, 58.0, 56.4, 55.0, 52.1, 50.3, 48.5, 48.5, 47.4, 47.0, 46.1, 33.3, 32.4, 30.6, 30.4, 30.3, 30.2, 28.6, 28.4, 28.3, 25.0, 24.8, 17.2, 16.5. HRMS (FAB) calcd for  $[C_{31}H_{41}N_3O_6 + Na]^+$  574.2893, found 574.2876



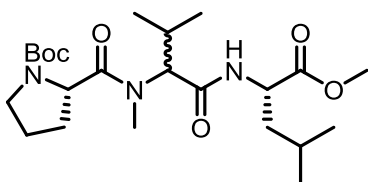


Ugi product derived from Boc-proline, benzylamine, isocyanoacetate derived from (*S*)-*N*-formylalanine methyl ester, and isobutyraldehyde (Table 4.3, Entry 3). Mixture of diastereomers and rotamers. Yield: 246 mg (96%). <sup>1</sup>H-NMR (CDCl<sub>3</sub>, 400 MHz) δ 8.19 (1 H, d, *J*=5.3 Hz) 7.80 (1 H, d, *J*=5.3 Hz) 7.09-7.42 (10 H, m), 4.79-5.03 (2 H, m) 4.25-4.60 (4 H, m), 4.13, 4.08 (1H, 2 singlets), 3.74, 3.72, 3.65 (6 H, singlets) 3.58-3.75 (1 H, m) 3.43-3.57 (2 H, m), 3.30-3.43 (1 H, m), 2.43-2.67 (1 H, m), 2.24-2.43 (1 H, m), 2.02-2.21 (2 H, m), 1.79-1.99 (2 H, m), 1.54-1.78 (2 H, m), 1.22-1.53 (21 H, m), 0.69-1.08 (17 H, m); <sup>13</sup>C-NMR (100 MHz, CDCl<sub>3</sub>) δ 176.1, 174.8, 173.4, 173.1, 170.3, 168.0, 154.6, 154.5, 137.9, 137.3, 128.6, 128.2, 127.7, 127.5, 127.4, 126.6, 80.3, 79.7, 77.5, 77.2, 77.0, 76.6, 65.8, 57.0, 54.5, 52.1, 52.0, 48.3, 48.1, 47.3, 47.3, 46.0, 30.7, 30.2, 28.6, 28.4, 28.3, 28.1, 26.4, 25.1, 24.5, 20.2, 19.9, 19.5, 19.1, 17.6, 16.7 HRMS (FAB) calcd for [C<sub>26</sub>H<sub>39</sub>N<sub>3</sub>O<sub>6</sub> + Na]<sup>+</sup> 512.2737, found 512.2752



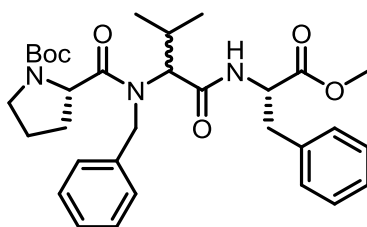
Ugi product derived from Boc-proline, benzylamine, isocyanoacetate derived from (*S*)-*N*-formylleucine methyl ester, and isobutyraldehyde (Table 4.3, Entry 4). Mixture of diastereomers and rotamers. Yield: 263 mg (95%). <sup>1</sup>H-NMR (CDCl<sub>3</sub>, 400 MHz) δ 8.15 (1H, 2 doublets, *J*=5.6 Hz), 7.86 (1 H, br s), 7.15-7.43 (10 H, m), 4.58-5.12 (1 H, m), 4.60-4.73 (1 H, m), 4.45-4.60 (3 H, m), 4.41, 4.38, 4.37, 4.33 (2 H, 4 singlets), 3.79-3.89 (1 H, m), 3.73, 3.72, 3.71, 4.67 (6 H, 4 singlets),

3.69-3.74 (.5 H, m), 3.58-3.69 (.5 H, m) 3.45-3.60 (2 H, m), 3.35-3.45 (1 H, m), 2.66-2.92 (1 H, m), 2.27-2.55 (1 H, m), 2.04-2.19 (2 H, m), 1.82-2.04 (2 H, m), 1.82-2.04 (2 H, m), 1.52-1.81 (7 H, m), 1.51, 1.49, 1.46, 1.44 (18 H 4 singlets), 1.12-1.35 (3 H, m) 0.88-1.03, (16 H, m), 0.73-0.87 (8 H, m);  $^{13}\text{C-NMR}$  (100 MHz,  $\text{CDCl}_3$ )  $\delta$  176.0, 174.8, 173.3, 173.0, 172.7, 170.8, 168.2, 154.6, 154.3, 138.0, 137.0, 128.6, 128.3, 127.8, 127.6, 127.5, 126.7, 108.4, 80.2, 79.6, 77.4, 76.6, 66.1, 63.8, 57.2, 54.5, 52.0, 51.8, 51.4, 50.6, 47.3, 47.1, 46.1, 40.6, 40.4, 31.3, 30.8, 29.9, 28.6, 28.4, 28.3, 27.9, 27.6, 26.7, 25.0, 24.8, 24.6, 24.3, 22.9, 22.8, 21.9, 21.4, 20.2, 19.8, 19.4, 19.1. HRMS (FAB) calcd for  $[\text{C}_{29}\text{H}_{45}\text{N}_3\text{O}_6 + \text{Na}]^+$  554.3206, found 554.3220

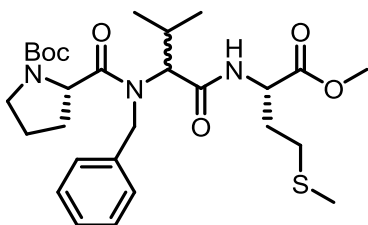


**Ugi product derived from Boc-proline, methylamine, isocynoacetate derived from (*S*)-*N*-formylleucine methyl ester, and isobutyraldehyde. Mixture of diastereomers and rotamers.**

Yield: 155 mg (68%).  $^1\text{H-NMR}$  ( $\text{CDCl}_3$ , 400 MHz) 8.38, 6.97, 6.57, 6.31 (2 H, 4 doublets,  $J=7.9$  Hz), 4.75-4.81 (1 H, m), 4.42-4.76 (4 H, m), 4.29 (1 H, d,  $J=10.7$  Hz), 3.71, 3.70 (6 H, 2 singlets) 4.42-4.76 (4 H, m), 3.04, 3.00, 2.98, 2.74 (6 H, 4 singlets), 2.10-2.46, (4 H, m), 2.00-2.10 (2 H, m), 1.79-1.99 (4 H, m), 1.54-1.74 (6 H, m), 1.44, 1.43, 1.40, 1.37 (18 H, 4 singlets), 1.00-1.09 (4 H, m), 0.86-0.97 (15 H, m) 0.77-0.84 (5 H, m).  $^{13}\text{C-NMR}$  (100 MHz,  $\text{CDCl}_3$ )  $\delta$  173.9, 173.4, 173.3, 170.5, 169.7, 168.8, 154.6, 154.5, 80.2, 79.6, 79.5, 77.2, 66.1, 56.2, 54.2, 52.0, 51.9, 51.0, 50.9, 50.3, 47.3, 47.0, 40.3, 40.2, 30.9, 29.4, 29.0, 28.4, 28.2, 26.1, 26.0, 24.9, 24.7, 24.6, 24.6, 22.8, 22.8, 22.6, 21.8, 21.4, 20.7, 20.4, 19.0, 18.5. HRMS (FAB) calcd for  $[\text{C}_{23}\text{H}_{41}\text{N}_3\text{O}_6 + \text{Na}]^+$  478.2893, found 478.2878

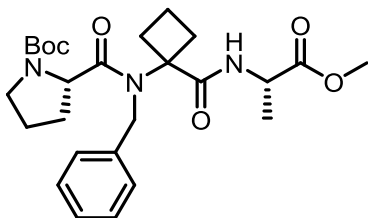


Ugi product derived from Boc-proline, benzylamine, isocyanoacetate derived from (*S*)-*N*-formylphenylalanine methyl ester, and isobutyraldehyde (Table 4.3, Entry 5). Mixture of diastereomers and rotamers. Yield: 238 mg (98%).  $^1\text{H-NMR}$  ( $\text{CDCl}_3$ , 400 MHz)  $\delta$  8.44 (1 H, d,  $J=6.5$  Hz) 7.78 (1 H, br s), 6.92-7.40 (20 H, m), 7.85 (.5 H, dd,  $J=7.2, 5.1$  Hz), 4.76, 4.72, (.5 H, 2 singlets), 4.49-4.69 (2 H, m), 4.31-4.48 (2 H, m), 4.23, (1 H, s), 4.09-4.21 (1 H, m), 3.61-3.75, (4 H, m), 3.43-3.60, (4 H, m), 3.27-3.43 (1H, m), 3.05-3.28 (1 H, m), 2.91-3.04 (1 H, m), 2.87 (1H, dd,  $J=13.4, 8.6$  Hz), 2.53-2.72 (1.5 H, m), 2.22-2.44 (1.5 H, m), 1.97-2.15 (2 H, m), 1.83-1.95 (1 H, m), 1.56-1.80 (2H, m), 1.49, 1.45, 1.44, 1.41 (18 H, 4 singlets), 0.95 (2 H, d,  $J=6.3$  Hz), 0.79-0.91 (8 H, m), 0.68, (2 H, d,  $J=6.8$  Hz);  $^{13}\text{C-NMR}$  (100 MHz,  $\text{CDCl}_3$ )  $\delta$  175.6, 174.7, 174.1, 172.3, 171.7, 168.1, 154.6, 154.3, 153.8, 145.2, 138.2, 136.6, 136.4, 129.0, 128.8, 128.6, 128.5, 128.4, 128.3, 127.8, 127.4, 127.2, 126.9, 126.7, 126.6, 126.3, 80.3, 80.1, 79.4, 66.3, 57.7, 57.1, 54.5, 54.2, 53.2, 52.9, 52.1, 52.0, 51.6, 47.3, 47.0, 45.9, 37.6, 37.6, 31.1, 30.8, 29.8, 28.5, 28.3, 27.6, 26.5, 25.0, 24.4, 22.6, 20.2, 19.7, 19.6, 19.2, 19.1. HRMS (FAB) calcd for  $[\text{C}_{32}\text{H}_{43}\text{N}_3\text{O}_6 + \text{Na}]^+$  485.2264, found 485.2288

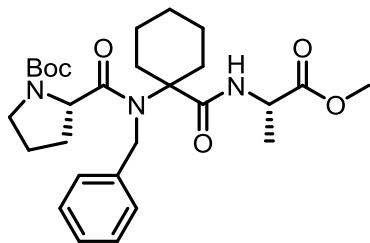


Ugi product derived from Boc-proline, benzylamine, isocyanoacetate derived from (*S*)-*N*-formylmethionine methyl ester, and isobutyraldehyde (Table 4.3, Entry 6). Mixture of diastereomers and rotamers. Yield: 274 mg (96%).  $^1\text{H-NMR}$  ( $\text{CDCl}_3$ , 400 MHz)  $\delta$  8.21 (1 H, d,  $J=6.1$

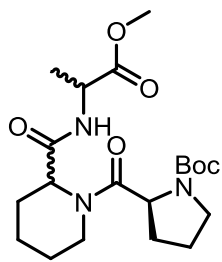
H<sub>z</sub>), 7.92 (1 H, br s), 7.09-7.45 (10 H, m), 4.81-5.10, (2 H, m), 4.66-4.78 (1 H, m), 4.46-4.66 (3 H, m), 4.37-4.45 (1 H, m), 4.32 4.29 (1 H, 2 singlets), 3.89 (1 H, q, J= 7.0 Hz), 3.74, 3.73, 3.67 (6 H, 3 singlets) 3.59-3.65 (1 H, m), 3.44-3.57 (2 H, m), 3.31-3.44 (1 H, m), 2.40-2.53 (3 H, m), 2.20-2.38 (3 H, m), 2.06 (3 H, s), 2.01 (3 H, s), 1.61-1.17 (12 H, m), 1.49, 1.48, 1.45, 1.42 (18 H, 4 singlets), 4.84-1.06 (9 H, m), 0.75 (3 H, d, J=6.8 Hz); <sup>13</sup>C-NMR (100 MHz, CDCl<sub>3</sub>) δ 175.8, 174.8, 174.4, 172.3, 172.0, 171.7, 170.5, 168.4, 154.7, 154.4, 137.9, 136.8, 128.6, 128.5, 128.4, 127.8, 127.5, 127.3, 127.1, 126.7, 126.5, 83.6, 80.3, 79.6, 79.4, 77.2, 66.1, 57.8, 57.2, 56.5, 54.5, 52.3, 52.2, 52.2, 52.0, 51.3, 51.2, 51.2, 47.4, 47.1, 46.1, 31.3, 31.0, 30.8, 30.1, 30.1, 29.8, 29.6, 28.5, 28.4, 27.7, 27.6, 27.5, 26.6, 25.0, 24.5, 24.4, 22.7, 20.2, 19.8, 19.7, 19.4, 19.2, 19.1, 18.8, 15.3. HRMS (FAB) [C<sub>28</sub>H<sub>43</sub>N<sub>3</sub>O<sub>6</sub>S + Na]<sup>+</sup>calcd. 572.2770, found 572.2780



Ugi product derived from Boc-proline, benzylamine, isocyanoacetate derived from (*S*)-*N*-formylalanine methyl ester, and cyclobutanone (Table 4.3, Entry 7). Mixture of rotamers. Yield: 207 mg (81%). <sup>1</sup>H-NMR (CDCl<sub>3</sub>, 400 MHz) δ 7.81, 7.75 (1 H, 2 doublets, J=7.0 Hz) 7.29 - 7.49 (5 H, m) 5.20, 5.14, (1 H, 2 singlets), 4.43-4.63 (1 H, m), 4.41, 4.35 (1 H, 2 singlets), 4.10-4.31 (1H, m), 3.75, 3.73, 3.71, 3.65, (3 H, 4 singlets), 3.29-3.56, (2 H, m), 2.55-2.94 (1 H, m) 2.00-2.54 (4 H, m), 1.59-1.99 (5 H, m), 1.49-1.57 (1 H, m), 1.32-1.45 (11 H, m); <sup>13</sup>C-NMR (100 MHz, CDCl<sub>3</sub>) δ 174.8, 173.7, 173.3, 154.7, 138.6, 128.9, 128.8, 127.3, 126.1, 125.9, 79.7, 77.2, 66.1, 56.8, 52.1, 49.5, 48.5, 47.4, 30.7, 28.7, 28.5, 28.4, 24.6, 17.5, 15.1 HRMS (FAB) calcd for [C<sub>26</sub>H<sub>37</sub>N<sub>3</sub>O<sub>6</sub> + Na]<sup>+</sup> 510.2580, found 510.2595

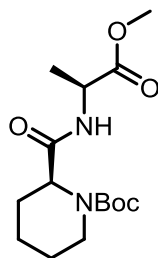


Ugi product derived from Boc-proline, benzylamine, isocyanoacetate derived from (*S*)-*N*-formylalanine methyl ester, and cyclohexanone (Table 4.3 Entry 8). Mixture of rotamers: Yield: 242 mg (90%). <sup>1</sup>H-NMR (CDCl<sub>3</sub>, 400 MHz) δ 7.18-7.61 (5 H, m), 7.65, 7.56 (1 H, 2 doublets, 7.0Hz), 5.05, 4.99, 4.84, 4.78 (1 H, 4 singlets), 4.33-4.72, (3 H, m), 3.75, 3.73, 3.71, (3 H, 3 singlets), 3.47-3.65 (1 H, m), 3.28-3.47 (1 H, m), 2.13-2.56, (2 H, m), 1.54-1.99 (10 H, m), 1.37-1.54 (14 H, s); <sup>13</sup>C-NMR (100 MHz, CDCl<sub>3</sub>) δ 175.1, 173.8, 173.4, 154.5, 139.3, 138.9, 129.0, 128.9, 127.3, 126.3, 126.2, 80.1, 79.4, 72.5, 66.3, 57.8, 52.1, 48.4, 48.3, 47.9, 47.3, 32.8, 30.5, 28.7, 28.5, 25.4, 24.3, 23.1, 22.7, 22.5, 17.8. HRMS (FAB) calcd for [C<sub>28</sub>H<sub>41</sub>N<sub>3</sub>O<sub>6</sub> + Na]<sup>+</sup> 538.2893, found 538.2876

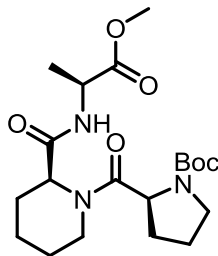


**Racemizing Joullié-Ugi Reaction General Procedure, Synthesis of mix-6:** A flask containing *N*-chloropiperidine (1.2mmol, 142.8mg) was charged with 25% sodium methoxide (1mmol, 0.23mL) in methanol and stirred for 30 minutes, over the course of which a white precipitate formed. The solution was then diluted with methanol (.67mL) followed by the addition of (*S*)-Boc-Pro-OH (1mmol, 215.3mg) and (*S*)-2-isocyano methyl propanoate (1mmol, 113.1mg). The reaction was allowed to stir for 48 hours after which the solvent was removed. The oily residue was dissolved in 7:3 ethyl acetate:hexanes and loaded onto a silica gel column (4"x.75"). The product was then eluted with 7:3 ethyl acetate:hexanes. Yield: 88.1mg (21.4%) The mixture of

diastereomers was analyzed/separated on a Higgins Analytical: Hasil C18 column (150mmx10mm). Solvent gradient: 20-60% acetonitrile in water over 20 minutes at 1.5mL/min. UV Detection: 214nm. <sup>1</sup>H NMR (CDCl<sub>3</sub>, mixture of diastereomers) 7.35-8.5 (4xd, 1H), 7.38 (d, 0.5H), 4.56 (m, 1H), 4.48 (m, 1H), 3.70 (m, 3H), 3.54 (m, 1H), 3.44 (m, 1H), 2.4-3.2 (3xm, 2H), 1.5-2.2 (m, 8H), 1.1-1.5(m,16H). LRMS (ESI) [M+H]<sup>+</sup> 412.22, [M+Na]<sup>+</sup> 434.43, [M-Boc]<sup>+</sup> 312.53



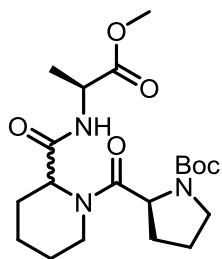
**Boc-(S)-Pip-(S)-Ala-Ome (9):** (S)-alanine methyl ester hydrochloride (.5mmol, 69.8mg), Boc-S-pipecolic acid (.5mmol, 114.7 mg) and HOBT (.7mmol 100mg) were dissolved in DCM (15mL). The solution was stirred for 15 minted before the addition of DCC(.7mmol, 144.33mg) and NMM(.58mmol, 60μL). The reaction proceeded for 16 hours after which the solution was concentrated to near dryness. The residue was suspended in ethyl acetate then filtered through silica gel. The filtrate was then washed with sodium bisulfate (2x10mL), sodium bicarbonate (2x10mL) and brine (1x10mL). The organic solution was dried over magnesium sulfate then filtered and concentrated to dryness to yield the product. Yeild 157.24mg (95.9%) <sup>1</sup>HNMR (CDCl<sub>3</sub>) 6.62(s broad, 1H), 4.81(s broad, 1H), 4.64(quint, 1H), 3.78 (s, 3H), 2.93(t, 1H), 2.33(d, 1H), 1.64(m, 6H), 1.53(s, 9H), 1.43(d, 3H). LRMS (ESI) [M+H]<sup>+</sup> 315.44, [M+Na]<sup>+</sup> 457.34, [M-Boc]<sup>+</sup> 215.58.



**Boc-(S)-Pro-(S)-Pip-(S)-Ala-Ome (SSS-6).** Boc-(S)-Pip-(S)-Ala-Ome (.21mmol, 65.9mg) was dissolved in DCM (1mL). TFA (.2mL) was added dropwise with stirring. After 1 hour the reaction was determined to be complete by TLC (1:1 ethyl acetate:hexanes, stained with ninhydrin). The reaction was then concentrated and the residue used without further purification.

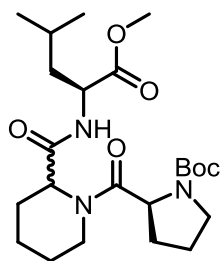
Boc-(S)-Proline (.23mmol, 50mg) and HATU (.21mmol, 79.8mg) were dissolved in DMF (0.5mL). To this solution was added DIPEA (.21mmol, 37 $\mu$ L). This solution was stirred for 30 minutes after which deprotected (S)-Pip-(S)-Ala-Ome dissolved in DMF (.5mL) with DIPEA (.21mmol, 37 $\mu$ L) was added. This reaction was stirred for 24 hours then concentrated to a viscous oil. The oil was loaded onto a silica gel column (4"x.75") and the product eluted with 7:3 ethyl acetate:hexanes. Yield: 71.2mg (82.5%)  $^1\text{H}$ NMR ( $\text{CDCl}_3$ ) 8.66(d, 1H) 4.59(m, 2H), 4.46(quint, 1H), 3.68(s, 3H), 3.57 (m, 1H), 3.45(m, 1H), 2.57(d, 1H), 2.47(t, 1H), 1.5-2.3(m, 10H) 1.4-1.5(m, 12H). LRMS (ESI)  $[\text{M}+\text{H}]^+$  412.44,  $[\text{M}+\text{Na}]^+$  434.63,  $[\text{M}-\text{Boc}]^+$  312.80.

**Non-Racemizing Joullié-Ugi Reaction General Procedure.** Tripiperidine (either .17 or .25 mmol) and Boc-Proline (.5mmol, 108 mg) were dissolved in methanol and stirred until the solution was homogeneous. Subsequently, the isocyanoacetate (.52mmol) was added to the reaction. It was stirred for 48 hours at room temperature, after which time the solvent was removed *in vacuo*. The oily residue were applied to a silica gel column and the product was purified via elution with a mobile phase of hexanes:ethyl acetate.



**Boc-(S)-Pro-Pip-(S)-Ala-Ome (Table 4.5, Entry 1). Mixture of diastereomers and rotamers. Yield:**

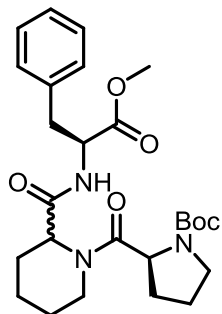
158 mg (73%)  $^1\text{H-NMR}$  ( $\text{CDCl}_3$ , 400 MHz)  $\delta$  8.45, 7.37, 6.62, 6.59 (2 H, 4 doublets,  $J=7.0$  Hz), 5.14-5.55 (1 H, m), 4.37-4.90 (5 H, m), 3.89 3.86 (2 H, 2 singlets), 3.71, 3.68 (6H, 2 singlets), 3.52-3.61 (2H, m), 3.39-3.51 (2H, m), 2.43-2.65 (2 H, m), 2.03-2.30 (5 H, m), 1.80-2.03 (6 H, m), 1.55-1.79 (7 H, m), 1.22-1.55 (26 H, m);  $^{13}\text{C-NMR}$  (100 MHz,  $\text{CDCl}_3$ )  $\delta$  173.7, 172.0, 171.5, 170.1, 169.8, 154.6, 79.9, 79.7, 56.3, 55.7, 55.6, 52.1, 52.1, 48.8, 48.3, 47.0, 46.8, 43.7, 39.7, 29.6, 29.5, 28.4, 26.1, 26.0, 24.8, 24.7, 20.6, 16.9, 16.5. HRMS (FAB) calcd for  $[\text{C}_{20}\text{H}_{33}\text{N}_3\text{O}_6 + \text{Na}]^+$  434.2267, found 434.2262



**Boc-(S)-Pro-Pip-(S)-Leu-Ome (Table 4.5, Entry 2). Mixture of diastereomers and rotamers. Yield:**

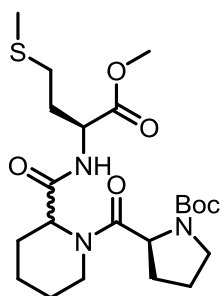
129 mg (54%)  $^1\text{H-NMR}$  ( $\text{CDCl}_3$ , 400 MHz)  $\delta$  8.33 (1 H, d,  $J=7.9$  Hz), 7.13 (1H, d,  $J=7.5$  Hz), 5.08-5.47 (1 H, m), 4.29-4.75 (4 H, m), 3.84 (.5 H, d,  $J=12.4$  Hz), 3.67, 3.65 (6 H, 2 singlets), 3.47-3.60 (2.5 H, m), 3.29-3.47 (3H, m), 2.31-2.60 (2 H, m), 1.97-2.23 (3 H, m), 1.76-1.95 (4 H, m), 1.54-1.76 (10 H, m), 1.17-1.54 (29 H, m), 0.75-0.99 (12 H, m);  $^{13}\text{C-NMR}$  (100 MHz,  $\text{CDCl}_3$ )  $\delta$  173.5, 173.3, 171.8, 170.2, 170.0, 154.5, 79.8, 79.5, 56.2, 55.7, 55.5, 51.9, 51.8, 51.6, 50.9, 46.9, 46.7, 43.5, 40.1, 39.6, 38.7, 29.5, 28.3, 28.2, 26.1, 25.9, 24.8, 24.7, 24.6, 22.9, 22.7, 22.5, 21.8, 20.9, 20.6. HRMS (FAB) calcd for  $[\text{C}_{23}\text{H}_{39}\text{N}_3\text{O}_6 + \text{Na}]^+$  476.2737, found 476.2720





**Boc-(S)-Pro-Pip-(S)-Phe-Ome (Table 4.5, Entry 3). Mixture of diastereomers and rotamers.**

Yield: 148 mg (58%)  $^1\text{H-NMR}$  ( $\text{CDCl}_3$ , 400 MHz)  $\delta$  8.50 (1 H, d,  $J=8.3$  Hz), 7.46 (1 H,  $J=7.7$  Hz), 7.05-7.38 (10 H, m), 5.04-5.41 (1 H, m), 4.78-4.04 (.5 H, m), 4.54-4.78 (3 H, m), 4.36-4.54 (1 H, m), 4.33, 4.30 (.5 H, 2 singlets), 3.86, 1.83 (1 H, 2 singlets), 3.63-3.78 (6 H, m), 3.52-3.63 (2 H, m), 3.53 -5.52 (2 H, m), 3.15-3.43 (3 H, m), 2.98- 3.15 (2 H, m), 2.34-2.57 (1 H, m), 1.99-2.28 (5 H, m), 1.80-1.99 (4 H, m), 1.58-1.80, (4 H, m), 1.00-1.58 (26 H, m);  $^{13}\text{C-NMR}$  (100 MHz,  $\text{CDCl}_3$ )  $\delta$  172.4, 172.1, 171.9, 171.3, 169.9, 169.7, 154.7, 137.5, 137.1, 129.2, 129.2, 128.4, 128.3, 127.0, 126.5, 126.5, 80.0, 79.7, 57.0, 56.2, 55.9, 55.6, 54.4, 54.2, 53.3, 52.1, 51.9, 47.0, 46.9, 43.5, 39.3, 37.4, 36.2, 29.6, 29.5, 28.4, 25.9, 25.9, 25.7, 24.8, 24.8, 24.7, 24.4, 20.5, 20.4. HRMS (FAB) calcd for  $[\text{C}_{26}\text{H}_{37}\text{N}_3\text{O}_6 + \text{Na}]^+$  510.2580, found 510.2566



**Boc-(S)-Pro-Pip-(S)-Met-Ome (Table 4.5, Entry 4). Mixture of diastereomers and rotamers.**

Yield: 135 mg (54%)  $^1\text{H-NMR}$  ( $\text{CDCl}_3$ , 400 MHz)  $\delta$  8.46 (1 H, d,  $J=7.7$  Hz), 7.30 (1 H, d, 8.2 Hz), 5.14-5.44 (1 H, m), 4.74 (1 H, td,  $J=8.6$ , 5.4 Hz), 4.52-4.67 (4 H, m), 3.89, 3.86 (1 H, 2 singlets), 3.72, 3.69, 3.65, (6 H, 3 singlets), 3.51-3.63 (2 H, m), 3.33-3.51 (3 H, m), 2.42-2.63 (6 H, m), 2.08, 2.06

(6 H, 2 singlets), 2.02-2.29 (8 H, m), 1.79-2.02 (6 H, m), 1.52-1.79 (4 H, m), 1.30-1.52 (24 H, m); <sup>13</sup>C-NMR (100 MHz, CDCl<sub>3</sub>) δ172.7, 171.9, 171.4, 170.4, 170.3, 154.7, 83.6, 80.0, 79.7, 56.3, 55.8, 55.6, 52.1, 51.5, 47.0, 46.9, 43.6, 39.7, 30.7, 30.0, 29.7, 29.6, 28.5, 28.4, 26.1, 26.0, 24.8, 20.6, 15.5, 15.3. HRMS (FAB) [C<sub>22</sub>H<sub>37</sub>N<sub>3</sub>O<sub>6</sub>S + Na]<sup>+</sup>calcd.494.2301, found 494.2311

### References

1. Hinzen, B. WO2003024996 A3, 2004.
2. Hinzen, B.; Raddatz, S.; Paulsen, H.; Lampe, T.; Schumacher, A.; Häbich, D.; Hellwig, V.; Benet-Buchholz, J.; Endermann, R.; Labischinski, H.; Brötz-Oesterhelt, H. Medicinal Chemistry Optimization of Acyldepsipeptides of the Enopeptin Class Antibiotics. *ChemMedChem* **2006**, *1*, 689-693.
3. Schmidt, U.; Neumann, K.; Schumacher, A.; Weinbrenner, S. Synthesis of Enopeptin B from *Streptomyces* sp RK-1051. *Angewandte Chemie International Edition in English* **1997**, *36*, 1110-1112.
4. Keenan, T. P.; Yaeger, D.; Holt, D. A. Synthesis of chiral nonracemic 4-trans-substituted pipercolic acid derivatives. *Tetrahedron: Asymmetry* **1999**, *10*, 4331-4341.
5. Passerini, M.; Simone, L. *Gazz. Chim. Ital.* **1921**, *51*, 126-129.
6. AnonymousVersammlungsberichte. *Angewandte Chemie* **1959**, *71*, 373-388.
7. Ugi, I.; Steinbrückner, C. Über ein neues Kondensations-Prinzip. *Angewandte Chemie* **1960**, *72*, 267-268.
8. Dömling, A. Recent Developments in Isocyanide Based Multicomponent Reactions in Applied Chemistry. *Chem. Rev.* **2006**, *106*, 17-89.
9. Scheuer, P. J. Isocyanides and cyanides as natural products. *Acc. Chem. Res.* **1992**, *25*, 433-439.
10. Edenborough, M. S.; Herbert, R. B. Naturally occurring isocyanides. *Nat. Prod. Rep.* **1988**, *5*, 229-245.
11. Dömling, A.; Ugi, I. Multicomponent Reactions with Isocyanides. *Angewandte Chemie International Edition* **2000**, *39*, 3168-3210.

12. Ugi, I.; Meyr, R. Neue Darstellungsmethode für Isonitrile. *Angewandte Chemie* **1958**, *70*, 702-703.
13. Zhu, J.; Wu, X.; Danishefsky, S. J. On the preparation of enantiomerically pure isonitriles from amino acid esters and peptides. *Tetrahedron Lett.* **2009**, *50*, 577-579.
14. Gulevich, A. V.; Zhdanko, A. G.; Orru, R. V. A.; Nenajdenko, V. G. Isocyanoacetate Derivatives: Synthesis, Reactivity, and Application. *Chem. Rev.* **2010**, *110*, 5235-5331.
15. Elders, N.; Ruijter, E.; Nenajdenko, V.; Orru, R. In  *$\alpha$ -Acidic Isocyanides in Multicomponent Chemistry*; Ruijter, E., Ed.; Synthesis of Heterocycles via Multicomponent Reactions I; Springer Berlin / Heidelberg: 2010; Vol. 23, pp 129-159; 159.
16. Wu, X.; Stockdill, J. L.; Wang, P.; Danishefsky, S. J. Total Synthesis of Cyclosporine: Access to N-Methylated Peptides via Isonitrile Coupling Reactions. *J. Am. Chem. Soc.* **2010**, *132*, 4098-4100.
17. Rao, Y.; Li, X.; Danishefsky, S. J. Thio FCMA Intermediates as Strong Acyl Donors: A General Solution to the Formation of Complex Amide Bonds. *J. Am. Chem. Soc.* **2009**, *131*, 12924-12926.
18. Fujii, K.; Ikai, Y.; Oka, H.; Suzuki, M.; Harada, K. A Nonempirical Method Using LC/MS for Determination of the Absolute Configuration of Constituent Amino Acids in a Peptide: Combination of Marfey's Method with Mass Spectrometry and Its Practical Application. *Anal. Chem.* **1997**, *69*, 5146-5151.
19. Ramón, D. J.; Yus, M. Asymmetric Multicomponent Reactions (AMCRs): The New Frontier. *Angewandte Chemie International Edition* **2005**, *44*, 1602-1634.
20. Owens, T. D.; Araldi, G.; Nutt, R. F.; Semple, J. E. Concise total synthesis of the prolyl endopeptidase inhibitor eurystatin A via a novel Passerini reaction–deprotection–acyl migration strategy. *Tetrahedron Lett.* **2001**, *42*, 6271-6274.
21. Berłożecki, S.; Szymanski, W.; Ostaszewski, R.  $\alpha$ -Amino acids as acid components in the Passerini reaction: influence of N-protection on the yield and stereoselectivity. *Tetrahedron* **2008**, *64*, 9780-9783.
22. Bowers, M. M.; Carroll, P.; Joullie, M. M. Model studies directed toward the total synthesis of 14-membered cyclopeptide alkaloids: synthesis of prolyl peptides via a four-component condensation. *J. Chem. Soc., Perkin Trans. 1* **1989**, 857-865.
23. Banfi, L.; Basso, A.; Guanti, G.; Merlo, S.; Repetto, C.; Riva, R. A convergent synthesis of enantiopure bicyclic scaffolds through multicomponent Ugi reaction. *Tetrahedron* **2008**, *64*, 1114-1134.
24. Failli, A.; Nelson, V.; Immer, H.; Götz, M. Model Experiments Directed towards the Synthesis of N-Aminoacetylpeptides. *Can. J. Chem.* **1973**, *51*, 2769-2775.

25. Bayer, T.; Riemer, C.; Kessler, H. A new strategy for the synthesis of cyclopeptides containing diaminoglutaric acid. *Journal of Peptide Science* **2001**, *7*, 250-261.
26. Berłożecki, S.; Szymański, W.; Ostaszewski, R. Application of Isocyanides Derived from  $\alpha$ -Amino Acids as Substrates for the Ugi Reaction. *Synthetic Communications* **2008**, *38*, 2714-2721.
27. Zhdanko, A. G.; Nenajdenko, V. G. Nonracemizable Isocyanoacetates for Multicomponent Reactions. *J. Org. Chem.* **2009**, *74*, 884-887.
28. Mroczkiewicz, M.; Winkler, K.; Nowis, D.; Placha, G.; Golab, J.; Ostaszewski, R. Studies of the Synthesis of All Stereoisomers of MG-132 Proteasome Inhibitors in the Tumor Targeting Approach. *J. Med. Chem.* **2010**, *53*, 1509-1518.
29. Bonne, D.; Dekhane, M.; Zhu, J. Modulating the Reactivity of  $\alpha$ -Isocyanoacetates: Multicomponent Synthesis of 5-Methoxyoxazoles and Fuopyrrolones. *Angewandte Chemie International Edition* **2007**, *46*, 2485-2488.
30. Lalli, C.; Bouma, M. J.; Bonne, D.; Masson, G.; Zhu, J. Exploiting the Divergent Reactivity of  $\alpha$ -Isocyanoacetate: Multicomponent Synthesis of 5-Alkoxyoxazoles and Related Heterocycles. *Chemistry: A European Journal* **2011**, *17*, 880-889.
31. Sun, X.; Janvier, P.; Zhao, G.; Bienaymé, H.; Zhu, J. A Novel Multicomponent Synthesis of Polysubstituted 5-Aminooxazole and Its New Scaffold-Generating Reaction to Pyrrolo[3,4-b]pyridine. *Org. Lett.* **2001**, *3*, 877-880.
32. Layer, R. W. The Chemistry of Imines. *Chem. Rev.* **1963**, *63*, 489-510.
33. Claxton, G. P.; Allen, L.; Grisar, M. J. 2,3,4,5-Tetrahydropyridine Trimer. *Org. Synth.* **1977**, *56*, 118.
34. De Kimpe, N.; Stevens, C. A convenient synthesis of 6-acetyl-1,2,3,4-tetrahydropyridine, the principle bread flavor component. *J. Org. Chem.* **1993**, *58*, 2904-2906.
35. Rouchaud, A.; Braekman, J. Synthesis of New Analogues of the Tetraopenerines. *European Journal of Organic Chemistry* **2009**, *2009*, 2666-2674.

## Chapter 5 – Synthesis of ADEPs with Conformationally Constrained Peptidolactones.

**Contents of this Chapter are Published in the following Manuscript:** Carney, D. W.; Schmitz, K. R.; Truong, J. V.; Sauer, R. T.; Sello, J. K.; *Restriction of the Conformational Dynamics of the Cyclic Acyldepsipeptide Antibiotics Improves Their Antibacterial Activity.* *J. Am. Chem. Soc.* **2014.** 136, 1922-1929. dx.doi.org/ 10.1021/ja410385c

### Introduction

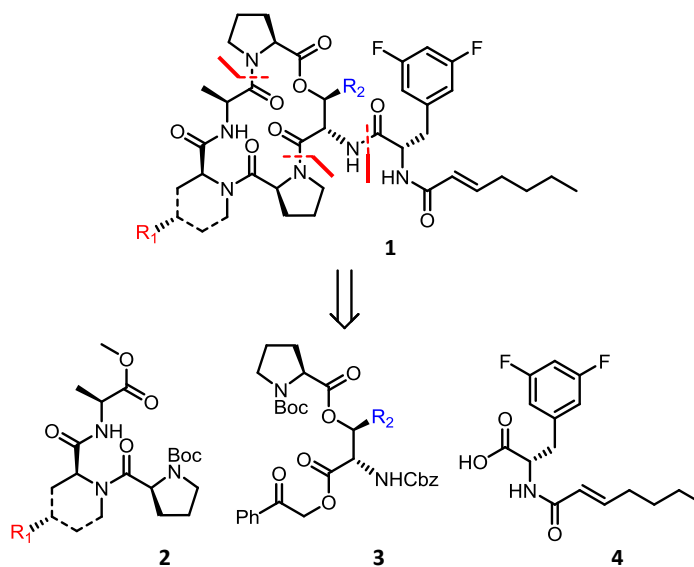


Figure 5.1 - Retrosynthetic analysis of ADEPs with conformationally constrained macrocycles

There are multiple precedents for the chemical syntheses of the cyclic acyldepsipeptide antibiotics and derivatives thereof.<sup>1-4</sup> In this study, we optimized a convergent strategy that was previously developed in our labs. It is based on retrosynthetic disconnection of the ADEP (**1**) into three fragments of similar size and complexity, namely a tripeptide (**2**), a prolyl ester (**3**), and an *N*-acyldifluorophenylalanine side chain (**4**) (Figure 5.1).<sup>4</sup> This convergent approach is most practical for solution-phase synthesis of ADEP derivatives and is amenable to the diversity-oriented synthesis required for this study. The following sections discuss the synthesis of each fragment and their coupling to construct the ADEP molecules.

## Results

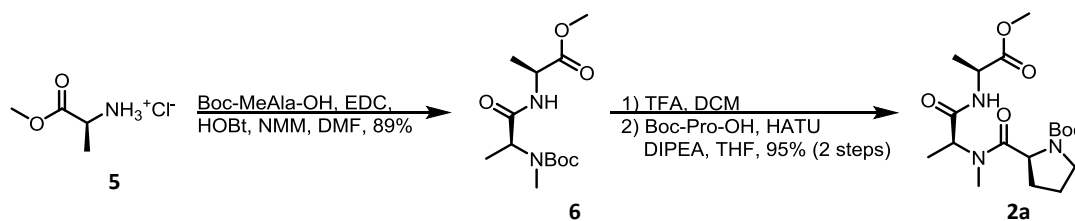


Figure 5.2 - Synthesis of *N*-methylalanine containing tripeptide

The peptidolactone of the natural product ADEPs, which we predicted would be the most conformationally flexible, required the synthesis of the tripeptide, Boc-Pro-*N*-MeAla-Ala-Ome (**2a**). Tripeptide **2a** was synthesized using standard peptide coupling (Figure 5.2). As discussed in chapter 4 however, the standard peptide coupling approach was not a viable option for the synthesis of piperolate containing tripeptides. With optimized Joullié-Ugi 3-component reaction (JU-3CR) conditions, we synthesized tripeptides containing piperolate (**2b**), 4-methylpiperolate (**2c**), and 4-isopropylpiperolate (**2d**). To generate the key piperolate residues in these tripeptides, we prepared cyclic imines derived from piperidine (**7a**), 4-methylpiperidine (**7b**), or 4-isopropylpiperidine (**7c**). While **7b** formed a crystalline trimer, **7c** did not. Fortunately, no isocyanoacetate epimerization was observed when **7c** was used in its crude form in the JU-3CR after diethylether extraction and concentration. All JU-3CR yielded separable 1:1 mixtures of diastereomeric tripeptides (**6a-c**) that were epimeric at C2 of the piperolate residue. (Figure 5.3A) This conserved product ratio indicates that reactions with C4-substituted cyclic imines are diastereoselective. Consistent with literature precedents,<sup>5,6</sup> these products had piperolate residues with a *trans*-relationship of the substituents at C2 and C4 as indicated by the crystal structures obtained for **epi-6b** and **epi-6a** (Figure 5.3B). The resulting substitution pattern strongly enforces a chair conformation for the piperolate 6-membered ring in which the carboxamide at C-2 is axially disposed due to allylic strain and the C4 alkyl substituent is in the equatorial position

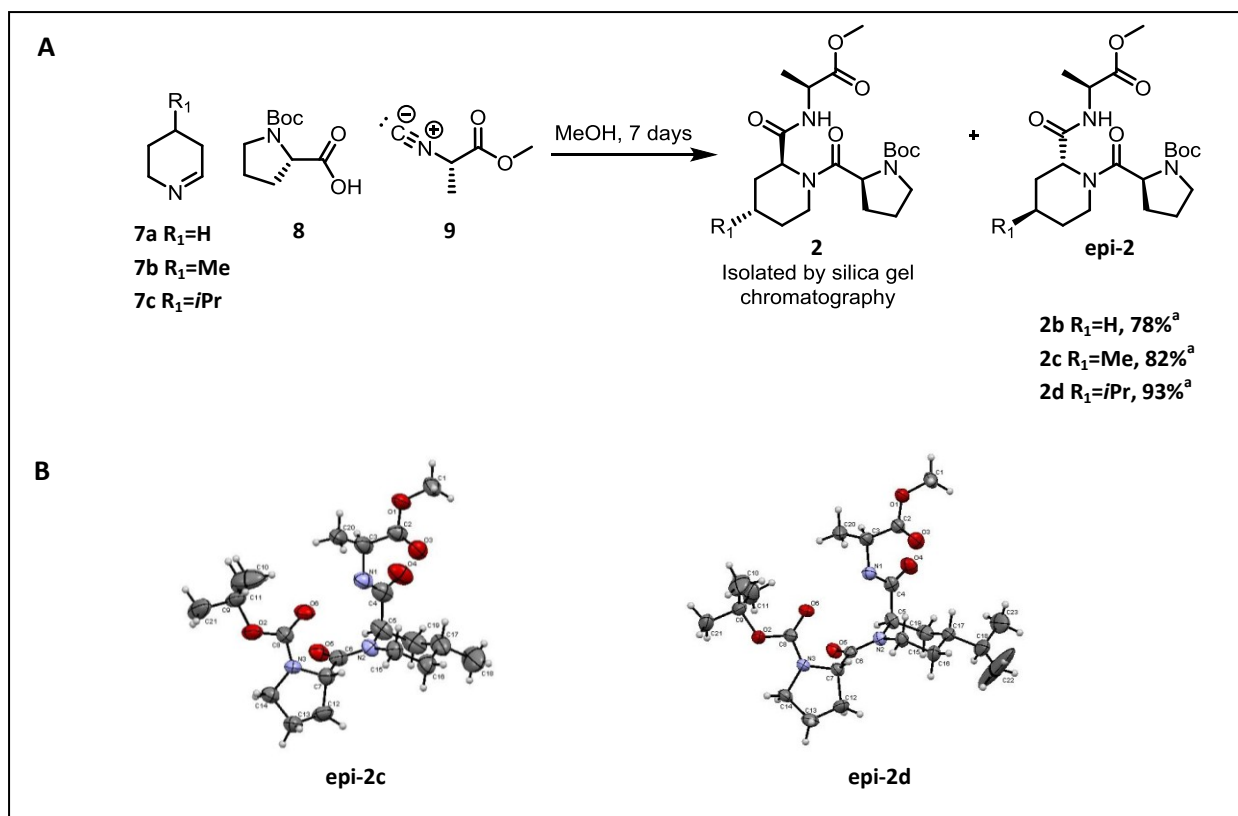
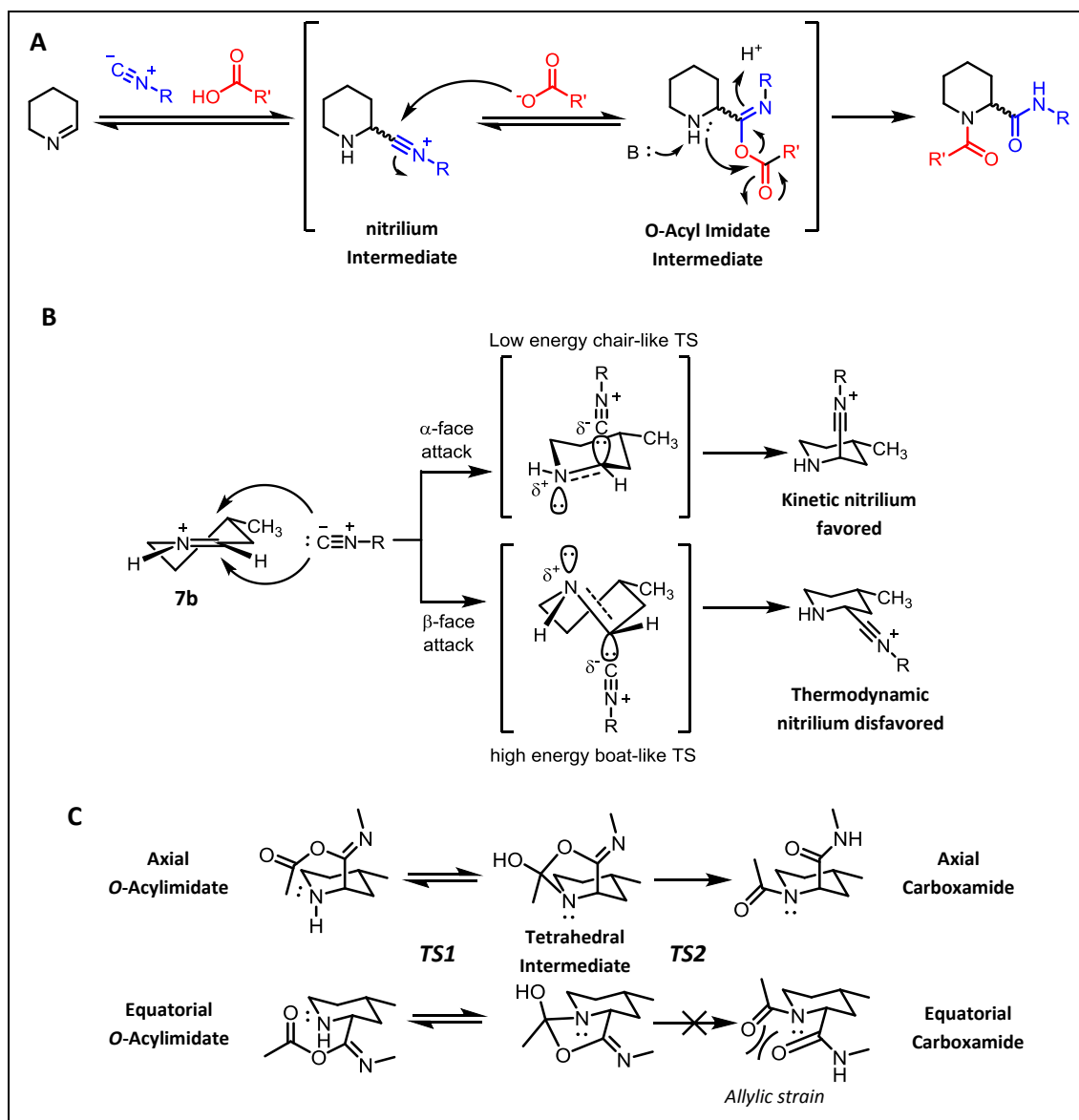


Figure 5.3 - A) Multicomponent synthesis of piperolate containing tripeptides <sup>a</sup>Combined isolated yield of both diastereomers B) crystal structures of epi-6b and epi-6c.

There are two transformations within the JU-3CR mechanism (Figure 3.4A) that might influence the diastereoselectivity in JU-3CR with 4-substituted dehydropiperidines. Stereoselectivity could arise as a result of kinetically controlled addition of the isocyanide to the cyclic imine  $\alpha$ -face through a chair-like transition state (Figure 3.3 B). However, in the Joullié-Ugi reaction mechanism, all steps, including nitrilium intermediate formation, are reversible except for the final *O*- to *N*-acyl transfer (Mumm Rearrangement).<sup>7,8</sup> Therefore, the Mumm rearrangement might be an important determinant of final product stereochemistry. The *O*- to *N*-acyl transfer is a 2 step, addition-elimination process (Figure 5.4C). First, the amine nitrogen attacks the carbonyl carbon of the *O*-acylimidate (*TS1*), forming a tetrahedral intermediate. The tetrahedral intermediate then collapses (*TS2*), transferring the acyl group from oxygen to the piperidine nitrogen as the resulting imidate tautomerizes to a carboxamide. The conformational

preference for nitrogen in *N*-unsubstituted piperidines is for the lone pair to be equatorially oriented.<sup>9,10</sup> Therefore, the difference in energy between nitrogen lone pair attack on an axially oriented versus an equatorially oriented C-2 *O*-acyl imidate (*TS1*) is probably small. However, there should be a significant difference in energy for the collapse tetrahedral intermediates (*TS2*) depending on the orientation of the forming carboxamide. A significant energetic penalty due to allylic strain ( $A^{1,3}$ ) is incurred if the C-2 carboxamide is disposed in an equatorial orientation. As a result, the Mumm rearrangement should have a strong preference for processing an axially oriented *O*-acylimidate. It therefore seems that formation of the iminium intermediate and the *O*- to *N*-acyl transfer synergistically influence the stereoselectivity of the JU-3CR with 4-substituted dehydropiperidines. This could explain why the reactions are completely diastereoselective.





**Figure 5.4 – Rationalization of the diastereoselectivity observed in JU-3CR with 4-substituted dehydropiperidines. A) JU-3CR reaction mechanism, B) diastereoselectivity could arise from kinetically controlled attack of the isocyanide on the cyclic imine. C) The *O*- to *N*-acyl transfer is selective for an axial *O*-acylimidate.**

With four distinct tripeptides (**2c-d**) in hand, our attention next turned to the proline esters (**3**). Esters of proline (**3**) with either serine or *allo*-threonine were prepared as described by Hinzen.<sup>2,3</sup> While the required Cbz-serine (**14a**) building block is commercially available at low cost, Cbz-*allo*-threonine (**14b**) is not commercially available and unprotected *allo*-threonine costs ~\$1000/gram. We therefore decided to synthesize Cbz-*allo*-threonine from commercial

threonine methyl ester (**10**). (Figure 5.5).<sup>11-13</sup> For this procedure, **10** was benzoylated with benzyl chloride to yield *N*-benzoylthreonine methyl ester (**11**). Upon activation of the  $\beta$ -hydroxyl of **11** with thionyl chloride, intramolecular nucleophilic attack of the amide oxygen at the threonine  $\beta$ -carbon forms an oxazole (**12**) with inversion of  $\beta$ -carbon stereocenter. Hydrolysis of **12** with 6M HCl gave unprotected *allo*-threonine (**13**), which was subsequently protected as the benzyl carbamate (**14b**).

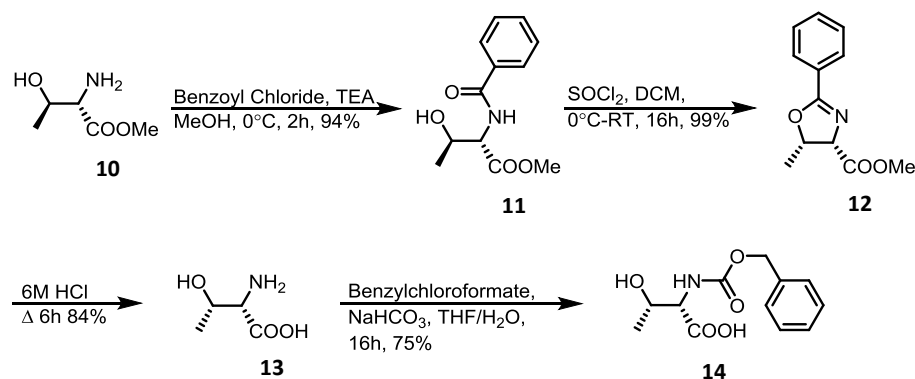


Figure 5.5 - Synthesis of protected *allo*-threonine.

*N*-Cbz protected amino acids (**14**) were protected as phenacyl esters (**15**) and subsequently coupled to Boc-proline using Steglich esterification conditions (Figure 5.6).<sup>14</sup> Curiously, these coupling reactions required a superstoichiometric amount (1.5-2 eq.) of EDC in order to reach completion. However, the excess EDC had to be added to the reaction in portions or else significant degradation of the product (**14**) was observed as a result of *E1cB* scission of the  $\beta$ -carbon – ester oxygen bond. This degradation reaction was most likely promoted by the basicity of the EDC reagent and was more prevalent for the serine-proline ester than the *allo*-threonine-proline ester. Regardless, with careful execution of the esterification reaction, **14a** and **14b** could be obtained in excellent yield.

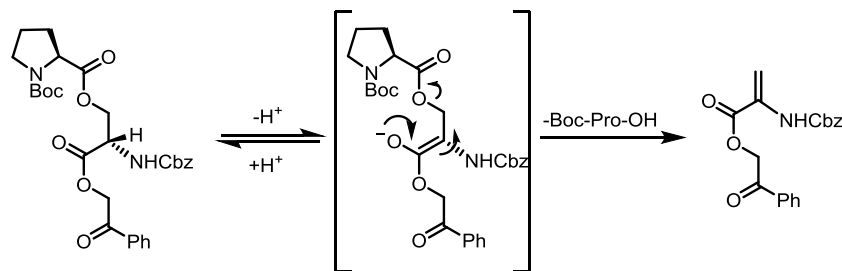
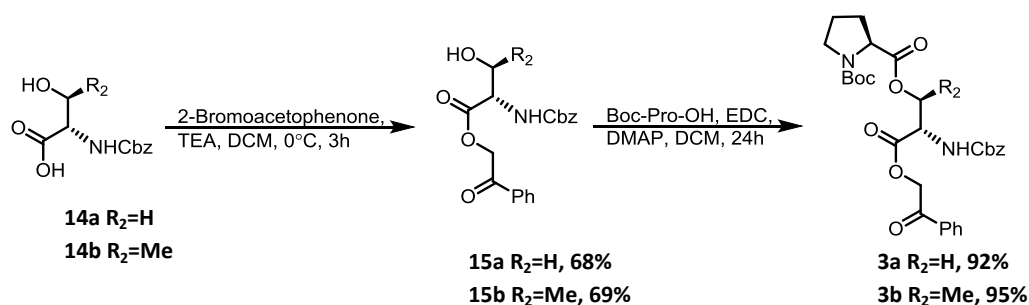
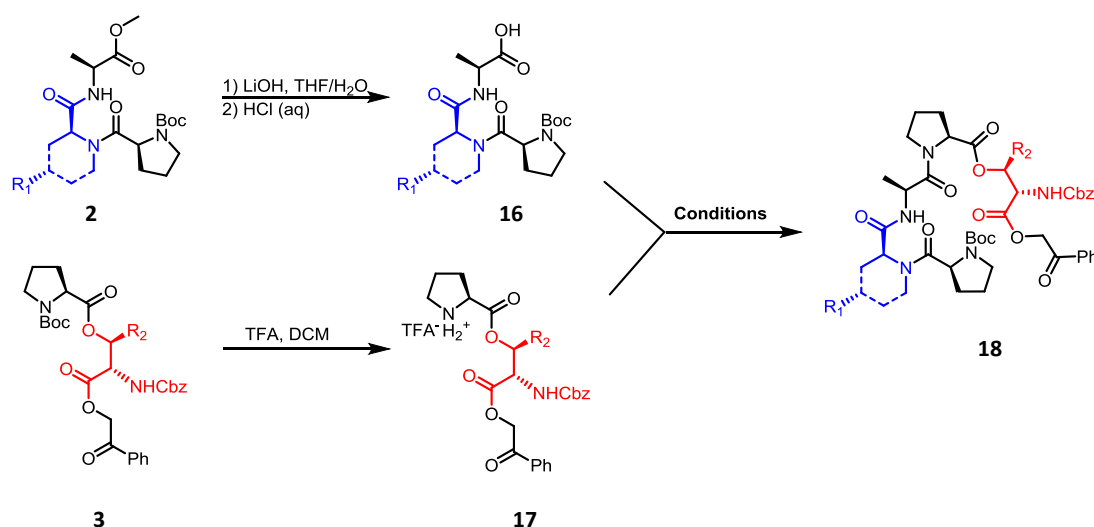


Figure 5.6 - Synthesis of proline esters and potential product degradation mechanism

The coupling of proline esters with the tripeptides was a problematic operation that required optimization (Table 5.1). Tripeptides (**2**) were saponified by treatment with lithium hydroxide in THF/water and proline esters (**3**) were Boc-deprotected by treatment with 40% TFA in DCM. The deprotected intermediates were combined and then coupled forming pentapeptolides (**18**) under various conditions. Originally, the segment coupling reaction was performed according to the published procedure using TPTU, HOBT, and DIPEA in DCM at room temperature (Table 5.1, entries 1-6)<sup>2</sup>. The reaction was allowed to proceed for 16 hours before workup and purification of the product by flash chromatography. Yields for this coupling procedure were disappointingly modest, ranging from 51-63%. LC-MS analysis of the reactions prior to purification indicated the formation of side products that could emerge from *E1cB* scission of  $\beta$ -carbon – ester oxygen bond in the same manner as observed in the proline ester synthesis.

Several steps were taken to optimize the segment coupling reaction. First, we conducted a simple experiment to study base promoted E1cB degradation of a proline ester. Compound **3a** was dissolved in either DCM or DMF and then treated with either 0, 1, or 2 equivalents of DIPEA. The samples were periodically visualized by TLC. The degradation of **3a** required DIPEA, a common base used in peptide coupling. It was also clear that the rate of degradation increased with increasing equivalents of base. Additionally, the rate of degradation was much faster in DCM than in DMF, consistent with the solvent effects expected for an E1cB mechanism. With these results in mind, we conducted the segment coupling reaction using an alternative coupling system. It was found that the yield of the coupling reaction was improved to 71% via the use of HATU/DIPEA in DMF with a reaction duration of 16 hours (Table 5.1, entry 7). Since both the proline ester starting materials (**3**) and the pentapeptolide products (**18**) are susceptible to E1cB mediated degradation, excessively long reaction durations can contribute to diminished product yields. We therefore optimized the segment coupling reaction duration using the HATU/DIPEA coupling system in DMF. Conversion of the proline ester was monitored using HPLC. By 1 hour, the reaction appeared to be complete, after which it was promptly subjected to aqueous workup. To our satisfaction, segment couplings conducted with HATU/DIPEA in DMF for 1 hour (Table 5.1, entries 8-13) proceeded in good to excellent yield.

Table 5.2 - Synthesis of pentapeptolides



Entry	Residue 1	Residue 2	Coupling Reagent / Base	Solvent	Time	Yield % <sup>a</sup>
1	<i>N</i> -MeAla	Ser	TPTU, HOBT / DIPEA	DCM	16 h	63
2	Pip	Ser	TPTU, HOBT / DIPEA	DCM	16 h	51
3	4-MePip	Ser	TPTU, HOBT / DIPEA	DCM	16 h	51
4	4- <i>i</i> PrPip	Ser	TPTU, HOBT / DIPEA	DCM	16 h	44
5	Pip	<i>allo</i> -Thr	TPTU, HOBT / DIPEA	DCM	16 h	61
6	4-MePip	<i>allo</i> -Thr	TPTU, HOBT / DIPEA	DCM	16 h	54
7	4-MePip	Ser	HATU / DIPEA	DMF	16 h	71
8	<i>N</i> -MeAla	Ser	HATU / DIPEA	DMF	1 h	91
9	Pip	Ser	HATU / DIPEA	DMF	1 h	75
10	4-MePip	Ser	HATU / DIPEA	DMF	1 h	79
11	4- <i>i</i> PrPip	Ser	HATU / DIPEA	DMF	1 h	80
12	<i>N</i> -MeAla	<i>allo</i> -Thr	HATU / DIPEA	DMF	1 h	84
13	Pip	<i>allo</i> -Thr	HATU / DIPEA	DMF	1 h	87
14	4-MePip	<i>allo</i> -Thr	HATU / DIPEA	DMF	1 h	80

All reactions were conducted at 2M concentration, in dry solvent, under ambient atmosphere, and at room temperature. <sup>a</sup>Isolated yields after flash chromatography

Pentapeptolides (**18**) were converted into peptidolactones (**19**) via the method reported by Schmidt in the synthesis of enopectin B.<sup>1</sup> First, the C-terminal phenacyl group was removed

by treatment with zinc in acetic acid, after which the C-terminus was activated as a pentafluorophenol ester. The N-terminal Boc-group was subsequently removed by treatment with 4M hydrogen chloride in dioxane. Macrocyclization proceeded upon neutralization of the hydrochloride salt under high dilution in a biphasic solution of DCM and 1 M aqueous sodium bicarbonate. Conversions of the fully protected pentapeptolides to the corresponding peptidolactones were carried out with no intermediate purification and in 36-59% yield over 4 steps (Table 3.2). Macrocyclization yields were, in general, lower for conformationally constrained peptidolactones than those that were relatively flexible.

**Table 5.3 - Synthesis of peptidolactones**

Entry	Residue 1	Residue 2	Yield % <sup>a</sup>	Entry	Residue 1	Residue 2	Yield % <sup>a</sup>
1	<i>N</i> -MeAla	Ser	59	5	<i>N</i> -MeAla	<i>allo</i> -Thr	40
2	Pip	Ser	55	6	Pip	<i>allo</i> -Thr	37
3	4-MePip	Ser	43	7	4-MePip	<i>allo</i> -Thr	36
4	4- <i>i</i> PrPip	Ser	45				

<sup>a</sup>Isolated yield over 4 steps after flash chromatography

Initially, we had hoped to complete the ADEP synthesis with a single deprotection and acylation of the peptidolactone (**19**) with fully formed *N*-E-2-heptenyldifluorophenylalanine (**20**). Unfortunately, complete racemization of the phenylalanine residue was observed in the coupling reaction when either TPTU and HOBt or HATU were used to activate the *N*-E-2-heptenyldifluorophenylalanine (Figure 5.7). We therefore elected to append the ADEP side

chain using a 4 step process of iterative *N*-terminal deprotections and HATU facilitated acylations, first with Boc-3,5-difluorophenylalanine and secondly with *E*-2-heptenoic acid (Table 5.3). The final ADEP products (**1a-g**) were isolated in >95% purity via silica gel chromatography in 50-71% yield over four steps from **19**.

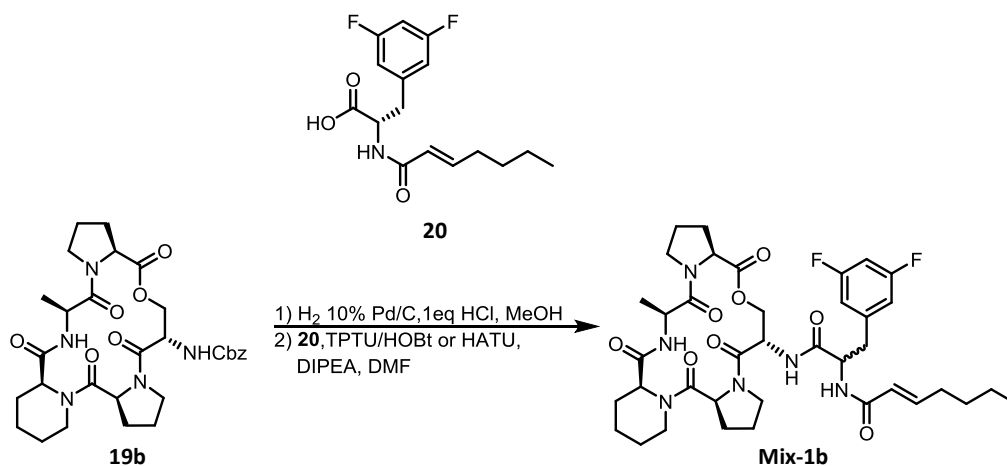


Figure 5.7 – Peptidolactone acylation with fully assembled side chain.

**Table 5.4 – Sequential acylation of peptidoactones**

1) H<sub>2</sub>, 10% Pd/C, 1eq HCl, MeOH  
2) N-Boc-(3,5-Difluoro)Phe-OH, HATU, DIPEA, DMF  
3) TFA, DCM  
4) (*E*)-2-heptenoic acid, HATU, DIPEA, DMF

**19** → **1**

Entry	Residue 1	Residue 2	Yield % <sup>a</sup>	Entry	Residue 1	Residue 2	Yield % <sup>a</sup>
1	<i>N</i> -MeAla	Ser	50	5	<i>N</i> -MeAla	<i>allo</i> -Thr	68
2	Pip	Ser	68	6	Pip	<i>allo</i> -Thr	71
3	4-MePip	Ser	61	7	4-MePip	<i>allo</i> -Thr	69
4	4- <i>i</i> PrPip	Ser	63				

<sup>a</sup>Isolated yield over 4 steps after flash chromatography

Although the strategy used to synthesize the ADEPs described in this study generally follows that which has been outlined in the literature,<sup>1-4</sup> some important advances were made in the course of our work. The use of isocyanide based multicomponent reactions to construct tripeptides containing a variety of substituted pipecolate residues has been demonstrated, and the configurational stability of chiral isocyanoacetates in Joullié-Ugi 3 component reactions has been rigorously validated. We have also optimized a key coupling reaction. Synthesis of the pentapeptolides (**18**) can now be achieved in greatly improved yield and in much shorter reaction duration. We have also exploited opportunities to execute multistep sequences of reactions without intermediate purification. These improvements to ADEP synthesis have greatly improved the overall efficiency of the process. It is now quite reasonable for an individual to produce up to 500 mg of **1a-g** (Figure 5.8) in a matter of 2-3 weeks.



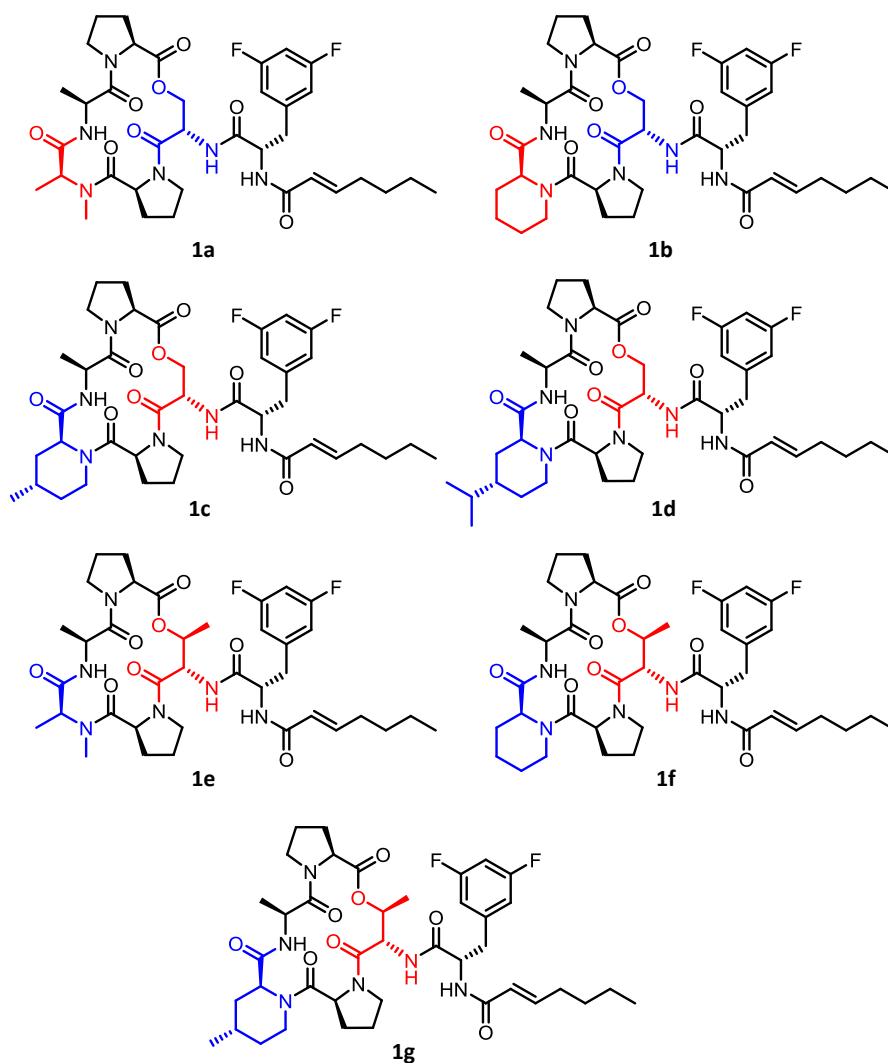


Figure 5.8 – Structures of ADEP molecules containing conformationally constrained amino acids

## Experimental Contributions

All synthesis and analysis was performed by Daniel Carney with the assistance of Brown University undergraduate student, Jonathan Truong.

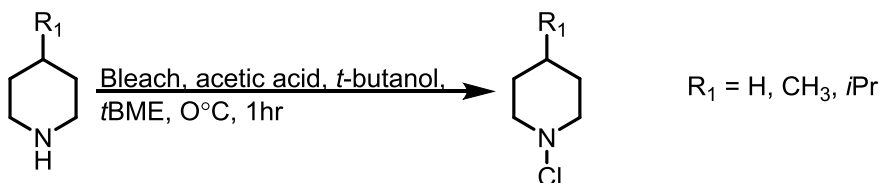
## Experimental

**Synthesis General:** All commercially available reagents were used without further purification.

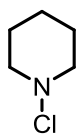
All reactions were conducted in oven dried glassware, under ambient atmosphere, using dry solvents unless otherwise stated. NMR chemical shifts were referenced to residual solvent peaks:  $\text{CDCl}_3$  ( $\delta = 7.27$  ppm for  $^1\text{H-NMR}$  and 77.00 ppm for  $^{13}\text{C-NMR}$ ), acetone- $d_6$  ( $\delta = 2.05$  for

$^1\text{H-NMR}$  and  $\delta = 29.92$  for  $^{13}\text{C-NMR}$ ). 2D NOSEY spectra were acquired for compounds existing as simple mixtures of rotamers in solution

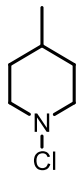
#### N-chlorination general procedure



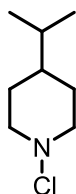
*N*-chloropiperidines were prepared according to literature procedures<sup>4</sup>. A piperidine (20 mmol) and *t*-butanol (.957 mL, 10 mmol) were dissolved in *t*-butyl methyl ether (tBME) (50 mL) and cooled to 0°C. The reaction was sealed with a septum and connected to a nitrogen line. Commercial bleach (0.5 M NaOCl) (40 mL, 20 mmol) and acetic acid (1.14 mL, 20 mmol) were added by syringe **slowly and simultaneously with vigorous stirring**. After 1 hour the reaction was quenched with water (25 mL) and the biphasic solution was transferred to a separatory funnel. The phases were partitioned and the organic phase washed once with brine. Evaporation of the solvent gave a colorless liquid, which was used without further purification.



***N*-chloropiperidine:** 2.02 g, 84% yield.  $^1\text{H-NMR}$  (300 MHz, chloroform-*d*)  $\delta = 3.83\text{-}2.53$  (br. m, 4 H), 1.72 (quin,  $J = 5.7$  Hz, 4 H), 1.61-1.24 (br. m, 2 H).  $^{13}\text{C-NMR}$  (101 MHz, chloroform-*d*)  $\delta = 63.9, 27.5, 22.9$ . LRMS (EI): 119  $[\text{M}]^+$ , 84  $[\text{M-Cl}]^+$ .

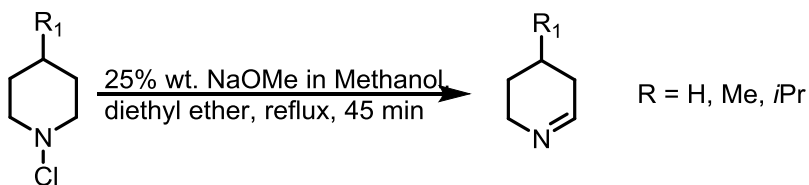


**4-methyl-N-chloropiperidine:** 2.38 g, 89% yield.  $^1\text{H-NMR}$  (400 MHz, chloroform-d)  $\delta$  = 3.42 (d,  $J$  = 10.1 Hz, 2 H), 2.97-2.76 (m, 2 H), 1.68 (d,  $J$  = 11.9 Hz, 2 H), 1.57 - 1.35 (m, 3 H), 0.91 (d,  $J$  = 5.8 Hz, 3 H).  $^{13}\text{C-NMR}$  (101 MHz, chloroform-d)  $\delta$  = 63.3, 36.0, 29.4, 21.2. LRMS (EI): 133  $[\text{M}]^+$ , 98  $[\text{M}-\text{Cl}]^+$ .



**4-isopropyl-N-chloropiperidine:** 2.76g, 84 % yield.  $^1\text{H-NMR}$  (400 MHz, chloroform-d)  $\delta$  = 3.47 (d,  $J$  = 11.1 Hz, 2 H), 2.82 (t,  $J$  = 11.0 Hz, 2 H), 1.70 (d,  $J$  = 14.0 Hz, 1 H), 1.57 - 1.43 (m, 2 H), 1.41 (sxt,  $J$  = 6.9 Hz, 1 H), 1.17 - 1.05 (m, 1 H), 0.86 (d,  $J$  = 6.7 Hz, 6 H).  $^{13}\text{C-NMR}$  (101 MHz, chloroform-d)  $\delta$  = 63.6, 40.9, 32.0, 31.3, 19.7. LRMS (EI): 161  $[\text{M}]^+$ , 126  $[\text{M}-\text{Cl}]^+$ .

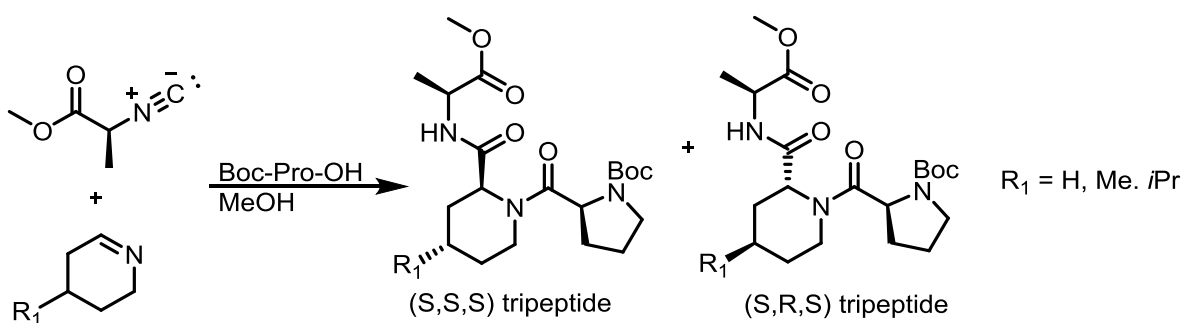
#### Dehydrohalogenation general procedure:



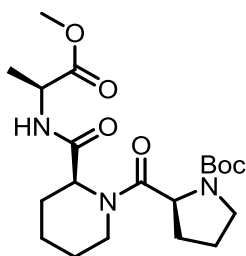
N-chloropiperidine (2.27 g, 17.0 mmol) was dissolved in diethyl ether (12 mL) and treated with sodium methoxide in methanol 25 wt. % (5 mL). The reaction was heated at reflux for 45 minutes, over the course of which a white precipitate formed. Once the reaction was complete, it was allowed to cool to room temperature after which a minimum volume of water was added

in order to dissolve the precipitate. The dehydropiperidine was extracted with diethyl ether (5 washes, ~1:1 water to ether in each wash) then dried over sodium sulfate. Removal of the solvent yielded a pale yellow oil, which was used immediately in Joullié-Ugi reactions assuming quantitative conversion.

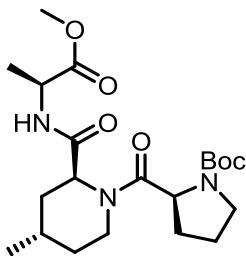
**Joullié-Ugi reaction general procedure:**



The crude dehydropiperidine (1 equivalent) was dissolved in methanol at a concentration of 1.0 M and then treated with Boc-Proline (1 equivalent) followed by methyl (*S*)-2-isocyanopropanoate (1 equivalent). The reaction was allowed to proceed for 7 days at room temperature, after which the solvent was removed and the concentrated reaction added directly to a silica gel column. The diastereomeric products are eluted with a hexanes/ethyl acetate solvent gradient. In each case, the undesired (*S,R,S*) tripeptide eluted first followed by the desired (*S,S,S*) tripeptide. Removal of the solvent from the (*S,S,S*) tripeptides revealed colorless oils, whereas the (*S,R,S*) tripeptides were white solids.

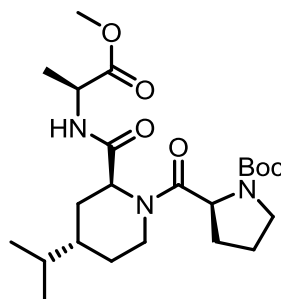


**tert-butyl (S)-2-((S)-2-(((S)-1-methoxy-1-oxopropan-2-yl)carbamoyl)piperidine-1-carbonyl)pyrrolidine-1-carboxylate (iv-a):** 39% yield.  $^1\text{H-NMR}$  mixture of 2 rotamers ~2:1 ratio (400 MHz, chloroform- $d$ )  $\delta$  = 8.46 (d,  $J$  = 7.3 Hz, 2 H), 6.67-6.52 (m, 1 H), 5.22-5.16 (m, 1 H), 4.77-4.56 (m, 6 H), 4.48 (quin,  $J$  = 7.3 Hz, 3 H), 3.93-3.78 (m, 1 H), 3.78-3.61 (m, 9 H), 3.61-3.52 (m, 2H), 3.52-3.38 (m, 3H), 3.21-3.07 (m, 1 H), 2.57 (d,  $J$  = 13.6 Hz, 2 H), 2.48 (dt,  $J$  = 2.6, 13.2 Hz, 2 H), 2.31-2.20 (m, 1 H), 2.20-2.04 (m, 5 H), 2.04-1.94 (m, 1H), 1.94-1.83 (m, 6H), 1.83-1.74 (m, 1H), 1.74-1.58 (m, 8 H) 1.58-1.51 (m, 1H), 1.51-1.33, (m, 38 H), 1.33-1.16 (m, 2 H), 0.92-0.80 (m, 1 H).  $^{13}\text{C-NMR}$  (101 MHz, chloroform- $d$ )  $\delta$  = 173.3, 171.5, 169.8, 154.5, 80.0, 56.3, 55.6, 52.1, 48.9, 46.8, 39.7, 29.6, 28.5, 28.4, 26.1, 24.9, 24.7, 20.6, 16.5. HRMS (FAB) predicted for  $[\text{C}_{20}\text{H}_{33}\text{N}_3\text{O}_6 + \text{Na}]^+$ :434.2267, Found: 434.2252.



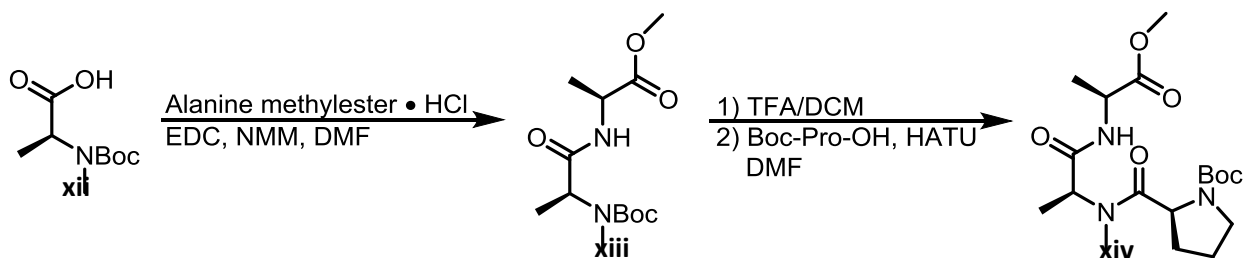
**tert-butyl (S)-2-((2S,4S)-2-(((S)-1-methoxy-1-oxopropan-2-yl)carbamoyl)-4-methylpiperidine-1-carbonyl)pyrrolidine-1-carboxylate (iv-b):** 41% yield.  $^1\text{H-NMR}$  mixture of 2 rotamers ~2:1 ratio (400 MHz, chloroform- $d$ )  $\delta$  = 8.46 (d,  $J$  = 7.0 Hz, 2 H), 6.66-6.56 (m, 1H), 5.27-5.17 (m, 1 H), 4.76-4.58 (m, 6 H), 4.52-4.41 (m, 2 H), 3.93-3.76 (m, 1 H), 3.76-3.67 (m, 9 H), 3.61-3.52 (m, 2 H), 3.50-3.38 (m, 3 H), 3.20-3.08 (m, 1 H), 2.6-2.43 (m, 4 H), 2.30-2.18 (m, 1 H), 2.18-2.05 (m, 5 H), 2.04-

1.93 (m, 2 H), 1.93-1.81 (m, 7 H), 1.79-1.69 (m, 2 H), 1.66-1.58 (m, 2 H), 1.49-1.44, (m, 13 H), 1.44-1.39 (m, 25 H), 1.37 (d,  $J = 7.0$  Hz, 3 H), 1.08-.98 (m, 4 H), .96-.89 (m, 9 H).  $^{13}\text{C}$ -NMR (101 MHz, chloroform- $d$ )  $\delta = 173.3, 171.5, 169.9, 154.5, 80.0, 56.4, 55.6, 52.1, 52.1, 48.9, 48.0, 46.8, 39.6, 34.3, 33.1, 29.6, 28.5, 28.4, 28.4, 27.1, 24.9, 21.8, 16.4$ . HRMS (FAB) Predicted for  $[\text{C}_{21}\text{H}_{35}\text{N}_3\text{O}_6 + \text{Na}]^+$ : 448.2424 Found: 448.2411.



**tert-butyl (S)-2-(((2S,4S)-4-isopropyl-2-(((S)-1-methoxy-1-oxopropan-2-yl)carbamoyl)piperidine-1-carbonyl)pyrrolidine-1-carboxylate (iv-c):** 44% yield.  $^1\text{H}$ -NMR mixture of 2 rotamers  $\sim 2:1$  ratio (600 MHz, chloroform- $d$ )  $\delta = 8.46$  (d,  $J = 7.0$  Hz, 2 H), 6.62 (d,  $J = 7.3$  Hz, 1 H), 5.28 - 5.20 (m, 1 H), 4.77 - 4.57 (m, 6 H), 4.50 - 4.40 (m, 2 H), 3.90 - 3.82 (m, 1 H), 3.77 - 3.61 (m, 9 H), 3.61 - 3.53 (m, 2 H), 3.51 - 3.39 (m, 3 H), 3.12 (q,  $J = 11.8$  Hz, 1 H), 2.59 (d,  $J = 13.2$  Hz, 2 H), 2.47 (dt,  $J = 2.9, 13.2$  Hz, 2 H), 2.28-2.19 (m, 1 H), 2.19 - 2.05 (m, 4 H), 2.02-1.92 (m, 1 H), 1.91 - 1.82 (m, 5 H), 1.77-1.53 (m, 4 H), 1.51-1.33 (m, 39 H), 1.32 - 1.18 (m, 5 H), 1.18 - 0.97 (m, 5 H), 0.92 - 0.84 (m, 20 H).  $^{13}\text{C}$ -NMR (151 MHz, chloroform- $d$ )  $\delta = 173.3, 171.4, 170.0, 154.5, 79.9, 57.4, 57.0, 56.5, 55.6, 52.4, 52.4, 52.1, 52.0, 48.9, 48.0, 46.8, 46.7, 46.5, 43.1, 39.7, 38.2, 37.7, 37.7, 32.3, 32.2, 31.9, 29.9, 29.9, 29.6, 28.9, 28.7, 28.4, 28.4, 28.3, 28.1, 24.9, 23.8, 23.3, 19.6, 19.5, 19.4, 19.3, 19.1, 16.4$ . HRMS (FAB) Predicted for  $[\text{C}_{23}\text{H}_{39}\text{N}_3\text{O}_6 + \text{Na}]^+$ : 476.2731, Found: 476.2742.

### Synthesis of *N*-Boc-Pro-*N*-MeAla-Ala-OMe



*N*-Boc-*N*-MeAla-OH (**xii**) (1.11 g, 5.46 mmol) and alanine methyl ester hydrochloride (0.762 g, 5.46 mmol) were dissolved in DMF (2.5 mL). Once homogeneous, EDC (1.20 g, 6.28 mmol) and HOBT (0.919 g, 6.00 mmol) were added followed by NMM (3.5 mmol). The reaction was allowed to proceed for 16 hours, after which the reaction solution was diluted with 100 mL of ethyl acetate. The ethyl acetate solution was extracted 3x 1M HCl, 3x saturated aqueous NaHCO<sub>3</sub>, 1x Brine, then dried over sodium sulfate. Final removal of solvent revealed the protected dipeptide (**xiii**) as a colorless oil, which was used without further purification. Yield: 1.17 g, 74%. <sup>1</sup>H-NMR (600 MHz, chloroform-*d*) δ = 6.84 - 6.26 (m, 1 H), 6.48 (m, 1 H), 4.91 - 4.62 (m, 1 H), 4.57 - 4.38 (m, 1 H), 3.73 (s, 3 H), 2.77 (br. s., 3 H), 1.48 (s, 9 H), 1.37 (d, *J* = 7.3 Hz, 3 H), 1.33 (d, *J* = 7.0 Hz, 3 H). <sup>13</sup>C-NMR (151 MHz, chloroform-*d*) δ = 173.1, 171.0, 156.3, 80.6, 53.4, 52.4, 47.9, 30.0, 28.3, 18.4, 13.5. HRMS (ESI) Predicted for [C<sub>13</sub>H<sub>24</sub>N<sub>2</sub>O<sub>5</sub> + Na]<sup>+</sup>: 311.1577, Found: 311.1573.

Boc removal from the protected dipeptide (**xiii**) was affected with 40% TFA in DCM. Upon complete conversion of the starting material, the reaction was concentrated by blowing with a stream of nitrogen followed by evaporation under high vacuum.

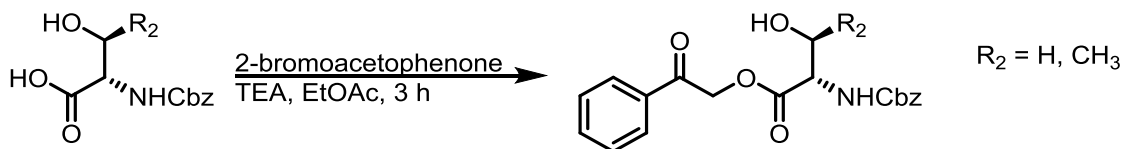
Without further purification, The TFA salt of the dipeptide free base was dissolved in DMF along with Boc-Pro-OH. Once homogenous, HATU was added to the solution followed by diisopropyl

ethylamine. The reaction was allowed to proceed over night, after which the DMF was removed *in vacuo*. The oily residue was diluted with ethyl acetate and subsequently extracted 3x 1M HCl, 3x saturated aqueous NaHCO<sub>3</sub>, 1x Brine, then dried over sodium sulfate. The protected tripeptide (**xiv**) was isolated by silica gel chromatography using an ethyl acetate in hexanes solvent gradient. Final removal of solvent revealed the desired product as a colorless oil. <sup>1</sup>H-NMR mixture of 3 rotamers ~ 1:1:0.6 ratio (600 MHz, acetone-d<sub>6</sub>) δ = 8.30 (d, *J* = 6.6 Hz, 1 H), 7.25 (d, *J* = 7.2 Hz, 1 H), 7.18 (d, *J* = 6.6 Hz, 1 H), 5.19 (q, *J* = 7.2 Hz, 1 H), 5.00 (q, *J* = 7.3 Hz, 1 H), 4.93 (q, *J* = 6.9 Hz, 1 H), 4.87 (dd, *J* = 5.1, 7.7 Hz, 1 H), 4.66 (dd, *J* = 3.4, 8.5 Hz, 2 H), 4.41 (sxt, *J* = 7.2 Hz, 3 H), 3.70 - 3.68 (m, 5 H), 3.66 (s, 4 H), 3.52 - 3.46 (m, 4 H), 3.44 - 3.33 (m, 2 H), 3.05 (s, 2 H), 3.01 (s, 3 H), 2.70 (s, 4 H), 2.35 - 2.28 (m, 1 H), 2.27 - 2.20 (m, 2 H), 2.15 - 2.10 (m, 1 H), 2.01 - 1.92 (m, 2 H), 1.92 - 1.82 (m, 6 H), 1.45 (s, 10 H), 1.45 - 1.42 (m, 7 H), 1.40 (d, *J* = 7.4 Hz, 4 H), 1.38 (s, 9 H), 1.37 - 1.28 (m, 15 H) <sup>13</sup>C-NMR (101 MHz, acetone-d<sub>6</sub>) δ = 164.3, 163.8, 163.7, 163.3, 161.9, 161.7, 161.1, 145.5, 144.8, 144.4, 70.6, 69.4, 69.4, 47.9, 46.1, 46.0, 44.0, 42.6, 42.5, 42.3, 39.3, 38.9, 37.9, 37.7, 37.4, 28.8, 21.7, 20.9, 20.7, 20.7, 18.8, 18.7, 18.7, 15.6, 14.8, 14.0, 7.9, 7.6, 5.1, 4.2, 4.0. HRMS (FAB) predicted for [C<sub>18</sub>H<sub>31</sub>N<sub>3</sub>O<sub>6</sub> + Na]<sup>+</sup>: 408.2111, Found: 408.2120.

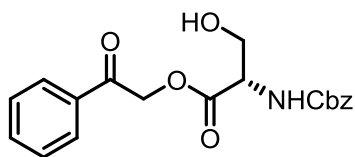
**Tripeptide Saponification General Procedure** The tripeptide (1 equivalent) was dissolved in 1:1 THF:water at a concentration of 0.4M. Once the solution was homogeneous, LiOH·H<sub>2</sub>O (2.75 equivalents) was added and allowed to react for 30 minutes. Upon complete conversion of the starting material, the reaction was quenched with 1M HCl (4.1 equivalents). The reaction mixture was then transferred to a separatory funnel and the product extracted by washing 4 times with DCM. DCM extracts were pooled and dried over sodium sulfate. The concentrated tripeptide free acid was used without further purification.



### Phenacyl protection

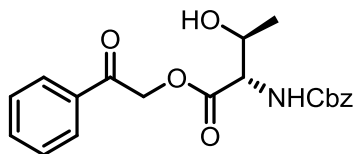


Cbz-amino acid (1 equivalent) was dissolved in ethyl acetate at a concentration of 0.4 M and cooled to 0°C. Once the solution was homogeneous, 2-bromoacetophenone (1.1 equivalent) was added followed by slow addition of triethylamine (2 equivalents) to initiate the reaction. The reaction was stirred at room temperature for 3 hours and then diluted to 3X the original reaction volume with ethyl acetate. The reaction solution was then transferred to a separatory funnel and extracted 3x 1M HCl, 1x saturated aqueous NaHCO<sub>3</sub>, 1x Brine, then dried over sodium sulfate. The z-serine phenacyl ester was purified by recrystallization from ethyl acetate. The Cbz-*allo*-threonine phenacyl ester was purified by silica gel chromatography using a solvent gradient of 40-60% EtOAc in hexanes. Final removal of solvent revealed a white solid.



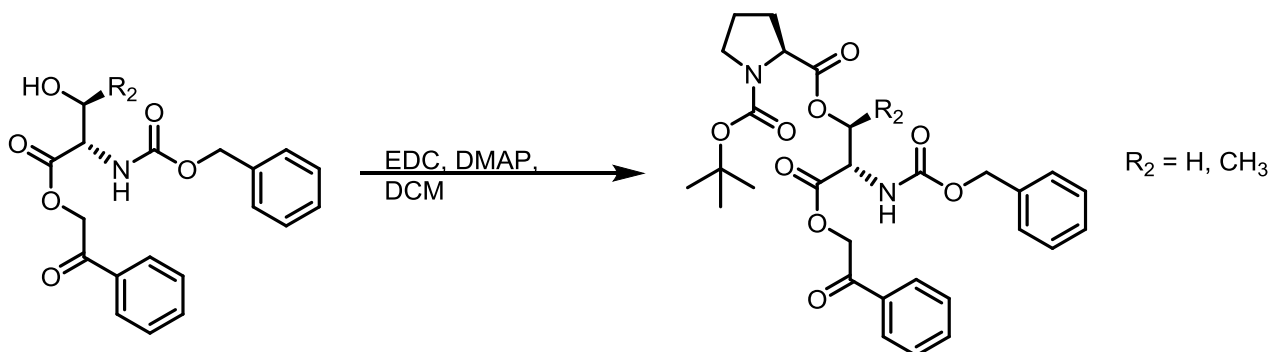
**Cbz-serine phenacyl ester (vi-a):** Yield: 68%. <sup>1</sup>H-NMR (400 MHz, chloroform-d)  $\delta = 7.93$  (d,  $J = 7.5$  Hz, 2 H), 7.67 (t,  $J = 7.4$  Hz, 1 H), 7.53 (t,  $J = 7.8$  Hz, 2 H), 7.46 - 7.30 (m, 5 H), 5.74 (d,  $J = 16.6$  Hz, 1 H), 5.80 (d,  $J = 8.3$  Hz, 1 H), 5.33 (d,  $J = 16.6$  Hz, 1 H), 5.15 (s, 2 H), 4.64 (d,  $J = 8.3$  Hz, 1 H), 4.35 (d,  $J = 11.8$  Hz, 1 H), 4.01 - 3.81 (m, 1 H), 3.66 (dd,  $J = 4.9, 10.4$  Hz, 1 H). <sup>13</sup>C-NMR (101 MHz, chloroform-d)  $\delta = 192.9, 170.4, 156.1, 145.5, 136.2, 134.7, 133.3, 129.1, 128.5, 128.2, 128.0,$

128.0, 77.2, 67.1, 66.7, 64.0, 56.5. HRMS (FAB) Predicted for  $[C_{19}H_{19}NO_6 + Na]^+$ : 380.1110, Found: 380.1104.



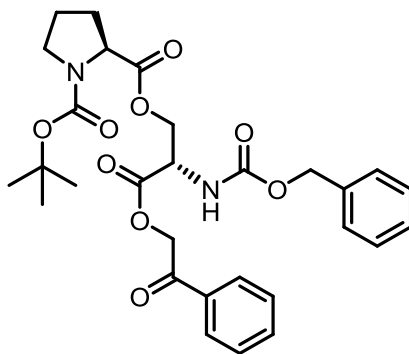
**Cbz-*allo*-threonine phenacyl ester (vi-b):** Yield: 69%.  $^1H$ -NMR (400 MHz, chloroform-*d*)  $\delta$  = 7.91 (d,  $J$  = 7.3 Hz, 2 H), 7.72 - 7.61 (m, 1 H), 7.58 - 7.47 (m, 2 H), 7.44 - 7.31 (m, 5 H), 5.88 (d,  $J$  = 8.3 Hz, 1 H), 5.50 (s, 2 H), 5.15 (s, 2 H), 4.51 (dd,  $J$  = 4.2, 8.5 Hz, 1 H), 4.25 - 4.08 (m, 1 H), 3.75 (d,  $J$  = 8.3 Hz, 1 H), 1.43 (d,  $J$  = 6.6 Hz, 3 H).  $^{13}C$ -NMR (101 MHz, chloroform-*d*)  $\delta$  = 192.5, 169.6, 156.1, 136.1, 134.5, 133.3, 129.0, 128.5, 128.1, 128.0, 127.9, 69.4, 67.1, 66.7, 60.0, 19.5. HRMS (FAB) Predicted for  $[C_{20}H_{21}NO_6 + Na]^+$ : 394.1267, Found: 394.1260.

### Proline esters



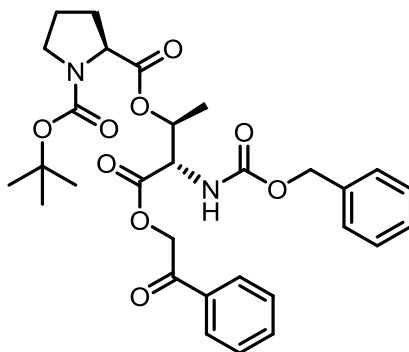
Cbz-amino acid phenacyl ester (1 equivalent) and Boc-proline (1.1 equivalents) were dissolved in DCM at a concentration of 2 M with respect to the Cbz-amino acid phenacyl ester. Once homogeneous, EDC (1 equivalent) and dimethylaminopyridine (0.1 equivalents) were added. Additional EDC-HCL (0.190 g, 0.25 equivalents) was added every 2 hours until the starting material was consumed. Upon completion of the reaction, the solvent was removed and the product residue was diluted with EtOAc and extracted 3 x 1 M HCl, 3 x Saturated  $NaHCO_3$ , 1 x

Brine, then dried over sodium sulfate. The product ester was isolated by silica gel chromatography (40-60% EtOAc in Hexanes). Final removal of the solvent yielded a colorless oil.



**2-((S)-2-(((benzyloxy)carbonyl)amino)-3-oxo-3-(2-oxo-2-phenylethoxy)propyl) 1-(tert-butyl)**

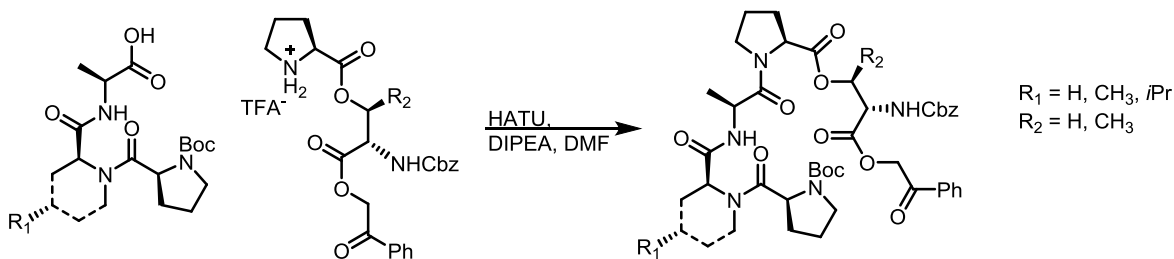
**(S)-pyrrolidine-1,2-dicarboxylate (vii-a):** Yield: 92% <sup>1</sup>H-NMR mixture of 2 rotamers ~1:1 ratio (600 MHz, chloroform-d) δ = 7.89 (t, *J* = 7.2 Hz, 4 H), 7.63 (q, *J* = 7.3 Hz, 2 H), 7.54 - 7.47 (m, 4 H), 7.41 - 7.30 (m, 10 H), 6.01 (d, *J* = 8.8 Hz, 1 H), 5.60 (d, *J* = 8.1 Hz, 1 H), 5.53 - 5.43 (m, 2 H), 5.38 (dd, *J* = 8.1, 16.1 Hz, 2 H), 5.22 - 5.07 (m, 4 H), 4.90-4.81 (m, 2 H), 4.71 - 4.60 (m, 3 H), 4.54 (dd, *J* = 3.7, 11.4 Hz, 1 H), 4.31 (dd, *J* = 4.0, 8.4 Hz, 1 H), 4.28 (dd, *J* = 4.0, 8.8 Hz, 1 H), 3.58 - 3.51 (m, 1 H), 3.48 (ddd, *J* = 5.1, 7.8, 10.2 Hz, 1 H), 3.46 - 3.40 (m, 1 H), 3.39 - 3.34 (m, 1 H), 2.26 - 2.13 (m, 2 H), 2.08 - 2.00 (m, 2 H), 1.99 - 1.93 (m, 1 H), 1.91 - 1.80 (m, 3 H), 1.42 (s, 9 H), 1.39 (s, 9 H). <sup>13</sup>C-NMR mixture of 2 rotamers ~1:1 ratio (151 MHz, chloroform-d) δ = 190.9, 190.6, 172.8, 172.4, 169.0, 168.9, 156.0, 155.7, 154.6, 153.7, 136.2, 135.9, 134.1, 133.9, 133.7, 128.9, 128.9, 128.5, 128.4, 128.2, 128.2, 128.0, 128.0, 127.7, 127.7, 80.0, 79.9, 67.2, 67.0, 66.9, 64.3, 64.3, 59.1, 58.9, 53.3, 46.6, 46.2, 30.7, 29.9, 28.3, 28.2, 24.3, 23.5. HRMS (FAB) Predicted for (C<sub>29</sub>H<sub>34</sub>N<sub>2</sub>O<sub>9</sub> + Na)<sup>+</sup>:577.2162 Found:577.2156.



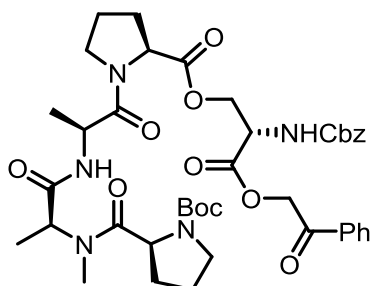
**2-((2S,3S)-3-(((benzyloxy)carbonyl)amino)-4-oxo-4-(2-oxo-2-phenylethoxy)butan-2-yl) 1-(tert-butyl) (S)-pyrrolidine-1,2-dicarboxylate (vii-b):** Yield: 95%. <sup>1</sup>H-NMR mixture of 2 rotamers ~ 1:1 ratio (600 MHz, chloroform-d)  $\delta$  = 7.90 (d,  $J$  = 7.7 Hz, 4 H), 7.68-7.60 (m, 2 H), 7.57 - 7.46 (m, 4 H), 7.43 - 7.29 (m, 10 H), 5.95 (d,  $J$  = 9.5 Hz, 1 H), 5.65 - 5.51 (m, 3 H), 5.49 - 5.40 (m, 2 H), 5.37 - 5.25 (m, 2 H), 5.21 - 5.04 (m, 4 H), 4.91 (dd,  $J$  = 2.9, 8.8 Hz, 1 H), 4.85 (dd,  $J$  = 2.9, 9.2 Hz, 1 H), 4.28 (dd,  $J$  = 4.0, 8.4 Hz, 1 H), 4.19 (dd,  $J$  = 4.0, 8.4 Hz, 1 H), 3.60 - 3.51 (br. s., 1 H), 3.50 - 3.39 (m, 2 H), 3.35 (td,  $J$  = 7.5, 10.4 Hz, 1 H), 2.16 - 2.08 (m, 2 H), 2.07 - 2.01 (m, 2 H), 2.00 - 1.91 (m, 2 H), 1.88 - 1.77 (m, 2 H), 1.56 - 1.45 (m, 8 H), 1.44 (s, 8 H), 1.42 (s, 8 H). <sup>13</sup>C-NMR mixture of 2 rotamers ~1:1 ratio (151 MHz, chloroform-d)  $\delta$  = 190.8, 172.5, 172.1, 168.7, 156.0, 155.9, 154.7, 153.8, 136.0, 134.2, 134.0, 133.9, 133.8, 129.0, 128.9, 128.5, 128.4, 128.2, 128.1, 128.0, 128.0, 127.7, 79.9, 71.2, 70.8, 67.2, 67.0, 66.9, 66.7, 59.0, 58.9, 56.9, 46.6, 46.3, 30.5, 29.8, 28.4, 28.3, 24.3, 23.5, 15.6, 15.3. HRMS (FAB) Predicted for  $[C_{30}H_{36}N_2O_9 + Na]^+$ : 591.2319, Found: 591.2335.

**Proline Ester Boc Group Removal General Procedure:** The Ser-Pro ester (or *allo*-Thr-Pro ester) was treated with 40% TFA in DCM at a concentration of 0.6 M. Upon complete conversion of the starting material, the reaction was concentrated by blowing with a stream of nitrogen then by evaporation under high vacuum. The ester free base was used without further purification.

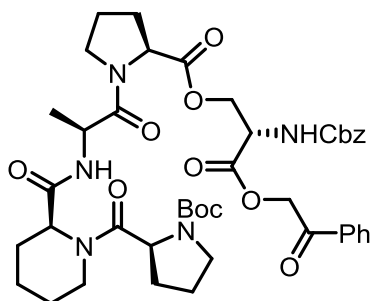
## Pentapeptolides



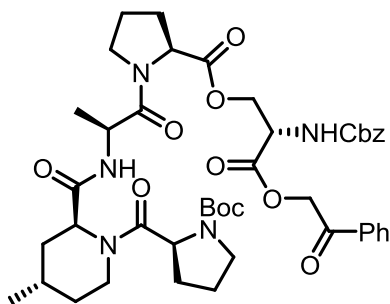
*Preparation General Procedure:* An equimolar amount of a tripeptide free acid and a proline ester free base were combined in DMF at a concentration of 0.25 M. Once the reaction solution was homogeneous, HATU (1.1 equivalents) was added followed by DIPEA (3.0 equivalents). The reaction solution turned bright yellow upon addition of the tertiary amine base. After 1 hour, the reaction was diluted with EtOAc (20x volume of DMF) and extracted 3 x 1 M HCl, 3 x saturated NaHCO<sub>3</sub>, 1 x Brine, then dried over sodium sulfate. The pentapeptolide products were purified by silica gel chromatography using a gradient of 0-20% acetone in EtOAc.



***tert*-butyl(S)-2-(((S)-1-(((S)-1-((S)-2-(((S)-2-(((benzyloxy)carbonyl)amino)-3-oxo-3-(2-oxo-2-phenylethoxy)propoxy)carbonyl)pyrrolidin-1-yl)-1-oxopropan-2-yl)amino)-1-oxopropan-2-yl)(methyl)carbamoyl)pyrrolidine-1-carboxylate:** Yield: 92%. HRMS (FAB) Predicted for [C<sub>41</sub>H<sub>53</sub>N<sub>5</sub>O<sub>12</sub> + Na]<sup>+</sup>: 830.3588, Found: 830.3568. Spectral data matched that previously reported.<sup>3</sup>

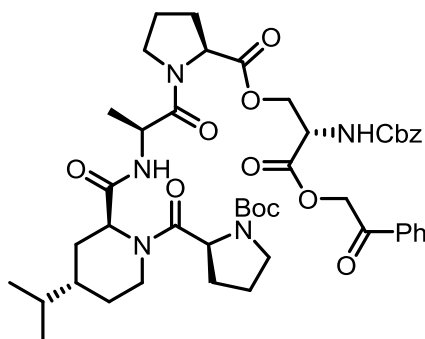


***tert*-butyl (S)-2-((S)-2-(((S)-1-((S)-2-(((S)-2-(((benzyloxy)carbonyl)amino)-3-oxo-3-(2-oxo-2-phenylethoxy)propoxy)carbonyl)pyrrolidin-1-yl)-1-oxopropan-2-yl)carbamoyl)piperidine-1-carbonyl)pyrrolidine-1-carboxylate:** Yield: 75%. HRMS (FAB) Predicted for  $[C_{43}H_{55}N_5O_{12} + Na]^+$ : 856.3745, Found: 856.3720. Spectral data matched that previously reported.<sup>3</sup>



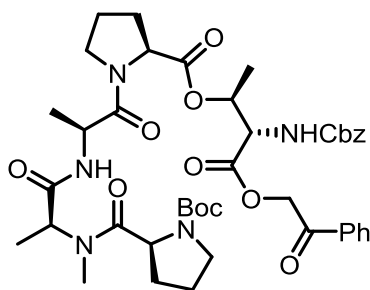
***tert*-butyl (2S)-2-((2S)-2-(((S)-1-((S)-2-(((S)-2-(((benzyloxy)carbonyl)amino)-3-oxo-3-(2-oxo-2-phenylethoxy)propoxy)carbonyl)pyrrolidin-1-yl)-1-oxopropan-2-yl)carbamoyl)-4-methylpiperidine-1-carbonyl)pyrrolidine-1-carboxylate.** Yield: 79% from protected tripeptide. HRMS (FAB) Predicted for  $[C_{44}H_{57}N_5O_{12} + Na]^+$ : 870.3901, Found: 870.3925. <sup>1</sup>H-NMR complex mixture of rotamers (600MHz, chloroform-*d*)  $\delta$  = 8.02-7.79 (m, 2 H), 7.72-7.79 (m 1 H), 7.57-7.43 (m, 2 H), 7.43-7.25 (m, 5 H), 6.92-6.34 (m, 1 H), 5.94-5.66 (m, 1 H), 5.65-4.92 (m, 5 H), 4.90-4.37 (m, 6 H), 3.94-2.94 (m, 6 H), 2.54-1.57 (m, 11 H), 1.50-1.33 (m, 10 H), 1.33-1.16 (m, 3 H), 1.10-0.66 (m, 4 H). <sup>13</sup>C-NMR (151 MHz, chloroform -*d*)  $\delta$  = 190.9, 172.3, 172.0, 171.8, 171.2, 171.2, 0.66 (m, 4 H).

170.1, 169.8, 168.9, 155.9, 154.5, 136.2, 134.1, 134.1, 134.0, 133.8, 129.1, 129.0, 128.9, 128.5, 128.2, 128.1, 128.0, 127.9, 127.9, 127.8, 127.7, 127.6, 80.0, 79.4, 79.3, 67.1, 66.9, 66.9, 64.3, 64.2, 59.1, 59.0, 58.9, 57.2, 57.0, 56.1, 55.5, 53.4, 53.2, 52.5, 52.4, 48.3, 46.9, 46.8, 46.7, 46.6, 46.5, 43.2, 42.9, 39.6, 38.6, 34.5, 34.0, 33.7, 33.4, 33.2, 30.1, 29.5, 29.0, 28.9, 28.8, 28.5, 28.4, 27.2, 27.0, 24.9, 24.8, 23.8, 23.2, 21.9, 21.8, 17.7, 15.8.



**tert-butyl (2S)-2-((2S)-2-(((S)-1-((S)-2-(((S)-2-(((benzyloxy)carbonyl)amino)-3-oxo-3-(2-oxo-2-phenylethoxy)propoxy)carbonyl)pyrrolidin-1-yl)-1-oxopropan-2-yl)carbonyl)-4-**

**isopropylpiperidine-1-carbonyl)pyrrolidine-1-carboxylate:** Yield: 80% from protected tripeptide. HRMS (FAB) Predicted for  $[C_{46}H_{61}N_5O_{12} + Na]^+$ :898.4215, Found: 898.4219.  $^1H$ -NMR complex mixture of rotamers (600 MHz, chloroform-d)  $\delta$  = 8.01-7.80 (m, 2 H), 7.71-7.58 (m, 1 H), 7.57-7.43 (m, 2 H), 7.42-7.29 (m, 5 H), 6.95-6.25 (m, 1 H), 5.95-5.64 (m, 1 H), 5.64-5.08 (m, 4 H), 5.06-4.20 (m, 7 H), 4.15-2.92 (m, 6 H), 2.58-1.52 (m, 10 H), 1.51-1.34 (m, 10 H), 1.34-1.14 (m, 5 H), 1.09-0.63 (m, 7 H).  $^{13}C$ -NMR (151 MHz, chloroform-d)  $\delta$  = 190.9, 171.2, 170.2, 169.8, 168.9, 156.0, 154.6, 136.2, 134.1, 133.8, 129.1, 129.0, 128.9, 128.5, 128.3, 128.2, 128.0, 127.9, 127.7, 127.7, 80.0, 79.5, 79.4, 67.1, 66.9, 64.3, 64.2, 59.1, 58.9, 57.4, 57.0, 56.2, 53.2, 52.6, 46.8, 46.7, 46.5, 43.4, 38.6, 38.1, 38.0, 32.4, 32.2, 30.1, 29.6, 29.0, 28.9, 28.6, 28.4, 28.4, 28.3, 28.0, 24.9, 24.8, 24.7, 23.8, 23.3, 19.7, 19.5, 19.4, 19.1, 19.1, 17.8.



**tert-butyl (S)-2-(((S)-1-(((S)-1-((S)-2-((((2S,3S)-3-(((benzyloxy)carbonyl)amino)-4-oxo-4-(2-oxo-2-phenylethoxy)butan-2-yl)oxy)carbonyl)pyrrolidin-1-yl)-1-oxopropan-2-yl)amino)-1-**

**oxopropan-2-yl)(methyl)carbamoyl)pyrrolidine-1-carboxylate:** Yield: 84% from protected

tripeptide. HRMS (FAB) Predicted for  $[C_{42}H_{55}N_5O_{12} + Na]^+$ : 844.3739, Found: 844.3755.  $^1H$ -NMR

complex mixture of rotamers (600 MHz, chloroform- $d$ )  $\delta$  = 7.98-7.83 (m, 2 H), 7.68-7.58 (m, 1 H),

7.57-7.45 (m, 2 H), 7.43-7.29 (m, 5 H), 7.04-6.60 (m, 1 H), 6.27-5.52 (m, 2 H), 5.50-5.06 (m, 5 H),

5.05-4.26 (m, 5 H), 3.91-3.30 (m, 4 H), 3.08-2.80 (m, 2 H), 2.29-2.12 (m, 2 H), 2.12-2.00 (m, 2 H),

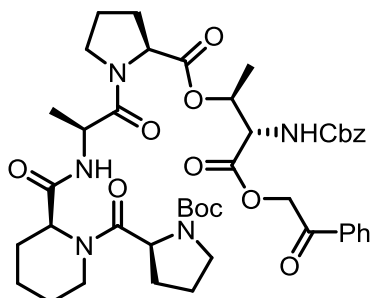
1.99-1.89 (m, 2 H), 1.89-1.72 (m, 2 H), 1.50-1.42 (m, 6 H), 1.42-1.36 (m, 7 H), 1.36-1.23 (m, 5 H).

$^{13}C$ -NMR (151 MHz, chloroform- $d$ )  $\delta$  = 190.8, 173.0, 171.5, 171.0, 168.8, 156.0, 154.5, 136.2,

134.1, 133.8, 129.0, 128.5, 128.2, 128.1, 128.1, 128.0, 127.9, 127.8, 127.7, 80.3, 79.4, 71.3, 71.0,

67.1, 66.9, 66.8, 59.4, 59.1, 59.0, 56.9, 56.7, 56.7, 55.2, 54.7, 47.5, 46.9, 46.8, 46.6, 30.2, 30.1,

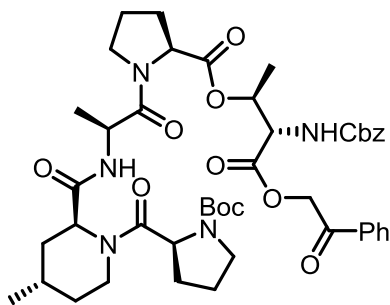
29.3, 29.1, 28.8, 28.6, 28.4, 28.4, 28.3, 24.9, 24.8, 24.0, 23.4, 17.6, 16.5, 15.3, 14.7, 13.3.



**tert-butyl (S)-2-(((S)-2-(((S)-1-((S)-2-((((2S,3S)-3-(((benzyloxy)carbonyl)amino)-4-oxo-4-(2-oxo-2-phenylethoxy)butan-2-yl)oxy)carbonyl)pyrrolidin-1-yl)-1-oxopropan-2-**



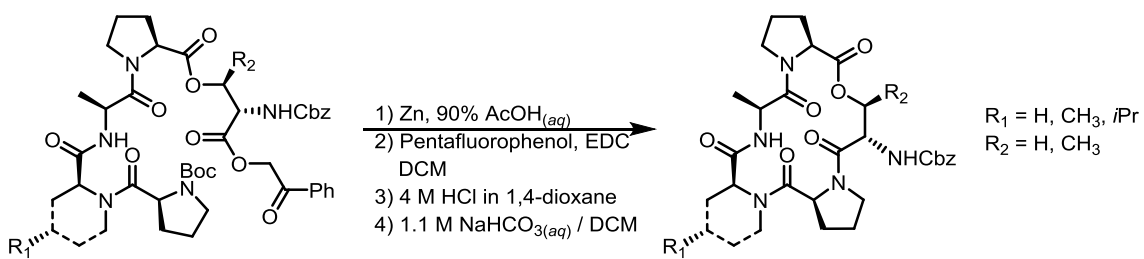
**yl)carbamoyl)piperidine-1-carbonyl)pyrrolidine-1-carboxylate:** Yield 87% from protected tripeptide. HRMS (FAB) Predicted for  $[C_{41}H_{57}N_5O_{12} + Na]^+$ : 870.3901, Found: 870.3925.  $^1H$ -NMR complex mixture of rotamers (600 MHz, chloroform -d)  $\delta$  = 8.08-7.83 (m, 2 H), 7.73-7.62 (m, 1 H), 7.59-7.49 (m, 2 H), 7.46-7.29 (m, 5 H), 7.07-6.02 (m, 1 H), 5.85-5.37 (m, 3 H), 5.37-5.02 (m, 4 H), 5.02-4.30 (m, 4 H), 3.97-2.99 (m, 5 H), 2.58-1.79 (m 10 H), 1.79-1.54 (m, 4 H), 1.54-1.34 (m, 15 H).  $^{13}C$ -NMR (151 MHz, chloroform -d)  $\delta$  = 190.8, 173.4, 172.4, 172.2, 171.5, 171.0, 170.6, 170.1, 169.8, 168.7, 156.0, 154.5, 153.9, 136.2, 134.1, 134.0, 133.8, 129.0, 128.9, 128.5, 128.2, 128.0, 127.7, 80.0, 79.4, 71.3, 70.9, 67.1, 66.8, 59.1, 58.8, 57.1, 56.7, 56.0, 55.5, 53.4, 52.2, 48.2, 46.9, 46.8, 46.7, 46.5, 43.5, 43.1, 39.8, 38.6, 30.1, 29.6, 29.1, 28.6, 28.5, 28.4, 28.4, 26.3, 25.8, 25.6, 25.3, 25.1, 24.9, 24.8, 23.9, 23.2, 20.7, 20.6, 20.5, 17.9, 15.9, 15.4, 15.3, 15.1.



**tert-butyl (2S)-2-((2S)-2-(((S)-1-((S)-2-((((2S,3S)-3-(((benzyloxy)carbonyl)amino)-4-oxo-4-(2-oxo-2-phenylethoxy)butan-2-yl)oxy)carbonyl)pyrrolidin-1-yl)-1-oxopropan-2-yl)carbamoyl)-4-methylpiperidine-1-carbonyl)pyrrolidine-1-carboxylate:** Yield: 80% from protected tripeptide. HRMS (FAB) Predicted for  $[C_{45}H_{59}N_5O_{12} + Na]^+$ : 884.4052, Found: 884.4034.  $^1H$ -NMR complex mixture of rotamers (600 MHz, chloroform-d)  $\delta$  = 8.02-7.81 (m, 2 H), 7.76-7.59 (m, 1 H), 7.59-7.44 (m, 2 H), 7.44-7.30 (m, 5 H), 7.20-5.96 (m, 1 H), 5.89-5.50 (m, 2 H), 5.50-5.34 (m, 1 H), 5.34-5.01 (m, 4 H), 4.97-4.32 (m, 4 H), 3.95-3.31 (m, 5 H), 3.24-2.39 (m, 1 H), 2.39-1.58 (m, 11 H), 1.57-1.20 (m, 16 H), 1.20-0.99 (m, 1 H), 0.99-0.79 (m, 3 H).  $^{13}C$ -NMR (151 MH, chloroform-d)  $\delta$  = 190.8, 190.7, 172.2, 172.0, 171.6, 171.5, 171.4, 170.9, 170.9, 170.1, 169.8, 169.7, 168.8, 168.7,

156.0, 154.4, 154.4, 153.8, 136.2, 134.1, 134.0, 133.8, 128.9, 128.9, 128.4, 128.3, 128.1, 128.1, 128.0, 127.9, 127.7, 127.6, 79.9, 79.3, 71.2, 70.9, 67.0, 66.8, 59.0, 59.0, 58.7, 57.1, 57.0, 56.6, 56.1, 55.5, 52.5, 52.4, 48.2, 46.9, 46.8, 46.7, 46.7, 46.6, 46.5, 43.2, 42.9, 39.6, 38.5, 34.5, 34.0, 33.7, 33.4, 33.2, 30.1, 29.5, 29.0, 28.6, 28.4, 28.4, 27.1, 27.0, 24.8, 24.7, 23.8, 23.2, 21.9, 21.8, 21.8, 17.8, 15.8, 15.3, 15.2, 15.0.

### Peptidolactones

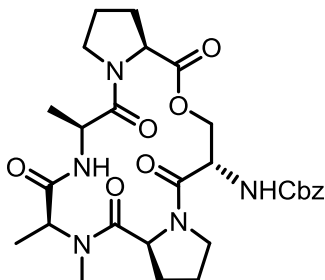


*Phenacyl deprotection general procedure:* The pentapeptolide was dissolved in 90% aqueous acetic acid at a concentration of 0.5M. Once homogeneous, Zinc dust (0.5g / mmol of peptolide) was added and allowed to react for 90 minutes, after which the reaction was diluted with ethyl acetate (5x reaction volume) and filtered through celite. The filtered zinc was then washed with additional ethyl acetate and water. The filtrate was transferred to a separatory funnel and partitioned. The Organic layer was subsequently washed 3 x 1M HCl and 1 x Brine. The organic layer was dried over sodium sulfate then concentrated *in vacuo* to a pale yellow oil. To remove residual acetic acid, the oily residue was diluted with toluene then concentrated *in vacuo*. This process was repeated a total of 3 times. The crude pentapeptolide free acid was then used without further purification.

*Pentafluorophenol esterification general procedure:* The pentapeptolide free acid was dissolved in DCM at a concentration of 0.4 M (based on the number of moles of protected pentapeptolide) and cooled to 0°C. Once the solution was homogeneous, pentafluorophenol (5

equivalents) was added followed by EDC·HCL (1.1 equivalents). The esterification was allowed to proceed for 1 hour, after which the solvent was removed *in vacuo* revealing a pale yellow oily residue. The crude pentafluorophenol ester was used without further purification.

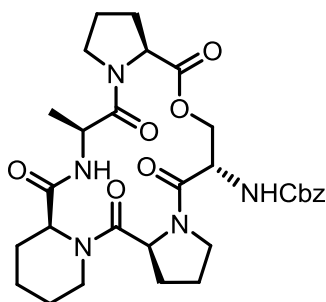
*Boc-removal / Macrocyclization:* The crude pentafluorophenol ester was treated with 4M HCl in 1,4-dioxane (2.5 mL / mmol of initial protected peptolide) and allowed to react for 30 minutes. The reaction solution was then diluted with DCM (160 mL/ mmol of initial protected peptolide) and added dropwise from an addition funnel into a flask containing DCM (225 mL / mmol of initial protected peptolide) and 1.1 M NaHCO<sub>3</sub> (140 mL/ mmol of initial protected peptolide) at a rate of ~2 drops / second. The reaction was allowed to proceed over night after which the reaction solution was transferred to a large separatory funnel and partitioned. The aqueous layer subsequently washed with fresh DCM. The organic layers were combined and dried over sodium sulfate. The macrocycle products were purified by silica gel chromatography with gradient of 0-30% acetone in EtOAc. Final removal of the solvent revealed a white foam.



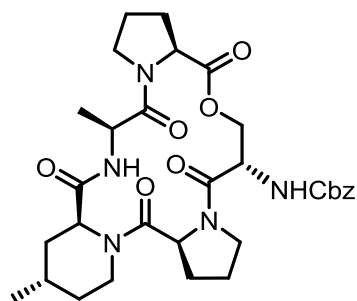
**benzyl ((6S,9S,11aS,17S,20aS)-6,9,10-trimethyl-5,8,11,16,20-pentaoxohexadecahydro-1H,5H,16H-dipyrrolo[2,1-c:2',1'-l][1]oxa[4,7,10,13]tetraazacyclohexadecin-17-yl)carbamate:**

Yield: 59% over 4 steps. <sup>1</sup>H-NMR (400 MHz, acetone-d<sub>6</sub>) δ = 7.43 (d, *J* = 9.5 Hz, 1 H), 6.76 - 6.69 (m, 2 H), 6.65 - 6.56 (m, 3 H), 6.21 (d, *J* = 9.8 Hz, 1 H), 4.51 (dd, *J* = 2.9, 8.4 Hz, 1 H), 4.43 (d, *J* = 11.8 Hz, 1 H), 4.30 (d, *J* = 11.8 Hz, 1 H), 4.21 - 4.12 (m, 2 H), 4.09 (q, *J* = 6.8 Hz, 1 H), 3.70 (d, *J* = 8.5 Hz, 1 H), 3.56 (dt, *J* = 1.8, 10.0 Hz, 1 H), 3.01 (dd, *J* = 10.2, 11.7 Hz, 1 H), 2.97 - 2.81 (m, 2 H),

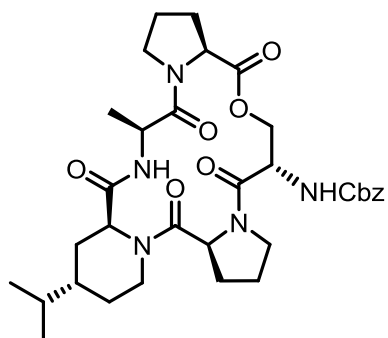
2.76 - 2.63 (m, 2 H), 2.00 (s, 3 H), 1.77 - 1.64 (m, 1 H), 1.57 - 1.43 (m, 1 H), 1.32 - 1.12 (m, 6 H), 0.73 (d,  $J = 7.0$  Hz, 3 H), 0.56 (d,  $J = 6.5$  Hz, 3 H).  $^{13}\text{C}$ -NMR (75 MHz, acetone- $d_6$ )  $\delta = 174.0, 173.3, 170.8, 169.4, 166.6, 157.6, 137.6, 129.6, 129.2, 128.9, 68.2, 65.3, 60.0, 57.1, 56.9, 55.1, 48.4, 47.6, 47.1, 38.8, 31.5, 31.4, 31.0, 23.7, 22.0, 18.0, 15.9$ . HRMS (FAB) Predicted for  $[\text{C}_{28}\text{H}_{37}\text{N}_5\text{O}_8 + \text{Na}]^+$ : 594.2540, Found: 594.2560.



**benzyl ((6S,8aS,14aS,20S,23aS)-6-methyl-5,8,14,19,23-pentaoxooctadecahydro-1H,5H,14H,19H-pyrido[2,1-i]dipyrrolo[2,1-c:2',1'-l][1]oxa[4,7,10,13]tetraazacyclohexadecin-20-yl)carbamate:** Yield 55% over 4 steps.  $^1\text{H}$ -NMR (600 MHz, chloroform- $d$ )  $\delta = 8.36$  (d,  $J = 9.5$  Hz, 1 H), 7.42 - 7.37 (m, 2 H), 7.37 - 7.33 (m, 2 H), 7.33 - 7.28 (m, 1 H), 5.68 (d,  $J = 9.5$  Hz, 1 H), 5.20 (dd,  $J = 2.9, 8.8$  Hz, 1 H), 5.12 - 5.05 (m, 2 H), 5.02 (dd,  $J = 6.8, 9.4$  Hz, 1 H), 4.79 (d,  $J = 11.4$  Hz, 1 H), 4.72 - 4.68 (m, 1 H), 4.57 - 4.45 (m, 2 H), 4.21 (t,  $J = 9.5$  Hz, 1 H), 3.81 - 3.69 (m, 2 H), 3.63 (dd,  $J = 9.9, 11.4$  Hz, 1 H), 3.58 - 3.48 (m, 2 H), 2.73 (d,  $J = 11.4$  Hz, 1 H), 2.56 (dt,  $J = 2.4, 13.3$  Hz, 1 H), 2.41 - 2.31 (m, 1 H), 2.27 - 2.18 (m, 1 H), 2.16 - 2.09 (m, 1 H), 2.01 - 1.90 (m, 4 H), 1.61 (d,  $J = 13.2$  Hz, 1 H), 1.48 - 1.43 (m, 2 H), 1.42 (d,  $J = 6.6$  Hz, 3 H), 1.39 - 1.31 (m, 1 H).  $^{13}\text{C}$ -NMR (151 MHz, chloroform- $d$ )  $\delta = 173.4, 171.5, 169.6, 168.5, 166.1, 156.2, 135.9, 128.5, 128.4, 128.1, 68.0, 65.8, 58.9, 57.1, 56.6, 53.9, 48.1, 46.9, 46.3, 41.1, 30.9, 30.6, 28.2, 24.8, 23.4, 23.1, 21.3, 18.1$ . HRMS (FAB) Predicted for  $[\text{C}_{30}\text{H}_{39}\text{N}_5\text{O}_8 + \text{Na}]$  620.2696, Found: 620.2681.

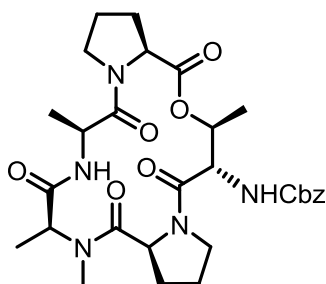


benzyl ((6S,8aS,10S,14aS,20S,23aS)-6,10-dimethyl-5,8,14,19,23-pentaoxooctadecahydro-1H,5H,14H,19H-pyrido[2,1-i]dipyrrolo[2,1-c:2',1'-l][1]oxa[4,7,10,13]tetraazacyclohexadecin-20-yl)carbamate: Yield 43% over 4 steps.  $^1\text{H-NMR}$  (400 MHz, chloroform-d)  $\delta$  = 8.34 (d,  $J$  = 9.6 Hz, 1 H), 7.43 - 7.28 (m, 5 H), 5.63 (d,  $J$  = 9.8 Hz, 1 H), 5.22 (dd,  $J$  = 3.3, 8.7 Hz, 1 H), 5.09 (d,  $J$  = 3.2 Hz, 2 H), 5.04 - 4.95 (m, 1 H), 4.80 (dd,  $J$  = 1.4, 11.6 Hz, 1 H), 4.72 (d,  $J$  = 5.3 Hz, 1 H), 4.57 - 4.48 (m, 2 H), 4.23 (dt,  $J$  = 1.4, 9.6 Hz, 1 H), 3.84 - 3.69 (m, 2 H), 3.64 (dd,  $J$  = 9.6, 11.7 Hz, 1 H), 3.60 - 3.47 (m, 2 H), 2.72 (d,  $J$  = 11.8 Hz, 1 H), 2.58 (dt,  $J$  = 2.6, 13.4 Hz, 1 H), 2.42 - 2.30 (m, 1 H), 2.29 - 2.09 (m, 2 H), 2.04 - 1.93 (m, 4 H), 1.71-1.61 (m, 3 H), 1.41 (d,  $J$  = 6.7 Hz, 3 H), 1.10 - 1.02 (m, 1 H), 0.95 (d,  $J$  = 6.3 Hz, 3 H).  $^{13}\text{C-NMR}$  (75 MHz, chloroform-d)  $\delta$  = 173.4, 171.6, 169.8, 168.6, 166.2, 156.2, 135.9, 128.5, 128.4, 128.1, 77.2, 68.0, 65.9, 58.9, 57.2, 56.7, 53.9, 48.1, 46.9, 46.3, 40.8, 36.4, 33.2, 30.9, 30.6, 28.0, 23.1, 21.9, 21.3, 18.1. HRMS (FAB) Predicted for  $[\text{C}_{31}\text{H}_{41}\text{N}_5\text{O}_8 + \text{Na}]^+$ : 634.3853, Found: 634.2868.



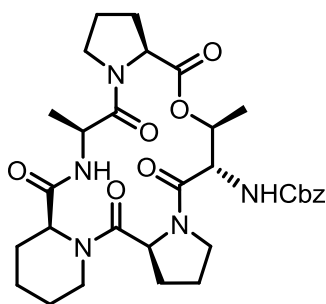
**benzyl** ((6S,8aS,10S,14aS,20S,23aS)-10-isopropyl-6-methyl-5,8,14,19,23-pentaoxooctadecahydro-1H,5H,14H,19H-pyrido[2,1-i]dipyrrolo[2,1-c:2',1'-

l][1]oxa[4,7,10,13]tetraazacyclohexadecin-20-yl)carbamate: Yield 45% over 4 steps. <sup>1</sup>H-NMR (400 MHz, chloroform-d)  $\delta$  = 8.33 (d,  $J$  = 9.8 Hz, 1 H), 7.43 - 7.31 (m, 5 H), 5.64 (d,  $J$  = 9.8 Hz, 1 H), 5.22 (dd,  $J$  = 3.1, 8.6 Hz, 1 H), 5.09 (d,  $J$  = 2.6 Hz, 2 H), 5.00 (dd,  $J$  = 6.6, 9.5 Hz, 1 H), 4.81 (dd,  $J$  = 1.5, 11.7 Hz, 1 H), 4.78 - 4.73 (m, 1 H), 4.57 (d,  $J$  = 14.0 Hz, 1 H), 4.53 (d,  $J$  = 8.2 Hz, 1 H), 4.27 - 4.17 (m, 1 H), 3.83 - 3.68 (m, 2 H), 3.64 (dd,  $J$  = 9.6, 11.7 Hz, 1 H), 3.55 (td,  $J$  = 7.1, 11.7 Hz, 2 H), 2.76 (d,  $J$  = 12.1 Hz, 1 H), 2.56 (dt,  $J$  = 2.6, 13.3 Hz, 1 H), 2.41-2.31 (m, 1 H), 2.29 - 2.19 (m, 1 H), 2.17 - 2.09 (m, 1 H), 2.04 - 1.90 (m, 5 H), 1.64 (d,  $J$  = 13.2 Hz, 1 H), 1.49 - 1.39 (m, 4 H), 1.34 - 1.21 (m, 1 H), 1.17 - 1.00 (m, 2 H), 0.92 (d,  $J$  = 6.7 Hz, 3 H), 0.88 (d,  $J$  = 6.7 Hz, 3 H). <sup>13</sup>C-NMR (101 MHz, chloroform-d)  $\delta$  = 173.4, 171.5, 169.8, 168.6, 166.2, 156.2, 135.9, 128.5, 128.4, 128.2, 83.6, 77.2, 68.0, 65.8, 58.9, 57.2, 56.6, 54.0, 48.1, 46.9, 46.3, 41.0, 39.0, 32.3, 31.9, 30.9, 30.7, 28.2, 23.1, 21.3, 19.5, 19.2, 18.2. HRMS (FAB) Predicted for [C<sub>33</sub>H<sub>45</sub>N<sub>5</sub>O<sub>8</sub> + Na]<sup>+</sup>:662.3166 Found: 662.3159.



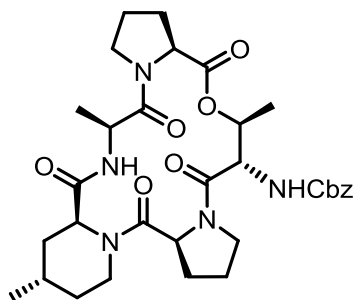
**benzyl** ((6*S*,9*S*,11*aS*,17*S*,18*S*,20*aS*)-6,9,10,18-tetramethyl-5,8,11,16,20-pentaoxohexadecahydro-1*H*,5*H*,16*H*-dipyrrolo[2,1-*c*:2',1'-

l][1]oxa[4,7,10,13]tetraazacyclohexadecin-17-yl)carbamate : Yield: 40% over 4 steps. <sup>1</sup>H-NMR (400 MHz, chloroform-*d*)  $\delta$  = 8.28 (d, *J* = 9.6 Hz, 1 H), 7.38 - 7.28 (m, 5 H), 5.58 (d, *J* = 9.6 Hz, 1 H), 5.30 (dd, *J* = 3.0, 8.8 Hz, 1 H), 5.15 - 5.07 (m, 1 H), 5.07 - 5.03 (m, 2 H), 4.89 (qd, *J* = 6.6, 9.5 Hz, 1 H), 4.75 (q, *J* = 6.8 Hz, 1 H), 4.40 (d, *J* = 7.6 Hz, 1 H), 4.30 (dd, *J* = 1.5, 9.6 Hz, 1 H), 3.81 - 3.73 (m, 1 H), 3.73 - 3.63 (m, 1 H), 3.52 - 3.43 (m, 2 H), 2.68 (s, 3 H), 2.38 - 2.27 (m, 1 H), 2.22 - 2.12 (m, 1 H), 2.12 - 1.98 (m, 2 H), 1.97 - 1.87 (m, 4 H), 1.48 (d, *J* = 7.1 Hz, 3 H), 1.35 (d, *J* = 6.6 Hz, 3 H), 1.23 (d, *J* = 6.6 Hz, 3 H). <sup>13</sup>C-NMR (101 MHz, chloroform-*d*)  $\delta$  = 173.0, 172.4, 170.2, 168.5, 166.5, 156.3, 135.8, 128.4, 128.4, 128.1, 77.2, 70.1, 68.1, 59.2, 56.4, 56.1, 56.0, 48.0, 47.0, 46.5, 31.2, 30.7, 30.6, 23.0, 21.3, 17.6, 15.7, 12.9.



**benzyl** ((6*S*,8*aS*,14*aS*,20*S*,21*S*,23*aS*)-6,21-dimethyl-5,8,14,19,23-pentaoxooctadecahydro-1*H*,5*H*,14*H*,19*H*-pyrido[2,1-*i*]dipyrrolo[2,1-*c*:2',1'-l][1]oxa[4,7,10,13]tetraazacyclohexadecin-20-yl)carbamate: Yield 37% over 4 steps. <sup>1</sup>H-NMR (600 MHz, chloroform-*d*)  $\delta$  = 8.41 (d, *J* = 9.5

Hz, 1 H), 7.45 - 7.35 (m, 4 H), 7.35 - 7.30 (m, 1 H), 5.59 (d,  $J = 9.5$  Hz, 1 H), 5.33 (dd,  $J = 3.1, 9.0$  Hz, 1 H), 5.14 - 5.07 (m, 3 H), 5.04 (qd,  $J = 6.7, 9.6$  Hz, 1 H), 4.73-4.69 (m, 1 H), 4.52 - 4.46 (m, 2 H), 4.34 (dd,  $J = 1.5, 9.5$  Hz, 1 H), 3.82 (ddd,  $J = 5.3, 8.3, 11.6$  Hz, 1 H), 3.74 (td,  $J = 8.6, 11.8$  Hz, 1 H), 3.57 - 3.49 (m, 2 H), 2.75 (d,  $J = 10.6$  Hz, 1 H), 2.60 - 2.51 (m, 1 H), 2.37 (dt,  $J = 5.1, 8.8$  Hz, 1 H), 2.26 - 2.19 (m, 1 H), 2.17 - 2.10 (m, 1 H), 2.07 - 2.03 (m, 1 H), 1.97 (qd,  $J = 5.3, 8.9$  Hz, 4 H), 1.80 - 1.74 (m, 1 H), 1.62 (d,  $J = 12.1$  Hz, 1 H), 1.50 - 1.45 (m, 2 H), 1.44 (d,  $J = 6.6$  Hz, 3 H), 1.40 - 1.31 (m, 1 H), 1.27 (d,  $J = 6.6$  Hz, 3 H).  $^{13}\text{C-NMR}$  (151 MHz, chloroform- $d$ )  $\delta = 173.0, 171.6, 169.7, 168.5, 166.7, 156.3, 135.9, 128.4, 128.4, 128.1, 70.3, 68.0, 59.0, 57.1, 56.6, 56.0, 48.1, 47.0, 46.4, 41.0, 31.2, 30.9, 30.6, 28.2, 24.9, 23.0, 21.3, 18.1, 12.9$ . HRMS (FAB) Predicted for  $[\text{C}_{31}\text{H}_{41}\text{N}_5\text{O}_8 + \text{Na}]^+$ : 634.3853, Found: 634.2861.



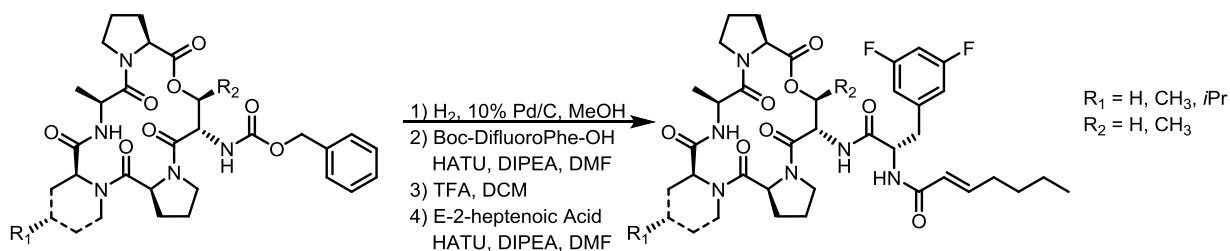
**benzyl** *((6S,8aS,10S,14aS,20S,21S,23aS)-6,10,21-trimethyl-5,8,14,19,23-pentaoxooctadecahydro-1H,5H,14H,19H-pyrido[2,1-*i*]dipyrrolo[2,1-*c:2',1'-l*][1]oxa[4,7,10,13]tetraazacyclohexadecin-20-yl)carbamate*

***l*][1]oxa[4,7,10,13]tetraazacyclohexadecin-20-yl)carbamate**: Yield: 36% over 4 steps.  $^1\text{H-NMR}$  (400 MHz, chloroform- $d$ )  $\delta = 8.37$  (d,  $J = 9.6$  Hz, 1 H), 7.45 - 7.29 (m, 5 H), 5.64 (d,  $J = 9.6$  Hz, 1 H), 5.39 - 5.25 (m, 1 H), 5.23 - 5.04 (m, 3 H), 5.04 - 4.94 (m, 1 H), 4.73 - 4.65 (m, 1 H), 4.47 (d,  $J = 8.3$  Hz, 2 H), 4.33 (d,  $J = 9.6$  Hz, 1 H), 3.84 - 3.65 (m, 2 H), 3.56 - 3.44 (m, 2 H), 2.70 (d,  $J = 12.9$  Hz, 1 H), 2.62 - 2.47 (m, 1 H), 2.42 - 2.28 (m, 1 H), 2.27 - 2.16 (m, 1 H), 2.15 - 2.01 (m, 2 H), 2.01 - 1.87 (m, 4 H), 1.58 (d,  $J = 11.6$  Hz, 2 H), 1.56 (s, 2 H), 1.39 (d,  $J = 6.6$  Hz, 3 H), 1.25 (d,  $J = 6.6$  Hz, 3 H), 1.18 - 0.96 (m, 2 H), 0.93 (d,  $J = 6.3$  Hz, 3 H).  $^{13}\text{C-NMR}$  (101 MHz, chloroform- $d$ )  $\delta = 172.8, 171.4,$



169.6, 168.4, 166.6, 156.2, 135.8, 128.3, 128.2, 127.9, 70.1, 67.8, 58.9, 56.9, 56.5, 55.9, 47.9, 46.8, 46.2, 40.6, 36.1, 33.1, 31.0, 30.4, 27.8, 22.8, 21.7, 21.2, 17.9, 12.7. HRMS (FAB) Predicted for  $[C_{32}H_{44}N_5O_8 + Na]^+$ : 648.3009, Found: 648.3030.

### Cyclic Acyldepsipeptides



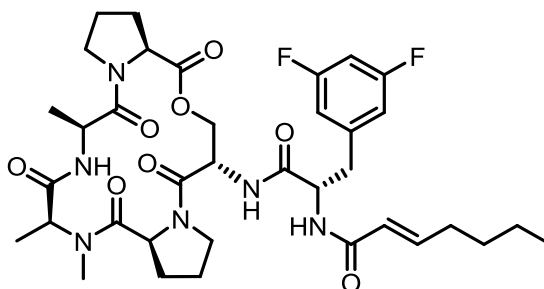
**Cbz removal:** The CBZ protected peptidolactone was dissolved in methanol at a concentration of 0.14 M. Once the solution was homogeneous, 10% Pd/C (130 mg / mmol peptidolactone) was added followed by 1M HCl (1 equivalent with respect to peptidolactone). With the reaction flask septum sealed, hydrogen gas was delivered to the reaction by a balloon affixed to a syringe. The reaction was allowed to proceed for 90 minutes after which it was filtered through celite in order to remove the Pd/C. Removal of solvent revealed the peptidolactone hydrochloride salt as an off white solid, which is used without further purification.

**Boc-DifluoroPhe acylation:** The peptidolactone hydrochloride salt was dissolved in DMF at a concentration of 0.25 M. Once the solution was homogeneous, Boc-difluorophenylalanine (1.1 equivalents) was added followed by HATU (1.1 equivalents). The reaction was initiated by the addition of DIPEA (2.2 equivalents) and allowed to proceed for 2 hours. Upon completion of the reaction the solvent was removed. The concentrated residue was diluted with ethyl acetate, and extracted 3x 1M HCl, 3x saturated  $NaHCO_3$ , 1x brine, then dried over sodium sulfate. The Boc-difluorophenylalanine acylated peptidolactones were isolated by silica gel chromatography

using an ethyl acetate / acetone solvent gradient. Final removal of the solvent revealed a fine white powder, which was used without further purification.

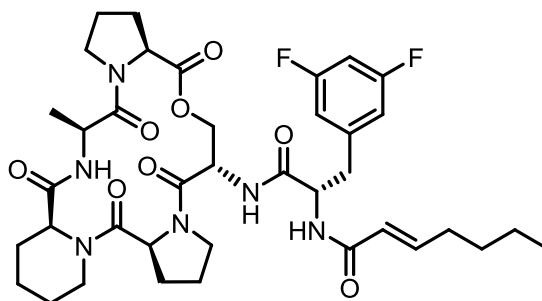
*Boc group removal:* The Boc-difluorophenylalanyl peptidolactones were treated with 40% TFA in DCM at a concentration of 0.6 M. Upon complete conversion of the starting material, the reaction was concentrated by blowing with a stream of nitrogen then by evaporation under high vacuum. The ester free base was used without further purification.

*E-2-Heptenoate Coupling* The difluorophenylalanyl peptidolactone TFA salts were dissolved in DMF at a concentration of 0.25 M. Once the solution was homogeneous, E-2-heptenoic acid (1.1 equivalents) was added followed by HATU (1.1 equivalents). The reaction was initiated by the addition of diisopropylethylamine (2.2 equivalents) and allowed to proceed for 16 hours. Upon completion of the reaction, the solvent was removed *in vacuo*. The concentrated residue was diluted with ethyl acetate and extracted 3x 1M HCl, 3x saturated NaHCO<sub>3</sub>, 1x brine, then dried over sodium sulfate. The ADEP final products were purified by silica gel chromatography using an ethyl acetate / acetone solvent gradient. Final removal of the solvent revealed the product as a white foam.



(E)-N-((S)-3-(3,5-difluorophenyl)-1-oxo-1-(((6S,9S,11aS,17S,20aS)-6,9,10-trimethyl-5,8,11,16,20-pentaoxohexadecahydro-1H,5H,16H-dipyrrolo[2,1-c:2',1'-l][1]oxa[4,7,10,13]tetraazacyclohexadecin-17-yl)amino)propan-2-yl)hept-2-enamide (1a):

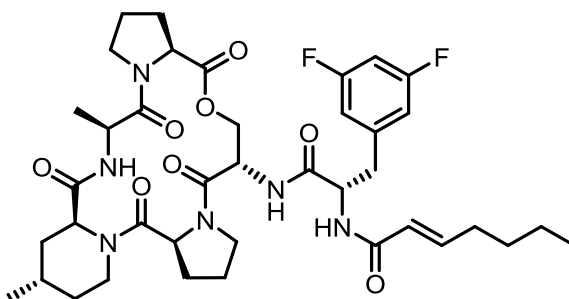
Yield: 50% over 4 steps.  $^1\text{H-NMR}$  (400 MHz, acetone- $d_6$ )  $\delta$  = 8.48 (d,  $J$  = 9.5 Hz, 1 H), 8.27 (d,  $J$  = 9.8 Hz, 1 H), 7.21 (d,  $J$  = 7.5 Hz, 1 H), 6.88 (s, 3 H), 6.77 (tt,  $J$  = 2.3, 9.3 Hz, 1 H), 6.33 (td,  $J$  = 1.5, 15.6 Hz, 1 H), 5.25 (dd,  $J$  = 3.0, 8.5 Hz, 1 H), 4.93 (dd,  $J$  = 2.0, 11.5 Hz, 1 H), 4.91 - 4.79 (m, 3 H), 4.61 (dt,  $J$  = 1.8, 9.9 Hz, 1 H), 4.48 (d,  $J$  = 8.5 Hz, 1 H), 3.74 - 3.58 (m, 3 H), 3.55 - 3.44 (m, 1 H), 3.40 - 3.29 (m, 1 H), 3.04 (dd,  $J$  = 8.2, 13.2 Hz, 1 H), 2.93 (dd,  $J$  = 4.9, 13.2 Hz, 1 H), 2.79 (s, 3 H), 2.57 - 2.45 (m, 1 H), 2.34 - 2.25 (m, 1 H), 2.22 (q,  $J$  = 7.5 Hz, 2 H), 2.03 - 1.88 (m, 6 H), 1.49 (d,  $J$  = 6.9 Hz, 3 H), 1.52 - 1.42 (m, 2 H), 1.42 - 1.34 (m, 2 H), 1.27 (d,  $J$  = 6.5 Hz, 3 H), 0.91 (t,  $J$  = 7.3 Hz, 3 H).  $^{13}\text{C-NMR}$  (75 MHz, acetone- $d_6$ )  $\delta$  = 173.9, 173.4, 172.4, 171.3, 171.0, 166.3, 166.1, 165.8, 165.6, 162.6, 162.4, 145.3, 143.1, 143.0, 142.8, 125.4, 114.1, 114.0, 113.9, 113.8, 103.3, 102.9, 102.6, 65.7, 60.7, 57.9, 57.3, 55.5, 52.8, 48.8, 48.2, 47.6, 39.9, 32.7, 32.1, 31.7, 31.5, 24.2, 23.3, 22.4, 18.2, 16.2, 14.6. HRMS (FAB) Predicted for  $[\text{C}_{36}\text{H}_{48}\text{F}_2\text{N}_6\text{O}_8 + \text{Na}]^+$ : 753.3399, Found: 753.3380.



**(E)-N-((S)-3-(3,5-difluorophenyl)-1-(((6S,8aS,14aS,20S,23aS)-6-methyl-5,8,14,19,23-pentaoxooctadecahydro-1H,5H,14H,19H-pyrido[2,1-i]dipyrrolo[2,1-c:2',1'-l][1]oxa[4,7,10,13]tetraazacyclohexadecin-20-yl)amino)-1-oxopropan-2-yl)hept-2-enamide**

**(1b):** Yield: 68% over 4 steps.  $^1\text{H-NMR}$  (400 MHz, acetone- $d_6$ )  $\delta$  = 8.57 (d,  $J$  = 9.3 Hz, 1 H), 8.25 (d,  $J$  = 9.5 Hz, 1 H), 7.22 (d,  $J$  = 7.5 Hz, 1 H), 6.93 - 6.80 (m, 3 H), 6.77 (tt,  $J$  = 2.3, 9.3 Hz, 1 H), 6.32 (td,  $J$  = 1.4, 15.5 Hz, 1 H), 5.21 (dd,  $J$  = 2.9, 8.7 Hz, 1 H), 5.05 - 4.94 (m, 1 H), 4.90 - 4.81 (m, 2 H), 4.77 - 4.71 (m, 1 H), 4.68 - 4.56 (m, 2 H), 4.52 (d,  $J$  = 8.5 Hz, 1 H), 3.73 - 3.66 (m, 1 H), 3.66 - 3.58

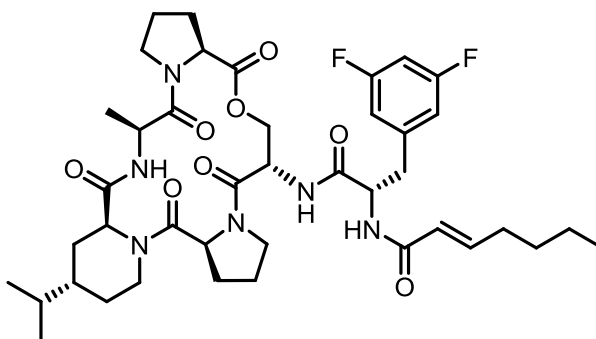
(m, 2 H), 3.55 - 3.45 (m, 1 H), 3.41 - 3.29 (m, 1 H), 3.04 (dd,  $J = 8.2, 13.2$  Hz, 1 H), 2.90 (dd,  $J = 4.9, 13.2$  Hz, 1 H), 2.69 - 2.57 (m, 2 H), 2.57 - 2.47 (m, 1 H), 2.36 - 2.26 (m, 1 H), 2.22 (q,  $J = 7.4$  Hz, 2 H), 2.05 - 1.85 (m, 6 H), 1.71 (d,  $J = 11.5$  Hz, 1 H), 1.65 - 1.53 (m, 2 H), 1.51 - 1.41 (m, 3 H), 1.41 - 1.32 (m, 3 H), 1.30 (d,  $J = 6.5$  Hz, 3 H), 0.91 (t,  $J = 7.3$  Hz, 3 H).  $^{13}\text{C-NMR}$  (75 MHz, acetone)  $\delta = 173.4, 172.3, 171.8, 170.8, 170.0, 165.9, 165.8, 165.2, 162.2, 162.0, 144.8, 142.7, 142.6, 125.1, 113.7, 113.4, 102.9, 102.5, 102.2, 65.5, 60.1, 57.8, 57.7, 55.1, 52.5, 52.4, 48.4, 47.7, 47.0, 41.6, 39.3, 32.3, 31.6, 31.3, 31.0, 28.4, 25.6, 23.8, 22.9, 22.1, 22.0, 18.3, 14.2$ . HRMS (FAB) Predicted for  $[\text{C}_{38}\text{H}_{50}\text{F}_2\text{N}_6\text{O}_8 + \text{Na}]^+$ : 779.3556, Found: 779.3526.



**(E)-N-((S)-3-(3,5-difluorophenyl)-1-(((6S,8aS,10S,14aS,20S,23aS)-6,10-dimethyl-5,8,14,19,23-pentaoxooctadecahydro-1H,5H,14H,19H-pyrido[2,1-i]dipyrrolo[2,1-c:2',1'-l][1]oxa[4,7,10,13]tetraazacyclohexadecin-20-yl)amino)-1-oxopropan-2-yl)hept-2-enamide**

**(1c):** Yield: 61% over 4 steps.  $^1\text{H-NMR}$  (400 MHz, acetone- $d_6$ )  $\delta = 8.56$  (d,  $J = 9.5$  Hz, 1 H), 8.30 (d,  $J = 9.5$  Hz, 1 H), 7.22 (d,  $J = 7.5$  Hz, 1 H), 6.93 - 6.80 (m, 3 H), 6.76 (tt,  $J = 2.3, 9.3$  Hz, 1 H), 6.33 (td,  $J = 1.4, 15.3$  Hz, 1 H), 5.23 (dd,  $J = 2.4, 8.7$  Hz, 1 H), 5.06 - 4.94 (m, 1 H), 4.93 - 4.83 (m, 2 H), 4.78 (d,  $J = 4.8$  Hz, 1 H), 4.70 - 4.58 (m, 2 H), 4.54 (d,  $J = 8.5$  Hz, 1 H), 3.71 (dd,  $J = 10.0, 11.5$  Hz, 1 H), 3.68 - 3.58 (m, 2 H), 3.56 - 3.45 (m, 1 H), 3.42 - 3.30 (m, 1 H), 3.04 (dd,  $J = 8.2, 13.2$  Hz, 1 H), 2.90 (dd,  $J = 4.9, 13.2$  Hz, 1 H), 2.71 - 2.57 (m, 2 H), 2.57 - 2.47 (m, 1 H), 2.35 - 2.25 (m, 1 H), 2.22 (q,  $J = 7.0$  Hz, 2 H), 2.04 - 1.85 (m, 6 H), 1.62 (d,  $J = 11.3$  Hz, 2 H), 1.52 - 1.42 (m, 2 H), 1.40 - 1.32 (m, 2 H), 1.28 (d,  $J = 6.5$  Hz, 3 H), 1.24 - 1.14 (m, 1 H), 1.08 - 0.95 (m, 1 H), 0.94 (d,  $J = 6.3$  Hz, 3

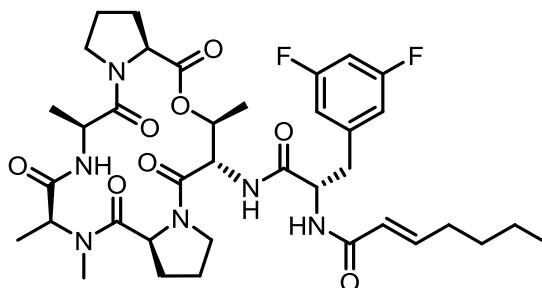
H), 0.91 (t,  $J = 7.3$  Hz, 3 H).  $^{13}\text{C-NMR}$  (75 MHz, acetone- $d_6$ )  $\delta = 163.5, 162.3, 162.0, 161.9, 160.8, 160.2, 156.0, 155.4, 155.2, 152.1, 152.0, 135.0, 132.7, 132.6, 132.5, 115.1, 103.8, 103.7, 103.6, 103.5, 92.9, 92.5, 92.2, 55.6, 50.2, 47.9, 45.1, 44.9, 42.5, 38.5, 37.8, 37.2, 31.4, 29.4, 26.7, 24.0, 22.4, 21.6, 21.4, 21.0, 20.8, 18.9, 13.9, 13.0, 12.3, 12.1, 8.3, 4.3$ . HRMS (FAB) Predicted for  $[\text{C}_{39}\text{H}_{52}\text{F}_2\text{N}_6\text{O}_8 + \text{Na}]^+$ : 793.3712, Found: 793.3728.



**(E)-N-((S)-3-(3,5-difluorophenyl)-1-(((6S,8aS,10S,14aS,20S,23aS)-10-isopropyl-6-methyl-5,8,14,19,23-pentaoxooctadecahydro-1H,5H,14H,19H-pyrido[2,1-i]dipyrrolo[2,1-c:2',1'-l][1]oxa[4,7,10,13]tetraazacyclohexadecin-20-yl)amino)-1-oxopropan-2-yl)hept-2-enamide**

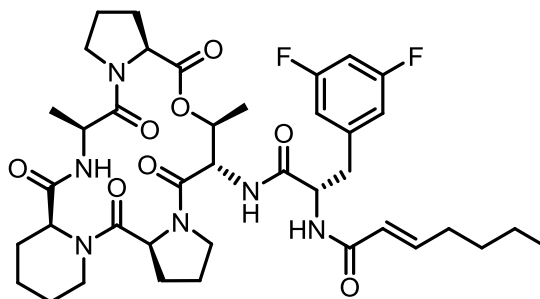
**(1d)**: Yield: 63% over 4 steps.  $^1\text{H-NMR}$  (400 MHz, acetone- $d_6$ )  $\delta = 8.55$  (d,  $J = 9.8$  Hz, 1 H), 8.18 (d,  $J = 9.3$  Hz, 1 H), 7.25 (d,  $J = 7.3$  Hz, 1 H), 6.93 - 6.84 (m, 3 H), 6.84 - 6.77 (m, 1 H), 6.33 (td,  $J = 1.5, 15.3$  Hz, 1 H), 5.25 (dd,  $J = 2.8, 8.5$  Hz, 1 H), 5.09 - 4.94 (m, 1 H), 4.89 (dd,  $J = 1.5, 11.5$  Hz, 1 H), 4.85 - 4.76 (m, 2 H), 4.72 (dd,  $J = 1.8, 13.6$  Hz, 1 H), 4.64 (dt,  $J = 1.6, 9.9$  Hz, 1 H), 4.55 (d,  $J = 8.5$  Hz, 1 H), 3.76 - 3.59 (m, 3 H), 3.56 - 3.44 (m, 1 H), 3.44 - 3.33 (m, 1 H), 3.07 (dd,  $J = 8.0, 13.3$  Hz, 1 H), 2.94 (dd,  $J = 5.0, 13.1$  Hz, 1 H), 2.89 (d,  $J = 12.0$  Hz, 1 H), 2.75 - 2.61 (m, 2 H), 2.61 - 2.49 (m, 1 H), 2.37 - 2.18 (m, 3 H), 2.06 - 1.89 (m, 6 H), 1.70 (d,  $J = 13.1$  Hz, 1 H), 1.54 - 1.44 (m, 3 H), 1.44 - 1.36 (m, 2 H), 1.32 (d,  $J = 6.5$  Hz, 4 H), 1.15 - 1.02 (m, 1 H), 0.96 - 0.90 (m, 9 H).  $^{13}\text{C-NMR}$  (75 MHz, acetone- $d_6$ )  $\delta = 173.4, 172.2, 171.9, 171.8, 170.8, 170.1, 165.9, 165.8, 165.4, 162.2, 162.0, 144.8, 142.7, 142.6, 142.5, 125.1, 113.7, 113.4, 102.9, 102.5, 102.2, 65.5, 60.1, 58.4, 57.9,$

57.7, 55.1, 52.5, 52.4, 48.4, 47.7, 47.0, 41.4, 40.1, 39.3, 33.3, 32.3, 32.1, 31.6, 31.3, 31.0, 23.8, 22.9, 22.0, 20.0, 19.8, 18.3, 14.2. HRMS (FAB) Predicted for  $[C_{41}H_{56}F_2N_6O_8 + Na]^+$ : 793.3712, Found: 793.3728.



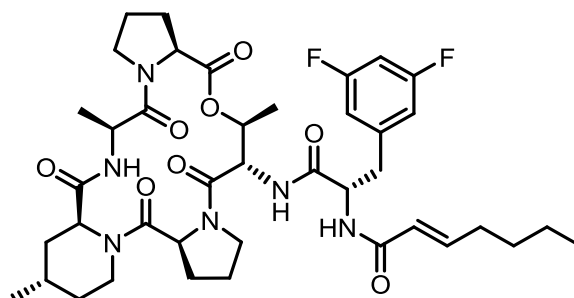
**(E)-N-((S)-3-(3,5-difluorophenyl)-1-oxo-1-(((6S,9S,11aS,17S,18S,20aS)-6,9,10,18-tetramethyl-5,8,11,16,20-pentaoxohexadecahydro-1H,5H,16H-dipyrrolo[2,1-c:2',1'-l][1]oxa[4,7,10,13]tetraazacyclohexadecin-17-yl)amino)propan-2-yl)hept-2-enamide (1e).**

Yield: 68% over 4 steps.  $^1H$ -NMR (600 MHz, acetone- $d_6$ )  $\delta$  = 8.47 (d,  $J$  = 9.2 Hz, 1 H), 8.12 (d,  $J$  = 9.5 Hz, 1 H), 7.21 (d,  $J$  = 7.3 Hz, 1 H), 6.89 - 6.81 (m, 3 H), 6.79 (tt,  $J$  = 2.5, 9.3 Hz, 1 H), 6.33 (td,  $J$  = 1.5, 15.4 Hz, 1 H), 5.32 - 5.23 (m, 2 H), 4.90 - 4.83 (m, 2 H), 4.78 (q,  $J$  = 6.7 Hz, 1 H), 4.74 (dd,  $J$  = 2.0, 9.7 Hz, 1 H), 4.40 (d,  $J$  = 8.1 Hz, 1 H), 3.69 - 3.64 (m, 1 H), 3.64 - 3.58 (m, 1 H), 3.47 - 3.40 (m, 1 H), 3.36 - 3.30 (m, 1 H), 3.04 (dd,  $J$  = 8.4, 13.2 Hz, 1 H), 2.95 (dd,  $J$  = 4.8, 13.2 Hz, 1 H), 2.77 (s, 3 H), 2.54 - 2.44 (m, 1 H), 2.30 - 2.23 (m, 1 H), 2.21 (q,  $J$  = 7.2 Hz, 2 H), 2.04 - 1.96 (m, 3 H), 1.96 - 1.87 (m, 3 H), 1.48 (d,  $J$  = 7.0 Hz, 3 H), 1.47 - 1.42 (m, 2 H), 1.39 - 1.32 (m, 2 H), 1.27 (d,  $J$  = 6.6 Hz, 3 H), 1.20 (d,  $J$  = 6.6 Hz, 3 H), 0.91 (t,  $J$  = 7.3 Hz, 3 H).  $^{13}C$ -NMR (151 MHz, acetone- $d_6$ )  $\delta$  = 173.1, 172.9, 172.3, 170.6, 170.4, 166.1, 166.0, 144.8, 125.1, 113.7, 113.6, 113.5, 113.5, 102.7, 102.6, 102.4, 70.5, 60.4, 57.4, 56.9, 55.1, 54.4, 48.4, 47.7, 47.2, 39.2, 32.3, 31.6, 31.4, 31.3, 31.1, 23.7, 22.9, 22.0, 17.8, 15.7, 14.2, 13.5. HRMS (FAB) Predicted for  $[C_{37}H_{50}F_2N_6O_8 + Na]^+$ : 767.3551, Found: 767.3548.



**(E)-N-((S)-3-(3,5-difluorophenyl)-1-(((6S,8aS,14aS,20S,21S,23aS)-6,21-dimethyl-5,8,14,19,23-pentaoxooctadecahydro-1H,5H,14H,19H-pyrido[2,1-i]dipyrrolo[2,1-c:2',1'-l][1]oxa[4,7,10,13]tetraazacyclohexadecin-20-yl)amino)-1-oxopropan-2-yl)hept-2-enamide**

**(1f).** Yield: 71% over 4 steps.  $^1\text{H-NMR}$  (400 MHz, acetone- $d_6$ )  $\delta$  = 8.55 (d,  $J$  = 9.5 Hz, 1 H), 8.24 (d,  $J$  = 9.8 Hz, 1 H), 7.24 (d,  $J$  = 7.3 Hz, 1 H), 6.91 (td,  $J$  = 7.0, 15.3 Hz, 1 H), 6.86 - 6.79 (m, 2 H), 6.79 - 6.72 (m, 1 H), 6.32 (td,  $J$  = 1.5, 15.3 Hz, 1 H), 5.29 (dd,  $J$  = 2.6, 8.7 Hz, 1 H), 5.21 (dq,  $J$  = 1.8, 6.6 Hz, 1 H), 5.04 - 4.90 (m, 2 H), 4.76 (dd,  $J$  = 1.9, 9.9 Hz, 1 H), 4.72 - 4.67 (m, 1 H), 4.62 (d,  $J$  = 13.6 Hz, 1 H), 4.44 (d,  $J$  = 8.0 Hz, 1 H), 3.76 - 3.66 (m, 1 H), 3.61 (td,  $J$  = 8.3, 11.7 Hz, 1 H), 3.49 (td,  $J$  = 6.8, 11.4 Hz, 1 H), 3.34 (dt,  $J$  = 4.4, 7.7 Hz, 1 H), 3.08 (dd,  $J$  = 7.8, 13.3 Hz, 1 H), 2.90 (dd,  $J$  = 4.8, 13.3 Hz, 1 H), 2.66 - 2.55 (m, 2 H), 2.52 (dt,  $J$  = 3.6, 8.0 Hz, 1 H), 2.33 - 2.17 (m, 3 H), 2.04 - 1.87 (m, 6 H), 1.70 (d,  $J$  = 12.3 Hz, 1 H), 1.63 - 1.52 (m, 2 H), 1.51 - 1.41 (m, 3 H), 1.41 - 1.31 (m, 3 H), 1.28 (d,  $J$  = 6.5 Hz, 3 H), 1.22 (d,  $J$  = 6.5 Hz, 3 H), 0.91 (t,  $J$  = 7.3 Hz, 3 H).  $^{13}\text{C-NMR}$  (75 MHz, acetone- $d_6$ )  $\delta$  = 172.9, 172.2, 172.2, 170.5, 169.8, 166.4, 166.2, 165.3, 165.1, 162.0, 161.9, 145.1, 142.6, 142.5, 142.4, 124.9, 113.8, 113.7, 113.6, 113.5, 102.8, 102.4, 102.1, 70.7, 60.2, 57.7, 54.6, 54.4, 48.4, 47.7, 47.2, 41.5, 38.9, 32.3, 31.5, 31.3, 31.2, 28.3, 25.6, 23.7, 22.9, 22.1, 22.0, 18.2, 14.2, 13.5. HRMS (FAB) Predicted for  $[\text{C}_{39}\text{H}_{52}\text{F}_2\text{N}_6\text{O}_8 + \text{Na}]^+$ : 793.3712, Found: 793.3731.



**(E)-N-((S)-3-(3,5-difluorophenyl)-1-oxo-1-(((6S,8aS,10S,14aS,20S,21S,23aS)-6,10,21-trimethyl-5,8,14,19,23-pentaoxooctadecahydro-1H,5H,14H,19H-pyrido[2,1-i]dipyrrolo[2,1-c:2',1'-l][1]oxa[4,7,10,13]tetraazacyclohexadecin-20-yl)amino)propan-2-yl)hept-2-enamide (1g).**

Yield: 69% over 4 steps. <sup>1</sup>H-NMR (400 MHz, acetone-d<sub>6</sub>) δ = 8.54 (d, *J* = 9.6 Hz, 1 H), 8.24 (d, *J* = 9.9 Hz, 1 H), 7.25 (d, *J* = 7.3 Hz, 1 H), 6.90 (td, *J* = 7.1, 15.4 Hz, 1 H), 6.86 - 6.81 (m, 2 H), 6.77 (tt, *J* = 2.3, 9.3 Hz, 1 H), 6.32 (td, *J* = 1.4, 15.4 Hz, 1 H), 5.29 (dd, *J* = 2.3, 8.6 Hz, 1 H), 5.21 (dq, *J* = 1.6, 6.5 Hz, 1 H), 5.01 - 4.90 (m, 2 H), 4.76 (dd, *J* = 1.8, 9.9 Hz, 1 H), 4.74 - 4.69 (m, 1 H), 4.68 - 4.59 (m, 1 H), 4.43 (d, *J* = 8.1 Hz, 1 H), 3.73 - 3.63 (m, 1 H), 3.63 - 3.55 (m, 1 H), 3.47 (td, *J* = 6.9, 11.5 Hz, 1 H), 3.33 (ddd, *J* = 4.0, 8.1, 11.6 Hz, 1 H), 3.07 (dd, *J* = 8.0, 13.3 Hz, 1 H), 2.90 (dd, *J* = 4.8, 13.1 Hz, 1 H), 2.67 - 2.56 (m, 2 H), 2.51 (dt, *J* = 3.4, 7.9 Hz, 1 H), 2.33 - 2.17 (m, 3 H), 2.03 - 1.87 (m, 6 H), 1.60 (d, *J* = 12.1 Hz, 2 H), 1.52 - 1.42 (m, 2 H), 1.42 - 1.28 (m, 3 H), 1.26 (d, *J* = 6.6 Hz, 3 H), 1.21 (d, *J* = 6.6 Hz, 3 H), 0.99 (dd, *J* = 3.7, 13.3 Hz, 1 H), 0.95 - 0.88 (m, 6 H). <sup>13</sup>C-NMR (101 MHz, acetone-d<sub>6</sub>) δ = 172.9, 172.3, 172.2, 170.5, 169.9, 166.4, 166.1, 164.9, 164.8, 162.5, 162.3, 145.0, 142.7, 142.6, 142.5, 125.0, 113.8, 113.7, 113.6, 113.5, 102.7, 102.5, 102.2, 70.7, 60.2, 57.8, 54.7, 54.4, 48.4, 47.7, 47.2, 41.3, 39.0, 36.5, 33.9, 32.3, 31.4, 31.3, 31.2, 28.8, 23.7, 22.9, 22.2, 22.0, 18.2, 14.2, 13.5. HRMS (FAB) Predicted for [C<sub>40</sub>H<sub>54</sub>F<sub>2</sub>N<sub>6</sub>O<sub>8</sub> + Na]<sup>+</sup>: 807.3869, Found: 807.3885.



## References

1. Schmidt, U.; Neumann, K.; Schumacher, A.; Weinbrenner, S. Synthesis of Enopeptin B from *Streptomyces* sp RK-1051. *Angewandte Chemie International Edition in English* **1997**, *36*, 1110-1112.
2. Hinzen, B. Antibacterial macrocycles. WO2003024996 A3. **2005**.
3. Hinzen, B.; Raddatz, S.; Paulsen, H.; Lampe, T.; Schumacher, A.; Häbich, D.; Hellwig, V.; Benet-Buchholz, J.; Endermann, R.; Labischinski, H.; Brötz-Oesterhelt, H. Medicinal Chemistry Optimization of Acyldepsipeptides of the Enopeptin Class Antibiotics. *ChemMedChem* **2006**, *1*, 689-693.
4. Socha, A. M.; Tan, N. Y.; LaPlante, K. L.; Sello, J. K. Diversity-oriented synthesis of cyclic acyldepsipeptides leads to the discovery of a potent antibacterial agent. *Bioorg. Med. Chem.* **2010**, *18*, 7193-7202.
5. Stevens, R. V. Nucleophilic additions to tetrahydropyridinium salts. Applications to alkaloid syntheses. *Acc. Chem. Res.* **1984**, *17*, 289-296.
6. Nguyen, T. B.; Wang, Q.; Guéritte, F. An Efficient One-Step Synthesis of Piperidin-2-yl and Pyrrolidin-2-yl Flavonoid Alkaloids through Phenolic Mannich Reactions. *European Journal of Organic Chemistry* **2011**, *2011*, 7076-7079.
7. Schwarz, J. P. Preparation of acyclic isoimides and their rearrangement rates to imides. *J. Org. Chem.* **1972**, *37*, 2906-2908.
8. Mumm, O. *Ber. Dtsch. Chem. Ges* **1910**, *43*, 886.
9. Lambert, J. B.; Keske, R. G. The Conformational Preference of the Nonbonding Electron Pair in Piperidine. *J. Am. Chem. Soc.* **1966**, *88*, 620-622.
10. Lambert, J. B.; Keske, R. G.; Carhart, R. E.; Jovanovich, A. P. The conformational rivalry between the nonbonding electron pair and the proton on nitrogen. *J. Am. Chem. Soc.* **1967**, *89*, 3761-3767.
11. Elliott, D. 15. Preparation of L-threonine. Interconversion of the four stereoisomeric  $\alpha$ -amino- $\beta$ -hydroxybutyric acids. *Journal of the Chemical Society (Resumed)* **1950**, 62-68.
12. Iwashita, M.; Makide, K.; Nonomura, T.; Misumi, Y.; Otani, Y.; Ishida, M.; Taguchi, R.; Tsujimoto, M.; Aoki, J.; Arai, H. Synthesis and evaluation of lysophosphatidylserine analogues as inducers of mast cell degranulation. Potent activities of lysophosphatidylthreonine and its 2-deoxy derivative. *J. Med. Chem.* **2009**, *52*, 5837-5863.
13. Aït-Haddou, H.; Hoarau, O.; Cramailere, D.; Pezet, F.; Daran, J.; Balavoine, G. G. New Dihydroxy Bis (Oxazoline) Ligands for the Palladium-Catalyzed Asymmetric Allylic Alkylation:

Experimental Investigations of the Origin of the Reversal of the Enantioselectivity.  
*Chemistry-A European Journal* **2004**, *10*, 699-707.

14. Neises, B.; Steglich, W. Simple method for the esterification of carboxylic acids. *Angewandte Chemie International Edition in English* **1978**, *17*, 522-524.

## Chapter 6 – Evaluation of ADEPs with Conformationally Constrained Peptidolactones

Contents of this Chapter are Published in the following Manuscript: Carney, D. W.; Schmitz, K. R.; Truong, J. V.; Sauer, R. T.; Sello, J. K.; *Restriction of the Conformational Dynamics of the Cyclic Acyldepsipeptide Antibiotics Improves Their Antibacterial Activity*. *J. Am. Chem. Soc.* **2014**. 136, 1922-1929. dx.doi.org/ 10.1021/ja410385c

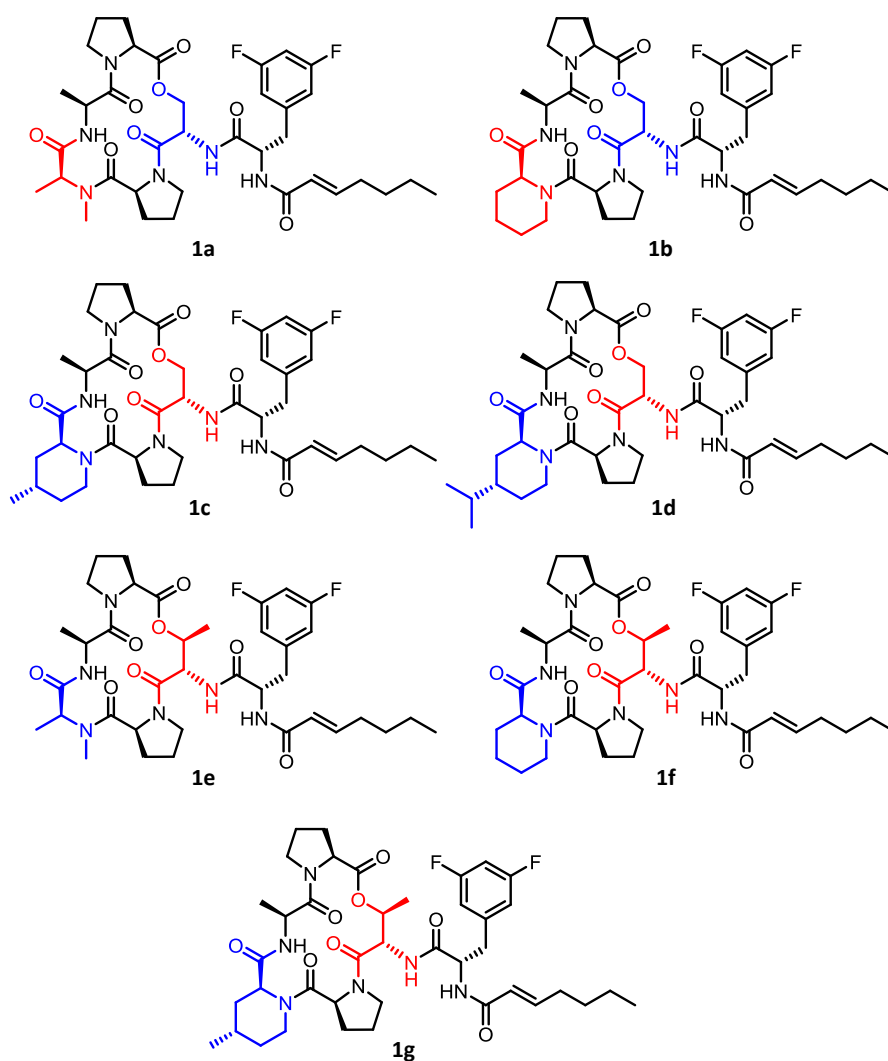
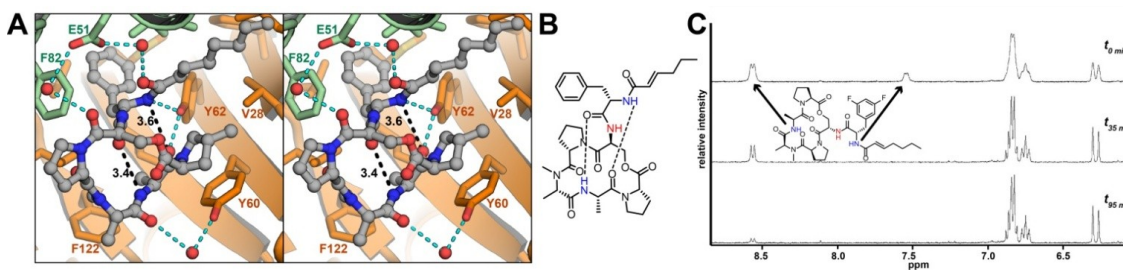


Figure 6.1 - Structures of ADEP molecules containing conformationally constrained amino acids

## Introduction

With a series of synthetic ADEPs in hand (Figure 6.1), we conducted a variety of experiments to study their conformational dynamics and biological activities. First, we sought to empirically test the hypothesis that incorporation of conformationally constrained amino acids into the ADEP peptidolactone imparts a rigidifying effect to the entire macrocycle. We could then correlate macrocycle rigidity to ClpP binding and activation as well as antibacterial activity. Insight into how ADEP peptidolactone rigidity could be measured experimentally was provided by published crystal structures of ADEP bound to ClpP<sup>1,2</sup> and of free ADEP from various organic solvents<sup>3</sup>.



**Figure 6.2 - Trans-annular hydrogen bonding in an ADEP.** A) Stereo-cartoon of an ADEP (gray ball-and-sticks) bound to *E. coli* ClpP (adjacent subunits in green and orange), generated from crystal structure 3MT6.<sup>2</sup> Two predicted hydrogen bonds are observed within the ADEP (black; distances in Å), and several hydrogen bond networks (cyan) occur either directly between the ADEP and ClpP or via ordered water molecules. B) Schematic representation of ADEP trans-annular hydrogen bonds C) Overlay of <sup>1</sup>H-NMR spectra of compound 1a over time in CD<sub>3</sub>OD. Amides participating in bonds are highlighted in blue and the non-bonding amide is highlighted in red. The half-lives of the hydrogens of the alanine and difluorophenylalanine residues were 26.8 minutes and 3.87 minutes, respectively.

In ADEP-ClpP complex structures, the ADEPs themselves adopt a compact conformation that appears to be enforced by two trans-annular hydrogen bonds between the peptidolactone and the appendant side chain (Figure 6.2 A).<sup>2</sup> Interestingly, a similar conformation is observed in crystals of free ADEP, where analogous hydrogen bonding between the peptidolactone and the side chain has been predicted.<sup>3</sup> We reasoned that the intramolecular hydrogen bonding exhibited within the ADEP molecule could be exploited in studies of peptidolactone rigidity. It is known that hydrogen bonding interactions slow down the rate of deuterium exchange with

amide hydrogen atoms. In the context of the ADEPs, intramolecular hydrogen bonding should attenuate the rate of deuterium exchange with specific amide hydrogens. Furthermore, the strength of the hydrogen bonding interaction should be dependent upon the conformational dynamics of the peptidolactone, which would also be reflected by the rate of deuterium exchange. Nevertheless, the existence of intramolecular hydrogen bonding within ADEP molecules in solution had not been previously validated.

To test the prediction that solvated ADEPs exhibit intramolecular hydrogen-bonding in solution, we performed experiments in which  $^1\text{H-NMR}$  was used to measure deuterium exchange rates of amide hydrogen atoms predicted to participate in the bonds (Figure 6.2 B). Hydrogen-deuterium exchange rates have been shown to be dependent upon the presence and strength of intramolecular hydrogen bonds in peptides.<sup>4</sup> Accordingly, we anticipated that deuterium exchange rates at the amide bonds engaged in hydrogen bonding would be slower than at non-hydrogen-bonded amides. Given the limited solubility of the ADEPs in water, we selected deuterio-methanol ( $\text{CD}_3\text{OD}$ ) as the solvent for the deuterium exchange experiments; accepting the possibility that the molecules' conformations could differ in organic and aqueous solvents. Immediately after preparation of a dilute solution of ADEP **1a** in  $\text{CD}_3\text{OD}$  (Figure 6.2B, Figure 6.3), we monitored attenuation of the amide proton resonances by  $^1\text{H-NMR}$  over a period of hours at 25 °C. As expected, the hydrogen atoms of the three secondary amides in the ADEP exchanged with deuterium at markedly different rates (Figure 6.2C). The amide hydrogen of the serine residue, which does not participate in a trans-annular hydrogen bond, exchanged completely in  $\text{CD}_3\text{OD}$  within several seconds and could never be observed in a  $^1\text{H-NMR}$  spectrum.

By comparison, the amide hydrogen of the side chain difluorophenylalanine residue required several minutes to completely exchange with deuterium; whereas, the macrocycle alanine amide hydrogen exchanged over the course of two hours (Figure 6.2C). These observations are consistent with the existence of trans-annular hydrogen bonds that are analogous to those inferred from the crystal structures of both free ADEP and ADEP in complex with ClpP.<sup>2,3,5</sup> These important similarities also suggest that the free ADEPs may be pre-disposed to adopt a conformation that is compatible with ClpP binding.

### Measurement of ADEP peptidolactone dynamics via <sup>1</sup>H-NMR Deuterium Exchange.

Since we had confirmed that ADEPs exhibit intramolecular hydrogen bonding in solution, we sought to examine the relative rigidities of the peptidolactones using D-exchange NMR experiments. As mentioned previously, we anticipated that the deuterium exchange rates for the hydrogens of the amides engaged in the hydrogen bonds would be dependent on the conformational dynamics of the ADEP peptidolactone. For all seven ADEPs, the alanine and difluorophenylalanine amide hydrogens' half-lives in CD<sub>3</sub>OD were measured from the rates at which their resonances in <sup>1</sup>H-NMR spectra attenuated relative to those of a non-exchanging reference signal in the same spectra. Compound **1a**, a known molecule<sup>3</sup> that is the closest analog of the natural products enopeptin B and A54556 B with *N*-methylalanine and serine residues in its peptidolactone, was expected to have the least rigid macrocycle and thus served as a point of comparison for the other ADEPs.

Using deuterium-exchange experiments, we systematically assessed the conformational consequences of replacing the *N*-methylalanine and serine residues in the ADEP macrocycle with conformationally constrained pipecolate and *allo*-threonine residues, respectively. Interestingly, pipecolate residues do not fortify both of the trans-annular bonds that are apparent in compounds containing *N*-methylalanine (compounds **1a** and **1e**) (Figure 6.3A). Indeed, we found

that difluorophenylalanine amide hydrogens of all compounds except for **1a** and **1e** exchanged completely within seconds in CD<sub>3</sub>OD (Figure 6.3B). Apparently, with the pipecolate residue in the macrocycle, the potential donor and acceptor atoms of the hydrogen bond are either too far apart or do not have appropriate trajectories for bonding. With respect to compounds **1a** and **1e**, we found that the inclusion of *allo*-threonine in the macrocycle attenuated the rate of deuterium exchange with the difluorophenylalanine amide hydrogen 2.8 fold (Figure 6.3C).

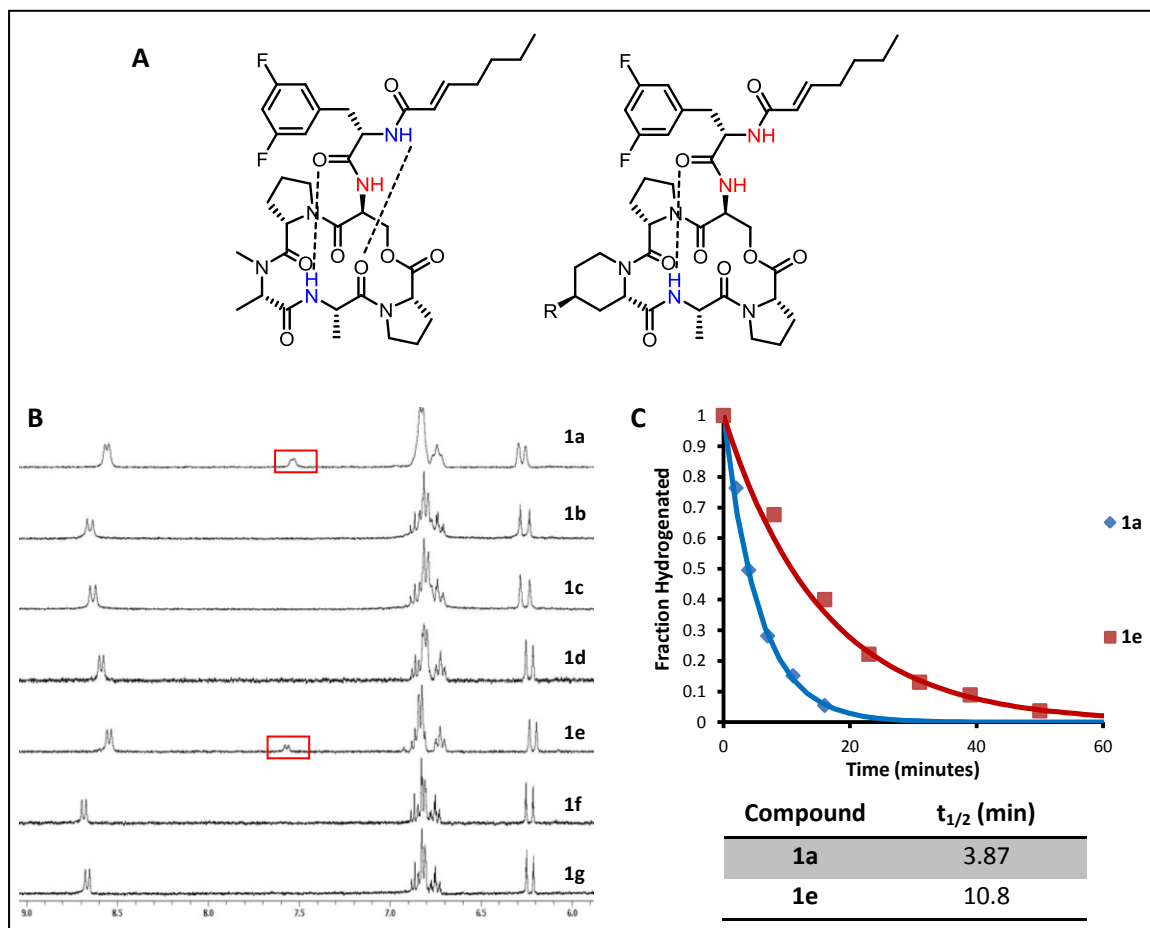


**Figure 6.3 – Effects of conformationally constrained amino acids on difluorophenylalanine amide deuterium exchange** A) *N*-methylalanine, but not pipecolic acid residues, in the peptidolactone enforce the trans-anular hydrogen bond from the macrocycle alanine carbonyl oxygen to the side chain difluorophenylalanine amide hydrogen. B) Overlay of <sup>1</sup>H-NMR spectra from D-exchange experiments acquired immediately after dissolving ADEP in CD<sub>3</sub>OD at 25 °C. The difluorophenylalanine amide proton signal is only observed for compounds that contain *N*-methylalanine in the macrocycle (**1a** and **1e**). C) ADEP Deuterium Exchange in CD<sub>3</sub>OD. Deuterium exchange rates were measured for 2mM solutions of each ADEP under pseudo-first order conditions in deuterated methanol at 25 °C. The amide hydrogen of the difluorophenylalanine amide in the compound with *allo*-threonine (**1e**) has a 2.8-fold longer half-life in CD<sub>3</sub>OD than the same hydrogen atom in the compound with serine in the same position (**1a**).

The transannular hydrogen bond in which the alanine amide is the donor is retained in all of the ADEPs and is strengthened by the presence of conformationally constrained amino acids within the peptidolactone (Figure 6.4). For instance, compound **1b** harboring a pipercolate residue in the peptidolactone had a slower rate of deuterium exchange rate than **1a**. Further, we found that the deuterium-exchange rate decreased as the steric bulk of the C4 substituent on the pipercolate increased (see data for compounds **1b**, **1c**, and **1d** in Figure 6.4). Substitution of *allo*-threonine for serine in the ADEP peptidolactone profoundly slows the deuterium-exchange rate. For instance, the half-lives of the alanine amide hydrogens in compound **1a**, which has serine, and compound **1e**, which has *allo*-threonine, are ~100-fold different at 25°C. Likewise, the deuterium exchange rate of the hydrogen atom of the difluorophenylalanine moieties in compounds **1a** and **1e** differed by 2.8-fold at 25°C. As expected, inclusion of both pipercolate and *allo*-threonine (**1f**) into the peptidolactone had a synergistic effect on deuterium exchange. Interestingly, the apparent relationship between rigidifying structural features and deuterium exchange rate was not observed when 4-methylpipercolate and *allo*-threonine were present together in the peptidolactone (**1g**). This compound had a faster rate of deuterium exchange than compounds with *allo*-threonine and either *N*-methylalanine (**1e**) or pipercolate (**1f**) in the peptidolactone. A reasonable explanation for this observation is that substituted pipercolate residues and *allo*-threonine each enforce slightly different low energy conformers. Accordingly, the opposing forces could prevent a single, low energy conformer from being reached. As expected, the rate of deuterium exchange increased for all compounds at an elevated temperature (*i.e.*, 40°C), whereas the trend for relative rates of deuterium exchange remained the same suggesting that the observed effects are the result of entropic factors. Overall, the general trend represented by these data support our hypothesis that the incorporation of conformationally constrained residues in the peptidolactone has a rigidifying effect.



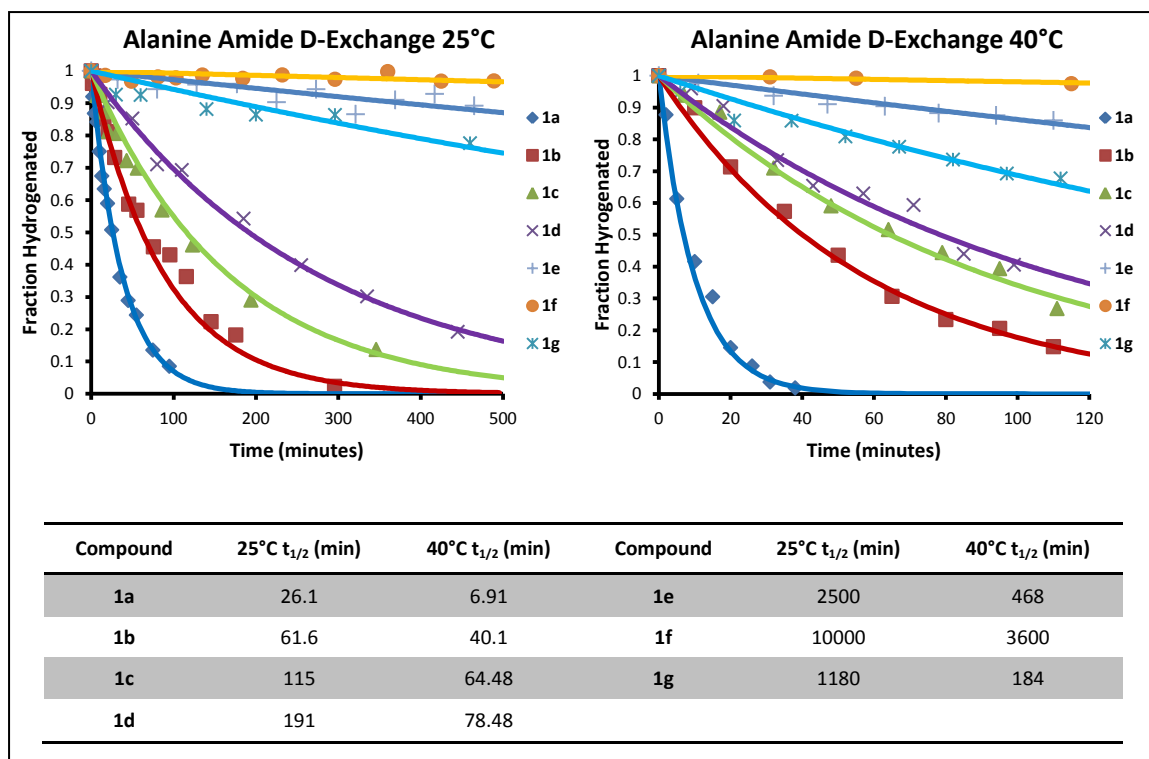
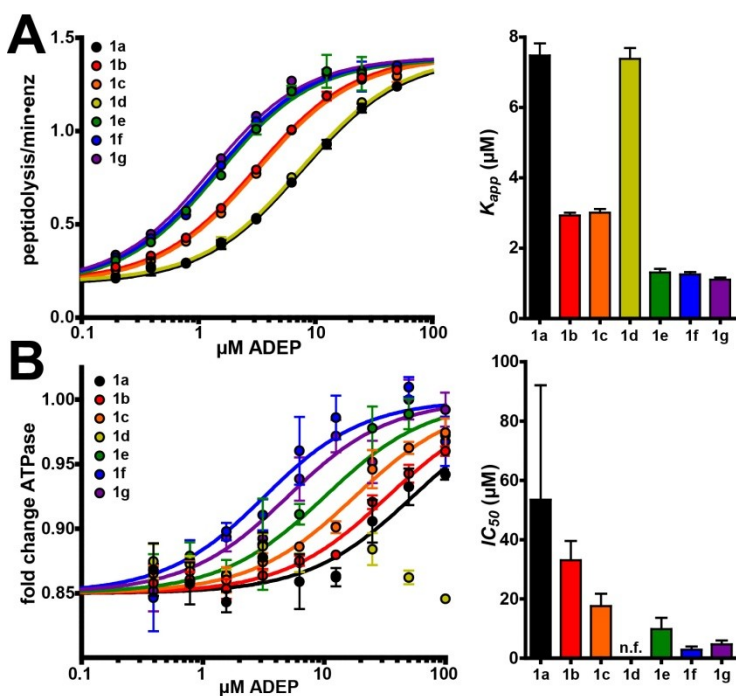


Figure 6.4 – Effects of conformationally constrained amino acids on alanine amide deuterium exchange. Deuterium exchange rates were measured for 2mM solutions of each ADEP under pseudo-first order conditions in deuterated methanol at 25 °C and 40°C.

### *In vitro* Assessment of ClpP Binding and Activation by the Rigidified ADEPs.

Binding of either the ADEPs or the regulatory ATPases to ClpP stabilizes an open conformation of the peptidase pore and stimulates degradation of oligopeptides.<sup>6,7</sup> Based on predictions that the entropic costs of ClpP binding would be lower for the conformationally constrained ADEP derivatives,<sup>3,8</sup> we expected that ADEP modifications that enhance macrocycle rigidity would improve ClpP binding and activation in a commensurate fashion. To test this hypothesis, we assayed ClpP catalyzed hydrolysis of an internally quenched fluorogenic decapeptide in the absence and presence of the ADEP derivatives. Cleavage between an aminobenzoic acid fluorophore and 2-nitrotyrosine quencher in this substrate relieves quenching, resulting in increased fluorescence that serves as a readout of peptidase activity. The capacities of each of the compounds to activate ClpP were assessed across a range of concentrations, and the

resulting activities were fit to yield apparent dissociation constants (Figure 6.5A, Table 6.1). As expected, we found a generally strong and positive correlation between the potency of the compounds as activators of ClpP and the deuterium exchange half-lives.  $K_{app}$  values range from 7.5  $\mu\text{M}$  for compound **1a**, the parental compound having the least rigid macrocycle, to 1.1  $\mu\text{M}$  for compound **1g**, which possesses a significantly more rigid macrocycle. Interestingly, compound **1d** was a weaker activator of ClpP than compounds **1b** and **1c** despite having a more rigid macrocycle. The bulky C4-isopropyl substituent may be poorly accommodated by the ClpP binding pocket. Nevertheless, structural modifications that rigidify the ADEP peptidolactone can improve ClpP activation up to  $\sim 7$ -fold *in vitro*.



**Figure 6.5 – Activation of ClpP and competition with ClpX by ADEPs *in vitro*.** (A) Rigidified ADEPs are more potent activators of ClpP peptide cleavage. Hydrolysis of a fluorogenic decapeptide substrate (15  $\mu\text{M}$ ) by *E. coli* ClpP (25 nM) was assayed in the presence of increasing concentrations of ADEP compounds, and activity was fit to a non-cooperative binding model (solid lines). Error bars represent standard deviation among three replicates or standard error of the fit. Tighter apparent affinities correlate with increased ADEP rigidity, with the exception of compound **1d**. See also Table 1. (B) ADEPs with greater macrocycle rigidity compete more strongly with ClpX for binding to ClpP. Fold change in ATPase activity of *E. coli* ClpX<sup>ΔN</sup> (10 nM) in the presence of *E. coli* ClpP (50 nM) was assayed over increasing concentrations of ADEPs, compared to the activity of ClpX<sup>ΔN</sup> alone, and was fit as above (no fit was obtained for **1d**). More rigid ADEPs better compete for binding to ClpP, and thus more effectively relieve ClpP-mediated repression of ClpX<sup>ΔN</sup> ATPase activity (Table 1).

In addition to modulating the quaternary structure of the ClpP tetradecamer, ADEPs and the accessory ATPases share the same binding sites and are known to compete for binding to ClpP.<sup>30-32</sup> As the rigidified ADEPs bound to ClpP more tightly, we predicted that these compounds would be stronger competitors for ATPase binding. We assayed binding competition by exploiting the observation that *E. coli* ClpX ATPase activity is depressed upon binding *E. coli* ClpP.<sup>7,9</sup> Accordingly, we inferred competition from the degree to which the ADEPs relieved depression of ATP hydrolysis by ClpX (Fig. 4.5B, Table. 4.2). As expected,  $IC_{50}$  values correlated with apparent affinities deduced from the peptidase activation experiments. The increased competition with ClpX indicates that the more rigid ADEPs bind more strongly to their original binding site on ClpP, rather than to novel sites. Interestingly, compound **1d** did not effectively compete with ClpX, despite the observation that it activated ClpP peptidase activity to the same extent as compound **1a**. Again, this weak suppression of ClpX ATPase activity can most likely be ascribed to poor accommodation of the isopropyl group in the ClpP binding pocket.

### Assessment of the Bioactivities of the Conformationally Constrained ADEPs in Antibacterial Assays.

As the ADEPs were synthesized, they were screened in house against a non-pathogenic Gram-positive bacterium, *Bacillus mycoides* (Table 6.1). Minimum inhibitory concentrations (MIC's) were determined using standard agar dilution methods.<sup>10</sup> These results helped to guide the design of compounds and were the primary reason that an ADEP analog containing a 4-isopropylpiperolate residue with *allo*-threonine in the peptidolactone was not synthesized. While the ADEPs with serine and either *N*-methylalanine (**1a**) or piperolate (**1b**) exhibited similar activity, the compound with serine and 4-methylpiperolate (**1c**) was slightly more potent. The ADEP with serine and 4-isopropylpiperolate was the least active of all the compounds. All three compounds with an *allo*-threonine residue in the peptidolactones were significantly more active

than analogs containing serine. Compounds with *allo*-threonine and either *N*-methylalanine (**1e**) and 4-methylpipercolate (**1g**) were 5x more active than the ADEP with the least rigid macrocycle (**1a**).

**Table 6.5 – Antibacterial activity of ADEPs against *B. mycooides***

	<b>1a</b>	<b>1b</b>	<b>1c</b>	<b>1d</b>	<b>1e</b>	<b>1f</b>	<b>1g</b>
<b><i>B. mycooides</i> MIC (µg/mL)</b>	0.5	0.5	0.4	0.6	0.1	0.2	0.1

The antibacterial activity of each compound was also assessed against three Gram-positive bacterial pathogens: *S. aureus*, *S. pneumoniae*, and *E. faecalis*. Minimum inhibitory concentrations (MICs) were determined by broth microdilution assays (Table 6.2). All seven synthetic ADEPs exhibited strong antibacterial activity. There were largely positive correlations between ADEP antibacterial activity, peptidolactone rigidity, and the apparent ClpP affinity. There were some exceptions. Compound **1d**, despite possessing a significantly more rigid peptidolactone, exhibited ClpP affinity and antibacterial activity similar to that of compound **1a**. Again, the presence of the large isopropyl substituent on the pipercolate residue most likely has a negative effect on binding to ClpP and thus antibacterial activity. In contrast, compound **1g**, bearing both a 4-methylpipercolate residue as well as an *allo*-threonine residue, was not the most rigid compound (compound **1f** in Table 6.1), yet it exhibited the most potent antibacterial activity in the series. While these exceptions cannot be completely explained, we do note that ADEPs whose hydrogens of the alanine residues have half-lives over 20 hours in the deuterium exchange experiments have the highest ClpP affinities and most antibacterial activity against all three species of bacterial pathogens. To the best of our knowledge, compound **1g** has the lowest MICs of any ADEP reported to date.<sup>27,29</sup> The antibacterial activity of **1g** was 32-fold more potent against *S. aureus*, 600-fold more potent against *E. faecalis*, and 1200-fold more potent against *S.*

*pneumoniae* than compound **1a**, which has the more flexible peptidolactone of the natural products.

Table 6.6 – Comparison of *in vitro* and *in vivo* ADEP properties

Compound	D- exchange $t_{1/2}$ 25°C (min)	ClpP Activation $K_{app}$ ( $\mu$ M)	ClpX Competition $IC_{50}$ ( $\mu$ M)	MIC		
				<i>S. aureus</i> ( $\mu$ g/mL)	<i>S. pneumoniae</i> ( $\mu$ g/mL)	<i>E. faecalis</i> ( $\mu$ g/mL)
<b>1a</b>	26.1	7.5 $\pm$ 0.34	53 $\pm$ 39	0.78	0.024	0.012
<b>1b</b>	61.6	2.9 $\pm$ 0.077	33 $\pm$ 6.5	0.39	0.006	0.015
<b>1c</b>	115	3.0 $\pm$ 0.10	18 $\pm$ 4.2	0.39	0.012	0.003
<b>1d</b>	191	7.4 $\pm$ 0.31	<i>no fit</i>	1.16	0.098	0.098
<b>1e</b>	2500	1.3 $\pm$ 0.10	9.8 $\pm$ 3.9	0.098	0.003	0.00076
<b>1f</b>	10000	1.3 $\pm$ 0.067	2.9 $\pm$ 1.0	0.098	$\leq$ 0.00002	$\leq$ 0.00002
<b>1g</b>	1180	1.1 $\pm$ 0.060	4.7 $\pm$ 1.3	0.024	$\leq$ 0.00002	$\leq$ 0.00002

The bacterial concentrations (colony forming units/mL) in each well of the dilution antimicrobial susceptibility tests were as follows: *S. aureus* ( $1.20 \times 10^6$ ), *E. faecalis* ( $8.5 \times 10^4$ ), and *S. pneumoniae* ( $3.65 \times 10^5$ ). The deuterium exchange rates for the hydrogen atoms of the alanine residues in the macrocycles are shown

### ADEP Activity in mouse models of infection

The remarkable activity that ADEPs exhibit *in vitro* has led to some preliminary *in vivo* studies in rodent models of bacterial infection. Bayer Healthcare AG examined the *in vivo* pharmacological, pharmacokinetic and toxicological properties of two of their optimized ADEPS, ADEP-2 and ADEP-4 (Figure 1).<sup>11</sup> Both compounds outperformed the clinically used drug, linezolid, while ADEP-4 exhibited the best overall efficacy in several mouse models of bacterial sepsis. Against a lethal challenge of *E. faecalis*, single doses as low as 1 mg/Kg of ADEP-2 and 0.5 mg/Kg of ADEP-4 were effective at saving 100% of mice in a 5 day study. Against a lethal challenge of *S. pneumoniae*, a single 12.5 mg/Kg dose of ADEP-4 saved 80% of rats in a 5 day study. ADEP-4 also significantly lowered bacterial loads on the liver, spleen, and lungs of mice with lethal *S. aureus* sepsis compared to an untreated control group. ADEP-4 was found to be non-toxic to mice with doses up to 100 mg/kg administered daily for 7 consecutive days. ADEP-4 half lives in mouse and dog ranged from 1-2 hours.

Although the initial *in vivo* efficacy of ADEP-4 appeared to be promising, Bayer Healthcare AG discontinued further ADEP development, probably because of the relatively high rate of spontaneous resistance resulting from loss of function mutations in the *clpP* gene.<sup>11</sup> It is likely that these concerns are unwarranted because bacteria without a functional *clpP* have compromised virulence and stress responses.<sup>12-17</sup> Accordingly, it is an interesting possibility that ADEPs could result in the selection of bacteria that cannot cause disease.<sup>15,18,19</sup>

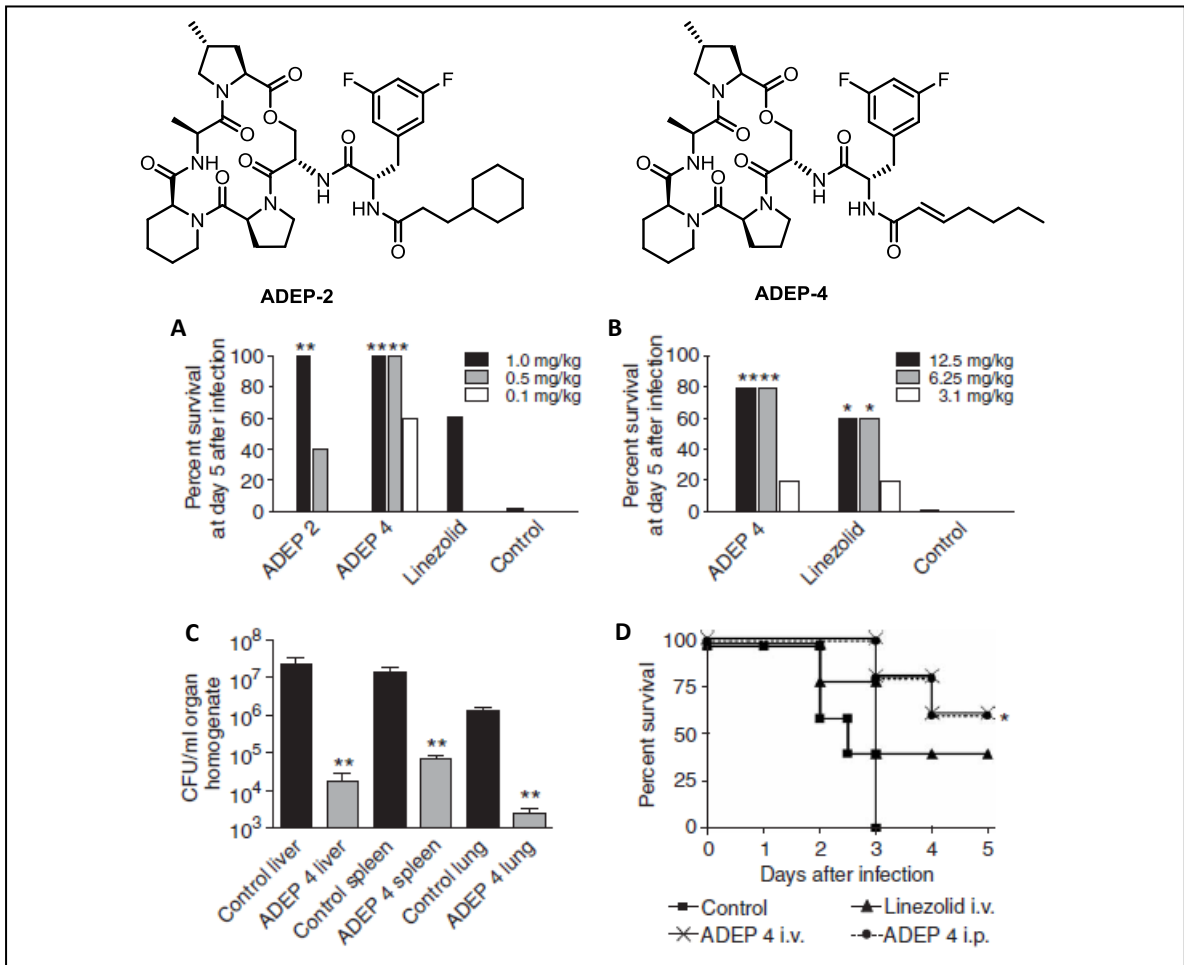


Figure 6.6 – Structures and *in vivo* activities of Bayer Healthcare AG optimized ADEPs<sup>11</sup> A) *In vivo* efficacy against mouse model of *E. faecalis* sepsis. B) *In vivo* efficacy against mouse model of *S. aureus* sepsis. C) Effects of ADEP-4 on viable bacterial organ load in mouse model of *S. aureus* sepsis. D) Effects of Intravenous (i.v.) and Intraperitoneal (i.p.) ADEP-4 therapy in mouse model of *S. pneumoniae* sepsis.

It has been proposed that concerns over SDEP resistance could be overcome by using the molecules in combination with other antibacterial agents. A recent study by the Lewis group has shown that ADEP-4 in combination with rifampicin is capable of eradicating chronic *S. aureus* biofilm infection.<sup>20</sup> This combination therapy was tested against several strains of *S. aureus* in a deep-seated mouse thigh infection model (Figure 2). In this model, mice are treated with the potent immunosuppressant, cyclophosphamide, and a large dose of a bacterial challenge is delivered directly to the thigh. The infection is allowed to progress for 24 hours before antibacterial agents are administered. The result is a recalcitrant and deep-seated infection that is much more difficult to treat than standard mouse models of bacterial sepsis. Remarkably, the combination of ADEP-4 and rifampicin was able to completely eradicate the infection within 24 hours. Other treatments such as vancomycin, vancomycin in combination with rifampicin, rifampicin alone, or ADEP alone were able to lower the viable bacterial counts but were unable to completely eradicate the infection.

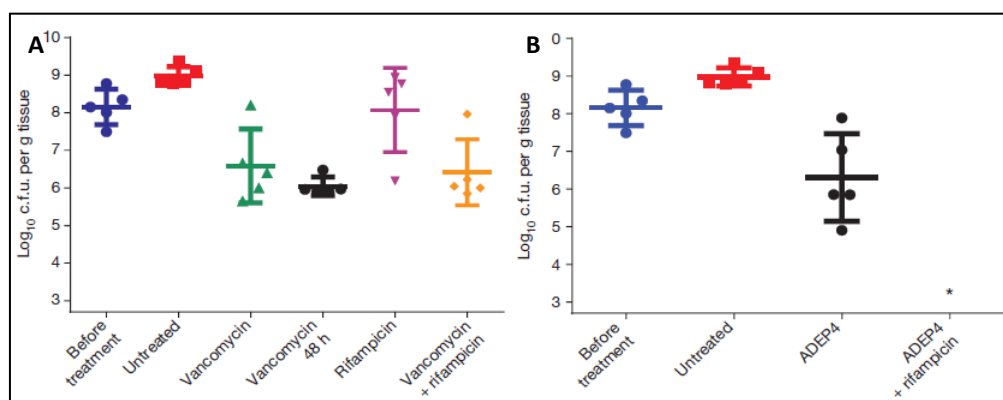


Figure 6.7 – Treatment of deep-seated *S. aureus* infection in mouse thigh.<sup>20</sup> A) Viable bacterial counts isolated from mouse thigh after treatment with vancomycin and rifampicin alone and in combination. B) Viable bacterial loads isolated from mouse thigh after treatment with ADEP-4 alone and in combination with rifampicin.

The potential for clinical development of the ADEPs seems quite promising. Since rigidified ADEPs exhibit dramatically improved potency, we selected a sample of our own optimized ADEPs for testing in mouse models of sepsis (**1b**, **1c**, **1e**, **1g**). Compound **1b** is our

closest analog to ADEP-4, which differs only by the presence of a 4-methylproline residue in the northern region of the peptidolactone. Compound **1c** was chosen to examine the effects of the pipercolic acid methyl group. Compound **1e** is highly potent, but does not contain a pipercolic acid residue in its peptidolactone. It is therefore the most amenable to large scale synthesis given the high cost of substituted pipercolic acids and the peculiarities of the IMCR. Compound **1g** is our most active ADEP analog containing both *allo*-threonine and 4-methylpipercolic acid in its peptidolactone. The clinically used antibiotic, vancomycin, was used as a positive control.

In the experiment, mice were injected intraperitoneally with a lethal inoculum of *S. aureus*. Mice were injected with 25 mg/Kg doses of the compounds 30 minutes before and again 1 hour after inoculation with *S. aureus*. The mice were then monitored for survival for 10 days (Figure 6.8). All mice in the vehicle treated control group died within 1 day whereas all mice treated with vancomycin survived for the duration of the experiment. All of the ADEPs were able to protect mice relative to the untreated control group. The efficacy of the ADEPs correlates well with the relative potencies in *in vitro* bacterial susceptibility assays (relative protection against *S. aureus* infection: vancomycin  $\approx$  **1b**>>**1e**>**1c**>**1g**). Remarkably, our most potent ADEP *in vitro* (**1g**), performed nearly as well as vancomycin in the mouse infection model experiment. These initial results are very encouraging. In future experiments, we will test a larger group of mice and determine viable bacterial counts from various organs after ADEP treatment. We will also conduct similar experiments in a mouse model of *E. faecalis*.



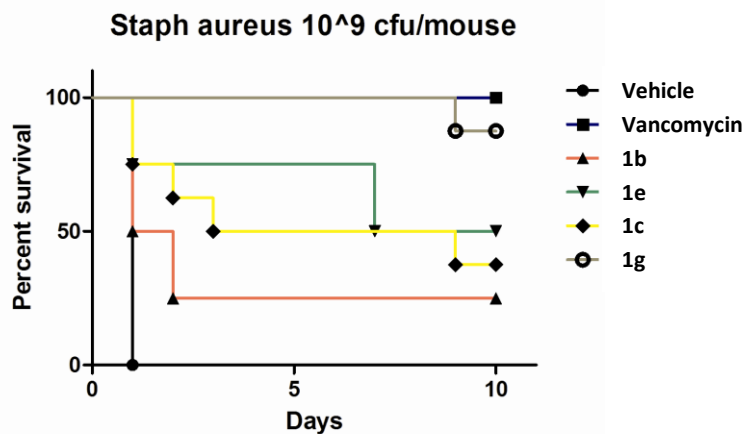


Figure 6.8 – Effect of optimized ADEPs in mouse model of *S. aureus* (ATCC 29213) infection. Mice (8 / compound) were injected with 25 mg/Kg of compound 30 min before and 1 h after inoculation and then monitored for survival over 10 days. All p values relative to vehicle treated control <0.05.

## Conclusion

The cyclic acyldepsipeptide antibiotics are a promising class of antibacterial agents that act by binding and dysregulating the activity of the ClpP peptidase. Reports by our group and others state that the activities of these compounds can be dramatically improved by replacing certain amino acid constituents of the peptidolactone core structure with more conformationally constrained counterparts.<sup>3,8</sup> It has been proposed that improvements in bioactivity are a consequence of these amino acids' capacity to stabilize a bioactive conformation of the ADEPs, which incurs a lower entropic cost upon binding to ClpP.<sup>3</sup> While compelling, this proposal had very little experimental support. Herein, we present data indicating that replacement of selected constituent amino acids in the ADEP peptidolactone core does indeed stabilize a bioactive conformation. Specifically, analyses of ADEPs harboring conformationally constrained amino acids via deuterium exchange experiments revealed that they exhibit the same trans-annular hydrogen bonds in solution that are inferred from the crystal structures of an ADEP in complex with ClpP. Our finding that replacement of the *N*-methylalanine residue of the ADEP natural products with a pipecolate attenuates deuterium exchange of only one of the two donors (*i.e.*,

amide hydrogen of alanine) in the trans-annular hydrogen bonds, whereas the substitution of the natural serine with *allo*-threonine suppresses deuterium exchange rates of both hydrogen bond donors indicates the position of the conformationally constrained amino acid within the macrocycle has important effects on molecular conformation. In molecules with either one or two trans-annular hydrogen bonds, the inverse correlations between the number of constrained amino acids constituting the depsipeptidolactone and the rates of deuterium exchange indicated that the amino acid substitutions lock the ADEPs into a conformation that is compatible with ClpP binding. The apparent enhancements of the conformationally constrained ADEPs' capacities to both activate ClpP and compete with its binding to the accessory ATPase, ClpX, corroborate the proposal that a bioactive conformation been fortified. These improvements are also consistent with the proposal that there is a lower entropic cost in the binding of the rigidified ADEPs to ClpP. The latter point is of particular interest because the commonly held view that rigid ligands suffer a lower entropic cost in receptor binding than flexible ones<sup>21-25</sup> has recently been challenged by cases wherein there are entropic penalties for ligand preorganization in receptor-ligand interactions.<sup>26,27</sup> In any case, the finding that ClpP activation by the ADEPs was enhanced by up to 7-fold via the introduction of conformational constraints, while these same changes enhanced antibacterial activity by up to 1,200-fold indicates that there are other factors involved. A likely explanation is that the constrained compounds are more cell-permeable. Indeed, peptides with enforced trans-annular hydrogen bonds exhibit dramatically enhanced cell-permeability and oral bioavailability because the bonding reduces the energetic costs of desolvation that accompanies membrane penetration in aqueous environments.<sup>28-31</sup> Apparently, the conformational constraints that we have introduced enhance the ADEPs' intrinsic trans-annular hydrogen bonding interactions that pre-dispose them for both ClpP binding and membrane penetration.

It is well-known that the conformational constraints of macrocyclic molecules can be further enhanced by judicious introduction of substituents on the ring.<sup>32,33</sup> In this case, it is notable that installation of small methyl substituents profoundly enhances the affinity of a large macrocycle for its biomolecular receptor and the molecules' bioactivities. Although replacement of hydrogen atoms with methyl groups is common in structure-activity relationship (SAR) studies and medicinal chemistry optimization programs,<sup>34</sup> the inclusion of a methyl group on a ligand typically is deleterious or minimally improves receptor binding. Indeed, a recent analysis of published SAR studies by Jorgensen and co-workers states that in 8% of cases the inclusion of a methyl group enhances bioactivity 10-fold or better.<sup>35</sup> In only 0.4% of cases did molecules with an additional methyl group have 100-fold enhanced bioactivity.<sup>35</sup> Their analysis also revealed that significant improvements in bioactivity are usually the result of the methyl group's capacity to fill a hydrophobic environment in the receptor and to influence the conformation of the ligand. Interestingly, the substituent effect strategy exploited in medicinal chemistry is mirrored in the ADEP natural products themselves. Specifically, enopeptin A, which has a 4-methyl proline residue in its macrocycle, has a two-fold lower MIC against *S. aureus*, *S. pneumoniae*, *E. faecalis*, and *E. faecium* than enopeptin B which has an unsubstituted proline residue at the same position.<sup>3</sup> In this study, we found that the position of the methyl substituent on the ADEP peptidolactone is very important. When comparing the ADEPs lacking methyl substituents (compounds **1a** and **1b**) to analogs harboring either 4-methyl pipecolate (compound **1c**) or *allo*-threonine (compound **1e**), we find that the *allo*-threonine residue exerts the strongest influence over conformational dynamics, ClpP affinity, and bioactivity. Furthermore, it should be noted that inclusion of *allo*-threonine in the ADEP peptidolactone improves the MIC ten-fold, while inclusion of 4-methyl proline improves the antibacterial activity only two-fold (as evidenced in the reported MICs of enopeptin A and enopeptin B).<sup>3</sup>

In this case, the unique characteristics of both the small molecule ligands as well as their receptor facilitated in-depth studies of a receptor-ligand interaction. Observations and modulations of the conformational dynamics of ADEPs were accompanied by measurements of their affinity for ClpP and antibacterial activity. A distinguishing feature of our multi-faceted study was the use of deuterium-exchange  $^1\text{H}$ -NMR experiments to assess relative differences in conformational rigidities of the ADEPs. We have shown that in such cases, trans-annular hydrogen bonding can be exploited to study the effects of structural modification on conformational rigidity. We anticipate that this approach to small-molecule dynamics could be applied to studies of many ligand-receptor interactions because many small molecules that interact with biological macromolecules exhibit trans-annular hydrogen bonds (especially peptides). It is a much simpler alternative to sophisticated multi-dimensional NMR experiments wherein  $^{15}\text{N}$ - and  $^{13}\text{C}$ -labeled compounds are used to assess the dynamics of small molecules.

The ADEP analogs reported herein constituted by the conformationally constrained amino acids *allo*-threonine and 4-methyl pipercolate have some of the lowest MICs ever reported for antibacterial agents. The most potent ADEP reported prior to this work, ADEP-4, was reported to cure *S. aureus* infections in mice and *S. pneumoniae* infections in rats with even greater efficacy than linezolid, a clinically used drug.<sup>3</sup> Given that our optimized analogs have MICs against *S. pneumoniae* and *E. faecalis* that are 200-fold lower than those reported for ADEP-4, it is tempting to speculate that a dramatically lower and potentially safer dose of our most potent compound could be efficacious in the treatment of various *Streptococcal* and *Enterococcal* infections in animals and humans. Preliminary mouse model experiment with our Rigidified ADEPs is very encouraging. Our most potent compound 1g was nearly as effective as vancomycin at protecting mice from lethal *S. aureus* sepsis.

An added advantage of the optimized compounds reported here with respect to drug development is that the key *allo*-threonine residue is much less expensive and easier to prepare than the 4-methylproline constituent of ADEP-4.<sup>3</sup> The promise of these molecules is further enhanced by the observations that peptides with strong trans-annular hydrogen bonds have enhanced oral bioavailability. Testing of these compounds in animal models of infection is currently underway. In total, our findings provide a compelling illustration of how the pharmacological properties of natural products can be improved by rational design.

### Experimental Contributions

ADEP deuterium exchange experiments were performed by Daniel Carney. ClpP binding and competition assays were performed by Karl Schmits from the Sauer lab in the MIT department of Biology. *B. mycoides* MIC were determined by Daniel Carney. *S. aureus*, *E. faecalis*, and *S. pneumoniae* were determined by C. Andersen and A. Onderdonk from the New England Regional Centers of Excellence in Biodefense at Harvard Medical School. Mouse model experiments were performed by Marios Arvanitis and Dedong Li from the Mylonakis lab in the Brown Medical School.

### Experimental Section

**H-D exchange kinetics.** NMR samples were prepared by dissolving thoroughly dried ADEP in ampule sealed CD<sub>3</sub>OD at a concentration of 2 mM. The ADEP in CD<sub>3</sub>OD was promptly transferred to a clean NMR tube, purged with an argon atmosphere, then capped and sealed with parafilm before being placed into the NMR spectrometer. Standard proton NMR spectra were acquired periodically over the course of several hours. The integration of the exchanging amide signal of interest was calibrated to a non-exchanging reference peak. Each data set was normalized such that the integral of the amide signal of interest in the first spectrum acquired was equal to 1.00

and designated as  $t_0$ . Data sets were plotted in Microsoft excel as normalized integrals vs. time. Plotted data sets were fit with exponential curves with Y intercepts set to 1. Exchange half-lives were calculated from the exponential functions.

**Protein expression and purification.** *E. coli* ClpP bearing a C-terminal His<sub>6</sub> tag and single-chain pseudo-hexameric *E. coli* ClpX<sup>ΔN</sup> (amino acids 62-424) were expressed and purified by metal affinity, anion exchange, and gel-filtration chromatography as described.<sup>5,5,36</sup>

**Activity and competition assays.** *In vitro* assays were performed at 30 °C in PD buffer (25 mM HEPES, pH 7.5, 100 mM KCl, 5 mM MgCl<sub>2</sub>, 1 mM DTT, 10% (wt/vol) glycerol, 10% (vol/vol) DMSO) using a SpectraMax M5 microplate reader (Molecular Devices). Peptidase activation was measured by incubating 25 nM of ClpP tetradecamer and ADEP analog with 15 μM of an internally quenched fluorogenic peptide substrate, Abz-KASPVSLGY<sup>NO2</sup>D,<sup>5</sup> incorporating a 2-aminobenzoic acid (Abz) fluorophore and 3-nitrotyrosine (Y<sup>NO2</sup>) quencher. Peptide hydrolysis by ClpP was monitored by following the increase in 420 nm fluorescence upon 320 nm excitation. Initial analysis of peptidase data showed negligible cooperativity, thus data were fit to a quadratic form of a non-cooperative binding equation, assuming 14 equivalent ADEP binding sites per ClpP tetradecamer.

To assay ADEP competition for ClpX binding to ClpP, 50 nM of ClpP tetradecamer, 10 nM of ClpX<sup>ΔN</sup> pseudo-hexamer, 0 - 100 μM of ADEP and 2.5 of mM ATP were incubated with an NADH-coupled ATP regeneration system.<sup>49</sup> ATP hydrolysis was monitored by following the coupled disappearance of NADH, via decrease in 340 nm absorbance. Pseudo-hexameric ClpX<sup>ΔN</sup> is functionally identical to monomerically encoded ClpX<sup>ΔN</sup>,<sup>32</sup> and was used to ensure hexamer stability at low ClpX concentrations. ATPase data were fit as above, assuming two ClpX binding sites per ClpP tetradecamer.

**MIC determinations:** MIC determinations for *B. mycooides* were performed in house using a standard agar dilution method. Difco Nutrient Agar (3 mL) was supplemented with an ADEP at a specified concentration. *B. mycooides* liquid cultures Difco Nutrient Broth (3 mL) was inoculated with single colonies of *B. mycooides* and grown overnight at 30°C. ADEP supplemented plates were inoculated with a 5 µL aliquot turbid overnight *B. mycooides* culture and then incubated at 30°C. After 48 hours, the agar plates were assessed for growth. MIC's were defined as the lowest concentration capable of inhibiting bacterial growth to fewer than 10 colonies. MIC determinations for pathogenic strains were performed BSL2+ conditions at the New England Center for Research Excellence (NERCE) in biodefense at Harvard Medical School following standard dilution antimicrobial susceptibility testing protocols.<sup>10</sup> Following incubation with the bacteria and the compound, each well was visually examined for growth with the unaided eye. The MIC is determined to be the first set of replicate wells of the dilution series exhibiting no growth when compared to the growth control wells.

**ADEP Stability Testing.** Stock solutions (3.3 mg/mL) of each ADEP in 75% PEG400 / 15% Water / 10% Ethanol were prepared. While **1A** and **2A** dissolved quickly in the vehicle, **2B** remained partially insoluble at 3.3 mg/mL even after mild heating. Each stock solution was split into 6 samples and labeled A-F. Samples A-C were stored at room temperature while samples D-F were stored at ~4°C. After 2, 5 and 7 days of storage, 25 µL aliquots of each sample were diluted ten-fold into 40% Acetonitrile / 60% Water and subsequently analyzed by HPLC.

HPLC analysis was carried out using and an Agilent 1260 Infinity series quaternary pump coupled to an Agilent 1260 Infinity series multi-wavelength detector. 10 µL injections of the diluted ADEP samples were made onto an Agilent Proshell 120 EC-C18 4.6x50 mm 2.7 µm column. The

samples were eluted with a solvent gradient of 40-80% acetonitrile in water over 10 minutes at 2.0 mL/min. Species elution was monitored at 214 nm and 254 nm.

**Survival assay.** To evaluate the *in vivo* efficacy of the compounds, murine peritonitis models were used as previously described.<sup>11</sup> Female 8 week-old CFW mice were used in all experiments. In brief, *S. aureus* ATCC 29213 was grown overnight in trypticase-soy (TS) broth at 37°C with agitation. Bacterial cells were then centrifuged, washed three times and resuspended in PBS at a concentration of 10<sup>9</sup> (concentrations similar to the LD<sub>90</sub> for this bacterial strain as determined by a pilot experiment). Subsequently, 100µl of this suspension was inoculated intraperitoneally to the mice. Approximately 30 minutes before and 1 hour following the inoculation, each group of mice was injected intraperitoneally with 100µl of a tested compound. All tested compounds were dissolved in 75% PEG400/10% Ethanol/15% water (the vehicle) with the exception of vancomycin which was dissolved in distilled water. Vancomycin and the vehicle were used as controls. Ten mice were used per group. All mice were evaluated daily for survival.

**Statistical analysis.** Survival was plotted using Kaplan Meier curves and p-values were calculated using the log-rank and Wilcoxon tests. Cfu counts were analyzed using non-parametric tests (Mann-Whitney). GraphPad 5.0 was used for all statistical calculations. A p value of <0.05 was considered statistically significant.

## References

1. Lee, B.; Park, E. Y.; Lee, K.; Jeon, H.; Sung, K. H.; Paulsen, H.; Rubsamen-Schaeff, H.; Brotz-Oesterhelt, H.; Song, H. K. Structures of ClpP in complex with acyldepsipeptide antibiotics reveal its activation mechanism. *Nat Struct Mol Biol* **2010**, *17*, 471-478.
2. Li, D. H. S.; Chung, Y. S.; Gloyd, M.; Joseph, E.; Ghirlando, R.; Wright, G. D.; Cheng, Y.; Maurizi, M. R.; Guarne, A.; Ortega, J. Acyldepsipeptide antibiotics induce the formation of a structured axial channel in ClpP: a model for the ClpX/ClpA-bound state of ClpP. *Chem. Biol.* **2010**, *17*, 959-969.



3. Hinzen, B.; Raddatz, S.; Paulsen, H.; Lampe, T.; Schumacher, A.; Häbich, D.; Hellwig, V.; Benet-Buchholz, J.; Endermann, R.; Labischinski, H.; Brötz-Oesterhelt, H. Medicinal Chemistry Optimization of Acyldepsipeptides of the Enopeptin Class Antibiotics. *ChemMedChem* **2006**, *1*, 689-693.
4. Steffel, L. R.; Cashman, T. J.; Reutershan, M. H.; Linton, B. R. Deuterium exchange as an indicator of hydrogen bond donors and acceptors. *J. Am. Chem. Soc.* **2007**, *129*, 12956-12957.
5. Lee, M. E.; Baker, T. A.; Sauer, R. T. Control of substrate gating and translocation into ClpP by channel residues and ClpX binding. *J. Mol. Biol.* **2010**, *399*, 707-718.
6. Singh, S. K.; Grimaud, R.; Hoskins, J. R.; Wickner, S.; Maurizi, M. R. Unfolding and internalization of proteins by the ATP-dependent proteases ClpXP and ClpAP. *Proceedings of the National Academy of Sciences of the United States of America* **2000**, *97*, 8898-8903.
7. Martin, A.; Baker, T. A.; Sauer, R. T. Distinct static and dynamic interactions control ATPase-peptidase communication in a AAA protease. *Mol. Cell* **2007**, *27*, 41-52.
8. Socha, A. M.; Tan, N. Y.; LaPlante, K. L.; Sello, J. K. Diversity-oriented synthesis of cyclic acyldepsipeptides leads to the discovery of a potent antibacterial agent. *Bioorg. Med. Chem.* **2010**, *18*, 7193-7202.
9. Joshi, S. A.; Hersch, G. L.; Baker, T. A.; Sauer, R. T. Communication between ClpX and ClpP during substrate processing and degradation. *Nature structural & molecular biology* **2004**, *11*, 404-411.
10. Willer, M.; Hindler, J.; Cockerill, F. Methods for dilution antimicrobial susceptibility tests for bacteria that grow aerobically; approved eighth. *CLSI* **2009**, *29*, 12-15.
11. Brotz-Oesterhelt, H.; Beyer, D.; Kroll, H.; Endermann, R.; Ladel, C.; Schroeder, W.; Hinzen, B.; Raddatz, S.; Paulsen, H.; Henninger, K.; Bandow, J. E.; Sahl, H.; Labischinski, H. Dysregulation of bacterial proteolytic machinery by a new class of antibiotics. *Nat. Med.* **2005**, *11*, 1082-1087.
12. Kwon, H.; Kim, S.; Choi, M.; Ogunniyi, A. D.; Paton, J. C.; Park, S.; Pyo, S.; Rhee, D. Effect of Heat Shock and Mutations in ClpL and ClpP on Virulence Gene Expression in *Streptococcus pneumoniae*. *Infect. Immun.* **2003**, *71*, 3757-3765.
13. Kwon, H.; Ogunniyi, A. D.; Choi, M.; Pyo, S.; Rhee, D.; Paton, J. C. The ClpP Protease of *Streptococcus pneumoniae* Modulates Virulence Gene Expression and Protects against Fatal Pneumococcal Challenge. *Infect. Immun.* **2004**, *72*, 5646-5653.
14. Frees, D.; Sorensen, K.; Ingmer, H. Global Virulence Regulation in *Staphylococcus aureus*: Pinpointing the Roles of ClpP and ClpX in the sar/agr Regulatory Network. *Infect. Immun.* **2005**, *73*, 8100-8108.

15. Butler, S. M.; Festa, R. A.; Pearce, M. J.; Darwin, K. H. Self-compartmentalized bacterial proteases and pathogenesis. *Mol. Microbiol.* **2006**, *60*, 553-562.
16. Robertson, G. T.; Ng, W.; Foley, J.; Gilmour, R.; Winkler, M. E. Global transcriptional analysis of clpP mutations of type 2 *Streptococcus pneumoniae* and their effects on physiology and virulence. *J. Bacteriol.* **2002**, *184*, 3508-3520.
17. Frees, D.; Qazi, S. N. A.; Hill, P. J.; Ingmer, H. Alternative roles of ClpX and ClpP in *Staphylococcus aureus* stress tolerance and virulence. *Mol. Microbiol.* **2003**, *48*, 1565-1578.
18. Böttcher, T.; Sieber, S. A.  $\beta$ -Lactones as Specific Inhibitors of ClpP Attenuate the Production of Extracellular Virulence Factors of *Staphylococcus aureus*. *J. Am. Chem. Soc.* **2008**, *130*, 14400-14401.
19. Böttcher, T.; Sieber, S. A. Structurally Refined  $\beta$ -Lactones as Potent Inhibitors of Devastating Bacterial Virulence Factors. *ChemBioChem* **2009**, *10*, 663-666.
20. Conlon, B.; Nakayasu, E.; Fleck, L.; LaFleur, M.; Isabella, V.; Coleman, K.; Leonard, S.; Smith, R.; Adkins, J.; Lewis, K. Activated ClpP kills persisters and eradicates a chronic biofilm infection. *Nature* **2013**, *503*, 365-370.
21. Böhm, H.; Klebe, G. What Can We Learn from Molecular Recognition in Protein–Ligand Complexes for the Design of New Drugs? *Angewandte Chemie International Edition in English* **1996**, *35*, 2588-2614.
22. Khan, A. R.; Parrish, J. C.; Fraser, M. E.; Smith, W. W.; Bartlett, P. A.; James, M. N. Lowering the entropic barrier for binding conformationally flexible inhibitors to enzymes. *Biochemistry (N. Y.)* **1998**, *37*, 16839-16845.
23. Nakanishi, H.; Kahn, M. In *Designin of Peptidomimetics*; The practice of medicinal chemistry; Academic Press: 2011; .
24. Searle, M. S.; Williams, D. H. The cost of conformational order: entropy changes in molecular associations. *J. Am. Chem. Soc.* **1992**, *114*, 10690-10697.
25. Vajda, S.; Wheng, Z.; Rosenfeld, R.; DeLisi, C. Effect of conformational flexibility and solvation on receptor-ligand binding free energies. *Biochemistry (N. Y.)* **1994**, *33*, 13977-13988.
26. Benfield, A. P.; Teresk, M. G.; Plake, H. R.; DeLorbe, J. E.; Millspaugh, L. E.; Martin, S. F. Ligand preorganization may be accompanied by entropic penalties in protein–ligand interactions. *Angewandte Chemie International Edition* **2006**, *45*, 6830-6835.
27. Udugamasooriya, D. G.; Spaller, M. R. Conformational constraint in protein ligand design and the inconsistency of binding entropy. *Biopolymers* **2008**, *89*, 653-667.

28. Rezai, T.; Yu, B.; Millhauser, G. L.; Jacobson, M. P.; Lokey, R. S. Testing the conformational hypothesis of passive membrane permeability using synthetic cyclic peptide diastereomers. *J. Am. Chem. Soc.* **2006**, *128*, 2510-2511.
29. Rezai, T.; Bock, J. E.; Zhou, M. V.; Kalyanaraman, C.; Lokey, R. S.; Jacobson, M. P. Conformational flexibility, internal hydrogen bonding, and passive membrane permeability: successful in silico prediction of the relative permeabilities of cyclic peptides. *J. Am. Chem. Soc.* **2006**, *128*, 14073-14080.
30. Veber, D. F.; Johnson, S. R.; Cheng, H.; Smith, B. R.; Ward, K. W.; Kopple, K. D. Molecular properties that influence the oral bioavailability of drug candidates. *J. Med. Chem.* **2002**, *45*, 2615-2623.
31. Bock, J. E.; Gavenonis, J.; Kritzer, J. A. Getting in Shape: Controlling Peptide Bioactivity and Bioavailability Using Conformational Constraints. *ACS chemical biology* **2012**, *8*, 488-499.
32. Marsault, E.; Peterson, M. L. Macrocycles are great cycles: applications, opportunities, and challenges of synthetic macrocycles in drug discovery. *J. Med. Chem.* **2011**, *54*, 1961-2004.
33. Giordanetto, F.; Kihlberg, J. Macrocyclic Drugs and Clinical Candidates: What Can Medicinal Chemists Learn from Their Properties? *J. Med. Chem.* **2013**.
34. Barreiro, E. J.; Kümmerle, A. E.; Fraga, C. A. The methylation effect in medicinal chemistry. *Chem. Rev.* **2011**, *111*, 5215-5246.
35. Leung, C. S.; Leung, S. S.; Tirado-Rives, J.; Jorgensen, W. L. Methyl Effects on Protein-Ligand Binding. *J. Med. Chem.* **2012**, *55*, 4489-4500.
36. Kim, Y.; Burton, R. E.; Burton, B. M.; Sauer, R. T.; Baker, T. A. Dynamics of substrate denaturation and translocation by the ClpXP degradation machine. *Mol. Cell* **2000**, *5*, 639-648.

## Chapter 7 – Synthesis and Evaluation of ADEPs with Modified side Chains

### Introduction

Structural studies have provided a wealth of information about the ADEP binding mode for ClpP.<sup>1,2</sup> While peptidolactones moiety binds at the surface of ClpP and is significantly solvent exposed, the ADEP acylphenylalanine side chain moiety binds in hydrophobic environments at the interface between ClpP monomers (Figure 7.1).<sup>1,2</sup> The phenylalanine aromatic ring occupies a deep hydrophobic pocket lined by the residues Tyr62, Ile90, Ile92, Leu114, and Leu189 of one ClpP monomer and residue Phe82 of the adjacent monomer. The fluorine atoms present on the aromatic ring of synthetic ADEP analogs are accommodated by the polar amide backbone environment. The phenylalanine amide nitrogen forms a hydrogen bond with the Tyr62 oxygen atom and the hydrophobic acyl cap snakes along a hydrophobic groove defined by Leu23 and Ile28 of one ClpP monomer and Leu48, Phe49, and Ala52 of the adjacent ClpP monomer. This structural information indicates that the side chain is a major facilitator of the ADEP-ClpP interaction.

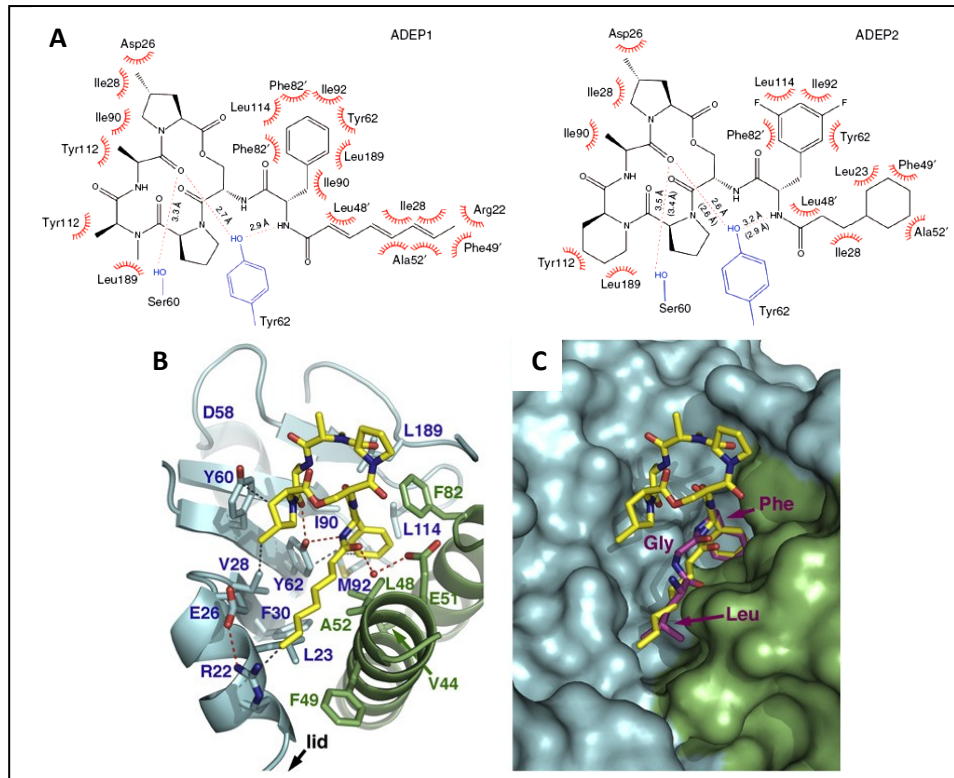


**Figure 7.1 – ADEP-ClpP binding Interactions** A) Schematic diagram showing the binding interactions between ADEP1 and ADEP2 with *B. subtilis* ClpP.<sup>1</sup> B Detailed 3-dimensional diagram of ADEP-1 (yellow stick) interactions with *E. coli* ClpP (blue and green ribbon). Hydrogen bonding is indicated by red lines and van der Waals interactions are indicated by grey lines.<sup>2</sup> C) Superimposition of ADEP-1 and the ClpX LGF motif bound to *E. coli* ClpP (Blue and Green Space filling diagram).<sup>2</sup>

Li *et al.* made the interesting observation that the acylphenylalanine side chain is nearly superimposable with a hypothetical binding mode for the highly conserved LGF/IGF loop motif of ClpX, a ClpP accessory ATPase (Figure 7.1C).<sup>2</sup> Although structures of the ClpX-ClpP complex have not been published, mutational analyses in the LGF/IGF loop of ClpX have indicated that this motif is essential for binding to ClpP.<sup>3</sup> The observation made by Li *et al.* led to the proposal that the ADEP side chain is a mimic of the LGF/IGF loop motif. Furthermore, Li *et al.* proposed that the “open” conformation of ClpP when it is in complex with an ADEP is a model for the conformation that ClpP must exist in when it is bound to an accessory ATPase. Since there is no structural information to validate this hypothesis, we hoped to test it empirically.

## ADEPs with peptidomimetic side chains

We hypothesized that if the ADEP acyldifluorophenylalanine moiety does indeed mimic the LGF/IGF loop motif, then it should be possible to replace the hydrophobic acyl-chain with a more peptide like moiety and retain affinity for ClpP and perhaps also antibacterial activity. We therefore designed a series of ADEPs with peptide side chains that closely resemble the LGF/IGF tripeptide (Figure 7.2). Specifically, we envisioned replacing the heptenoyl acyl group with either a *N*-acetyl dipeptide (**2a** and **2b**) or *N*-acylglycine (**2c** and **2d**) where the *N*-acyl group mimics the side chain of either leucine or isoleucine. The natural product peptidolactone was chosen as the anchor for these side chains because it is the most expedient macrocycle to prepare synthetically on a scale large enough for late stage diversification.

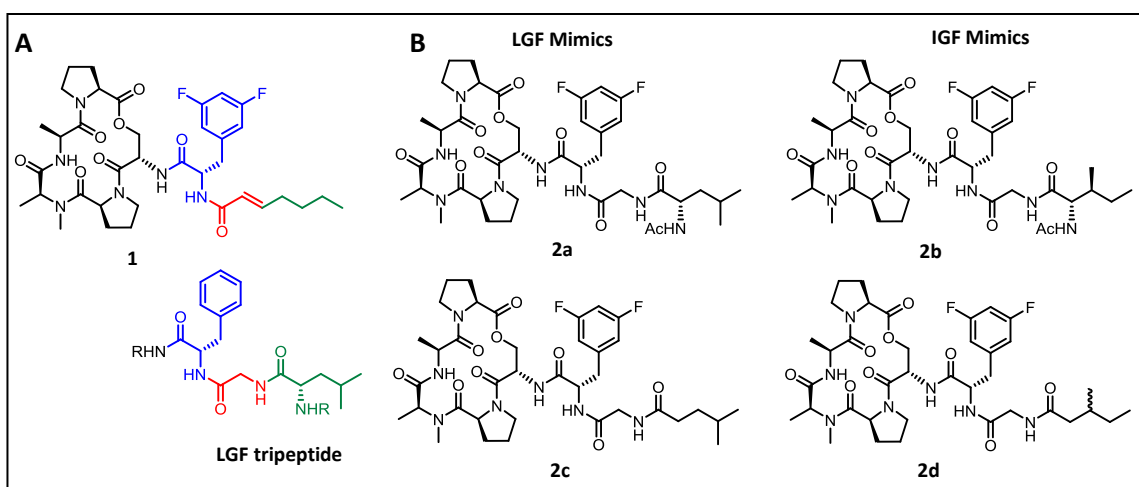


Figure 7.2 – ADEP Peptidomimetics A) Side by side view of the LGF tripeptide (top) and the ADEP acyldifluorophenylalanine side chain (bottom) B) ADEP molecule with peptide side chains.

ADEPs **2a-d** were prepared according to Figure (5.3). Boc-Leu-OH or Boc-Ile-OH was coupled to Glycine methyl ester with Dicyclohexylcarbodiimide (DCC), HOBT, and *N*-methylmorpholine (NMM) in DCM. The *N*-terminal Boc group was removed with 40% TFA in DCM and then the *N*-terminus was acetylated with acetic anhydride. The dipeptide C-terminus was saponified with LiOH in THF/H<sub>2</sub>O and then coupled to difluorophenylalanyl-macrocycle **3** to

give ADEPs **2a** and **2b**. For ADEPs **2c** and **2d** glycine methyl ester was acylated with either 4-methylvaleric acid or racemic 3-methylvaleric acid using DCC and NMM in DCM. The glycine C-terminus was then saponified with LiOH in THF/H<sub>2</sub>O and then coupled to **3** using HATU and DIPEA in DMF.

ADEPs **2a-d** were screened against *B. mycooides* for antibacterial activity using standard agar dilution methods. Unfortunately, none of the compounds exhibited antibacterial activity up to 100 µg/mL (figure 7.3). These results suggest that ADEPs with peptide side chains do not bind to ClpP and therefore that the ADEP side chain does not mimic the ClpX LGF/IGF loop motif. However, it is possible that **1a-d** do not exhibit antibacterial activity because they have difficulty crossing the bacterial cell membrane due to decreased lipophilicity or because they are degraded by endogenous peptidases. The compounds were therefore tested for ClpP activation *in vitro* using experiments described in chapter 6. Unfortunately, ADEPs **2a-d** exhibited little to no ability to activate *E. coli* ClpP peptolytic activity (figure 7.5.)

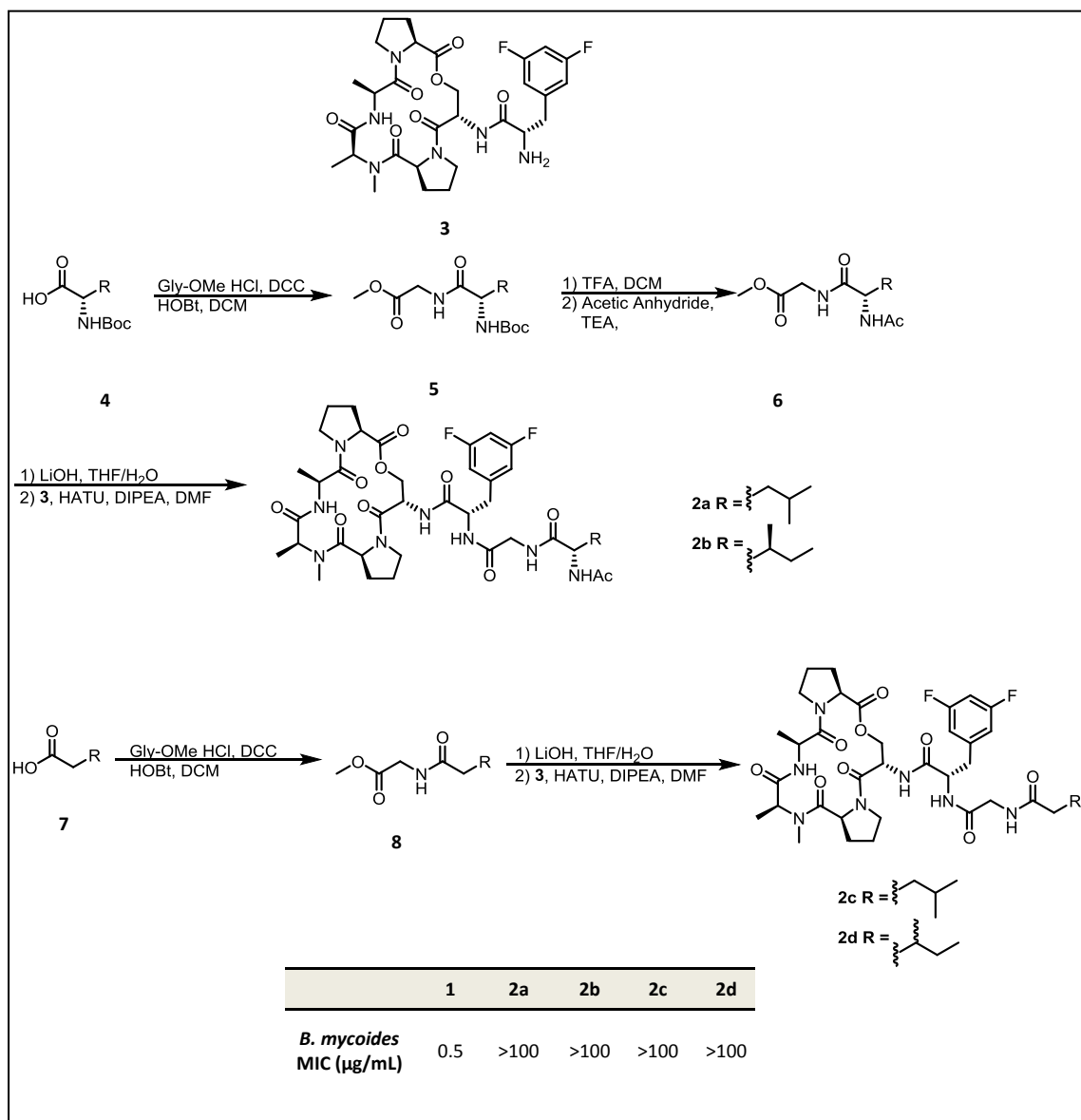


Figure 7.3 – Synthesis and antibacterial activity of ADEPs with peptide side chains.

Since the LGF/IGF functionalized ADEPs were much less active than ADEPs with lipophilic side chains, we envisioned one additional strategy to mimic the LGF/IGF motif, which involved stripping away most of the peptide functionality from the LGF/IGF motif. We synthesized ADEPs with simple *N*-acyldifluorophenylalanyl side chains that have carbon chain branching in similar patterns as the leucine and isoleucine R-groups (Figure 7.4). These compounds were prepared



as follows. A primary alcohol (**8**) was oxidized by PCC to the corresponding aldehyde, which was then engaged in a Horner-Wadsworth-Emmons olefination with the anion of trimenthylphosphonoacetate to yield an  $\alpha,\beta$ -unsaturated ester (**9**). The ester was saponified with LiOH in THF/Water under microwave irradiation to 100°C for 1 hour and then coupled to macrocycle **3** using HATU and DIPEA in DMF. ADEPs **2e-g** were screened against *B. mycooides* and found to be more active than the parent ADEP **1**. All three analogs were also able to strongly activate *E. coli* ClpP *in vitro* (Figure 7.5). However, the correlation between antibacterial activity and carbon branching pattern with respect to the IGF/LGF tripeptide was weak. The least active compound of the three (**2e**, MIC = 0.3  $\mu\text{g/mL}$ ) has a branching pattern corresponding to the leucine R-group. ADEP **2f** (MIC = 0.2  $\mu\text{g/mL}$ ) has a branching pattern that is similar to the isoleucine R-group and is more active than **2e**, which could be an indication that *B. mycooides* ClpP binds the IGF motif slightly better than the LGF motif. However, **2g** (MIC = 0.2  $\mu\text{g/mL}$ ) is just as active as **2f** and has a carbon branching pattern that corresponds to neither the leucine nor the isoleucine R-groups. While the ADEPs **2e-g** are interesting from a medicinal chemistry standpoint, they do not provide any compelling evidence of LGF/IGF mimicry.

These results have important implications for the proposals put forth by Li *et al.* Chemical evidence suggests that the ADEP acylphenylalanine side chain does not mimic the ClpX LGF/IGF loop. The fact that the two structures are nearly superimposable may only be coincidence and that the IGF/LGF loop exhibits a ClpP binding mode that is distinct from the ADEP side chain binding mode. Most importantly, we conclude that it is inappropriate to use the ADEP-ClpP complex as a model for ClpP when it is bound to its accessory ATPases until further empirical evidence is presented to validate the proposal by Li *et al.*

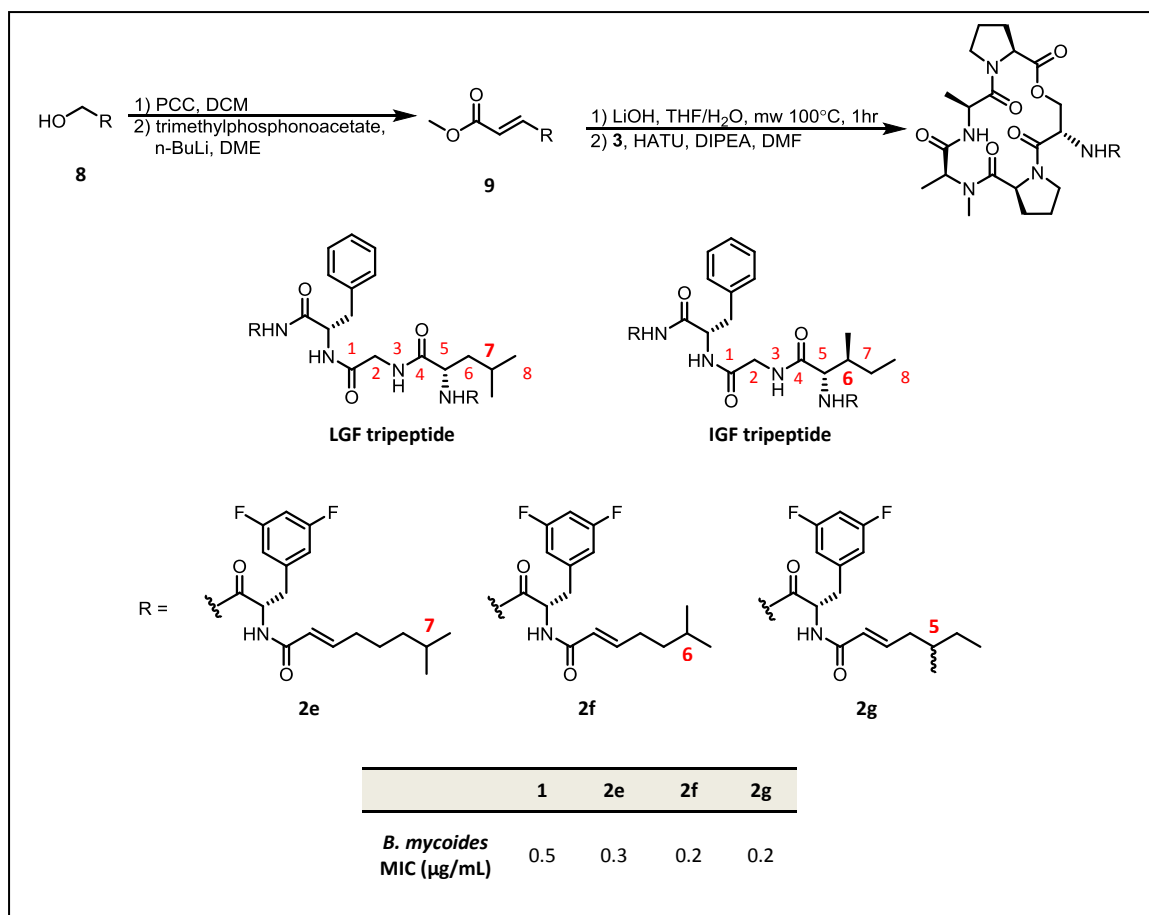


Figure 7.4 – Synthesis and evaluation of ADEP with side chain carbon branching. The carbon chain of Gly-Leu and Gly-Ile moieties are numbered for comparison to the carbon branching pattern in the side chains of ADEPs 2e-2g

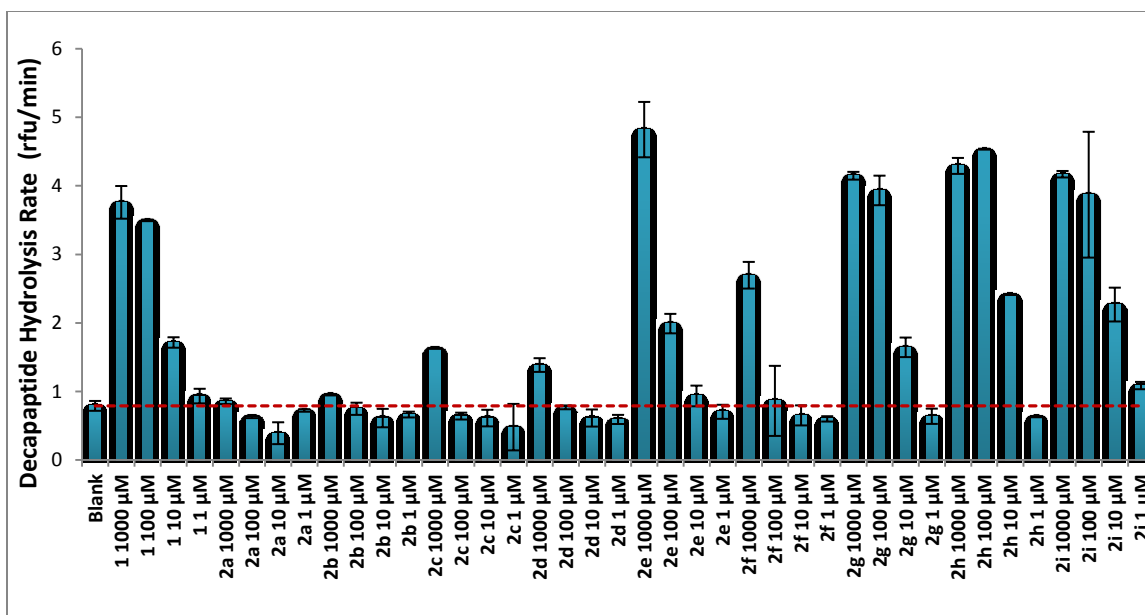


Figure 7.5 – Activation of ClpP by ADEPs with IGF/LGF mimic side chains. Hydrolysis of a fluorogenic decapeptide substrate (15 μM) by *E. coli* ClpP (25 nM) was assayed in the presence of increasing concentrations of ADEP compounds. Bars represent initial rates of decapeptide hydrolysis (average of 2 experiments). Error bars indicate standard deviation. Horizontal red dashed line indicates decapeptide hydrolysis rate in the absence of ADEP.

### Side Chain Medicinal Chemistry

We were also interested in studying the *N*-acylphenylalanine moiety from a medicinal chemistry standpoint. Since the side chain is involved in many key interactions that facilitate ADEP binding to ClpP, we anticipated that structural modifications to this moiety would modulate ADEP activity. In an effort to further improve ADEP potency, we explored the possibility of engaging residue R22 (Figure 7.1B) in a hydrogen bonding interaction by installing a hydroxyl functional group at the terminus of the *N*-acylgroup.

ADEPs bearing sidechains with terminal hydroxyl groups were synthesized according to Figure 7.6. A symmetrical diol (**10**) was mono-TBS protected by treatment with TBSCl in the presence of imidazole and DMAP. After isolation of the mono-TBS protected product (**11**) by flash chromatography, the free hydroxyl was oxidized with pyridinium chlorochromate (PCC) to the corresponding aldehyde. Without intermediate purification, the aldehyde was used in a

Horner-Wadsworth-Emmons olefination with the anion of trimethylphosphonoacetate to yield an  $\alpha,\beta$ -unsaturated ester (**12**). The ester was saponified with LiOH in THF/Water under microwave irradiation to 100°C for 1 hour and then coupled to macrocycle **3** using HATU and DIPEA in DMF. While the saponification/coupling sequence for 7 carbon chain and 8 carbon chain esters (**12**,  $n = 3$  or 4) were successful, no coupling product was observed for the 6 carbon chain ester (**12**,  $n = 2$ ). Interestingly, the major products after purification of the coupling reaction were free hydroxyl ADEPs **2h-i**. We assume that the TBS group is removed during the saponification, a fortuitous occurrence as we were saved from the burden of a discrete TBS deprotection step in order to complete our synthesis. Unlike other ADEP syntheses, HPLC was required to purify **2h-i** to homogeneity. Unfortunately, when screened against *B. mycooides* for antibacterial activity, ADEPs **2h-i** were inactive up to concentrations as high as 10  $\mu\text{g/mL}$ .

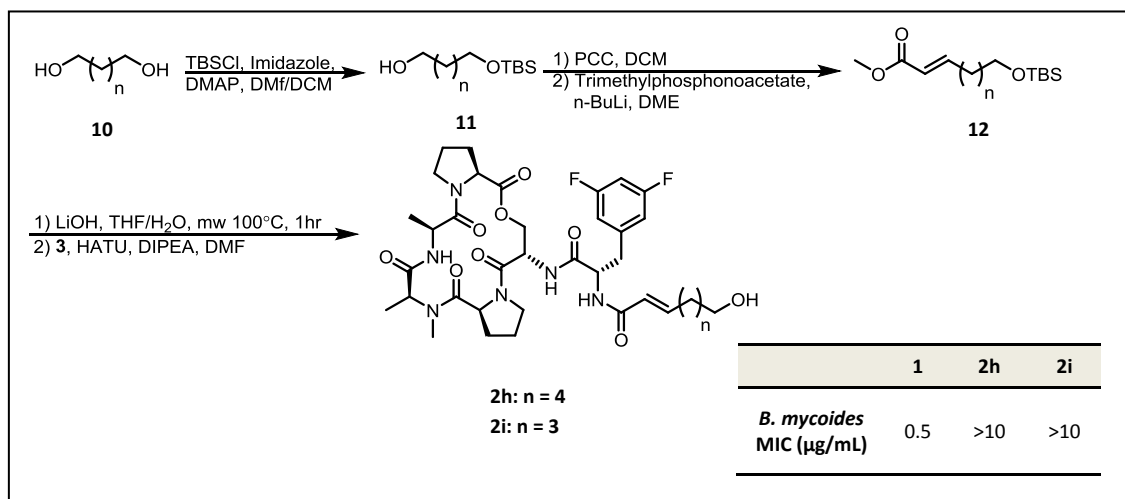
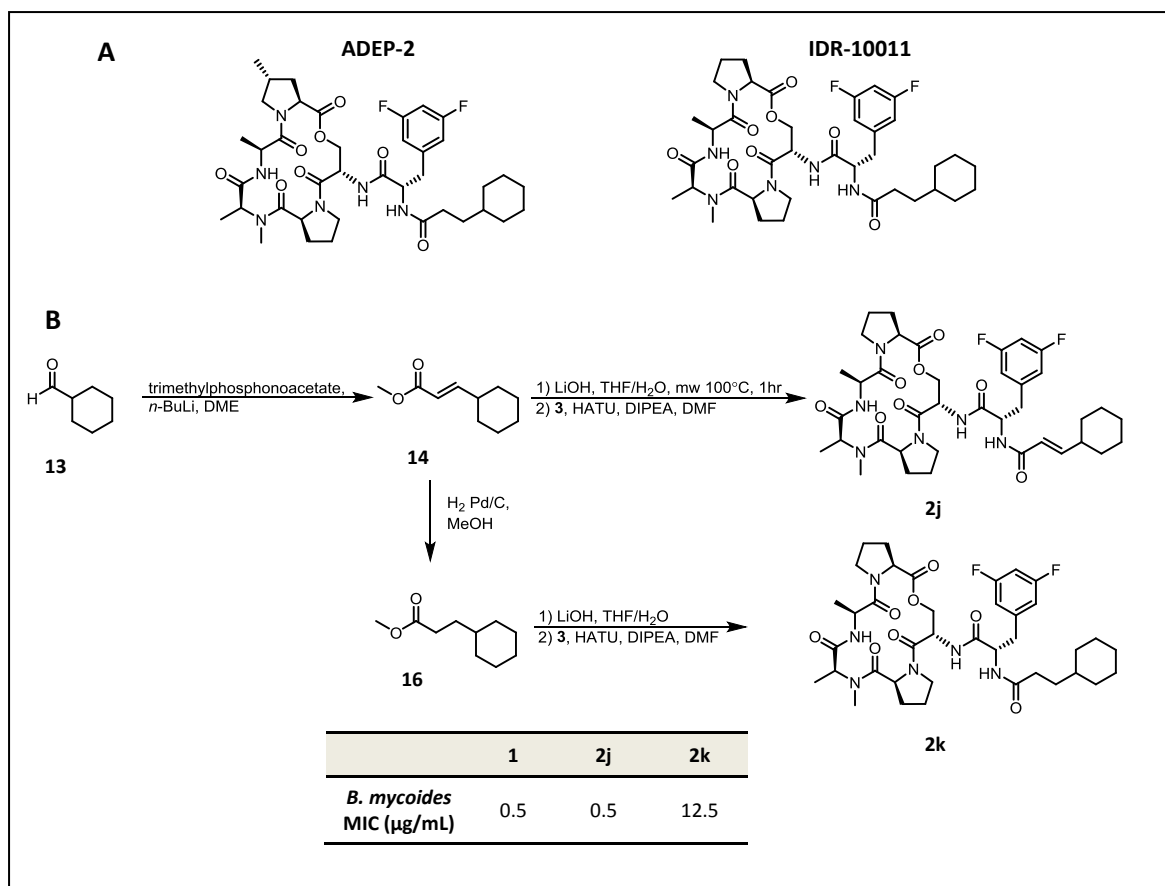


Figure 7.6 – Synthesis and antibacterial activity of ADEPs with hydroxyl terminating side chains

We were also prompted to study a controversial structure-activity relationship described in the literature. There have been two reports of highly active ADEPs that bear saturated 3-cyclohexylpropanoyl side chain acyl groups (Figure 7.7A).<sup>4,5</sup> This is peculiar because Hinzen *et al.* reported that  $\alpha,\beta$ -unsaturation in the side chain acyl group is very important for

activity.<sup>6</sup> We synthesized two ADEPs with either an unsaturated cyclohexyl-E-2-propenoyl (**2j**) or a saturated 3-cyclohexylpropanoyl (**2k**) side chain acyl group (Figure 7.7B). Commercially available cyclohexanal (**13**) was converted to  $\alpha,\beta$ -unsaturated ester (**14**) via Horner-Wadsworth-Emmons olefination. Ester **14** was either saponified and coupled to **3** yielding ADEP **2j**, or hydrogenated using palladium on carbon to give saturated ester **15**. This ester was saponified at room temperature and coupled to macrocycle **3** yielding ADEP **2k**.

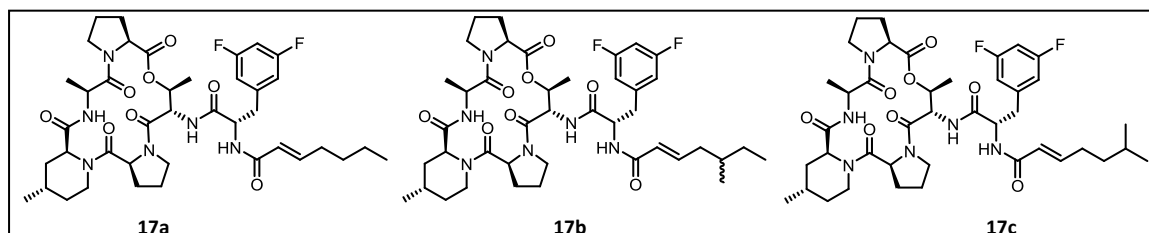
ADEP's **2j** and **2k** were screened for antibacterial activity against *B. mycooides*. The ADEP with the unsaturated cyclohexyl-E-2-propenoyl (**2j**) side chain group was equally as active as the parent ADEP **1**. However, the ADEP with the saturated 3-cyclohexylpropanoyl (**2k**) side chain acyl group was 25 fold less active than **1** and **2j**. This structure activity relationship is consistent with the report by Hinzen *et al*,<sup>6</sup> which originally pointed out the importance of the  $\alpha,\beta$ -unsaturated amide moiety in the side chain for antibacterial activity.



**Figure 7.7 –  $\alpha,\beta$ -unsaturation in ADEP side chain acyl groups** A) Reported ADEPs that lack  $\alpha,\beta$ -unsaturation in side chain acyl groups. B) Synthesis and antibacterial activity of corresponding ADEPs with and without  $\alpha,\beta$ -unsaturation in side chain acyl groups

With the discovery of improved ADEP side chains from our IGF/LGF peptidomimicry studies, we wished to synthesize fully optimized ADEPs that combined our most potent conformationally constrained peptidolactone with the improved side chains. In the same manner as **2f-g** were synthesized, carbon branched side chains were coupled to the peptidolactone containing 4-methylpipercolate and *allo*-threonine (see chapters 5 and 6). These optimized ADEPs were evaluated with *in vitro* ClpP binding experiments, and screening for activity against non-pathogenic and pathogenic bacteria (Figure 7.8). As expected, all ADEPs with the rigidified peptidolactones containing 4-methylpipercolate and *allo*-threonine residues bound ClpP more tightly and were far more potent antibacterial agents than the ADEP with the

natural product peptidolactones (**1**). Compound **17c** with an acyl-moiety C-5 methyl group was indeed a slightly tighter binder of *E. coli* ClpP and also competed with ClpX more effectively than the unbranched analog (**17a**). In contrast, **17c** with an acyl-moiety C-6 methyl group was a slightly weaker binder of *E. coli* ClpP and competed with ClpX less effectively than the unbranched analog (**17a**). Against *B. mycoides*, both **17b** and **17c** were more potent antibacterial agents than **17a**, with **17b** being the most potent of the three analogs. Interestingly, **17a** was the most potent antibacterial agent against *S. aureus*. Against *S. pneumoniae*, and *E. faecalis*, minimum inhibitory concentrations for **17a-c** were all below the limits of detection for the assay. The effects of side chain branching on ADEP antibacterial potency seems to be organism dependent. Perhaps subtle differences exist in the chemical environment of the ADEP binding site of ClpP from organism to organism. Nevertheless, against some organisms, ADEPs with branched side chains have the potential to significantly lower the effective dose required to treat bacterial infections.



	<b>1</b>	<b>17a</b>	<b>17b</b>	<b>17c</b>
ClpP Activation K <sub>app</sub> (μM)	7.5±0.34	1.1±0.060	0.811±0.066	1.35±0.046
ClpX Competition IC <sub>50</sub> (μM)	53±39	4.7±1.3	3.25±0.85	8.80±1.7
<b>MIC (μg/mL)</b>				
<i>B. mycoides</i>	0.5	0.1	0.05	0.075
<i>S. aureus</i>	0.78	0.024	0.098	0.195
<i>S. pneumoniae</i>	0.024	≤0.00002	≤0.00002	≤0.00002
<i>E. faecalis</i>	0.012	≤0.00002	≤0.00002	≤0.00002

Figure 7.8 – Structure and biological activity of fully optimized ADEPs

## ADEP binding and activation of *M. tuberculosis* ClpP

*Mycobacterium tuberculosis* (Mtb), the causative agent of the disease tuberculosis, is one of the most problematic human bacterial pathogens facing modern medicine. Tuberculosis is the cause of nearly 2 million deaths worldwide each year and it is estimated that one third of the world's population is infected with a latent form of the disease.<sup>7</sup> Multidrug resistant forms of Mtb are emerging with increasing frequency.<sup>8</sup> There is a critical need for new drug targets and new classes of antibacterial agents to treat this infectious disease. Recently, it was shown that ClpP activation is toxic to Mtb.<sup>5</sup> ADEPs exhibited potent antibacterial activity against these pathogenic bacteria in the presence of efflux pump inhibitors. We were therefore curious about the activity of our optimized ADEPs against *M. tuberculosis*.

In collaboration with Sauer group at MIT, we decided to first study activation of the Mtb ClpP. Unlike most bacteria, ClpP is essential for survival in Mycobacteria.<sup>9</sup> Another distinguishing feature is that the functional ClpP in mycobacteria is a heterotetradecamer composed of two distinct ClpP monomers, ClpP1 and ClpP2.<sup>9,10</sup> ClpP1 and ClpP2 each form homoheptameric rings that associate to form the heterotetradecamer, ClpP1P2. Homotetradecamers can form, but are catalytically inactive.<sup>11,12</sup> Interestingly, the two ClpP proteins exhibit different substrate selectivities, the molecular basis for which is not entirely understood.<sup>13</sup> In addition to providing important information about the therapeutic potential of the ADEPs in fighting MTB infections, a study of MTB ClpP activation by ADEPs might also shed light on the molecular mechanisms that control the independent ClpP1 and ClpP2 activities.

Both Mtb ClpP1 and ClpP2 were over-expressed and purified by Dr. Karl Schmitz from the Sauer group. ADEPs 1 and 17a-c all exhibited concentration dependent activation of the MTB ClpP1P2 decapeptidase activity (see chapter 6) in the presence of *N*-blocked dipeptide



agonist (Z-LLNva-CHO),<sup>10</sup> which is required to induce heterotetradecamer formation (Figure 7.9). All four compounds were able to Activate MTB ClpP1P2. However, **17a** and **17c** were significantly tighter binders than 1 and 17c as indicated by the apparent dissociation constants ( $K_{app}$ ). The most potent activator of MTB ClpP1P2 was ADEP **17c** ( $K_{app} = 4.5 \pm 0.1 \mu\text{M}$ ). Binding of ADEPs to MTB ClpP1P2 was slightly cooperative as indicated by the Hill coefficients, which ranged from 1.7 – 2.0. Mtb susceptibility assays to determine the antibacterial activity of these ADEPs against *M. tuberculosis* will be performed in the near future.

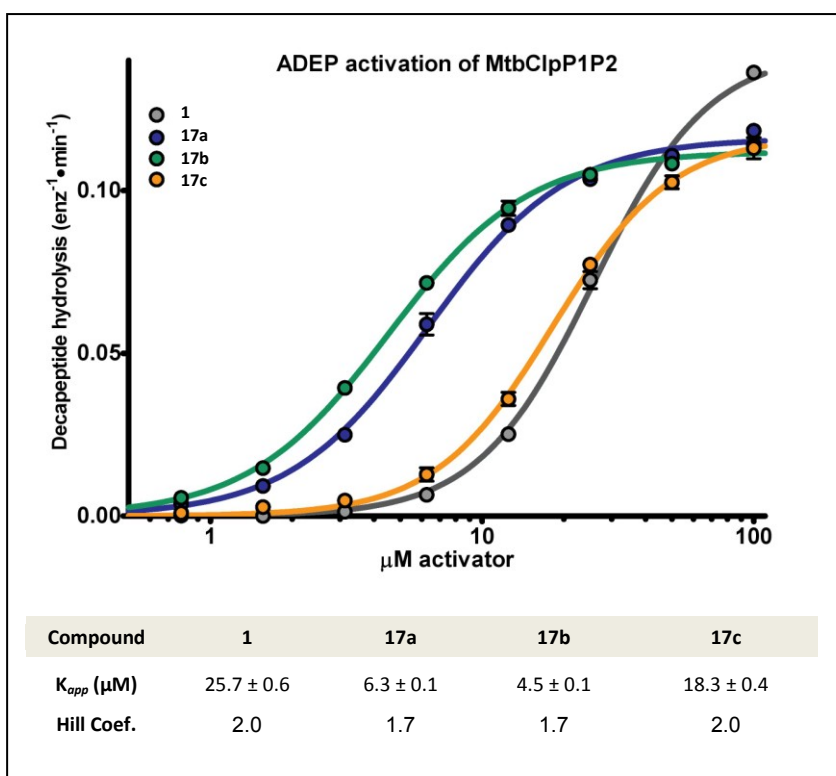


Figure 7.9 – Activation of Mtb ClpP1P2 by Optimized ADEPs: ADEPs were incubated with Mtb ClpP1P2, fluorogenic decapeptide, and *N*-blocked dipeptide agonist Z-LLNva-CHO. Apparent dissociation constants  $K_{app}$  were calculated from plots of decapeptidase rate vs. ADEP concentration that were fit to the Hill equation for cooperative binding.

In addition to studying ADEP activation of Mtb ClpP1P2, we have also obtained an X-ray crystal structure of ADEP **17c** bound to heterotetradecameric complex. This is the first known structure of an ADEP bound to a mycobacterial ClpP, as well as the first structure of an Mtb ClpP heterotetradecamer. To date, only a homotetradecameric structure of Mtb ClpP1 has been

reported.<sup>12</sup> Interestingly, our crystal structure shows that ADEP is only bound to ClpP2 and not ClpP1 (Figure 7.10 A). The ClpP2 N-terminal loops, which gate entrance to the proteolytic chamber,<sup>2</sup> are observed in an ordered “open” conformation, which is indicative of ClpP in an activated state. In the close up view of the ClpP2 – ADEP binding interaction, it is seen that the ADEP molecule is deeply buried in a mostly hydrophobic cleft at the interface of ClpP2 monomers (Figure 7.10B). There is one potentially unfavorable steric interaction between ClpP2 and the ADEP methyl group of the 4-methylpiperolate residue. The *allo*-threonine methyl group is pointed away from the surface of ClpP2 and as such is very well accommodated. The methyl branching in the side chain acyl group also appears to be well accommodated. These observations suggest that an ADEP analog with with piperolic acid and *allo*-threonine in its peptidolactone along with a carbon branched side chain acyl group might be ideally suited for binding to MTB ClpP2.

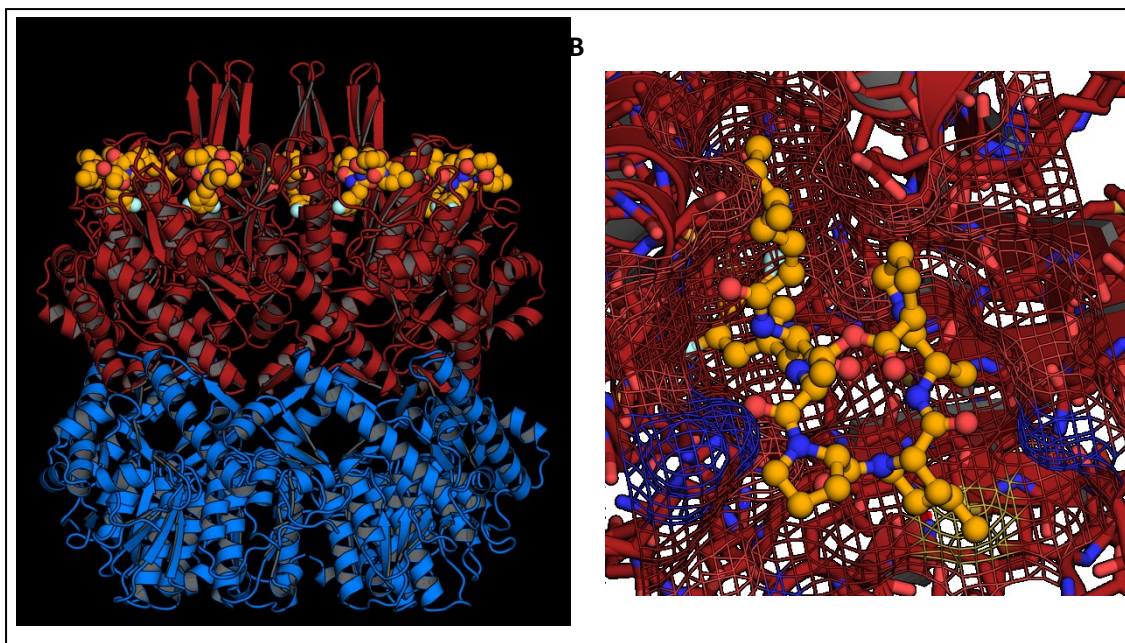


Figure 7.10 – X-ray crystal structure of ADEP 17c bound to MTB ClpP1P2. A) Side on view of ClpP1P2 heterotetradecamer with bound ADEP. ClpP1 is shown in blue. ClpP2 in shown in red. ADEP shown as CPK model. B) Close up view of the ClpP2 ADEP binding interaction: Red mesh indicates hydrophobic region, Blue mesh indicates polar region, yellow mesh indicates unfavorable steric interaction.

Analysis of the ADEP-ClpP1P2 crystal structure is ongoing. We would like to formulate hypotheses as to why ADEPs bind only to ClpP2 and not ClpP1. Specifically we would like to predict point mutations that could be made to ClpP1 that would allow ADEPs to bind to it. Additionally, we are interested in ClpP2 point mutations that preclude ADEP binding without affecting proteolytic activity. These mutations could lead to ADEP resistance in Mtb. With this crystal structure and a reliable *in vitro* ClpP activation assay, we can now use structure based design to discover ADEPs that are ideally suited for MTB ClpP2 binding. We are very excited about the future prospects of ADEP antibacterial therapy for tuberculosis.

### Experimental Contributions

All compounds were synthesized by Daniel Carney with the assistance of Morehouse College undergraduate student, Anthony Scrusse. *B. mycooides* MIC were determined by Daniel Carney with the assistance of Anthony Scrusse and Brown University graduate student Corey Compton. *S. aureus*, *E. faecalis*, and *S. pneumoniae* were determined by C. Andersen and A. Onderdonk from the New England Regional Centers of Excellence in Biodefense at Harvard Medical School. ClpP activation assays were performed by Karl Schmitz from the Sauer lab in the MIT department of Biology. ADEP-MBT ClpP1P2 crystal structure was obtained and solved by Karl Schmitz.

### Experimental Procedures

**ClpP Activation Assays.** *In vitro* assays were performed at 30 °C in PD buffer (25 mM HEPES, pH 7.5, 100 mM KCl, 5 mM MgCl<sub>2</sub>, 1 mM DTT, 10% (wt/vol) glycerol, 10% (vol/vol) DMSO) using a SpectraMax M5 microplate reader (Molecular Devices). Peptidase activation was measured by incubating 25 nM of ClpP tetradecamer and ADEP analog with 15 μM of an internally quenched fluorogenic peptide substrate, Abz-KASPVSLGY<sup>NO<sub>2</sub>D</sup>,<sup>14</sup> incorporating a 2-aminobenzoic acid (Abz)

fluorophore and 3-nitrotyrosine ( $\text{Y}^{\text{NO}_2}$ ) quencher. In MBT ClpP1P2 activation assays, the *N*-blocked dipeptide agonist Z-LLNva-CHO was included as well. Peptide hydrolysis by ClpP was monitored by following the increase in 420 nm fluorescence upon 320 nm excitation. Initial analysis of peptidase data showed negligible cooperativity, thus data were fit to a quadratic form of a non-cooperative binding equation, assuming 14 equivalent ADEP binding sites per ClpP tetradecamer.

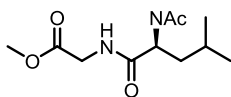
**MIC determinations:** MIC determinations for *B. mycooides* were performed in house using a standard agar dilution method. Difco Nutrient Agar (3 mL) was supplemented with an ADEP at a specified concentration. *B. mycooides* liquid cultures Difco Nutrient Broth (3 mL) was inoculated with single colonies of *B. mycooides* and grown overnight at 30°C. ADEP supplemented plates were inoculated with a 5  $\mu\text{L}$  aliquot turbid overnight *B. mycooides* culture and then incubated at 30°C. After 48 hours, the agar plates were assessed for growth. MIC's were defined as the lowest concentration capable of inhibiting bacterial growth to fewer than 10 colonies. MIC determinations for pathogenic strains were performed BSL2+ conditions at the New England Center for Research Excellence (NERCE) in biodefense at Harvard Medical School following standard dilution antimicrobial susceptibility testing protocols.<sup>15</sup> Following incubation with the bacteria and the compound, each well was visually examined for growth with the unaided eye. The MIC is determined to be the first set of replicate wells of the dilution series exhibiting no growth when compared to the growth control wells.

**Synthesis General:** All commercially available reagents were used without further purification. All reactions were conducted in oven dried glassware, under ambient atmosphere, using dry solvents unless otherwise stated. NMR chemical shifts were referenced to residual solvent peaks:  $\text{CDCl}_3$  ( $\delta = 7.27$  ppm for  $^1\text{H}$ -NMR and 77.00 ppm for  $^{13}\text{C}$ -NMR), acetone- $d_6$  ( $\delta = 2.05$  for

$^1\text{H-NMR}$  and  $\delta = 29.92$  for  $^{13}\text{C-NMR}$ ). 2D NOSEY spectra were acquired for compounds existing as simple mixtures of rotamers in solution

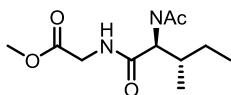
**Synthesis of *N*-acetyldipeptides general procedure:** Dicyclohexylcarbodiimide (206 mg, 1 mmol) was dissolved in Dichloromethane (5 mL). To this solution was added in order: Boc-protected leucine or isoleucine (249 mg, 1.00 mmol), HOBT·H<sub>2</sub>O (156 mg, 1 mmol), glycine methylester hydrochloride (126 mg, 1 mmol), and *N*-methylmorpholine (0.112 mL, 1 mmol). The coupling reaction was allowed to proceed for 16 hours after which, the solvent was removed in vacuo and the residue was diluted in ethyl acetate (20 mL). The solution was filtered through a silica gel plug to remove the dicyclohexylurea byproduct and the filtrate was extracted: 3 x 1 M HCl, 3 x saturated NaHCO<sub>3</sub>, 1 x Brine. The organic phase was then dried over sodium sulfate and after final removal of solvent, the dipeptide products were used without further purification.

The crude dipeptide products were Boc-protected with 40% trifluoroacetic acid in dichloromethane (4 mL). Upon complete conversion of the protected dipeptide, the solvent was removed, first by blowing with a stream of nitrogen followed by drying under high vacuum. Once dry, the deprotected dipeptides were dissolved in dichloromethane (5 mL) and acetylated with acetic anhydride (0.189 mL, 2 mmol) and triethylamine (0.277 mL, 2 mmol). After a 1 hour reaction time, the solvent was removed in vacuo, and the *N*-acetyldipeptides were isolated by silica gel flash chromatography using a 10% acetone in ethyl acetate mobile phase.



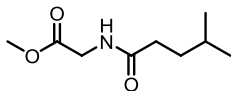
***N*-acetyl-Leu-Gly-OMe (6a):** Yield: 154 mg 63% over 3 steps. HRMS (FAB) Predicted for [C<sub>11</sub>H<sub>20</sub>N<sub>2</sub>O<sub>4</sub> + Na]<sup>+</sup>: 267.1321, Found: 267.1315.  $^1\text{H NMR}$  (400MHz, CHLOROFORM-*d*)  $\delta = 7.59$  (t,  $J = 5.5$  Hz, 1 H), 7.12 (d,  $J = 8.5$  Hz, 1 H), 4.57 (dt,  $J = 5.8, 8.5$  Hz, 1 H), 3.99 (dd,  $J = 6.0, 17.8$  Hz, 1

H), 3.87 (dd,  $J = 5.5, 17.8$  Hz, 1 H), 3.67 (s, 3 H), 1.92 (s, 3 H), 1.73 - 1.57 (m, 2 H), 1.57 - 1.46 (m, 1 H), 0.89 (d,  $J = 6.3$  Hz, 3 H), 0.87 (d,  $J = 6.3$  Hz, 3 H).  $^{13}\text{C}$  NMR (101MHz, CHLOROFORM-d)  $\delta = 173.2, 170.5, 170.0, 52.0, 51.4, 41.0, 40.9, 24.5, 22.7, 22.7, 22.0$ .

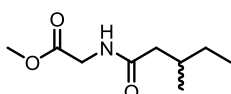


**N-acetyl-Ile-Gly-OMe (6b):** Yield: 139 mg, 57% over 3 steps. HRMS (FAB) Predicted for  $[\text{C}_{11}\text{H}_{20}\text{N}_2\text{O}_4 + \text{Na}]^+$ : 267.1321, Found: 267.1330.  $^1\text{H}$  NMR (400MHz, CHLOROFORM-d)  $\delta = 6.75$  (br. s., 1 H), 6.28 (d,  $J = 8.3$  Hz, 1 H), 4.37 (dd,  $J = 7.8, 8.5$  Hz, 1 H), 4.10 (dd,  $J = 5.5, 18.1$  Hz, 1 H), 3.97 (dd,  $J = 5.3, 18.3$  Hz, 1 H), 3.76 (s, 3 H), 2.02 (s, 3 H), 1.95 - 1.75 (m, 2 H), 1.66 - 1.45 (m, 1 H), 1.25 - 1.09 (m, 1 H), 0.95 (d,  $J = 6.8$  Hz, 3 H), 0.92 (t,  $J = 7.5$  Hz, 3 H).  $^{13}\text{C}$  NMR (101MHz, CHLOROFORM-d)  $\delta = 171.7, 170.3, 170.0, 57.6, 52.4, 41.1, 37.2, 25.0, 23.2, 15.3, 11.2$ .

**Synthesis of N-acylglycine methyl esters general procedure:** Dicyclohexylcarbodiimide (206 mg, 1 mmol) was dissolved in Dichloromethane (5 mL). To this solution was added in order: 4-methylvaleric acid or 3-methylvaleric acid (116 g, 1 mmol), glycine methyl ester hydrochloride (126 mg, 1 mmol), and N-methylmorpholine (0.112 mL, 1 mmol). The coupling reaction was allowed to proceed for 16 hours after which, the solvent was removed in vacuo and the residue was diluted in ethyl acetate (20 mL). The solution was filtered through a silica gel plug to remove the dicyclohexylurea byproduct and the filtrate was extracted: 3 x 1 M HCl, 3 x saturated  $\text{NaHCO}_3$ , 1 x Brine. After drying and removal of solvent, the N-acylglycine methyl esters were used without further purification.



**N-(4-methylvaleryl)-Gly-OMe (8a):** Yield: 173 mg, 93%. HRMS (FAB) Predicted for  $[C_9H_{17}NO_3 + Na]^+$ : 210.1106, Found: 210.1112.  $^1H$  NMR (400MHz, CHLOROFORM-d)  $\delta$  = 6.72 (br. s., 1 H), 3.90 (d,  $J$  = 5.6 Hz, 2 H), 3.63 (s, 3 H), 2.30 - 2.05 (m, 2 H), 1.59 - 1.35 (m, 3 H), 0.79 (d,  $J$  = 6.3 Hz, 1 H).  $^{13}C$  NMR (101MHz, CHLOROFORM-d)  $\delta$  = 173.7, 170.3, 51.9, 40.8, 34.1, 33.9, 27.5, 22.0.

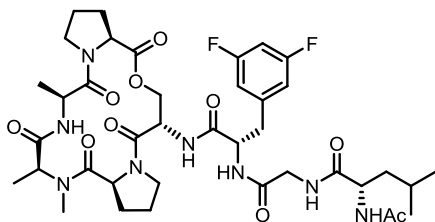


**N-(3-methylvaleryl)-Gly-OMe (8b):** Yield: 166 mg, 89%. HRMS (FAB) Predicted for  $[C_9H_{17}NO_3 + Na]^+$ : 210.1106, Found: 210.1115.  $^1H$  NMR (400MHz, CHLOROFORM-d)  $\delta$  = 6.30 (br. s., 1 H), 4.00 (d,  $J$  = 5.3 Hz, 2 H), 3.71 (s, 3 H), 2.22 (dd,  $J$  = 6.1, 13.9 Hz, 1 H), 2.04 - 1.93 (m, 1 H), 1.93 - 1.79 (m, 1 H), 1.44 - 1.26 (m, 1 H), 1.25 - 1.10 (m, 1 H), 0.90 (d,  $J$  = 6.6 Hz, 3 H), 0.85 (t,  $J$  = 7.5 Hz, 3 H).  $^{13}C$  NMR (101MHz, CHLOROFORM-d)  $\delta$  = 173.0, 170.5, 52.2, 43.5, 41.0, 32.2, 29.3, 19.0, 11.2.

**Synthesis of LGF/IGF sidechain mimic ADEPs General Procedure:** Acylated glycine methyl esters **6** and **7** (0.5 mmol) were saponified by treatment with lithium hydroxide mono-hydrate (70 mg, 1.7 mmol) in 1:1 THF:Water (2.5 mL). After complete conversion of the methyl ester, the reaction was quenched with 1 M HCl(aq) (2 mL). The saponified products were extracted with ethyl acetate and dried over sodium sulfate. After final removal of solvent the free acids were used without further purification.

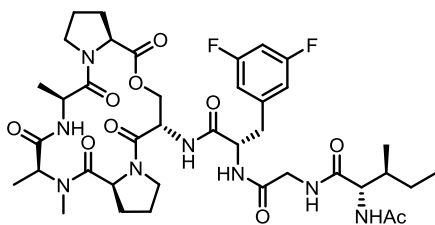
The free acids were dissolved in DMF (2 mL) along with the free base difluorophenylalanyl macrocycle **3** (310 mg, 0.5 mmol). The solution was then treated with HATU (190 mg 0.5 mmol) and DIPEA (0.26 mL, 1.5 mmol). The acylation reaction was allowed to proceed over night, after which the DMF was removed in vacuo. The concentrated residue was diluted in ethyl acetate

(~40 mL), extracted: 2 x 1 M HCl aq. 2 x saturated NaHCO<sub>3</sub> aq, 1 x Brine, then dried over sodium sulfate. The ADEP products were isolated by silica gel flash chromatography using an acetone/ethyl acetate solvent gradient.



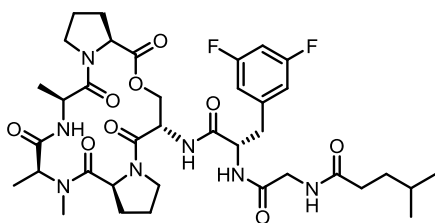
**LGF Sidechain Mimic ADEP 2a:** Yield: 137 mg, 34%. HRMS (ESI) Predicted for [C<sub>39</sub>H<sub>54</sub>F<sub>2</sub>N<sub>8</sub>O<sub>10</sub> + H]<sup>+</sup>: 833.4009 Found: 833.4020 <sup>1</sup>H NMR (600MHz, Acetone) δ = 8.57 (d, *J* = 9.2 Hz, 1 H), 8.29 - 8.18 (m, 2 H), 7.63 (d, *J* = 8.8 Hz, 1 H), 7.55 (d, *J* = 6.6 Hz, 1 H), 6.93 (dd, *J* = 2.0, 8.3 Hz, 2 H), 6.80 - 6.71 (m, 1 H), 5.27 (dd, *J* = 3.5, 8.6 Hz, 1 H), 4.97 - 4.86 (m, 3 H), 4.86 - 4.79 (m, 1 H), 4.60 (dt, *J* = 1.5, 9.7 Hz, 1 H), 4.45 (d, *J* = 8.8 Hz, 1 H), 4.41 - 4.33 (m, 1 H), 4.23 (dd, *J* = 7.7, 16.9 Hz, 1 H), 3.73 (dd, *J* = 10.1, 11.6 Hz, 1 H), 3.68 - 3.57 (m, 3 H), 3.53 - 3.45 (m, 1 H), 3.34 (br. s., 1 H), 3.05 - 2.95 (m, 2 H), 2.80 - 2.75 (m, 3 H), 2.55 - 2.45 (m, 1 H), 2.25 (d, *J* = 7.3 Hz, 1 H), 2.01 - 1.87 (m, 9 H), 1.73 (dd, *J* = 6.8, 7.5 Hz, 1 H), 1.58 (ddd, *J* = 6.4, 8.1, 14.1 Hz, 2 H), 1.52 - 1.43 (m, 3 H), 1.39 - 1.31 (m, 3 H), 0.99 - 0.93 (m, 3 H), 0.92 (d, *J* = 6.6 Hz, 3 H). <sup>13</sup>C NMR (151MHz, Acetone) δ = 174.0, 174.0, 173.5, 172.8, 171.6, 171.2, 171.0, 170.3, 166.5, 164.9, 164.8, 163.3, 163.2, 143.5, 114.0, 114.0, 113.9, 113.8, 103.0, 102.9, 102.7, 66.3, 60.9, 57.9, 57.4, 54.9, 54.3, 52.8, 49.1, 47.9, 47.6, 43.8, 41.9, 39.4, 39.2, 32.1, 31.7, 31.6, 25.8, 24.3, 23.6, 23.3, 22.9, 22.4, 18.4, 16.4.





**IGF Sidechain Mimic ADEP 2b:** Yield 159 mg, 41%. HRMS (ESI) Predicted for  $[C_{39}H_{54}F_2N_8O_{10} + H]^+$ :

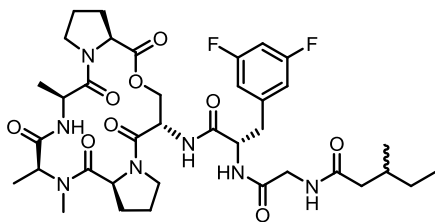
833.4009 Found: 833.4107.  $^1H$  NMR (600MHz, Acetone)  $\delta$  = 8.55 (d,  $J$  = 9.2 Hz, 1 H), 8.32 (d,  $J$  = 9.5 Hz, 1 H), 8.24 (dd,  $J$  = 4.4, 7.3 Hz, 1 H), 7.63 (d,  $J$  = 8.8 Hz, 1 H), 7.51 (d,  $J$  = 7.0 Hz, 1 H), 6.98 - 6.88 (m, 2 H), 6.81 - 6.72 (m, 1 H), 5.27 (dd,  $J$  = 3.5, 8.6 Hz, 1 H), 4.99 - 4.87 (m, 3 H), 4.84 (q,  $J$  = 6.7 Hz, 1 H), 4.60 (dt,  $J$  = 1.8, 9.7 Hz, 1 H), 4.45 (d,  $J$  = 8.8 Hz, 1 H), 4.32 - 4.22 (m, 2 H), 3.75 - 3.68 (m, 2 H), 3.68 - 3.61 (m, 2 H), 3.54 - 3.45 (m, 1 H), 3.40 - 3.29 (m, 1 H), 3.02 (dd,  $J$  = 5.7, 13.8 Hz, 1 H), 2.98 - 2.94 (m, 1 H), 2.77 (s, 3 H), 2.57 - 2.46 (m, 1 H), 2.30 - 2.20 (m, 1 H), 2.04 - 1.86 (m, 9 H), 1.85 - 1.77 (m, 1 H), 1.69 - 1.56 (m, 1 H), 1.48 (d,  $J$  = 7.0 Hz, 3 H), 1.35 (d,  $J$  = 6.6 Hz, 3 H), 1.28 - 1.21 (m, 1 H), 0.94 (d,  $J$  = 7.0 Hz, 3 H), 0.89 (t,  $J$  = 7.3 Hz, 3 H).  $^{13}C$  NMR (151MHz, Acetone)  $\delta$  = 174.1, 173.5, 173.0, 172.7, 171.5, 171.2, 171.0, 170.4, 166.5, 165.0, 164.9, 163.3, 163.3, 143.5, 114.0, 113.8, 103.1, 102.9, 102.8, 66.3, 60.9, 60.1, 58.0, 57.4, 54.8, 52.8, 49.1, 47.9, 47.6, 43.7, 39.5, 37.7, 32.1, 31.7, 31.6, 26.5, 24.3, 23.3, 22.4, 18.5, 16.4, 16.4, 11.9.



**LGF Sidechain Mimic ADEP 2c:** Yield: 203 mg 52%. HRMS (ESI) Predicted for  $[C_{37}H_{51}F_2N_7O_9 + H]^+$ :

776.3795, Found: 776.3795.  $^1H$  NMR (600MHz, Acetone)  $\delta$  = 8.36 (d,  $J$  = 9.2 Hz, 1 H), 8.12 (d,  $J$  =

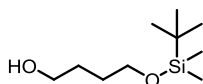
9.2 Hz, 1 H), 7.70 - 7.59 (m, 1 H), 7.06 (d,  $J = 7.7$  Hz, 1 H), 6.85 (dd,  $J = 2.4, 8.3$  Hz, 2 H), 6.79 (tt,  $J = 2.2, 9.3$  Hz, 1 H), 5.23 (dd,  $J = 3.5, 8.6$  Hz, 1 H), 4.96 - 4.86 (m, 2 H), 4.86 - 4.75 (m, 2 H), 4.59 - 4.52 (m, 1 H), 4.45 (d,  $J = 8.4$  Hz, 1 H), 4.25 (dd,  $J = 7.0, 16.9$  Hz, 1 H), 3.75 - 3.59 (m, 4 H), 3.46 (td,  $J = 7.0, 11.3$  Hz, 1 H), 3.38 - 3.29 (m, 1 H), 2.96 (dd,  $J = 7.3, 13.6$  Hz, 1 H), 2.86 (dd,  $J = 5.5, 13.6$  Hz, 1 H), 2.75 (s, 3 H), 2.55 - 2.46 (m, 1 H), 2.31 - 2.23 (m, 3 H), 2.03 - 1.86 (m, 6 H), 1.62 - 1.54 (m, 1 H), 1.54 - 1.49 (m, 2 H), 1.48 (d,  $J = 6.6$  Hz, 3 H), 1.28 (d,  $J = 6.2$  Hz, 3 H), 0.90 (d,  $J = 3.7$  Hz, 3 H), 0.89 (d,  $J = 3.3$  Hz, 3 H).  $^{13}\text{C}$  NMR (151MHz, Acetone)  $\delta = 173.9, 173.6, 172.3, 171.1, 171.1, 170.3, 166.2, 165.0, 163.4, 142.5, 114.2, 114.1, 114.1, 103.3, 103.2, 103.0, 65.9, 60.9, 57.9, 57.4, 54.7, 52.9, 49.0, 48.1, 47.6, 43.8, 40.2, 35.8, 35.3, 32.1, 31.7, 31.5, 30.9, 29.1, 24.3, 23.2, 23.2, 22.5, 18.5, 16.3$ .



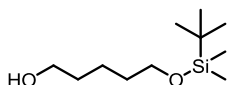
**IGF Sidechain Mimic ADEP 2d:** Yield: 177 mg 47%. HRMS (ESI) Predicted for  $[\text{C}_{37}\text{H}_{51}\text{F}_2\text{N}_7\text{O}_9 + \text{H}]^+$ : 776.3795 Found: 776.3801.  $^1\text{H}$  NMR (600MHz, Acetone)  $\delta = 8.37$  (d,  $J = 9.2$  Hz, 1 H), 8.31 (d,  $J = 9.5$  Hz, 1 H), 7.76 - 7.65 (m, 1 H), 7.15 (d,  $J = 5.1$  Hz, 1 H), 6.84 (d,  $J = 7.0$  Hz, 2 H), 6.77 (tt,  $J = 2.3, 9.2$  Hz, 1 H), 5.24 (dd,  $J = 3.5, 8.6$  Hz, 1 H), 4.97 - 4.85 (m, 3 H), 4.81 (q,  $J = 6.8$  Hz, 1 H), 4.56 (t,  $J = 9.7$  Hz, 1 H), 4.45 (dd,  $J = 1.7, 8.6$  Hz, 1 H), 4.29 (ddd,  $J = 2.4, 6.7, 17.0$  Hz, 1 H), 3.76 (td,  $J = 5.4, 17.1$  Hz, 1 H), 3.71 - 3.58 (m, 3 H), 3.49 (td,  $J = 7.0, 11.4$  Hz, 1 H), 3.32 (t,  $J = 8.8$  Hz, 1 H), 2.97 (dd,  $J = 7.3, 13.2$  Hz, 1 H), 2.85 (dd,  $J = 5.7, 13.4$  Hz, 1 H), 2.76 - 2.72 (m, 3 H), 2.55 - 2.45 (m, 1 H), 2.31 - 2.18 (m, 2 H), 2.10 - 2.05 (m, 1 H), 2.02 - 1.84 (m, 7 H), 1.47 (d,  $J = 7.0$  Hz, 3 H), 1.42 - 1.34 (m, 1 H), 1.27 (t,  $J = 6.1$  Hz, 3 H), 1.22 - 1.16 (m, 1 H), 0.90 (dd,  $J = 0.9, 6.8$  Hz, 3 H), 0.87 (t,  $J = 7.5$  Hz, 3 H)  $^{13}\text{C}$  NMR (151MHz, Acetone)  $\delta = 173.8, 173.8, 173.5, 173.3, 172.2, 171.1, 171.0, 170.4$ ,

166.3, 165.0, 164.9, 163.3, 163.2, 142.4, 114.2, 114.1, 114.0, 114.0, 103.2, 103.1, 102.9, 65.9, 65.9, 60.8, 57.9, 57.3, 54.6, 52.8, 48.9, 48.0, 47.7, 44.4, 44.3, 43.7, 40.2, 40.1, 33.4, 33.3, 32.1, 31.6, 31.5, 24.3, 22.4, 20.0, 18.4, 18.4, 16.3, 12.1, 12.1.

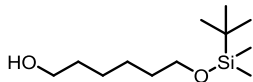
**Mono-TBS Protection of Diols General Procedure:** A diol (5 mmol), imidazole (885 mg, 13 mmol), and DMAP (61 mg, 0.50 mmol) were dissolved in DMF (15 mL) and cooled to 0°C. A solution of TBSCl (754 mg 5 mmol) in DCM (5 mL) was then added to the DMF solution. The reaction was allowed to proceed for 24 hours, after which the reaction was quenched with water (50 mL). The aqueous layer was extracted three times with DCM to isolate the organic products, which consisted mainly of the monosilated diol, some disilated by product, and unreacted starting material. The mono-TBS protected diols were cleanly isolated by silica gel flash chromatography using 20-40% ethyl acetate in hexanes at the mobile phase.



**Mono-OTBS butane-1,4-diol:** Yield: 440 mg, 43%. HRMS (FAB) Predicted for  $[C_{10}H_{24}O_2Si + Na]^+$ : 227.1443, Found: 227.1452.  $^1H$  NMR (400MHz, CHLOROFORM-d)  $\delta$  = 3.68 (t,  $J$  = 5.1 Hz, 2 H), 3.66 - 3.62 (m, 2 H), 2.57 (br. s., 1 H), 1.76 - 1.57 (m, 4 H), 0.91 (s, 9 H), 0.08 (s, 6 H).  $^{13}C$  NMR (101MHz, CHLOROFORM-d)  $\delta$  = 63.3, 62.8, 30.3, 29.9, 25.9, 18.3, -5.4.



**Mono-OTBS pentane-1,5-diol:** Yield: 528 mg, 48%. HRMS (FAB) Predicted for  $[C_{11}H_{26}O_2Si + Na]^+$ : 241.1600, Found: 241.1605.  $^1H$  NMR (400MHz, CHLOROFORM-d)  $\delta$  = 3.69 - 3.64 (m, 2 H), 3.62 (t,  $J$  = 5.6 Hz, 2 H), 1.64 - 1.52 (m, 4 H), 1.51 (br. s., 1 H), 1.47 - 1.36 (m, 2 H), 0.90 (s, 9 H), 0.05 (s, 6 H).  $^{13}C$  NMR (101MHz, CHLOROFORM-d)  $\delta$  = 63.1, 62.9, 32.5, 26.0, 22.0, 18.4, -5.3.



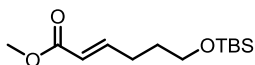
**Mono-OTBS hexane-1,6-diol:** Yield: 580 mg, 50%. HRMS (FAB) Predicted for  $[C_{12}H_{28}O_2Si + Na]^+$ : 255.1756, Found: 255.1760.  $^1H$  NMR (400MHz, CHLOROFORM-d)  $\delta$  = 3.65 (t, J = 6.6 Hz, 2 H), 3.61 (t, J = 6.6 Hz, 2 H), 1.60 - 1.49 (m, 4 H), 1.47 (br. s., 1 H), 1.42 - 1.30 (m, 4 H), 0.90 (s, 9 H), 0.05 (s, 6 H).  $^{13}C$  NMR (101MHz, CHLOROFORM-d)  $\delta$  = 63.2, 63.0, 32.8, 26.0, 25.6, 25.5, 18.4, -5.3.

**Oxidation/Horner-Emmons-Wadsworth Olefination of Mono-TBS Diols General Procedure:**

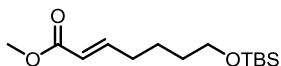
Pyridinium chlorochromate (PCC) (323 mg, 1.5 mmol) and 3Å molecular sieves (1 g) were suspended in Dichloromethane with stirring. To the suspension was added a mono-TBS diol (1 mmol) and was allowed to react until completely consumed, as indicated by TLC (1-2 hours). Upon completion, the reaction was filtered through a silica gel plug, rinsing with dichloromethane. The dichloromethane was carefully evaporated in vacuo at 30°C yielding the concentrated aldehydes. The aldehydes were used without further purification.  $^1HNMR$  was used to quantify residual DCM in order to accurately determine aldehyde stoichiometry for the subsequent olefination.

The crude aldehyde was added to an oven dried flask and sealed with a septum. The atmosphere was purged with nitrogen and then charged with dimethoxyethane. A separate oven dried flask with a stir bar was sealed with a septum and purged with dry nitrogen. Once the flask has cooled to room temperature, trimethylphosphonoacetate (1.2 equivalents w.r.t aldehyde) was added to the flask via syringe followed by dimethoxyethane (DME) (concentration 0.5 M w.r.t trimethylphosphonoacetate). The reaction was cooled to 0°C with an ice bath (-78°C for reactions >5 mmol scale) after which, n-butyllithium (2.5 M solution) (1.2

equivalents w.r.t. aldehyde) was added. The reaction was then allowed to warm to room temperature. The aldehyde solution was added via syringe to the room temperature reaction solution dropwise. A white precipitate began to form within seconds. The reaction was allowed to proceed for 2.5 hours, after which it was quenched by the addition of water (same volume of the reaction), dissolving the white precipitate. The phases were partitioned and the aqueous phase was washed once with diethyl ether. The combined organic layers were washed once with brine and dried over sodium sulfate. E/Z selectivity was typically ~13/1. In most cases, the geometric isomers were difficult to separate cleanly. However, the E- $\alpha,\beta$ -unsaturated ester was enriched to at least 95% purity by silica gel chromatography using a DCM/Hexanes solvent gradient. Fractions containing mixtures of the two geometric isomers were rechromatographed if substantial or discarded. Reported yields are of purified E-isomer only.

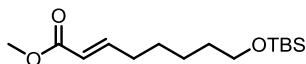


**Methyl (E)-6-((tert-butyldimethylsilyl)oxy)hex-2-enoate:** (2 mmol scale) Yield 221 mg, 43% over 2 steps. HRMS (FAB) Predicted for  $[C_{13}H_{26}O_3Si + Na]^+$ : 281.1549, Found: 281.1539.  $^1H$  NMR (400MHz, CHLOROFORM-d)  $\delta$  = 7.00 (td,  $J$  = 6.9, 15.7 Hz, 1 H), 5.84 (td,  $J$  = 1.6, 15.7 Hz, 1 H), 3.73 (s, 3 H), 3.63 (t,  $J$  = 6.2 Hz, 2 H), 2.33 - 2.24 (m, 2 H), 1.71 - 1.63 (m, 2 H), 0.89 (s, 12 H), 0.05 (s, 6 H).  $^{13}C$  NMR (101MHz, CHLOROFORM-d)  $\delta$  = 167.1, 149.3, 121.0, 62.1, 51.4, 31.1, 28.7, 25.9, 18.3, -5.4.



**Methyl (E)-7-((tert-butyldimethylsilyl)oxy)hept-2-enoate:** Yield: 110 mg, 40% over 2 steps. HRMS (FAB) Predicted for  $[C_{14}H_{28}O_3Si + Na]^+$ : 295.1705, Found: 295.1711.  $^1H$  NMR (400MHz, CHLOROFORM-d)  $\delta$  = 6.97 (td,  $J$  = 7.0, 15.5 Hz, 1 H), 5.82 (td,  $J$  = 1.6, 15.7 Hz, 1 H), 3.72 (s, 3 H),

3.65 - 3.58 (m, 2 H), 2.22 (dq,  $J = 1.5, 7.1$  Hz, 2 H), 1.57 - 1.45 (m, 4 H), 0.89 (s, 9 H), 0.04 (s, 6 H).  
 $^{13}\text{C}$  NMR (101MHz, CHLOROFORM-d)  $\delta = 167.1, 149.5, 120.9, 62.7, 51.4, 32.2, 31.9, 25.9, 24.3, 18.3, -5.4$ .



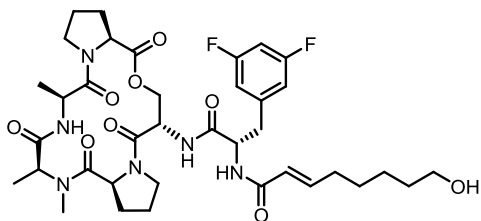
**Methyl (E)-8-((tert-butyldimethylsilyl)oxy)oct-2-enoate:** Yield: 156 mg, 54% over 2 steps. HRMS (FAB) Predicted for  $[\text{C}_{15}\text{H}_{30}\text{O}_3\text{Si} + \text{Na}]^+$ : 309.1862, Found: 309.1850.  $^1\text{H}$  NMR (400MHz, CHLOROFORM-d)  $\delta = 6.96$  (td,  $J = 7.0, 15.6$  Hz, 1 H), 5.81 (td,  $J = 1.5, 15.7$  Hz, 1 H), 3.72 (s, 3 H), 3.59 (t,  $J = 6.4$  Hz, 2 H), 2.20 (dq,  $J = 1.5, 7.2$  Hz, 2 H), 1.55 - 1.43 (m, 4 H), 1.40 - 1.32 (m, 2 H), 0.88 (s, 9 H), 0.04 (s, 6 H).  $^{13}\text{C}$  NMR (101MHz, CHLOROFORM-d)  $\delta = 167.1, 149.6, 120.9, 63.0, 51.3, 32.5, 32.2, 27.8, 25.9, 25.3, 18.3, 9.6, -5.3$ .

**Synthesis of ADEPs with Hydroxyl Terminating Side Chains General Procedure:** TBS protected methyl esters (0.15 mmol) were dissolved in 1:1 THF/water (0.4 mL) and treated with lithium hydroxide mono-hydrate (20 mg, 0.48 mmol). The reactions were heated to 100°C by microwave irradiation for 1 hour. The reactions were checked by TLC for conversion of the starting material, additional heating cycles were conducted if necessary. The reactions were quenched by the addition of 1M  $\text{HCl}_{\text{aq}}$  (1.5 mL). The saponified products were extracted with ethyl acetate and dried over sodium sulfate. After final removal of solvent the free acids were used without further purification.

The free acids were dissolved in DMF (1 mL) along with the free base difluorophenylalanyl macrocycle 3 (68 mg, 0.11 mmol). The solution was then treated with HATU (42 mg 0.11 mmol) and DIPEA (58  $\mu\text{L}$ , 0.33 mmol). The acylation reaction was allowed to proceed over night, after which the DMF was removed *in vacuo*. The concentrated residue was diluted in ethyl acetate

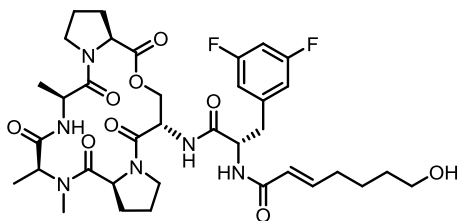
(~10 mL), extracted: 2 x 1 M HCl<sub>aq</sub>, 2 x saturated NaHCO<sub>3aq</sub>, 1 x Brine, then dried over sodium sulfate. The ADEP products were isolated by silica gel flash chromatography using an acetone/ethyl acetate solvent gradient. HPLC was used to purify ADEPs with hydroxyl terminating side chains to >95%. Acetonitrile was removed from the combined HPLC fractions in vacuo and then the purified ADEPs were extracted from the remaining water with ethyl acetate and dried over sodium sulfate. After final removal of solvent, the ADEPs were revealed as white solids.

- HPLC Parameters: Column – Agilent Eclipse XBD-C8 9.4 x 250 mm. Gradient – 30-85% acetonitrile in water over 15 minutes. Flow Rate – 4 mL/min.



**ADEP 2h:** Yield: 19 mg 24% over 2 steps. HRMS (FAB) Predicted for [C<sub>37</sub>H<sub>50</sub>F<sub>2</sub>N<sub>6</sub>O<sub>9</sub> + Na]<sup>+</sup>: 783.3505, Found: 783.3520. <sup>1</sup>H NMR (400MHz, Acetone) δ = 8.47 (d, *J* = 9.0 Hz, 1 H), 8.17 (d, *J* = 9.8 Hz, 1 H), 7.21 (d, *J* = 7.5 Hz, 1 H), 6.93 - 6.81 (m, 3 H), 6.78 (tt, *J* = 2.3, 9.3 Hz, 1 H), 6.33 (td, *J* = 1.5, 15.6 Hz, 1 H), 5.24 (dd, *J* = 3.0, 8.5 Hz, 1 H), 4.97 - 4.86 (m, 2 H), 4.86 - 4.74 (m, 2 H), 4.60 (dt, *J* = 2.0, 9.9 Hz, 1 H), 4.47 (d, *J* = 8.3 Hz, 1 H), 3.73 - 3.60 (m, 3 H), 3.54 (t, *J* = 6.1 Hz, 2 H), 3.47 (td, *J* = 7.1, 11.4 Hz, 2 H), 3.41 - 3.29 (m, 1 H), 3.03 (dd, *J* = 8.2, 13.2 Hz, 1 H), 2.93 (dd, *J* = 5.0, 13.1 Hz, 1 H), 2.79 (s, 3 H), 2.59 - 2.42 (m, 1 H), 2.35 - 2.18 (m, 3 H), 2.03 - 1.86 (m, 6 H), 1.58 - 1.46 (m, 7 H), 1.45 - 1.38 (m, 2 H), 1.28 (d, *J* = 6.5 Hz, 3 H). <sup>13</sup>C NMR (151MHz, Acetone) δ = 173.5, 173.1, 172.0, 170.9, 170.6, 165.9, 165.6, 164.6, 163.0, 162.9, 144.7, 125.1, 113.6, 113.5,

102.6, 102.4, 65.3, 62.4, 60.3, 57.4, 57.0, 55.3, 52.4, 48.5, 47.8, 47.2, 39.5, 33.7, 32.7, 31.7, 31.1, 31.1, 29.1, 26.3, 23.8, 22.0, 17.8, 15.8.



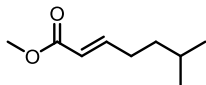
**ADEP 2i:** Yield: 28 mg 34% over 2 steps. HRMS (FAB) Predicted for  $[C_{36}H_{48}F_2N_6O_9 + Na]^+$ : 769.3349, Found: 769.3331.  $^1H$  NMR (400MHz, Acetone)  $\delta$  = 8.47 (d,  $J$  = 9.3 Hz, 1 H), 8.23 (d,  $J$  = 9.6 Hz, 1 H), 7.32 - 7.17 (m, 1 H), 6.94 - 6.82 (m, 3 H), 6.82 - 6.72 (m, 1 H), 6.34 (d,  $J$  = 15.4 Hz, 1 H), 5.34 - 5.16 (m, 1 H), 5.00 - 4.85 (m, 2 H), 4.85 - 4.73 (m, 2 H), 4.60 (t,  $J$  = 9.3 Hz, 1 H), 4.47 (d,  $J$  = 8.1 Hz, 1 H), 3.73 - 3.60 (m, 3 H), 3.60 - 3.53 (m, 2 H), 3.53 - 3.39 (m, 2 H), 3.39 - 3.25 (m, 1 H), 3.08 - 2.98 (m, 1 H), 2.98 - 2.92 (m, 1 H), 2.79 (s, 3 H), 2.58 - 2.42 (m, 1 H), 2.35 - 2.17 (m, 3 H), 2.04 - 1.87 (m, 6 H), 1.55 (br. s., 4 H), 1.48 (d,  $J$  = 6.8 Hz, 3 H), 1.28 (d,  $J$  = 6.6 Hz, 3 H).  $^{13}C$  NMR (101MHz, Acetone)  $\delta$  = 173.5, 173.1, 172.0, 170.9, 170.6, 166.1, 166.0, 165.7, 144.8, 142.6, 125.1, 113.7, 113.5, 102.8, 102.6, 102.3, 65.3, 62.2, 60.3, 57.5, 57.0, 55.2, 52.4, 48.5, 47.8, 47.2, 39.5, 33.2, 32.4, 31.7, 31.1, 30.5, 25.6, 23.8, 22.0, 17.8, 15.8.

**Synthesis of Carbon Branched  $\alpha,\beta$ -Unsaturated Methyl Esters:** Pyridinium chlorochromate (PCC) (3.23 g, 15 mmol) was suspended in Dichloromethane with stirring. To the suspension was added a primary alcohol (10 mmol) and was allowed to react until completely consumed, as indicated by TLC (1-2 hours). Upon completion, the reaction was filtered through a silica gel plug, rinsing with dichloromethane. The dichloromethane was carefully evaporated in vacuo at 30°C yielding the concentrated aldehydes. The aldehydes were used without further

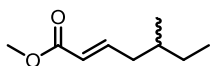


purification.  $^1\text{H}$ NMR was used to quantify residual DCM in order to accurately determine aldehyde stoichiometry for the subsequent olefination.

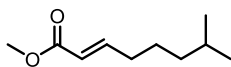
The crude aldehyde was added to an oven dried flask and sealed with a septum. The atmosphere was purged with nitrogen and then charged with dimethoxyethane. A separate oven dried flask with a stir bar was sealed with a septum and purged with dry nitrogen. Once the flask has cooled to room temperature, trimethylphosphonoacetate (1.2 equivalents w.r.t aldehyde) was added to the flask via syringe followed by dimethoxyethane (DME) (concentration 0.5 M w.r.t trimethylphosphonoacetate). The reaction was cooled to 0°C with an ice bath (-78°C for reactions >5 mmol scale) after which, n-butyllithium (2.5 M solution) (1.2 equivalents w.r.t. aldehyde) was added. The reaction was then allowed to warm to room temperature. The aldehyde solution was added via syringe to the room temperature reaction solution dropwise. A white precipitate began to form within seconds. The reaction was allowed to proceed for 2.5 hours, after which it was quenched by the addition of water (same volume of the reaction), dissolving the white precipitate. The phases were partitioned and the aqueous phase was washed once with diethyl ether. The combined organic layers were washed once with brine and dried over sodium sulfate. E/Z selectivity was typically ~13/1. In most cases, the geometric isomers were difficult to separate cleanly. However, the E- $\alpha,\beta$ -unsaturated ester was enriched to at least 95% purity by silica gel chromatography using a DCM/Hexanes solvent gradient. Fractions containing mixtures of the two geometric isomers were rechromatographed if substantial or discarded. Reported yields are of purified E-isomer only.



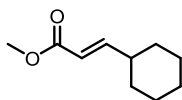
**Methyl (E)-6-methylhept-2-enoate:** Yield 640, 41% over 2 steps.  $^1\text{H}$  NMR (400MHz, CHLOROFORM-d)  $\delta$  = 6.98 (td,  $J$  = 7.0, 15.6 Hz, 1 H), 5.82 (td,  $J$  = 1.6, 15.7 Hz, 1 H), 3.73 (s, 3 H), 2.26 - 2.15 (m, 2 H), 1.58 (non,  $J$  = 6.6 Hz, 1 H), 1.38 - 1.30 (m, 2 H), 0.90 (d,  $J$  = 6.5 Hz, 6 H).



**Methyl (E)-5-methylhept-2-enoate:** Yield 492 mg, 31% over 2 steps.  $^1\text{H}$  NMR (400MHz, CHLOROFORM-d)  $\delta$  = 6.96 (td,  $J$  = 7.5, 15.8 Hz, 1 H), 5.82 (td,  $J$  = 1.3, 15.7 Hz, 1 H), 3.73 (s, 3 H), 2.27 - 2.16 (m, 1 H), 2.09 - 1.99 (m, 1 H), 1.60 - 1.48 (m, 1 H), 1.44 - 1.32 (m, 1 H), 1.25 - 1.14 (m, 1 H), 0.91 - 0.87 (m, 6 H).

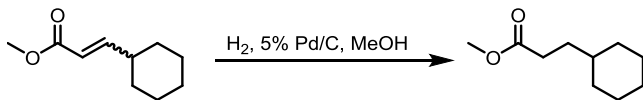


**Methyl (E)-7-methyloct-2-enoate:** (2 mmol scale) Yield, 100 mg, 64% over 2 steps.  $^1\text{H}$  NMR (400MHz, CHLOROFORM-d)  $\delta$  = 6.98 (td,  $J$  = 7.0, 15.6 Hz, 1 H), 5.82 (td,  $J$  = 1.6, 15.6 Hz, 1 H), 3.73 (s, 3 H), 2.19 (dq,  $J$  = 1.6, 7.2 Hz, 2 H), 1.55 (td,  $J$  = 6.7, 13.3 Hz, 1 H), 1.50 - 1.41 (m, 2 H), 1.24 - 1.17 (m, 2 H), 0.88 (d,  $J$  = 6.8 Hz, 6 H).



**methyl (E)-3-cyclohexylacrylate:** (5 mmol scale from commercially available cyclohexane carbaldehyde) Yield: 428 mg, 51%.  $^1\text{H}$  NMR (600MHz, CHLOROFORM-d)  $\delta$  = 6.93 (dd,  $J$  = 7.0, 15.8 Hz, 1 H), 5.77 (dd,  $J$  = 1.5, 15.8 Hz, 1 H), 3.73 (s, 3 H), 2.20 - 2.06 (m, 1 H), 1.82 - 1.70 (m, 4 H),

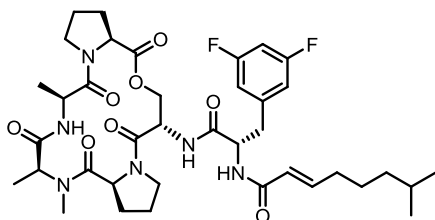
1.70 - 1.63 (m, 1 H), 1.35 - 1.24 (m, 2 H), 1.22 - 1.09 (m, 3 H).  $^{13}\text{C}$  NMR (151MHz, CHLOROFORM-d)  $\delta$  = 167.6, 154.7, 118.4, 51.4, 40.4, 31.6, 25.9, 25.7.



**methyl 3-cyclohexylpropanoate:** Methyl (E/Z)-3-cyclohexylacrylate (298 mg, 1.75 mmol) was dissolved in methanol (5 mL) and then treated with 5% palladium on carbon (40 mg). The reaction flask was sealed with a septum through which hydrogen gas was supplied from a balloon affixed to a syringe. Consumption of the starting material was monitored by TLC (30% DCM / 70% hexanes). Once the starting material was completely consumed, the reaction was filtered through celite, rinsing with methanol. Pure methyl 3-cyclohexylpropanoate was revealed upon removal of the solvent and was used without further purification. Yield 273 mg, 89%.  $^1\text{H}$  NMR (600MHz, CHLOROFORM-d)  $\delta$  = 3.67 (s, 3 H), 2.36 - 2.28 (m, 2 H), 1.69 (d,  $J$  = 10.6 Hz, 4 H), 1.66 - 1.62 (m, 1 H), 1.55 - 1.49 (m, 2 H), 1.25 - 1.10 (m, 4 H), 0.93 - 0.83 (m, 2 H).  $^{13}\text{C}$  NMR (151MHz, CHLOROFORM-d)  $\delta$  = 174.7, 51.5, 37.2, 32.9, 32.3, 31.6, 26.5, 26.2.

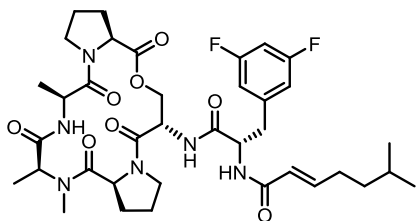
**Synthesis of ADEPs with Carbon Branched Side Chains:** Methyl esters (0.15 mmol) were dissolved in 1:1 THF/water (0.4 mL) and treated with lithium hydroxide mono-hydrate (20 mg, 0.48 mmol). The reactions were heated to 100°C by microwave irradiation for 1 hour. The reactions were checked by TLC for conversion of the starting material, additional heating cycles were conducted if necessary. The reactions were quenched by the addition of 1M HCl<sub>aq</sub> (1.5 mL). The saponified products were extracted with ethyl acetate and dried over sodium sulfate. After final removal of solvent the free acids were used without further purification. Saponification of methyl 3-cyclohexylpropanoate was conducted similarly, but without microwave irradiation.

The free acids were dissolved in DMF (1 mL) along with the free base difluorophenylalanyl macrocycle 3 (68 mg, 0.11 mmol). The solution was then treated with HATU (42 mg 0.11 mmol) and DIPEA (58  $\mu$ L, 0.33 mmol). The acylation reaction was allowed to proceed over night, after which the DMF was removed *in vacuo*. The concentrated residue was diluted in ethyl acetate (~10 mL), extracted: 2 x 1 M HCl<sub>aq</sub>, 2 x saturated NaHCO<sub>3aq</sub>, 1 x Brine, then dried over sodium sulfate. The ADEP products were isolated by silica gel flash chromatography using an acetone/ethyl acetate solvent gradient. HPLC was used to purify ADEPs with hydroxyl terminating side chains to >95%. Acetonitrile was removed from the combined HPLC fractions *in vacuo* and then the purified ADEPs were extracted from the remaining water with ethyl acetate and dried over sodium sulfate. After final removal of solvent, the ADEPs were revealed as white solids.

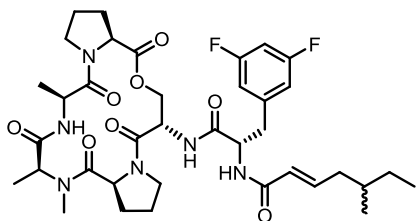


**ADEP 2e:** Yield 39 mg, 46% over 2 steps. <sup>1</sup>H NMR (400MHz, Acetone)  $\delta$  = 8.47 (d,  $J$  = 9.3 Hz, 1 H), 8.23 (d,  $J$  = 9.5 Hz, 1 H), 7.21 (d,  $J$  = 7.3 Hz, 1 H), 6.94 - 6.82 (m, 3 H), 6.81 - 6.71 (m, 1 H), 6.33 (td,  $J$  = 1.4, 15.5 Hz, 1 H), 5.24 (dd,  $J$  = 2.9, 8.4 Hz, 1 H), 5.00 - 4.86 (m, 2 H), 4.86 - 4.77 (m, 2 H), 4.68 - 4.56 (m, 1 H), 4.48 (d,  $J$  = 8.8 Hz, 1 H), 3.75 - 3.57 (m, 3 H), 3.48 (td,  $J$  = 7.0, 11.3 Hz, 1 H), 3.42 - 3.27 (m, 1 H), 3.04 (dd,  $J$  = 8.2, 13.2 Hz, 1 H), 2.93 (dd,  $J$  = 4.9, 13.2 Hz, 1 H), 2.79 (s, 3 H), 2.58 - 2.44 (m, 1 H), 2.35 - 2.24 (m, 1 H), 2.24 - 2.16 (m, 2 H), 2.03 - 1.85 (m, 5 H), 1.62 - 1.36 (m, 7 H), 1.30 - 1.26 (m, 3 H), 1.26 - 1.19 (m, 2 H), 0.88 (d,  $J$  = 6.8 Hz, 6 H). <sup>13</sup>C NMR (101MHz, CHLOROFORM-d)  $\delta$  = 173.5, 173.1, 172.0, 170.9, 170.6, 165.9, 165.7, 165.0, 164.9, 162.6, 162.4,

144.9, 142.6, 142.6, 125.1, 113.7, 113.6, 113.5, 113.5, 102.8, 102.5, 102.3, 65.3, 60.3, 57.5, 56.9, 55.1, 52.4, 48.4, 47.7, 47.2, 39.5, 39.2, 32.9, 31.7, 31.1, 28.7, 27.1, 23.8, 22.9, 22.0, 17.8, 15.8.

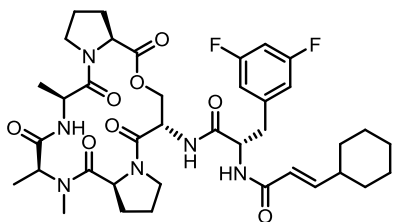


**ADEP 2f** Yield 25 mg, 30% over 2 steps.  $^1\text{H}$  NMR (400MHz, Acetone)  $\delta$  = 8.46 (d,  $J$  = 9.3 Hz, 1 H), 8.14 (d,  $J$  = 9.5 Hz, 1 H), 7.20 (d,  $J$  = 7.5 Hz, 1 H), 6.94 - 6.81 (m, 3 H), 6.81 - 6.74 (m, 1 H), 6.33 (td,  $J$  = 1.5, 15.3 Hz, 1 H), 5.23 (dd,  $J$  = 3.1, 8.4 Hz, 1 H), 4.96 - 4.86 (m, 2 H), 4.86 - 4.72 (m, 2 H), 4.60 (dt,  $J$  = 1.9, 10.0 Hz, 1 H), 4.47 (d,  $J$  = 8.5 Hz, 1 H), 3.72 - 3.57 (m, 3 H), 3.46 (td,  $J$  = 7.1, 11.4 Hz, 1 H), 3.35 (ddd,  $J$  = 3.6, 9.0, 12.2 Hz, 1 H), 3.03 (dd,  $J$  = 8.2, 13.2 Hz, 1 H), 2.94 (dd,  $J$  = 5.0, 13.1 Hz, 1 H), 2.79 (s, 3 H), 2.55 - 2.44 (m, 1 H), 2.33 - 2.19 (m, 3 H), 2.03 - 1.85 (m, 6 H), 1.66 - 1.54 (m, 1 H), 1.49 (d,  $J$  = 7.0 Hz, 3 H), 1.40 - 1.33 (m, 2 H), 1.28 (d,  $J$  = 6.5 Hz, 3 H), 0.90 (d,  $J$  = 6.8 Hz, 3 H), 0.91 (d,  $J$  = 6.5 Hz, 3 H).  $^{13}\text{C}$  NMR (101MHz, Acetone)  $\delta$  = 173.5, 173.1, 172.0, 170.9, 170.6, 165.9, 165.6, 144.9, 142.6, 125.0, 113.7, 113.4, 102.8, 102.6, 102.3, 65.3, 60.3, 57.4, 56.9, 55.3, 52.4, 48.4, 47.7, 47.1, 39.5, 38.3, 31.7, 31.1, 30.5, 28.2, 23.8, 22.8, 22.7, 22.0, 17.8, 15.8.

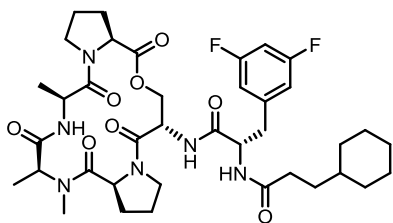


**ADEP 2g** Yield: 34 mg, 41% over 2 steps.  $^1\text{H}$  NMR (400MHz, Acetone)  $\delta$  = 8.46 (d,  $J$  = 9.3 Hz, 1 H), 8.17 (d,  $J$  = 9.8 Hz, 1 H), 7.22 (d,  $J$  = 7.3 Hz, 1 H), 6.91 - 6.81 (m, 3 H), 6.81 - 6.73 (m, 1 H), 6.32 (dd,  $J$  = 0.8, 15.3 Hz, 1 H), 5.24 (dd,  $J$  = 3.1, 8.7 Hz, 1 H), 4.97 - 4.86 (m, 2 H), 4.86 - 4.75 (m, 2 H),

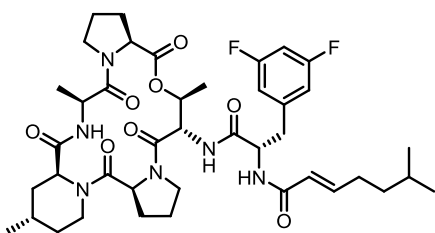
4.60 (dt,  $J = 1.9, 10.0$  Hz, 1 H), 4.47 (d,  $J = 8.5$  Hz, 1 H), 3.72 - 3.57 (m, 3 H), 3.47 (td,  $J = 7.0, 11.3$  Hz, 1 H), 3.40 - 3.29 (m, 1 H), 3.03 (dd,  $J = 8.2, 13.2$  Hz, 1 H), 2.93 (dd,  $J = 4.9, 13.2$  Hz, 1 H), 2.79 (s, 3 H), 2.57 - 2.44 (m, 1 H), 2.35 - 2.08 (m, 3 H), 2.03 - 1.83 (m, 6 H), 1.61 - 1.51 (m, 1 H), 1.49 (d,  $J = 7.0$  Hz, 3 H), 1.43 - 1.38 (m, 1 H), 1.28 (d,  $J = 6.5$  Hz, 3 H), 1.22 - 1.16 (m, 1 H), 0.94 - 0.86 (m, 6 H).  $^{13}\text{C}$  NMR (101MHz, Acetone)  $\delta = 173.4, 173.1, 171.9, 170.9, 170.6, 165.7, 165.6, 164.9, 162.6, 143.5, 142.7, 142.6, 126.2, 126.2, 113.7, 113.6, 113.4, 102.8, 102.6, 102.3, 65.2, 60.3, 57.4, 56.9, 55.2, 52.4, 48.4, 47.8, 47.2, 39.8, 39.5, 35.2, 35.1, 31.7, 31.1, 30.0, 23.8, 21.9, 19.6, 17.8, 15.8, 11.8.$



**ADEP 2j:** (0.34 mmol scale) Yield: 139 mg, 54% over 2 steps.  $^1\text{H}$  NMR (400MHz, Acetone)  $\delta = 8.48$  (d,  $J = 9.3$  Hz, 1 H), 8.33 - 8.14 (m, 1 H), 7.22 (d,  $J = 7.3$  Hz, 1 H), 6.92 - 6.81 (m, 3 H), 6.81 - 6.73 (m, 1 H), 6.38 - 6.24 (m, 1 H), 5.30 - 5.19 (m, 1 H), 4.98 - 4.86 (m, 2 H), 4.86 - 4.76 (m, 2 H), 4.60 (t,  $J = 9.9$  Hz, 1 H), 4.47 (d,  $J = 8.3$  Hz, 1 H), 3.73 - 3.56 (m, 3 H), 3.54 - 3.42 (m, 1 H), 3.41 - 3.29 (m, 1 H), 3.08 - 2.98 (m, 1 H), 2.96 - 2.86 (m, 2 H), 2.78 (s, 3 H), 2.58 - 2.43 (m, 1 H), 2.37 - 2.22 (m, 1 H), 2.22 - 2.13 (m, 1 H), 2.02 - 1.88 (m, 5 H), 1.87 - 1.70 (m, 4 H), 1.66 (d,  $J = 13.9$  Hz, 1 H), 1.48 (d,  $J = 7.1$  Hz, 3 H), 1.40 - 1.25 (m, 5 H), 1.25 - 1.12 (m, 3 H).  $^{13}\text{C}$  NMR (101MHz, Acetone)  $\delta = 173.4, 173.1, 172.0, 170.9, 170.6, 166.2, 165.6, 162.6, 149.8, 142.6, 142.5, 122.7, 113.7, 113.6, 113.5, 113.4, 102.8, 102.5, 102.3, 65.3, 60.3, 57.5, 56.9, 55.2, 52.4, 48.4, 47.8, 47.2, 41.0, 39.6, 32.9, 32.8, 31.7, 31.1, 26.8, 26.6, 23.8, 21.9, 17.8, 15.8.$

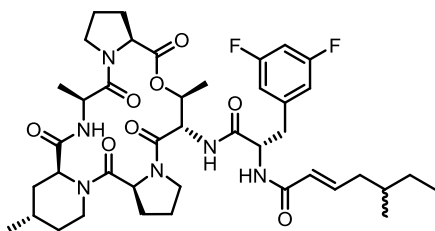


**ADEP 2k:** (0.34 mmol scale) Yield: 152 mg, 59% over 2 steps.  $^1\text{H}$  NMR (400MHz, Acetone)  $\delta$  = 8.46 (d,  $J$  = 9.6 Hz, 1 H), 8.10 (d,  $J$  = 9.6 Hz, 1 H), 7.08 (d,  $J$  = 7.1 Hz, 1 H), 6.90 - 6.82 (m, 2 H), 6.82 - 6.75 (m, 1 H), 5.24 (dd,  $J$  = 3.0, 8.6 Hz, 1 H), 4.92 (dd,  $J$  = 1.8, 11.6 Hz, 1 H), 4.89 - 4.77 (m, 2 H), 4.69 (dt,  $J$  = 5.4, 7.5 Hz, 1 H), 4.63 - 4.54 (m, 1 H), 4.45 (d,  $J$  = 8.6 Hz, 1 H), 3.74 - 3.57 (m, 3 H), 3.51 - 3.42 (m, 1 H), 3.42 - 3.32 (m, 1 H), 3.00 (dd,  $J$  = 7.8, 13.1 Hz, 1 H), 2.91 (dd,  $J$  = 5.3, 13.1 Hz, 1 H), 2.78 (s, 3 H), 2.57 - 2.44 (m, 1 H), 2.41 - 2.35 (m, 2 H), 2.34 - 2.21 (m, 1 H), 2.04 - 1.87 (m, 6 H), 1.81 - 1.61 (m, 5 H), 1.57 - 1.43 (m, 5 H), 1.29 - 1.24 (m, 4 H), 1.24 - 1.12 (m, 3 H).  $^{13}\text{C}$  NMR (101MHz, Acetone)  $\delta$  = 173.5, 173.4, 173.1, 172.1, 172.0, 170.6, 170.6, 165.6, 165.0, 164.9, 162.6, 162.4, 142.6, 113.7, 113.7, 113.5, 113.5, 102.8, 102.6, 102.3, 65.3, 60.3, 57.4, 56.9, 55.1, 52.4, 52.3, 48.4, 47.7, 47.1, 39.5, 38.3, 34.1, 34.0, 33.9, 33.9, 31.7, 31.1, 31.1, 27.4, 27.1, 23.8, 22.0, 17.8, 15.8.



**ADEP 15b:** (0.07 mmol scale) Yield: 17 mg, 30% over 2 steps.  $^1\text{H}$  NMR (600MHz, CHLOROFORM-d)  $\delta$  = 8.51 (d,  $J$  = 9.5 Hz, 1 H), 7.24 - 7.05 (m, 1 H), 7.01 - 6.89 (m, 2 H), 6.71 (d,  $J$  = 5.9 Hz, 2 H), 6.67 - 6.59 (m, 1 H), 6.18 (dd,  $J$  = 1.3, 15.2 Hz, 1 H), 5.24 (d,  $J$  = 8.4 Hz, 1 H), 5.17 - 5.05 (m, 1 H), 5.00 - 4.89 (m, 1 H), 4.85 - 4.74 (m, 1 H), 4.74 - 4.61 (m, 3 H), 4.46 (d,  $J$  = 8.4 Hz, 1 H), 3.85 - 3.73 (m, 1 H), 3.65 - 3.51 (m, 2 H), 3.35 - 3.24 (m, 1 H), 3.06 - 2.97 (m, 1 H), 2.91 (dd,  $J$  = 5.1, 13.6 Hz,

1 H), 2.69 (d,  $J = 12.1$  Hz, 1 H), 2.65 - 2.55 (m, 1 H), 2.41 - 2.30 (m, 1 H), 2.25 - 2.20 (m, 2 H), 2.14 - 2.08 (m, 1 H), 2.03 - 1.91 (m, 4 H), 1.91 - 1.80 (m, 2 H), 1.68 - 1.56 (m, 3 H), 1.38 - 1.30 (m, 5 H), 1.19 (d,  $J = 6.6$  Hz, 3 H), 1.06 (dt,  $J = 5.5, 12.7$  Hz, 1 H), 1.02 - 0.98 (m, 1 H), 0.95 (d,  $J = 5.9$  Hz, 3 H), 0.92 - 0.85 (m, 6 H).  $^{13}\text{C}$  NMR (151MHz, CHLOROFORM-d)  $\delta = 172.1, 171.2, 171.0, 169.6, 169.4, 166.1, 165.5, 163.7, 163.6, 162.0, 161.9, 146.0, 140.3, 123.2, 112.6, 112.5, 102.4, 102.2, 102.1, 69.9, 59.0, 57.1, 56.9, 54.0, 53.2, 47.7, 46.9, 46.5, 40.7, 37.9, 37.4, 36.0, 33.3, 30.7, 30.0, 27.9, 27.5, 22.9, 22.4, 22.3, 21.9, 21.2, 17.8, 13.0$ .



**ADEP 15c:** (0.07 mmol scale) Yield: 48 mg, 86% over 2 steps.  $^1\text{H}$  NMR (600MHz, CHLOROFORM-d)  $\delta = 8.51$  (d,  $J = 9.5$  Hz, 1 H), 7.01 (d,  $J = 9.2$  Hz, 1 H), 6.99 - 6.88 (m, 2 H), 6.79 - 6.68 (m, 2 H), 6.68 - 6.58 (m, 1 H), 6.17 (d,  $J = 15.0$  Hz, 1 H), 5.24 (dd,  $J = 2.8, 8.6$  Hz, 1 H), 5.17 - 5.06 (m, 1 H), 5.03 - 4.90 (m, 1 H), 4.76 (dt,  $J = 5.3, 8.0$  Hz, 1 H), 4.72 - 4.63 (m, 3 H), 4.46 (d,  $J = 8.1$  Hz, 1 H), 3.86 - 3.74 (m, 1 H), 3.66 - 3.50 (m, 2 H), 3.35 - 3.25 (m, 1 H), 3.01 (dd,  $J = 8.3, 13.4$  Hz, 1 H), 2.93 (dd,  $J = 5.1, 13.6$  Hz, 1 H), 2.70 (d,  $J = 11.7$  Hz, 1 H), 2.66 - 2.57 (m, 1 H), 2.40 - 2.31 (m, 1 H), 2.28 - 2.16 (m, 2 H), 2.16 - 2.03 (m, 2 H), 2.03 - 1.92 (m, 3 H), 1.90 - 1.83 (m, 2 H), 1.69 - 1.58 (m, 2 H), 1.54 (qd,  $J = 6.5, 13.0$  Hz, 1 H), 1.42 - 1.28 (m, 4 H), 1.25 - 1.12 (m, 4 H), 1.07 (dt,  $J = 5.5, 12.7$  Hz, 1 H), 1.01 (dd,  $J = 3.7, 12.8$  Hz, 1 H), 0.96 (d,  $J = 6.2$  Hz, 3 H), 0.93 - 0.79 (m, 6 H).  $^{13}\text{C}$  NMR (151MHz, CHLOROFORM-d)  $\delta = 172.1, 171.2, 171.0, 169.6, 169.4, 166.0, 165.5, 163.7, 163.6, 162.1, 162.0, 144.7, 140.3, 140.2, 124.3, 112.6, 112.6, 112.5, 112.4, 102.5, 102.3, 102.1, 69.8, 59.0, 57.1, 56.8, 54.1, 53.2, 47.7, 47.0, 46.5, 40.8, 39.2, 39.2, 37.9, 36.0, 34.2, 34.2, 33.3, 30.7, 29.2, 29.1, 28.0, 22.9, 21.9, 21.2, 19.1, 19.1, 17.8, 13.0, 11.4, 11.3$



## References

1. Lee, B.; Park, E. Y.; Lee, K.; Jeon, H.; Sung, K. H.; Paulsen, H.; Rubsamen-Schaeff, H.; Brotz-Oesterhelt, H.; Song, H. K. Structures of ClpP in complex with acyldepsipeptide antibiotics reveal its activation mechanism. *Nat Struct Mol Biol* **2010**, *17*, 471-478.
2. Li, D. H. S.; Chung, Y. S.; Gloyd, M.; Joseph, E.; Ghirlando, R.; Wright, G. D.; Cheng, Y.; Maurizi, M. R.; Guarne, A.; Ortega, J. Acyldepsipeptide antibiotics induce the formation of a structured axial channel in ClpP: a model for the ClpX/ClpA-bound state of ClpP. *Chem. Biol.* **2010**, *17*, 959-969.
3. Kim, Y.; Levchenko, I.; Fraczkowska, K.; Woodruff, R. V.; Sauer, R. T.; Baker, T. A. Molecular determinants of complex formation between Clp/Hsp100 ATPases and the ClpP peptidase. *Nature Structural & Molecular Biology* **2001**, *8*, 230-233.
4. Brotz-Oesterhelt, H.; Beyer, D.; Kroll, H.; Endermann, R.; Ladel, C.; Schroeder, W.; Hinzen, B.; Raddatz, S.; Paulsen, H.; Henninger, K.; Bandow, J. E.; Sahl, H.; Labischinski, H. Dysregulation of bacterial proteolytic machinery by a new class of antibiotics. *Nat. Med.* **2005**, *11*, 1082-1087.
5. Ollinger, J.; O'Malley, T.; Kesicki, E. A.; Odingo, J.; Parish, T. Validation of the essential ClpP protease in *Mycobacterium tuberculosis* as a novel drug target. *J. Bacteriol.* **2012**, *194*, 663-668.
6. Hinzen, B.; Raddatz, S.; Paulsen, H.; Lampe, T.; Schumacher, A.; Häbich, D.; Hellwig, V.; Benet-Buchholz, J.; Endermann, R.; Labischinski, H.; Brötz-Oesterhelt, H. Medicinal Chemistry Optimization of Acyldepsipeptides of the Enopeptin Class Antibiotics. *ChemMedChem* **2006**, *1*, 689-693.
7. Global Tuberculosis Control: WHO report **2010**.
8. Gandhi, N. R.; Nunn, P.; Dheda, K.; Schaaf, H. S.; Zignol, M.; Van Soolingen, D.; Jensen, P.; Bayona, J. Multidrug-resistant and extensively drug-resistant tuberculosis: a threat to global control of tuberculosis. *The Lancet* **2010**, *375*, 1830-1843.
9. Raju, R. M.; Unnikrishnan, M.; Rubin, D. H.; Krishnamoorthy, V.; Kandror, O.; Akopian, T. N.; Goldberg, A. L.; Rubin, E. J. *Mycobacterium tuberculosis* ClpP1 and ClpP2 function together in protein degradation and are required for viability in vitro and during infection. *PLoS pathogens* **2012**, *8*, e1002511.
10. Akopian, T.; Kandror, O.; Raju, R. M.; Unnikrishnan, M.; Rubin, E. J.; Goldberg, A. L. The active ClpP protease from *M. tuberculosis* is a complex composed of a heptameric ClpP1 and a ClpP2 ring. *EMBO J.* **2012**, *31*, 1529-1541.

11. Akopian, T.; Kandrор, O.; Raju, R. M.; UnniKrishnan, M.; Rubin, E. J.; Goldberg, A. L. The active ClpP protease from *M. tuberculosis* is a complex composed of a heptameric ClpP1 and a ClpP2 ring. *EMBO J.* **2012**, *31*, 1529-1541.
12. Ingvarsson, H.; Mate, M. J.; Hogbom, M.; Portnoi, D.; Benaroudj, N.; Alzari, P. M.; Ortiz-Lombardia, M.; Unge, T. Insights into the inter-ring plasticity of caseinolytic proteases from the X-ray structure of *Mycobacterium tuberculosis* ClpP1. *Acta Crystallographica Section D: Biological Crystallography* **2007**, *63*, 249-259.
13. Personne, Y.; Brown, A. C.; Schuessler, D. L.; Parish, T. *Mycobacterium tuberculosis* ClpP proteases are co-transcribed but exhibit different substrate specificities. *PLoS one* **2013**, *8*, e60228.
14. Lee, M. E.; Baker, T. A.; Sauer, R. T. Control of substrate gating and translocation into ClpP by channel residues and ClpX binding. *J. Mol. Biol.* **2010**, *399*, 707-718.
15. Willer, M.; Hindler, J.; Cockerill, F. Methods for dilution antimicrobial susceptibility tests for bacteria that grow aerobically; approved eighth. *CLSI* **2009**, *29*, 12-15.

## Chapter 8 – The Acyldepsipeptide *N*-Acyl difluorophenylalanine Moiety is Necessary and Sufficient for ClpP Activation.

### Introduction

While ADEPs are promising candidates for clinical development, peptide antibiotics often times suffer from poor stability *in vivo* because of the many peptidases expressed by both the host and the pathogen that could potentially hydrolyze the backbone amide bonds of antibacterial agent.<sup>1-3</sup> Additionally, peptides exhibit low lipophilicity due to the polarity of the backbone amides. This often leads to a reduced ability to cross cell membranes leading to low oral bioavailability.<sup>4,5</sup> The macrocyclic structure of the ADEPs and its inherent trans-annular hydrogen bonding appear to be critical for their cell permeability and their bioactivity.<sup>6-8</sup> Questions about the *in vivo* stability of the ADEPs remain, as a comprehensive pharmacokinetic study of the ADEPs has yet to be conducted.

Regardless of the ultimate clinical utility of the ADEPs, activation of ClpP by small molecules is a promising strategy in antibacterial drug development.<sup>9-13</sup> Given the potential liabilities of the peptide core structure of the ADEPs, it is a worthwhile endeavor to search for non-peptide activators of ClpP that could be used as antibacterial agents. Interest in this strategy is evident in a high throughput screen for ClpP activators that yielded 4 new structural classes of ClpP activators.<sup>10</sup> Curiously, no subsequent development of these new structural classes has been published. However, it is noteworthy that ongoing studies in our lab have shown that at least one the new structural classes may be a false positive for ClpP activation (see chapter 11). An alternate to high throughput screening for new ClpP activators is to search for simple fragments that may only weakly activate ClpP but can be structurally elaborated into higher affinity ligands.<sup>14-17</sup> Fragment based drug design differs from HTS in that smaller

collections of molecular fragments are screened initially in search of low affinity or potency hits. Hit to lead development of the fragments relies heavily on rational and structure-based design. Although fragment based drug design a relatively new strategy, it has become widely accepted as powerful tool in drug discovery.<sup>17</sup>

## Results

Our lab has undertaken an effort to elucidate and validate a minimal structure that is able to activate ClpP, which would provide a scaffold from which new ClpP activators could be designed. To begin, we broke the ADEP structure down into several smaller fragments and then chemically synthesized and tested each for antibacterial activity against *B. subtilis*, a highly ADEP susceptible bacterium. Fragments included an ADEP peptidolactone with the serine residue acylated with an acetyl group (**2**), an *N*-acetyldifluorophenylalanyl peptidolactone (**3**), a serine-proline ester coupled to the *N*-E-2-heptenoyldifluorophenylalanine (**4**), and *N*-E-2-heptenoyldifluorophenylalanine methyl ester (**5**) (Figure 8.1). Fragments **4** and **5** but not **2** and **3** exhibited antibacterial activity, albeit with much lower potency than intact ADEP **1** (Table 8.1). These observations can be explained by crystal structures of ADEPs bound to ClpP in which there are complimentary, non-covalent interactions between the molecule and the protein.<sup>18,19</sup> Interestingly, fragment **4**, which contains a portion of the ADEP peptidolactone coupled to the ADEP side chain, is less active than fragment **5**, which is composed only of the side chain portion of the ADEP molecule. A possible explanation for this observation is that the peptide based structure of **4** exhibits poor cell permeability.

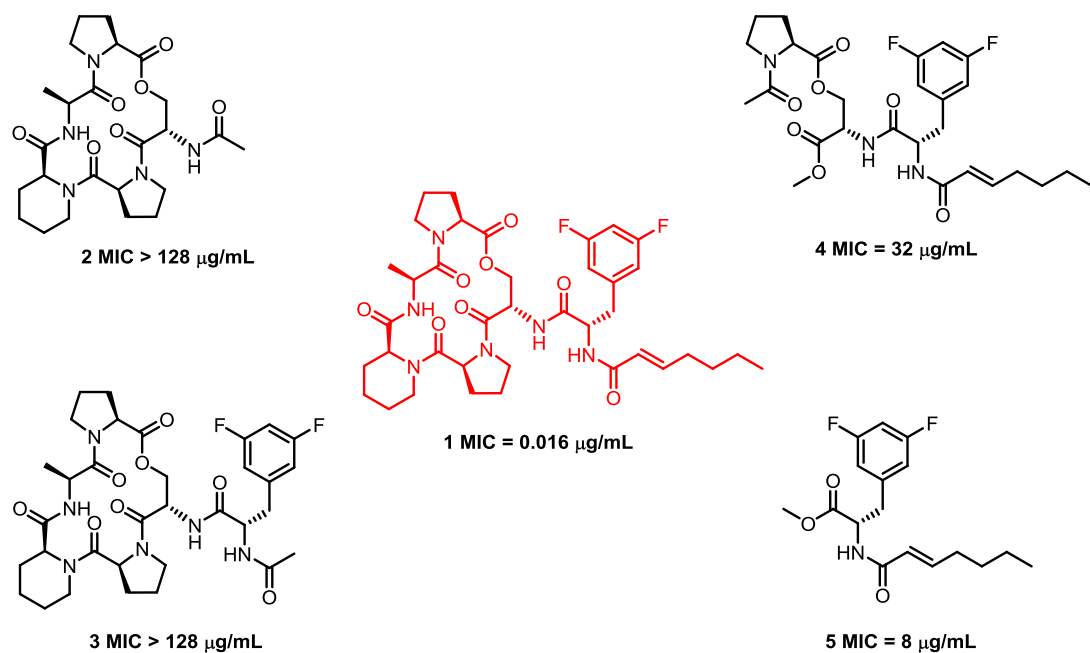


**Figure 8.110** - Deconstruction of an acyldepsipeptide in search of fragments with antibacterial activity against *B. subtilis*

With active fragments **4** and **5** identified, we undertook efforts to establish their basic structure-activity relationships (SAR) beginning with fragment **4**, which is composed of a portion of the ADEP peptidolactone. We recently reported that substitution of the serine residue within the ADEP peptidolactone with *allo*-threonine resulted in a substantial improvement in ADEP activity due to conformational restriction of the peptidolactone.<sup>8</sup> We hypothesized that the same SAR may hold true for fragment **4** as well. Compounds **6-7** are analogs of **4** wherein the serine residue has been replaced with either *allo*-threonine (**6**) or threonine (**7**). To our surprise, both analogs had the same antibacterial activity against *B. subtilis* as fragment **4** (MIC = 32  $\mu\text{g/mL}$ ). Perhaps the *allo*-threonine and threonine residues do not significantly restrict the conformations of the acyclic fragments. In any case, fragment **4** is not as attractive for hit to lead development as fragment **5**, which is both more active and structurally less complex than **4**.

A positional scanning approach was used to study the SAR of fragment **5**. First, we synthesized a series of analogs with varied acyl chains (**8-10**). Fragment **8** bears an acyl chain

that is common to several previously reported synthetic ADEPs<sup>20</sup> and Fragment **9** bears the acyl chain of the A54556 ADEP natural products.<sup>21</sup> Fragment **10** is an analog that we synthesized to test the effects of side chain branching. Fragments **5**, **8**, and **10** are all equally potent (MIC = 8 µg/mL) while fragment **9** exhibited attenuated activity (MIC = 32 µg/mL). This is consistent with ADEP SAR, wherein analogs with polyunsaturated side chains are less active compared to analogs with  $\alpha,\beta$ -unsaturated analogs.<sup>7,22</sup> Fragments **11** and **12** are saturated analogs of **5** and **8** respectively and exhibit significantly attenuate antibacterial activity, which is also consistent with reported ADEP SAR.<sup>7</sup> We next studied a series of analogs, in which the difluorophenylalanine was replaced. Fragments **13** and **14** are analogs in which the difluorophenylalanine is substituted by either phenylalanine or leucine, respectively. The analog with the phenylalanine residue (**11**, MIC = 64 µg/mL) is less active than that with difluorophenylalanine. In contrast, the analog containing leucine is completely inactive. This result is once again consistent with the known ADEP SAR.<sup>7</sup>

Additional analogs of **5** were prepared in order to probe SAR unique to the *N*-acyldifluorophenylalanine moiety and perhaps suggest strategies for improving potency. The most logical strategy for elaborating fragment **5** is build out from its *C*-terminus. As such, we explored the effects of several *C*-terminus structural manipulations on fragment antibacterial activity. Fragment **15** is the carboxylic acid derivative of methyl ester **5**. While **15** is still active (MIC = 64 µg/mL), it is considerably less potent than **5**, perhaps as a result of poor membrane permeability. Fragments **16-18** are the primary, methyl, and dimethyl amide analogs, respectively, of **5**. These analogs are also less active than **5**, with **16** and **17** (MIC = 32 µg/mL) being slightly more potent than **18** (MIC = 64 µg/mL). Three additional ester analogs (**19-21**) were prepared. The furfuryl ester **19** (MIC = 32 µg/mL) exhibited attenuated activity compared to **5** while the benzyl ester (**20**) was completely inactive. Interestingly, the propargyl ester **21**

(MIC = 2) was 4 fold more potent than **5**. This finding was encouraging since we envisioned using **21** to assist in target validation (*vide infra*).

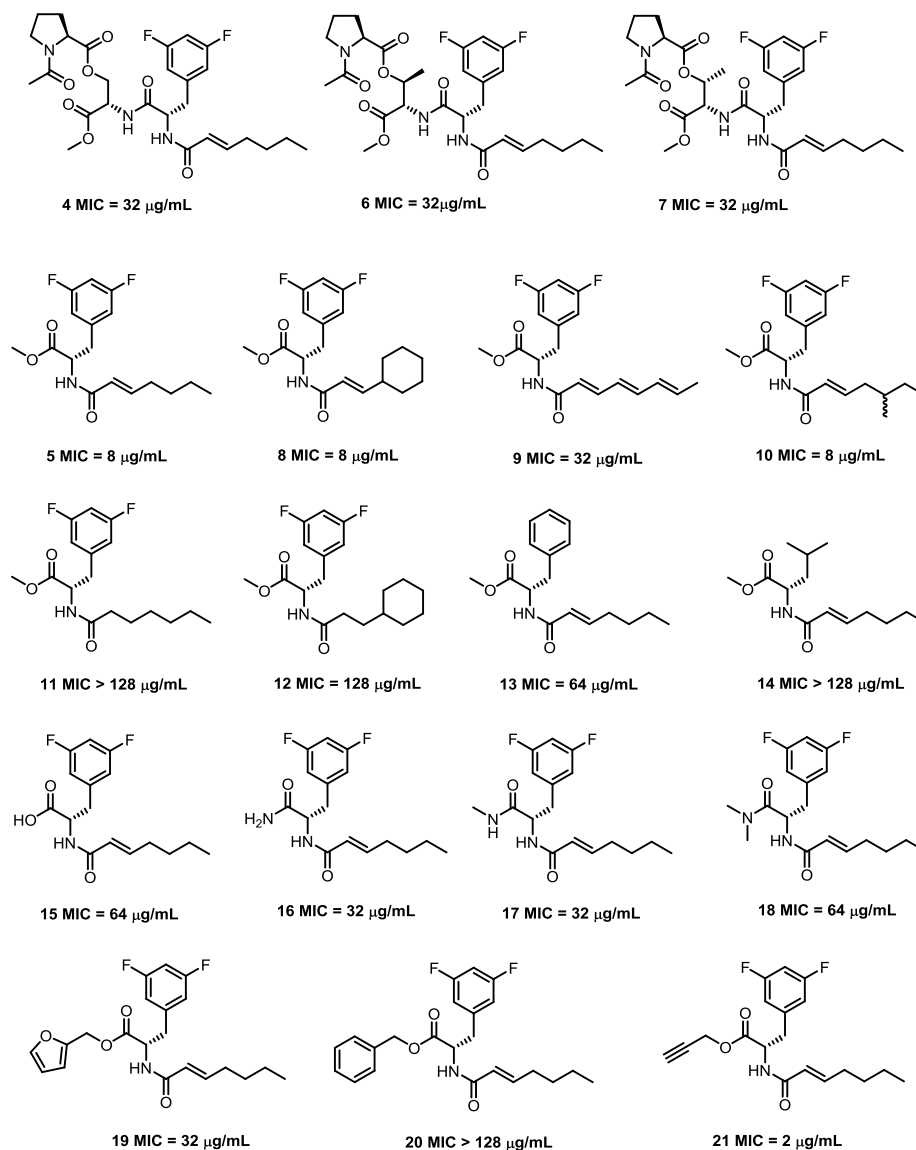


Figure 8.2 –Structures and antibacterial activity of *N*-acyldifluorophenylalanine fragment analogs against *B. subtilis*

Indeed, the operating assumption is that the ADEPs and the *N*-acyldifluorophenylalanine fragments have the same mechanism of action. However, a series of genetic and biochemical experiments were performed to conclusively validate the target of the bioactive fragments. First, compound **1** and Fragment **5** were tested for antibacterial activity against two mutant

strains of *B. subtilis* donated by the Grossman lab at MIT. One strain was  $\Delta spx$  null strain (BOSE 1227 *spx::neo*) and the second was a  $\Delta spx-clpP$  double null strain (BOSE 1246 *spx::neo* and *clpP::cat*).<sup>23</sup> The *spx* gene encodes a transcriptional regulator protein that is normally degraded by ClpP.<sup>24</sup> Inactivation of the *spx* gene restores developmental competency to *clpP* null strains of *B. subtilis*. Loss of function mutations in the *spx* gene were not predicted to affect *B. subtilis* susceptibility to ClpP activators. As expected, the antibacterial activities of **1** and **5** against the  $\Delta spx$  null strain were identical to their activities against wild type *B. subtilis*. Additionally, both **1** and **5** were completely inactive against the *B. subtilis* strain lacking both *spx* and *clpP*. This activity profile is precisely what should be expected for compounds that activate ClpP.

To biochemically validate the proposal that ADEP fragments activate ClpP, a series of fragments were tested for their ability to activate *B. subtilis* ClpP *in vitro* (Figure 8.3.). Fragments were incubated with *B. subtilis* ClpP and a fluorogenic decapeptide and the initial rates of decapeptide hydrolysis were measured. All of the fragments exhibited concentration dependent activation of ClpP decapeptidase activity and exhibited similar apparent binding affinities ( $K_{app}$ ) ranging from 3.9 – 7.9  $\mu$ M. As expected, fragment binding to ClpP was much weaker than ADEP binding to ClpP ( $K_{app} = 29 \pm 1$  nm). This biochemical evidence conclusively demonstrates that *N*-acyldifluorophenyllanine fragments are a minimal structure that is capable of binding to and activating ClpP.



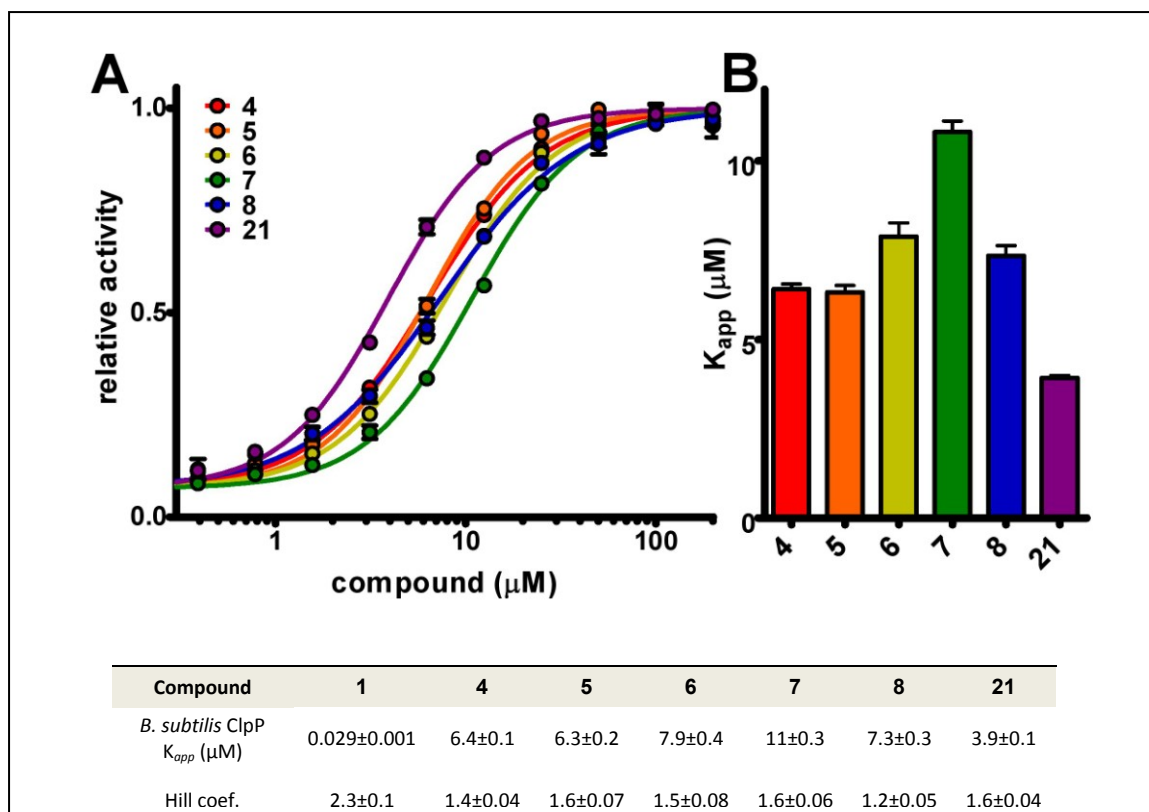


Figure 8.3 - ClpP Binding of Key *N*-acyldifluorophenylalanine Fragment Analogs: ADEPs and fragments were incubated with *B. subtilis* ClpP and fluorogenic decapeptide. Apparent dissociation constants  $K_{app}$  were calculated from plots of decapeptidase rate vs. ADEP concentration that were fit to the Hill equation for cooperative binding.

A final biochemical experiment was conducted to rule out the possibility that fragment antibacterial activity was an off target effect independent of ClpP activation. We chemically synthesized an activity reagent to identify the targets of Fragment **21** using chemical proteomics.<sup>25</sup> The affinity reagent was prepared by coupling fragment **21** to a biotin-azide conjugate via Cu(I) catalyzed Azide-Alkyne Huisgen Cycloaddition<sup>26</sup>. This *N*-E-2-heptenyldifluorophenylalanine – biotin conjugate was incubated with cell lysates of *B. subtilis* and *S. coelicolor*, a distinct relative with a ClpP peptidase. Streptavidin beads were then added to the cell lysates in order to sequester the probe and the proteins that were bound to it. The beads were washed several times with buffer to remove non-specific binders, and then proteins specifically bound to the beads were eluted using a buffer containing free fragment **5**. These

eluates were submitted for proteomic analysis and all specifically bound proteins were identified.

Using our affinity reagent, we isolated and positively identified 17 unique proteins from the *B. subtilis* lysate and 11 unique proteins from the *S. coelicolor* lysate (Figure 8.4). Only 2 proteins, ClpP and the essential cell division protein, FtsZ, were common to both lists. The isolation of FtsZ from both lysates was an interesting finding. It is possible that inhibition of FtsZ is an alternate mechanism of action for the ADEP fragments.<sup>27-29</sup> However, recent reports indicate that ADEP activated ClpP degrades FtsZ, which explained the observation that ADEP treated cells are unable to undergo cell division and are observed as extended filaments or bloated cocci depending on the organism.<sup>30</sup> It is interesting to speculate whether that the affinity reagent is capturing ClpP with incompletely degraded substrates in its active site. It is possible that all of the sequestered proteins other than ClpP itself are in fact ClpP substrates.

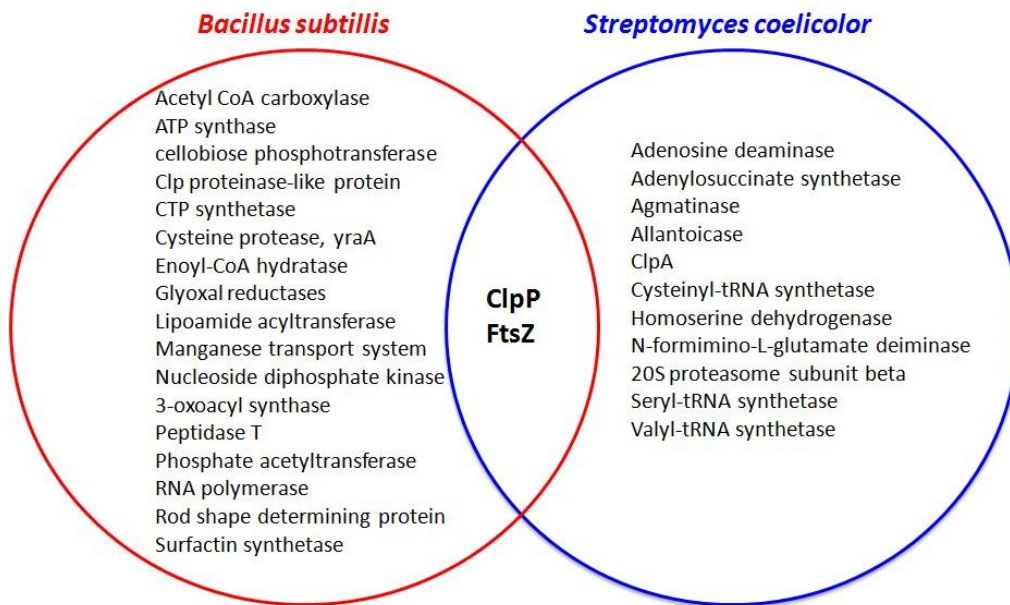


Figure 8.4 – Lists of proteins positively identified as specifically bound to N-E-2-heptenyldifluorophenylalanine affinity matrix: ClpP and FtsZ are the only proteins isolated from *B. subtilis* and *S. coelicolor* cell lysates.

## Conclusions

In summary, we sought to discover an ADEP fragment that was necessary and sufficient for ClpP activation and bacterial killing. To this end we deconstructed the ADEP structure in search of its pharmacophore. Ultimately, we found that the *N*-acyldifluorophenylalanine moiety was the minimal structure required for antibacterial activity. We then undertook a multifaceted approach to confirm that the fragment exhibited the same mechanism of action as the ADEPs. We synthesized a library of fragment analogs in order to study the *N*-acyldifluorophenylalanine structure-activity relationships and found that they were highly consistent with the SAR reported for the ADEPs.<sup>7</sup> Genetic approaches were used to validate that the *N*-acyldifluorophenylalanine fragments target ClpP. We found that both an ADEP (**1**) and fragment **5** were inactive against a *B. subtilis*  $\Delta$ spx-clpP null strain. We also selected a small group of fragments to their ability to activate *B. subtilis* ClpP *in vitro*. Indeed, all compounds bearing the *N*-acyldifluorophenylalanine moiety were able to activate ClpP peptidolysis of a fluorogenic decapeptide in a dose dependant manner. Finally, using a chemical proteomics strategy utilizing an *N*-acyldifluorophenylalanine affinity reagent, we were able to isolate and identify ClpP from *B. subtilis* and *S. coelicolor* cell lysates. As a result of our exhaustive investigation, we can be very confident that the *N*-acyldifluorophenylalanine moiety is necessary and sufficient for antibacterial activity as a result of ClpP activation.

ClpP activation is a very promising strategy for antibacterial drug development. This study should serve as the foundation for the discovery of many more ClpP activators. The *N*-acyldifluorophenylalanine moiety is highly amenable to combinatorial library synthesis as it poses a reactive carboxylate functionality that can be easily coupled to various scaffolds and rapidly diversified. To add to the attractiveness of the *N*-acyldifluorophenylalanine moiety for future development, in general the reported fragments are highly stable and can be stored on

the bench top at room temperature for weeks without any detectable degradation, there being only a couple of exceptions (**7**: light sensitive and **18**: acid sensitive). Although the fragments themselves exhibit only modest antibacterial activity, we expect that development of this pharmacophore in medicinal chemistry programs will yield novel antibacterial drug leads.

### Experimental Contributions

Synthesis of all compounds was completed by Daniel Carney with assistance from Brown University undergraduate student Julia Stevens. MIC assays with *B. Subtilis* were performed by Daniel Carney. ClpP activation assay was performed by Karl Schmitz from the Sauer lab in the MIT department of Biology. Chemical proteomics experiments were performed by Daniel Carney, Brown University graduate student, Corey Compton, and Brown University Proteomics core facility manager, Jim Clifton.

### Experimental Methods

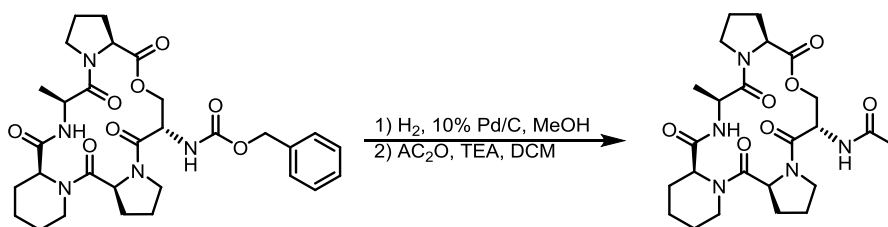
**Minimum inhibitory concentration determinations:** *B. subtilis* MICs were determined using standard agar dilution techniques. Liquid cultures (LB Broth) inoculated from a fresh single colony were grown for 6 hours at 37°C. LB Agar plates supplemented with varying concentrations of test compound were inoculated with 5 uL of the liquid culture and then incubated at 37°C for 48 hours, after which the agar plates were inspected for growth. Because of the relatively high rate of spontaneous resistance observed, the MIC was determined to be lowest concentration of compound able to inhibit *B. subtilis* growth to less than 10 single colonies.

**Chemical proteomics:** Liquid cultures (2 x 15 mL of each organism) of *B. subtilis* and *S. coelicolor* were grown to stationary phase and then lysed by lysozyme treatment. To remove proteins that

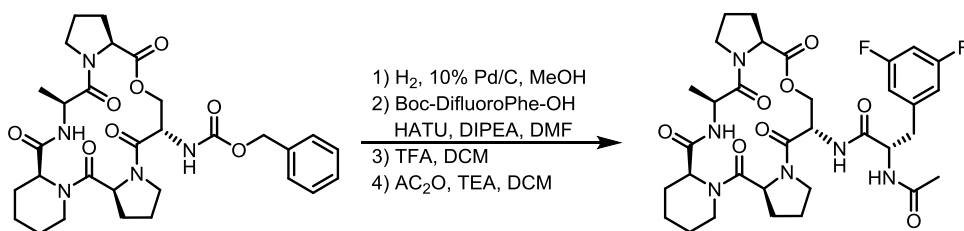
would bind non-specifically to our affinity matrix, the lysed cells were incubated with a commercially available avidin-agarose bead suspension (Sigma-Aldrich) (50  $\mu$ L) then centrifuged (13,000 rpm, 10 min, 4°C). The supernatant was subsequently isolated from the pelleted beads were discarded. The cell lysae was then incubated with the N-E-heptenoyldifluorophenylalanine – biotin conjugate (100  $\mu$ L of 8.2 mM solution in 1:1 ethanol water) and avadin-agarose bead suspension (400  $\mu$ L) for 30 minutes. After incubation, the beads were isolate and eluted twice with PBS buffer and then once with a 0.3 mM solution of fragment **5** in BPS Buffer. Eluates were tryptically digested, and the resulting peptides were loaded onto a reverse phase column and separated by an Agilent 1200 HPLC. The peptides were identified by tandem, high-resolution MS/MS analyses using a coupled LTQ Orbitrap Velos mass spectrometer at the Brown University Center for Genomics and Proteomics. The mass spectral data were searched using the MASCOT software algorithm against the corresponding bacterial protein databases. In the bioinformatic identifications of the peptide fragments, trypsin specificity with two missed cleavage sites was allowed and the MS mass tolerance was 7 ppm while the MS/MS tolerance was 0.5 Da. Identifications were contingent on at least one unique peptide spectrum match (PSM) in the molecular weight search (MOWSE) with a protein score cutoff of 32.8. Positive hits from the PBS buffer eluates were subtracted from the positive hits from the fragment 5 solution eluates in order to generate a list of proteins that were bound specifically to our affinity matrix.

**Synthesis General:** <sup>28,29</sup>

All commercially available reagents were used without further purification. All reactions were conducted in oven dried glassware, under ambient atmosphere, using dry solvents unless otherwise stated. NMR chemical shifts were referenced to residual solvent peaks:  $\text{CDCl}_3$  ( $\delta$  = 7.27 ppm for  $^1\text{H-NMR}$  and 77.00 ppm for  $^{13}\text{C-NMR}$ ), acetone- $d_6$  ( $\delta$  = 2.05 for  $^1\text{H-NMR}$  and  $\delta$  = 29.92 for  $^{13}\text{C-NMR}$ ).



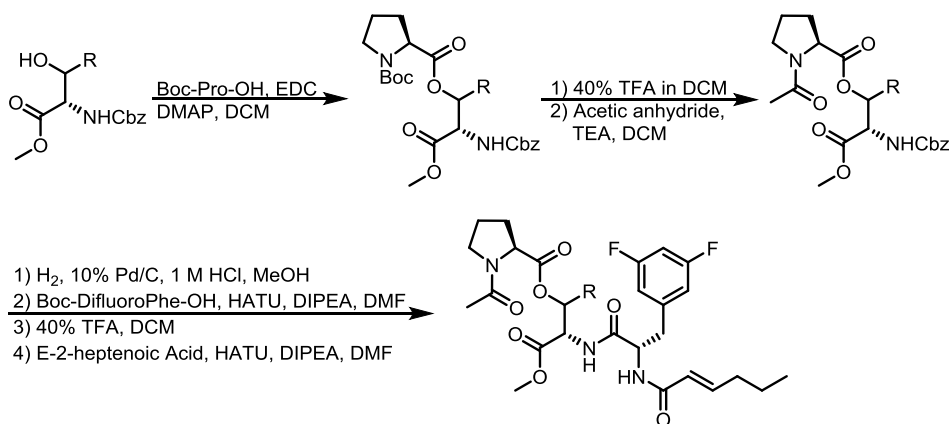
**Synthesis of *N*-acetyl ADEP peptidolactones (2):** Previously reported Cbz ADEP peptidolactone<sup>8</sup> (58 mg, 0.10 mmol) was dissolved in MeOH (1 mL) and treated with 10% Pd/C (13 mg) and 1 M HCl (0.10 mL). The reaction flask was sealed with a septum through which H<sub>2</sub> was delivered from a balloon. Upon complete conversion of the starting material, the reaction was filtered through celite, rinsing with methanol. The crude product was then concentrated and subsequently dissolved in DCM (0.33 mL) and treated with acetic anhydride (20  $\mu$ L, 0.20 mmol) and triethylamine (28  $\mu$ L, .20 mmol). The acetylation reaction was allowed to proceed for 3 hours after which the reaction solution was transferred directly to a silica gel column and chromatographed with 80% acetone in ethyl acetate. The product was isolated as a white solid: 39 mg, 78% yield. HRMS (ESI) predicted for [C<sub>24</sub>H<sub>35</sub>N<sub>5</sub>O<sub>7</sub> + H]<sup>+</sup>: 506.2615, found:506.2607. <sup>1</sup>H NMR (600MHz, CHLOROFORM-d)  $\delta$  = 8.62 (d, *J* = 9.5 Hz, 1 H), 6.44 (d, *J* = 9.5 Hz, 1 H), 5.22 (dd, *J* = 3.1, 9.0 Hz, 1 H), 4.99 (qd, *J* = 6.6, 9.5 Hz, 1 H), 4.80 (dd, *J* = 1.5, 11.7 Hz, 1 H), 4.73 - 4.64 (m, 1 H), 4.62 - 4.55 (m, 1 H), 4.55 - 4.45 (m, 2 H), 3.78 (ddd, *J* = 5.1, 8.2, 11.6 Hz, 1 H), 3.72 - 3.61 (m, 2 H), 3.58 - 3.45 (m, 2 H), 2.73 (d, *J* = 11.7 Hz, 1 H), 2.63 (dt, *J* = 2.6, 13.3 Hz, 1 H), 2.41 - 2.29 (m, 1 H), 2.26 - 2.10 (m, 2 H), 2.04 - 1.99 (m, 1 H), 1.97 (s, 3 H), 1.96 - 1.92 (m, 3 H), 1.78 - 1.71 (m, 2 H), 1.62 (d, *J* = 14.3 Hz, 1 H), 1.53 - 1.42 (m, 2 H), 1.41 (d, *J* = 6.6 Hz, 3 H), 1.38 - 1.29 (m, 1 H). <sup>13</sup>C NMR (151MHz, CHLOROFORM-d)  $\delta$  = 173.5, 171.2, 170.1, 169.8, 168.6, 166.4, 65.5, 58.7, 57.2, 56.5, 51.4, 48.1, 46.9, 46.4, 41.1, 31.0, 30.6, 28.4, 24.8, 23.1, 23.0, 21.3, 21.3, 17.9.



**Synthesis of N-acetyl-3,5-difluorophenylalanyl ADEP peptidolactones (3):** Previously reported Cbz ADEP peptidolactone<sup>8</sup> (58 mg, 0.10 mmol) was dissolved in MeOH (1 mL) and treated with 10% Pd/C (13 mg) and 1 M HCl (0.10 mL). The reaction flask was sealed with a septum through which H<sub>2</sub> was delivered from a balloon. Upon complete conversion of the starting material, the reaction was filtered through celite, rinsing with methanol. The crude product was then concentrated and subsequently dissolved in DMF (0.33 mL) and combined with Boc-3,5-difluorophenylalanine. Once homogeneous, the reaction solution was treated with HATU (38 mg, 0.10 mmol) and DIPEA (35  $\mu$ L, 0.20 mmol) and allowed to react over night. The reaction was then diluted with ethyl acetate (3 mL) and extracted: 3x 1M HCl, 3x sat NaHCO<sub>3</sub>, 1x brine, and then dried over sodium sulfate. After removal of the solvent, the crude Boc-3,5-difluorophenylalanyl ADEP peptidolactone was used without further purification.

The crude Boc-3,5-difluorophenylalanyl ADEP peptidolactone was deprotected by treatment with 40% TFA in DCM (0.5 mL). Upon complete conversion of the starting material, the reaction was concentrated first by blowing with a stream of nitrogen and then by placing the residue under high vacuum. Once dry, the Boc- deprotected 3,5-difluorophenylalanyl ADEP peptidolactone was dissolved in DCM (0.5 mL) and treated with acetic anhydride (16  $\mu$ L, 0.17 mmol) and triethylamine (24  $\mu$ L, 0.17 mmol). The reaction was allowed to proceed for 3 hours, after which the reaction solution was added directly to a silica gel column and chromatographed with 50-100% acetone in ethyl acetate. The final product was isolated as a white solid: 41 mg, 59% over 4 steps. HRMS (ESI) predicted for [C<sub>33</sub>H<sub>42</sub>F<sub>2</sub>N<sub>6</sub>O<sub>8</sub> + H]<sup>+</sup>: 689.3110, found: 689.3097. <sup>1</sup>H

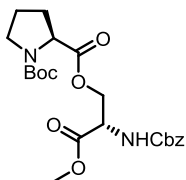
NMR (600MHz ,CHLOROFORM-d)  $\delta$  = 8.54 (d,  $J$  = 9.5 Hz, 1 H), 7.51 (d,  $J$  = 9.5 Hz, 1 H), 6.99 (d,  $J$  = 8.1 Hz, 1 H), 6.76 - 6.68 (m, 2 H), 6.64 (tt,  $J$  = 2.3, 9.0 Hz, 1 H), 5.16 (dd,  $J$  = 2.9, 8.8 Hz, 1 H), 5.01 - 4.91 (m, 1 H), 4.79 (dd,  $J$  = 1.7, 11.6 Hz, 1 H), 4.74 (dt,  $J$  = 5.1, 7.9 Hz, 1 H), 4.71 - 4.66 (m, 2 H), 4.56 - 4.47 (m, 2 H), 3.77 (ddd,  $J$  = 5.5, 8.1, 11.7 Hz, 1 H), 3.71 - 3.59 (m, 2 H), 3.56 (dd,  $J$  = 10.1, 11.6 Hz, 1 H), 3.41 - 3.32 (m, 1 H), 2.95 (dd,  $J$  = 8.4, 13.2 Hz, 1 H), 2.88 (dd,  $J$  = 4.8, 13.6 Hz, 1 H), 2.71 (d,  $J$  = 10.3 Hz, 1 H), 2.65 - 2.57 (m, 1 H), 2.38 (dt,  $J$  = 5.1, 8.8 Hz, 1 H), 2.26 - 2.16 (m, 2 H), 2.15 (s, 3 H), 2.06 - 1.90 (m, 5 H), 1.79 - 1.74 (m, 1 H), 1.65 (d,  $J$  = 12.5 Hz, 1 H), 1.53 - 1.44 (m, 2 H), 1.44 - 1.36 (m, 1 H), 1.33 (d,  $J$  = 6.6 Hz, 3 H).  $^{13}\text{C}$  NMR (151MHz ,CHLOROFORM-d)  $\delta$  = 172.5, 171.1, 170.8, 170.5, 169.8, 169.4, 165.0, 163.6, 162.0, 140.2, 112.6, 112.6, 112.4, 102.4, 102.3, 65.1, 59.0, 57.1, 56.9, 54.2, 51.2, 47.8, 46.8, 46.5, 41.0, 38.5, 30.8, 30.4, 29.2, 27.9, 25.0, 23.1, 22.8, 21.3, 21.2, 17.9.



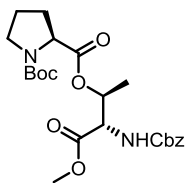
**Synthesis of Boc-Proline Esters General Procedure:** An *N*-Cbz amino acid methyl ester (1 equivalent) and Boc proline (1.1 equivalent) were dissolved in DCM at a concentration of 0.2 M with respect to the *N*-Cbz amino acid. The solution was treated with DMAP (0.1 equivalents) and EDC-HCl (1.5-2.0 equivalents), which was added in portions until the starting material was completely consumed (monitoring with TLC 1:1 EtOAc/Hexanes). After 24 hours the reaction was concentrated *in vacuo* and then diluted with ethyl acetate (50 mL). The ethyl acetate



solution was extracted 3 x 1M HCl<sub>aq</sub>, 3 x saturated NaHCO<sub>3aq</sub>, and 1 x Brine then dried over sodium sulfate. The proline ester products were isolated by silica gel chromatography using a 30-50% ethyl acetate in hexanes solvent gradient.

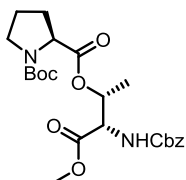


**N-Cbz-O-Boc-prolyl-serine methyl ester:** Product isolated as a white solid 97% yield. HRMS (FAB) Predicted for [C<sub>22</sub>H<sub>30</sub>N<sub>2</sub>O<sub>8</sub> + Na]<sup>+</sup>: 473.18999, Found: 473.1885. 1:1 Mixture of amide rotamers <sup>1</sup>H NMR (600MHz, CHLOROFORM-d) δ = 7.42 - 7.27 (m, 10 H), 5.97 (d, J = 8.4 Hz, 1 H), 5.54 (d, J = 8.1 Hz, 1 H), 5.20 - 5.02 (m, 4 H), 4.69 - 4.56 (m, 3 H), 4.52 - 4.38 (m, 3 H), 4.28 (dd, J = 4.0, 8.4 Hz, 1 H), 4.20 (dd, J = 3.9, 8.6 Hz, 1 H), 3.76 (s, 6 H), 3.52 (ddd, J = 5.1, 7.4, 10.5 Hz, 1 H), 3.47 - 3.40 (m, 2 H), 3.40 - 3.34 (m, 1 H), 2.25 - 2.11 (m, 2 H), 1.98 - 1.81 (m, 6 H), 1.43 (s, 9 H), 1.38 (s, 9 H). <sup>13</sup>C NMR (151MHz, CHLOROFORM-d) δ = 172.7, 172.3, 169.9, 169.6, 156.0, 155.6, 154.6, 153.5, 136.2, 135.9, 128.5, 128.4, 128.2, 128.1, 128.0, 80.1, 80.0, 67.2, 67.0, 64.3, 64.2, 58.9, 58.8, 53.3, 52.8, 52.7, 46.5, 46.2, 30.8, 29.9, 28.3, 28.2, 24.3, 23.4.



**N-Cbz-O-Boc-prolyl-allo-threonine methyl ester:** Product isolated as a colorless oil 79% yield. HRMS (ESI) Predicted for C<sub>22</sub>H<sub>30</sub>N<sub>2</sub>O<sub>8</sub> + H]<sup>+</sup>: 465.2236, Found: 465.2237. 1:1 Mixture of amide rotamers. <sup>1</sup>H NMR (600MHz, CHLOROFORM-d) δ = 7.39 - 7.30 (m, 10 H), 5.97 (d, J = 9.2 Hz, 1 H), 5.55 (d, J = 8.8 Hz, 1 H), 5.31 - 5.21 (m, 2 H), 5.16 - 5.07 (m, 4 H), 4.64 (dd, J = 3.5, 8.6 Hz, 1 H), 4.61 (dd, J = 2.9, 9.2 Hz, 1 H), 4.25 (dd, J = 4.2, 8.6 Hz, 1 H), 4.15 (dd, J = 3.9, 8.6 Hz, 1 H), 3.78 (s,

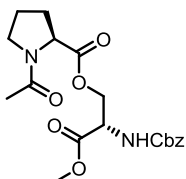
3 H), 3.76 (s, 3 H), 3.58 - 3.50 (m, 1 H), 3.50 - 3.35 (m, 3 H), 2.19 - 2.08 (m, 2 H), 2.03 - 1.87 (m, 4 H), 1.87 - 1.79 (m, 2 H), 1.45 (s, 9 H), 1.40 (s, 9 H), 1.33 (d,  $J = 6.6$  Hz, 3 H), 1.31 (d,  $J = 6.6$  Hz, 3 H).  $^{13}\text{C}$  NMR (151MHz, CHLOROFORM-d)  $\delta = 172.4, 172.0, 169.5, 155.9, 155.7, 154.7, 153.7, 136.2, 136.0, 128.9, 128.5, 128.4, 128.2, 128.1, 128.0, 128.0, 127.7, 80.0, 79.8, 71.3, 70.8, 67.2, 66.9, 59.0, 58.8, 57.2, 57.1, 52.7, 52.3, 46.6, 46.3, 30.6, 29.8, 28.4, 28.3, 24.3, 23.5, 16.3, 16.1.$



**N-Cbz-O-Boc-prolyl-threonine methyl ester:** Product Isolated as a colorless oil, 96% yield. HRMS (ESI) Predicted for  $\text{C}_{22}\text{H}_{30}\text{N}_2\text{O}_8 + \text{H}]^+$ : 465.2236, Found: 465.2239. 1:1 Mixture of amide rotamers.  $^1\text{H}$  NMR (600MHz, CHLOROFORM-d)  $\delta = 7.39 - 7.31$  (m, 10 H), 5.85 (d,  $J = 9.5$  Hz, 1 H), 5.44 - 5.29 (m, 3 H), 5.17 - 5.11 (m, 4 H), 4.52 (dd,  $J = 2.6, 9.5$  Hz, 1 H), 4.48 (dd,  $J = 2.6, 9.5$  Hz, 1 H), 4.24 - 4.17 (m, 2 H), 3.73 (s, 3 H), 3.72 (s, 3 H), 3.53 - 3.47 (m, 1 H), 3.47 - 3.40 (m, 2 H), 3.39 - 3.31 (m, 1 H), 2.25 - 2.15 (m, 1 H), 2.15 - 2.06 (m, 1 H), 1.95 - 1.79 (m, 6 H), 1.49 - 1.35 (m, 18 H), 1.34 - 1.30 (m, 6 H).  $^{13}\text{C}$  NMR (151MHz, CHLOROFORM-d)  $\delta = 172.0, 171.7, 170.3, 170.1, 156.7, 156.4, 154.2, 153.6, 136.1, 135.9, 128.5, 128.4, 128.4, 128.2, 128.1, 128.1, 128.0, 80.0, 79.9, 71.1, 70.9, 67.3, 67.1, 67.0, 66.5, 59.2, 59.1, 59.0, 58.8, 57.6, 57.4, 52.6, 52.4, 46.4, 46.3, 46.2, 30.9, 30.8, 29.6, 28.4, 28.2, 28.2, 24.4, 23.5, 23.3, 19.9, 17.1, 16.8.$

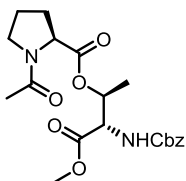
**Proline Deprotection and Acetylation General Procedure:** Boc-Proline esters (1 equivalent) were deprotected by treatment with 40% TFA in DCM. Upon complete conversion of the starting material, the reaction was concentrated first by blowing with a stream of nitrogen and then by placing the residue under high vacuum. Once dry, the residue was dissolved in DCM to a

concentration of 0.2 M and treated with triethylamine (2 equivalents) and acetic anhydride (2 equivalents). The reactions were allowed to proceed for 16 hours after which the solvent was removed in vacuo. The N-acetyl Proline esters were isolated by silica gel chromatography 100% ethyl acetate.



**(S)-2-(((benzyloxy)carbonyl)amino)-3-methoxy-3-oxopropyl acetyl-L-prolinate:** Product

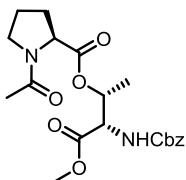
Isolated as a colorless oil 85%. HRMS (FAB) Predicted for:  $[C_{19}H_{24}N_2O_7 + Na]^+$ : 415.1481, Found 415.1472.  $^1H$  NMR (400MHz, CHLOROFORM-d)  $\delta$  = 7.42 - 7.28 (m, 5 H), 6.10 (d,  $J$  = 8.5 Hz, 1 H), 5.14 (d,  $J$  = 2.8 Hz, 2 H), 4.68 (dd,  $J$  = 3.3, 11.3 Hz, 1 H), 4.61 (td,  $J$  = 3.3, 8.7 Hz, 1 H), 4.45 - 4.39 (m, 1 H), 4.35 (dd,  $J$  = 3.6, 11.2 Hz, 1 H), 3.77 (s, 3 H), 3.62 - 3.52 (m, 1 H), 3.52 - 3.43 (m, 1 H), 2.28 - 2.11 (m, 1 H), 2.07 (s, 3 H), 2.02 - 1.91 (m, 3 H).  $^{13}C$  NMR (101MHz, CHLOROFORM-d)  $\delta$  = 171.5, 170.1, 169.9, 156.1, 136.3, 128.5, 128.4, 128.2, 127.9, 127.9, 66.9, 64.2, 58.7, 53.4, 52.7, 47.7, 29.2, 24.8, 22.1.



**(2S,3S)-3-(((benzyloxy)carbonyl)amino)-4-methoxy-4-oxobutan-2-yl acetyl-L-prolinate:** Product

Isolated as a white foam, 52 % yield. HRMS (ESI) Predicted for  $[C_{20}H_{26}N_2O_7 + H]^+$ : 407.1818, Found: 407.1816.  $^1H$  NMR (400MHz, CHLOROFORM-d)  $\delta$  = 7.38 - 7.27 (m, 5 H), 6.11 (d,  $J$  = 9.3 Hz, 1 H), 5.21 (dq,  $J$  = 3.1, 6.7 Hz, 1 H), 5.11 (s, 2 H), 4.55 (dd,  $J$  = 3.1, 9.2 Hz, 1 H), 4.37 (dd,  $J$  = 4.0, 8.3 Hz, 1 H), 3.75 (s, 3 H), 3.60 - 3.52 (m, 1 H), 3.52 - 3.45 (m, 1 H), 2.20 - 2.13 (m, 1 H), 2.10

(s, 3 H), 2.02 - 1.91 (m, 3 H), 1.32 (d,  $J = 6.8$  Hz, 3 H).  $^{13}\text{C}$  NMR (151MHz, CHLOROFORM-d)  $\delta =$  171.3, 170.3, 169.6, 156.1, 136.5, 129.0, 128.5, 128.4, 128.1, 127.9, 127.8, 127.6, 71.3, 66.8, 58.9, 57.2, 52.3, 47.8, 29.2, 24.8, 22.2, 16.4.



**(2R,3S)-3-(((benzyloxy)carbonyl)amino)-4-methoxy-4-oxobutan-2-yl acetyl-L-prolinate:**

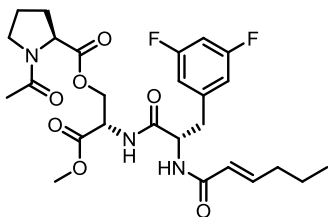
Product isolated as a white foam, 91 % yield. Predicted for  $[\text{C}_{20}\text{H}_{26}\text{N}_2\text{O}_7 + \text{H}]^+$ : 407.1818, Found: 407.1806. ~2:1 mixture of amide rotamers.  $^1\text{H}$  NMR (600MHz, CHLOROFORM-d)  $\delta =$  7.42 - 7.28 (m, 5 H), 5.69 (d,  $J = 9.2$  Hz, 1 H), 5.50 - 5.36 (m, 1 H), 5.18 - 5.09 (m, 2 H), 4.57 - 4.46 (m, 1 H), 4.36 (dd,  $J = 4.2, 8.6$  Hz, 1 H), 3.77 (s, 2 H), 3.71 (s, 1 H), 3.59 (qd,  $J = 4.9, 7.7$  Hz, 1 H), 3.53 - 3.41 (m, 1 H), 2.21 - 2.10 (m, 1 H), 2.05 (s, 3 H), 2.01 - 1.83 (m, 3 H), 1.34 - 1.23 (m, 3 H).  $^{13}\text{C}$  NMR (151MHz, CHLOROFORM-d)  $\delta =$  171.1, 171.0, 170.0, 169.3, 169.2, 156.5, 156.3, 136.1, 135.8, 128.5, 128.4, 128.3, 128.2, 128.1, 128.0, 127.9, 71.4, 71.1, 67.4, 67.1, 66.6, 59.9, 58.5, 58.3, 57.5, 57.2, 52.8, 52.7, 47.6, 46.2, 31.4, 29.3, 29.1, 24.7, 22.6, 22.1, 22.0, 16.8, 16.7.

**Side Chain Synthesis General Procedure: Cbz removal:** The CBZ protected proline ester was dissolved in methanol at a concentration of 0.14 M. Once the solution was homogeneous, 10% Pd/C (130 mg / mmol peptidolactone) was added followed by 1M HCl (1 equivalent with respect to proline ester). With the reaction flask septum sealed, hydrogen gas was delivered to the reaction by a balloon affixed to a syringe. The reaction was allowed to proceed for 90 minutes after which it was filtered through celite in order to remove the Pd/C. Removal of solvent revealed the proline hydrochloride salt as an off white foam, which is used without further purification.

*Boc-DifluoroPhe acylation:* The proline ester hydrochloride salt was dissolved in DMF at a concentration of 0.25 M. Once the solution was homogeneous, Boc-difluorophenylalanine (1.1 equivalents) was added followed by HATU (1.1 equivalents). The reaction was initiated by the addition of DIPEA (2.2 equivalents) and allowed to proceed for 2 hours. After the reaction, the DMF solution was diluted ~10 x the reaction volume with ethyl acetate, and extracted 3x 1M HCl, 3x saturated NaHCO<sub>3</sub>, 1x brine, then dried over sodium sulfate. The Boc-difluorophenylalanine acylated proline esters were isolated by silica gel chromatography using an ethyl acetate / acetone solvent gradient. Final removal of the solvent revealed a fine white powder, which was used without further purification.

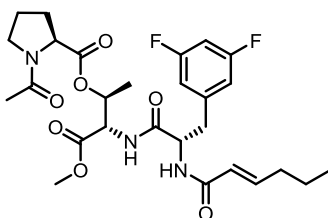
*Boc group removal:* The Boc-difluorophenylalanyl proline esters were treated with 40% TFA in DCM at a concentration of 0.3 M. Upon complete conversion of the starting material, the reaction was concentrated by blowing with a stream of nitrogen then by evaporation under high vacuum. The deprotected product was used without further purification.

*E-2-Heptenoate Coupling:* The difluorophenylalanyl proline ester TFA salts were dissolved in DMF at a concentration of 0.2 M. Once the solution was homogeneous, E-2-heptenoic acid (1.1 equivalents) was dissolved in DMF at a concentration of 0.2 M. The acid was then treated with HATU (1.1 equivalents) and DIPEA (1.1 equivalents) and allowed to stir for 15 minutes. The preactivated acid was then added to a solution of the difluorophenylalanyl proline ester TFA salts followed by additional DIPEA (1.1 equivalents). The reaction was allowed to proceed for 2 hours, after which it was diluted ~10x with ethyl acetate and extracted 3x 1M HCl, 3x saturated NaHCO<sub>3</sub>, 1x brine, then dried over sodium sulfate. The final products were purified by silica gel chromatography using an ethyl acetate / acetone solvent gradient. Final removal of the solvent revealed the products as white foams.



**(S)-2-((S)-3-(3,5-difluorophenyl)-2-((E)-hex-2-enamido)propanamido)-3-methoxy-3-oxopropyl**

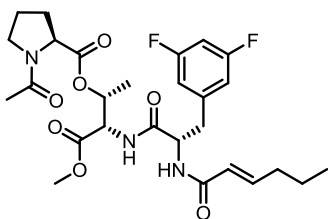
**acetyl-L-prolinate (4):** 0.46 mmol scale, yield: 185 mg, 72% over 4 steps. HRMS (FAB) Predicted for  $[C_{27}H_{35}F_2N_3O_7 + Na]^+$ : 574.2341, Found: 574.2358.  $^1H$  NMR (600MHz, CHLOROFORM-d)  $\delta$  = 7.29 (d,  $J$  = 8.8 Hz, 1 H), 7.24 (d,  $J$  = 7.7 Hz, 1 H), 6.83 (td,  $J$  = 7.0, 15.4 Hz, 1 H), 6.79 (dd,  $J$  = 2.2, 8.1 Hz, 2 H), 6.62 (tt,  $J$  = 2.3, 9.0 Hz, 1 H), 5.87 (td,  $J$  = 1.5, 15.3 Hz, 1 H), 5.03 - 4.92 (m, 1 H), 4.89 - 4.78 (m, 2 H), 4.32 (dd,  $J$  = 5.0, 8.6 Hz, 1 H), 4.27 - 4.21 (m, 1 H), 3.77 (s, 3 H), 3.60 - 3.51 (m, 2 H), 3.26 (dd,  $J$  = 5.3, 14.1 Hz, 1 H), 3.06 (dd,  $J$  = 8.1, 13.9 Hz, 1 H), 2.31 - 2.21 (m, 1 H), 2.20 - 2.13 (m, 2 H), 2.13 (s, 3 H), 2.07 - 1.95 (m, 3 H), 1.46 - 1.38 (m, 2 H), 1.36 - 1.29 (m, 2 H), 0.90 (t,  $J$  = 7.3 Hz, 3 H).  $^{13}C$  NMR (151MHz, CHLOROFORM-d)  $\delta$  = 171.2, 170.6, 170.4, 169.4, 165.9, 163.6, 163.5, 161.9, 161.9, 145.4, 141.3, 141.3, 141.2, 123.2, 112.5, 112.5, 112.4, 112.4, 102.1, 101.9, 101.7, 63.0, 59.2, 53.6, 52.7, 51.7, 48.0, 37.6, 31.8, 30.2, 29.2, 25.0, 22.3, 22.2, 13.8.



**(2S,3S)-3-((S)-3-(3,5-difluorophenyl)-2-((E)-hex-2-enamido)propanamido)-4-methoxy-4-**

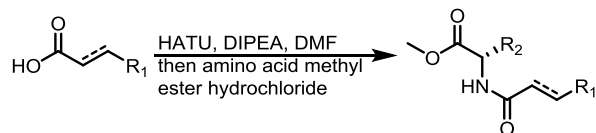
**oxobutan-2-yl acetyl-L-prolinate (6):** 0.52 mmol scale, yield: 212 mg, 72% over 4 steps. HRMS (ESI) Predicted for  $[C_{28}H_{37}F_2N_3O_7 + H]^+$ : 566.2679, Found: 566.2659.  $^1H$  NMR (600MHz, CHLOROFORM-d)  $\delta$  = 7.39 - 7.29 (m, 2 H), 6.82 (td,  $J$  = 7.0, 15.4 Hz, 1 H), 6.79 - 6.74 (m, 2 H), 6.63 (tt,  $J$  = 2.3, 9.0 Hz, 1 H), 5.90 (td,  $J$  = 1.7, 15.4 Hz, 1 H), 5.33 (dq,  $J$  = 2.9, 6.7 Hz, 1 H), 4.92 (dt,

$J = 5.1, 8.8 \text{ Hz}, 1 \text{ H}$ ),  $4.66 \text{ (dd, } J = 2.9, 8.4 \text{ Hz}, 1 \text{ H)}$ ,  $4.40 \text{ (dd, } J = 4.4, 8.8 \text{ Hz}, 1 \text{ H)}$ ,  $3.76 \text{ (s, } 3 \text{ H)}$ ,  $3.61 - 3.51 \text{ (m, } 2 \text{ H)}$ ,  $3.24 \text{ (dd, } J = 5.1, 14.3 \text{ Hz}, 1 \text{ H)}$ ,  $3.00 \text{ (dd, } J = 8.6, 14.1 \text{ Hz}, 1 \text{ H)}$ ,  $2.33 - 2.23 \text{ (m, } 1 \text{ H)}$ ,  $2.19 \text{ (s, } 3 \text{ H)}$ ,  $2.17 - 2.13 \text{ (m, } 2 \text{ H)}$ ,  $2.07 - 1.93 \text{ (m, } 3 \text{ H)}$ ,  $1.46 - 1.37 \text{ (m, } 2 \text{ H)}$ ,  $1.36 - 1.26 \text{ (m, } 5 \text{ H)}$ ,  $0.89 \text{ (t, } J = 7.2 \text{ Hz}, 3 \text{ H})$ .  $^{13}\text{C NMR (151MHz, CHLOROFORM-d)}$   $\delta = 171.1, 170.7, 170.3, 168.7, 165.8, 163.6, 163.6, 162.0, 161.9, 145.4, 141.3, 141.2, 141.1, 123.2, 112.3, 112.3, 112.2, 112.2, 102.2, 102.0, 101.9, 70.4, 59.5, 55.3, 53.9, 52.2, 48.0, 38.0, 31.7, 30.2, 29.4, 24.9, 22.4, 22.2, 16.9, 13.8$ .

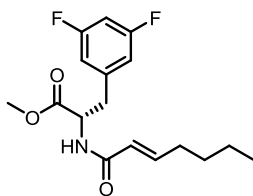


**(2R,3S)-3-((S)-3-(3,5-difluorophenyl)-2-((E)-hex-2-enamido)propanamido)-4-methoxy-4-**

**oxobutan-2-yl acetyl-L-prolinate (7):** 0.50 mmol scale, Yield: 222 mg 79% over 4 steps. HRMS (ESI) Predicted for  $[\text{C}_{28}\text{H}_{37}\text{F}_2\text{N}_3\text{O}_7 + \text{H}]^+$ : 566.2679, Found: 566.2667.  $^1\text{H NMR (400MHz, CHLOROFORM-d)}$   $\delta = 7.28 \text{ (d, } J = 8.8 \text{ Hz}, 1 \text{ H)}$ ,  $7.13 \text{ (d, } J = 8.8 \text{ Hz}, 1 \text{ H)}$ ,  $6.87 - 6.75 \text{ (m, } 3 \text{ H)}$ ,  $6.60 \text{ (tt, } J = 2.3, 9.0 \text{ Hz}, 1 \text{ H)}$ ,  $5.84 \text{ (td, } J = 1.5, 15.3 \text{ Hz}, 1 \text{ H)}$ ,  $5.18 \text{ (quin, } J = 6.5 \text{ Hz}, 1 \text{ H)}$ ,  $5.01 \text{ (ddd, } J = 5.4, 7.2, 8.8 \text{ Hz}, 1 \text{ H)}$ ,  $4.67 \text{ (dd, } J = 6.5, 8.5 \text{ Hz}, 1 \text{ H)}$ ,  $4.12 \text{ (dd, } J = 5.0, 8.0 \text{ Hz}, 1 \text{ H)}$ ,  $3.74 \text{ (s, } 3 \text{ H)}$ ,  $3.68 - 3.59 \text{ (m, } 1 \text{ H)}$ ,  $3.57 - 3.47 \text{ (m, } 1 \text{ H)}$ ,  $3.23 \text{ (dd, } J = 5.4, 13.9 \text{ Hz}, 1 \text{ H)}$ ,  $3.13 \text{ (dd, } J = 7.2, 13.9 \text{ Hz}, 1 \text{ H)}$ ,  $2.26 - 2.11 \text{ (m, } 4 \text{ H)}$ ,  $2.10 \text{ (s, } 3 \text{ H)}$ ,  $2.03 - 1.91 \text{ (m, } 2 \text{ H)}$ ,  $1.45 - 1.37 \text{ (m, } 2 \text{ H)}$ ,  $1.36 - 1.27 \text{ (m, } 5 \text{ H)}$ ,  $0.92 - 0.87 \text{ (m, } 3 \text{ H})$ .  $^{13}\text{C NMR (151MHz, CHLOROFORM-d)}$   $\delta = 171.7, 171.1, 169.7, 169.4, 166.3, 163.5, 163.4, 161.9, 161.8, 145.6, 141.3, 141.2, 123.0, 112.8, 112.8, 112.6, 102.0, 101.8, 101.6, 70.2, 58.6, 56.2, 53.4, 52.7, 48.0, 37.1, 31.8, 30.2, 29.1, 25.0, 22.2, 18.0, 13.8$ .

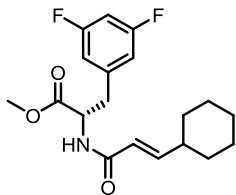


**Synthesis of ADEP side chain methyl esters general procedure:** The carboxylic acid (1 equivalent) was dissolved in DMF at a concentration of 0.2 M. The acid was then treated with HATU (1.1 equivalents) and DIPEA (2.2 equivalents) and allowed to stir for 15 minutes after which, an amino acid methyl ester hydrochloride was added. The coupling reaction was allowed to proceed for 3 hours, after which the reaction solution was diluted to 5x original volume with ethyl acetate and extracted 3x 1M HCl, 3x sat NaHCO<sub>3</sub>, 1x Brine. The organic layer was then dried over sodium sulfate and purified by silica gel flash chromatography using a hexanes/ethyl acetate solvent gradient.

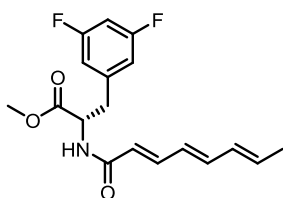


**Methyl (S,E)-3-(3,5-difluorophenyl)-2-(hept-2-enamido)propanoate (5).** Compound isolated as white solid: 80% yield. HRMS (ESI) predicted for [C<sub>17</sub>H<sub>21</sub>F<sub>2</sub>NO<sub>3</sub> + H]<sup>+</sup>: 326.1568, found:326.1559. <sup>1</sup>H NMR (400MHz, CHLOROFORM-d) δ = 6.87 (td, J = 7.0, 15.3 Hz, 1 H), 6.73 - 6.66 (m, 1 H), 6.66 - 6.60 (m, 2 H), 6.02 (d, J = 6.8 Hz, 1 H), 5.80 (td, J = 1.5, 15.3 Hz, 1 H), 4.95 (td, J = 5.7, 7.4 Hz, 1 H), 3.79 - 3.73 (m, 3 H), 3.19 (dd, J = 5.8, 13.8 Hz, 1 H), 3.11 (dd, J = 5.3, 13.8 Hz, 1 H), 2.19 (dq, J = 1.4, 7.2 Hz, 2 H), 1.49 - 1.39 (m, 2 H), 1.38 - 1.29 (m, 2 H), 0.91 (t, J = 7.3 Hz, 3 H). <sup>13</sup>C NMR (75MHz, CHLOROFORM-d) δ = 171.6, 165.5, 164.6, 164.5, 161.3, 161.2, 146.4, 140.0, 139.9, 139.7, 122.6, 112.4, 112.3, 112.1, 112.0, 103.0, 102.6, 102.3, 52.8, 52.5, 37.6, 31.7, 30.2, 22.2, 13.8.

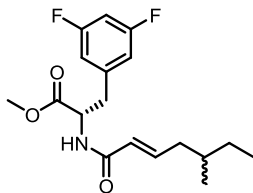




**Methyl (S,E)-2-(3-cyclohexylacrylamido)-3-(3,5-difluorophenyl)propanoate (8).** Compound isolated as white solid: 83% yield. HRMS (ESI) predicted for  $[C_{19}H_{23}F_2NO_3 + H]^+$ : 352.1724, found:352.1716.  $^1H$  NMR (400MHz, CHLOROFORM-d)  $\delta$  = 6.83 (dd,  $J$  = 6.8, 15.3 Hz, 1 H), 6.70 (tt,  $J$  = 2.1, 9.0 Hz, 1 H), 6.67 - 6.60 (m, 2 H), 6.00 (d,  $J$  = 7.0 Hz, 1 H), 5.74 (dd,  $J$  = 1.3, 15.3 Hz, 1 H), 5.00 - 4.91 (m, 1 H), 3.76 (s, 3 H), 3.19 (dd,  $J$  = 5.8, 13.8 Hz, 1 H), 3.12 (dd,  $J$  = 5.3, 13.8 Hz, 1 H), 2.20 - 2.06 (m, 1 H), 1.80-1.72 (m, 4 H), 1.68 (d,  $J$  = 12.5 Hz, 1 H), 1.37 - 1.24 (m, 2 H), 1.24 - 1.07 (m, 3 H).  $^{13}C$  NMR (101MHz, CHLOROFORM-d)  $\delta$  = 171.6, 165.8, 164.2, 164.1, 161.7, 161.6, 151.4, 139.9, 139.9, 120.2, 112.3, 112.3, 112.2, 112.1, 102.9, 102.7, 102.4, 52.9, 52.5, 40.3, 37.6, 31.8, 25.9, 25.7

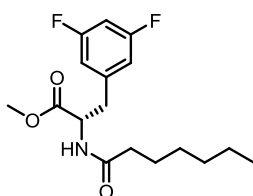


**Methyl (S)-3-(3,5-difluorophenyl)-2-((2E,4E,6E)-octa-2,4,6-trienamido)propanoate (9).** Compound isolated as white solid: 77% yield. HRMS (ESI) predicted for  $[C_{18}H_{19}F_2NO_3 + H]^+$ : 336.1411, found:336.1405.  $^1H$  NMR (400MHz, CHLOROFORM-d)  $\delta$  = 7.33 - 7.22 (m, 1 H), 6.71 (t,  $J$  = 9.0 Hz, 1 H), 6.68 - 6.62 (m, 2 H), 6.53 (dd,  $J$  = 10.8, 14.8 Hz, 1 H), 6.24 - 6.11 (m, 2 H), 6.09 (d,  $J$  = 7.5 Hz, 1 H), 6.02 - 5.89 (m, 1 H), 5.86 (d,  $J$  = 15.1 Hz, 1 H), 5.07 - 4.90 (m, 1 H), 3.77 (s, 3 H), 3.21 (dd,  $J$  = 5.8, 13.8 Hz, 1 H), 3.13 (dd,  $J$  = 5.3, 13.8 Hz, 1 H), 1.84 (d,  $J$  = 6.5 Hz, 3 H).  $^{13}C$  NMR (101MHz, CHLOROFORM-d)  $\delta$  = 171.6, 165.7, 164.2, 164.1, 161.7, 161.6, 142.4, 140.7, 139.8, 134.7, 131.2, 127.3, 121.4, 112.3, 112.3, 112.1, 112.1, 102.9, 102.7, 102.4, 52.9, 52.5, 37.6, 18.5.



**Methyl (2S)-3-(3,5-difluorophenyl)-2-((E)-5-methylhept-2-enamido)propanoate (10).**

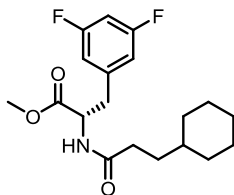
Compound isolated as white solid: 78% yield. HRMS (ESI) predicted for  $[C_{18}H_{23}F_2NO_3 + H]^+$ : 340.1724, found:340.1715.  $^1H$  NMR (400MHz, CHLOROFORM-d)  $\delta$  = 6.87 (td,  $J$  = 7.5, 15.1 Hz, 1 H), 6.70 (tt,  $J$  = 2.3, 9.0 Hz, 1 H), 6.67 - 6.59 (m, 2 H), 5.99 (d,  $J$  = 7.0 Hz, 1 H), 5.80 (d,  $J$  = 15.6 Hz, 1 H), 5.00 - 4.89 (m, 1 H), 3.76 (s, 3 H), 3.21 (dd,  $J$  = 5.8, 13.8 Hz, 1 H), 3.12 (dd,  $J$  = 5.3, 13.8 Hz, 1 H), 2.25 - 2.15 (m, 1 H), 2.08 - 1.98 (m, 1 H), 1.59-1.49 (m, 1 H), 1.44 - 1.32 (m, 1 H), 1.23 - 1.13 (m, 1 H), 0.92 - 0.86 (m, 6 H).  $^{13}C$  NMR (101MHz, CHLOROFORM-d)  $\delta$  = 171.6, 165.4, 164.2, 164.1, 161.7, 161.6, 145.4, 139.9, 139.8, 123.7, 112.3, 112.3, 112.2, 112.1, 102.9, 102.7, 102.4, 52.8, 52.6, 39.2, 37.6, 34.2, 29.2, 29.1, 19.1, 11.3.



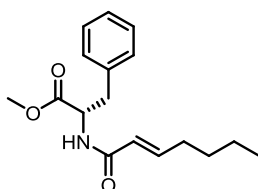
**Methyl (S,E)-3-(3,5-difluorophenyl)-2-(hept-2-enamido)propanoate (11).**

Compound isolated as white solid: 80% yield. HRMS (ESI) predicted for  $[C_{17}H_{21}F_2NO_3 + H]^+$ : 326.1568, found:326.1559.  $^1H$  NMR (400MHz, CHLOROFORM-d)  $\delta$  = 6.87 (td,  $J$  = 7.0, 15.3 Hz, 1 H), 6.73 - 6.66 (m, 1 H), 6.66 - 6.60 (m, 2 H), 6.02 (d,  $J$  = 6.8 Hz, 1 H), 5.80 (td,  $J$  = 1.5, 15.3 Hz, 1 H), 4.95 (td,  $J$  = 5.7, 7.4 Hz, 1 H), 3.79 - 3.73 (m, 3 H), 3.19 (dd,  $J$  = 5.8, 13.8 Hz, 1 H), 3.11 (dd,  $J$  = 5.3, 13.8 Hz, 1 H), 2.19 (dq,  $J$  = 1.4, 7.2 Hz, 2 H), 1.49 - 1.39 (m, 2 H), 1.38 - 1.29 (m, 2 H), 0.91 (t,  $J$  = 7.3 Hz, 3 H).  $^{13}C$  NMR (75MHz, CHLOROFORM-d)  $\delta$  = 171.6, 165.5, 164.6, 164.5, 161.3, 161.2, 146.4, 140.0, 139.9,

139.7, 122.6, 112.4, 112.3, 112.1, 112.0, 103.0, 102.6, 102.3, 52.8, 52.5, 37.6, 31.7, 30.2, 22.2, 13.8.

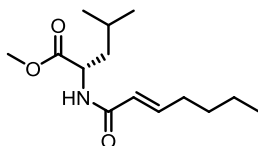


**Methyl (S)-2-(3-cyclohexylpropanamido)-3-(3,5-difluorophenyl)propanoate (12).** Compound isolated as white solid: 84% yield. HRMS (ESI) predicted for  $[C_{19}H_{25}F_2NO_3 + H]^+$ : 354.1881, found:354.1873.  $^1H$  NMR (400MHz, CHLOROFORM-d)  $\delta$  = 6.74 - 6.68 (m, 1 H), 6.66 - 6.60 (m, 2 H), 5.95 (d,  $J$  = 6.8 Hz, 1 H), 4.92 - 4.86 (m, 1 H), 3.77 (s, 3 H), 3.17 (dd,  $J$  = 5.8, 13.9 Hz, 1 H), 3.07 (dd,  $J$  = 5.4, 13.8 Hz, 1 H), 2.26 - 2.19 (m, 2 H), 1.68 (s, 3 H), 1.71 (s, 2 H), 1.55 - 1.47 (m, 2 H), 1.28 - 1.11 (m, 4 H), 0.89 (q,  $J$  = 11.4 Hz, 2 H).  $^{13}C$  NMR (101MHz, CHLOROFORM-d)  $\delta$  = 173.0, 171.7, 164.2, 161.7, 139.9, 139.8, 112.3, 112.2, 112.1, 112.1, 102.9, 102.7, 102.4, 52.6, 52.6, 37.6, 37.2, 34.0, 33.0, 32.9, 26.5, 26.1.

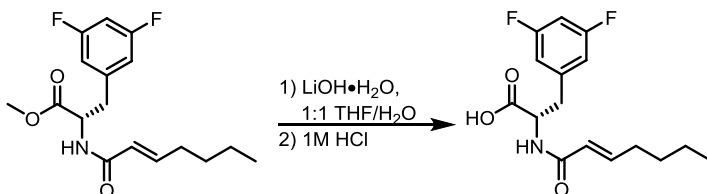


**Methyl (E)-hept-2-enoyl-L-phenylalaninate (13).** Compound isolated as a white solid: 97% yield. HRMS (ESI) predicted for  $[C_{17}H_{23}NO_3 + H]^+$ : 290.1756, found:290.1750.  $^1H$  NMR (400MHz, CHLOROFORM-d)  $\delta$  = 7.37 - 7.19 (m, 3 H), 7.14 - 7.05 (m, 2 H), 6.86 (td,  $J$  = 7.0, 15.1 Hz, 1 H), 5.96 (d,  $J$  = 7.5 Hz, 1 H), 5.77 (td,  $J$  = 1.5, 15.1 Hz, 1 H), 4.97 (td,  $J$  = 5.6, 7.8 Hz, 1 H), 3.73 (s, 3 H), 3.24 - 3.09 (m, 2 H), 2.25 - 2.10 (m, 2 H), 1.48 - 1.38 (m, 2 H), 1.38 - 1.28 (m, 2 H), 0.90 (t,  $J$  = 7.0

Hz, 3 H).  $^{13}\text{C}$  NMR (101MHz, CHLOROFORM-d)  $\delta$  = 172.1, 165.4, 145.9, 135.8, 129.2, 128.5, 127.0, 122.8, 53.0, 52.3, 37.8, 31.7, 30.2, 22.2, 13.8.

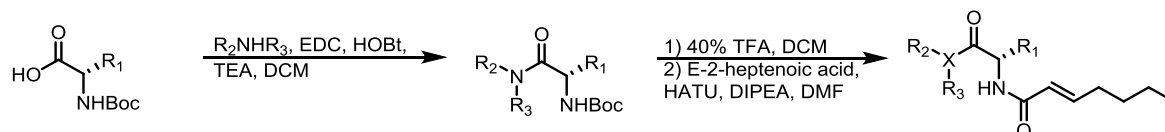


**methyl (E)-hept-2-enoyl-L-leucinate (14).** Compound isolated as a colorless oil: 95% yield. HRMS (ESI) predicted for  $[\text{C}_{14}\text{H}_{25}\text{NO}_3 + \text{H}]^+$ : 256.1913, found:256.1904.  $^1\text{H}$  NMR (600MHz, CHLOROFORM-d)  $\delta$  = 6.87 (td,  $J$  = 7.0, 15.4 Hz, 1 H), 5.91 - 5.83 (m, 1 H), 5.81 (td,  $J$  = 1.5, 15.3 Hz, 1 H), 4.73 (dt,  $J$  = 4.8, 8.6 Hz, 1 H), 3.74 (s, 3 H), 2.19 (dq,  $J$  = 1.5, 7.2 Hz, 2 H), 1.70 - 1.65 (m, 2 H), 1.60 - 1.53 (m, 1 H), 1.47 - 1.39 (m, 2 H), 1.39 - 1.30 (m, 2 H), 0.96 (d,  $J$  = 5.9 Hz, 3 H), 0.94 (d,  $J$  = 6.2 Hz, 3 H), 0.91 (t,  $J$  = 7.2 Hz, 3 H).  $^{13}\text{C}$  NMR (151MHz, CHLOROFORM-d)  $\delta$  = 173.8, 165.7, 145.9, 122.9, 52.3, 50.5, 41.9, 31.7, 30.2, 24.8, 22.8, 22.2, 22.0, 13.8.



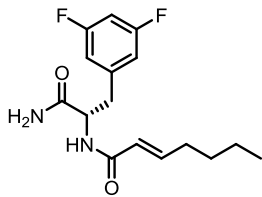
**Synthesis of ADEP Side Chain Free Acid (15).** Methyl (S,E)-3-(3,5-difluorophenyl)-2-(hept-2-enamido)propanoate (50 mg, 0.15 mmol) was dissolved in 1:1 THF/ $\text{H}_2\text{O}$  (0.5 mL) and treated with lithium hydroxide monohydrate (17 mg, 0.41 mmol). The reaction was allowed to proceed for 45 minutes, after which 1 M HCl (0.62 mL) was added. The reaction solution was then transferred to a separatory funnel and extracted 3x DCM. The DCM extracts were combined and dried over sodium sulfate. After removal of solvent, the ADEP side chain free acid was revealed as a white solid and used without further purification: 43 mg, 93% yield. HRMS (ESI) predicted for  $[\text{C}_{16}\text{H}_{19}\text{F}_2\text{NO}_3 + \text{H}]^+$ : 311.1411, found:312.1402.  $^1\text{H}$  NMR (600MHz, CHLOROFORM-d)  $\delta$  = 10.12

(br. s., 1 H), 6.89 (td,  $J = 7.0, 15.4$  Hz, 1 H), 6.77 - 6.58 (m, 3 H), 6.27 (d,  $J = 7.0$  Hz, 1 H), 5.82 (td,  $J = 1.5, 15.3$  Hz, 1 H), 4.93 (td,  $J = 5.7, 7.3$  Hz, 1 H), 3.26 (dd,  $J = 5.7, 14.1$  Hz, 1 H), 3.15 (dd,  $J = 5.7, 14.1$  Hz, 1 H), 2.24 - 2.11 (m, 2 H), 1.48 - 1.37 (m, 2 H), 1.37 - 1.24 (m, 2 H), 0.90 (t,  $J = 7.3$  Hz, 3 H).  $^{13}\text{C}$  NMR (151MHz, CHLOROFORM- $d$ )  $\delta = 173.6, 166.7, 163.8, 163.7, 162.1, 162.0, 147.6, 139.7, 139.6, 122.1, 112.4, 112.4, 112.3, 112.3, 102.9, 102.7, 102.5, 53.1, 37.0, 31.8, 30.1, 22.2, 13.8$ .

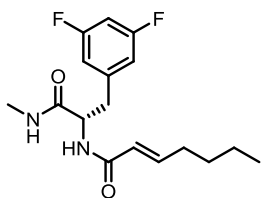


**Synthesis of ADEP side chain methyl amides general procedure:** A Boc-amino acid (1 equivalent) and either 7 M ammonia in methanol (1 equivalent), 2 M methyl amine in methanol (1 equivalent), or dimethylamine hydrochloride (1 equivalent) were dissolved in dichloromethane at a concentration of 0.1 M with respect to the Boc-amino acid. The solution was then treated with EDC (1.1 equivalents), HOBt (1.1 equivalents), and TEA (1.1 equivalents for free base amines, 2.1 equivalents for dimethyl amine HCl). The coupling reactions were allowed to run over night after which solvent was removed and the residue was diluted in ethyl acetate to twice the original reaction volume. The ethyl acetate solution was extracted 3x 1M HCl, 3x sat  $\text{NaHCO}_3$ , 1x brine, and then dried over sodium sulfate. The concentrated crude Boc-amino amides were advanced without further purification.

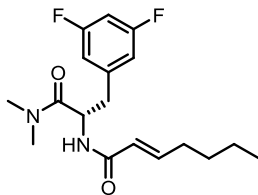
Crude Boc-amino amides were deprotected by treatment with 40% TFA in DCM. Upon complete conversion of the starting material, the reaction was concentrated first by blowing with a stream of nitrogen and then by placing the residue under high vacuum. Once dry, the free base amino amides were subjected to HATU mediated coupling with a carboxylic acid and purified as described in the general procedure for the synthesis of side chain methyl esters.



**(S,E)-N-(1-amino-3-(3,5-difluorophenyl)-1-oxopropan-2-yl)hept-2-enamide (16).** Compound isolated as white solid: 69% yield over 3 steps. HRMS (ESI) predicted for  $[C_{16}H_{20}F_2N_2O_2 + H]^+$ : 311.1571, found:311.1562.  $^1H$  NMR (400MHz, DMSO- $d_6$ )  $\delta$  = 8.12 (d,  $J$  = 9.0 Hz, 1 H), 7.50 (s, 1 H), 7.11 (s, 1 H), 7.04 (tt,  $J$  = 2.4, 9.4 Hz, 1 H), 7.00 - 6.90 (m, 2 H), 6.54 (td,  $J$  = 7.0, 15.1 Hz, 1 H), 6.03 - 5.83 (m, 1 H), 4.61 - 4.42 (m, 1 H), 3.02 (dd,  $J$  = 4.5, 13.6 Hz, 1 H), 2.78 (dd,  $J$  = 10.0, 14.1 Hz, 1 H), 2.17 - 2.06 (m, 2 H), 1.40 - 1.31 (m, 2 H), 1.31 - 1.22 (m, 2 H), 0.86 (t,  $J$  = 7.3 Hz, 3 H).  $^{13}C$  NMR (101MHz, DMSO- $d_6$ )  $\delta$  = 172.7, 164.8, 163.3, 163.2, 160.9, 160.7, 143.0, 142.9, 142.8, 142.7, 124.1, 112.4, 112.3, 112.2, 112.1, 102.0, 101.8, 101.5, 53.3, 37.3, 30.8, 29.9, 21.6, 13.7.

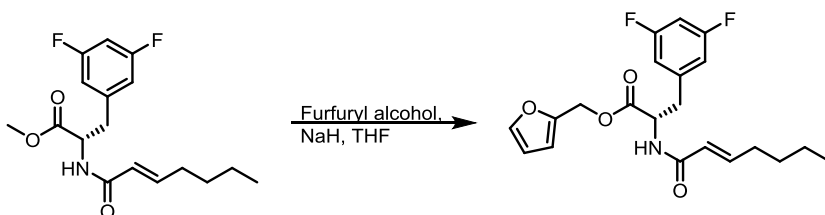


**(S,E)-N-(3-(3,5-difluorophenyl)-1-(methylamino)-1-oxopropan-2-yl)hept-2-enamide (17).** Compound isolated as white solid: 72% yield over 3 steps. HRMS (ESI) predicted for  $[C_{17}H_{22}F_2N_2O_2 + H]^+$ : 325.1727, found:325.1719.  $^1H$  NMR (400MHz, CHLOROFORM- $d$ )  $\delta$  = 6.89 - 6.78 (m, 1 H), 6.76 (d,  $J$  = 6.3 Hz, 2 H), 6.67 (dt,  $J$  = 2.4, 9.0 Hz, 1 H), 6.55 (d,  $J$  = 7.5 Hz, 2 H), 5.79 (d,  $J$  = 15.3 Hz, 1 H), 4.77 (q,  $J$  = 7.5 Hz, 1 H), 3.15 - 2.99 (m, 2 H), 2.74 (d,  $J$  = 4.8 Hz, 3 H), 2.18 (q,  $J$  = 6.9 Hz, 2 H), 1.48 - 1.38 (m, 2 H), 1.37 - 1.28 (m, 2 H), 0.90 (t,  $J$  = 7.3 Hz, 3 H).  $^{13}C$  NMR (101MHz, CHLOROFORM- $d$ )  $\delta$  = 171.3, 166.0, 146.3, 140.7, 140.6, 122.7, 112.3, 112.0, 102.4, 54.1, 38.1, 31.7, 30.2, 26.2, 22.2, 13.8.



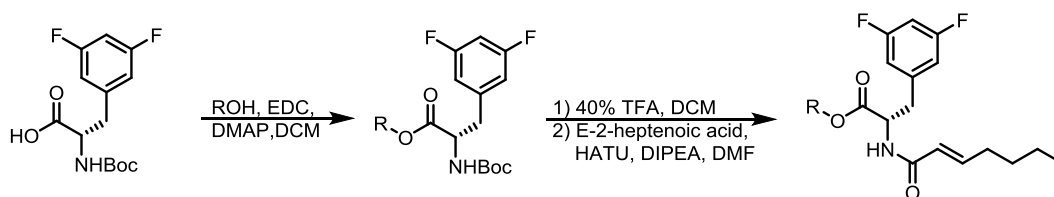
**(S,E)-N-(3-(3,5-difluorophenyl)-1-(dimethylamino)-1-oxopropan-2-yl)hept-2-enamide (18).**

Compound isolated as white solid: 82% yield over 3 steps. HRMS (ESI) predicted for  $[C_{18}H_{24}F_2N_2O_2 + H]^+$ : 339.1884, found:339.1874.  $^1H$  NMR (400MHz, CHLOROFORM-d)  $\delta$  = 6.92 - 6.79 (m, 1 H), 6.77 - 6.65 (m, 3 H), 6.47 (d,  $J$  = 8.0 Hz, 1 H), 5.80 (d,  $J$  = 15.1 Hz, 1 H), 5.22 (dt,  $J$  = 6.0, 7.8 Hz, 1 H), 3.01 (t,  $J$  = 6.3 Hz, 2 H), 2.92 (s, 3 H), 2.86 - 2.79 (m, 3 H), 3.07-2.95 (m, 2 H), 1.49 - 1.40 (m, 2 H), 1.38 - 1.30 (m, 2 H), 0.91 (t,  $J$  = 7.3 Hz, 4 H).  $^{13}C$  NMR (101MHz, CHLOROFORM-d)  $\delta$  = 170.7, 165.3, 164.2, 164.0, 161.7, 161.6, 145.8, 140.3, 140.2, 123.0, 112.4, 112.3, 112.2, 112.1, 102.8, 102.5, 102.3, 49.6, 39.1, 37.0, 35.6, 31.7, 30.2, 22.2, 13.8.



**Synthesis of ADEP side chain furfuryl ester (19):** furfuryl alcohol (26  $\mu$ L, 0.3 mmol) was dissolved in THF (2 mL) and treated with NaH 60% in mineral oil (1 mg, 0.03 mmol) and allowed to react for 5 minutes before the addition of SC1 (65 mg, 0.2 mmol). After reacting for 6 hours, the reaction was concentrated and the crude product residue was loaded directly onto a silica gel column and chromatographed with 20% ethyl acetate in hexanes. The product was isolated as a white solid: 29 mg, 37% yield. HRMS (ESI) predicted for  $[C_{21}H_{23}F_2NO_4 + H]^+$ : 391.1673, found:392.1669.  $^1H$  NMR (400MHz, CHLOROFORM-d)  $\delta$  = 7.47 (s, 1 H), 6.96 - 6.81 (m, 1 H), 6.67 (tt,  $J$  = 2.3, 9.0 Hz, 1 H), 6.59 - 6.48 (m, 2 H), 6.45 (d,  $J$  = 3.0 Hz, 1 H), 6.42 - 6.36 (m, 1 H), 5.98 (d,

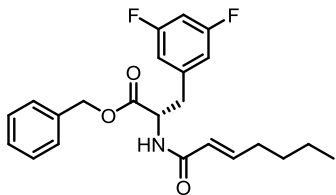
$J = 7.5$  Hz, 1 H), 5.80 (d,  $J = 15.6$  Hz, 1 H), 5.25 (d,  $J = 13.0$  Hz, 1 H), 5.04 (d,  $J = 13.1$  Hz, 1 H), 5.00 - 4.89 (m, 1 H), 3.25 - 3.06 (m, 2 H), 2.20 (q,  $J = 7.2$  Hz, 2 H), 1.50 - 1.40 (m, 2 H), 1.40 - 1.31 (m, 2 H), 0.91 (t,  $J = 7.0$  Hz, 3 H).  $^{13}\text{C}$  NMR (101MHz, CHLOROFORM- $d$ )  $\delta = 170.8, 165.4, 164.1, 164.0, 161.6, 161.5, 148.3, 146.5, 143.7, 139.7, 139.6, 139.5, 122.7, 112.5, 112.4, 112.3, 112.2, 111.7, 110.7, 102.9, 102.6, 102.4, 59.0, 52.7, 37.5, 31.7, 30.2, 22.2, 13.8$ .



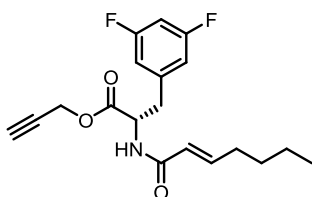
**Synthesis of side chain benzyl and propargyl esters:** Boc-3,5-Difluorophenylalanine (1 equivalent) and an alcohol (1 equivalent) were dissolved in DCM at a concentration of 0.2 M. The solution was treated with EDC and DMAP and allowed to react for 3 hours. after which solvent was removed and the residue was diluted in ethyl acetate to twice the original reaction volume. The ethyl acetate solution was extracted 3x 1M HCl, 3x sat  $\text{NaHCO}_3$ , 1x brine, and then dried over sodium sulfate. The concentrated crude Boc-amino acid esters were advanced without further purification.

Crude Boc-amino acid esters were deprotected by treatment with 40% TFA in DCM. Upon complete conversion of the starting material, the reaction was concentrated first by blowing with a stream of nitrogen and then by placing the residue under high vacuum. Once dry, the free base amino amides were subjected to HATU mediated coupling with a carboxylic acid and purified as described in the general procedure for the synthesis of side chain methyl esters.



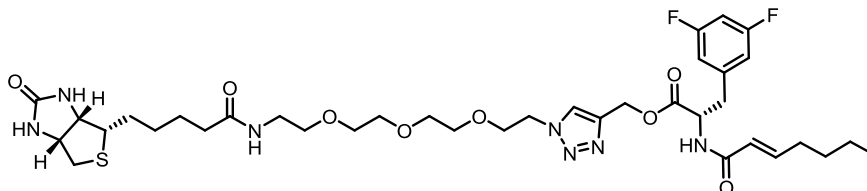


**Benzyl (S,E)-3-(3,5-difluorophenyl)-2-(hept-2-enamido)propanoate (20).** Compound isolated as a white solid: 55% yield over 3 steps. HRMS (ESI) predicted for  $[C_{23}H_{25}F_2NO_3 + H]^+$ : 401.1881, found: 401.1870.  $^1H$  NMR (400MHz, CHLOROFORM-d)  $\delta$  = 7.43 - 7.36 (m, 3 H), 7.36 - 7.30 (m, 2 H), 6.88 (td,  $J$  = 7.0, 15.6 Hz, 1 H), 6.66 (tt,  $J$  = 2.3, 9.0 Hz, 1 H), 6.58 - 6.46 (m, 2 H), 6.01 (d,  $J$  = 7.0 Hz, 1 H), 5.80 (td,  $J$  = 1.5, 15.1 Hz, 1 H), 5.21 (d,  $J$  = 12.0 Hz, 1 H), 5.13 (d,  $J$  = 12.0 Hz, 1 H), 4.98 (td,  $J$  = 5.4, 7.3 Hz, 1 H), 3.17 (dd,  $J$  = 6.0, 14.1 Hz, 1 H), 3.10 (dd,  $J$  = 5.0, 14.1 Hz, 1 H), 2.26 - 2.11 (m, 2 H), 1.52 - 1.39 (m, 2 H), 1.39 - 1.29 (m, 2 H), 0.91 (t,  $J$  = 7.2 Hz, 3 H).  $^{13}C$  NMR (101MHz, CHLOROFORM-d)  $\delta$  = 171.0, 165.4, 164.1, 164.0, 161.6, 161.5, 146.4, 139.8, 139.7, 134.7, 128.8, 128.7, 128.7, 122.7, 112.4, 112.3, 112.2, 112.2, 102.8, 102.6, 102.3, 67.6, 52.8, 37.5, 31.7, 30.2, 22.2, 13.8.



**Prop-2-yn-1-yl (S,E)-3-(3,5-difluorophenyl)-2-(hept-2-enamido)propanoate (21).** Compound isolated as a white solid 36% yield over 3 steps. HRMS (ESI) predicted for  $[C_{19}H_{21}F_2NO_3 + H]^+$ : 350.1568, found: 350.1560.  $^1H$  NMR (400MHz, CHLOROFORM-d)  $\delta$  = 6.88 (td,  $J$  = 7.0, 15.6 Hz, 1 H), 6.80 - 6.60 (m, 3 H), 6.01 (d,  $J$  = 7.5 Hz, 1 H), 5.80 (td,  $J$  = 1.5, 15.1 Hz, 1 H), 4.99 (td,  $J$  = 5.5, 7.5 Hz, 1 H), 4.91 - 4.78 (m, 1 H), 4.67 (dd,  $J$  = 2.5, 15.6 Hz, 1 H), 3.25 - 3.12 (m, 2 H), 2.56 (t,  $J$  = 2.5 Hz, 1 H), 2.25 - 2.14 (m, 2 H), 1.49 - 1.39 (m, 2 H), 1.39 - 1.29 (m, 2 H), 0.93 - 0.87 (m, 3 H).  $^{13}C$  NMR (101MHz, CHLOROFORM-d)  $\delta$  = 170.4, 165.5, 164.2, 164.1, 161.7, 161.6, 146.6, 139.5,

139.4, 139.3, 122.5, 112.6, 112.5, 112.4, 112.3, 103.0, 102.7, 102.5, 75.9, 52.9, 52.6, 37.4, 31.7, 30.2, 22.2, 13.8.



**N-E-2-Heptenylidifluorophenylalanine – Biotin Conjugate:** Compound **21** (17 mg, 0.05 mmol) and commercially available Azido-Biotin Conjugate (SigmaAldrich) (16 mg, 0.04 mmol) were dissolved in 1:1 water / ethanol (1 mL) and treated with Cu(II) sulfate (1 mg, 0.006 mmol), TCEP (2 mg, 0.007 mmol), and 2,6-lutidine (50  $\mu$ L, 0.43 mmol). The reaction solution turned blue/green after the addition of 2,6-lutidine, an indication of Cu(I) formation. The reaction was allowed to proceed over night, over the course of which, a blue/green precipitate had formed. The reaction solution was filtered and diluted with 1:1 water/ethanol to a final theoretical concentration of 8.2 mM (4.8 mL) with respect to the N-acyldifluorophenylalanine – biotin conjugate. This solution was used directly in chemical proteomics experiments without further purification. Formation of the conjugate was confirmed by ESI MS analysis.

## References

1. Edwards, C. M.; Cohen, M. A.; Bloom, S. R. Peptides as drugs. *QJM* **1999**, *92*, 1-4.
2. Loffet, A. Peptides as drugs: is there a market? *Journal of Peptide Science* **2002**, *8*, 1-7.

3. Vlieghe, P.; Lisowski, V.; Martinez, J.; Khrestchatsky, M. Synthetic therapeutic peptides: science and market. *Drug Discov. Today* **2010**, *15*, 40-56.
4. Hamman, J. H.; Enslin, G. M.; Kotzé, A. F. Oral delivery of peptide drugs. *BioDrugs* **2005**, *19*, 165-177.
5. Morishita, M.; Peppas, N. A. Is the oral route possible for peptide and protein drug delivery? *Drug Discov. Today* **2006**, *11*, 905-910.
6. Veber, D. F.; Johnson, S. R.; Cheng, H.; Smith, B. R.; Ward, K. W.; Kopple, K. D. Molecular properties that influence the oral bioavailability of drug candidates. *J. Med. Chem.* **2002**, *45*, 2615-2623.
7. Hinzen, B.; Raddatz, S.; Paulsen, H.; Lampe, T.; Schumacher, A.; Häbich, D.; Hellwig, V.; Benet-Buchholz, J.; Endermann, R.; Labischinski, H.; Brötz-Oesterhelt, H. Medicinal Chemistry Optimization of Acyldepsipeptides of the Enopeptin Class Antibiotics. *ChemMedChem* **2006**, *1*, 689-693.
8. Carney, D. W.; Schmitz, K. R.; Truong, J. V.; Sauer, R. T.; Sello, J. K. Restriction of the Conformational Dynamics of the Cyclic Acyldepsipeptide Antibiotics Improves Their Antibacterial Activity. *J. Am. Chem. Soc.* **2014**.
9. Compton, C. L.; Schmitz, K. R.; Sauer, R. T.; Sello, J. K. Antibacterial Activity of and Resistance to Small Molecule Inhibitors of the ClpP Peptidase. *ACS Chemical Biology* **2013**.
10. Leung, E.; Datti, A.; Cossette, M.; Goodreid, J.; McCaw, S. E.; Mah, M.; Nakhamchik, A.; Ogata, K.; El Bakkouri, M.; Cheng, Y. Activators of cylindrical proteases as antimicrobials: identification and development of small molecule activators of ClpP protease. *Chem. Biol.* **2011**, *18*, 1167-1178.
11. Raju, R. M.; Goldberg, A. L.; Rubin, E. J. Bacterial proteolytic complexes as therapeutic targets. *Nature Reviews Drug Discovery* **2012**, *11*, 777-789.
12. Roberts, D. M.; Personne, Y.; Ollinger, J.; Parish, T. Proteases in Mycobacterium tuberculosis pathogenesis: potential as drug targets. *Future microbiology* **2013**, *8*, 621-631.
13. Brötz-Oesterhelt, H.; Sass, P. Bacterial caseinolytic proteases as novel targets for antibacterial treatment. *International Journal of Medical Microbiology* **2013**.
14. Erlanson, D. A.; McDowell, R. S.; O'Brien, T. Fragment-based drug discovery. *J. Med. Chem.* **2004**, *47*, 3463-3482.
15. Hajduk, P. J.; Greer, J. A decade of fragment-based drug design: strategic advances and lessons learned. *Nature reviews Drug discovery* **2007**, *6*, 211-219.
16. Congreve, M.; Chessari, G.; Tisi, D.; Woodhead, A. J. Recent developments in fragment-based drug discovery. *J. Med. Chem.* **2008**, *51*, 3661-3680.

17. Scott, D. E.; Coyne, A. G.; Hudson, S. A.; Abell, C. Fragment-based approaches in drug discovery and chemical biology. *Biochemistry (N. Y.)* **2012**, *51*, 4990-5003.
18. Lee, B.; Park, E. Y.; Lee, K.; Jeon, H.; Sung, K. H.; Paulsen, H.; Rubsamen-Schaeff, H.; Brotz-Oesterhelt, H.; Song, H. K. Structures of ClpP in complex with acyldepsipeptide antibiotics reveal its activation mechanism. *Nat Struct Mol Biol* **2010**, *17*, 471-478.
19. Li, D. H. S.; Chung, Y. S.; Gloyd, M.; Joseph, E.; Ghirlando, R.; Wright, G. D.; Cheng, Y.; Maurizi, M. R.; Guarne, A.; Ortega, J. Acyldepsipeptide antibiotics induce the formation of a structured axial channel in ClpP: a model for the ClpX/ClpA-bound state of ClpP. *Chem. Biol.* **2010**, *17*, 959-969.
20. Brotz-Oesterhelt, H.; Beyer, D.; Kroll, H.; Endermann, R.; Ladel, C.; Schroeder, W.; Hinzen, B.; Raddatz, S.; Paulsen, H.; Henninger, K.; Bandow, J. E.; Sahl, H.; Labischinski, H. Dysregulation of bacterial proteolytic machinery by a new class of antibiotics. *Nat. Med.* **2005**, *11*, 1082-1087.
21. Michel, K. H.; Kastner, R. E. *A54556 antibiotics and process for production thereof* **1985**.
22. Hinzen, B. WO2003024996 A3, 2004.
23. Nakano, M. M.; Hajarizadeh, F.; Zhu, Y.; Zuber, P. Loss-of-function mutations in yjbD result in ClpX-and ClpP-independent competence development of *Bacillus subtilis*. *Mol. Microbiol.* **2001**, *42*, 383-394.
24. Nakano, S.; Zheng, G.; Nakano, M. M.; Zuber, P. Multiple pathways of Spx (YjbD) proteolysis in *Bacillus subtilis*. *J. Bacteriol.* **2002**, *184*, 3664-3670.
25. Rix, U.; Superti-Furga, G. Target profiling of small molecules by chemical proteomics. *Nature Chemical Biology* **2009**, *5*, 616-624.
26. Rostovtsev, V. V.; Green, L. G.; Fokin, V. V.; Sharpless, K. B. A stepwise Huisgen cycloaddition process: copper (I)-catalyzed regioselective "ligation" of azides and terminal alkynes. *Angewandte Chemie* **2002**, *114*, 2708-2711.
27. Wang, J.; Galgoci, A.; Kodali, S.; Herath, K. B.; Jayasuriya, H.; Dorso, K.; Vicente, F.; Gonzalez, A.; Cully, D.; Bramhill, D.; Singh, S. Discovery of a small molecule that inhibits cell division by blocking FtsZ, a novel therapeutic target of antibiotics. *J. Biol. Chem.* **2003**, *278*, 44424-44428.
28. Kapoor, S.; Panda, D. Targeting FtsZ for antibacterial therapy: a promising avenue. **2009**.
29. Rai, D.; Singh, J.; Roy, N.; Panda, D. Curcumin inhibits FtsZ assembly: an attractive mechanism for its antibacterial activity. *Biochem. J.* **2008**, *410*, 147-155.

30. Sass, P.; Josten, M.; Famulla, K.; Schiffer, G.; Sahl, H.; Hamoen, L.; Brötz-Oesterhelt, H. Antibiotic acyldepsipeptides activate ClpP peptidase to degrade the cell division protein FtsZ. *Proceedings of the National Academy of Sciences* **2011**, *108*, 17474-17479.

## Chapter 9 – *N*-Acyldifluorophenylalanine Fragment Hit to lead development.

### Introduction.

In the previous chapter we discussed the discovery that the *N*-acyldifluorophenylalanine moiety of the ADEP molecules necessary and sufficient for ClpP activation (Figure 9.1). Fragments (**2**, **3**) based on this scaffold exhibited modest antibacterial activity against *B. subtilis*. However, even the most potent fragments were at least 100 fold less potent than the parent ADEPs against *B. subtilis*. The *N*-acyldifluorophenylalanine moiety requires significant structural elaboration before achieving a level of activity that is acceptable for drug lead development.

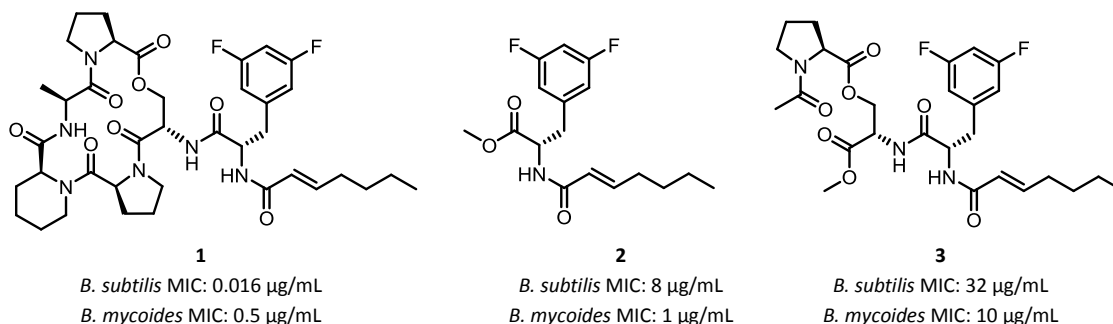


Figure 9.1 – Structures and antibacterial activity of a Prototypical ADEP and *N*-heptenoyldifluorophenylalanine fragments.

Diversity-oriented synthesis<sup>1-3</sup> has become mainstay strategy used to develop highly active drug leads from low potency fragments and hits. Combinatorial chemistry and rational design are two distinct diversity-oriented synthetic strategies that are commonly utilized to in hit to lead drug development. We have recently initiated efforts using both approaches in an attempt to improve the potency of the *N*-acyldifluorophenylalanine fragments.

### Results

Isocyanide based multicomponent reactions (IMCR) are particularly useful in diversity oriented combinatorial synthesis. These reactions are characterized by their, simple execution, high atom economies, versatility in terms of tolerated functionality, and their ability to build

significant complexity from simple and commercially available substrates.<sup>4,5</sup> Two of the most prominent IMCR are the Passerini 3-component reaction (P-3CR)<sup>6</sup> and the Ugi 4-component reaction (U-4CR),<sup>7,8</sup> which were both discussed extensively in chapter 4. Both reactions incorporate a carboxylic acid, an oxo-compound, and an isocyanide. The U-4CR reaction is distinguished from the P-3CR reaction by the inclusion of a fourth substrate, a primary amine.

IMCR could be potentially useful for diversifying the *N*-acyldifluorophenylalanine fragment and building chemical libraries. A carboxylic acid analog (**4**) of this fragment could serve as a substrate for both the U-4CR as well as the P-3CR. With the P-3CR, the combination of **1** with 10 different aldehydes or ketones and 10 isocyanides, would provide 100 unique compounds. With the U-4CR, the combination of **4** with 10 different amines, 10 different aldehydes or ketones and 10 isocyanides, would provide 1,000 unique compounds.

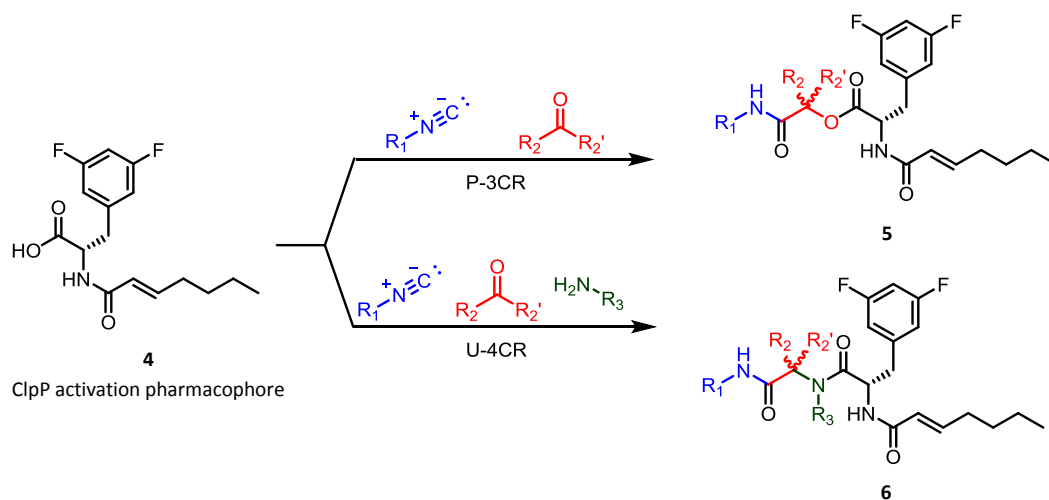


**Figure 9.2 – IMCR for the synthesis or combinatorial libraries bearing the *N*-heptenoyldifluorophenylalanine ClpP activation pharmacophore.**

In collaboration with two undergraduate students in our lab, Julia Stevens and Arianna Kazez, we used IMCRs to construct a library of compounds bearing the *N*-heptenoyldifluorophenylalanine moiety. A collection of 24 U-4CR products (**5**) and 4 P-3CR products (**6**) was synthesized and tested for antibacterial against *B. mycoides* over the course of

one summer. Of the 28 compound collection, only 4 analogs (**5h**, **5x**, **6a**, **6d**) exhibited modest antibacterial activity. Compounds **5h** and **6a**, as well as **5x** and **6d** are pairs of corresponding U-4CR and P-3CR products. The U-4CR products contain an *N*-propylamide whereas the P-3CR products contain an ester. In both cases, the P-3CR product is more potent than the corresponding U-4CR product. In any case, none of the IMCR products were more potent than the *N*-heptenoyldifluorophenylalanine methyl ester **2** (*B. mycooides* MIC = 1 µg/mL). This project highlights an important drawback to diversity oriented combinatorial chemistry that is problematic for labs that do not specialize in high throughput chemistry. Much larger combinatorial libraries and HTS capabilities are required in order to have a strong likelihood of discovering a highly active analog.



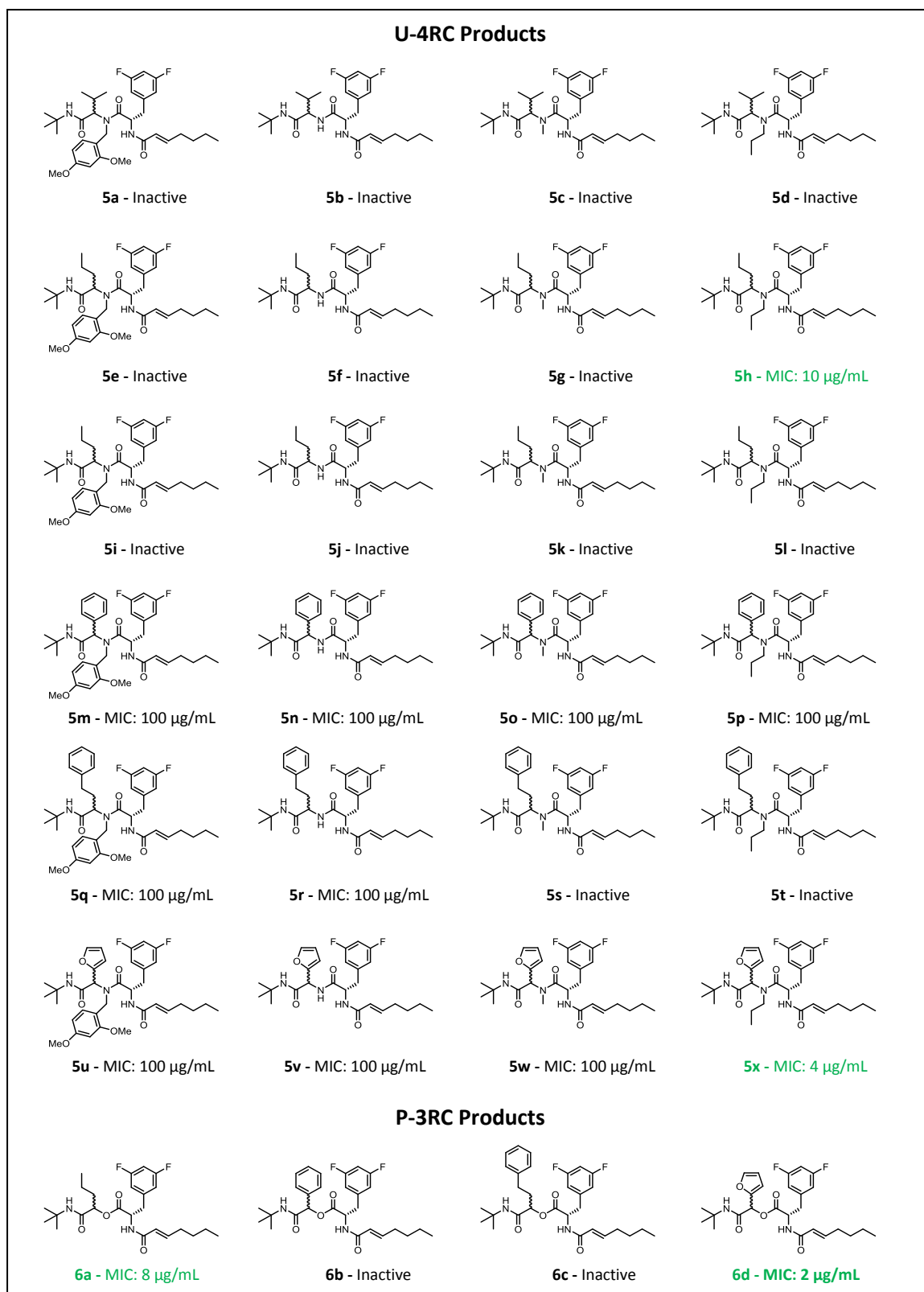


Figure 9.3 – IMCR library containing the *N*-heptenoyldifluorophenylalanine ClpP activation pharmacophore and antibacterial activity against *B. mycoides*.

We have also explored rational design approaches for improving the activity of *N*-acyldifluorophenylalanine fragments. Our goal was design a handle for the *N*-heptenoyldifluorophenylalanine moiety that would mimic the binding mode of the ADEP peptidolactones, while also being structurally much less complex. In the simplest sense, we hypothesized that the ADEP peptidolactone provides a hydrophobic moiety that mediates van der Waal's interactions with the solvent exposed surface of ClpP. Therefore, we reasoned that ADEP peptidolactones could be replaced by a simple carbocycle. Initially, we acylated a variety of carbocycles bearing primary amino groups with carboxylic acid **4**, generating a collection *N*-E-heptenoyldifluorophenylalanineamides (**7**) (Figure 4). Unfortunately, none of these analogs exhibited antibacterial activity against *B. mycoides*. Not surprisingly, our first hypothesis overlooks the nuances of the ADEP peptidolactone in facilitating the ADEP-ClpP binding interaction.

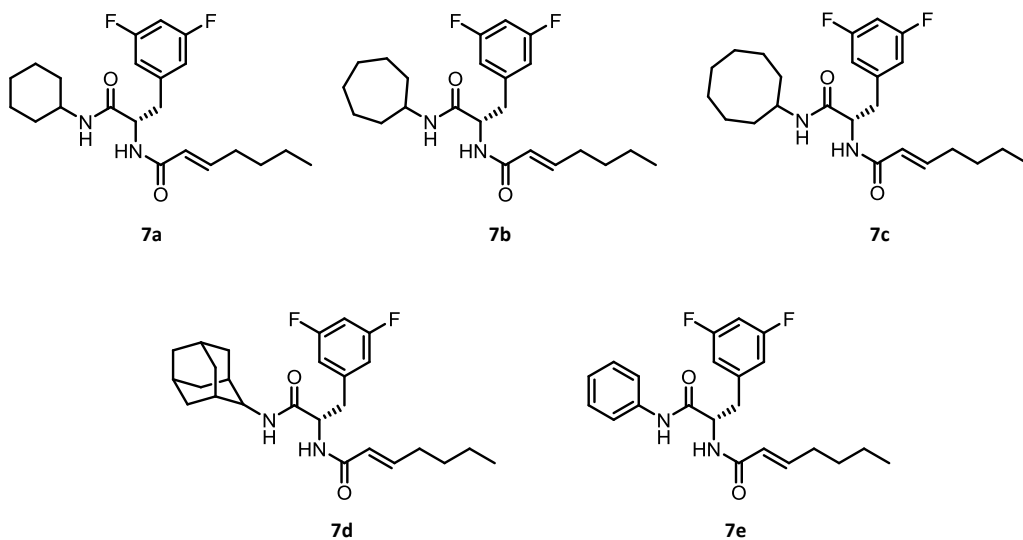
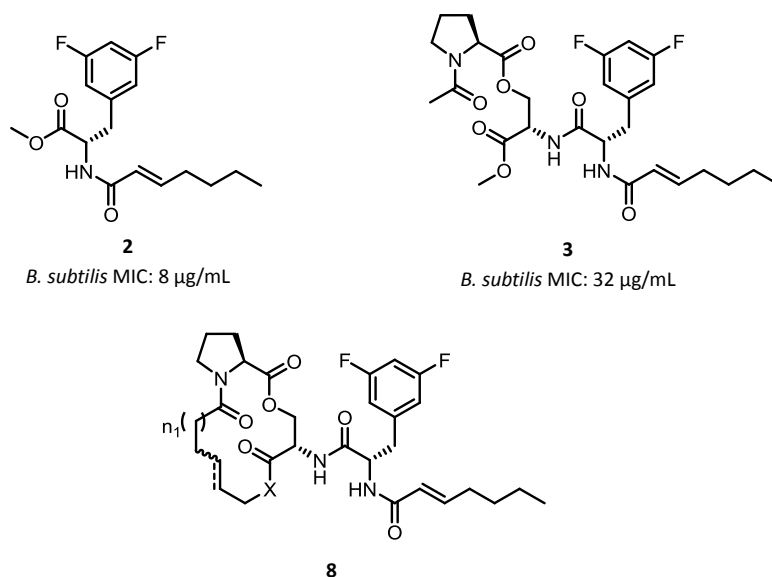


Figure 9.4 – Analogs of *N*-heptenoyldifluorophenylalanine coupled to carbocyclic amines do not exhibit antibacterial activity against *B. mycoides*.

In a separate rational design approach, we hypothesized that antibacterial activity of the

*N*-E-2-heptenoyldifluorophenylalanine moiety could be improved by reintroducing a portion of the ADEP-peptidolactone to the *N*-E-2-heptenoyldifluorophenylalanine moiety (Figure 5). As discussed in the previous chapter however, a fragment (**3**) composed of the *N*-E-2-heptenoyldifluorophenylalanine moiety coupled to a serine-proline ester was less active than the structurally less complex fragment **2**. Fragment 3 is very conformationally flexible. Therefore, it probably incurs a significant entropic penalty when binding to ClpP. We hypothesized that the entropic penalty for fragment **3** binding to ClpP could be reduced by tethering the two ends of the serine-proline ester moiety to each other. As such, we envisioned synthesizing a collection of compounds based on structure **8**. We also wanted to design a modular synthesis that would allow us to easily diversify the structures of the products. Some important features of the structure that we wanted to vary were ring size, the presence and geometry of a unit of unsaturation, and the identity of the linker heteroatom. Our strategy was to use a ring closing metathesis (RCM) route.



**Figure 9.5 – Antibacterial activity of ADEP fragments and a circularization strategy to minimize entropic penalties for binding to ClpP**

To date, we have synthesized 3 circularized ADEP fragments (**8a-c**) as shown in Figure 9.6. First, the carboxylate anion of Fmoc-serine (**9**) was engaged in a SN2 reaction with allylbromide yielding allyl ester **10**, which was subsequently esterified with Boc proline. Ester **11** was then Boc-protected by treatment with trifluoroacetic acid in dichloromethane. In turn, the deprotected amine was acylated with 4-pentenoic acid yielding compound **12**. Treatment of **12** with Grubbs second generation catalyst promoted a ring-closing metathesis reaction with 4.5:1 E/Z - selectivity in favor of the *E*-alkene (**13b**). The geometric isomers were cleanly separated by silica gel chromatography and a portion of the *E*-alkene RCM product (**13b**) was hydrogenated generating a macrocycle with a saturated tether (**13c**). The three macrocycles were advanced in parallel through a four step sequence to append the *N*-E-2-heptenoyldifluorophenylalanine side chain. First, the macrocycles were Fmoc-protected with 10% piperidine in DMF then acylated with Boc-difluorophenylalanine. Construction of the side chain was completed after *N*-terminal Boc-deprotection followed by acylation with *E*-2-heptenoic acid.

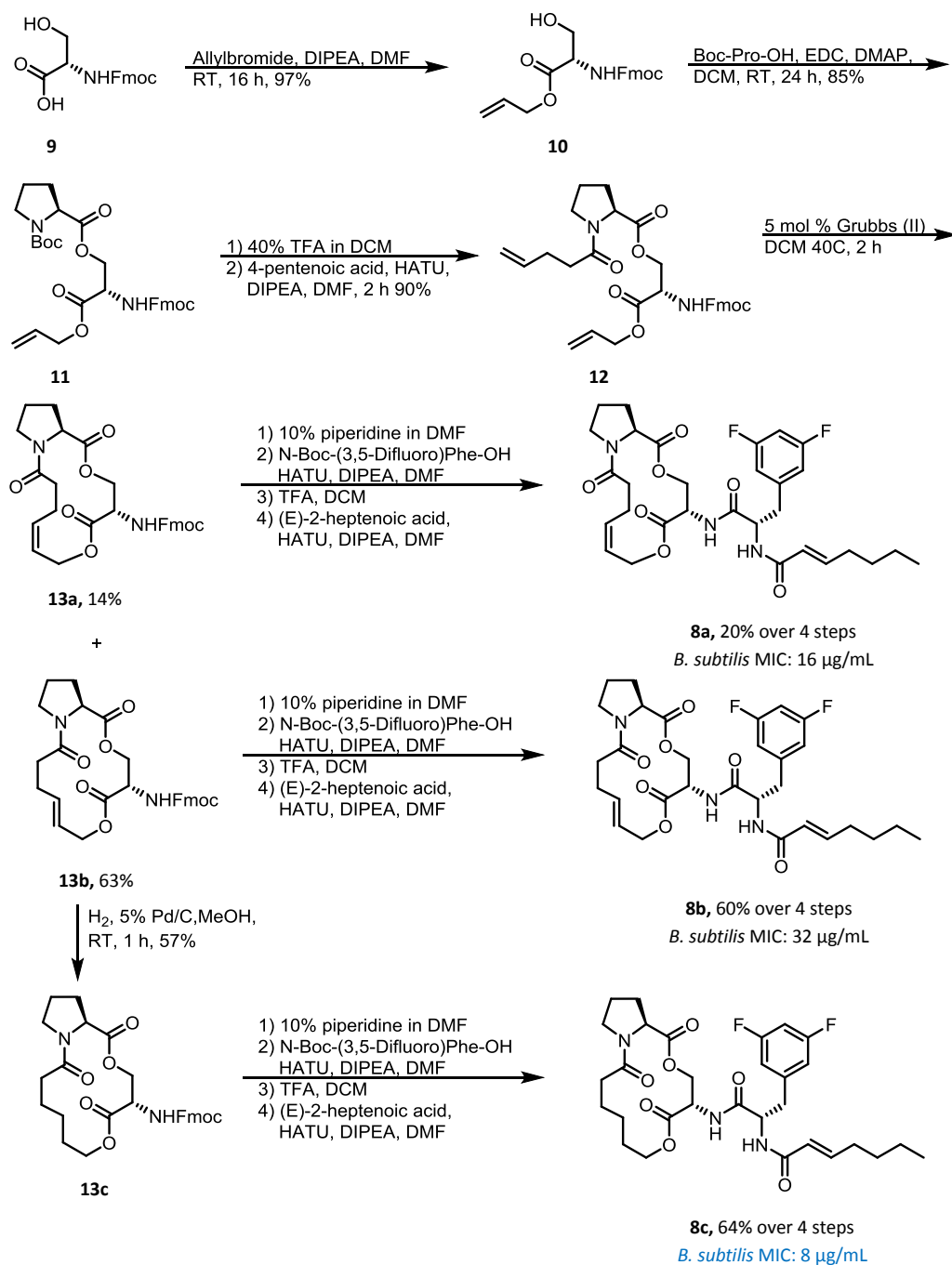


**Figure 9.6 – Diversity oriented synthesis and antibacterial activity of circularized ADEP fragments**

The three circularized ADEP fragments (**8a-c**) were tested for antibacterial activity against *B. subtilis*. Rewardingly, all three analogs were active. Compound **8b** (*B. subtilis* MIC: 32  $\mu\text{g/mL}$ ), which has an *E*-alkenyl tether was equally as potent as acyclic fragment **3** while compound **8a** (*B. subtilis* MIC: 16  $\mu\text{g/mL}$ ), which has a *Z*-alkenyl tether was slightly more potent

than **3**. Compound **8c** (*B. subtilis* MIC: 8 µg/mL) was the most active in the group and was equally as potent as fragment **2**. These initial results are encouraging and indicate that circularization of fragment **8** can improve its activity. It is our hope that this diversity oriented synthesis will eventually lead to the discovery of circularized fragments that exceed the activity of fragment **2** or even approach the activity of ADEPs.

## Discussion

After the discovery of ADEP fragments that retain antibacterial activity, we set out to discover new ClpP activator drug leads that contain the ClpP activation pharmacophore derived from the ADEPs. We utilized both combinatorial chemistry and rational design strategies to develop diversity oriented syntheses of new fragment analogs. In our combinatorial approach, we used isocyanide based multicomponent reactions to prepare a collection of 28 unique compounds. Unfortunately, none of these analogs were as potent as our lead fragments. Success with combinatorial hit to lead development typically requires the preparation of much larger compound libraries and high throughput screening capabilities. Our hypothesis driven rational design strategies appear to be more promising.

While our attempts to replace the ADEP peptidolactones with simple carbocycles did not lead to active compounds, circularization of fragments composed of the heptenoyldifluorophenylalanine moiety coupled to a proline ester moiety led to the discovery of analogs that were as active as lead fragment **2**. The diversity oriented synthesis and evaluation of additional circularized fragments is ongoing. The RCM route that we have developed could be used to prepare a structurally diverse library of macrocycles. For instance, the ring size can be adjusted by changing the carboxylic acid that is used to acylate the proline nitrogen of **11**. By using the ring closing metathesis reaction as a diversification step, we can access both geometric

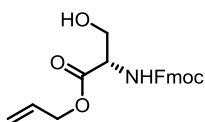
isomers as well as a saturated analog of each macrocycle ring size. We can also prepare primary and secondary serine amides in the first step instead of an ester. These are only a few of the possibilities that one could imagine. It is our hope that we will eventually discover analogs with potencies similar to that of the ADEPs.

## Experimental Contributions

Synthesis and biological evaluation of all compounds was completed by Daniel Carney with the assistance of Brown University Undergraduate students, Julia Stevens and Arianna Kazez.

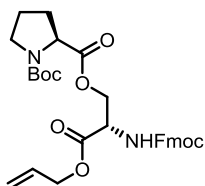
## Experimental Methods

**Synthesis General:** All commercially available reagents were used without further purification. All reactions were conducted in oven dried glassware, under ambient atmosphere, using dry solvents unless otherwise stated. NMR chemical shifts were referenced to residual solvent peaks: CDCl<sub>3</sub> ( $\delta$  = 7.27 ppm for <sup>1</sup>H-NMR and 77.00 ppm for <sup>13</sup>C-NMR), acetone-d<sub>6</sub> ( $\delta$  = 2.05 for <sup>1</sup>H-NMR and  $\delta$  = 29.92 for <sup>13</sup>C-NMR).



**Fmoc-Serine Allyl ester (10).** Fmoc-Serine-OH mono hydrate (1.72 g, 5 mmol) and allyl bromide (0.85 mL 10 mmol) were dissolved in DMF (20 mL) and cooled to 0°C. To the cooled solution was added DIPEA (1.75 mL, 10 mmol) and allowed to react for 16 hours. Upon completion, the reaction was diluted with ethyl acetate (100 mL), extracted 3 x water and 1 x brine, and then dried over sodium sulfate. The product was purified by flash chromatography on silica gel with a 50-60% ethyl acetate in hexanes solvent gradient. Yield 1.78 g, 97%. HRMS (ESI) Predicted for [C<sub>21</sub>H<sub>21</sub>NO<sub>5</sub> + H]<sup>+</sup>:368.1498, Found: 368.1490. <sup>1</sup>H NMR (600MHz, CHLOROFORM-d)  $\delta$  = 7.78 (d, J =

7.7 Hz, 2 H), 7.68 - 7.52 (m, 2 H), 7.41 (t,  $J = 7.5$  Hz, 2 H), 7.32 (t,  $J = 7.3$  Hz, 2 H), 5.99 - 5.85 (m, 1 H), 5.81 (br. s., 1 H), 5.35 (d,  $J = 17.2$  Hz, 1 H), 5.27 (d,  $J = 10.3$  Hz, 1 H), 4.70 (d,  $J = 5.1$  Hz, 2 H), 4.57 - 4.38 (m, 3 H), 4.24 (t,  $J = 7.0$  Hz, 1 H), 4.04 (d,  $J = 11.0$  Hz, 1 H), 3.95 (d,  $J = 9.2$  Hz, 1 H), 2.36 (br. s., 1 H).  $^{13}\text{C}$  NMR (151MHz, CHLOROFORM-d)  $\delta = 170.2, 156.2, 143.8, 143.6, 141.3, 141.3, 131.3, 127.7, 127.1, 127.0, 125.1, 120.0, 120.0, 119.0, 67.2, 66.4, 63.3, 56.1, 47.1.$



**2-((S)-2-(((9H-fluoren-9-yl)methoxy)carbonyl)amino)-3-(allyloxy)-3-oxopropyl)-1-(tert-butyl)**

**(S)-pyrrolidine-1,2-dicarboxylate (11).** Fmoc-Serine Allyl ester (1.78 g, 4.83 mmol) (10) and Boc-

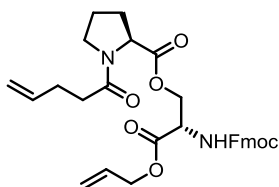
Pro-OH were dissolved in dichloromethane (25 mL). The solution was treated with DMAP (61 mg, 0.5 mmol) and EDC (1.44 g, 7.5 mmol, in 2.5 mmol portions over 3 hours). Upon complete conversion of the starting material, the solvent was removed in vacuo and the residue was diluted in ethyl acetate (50 mL). The ethyl acetate solution was washed 3 x 1M HCl<sub>aq</sub>, 3 x Saturated NaHCO<sub>3aq</sub>, and 1 x Brine then dried over sodium sulfate. The product was purified by flash chromatography on silica gel with a 30-50% ethyl acetate in hexanes solvent gradient.

Yield: 2.32 grams, 85%. HRMS (ESI) Predicted for [C<sub>31</sub>H<sub>36</sub>N<sub>2</sub>O<sub>8</sub> + H]<sup>+</sup>:565.2550, Found: 565.2540.

$^1\text{H}$  NMR, ~5:4 mixture of amide rotamers, (400MHz, CHLOROFORM-d)  $\delta = 7.78$  (dd,  $J = 2.9, 7.5$  Hz, 2 H), 7.66 (dd,  $J = 8.0, 10.5$  Hz, 1 H), 7.61 (d,  $J = 7.3$  Hz, 1 H), 7.47 - 7.37 (m, 2 H), 7.37 - 7.29 (m, 2 H), 6.11 (d,  $J = 8.3$  Hz, .5 H), 6.01 - 5.83 (m, 1 H), 5.58 (d,  $J = 7.8$  Hz, .5 H) 5.40 - 5.32 (m, 1 H), 5.32 - 5.25 (m, 1 H), 4.74 - 4.59 (m, 3 H), 4.59 - 4.30 (m, 4 H), 4.30 - 4.22 (m, 2 H), 3.60 - 3.36 (m, 2 H), 2.30 - 2.11 (m, 1 H), 2.04 - 1.79 (m, 3 H), 1.50 (s, 5 H), 1.41 (s, 4 H).  $^{13}\text{C}$  NMR (101MHz, CHLOROFORM-d)  $\delta = 172.8, 172.4, 169.1, 156.1, 155.7, 154.7, 153.6, 143.9, 143.8, 143.6, 141.2,$



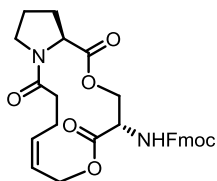
131.5, 131.1, 127.7, 127.6, 127.1, 125.4, 125.2, 125.1, 120.0, 119.9, 119.3, 118.9, 80.2, 80.0, 67.4, 66.6, 66.4, 64.4, 64.3, 58.9, 53.5, 47.1, 46.6, 46.3, 30.9, 30.0, 28.4, 28.3, 24.4, 23.5.



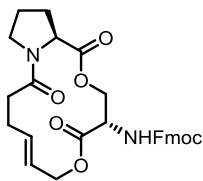
**(S)-2-((((9H-fluoren-9-yl)methoxy)carbonyl)amino)-3-(allyloxy)-3-oxopropyl pent-4-enoate (12).** Ester **11** (464 mg, 1 mmol) was Boc-protected by treatment with 40% TFA in DCM (2 mL). Upon complete conversion of the starting material, the solvent was removed first by blowing with nitrogen then under high vacuum. Once dry, the Boc-protected **12** was dissolved in DMF (2 mL) and excess TFA was neutralized with DIPEA (750  $\mu$ L). In a separate flask, 4-pentenoic acid (102  $\mu$ L, 1 mmol) was dissolved in DMF (2 mL) and preactivated by treatment with HATU (380 mg, 1 mmol) and DIPEA (175  $\mu$ L, 1 mmol). After 10 minutes, the preactivated acid solution was added to the solution containing Boc-protected **12** and allowed to react for 2 hours. Upon completion, the reaction was diluted with ethyl acetate (50 mL) and extracted: 3 x 1M HCl<sub>aq</sub>, 1 x NaHCO<sub>3aq</sub>, and 1 x Brine, then dried over sodium sulfate. The product was purified by flash chromatography on silica gel with a 50-60% ethyl acetate in hexanes solvent gradient. Yield: 491 mg, 90%. HRMS (ESI) Predicted for [C<sub>31</sub>H<sub>34</sub>N<sub>2</sub>O<sub>7</sub> + H]<sup>+</sup>: 547.2444, Found: 547.2435. <sup>1</sup>H NMR (400MHz, CHLOROFORM-d)  $\delta$  = 7.77 (d, *J* = 7.6 Hz, 2 H), 7.70 (d, *J* = 7.3 Hz, 2 H), 7.44 - 7.36 (m, 2 H), 7.36 - 7.28 (m, 2 H), 6.38 (d, *J* = 9.1 Hz, 1 H), 6.00 - 5.84 (m, 2 H), 5.40 - 5.30 (m, 1 H), 5.27 (qd, *J* = 1.3, 10.6 Hz, 1 H), 5.12 - 5.04 (m, 1 H), 5.04 - 4.97 (m, 1 H), 4.85 (dd, *J* = 3.2, 11.2 Hz, 1 H), 4.78 - 4.61 (m, 3 H), 4.49 (dd, *J* = 3.9, 8.5 Hz, 1 H), 4.41 - 4.33 (m, 3 H), 4.31 - 4.23 (m, 1 H), 3.62 - 3.47 (m, 2 H), 2.57 - 2.49 (m, 2 H), 2.49 - 2.34 (m, 2 H), 2.28 - 2.18 (m, 1 H), 2.07 - 1.94 (m,

3 H).  $^{13}\text{C}$  NMR (101MHz, CHLOROFORM-d)  $\delta$  = 172.0, 171.5, 169.2, 156.2, 143.9, 141.2, 137.5, 131.5, 127.6, 127.1, 127.0, 125.4, 119.8, 118.7, 115.2, 67.4, 66.2, 64.3, 59.1, 53.5, 47.0, 33.8, 29.1, 28.5, 24.9.

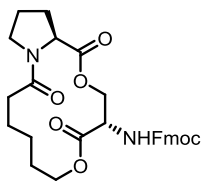
**Ring Closing Metathesis Reaction:** Ester **12** (491 mg, 0.9 mmol) was dissolved in DCM (300 mL) and heated to 40°C. Once at stable temperature, Grubbs second generation catalyst (42 mg, 0.05 mmol) was added and allowed to react for 2 hours. Upon completion, the reactions was concentrated *in vacuo* and the products were isolated by flash chromatography on silica gel with a 60-100% ethyl acetate in hexanes solvent gradient.



**(9H-fluoren-9-yl)methyl ((4S,16aS,Z)-1,5,12-trioxo-4,5,7,10,11,12,14,15,16,16a-decahydro-1H,3H-pyrrolo[2,1-c][1,11]dioxo[4]azacyclotetradecin-4-yl)carbamate (13a).** Yield 68.2 mg, 14%. HRMS (ESI) Predicted for  $[\text{C}_{29}\text{H}_{30}\text{N}_2\text{O}_7 + \text{H}]^+$ : 519.2131, Found: 519.2120.  $^1\text{H}$  NMR, minor rotameric effects, (400MHz, CHLOROFORM-d)  $\delta$  = 7.82 - 7.67 (m, 3 H), 7.46 - 7.37 (m, 2 H), 7.37 - 7.29 (m, 2 H), 6.85 (d,  $J$  = 9.6 Hz, 1 H), 6.05 - 5.83 (m, 1 H), 5.71 (dt,  $J$  = 4.4, 10.8 Hz, 1 H), 4.95 (dd,  $J$  = 3.5, 11.1 Hz, 1 H), 4.76 (dd,  $J$  = 8.1, 11.6 Hz, 1 H), 4.71 - 4.64 (m, 1 H), 4.60 (dd,  $J$  = 6.6, 11.6 Hz, 1 H), 4.55 - 4.44 (m, 2 H), 4.41 - 4.32 (m, 2 H), 4.32 - 4.21 (m, 1 H), 3.74 - 3.49 (m, 2 H), 3.13 (dtd,  $J$  = 2.1, 11.4, 13.9 Hz, 1 H), 2.63 (ddd,  $J$  = 2.8, 11.5, 14.0 Hz, 1 H), 2.50 (ddd,  $J$  = 2.7, 7.0, 14.1 Hz, 1 H), 2.38 - 2.16 (m, 2 H), 2.13 - 1.95 (m, 4 H).  $^{13}\text{C}$  NMR (101MHz, CHLOROFORM-d)  $\delta$  = 172.1, 171.6, 169.7, 156.3, 144.1, 143.9, 141.2, 136.4, 127.6, 127.5, 127.0, 126.9, 125.7, 125.5, 124.7, 119.8, 119.8, 67.3, 64.5, 60.4, 59.6, 54.0, 47.9, 47.1, 33.3, 29.3, 25.0, 24.5.



**(9H-fluoren-9-yl)methyl ((4S,16aS,E)-1,5,12-trioxo-4,5,7,10,11,12,14,15,16,16a-decahydro-1H,3H-pyrrolo[2,1-c][1,11]dioxo[4]azacyclotetradecin-4-yl)carbamate (13b).** Yield: 297 mg, 64%. HRMS (ESI) Predicted for  $[C_{29}H_{30}N_2O_7 + H]^+$ : 519.2131, Found: 519.2119.  $^1H$  NMR (400MHz, CHLOROFORM-d)  $\delta$  = 7.77 (d, J = 7.3 Hz, 2 H), 7.67 (t, J = 8.5 Hz, 2 H), 7.41 (t, J = 7.5 Hz, 2 H), 7.33 (dt, J = 3.2, 7.4 Hz, 2 H), 6.10 - 6.00 (m, 1 H), 5.97 - 5.85 (m, 1 H), 5.61 (td, J = 5.8, 15.6 Hz, 1 H), 4.82 (dd, J = 5.9, 12.3 Hz, 1 H), 4.70 - 4.59 (m, 3 H), 4.56 - 4.45 (m, 2 H), 4.45 - 4.33 (m, 2 H), 4.32 - 4.25 (m, 1 H), 3.71 - 3.58 (m, 1 H), 3.57 - 3.45 (m, 1 H), 2.69 - 2.49 (m, 2 H), 2.47 - 2.36 (m, 1 H), 2.31 - 2.22 (m, 1 H), 2.22 - 2.13 (m, 1 H), 2.13 - 2.04 (m, 2 H), 2.04 - 1.95 (m, 1 H).  $^{13}C$  NMR (101MHz, CHLOROFORM-d)  $\delta$  = 171.7, 170.9, 168.9, 155.9, 143.9, 143.8, 141.2, 134.7, 127.6, 127.1, 125.4, 125.3, 124.4, 119.9, 67.3, 65.0, 63.7, 59.0, 53.4, 47.1, 47.0, 33.8, 29.2, 26.6, 24.8.



**(9H-fluoren-9-yl)methyl ((4S,16aS)-1,5,12-trioxododecahydro-1H,3H-pyrrolo[2,1-c][1,11]dioxo[4]azacyclotetradecin-4-yl)carbamate (13c).** Macrocycle **13b** (233 mg, 0.45 mmol) was dissolved in MeOH (2 mL). To the solution was added 5% Pd/C (30 mg). The reaction was then sealed with a septum through which hydrogen gas was delivered via a syringe fixed to an  $H_2$  filled balloon. The atmosphere was allowed to purge with hydrogen for 1 minute, then allowed to react for 1 hour. Upon completion, the reaction was filtered through celite to remove the Pd/C. The filtrate was concentrated in vacuo and then the product was purified by flash

chromatography on silica gel with a 70-100% ethyl acetate in hexanes solvent gradient. Yield 138 mg, 57%. HRMS (ESI) Predicted for  $[C_{29}H_{32}N_2O_7 + H]^+$ : 521.2288, Found: 519.2281. <sup>1</sup>H NMR (600MHz, CHLOROFORM-d)  $\delta$  = 7.82 - 7.71 (m, 4 H), 7.43 - 7.37 (m, 2 H), 7.35 - 7.28 (m, 2 H), 6.67 (d, J = 9.9 Hz, 1 H), 5.12 (dd, J = 4.4, 11.0 Hz, 1 H), 4.74 - 4.67 (m, 1 H), 4.61 (dd, J = 5.5, 8.4 Hz, 1 H), 4.57 (ddd, J = 4.6, 6.4, 11.0 Hz, 1 H), 4.42 - 4.37 (m, 2 H), 4.35 - 4.29 (m, 2 H), 4.07 (ddd, J = 4.2, 7.9, 11.0 Hz, 1 H), 3.69 - 3.56 (m, 2 H), 2.51 (ddd, J = 3.3, 10.7, 14.2 Hz, 1 H), 2.38 (ddd, J = 3.7, 6.8, 14.1 Hz, 1 H), 2.28 (qd, J = 7.6, 12.5 Hz, 1 H), 2.14 - 2.07 (m, 1 H), 2.04 - 1.99 (m, 2 H), 1.93 - 1.85 (m, 1 H), 1.79 - 1.70 (m, 1 H), 1.70 - 1.56 (m, 3 H), 1.40 - 1.32 (m, 1 H). <sup>13</sup>C NMR (151MHz, CHLOROFORM-d)  $\delta$  = 173.0, 171.4, 170.2, 156.4, 144.2, 143.9, 141.3, 127.6, 127.5, 127.0, 127.0, 125.8, 125.5, 119.8, 119.8, 67.4, 64.3, 63.9, 59.5, 53.7, 47.8, 47.1, 33.3, 29.5, 26.2, 25.0, 23.6, 23.3

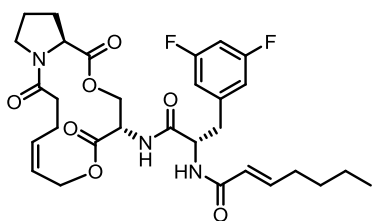
#### **Side Chain Synthesis General Procedure:**

*Fmoc removal:* A Fmoc-macrocycle (14a-c) (1 equivalent) was treated with 10% piperidine in DMF at a concentration of 0.1 M and allowed to react 30 minutes. Upon completion the DMF and piperidine were removed by short path vacuum distillation.

*Boc-Difluorophenylalanine acylation:* The deprotected macrocycle and Boc-Difluorophenylalanine (1.1 equivalents) were dissolved in DMF (2 mL) and treated with HATU (1.1 equivalents) and DIPEA (1.1 equivalents). The reaction was allowed to proceed for 3 hours after which the reaction was diluted with ethyl acetate (20 mL). The ethyl acetate solution was extracted 2 x 1M HCl<sub>aq</sub>, 1 x NaHCO<sub>3aq</sub>, and 1 x Brine, then dried over sodium sulfate. The product was purified by flash chromatography on silica gel with 80-100% ethyl acetate in hexanes.

*Boc-deprotection and E-2-heptenoic acid acylation:* The Boc-difluorophenylalanyl macrocycle was treated with 40% TFA in DCM at a concentration of 0.25 M. Upon complete conversion of

the starting material, the solvent was removed first by blowing with nitrogen then under high vacuum. Once dry, the Boc-protected difluorophenylalanyl macrocycle was dissolved in DMF to a concentration of 0.5 M and excess TFA was neutralized with DIPEA (determined gravimetrically). In a separate flask, E-2-heptenoic acid (1 equivalent) was dissolved in DMF to a concentration of 0.5 M and preactivated by treatment with HATU (1 equivalent) and DIPEA (1 equivalent). After 10 minutes, the preactivated acid solution was added to the solution containing Boc-protected difluorophenylalanyl macrocycle and allowed to react for 2 hours. Upon completion, the reaction was diluted with ethyl acetate (10 x original reaction volume) and extracted: 2 x 1M HCl<sub>aq</sub>, 2 x NaHCO<sub>3aq</sub>, and 1 x Brine, then dried over sodium sulfate. The product was purified by flash chromatography on silica gel with 100% ethyl acetate.



**(E)-N-((S)-3-(3,5-difluorophenyl)-1-oxo-1-(((4S,16aS,Z)-1,5,12-trioxo-**

**4,5,7,10,11,12,14,15,16,16a-decahydro-1H,3H-pyrrolo[2,1-c][1,11]dioxo[4]azacyclotetradecin-**

**4-yl)amino)propan-2-yl)hept-2-enamide (8a).** Yield: 14.7 mg, 20% over 4 steps. HRMS (ESI)

Predicted for [C<sub>30</sub>H<sub>37</sub>F<sub>2</sub>N<sub>3</sub>O<sub>7</sub> + H]<sup>+</sup>: 590.2678, Found: 590.2668. <sup>1</sup>H NMR (600MHz, Acetone-d<sub>6</sub>) δ

= 7.82 (d, J = 9.2 Hz, 1 H), 7.38 (d, J = 8.8 Hz, 1 H), 7.08 - 6.93 (m, 2 H), 6.90 - 6.81 (m, 1 H), 6.72

(td, J = 6.9, 15.2 Hz, 1 H), 6.03 (td, J = 1.5, 15.4 Hz, 1 H), 5.88 - 5.81 (m, 2 H), 4.97 (dd, J = 4.0,

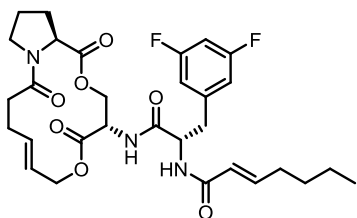
11.0 Hz, 1 H), 4.83 (dt, J = 5.0, 9.1 Hz, 1 H), 4.77 (ddd, J = 1.5, 4.0, 9.2 Hz, 1 H), 4.71 - 4.58 (m, 1

H), 4.53 - 4.45 (m, 1 H), 4.44 - 4.38 (m, 1 H), 4.26 (dd, J = 1.5, 11.0 Hz, 1 H), 3.83 (td, J = 6.7, 10.0

Hz, 1 H), 3.68 (td, J = 6.9, 10.0 Hz, 1 H), 3.33 (dd, J = 5.1, 13.9 Hz, 1 H), 3.02 - 2.92 (m, 2 H), 2.90 -

2.82 (m, 3 H), 2.44 - 2.39 (m, 1 H), 2.37 - 2.32 (m, 1 H), 2.32 - 2.25 (m, 1 H), 2.24 - 2.09 (m, 3 H),

2.09 - 2.05 (m, 2 H), 2.02 - 1.86 (m, 2 H), 1.45 - 1.37 (m, 2 H), 1.36 - 1.30 (m, 2 H), 0.89 (t, J = 7.3 Hz, 3 H). <sup>13</sup>C NMR (151MHz, Acetone-d<sub>6</sub>) δ = 173.9, 172.3, 171.1, 170.0, 165.7, 164.6, 164.5, 163.0, 162.9, 144.7, 138.5, 125.2, 125.0, 113.4, 113.4, 113.3, 113.2, 102.7, 102.5, 102.3, 64.8, 61.0, 60.3, 55.1, 52.6, 52.5, 49.2, 38.8, 34.1, 32.3, 31.3, 30.2, 25.8, 25.7, 23.0, 14.2.

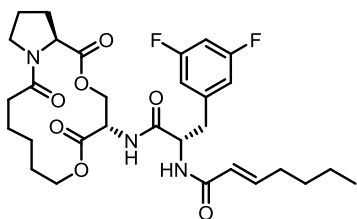


**(E)-N-((S)-3-(3,5-difluorophenyl)-1-oxo-1-(((4S,16aS,E)-1,5,12-trioxo-**

**4,5,7,10,11,12,14,15,16,16a-decahydro-1H,3H-pyrrolo[2,1-c][1,11]dioxazacyclotetradecin-**

**4-yl)amino)propan-2-yl)hept-2-enamide (8b).** Yield: 35.3 mg, 60% over 4 steps. HRMS (ESI)

Predicted for [C<sub>30</sub>H<sub>37</sub>F<sub>2</sub>N<sub>3</sub>O<sub>7</sub> + H]<sup>+</sup>: 590.2678, Found: 590.2670. <sup>1</sup>H NMR (600MHz, Acetone-d<sub>6</sub>) δ = 7.70 (d, J = 8.4 Hz, 1 H), 7.30 (d, J = 8.4 Hz, 1 H), 6.97 - 6.89 (m, 2 H), 6.84 (tt, J = 2.5, 9.3 Hz, 1 H), 6.72 (td, J = 7.0, 15.0 Hz, 1 H), 6.01 (td, J = 1.5, 15.3 Hz, 1 H), 5.77 (td, J = 6.8, 15.4 Hz, 1 H), 5.63 - 5.53 (m, 1 H), 4.86 - 4.78 (m, 2 H), 4.78 - 4.72 (m, 1 H), 4.46 - 4.42 (m, 1 H), 4.42 - 4.35 (m, 2 H), 4.35 - 4.32 (m, 1 H), 3.65 (t, J = 6.8 Hz, 2 H), 3.24 (dd, J = 5.3, 13.8 Hz, 1 H), 2.97 (dd, J = 8.8, 13.9 Hz, 1 H), 2.68 - 2.57 (m, 1 H), 2.53 - 2.42 (m, 1 H), 2.34 (ddd, J = 3.7, 6.2, 15.0 Hz, 1 H), 2.28 - 2.19 (m, 2 H), 2.15 (dq, J = 1.8, 7.2 Hz, 2 H), 2.12 - 2.05 (m, 2 H), 2.02 - 1.94 (m, 2 H), 1.44 - 1.36 (m, 2 H), 1.36 - 1.27 (m, 2 H), 0.89 (t, J = 7.2 Hz, 3 H). <sup>13</sup>C NMR (101MHz, Acetone-d<sub>6</sub>) δ = 172.5, 171.9, 171.3, 171.2, 169.6, 165.9, 165.0, 164.9, 162.6, 144.9, 143.4, 135.2, 125.5, 124.8, 113.4, 113.4, 113.2, 113.2, 102.6, 102.3, 65.1, 63.8, 60.4, 54.8, 52.4, 52.3, 48.1, 38.6, 34.2, 32.3, 31.3, 27.5, 25.6, 22.9, 14.2.



**(E)-N-((S)-3-(3,5-difluorophenyl)-1-oxo-1-(((4S,16aS)-1,5,12-trioxododecahydro-1H,3H-pyrrolo[2,1-c][1,11]dioxo[4]azacyclotetradecin-4-yl)amino)propan-2-yl)hept-2-enamide (8c).**

Yield: 80.9 mg, 68% over 4 steps. <sup>1</sup>H NMR (400MHz, CHLOROFORM-d) δ = 7.48 (d, J = 8.6 Hz, 1 H), 6.94 (d, J = 8.6 Hz, 1 H), 6.88 - 6.75 (m, 3 H), 6.63 (tt, J = 2.3, 9.1 Hz, 1 H), 5.90 (td, J = 1.4, 15.3 Hz, 1 H), 5.14 (dd, J = 4.0, 11.4 Hz, 1 H), 4.91 (dt, J = 5.2, 8.5 Hz, 1 H), 4.86 (dd, J = 3.0, 8.6 Hz, 1 H), 4.50 (td, J = 5.4, 10.9 Hz, 1 H), 4.41 (dd, J = 4.8, 8.1 Hz, 1 H), 4.25 (dd, J = 1.0, 11.1 Hz, 1 H), 4.08 - 3.99 (m, 1 H), 3.62 (t, J = 6.3 Hz, 2 H), 3.31 (dd, J = 5.1, 14.1 Hz, 1 H), 3.00 (dd, J = 8.3, 14.1 Hz, 1 H), 2.51 (ddd, J = 2.9, 10.7, 13.9 Hz, 1 H), 2.33 - 2.23 (m, 2 H), 2.19 - 2.11 (m, 2 H), 2.09 - 1.97 (m, 3 H), 1.93 - 1.77 (m, 2 H), 1.69 - 1.48 (m, 3 H), 1.44 - 1.35 (m, 2 H), 1.35 - 1.28 (m, 2 H), 1.28 - 1.18 (m, 1 H), 0.95 - 0.83 (m, 3 H). <sup>13</sup>C NMR (101MHz, CHLOROFORM-d) δ = 173.3, 171.6, 170.3, 169.3, 165.9, 164.1, 163.9, 161.6, 161.5, 145.6, 141.2, 141.2, 141.1, 123.0, 112.3, 112.3, 112.2, 112.1, 102.3, 102.1, 101.8, 64.1, 63.2, 59.7, 54.0, 51.9, 48.1, 37.8, 33.3, 31.8, 30.3, 29.4, 25.8, 25.0, 23.4, 22.9, 22.2, 13.8.

## References

- Schreiber, S. L. Target-oriented and diversity-oriented organic synthesis in drug discovery. *Science* **2000**, *287*, 1964-1969.
- Burke, M. D.; Schreiber, S. L. A Planning Strategy for Diversity-Oriented Synthesis. *Angewandte Chemie International Edition* **2004**, *43*, 46-58.
- O'Connor, C. J.; Beckmann, H. S.; Spring, D. R. Diversity-oriented synthesis: producing chemical tools for dissecting biology. *Chem. Soc. Rev.* **2012**, *41*, 4444-4456.
- Dömling, A.; Ugi, I. Multicomponent Reactions with Isocyanides. *Angewandte Chemie International Edition* **2000**, *39*, 3168-3210.

5. Dömling, A. Recent Developments in Isocyanide Based Multicomponent Reactions in Applied Chemistry. *Chem. Rev.* **2006**, *106*, 17-89.
6. Passerini, M.; Simone, L. *Gazz. Chim. Ital.* **1921**, *51*, 126-129.
7. Ugi, I.; Meyr, R. Neue Darstellungsmethode für Isonitrile. *Angewandte Chemie* **1958**, *70*, 702-703.
8. Versammlungsberichte. *Angewandte Chemie* **1959**, *71*, 373-388.



## Chapter 10 – Fragment based potentiation of ADEP antibacterial activity.

### Background

The underlying motivation for the research described in this thesis dissertation is the problem of antibacterial drug resistance. In previous chapters, we have extensively discussed medicinal chemistry studies directed towards the ADEPs, a new class of antibacterial agents that have a mechanism of action that is distinct from all clinically used antibacterial drugs. The discovery of new classes of antibacterial agents will continue to be an essential area of scientific research. However, there may also be opportunities to restore or potentiate the activity of antibacterial drugs that are becoming obsolete due to resistance.

A major component of multidrug resistant phenotypes is the presence of membrane-bound efflux pumps.<sup>1-6</sup> With nearly all classes of antibacterial compounds known to be substrates of one or more efflux pumps<sup>1,2,4,5,7,8</sup>, drug efflux is a major challenge in antibacterial therapy. Many efflux pumps exhibit promiscuous substrate selectivity and can even export molecules from unrelated structural classes.<sup>1-3,9</sup> Given the significance of efflux pumps in many multidrug resistant phenotypes of pathogenic bacteria, there is much interest in either circumventing or directly inhibiting their activity. The former strategy typically focuses on developing new analogues of existing antibacterial agents that are poor substrates of efflux pumps<sup>10,11</sup>, while the latter is focused on identifying efflux pump inhibitors.<sup>7,12-16</sup> A new and unexplored strategy is elucidation of efflux recognition elements within a given antibacterial compound and designing fragments that are strongly recognized by the key efflux pump. If a simple fragment of a bioactive molecule is preferentially recognized by an efflux pump, then the presence of this fragment should preclude export of its bioactive counterpart by competing for occupancy of the efflux pump.

The ADEPs themselves offer an intriguing opportunity to test this fragment based potentiation strategy. It was recently reported that ADEP resistance in *Streptomyces* is partially mediated by the efflux pump SclAB.<sup>17</sup> Additionally, Parish and co-workers recently reported that ADEPs are toxic to *Mycobacterium tuberculosis*.<sup>18</sup> However, low MICs were only realized when the ADEPs were used in combination with efflux pump inhibitors. The identities of specific efflux pumps in *M. tuberculosis* that recognize and export the ADEPs have not yet been elucidated. In light of these results, we reasoned that an ADEP would serve as a good system with which to test our hypothesis that a small ADEP fragment could be used to potentiate ADEP antibacterial activity in *Streptomyces* and *Mycobacteria*.

## Results

In the same manner as in chapter 6, we designed and synthesized a collection of molecular fragments based on the structure of a known synthetic ADEP (**1**). To test their ability to potentiate ADEP activity, these fragments were combined at a 2.5 : 1, 5 : 1, 10 : 1, or 20 : 1 molar ratio with the parent ADEP (**1**) and the minimum inhibitory concentration (MIC) for each mixture was measured in the model Actinomycete, *Streptomyces coelicolor* (Figure 10.1). Importantly, none of the ADEP fragments exhibited antibacterial activity by themselves at the concentrations tested for potentiation activity. Fragments composed primarily of the ADEP peptidolactone (**2-3**) or just a portion of the side chain (**4**) exhibited no potentiation activity. To our delight, one fragment, a methyl ester of the *N*-E-2-heptenoyldifluorophenylalanine side chain (**5**), was able to potentiate the activity of ADEP **1** against *S. coelicolor* in a molar ratio dependent manner (Figure 10. 1). At a 20:1 molar ratio with **5**, the ADEP **1** MIC was 44% lower than the MIC of ADEP **1** alone. Although we have shown that **5** exhibits antibacterial activity against *B. subtilis*, **5** is 500 fold less potent than ADEP **1**. It is therefore unlikely that the apparent reduction in ADEP MIC in *S. coelicolor* is due to ClpP activation by **5**.

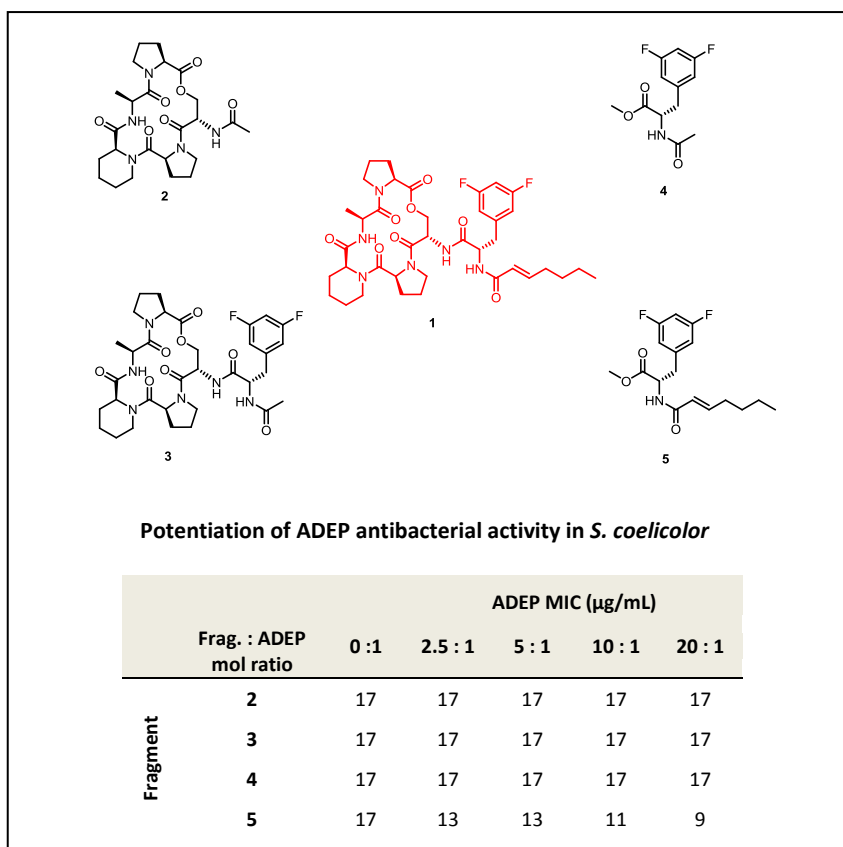


**Figure 10.1 – Potentiation of ADEP antibacterial activity in *S. coelicolor* by various fragments.** Mixtures of ADEP 1 and each fragment were combined at the indicated molar ratios. The *S. coelicolor* MIC with respect to each ADEP was determined by the agar dilution method. Fragment 5 exhibits a molar ratio dependent potentiation of ADEP antibacterial activity.

Using a positional scanning approach, we set out to optimize the *N*-acyldifluorophenylalanine fragment's ability to potentiate ADEP antibacterial activity in *S. coelicolor* (Figure 2, Table 1). First, the *N*-terminal acyl group was varied to include straight chain and cyclic structures, as well as variations in the degree of unsaturation. In total, analogs of **5** with five different *N*-terminal acyl groups (**6-10**) were synthesized and tested for potentiation activity. Interestingly, none of the *N*-terminal acyl group analogs other than **5** exhibited ADEP potentiation activity. This includes fragment **10**, which bears the polyunsaturated *N*-acyl group that is found in ADEP natural products.<sup>19</sup> It is curious that an element of the natural ADEPs is not strongly recognized by the ADEP efflux pump(s). This is perhaps a consequence of the intrinsic chemical instability of the triene moiety in **10**.<sup>20</sup> Next, we sought to identify the structural

requirements of the amino acid residue for efflux recognition. Substitution of phenylalanine (**11**) in place of difluorophenylalanine retained weak potentiation activity, whereas substitution of leucine (**12**) for difluorophenylalanine completely abolished potentiation activity. This is a clear indication that fragment based potentiation requires that the fragment must maintain significant structural similarities to its parent in order to be an effective potentiator.

In a final set of fragment **5** analogs, the C-terminal functional group was varied. In total, analogs with five different functionalities were synthesized and tested for ADEP potentiation activity. The C-terminal functional groups of these analogs included, a carboxylic acid (**13**), primary (**14**), secondary (**15**), and tertiary (**16**) amides, and a benzyl ester (**17**). Most of these analogs with varied C-terminal functional groups were unable to potentiate ADEP activity. However, significantly improved ADEP potentiation activity was observed when the methyl ester functionality (**3**) was changed to either a primary amide (**14**) or a secondary *N*-methylamide (**15**). At a 20:1 molar ratio, both fragments **14** and **15** individually lowered the MIC of ADEP **1** by 67%. Both of these analogs have hydrogen bond donors at their C-termini, which may be an important functionality for efflux pump recognition. Fragment **15** appeared to be slightly more effective than **14** at lower molar ratios, so **15** was chosen as our lead potentiator for subsequent experiments.

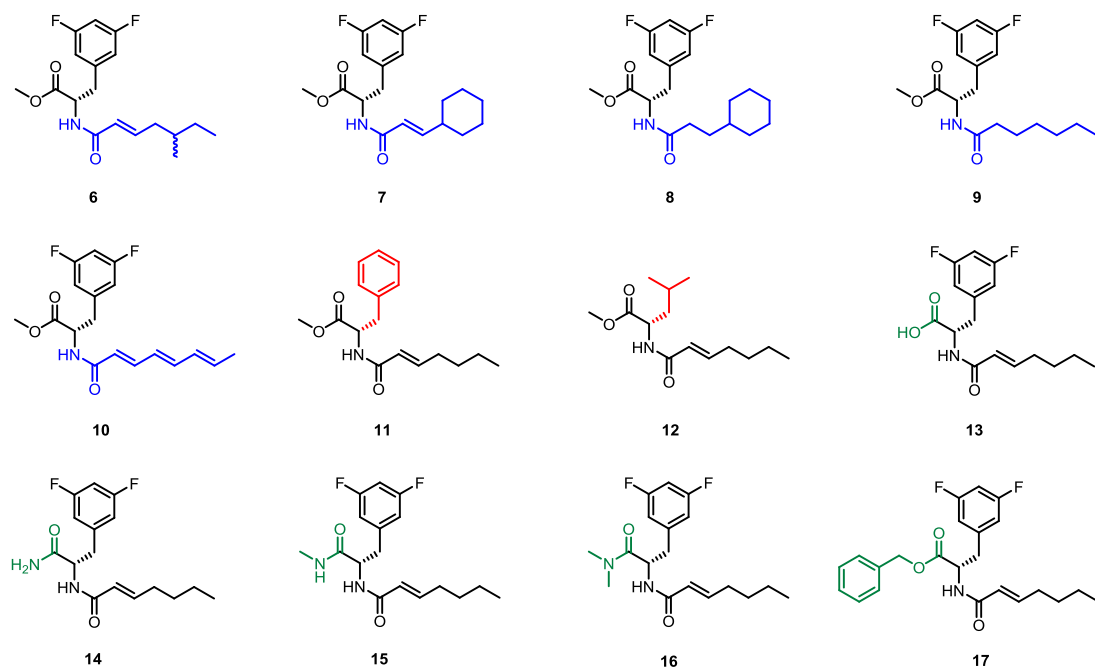


Figure 10.2 - Structures of *N*-acyldifluorophenylalanine analogs. *N*-terminal acyl group variants highlighted in blue, amino acid variants highlighted in red, C-terminal functional group variants highlighted in green.

Table 10.1 - Potentiation of ADEP antibacterial activity in *S. coelicolor* by *N*-acyldifluorophenylalanine analogs

	Frag. : ADEP mol ratio	ADEP MIC ( $\mu\text{g}/\text{mL}$ )				
		0 : 1	2.5 : 1	5 : 1	10 : 1	20 : 1
Compound	6	17	17	17	17	17
	7	17	17	17	17	17
	8	17	17	17	17	17
	9	17	17	17	17	17
	10	17	17	17	17	17
	11	17	17	17	13	13
	12	17	17	17	17	17
	13	17	17	17	17	17
	14	17	15	11	7.5	5.6
	15	17	13	9.4	7.5	5.6
	16	17	17	17	17	17
	17	17	17	17	17	17
	Reserpine	17	17	17	11	9.4

Mixtures of ADEP 1 and each fragment were combined at the indicated molar ratios. The *S. coelicolor* MIC with respect to each ADEP was determined by the agar dilution method.

While the fragment based potentiation strategy appears to be remarkably effective against *S. coelicolor*, questions remained about the specificity of this approach. We were curious to know if ADEP fragments could be used to potentiate the activity of other antibacterial compounds with known efflux pump mediated resistance in Streptomyces. The MICs of two antibacterial agents with known efflux mediated resistance in *S. coelicolor* were determined in the presence and absence of 50 µg/mL of fragment **15** (Table 10.2).<sup>21</sup> Fragment **15** did not potentiate the activity of either Chloramphenicol or Spiramycin, which suggests that either these compounds are not affected by the same efflux pumps as the ADEPs or that the fragments are specific for potentiating ADEPs. This result corroborates our finding from the SAR studies that fragments must resemble its parent compound in order to potentiate the parent compound's biological activity.

**Table 10.2 – Potentiation activity of fragment 15 toward various antibacterial agents.**

Compound	ADEP MIC (µg/mL)	
	-Fragment 15	+ Fragment 15
ADEP	18	10
Chloramphenicol	80	80
Spiramycin	225	225

The MICs of various antibacterial agents against *S. coelicolor* were calculated in the presence and absence of 50 µg/mL compound **14**

Although *S. coelicolor* is a useful model organism, it is not pathogenic to humans and is not medically relevant. We therefore wished to study our fragment based potentiation strategy in Mycobacteria. *M. tuberculosis*, the causative agent of the disease, tuberculosis, is one of the most problematic human bacterial pathogens facing modern medicine. Tuberculosis is the cause of nearly 2 million deaths worldwide each year and it is estimated that one third of the world's population is infected with a latent form of the disease.<sup>22</sup> Additionally, multidrug resistant forms of MTB are emerging with increasing frequency.<sup>23</sup> There is a critical need for new drug targets

and new classes of antibacterial agents to treat this infectious disease. Since it has recently been reported that *M. tuberculosis* is susceptible to ClpP activation and that ADEP resistance in these bacteria is mediated by efflux pumps,<sup>18</sup> we hypothesized that these *Mycobacteria* would be susceptible to fragment based ADEP potentiation.

To test this hypothesis, our lead fragment potentiator (**15**), and the known efflux pump inhibitor, reserpine,<sup>16,18,24</sup> were evaluated for their ability to potentiate ADEP activity in *Mycobacteria* (Table 10.2). In these experiments, ADEP MICs were determined with fixed concentrations of the potentiators. Against *M. smegmatis*, the lead potentiator (**15**) was a more effective ADEP potentiator than reserpine at high concentrations. Against *M. tuberculosis*, **15** was a more effective ADEP potentiator than reserpine at all concentrations. Overall the fragment based potentiation strategy was very effective against mycobacteria. At its highest concentration (50 µg/mL) fragment **15** lowered the ADEP MIC by 75% against *M. smegmatis* and by 80% against *M. tuberculosis*.

**Table 10.3 - Potentiation of ADEP antibacterial activity in *Mycobacteria***

Compound	Potentiator Conc. (µg/mL)	ADEP MIC (µg/mL)							
		<i>M. smegmatis</i>				<i>M. tuberculosis</i>			
		0	12.5	25	50	0	12.5	25	50
	Reserpine	120	75	75	60	50	40	40	40
	<b>15</b>	120	90	75	30	50	20	20	10

ADEP MICs were determined in the presence of fixed concentrations of a potentiator. *M. smegmatis* MICs were determined by the agar dilution method. *M. tuberculosis* MICs were determined by the agar dilution method.

## Conclusions

Herein we report an original and versatile strategy to circumvent resistance caused by drug efflux. A key feature of this strategy is that it is unnecessary to identify the the efflux

pump(s) that act on the small-molecule therapeutic of interest. Historically, efflux has been combated with combination therapies involving efflux pump inhibitors.<sup>7,7,11-16,24,25</sup> Led by MPEX pharmaceuticals, several of these EPIs have progressed into clinical trials.<sup>13</sup> Our fragment based approach represents a fundamentally new strategy to for circumventing the action of efflux pumps. We have shown that ADEP activity against *Streptomyces* and *Mycobacteria* can be significantly improved when used in combination with fragments that are selectively recognized by the efflux pumps that normally export ADEP. We have shown, via an extensive SAR study, that fragments must bear close resemblance to their parent compound in order to effectively potentiate the parent's biological activity. This is corroborated by the finding that ADEP fragments do not potentiate Chloramphenicol or Spiramycin antibacterial activity in *S. coelicolor*. In principle, this approach should be generalizable to all small molecule therapeutics that are acted on by efflux pumps. Access to the efflux recognition elements of any bioactive small-molecule should enable specific potentiation of their biological effects. This new approach for circumventing efflux mediated resistance will undoubtedly prove useful in a wide range of therapeutic applications.

### Experimental Contributions

Chemical synthesis of all compounds was completed by Daniel Carney. All biological evaluation was performed by Brown University Graduate Student, Corey Compton.

### Experimental Procedures

**Strains, Media and Culture Conditions.** *Streptomyces coelicolor* M145 was grown at 30 °C on mannitol soya flour medium (SFM), Difco nutrient agar medium (DNA), yeast extract-malt extract medium (YEME), or minimal liquid medium (NMMP).<sup>26</sup> *Mycobacterium smegmatis* MC2155 was grown in Luria–Bertani medium supplemented with 0.2% (v/v) glycerol at 37 °C.



*Mycobacterium tuberculosis* H37Rv was maintained in Middlebrook 7H9 broth supplemented with 0.2% (v/v) glycerol, 0.05% Tween 80, and 10% (v/v) oleic acid-albumin-dextrose-catalase.

**MIC assays.** *S. coelicolor* M145 MIC assays were performed on Difco nutrient agar medium supplemented with the indicated concentrations of compound. Growth was assessed after incubation at 30°C for 48 h. The lowest drug concentration that inhibited  $\geq 90\%$  growth was considered to be the MIC.

*Mycobacterium smegmatis* MIC assays were performed on Difco nutrient agar medium supplemented with 0.2% glycerol and the indicated concentrations of compound. Growth was assessed after incubation at 30°C for 72 h. The lowest drug concentration that inhibited  $\geq 90\%$  growth was considered to be the MIC.

To determine the MICs of compounds for *M. tuberculosis*, OD600-based assays were used. Bacteria were grown to midlog phase and plated in 96-well plates at OD600 = 0.025 in the presence of small molecule inhibitors for indicated time periods, and growth was assessed by reading OD600. The MIC value was determined as the lowest concentration that inhibited growth by  $>90\%$  relative to the DMSO control

***For Chemical synthesis of ADEP Fragments, see chapter 8.***

## References

1. Poole, K. Efflux-mediated antimicrobial resistance. *J. Antimicrob. Chemother.* **2005**, *56*, 20-51.
2. Webber, M. A.; Piddock, L. J. The importance of efflux pumps in bacterial antibiotic resistance. *J. Antimicrob. Chemother.* **2003**, *51*, 9-11.
3. Lomovskaya, O.; Zgurskaya, H. I.; Totrov, M.; Watkins, W. J. Waltzing transporters and 'the dance macabre' between humans and bacteria. *Nature reviews Drug discovery* **2007**, *6*, 56-65.

4. Mahamoud, A.; Chevalier, J.; Alibert-Franco, S.; Kern, W. V.; Pages, J. M. Antibiotic efflux pumps in Gram-negative bacteria: the inhibitor response strategy. *J. Antimicrob. Chemother.* **2007**, *59*, 1223-1229.
5. Nikaido, H. Broad-specificity efflux pumps and their role in multidrug resistance of Gram-negative bacteria. *FEMS Microbiol. Rev.* **2012**, *36*, 340-363.
6. Rouveix, B. Clinical implications of multiple drug resistance efflux pumps of pathogenic bacteria. *J. Antimicrob. Chemother.* **2007**, *59*, 1208-1209.
7. Lomovskaya, O.; Warren, M. S.; Lee, A.; Galazzo, J.; Fronko, R.; Lee, M.; Blais, J.; Cho, D.; Chamberland, S.; Renau, T.; Leger, R.; Hecker, S.; Watkins, W.; Hoshino, K.; Ishida, H.; Lee, V. J. Identification and characterization of inhibitors of multidrug resistance efflux pumps in *Pseudomonas aeruginosa*: novel agents for combination therapy. *Antimicrob. Agents Chemother.* **2001**, *45*, 105-116.
8. Poirel, L.; Bonnin, R. A.; Nordmann, P. Analysis of the resistome of a multidrug-resistant NDM-1-producing *Escherichia coli* strain by high-throughput genome sequencing. *Antimicrob. Agents Chemother.* **2011**, *55*, 4224-4229.
9. Wong, K.; Ma, J.; Rothnie, A.; Biggin, P. C.; Kerr, I. D. Towards understanding promiscuity in multidrug efflux pumps. *Trends Biochem. Sci.* **2014**, *39*, 8-16.
10. Testa, R. T.; Petersen, P. J.; Jacobus, N. V.; Sum, P. E.; Lee, V. J.; Tally, F. P. In vitro and in vivo antibacterial activities of the glycylcyclines, a new class of semisynthetic tetracyclines. *Antimicrob. Agents Chemother.* **1993**, *37*, 2270-2277.
11. Ince, D.; Zhang, X.; Silver, L. C.; Hooper, D. C. Dual targeting of DNA gyrase and topoisomerase IV: target interactions of garenoxacin (BMS-284756, T-3811ME), a new desfluoroquinolone. *Antimicrob. Agents Chemother.* **2002**, *46*, 3370-3380.
12. Renau, T. E.; Léger, R.; Flamme, E. M.; Sangalang, J.; She, M. W.; Yen, R.; Gannon, C. L.; Griffith, D.; Chamberland, S.; Lomovskaya, O. Inhibitors of Efflux Pumps in *Pseudomonas aeruginosa* Potentiate the Activity of the Fluoroquinolone Antibacterial Levofloxacin. *J. Med. Chem.* **1999**, *42*, 4928-4931.
13. Renau, T. E.; Léger, R.; Flamme, E. M.; She, M. W.; Gannon, C. L.; Mathias, K. M.; Lomovskaya, O.; Chamberland, S.; Lee, V. J.; Ohta, T. Addressing the stability of C-capped dipeptide efflux pump inhibitors that potentiate the activity of levofloxacin in *Pseudomonas aeruginosa*. *Bioorg. Med. Chem. Lett.* **2001**, *11*, 663-667.
14. Nelson, M. L.; Park, B. H.; Levy, S. B. Molecular requirements for the inhibition of the tetracycline antiport protein and the effect of potent inhibitors on the growth of tetracycline-resistant bacteria. *J. Med. Chem.* **1994**, *37*, 1355-1361.

15. Okandeji, B. O.; Greenwald, D. M.; Wroten, J.; Sello, J. K. Synthesis and evaluation of inhibitors of bacterial drug efflux pumps of the major facilitator superfamily. *Bioorg. Med. Chem.* **2011**, *19*, 7679-7689.
16. Stavri, M.; Piddock, L. J.; Gibbons, S. Bacterial efflux pump inhibitors from natural sources. *J. Antimicrob. Chemother.* **2007**, *59*, 1247-1260.
17. Gominet, M.; Seghezzi, N.; Mazodier, P. Acyl depsipeptide (ADEP) resistance in *Streptomyces*. *Microbiology* **2011**, *157*, 2226-2234.
18. Ollinger, J.; O'Malley, T.; Kesicki, E. A.; Odingo, J.; Parish, T. Validation of the essential ClpP protease in *Mycobacterium tuberculosis* as a novel drug target. *J. Bacteriol.* **2012**, *194*, 663-668.
19. Michel, K. H.; Kastner, R. E. *A54556 antibiotics and process for production thereof* **1985**.
20. Hinzen, B.; Raddatz, S.; Paulsen, H.; Lampe, T.; Schumacher, A.; Häbich, D.; Hellwig, V.; Benet-Buchholz, J.; Endermann, R.; Labischinski, H.; Brötz-Oesterhelt, H. Medicinal Chemistry Optimization of Acyldepsipeptides of the Enopeptin Class Antibiotics. *ChemMedChem* **2006**, *1*, 689-693.
21. Vecchione, J. J.; Sello, J. K. Characterization of an inducible, antibiotic-resistant aminoacyl-tRNA synthetase gene in *Streptomyces coelicolor*. *J. Bacteriol.* **2008**, *190*, 6253-6257.
22. Anonymous Global Tuberculosis Control 2010. **2010**.
23. Gandhi, N. R.; Nunn, P.; Dheda, K.; Schaaf, H. S.; Zignol, M.; Van Soolingen, D.; Jensen, P.; Bayona, J. Multidrug-resistant and extensively drug-resistant tuberculosis: a threat to global control of tuberculosis. *The Lancet* **2010**, *375*, 1830-1843.
24. Schmitz, F. J.; Fluit, A. C.; Luckefahr, M.; Engler, B.; Hofmann, B.; Verhoef, J.; Heinz, H. P.; Hadding, U.; Jones, M. E. The effect of reserpine, an inhibitor of multidrug efflux pumps, on the in-vitro activities of ciprofloxacin, sparfloxacin and moxifloxacin against clinical isolates of *Staphylococcus aureus*. *J. Antimicrob. Chemother.* **1998**, *42*, 807-810.
25. Markham, P. N.; Neyfakh, A. A. Inhibition of the multidrug transporter NorA prevents emergence of norfloxacin resistance in *Staphylococcus aureus*. *Antimicrob. Agents Chemother.* **1996**, *40*, 2673-2674.
26. Kieser, T. Practical streptomyces genetics. **2000**.

## Chapter 11 – Antibacterial Phenylcyclohexane Carboxylates (PCHCs).

### Introduction

As discussed in previous chapters, the discovery of ClpP as an antibacterial drug target<sup>1-4</sup> has encouraged efforts to find new structural classes of ClpP activators that are distinct from the ADEPs. Leung *et al.* recently reported the results of a high throughput screen (HTS) for ClpP activators.<sup>5</sup> Using a fluorescence based assay that measured compounds' capacities to activate *E. coli* ClpP-mediated degradation of fluorescein isothiocyanate (FITC) labeled casein *in vitro*. The fluorescence of FITC labeled casein is internally quenched, but quenching is relieved upon hydrolysis of the protein into smaller peptide fragments. From a diverse collection of ~60,000 drug like compounds, 5 hits termed **ACP1-5 (Activators of self-Compartmentalizing Proteases)** were identified (Figure 11.1A). Each "hit" was then independently validated to activate ClpP mediated degradation of FITC labeled casein in a dose dependent manner (Figure 11.1B). What was most intriguing about these ClpP activators was that docking studies suggested that they allbind to ClpP at a site that is distinct that to which the ADEPs bind.

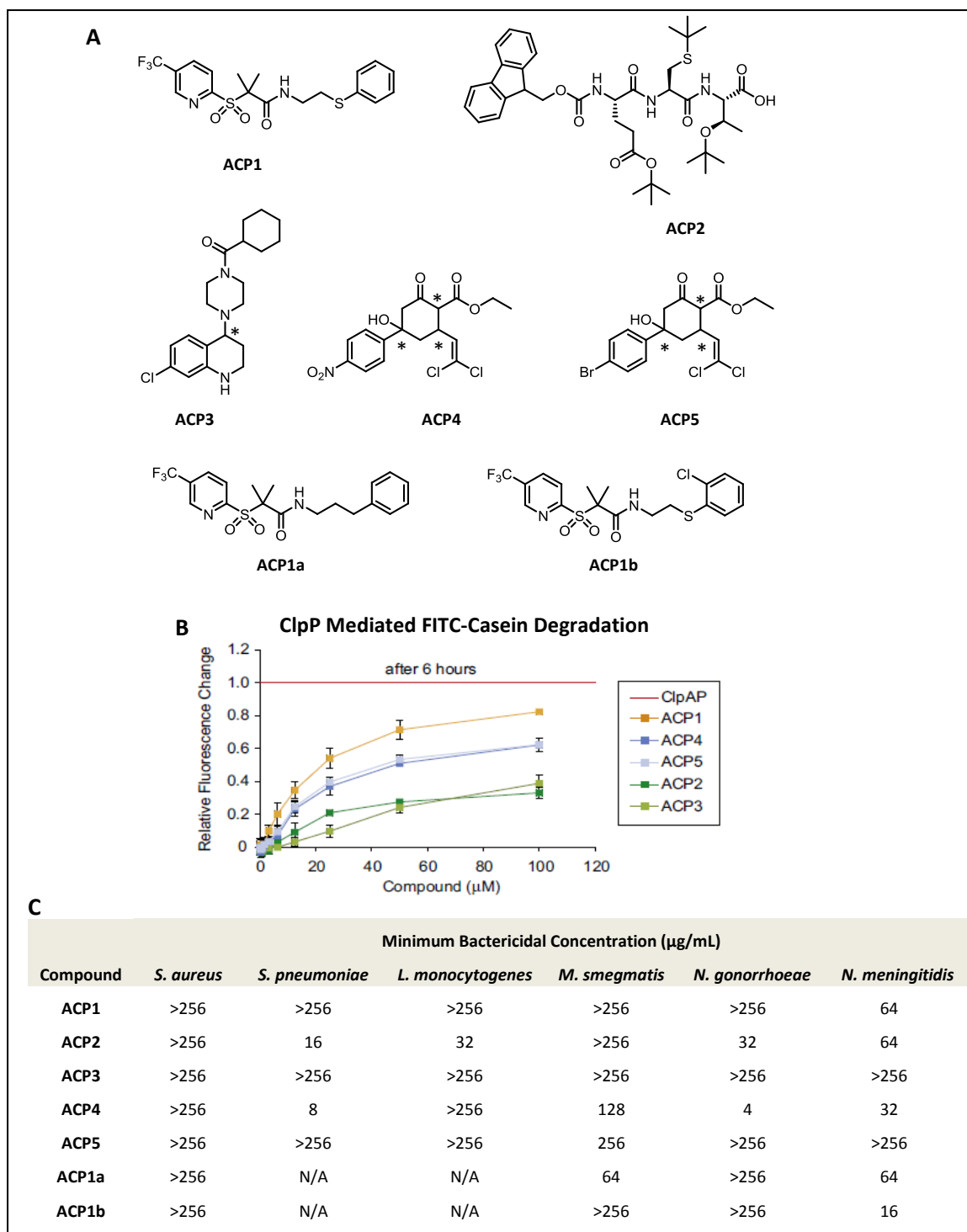


Figure 11.1 – Activators of self-Compartmentalized Proteases (ACPs) identified in HTS<sup>5</sup> A) Structures of HTS hit compounds. Neither absolute nor relative stereochemistry was indicated for chiral compounds ACP3-5. \* Indicates stereocenters of unknown configuration. B) ClpP mediated FITC-Casein Degradation: Compounds at varying concentrations were incubated at with ClpP and FITC labeled casein. The change in fluorescence due to FITC labeled casein degradation over 6 hours was measured and compared to the change in fluorescence over 6 hours associated with FITC labeled casein degradation by the proteolytically active complex (ClpAP) of ClpP and AAA+ partner ClpA. C) Selected minimum bactericidal concentrations of ACP compounds.

While the ACP hits were all able to activate ClpP *in vitro*, antibacterial activity was generally low with only a few exceptions (Figure 11.1C). Due to its high activity *in vitro*, high satisfaction of Lipinski's rules,<sup>6,7</sup> and ease of synthesis, Leung *et al.* selected **ACP1** for drug lead development and also reported the synthesis and evaluation of additional analogs, two of which (Figure 11.1A) exhibited slightly improved antibacterial activity. Despite exhibiting the best overall antibacterial activity, **ACP2** was rejected for lead development because small protected peptides do not typically perform well as drugs.<sup>8-11</sup> Like **ACP1**, **ACP3** also possesses a drug-like structure that satisfies Lipinski's rules. However, it was rejected because of its modest ClpP activation activity *in vitro* and complete lack of antibacterial activity. Lastly, **ACP4** and **ACP5** were rejected for lead development despite exhibiting relatively strong ClpP activation *in vitro* and modest antibacterial activity because their synthesis is a challenge. Since their disclosure, no further developments of the ACP compounds have been reported.

Upon reviewing the disclosure of the ACP compounds by Leung *et al.*, we were in fact quite interested in the phenylcyclohexane carboxylates (PCHCs), **ACP4** and **ACP5**. The reported antibacterial activity of these hit compounds was indeed significant enough to warrant lead development. Given our interests in ClpP activators, we were also interested in studying compounds with a potentially unique mode of ClpP activation. We anticipated that the syntheses of **ACP4** and **ACP5** would be more challenging than **ACP1**, but not restrictively so. We envisioned that the PCHC core structure (**1**) could be constructed via Robinson annulation<sup>12,13</sup> from an  $\alpha,\beta$ -unsaturated-phenylketone (**2**) and ethylacetoacetate (**3**).  $\alpha,\beta$ -unsaturated-phenylketones could be prepared via crossed aldol condensation of an acetophenone (**4**) and a non-enolizable aldehyde (**5**). This synthetic scheme (Figure 11.2) opens the door to diversity oriented synthesis of PCHCs that could be evolved in SAR studies. Indeed, a wide variety of

acetophenones and non-enolizable aldehydes could be used to diversify the functionality on the PCHP phenyl group ( $R_1$ ) and at the cyclohexanone C-3 ( $R_2$ ), respectively.

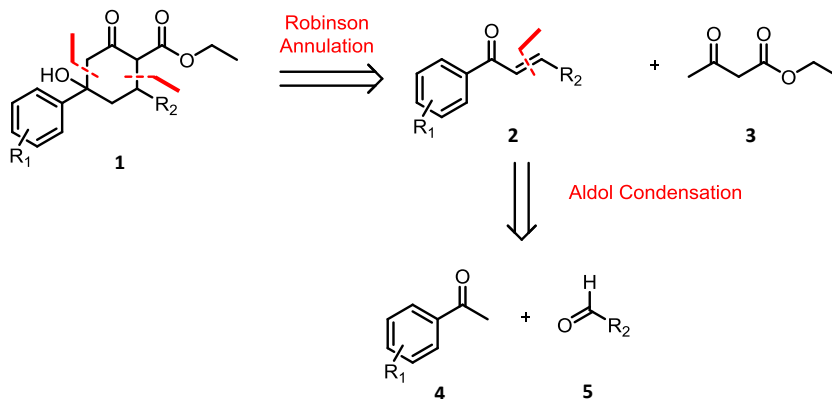


Figure 11.2 – Retrosynthesis of phenylcyclohexane carboxylates

While many non-enolizable vinylic and aromatic aldehydes are commercially available, Synthesis of **ACP4** and **ACP5** requires dichloroacrolein<sup>14</sup> (**6**), a previously reported, but non-commercially available aldehyde. Dichloroacrolein was synthesized on multi-gram scale in a one-pot two-step procedure from isobutyl vinyl ether (**7**) (Figure 11.3). First, **7** was refluxed with catalytic benzoyl peroxide in carbon tetrachloride for 48 hours forming the radical addition product (**8**). After removal of the excess carbon tetrachloride *in vacuo*, **8** was pyrolyzed by gradual heating from 170C-220°C, over the course of which a distillate was collected composed of a mixture of dichloroacrolein (**6**) and isobutylchloride byproduct (**9**). Dichloroacrolein was ultimately isolated by fractional distillation.

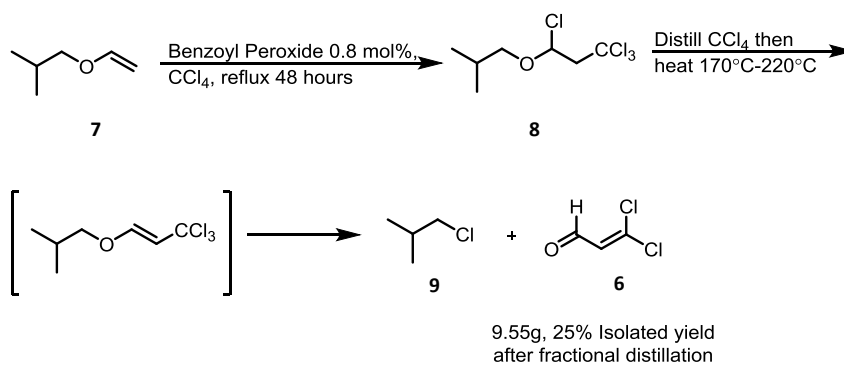


Figure 11.3 – Synthesis of dichloroacrolein

For the diversity-oriented synthesis of PCHC analogs (Figure 4), acetophenones (**4**) were condensed with **6** or other commercially available aldehydes (**5**) under acidic conditions and then engaged in a sodium ethoxide promoted Robinson annulation with **3** forming PCHC analogs as single diastereomers. Isolation of the annulation products (**1**) was complicated by facile  $\beta$ -elimination of the C-5 hydroxyl group under both basic and acidic conditions. This problem was circumvented by keeping reaction durations short (<2 hours) thus minimizing product exposure to sodium ethoxide and also by chromatographing the products on deactivated silica gel. Using this procedure, visiting researcher Dele Olubanwo synthesized a library of PCHC analogs in order to probe structure activity relationships.

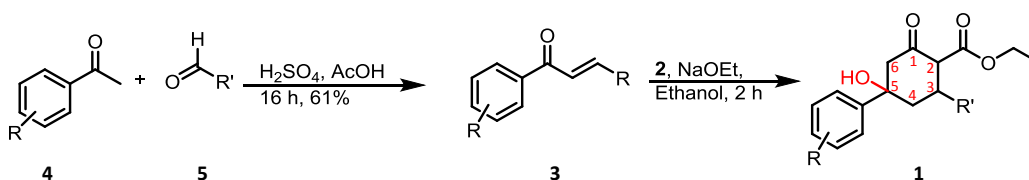


Figure 11.4 – Synthesis of phenylcyclohexyl carboxylates

One bioactive PCHC analog (**1a**), was selected for in-depth NMR analysis in order to solve the unresolved issue of relative stereochemistry, which was never addressed in the report by Leung *et al.* First, a full assignment of the  $^1\text{H-NMR}$  spectrum (Figure 11.5) was facilitated by analysis of the 2-D COSEY and HSQC spectra (see appendix). The first important piece of stereochemical information that could be gleaned from the  $^1\text{H-NMR}$  spectrum is the large



coupling constant for the protons g and f ( $J_{gf} = 11.7\text{-}11.9$  Hz), which is indicative of a *trans*-diaxial relationship. Since there are no protons bonded directly to C-5, the stereochemistry at this center relative to C-1 and C-2 could not be determined directly from  $^1\text{H-NMR}$  coupling constants. It was therefore necessary to use Nuclear Overhauser Effect (NOE) correlations in order to determine the stereochemistry at C-5. First, we needed to determine which signals in the  $^1\text{H-NMR}$  spectrum corresponded to the axial protons as well as which signals corresponded to the equatorial protons on C-4 and C-6. In the  $^1\text{H-NMR}$  spectrum, we observe a 4-bond coupling interaction between proton-b and proton-d ( $J_{bd} = 2.2$  Hz). This is a classic long range coupling interaction that is typically observed between equatorial protons that are separated by 4 bonds on a conformationally constrained 6-membered ring. It was additionally deduced that signals c and e must correspond to the axial protons on C-4 and C-6. Inspection of the **1a** 2D NOSEY spectrum reveals 3 key NOE correlations for the C-5 hydroxyl proton (Figure 11.6). The C-5 hydroxyl proton exhibits strong NOE correlations to the equatorial protons on C-4 and C-6, but not the axial protons on these carbons. This indicates that the C-5 hydroxyl group must be *cis* to the equatorial protons on C-4 and C-6 and therefore is axially disposed. There is also a weak NOE correlation between the C-5 hydroxyl proton and the C-3 axial proton, which is further evidence of the hydroxyl group's axial orientation.

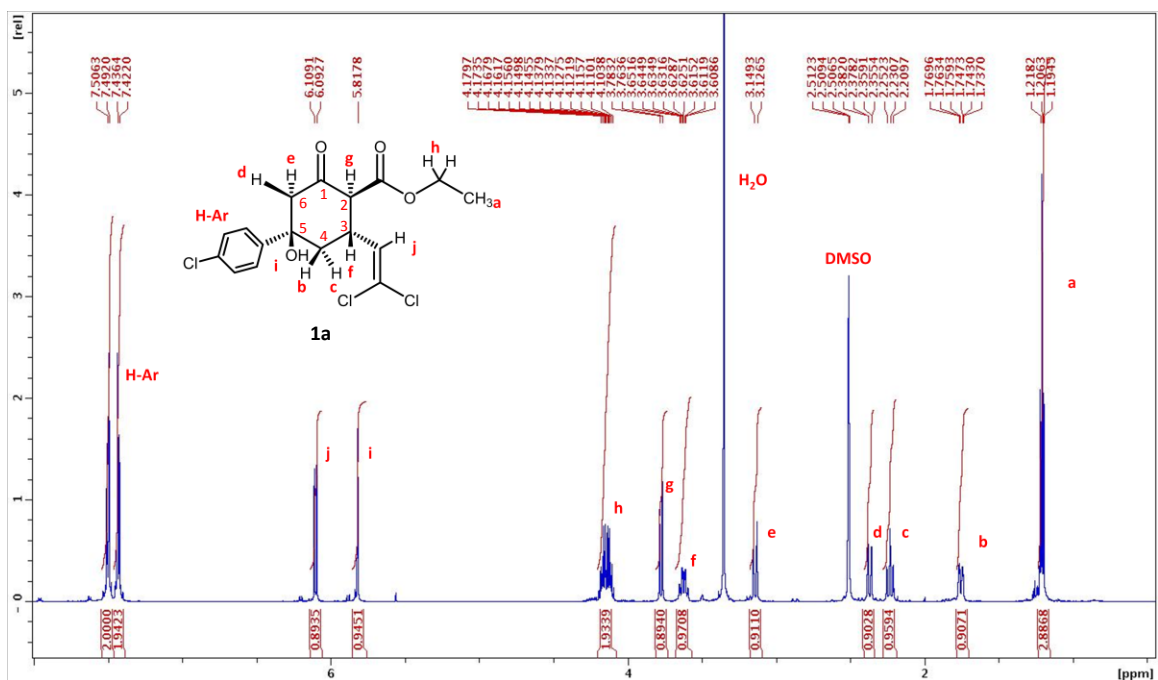


Figure 11.5 – Compound 1a  $^1\text{H}$  NMR (600MHz,  $\text{DMSO-d}_6$ )  $\delta$  = 7.57 - 7.45 (m,  $J$  = 8.8 Hz, 2 H, H-Ar), 7.45 - 7.36 (m,  $J$  = 8.8 Hz, 2 H, H-Ar), 6.09 (d,  $J$  = 9.9 Hz, 1 H, j), 5.81 (s, 1 H, i), 4.21 - 4.04 (m, 2 H, h), 3.76 (d,  $J$  = 11.7 Hz, 1 H, g), 3.61 (ddt,  $J$  = 4.0, 9.9, 11.9 Hz, 1 H, f), 3.13 (d,  $J$  = 13.6 Hz, 1 H, e), 2.36 (dd,  $J$  = 2.2, 13.6 Hz, 1 H, d), 2.22 (t,  $J$  = 12.7 Hz, 1 H, c), 1.81 - 1.68 (m, 1 H, b), 1.20 (t,  $J$  = 7.2 Hz, 3 H, a).

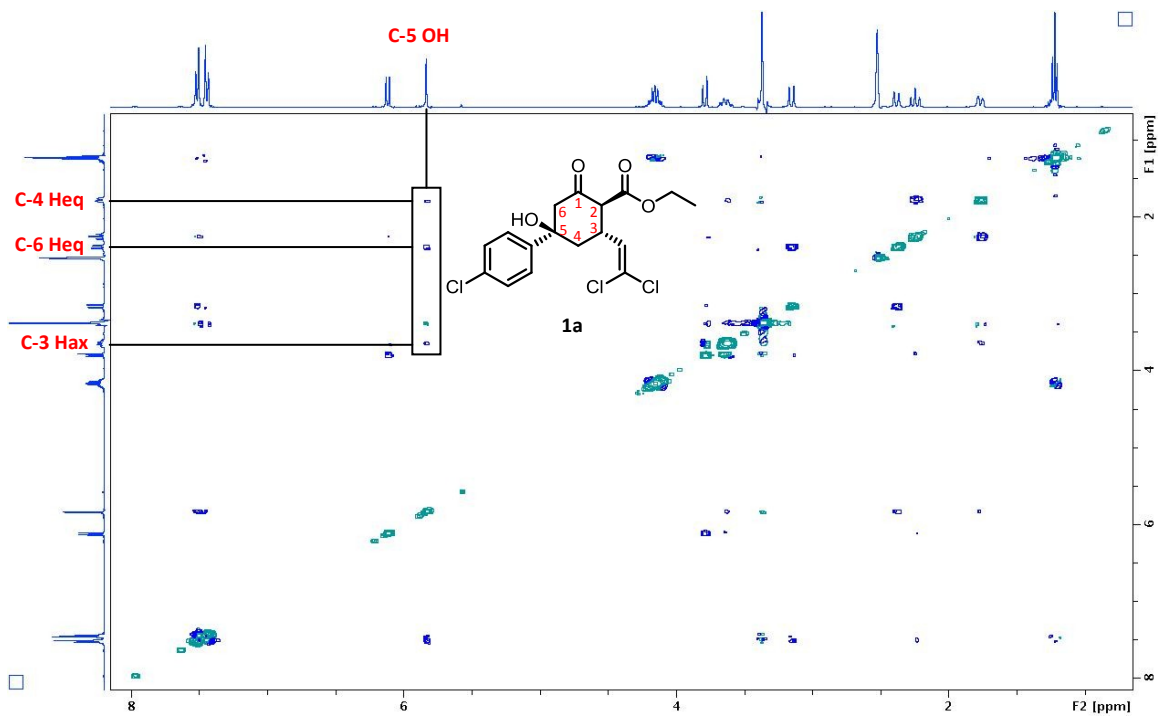


Figure 11.6 - Compound 1a 2D NOESY spectrum. NOE correlations to the C-5 hydroxyl proton are highlighted

These NMR studies allowed us to unambiguously assign the relative stereochemistry at all the stereocenters in the bioactive PCHC compounds (Figure 11.7). The Robinson annulation reactions appear to be under complete thermodynamic control, placing all large ring substituents into equatorial positions. The absolute configuration of the bioactive PCHC molecules has not yet been determined and all compounds synthesized to date are racemic.

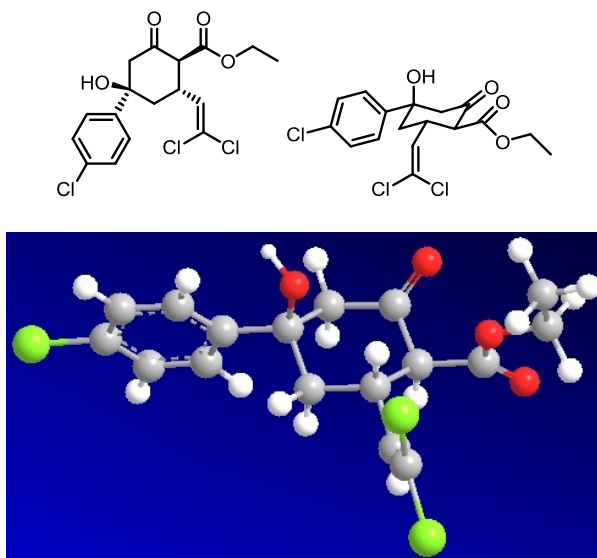


Figure 11.7 – PCHC relative stereochemistry A) 2-dimentional models with stereochemistry indicated either by wedges and dashes or as axial and equatorial substituents on a cyclohexane chair conformation. B) 3-dimentional model showing MM2 minimized conformation in Chem3D Pro.

For SAR studies of the PCHCs, a reduced compound was prepared via the treatment of **1a** with sodium borohydride. This reaction led to chemoselective reduction of the C-1 ketone to a secondary alcohol as a single diastereomer (Figure 11.8). Again, there were questions about the structure of the reduced compound, which were resolved by NMR experiments. Complete assignment of the <sup>1</sup>H-NMR spectrum (Figure 11.9) was facilitated by analysis of the 2-D COSEY and HSQC spectra (see appendix). Signal I, which corresponded to the proton arising from the addition of hydride to the ketone in **1a**, did not exhibit any large *trans*-diaxial coupling constants, which suggested that the C-1 proton was in an equatorial position. Therefore the C-1 hydroxyl group is most likely in an axial position. This conclusion was further supported by

evidence from the 2D-NOSEY spectrum (Figure 11.10). A NOE correlation was observed between the C-1 hydroxyl proton and the C-6 equatorial proton and not between the C-6 or C-2 axial protons. A NOE correlation was also observed between the C-1 equatorial proton and the C-2 axial proton. From these observations one can conclude that sodium borohydride delivers hydride exclusively to the sterically more accessible face of the C-1 ketone (*anti* to the C-2 carboxylate).

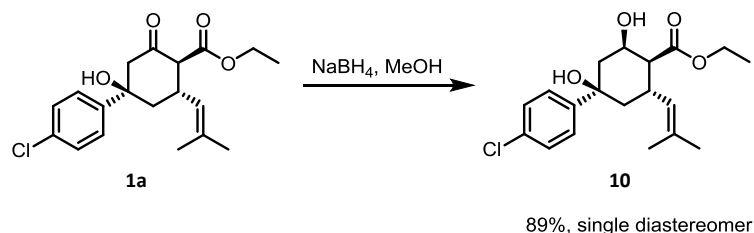


Figure 11.8 – Stereoselective and chemoselective reduction of **1a**

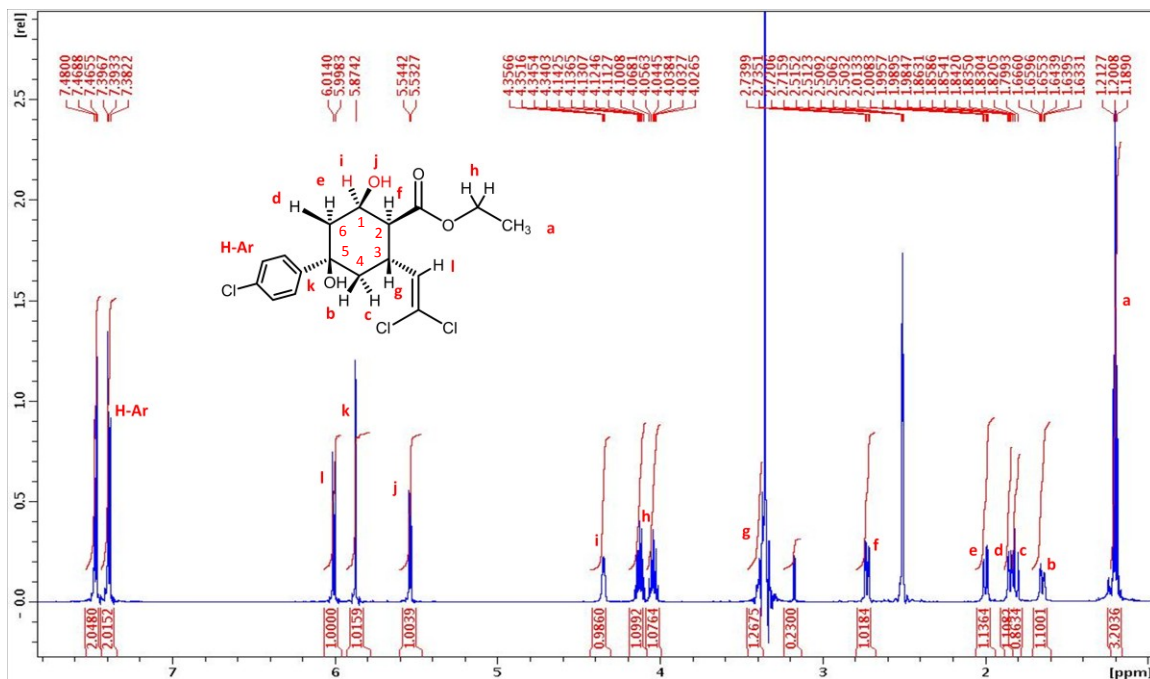


Figure 11.9 – Compound **10**,  $^1\text{H NMR}$  (600MHz,  $\text{DMSO-d}_6$ )  $\delta$  = 7.46 (d,  $J$  = 8.8 Hz, 2 H, H-Ar), 7.38 (d,  $J$  = 8.8 Hz, 2 H, H-Ar), 6.00 (d,  $J$  = 9.5 Hz, 1 H, l), 5.87 (s, 1 H, k), 5.53 (d,  $J$  = 6.6 Hz, 1 H, j), 4.34 (qd,  $J$  = 3.1, 6.5 Hz, 1 H, i), 4.12 (qd,  $J$  = 7.0, 10.8 Hz, 1 H, h), 4.03 (qd,  $J$  = 7.0, 10.9 Hz, 1 H, h), 3.41 - 3.36 (m, 1 H, g), 2.72 (dd,  $J$  = 2.8, 11.6 Hz, 1 H, f), 1.99 (dd,  $J$  = 2.9, 14.3 Hz, 1 H, e), 1.87 - 1.82 (m, 1 H, d), 1.81 (t,  $J$  = 12.5 Hz, 1 H, c), 1.68 - 1.61 (m, 1 H, b), 1.19 (t,  $J$  = 7.2 Hz, 3 H, a).

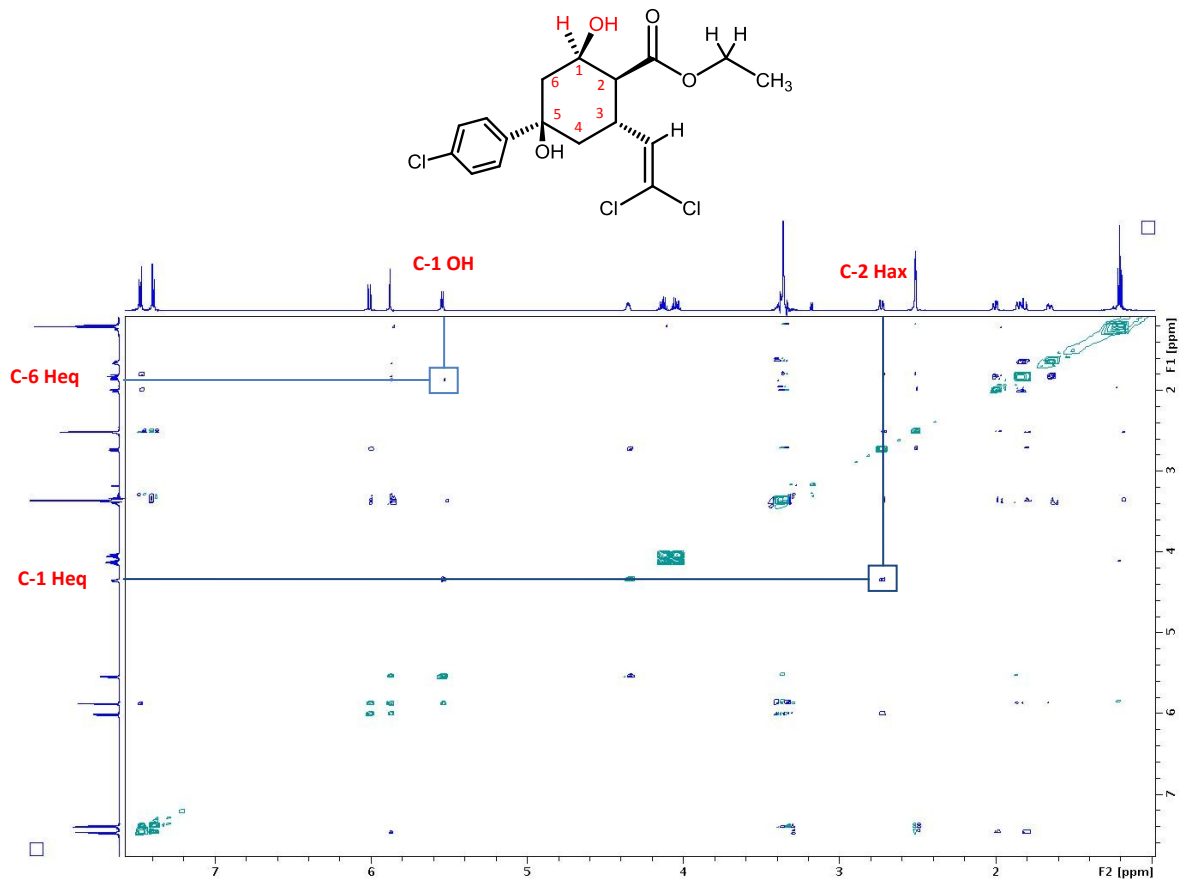
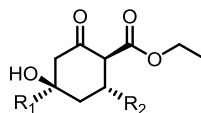


Figure 11.10 - Compound 1a 2D NOSEY spectrum

The library of PCHCs was screened against *B. subtilis* for antibacterial activity. Most of the compounds exhibited modest activity. Interestingly, **ACP5** (Table 1: entry 4, MIC = 100  $\mu\text{g/mL}$ ) was more active than **ACP4** (Table 11.1: entry 1, MIC >200  $\mu\text{g/mL}$ ). This result is in contrast to data reported by Leung *et al.* Compound **1a** (Table 11.1: entry 6, MIC 100  $\mu\text{g/mL}$ ) was equally as potent as **ACP5** and derived from a less expensive, 4-chloro substituted acetophenone. An analog with a *m*-nitrophenyl substituent was the most active compound in the library (Table 1: entry 2, MIC = 50  $\mu\text{g/mL}$ ). However, nitro groups are often times regarded as a liability in medicinal chemistry. Another potential liability is the dichlorovinyl moiety. Fortunately, compounds wherein the dichlorovinyl moiety is replaced with a furfuryl moiety retain activity (Table 11.1: entry 12, MIC = 100  $\mu\text{g/mL}$ ; entry 14, MIC = 200  $\mu\text{g/mL}$ ). These compounds are the most promising for continued drug lead development.

Table 11.7 – Antibacterial Activity of CPHCs against *B. subtilis*



Entry	R <sub>1</sub>	R <sub>2</sub>	<i>B. subtilis</i> MIC (µg/mL)	Entry	R <sub>1</sub>	R <sub>2</sub>	<i>B. subtilis</i> MIC (µg/mL)
1	<i>p</i> -Nitrophenyl	2,2-dichlorovinyl	>200	8	<i>o</i> -Chlorophenyl	2,2-dichlorovinyl	100
2	<i>m</i> -Nitrophenyl	2,2-dichlorovinyl	50	9	<i>p</i> -Methylphenyl	2,2-dichlorovinyl	200
3	<i>o</i> -Nitrophenyl	2,2-dichlorovinyl	>200	10	phenyl	2,2-dichlorovinyl	>200
4	<i>p</i> -Bromophenyl	2,2-dichlorovinyl	100	11	<i>p</i> -Bromophenyl	2-thiophenyl	>200
5	<i>m</i> -Bromophenyl	2,2-dichlorovinyl	100	12	<i>p</i> -Bromophenyl	2-furfuryl	100
6	<i>p</i> -Chlorophenyl	2,2-dichlorovinyl	100	13	<i>p</i> -Bromophenyl	2-(5-methylfurfuryl)	>200
7	<i>m</i> -Chlorophenyl	2,2-dichlorovinyl	100	14	<i>p</i> -Chlorophenyl	2-furfuryl	200

Minimum Inhibitory concentration (MIC) was defined as the lowest compound concentration able to completely inhibit bacterial growth for up to 48 hours.

The activities of the PCHPs were assessed in antibacterial assays. Minimum inhibitory concentrations (MIC) were determined by the agar dilution method.<sup>15</sup> When the agar plates were inspected at 24, 48, and 72 hours, the bacterial growth tended to steadily increase over time. In typical agar dilution MIC assays, there is little change in bacterial growth from 24 to 48 hours and no change from 48 to 72 hours. Activity for a subset of these compounds seemed to diminish over time. The peculiar activity of the PCHC's is indicative of gradual compound degradation in the growth medium. As the concentration of active compound decreases over time, persistent bacterial cells are eventually able to proliferate.

We reasoned that the loss in activity over time could be a result of compound dehydration. Dehydration could occur either by a base promoted E1cB mechanism or an acid promoted E1 mechanism (Figure 11.11A). In the growth media, both mechanisms could be operative. To test the effect of dehydration on PCHC activity, compound **11**, which was recovered as a byproduct from syntheses of **1a**, was tested against *B. subtilis* and found to be completely inactive. Apparently, the tertiary alcohol is absolutely essential for antibacterial

activity. Consistent with our elimination proposal, compound **10**, which cannot undergo *E1cB* mediated dehydration, exhibited stable activity (Figure 11.11B). Importantly, **10** was also more potent than any of the PCHPs.

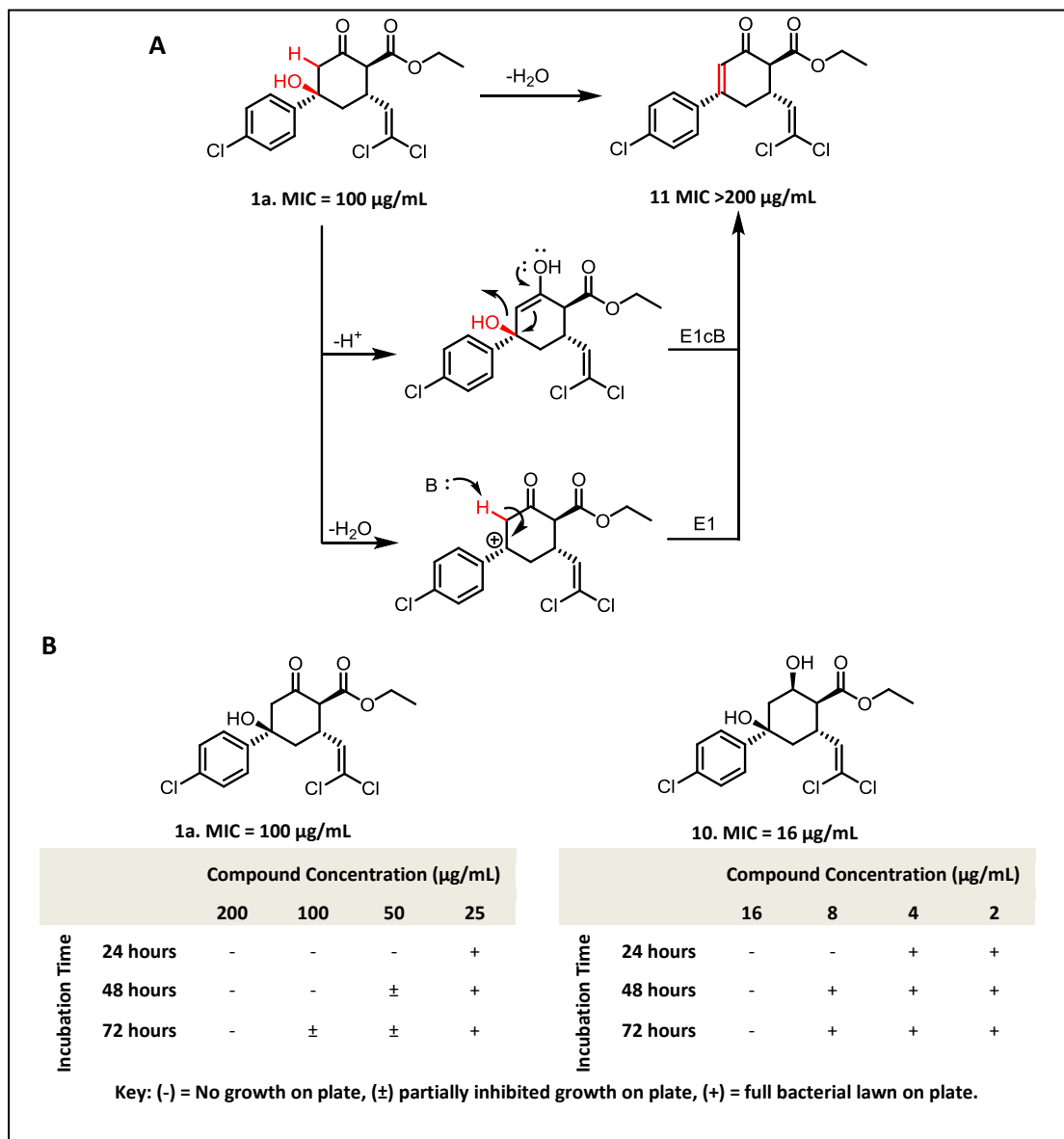


Figure 11.11 – Effects of PCHC dehydration and reduction on antibacterial activity A) possible mechanisms of PCHC dehydration and effect on antibacterial activity B) effect of PCHC reduction on antibacterial potency and stability.

The report by Leung and co-workers suggests that antibacterial activity of ACP-4 and ACP-5 was due to activation of the peptolytic activity of ClpP. To confirm this mechanism of

action, we tested tested ACP-5 and compound 10 against a  $\Delta clpP$ -*spx* null strain of *B. subtilis* that is not susceptible to the ADEPs (see chapter 8).<sup>16,17</sup> To our surprise, CPHCs were all active against the *B. subtilis*  $\Delta spx$  null strain and  $\Delta clpP$ -*spx* double null strain of *B. subtilis* (Figure 11.12A). These data suggest that CPHC's have targets other than ClpP. We also tested CPHC's for their ability to activate ClpP *in vitro*. We found that CPHC's mediated very weak ClpP activation compared to **ADEP1** (Figure 11.12B). At the highest concentration tested (1000  $\mu$ M), **ACP5** induced decapeptide hydrolysis was only slightly more than in blank samples with no activator. **ADEP1A** on the other hand appears to saturate ClpP at 1000  $\mu$ M.

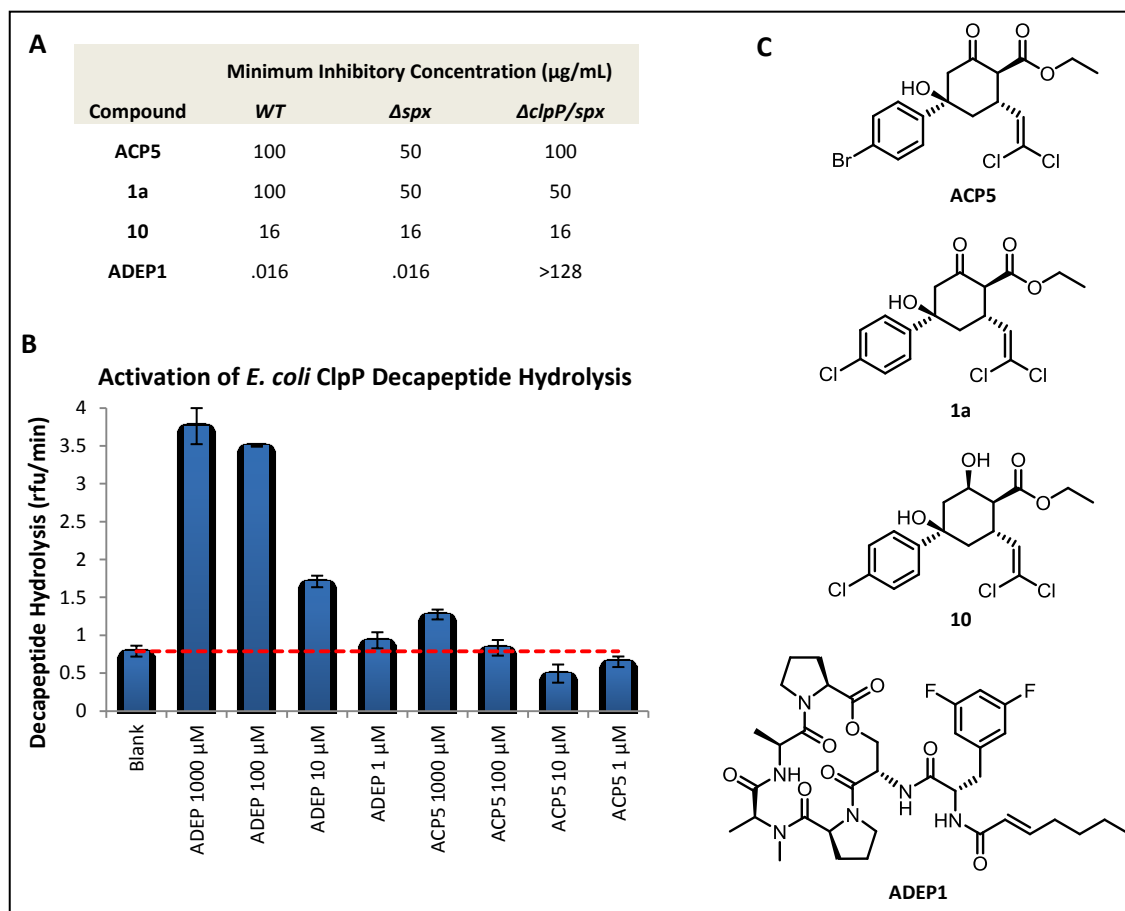


Figure 11.1211 – Attempts to Validate ClpP as CPHC target A) Antibacterial activity against *B. subtilis*, wild type, *spx* null strain and *clpP/spx* double null strain. B) Hydrolysis of a fluorogenic decapeptide substrate (15  $\mu$ M) by *E. coli* ClpP (25 nM) was assayed in the presence of increasing concentrations of ADEP1 or ACP5. Bars represent initial rates of decapeptide hydrolysis (average of 2 experiments). Error bars indicate standard deviation. Horizontal red dashed line indicates decapeptide hydrolysis rate in the absence of ADEP. C) Structures of tested compounds



## Conclusions

Lead development of the CPHC's is an ongoing endeavor in our lab. The primary objectives that lay ahead are continued investigation of structure-activity relationships and potency optimization, asymmetric synthesis to identify the bioactive enantiomer, and most importantly, alternate target identification and validation. Our genetic data strongly suggests that the CPHC's have a target other than ClpP that is responsible for antibacterial activity. We are currently designing and synthesizing affinity reagents for chemical proteomics experiments, which will allow us identify all of the proteins that the CPHCs interact with.<sup>18</sup> Additionally we will use bacterial cytological profiling experiments as a complementary target identification method to determine the cellular pathway that is modulated by the CPHCs.<sup>19</sup> The results of chemical proteomics experiments and bacterial cytological profiling should implicate a small number of proteins as CPHC targets that can be validated by genetic and biochemical methods.

## Experimental Contributions

Stereochemical analysis of compounds **1a** and **10** were completed by Daniel Carney. Chemical synthesis of compounds was completed by visiting researcher, Dr. Dele Olubanwu with assistance from Daniel Carney and Brown undergraduate student, Arianna Kazez. Antibacterial testing with *B. subtilis* was completed by Daniel Carney with assistance from Arianna Kazez. ClpP activation assays were conducted by Karl Schmitz with assistance from Daniel Carney.

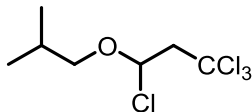
## Experimental Procedures

**Minimum inhibitory concentration determinations:** *B. subtilis* MICs were determined using standard agar dilution techniques. Liquid cultures (LB Broth) inoculated from a fresh single colony were grown for 6 hours at 37°C. LB agar plates supplemented with varying concentrations of test compound were inoculated with 5 µL of the liquid culture and then

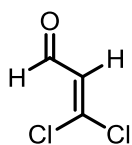
incubated at 37°C for up to 72 hours. The agar plates were inspected for growth at 24 hour intervals. The MIC was determined to be lowest concentration of compound able to completely inhibit *B. subtilis* growth after 48 hours.

**Synthesis General:** All commercially available reagents were used without further purification. All reactions were conducted in oven dried glassware, under ambient atmosphere, using dry solvents unless otherwise stated. NMR chemical shifts were referenced to residual solvent peaks: CDCl<sub>3</sub> ( $\delta$  = 7.27 ppm for <sup>1</sup>H-NMR and 77.00 ppm for <sup>13</sup>C-NMR), DMSO-d<sub>6</sub> ( $\delta$  = 2.50 for <sup>1</sup>H-NMR and  $\delta$  = 39.51 for <sup>13</sup>C-NMR).

**Synthesis of dichloroacrolein:** Isobutyl vinyl ether (39 mL, 300 mmol) was dissolved in freshly distilled carbon tetrachloride (200 mL) and then treated with benzoyl chloride (606 mg, 2.5 mmol). The solution was then refluxed for 48 hours. Formation of the radical addition product can be monitored by <sup>1</sup>H-NMR. Although the Isobutyl vinyl ether was usually completely consumed by 24 hours, advancing to the second stage of the reaction before 48 hours led to significant degradation of the intermediate and formation of a viscous tar. Presumably, the additional 24 hours of reaction is necessary to allow termination of residual radical intermediates. After the 48 hours of refluxing, the solvent was removed by distillation. The remaining residue was transferred to a fractional distillation apparatus and heated to 170°C for 1 hour. The temperature was then raised to 220°C over 30 minutes under slightly reduced pressure, over the course of which distillate was collected in fractions. The fractions were analyzed <sup>1</sup>H-NMR and those that contained dichloroacrolein were combined. Dichloroacrolein containing fractions also contained some of the isobutylchloride byproduct. The isobutyl chloride and dichloroacrolein were separated by fractional vacuum distillation.

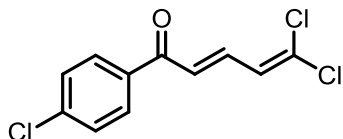


**Dichloroacrolein Intermediate.**  $^1\text{H}$  NMR (400MHz, CHLOROFORM-d)  $\delta$  = 5.94 (dd,  $J$  = 2.3, 7.5 Hz, 1 H), 3.76 (dd,  $J$  = 6.3, 8.8 Hz, 1 H), 3.56 (dd,  $J$  = 7.7, 15.2 Hz, 1 H), 3.44 (dd,  $J$  = 2.3, 15.3 Hz, 1 H), 3.31 (dd,  $J$  = 6.5, 9.0 Hz, 1 H), 2.02 - 1.87 (m, 1 H), 0.97 (d,  $J$  = 2.5 Hz, 3 H), 0.95 (d,  $J$  = 2.5 Hz, 3 H).



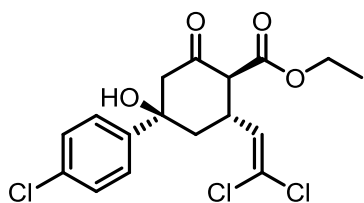
**Dichloroacrolein.** Yield: 9.55g, 25% from Isobutyl vinyl ether.  $^1\text{H}$  NMR (400MHz, CHLOROFORM-d)  $\delta$  = 9.88 (d,  $J$  = 6.8 Hz, 1 H), 6.45 (d,  $J$  = 6.8 Hz, 1 H).

**Synthesis of  $\alpha,\beta$ -unsaturated-phenylketones general Procedure:** An acetophenone (8.7 mmol) and an aldehyde (8 mmol) were dissolved in acetic acid (10 mL) and then treated with sulfuric acid (1.2 mL). The reaction was allowed to proceed for 16 hours, over the course of which a precipitate typically formed. The reaction was then poured over ice and allowed to stand until the ice was melted. The solidified product was then collected by filtration and washed with cold acetic acid and water. Once dry, the  $\alpha,\beta$ -unsaturated-phenylketones were used without further purification.



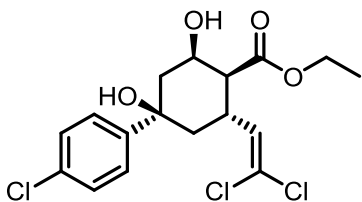
**Representative Example - (E)-5,5-dichloro-1-(4-chlorophenyl)penta-2,4-dien-1-one (3a).** Yield: 1.50 g, 61%.  $^1\text{H}$  NMR (400MHz, DMSO- $d_6$ )  $\delta$  = 8.02 (d,  $J$  = 8.8 Hz, 2 H), 7.66 (d,  $J$  = 8.5 Hz, 2 H), 7.57 (d,  $J$  = 14.8 Hz, 1 H), 7.34 (dd,  $J$  = 11.0, 14.8 Hz, 1 H), 7.15 (d,  $J$  = 10.8 Hz, 1 H).

**Synthesis of CPHCs general procedure:** An  $\alpha,\beta$ -unsaturated-phenylketone (0.65 mmol) and ethyl acetoacetate (0.78) were dissolved in ethanol (3.25 mL) and treated with 21% by weight sodium ethoxide in ethanol (0.48 mL, 1.3 mmol). The reaction was allowed to proceed for 2 hours after which the reaction was quenched by the addition of 3:1 distilled water / brine. The aqueous solution as then extracted with dichloromethane. The organic extracts were combined and dried over sodium slufate. The CPHC's were then isolated by flash chromatography on deactivated silica gel. Silica gel was deactivated by flushing the column with 1% triethylamine in hexanes before loading the crude reaction product. The CPHCs were eluted with 30-50% ethyl acetate in hexanes.



**Representative example - ethyl (1S,2R,4R)-4-(4-chlorophenyl)-2-(2,2-dichlorovinyl)-4-hydroxy-6-oxocyclohexane-1-carboxylate + enantiomer (1a).** Yield: 143 mg, 56%. HRMS (ESI) Predicted for  $[\text{C}_{17}\text{H}_{17}\text{Cl}_3\text{O}_4 + \text{H}]^+$ : 391.0271, found 391.0260.  $^1\text{H}$  NMR (600MHz, DMSO- $d_6$ )  $\delta$  = 7.57 - 7.45 (m,  $J$  = 8.8 Hz, 2 H), 7.45 - 7.36 (m,  $J$  = 8.8 Hz, 2 H), 6.09 (d,  $J$  = 9.9 Hz, 1 H), 5.81 (s, 1 H), 4.21 - 4.04 (m, 2 H), 3.76 (d,  $J$  = 11.7 Hz, 1 H), 3.61 (ddt,  $J$  = 4.0, 9.9, 11.9 Hz, 1 H), 3.13 (d,  $J$  = 13.6 Hz, 1 H),

2.36 (dd,  $J = 2.2, 13.6$  Hz, 1 H), 2.22 (t,  $J = 12.7$  Hz, 1 H), 1.81 - 1.68 (m, 1 H), 1.20 (t,  $J = 7.2$  Hz, 3 H).  $^{13}\text{C}$  NMR (151MHz, DMSO- $d_6$ )  $\delta = 203.0, 168.5, 146.3, 131.6, 131.4, 128.0, 126.6, 120.0, 74.9, 60.4, 59.8, 52.5, 40.6, 37.9, 14.1$ .



**ethyl (1S,2R,4R,6R)-4-(4-chlorophenyl)-2-(2,2-dichlorovinyl)-4,6-dihydroxycyclohexane-1-carboxylate + enantiomer (10).** PCHC **1a** (143 mg, 0.37 mmol) was dissolved in methanol (2 mL) and treated with sodium borohydride (27 mg, 0.72 mmol). The reaction was allowed to proceed for 15 minutes, after which the solvent was removed in vacuo. The concentrated residue was diluted with ethyl acetate (~10 mL) and extracted once with saturated aqueous ammonium chloride. The aqueous extract was back extracted once with ethyl acetate and the combined organic phases were dried over sodium sulfate. The desired product was isolated by flash chromatography on silica gel using a 30% ethyl acetate in hexanes mobile phase. Yield: 129 mg, 89%. HRMS (ESI) Predicted for  $[\text{C}_{17}\text{H}_{19}\text{Cl}_3\text{O}_4 + \text{Na}]^+$ : 415.0247, found 415.0239.  $^1\text{H}$  NMR (600MHz, DMSO- $d_6$ )  $\delta = 7.46$  (d,  $J = 8.8$  Hz, 2 H), 7.38 (d,  $J = 8.8$  Hz, 2 H), 6.00 (d,  $J = 9.5$  Hz, 1 H), 5.87 (s, 1 H), 5.53 (d,  $J = 6.6$  Hz, 1 H), 4.34 (qd,  $J = 3.1, 6.5$  Hz, 1 H), 4.12 (qd,  $J = 7.0, 10.8$  Hz, 1 H), 4.03 (qd,  $J = 7.0, 10.9$  Hz, 1 H), 3.41 - 3.36 (m, 1 H), 2.72 (dd,  $J = 2.8, 11.6$  Hz, 1 H), 1.99 (dd,  $J = 2.9, 14.3$  Hz, 1 H), 1.87 - 1.82 (m, 1 H), 1.81 (t,  $J = 12.5$  Hz, 1 H), 1.68 - 1.61 (m, 1 H), 1.19 (t,  $J = 7.2$  Hz, 3 H).  $^{13}\text{C}$  NMR (151MHz, DMSO- $d_6$ )  $\delta = 171.6, 147.1, 133.8, 131.2, 127.9, 126.5, 118.2, 72.9, 68.3, 59.8, 50.5, 41.9, 41.5, 31.4, 14.1$ .

## References

1. Brotz-Oesterhelt, H.; Beyer, D.; Kroll, H.; Endermann, R.; Ladel, C.; Schroeder, W.; Hinzen, B.; Raddatz, S.; Paulsen, H.; Henninger, K.; Bandow, J. E.; Sahl, H.; Labischinski, H. Dysregulation of bacterial proteolytic machinery by a new class of antibiotics. *Nat. Med.* **2005**, *11*, 1082-1087.
2. Kirstein, J.; Hoffmann, A.; Lilie, H.; Schmidt, R.; Rübsamen-Waigmann, H.; Brötz-Oesterhelt, H.; Mogk, A.; Turgay, K. The antibiotic ADEP reprogrammes ClpP, switching it from a regulated to an uncontrolled protease. *EMBO Molecular Medicine* **2009**, *1*, 37-49.
3. Ollinger, J.; O'Malley, T.; Kesicki, E. A.; Odingo, J.; Parish, T. Validation of the essential ClpP protease in *Mycobacterium tuberculosis* as a novel drug target. *J. Bacteriol.* **2012**, *194*, 663-668.
4. Brötz-Oesterhelt, H.; Sass, P. Bacterial caseinolytic proteases as novel targets for antibacterial treatment. *International Journal of Medical Microbiology* **2013**.
5. Leung, E.; Datti, A.; Cossette, M.; Goodreid, J.; McCaw, S. E.; Mah, M.; Nakhamchik, A.; Ogata, K.; El Bakkouri, M.; Cheng, Y. Activators of cylindrical proteases as antimicrobials: identification and development of small molecule activators of ClpP protease. *Chem. Biol.* **2011**, *18*, 1167-1178.
6. Lipinski, C. A. Lead-and drug-like compounds: the rule-of-five revolution. *Drug Discovery Today: Technologies* **2004**, *1*, 337-341.
7. Lipinski, C. A.; Lombardo, F.; Dominy, B. W.; Feeney, P. J. Experimental and computational approaches to estimate solubility and permeability in drug discovery and development settings. *Adv. Drug Deliv. Rev.* **2012**, *64*, 4-17.
8. Loffet, A. Peptides as drugs: is there a market? *Journal of Peptide Science* **2002**, *8*, 1-7.
9. Hamman, J. H.; Enslin, G. M.; Kotzé, A. F. Oral delivery of peptide drugs. *BioDrugs* **2005**, *19*, 165-177.
10. Edwards, C. M.; Cohen, M. A.; Bloom, S. R. Peptides as drugs. *QJM* **1999**, *92*, 1-4.
11. Vlieghe, P.; Lisowski, V.; Martinez, J.; Khrestchatsky, M. Synthetic therapeutic peptides: science and market. *Drug Discov. Today* **2010**, *15*, 40-56.
12. Rapson, W. S.; Robinson, R.; Schlittler, E.; Achmatowicz, O.; Clemo, G.; Macdonald, J. M.; Juliusburger, F.; Topley, B.; Weiss, J.; Blair, R. D. 307. Experiments on the synthesis of substances related to the sterols. Part II. A new general method for the synthesis of substituted cyclohexenones. *J.Chem.Soc* **1935**, *1285*, 1288.
13. Gawley, R. E. The Robinson annelation and related reactions. *Synthesis* **1976**, *1976*, 777-794.

14. Soulen, R. L.; Clifford, D. B.; Crim, F. F.; Johnston, J. A. Nucleophilic vinylic substitution. I. Synthesis and reactions of 2-substituted 3, 3-dichloroacrylonitriles. *J. Org. Chem.* **1971**, *36*, 3386-3391.
15. Wiegand, I.; Hilpert, K.; Hancock, R. E. Agar and broth dilution methods to determine the minimal inhibitory concentration (MIC) of antimicrobial substances. *Nature protocols* **2008**, *3*, 163-175.
16. Nakano, M. M.; Hajarizadeh, F.; Zhu, Y.; Zuber, P. Loss-of-function mutations in yjbD result in ClpX-and ClpP-independent competence development of *Bacillus subtilis*. *Mol. Microbiol.* **2001**, *42*, 383-394.
17. Nakano, S.; Zheng, G.; Nakano, M. M.; Zuber, P. Multiple pathways of Spx (YjbD) proteolysis in *Bacillus subtilis*. *J. Bacteriol.* **2002**, *184*, 3664-3670.
18. Rix, U.; Superti-Furga, G. Target profiling of small molecules by chemical proteomics. *Nature Chemical Biology* **2009**, *5*, 616-624.
19. Nonejuie, P.; Burkart, M.; Pogliano, K.; Pogliano, J. Bacterial cytological profiling rapidly identifies the cellular pathways targeted by antibacterial molecules. *Proc. Natl. Acad. Sci. U. S. A.* **2013**, *110*, 16169-16174.

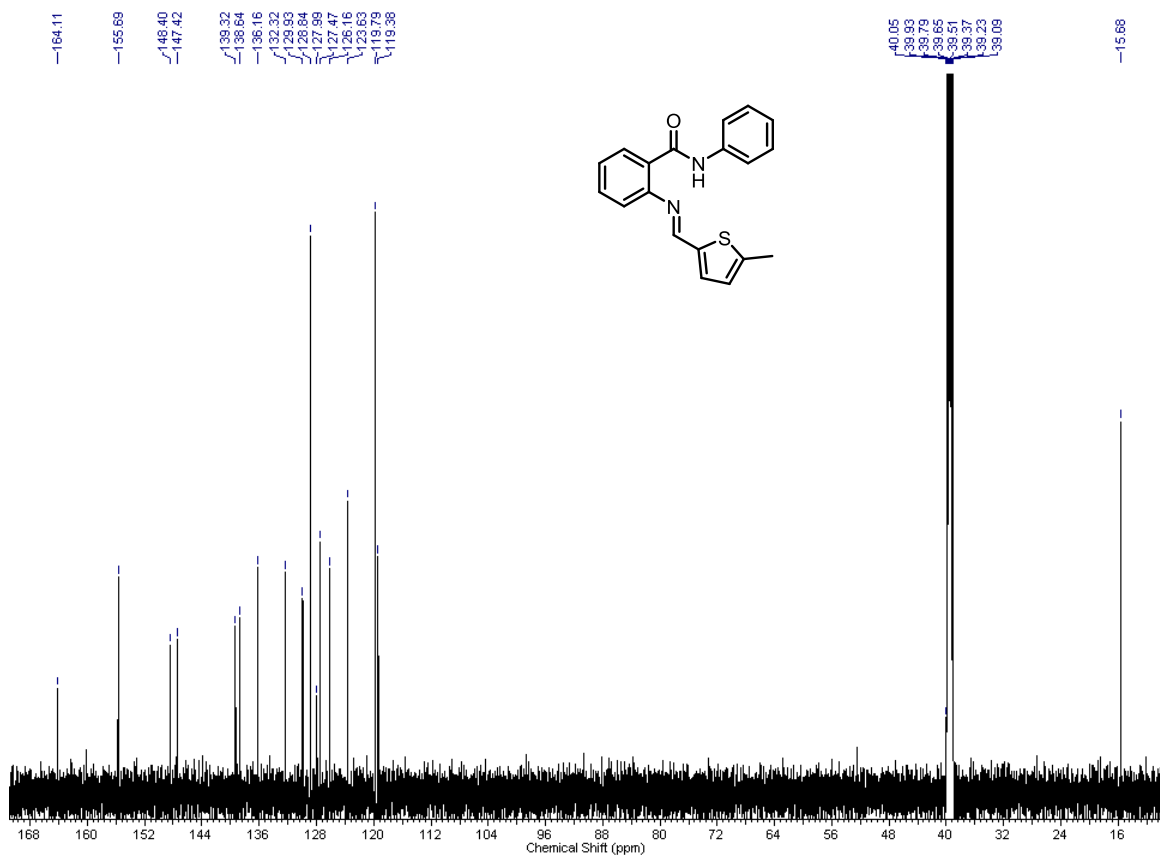
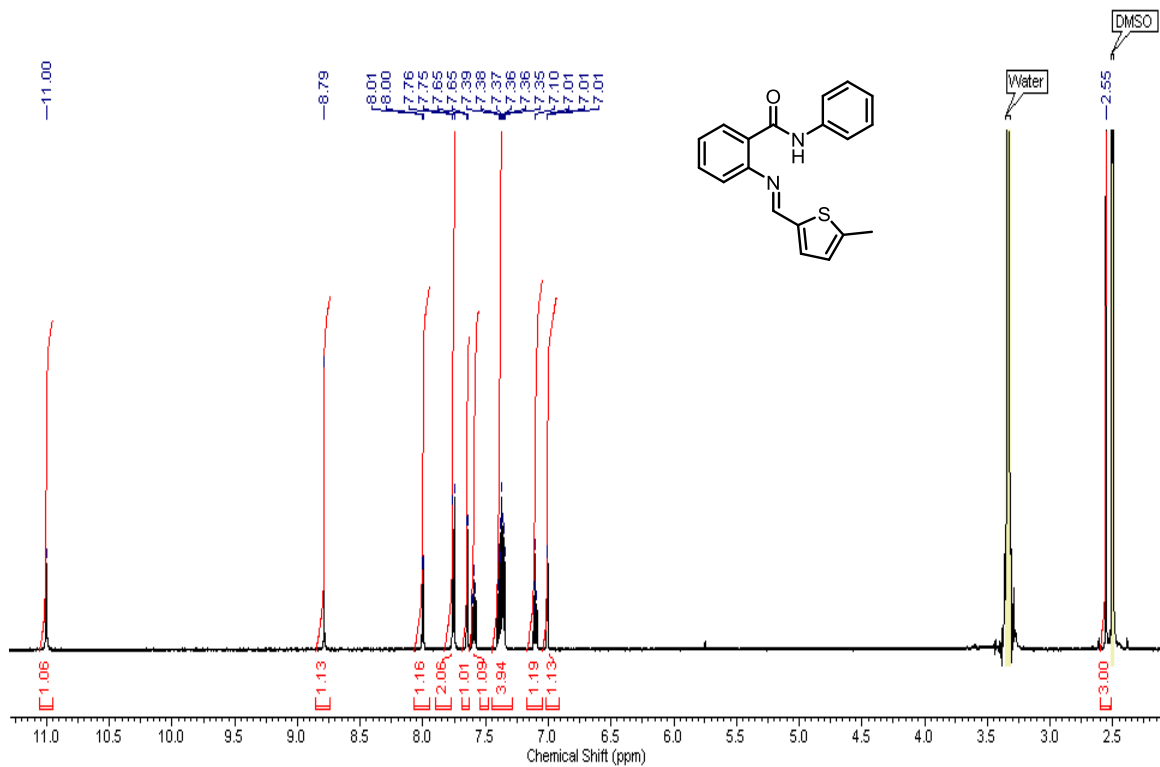
## Appendix of Compound Spectra

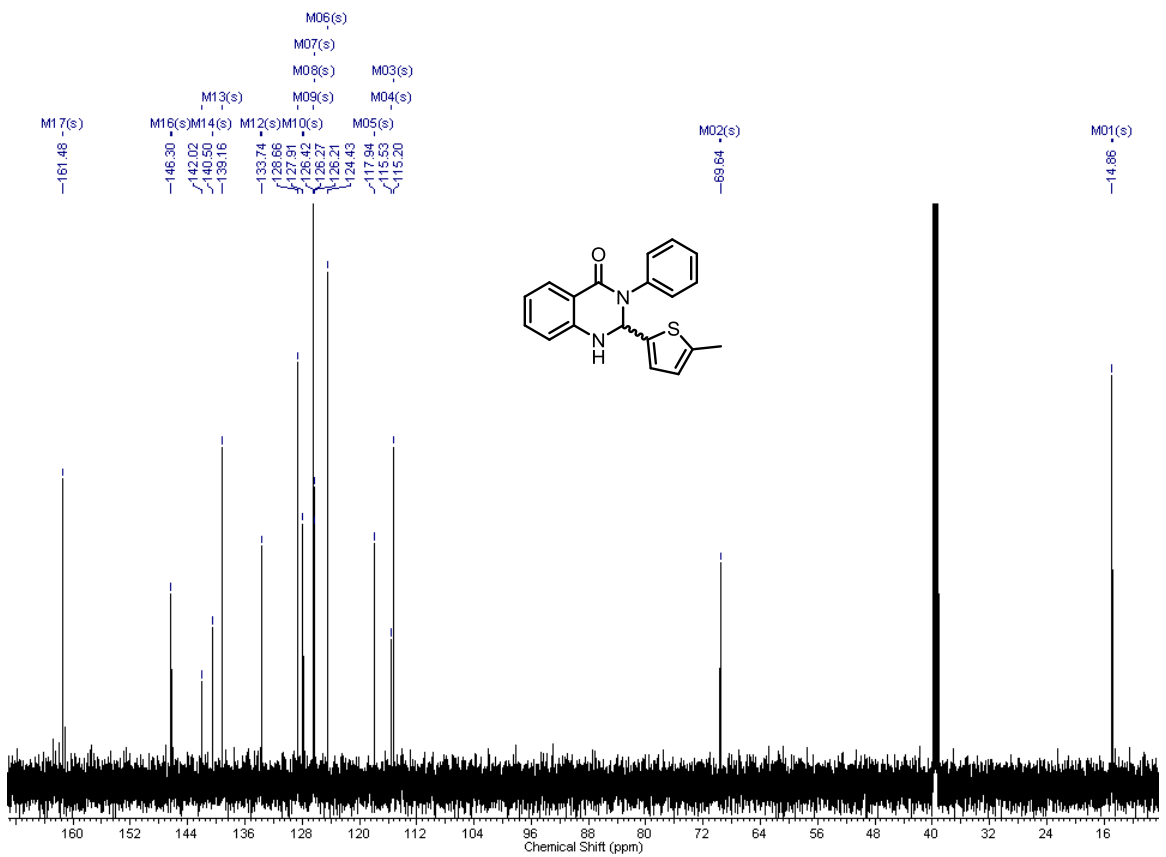
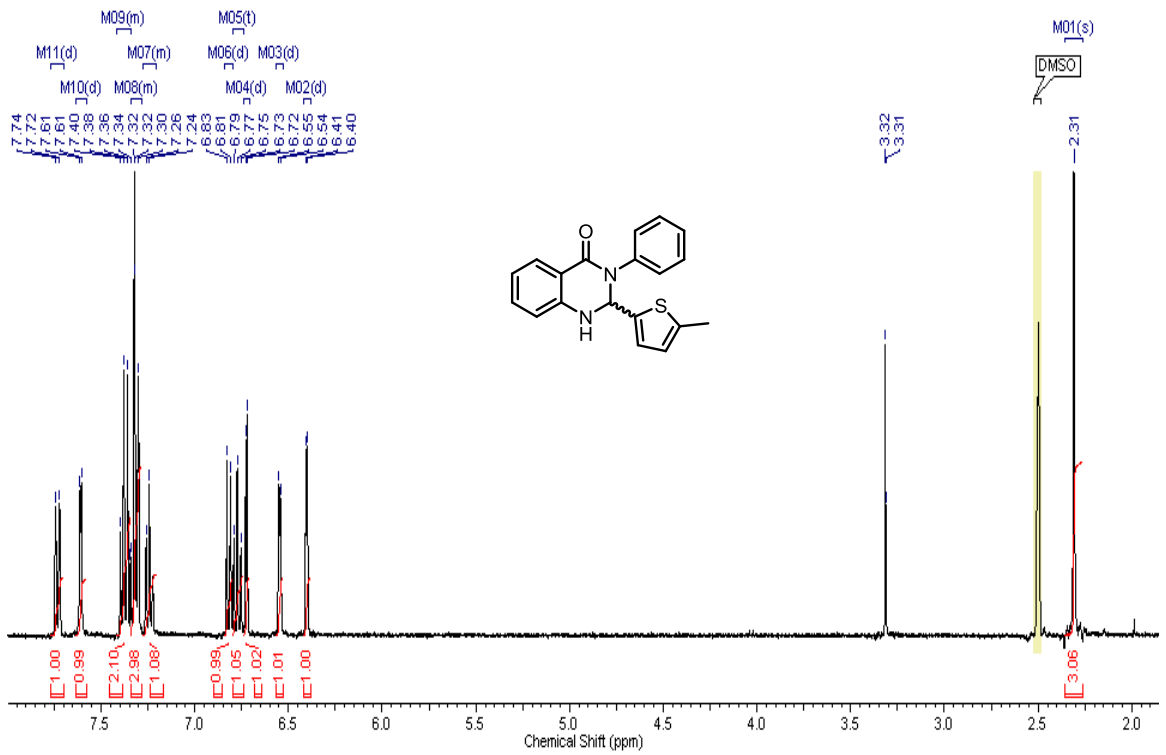
### Contents

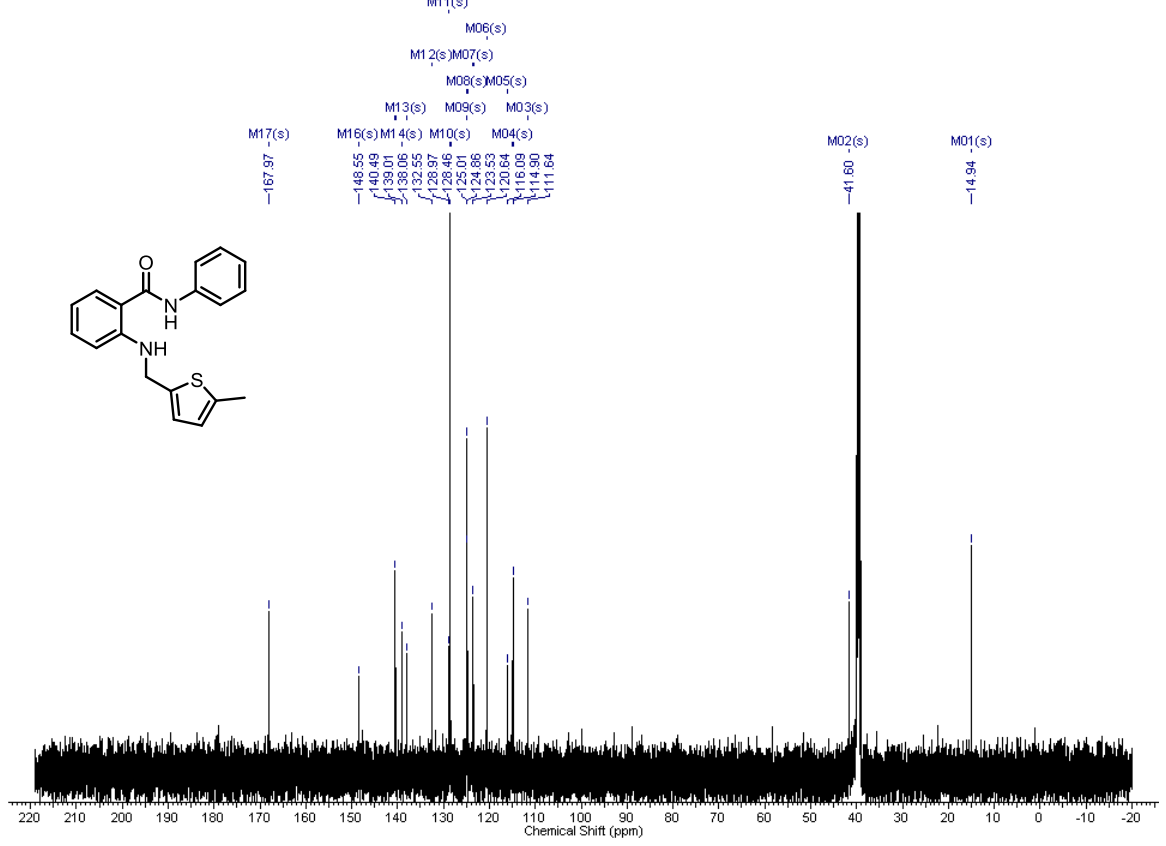
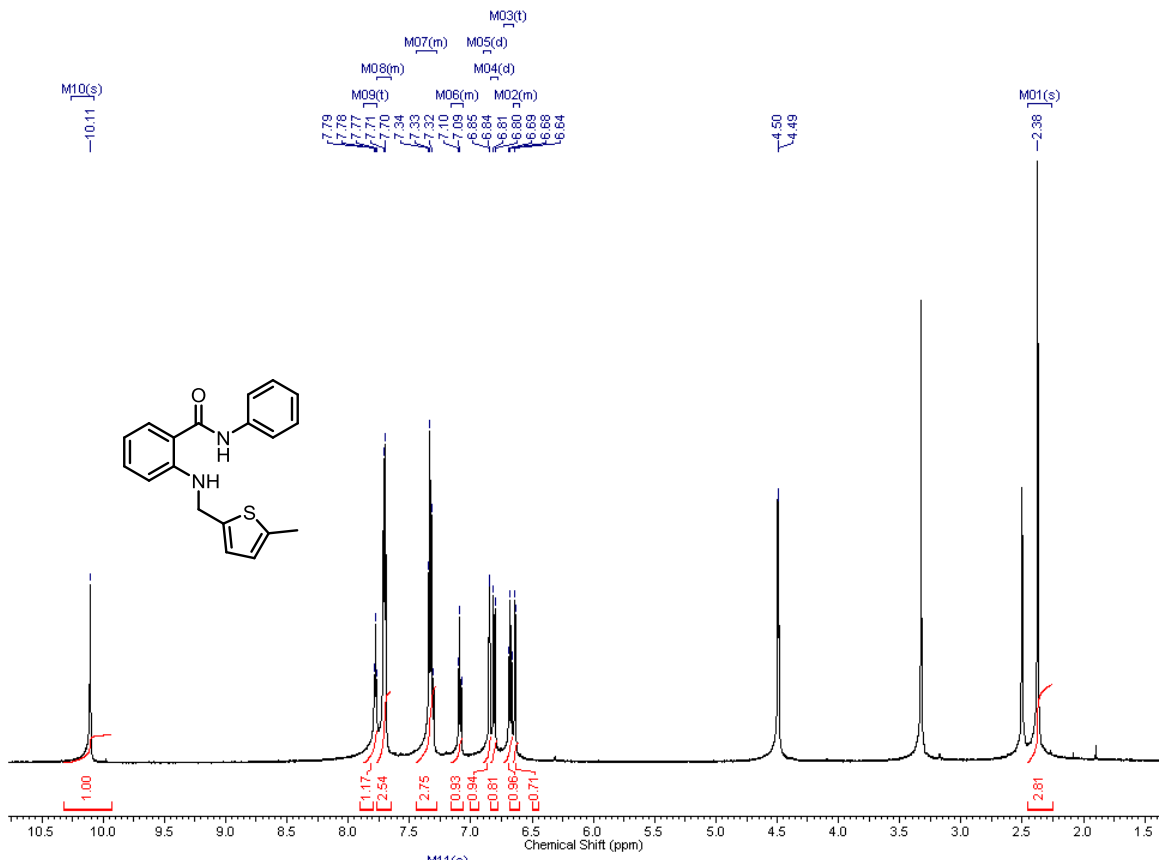
Appendix of Compound Spectra .....	312
Chapter 2 – Dihydroquinazolinone Retrograde Transport Inhibitors.....	313
Chapter 4 – Isocyanide Based Multicomponent Reactions and Synthesis of Pipecolate Containing Peptides. ....	357
NMR and MassSpectra.....	357
Isocyanoacetate Epimerization Chromatograms.....	388
Advanced Marfey Analysis Chromatograms.....	403
LC Chromatograms.....	418
Chapter 5 – Synthesis of ADEPs with Conformationally Constrained Peptidolactones .....	420
Chapter 7 – Synthesis and Evaluation of ADEPs with Modified side Chains .....	457
Chapter 8 – The <i>N</i> -Acyldifluorophenyllanine Moiety is Necessary and Sufficient for ClpP Activation.....	485
Chapter 9 – <i>N</i> -Acyldifluorophenylalanine Fragment Hit to lead development.....	512
Chapter 11 – Antibacterial Phenylcyclohexane Caboxylates (PCHCs) .....	523

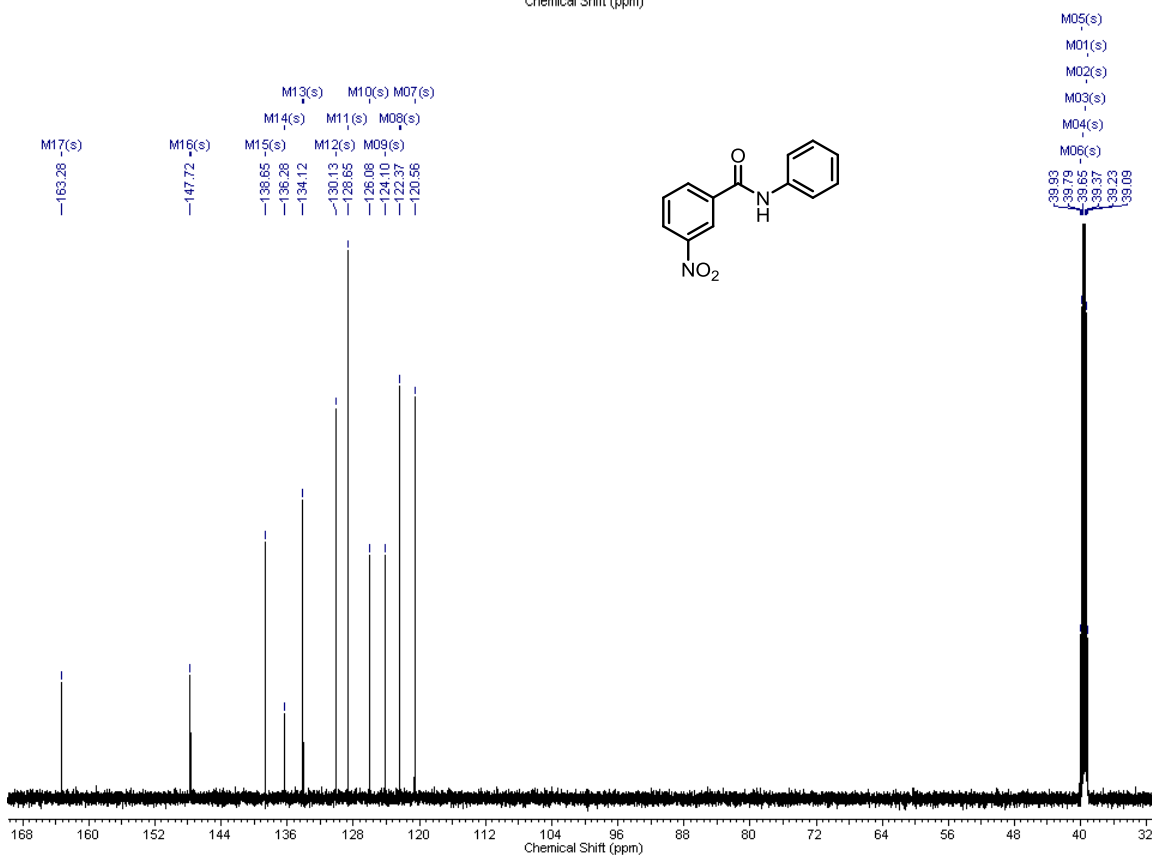
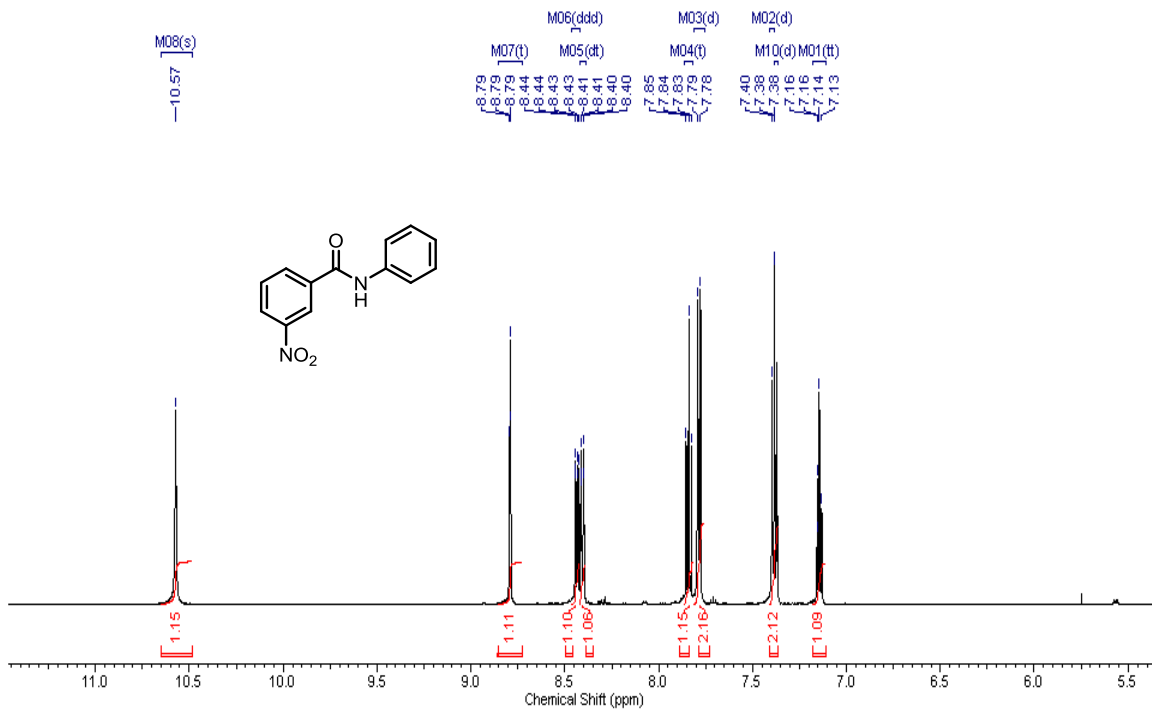


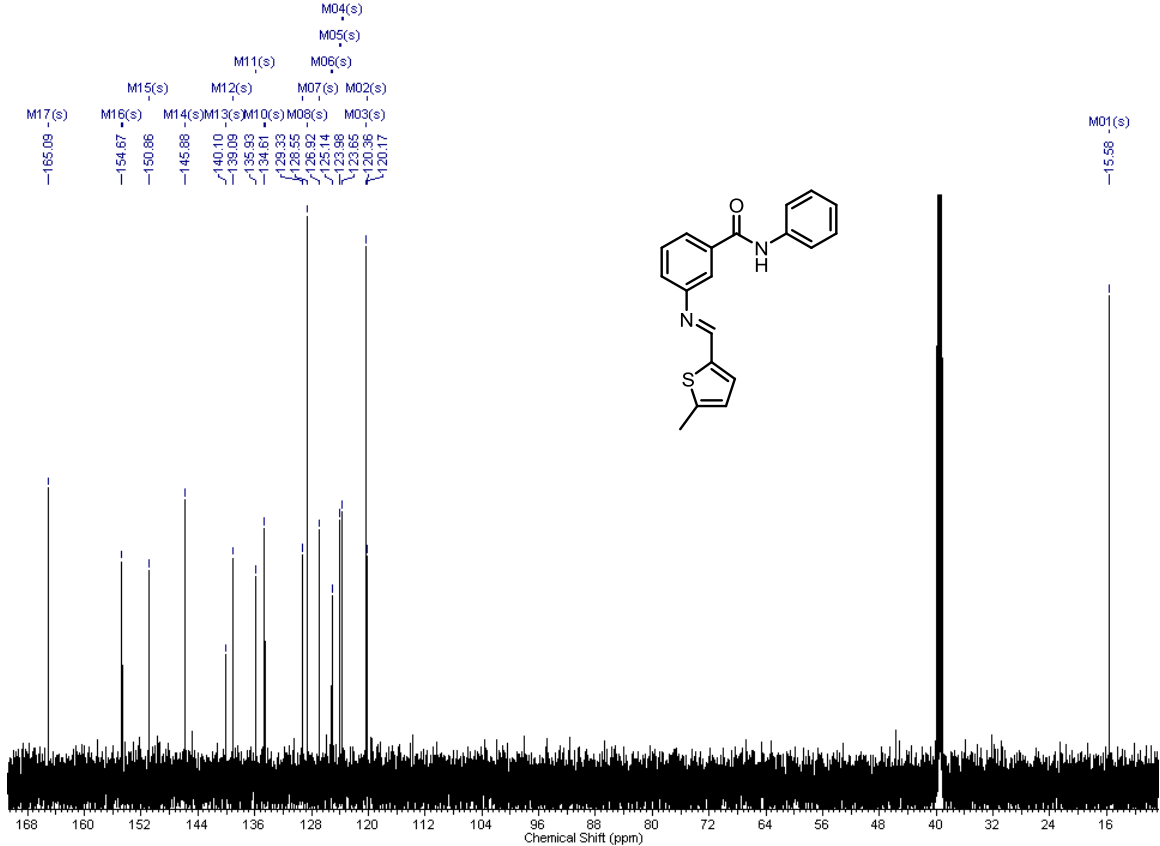
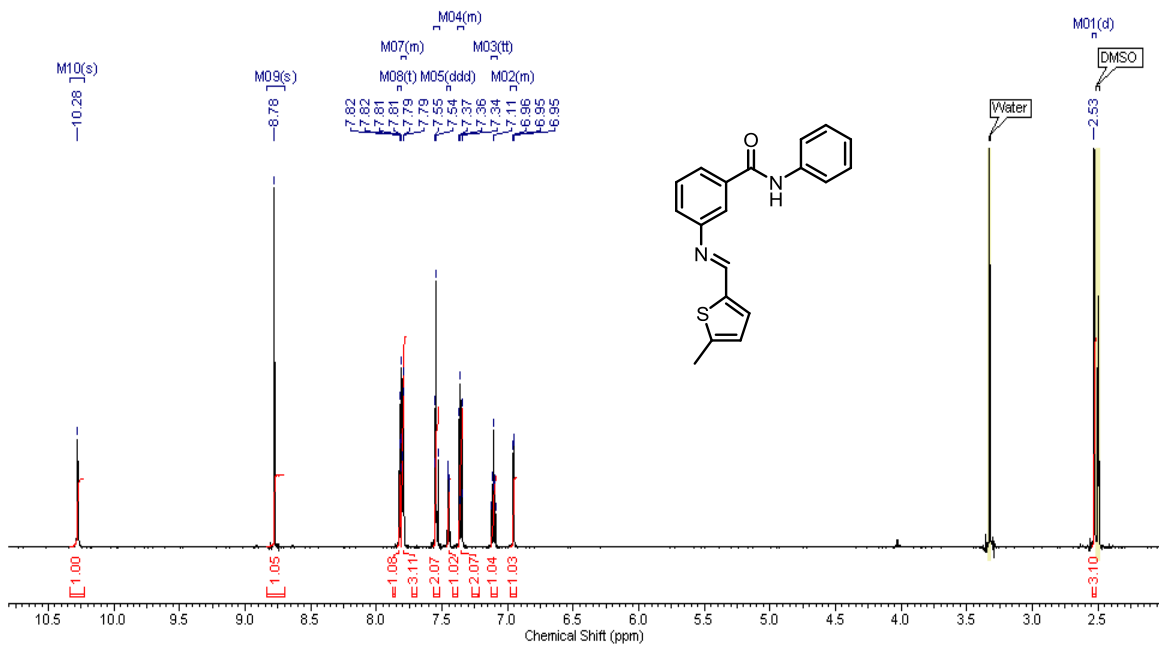
## Chapter 2 - Dihydroquinazolinone Retrograde Transport Inhibitors

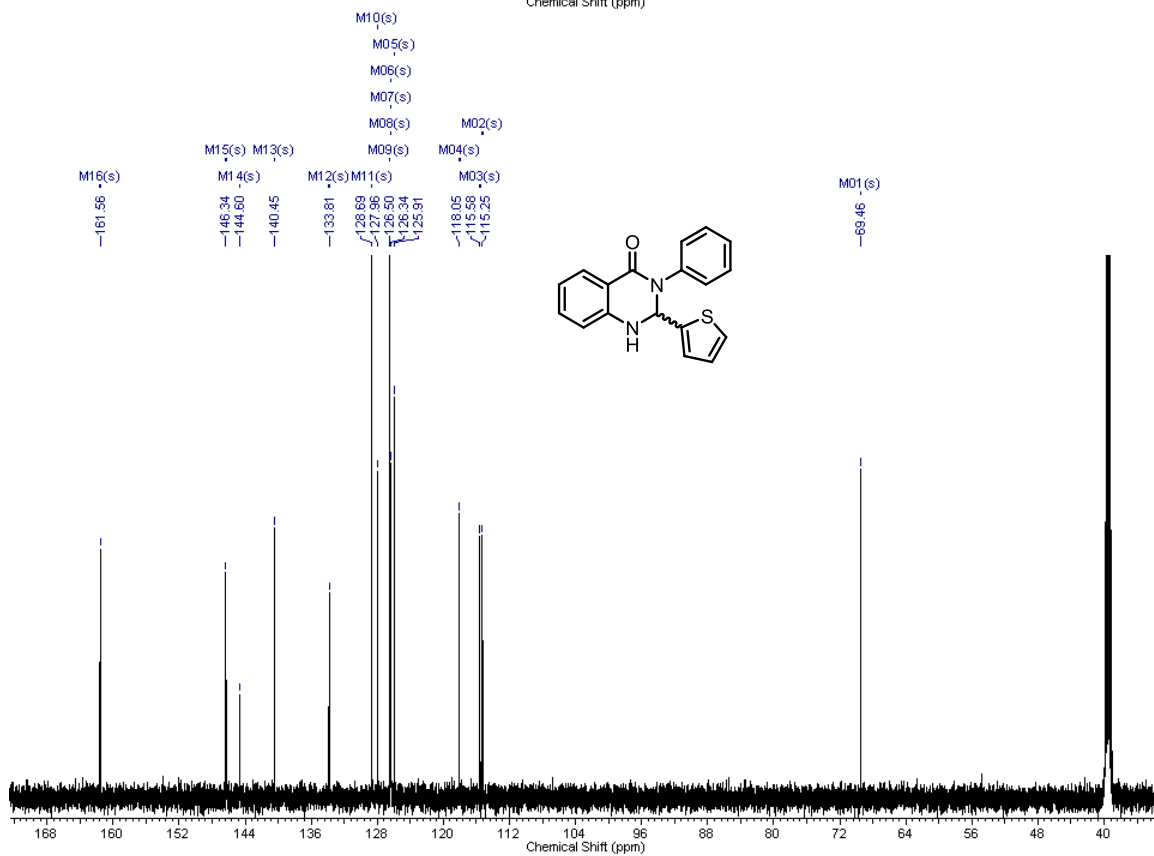
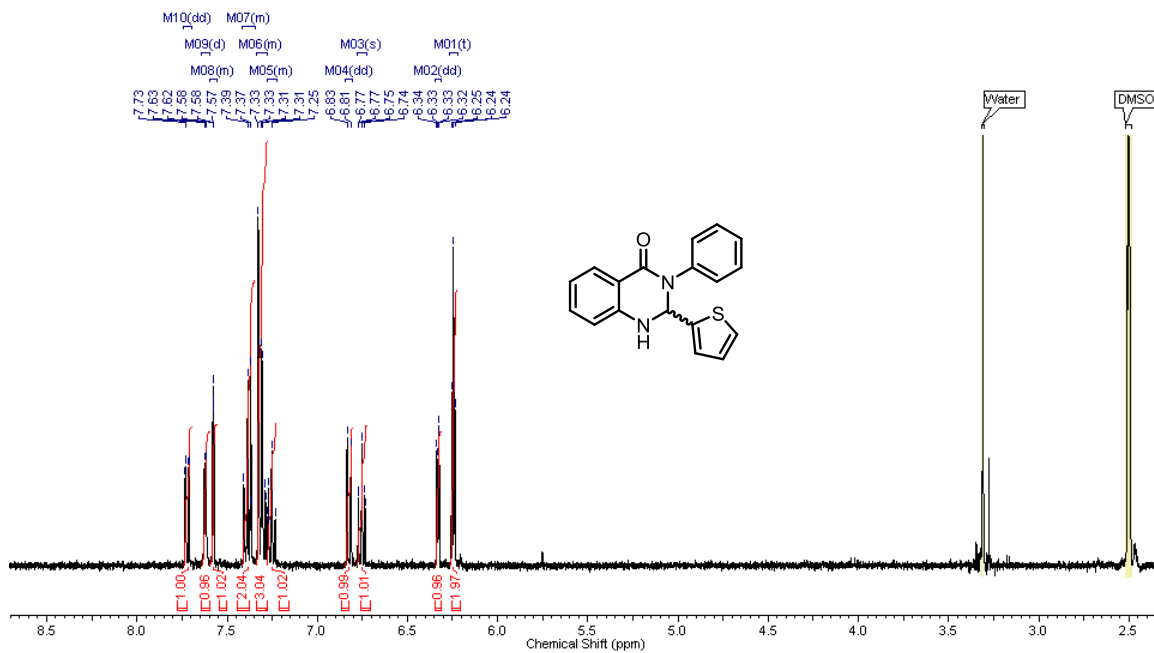


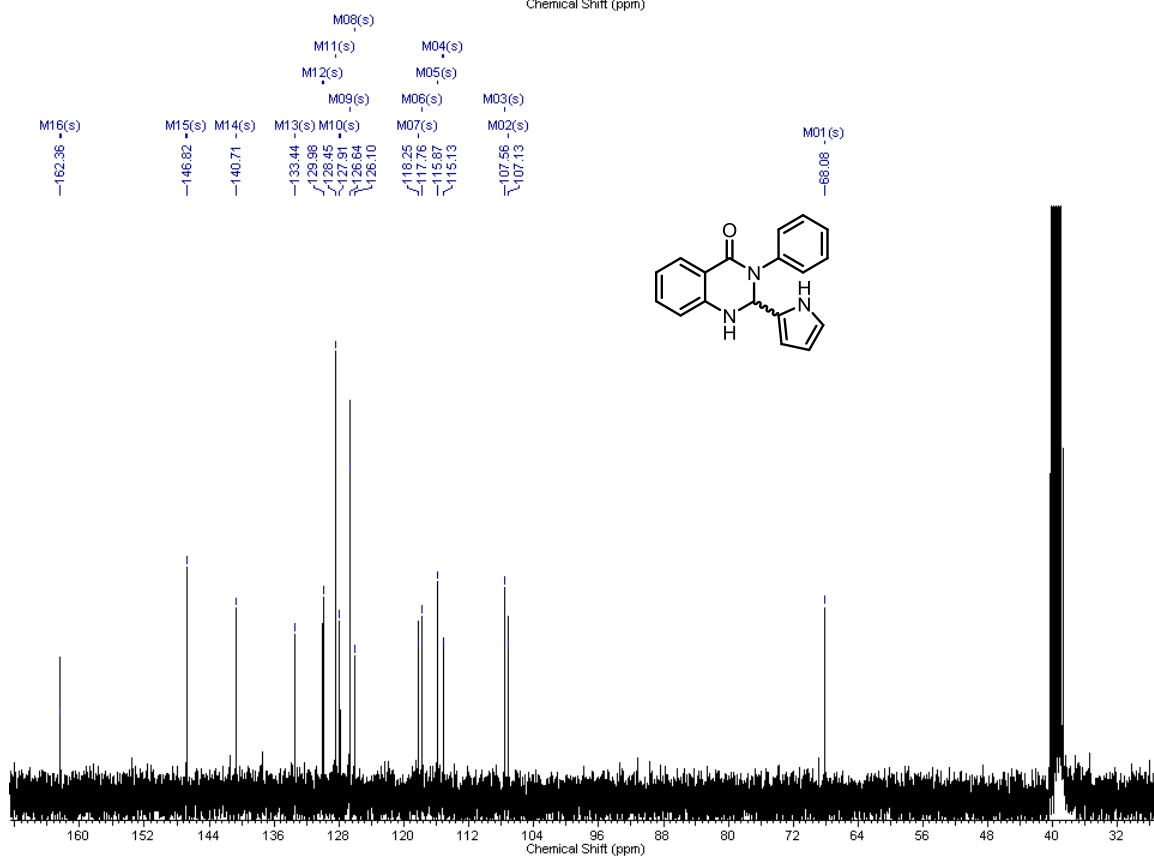
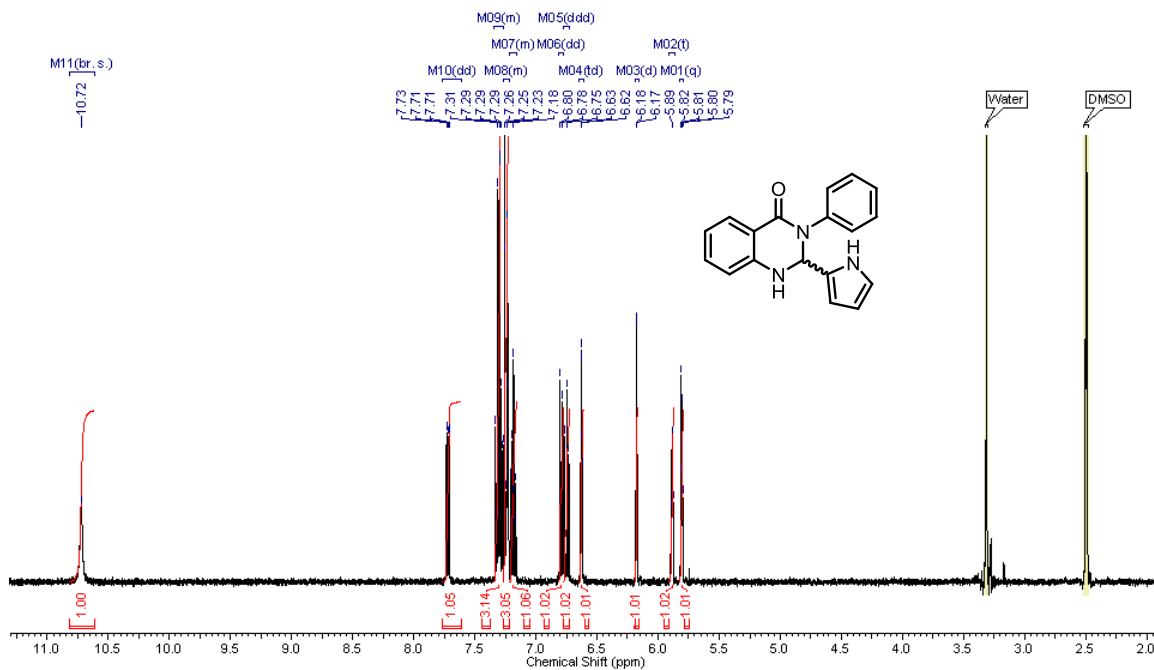


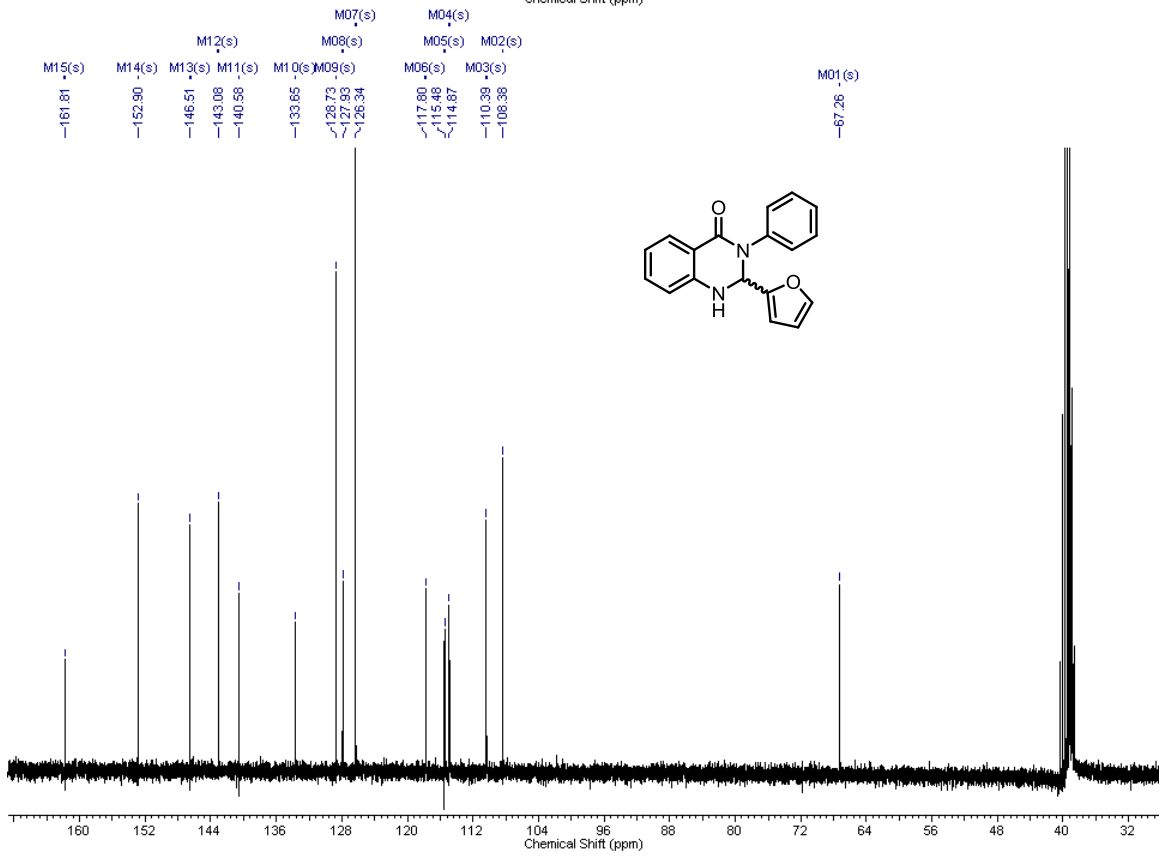
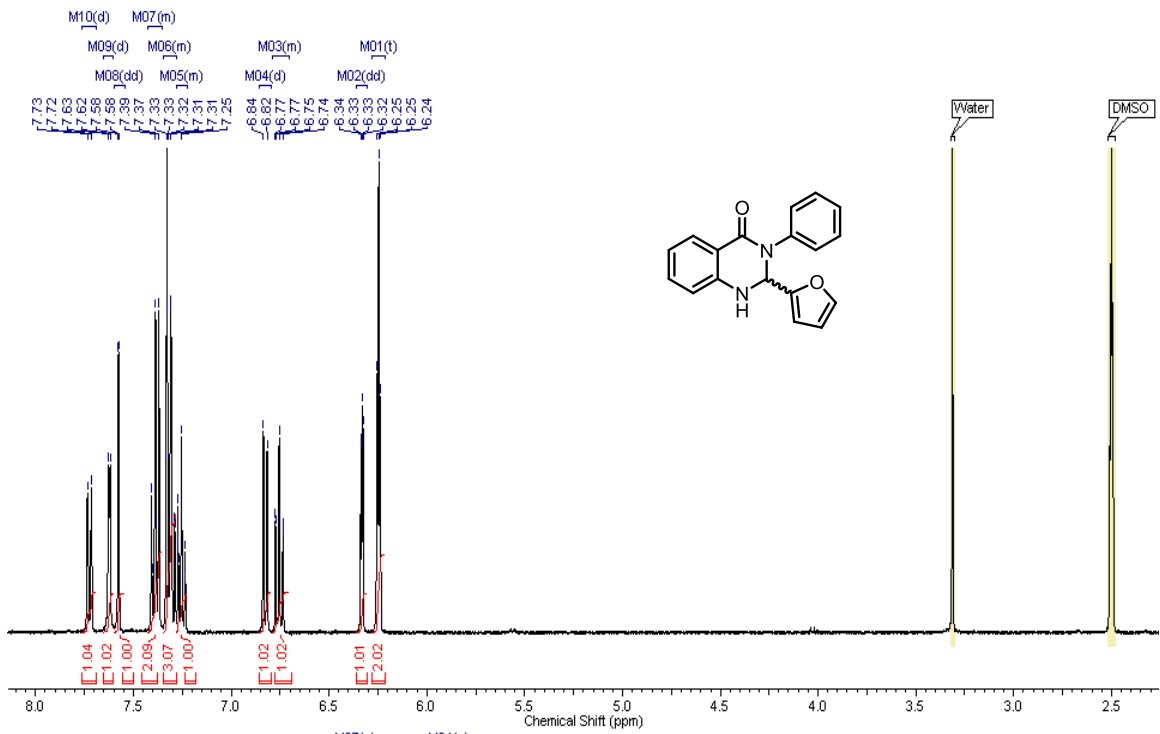




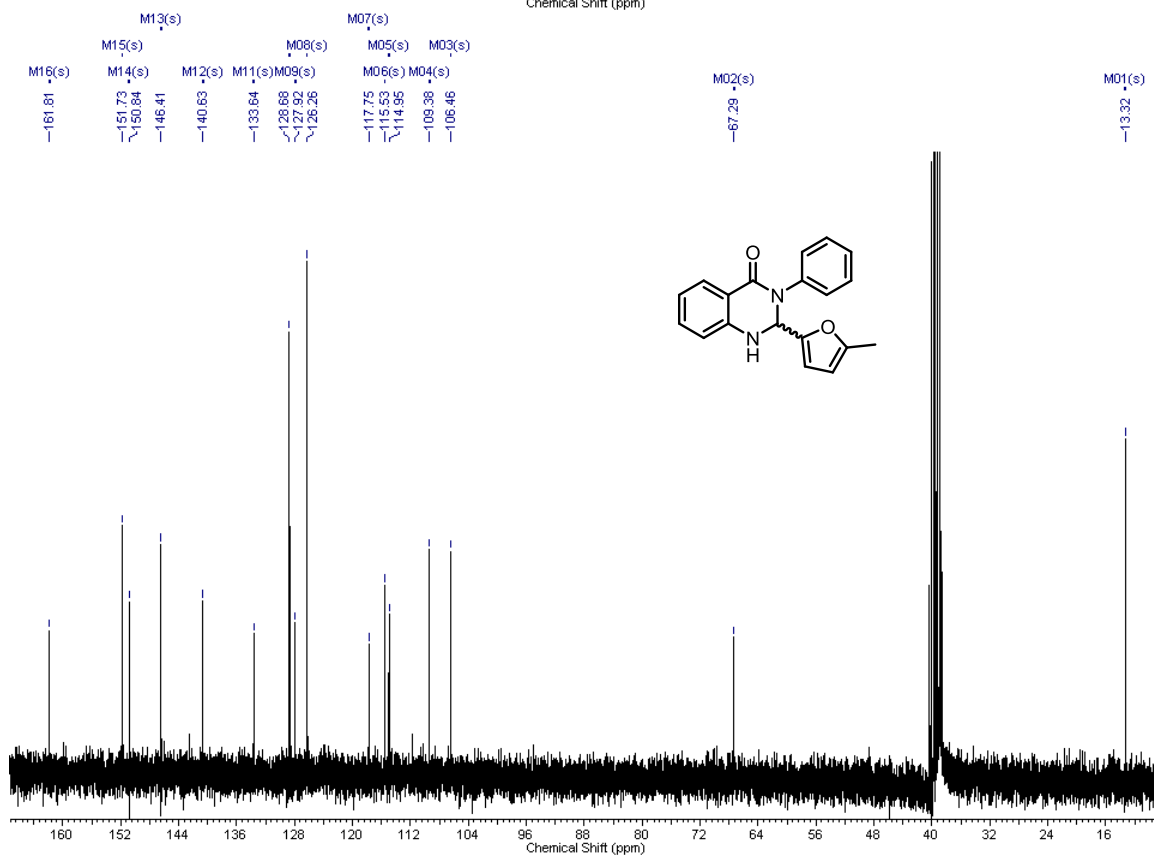
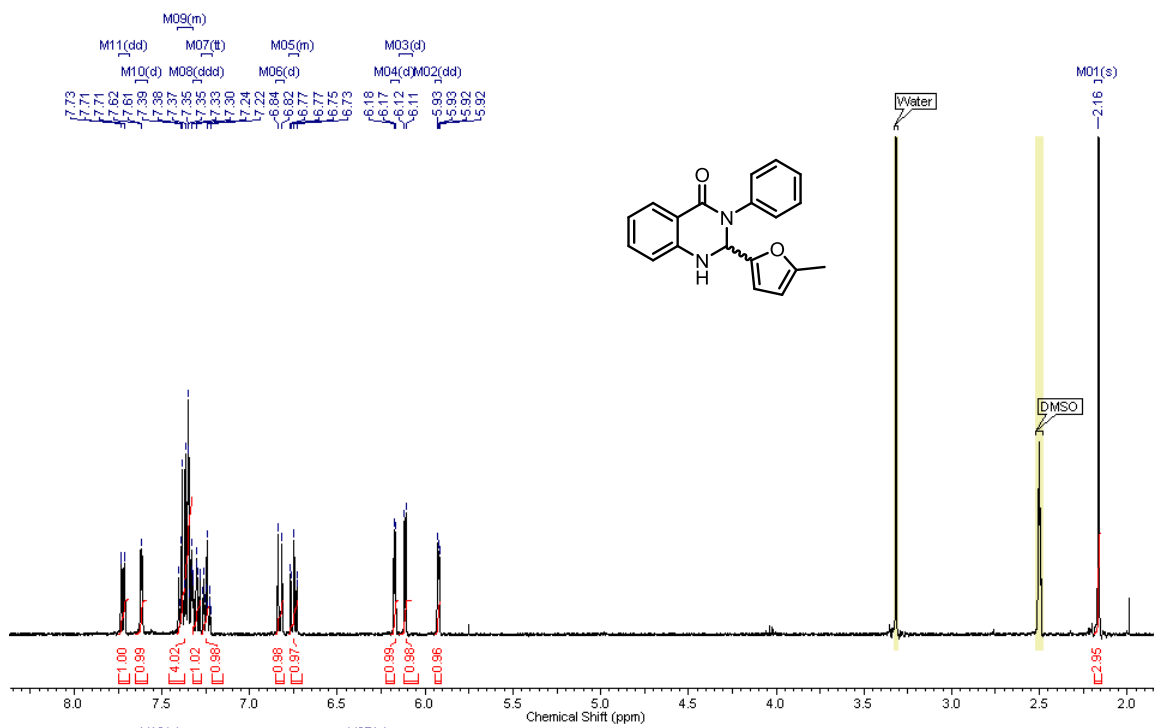


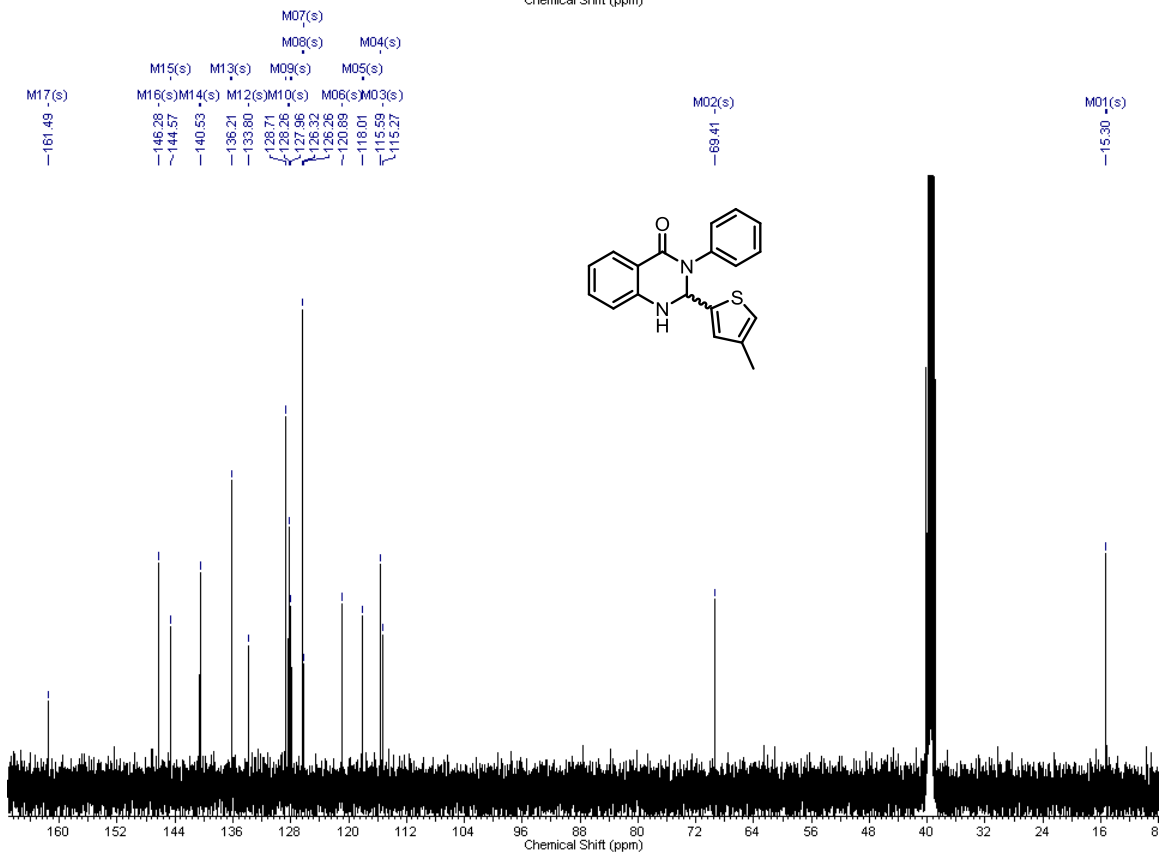
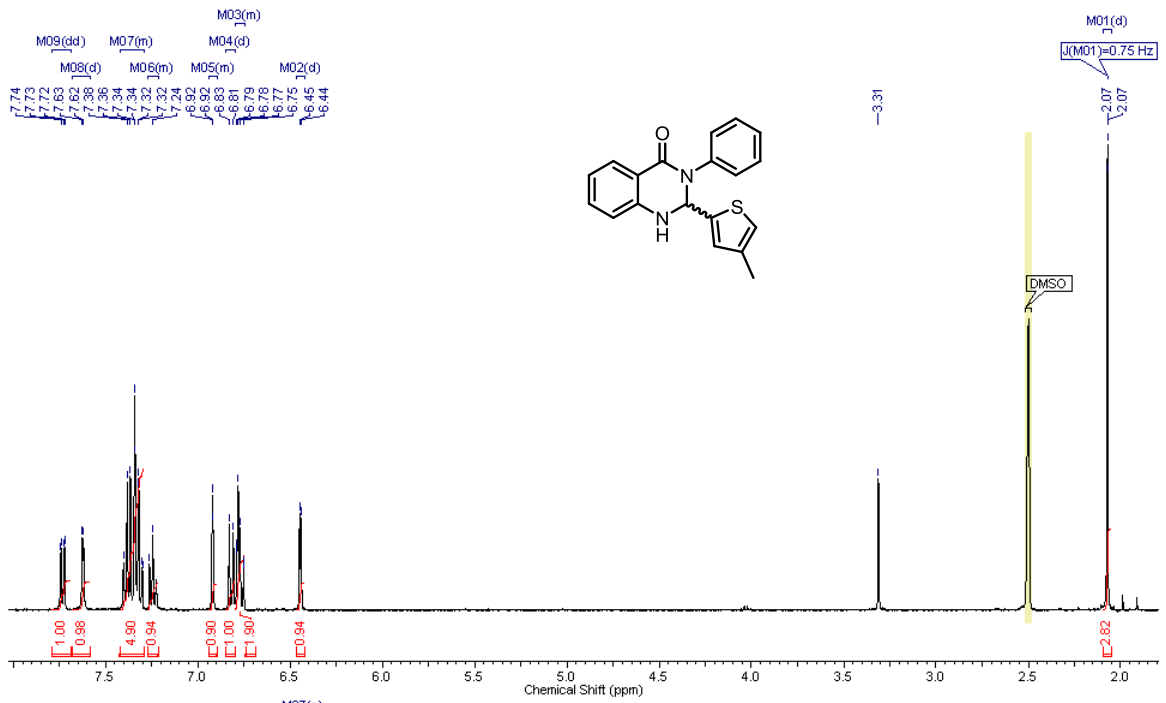


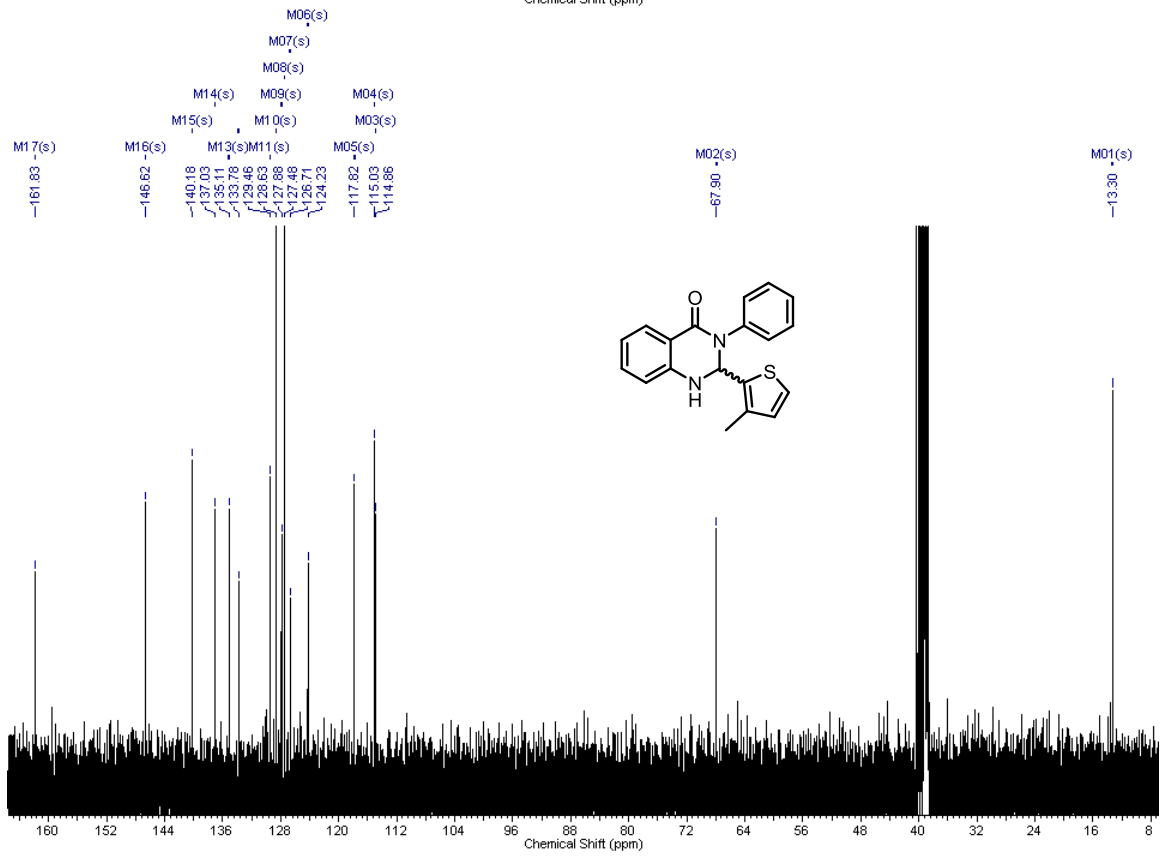
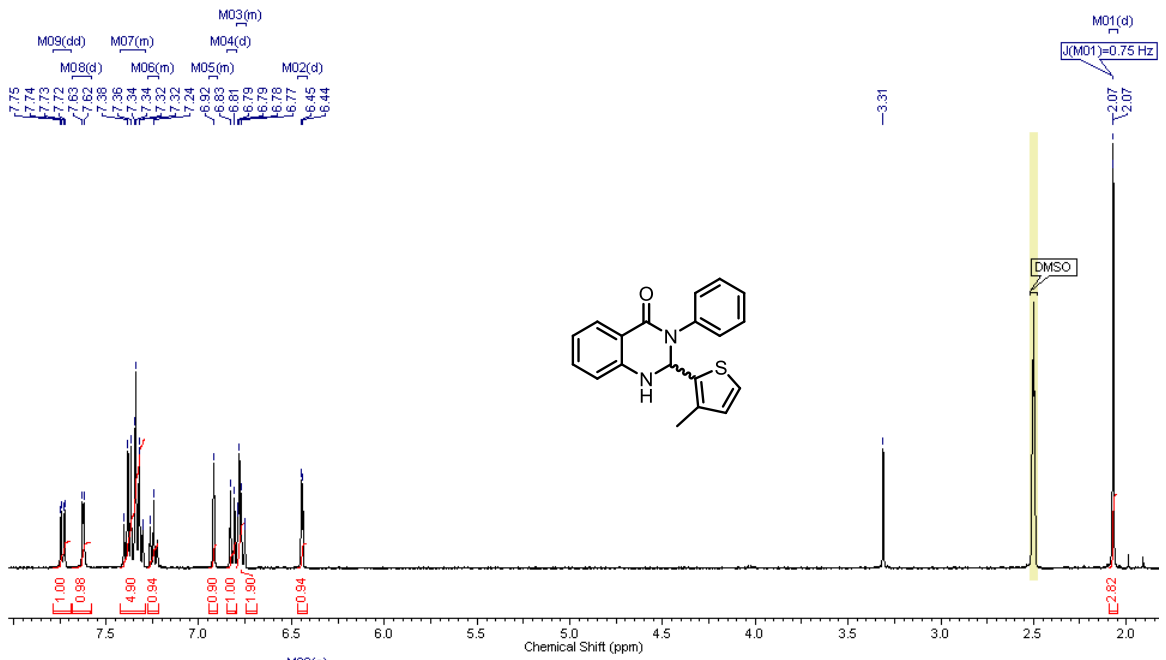


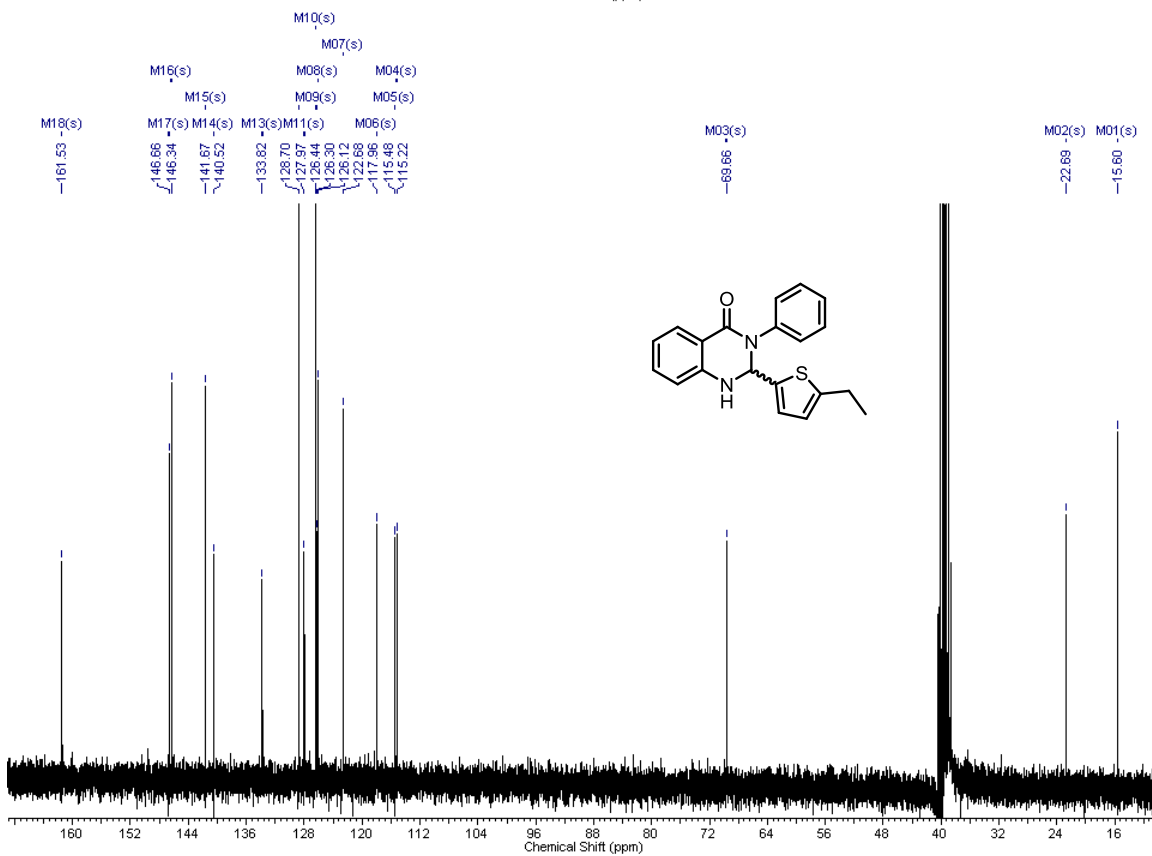
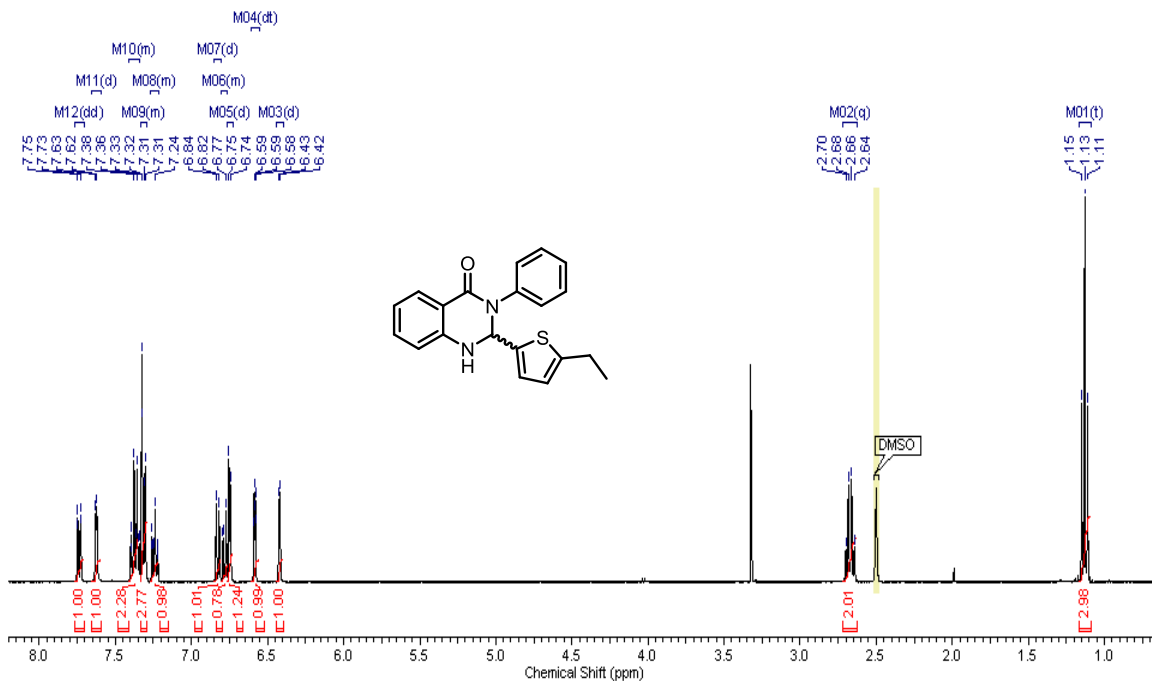


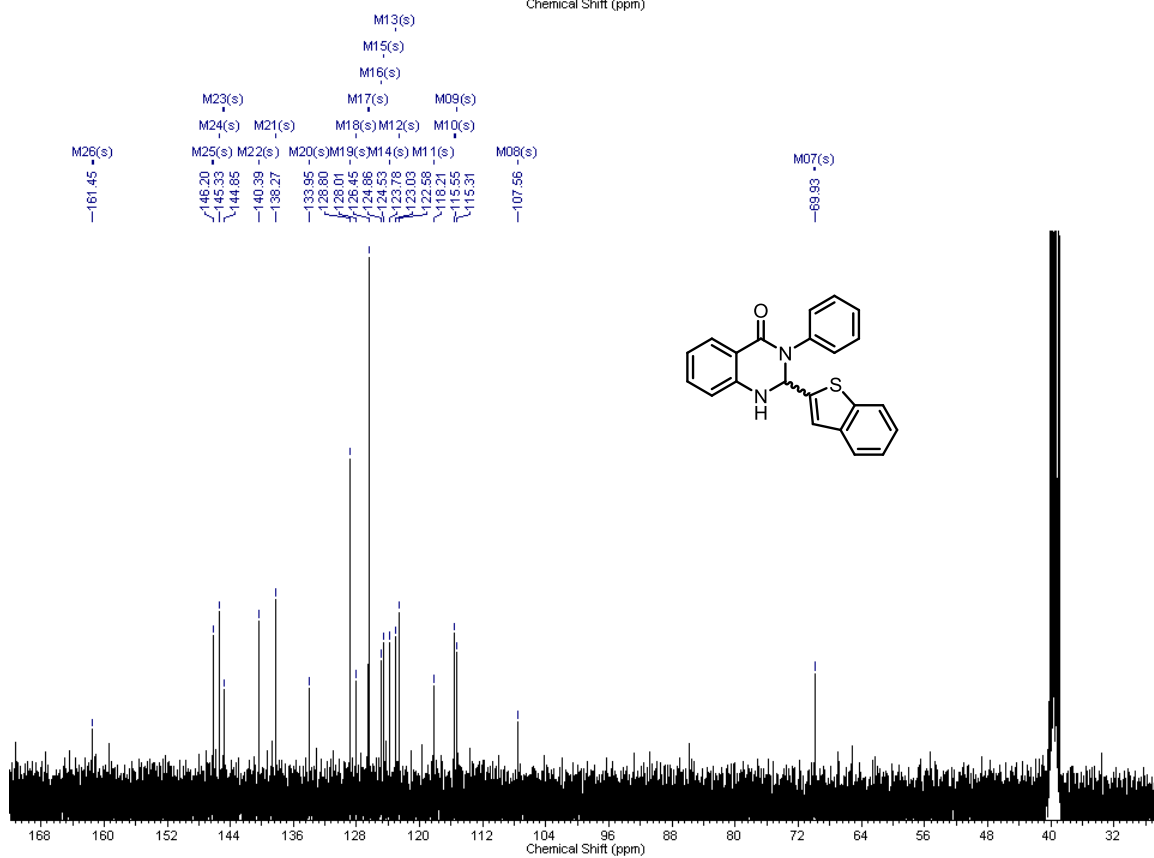
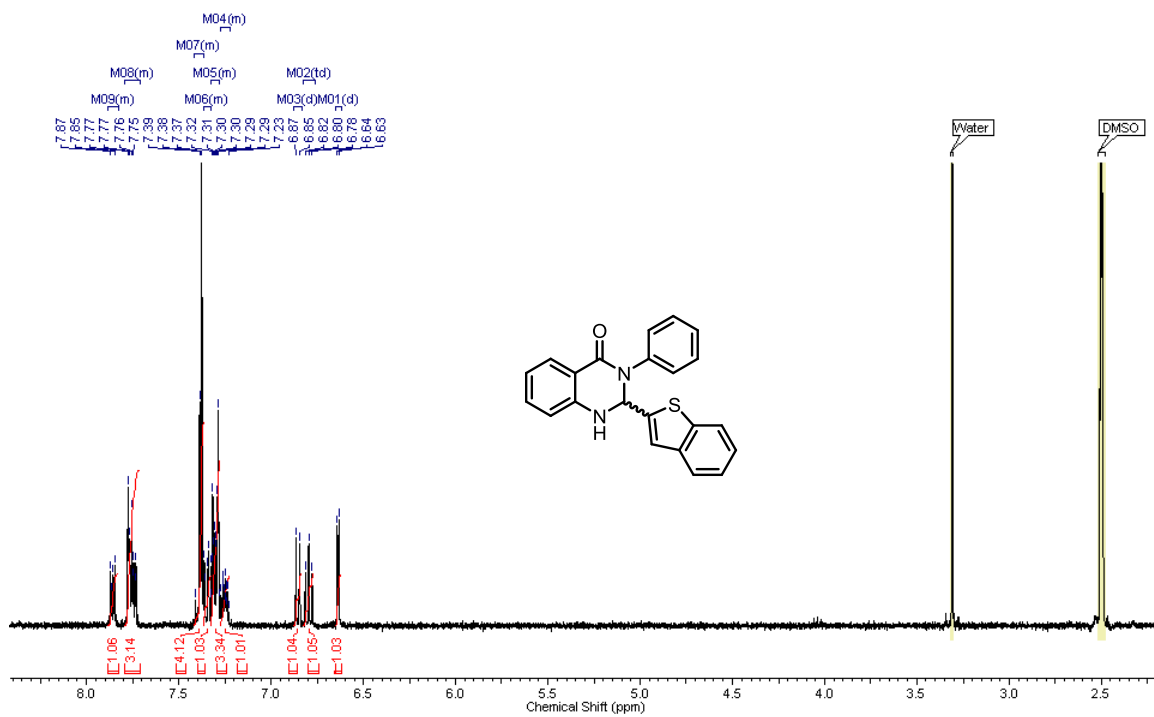


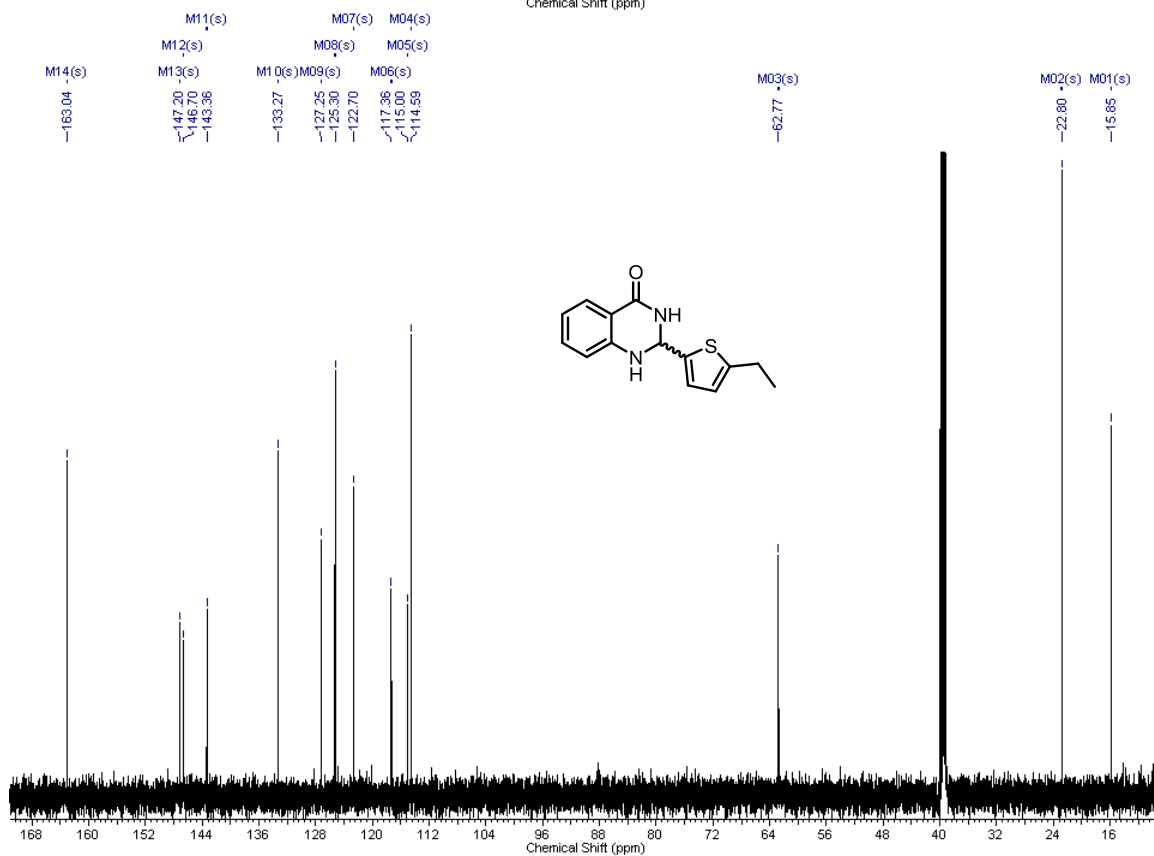
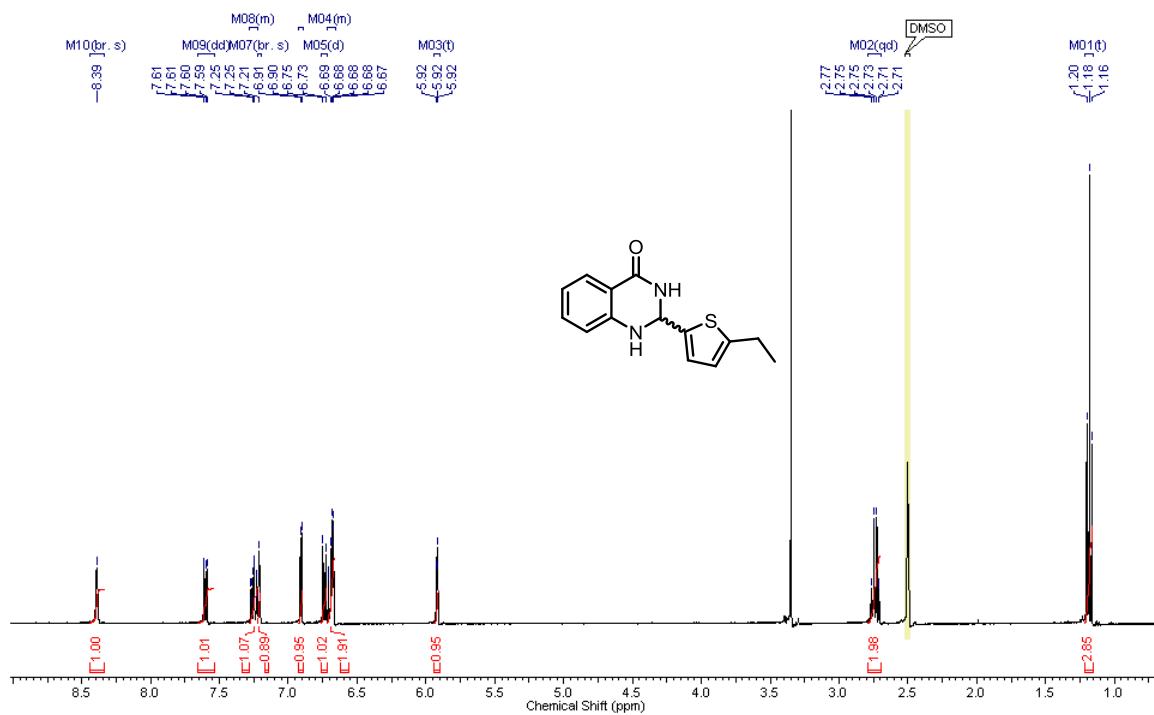


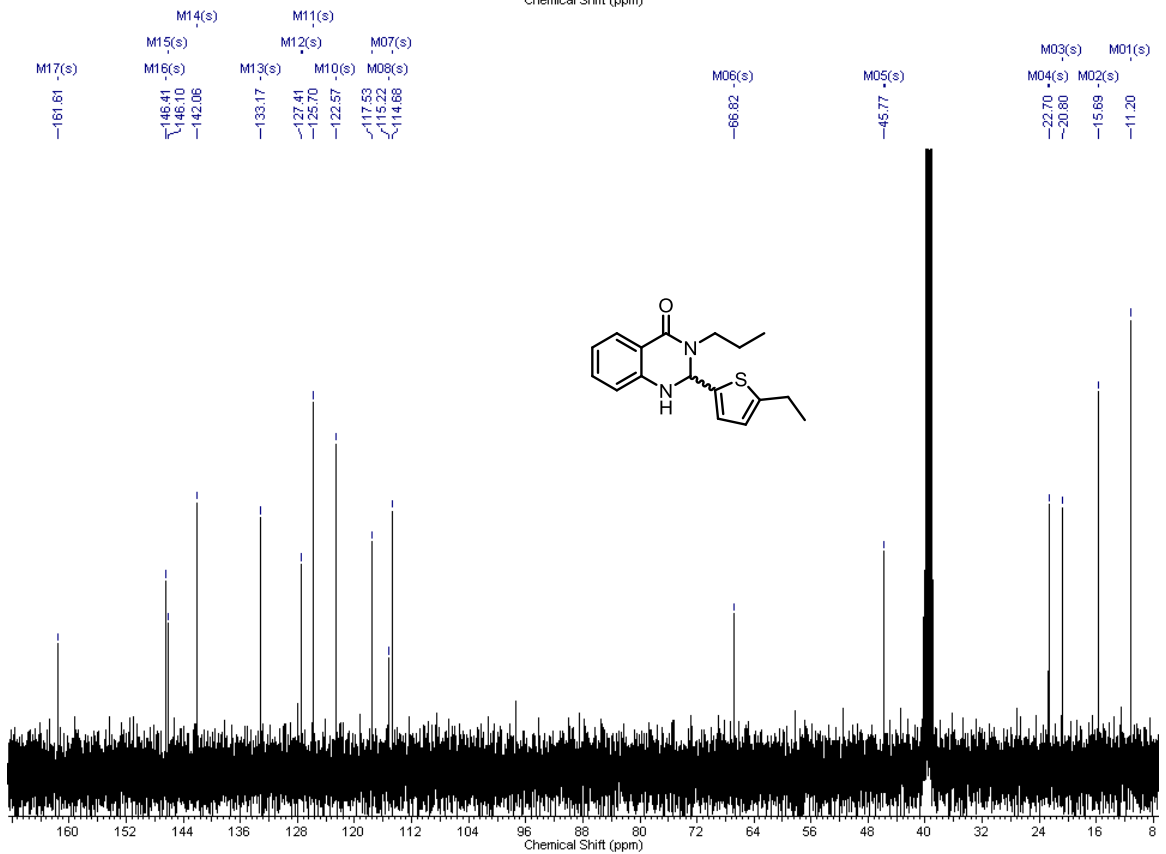
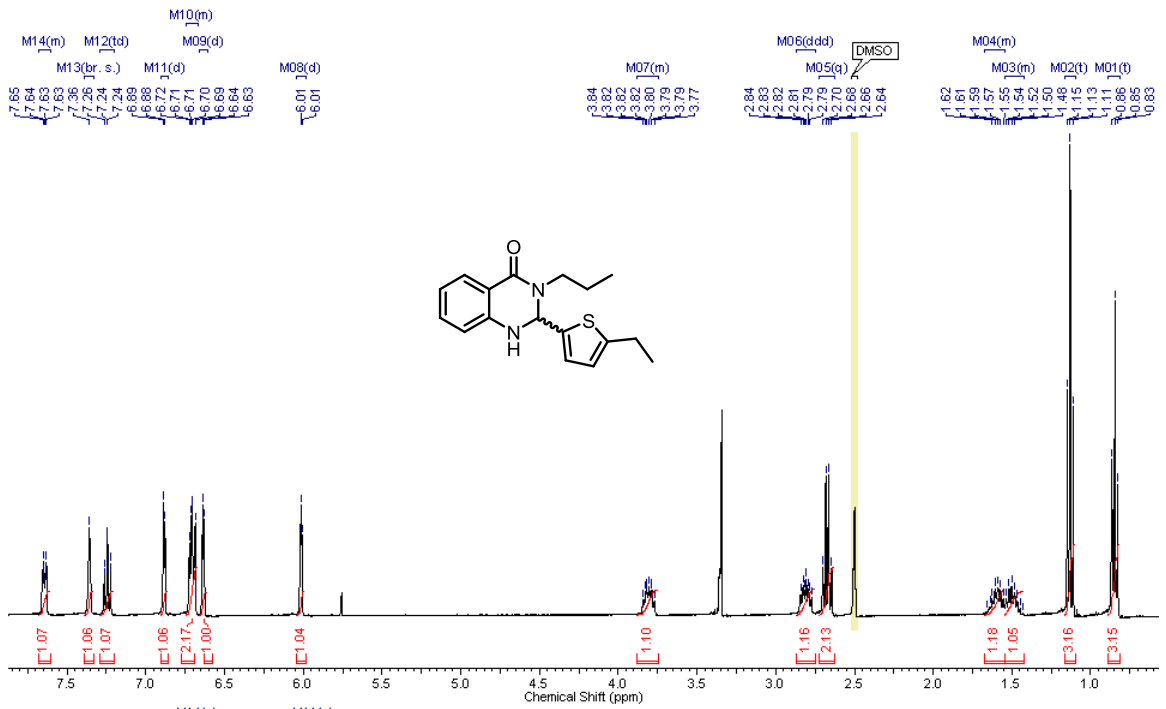


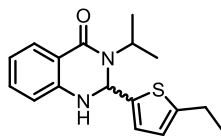
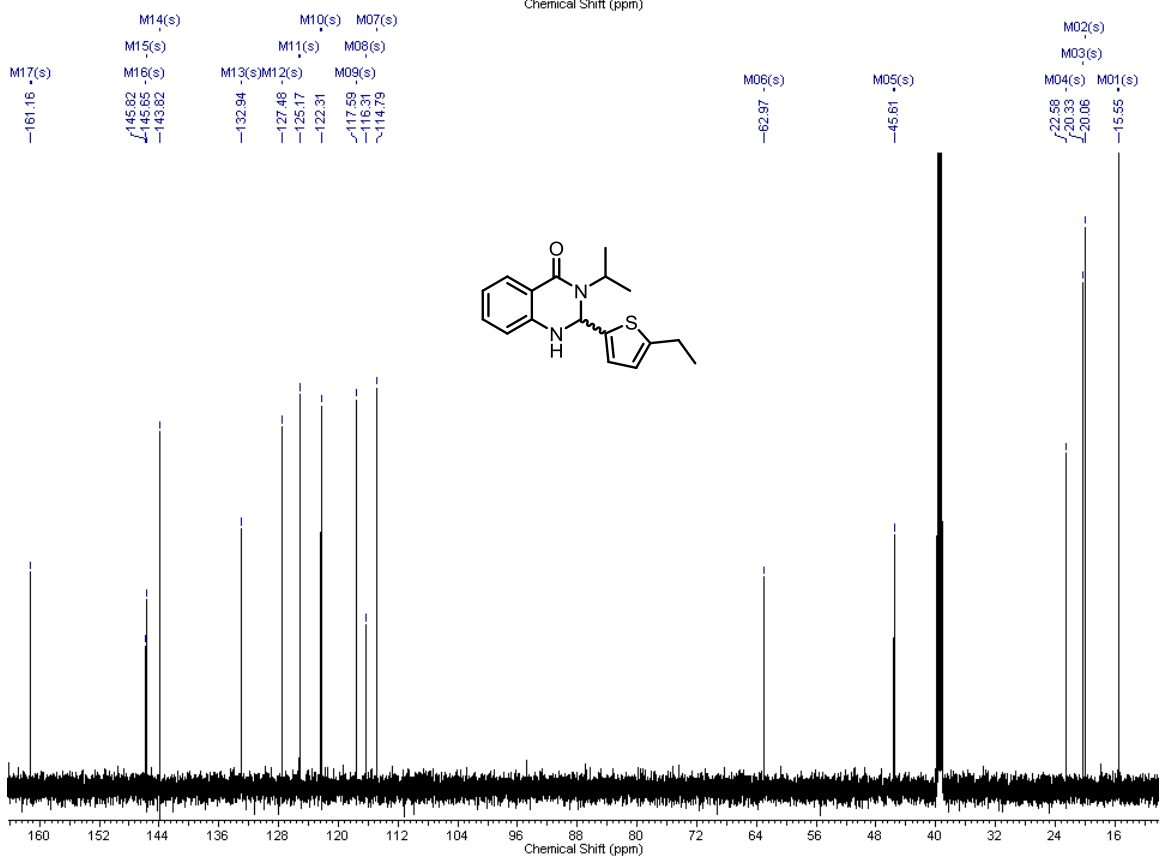
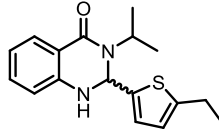
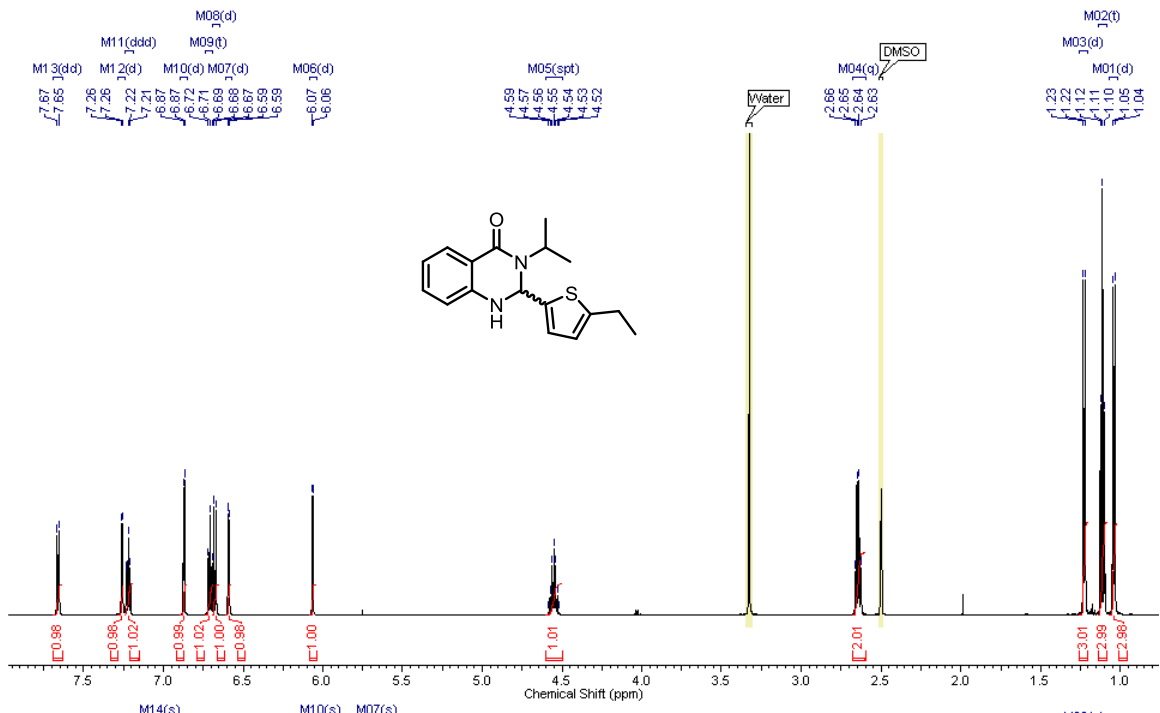




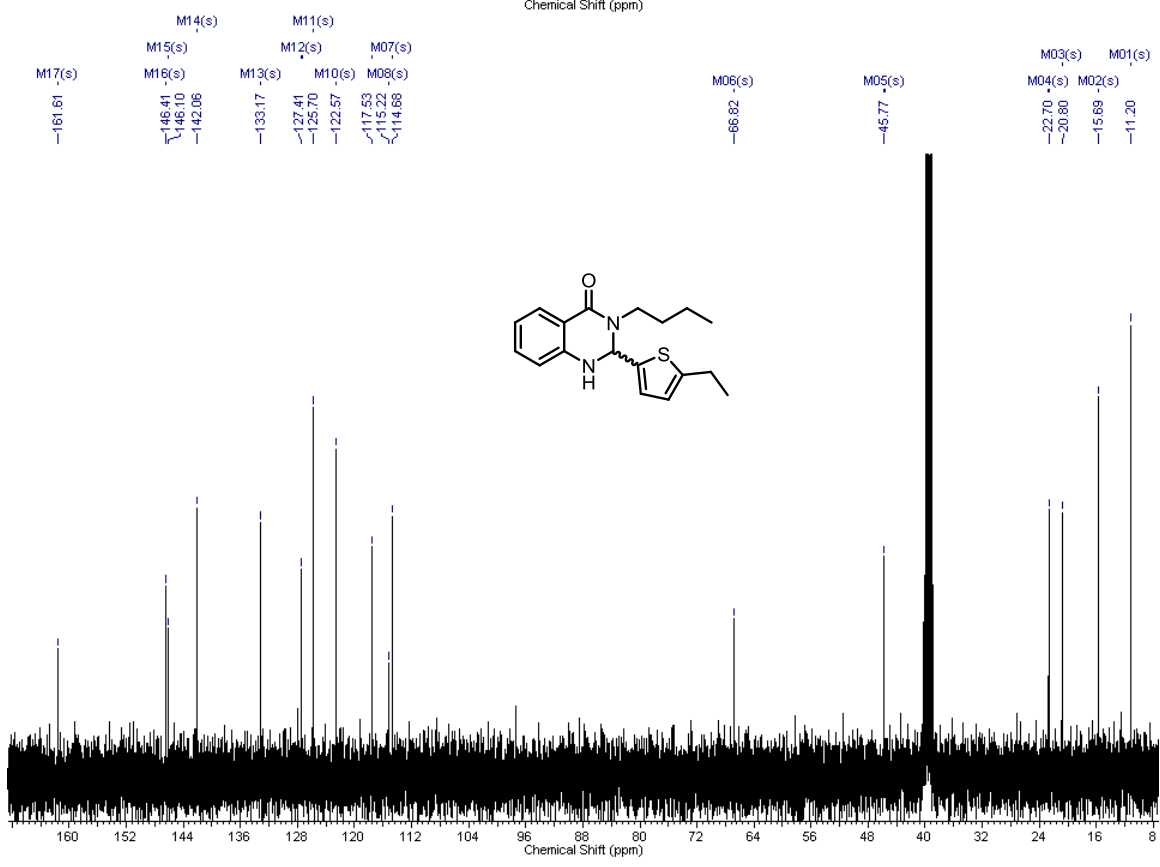
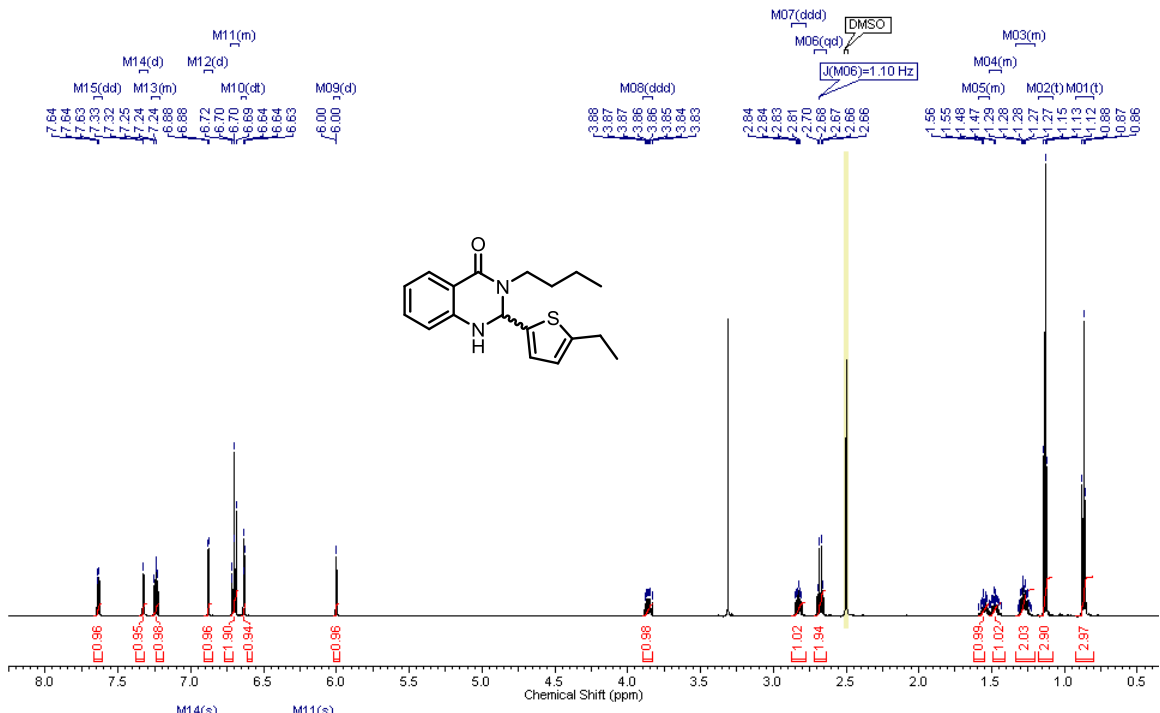


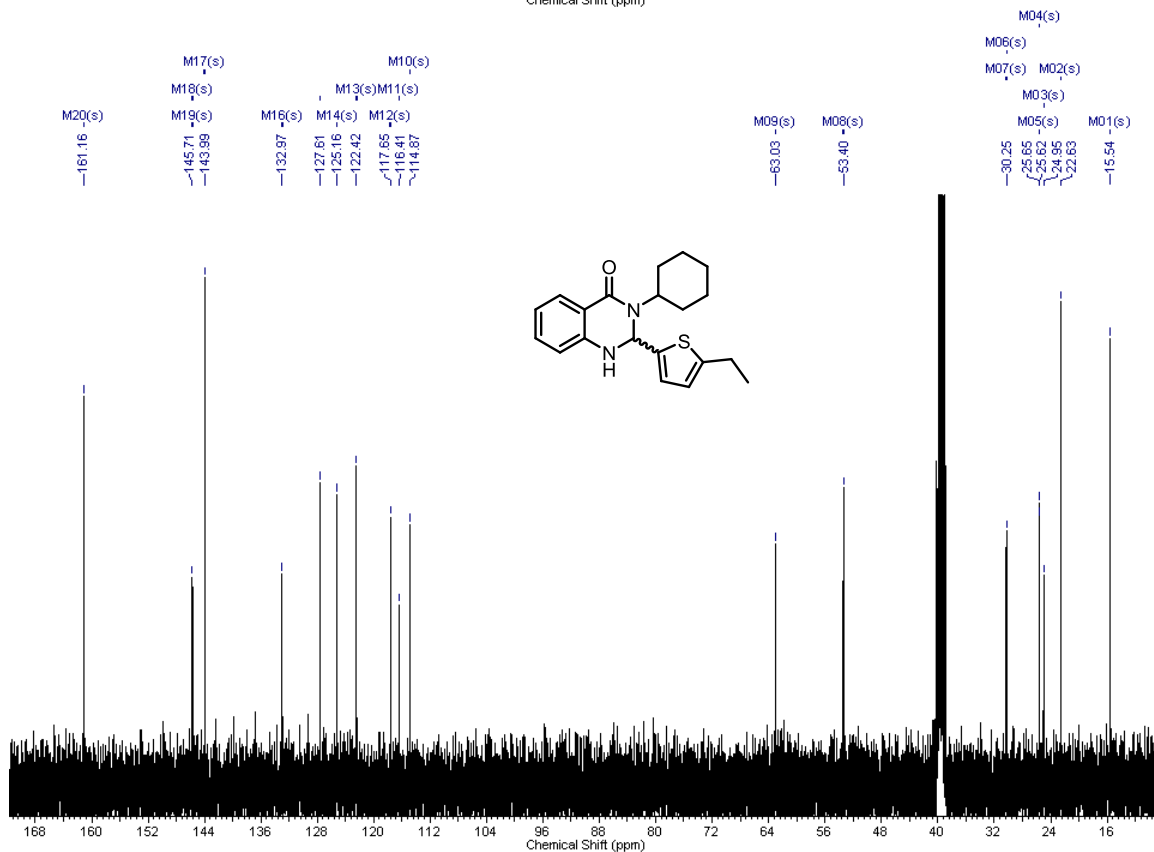
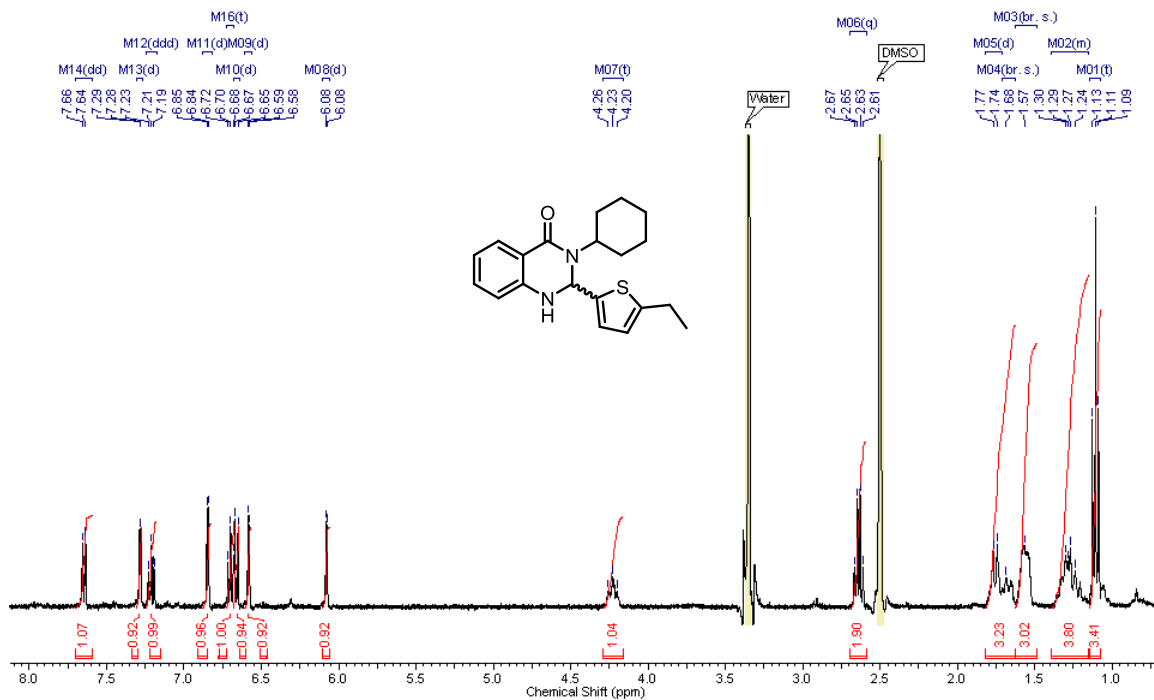


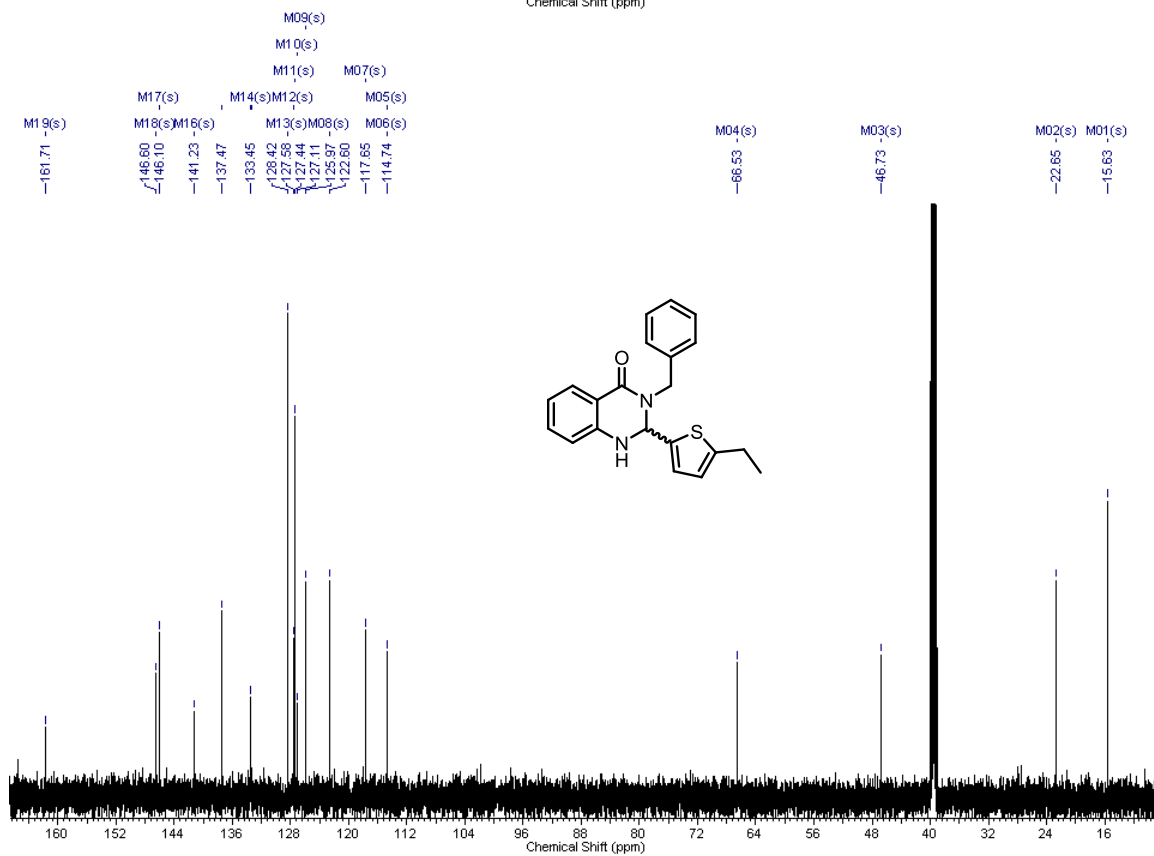
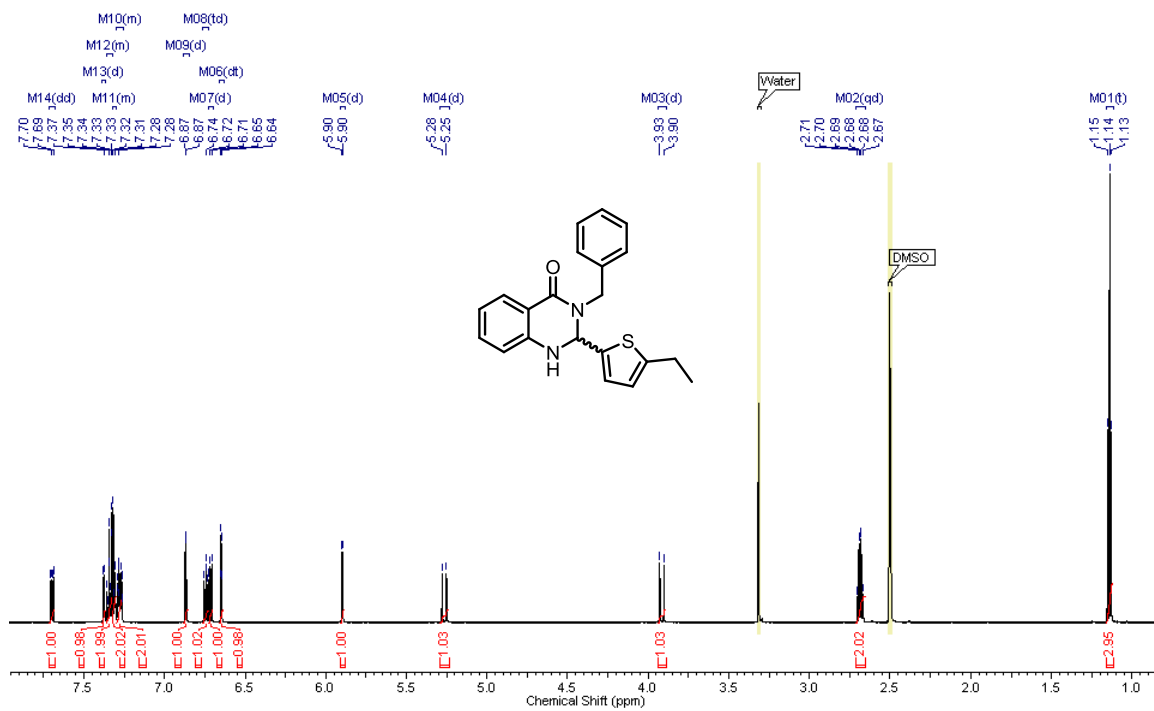


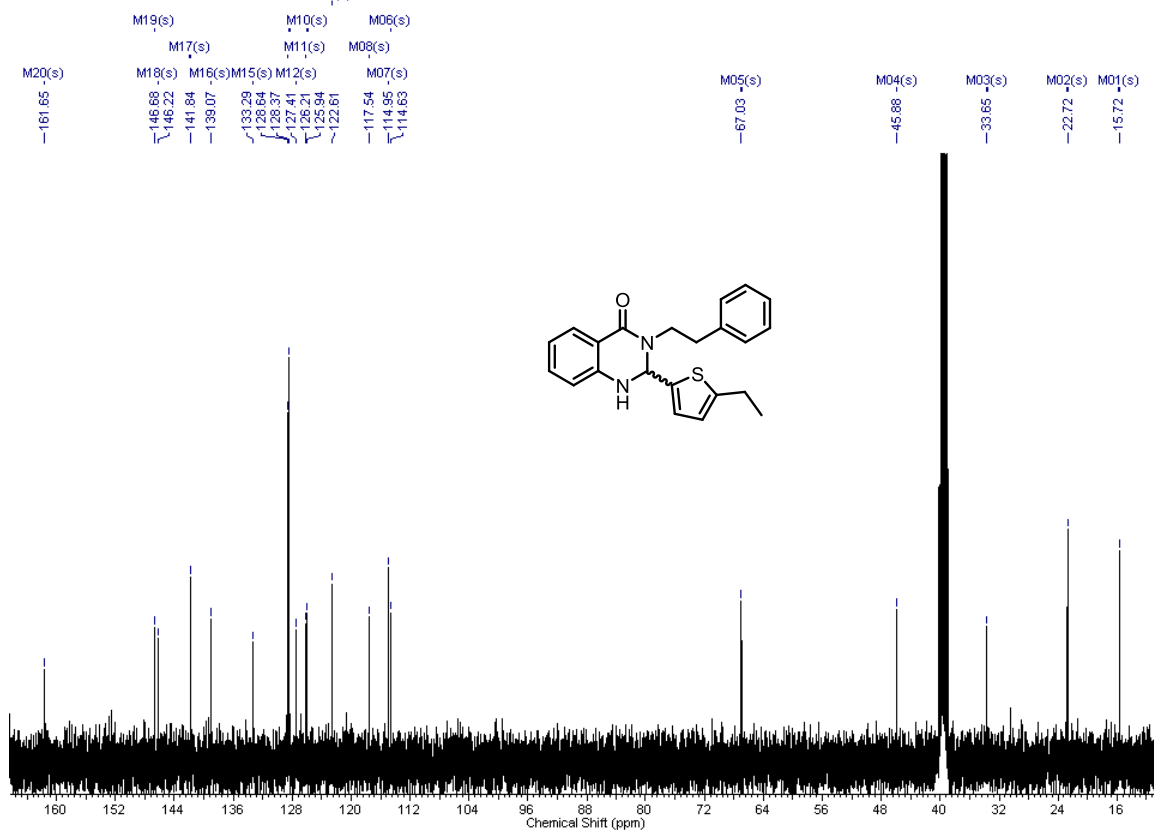
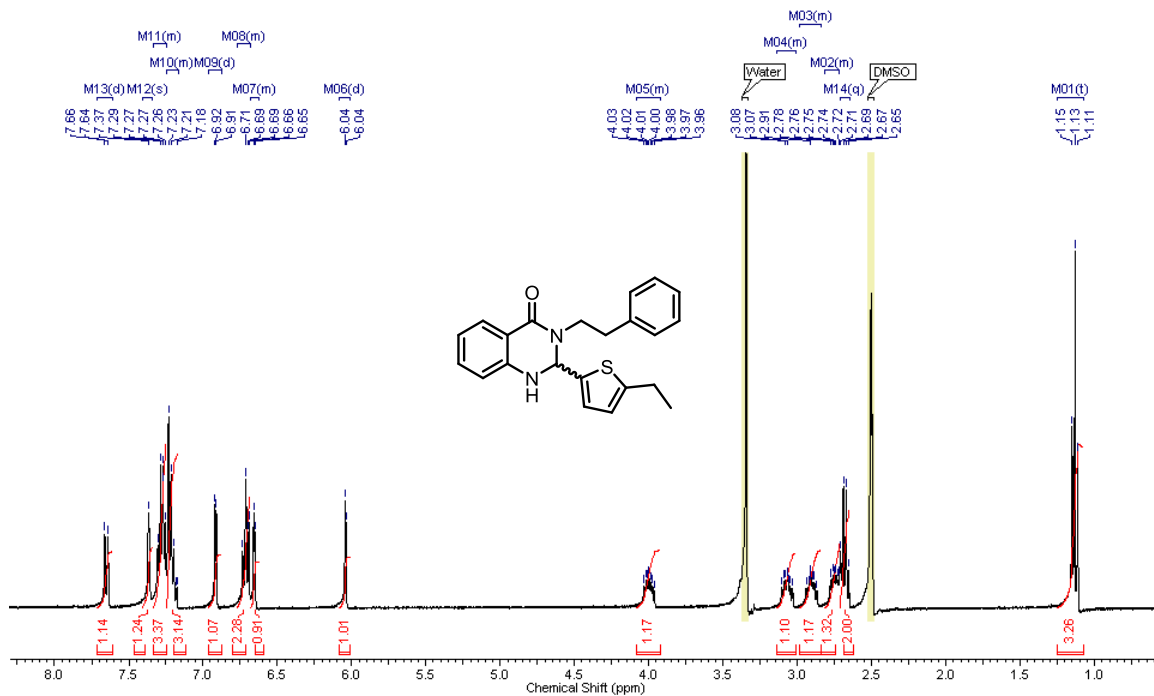


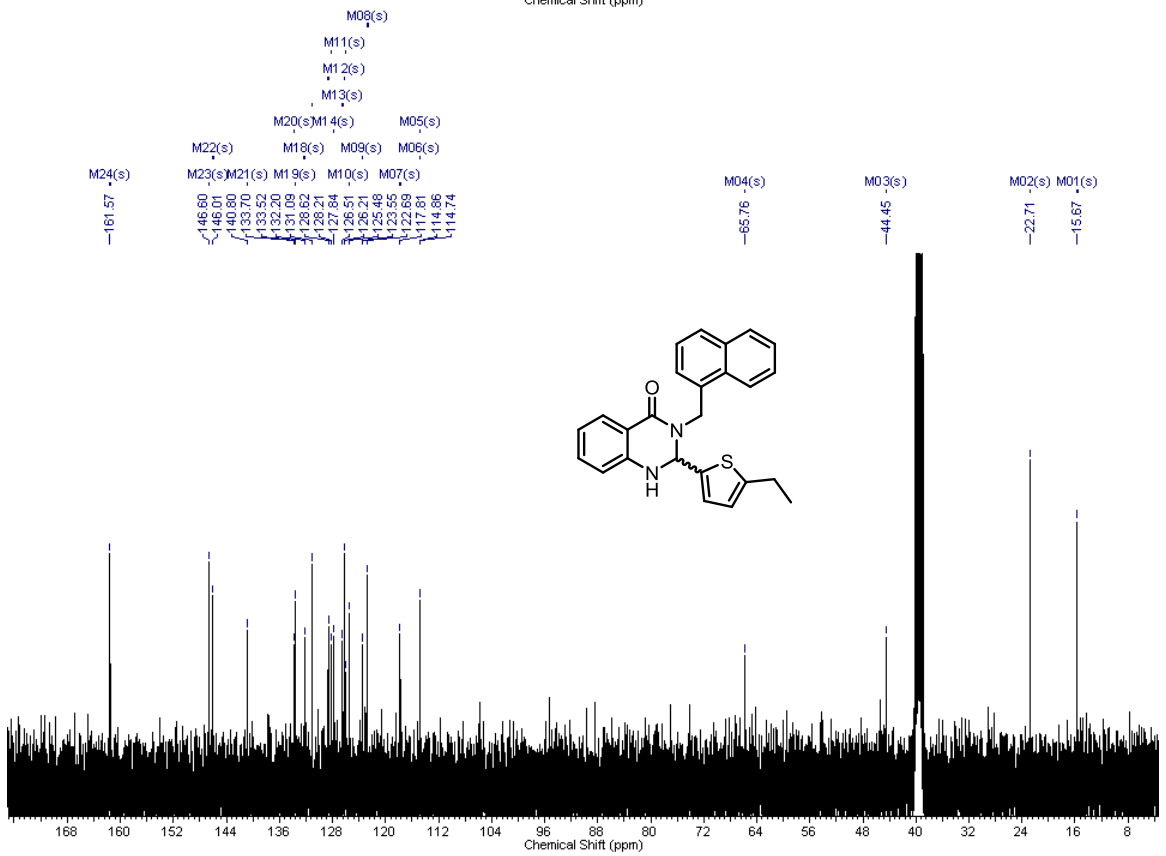
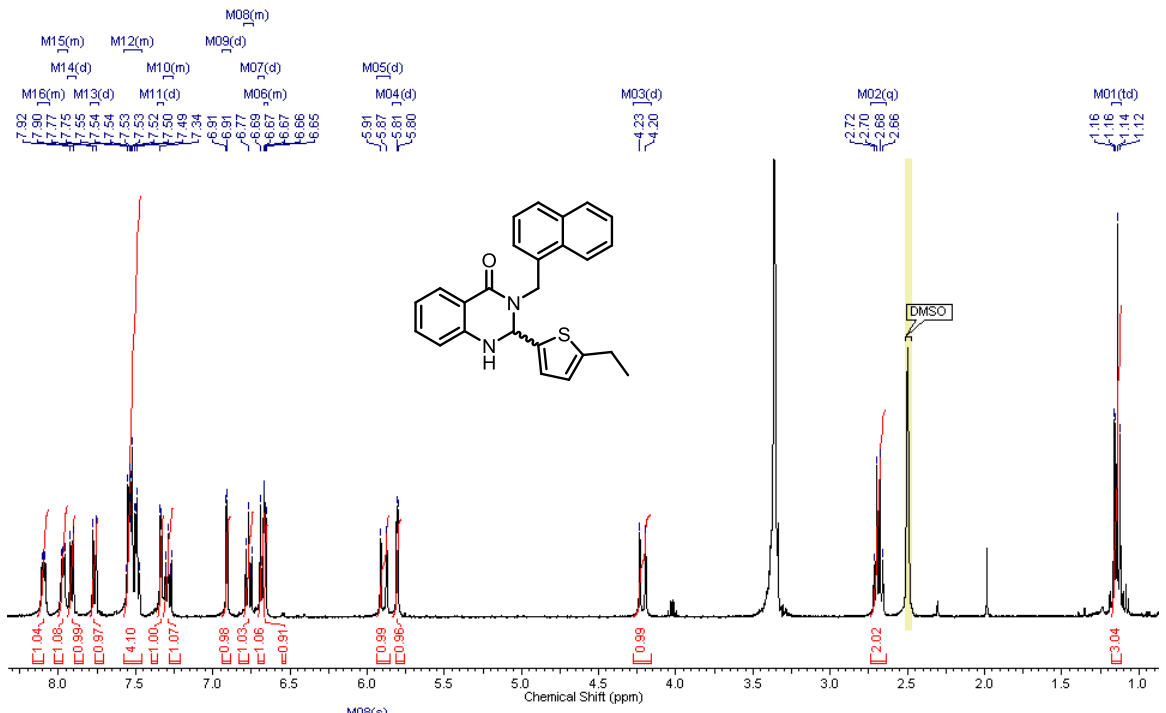


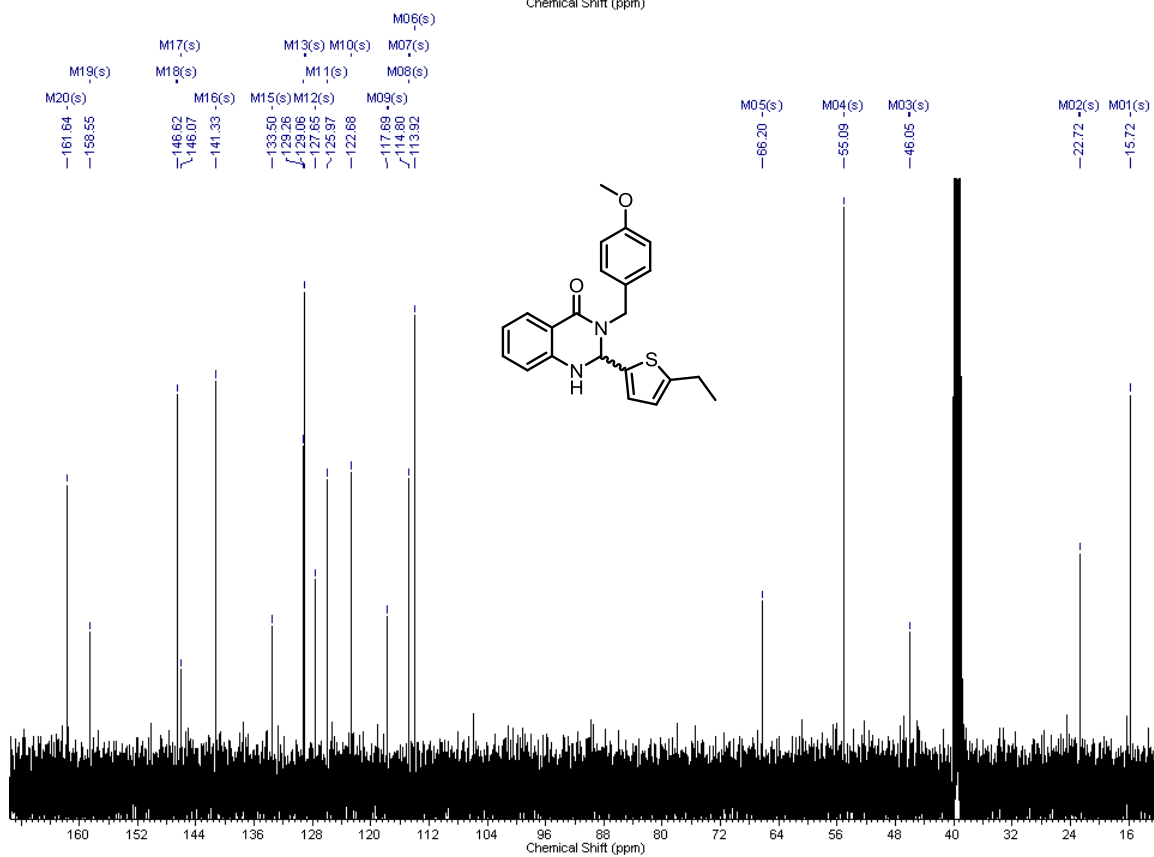
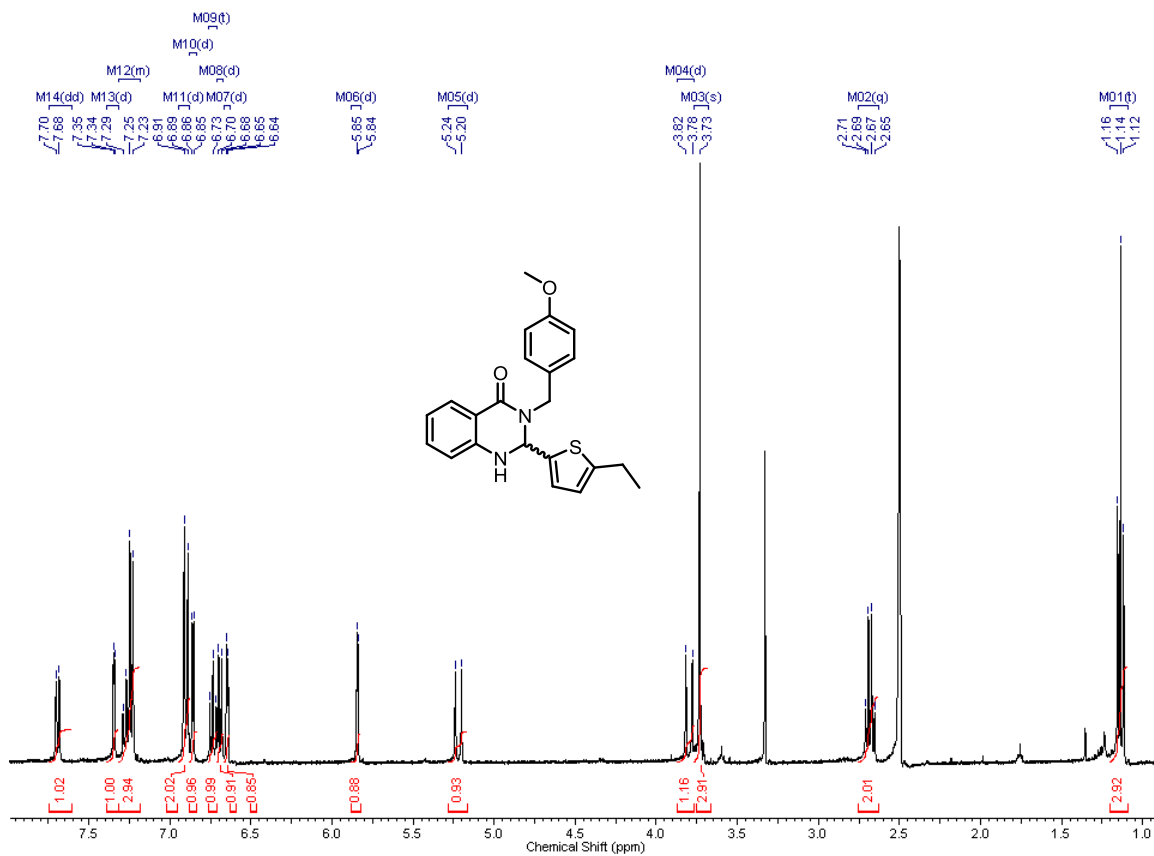


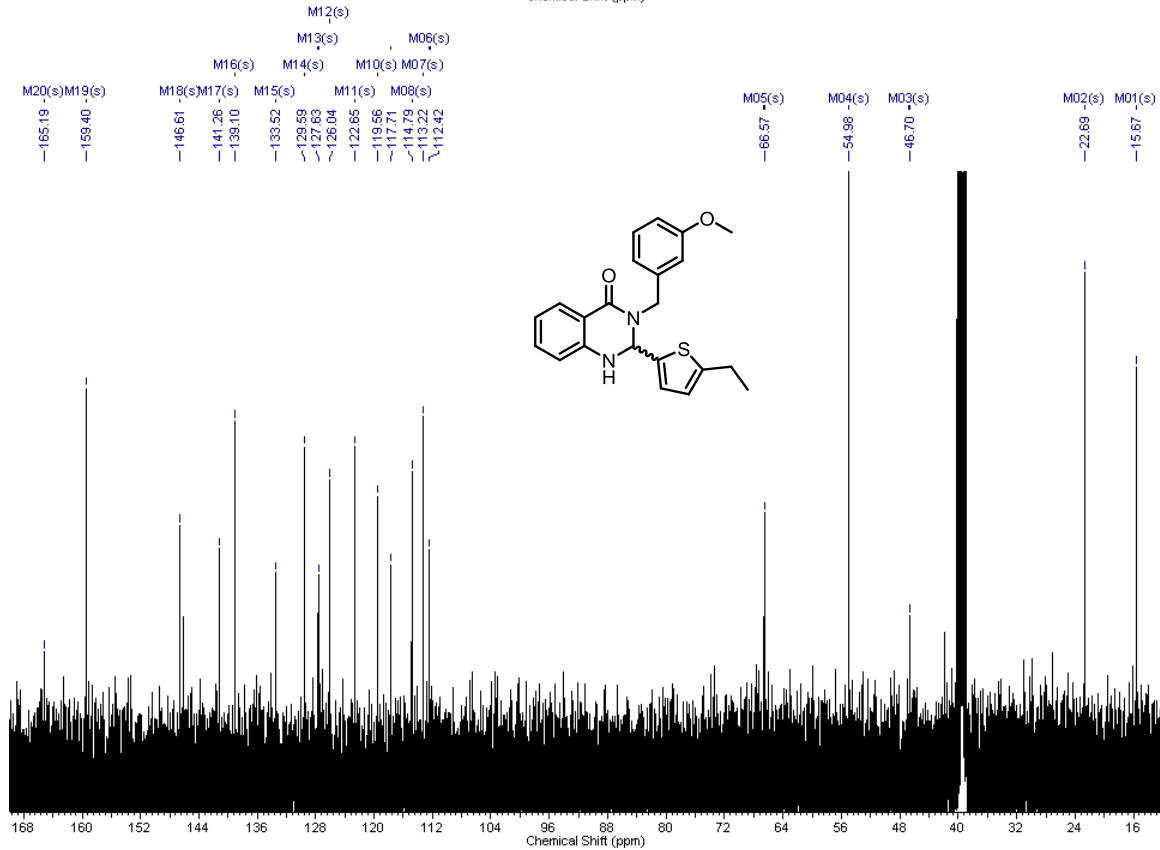
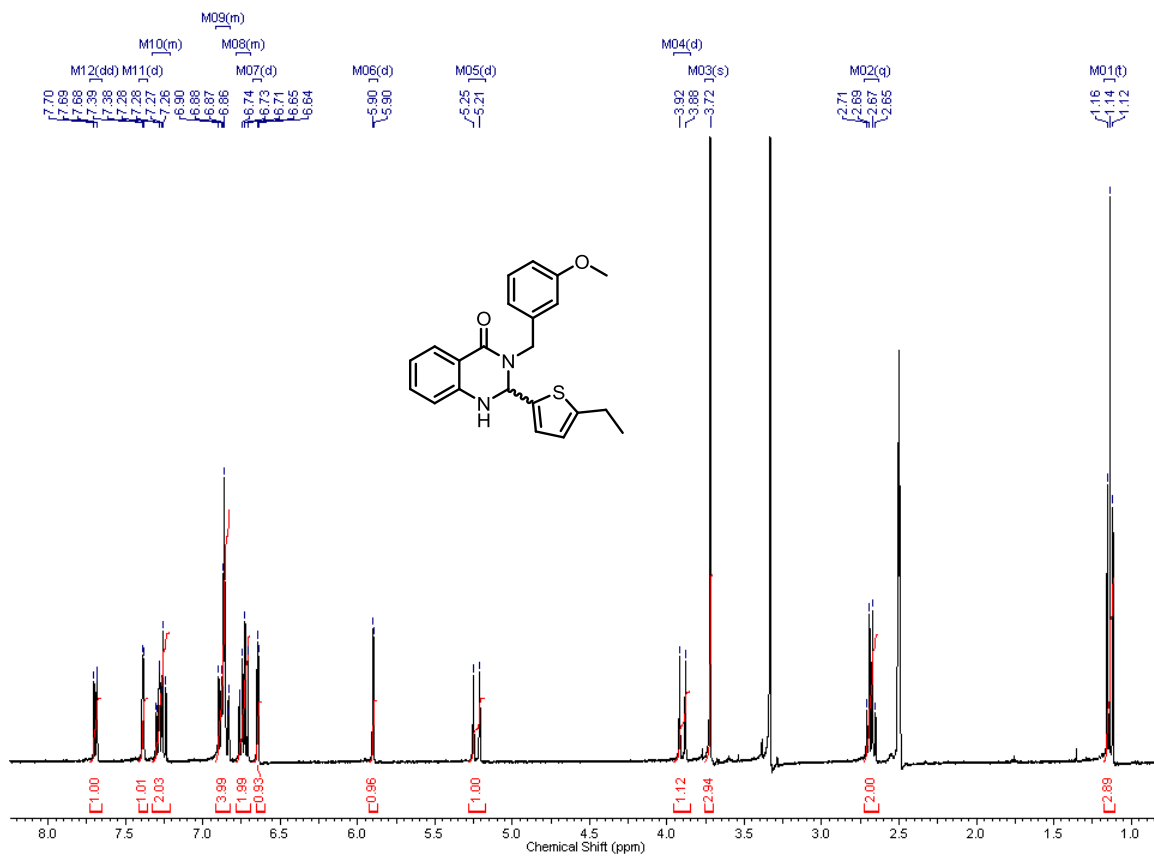


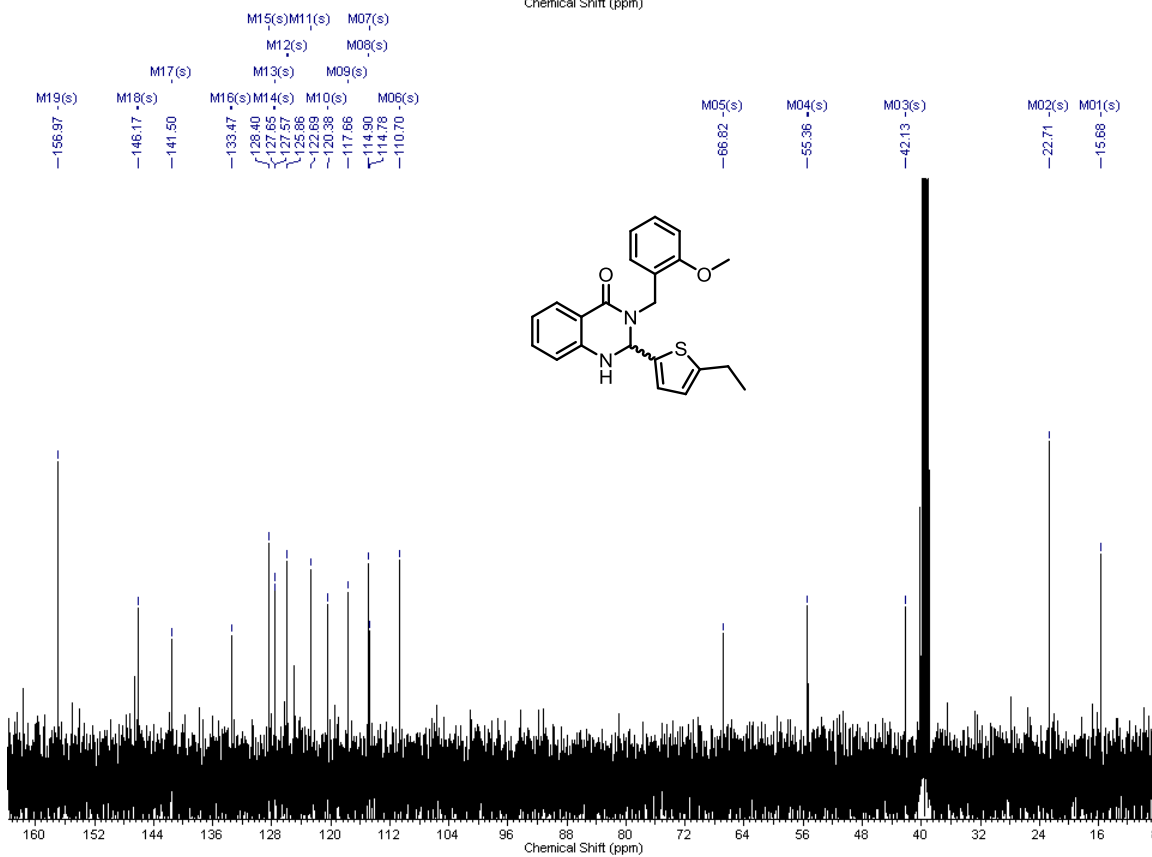
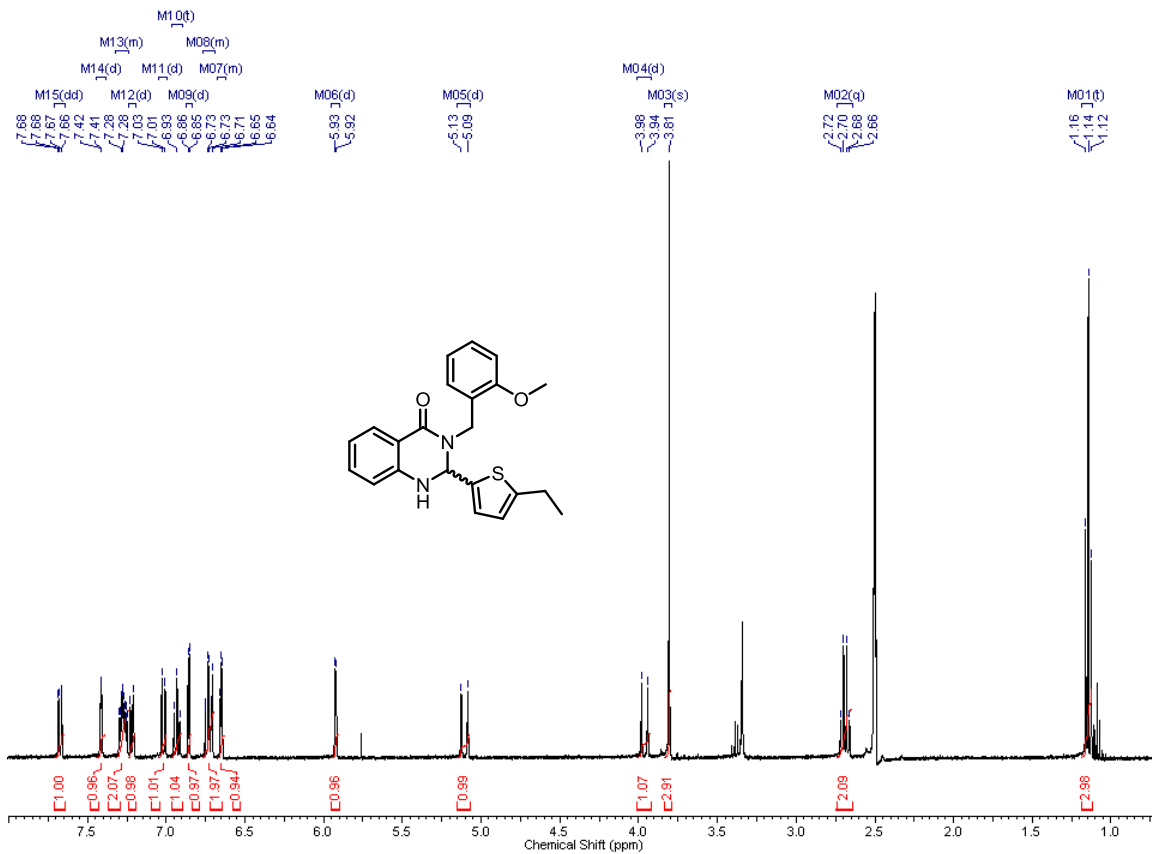




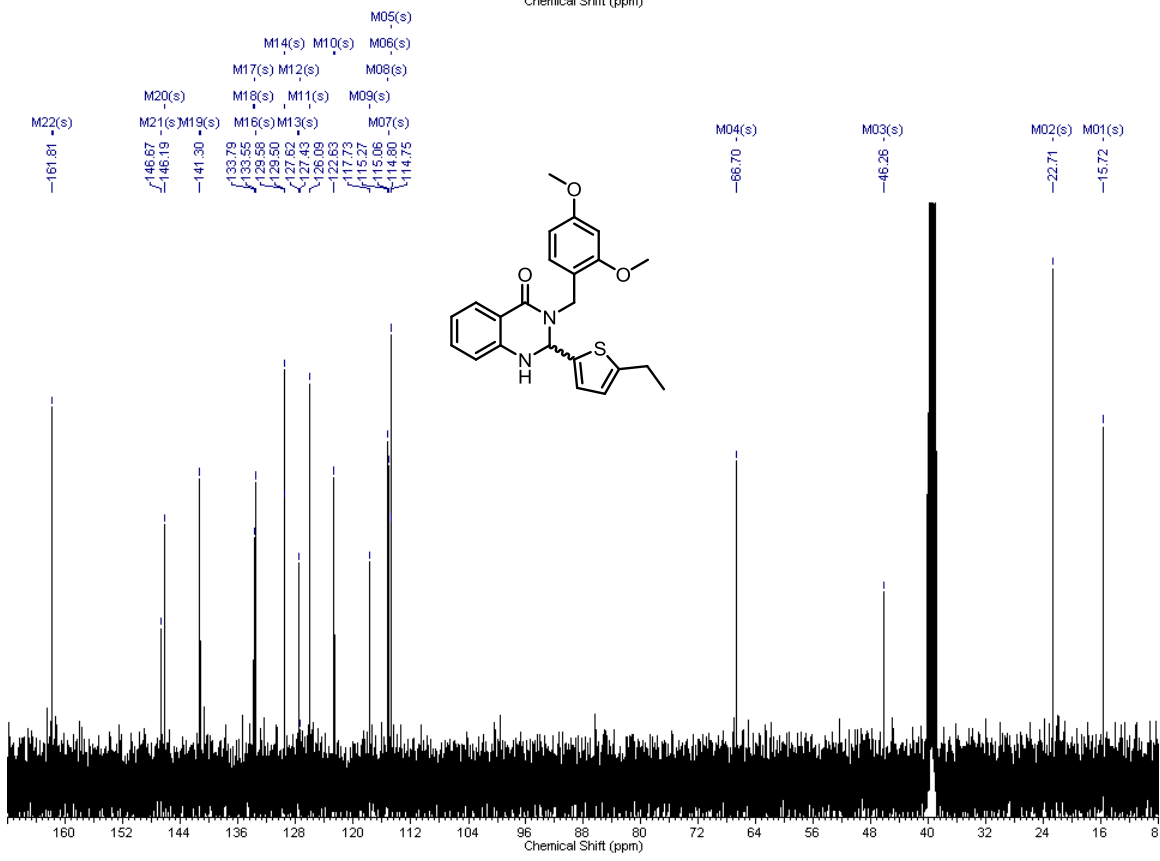
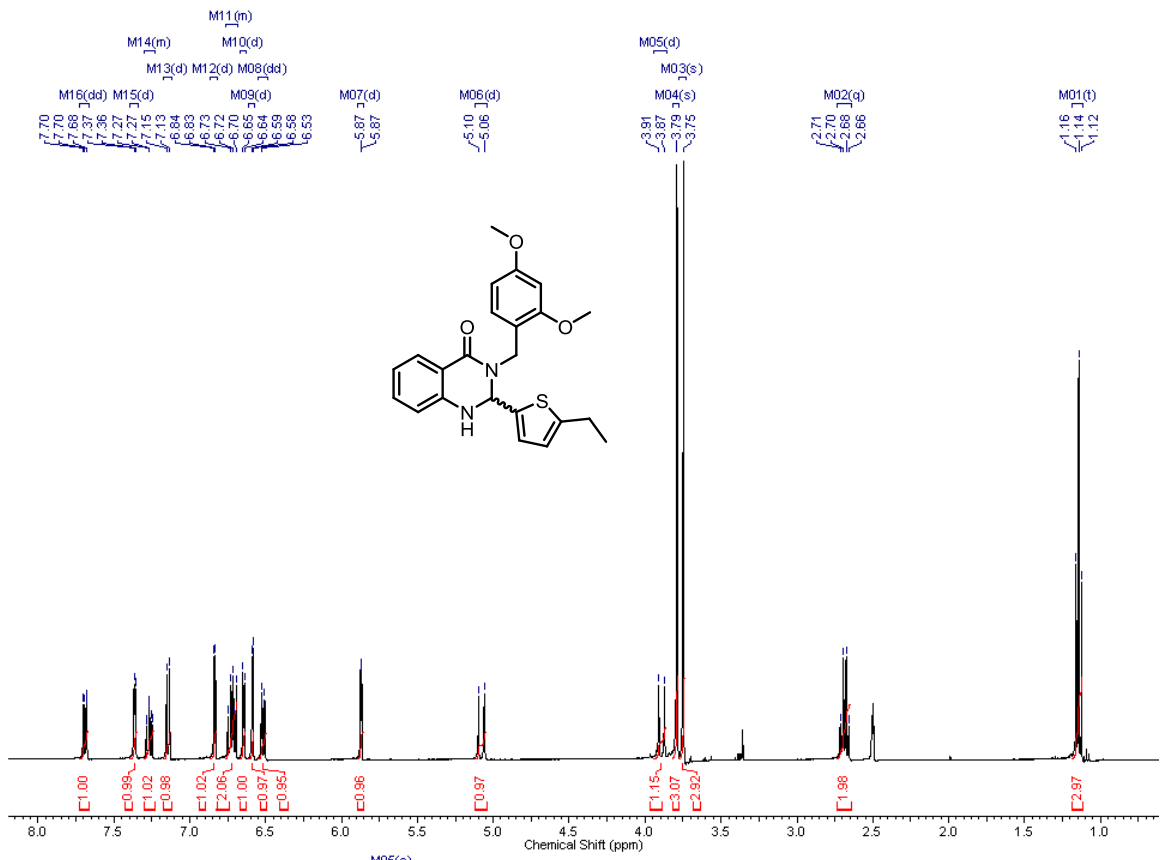


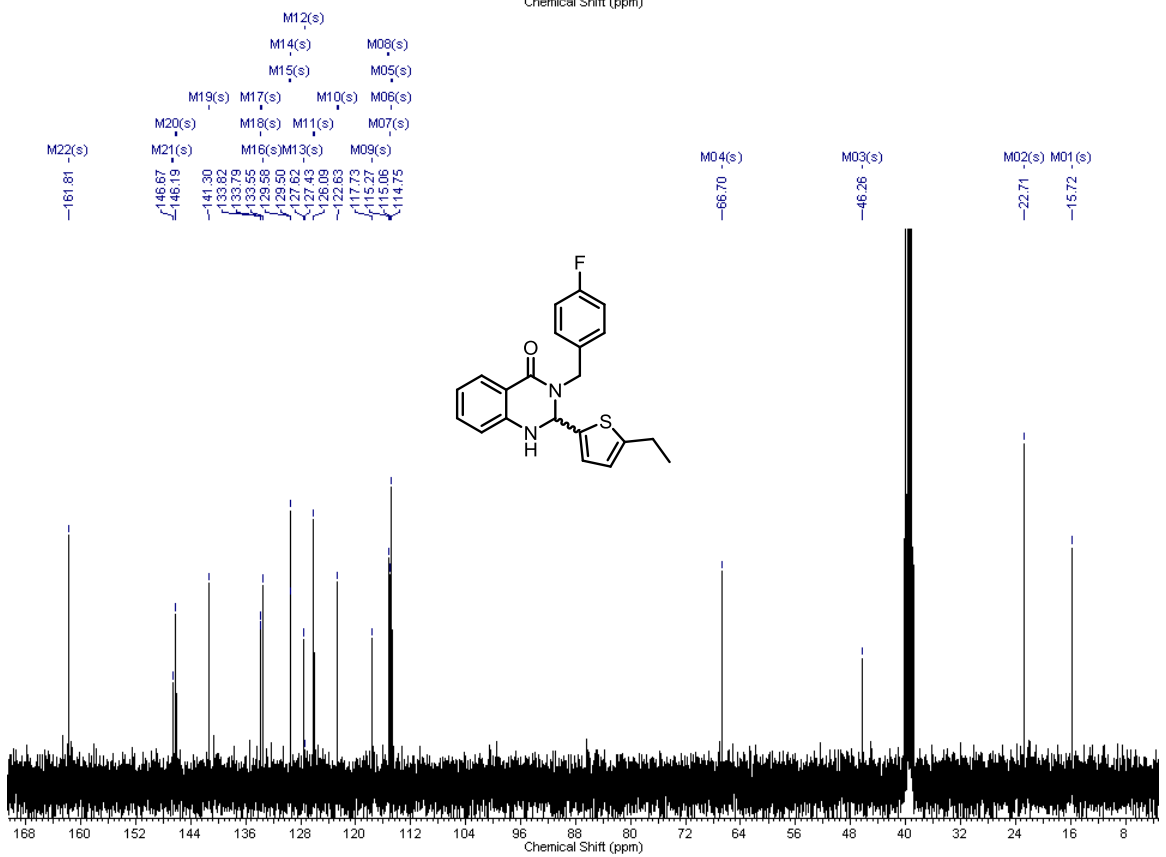
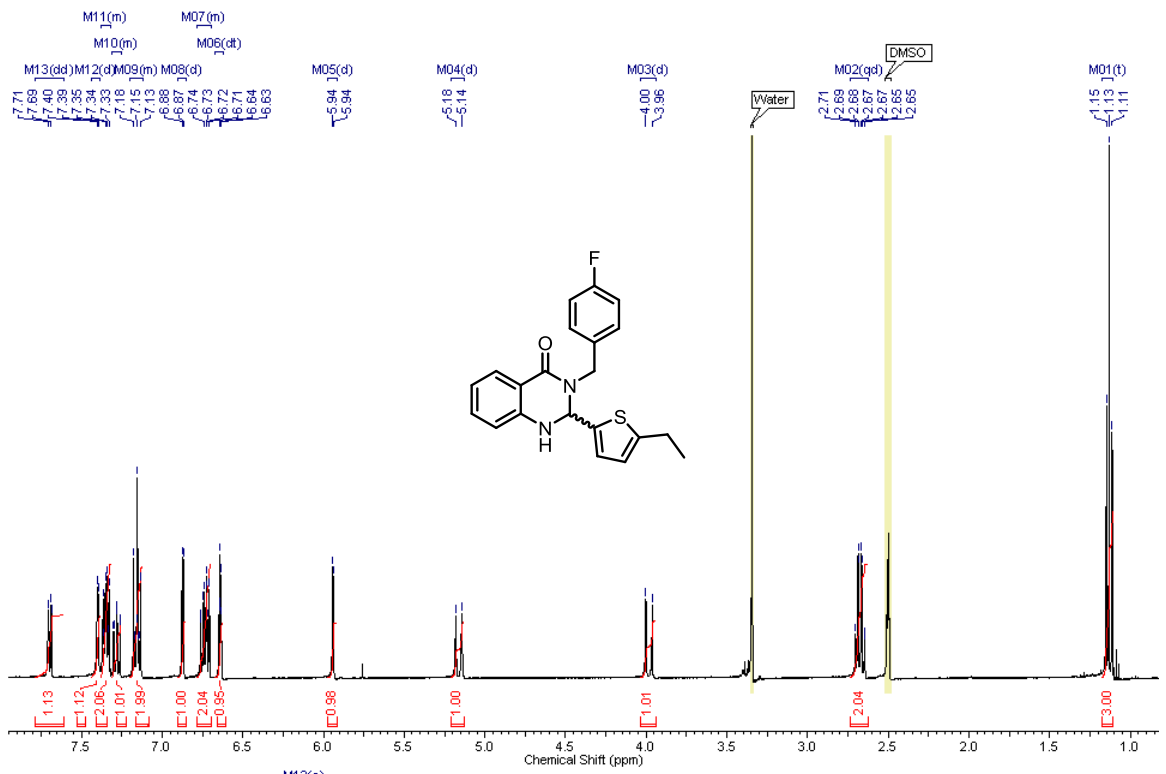


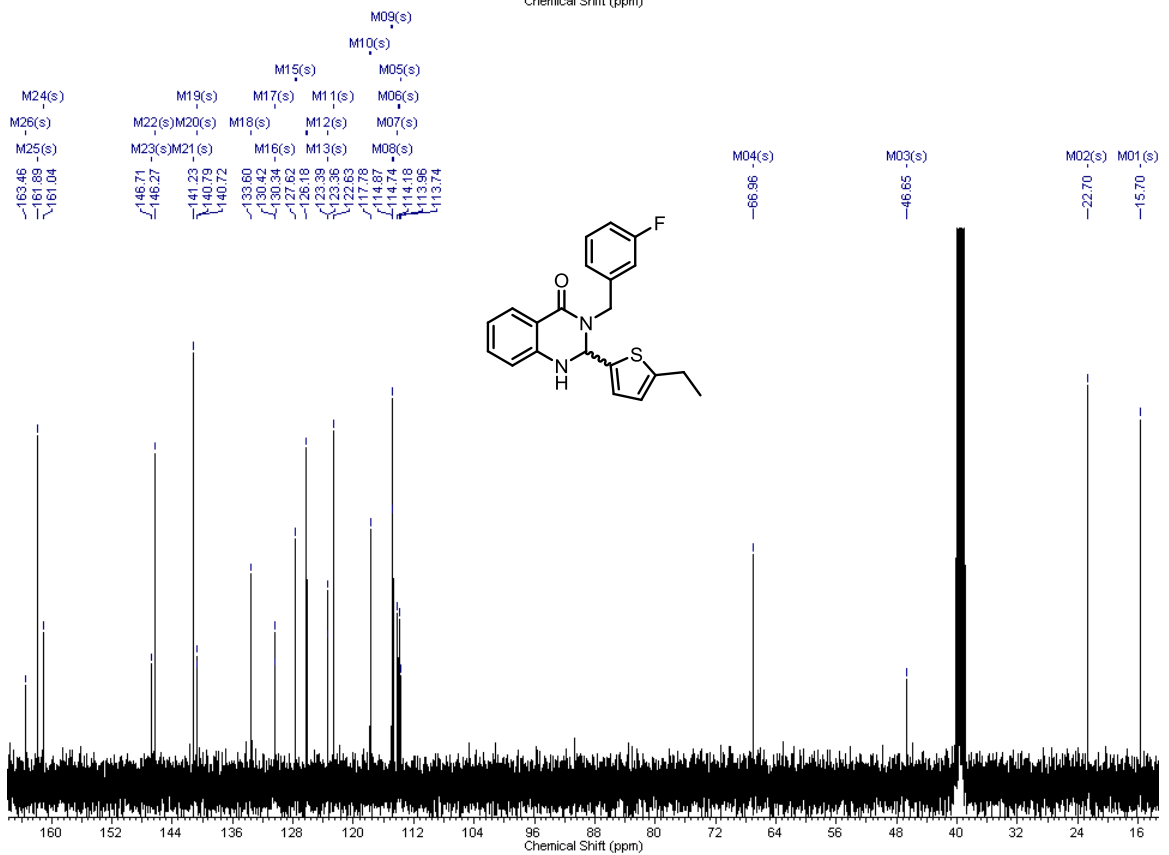
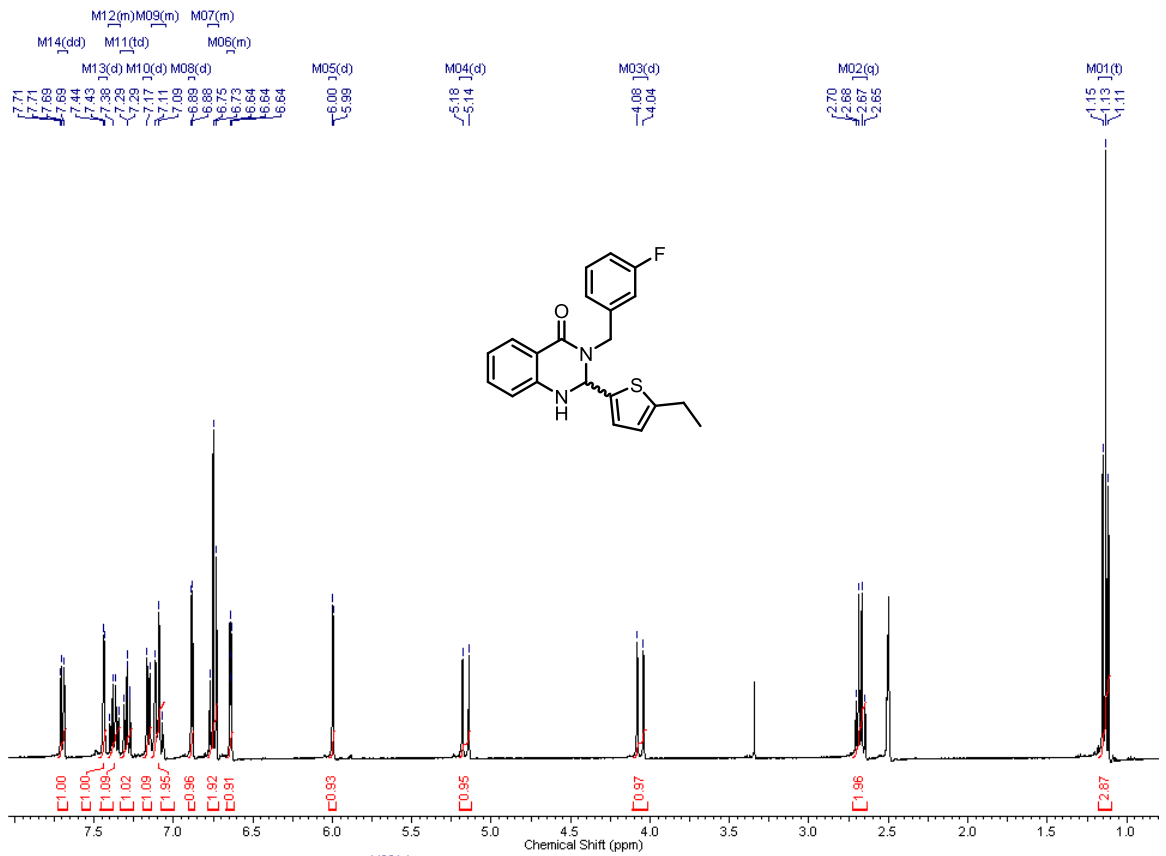


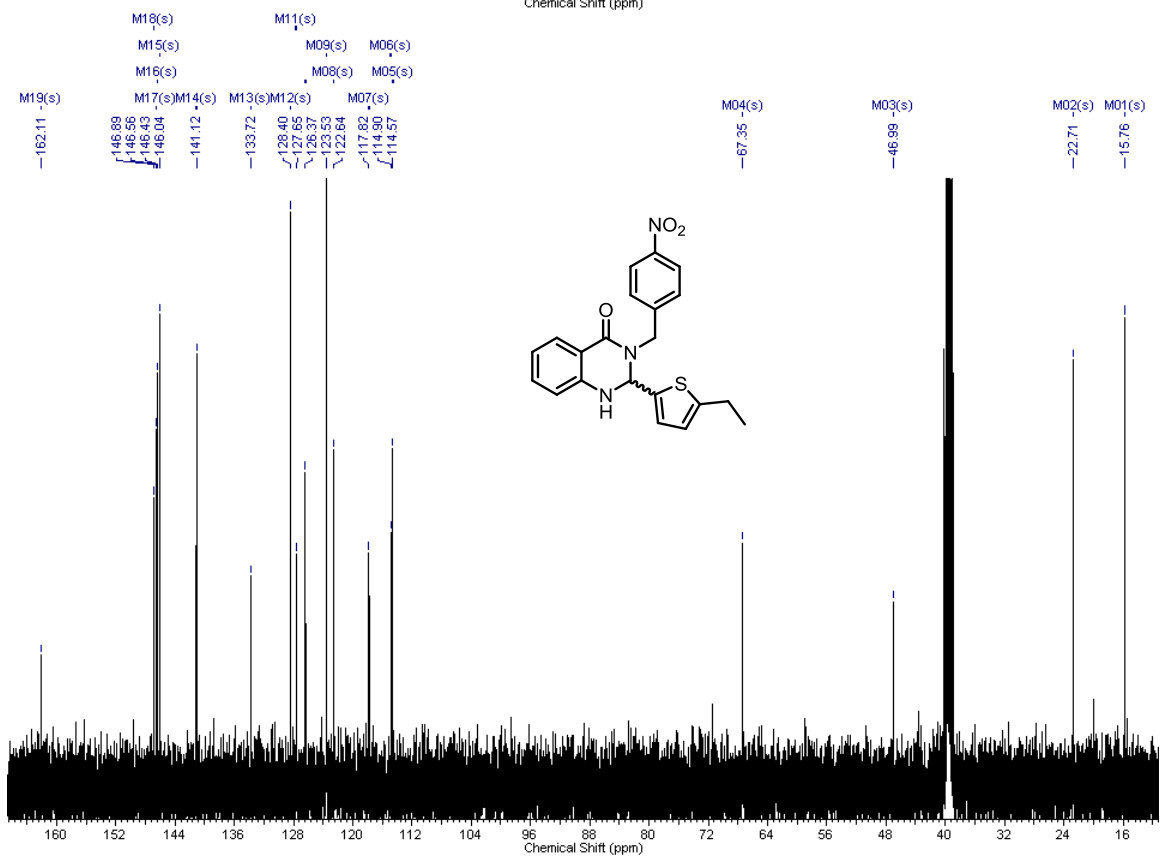
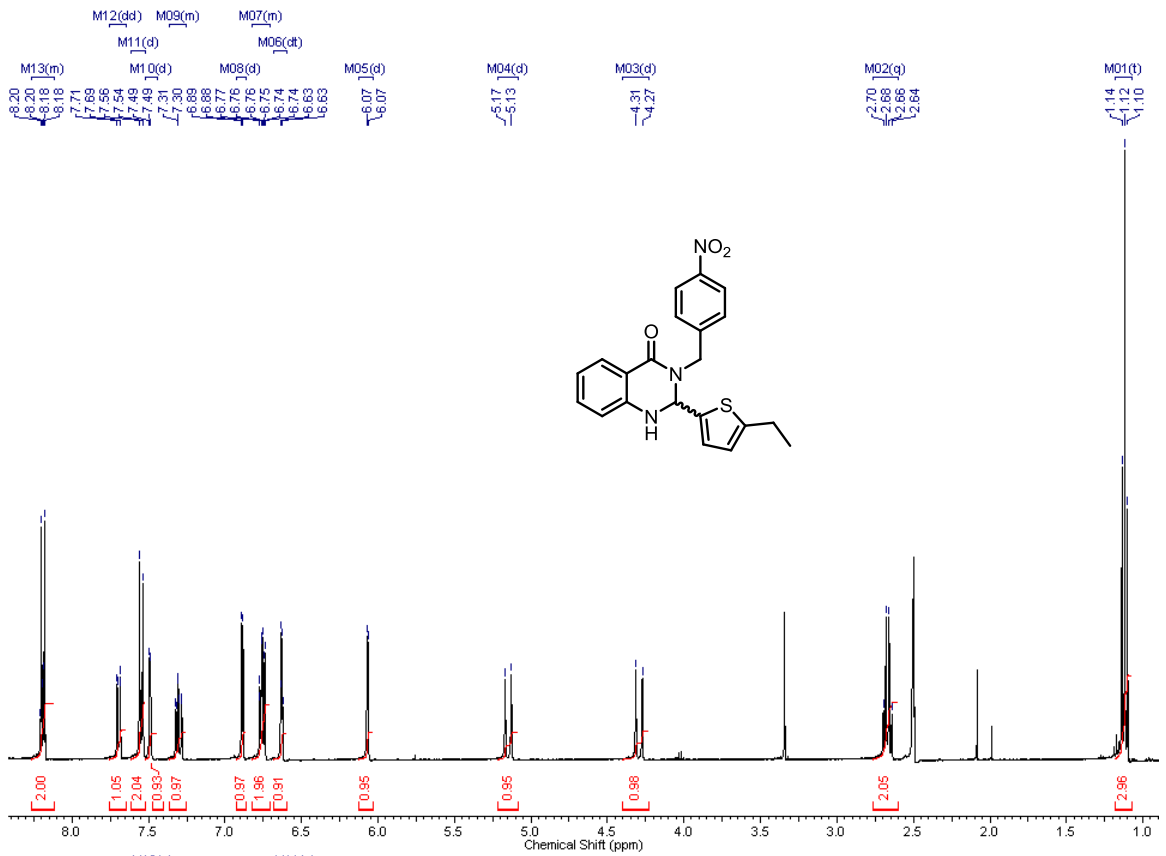


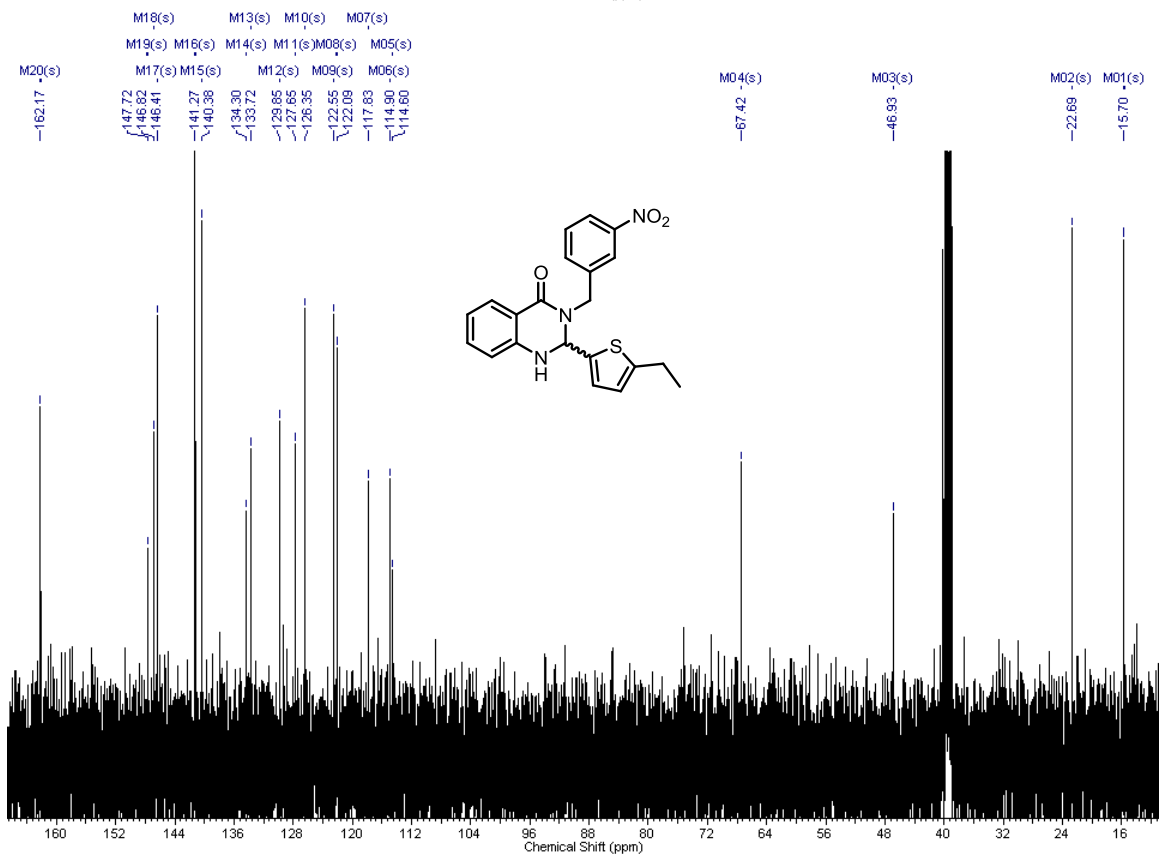
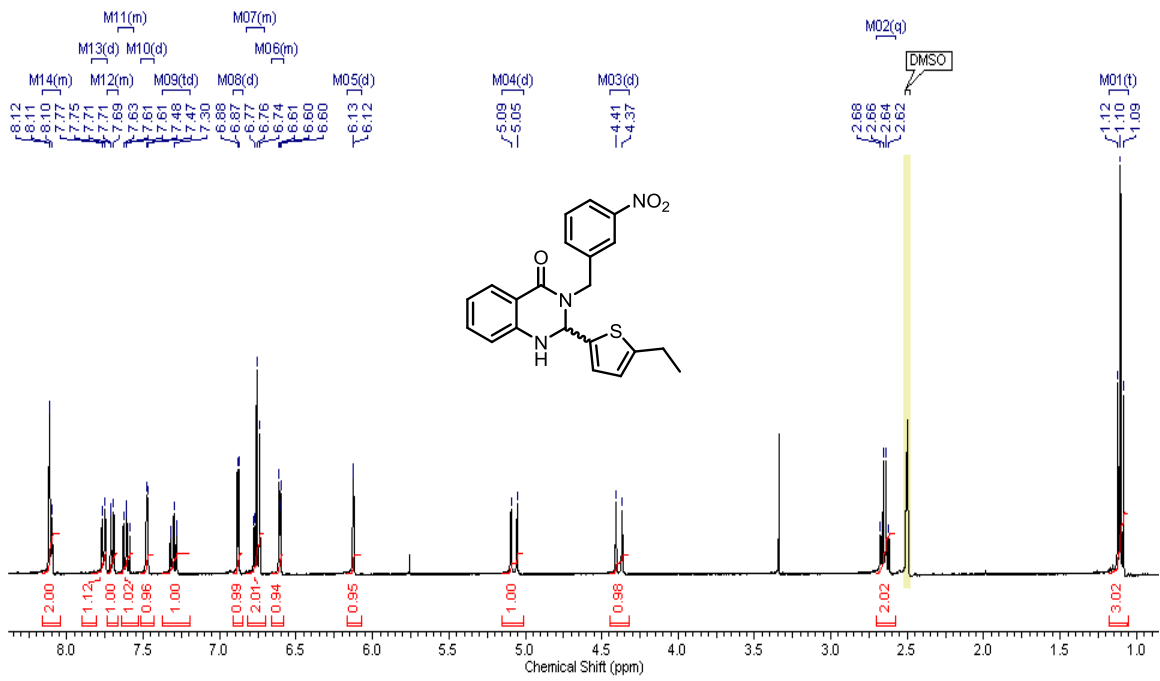


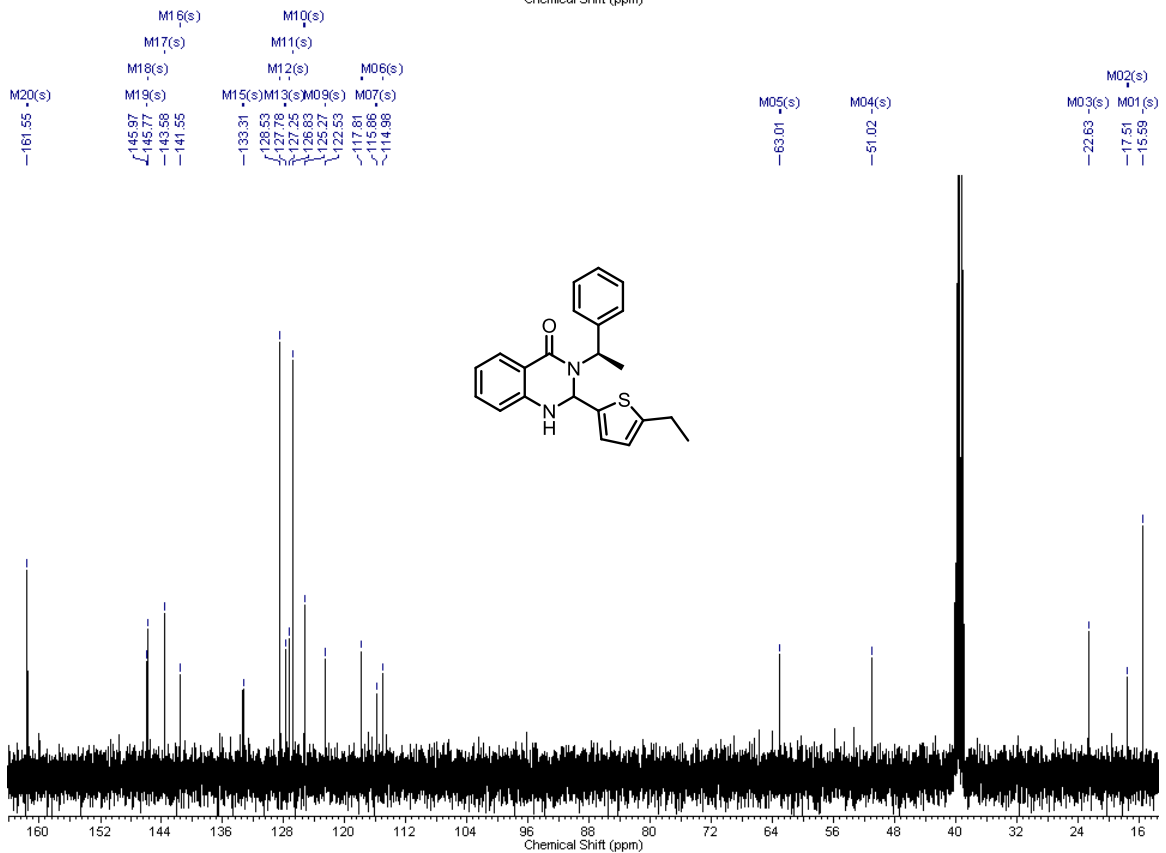
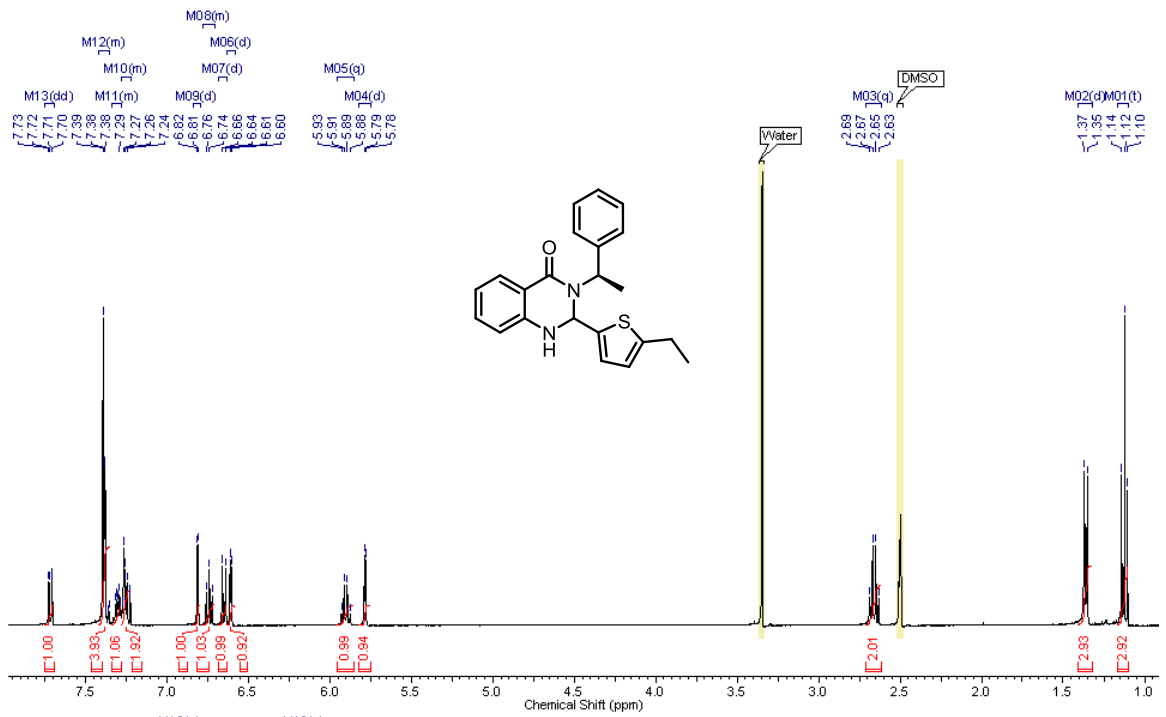


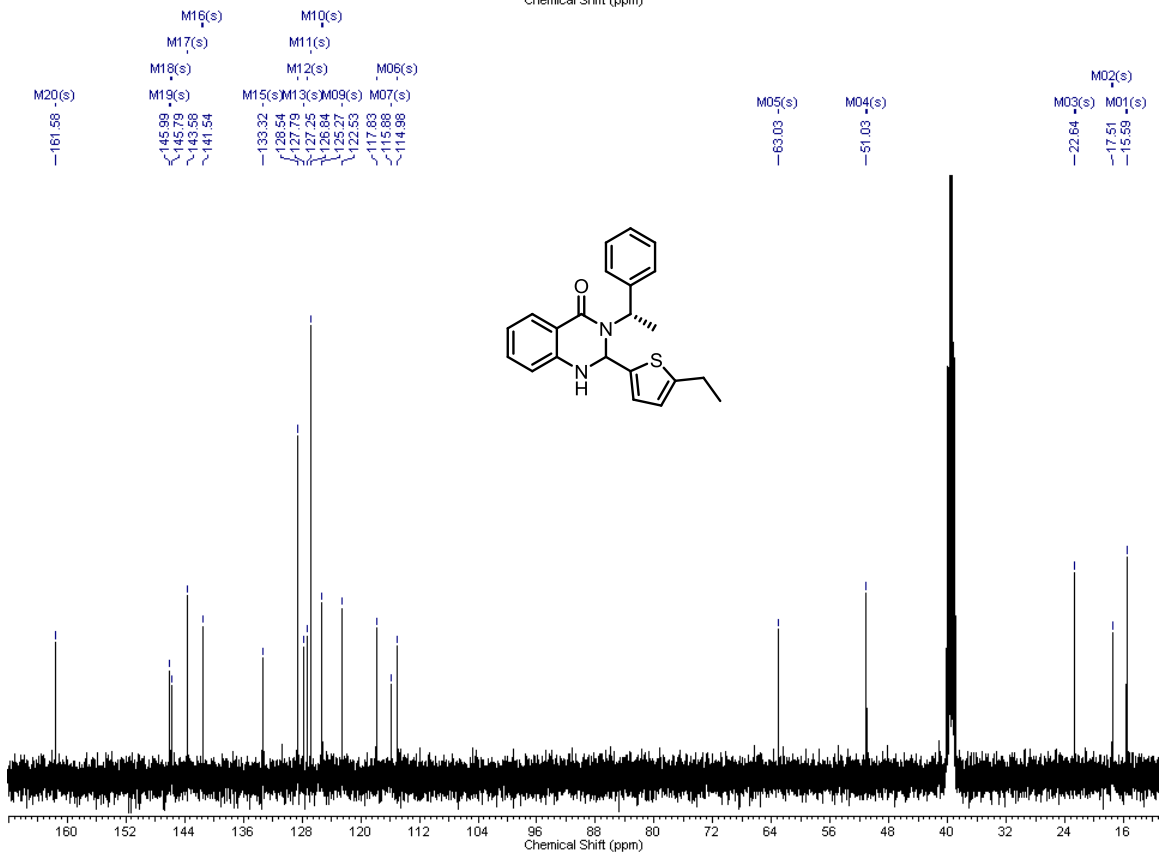
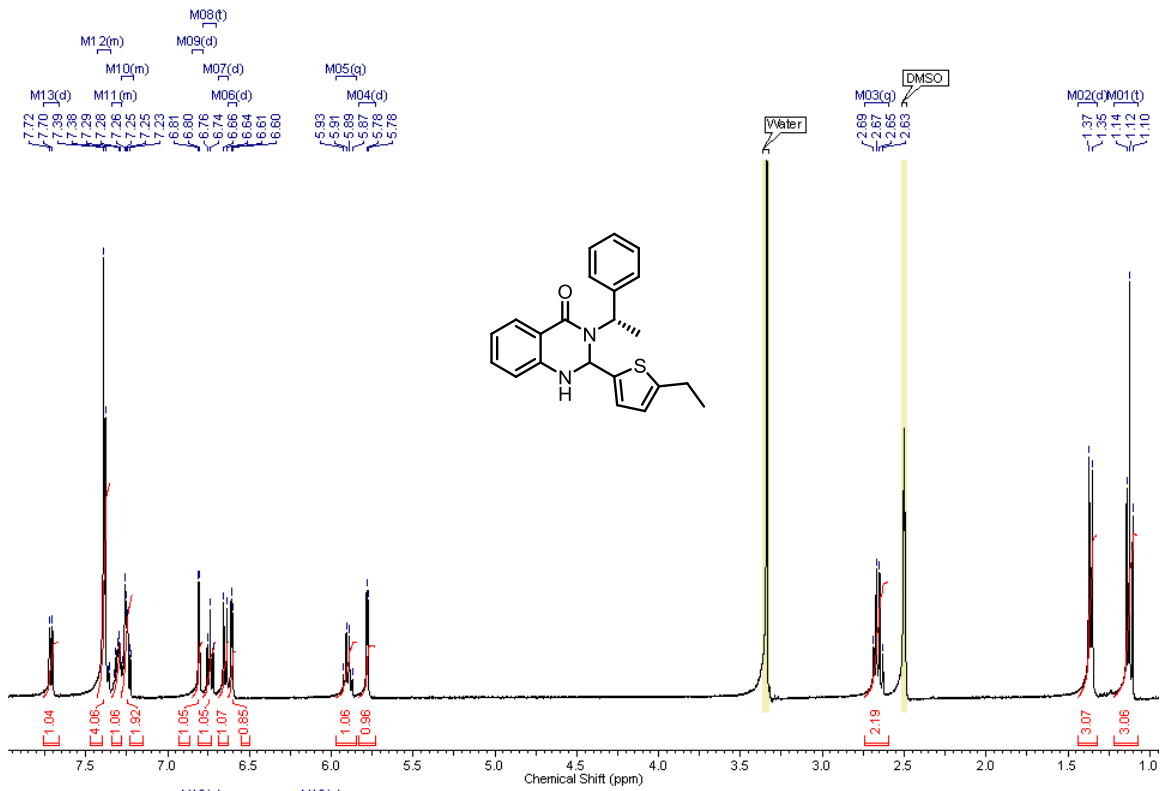


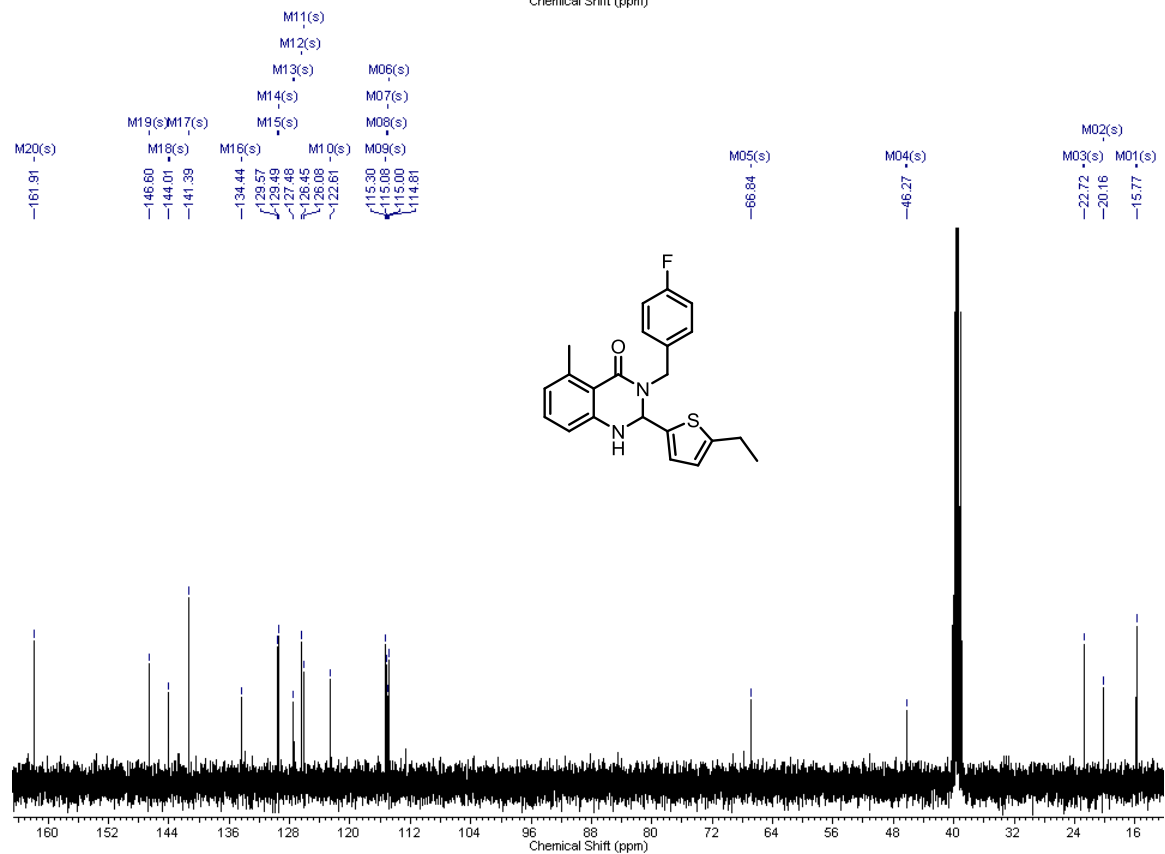
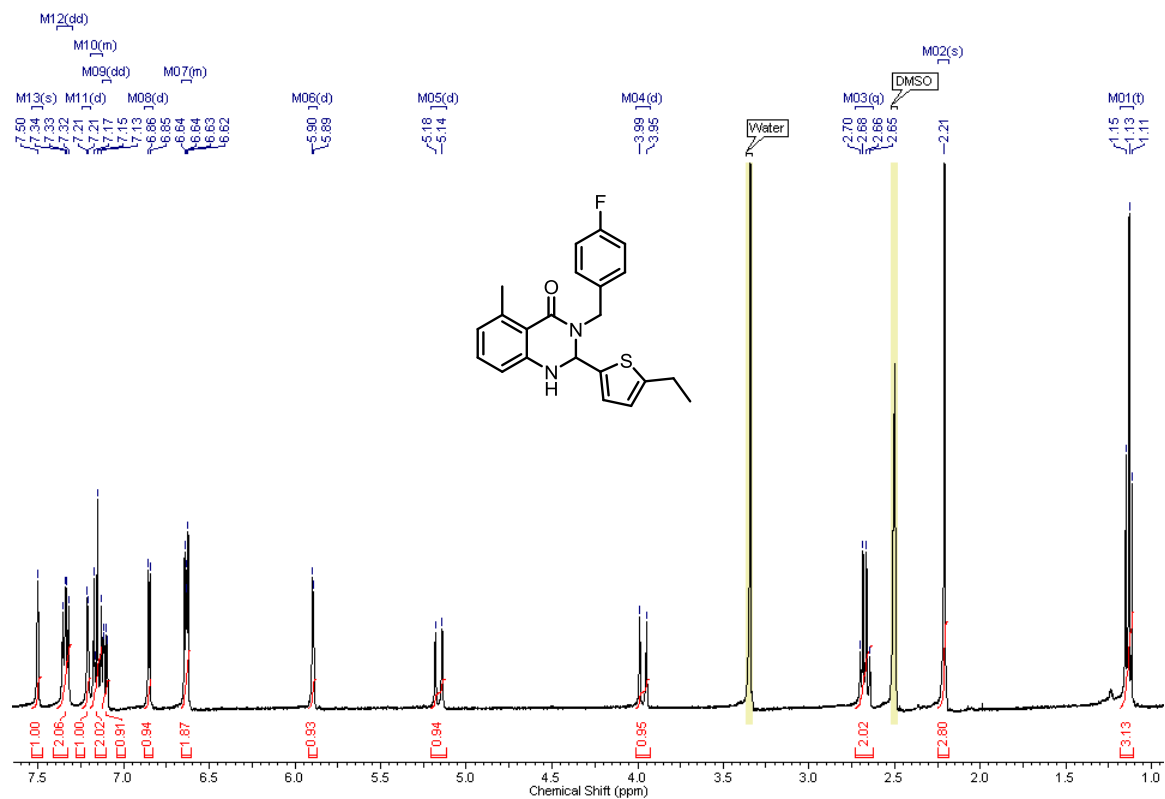




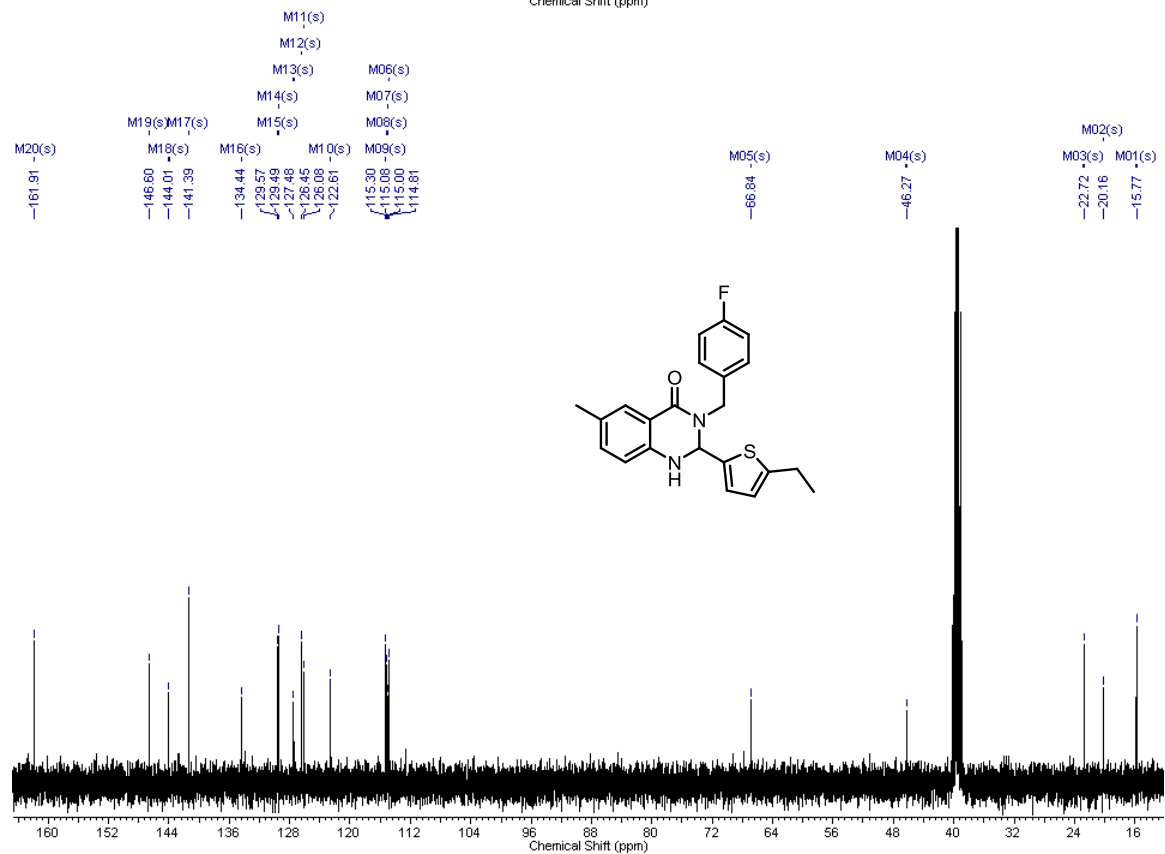
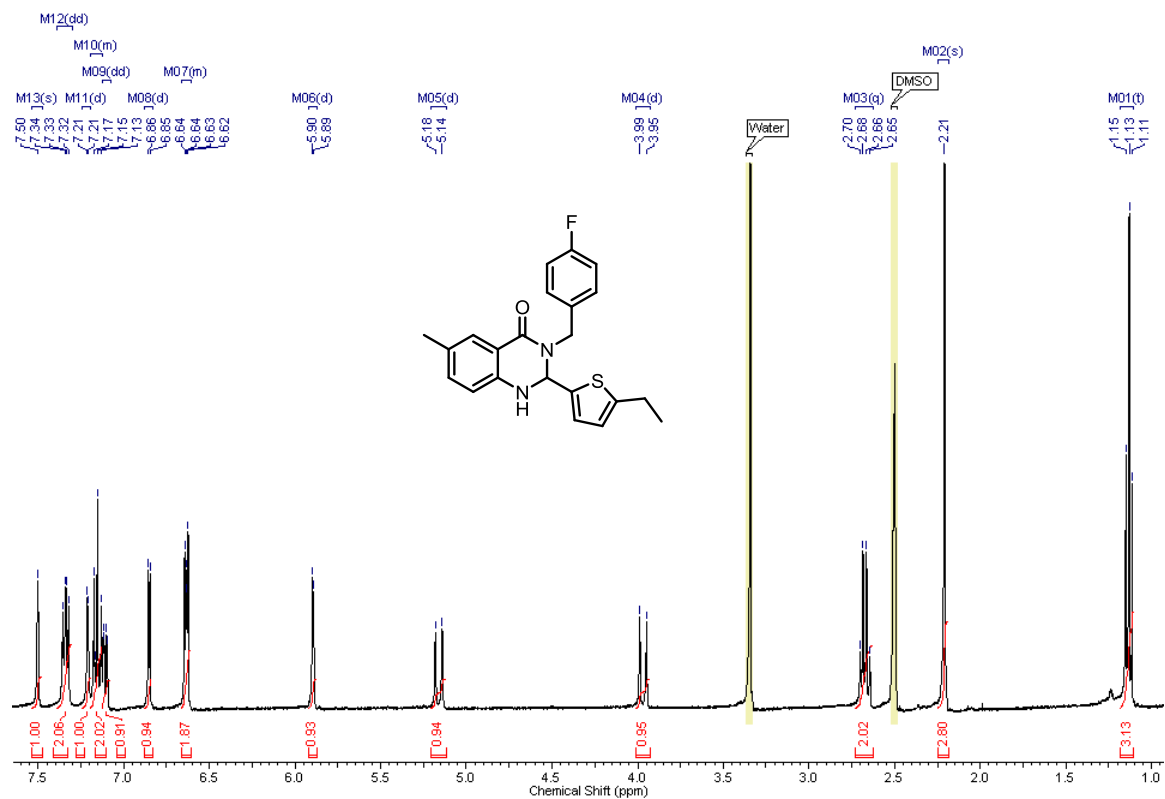


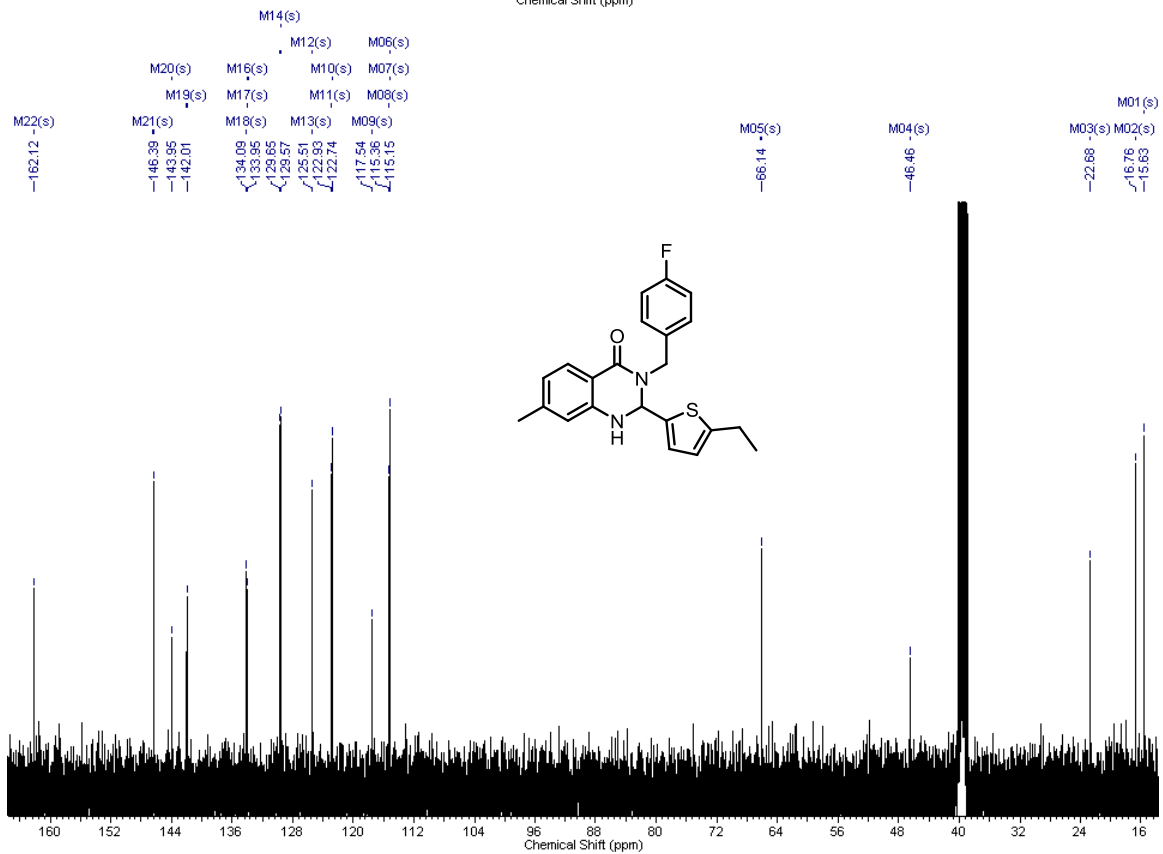
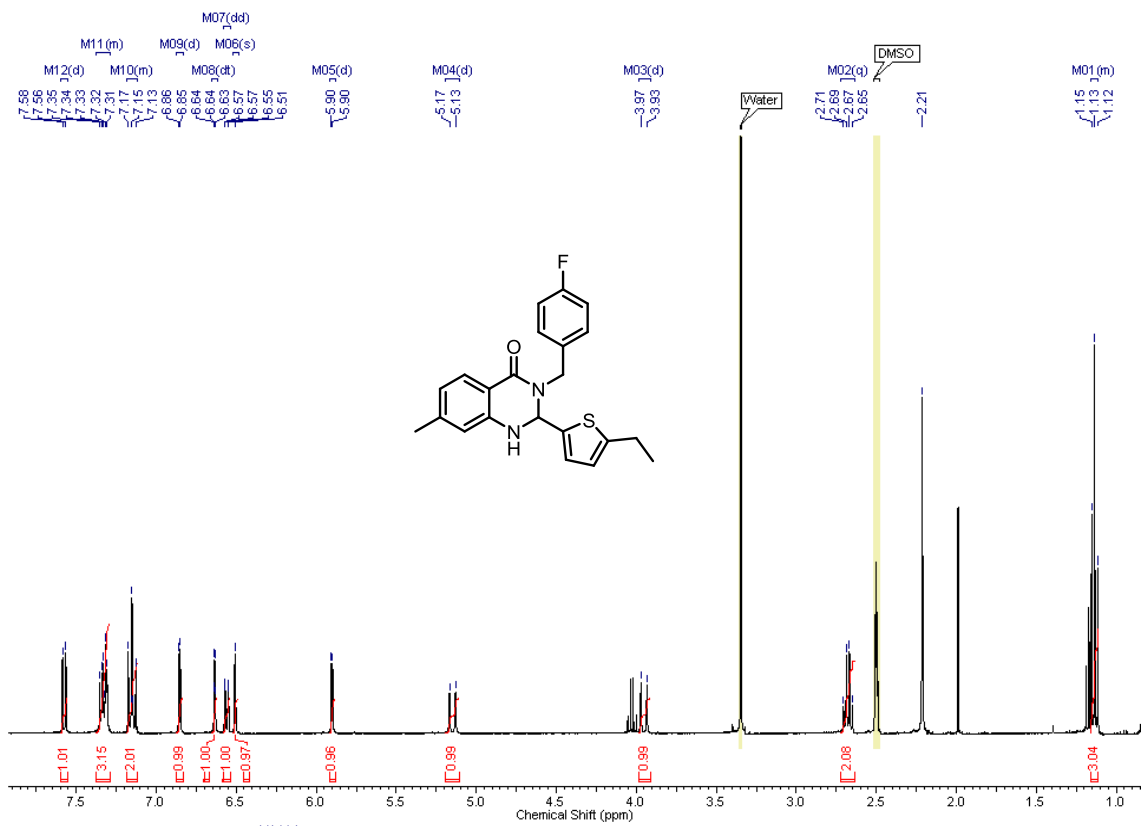


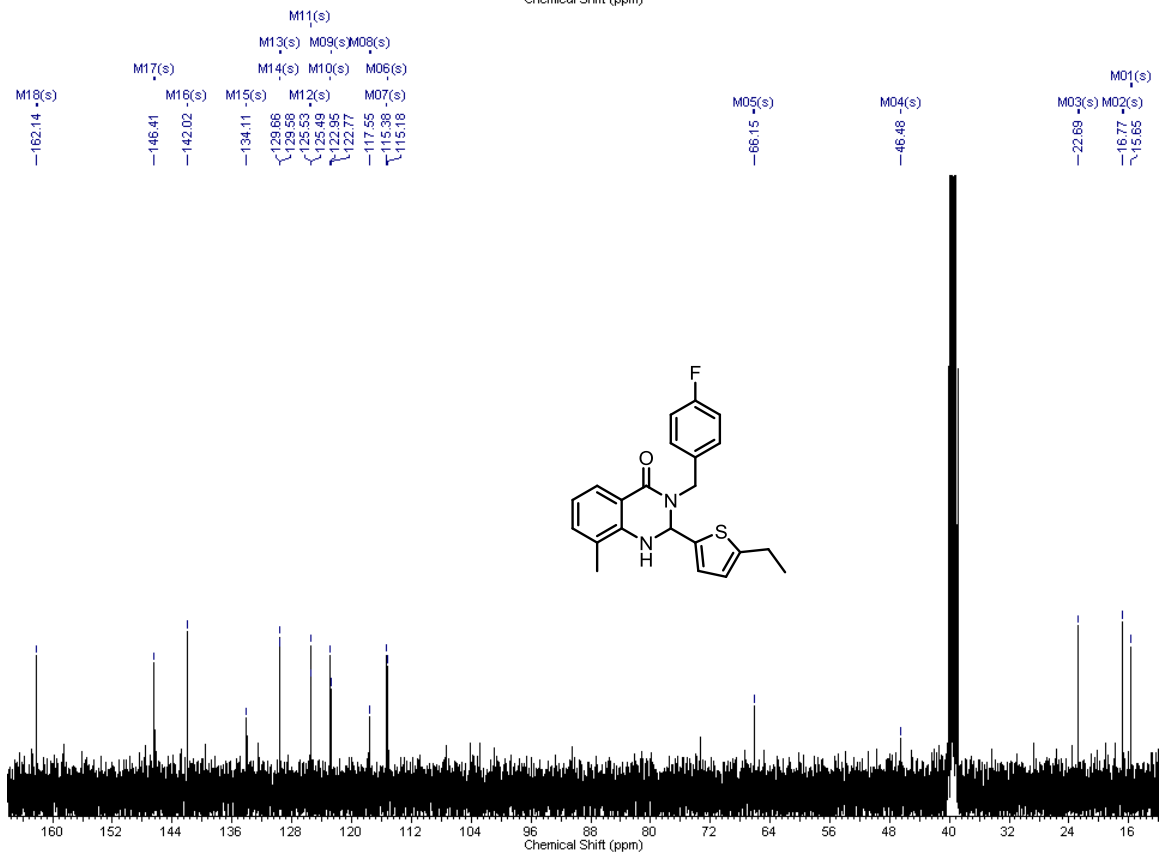
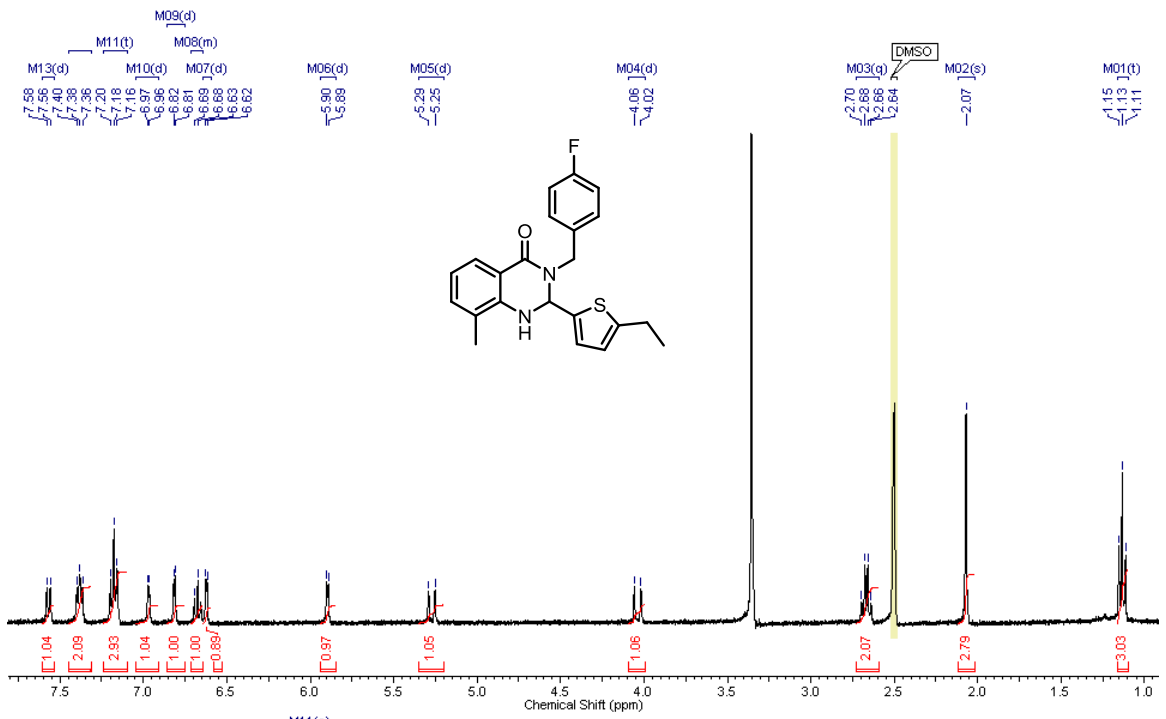


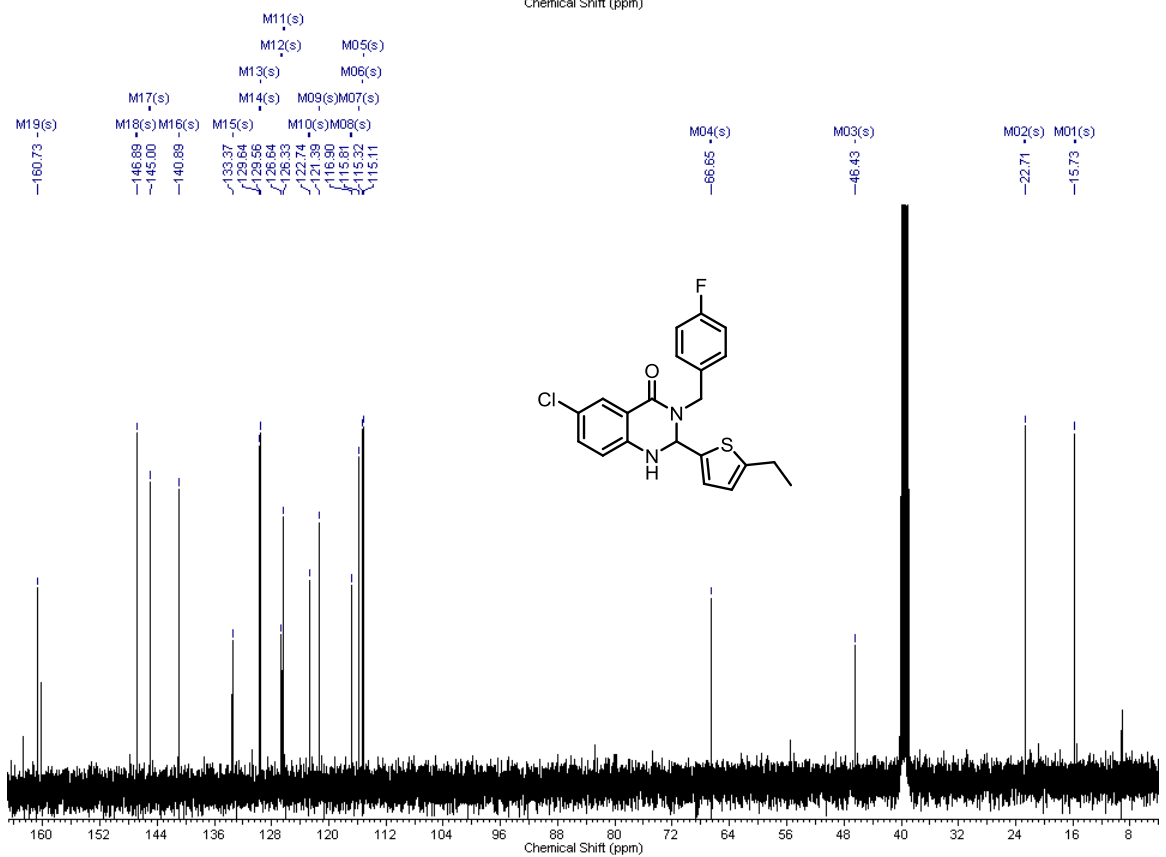
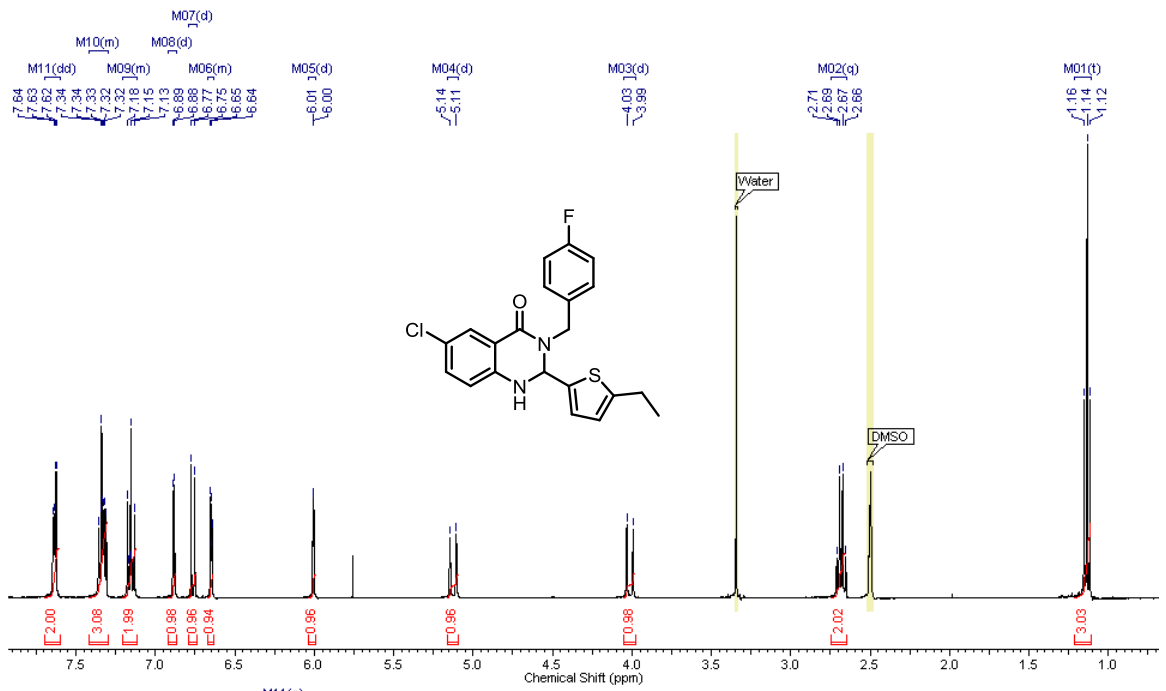


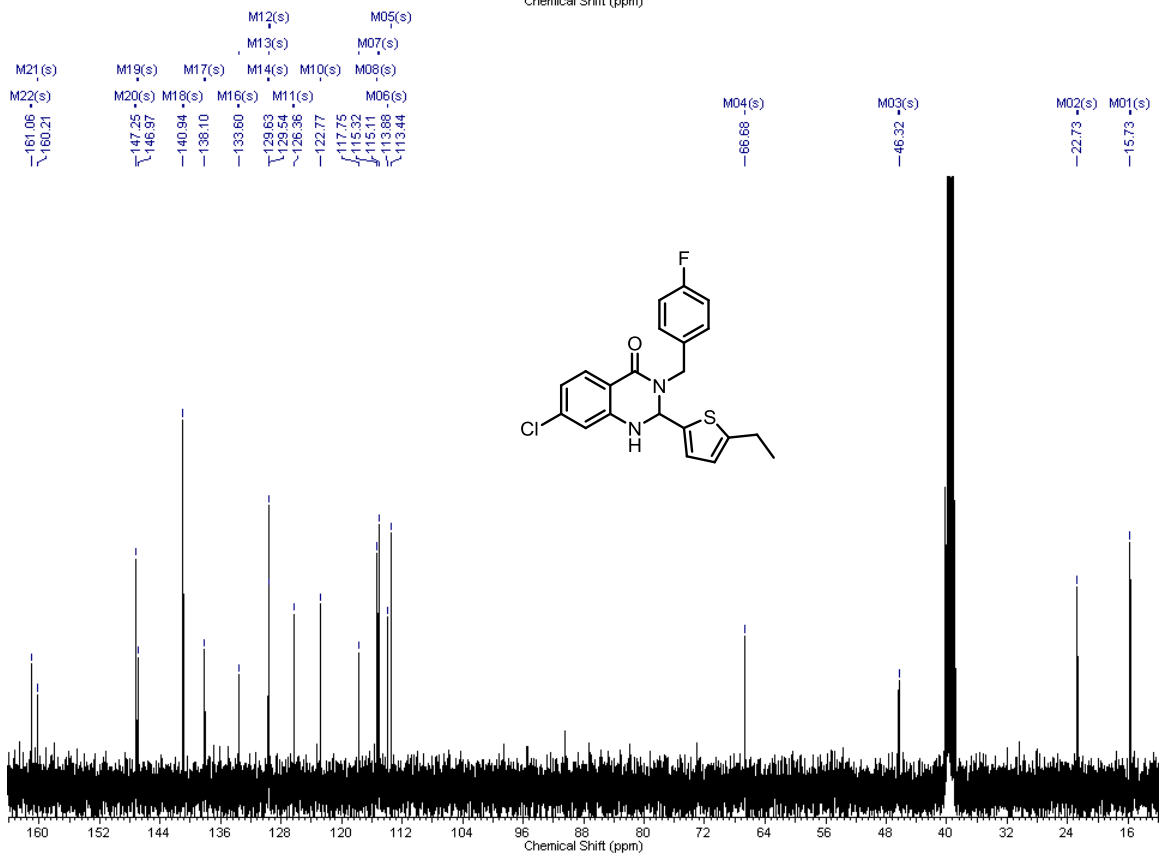
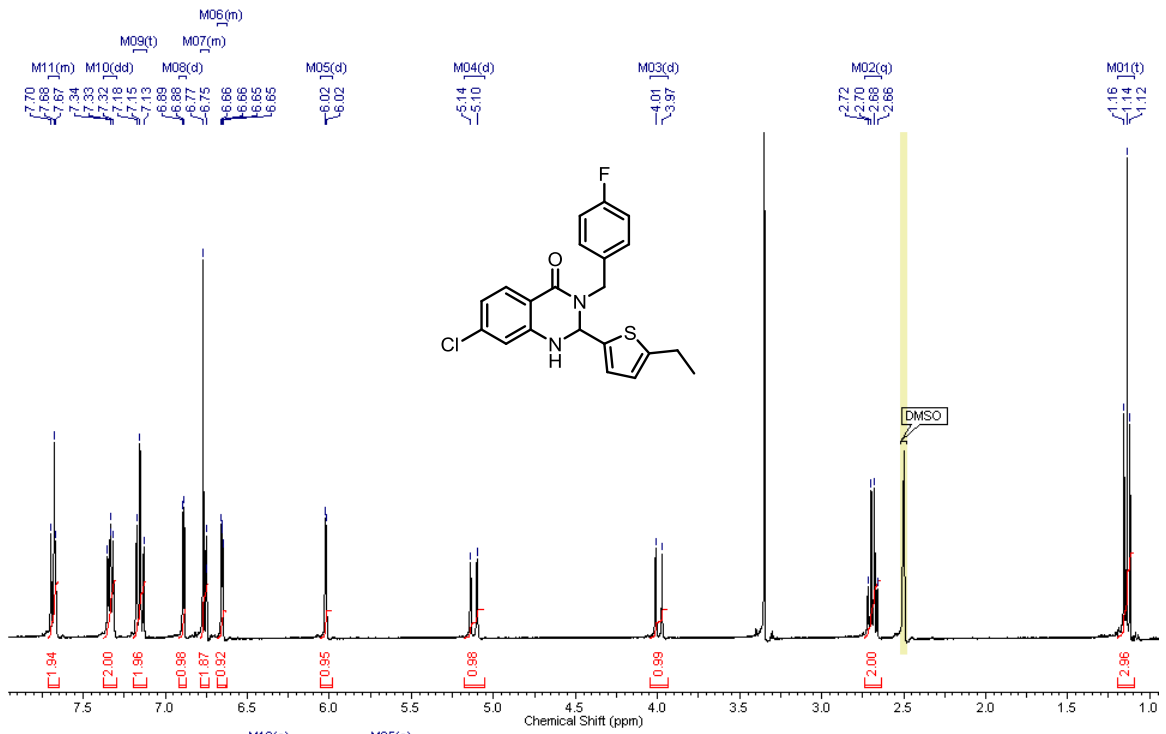


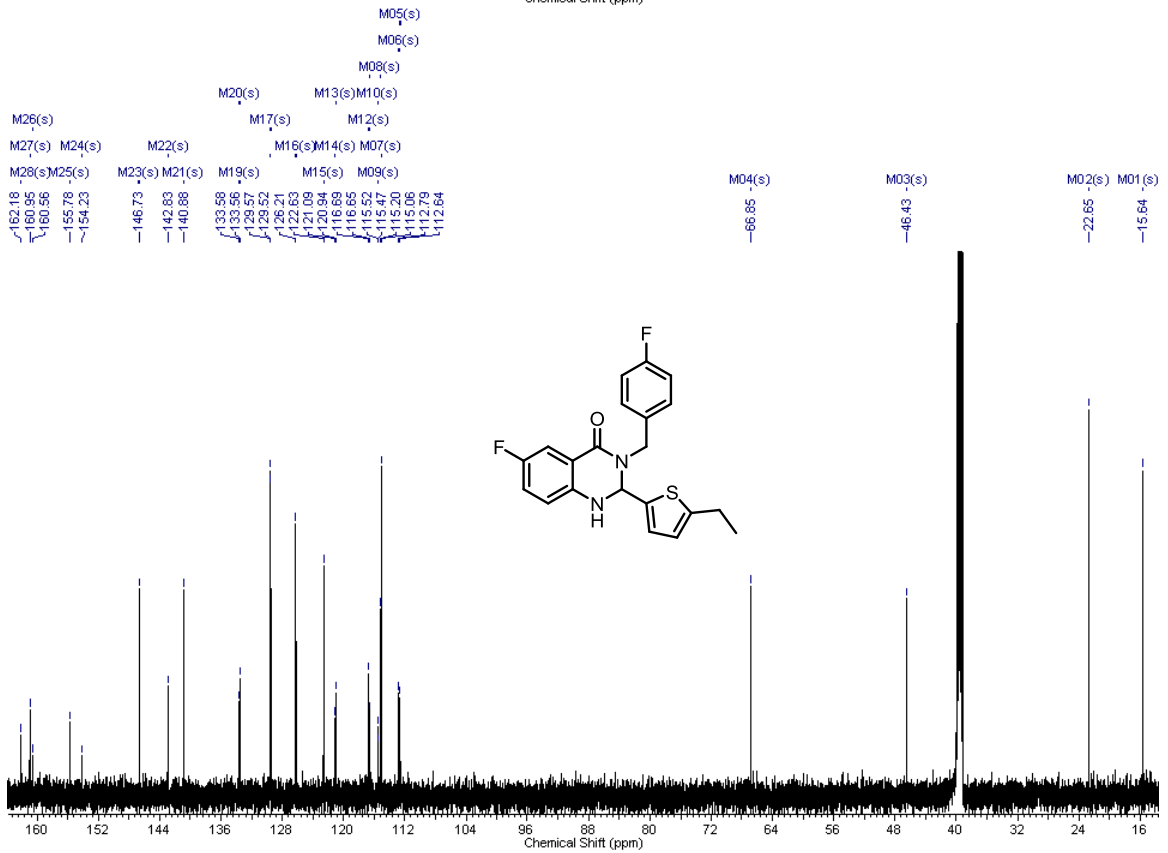
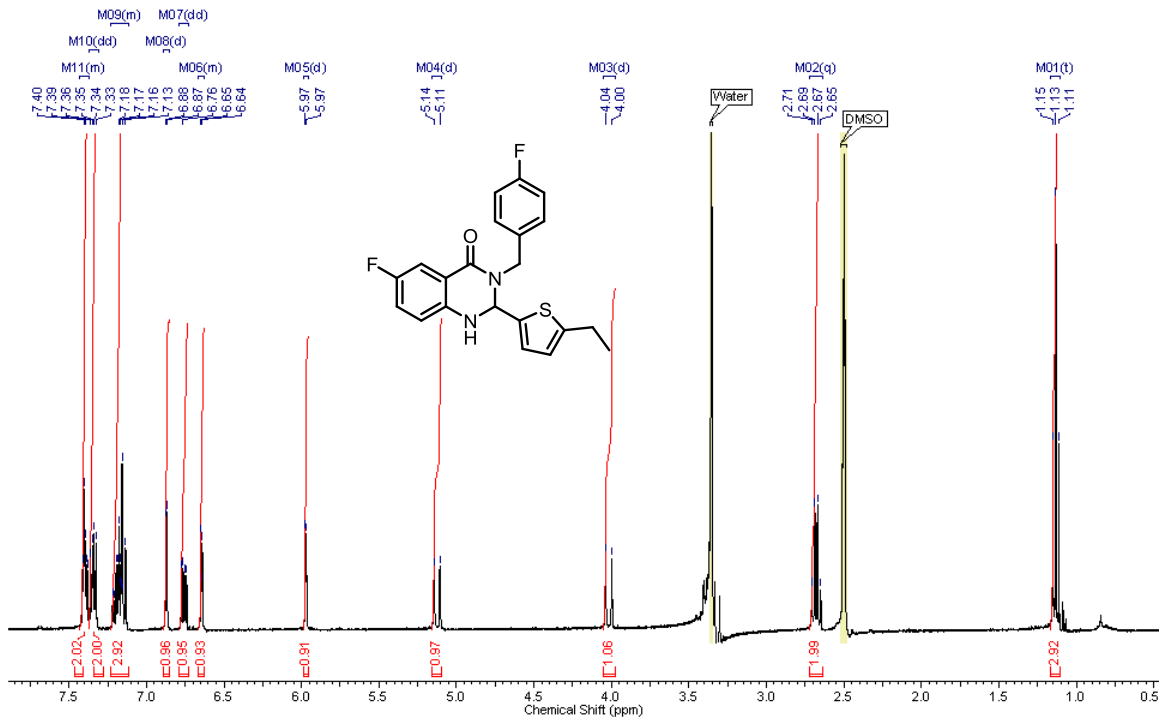


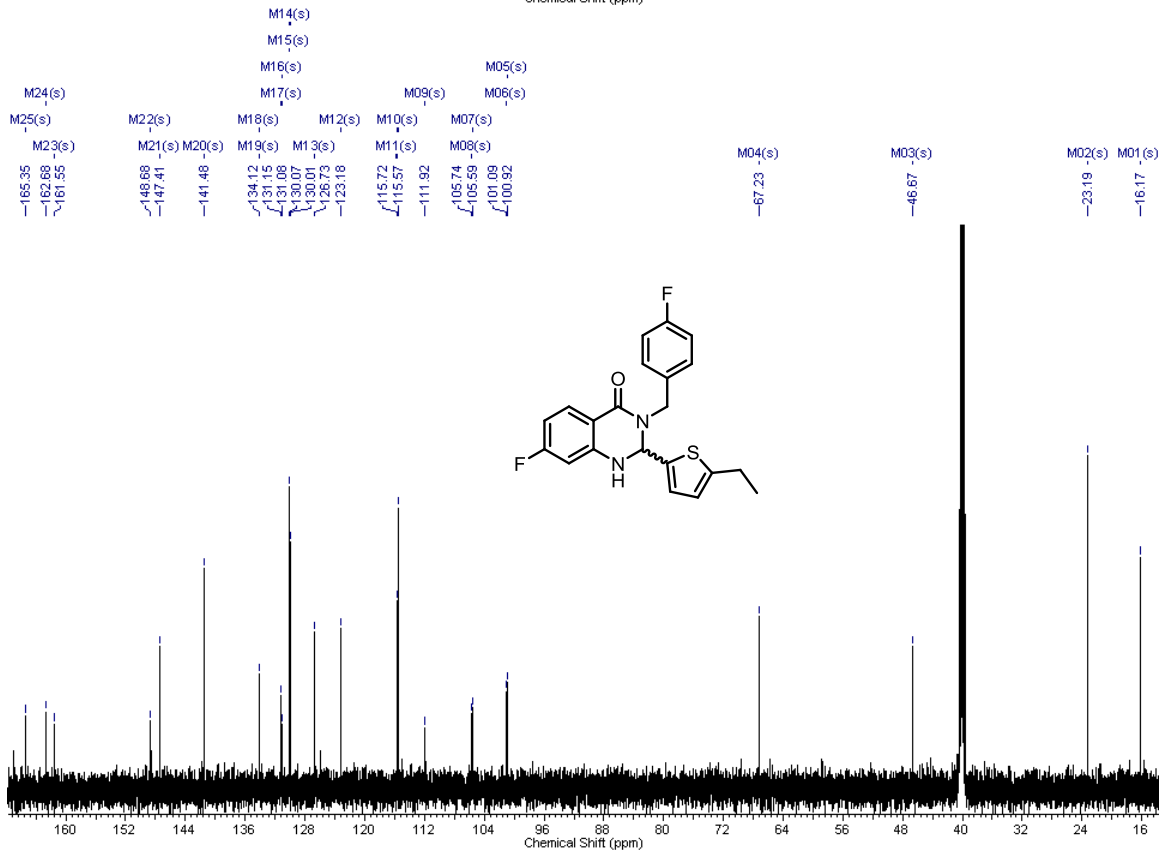
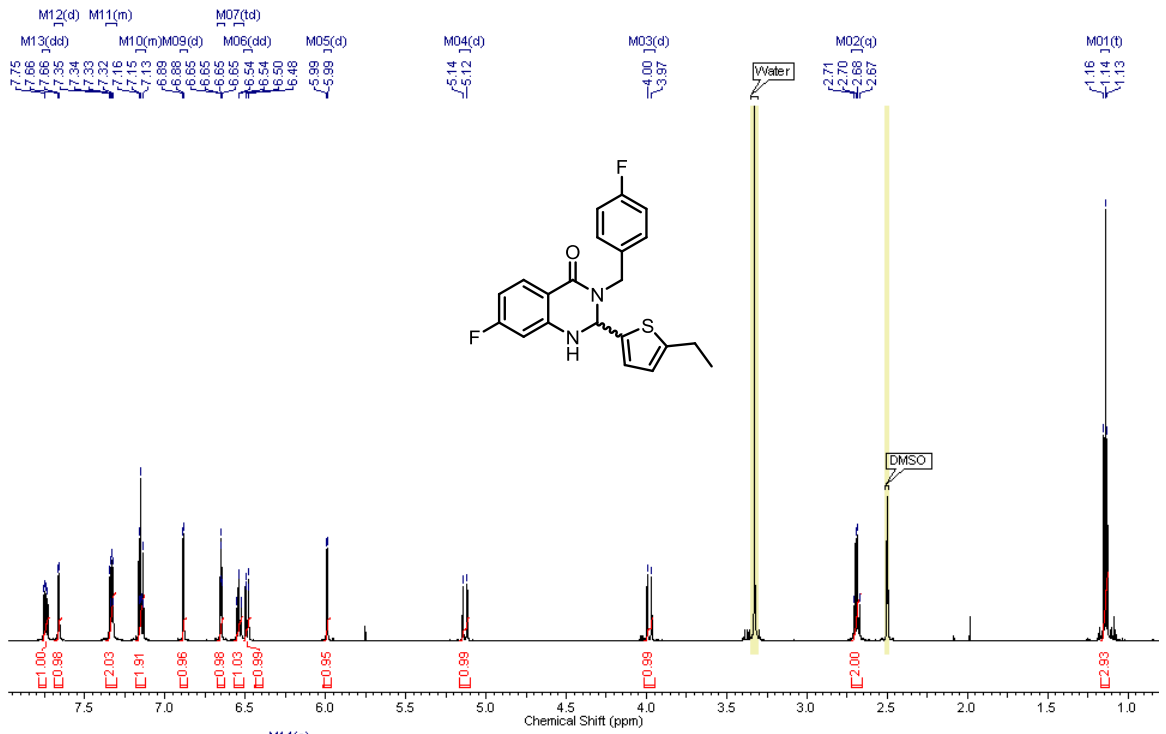


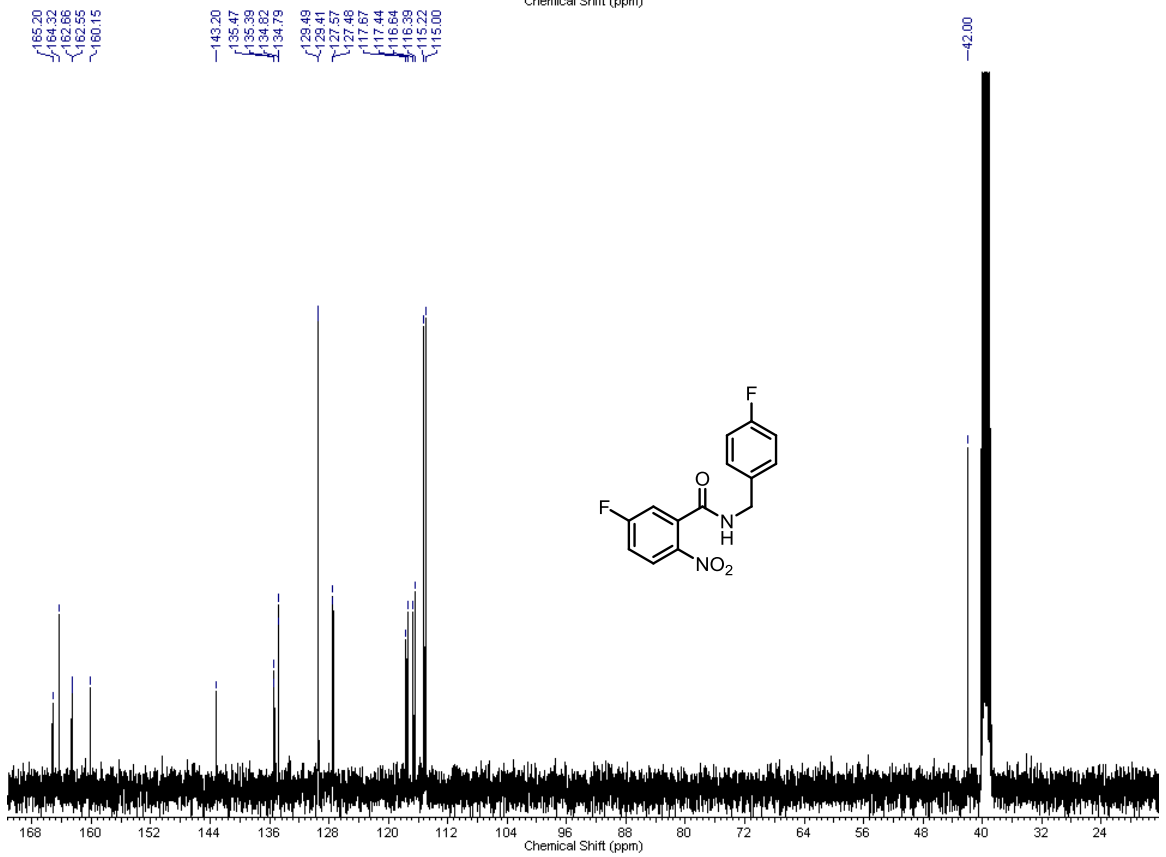
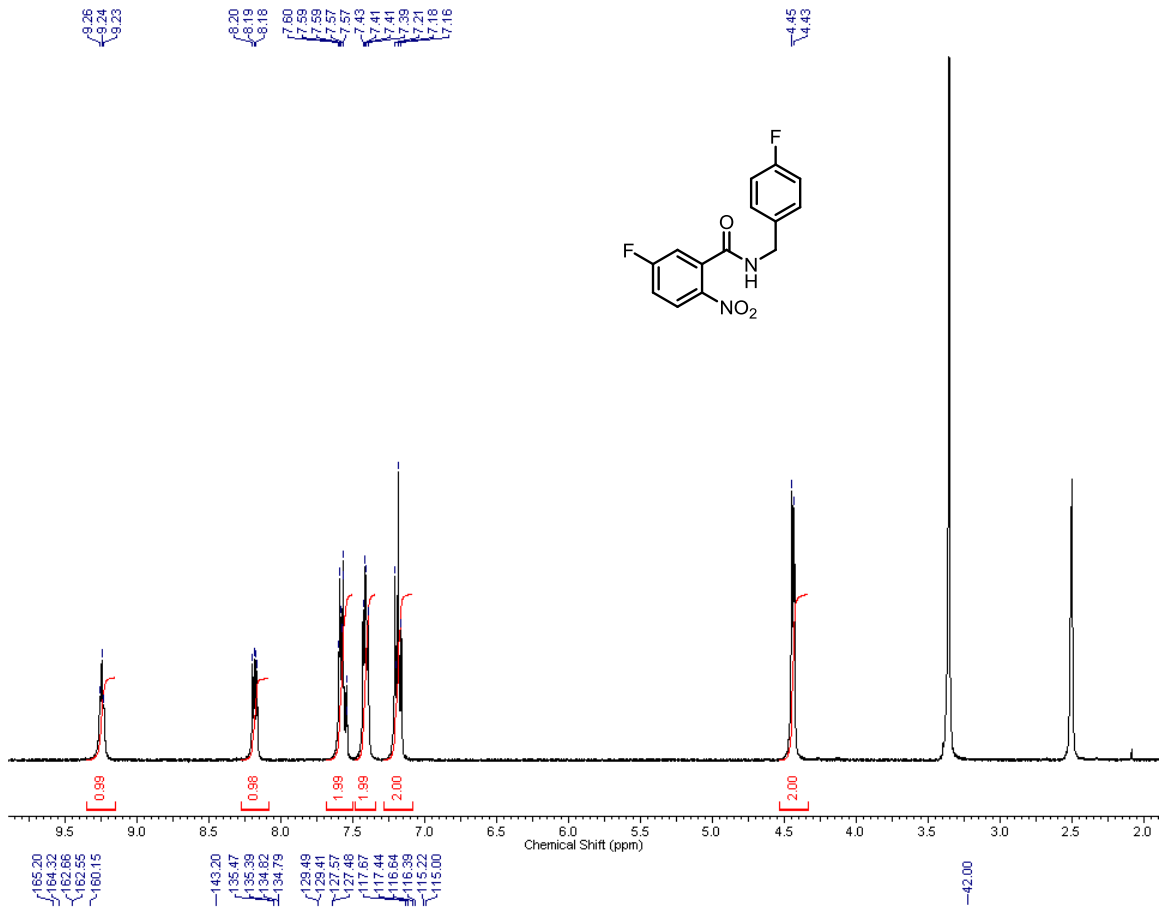




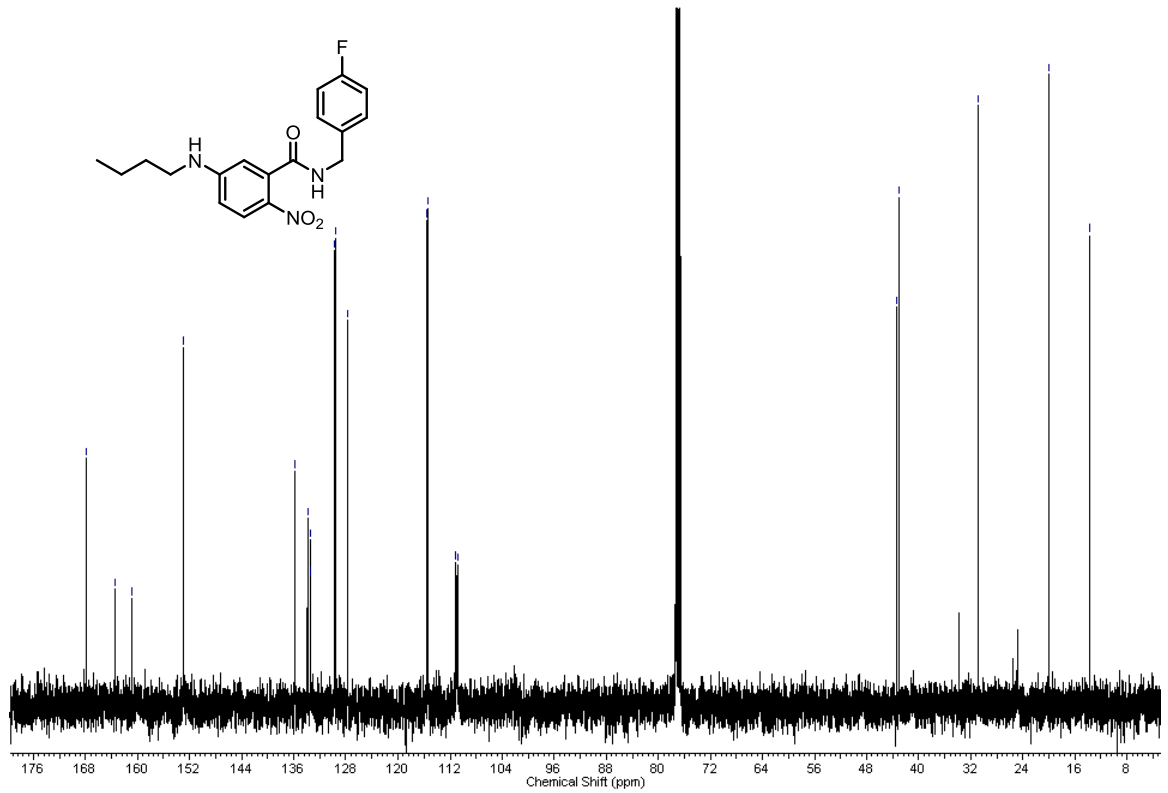
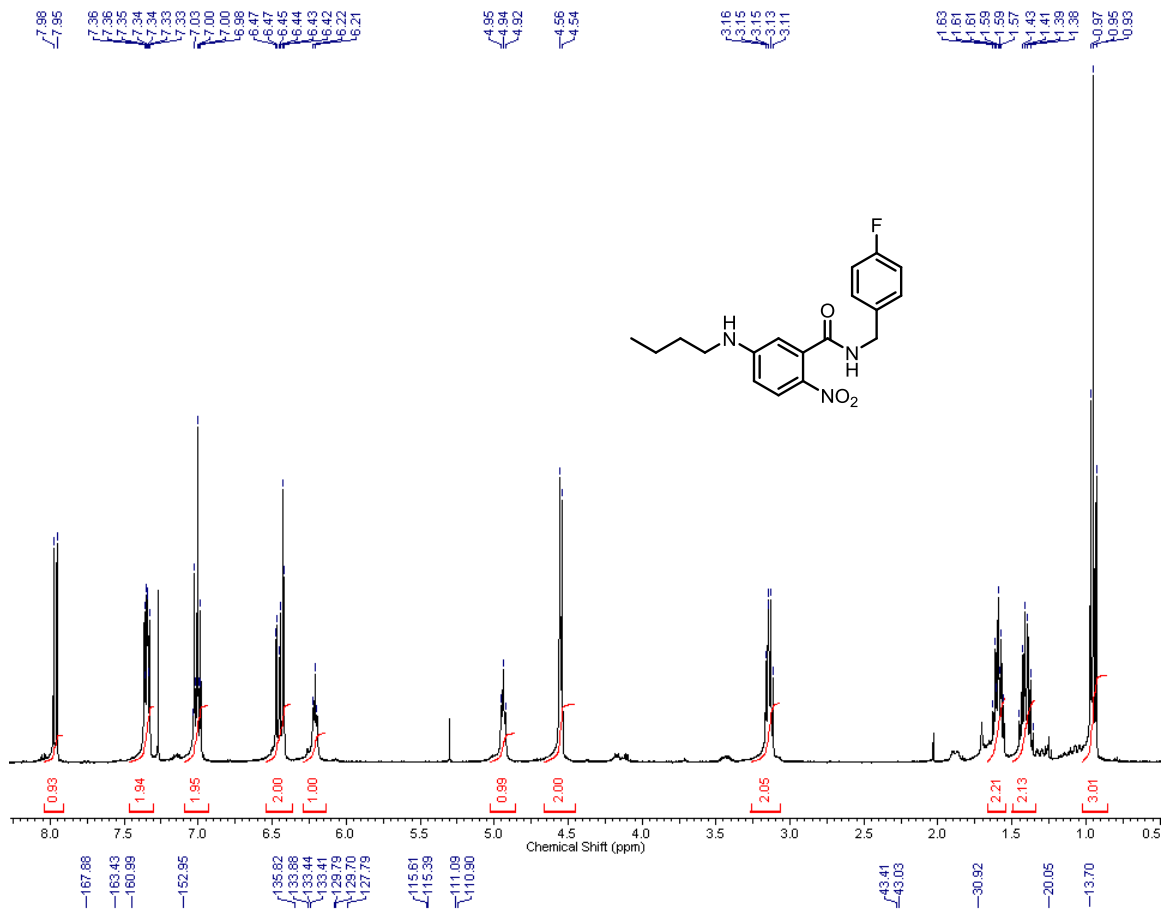


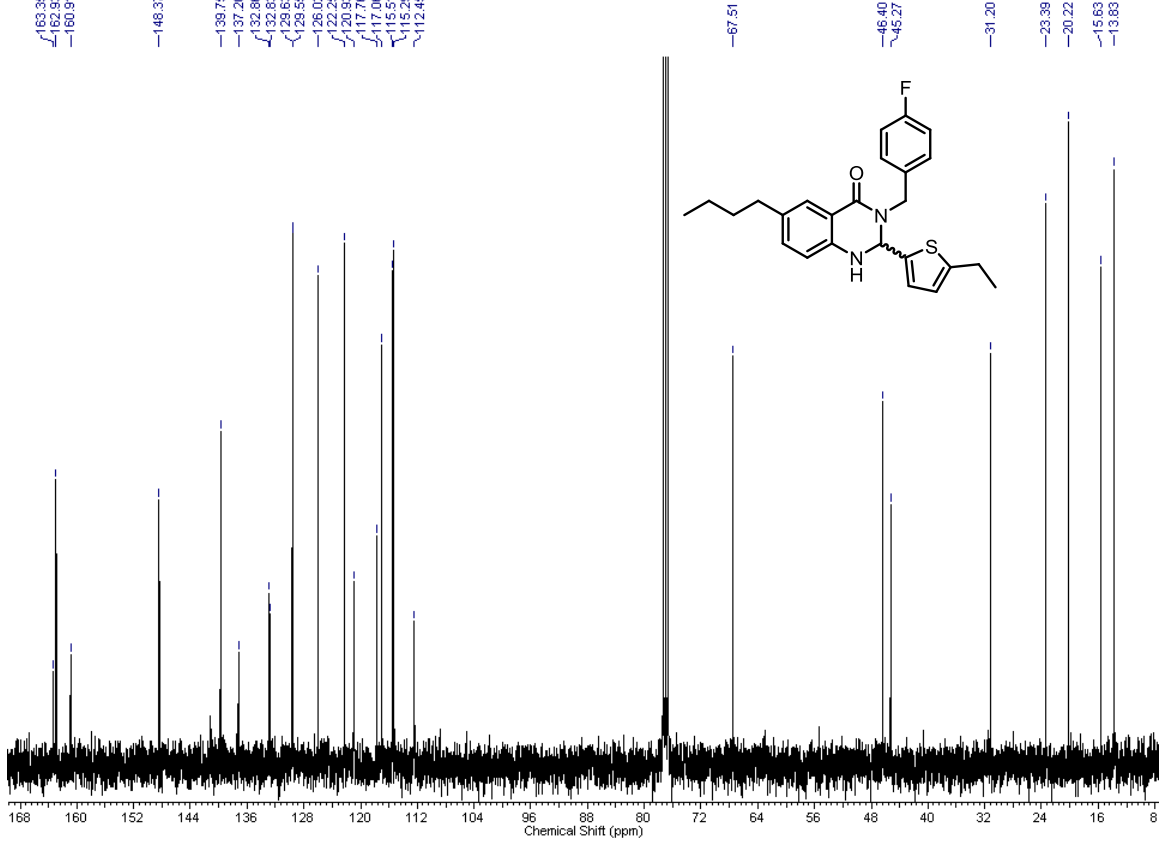
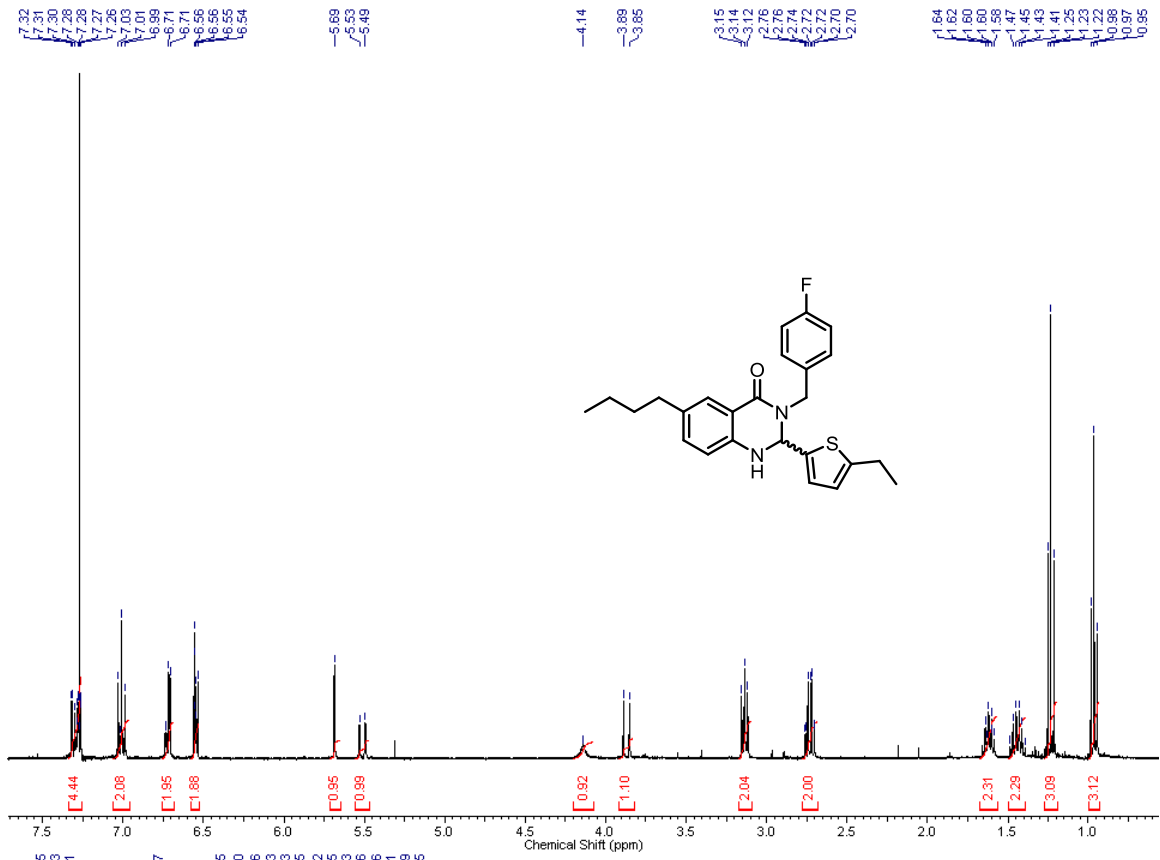


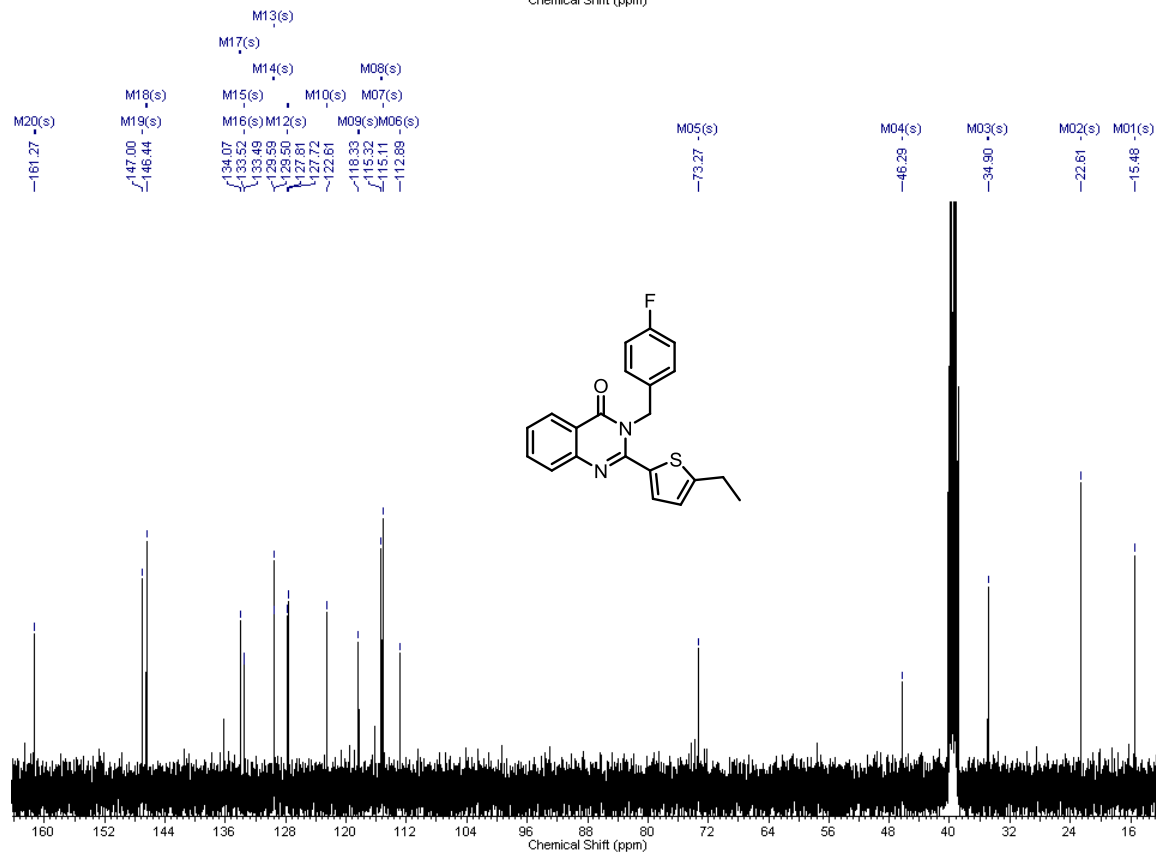
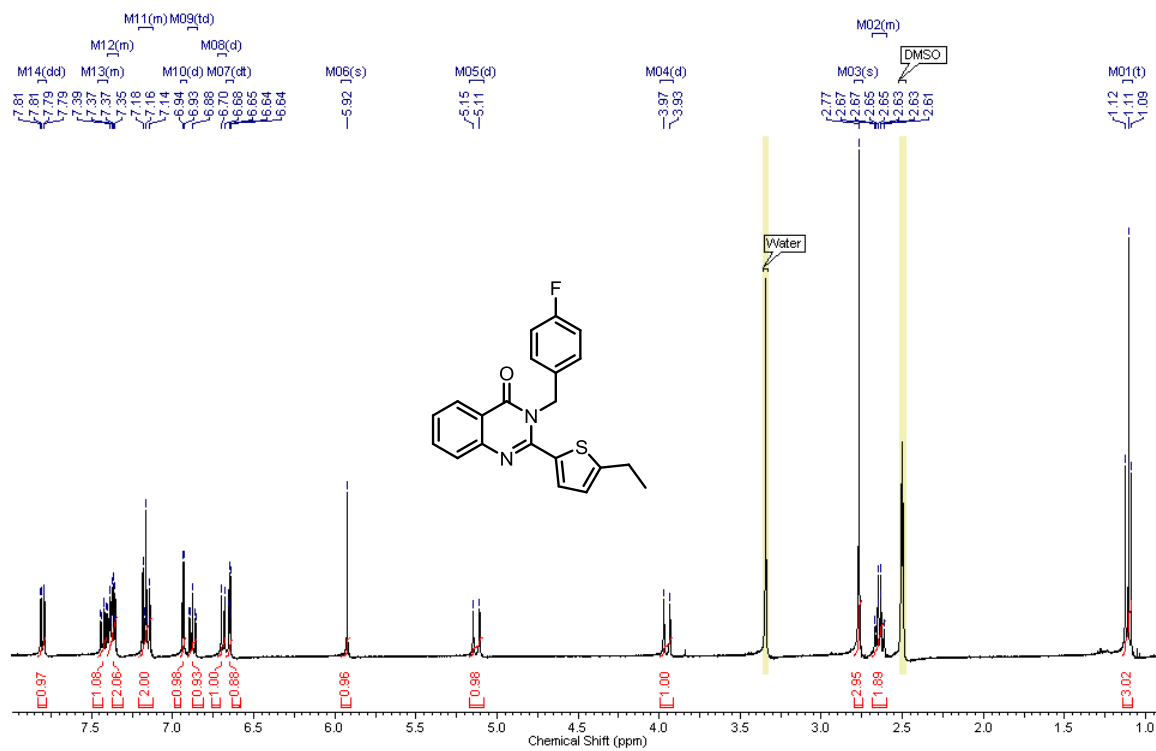


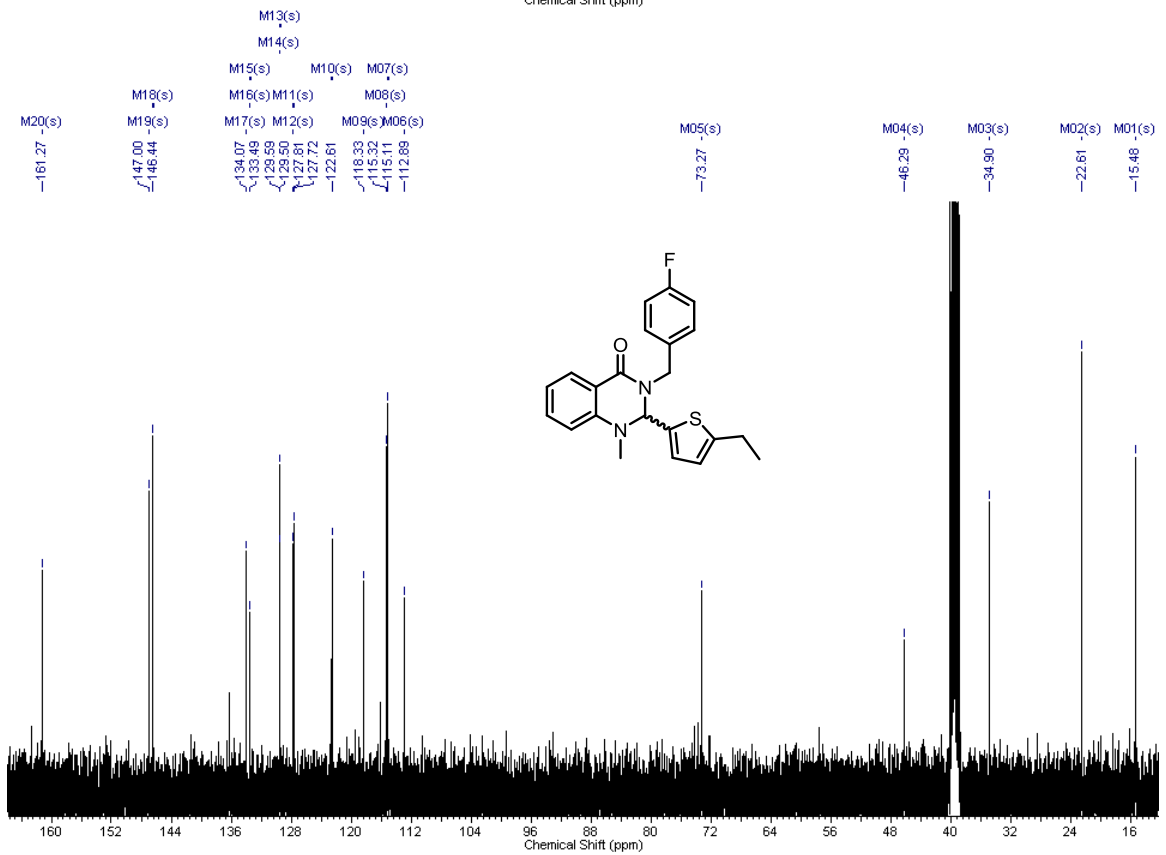
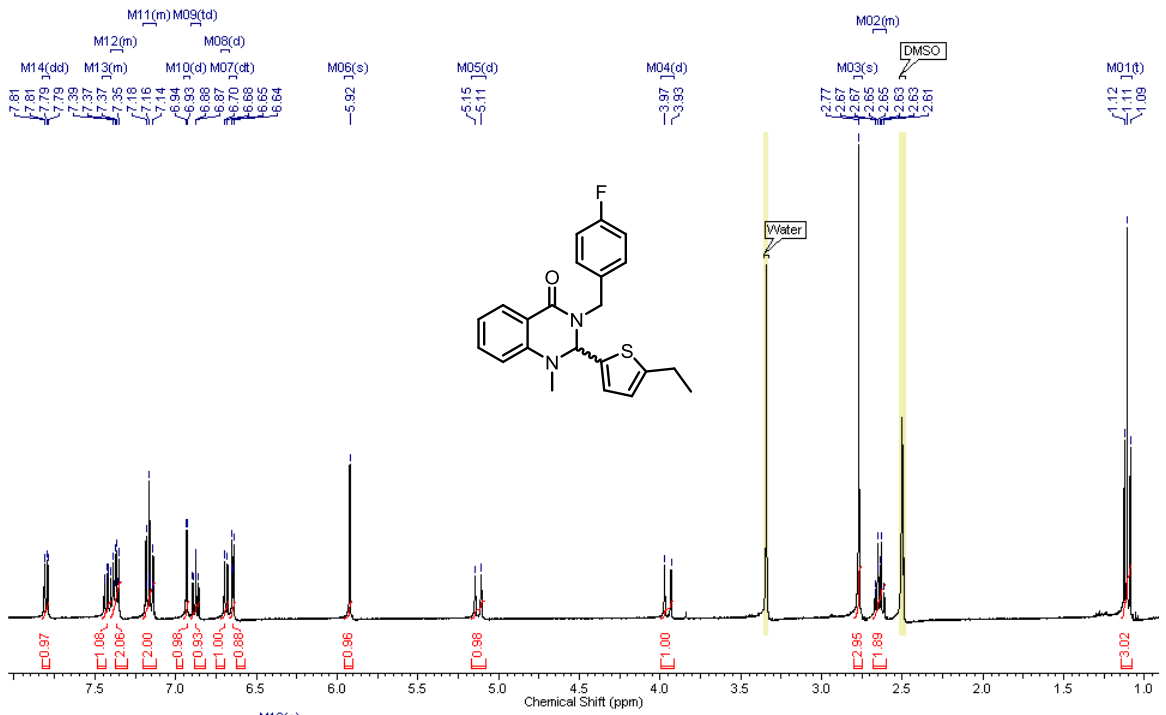






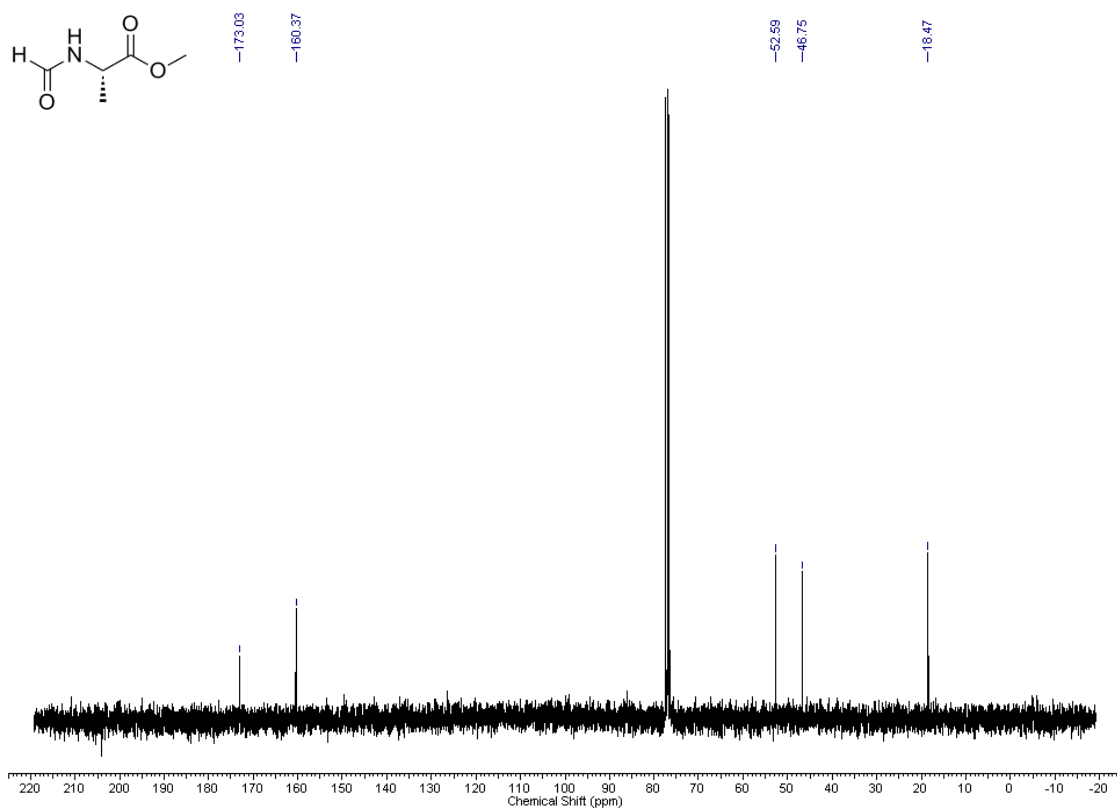
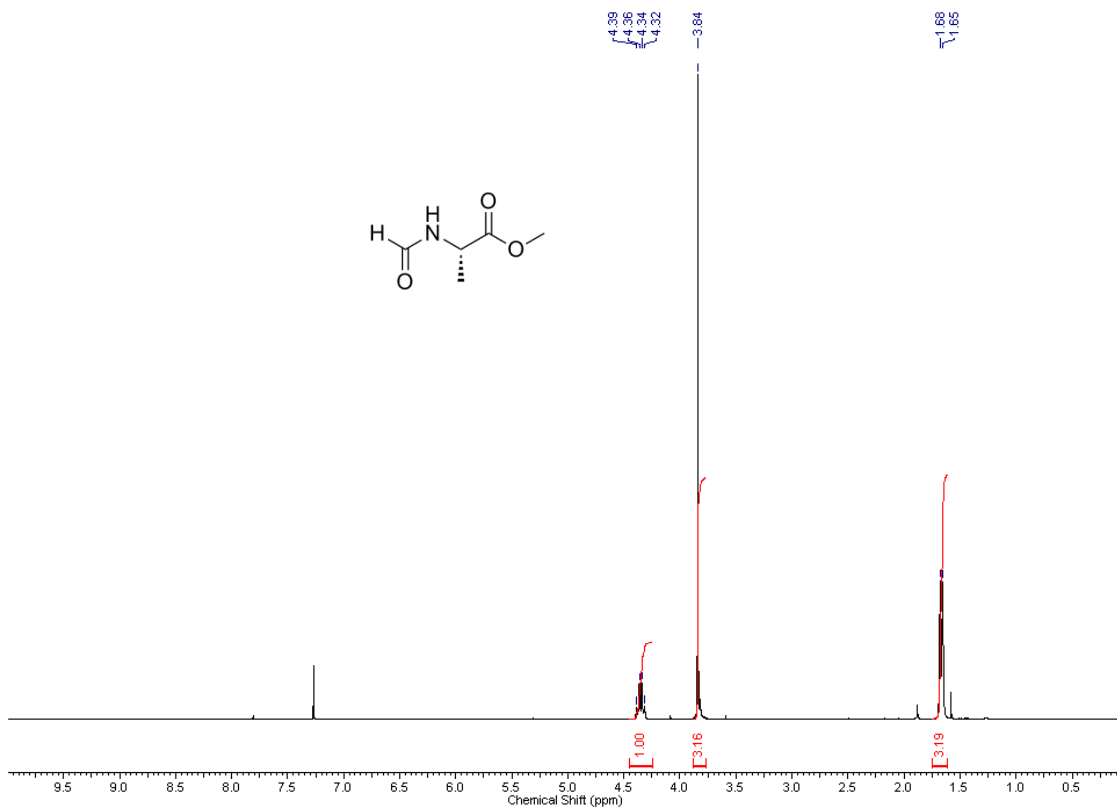


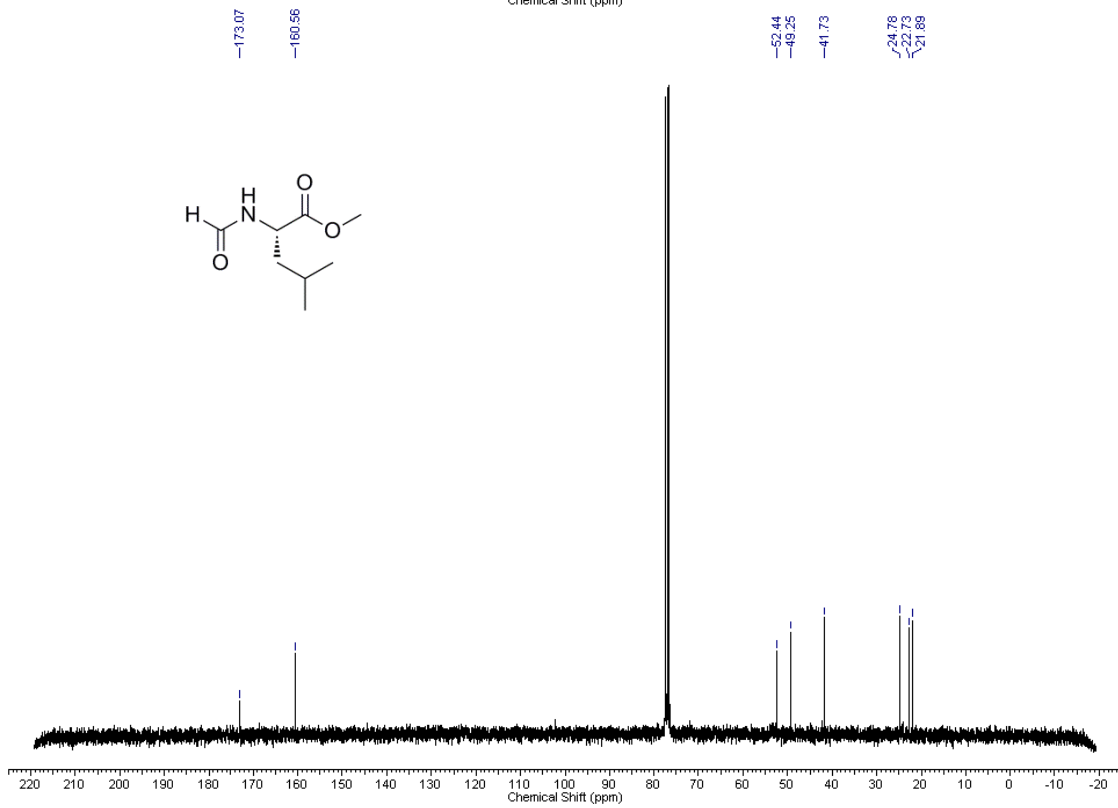
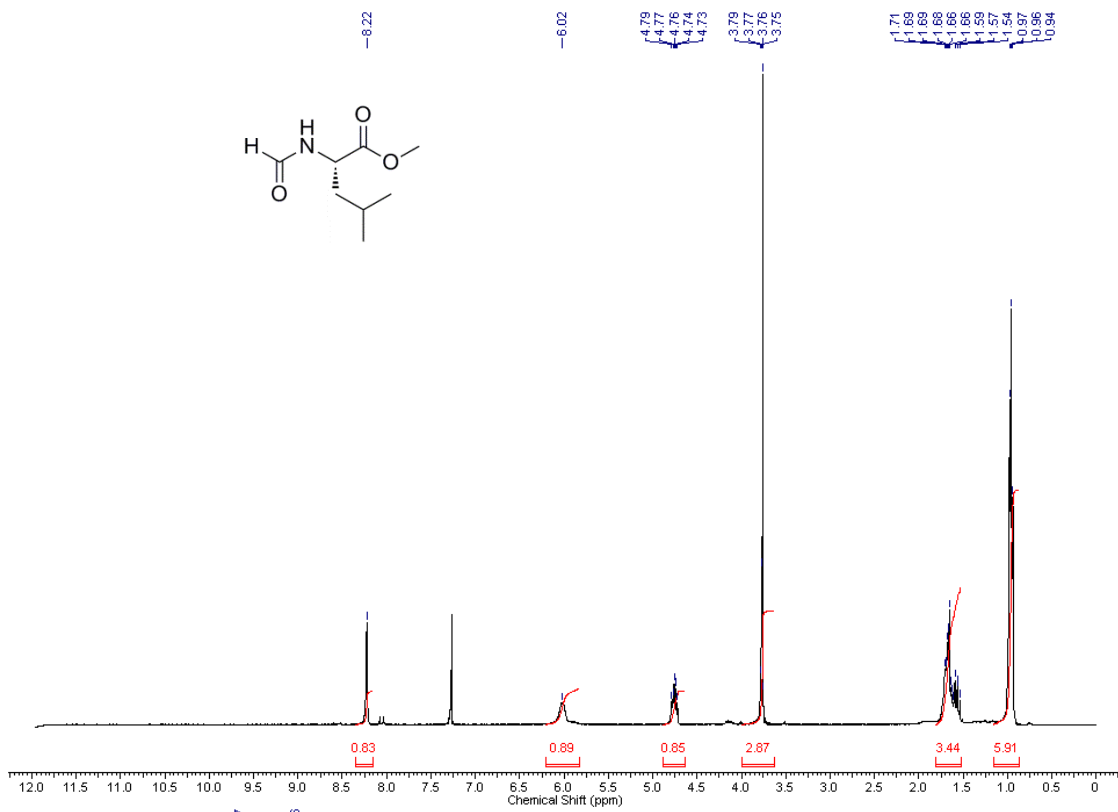


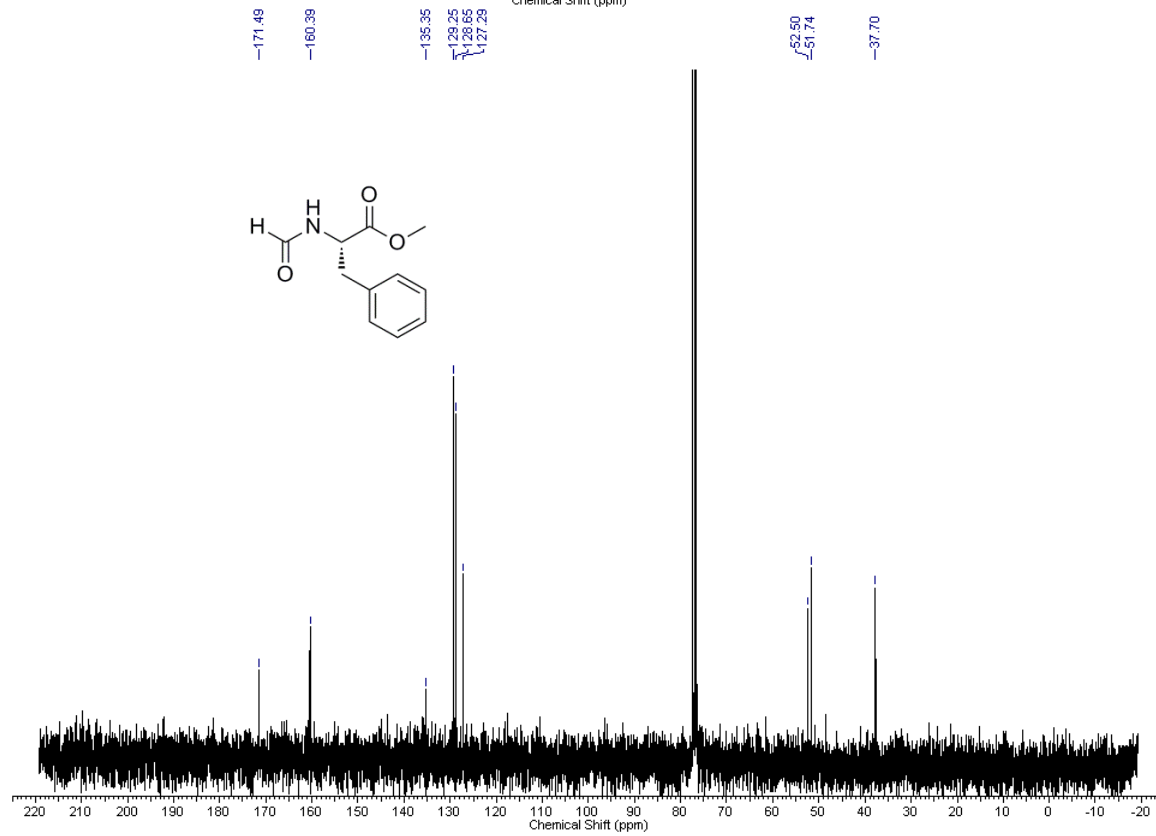
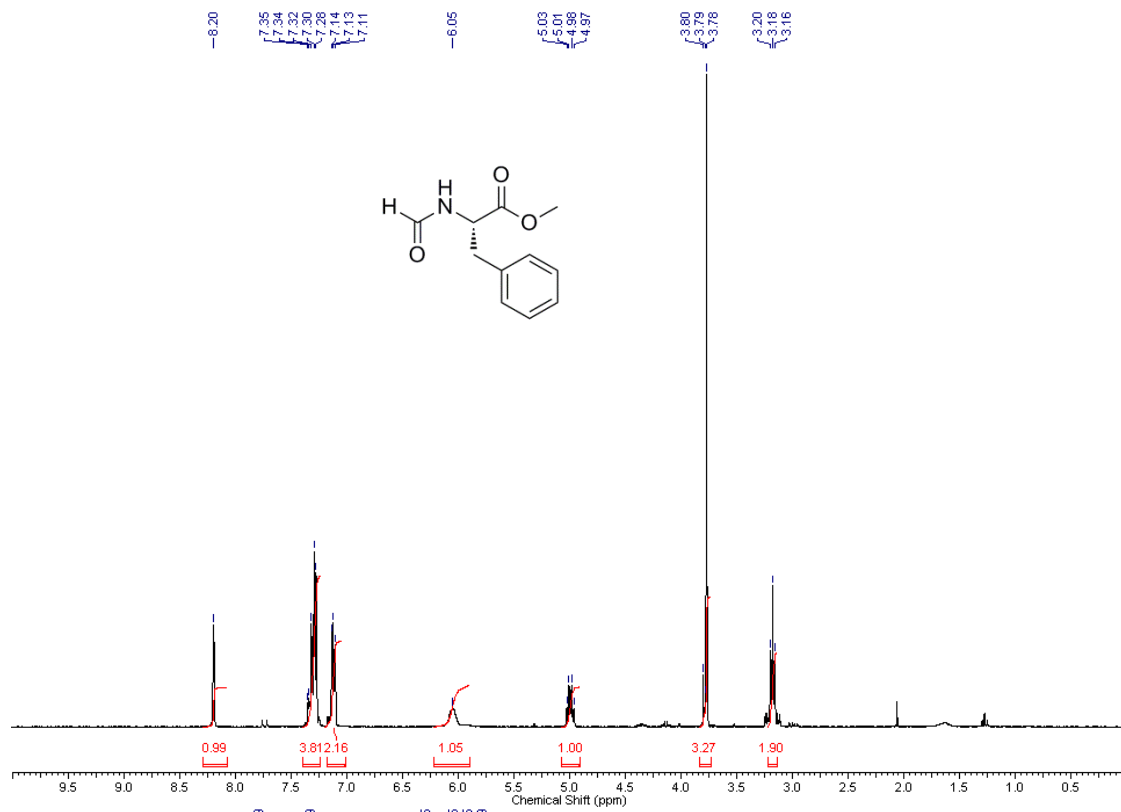


## **Chapter 4 – Isocyanide Based Multicomponent Reactions and Synthesis of Pipecolate Containing Peptides.**

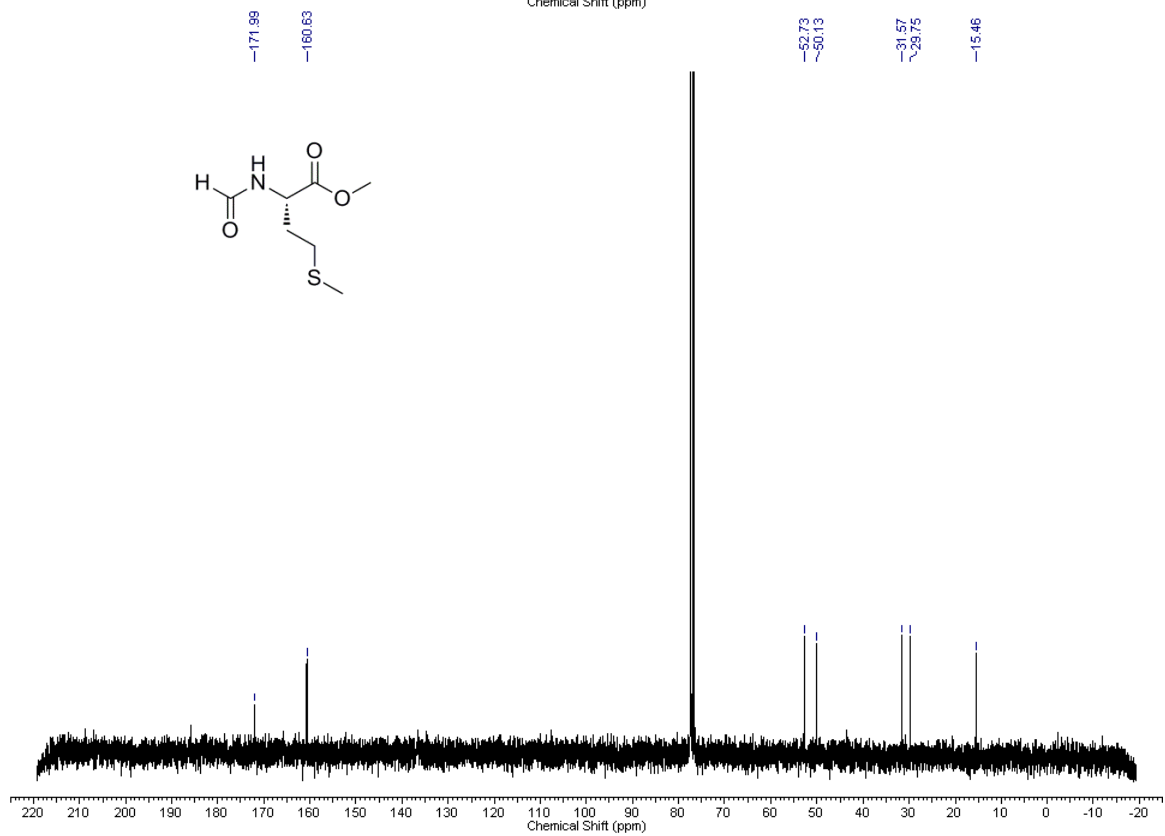
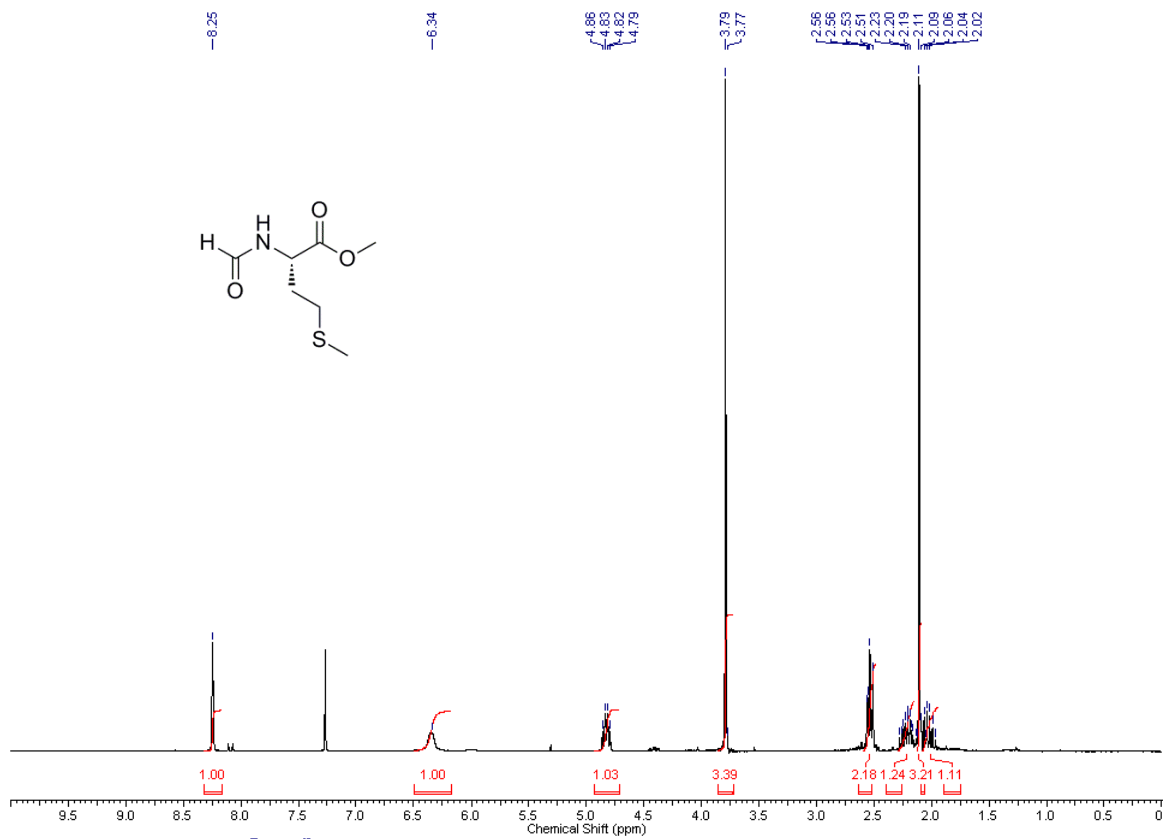
### **NMR and MassSpectra**

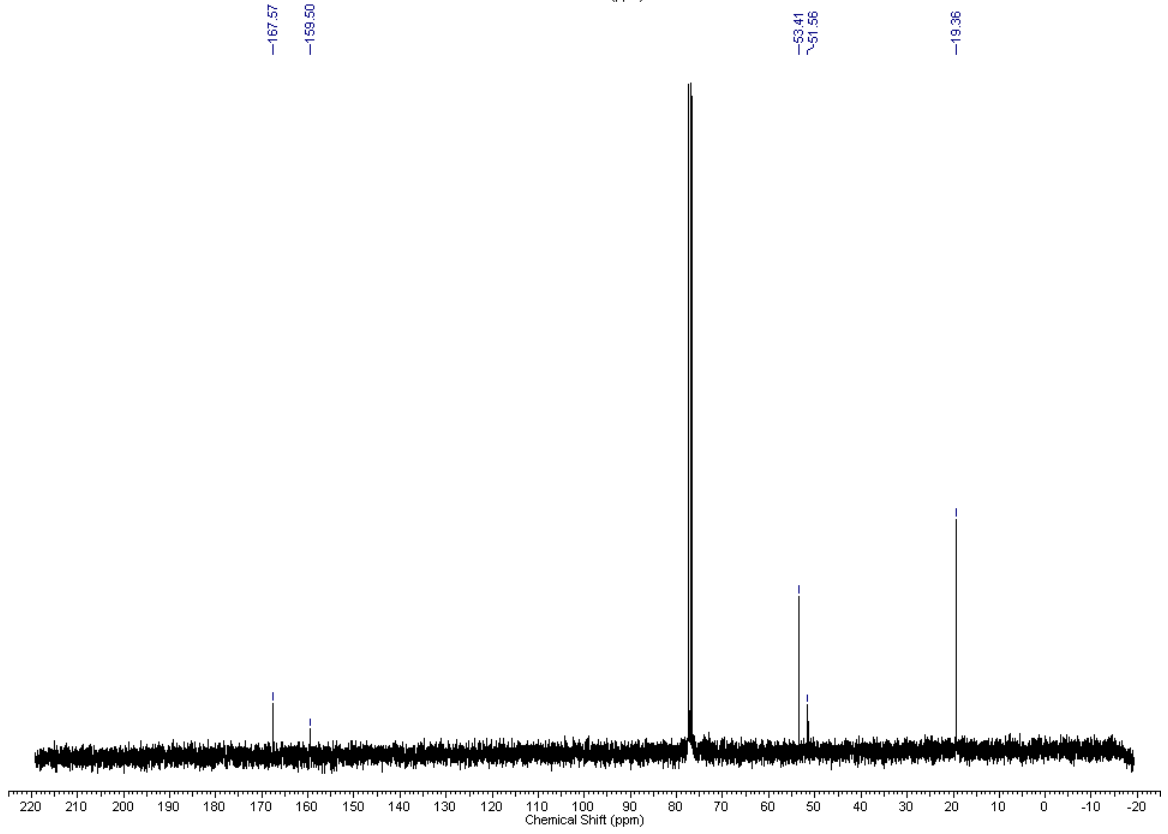
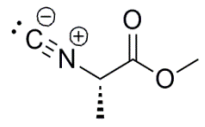
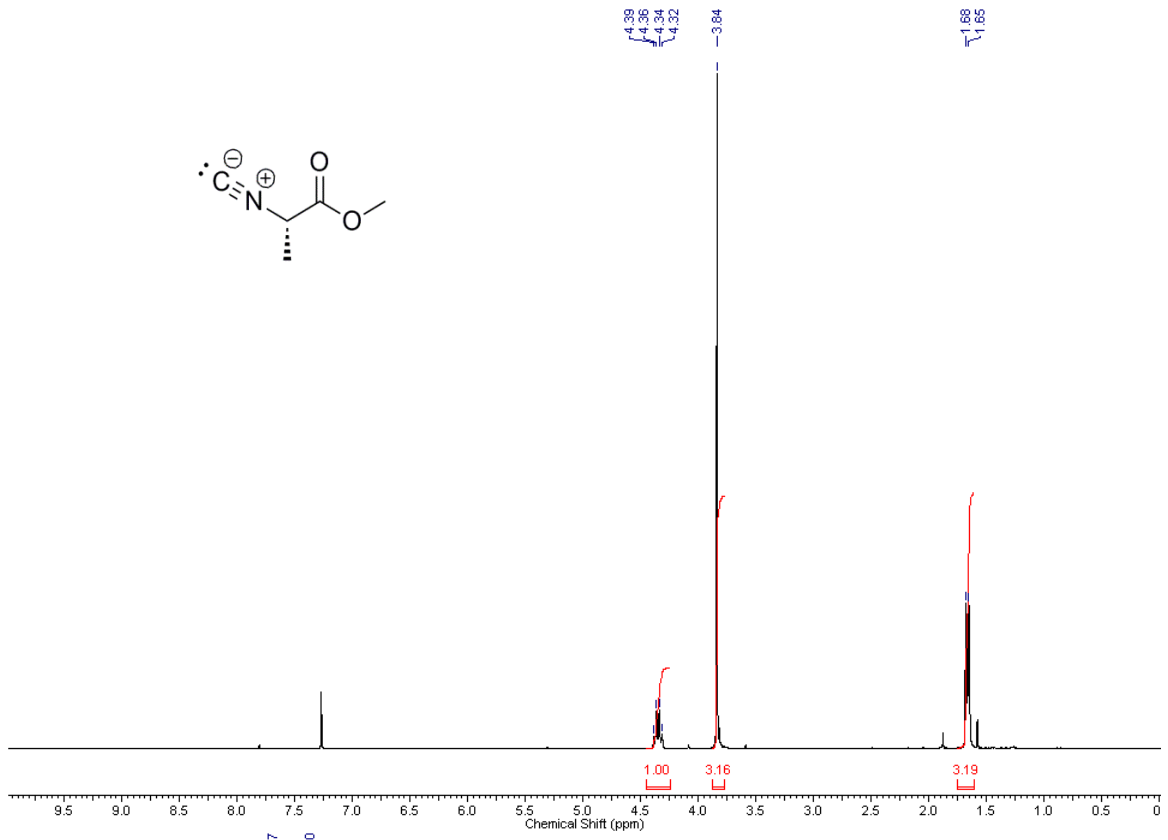




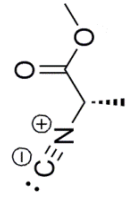
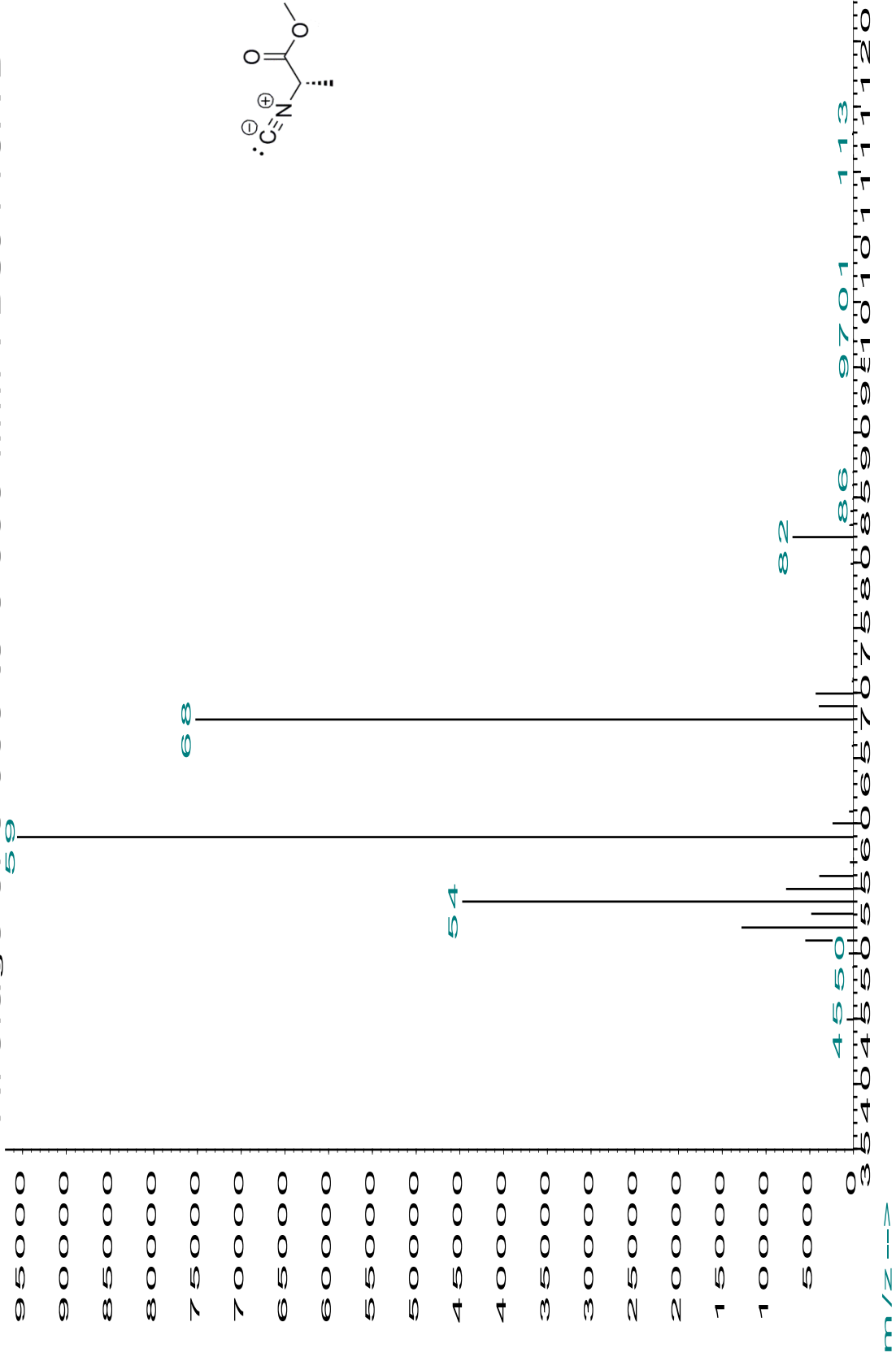


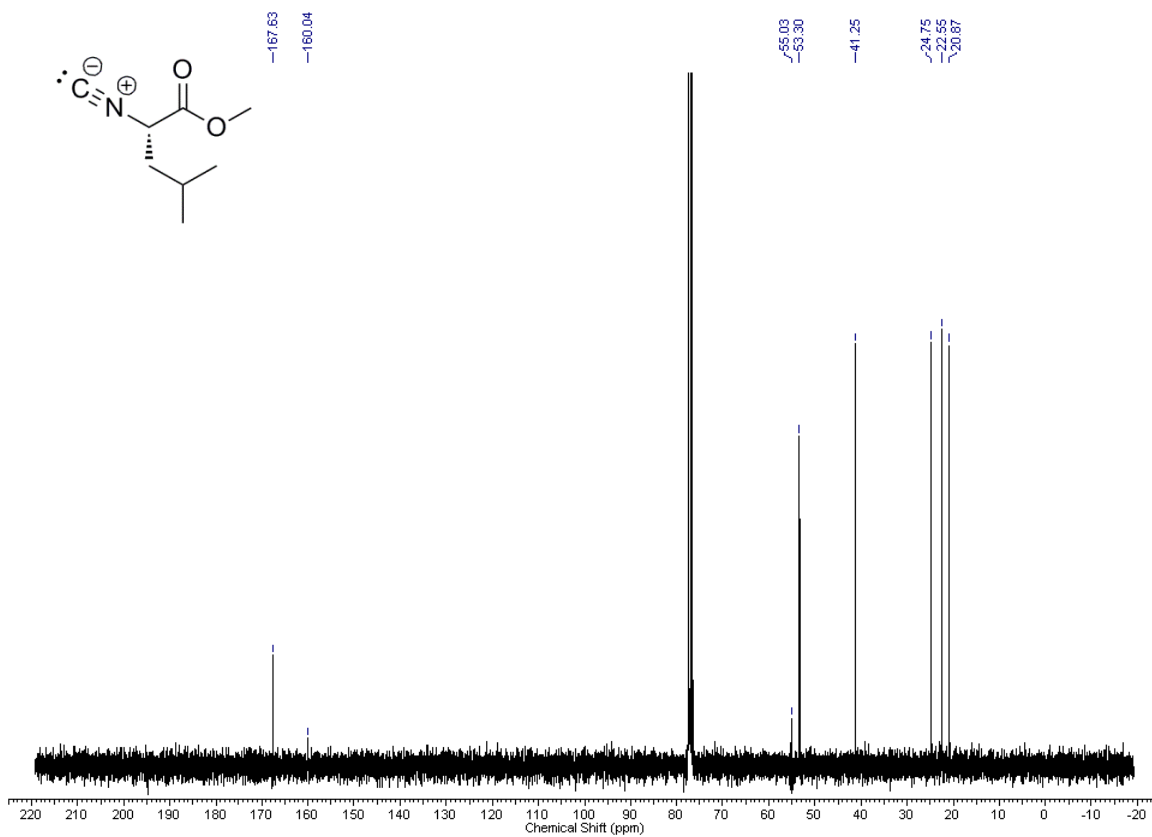
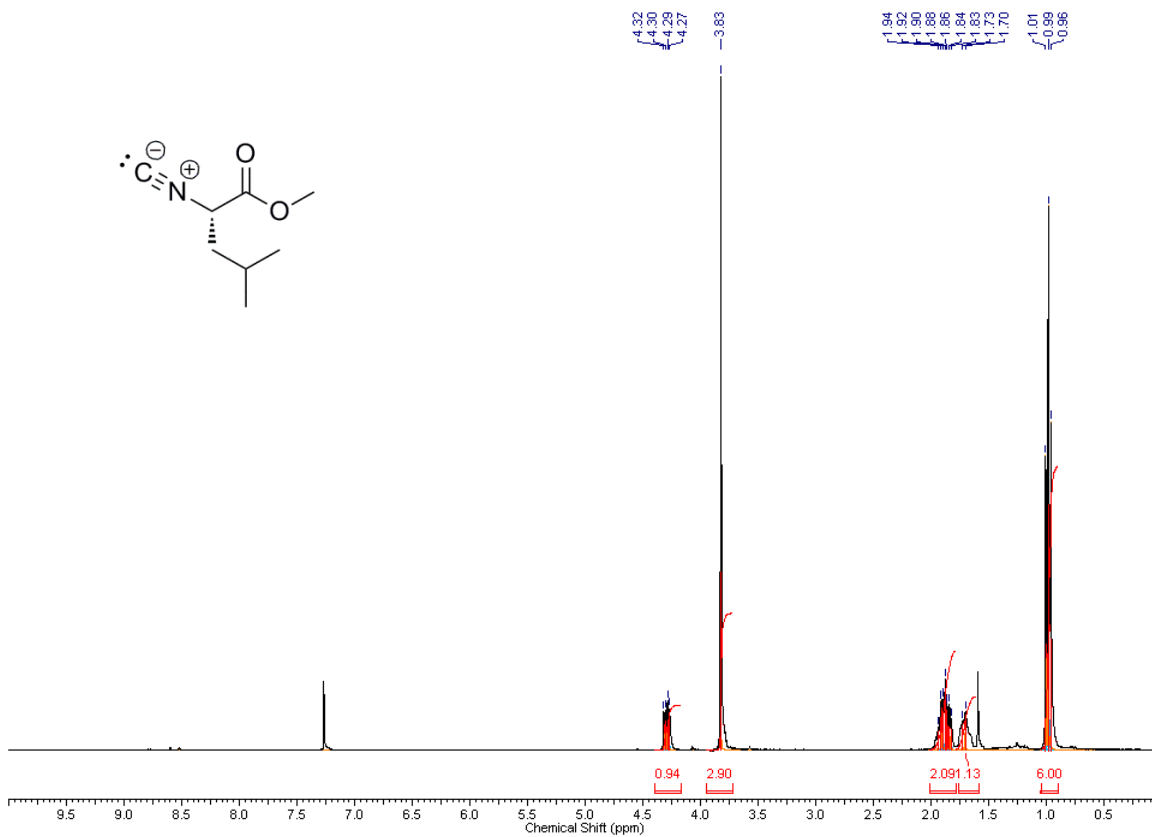




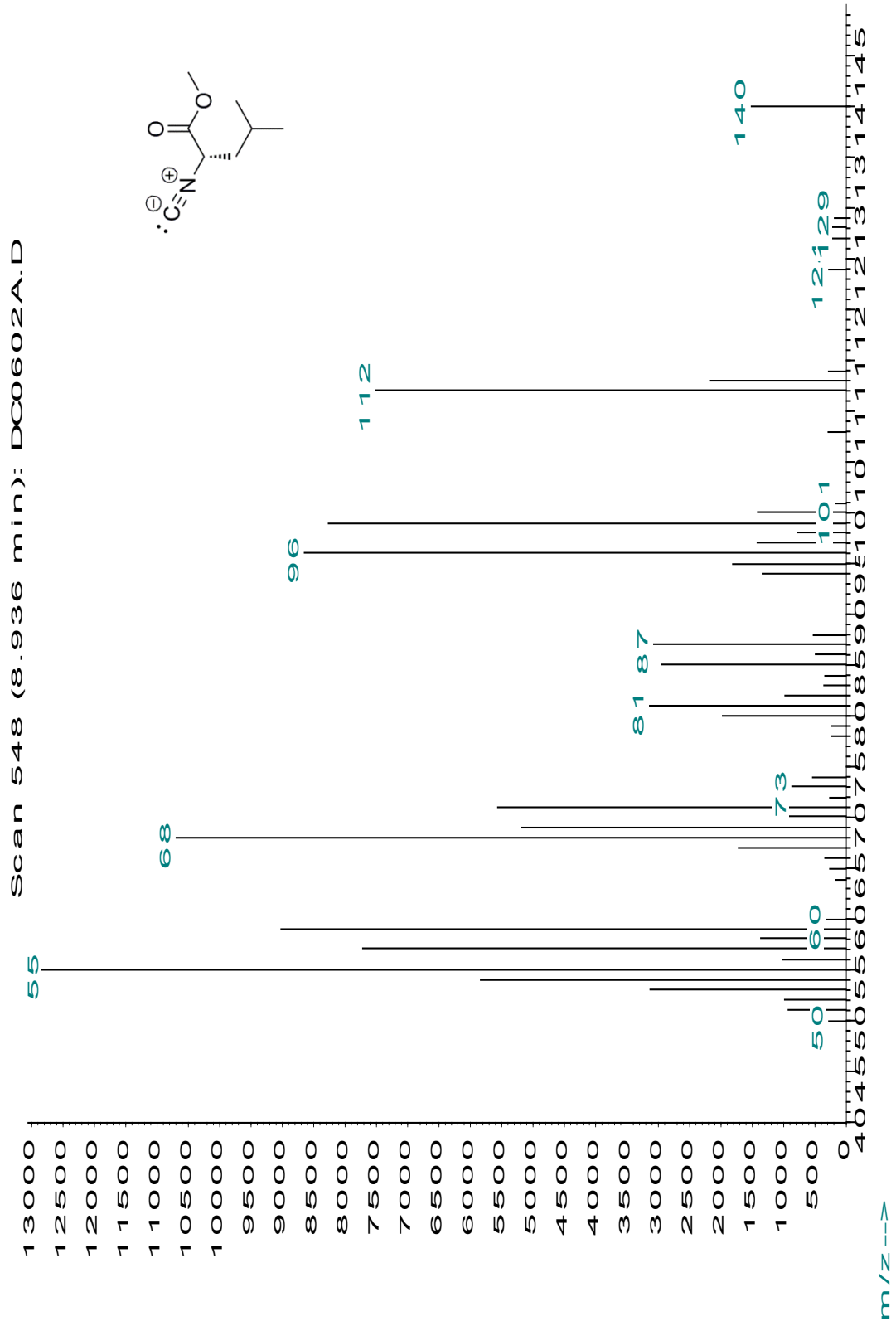


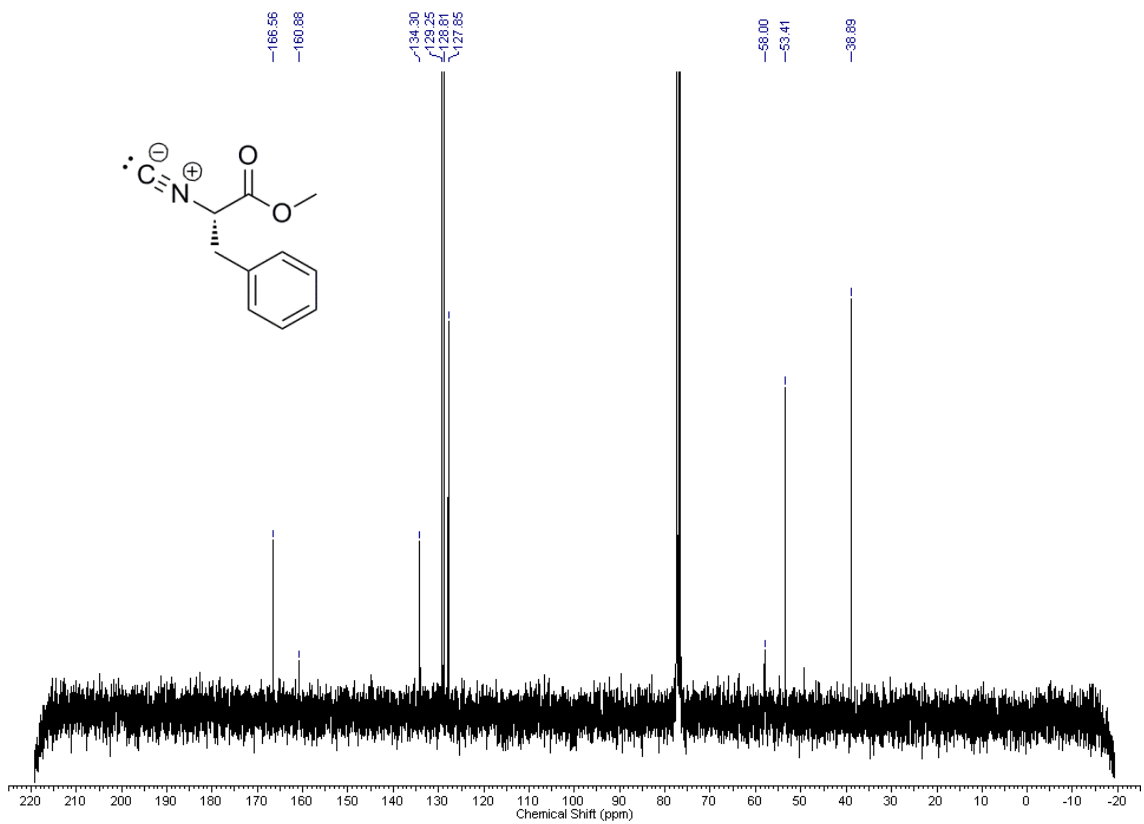
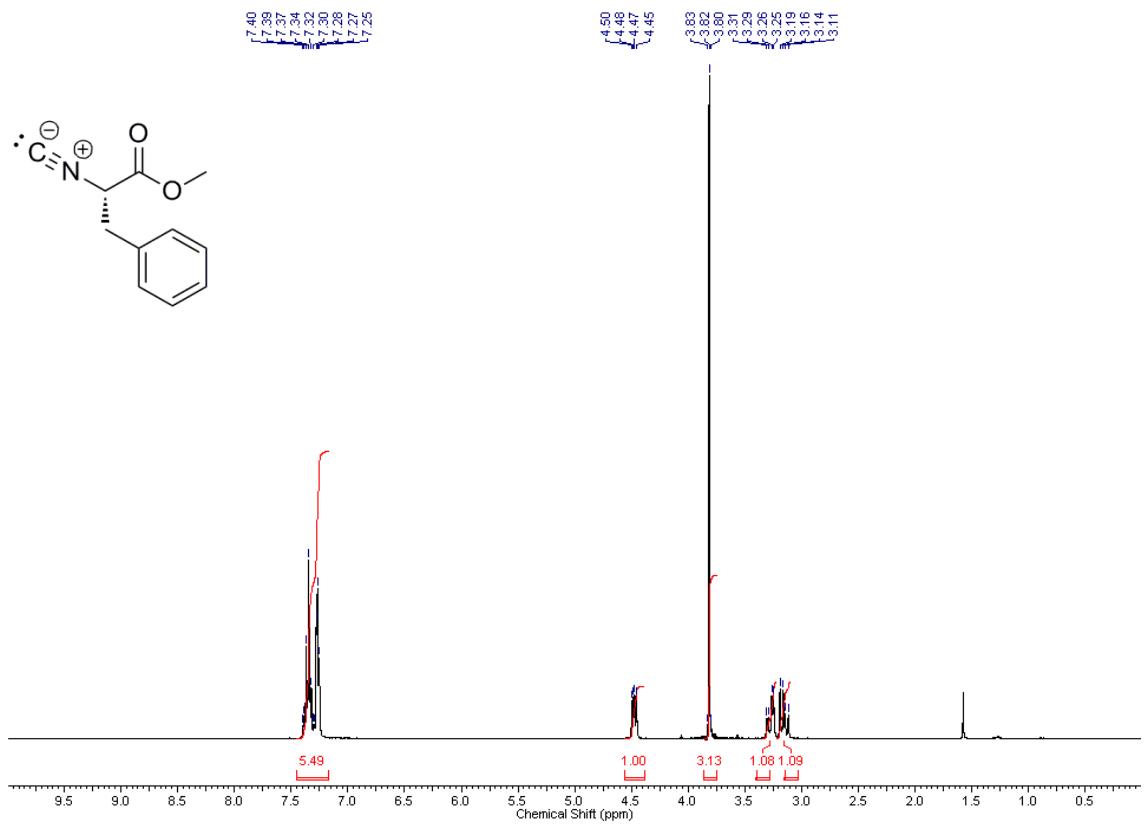
Average of 6.050 to 6.390 min.: DC0113A.D



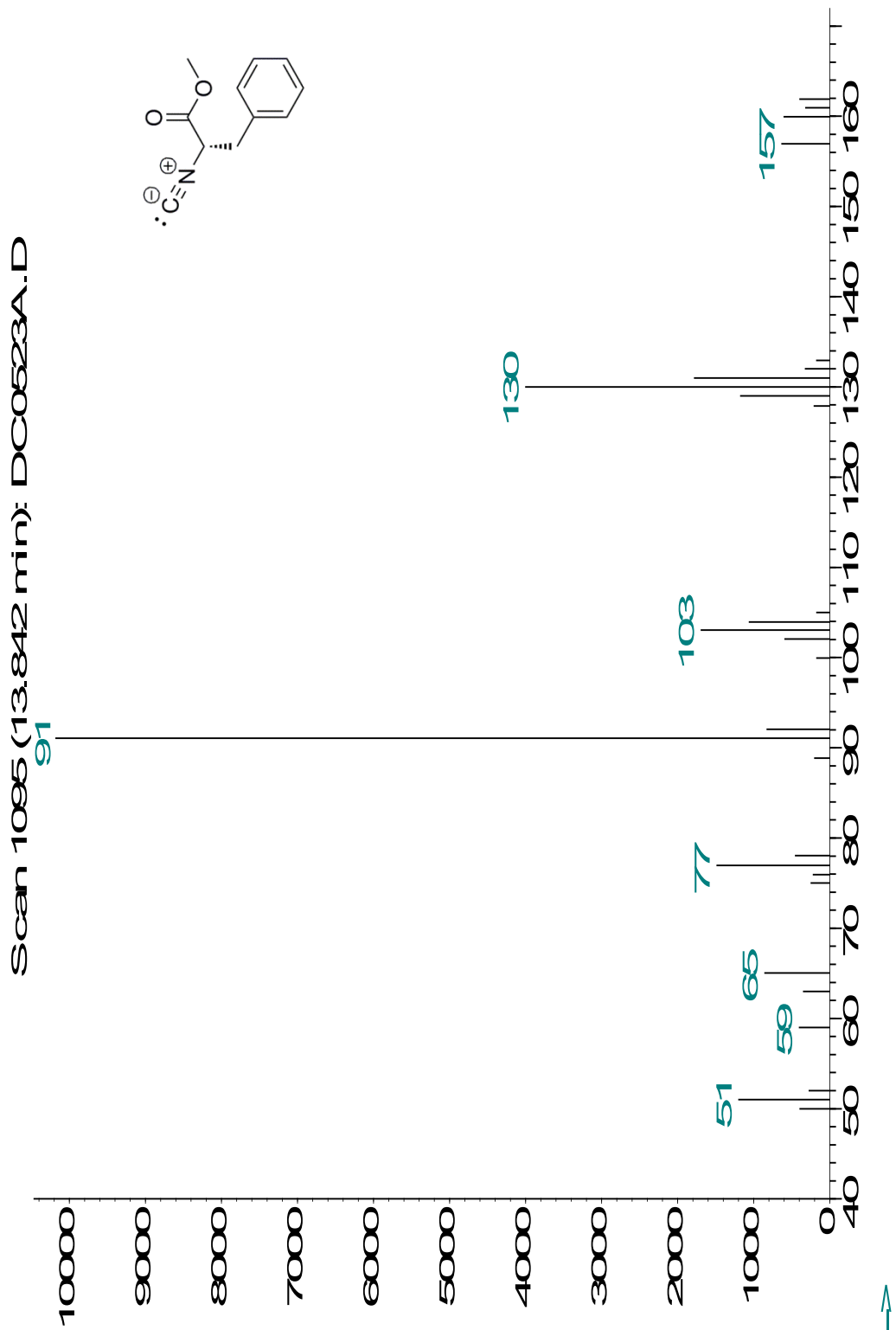


Abundance

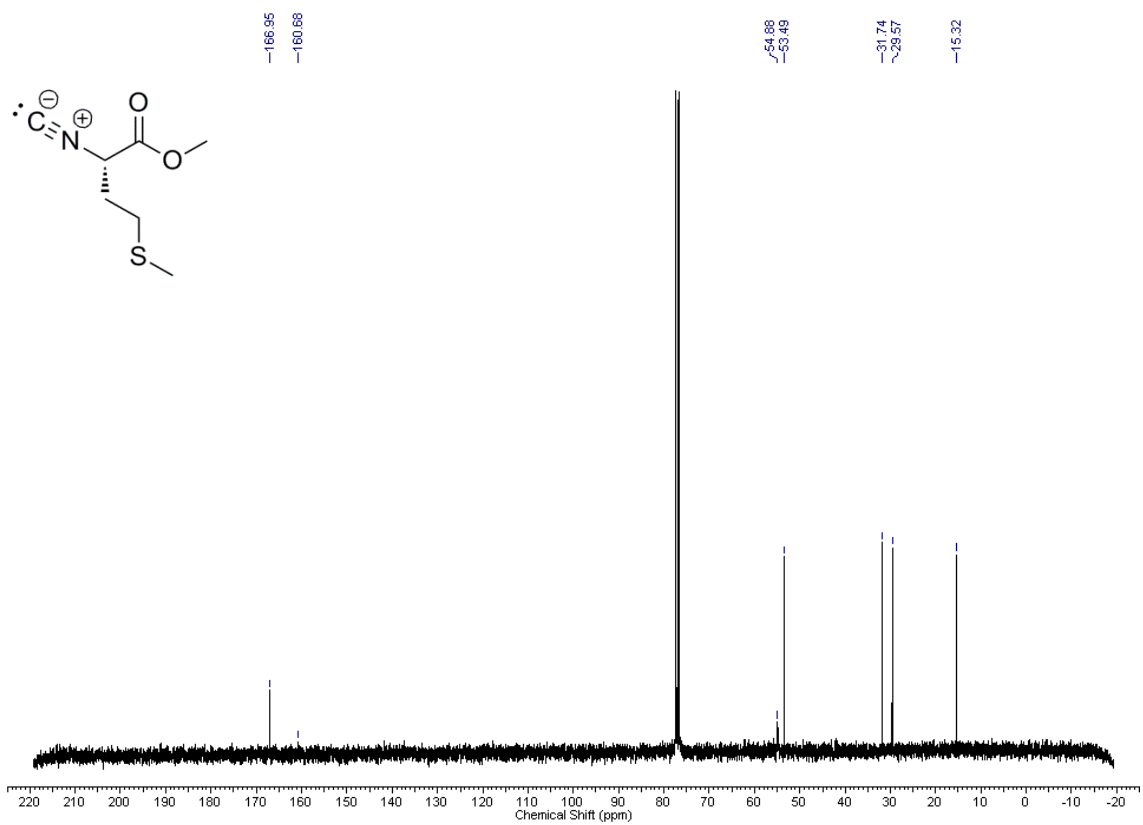
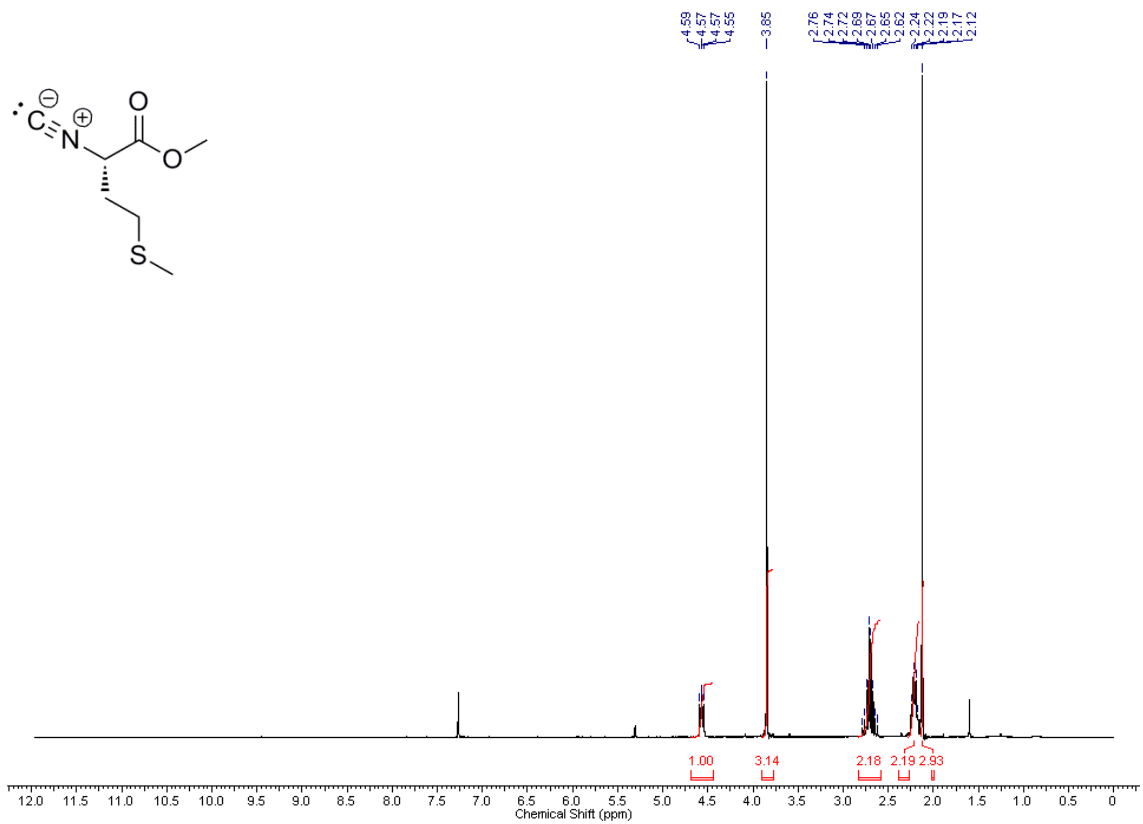




Abundance

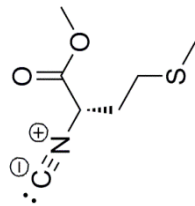
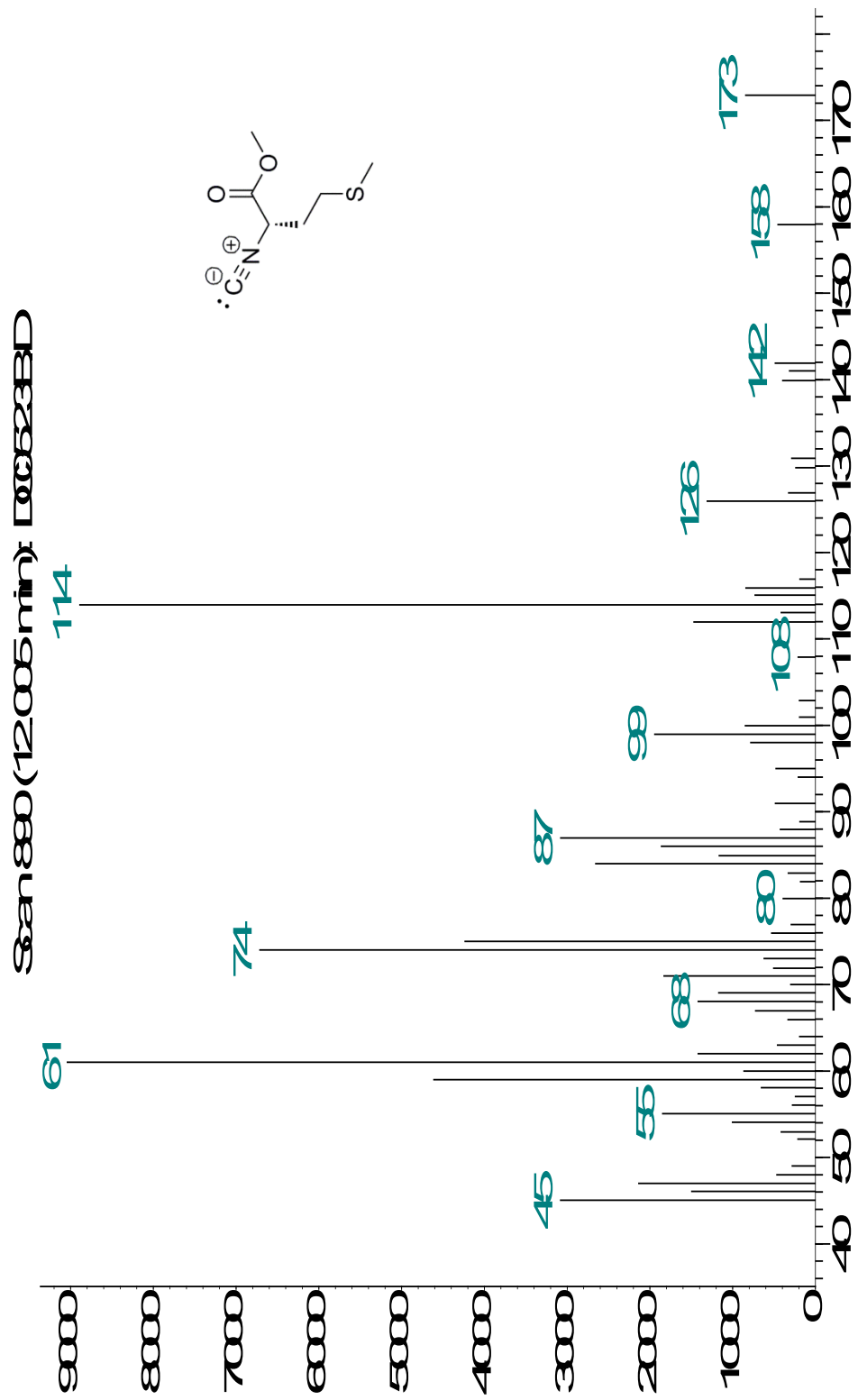


m/z→

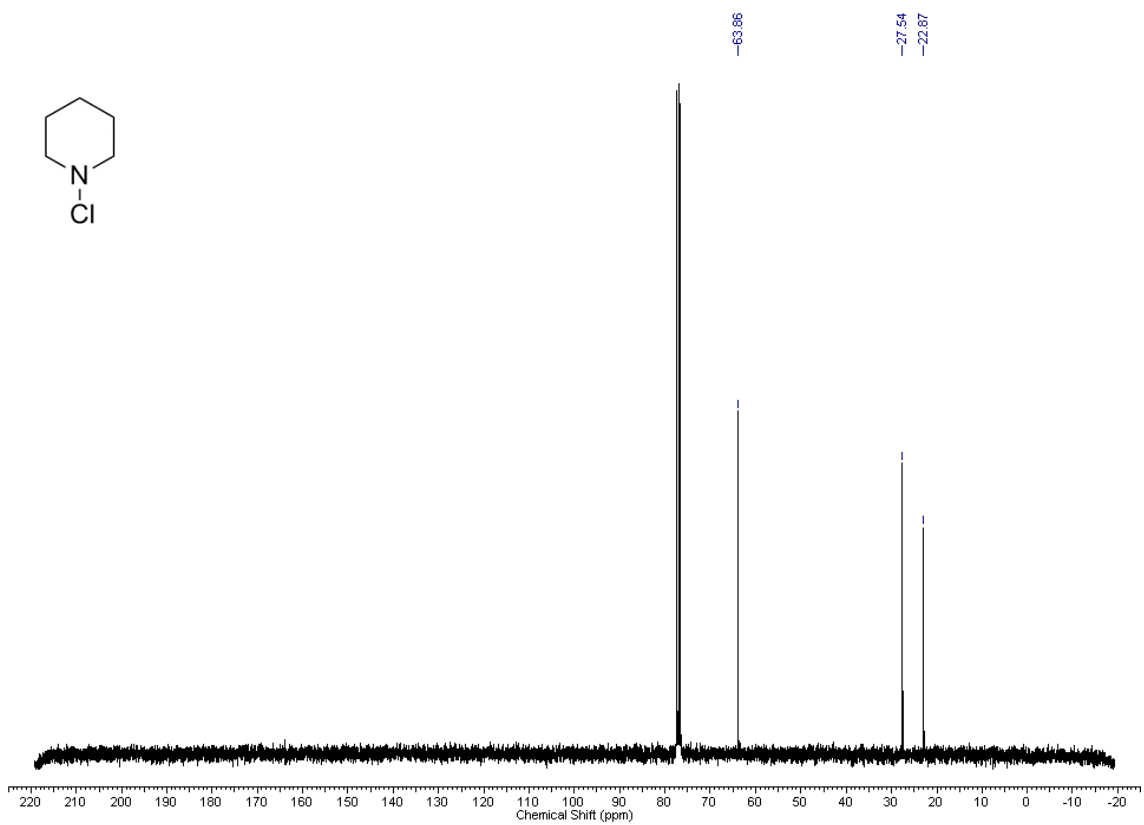
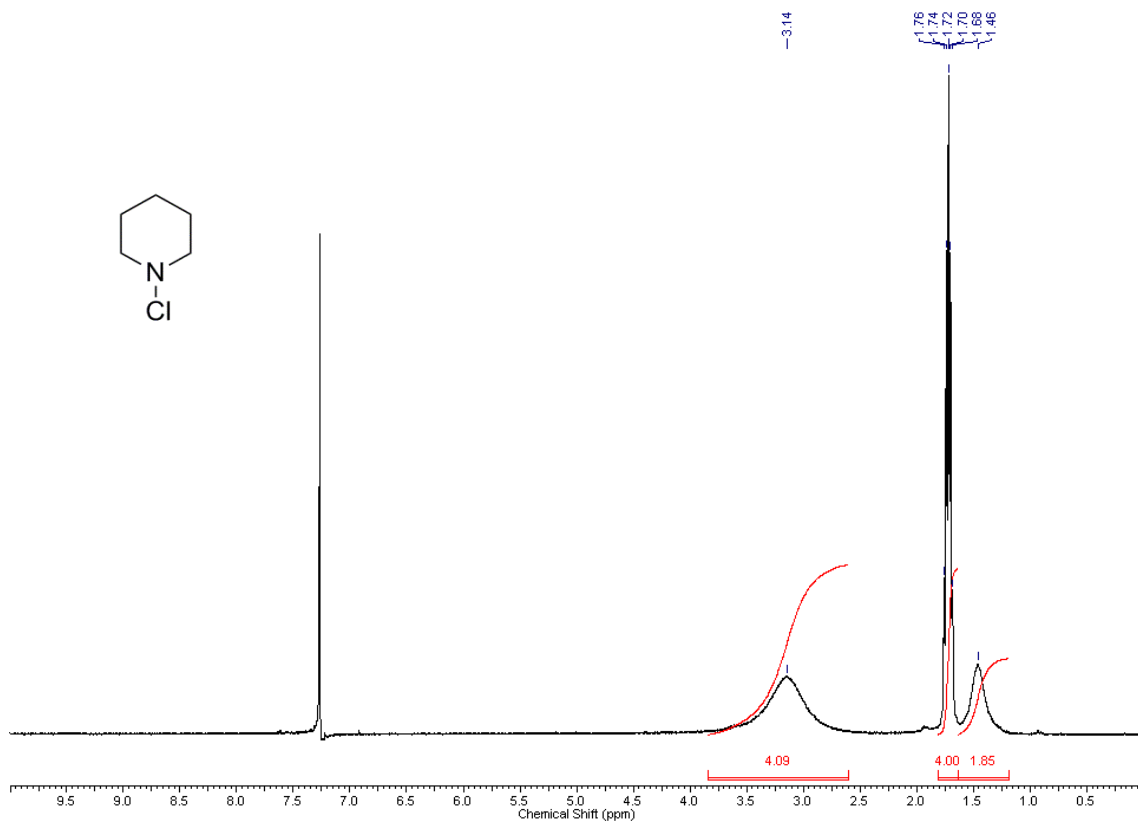


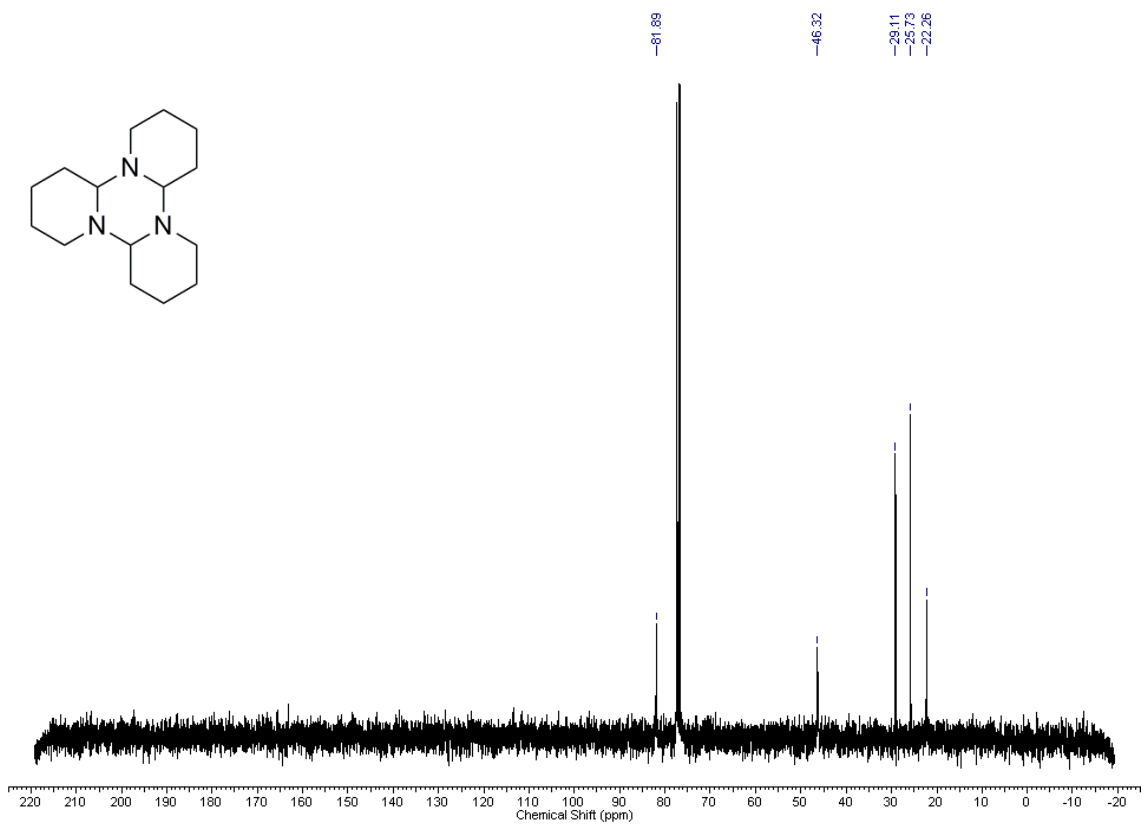
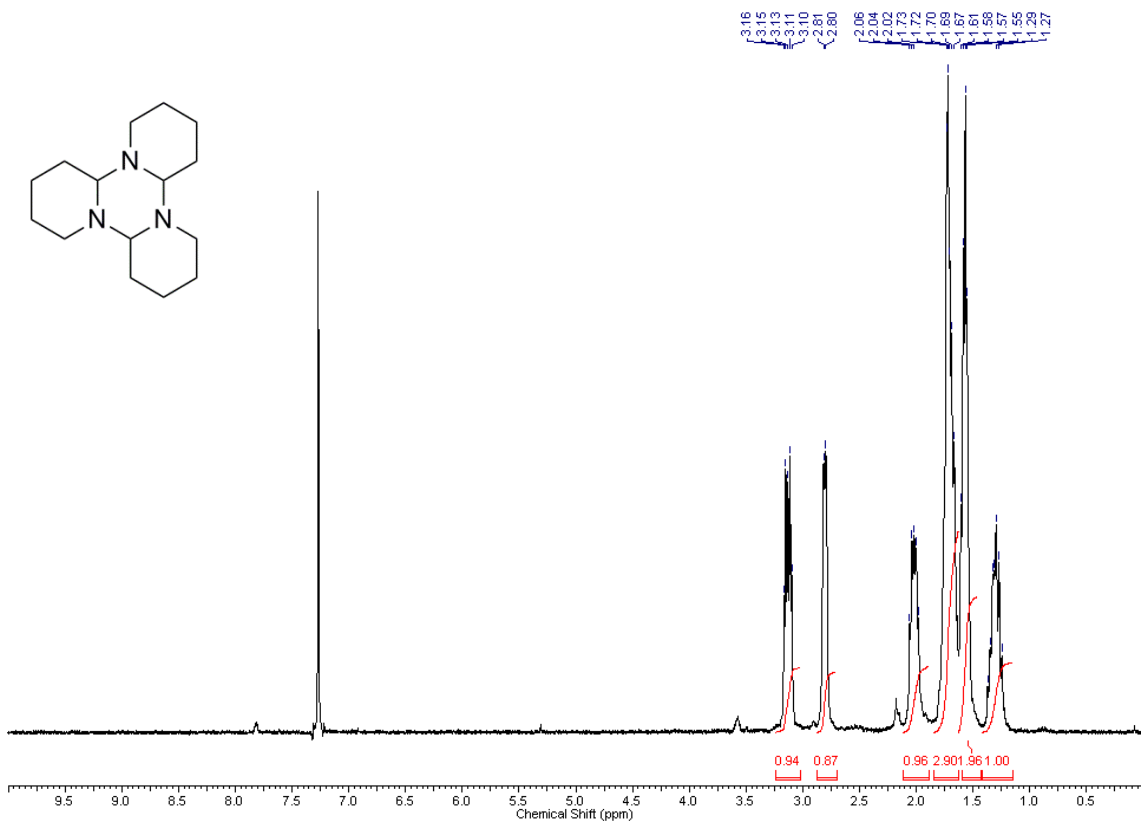


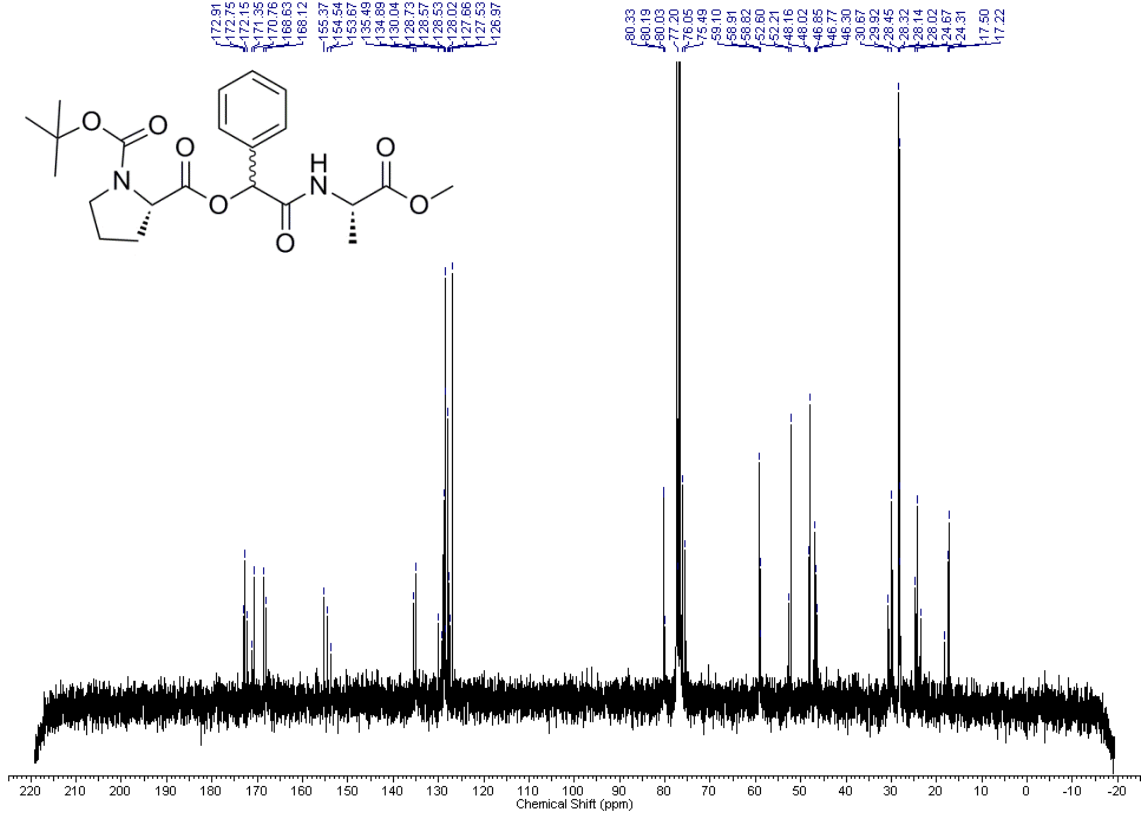
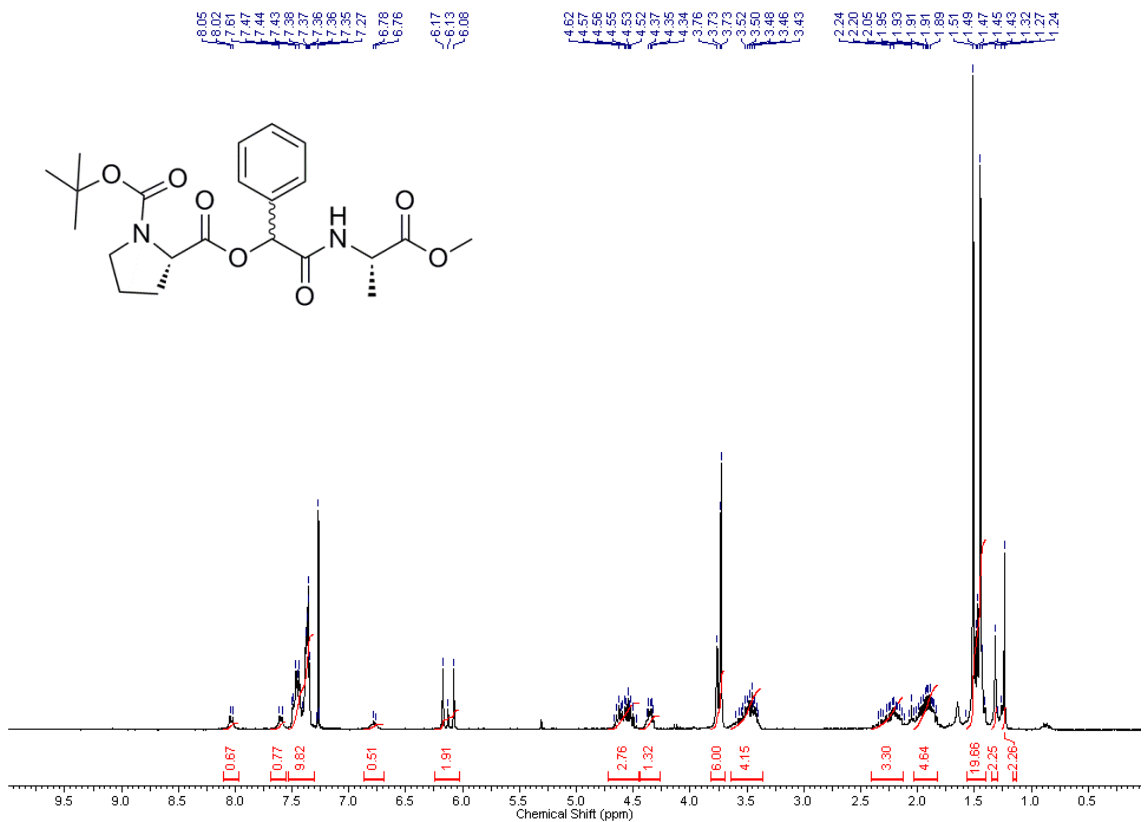
Abundance

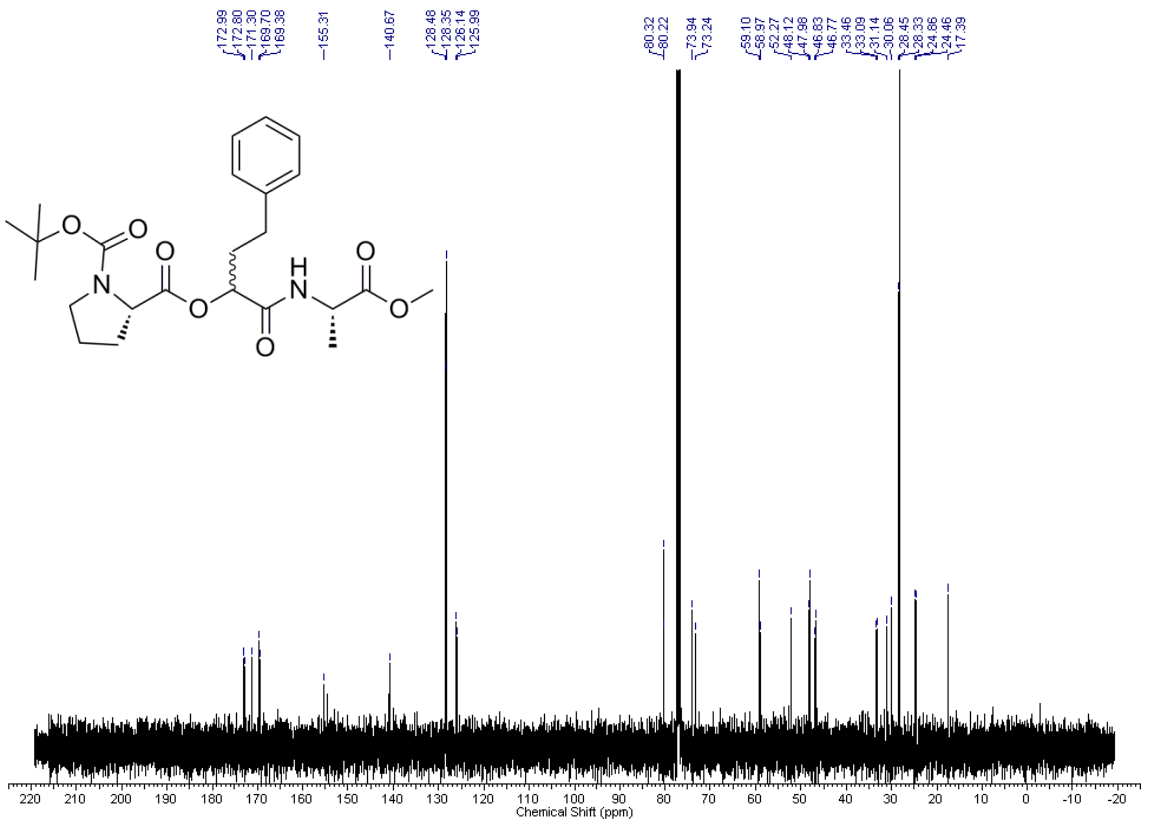
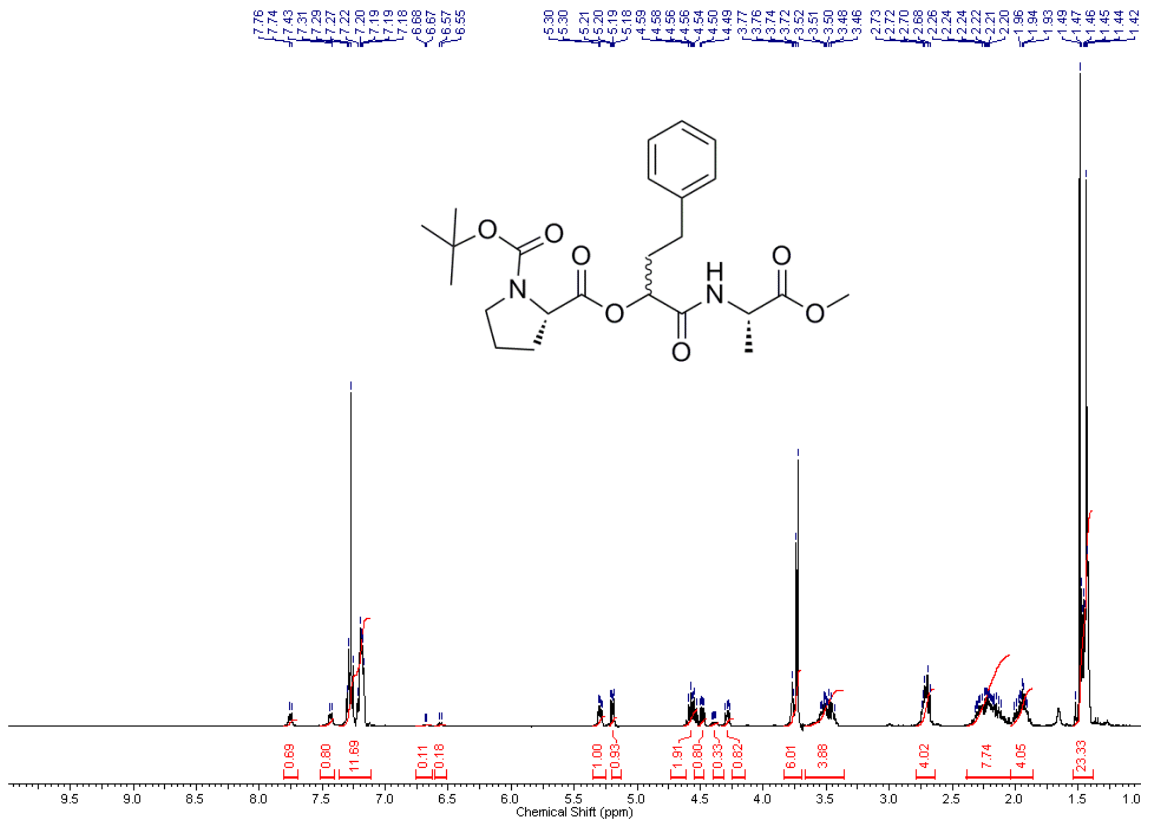


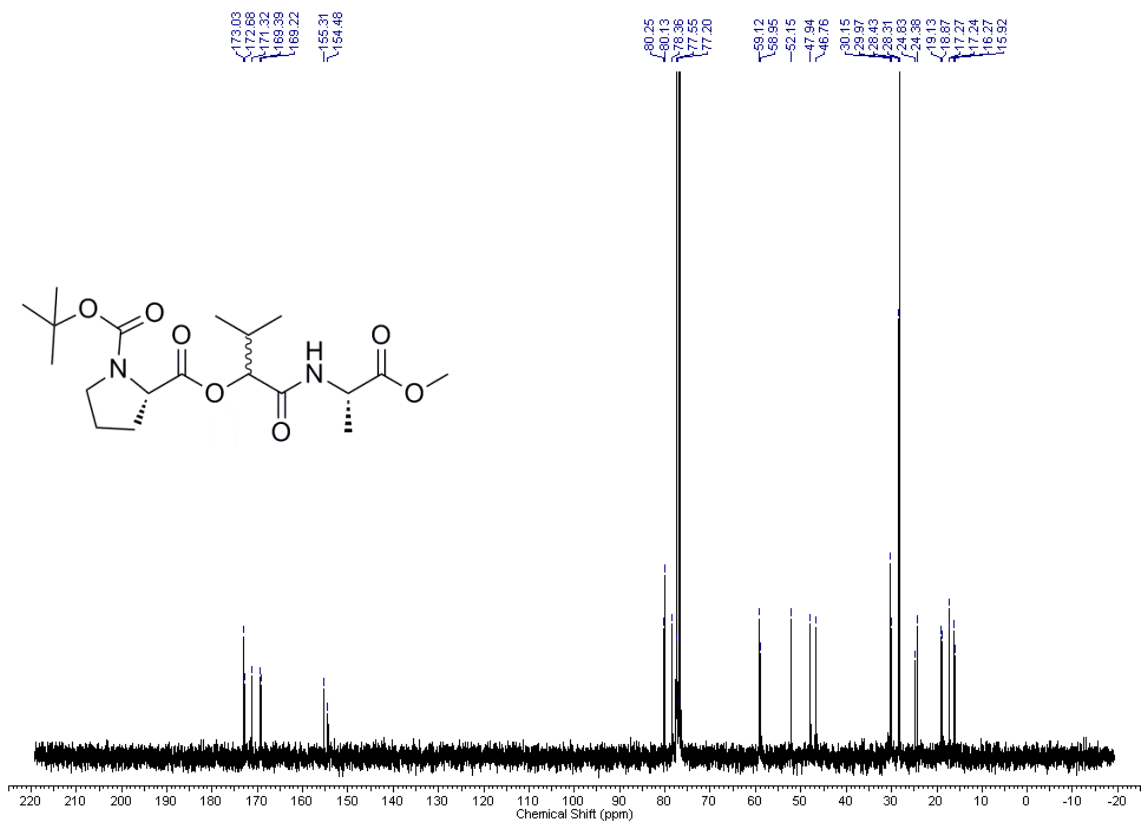
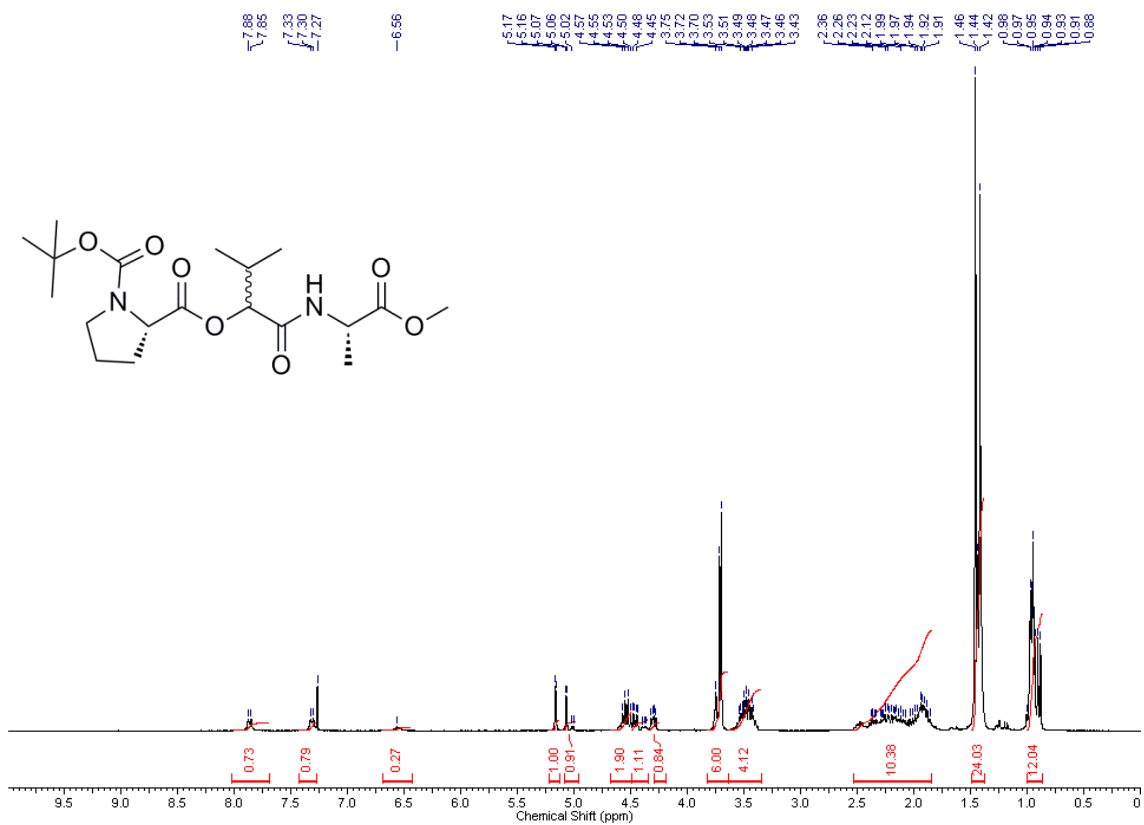
m/z →

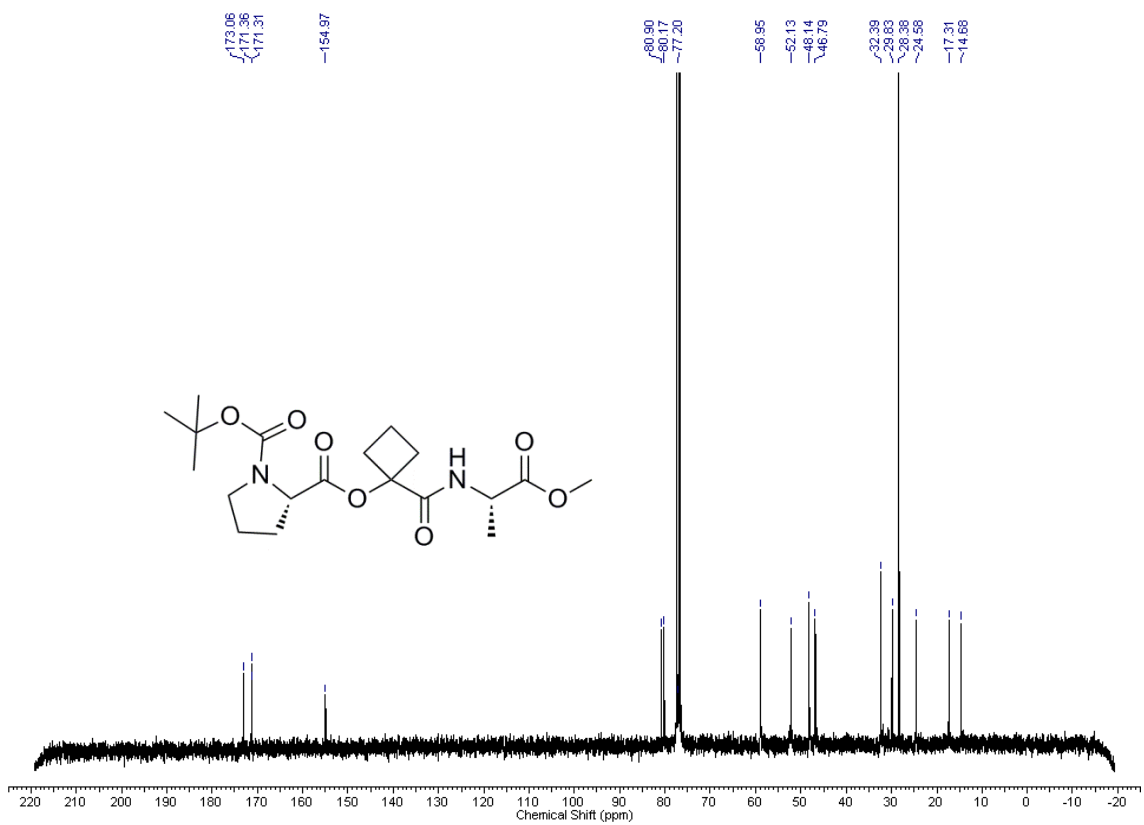
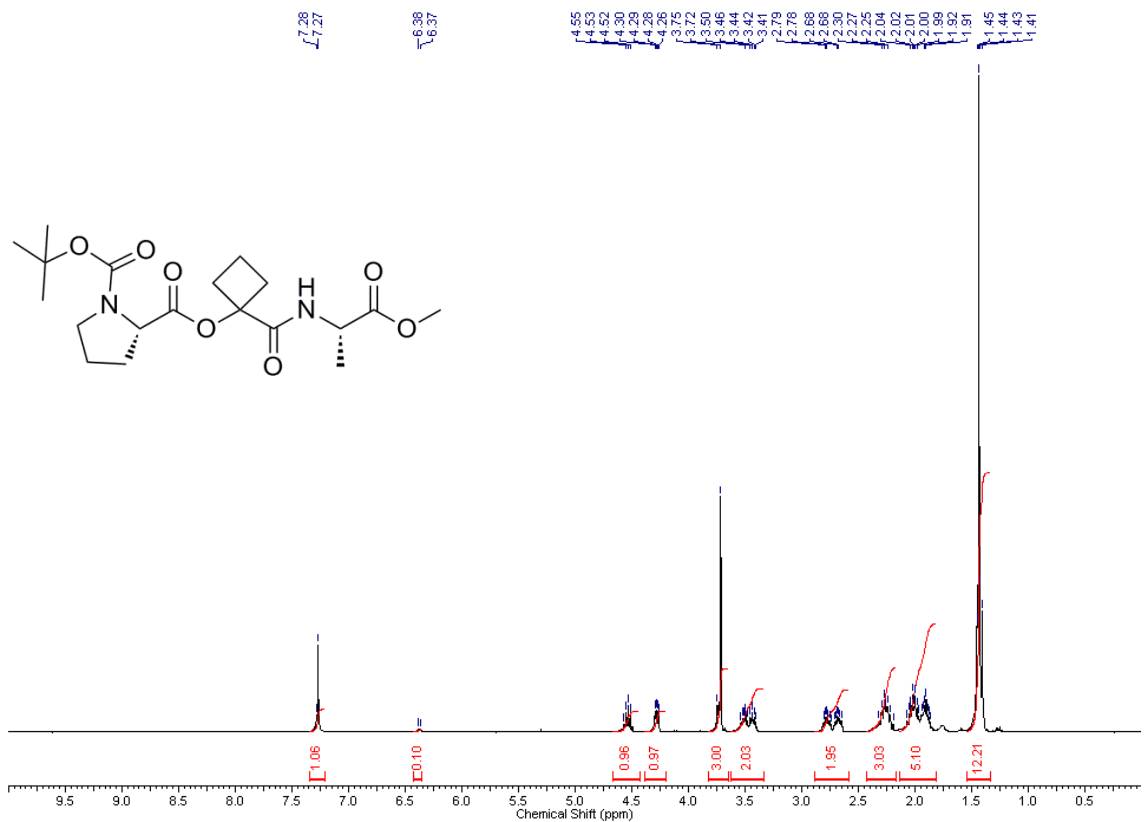


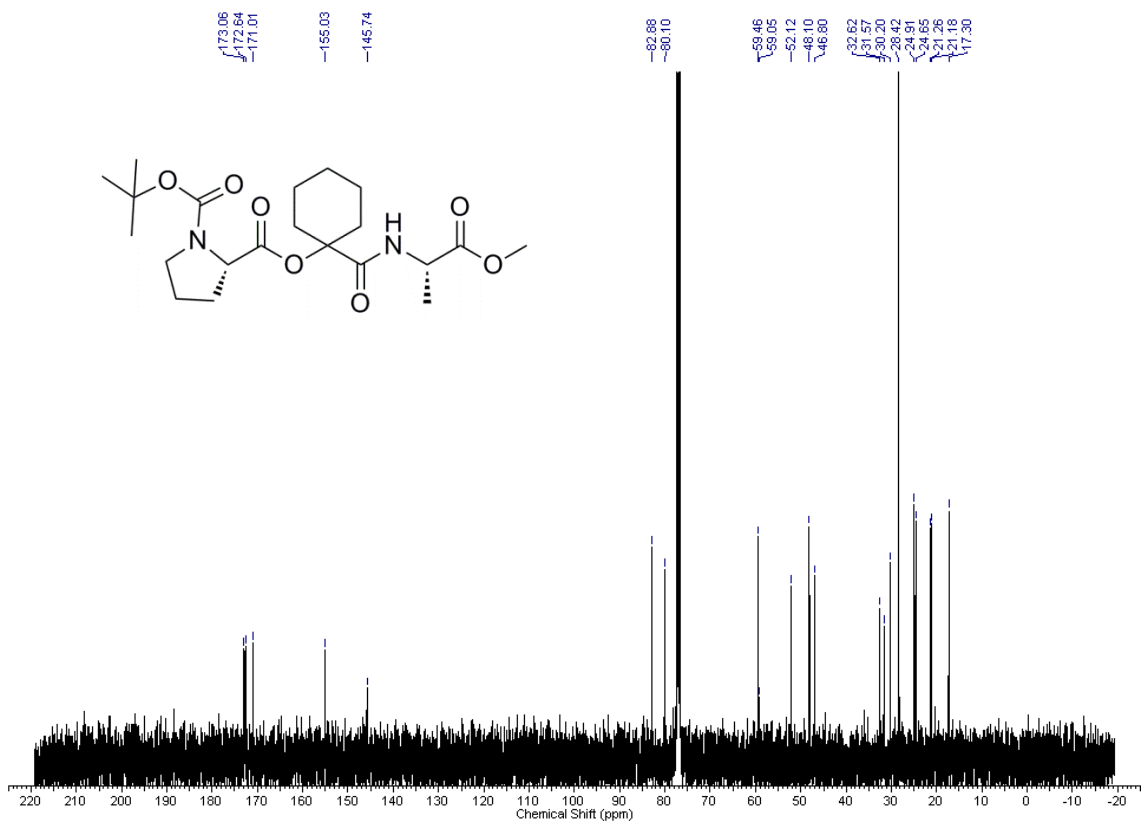
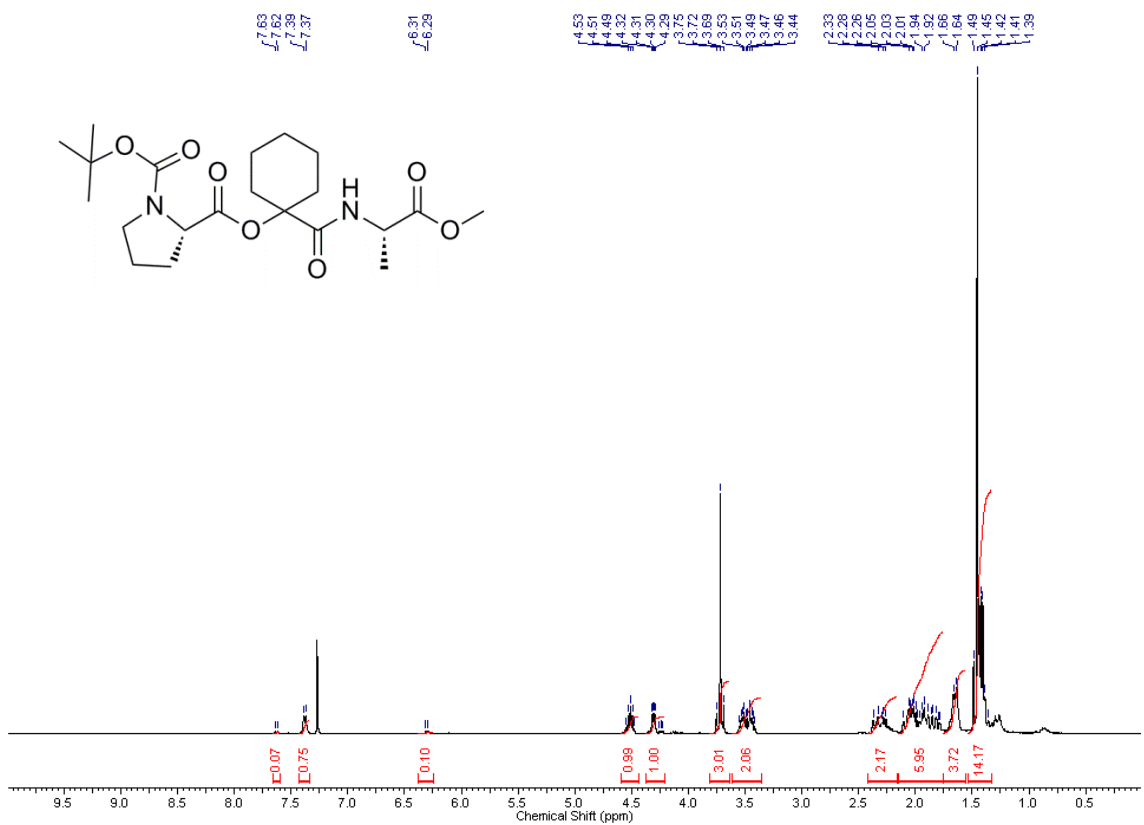




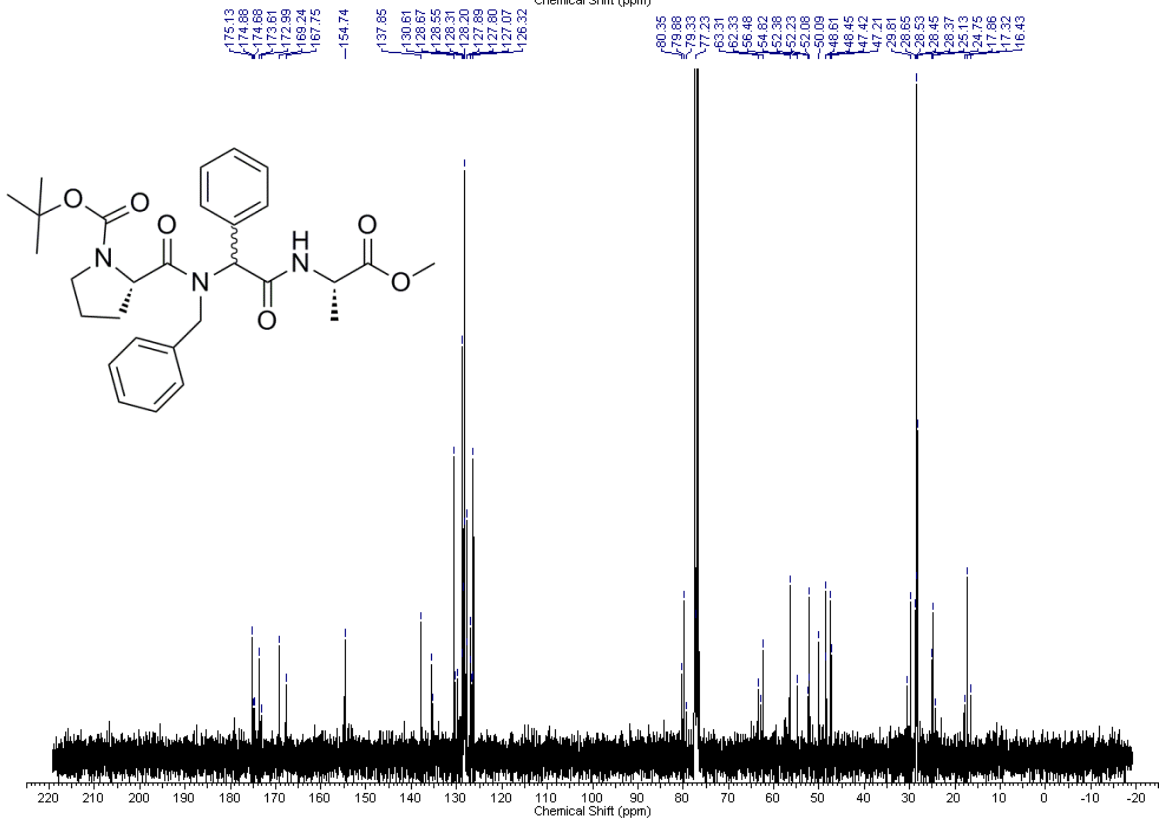
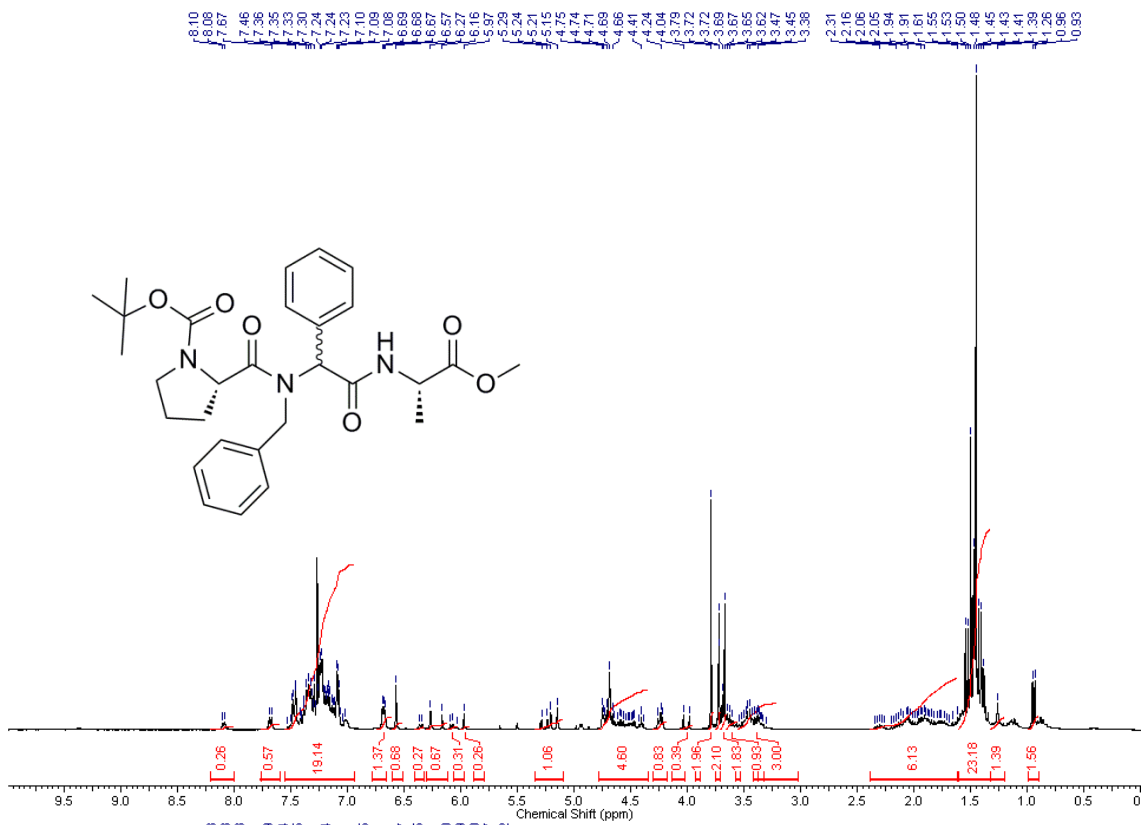


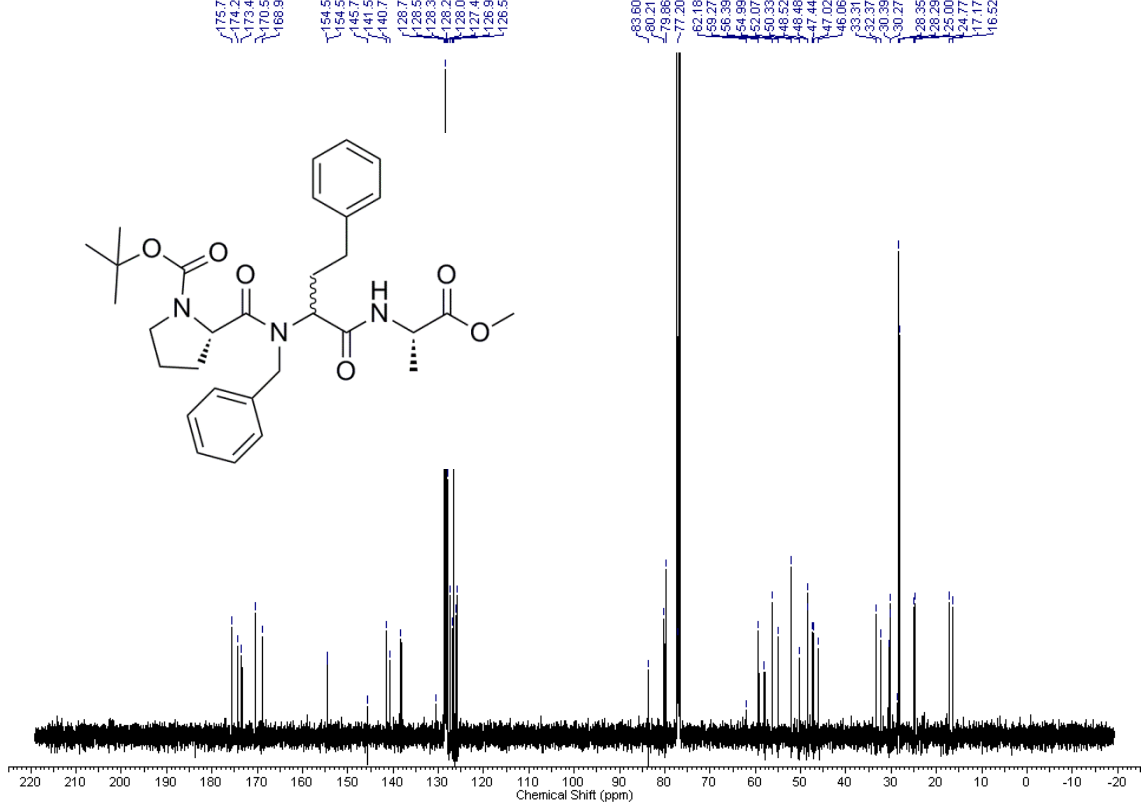
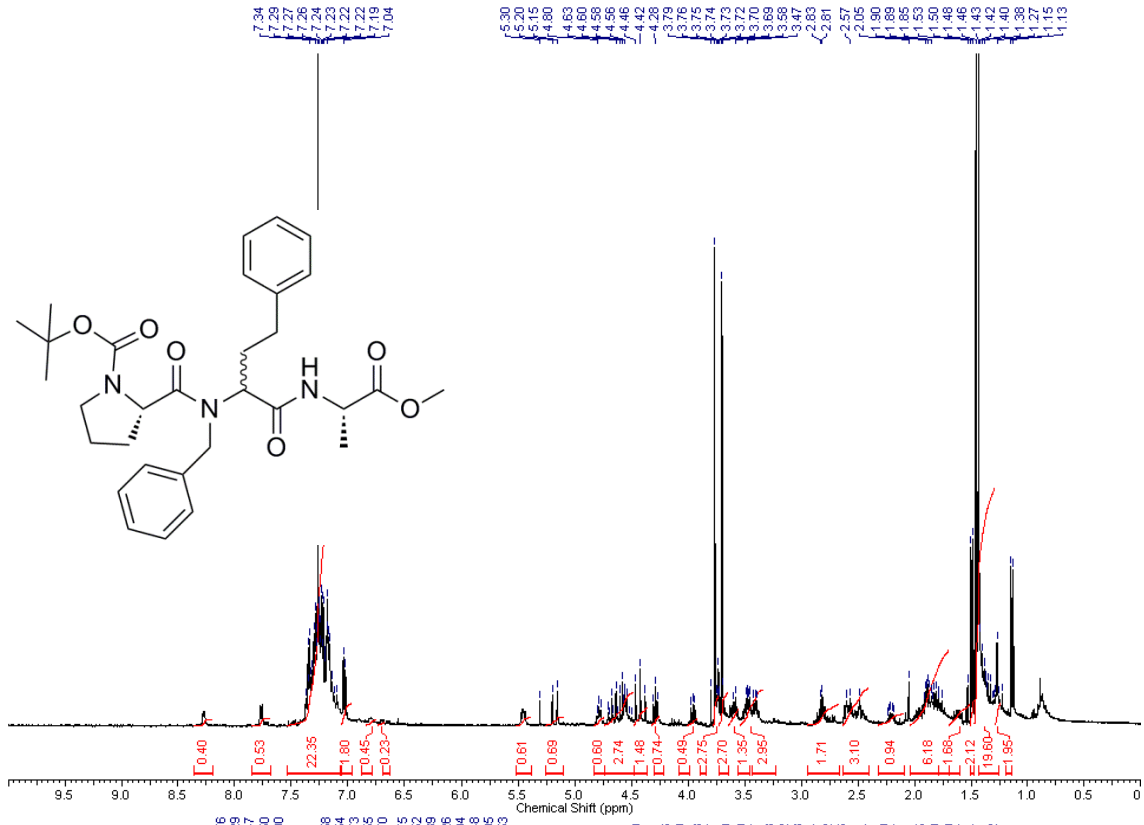


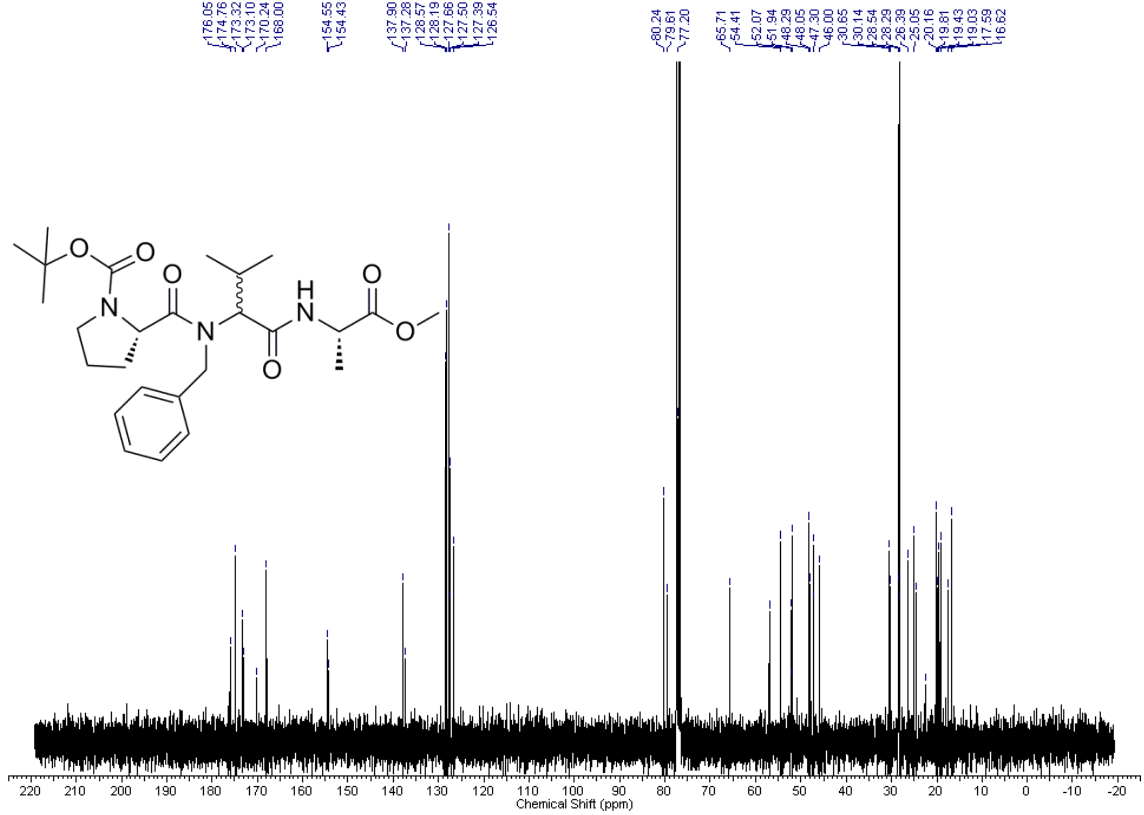
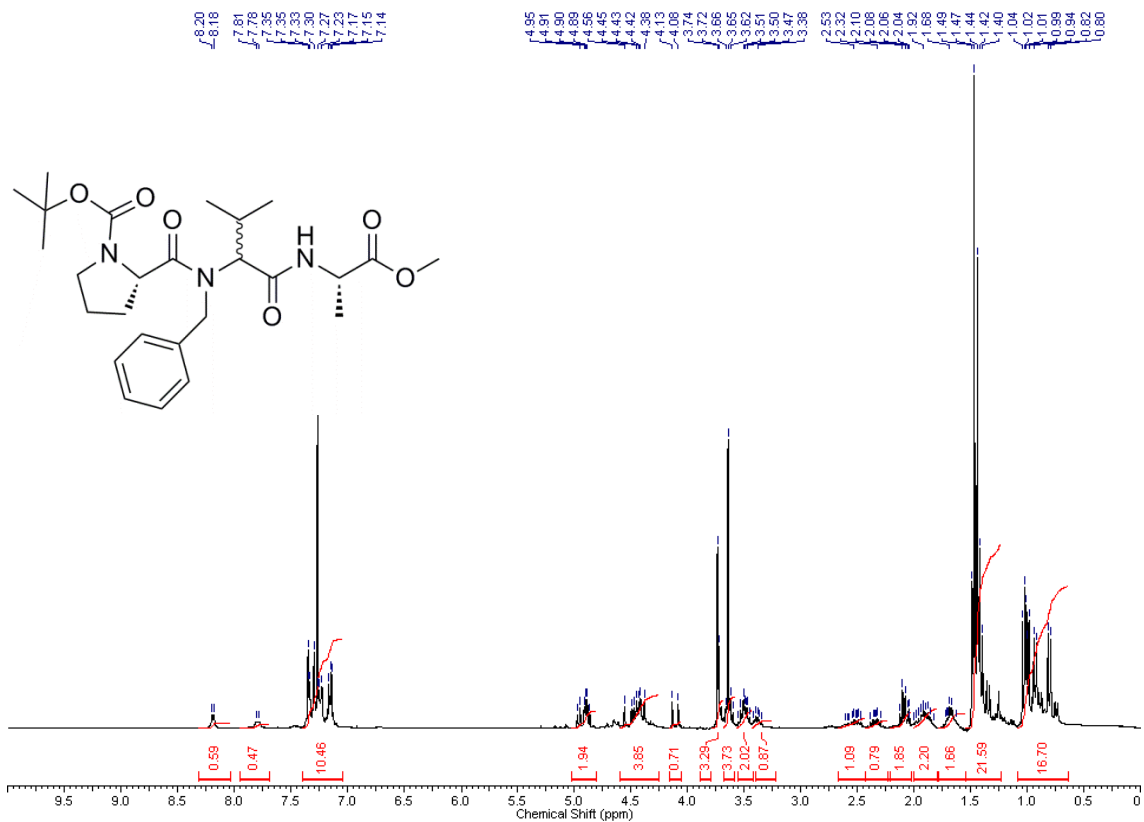


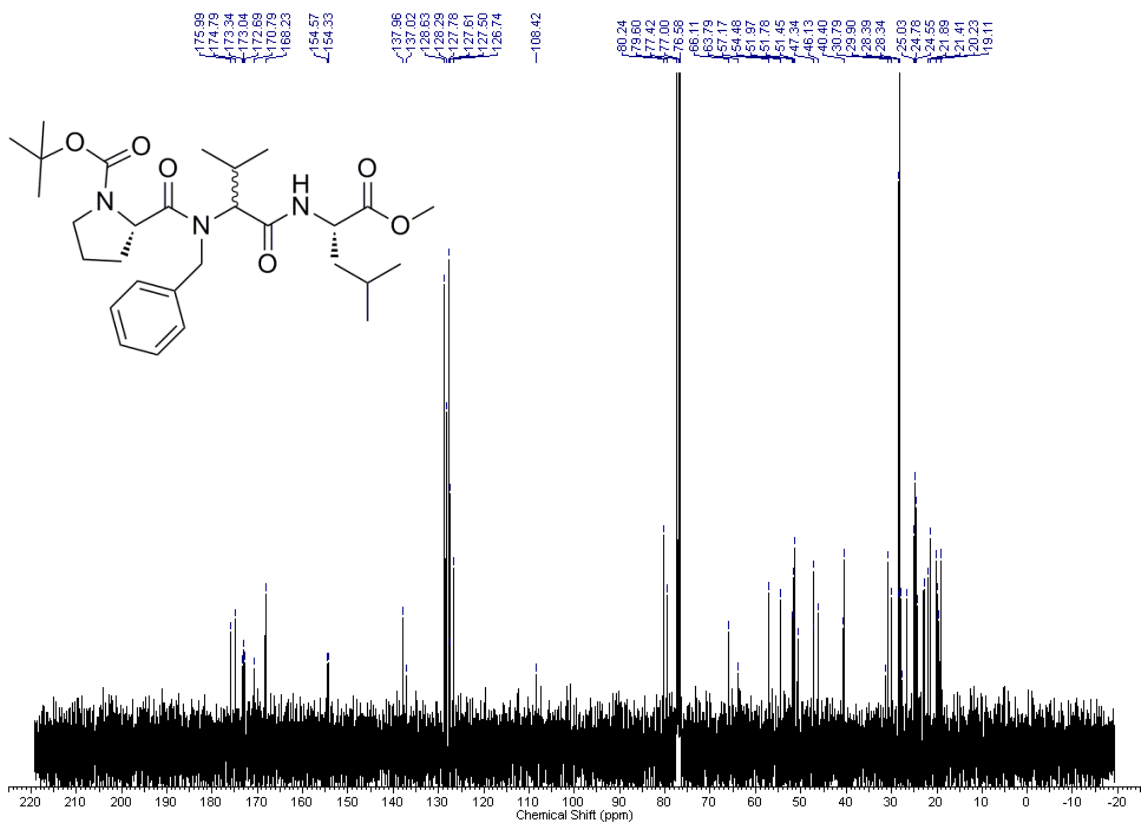
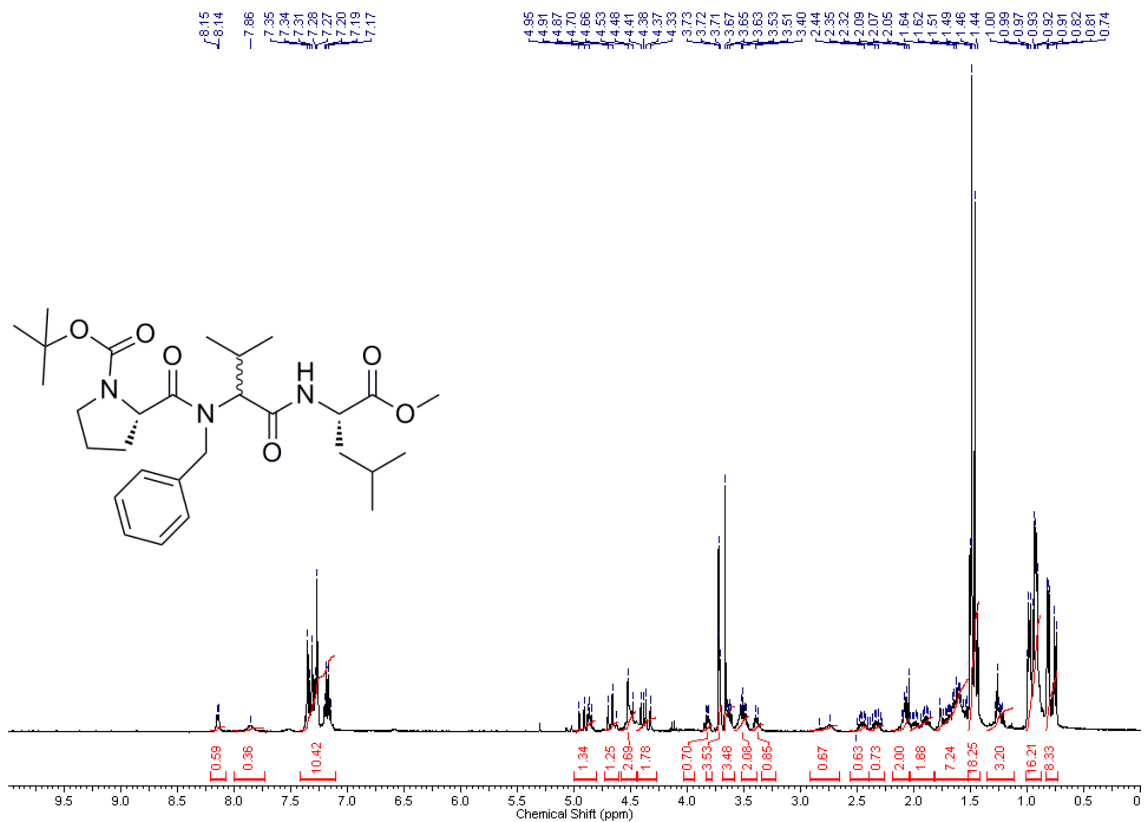


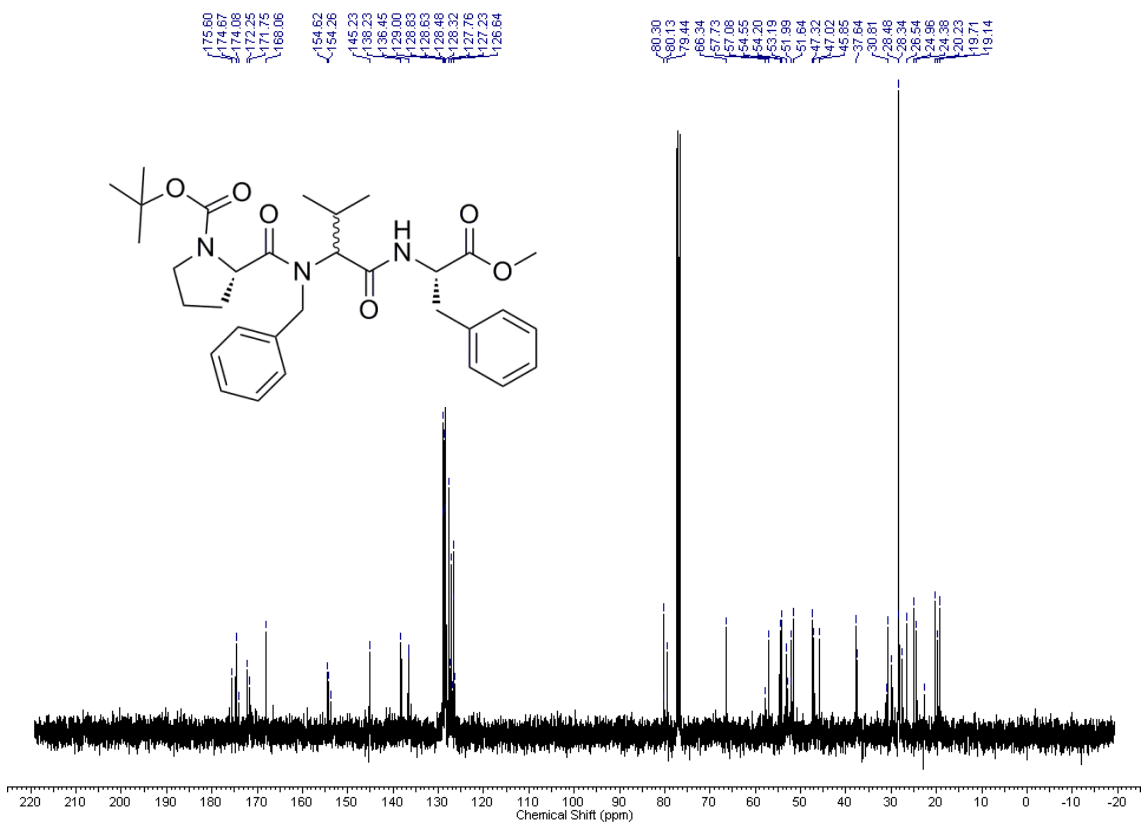
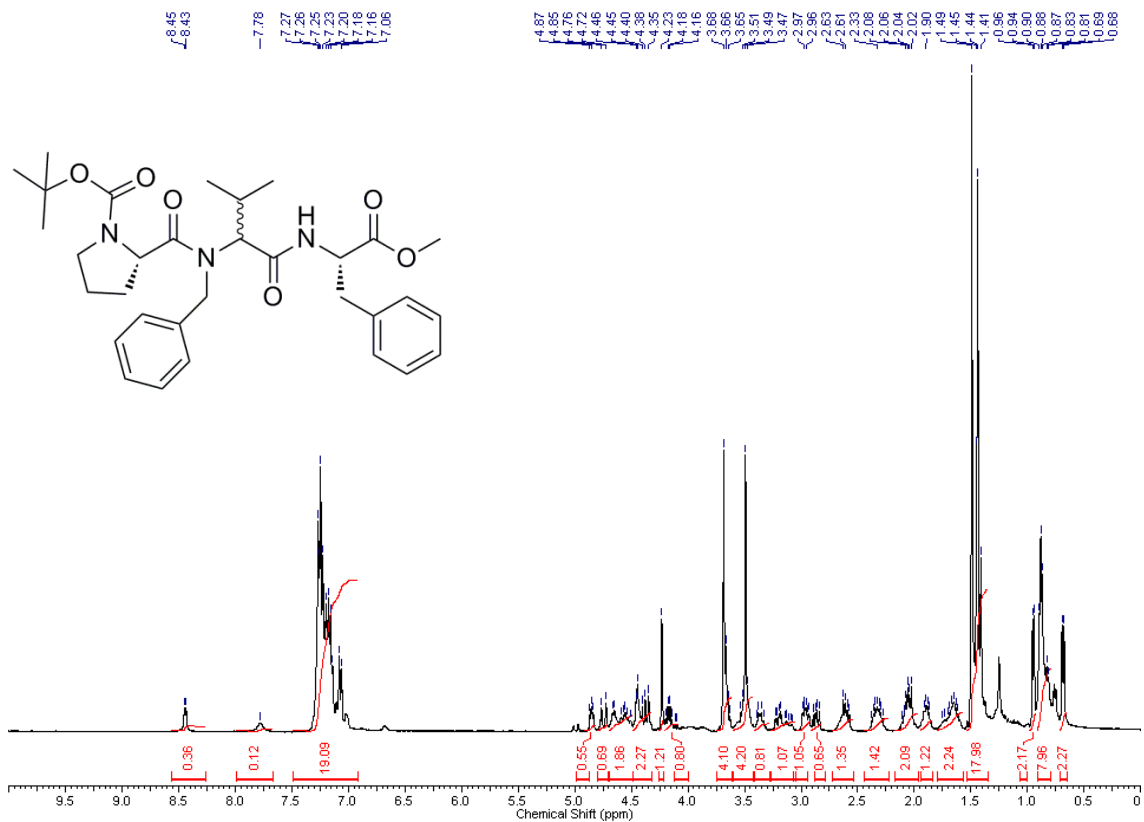


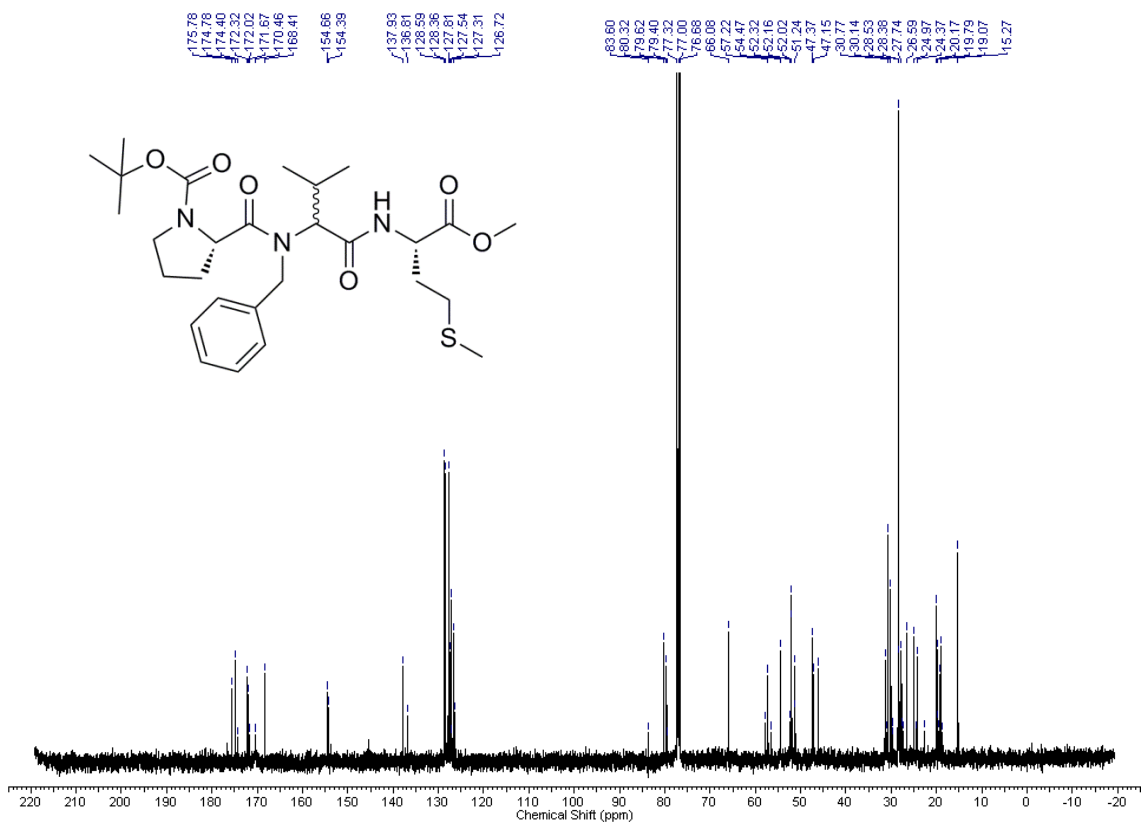
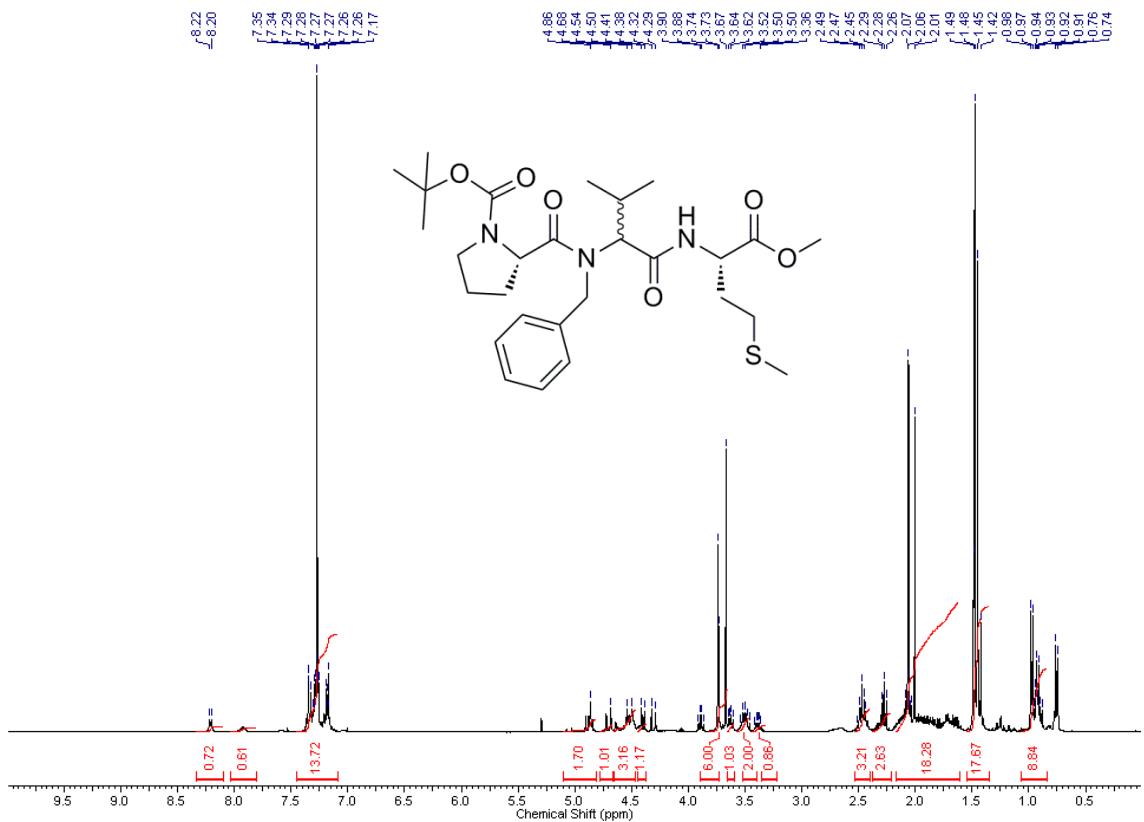


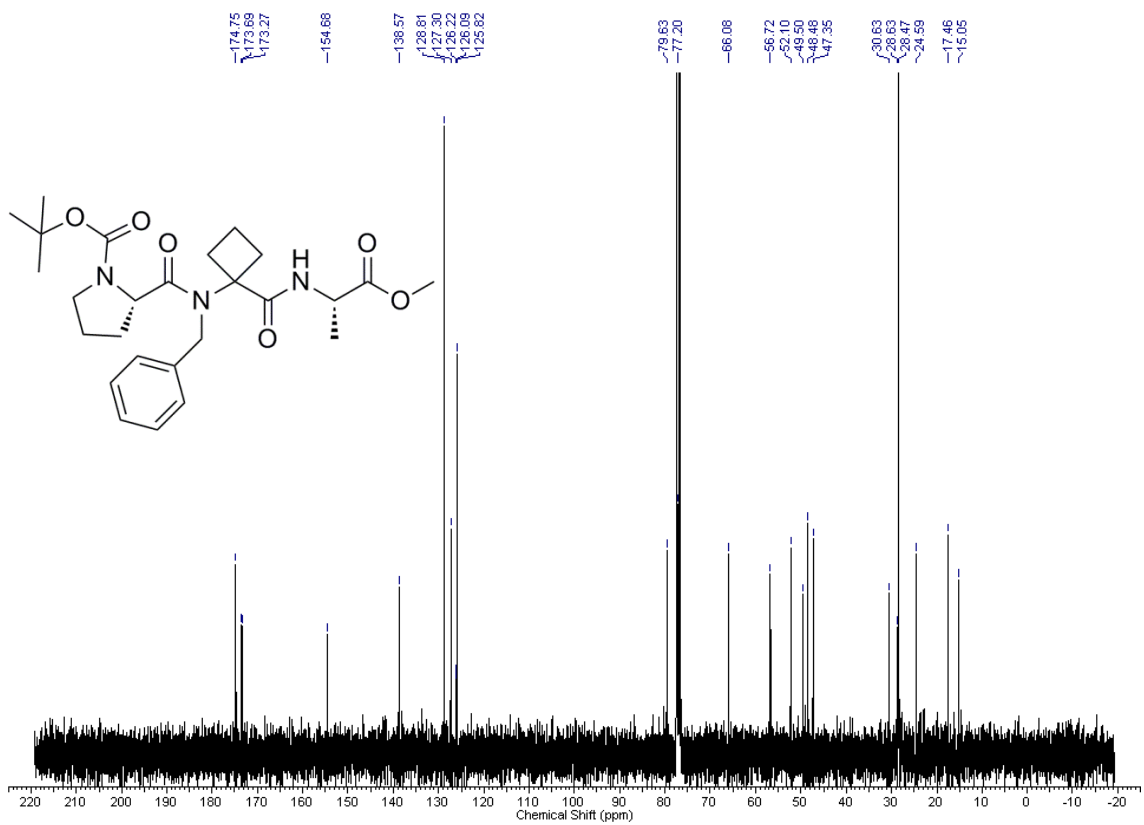
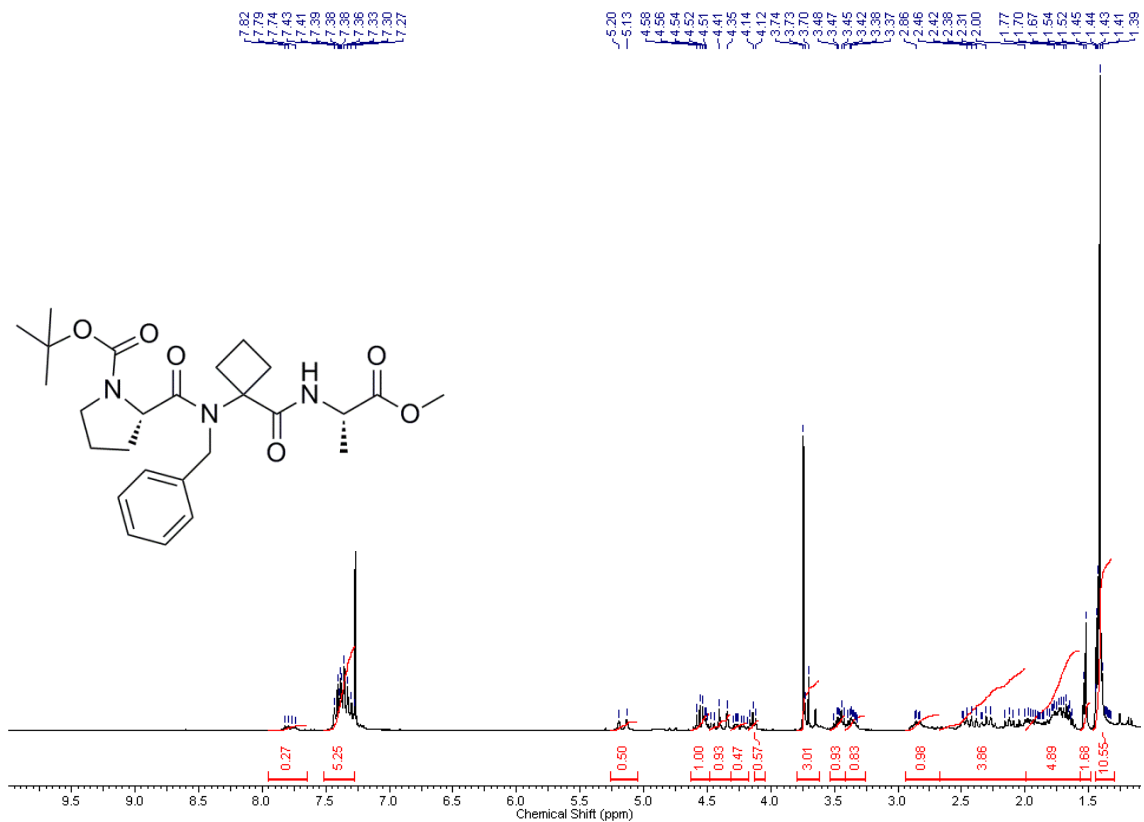


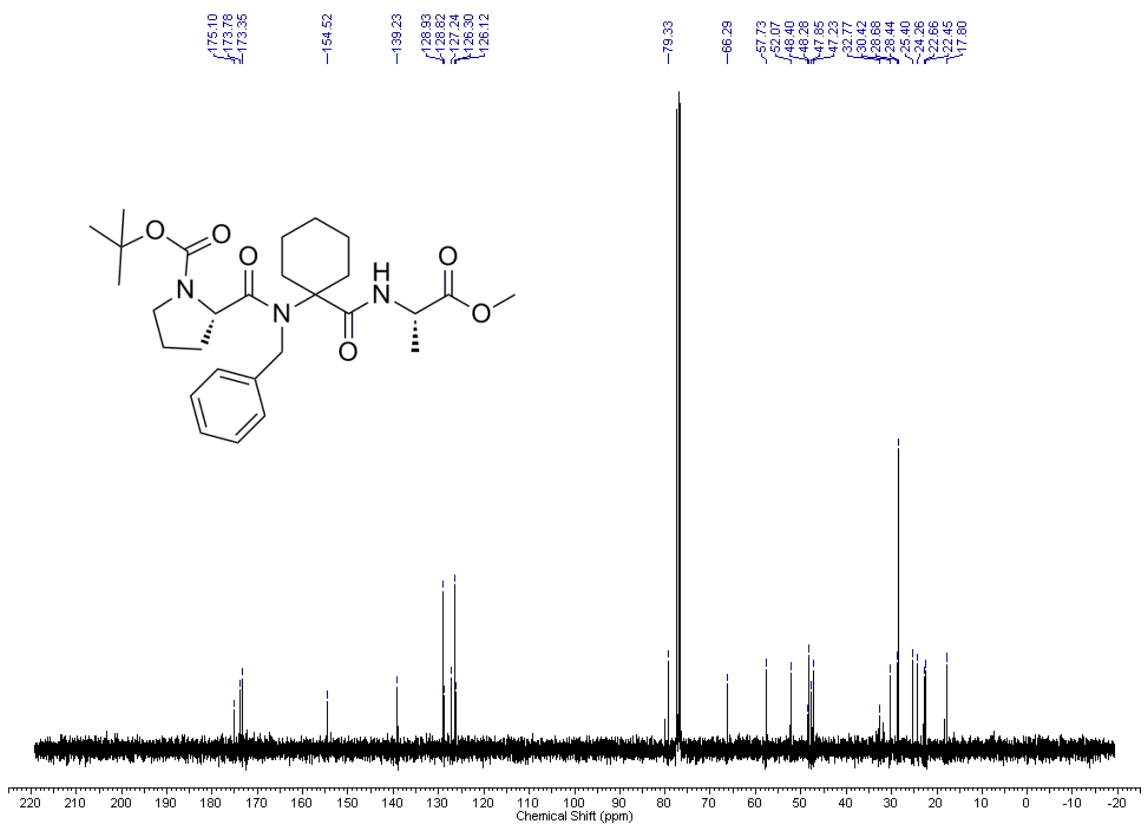
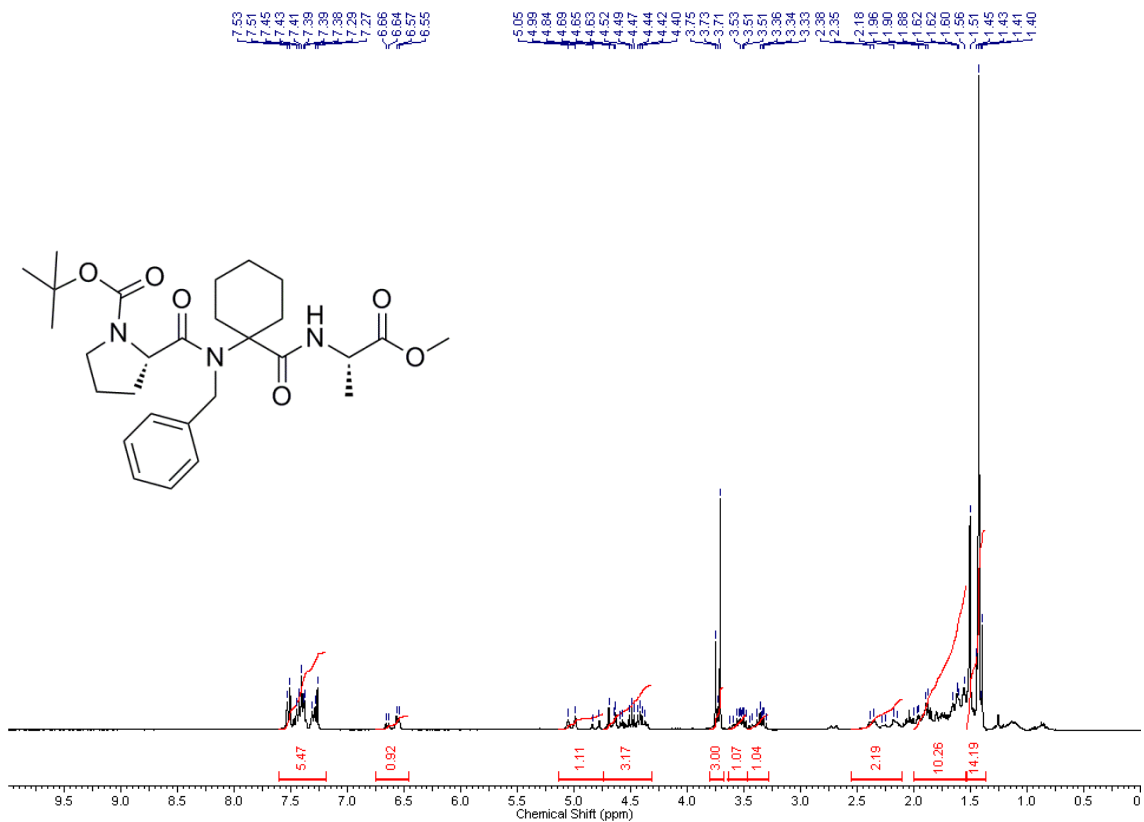




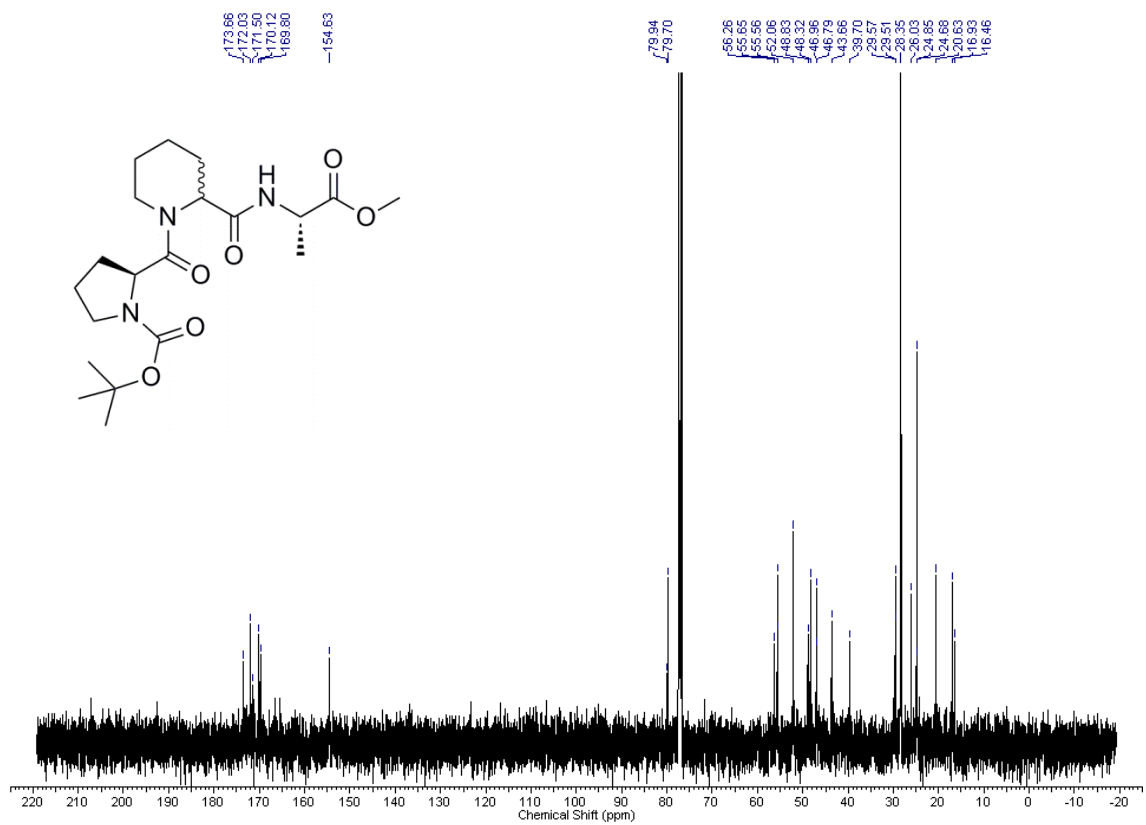
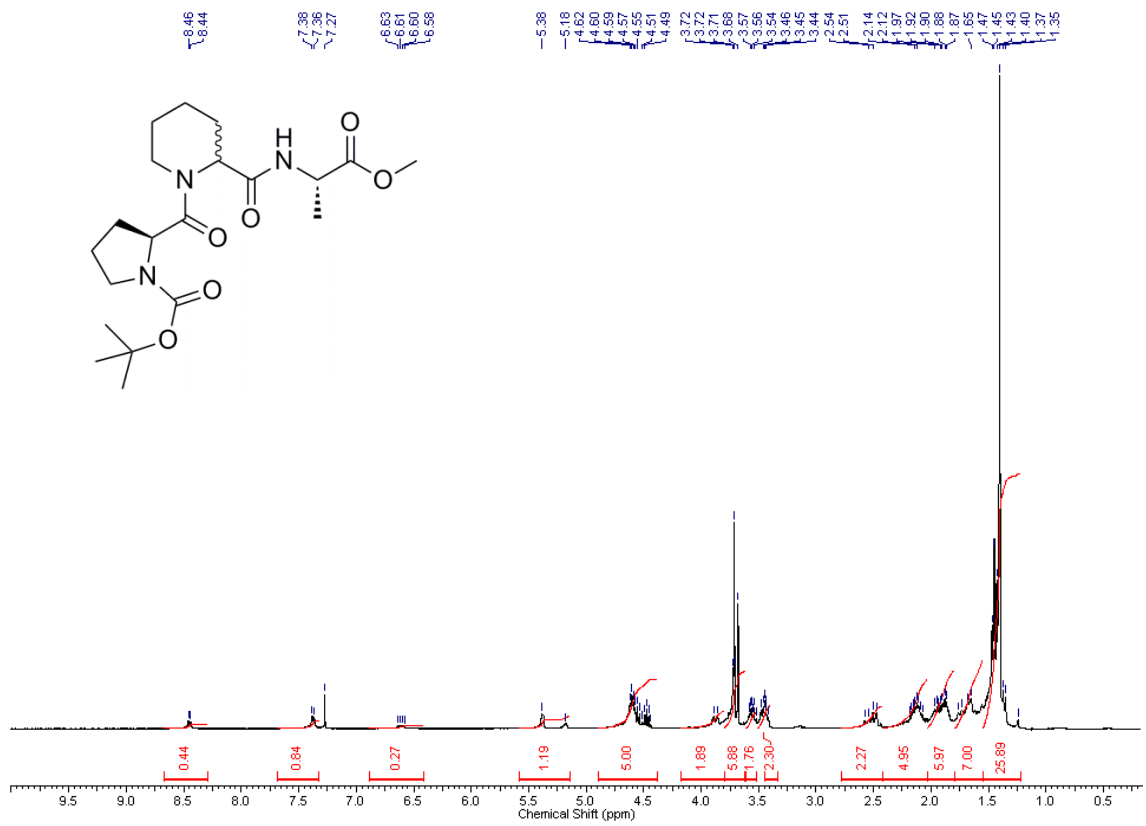


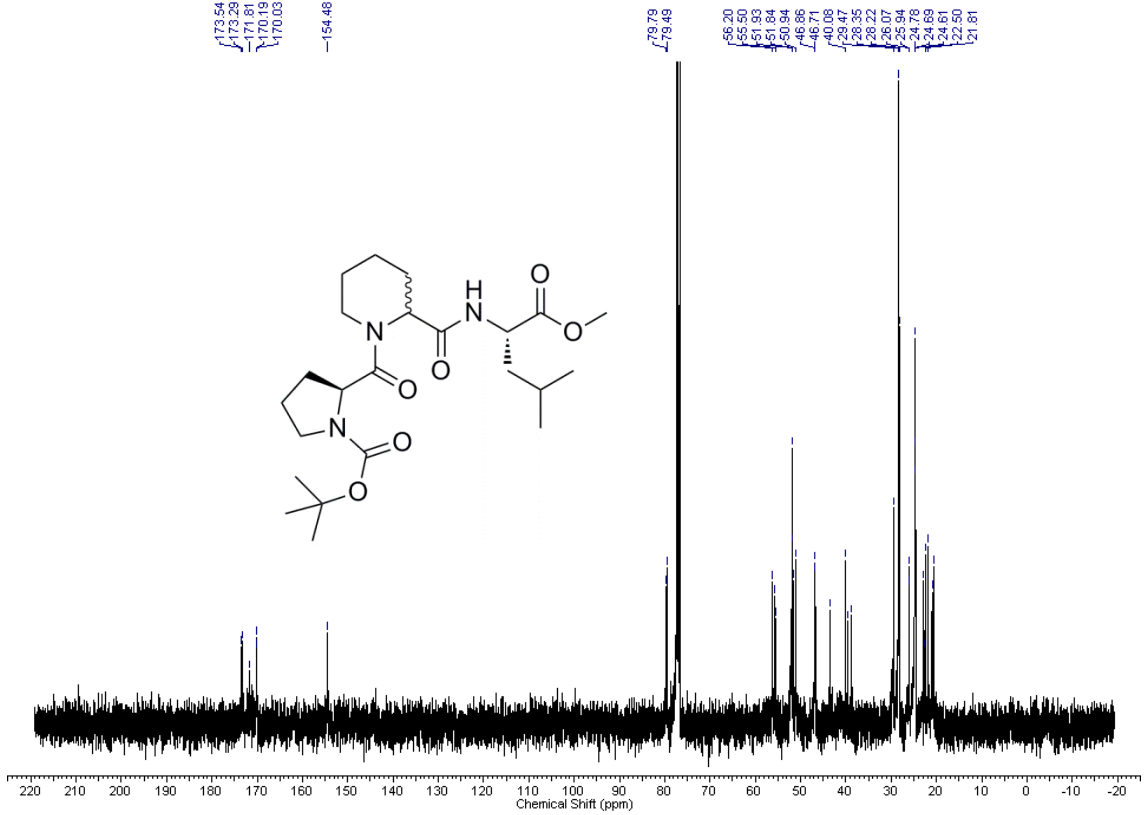
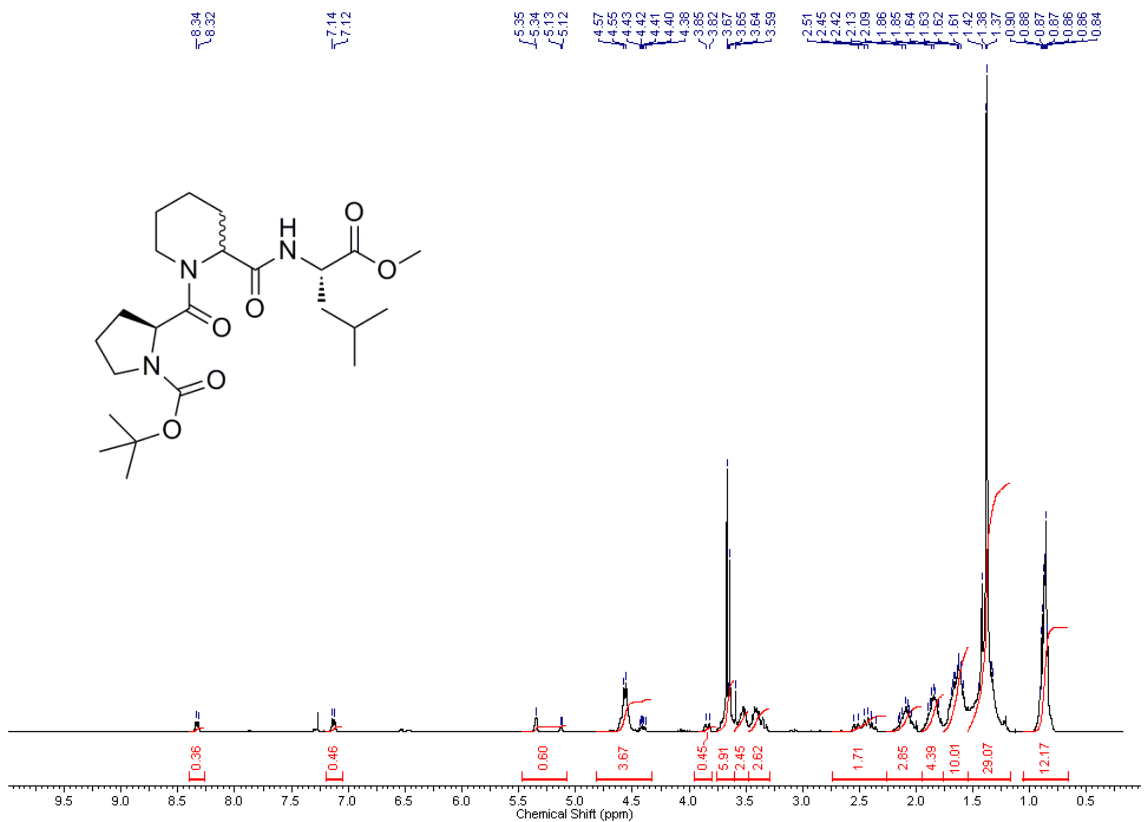


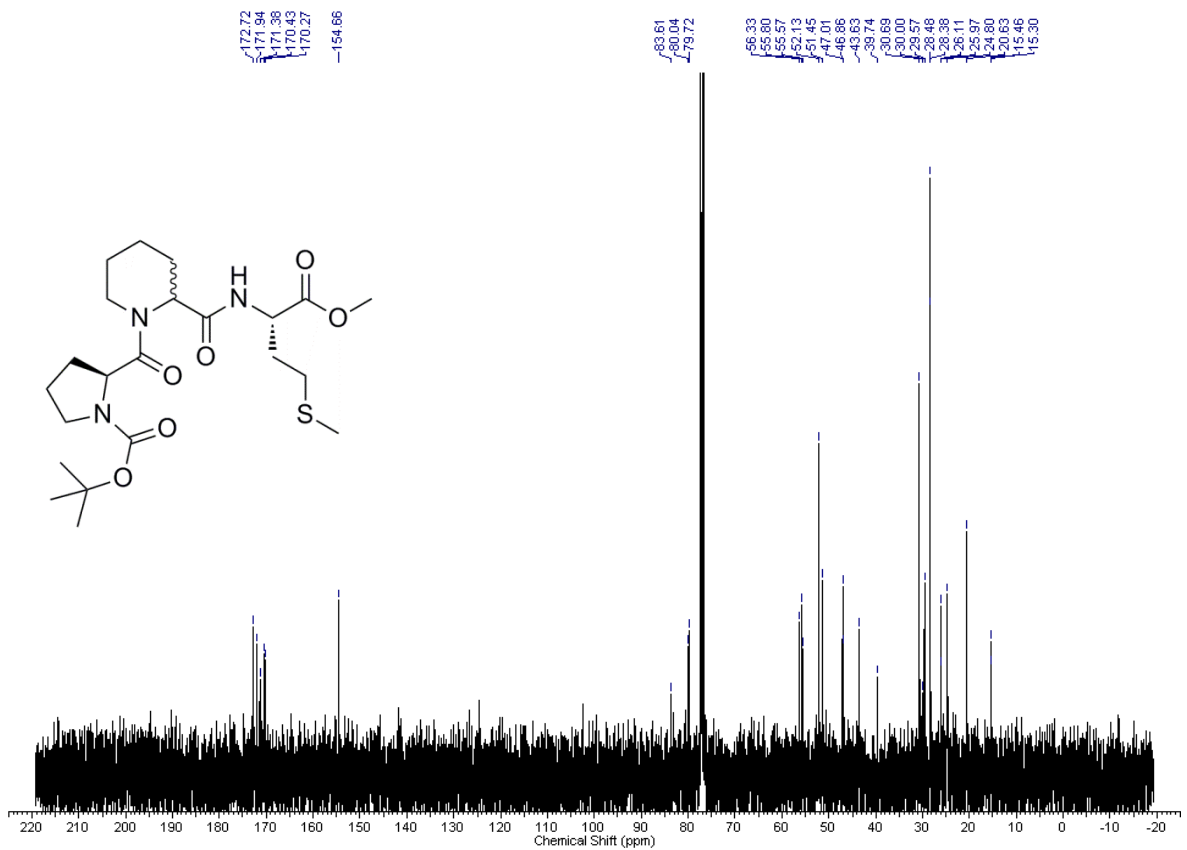
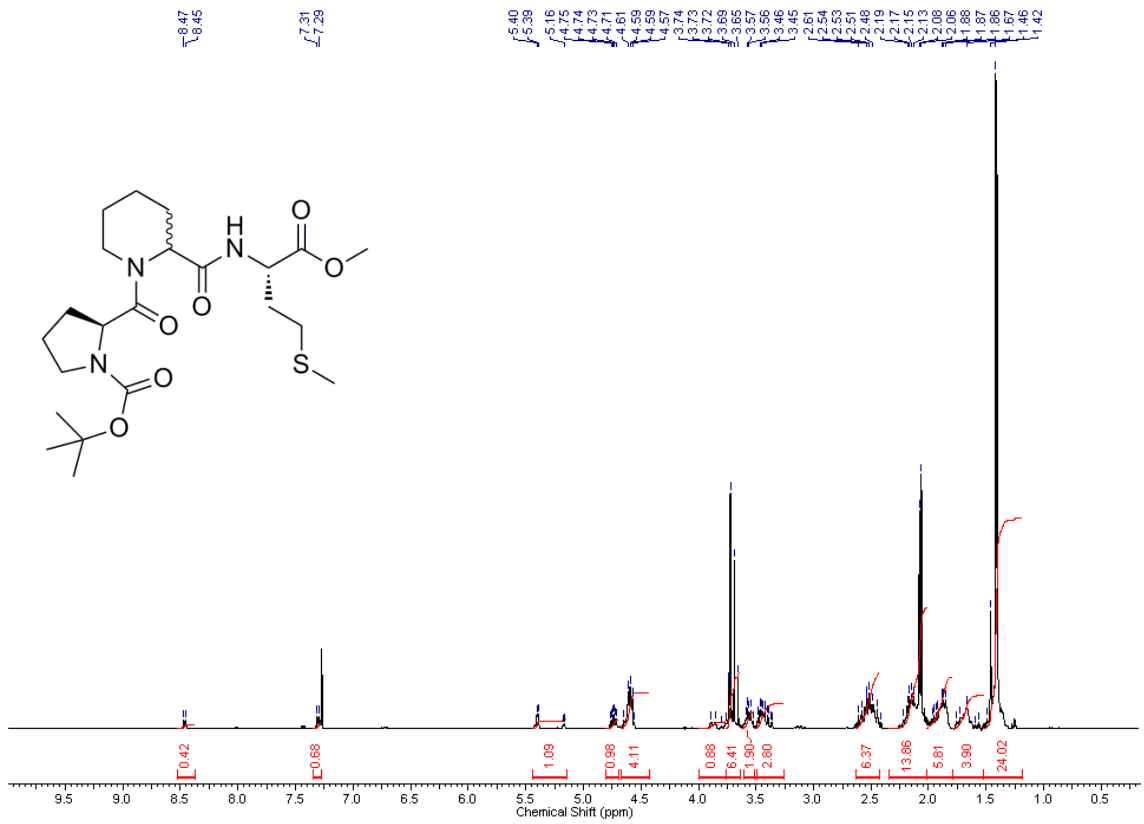






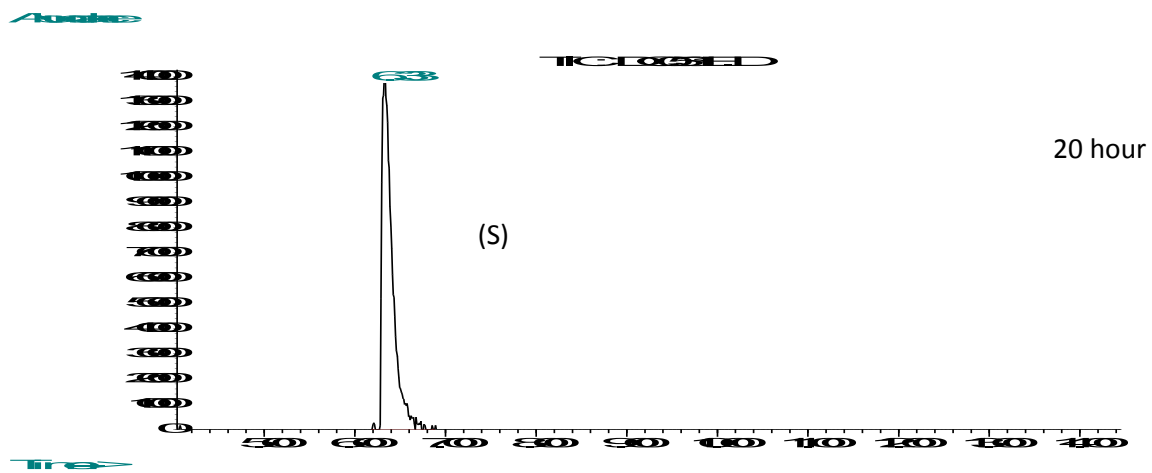
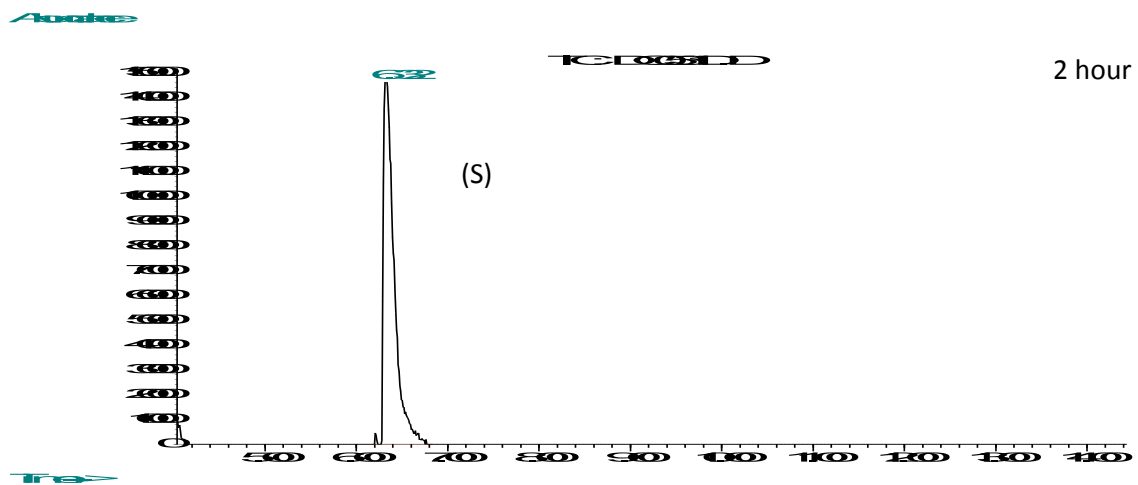
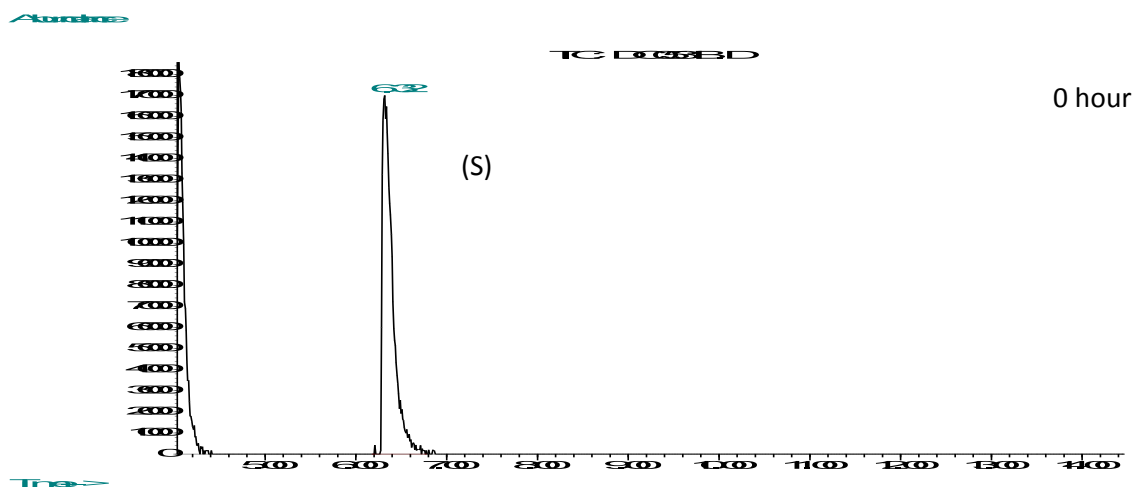




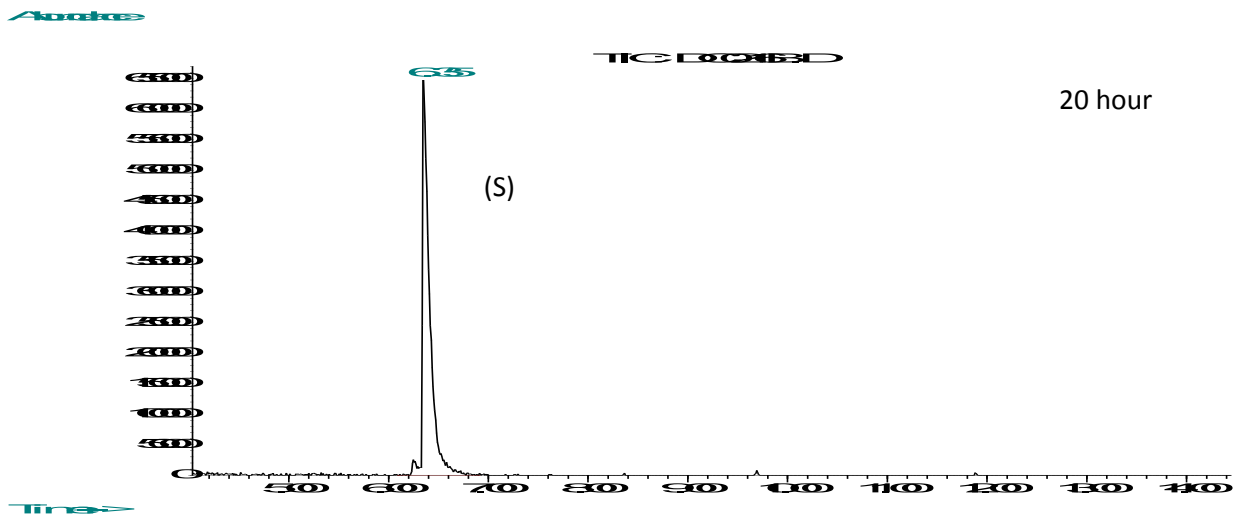
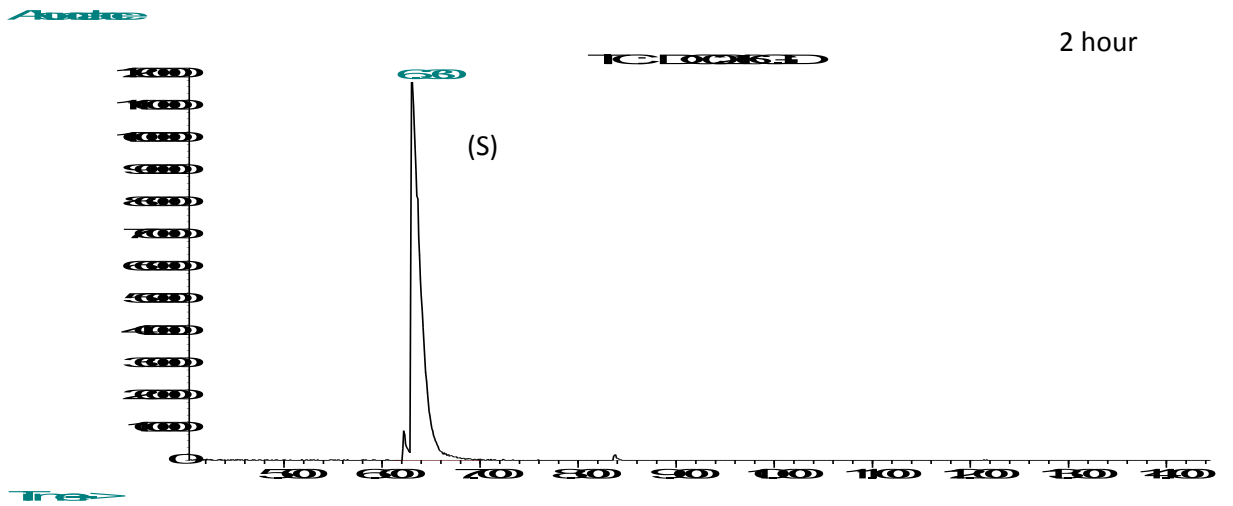
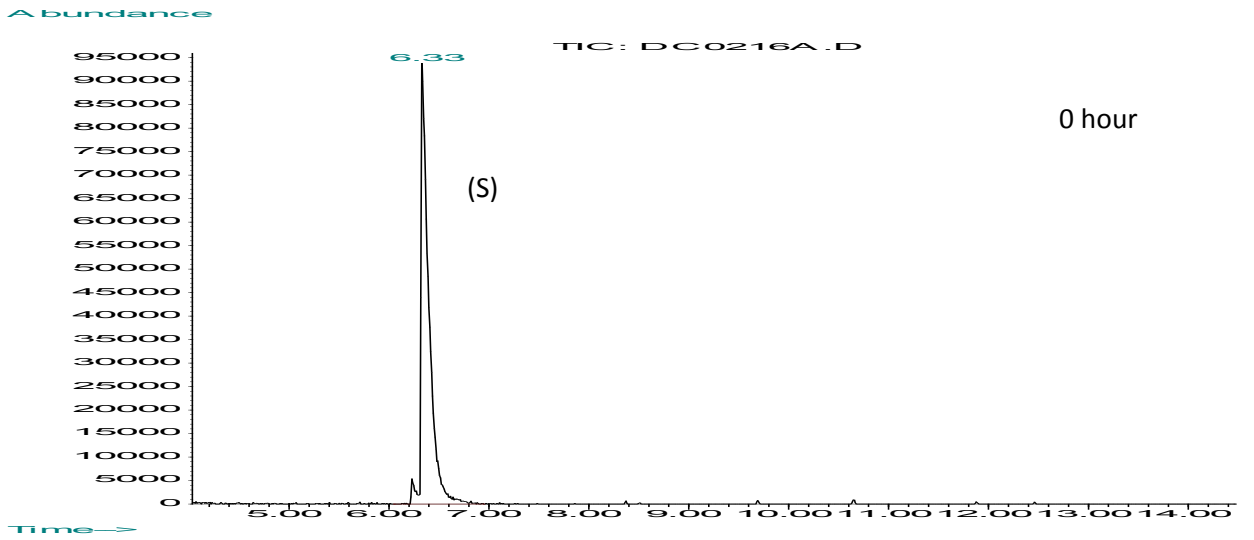


## **Isocyanoacetate Epimerization Chromatograms**

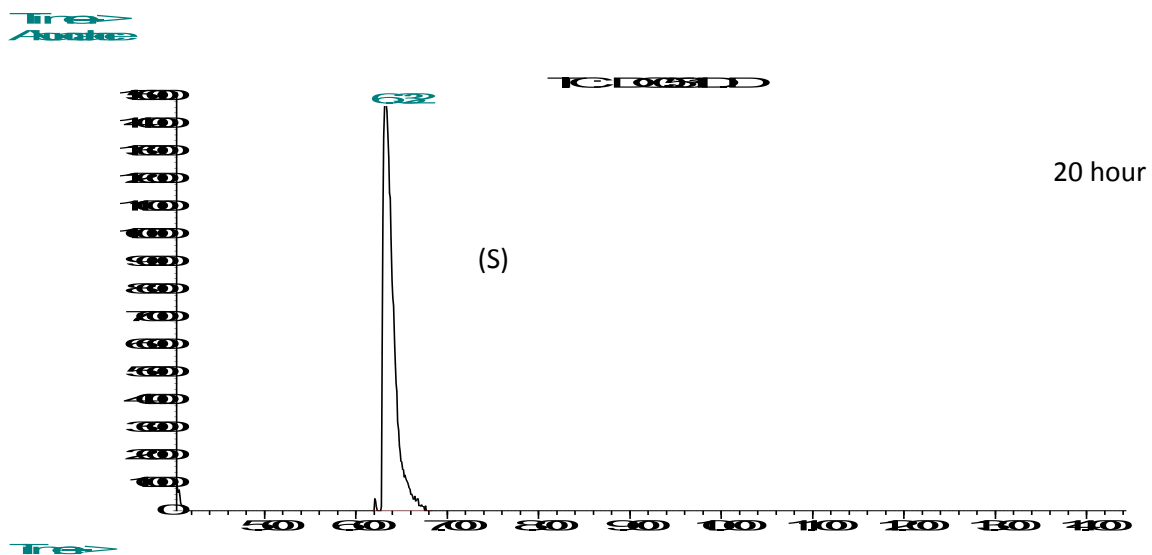
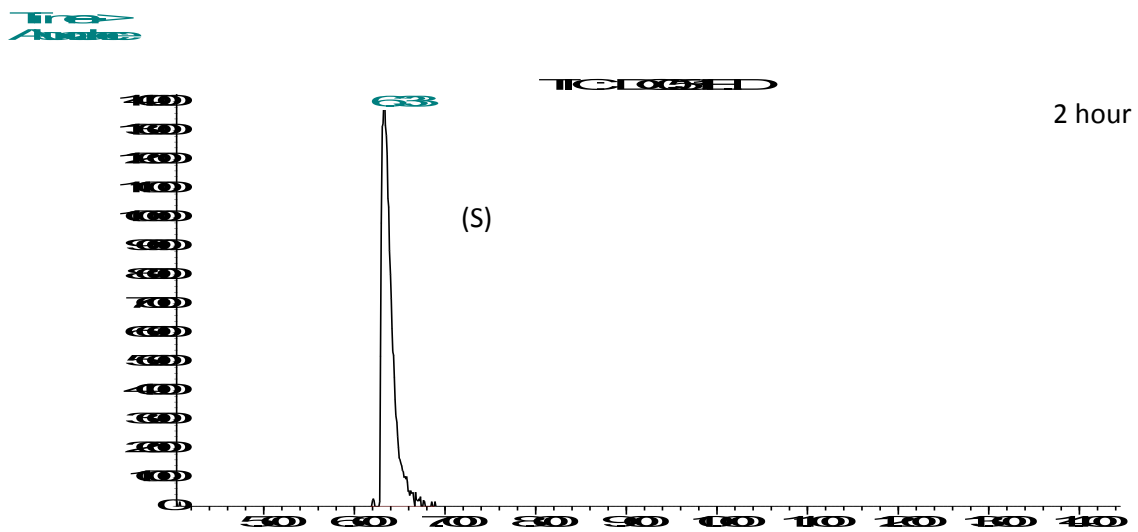
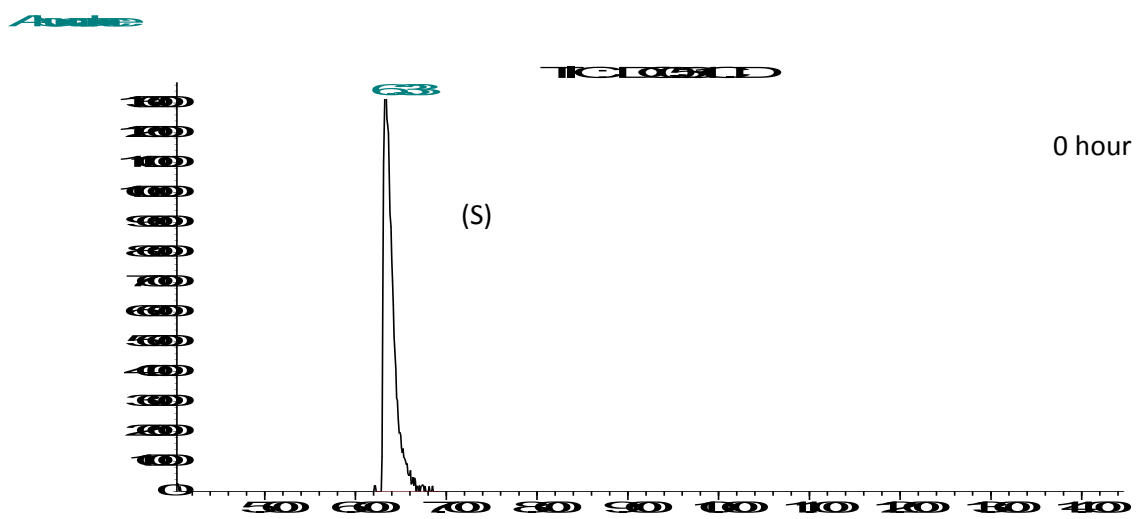
Isocyanoacetate derived from (S)-N-formylalanine methyl ester control  
in methanol



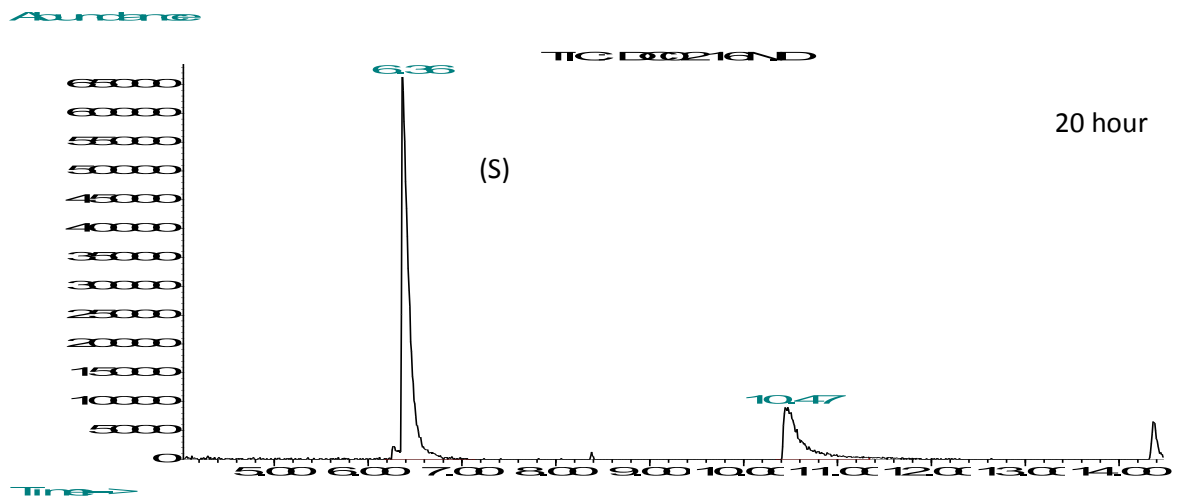
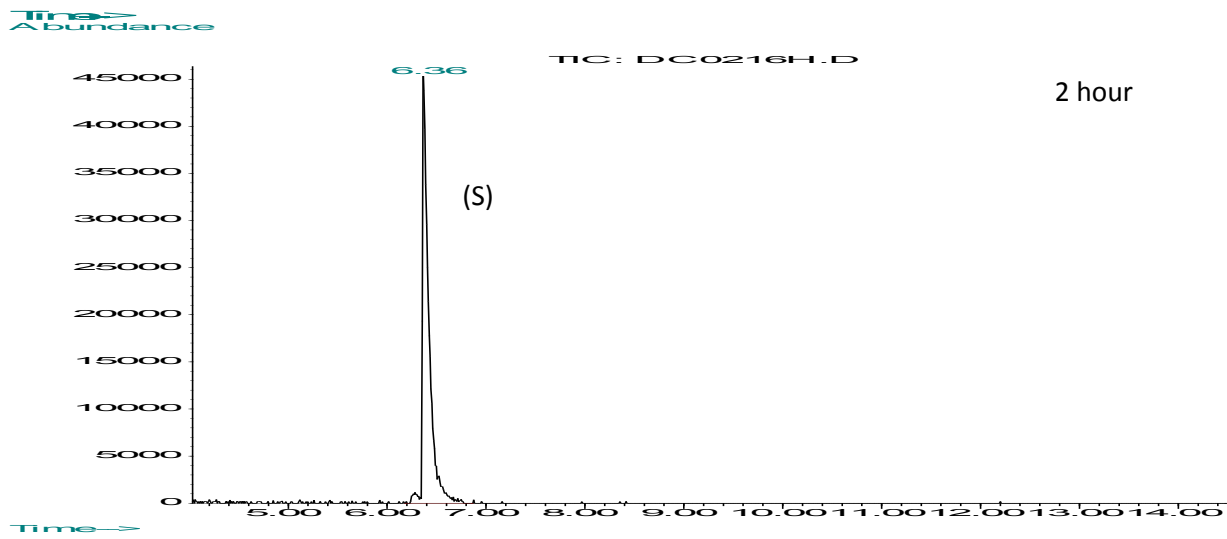
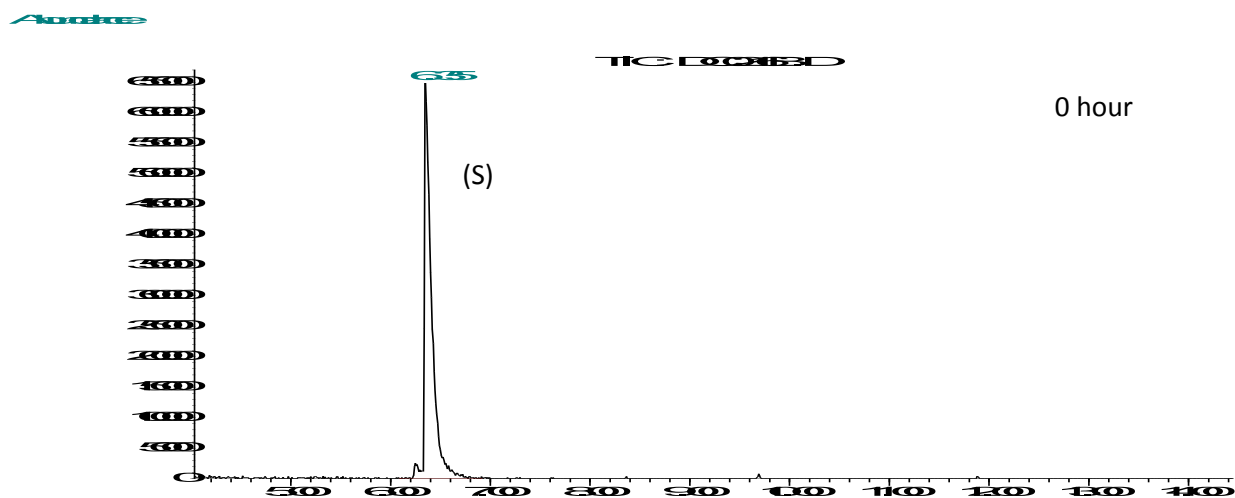
**Isocyanoacetate derived from (S)-N-formylalanine methyl ester control  
in Dichloromethane**



Isocyanoacetate derived from (S)-N-formylalanine methyl ester + Boc-Proline in methanol

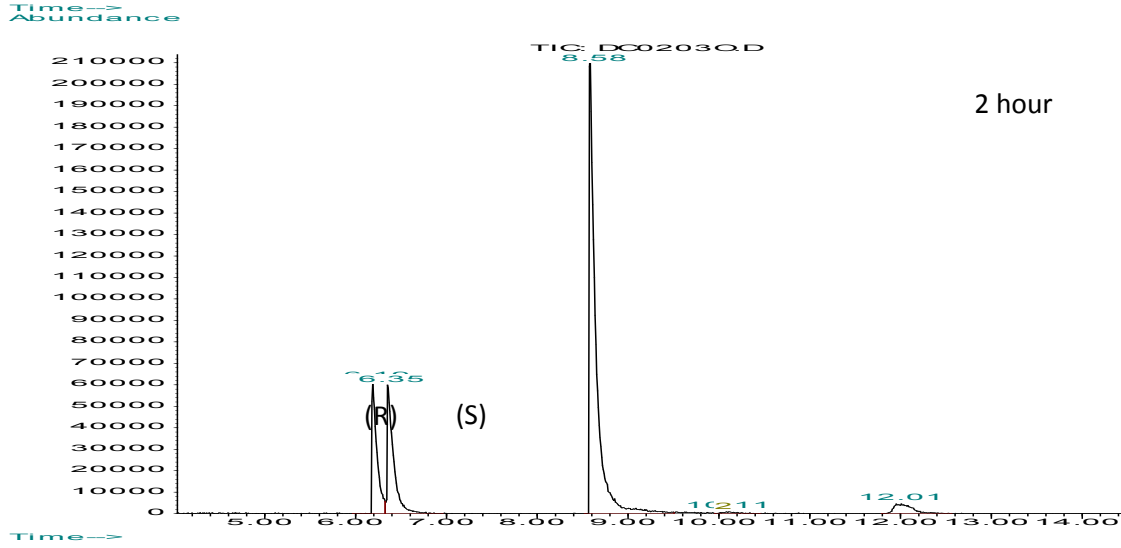
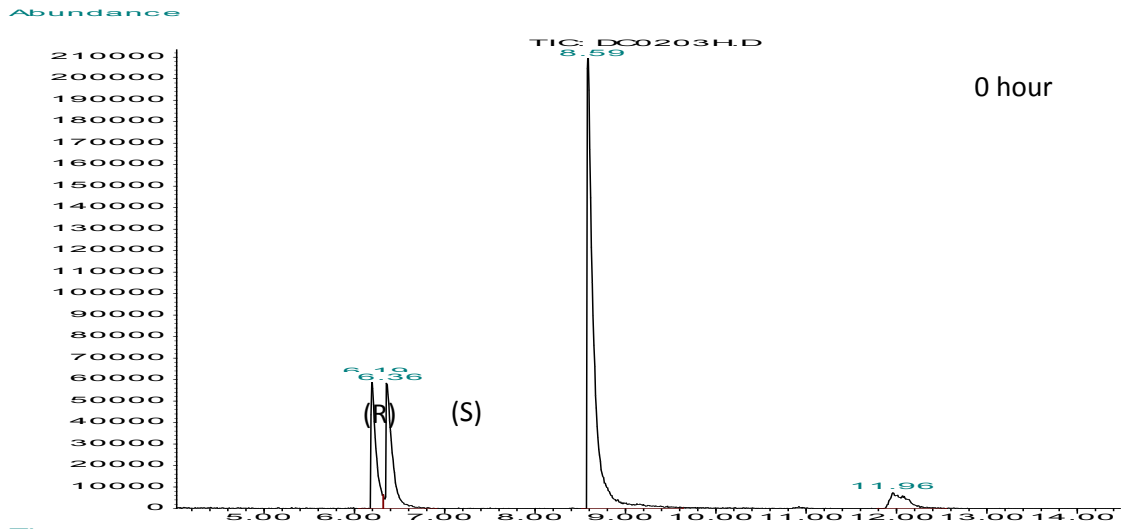


Isocyanoacetate derived from (S)-N-formylalanine methyl ester + Boc-Proline in dichloromethane

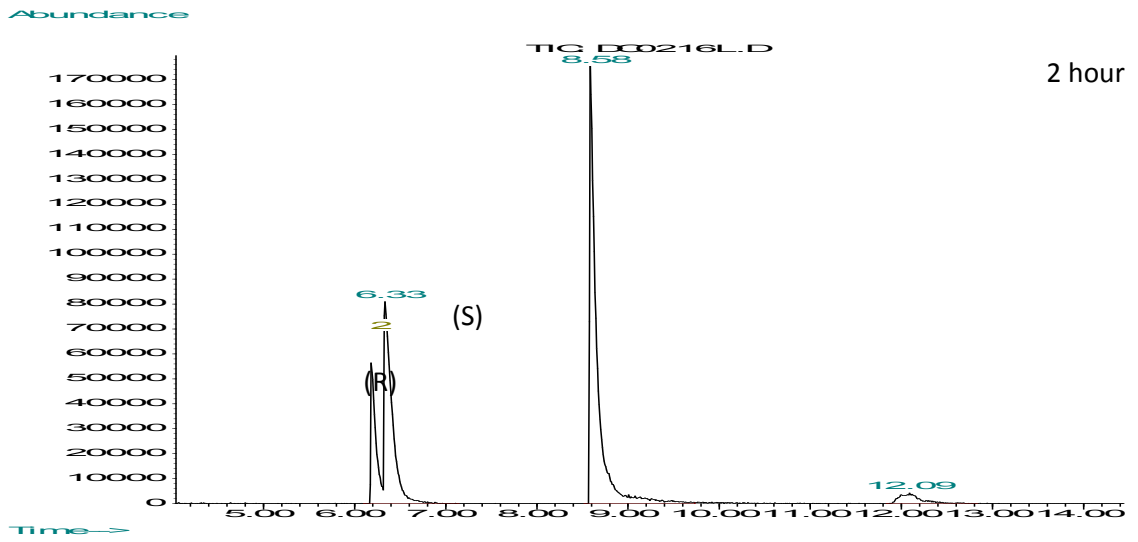
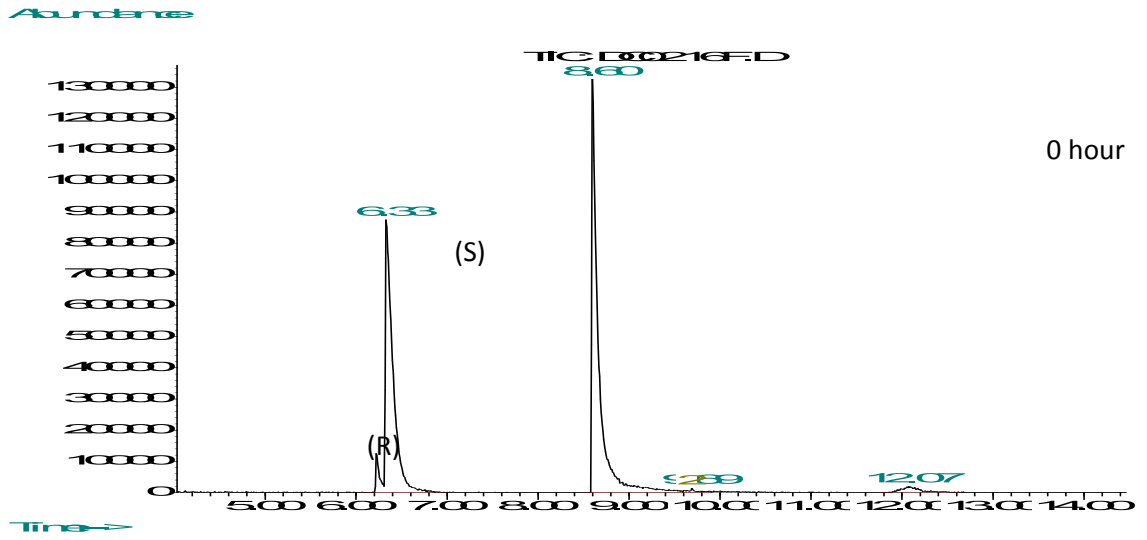




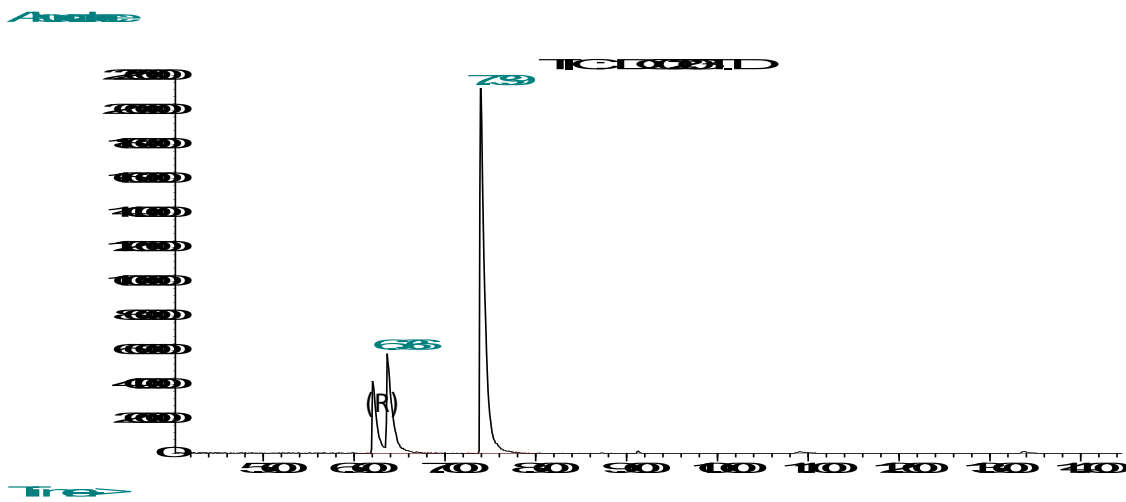
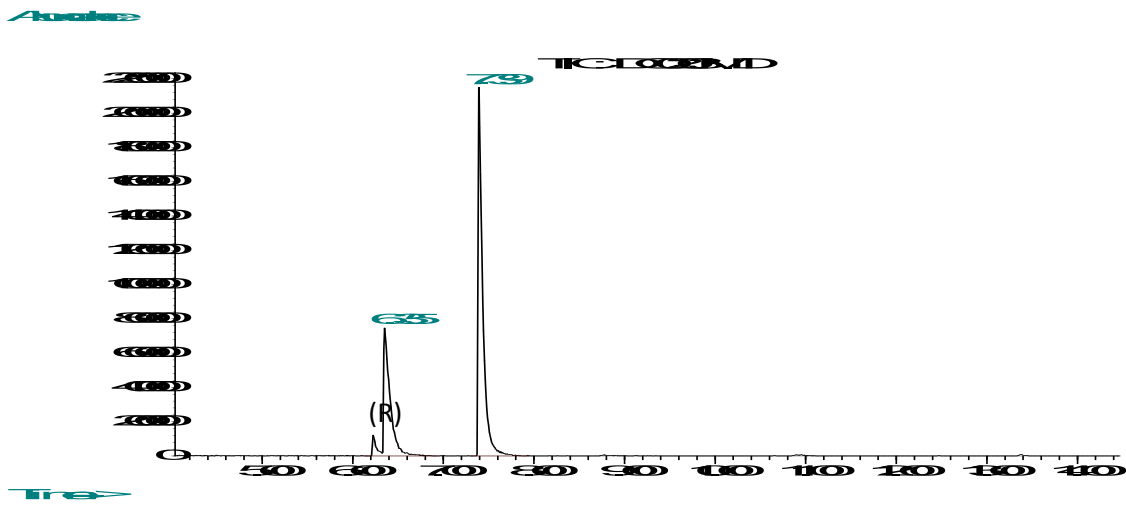
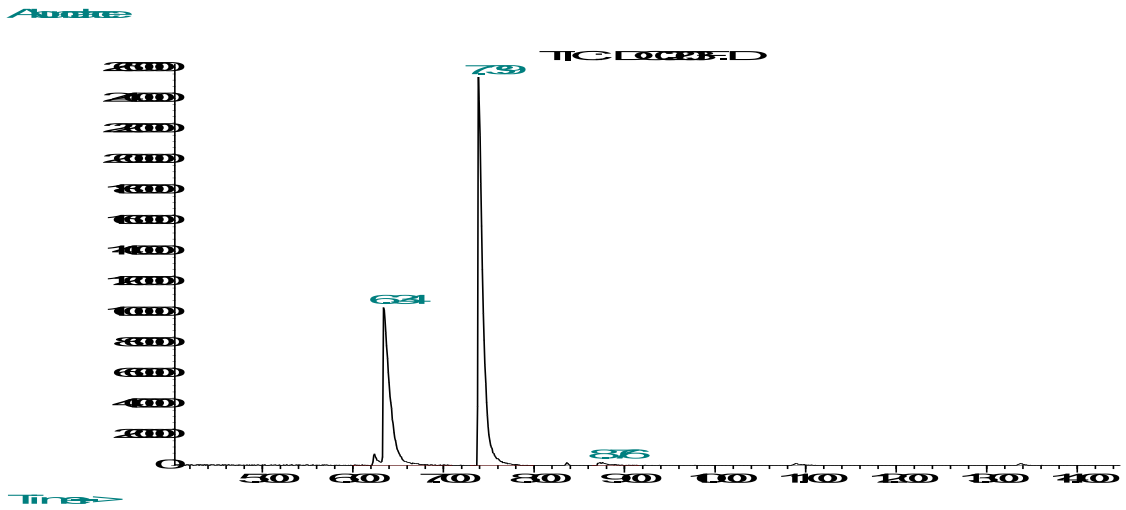
**Isocyanoacetate derived from (S)-N-formylalanine methyl ester + benzylamine in methanol**



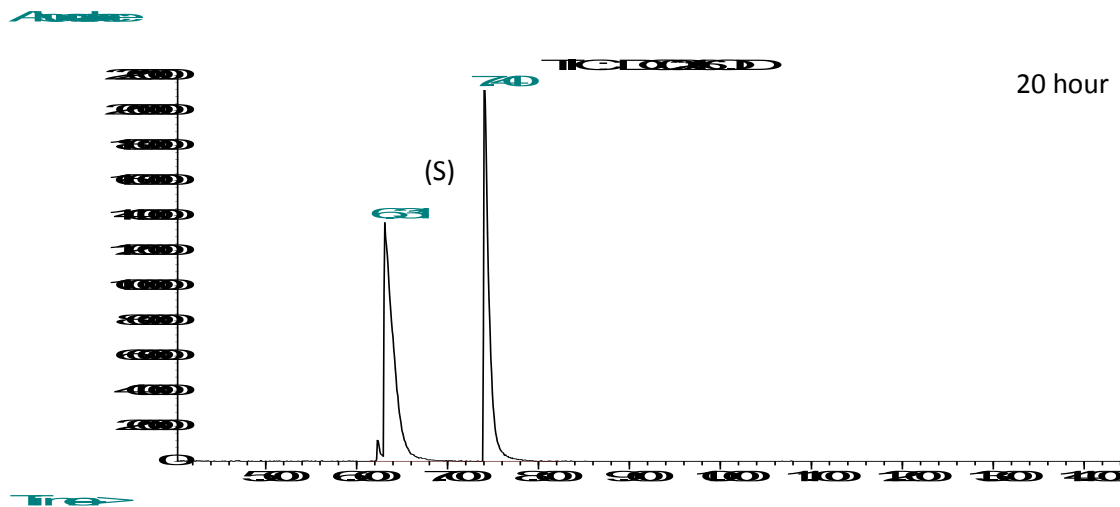
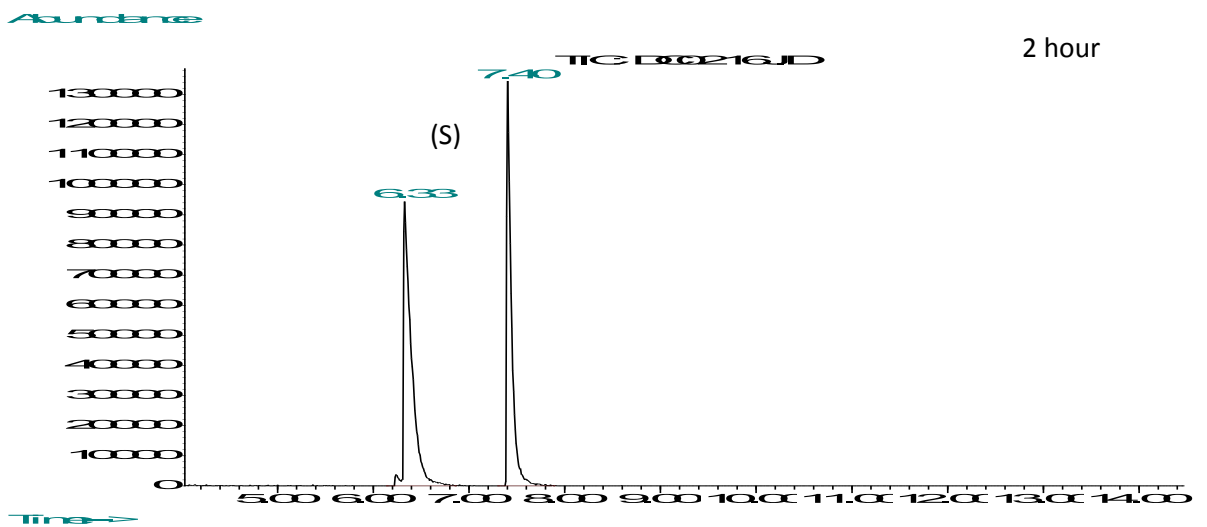
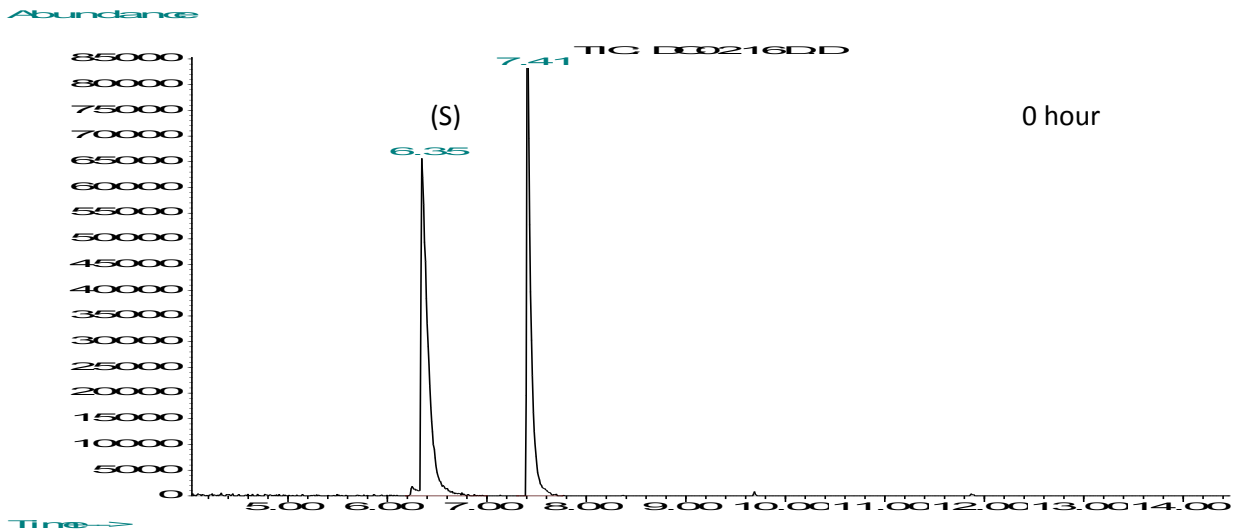
Isocyanoacetate derived from (S)-N-formylalanine methyl ester + benzylamine in dichloromethane



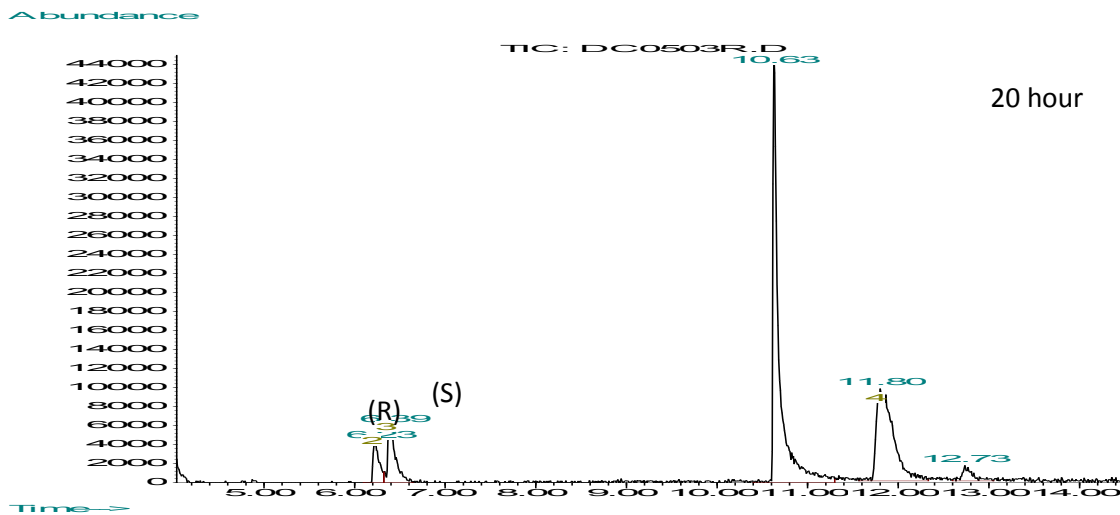
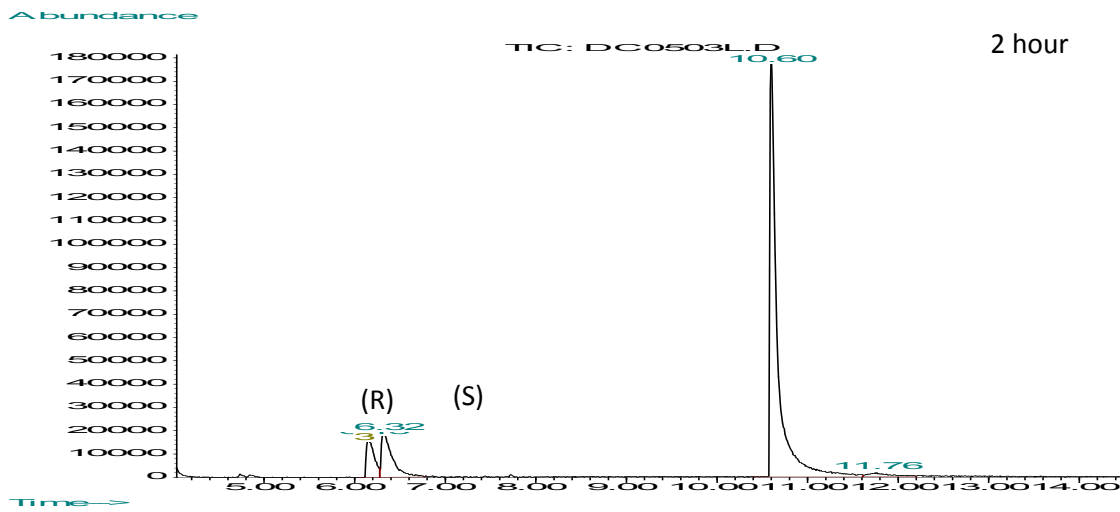
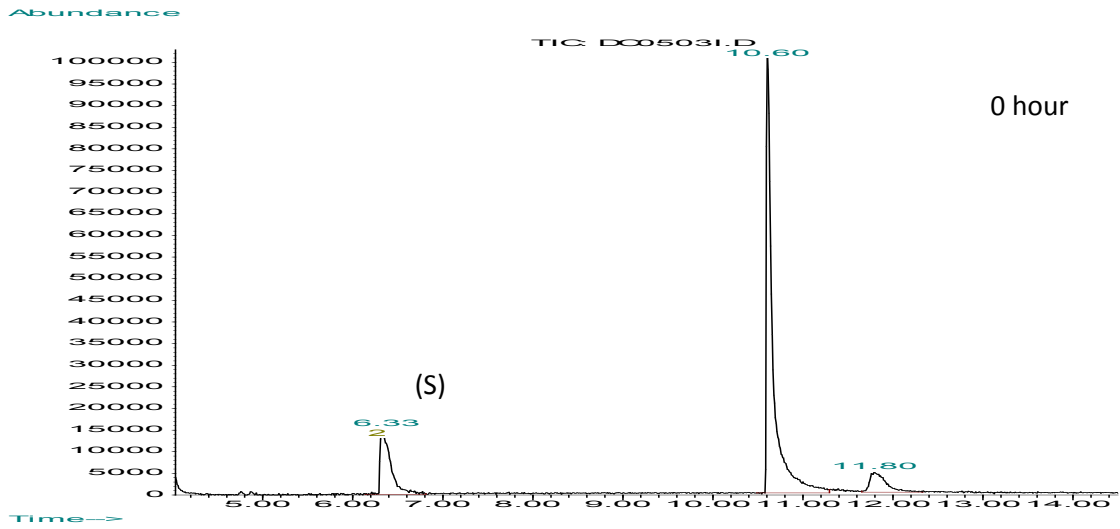
Isocyanoacetate derived from (S)-N-formylalanine methyl ester + benzylamine+ benzaldehydin methanol



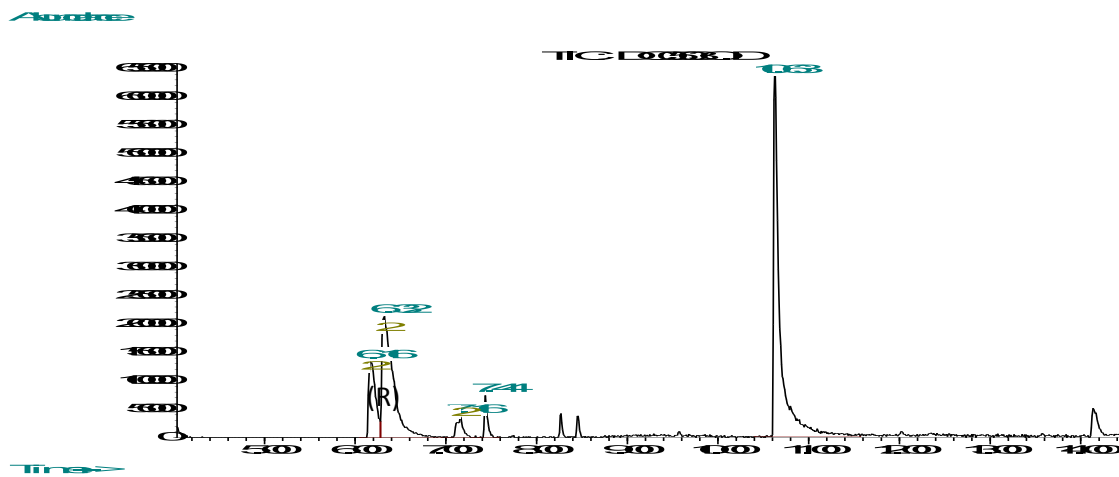
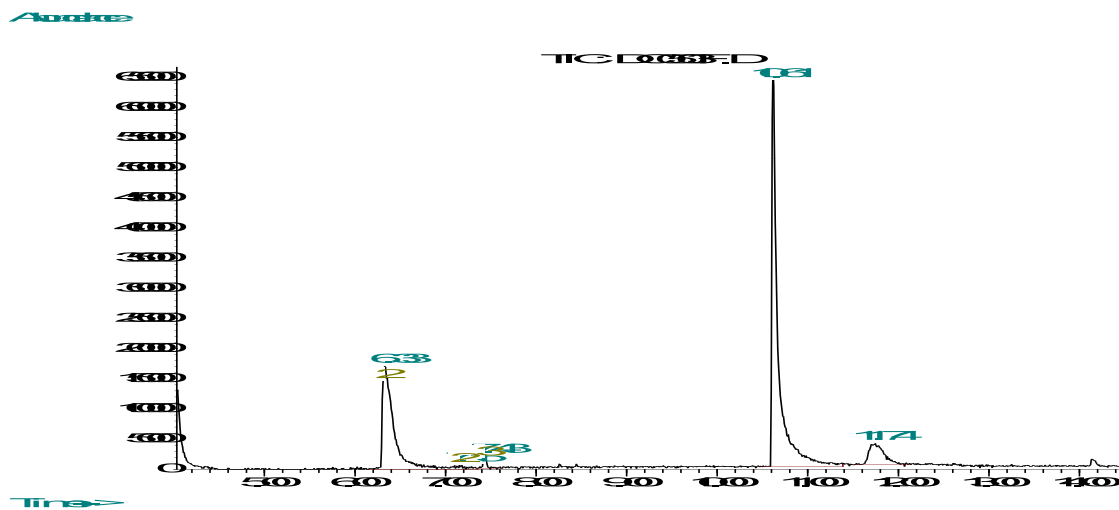
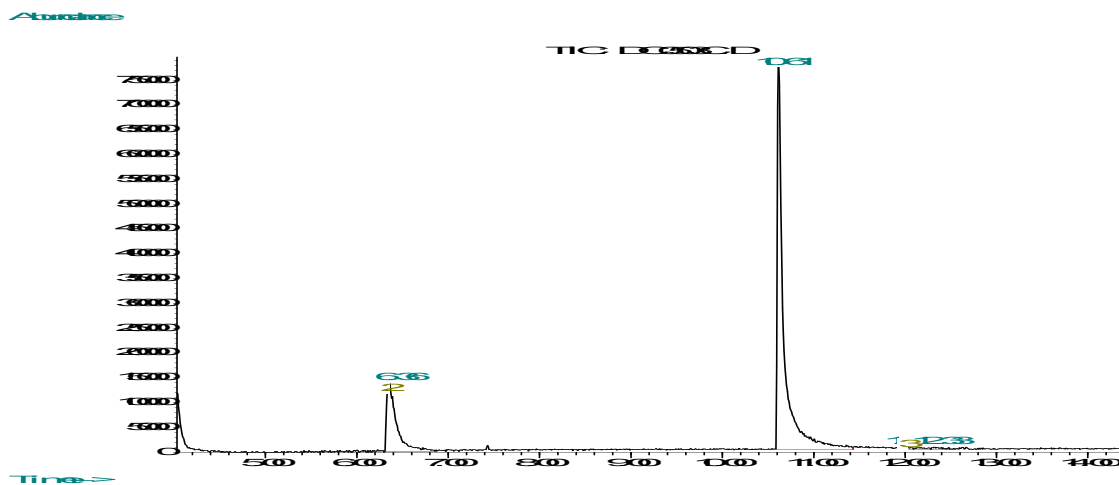
**Isocyanoacetate derived from (S)-N-formylalanine methyl ester + benzylamine + benzaldehyde in dichloromethane**



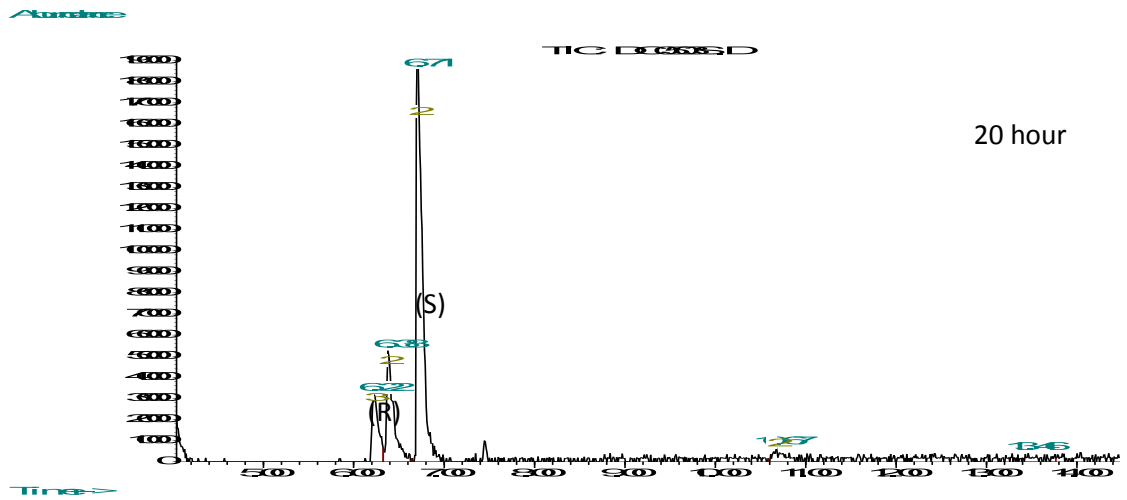
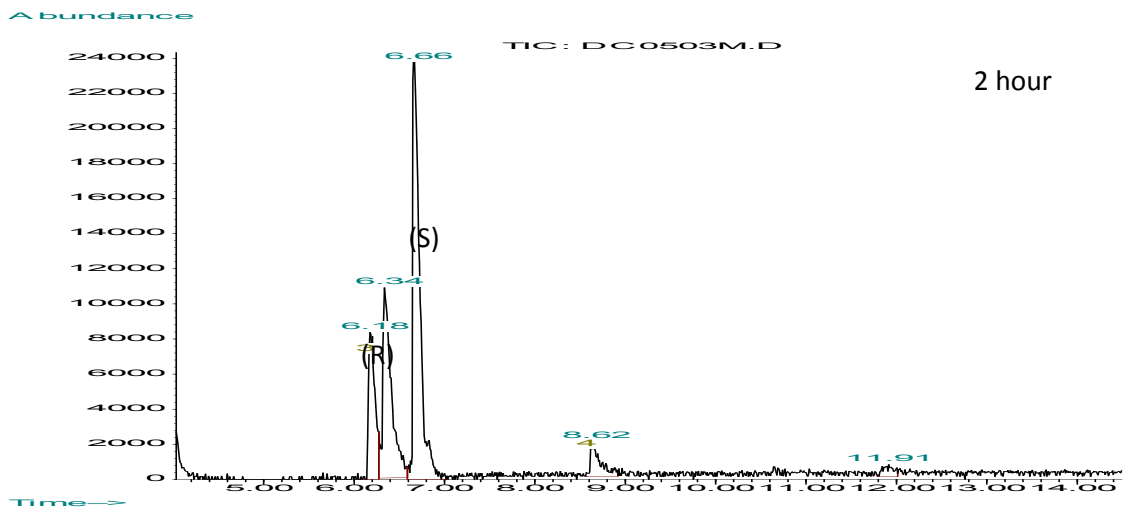
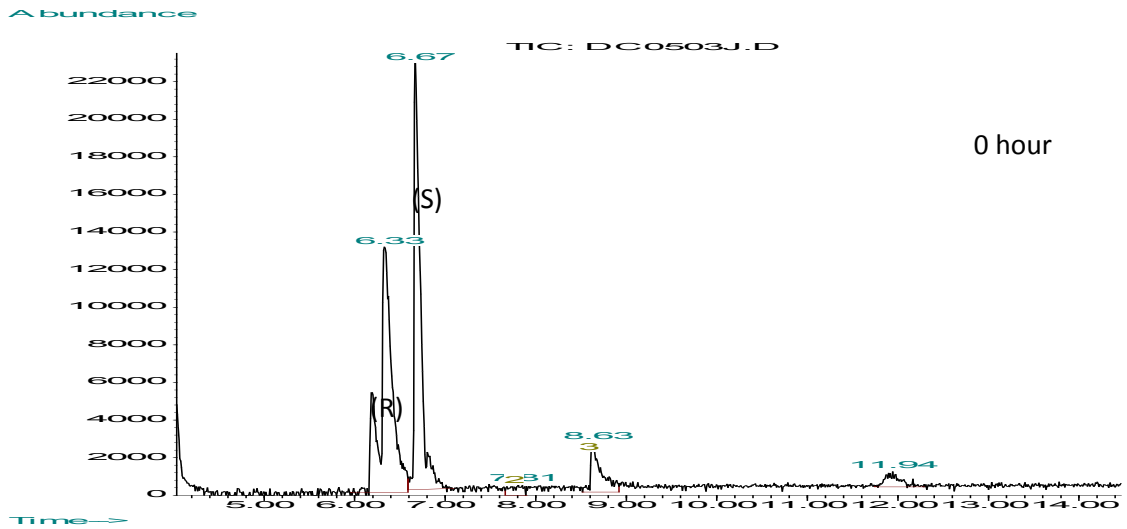
**Isocyanoacetate derived from (S)-N-formylalanine methyl ester + benzylamine + isobutyraldehyde in methanol**



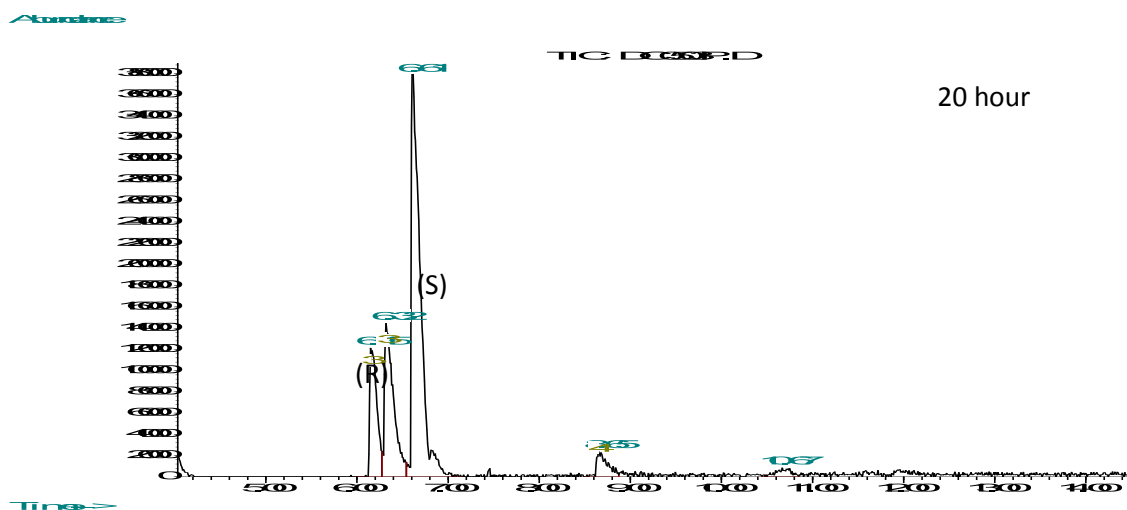
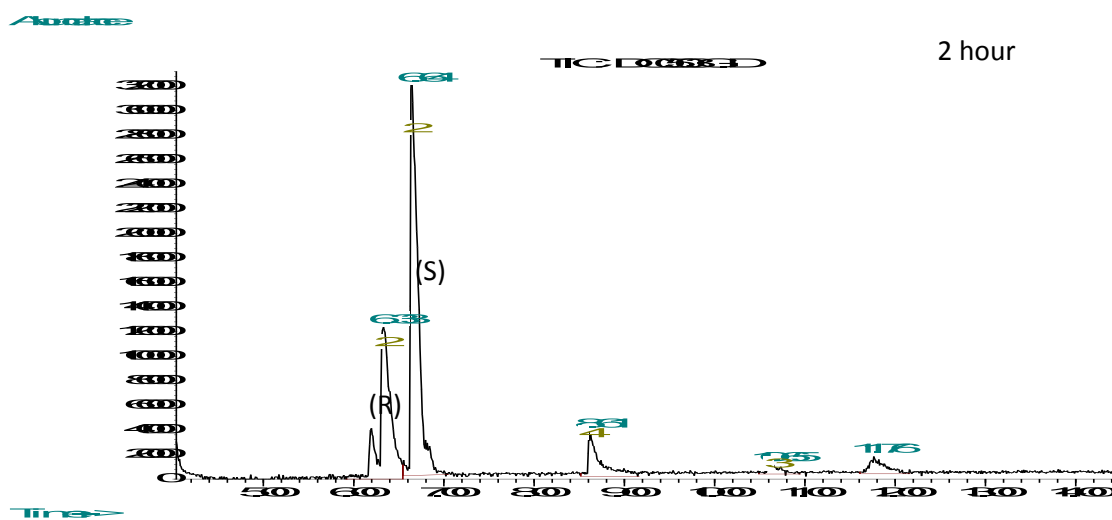
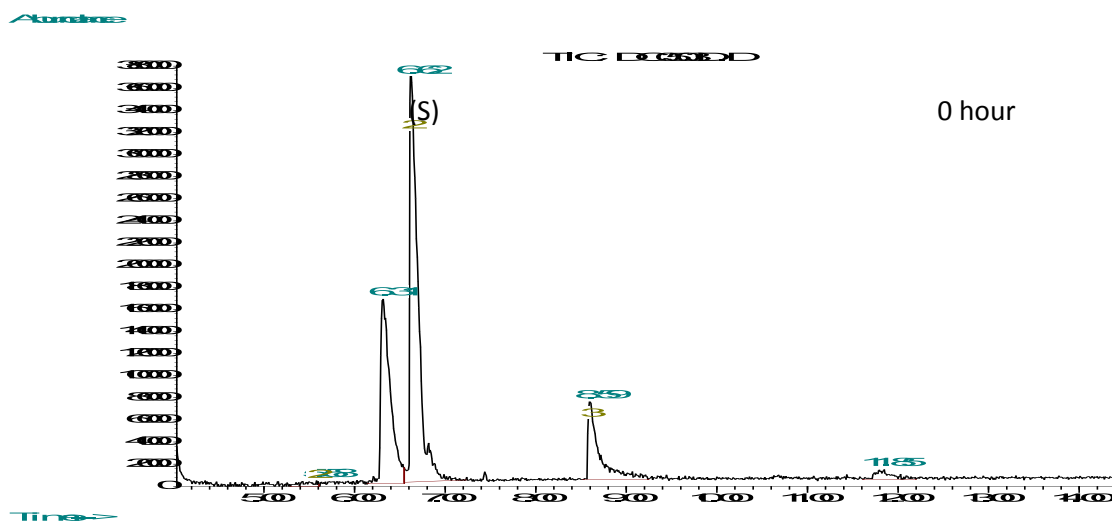
Isocyanacetate derived from (S)-N-formylalanine methyl ester + benzylamine + isobutyraldehyde in dichloromethane



**Isocyanoacetate derived from (S)-N-formylalanine methyl ester + benzylamine + cyclohexanone in methanol**

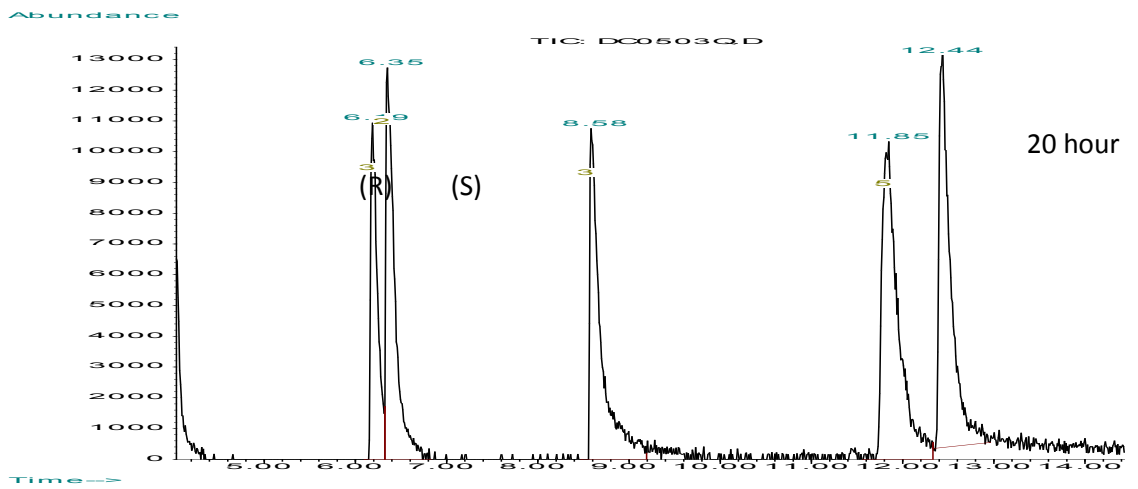
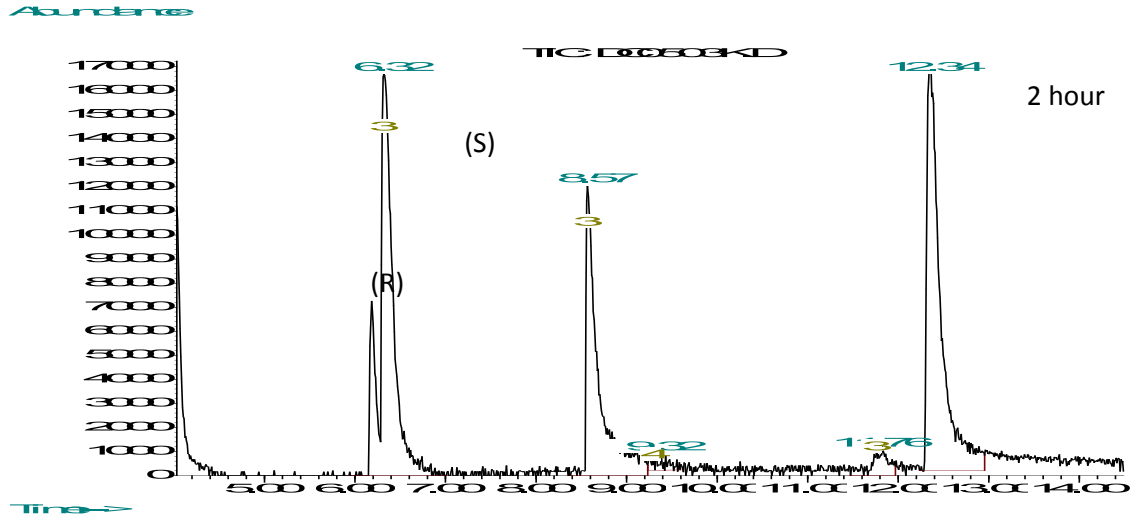
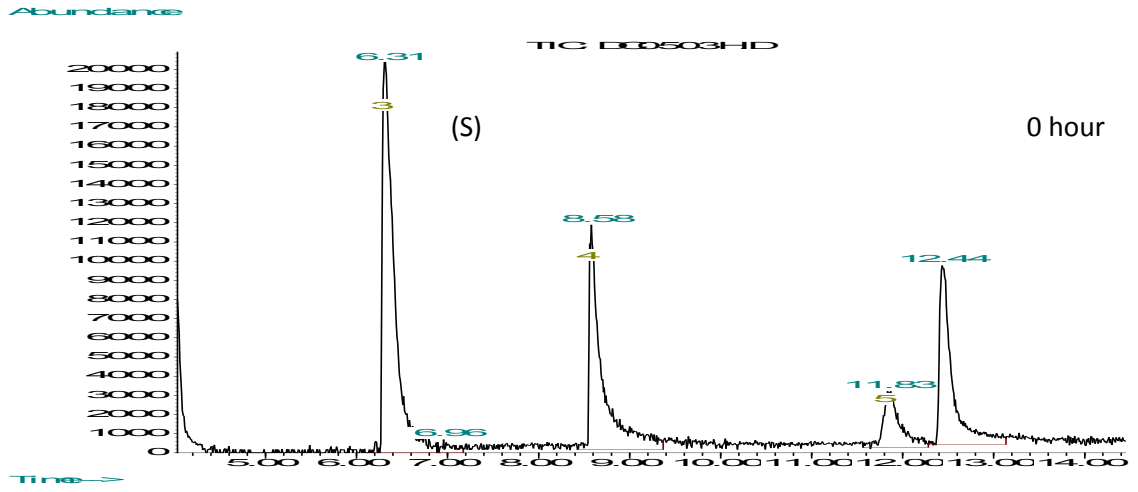


Isocyanoacetate derived from (S)-N-formylalanine methyl ester + benzylamine + cyclohexanone in dichloromethane

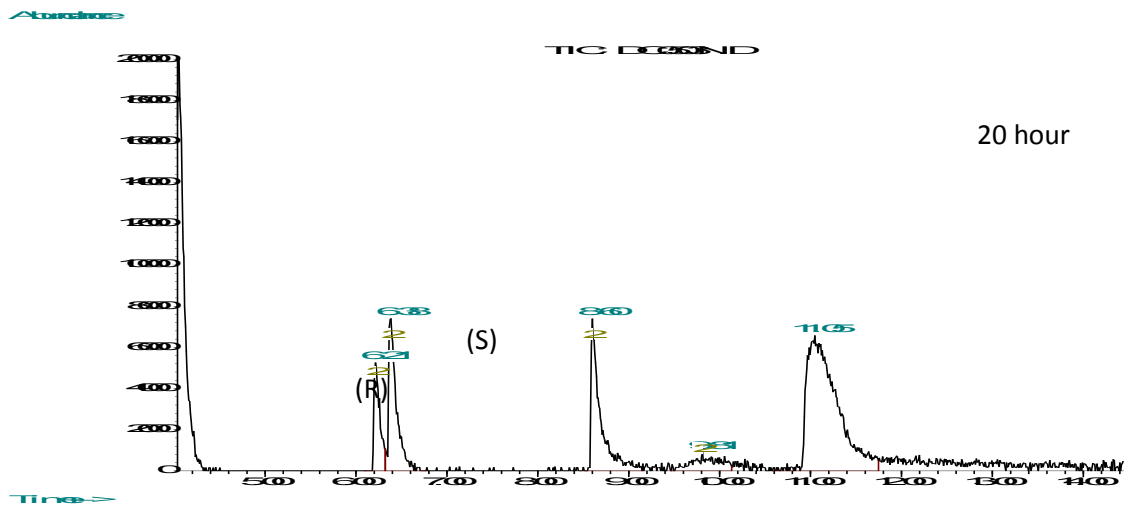
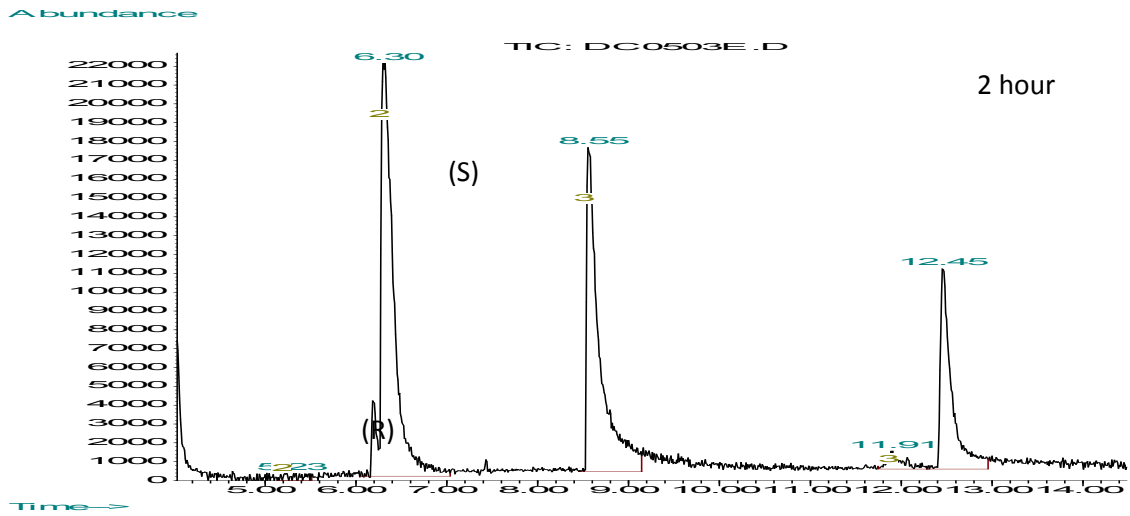
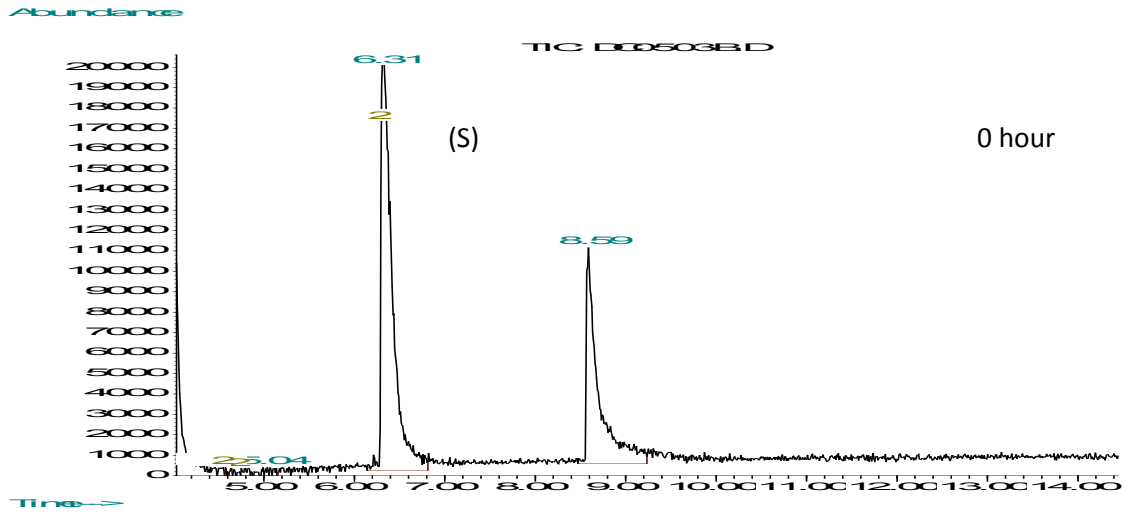




Isocyanoacetate derived from (S)-N-formylalanine methyl ester + benzylamine + Boc-proline in methanol



Isocyanoacetate derived from (S)-N-formylalanine methyl ester + benzylamine + Boc-proline in dichloromethane

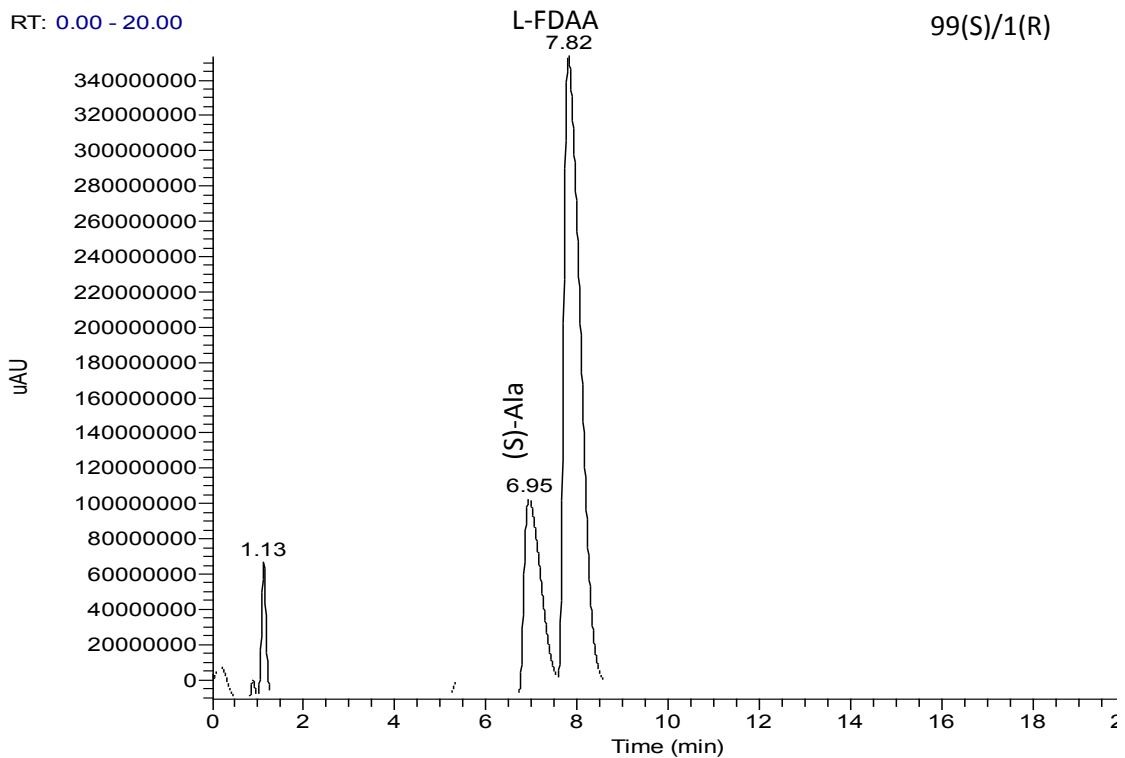


## **Advanced Marfey Analysis Chromatograms**

# Alanine Limits of Detection

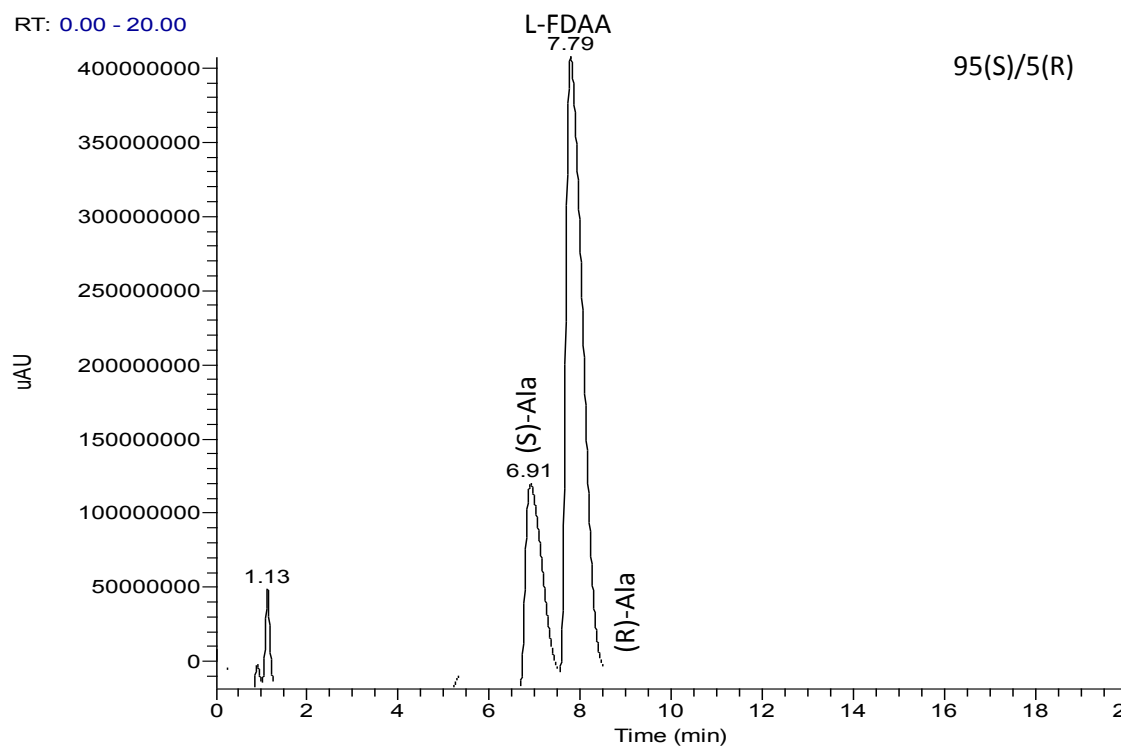
RT: 0.00 - 20.00

99(S)/1(R)

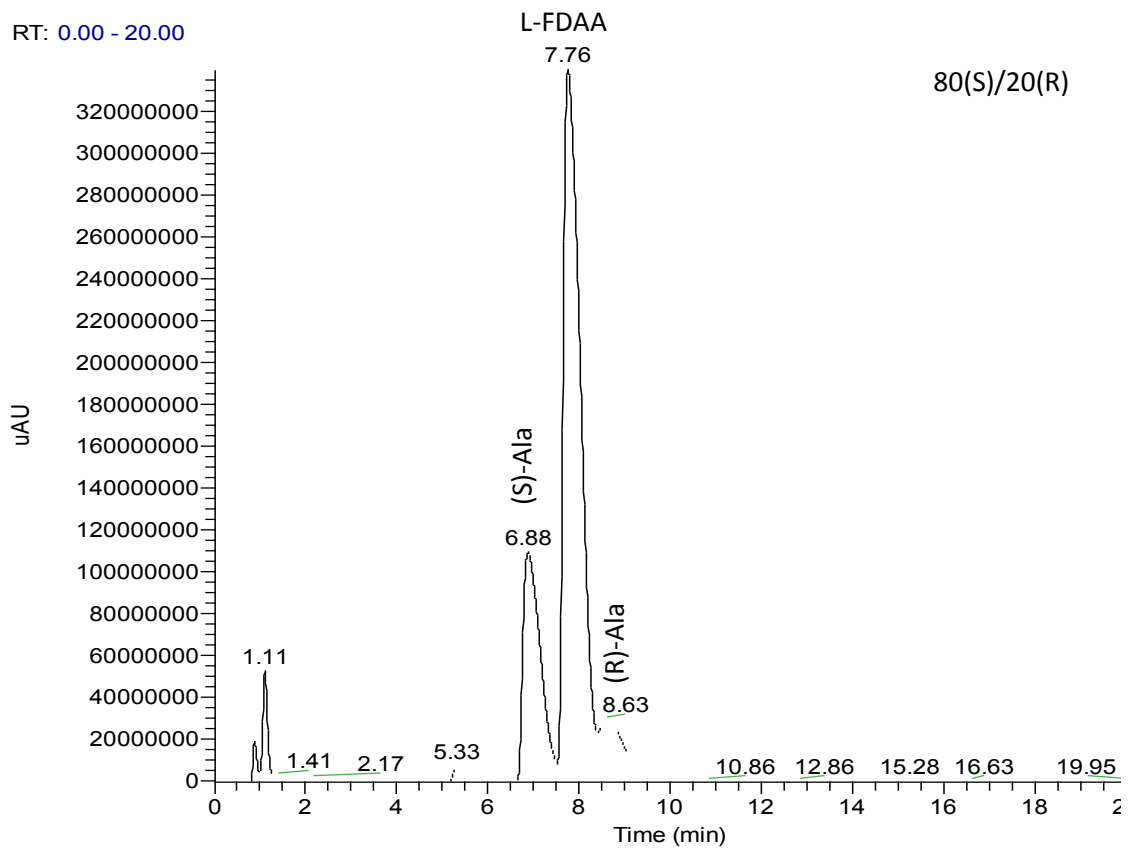
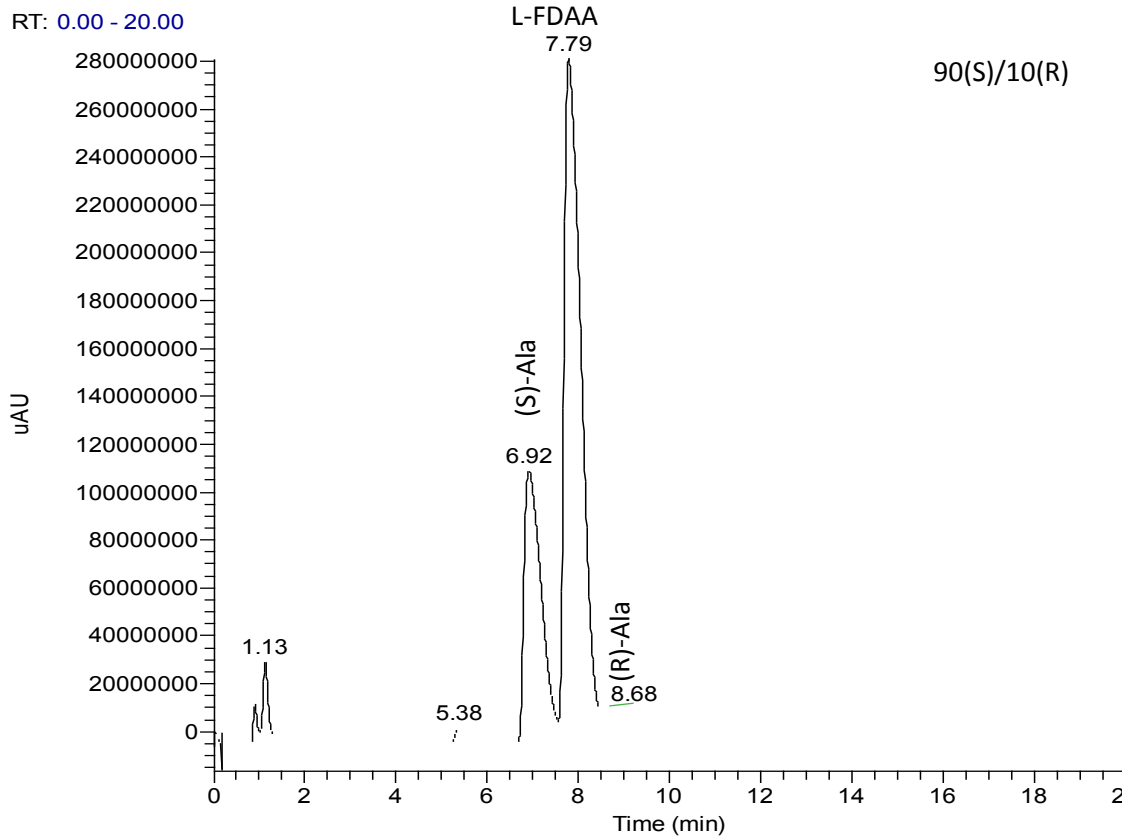


RT: 0.00 - 20.00

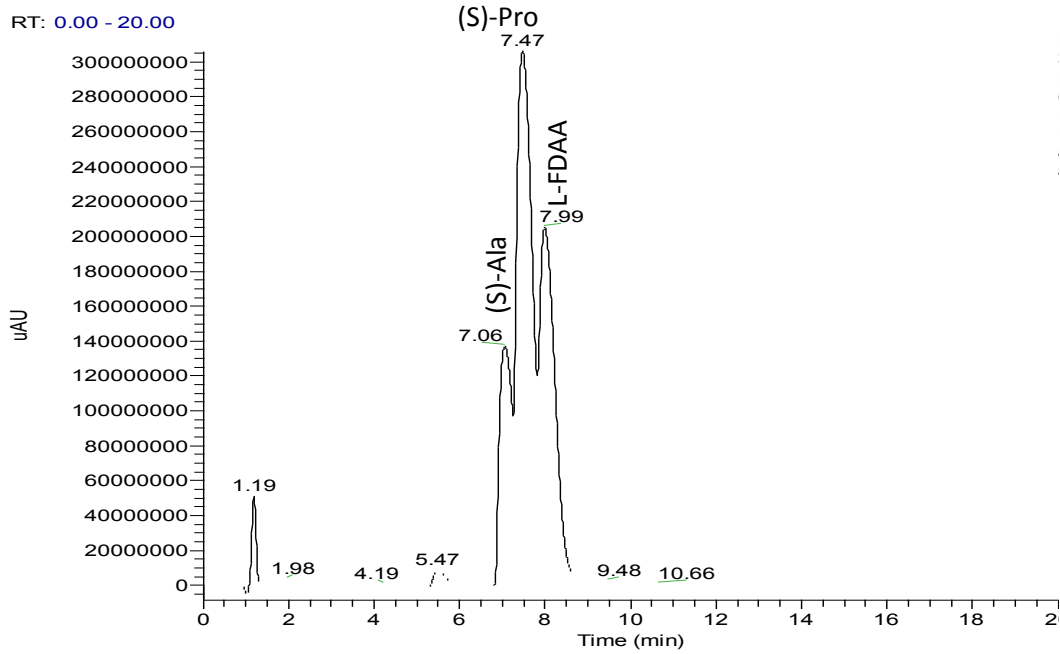
95(S)/5(R)



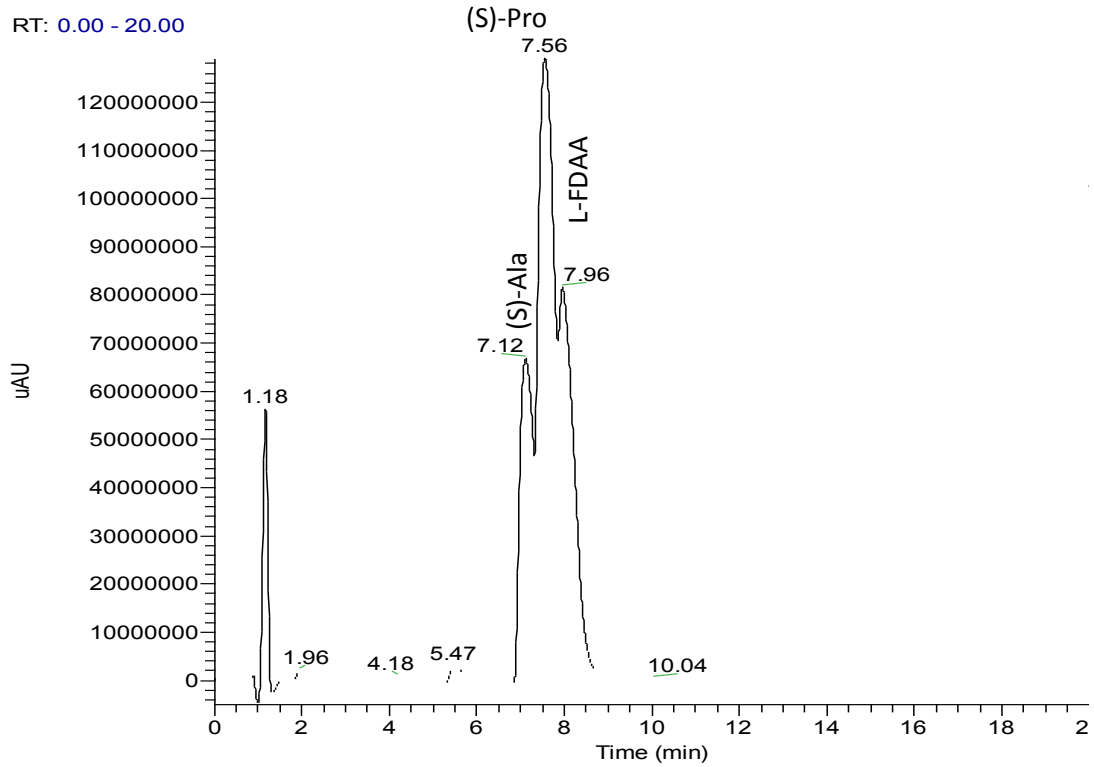
95(S)/5(R)



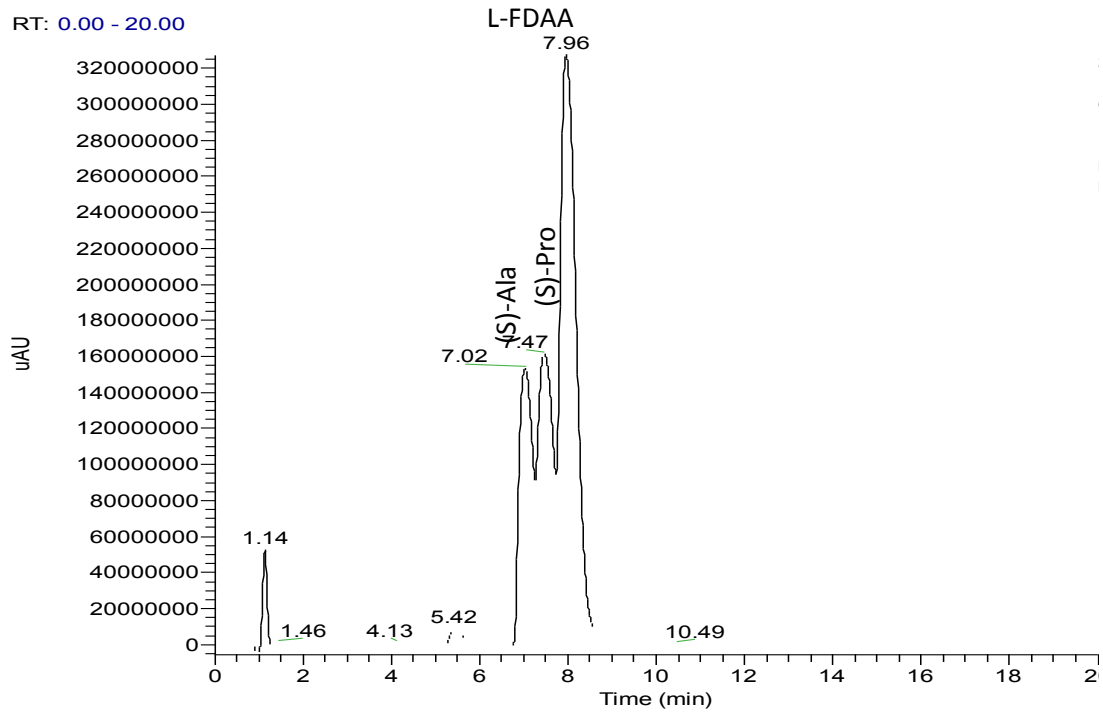
**Passeriniproduct derived from Boc-proline, isocyanide derived from (S)-N-formylalanine methyl ester, and benzaldehyde.**



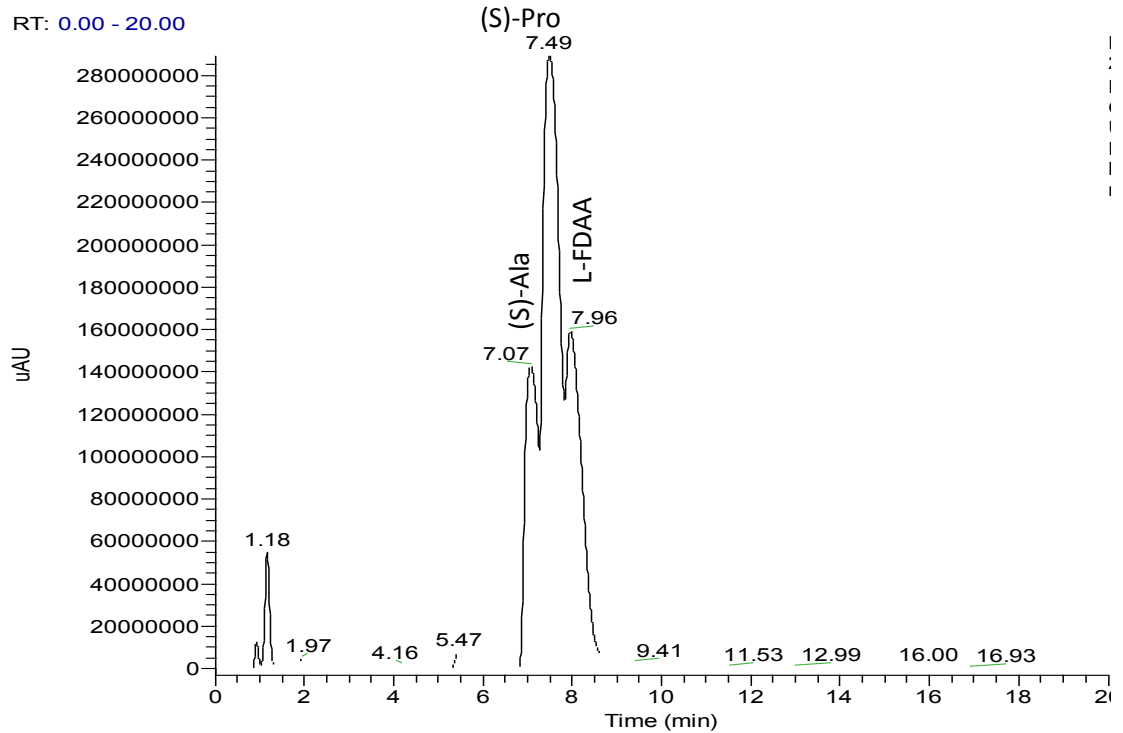
**Passeriniproduct derived from Boc-proline, isocyanide derived from (S)-N-formylalanine methyl ester, and hydrocinnamaldehyde.**



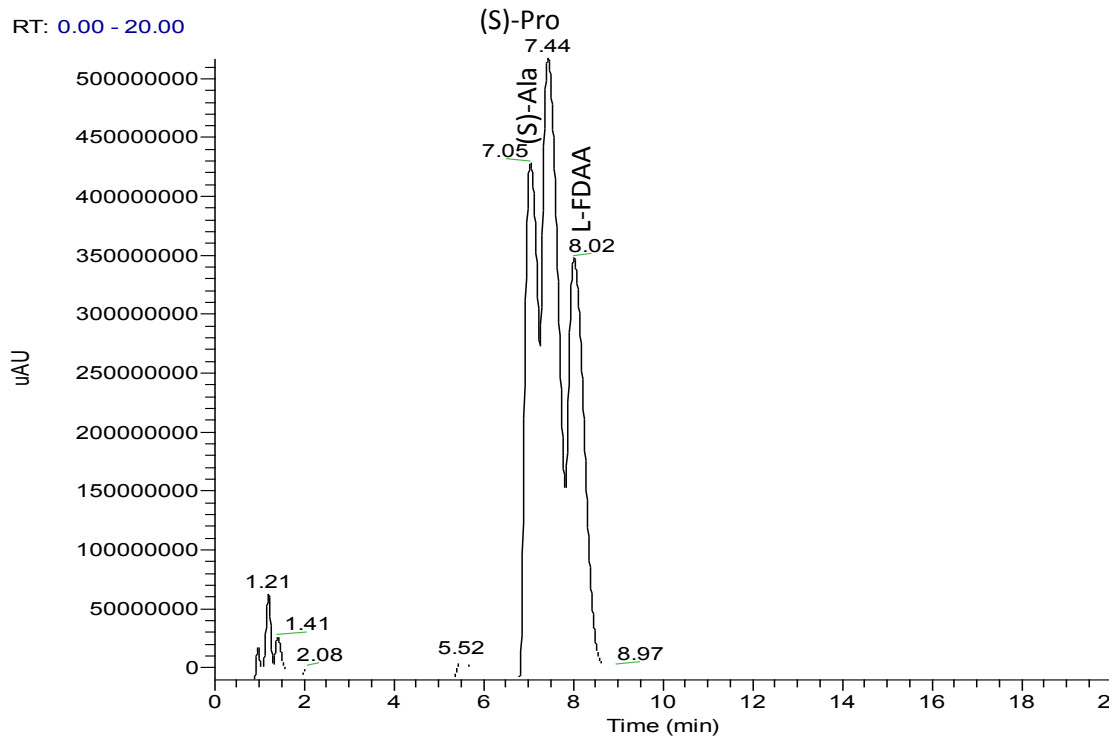
**Passeriniproduct derived from Boc-proline, isocyanide derived from (S)-N-formylalanine methyl ester, and isobutyraldehyde.**



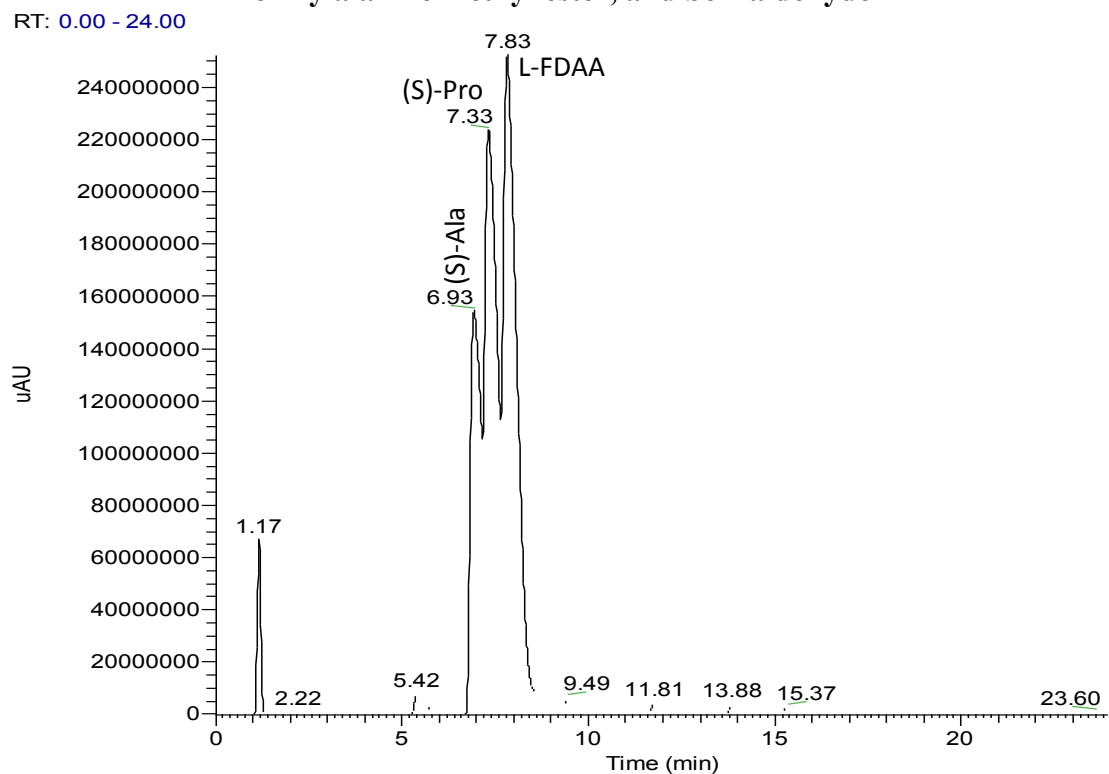
**Passeriniproduct derived from Boc-proline, isocyanide derived from (S)-N-formylalanine methyl ester, and cyclobutanone**



**Passeriniproduct derived from Boc-proline, isocyanide derived from (S)-N-formylalanine methyl ester, and cyclohexanone**

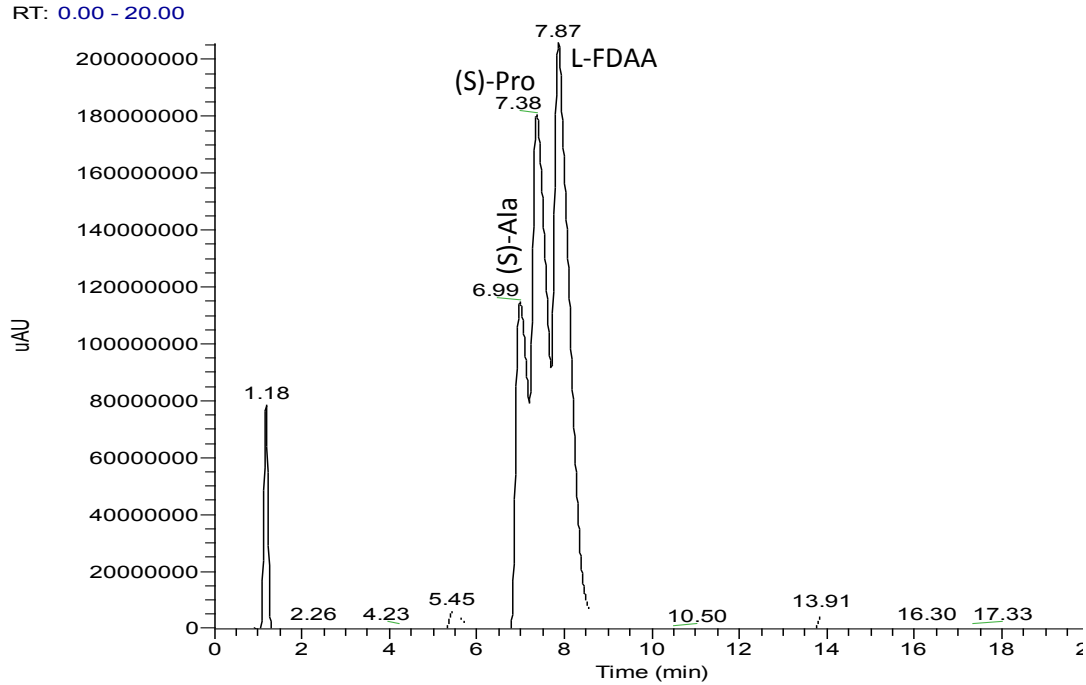


**Ugi product derived from Boc-proline, benzylamine, isocyanide derived from (S)-N-formylalanine methyl ester, and benzaldehyde**

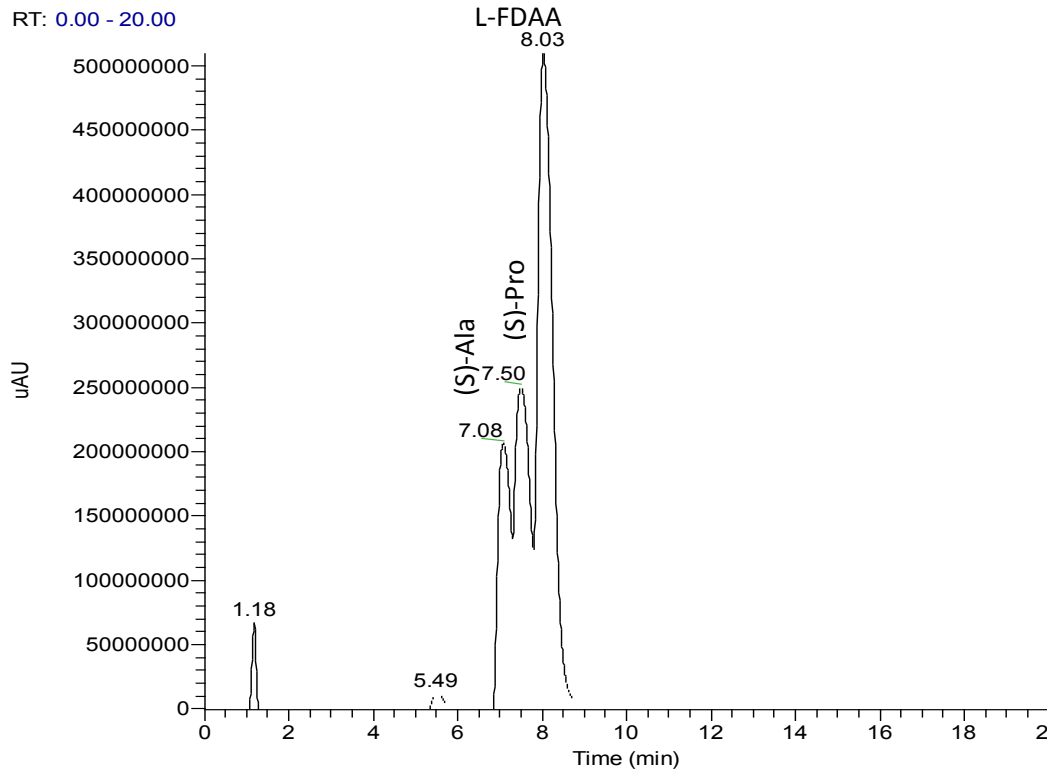




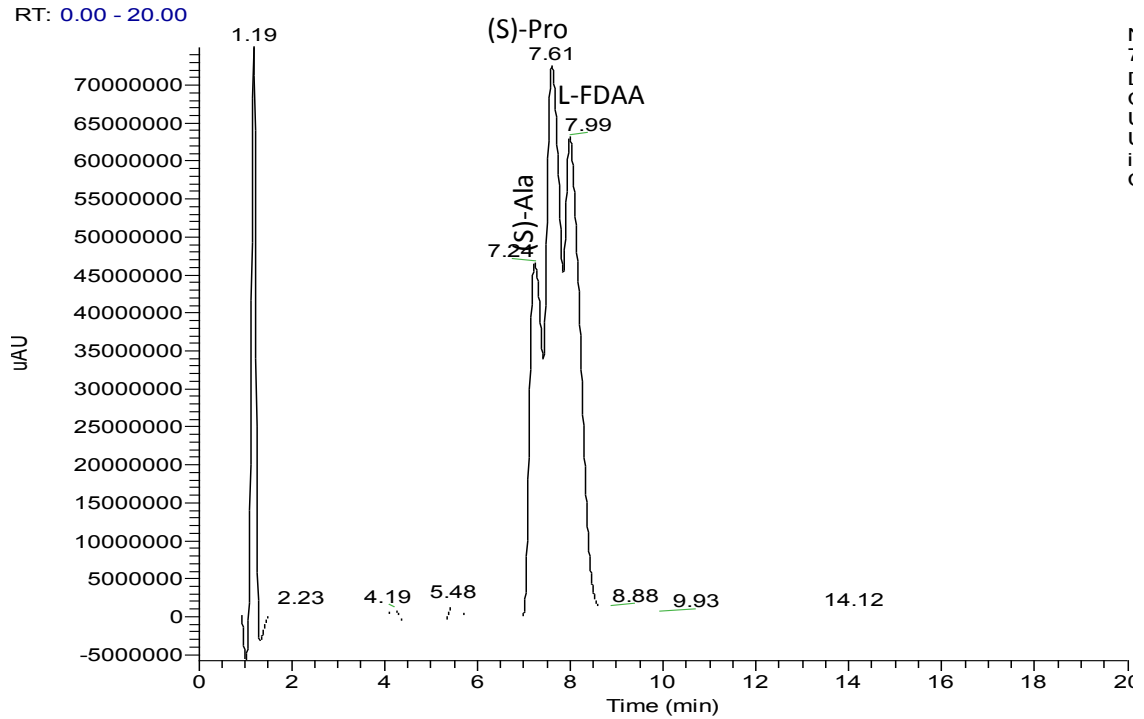
**Ugi product derived from Boc-proline, benzylamine, isocyanide derived from (S)-N-formylalanine methyl ester, and hydrocinnamaldehyde**



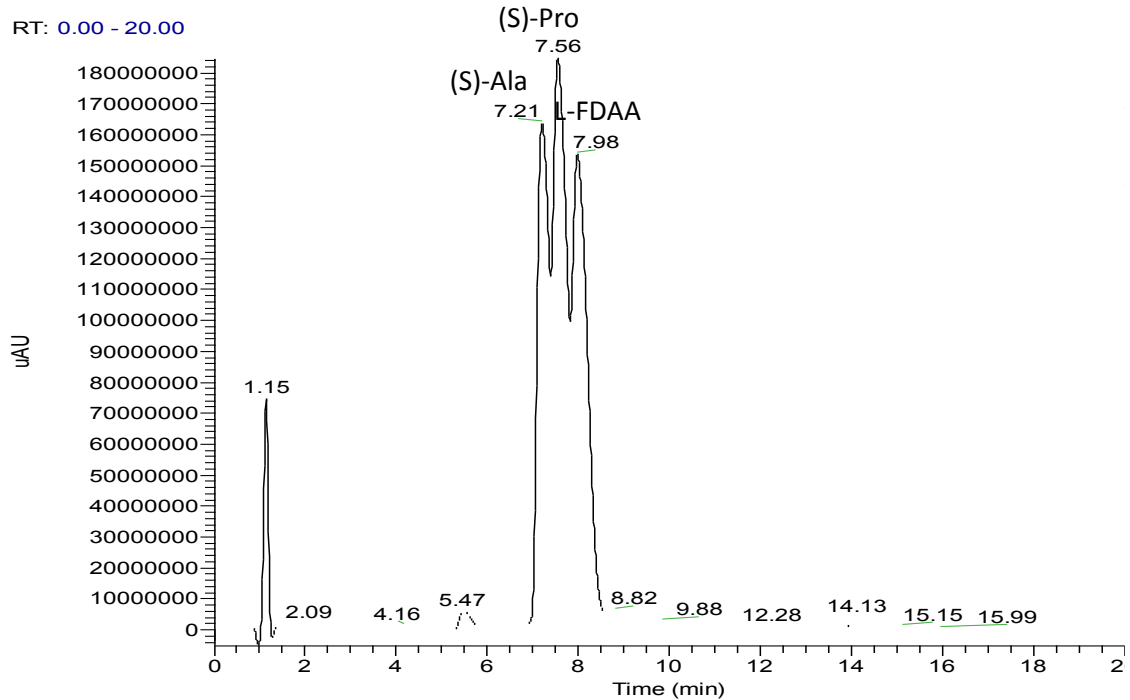
**Ugi product derived from Boc-proline, benzylamine, isocyanide derived from (S)-N-formylalanine methyl ester, and Isobutyraldehyde (120 min precondensation)**



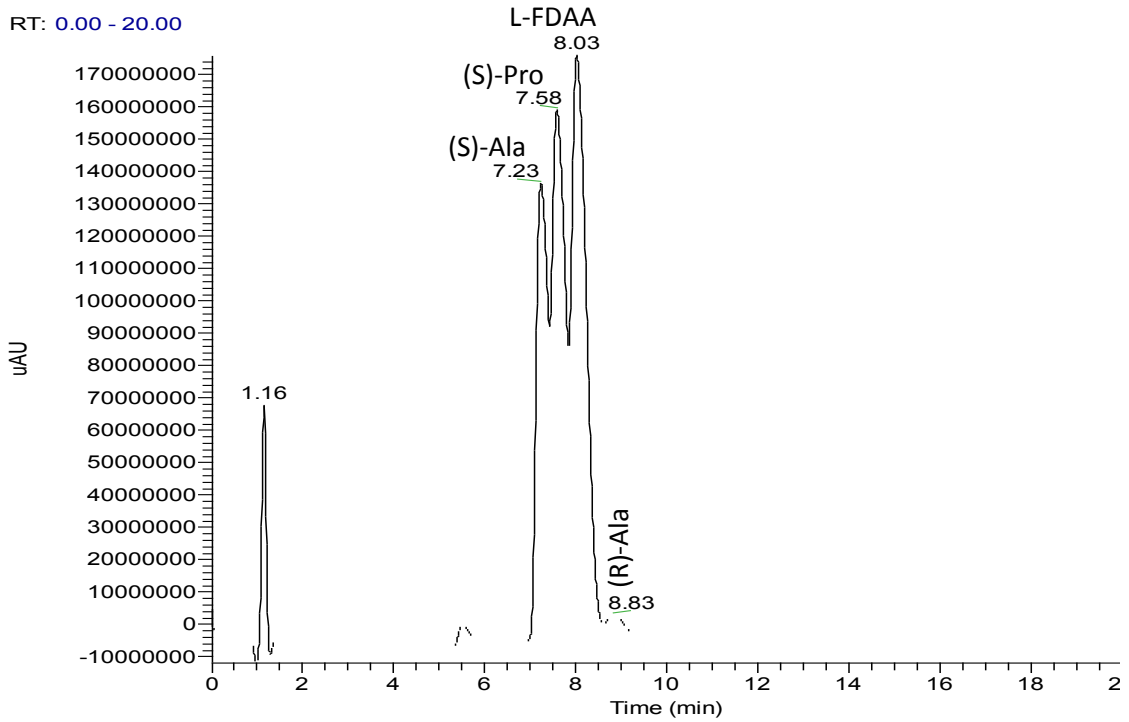
**Ugi product derived from Boc-proline, benzylamine, isocyanide derived from (S)-N-formylalanine methyl ester, and Isobutyraldehyde (60 min precondensation)**



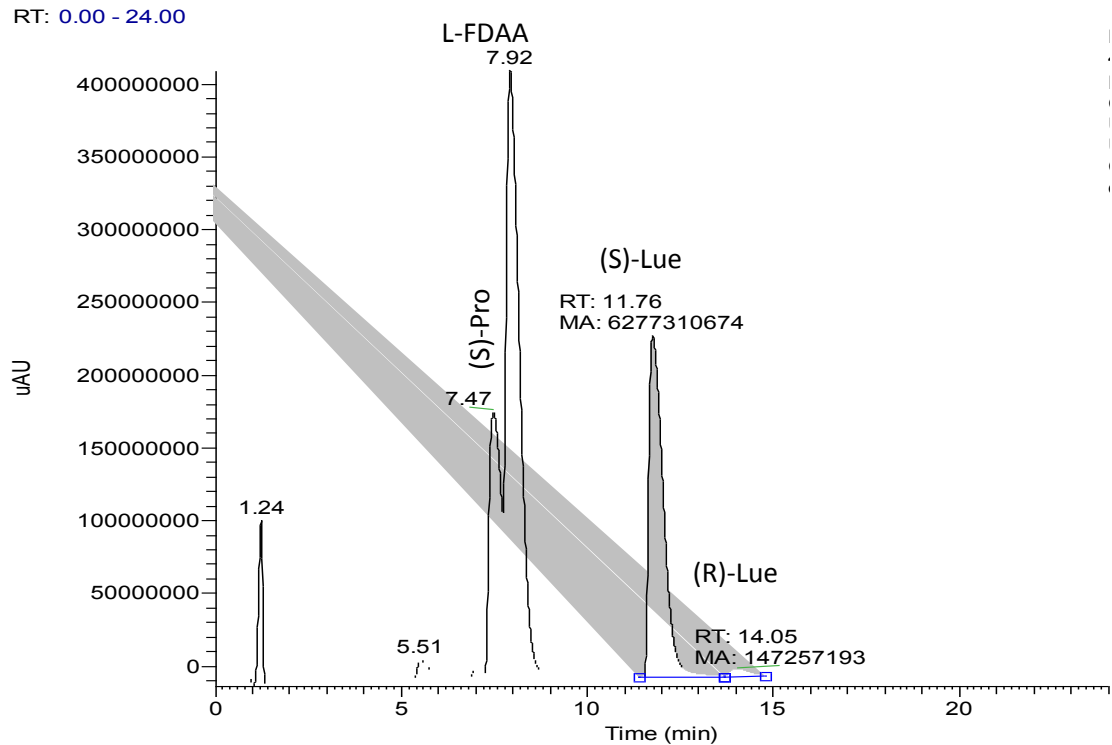
**Ugi product derived from Boc-proline, benzylamine, isocyanide derived from (S)-N-formylalanine methyl ester, and Isobutyraldehyde (30 min precondensation)**



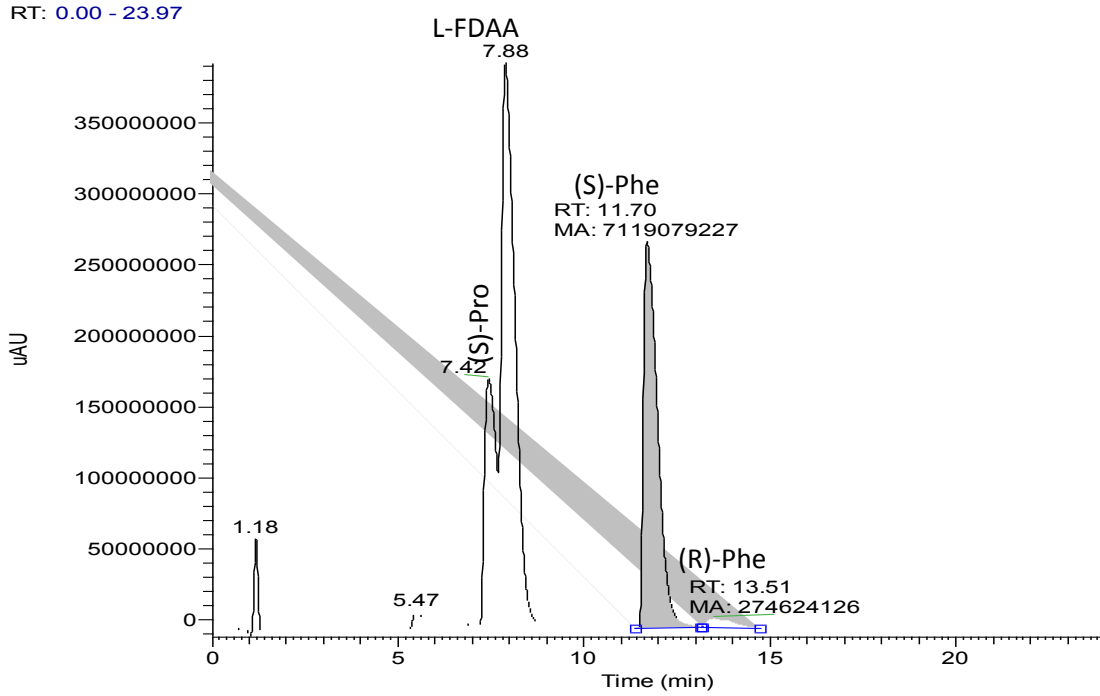
**Ugi product derived from Boc-proline, benzylamine, isocyanide derived from (S)-N-formylalanine methyl ester, and Isobutyraldehyde (0 min precondensation)**



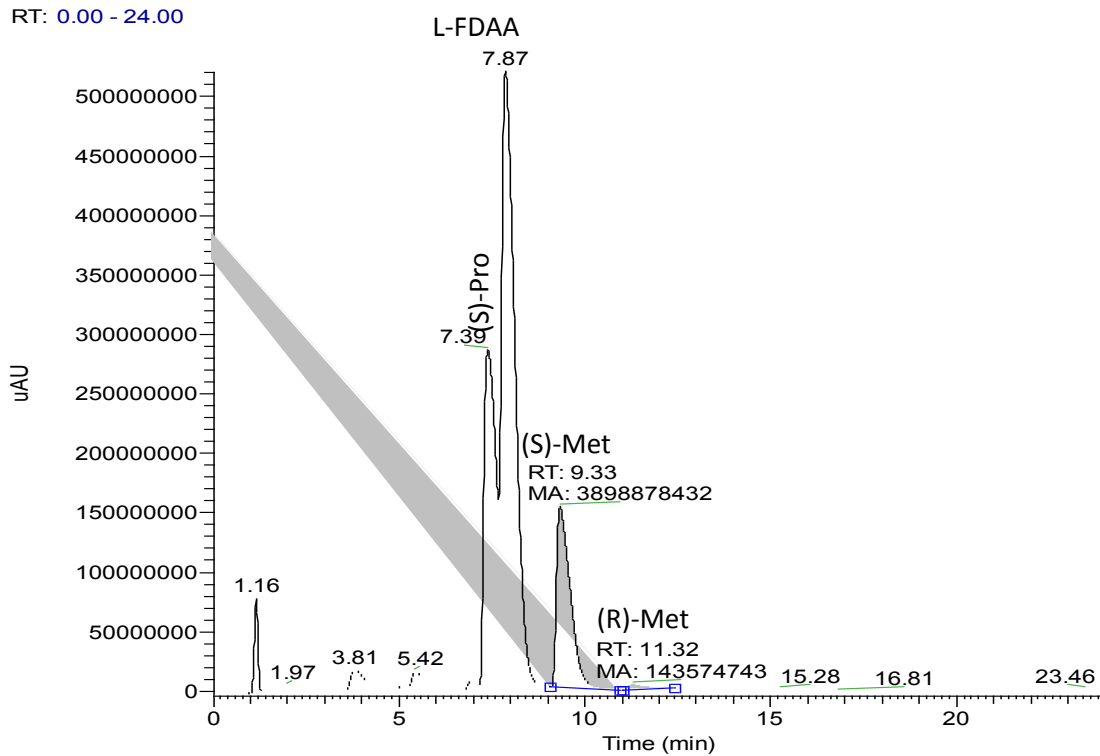
**Ugi product derived from Boc-proline, benzylamine, isocyanide derived from (S)-N-formylleucine methyl ester, and Isobutyraldehyde**



**Ugi product derived from Boc-proline, benzylamine, isocyanide derived from (S)-N-formylphenylalanine methyl ester, and Isobutyraldehyde**

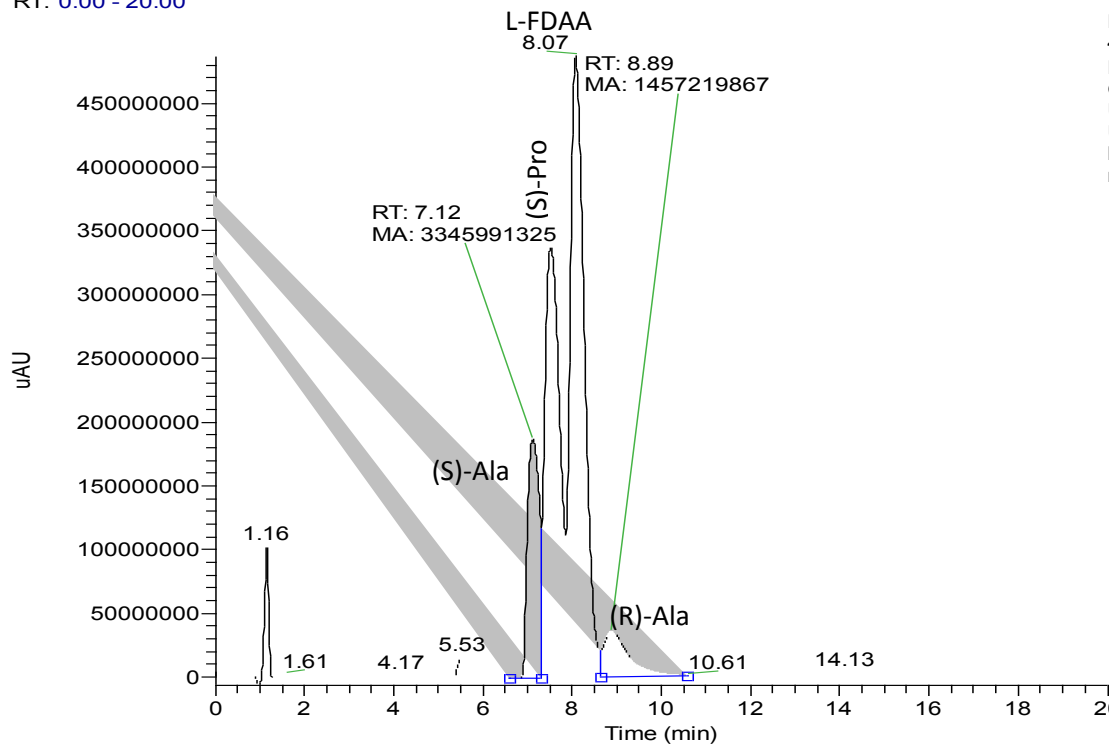


**Ugi product derived from Boc-proline, benzylamine, isocyanide derived from (S)-N-formylmethionine methyl ester, and Isobutyraldehyde**



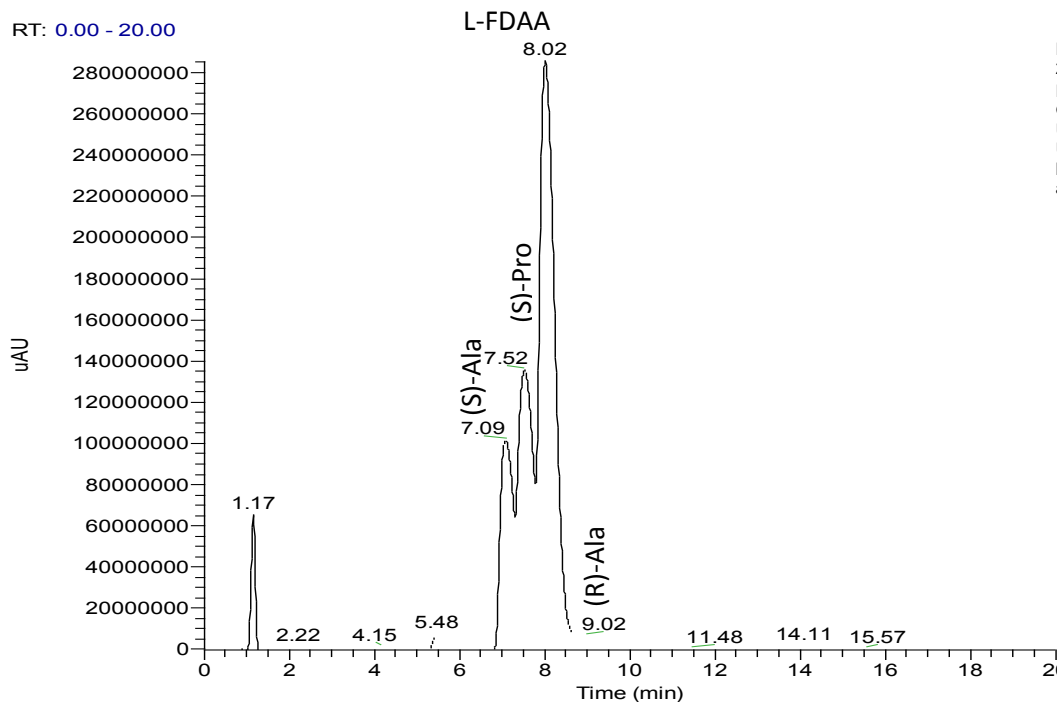
**Ugi product derived from Boc-proline, benzylamine, isocyanide derived from (S)-N-formylalanine methyl ester, and cyclobutanone**

RT: 0.00 - 20.00

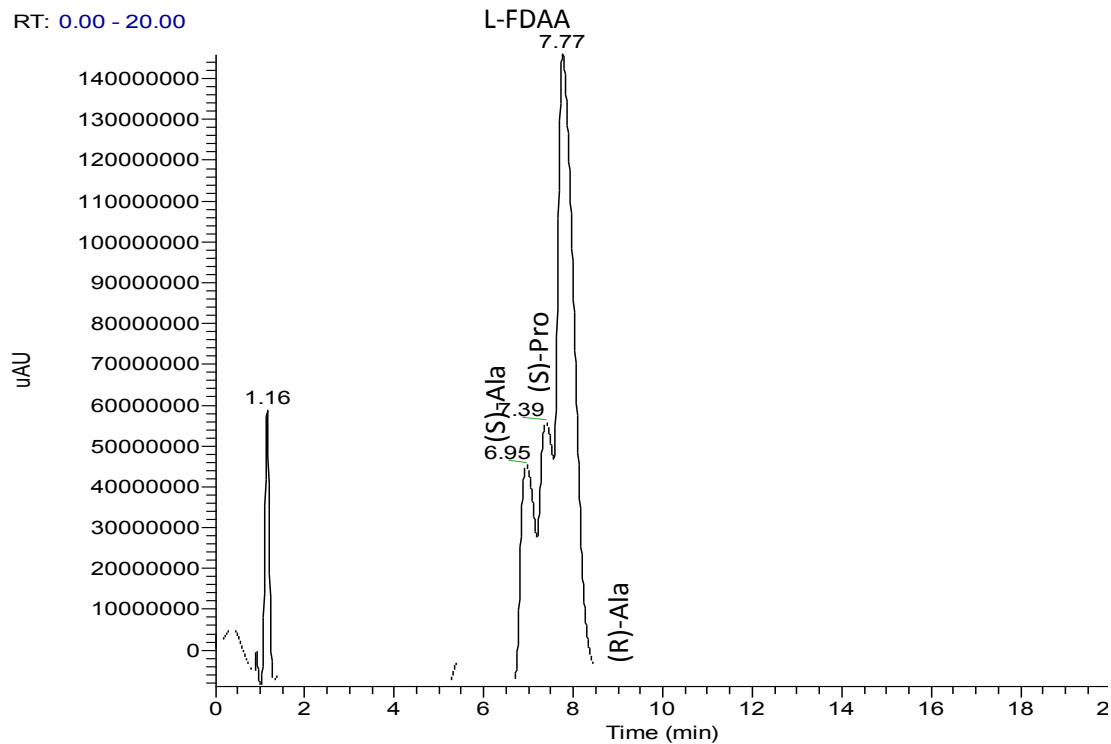


**Ugi product derived from Boc-proline, benzylamine, isocyanide derived from (S)-N-formylalanine methyl ester, and cyclohexanone (120 min precondensation)**

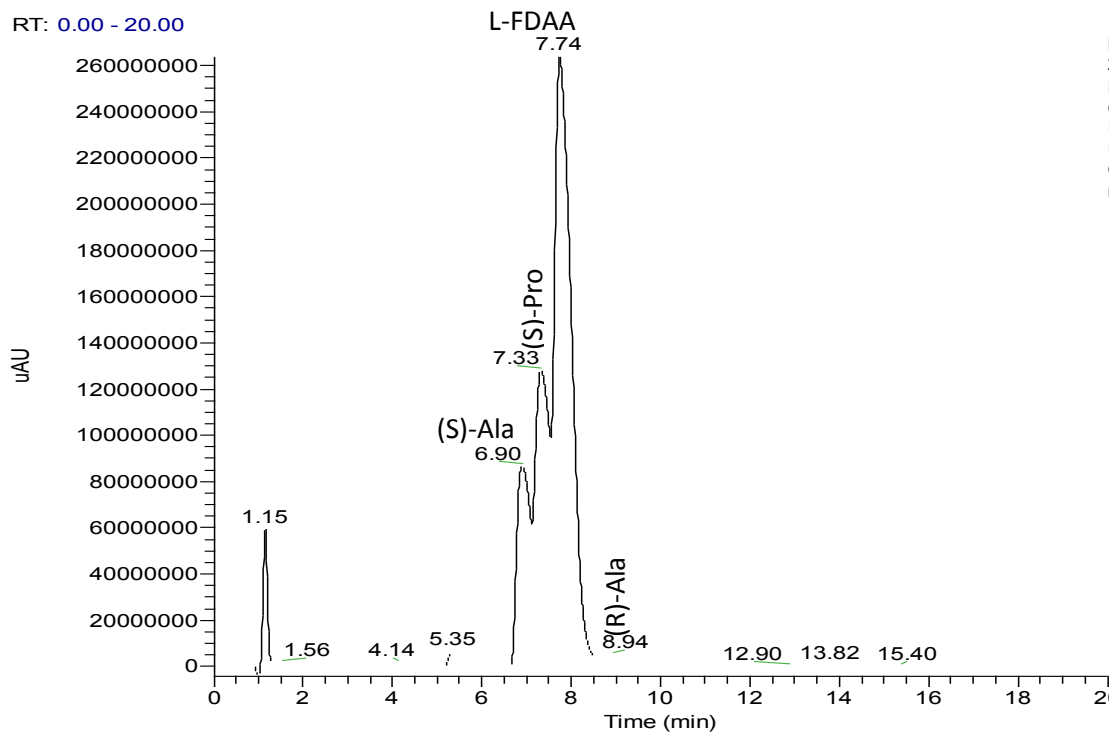
RT: 0.00 - 20.00



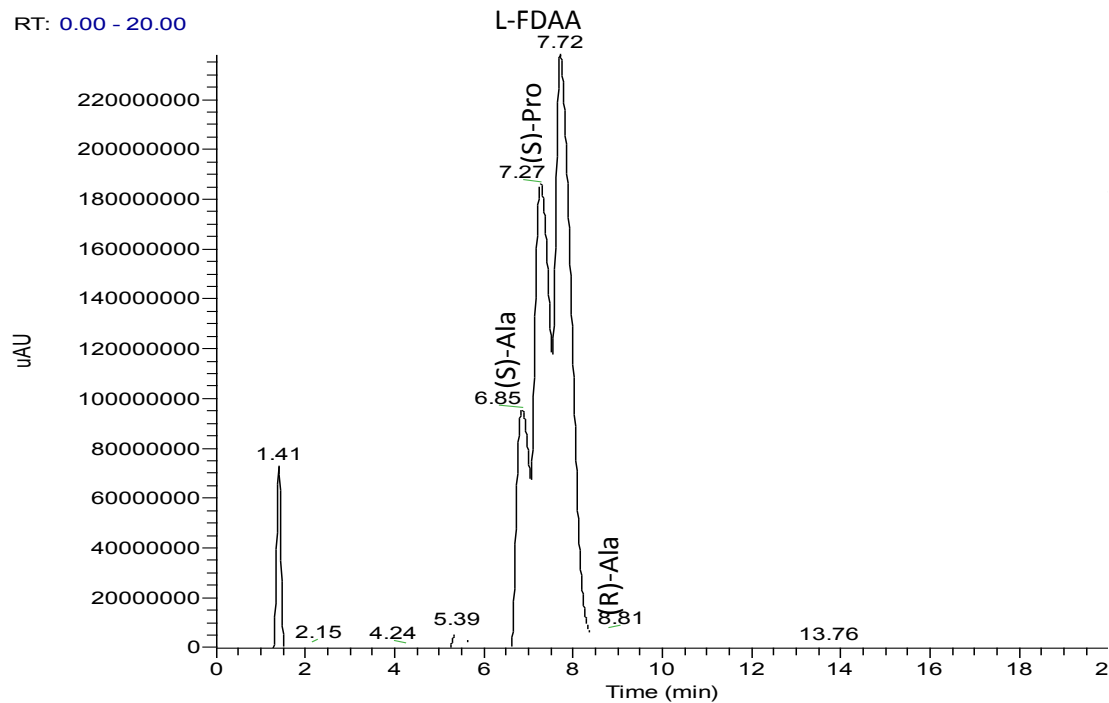
**Ugi product derived from Boc-proline, benzylamine, isocyanide derived from (S)-N-formylalanine methyl ester, and cyclohexanone (60 min precondensation)**



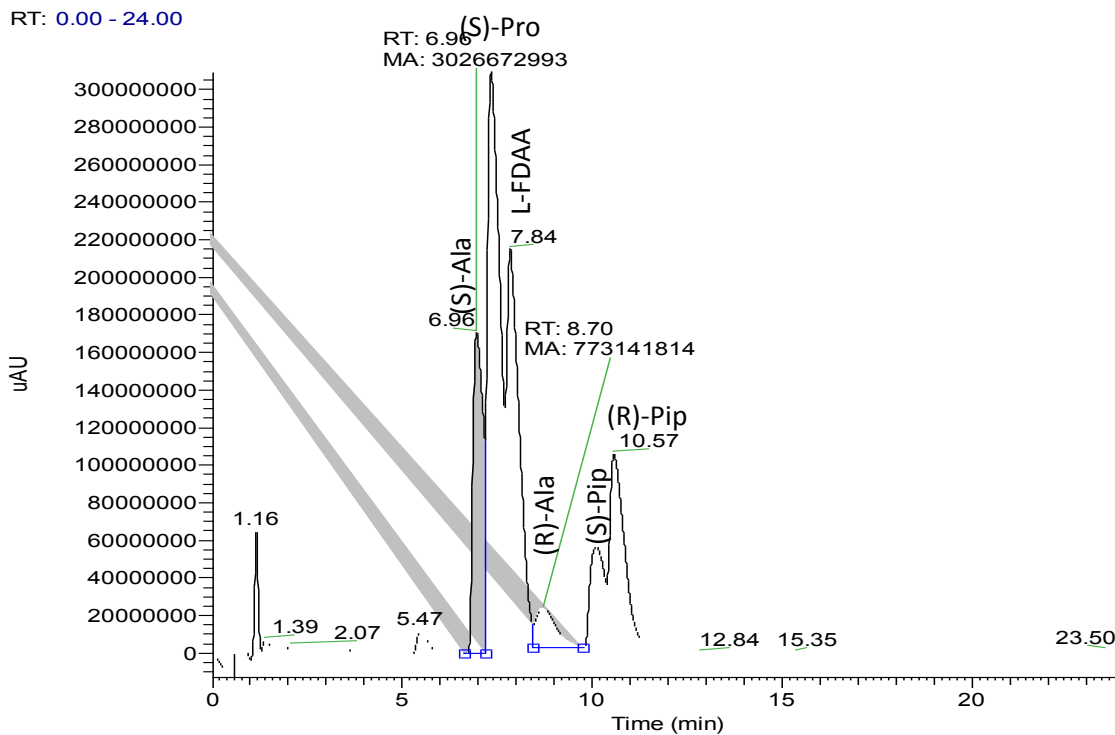
**Ugi product derived from Boc-proline, benzylamine, isocyanide derived from (S)-N-formylalanine methyl ester, and cyclohexanone (30 min precondensation)**



**Ugi product derived from Boc-proline, benzylamine, isocyanide derived from (S)-N-formylalanine methyl ester, and cyclohexanone (0 min precondensation)**

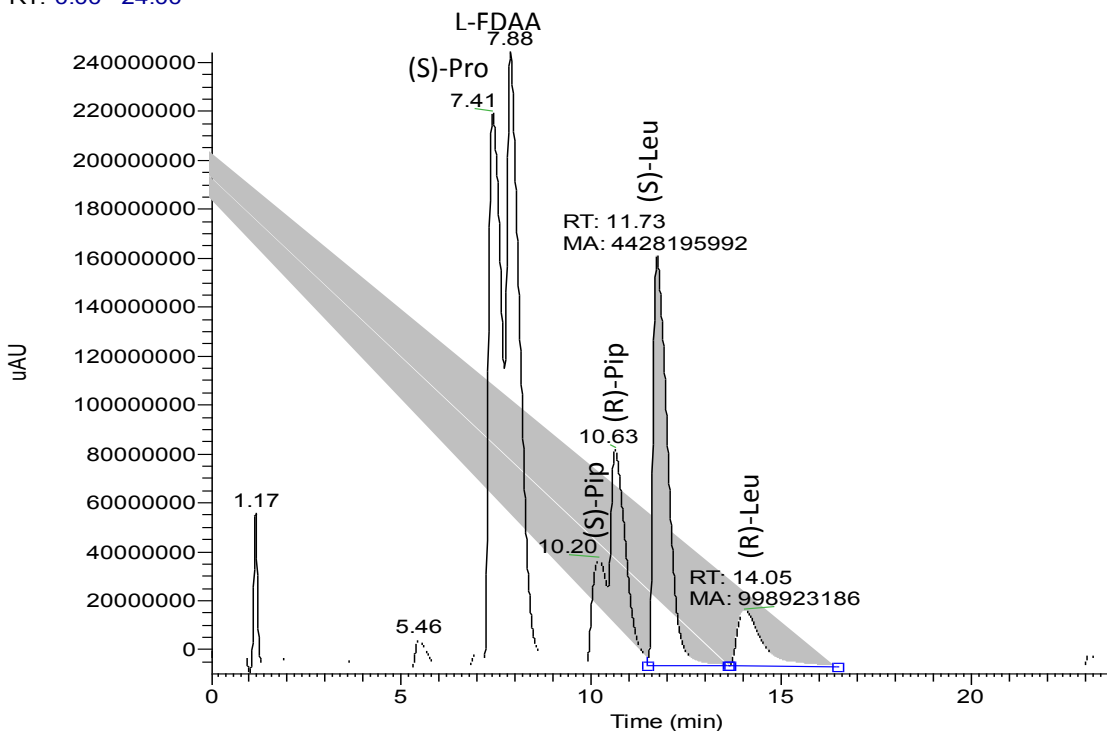


**Joullié-Ugi product derived from Boc-proline, isocyanide derived from (S)-N-formylalanine methyl ester, and excess triperideine**



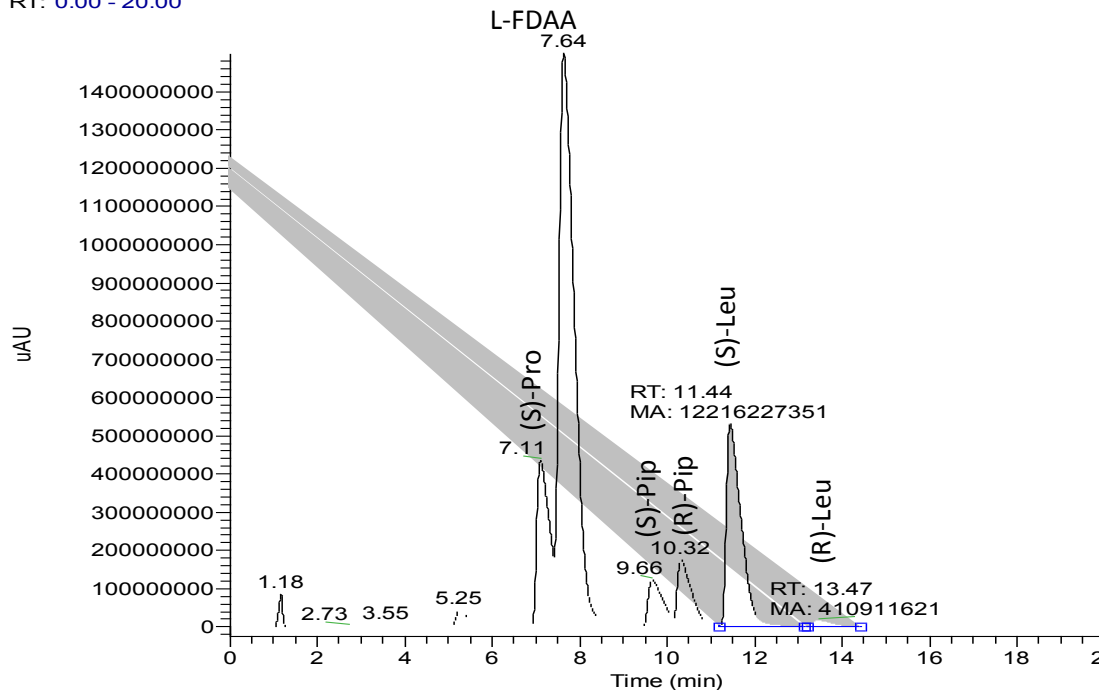
**Joullié-Ugi product derived from Boc-proline, isocyanide derived from (S)-N-formylleucine methyl ester, and excess triperideine**

RT: 0.00 - 24.00



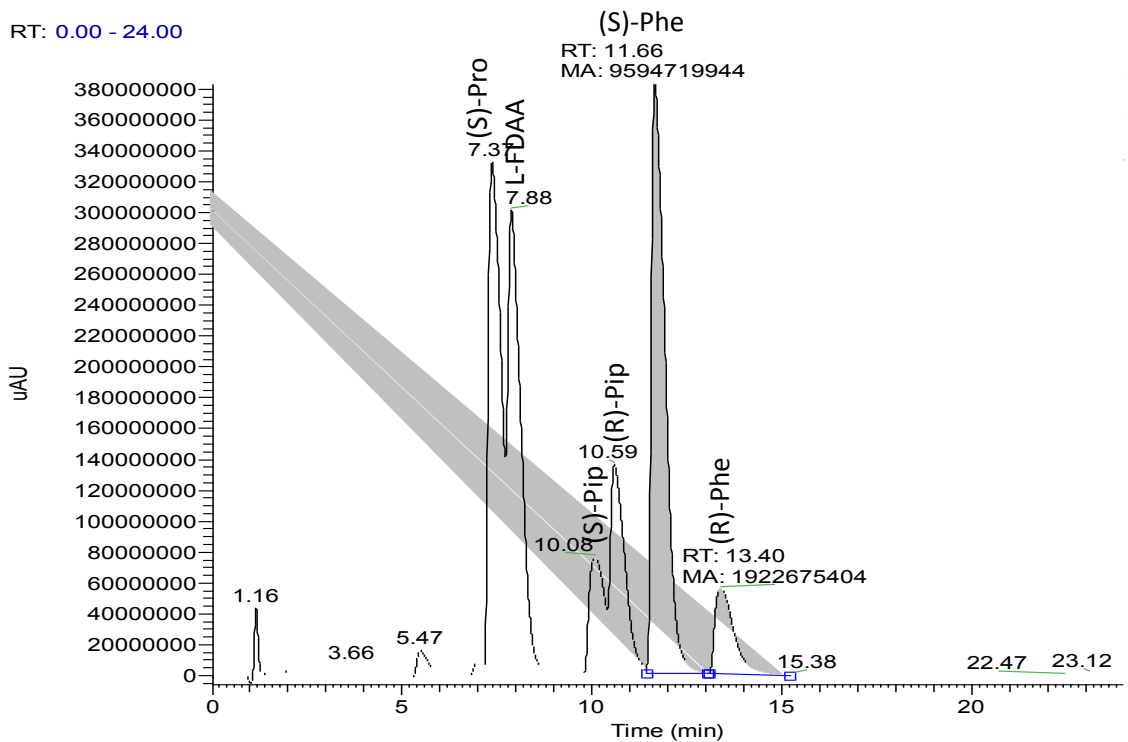
**Joullié-Ugi product derived from Boc-proline, isocyanide derived from (S)-N-formylleucine methyl ester, and equimolar triperideine**

RT: 0.00 - 20.00

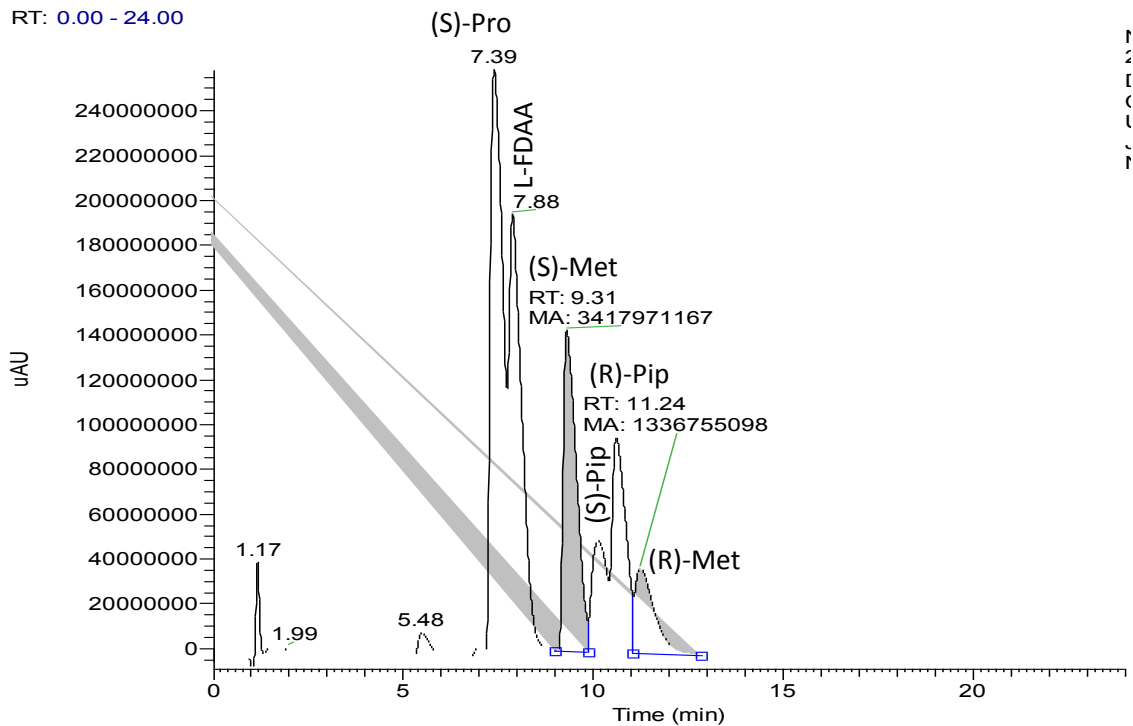




**Joullié-Ugi product derived from Boc-proline, isocyanide derived from (S)-*N*-formylphenylalanine methyl ester, and excess triperideine**



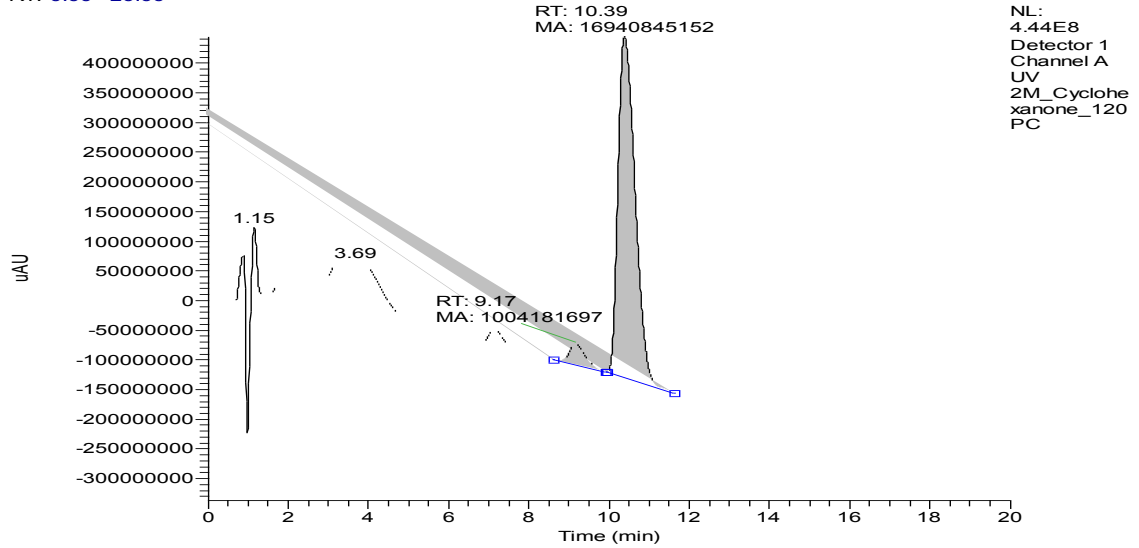
**Joullié-Ugi product derived from Boc-proline, isocyanide derived from (S)-*N*-formylmethionine methyl ester, and excess triperideine**



## LC Chromatograms

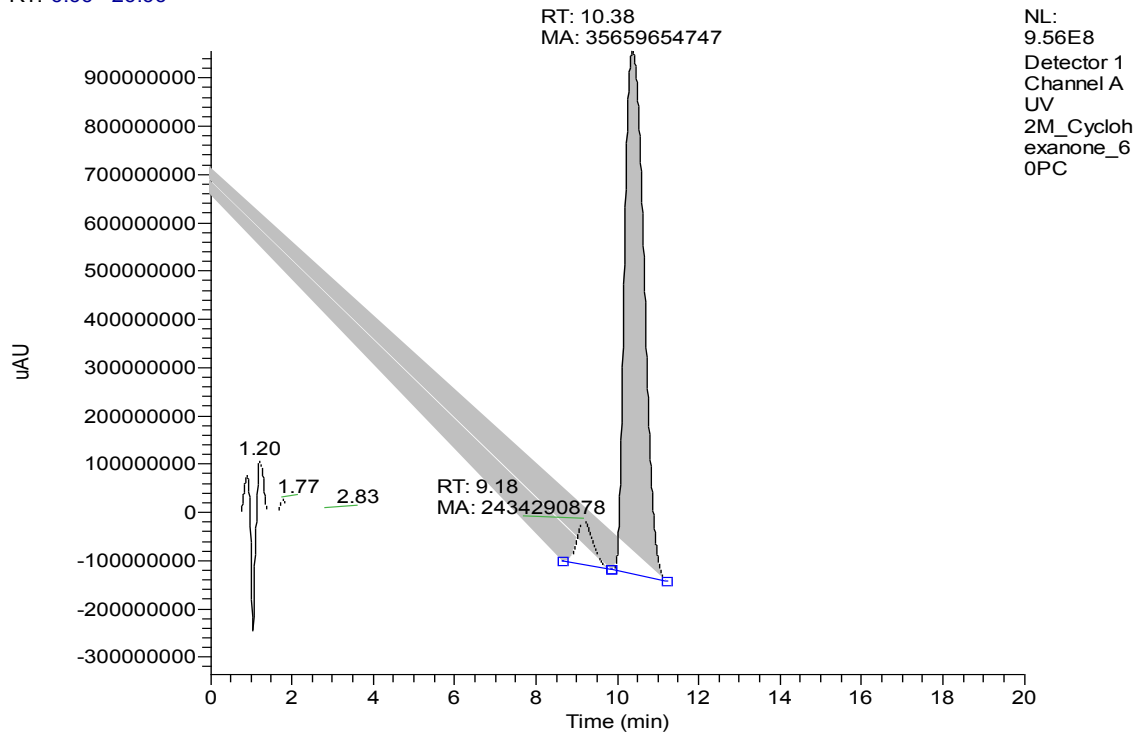
**Ugi product derived from Boc-proline, benzylamine, isocyanide derived from (S)-N-formylalanine methyl ester, and cyclohexanone (120 min precondensation)**

RT: 0.00 - 20.00



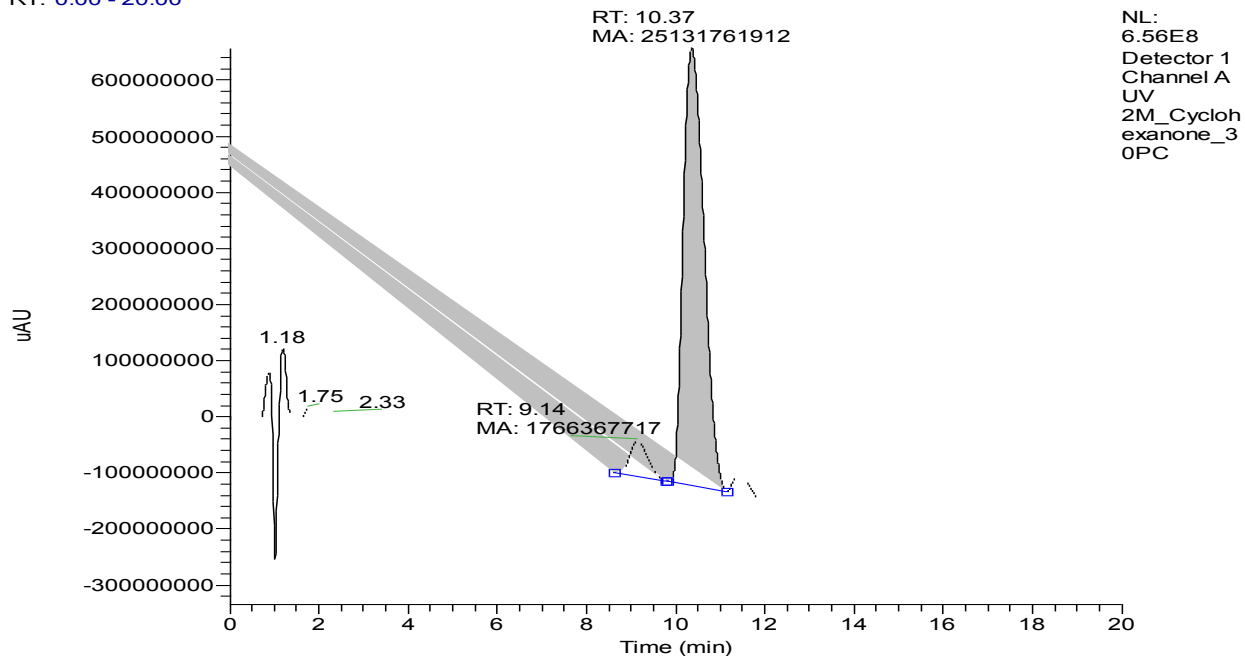
**Ugi product derived from Boc-proline, benzylamine, isocyanide derived from (S)-N-formylalanine methyl ester, and cyclohexanone (60 min precondensation)**

RT: 0.00 - 20.00



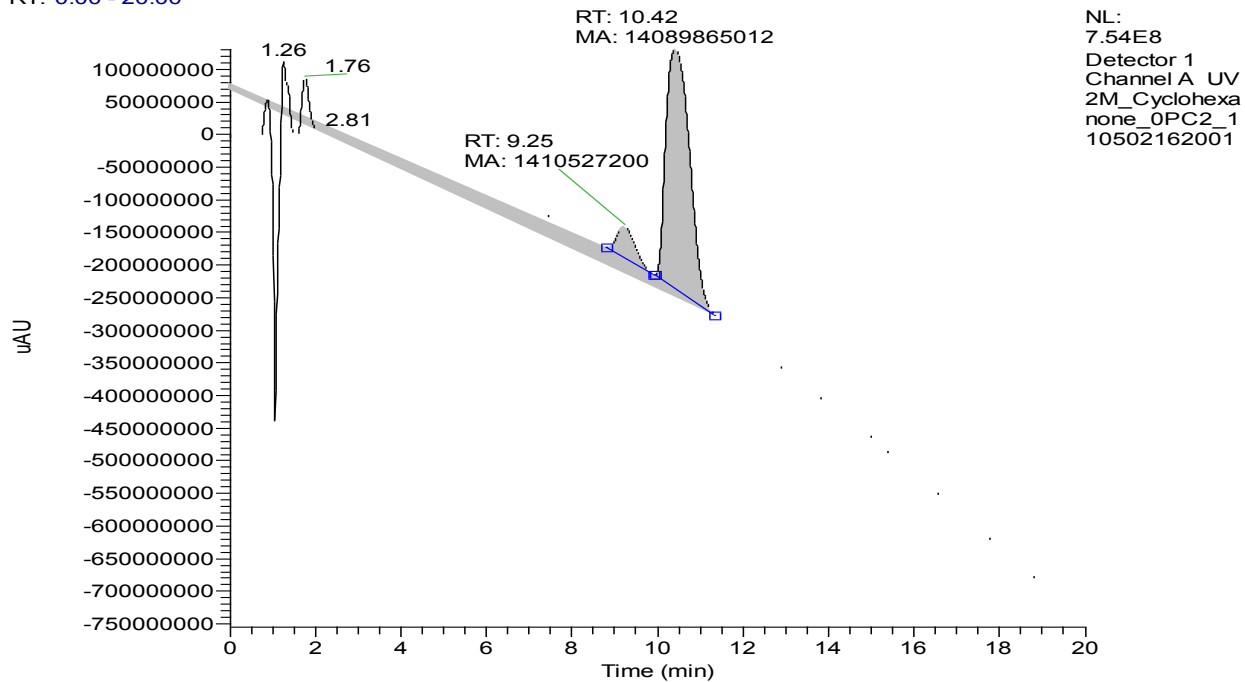
**Ugi product derived from Boc-proline, benzylamine, isocyanide derived from (S)-N-formylalanine methyl ester, and cyclohexanone (30 min precondensation)**

RT: 0.00 - 20.00



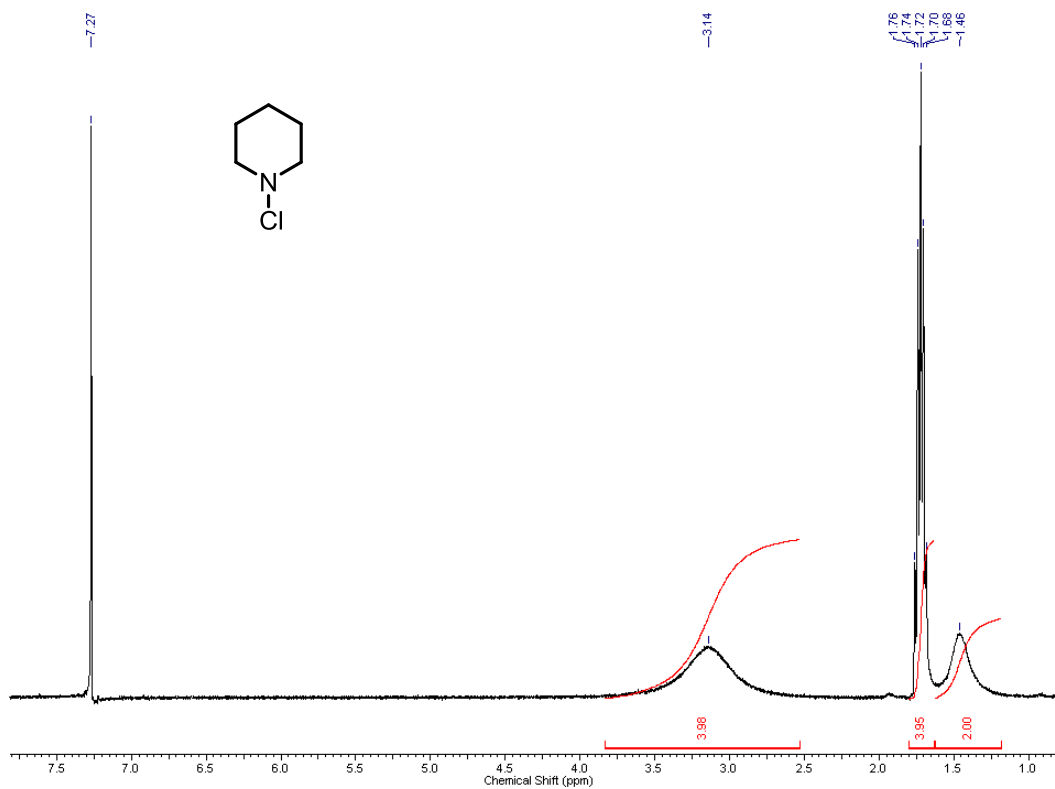
**Ugi product derived from Boc-proline, benzylamine, isocyanide derived from (S)-N-formylalanine methyl ester, and cyclohexanone (0 min precondensation)**

RT: 0.00 - 20.00

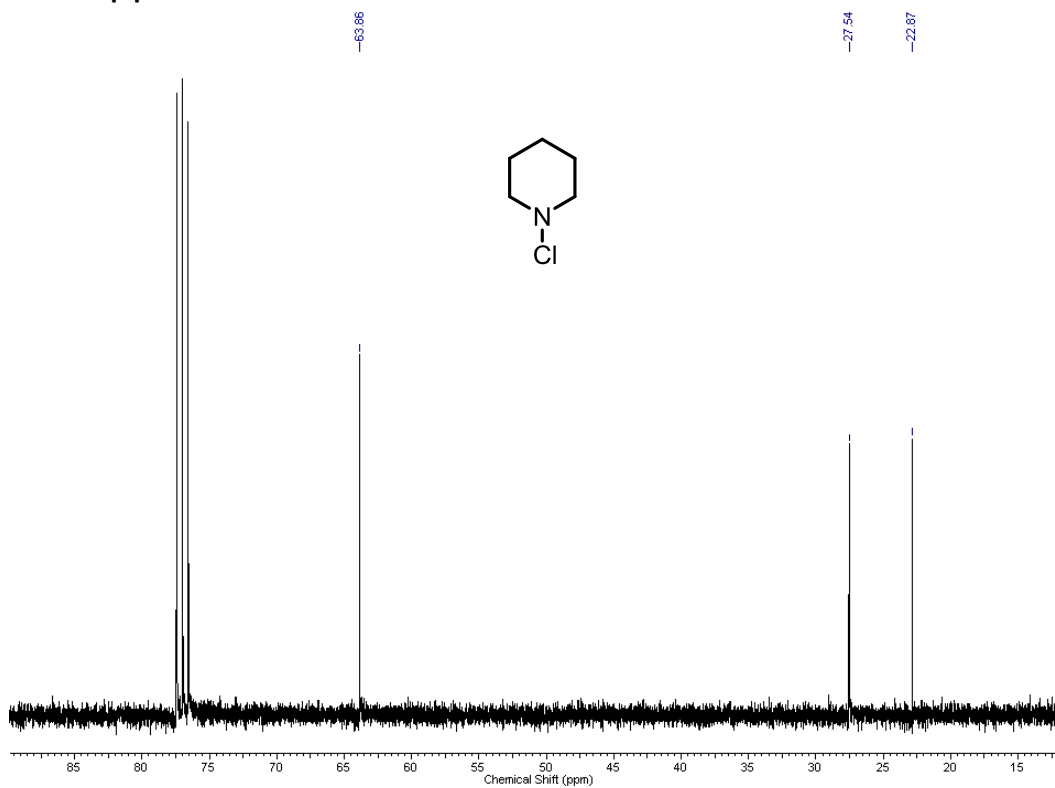


## **Chapter 5 – Synthesis of ADEPs with Conformationally Constrained Peptidolactones**

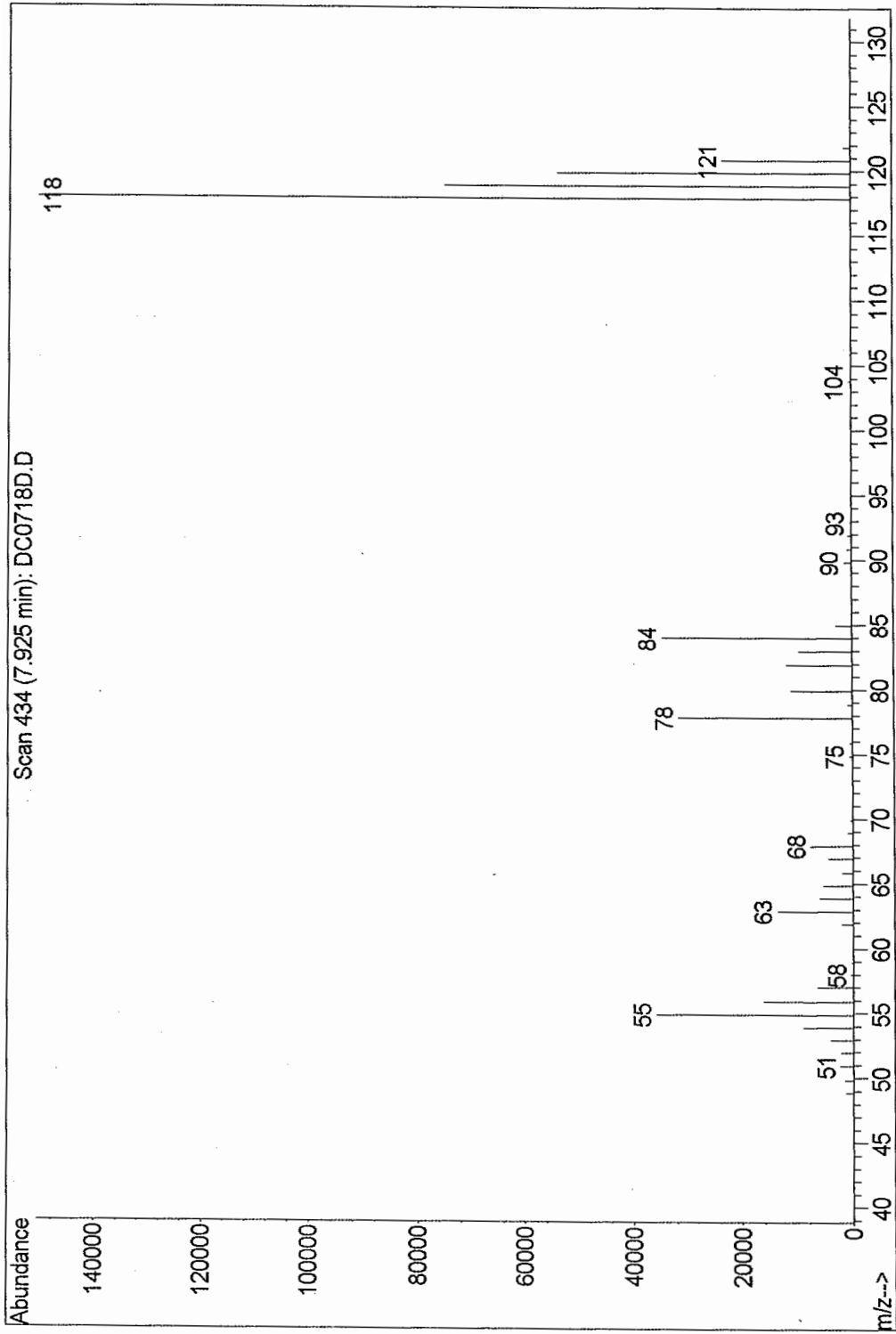
### *N*-chloropiperidine <sup>1</sup>H NMR



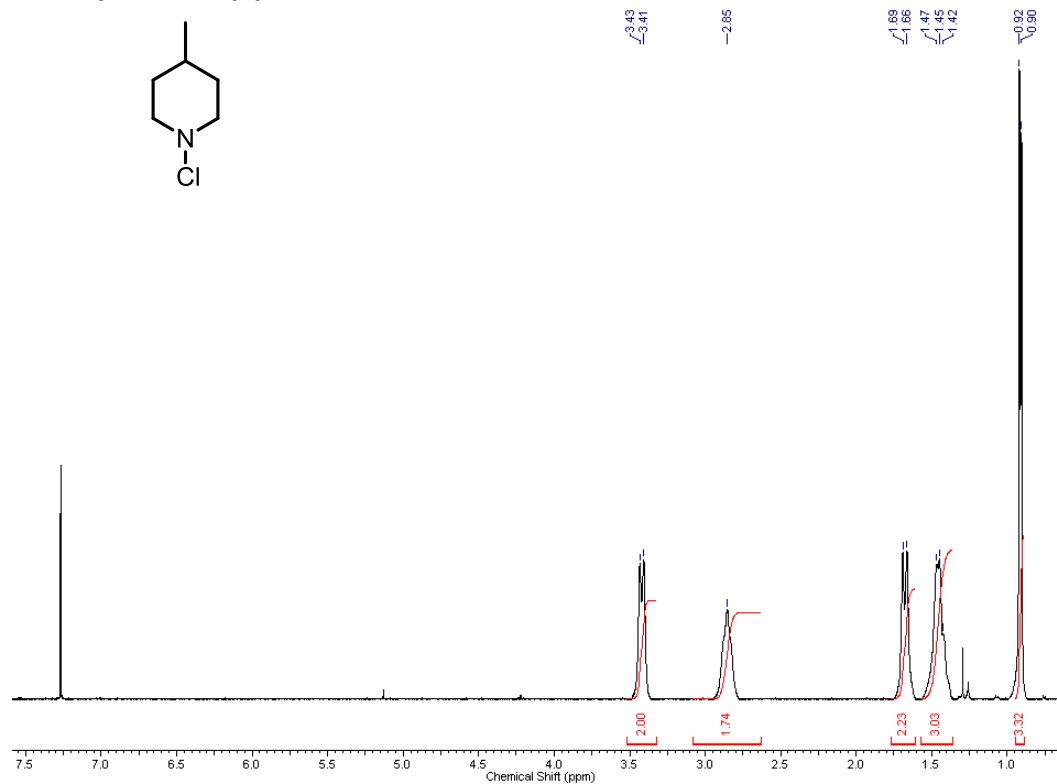
### *N*-chloropiperidine <sup>13</sup>C NMR



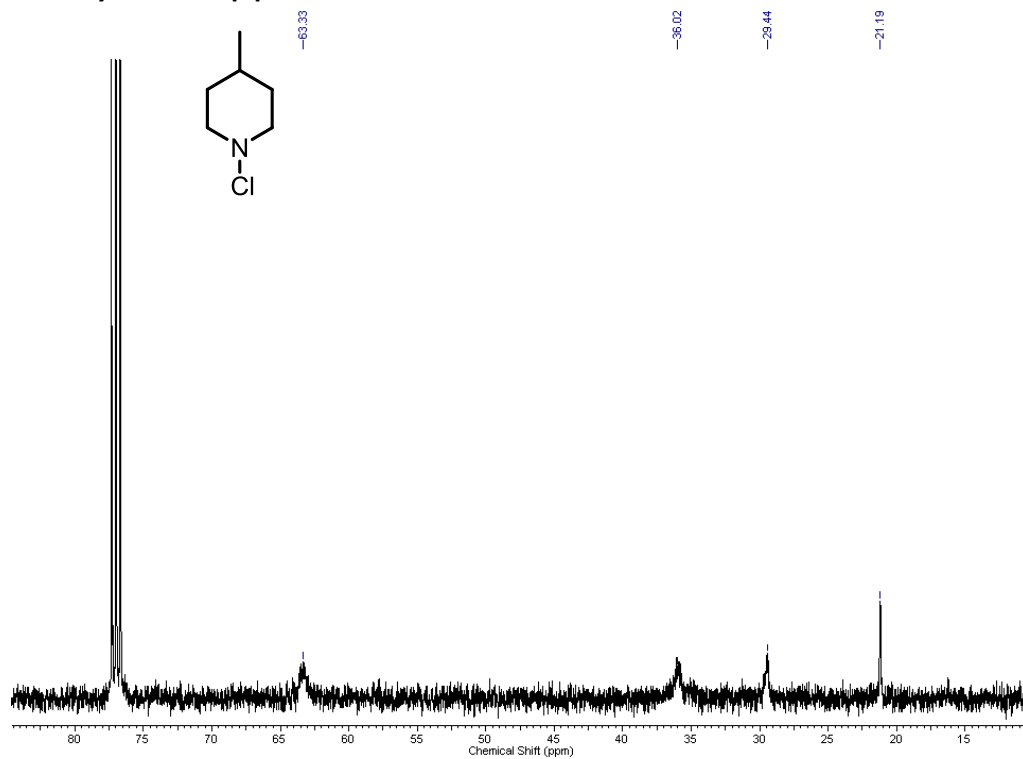
N-chloropiperidine EI mas spectrum



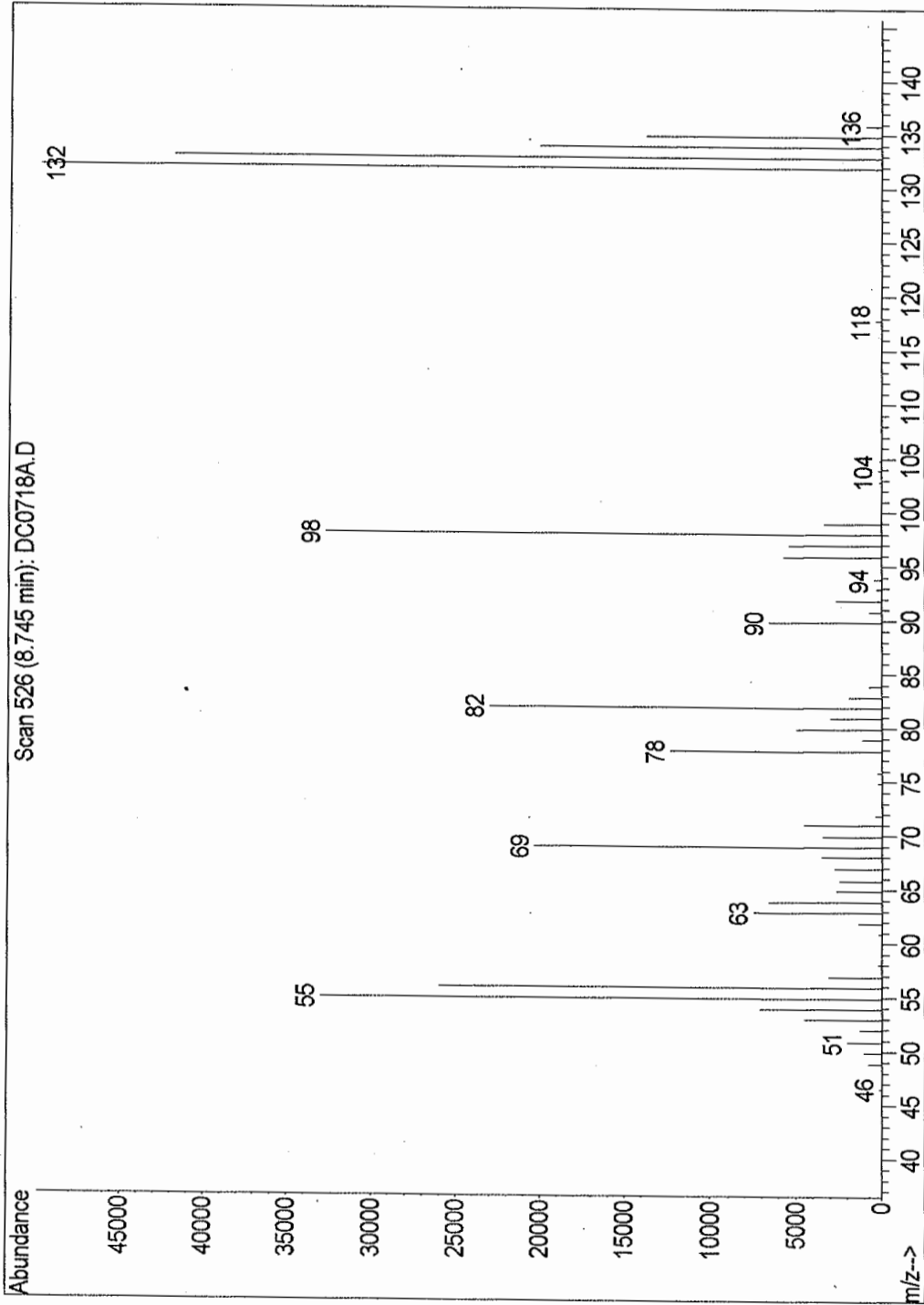
### 4-methyl-N-chloropiperidine <sup>1</sup>HNMR



### 4-methyl-N-chloropiperidine <sup>13</sup>CNMR

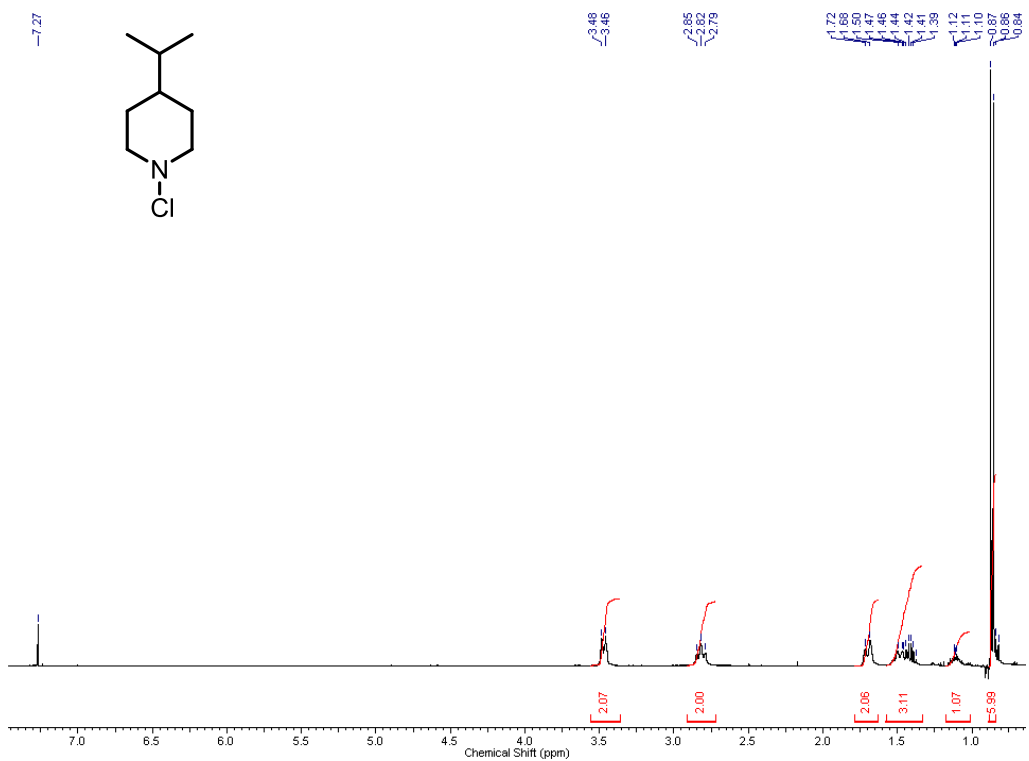


4-methyl-N-chloropiperidine EI mass spectrum

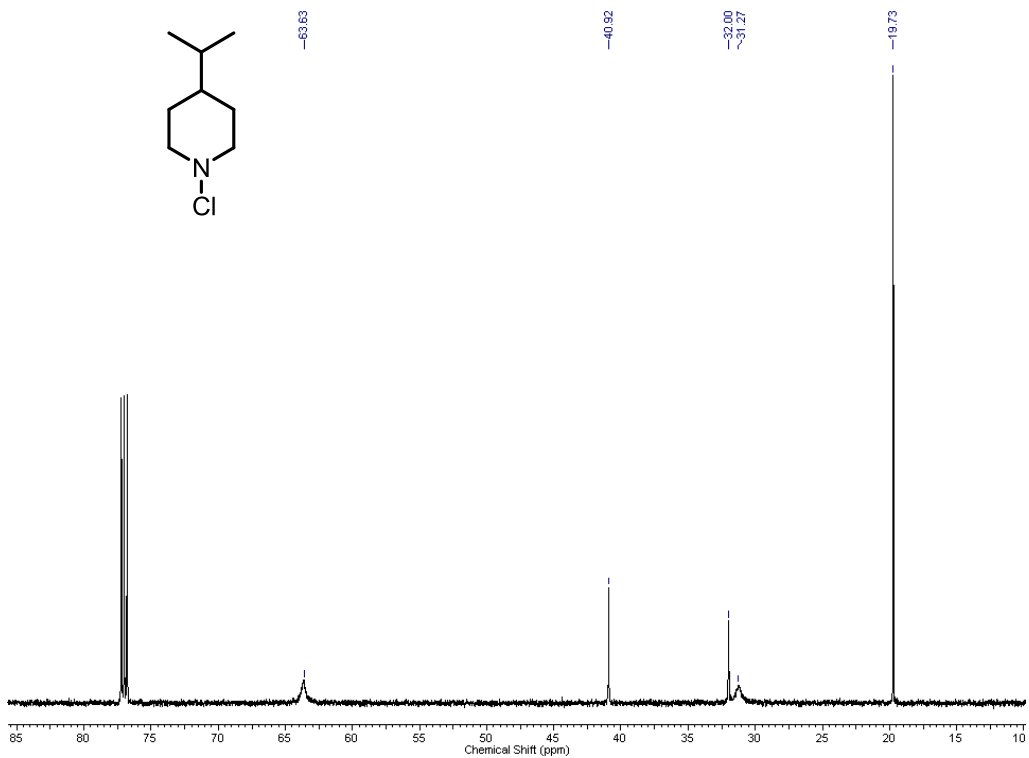




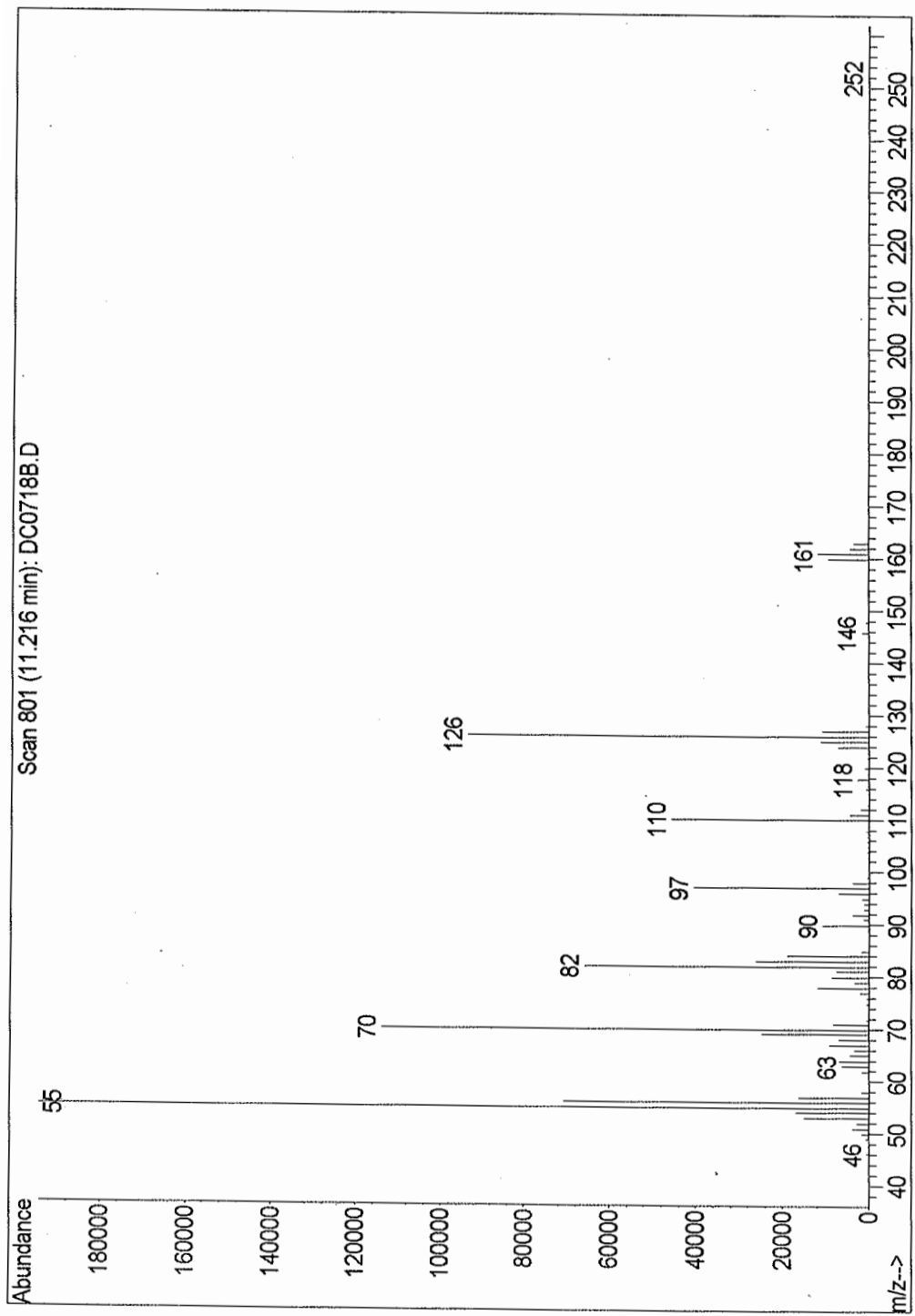
### 4-isopropyl-N-chloropiperidine <sup>1</sup>H NMR

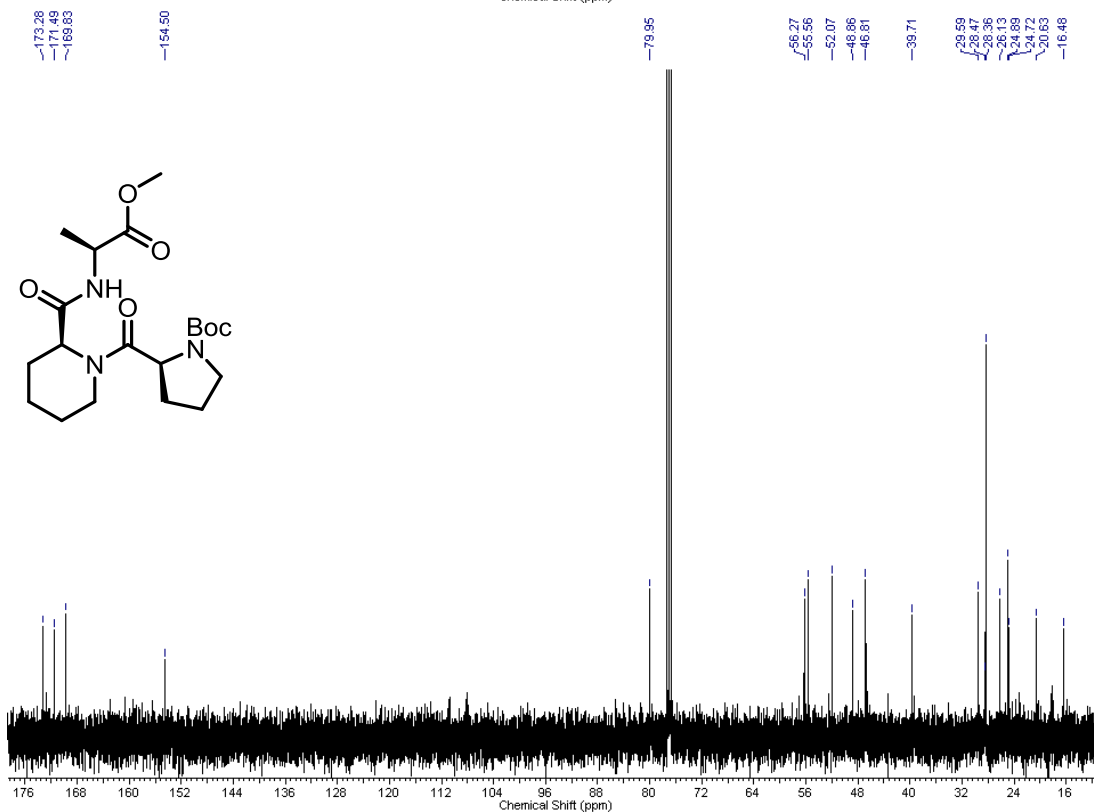
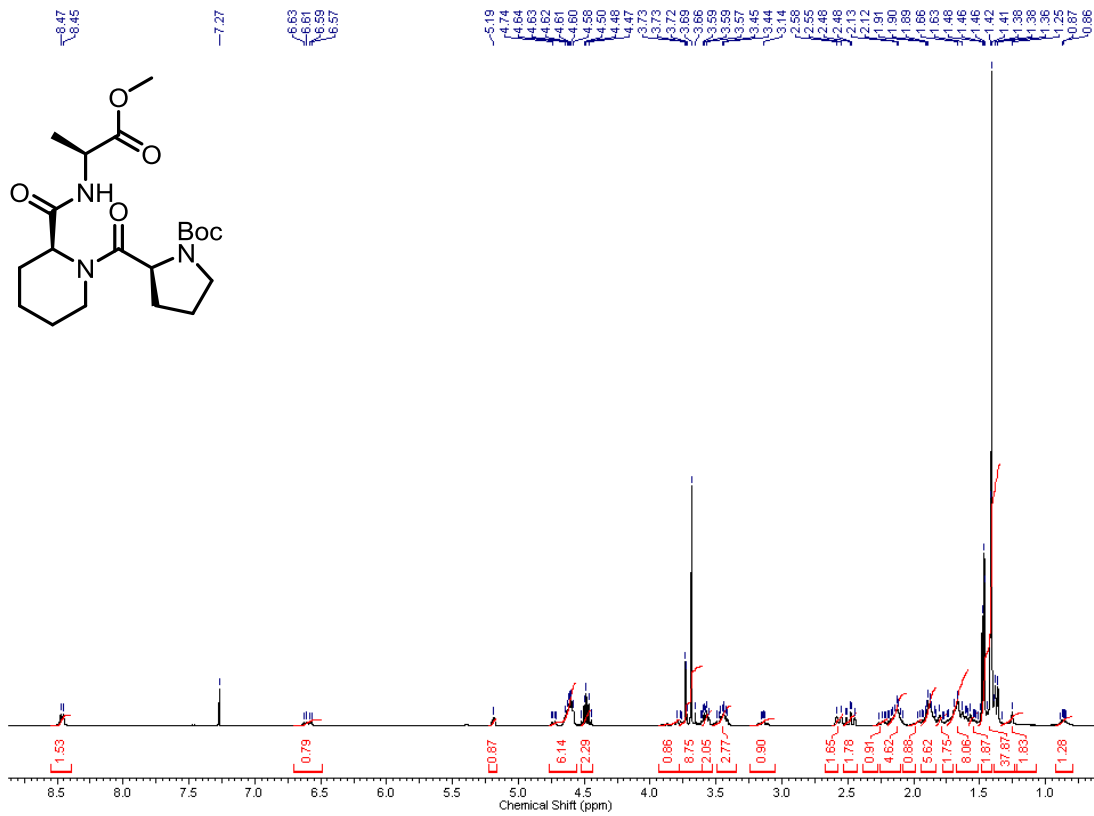


### 4-isopropyl-N-chloropiperidine <sup>13</sup>C NMR

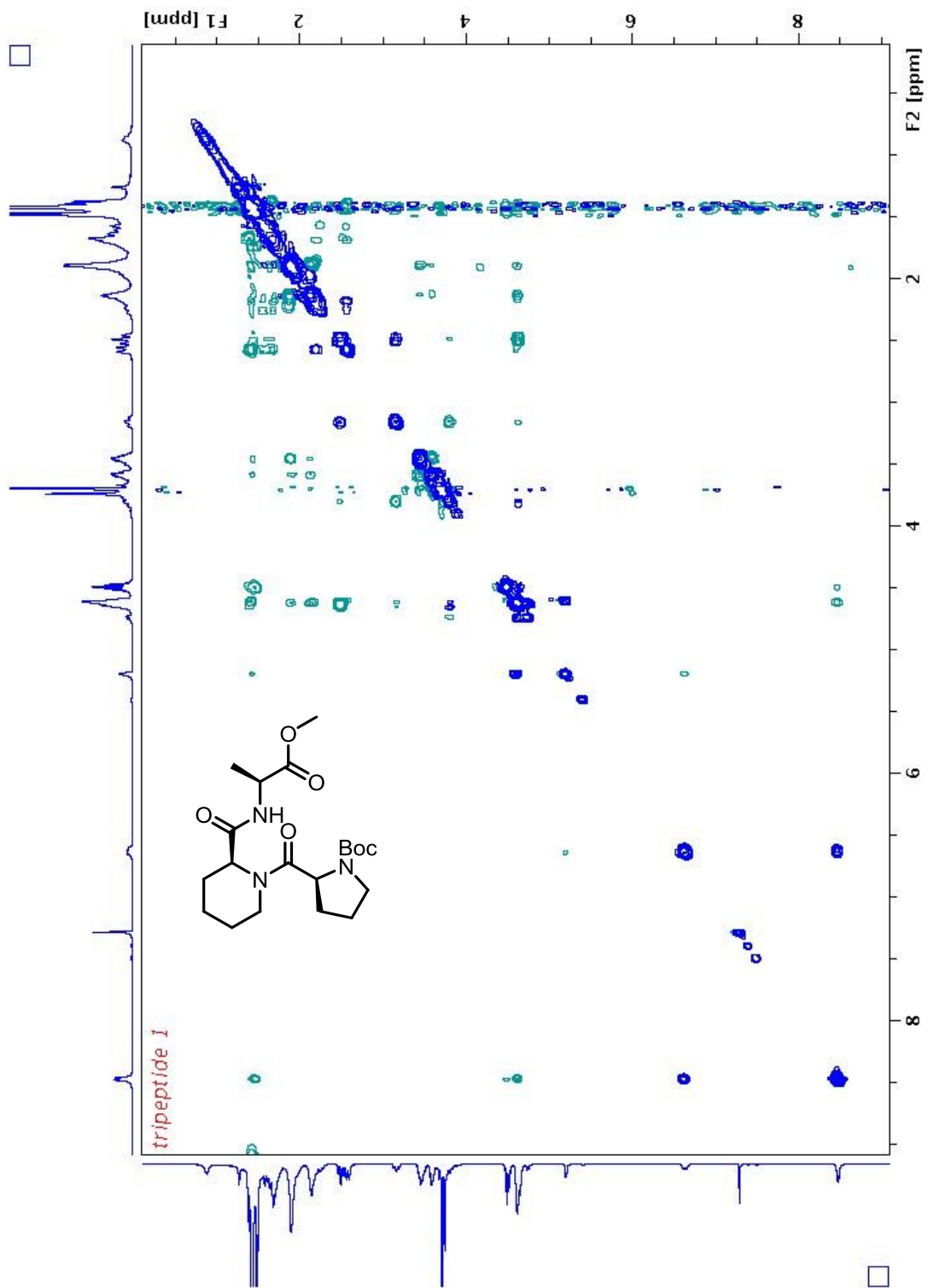


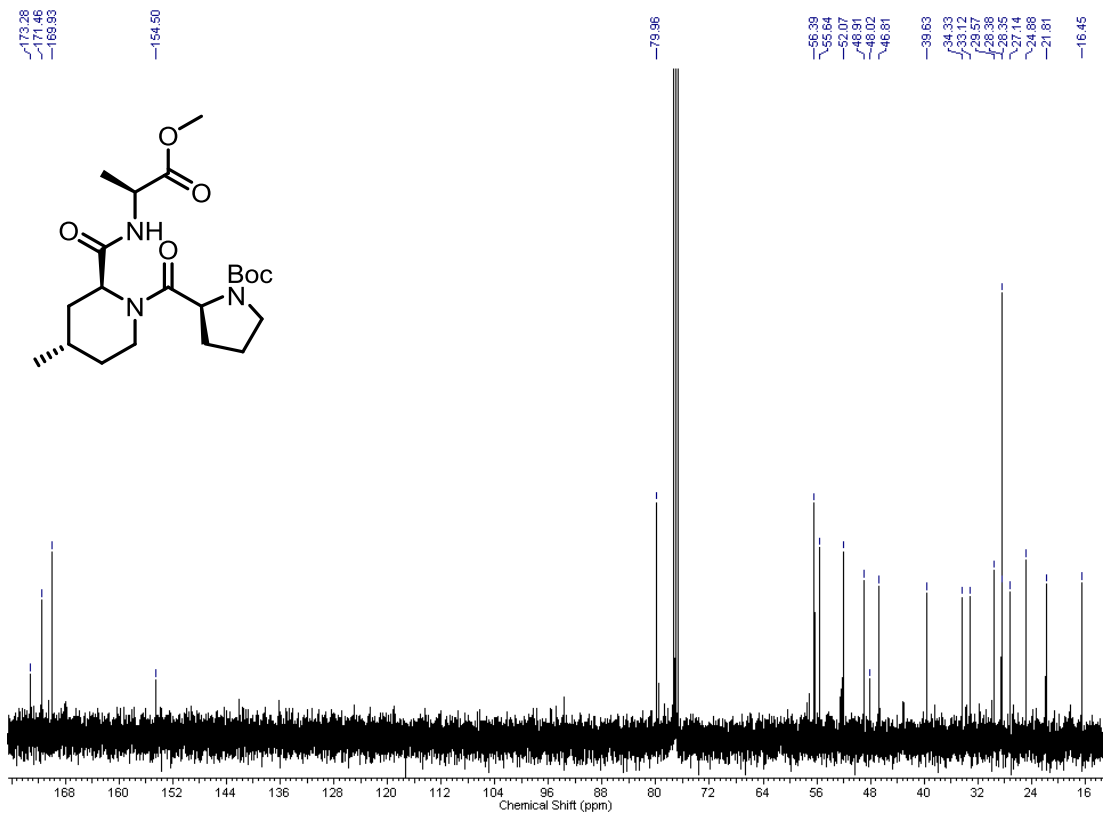
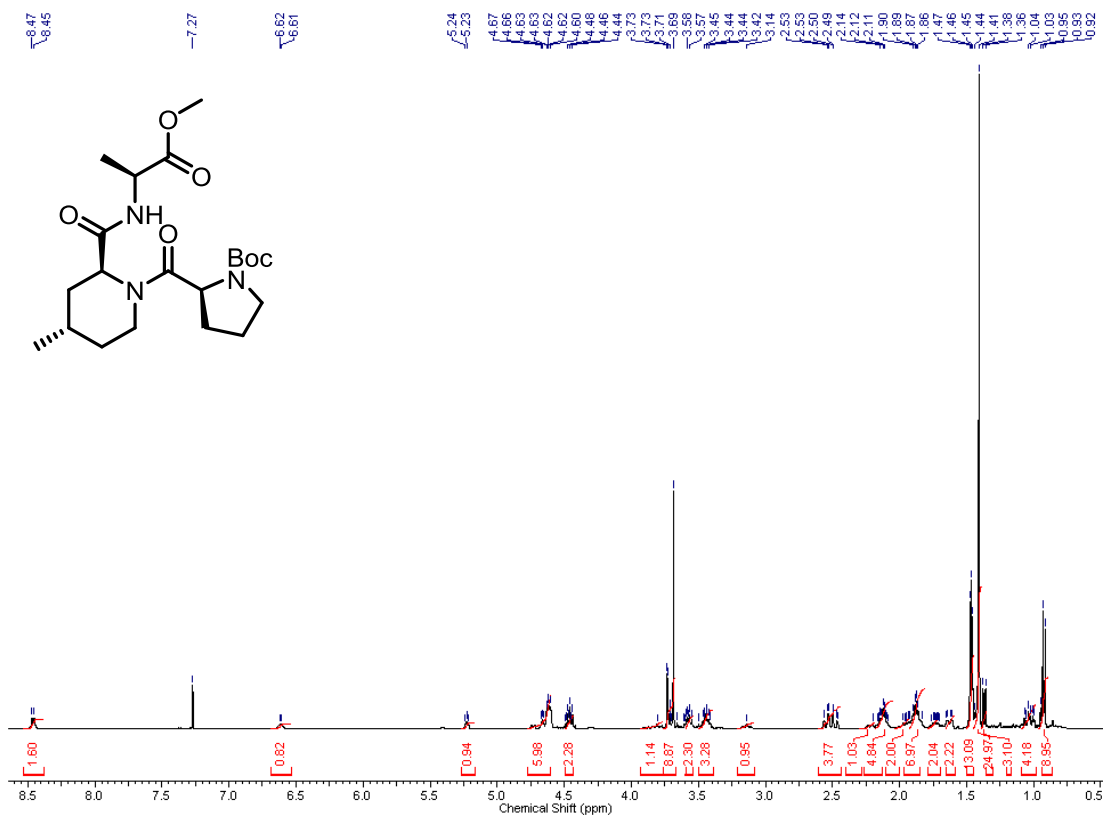
4-isopropyl-N-chloropiperidine EI mass spectrum



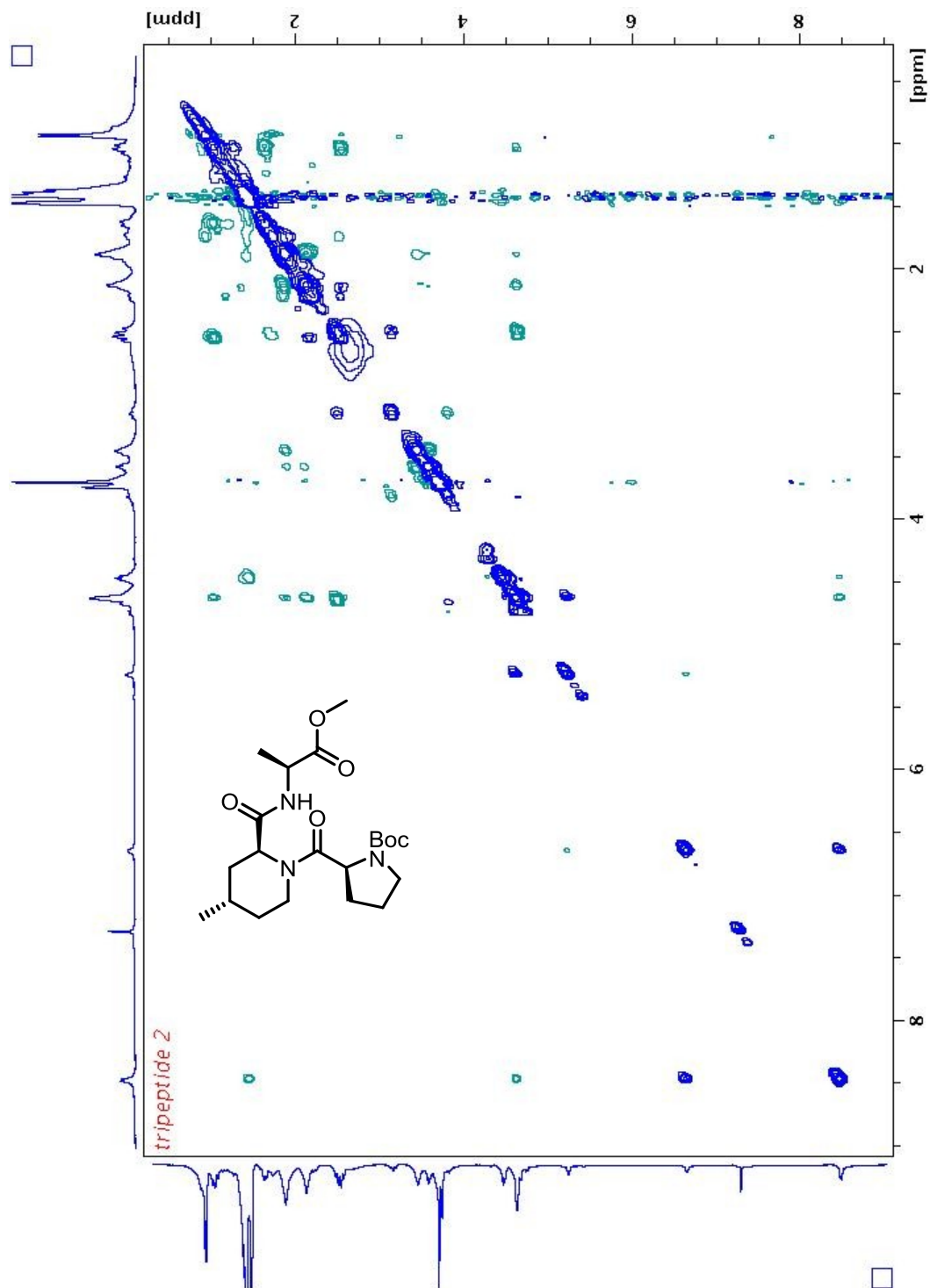


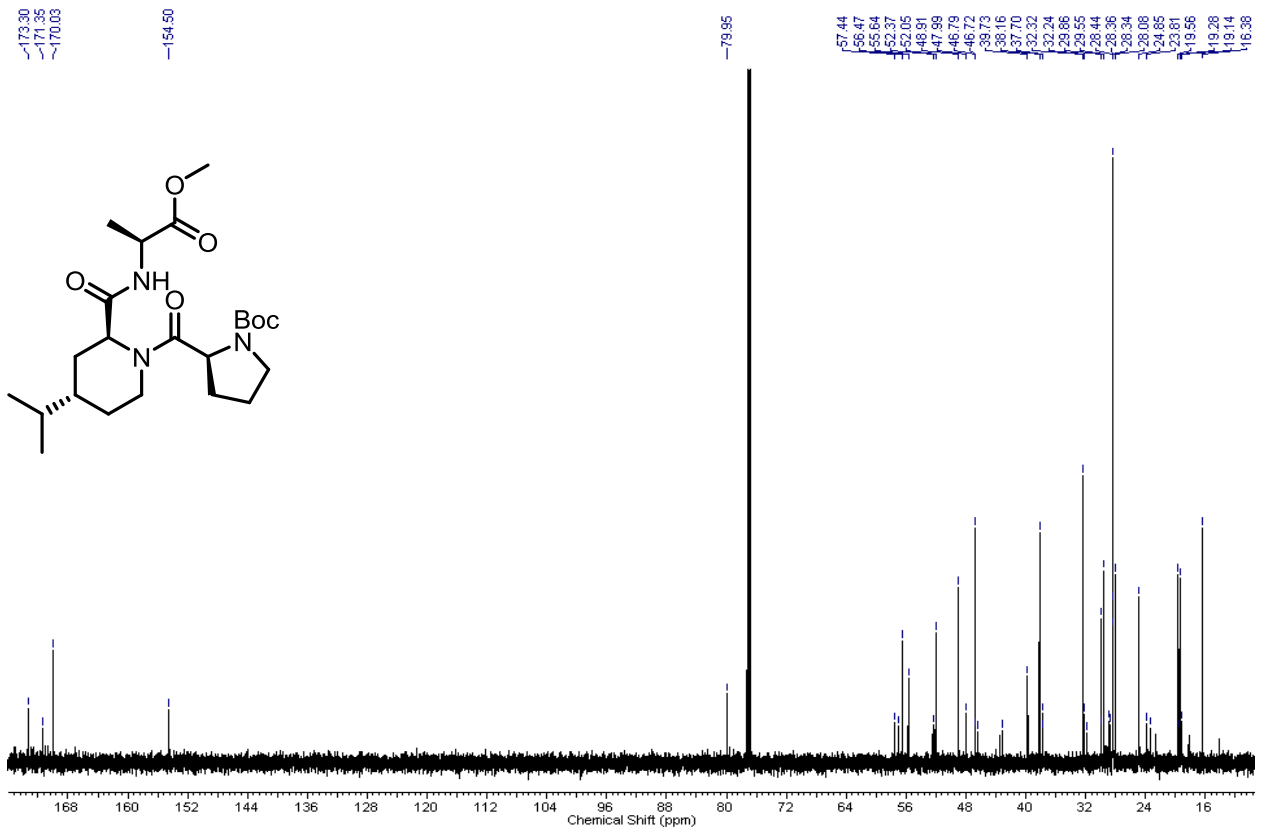
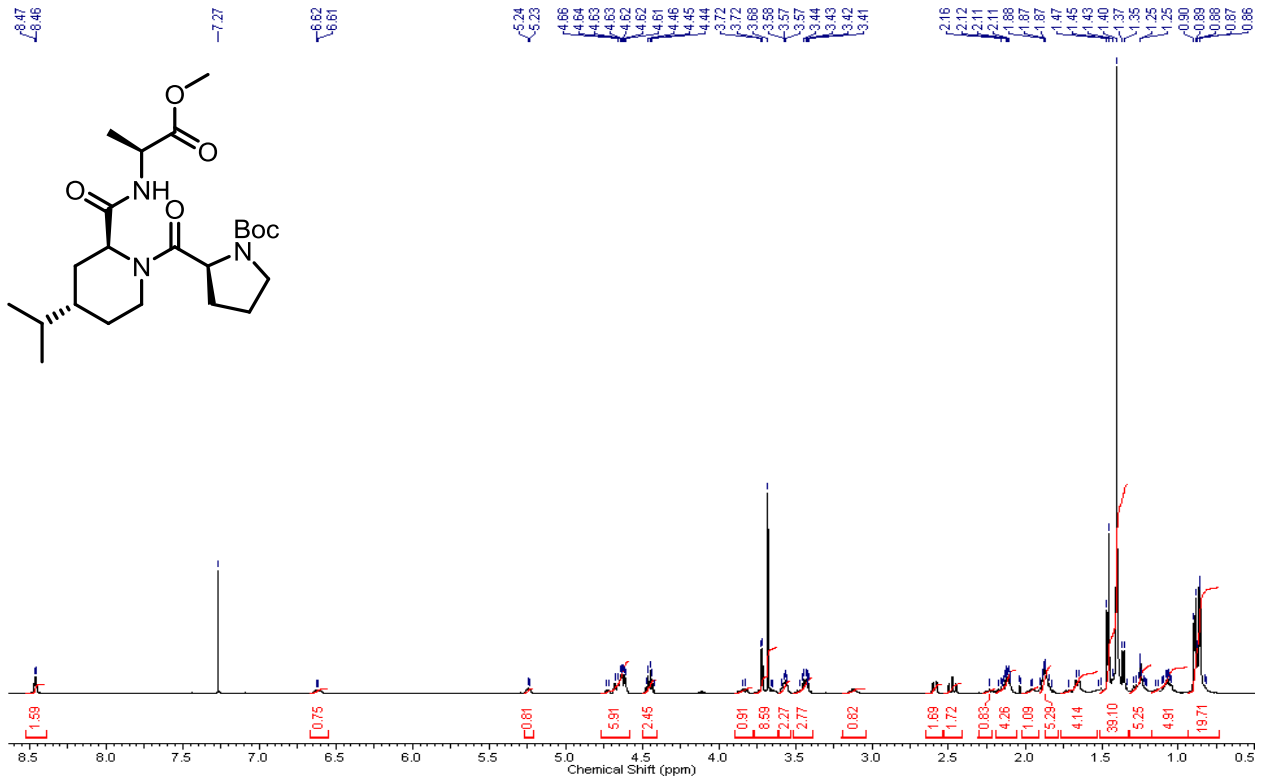
NOSEY spectrum: Exchange cross-peaks shown in blue, NOE cross-peaks shown in teal



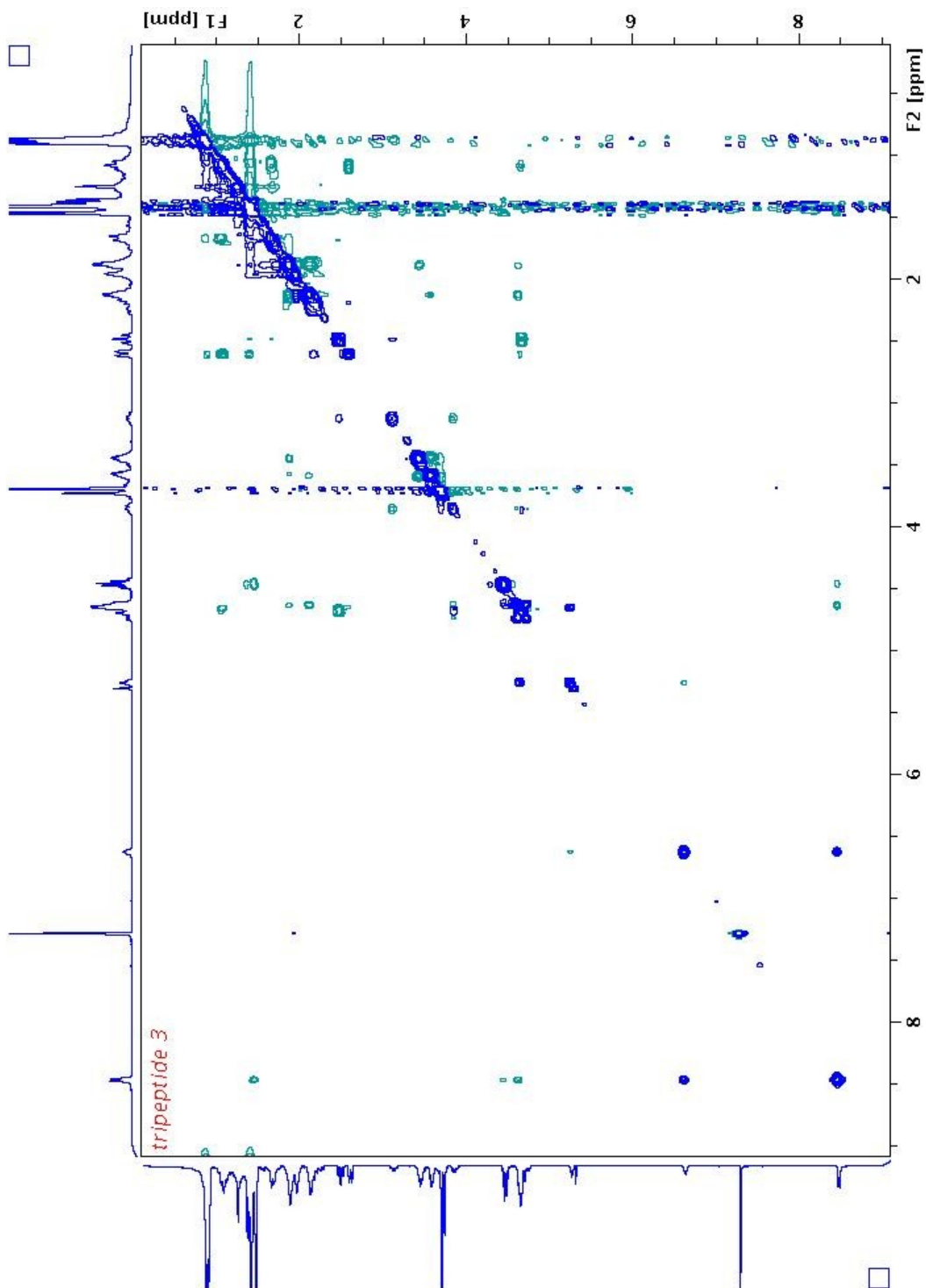


NOSEY spectrum: Exchange cross-peaks shown in blue, NOE cross-peaks shown in teal

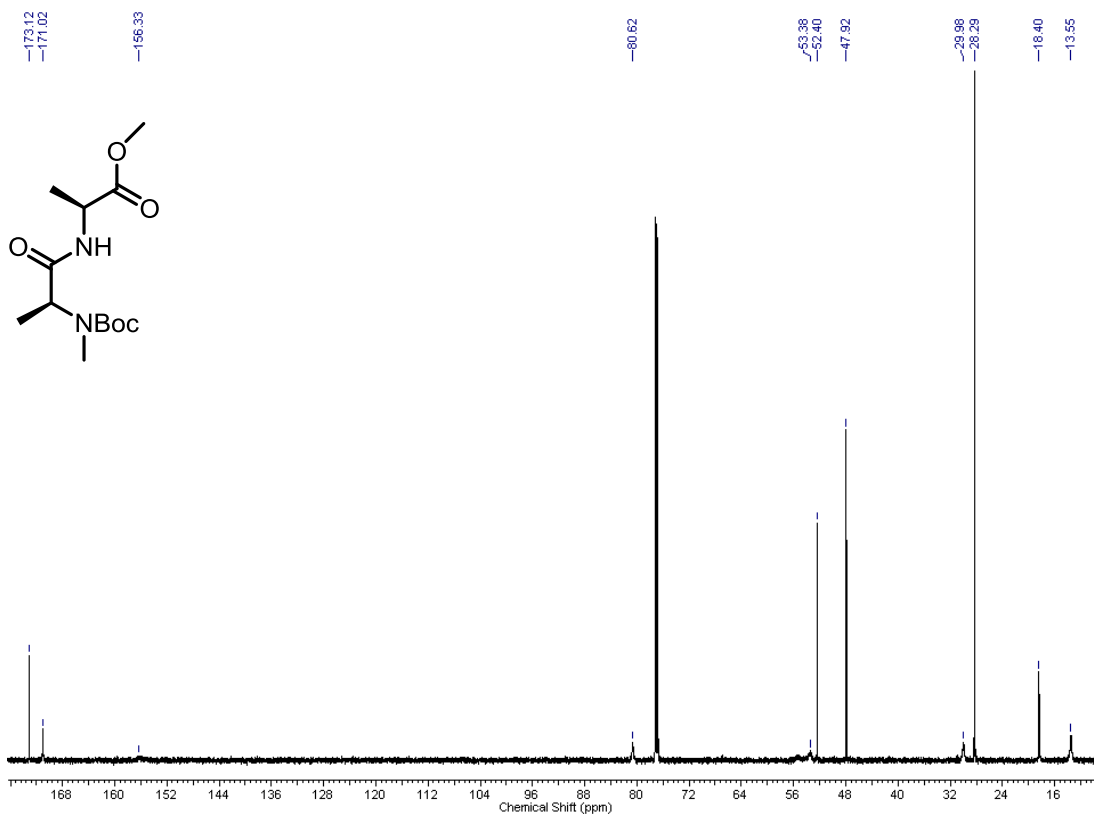
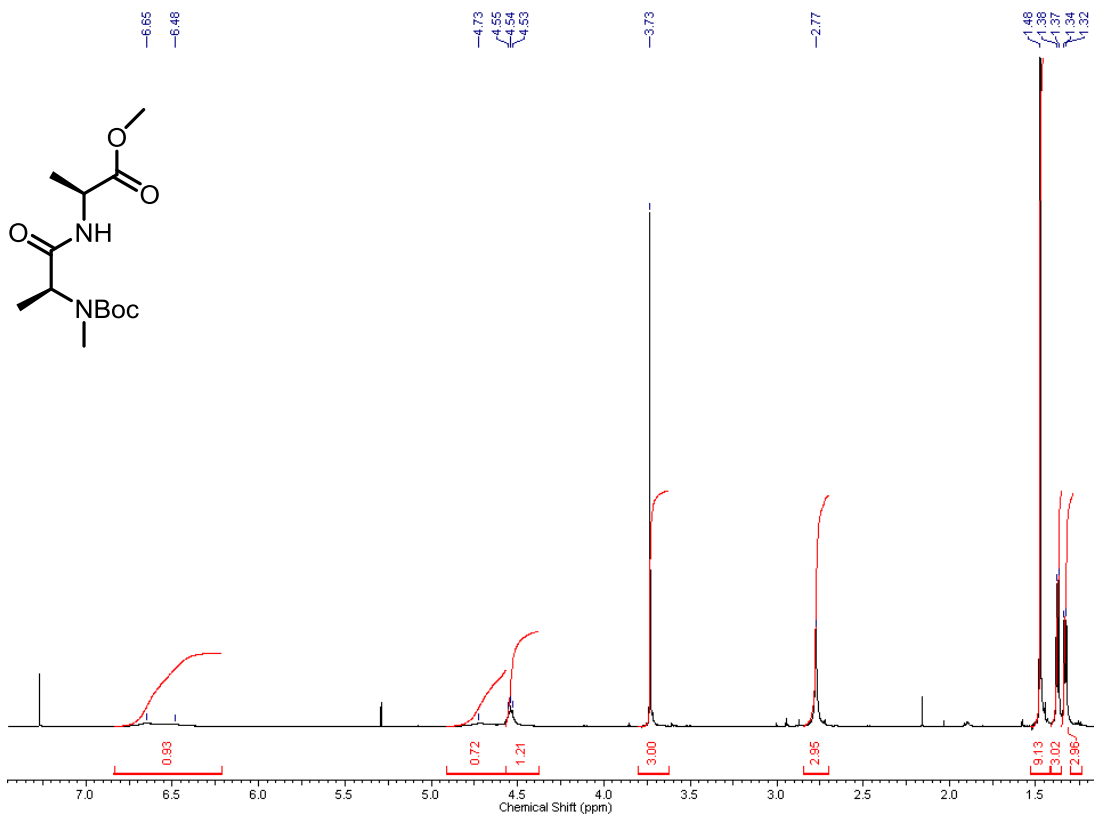


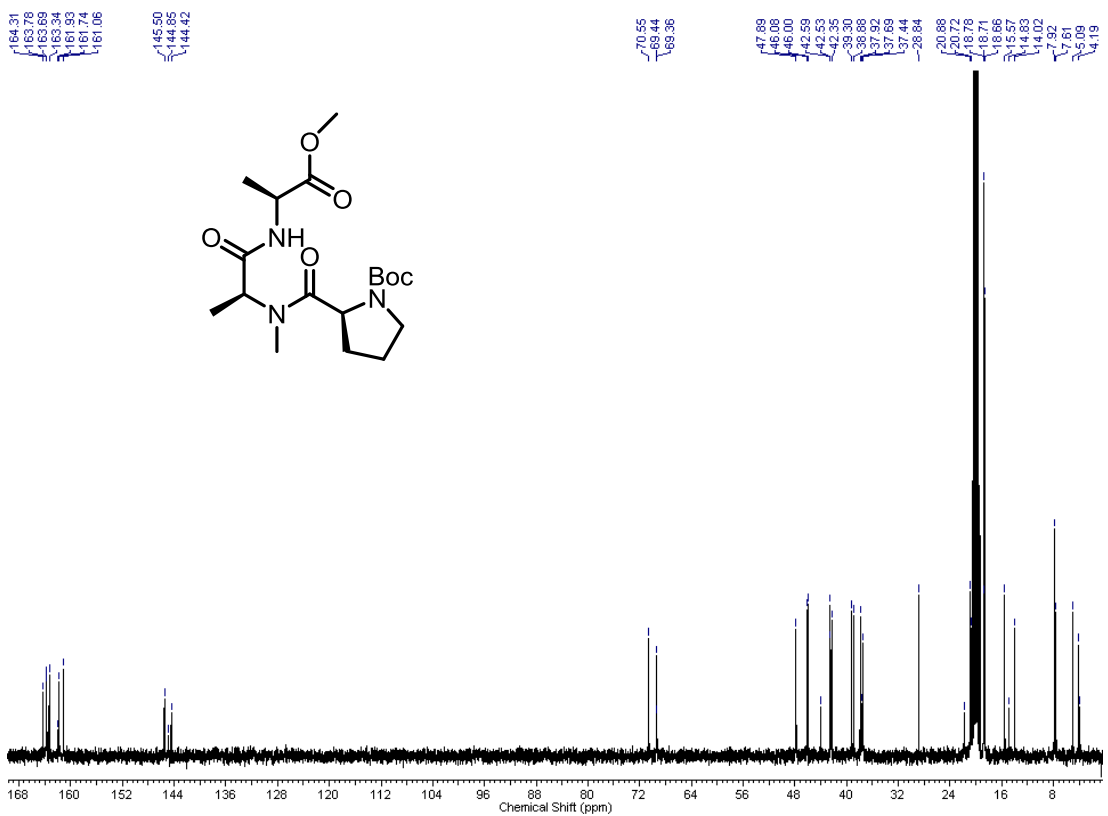
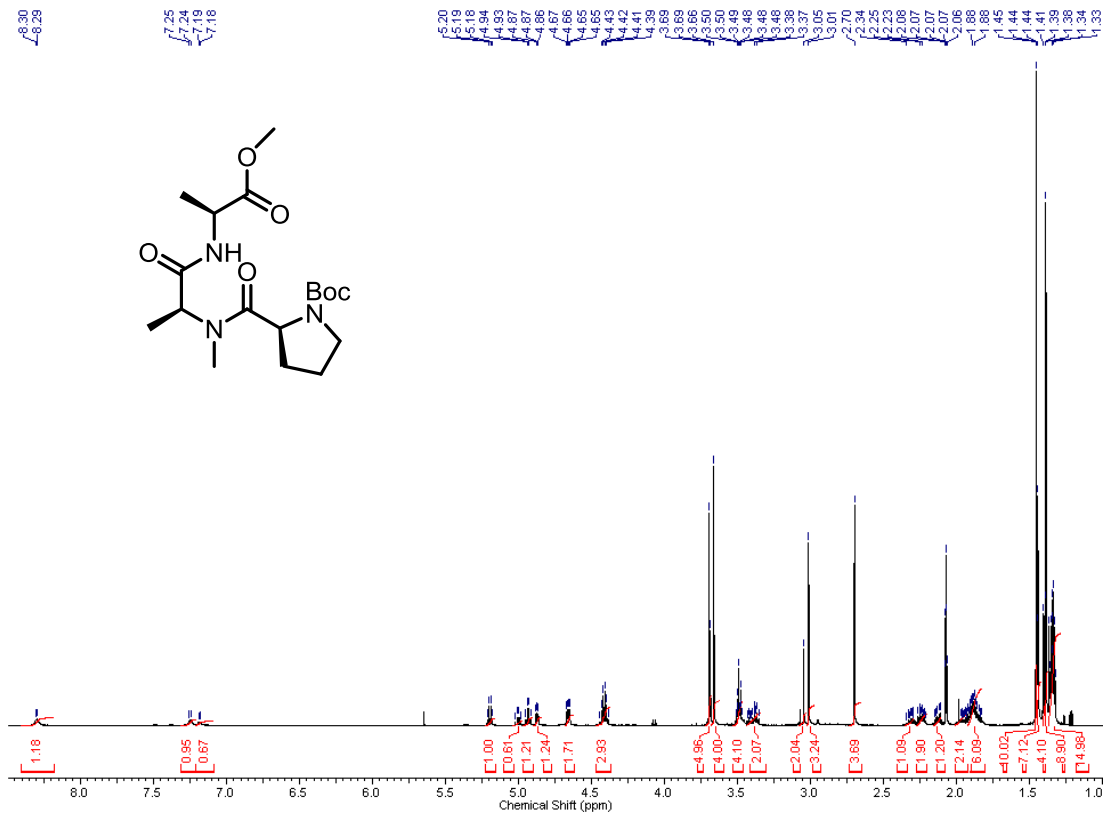


NOSEY spectrum: Exchange cross-peaks shown in blue, NOE cross-peaks shown in teal

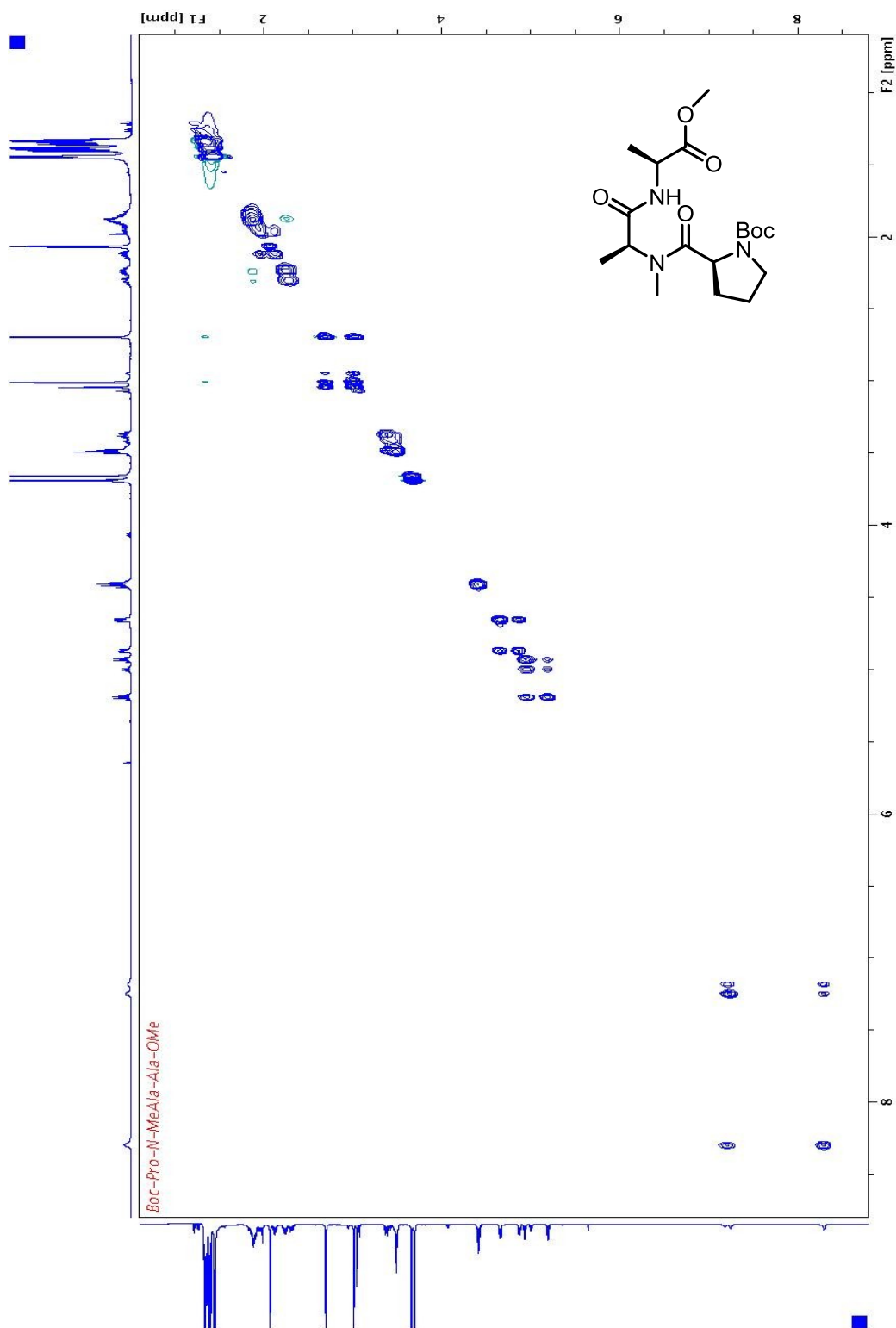


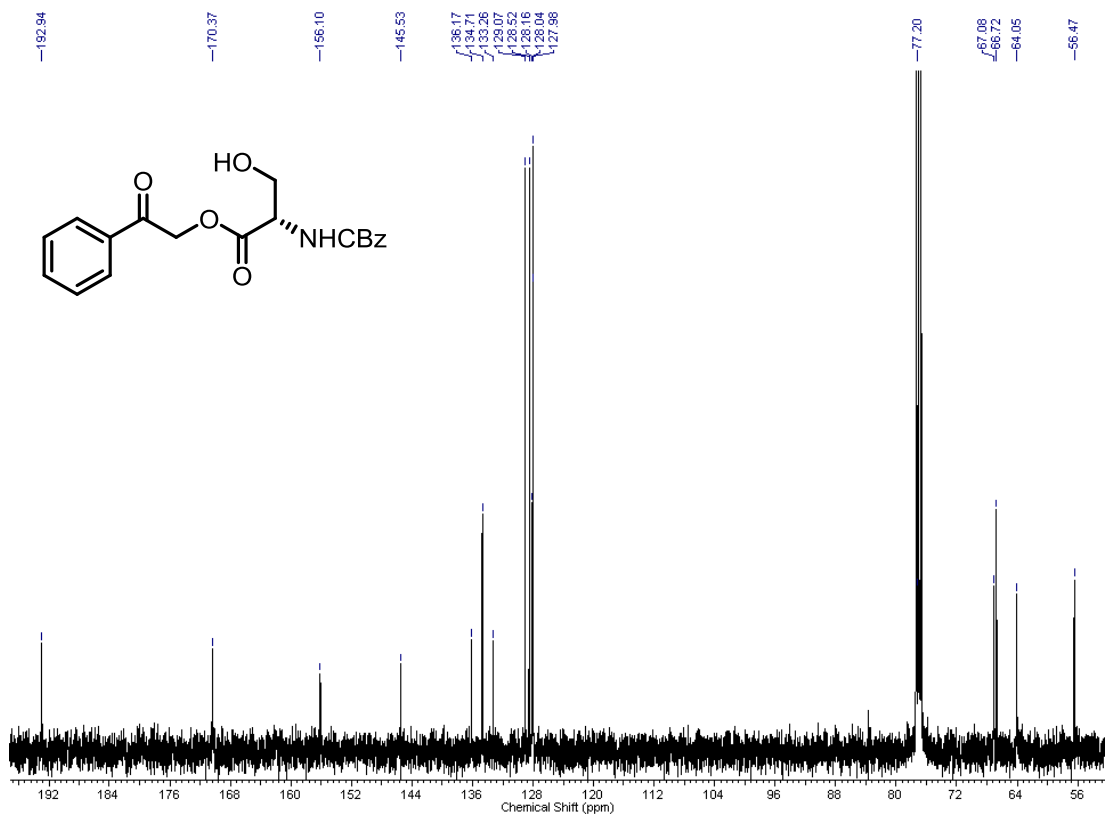
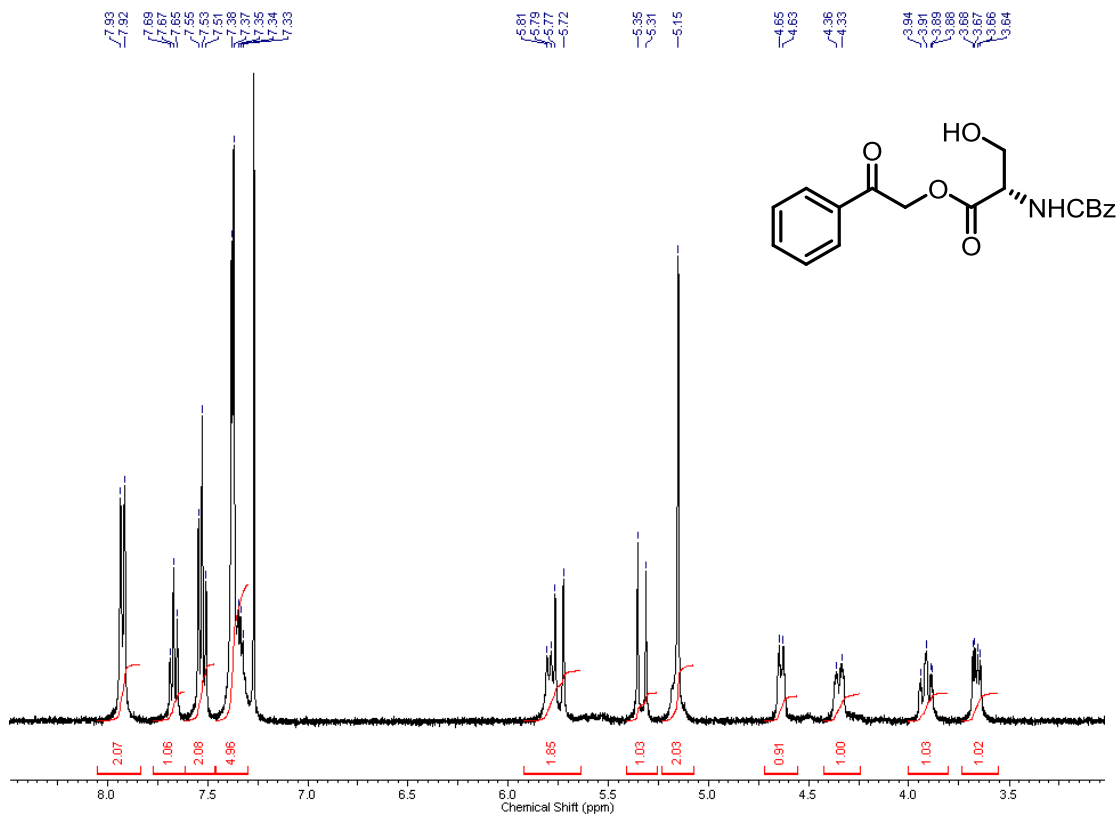


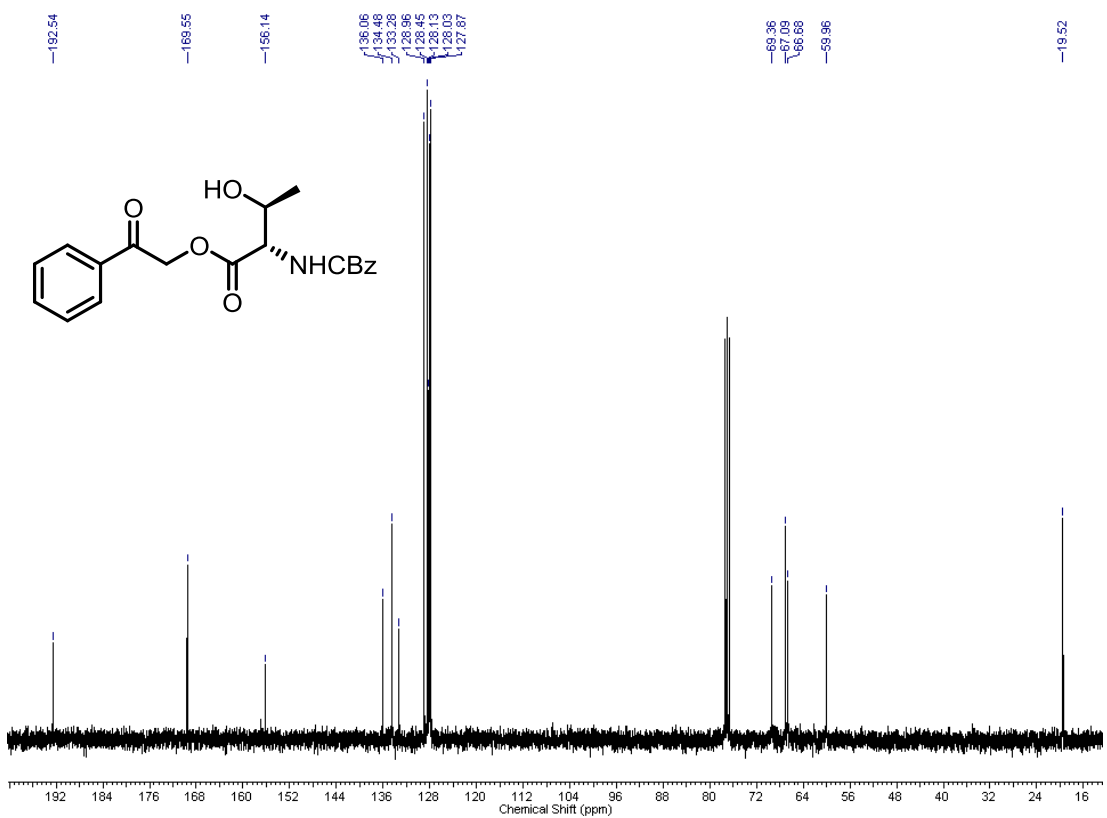
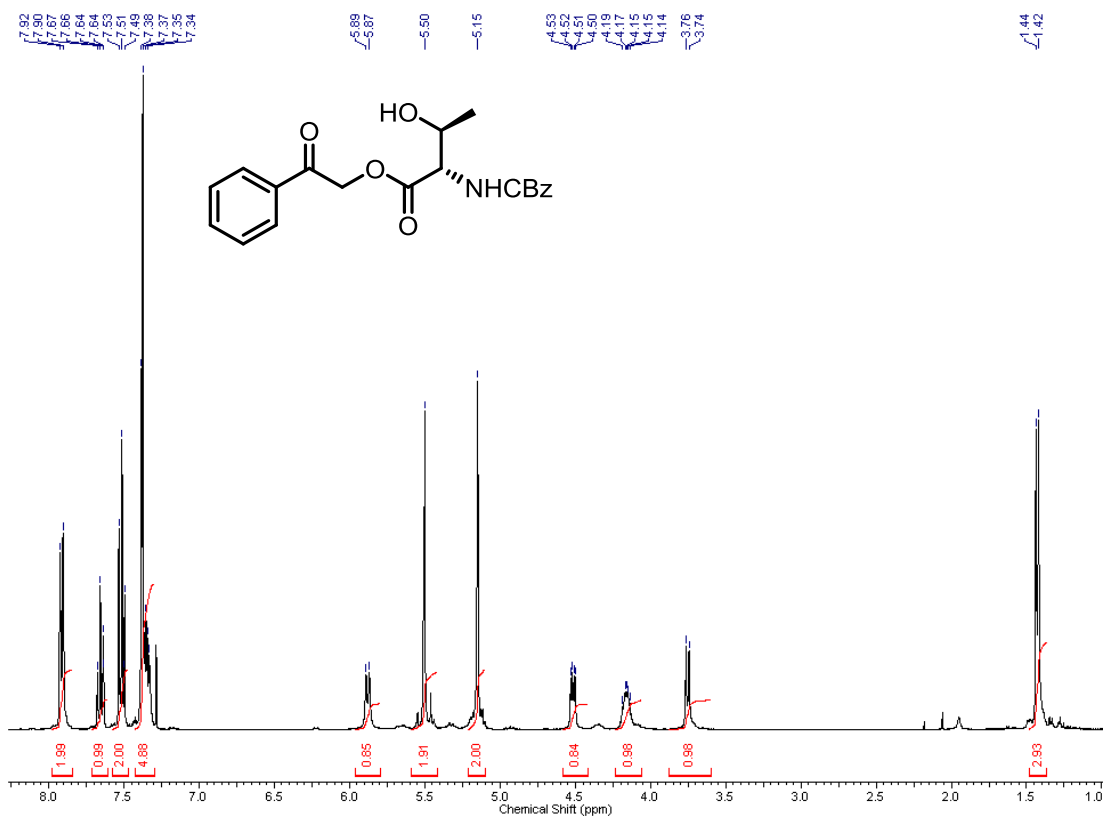


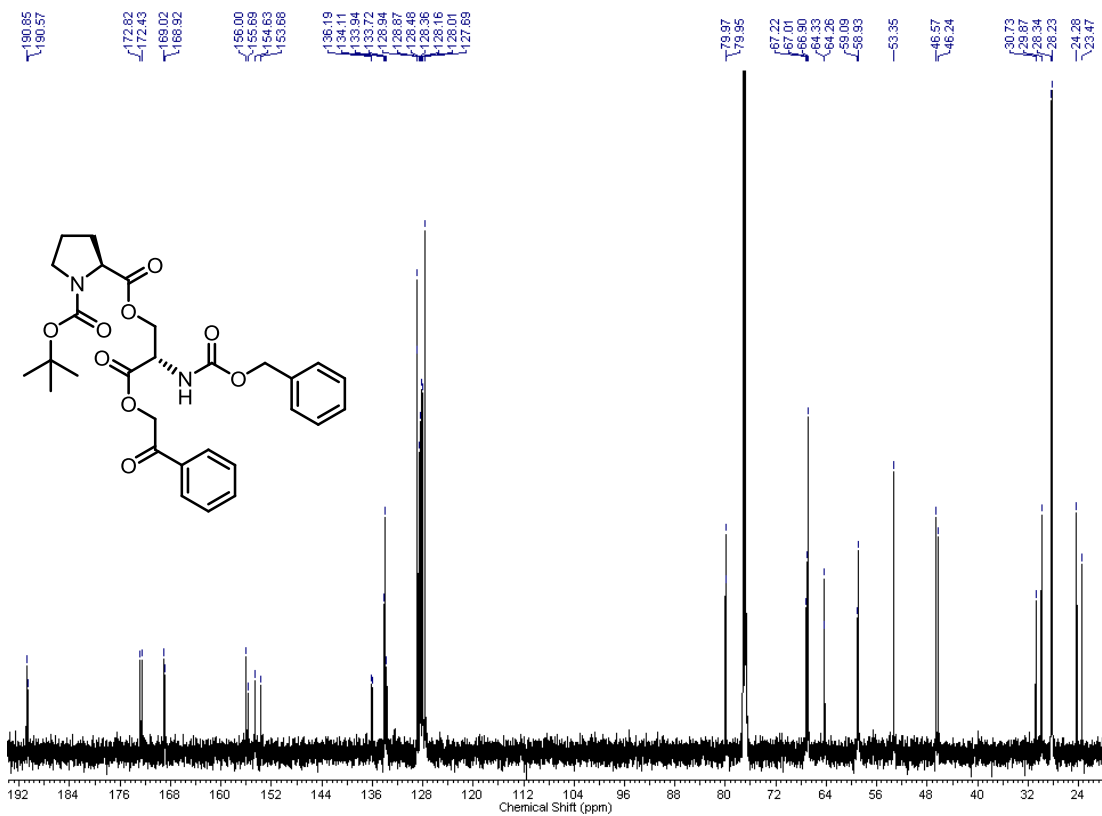
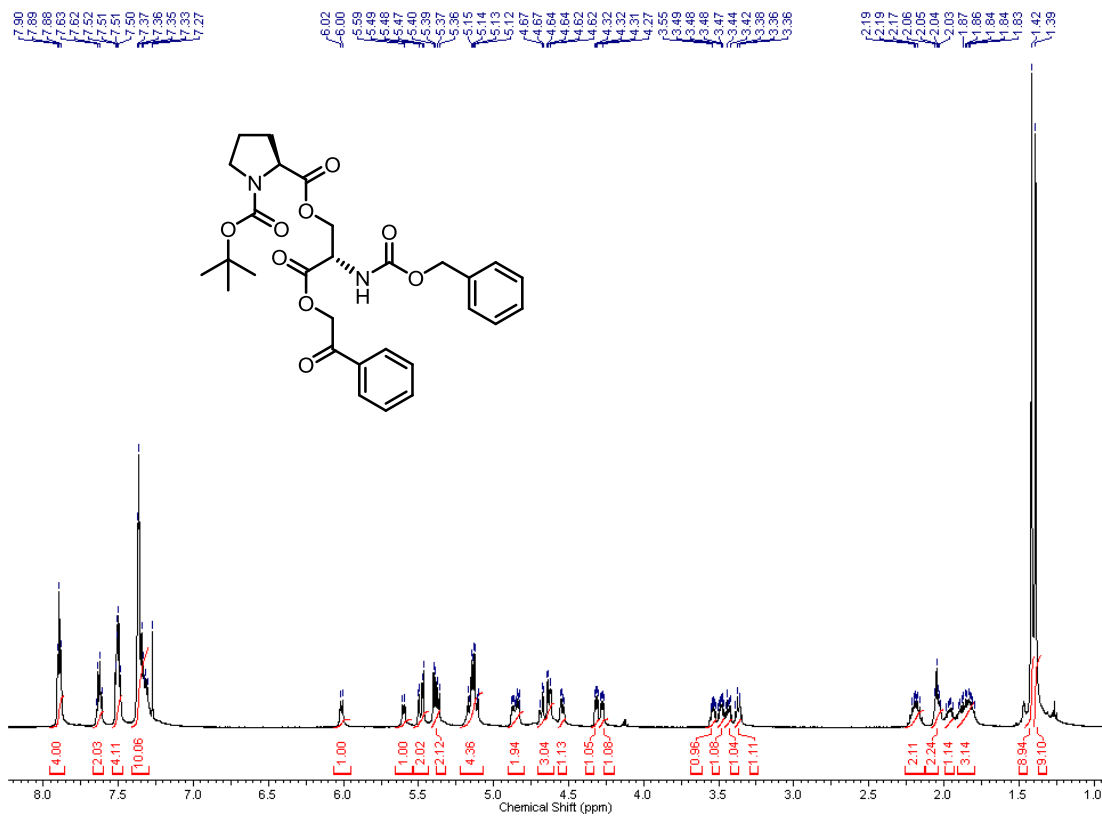


NOSEY Exchange cross-peaks shown in blue, NOE cross-peaks shown in teal

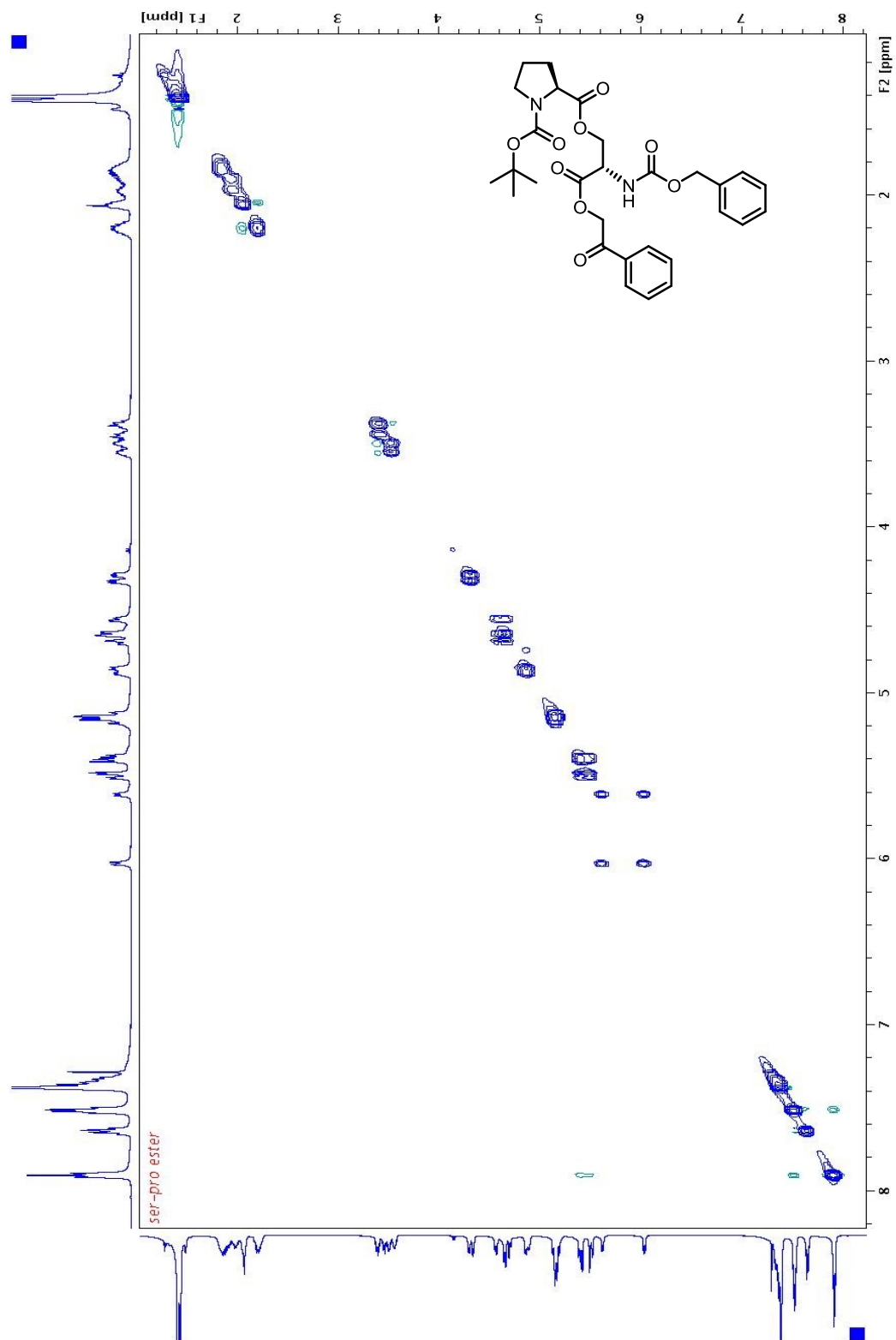


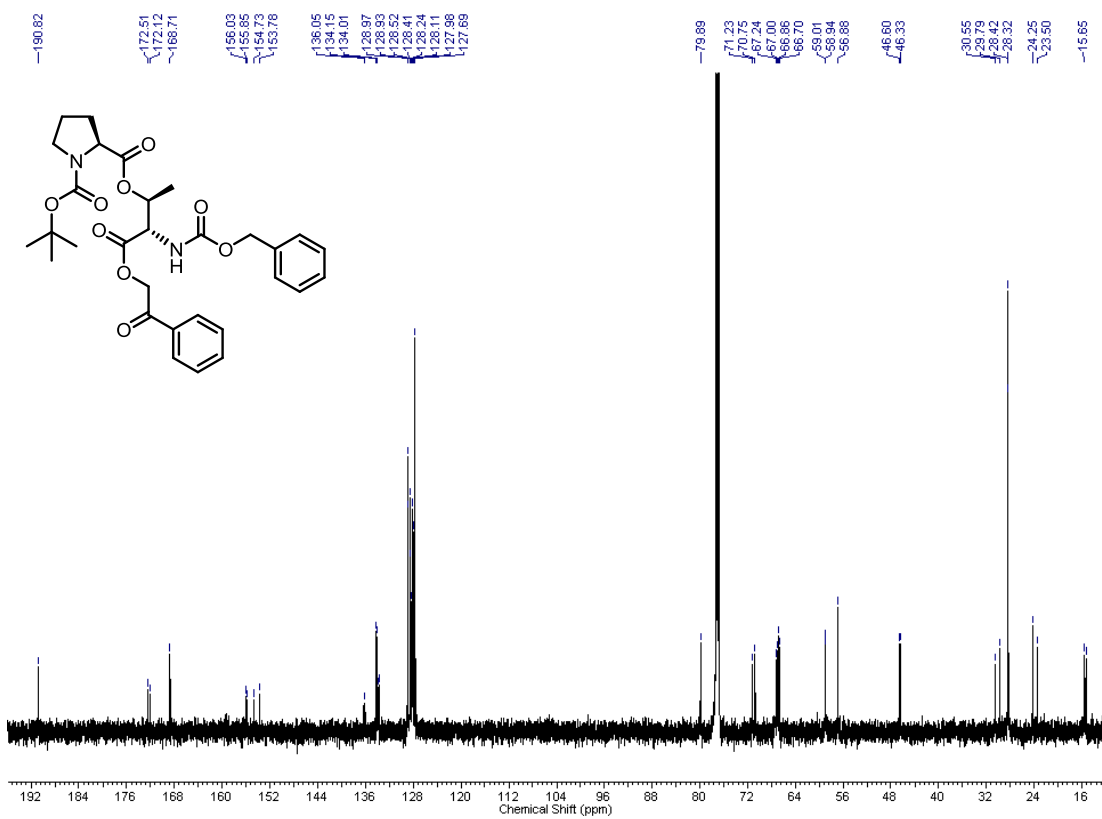
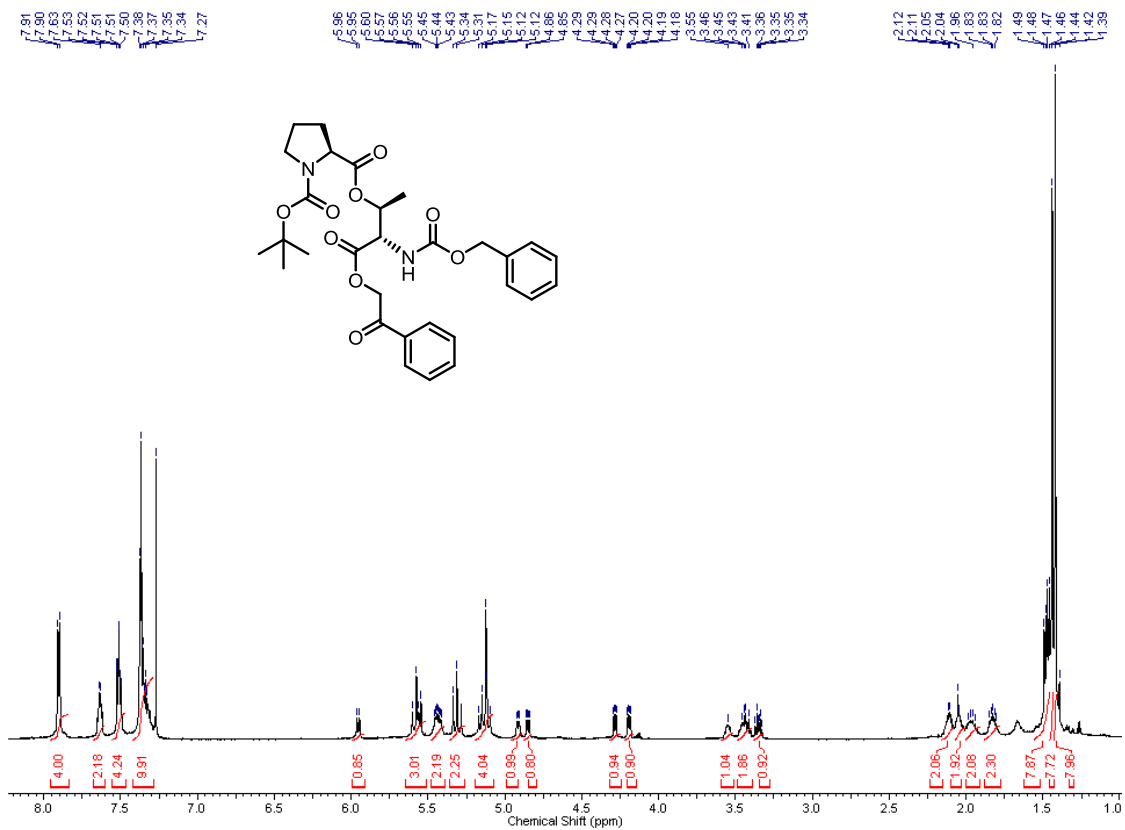






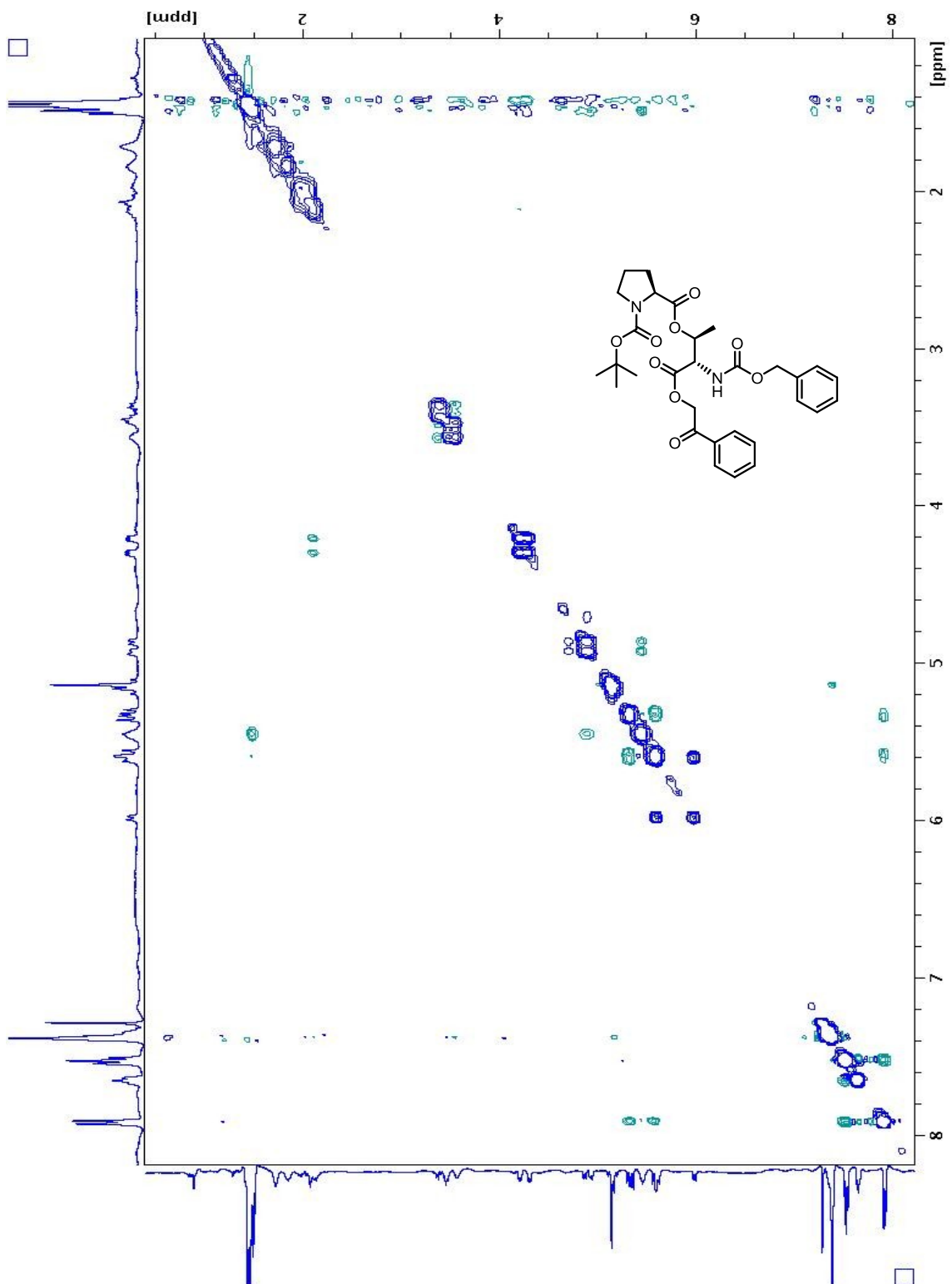
NOSEY: Exchange cross-peaks shown in blue, NOE cross-peaks shown in teal

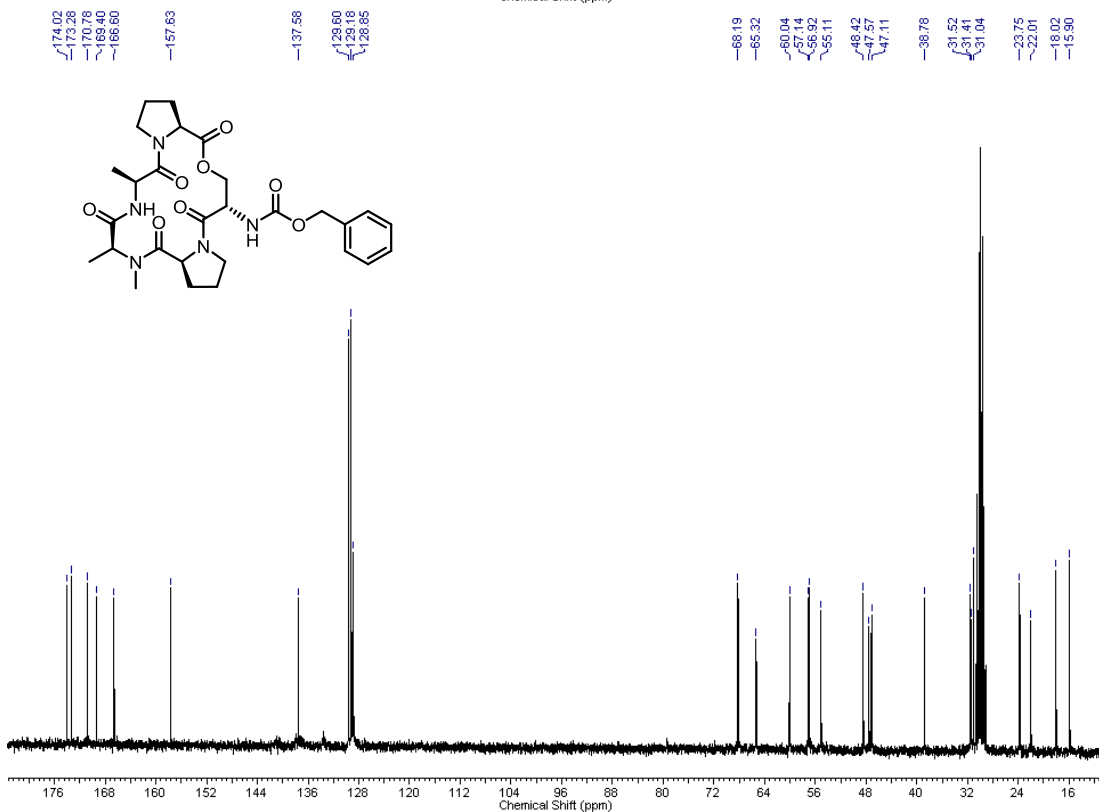
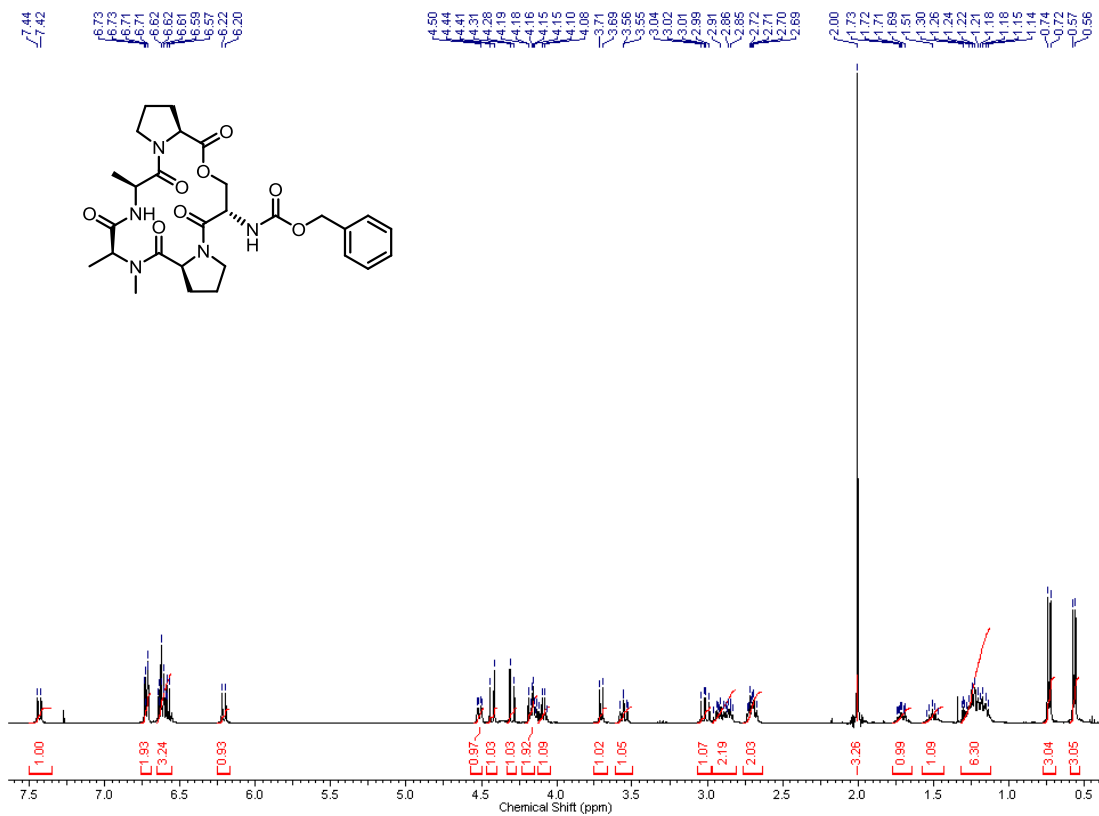


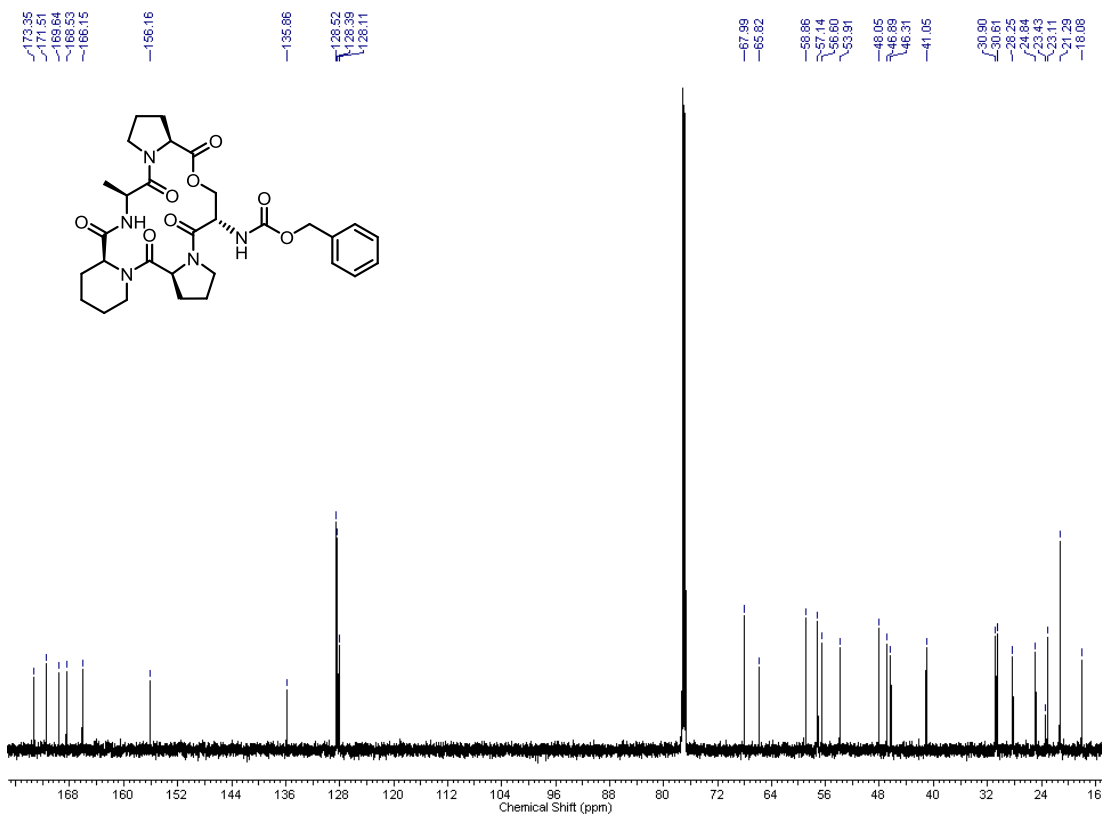
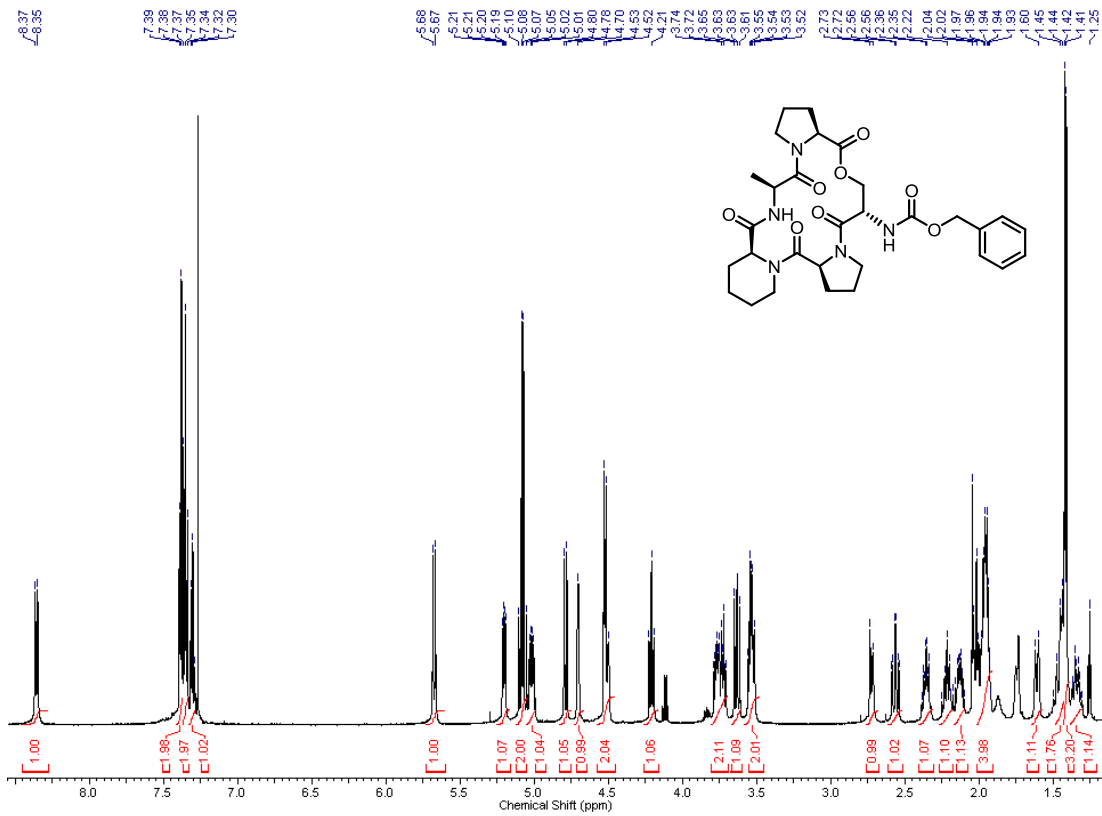




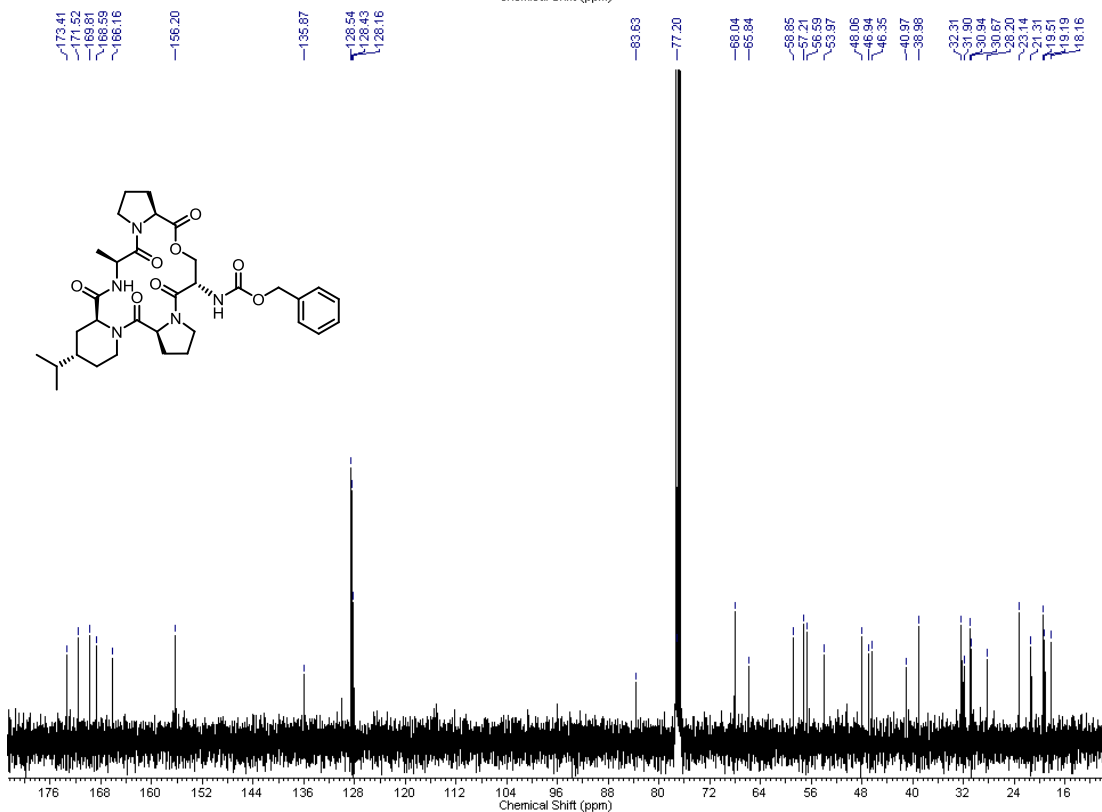
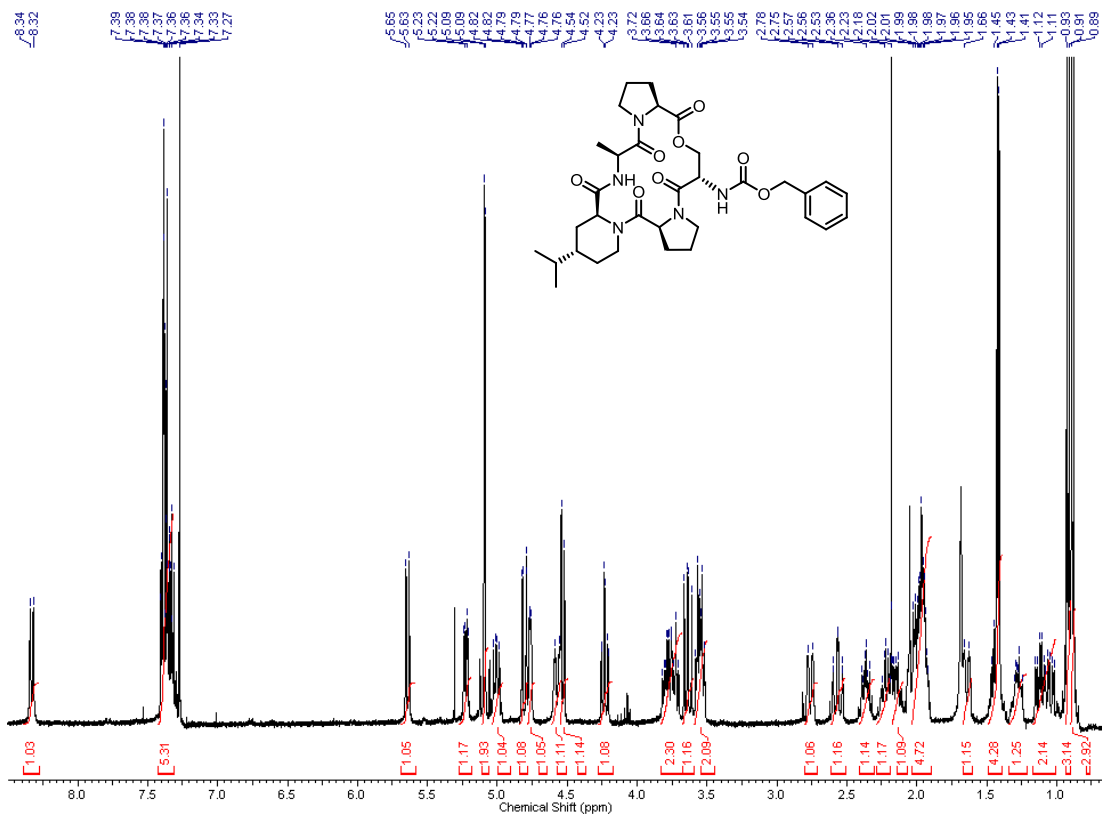
**NOSEY: Exchange cross-peaks shown in blue, NOE cross-peaks shown in teal**

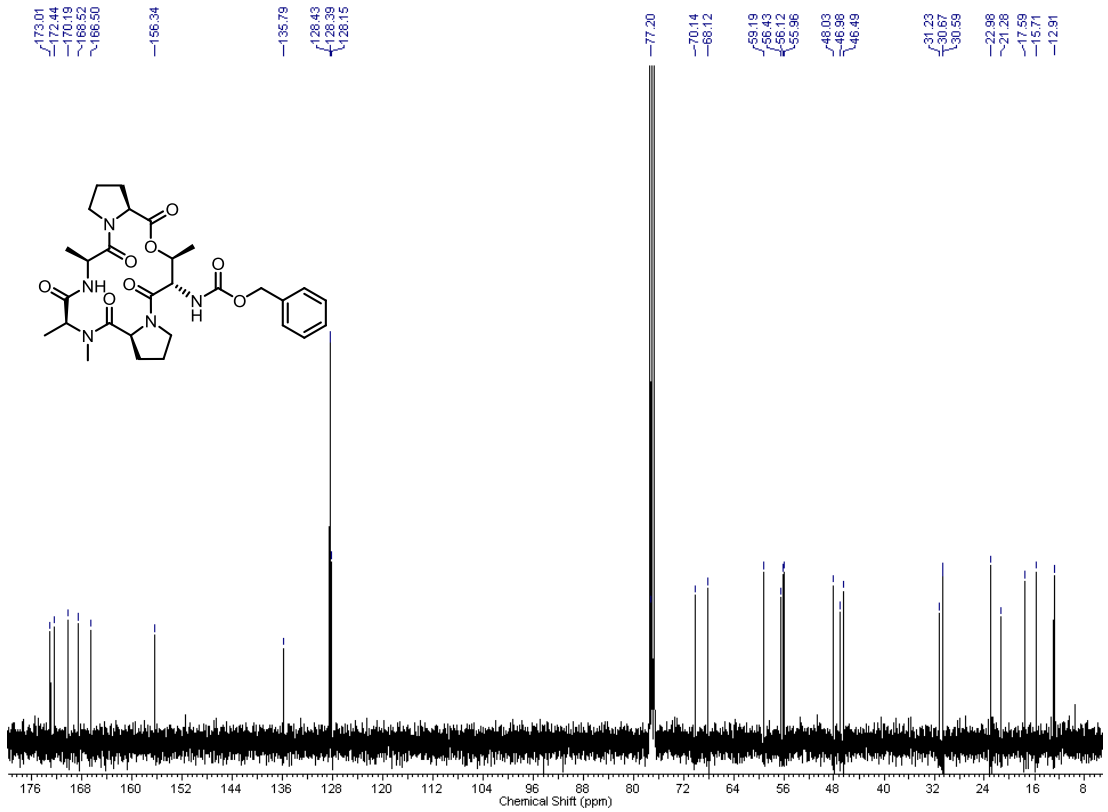
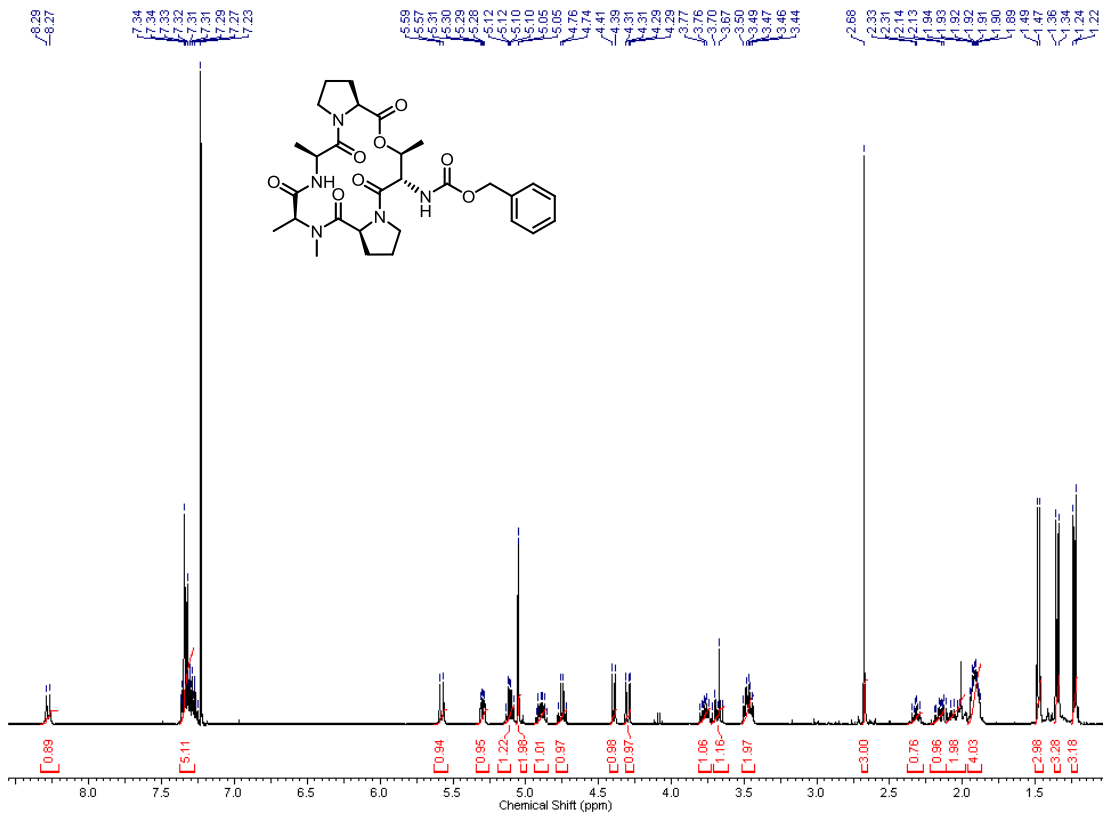






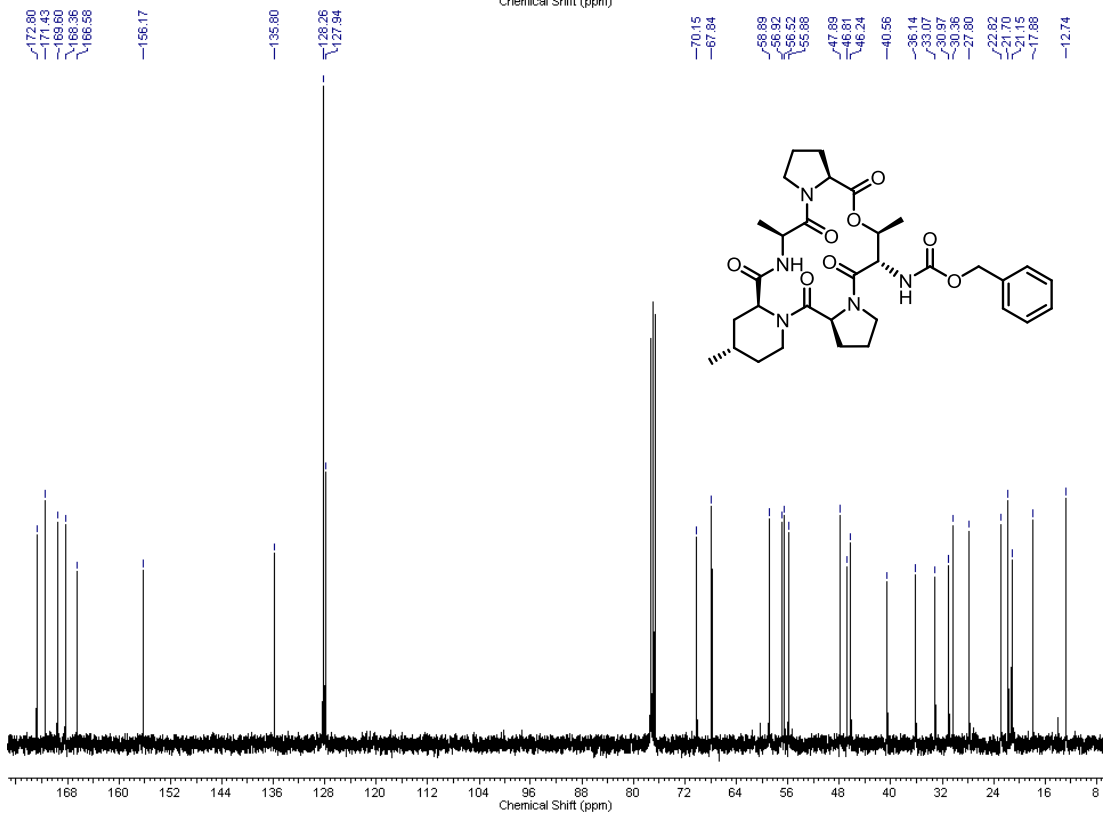
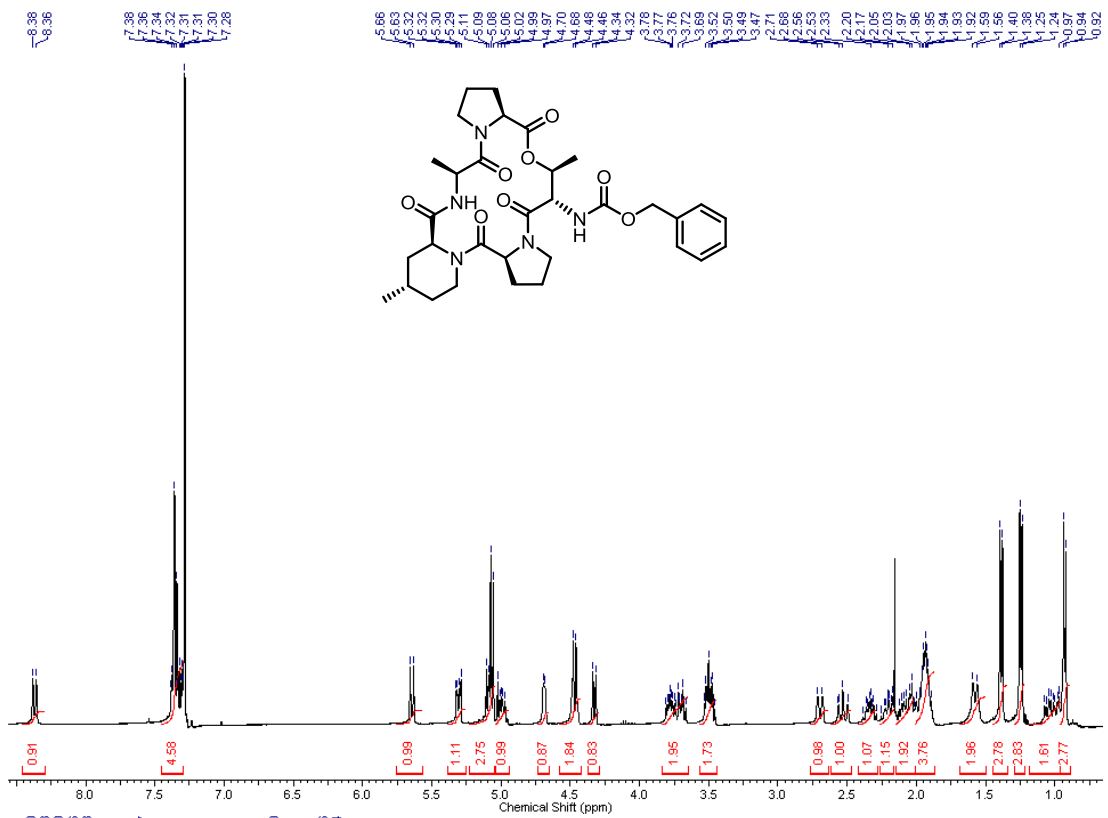


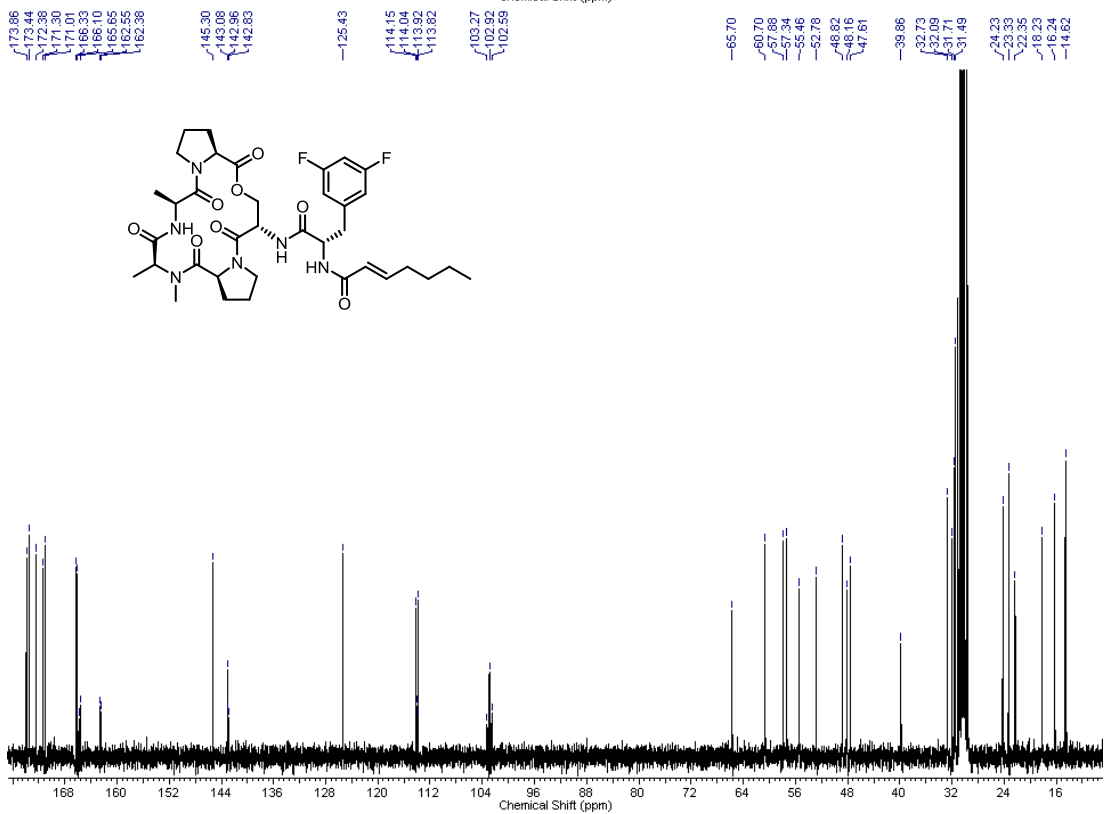
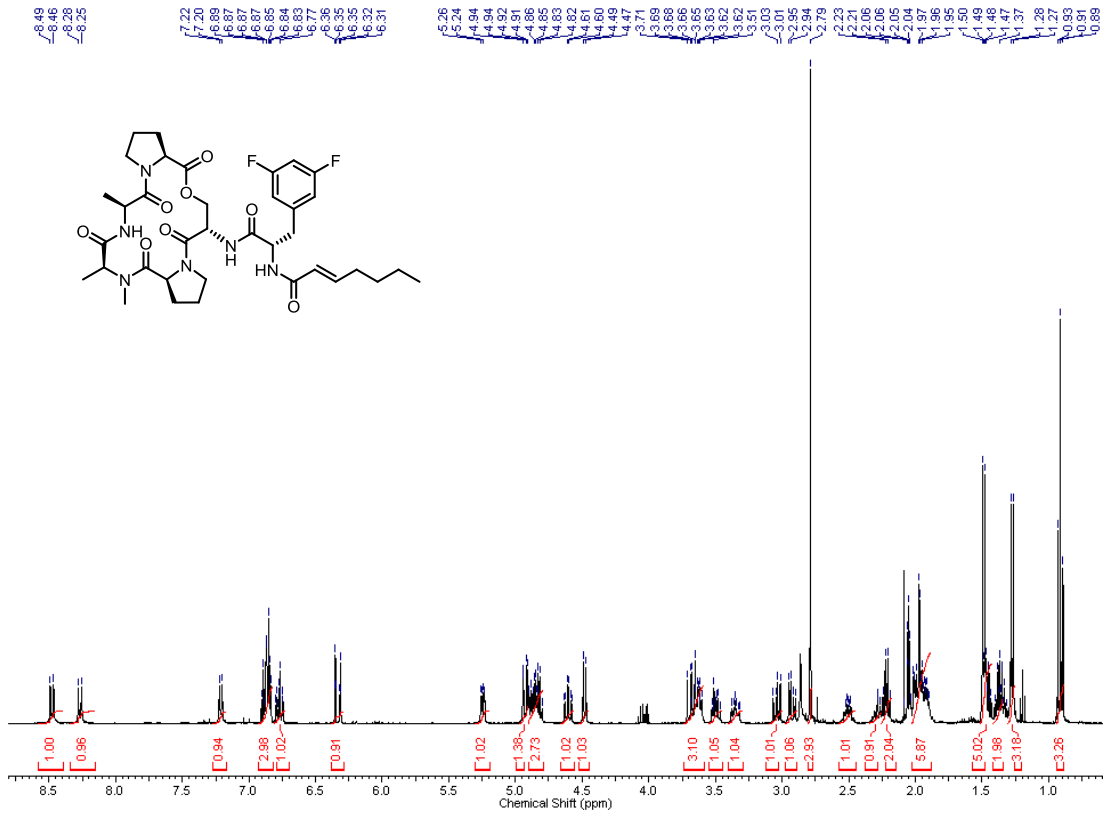


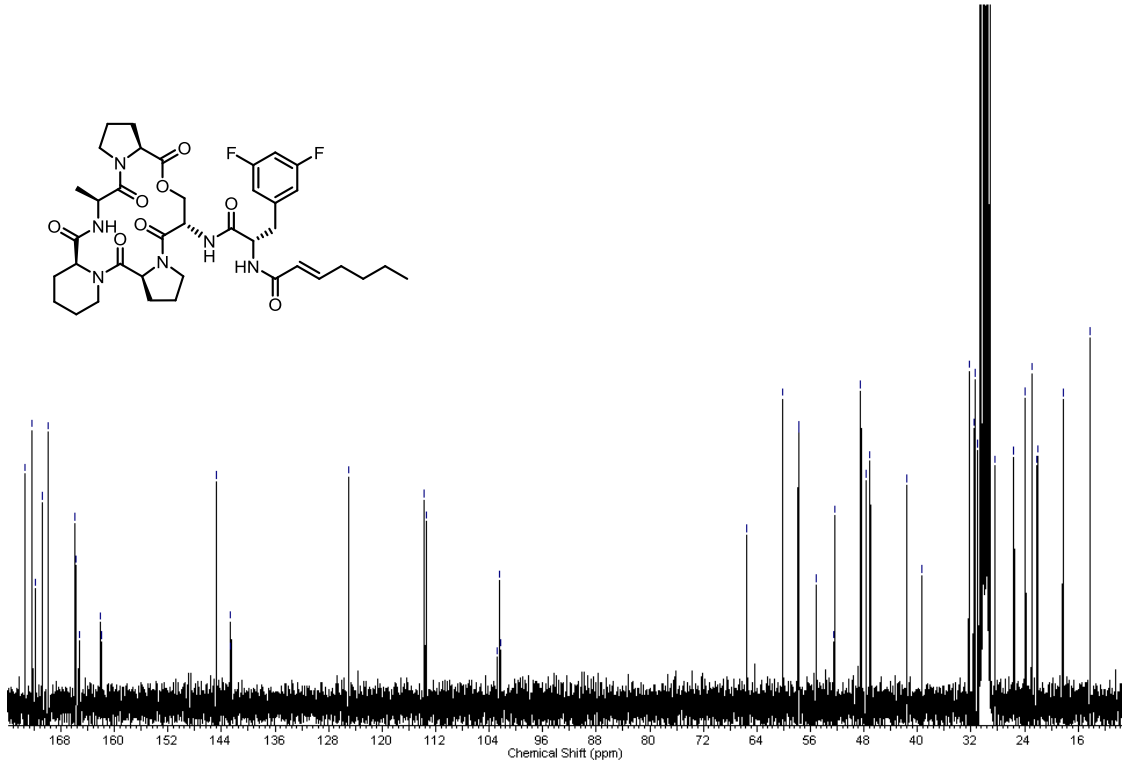
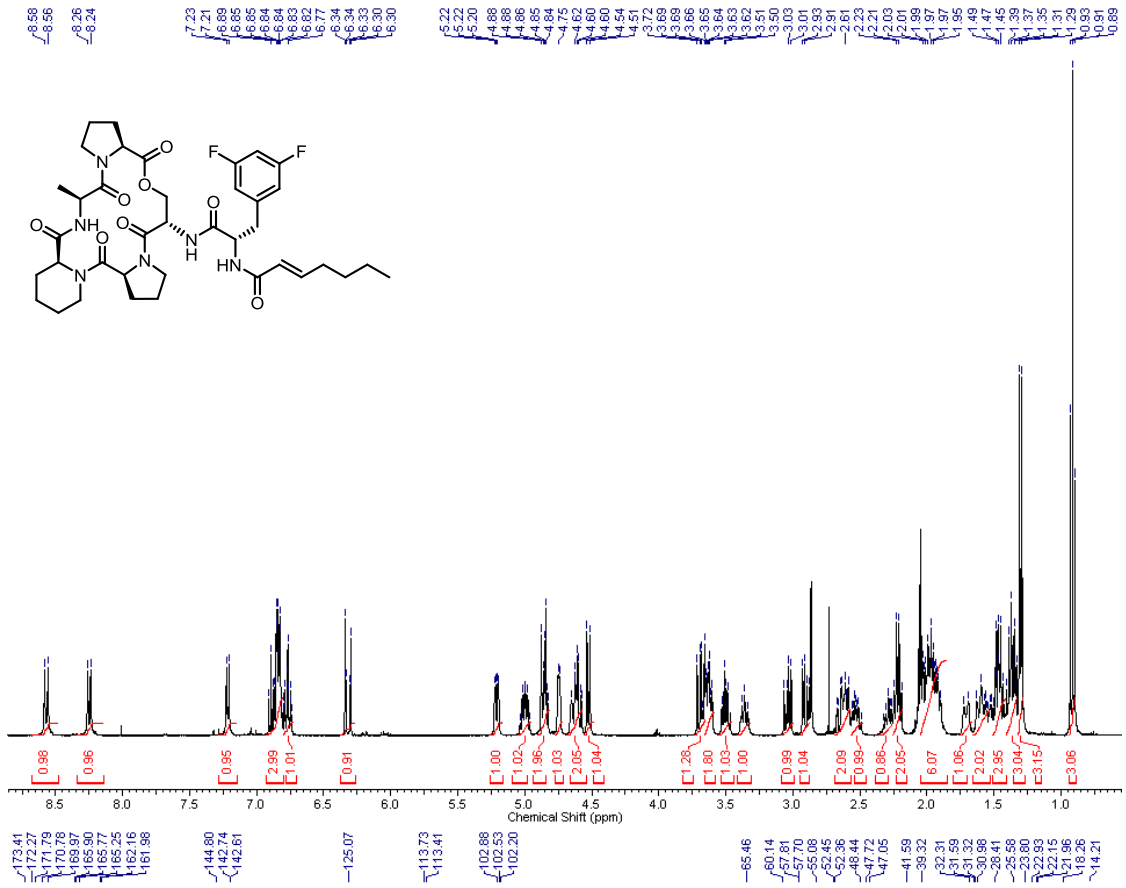


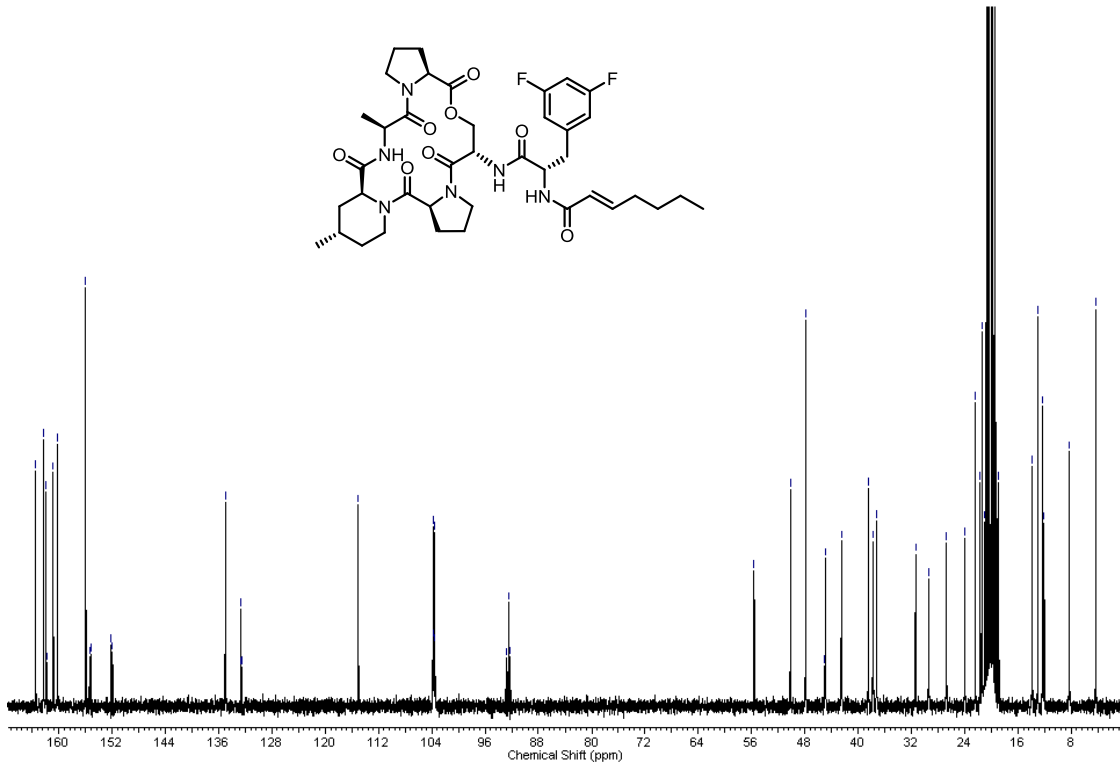
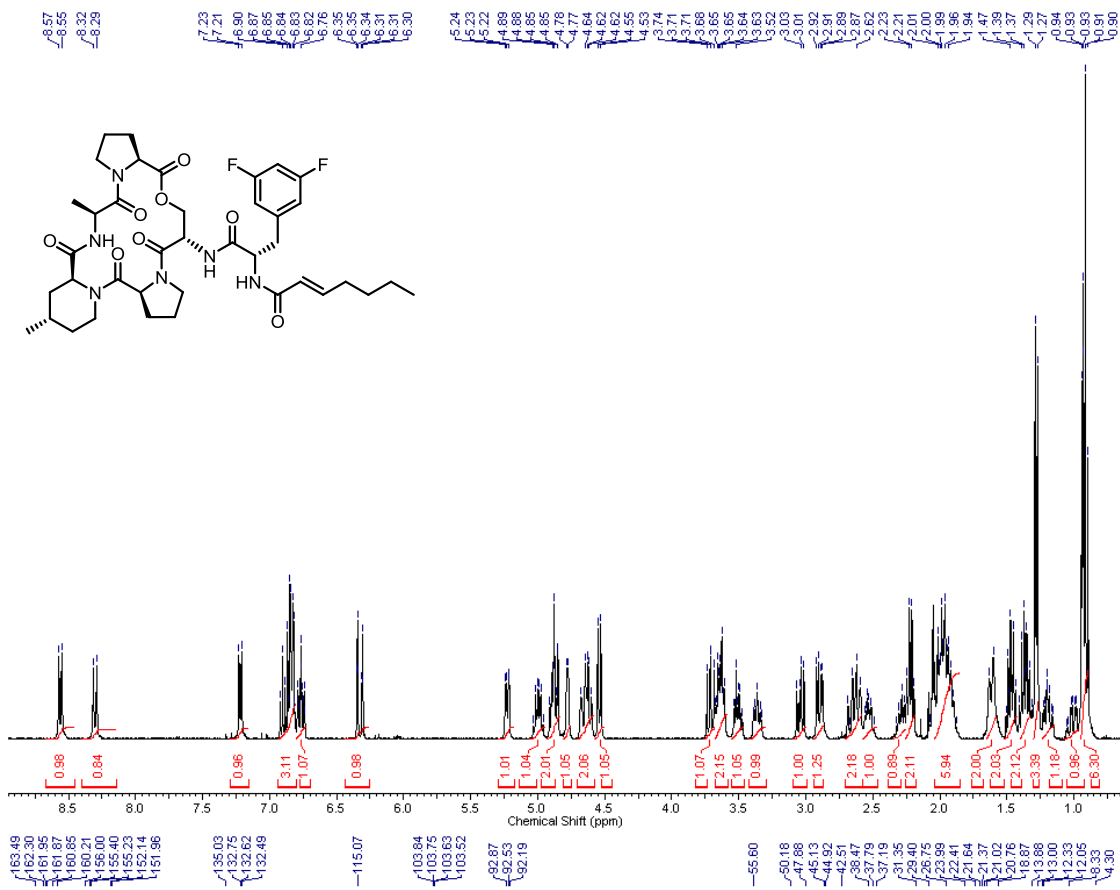


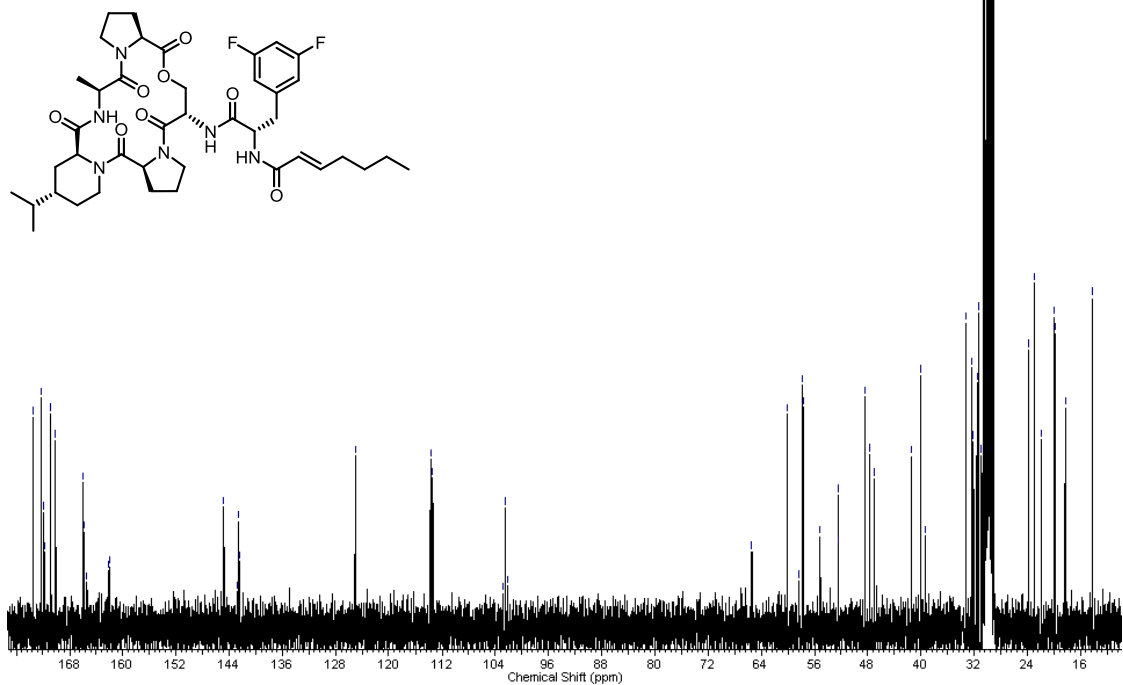
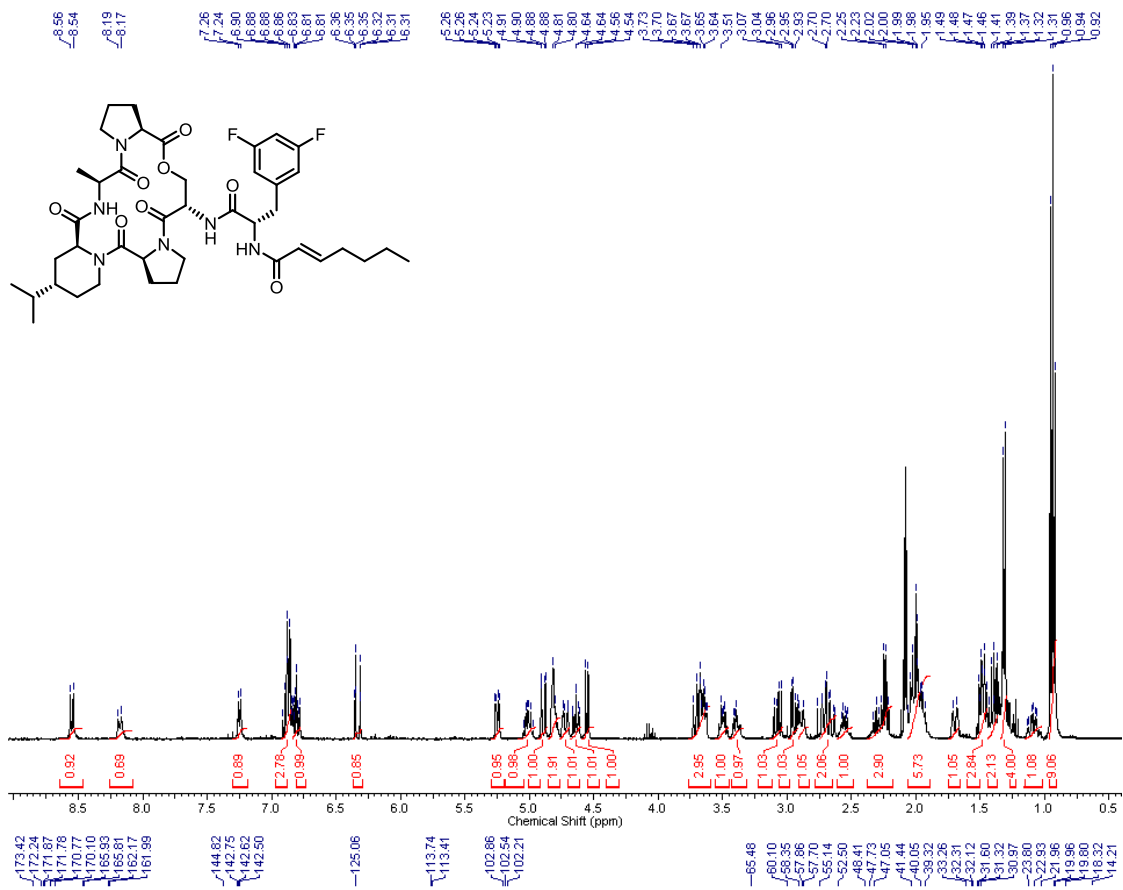


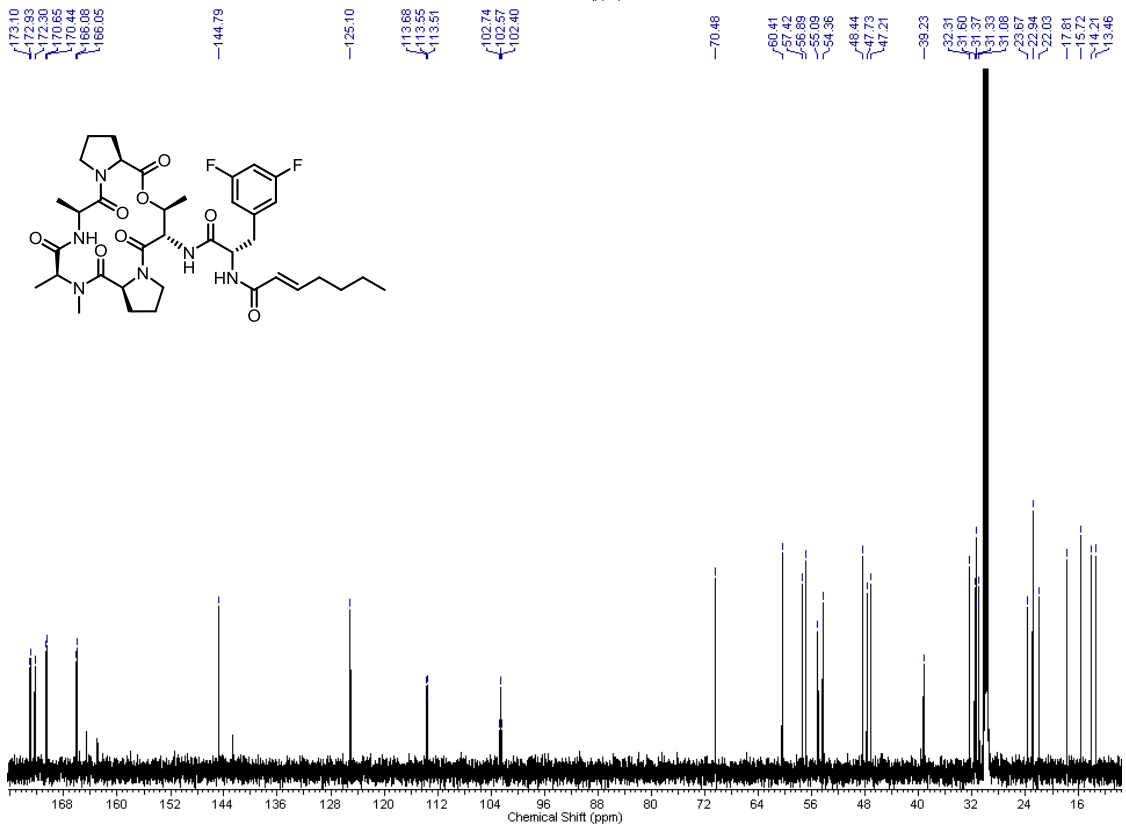
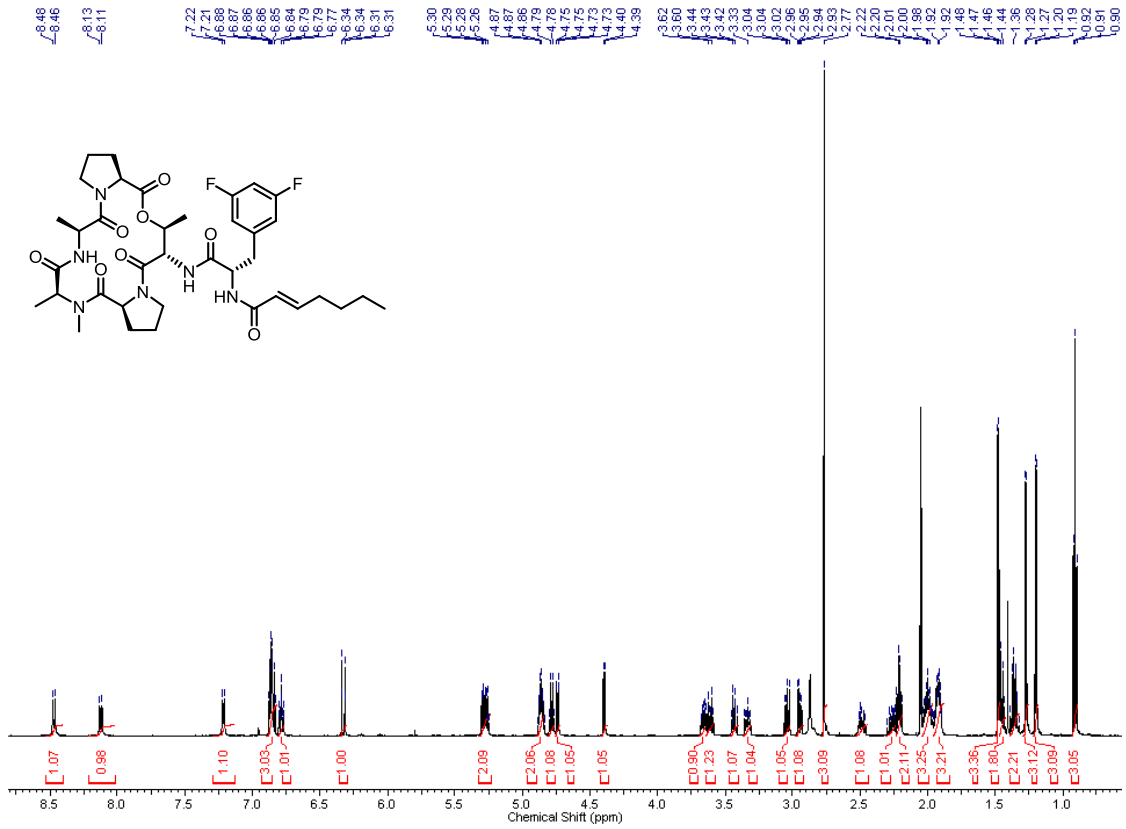


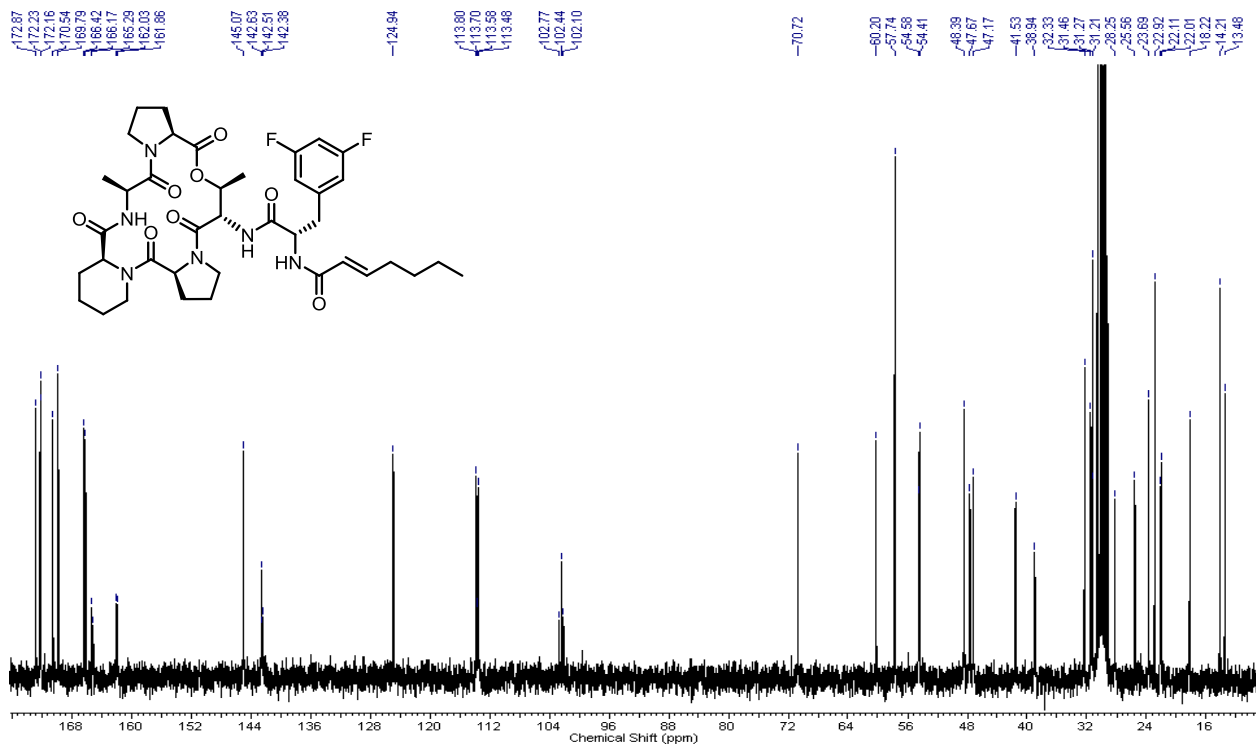
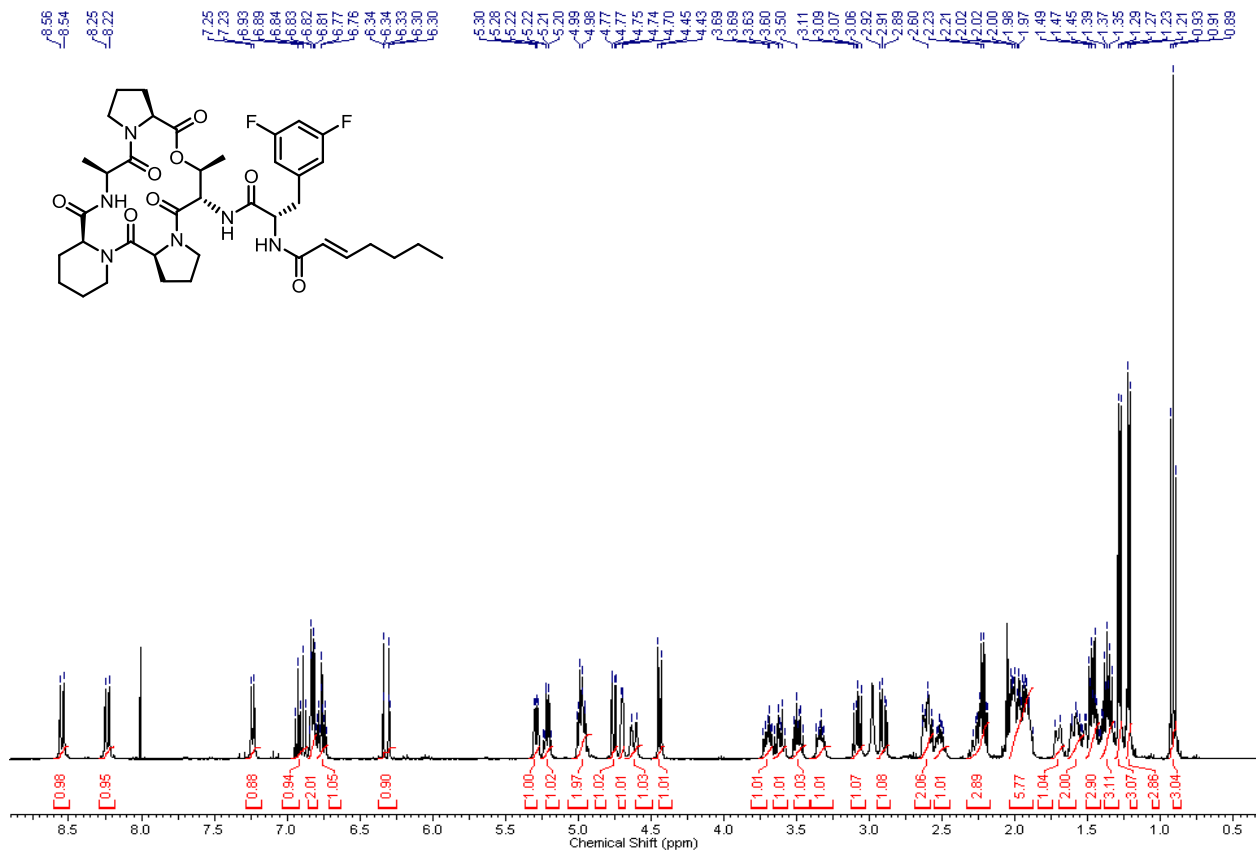


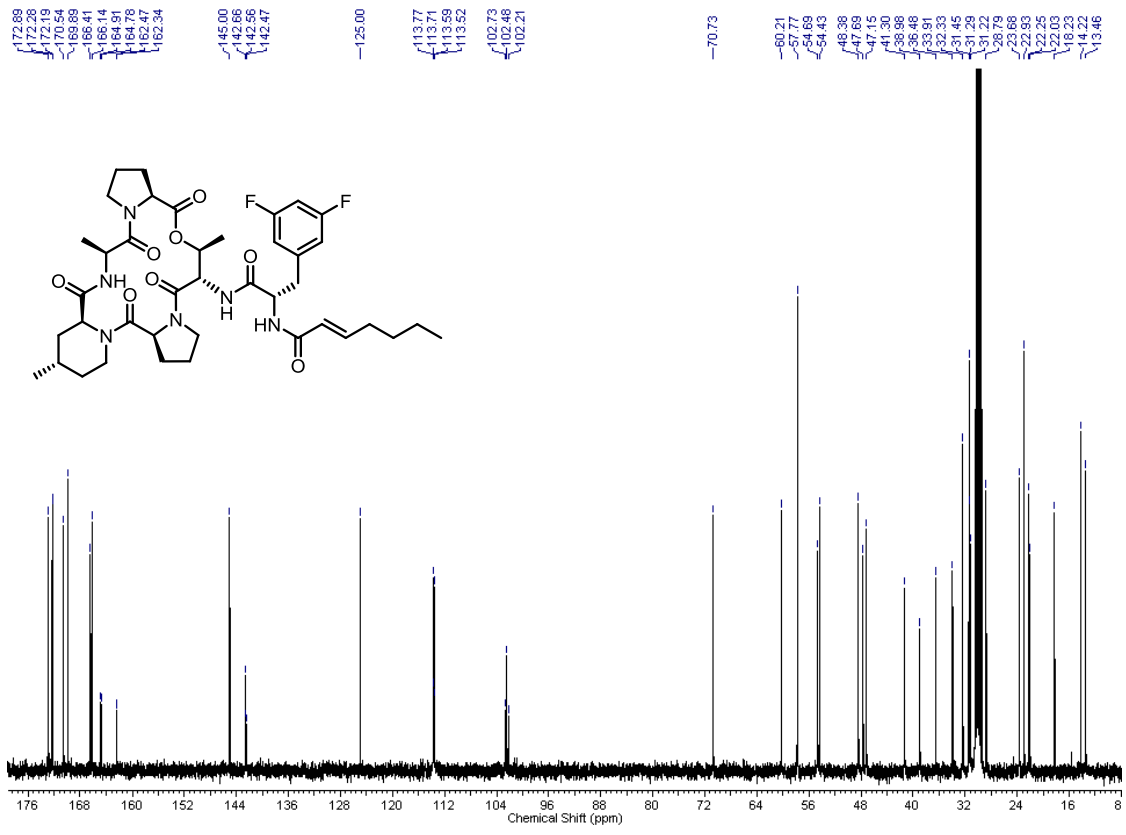
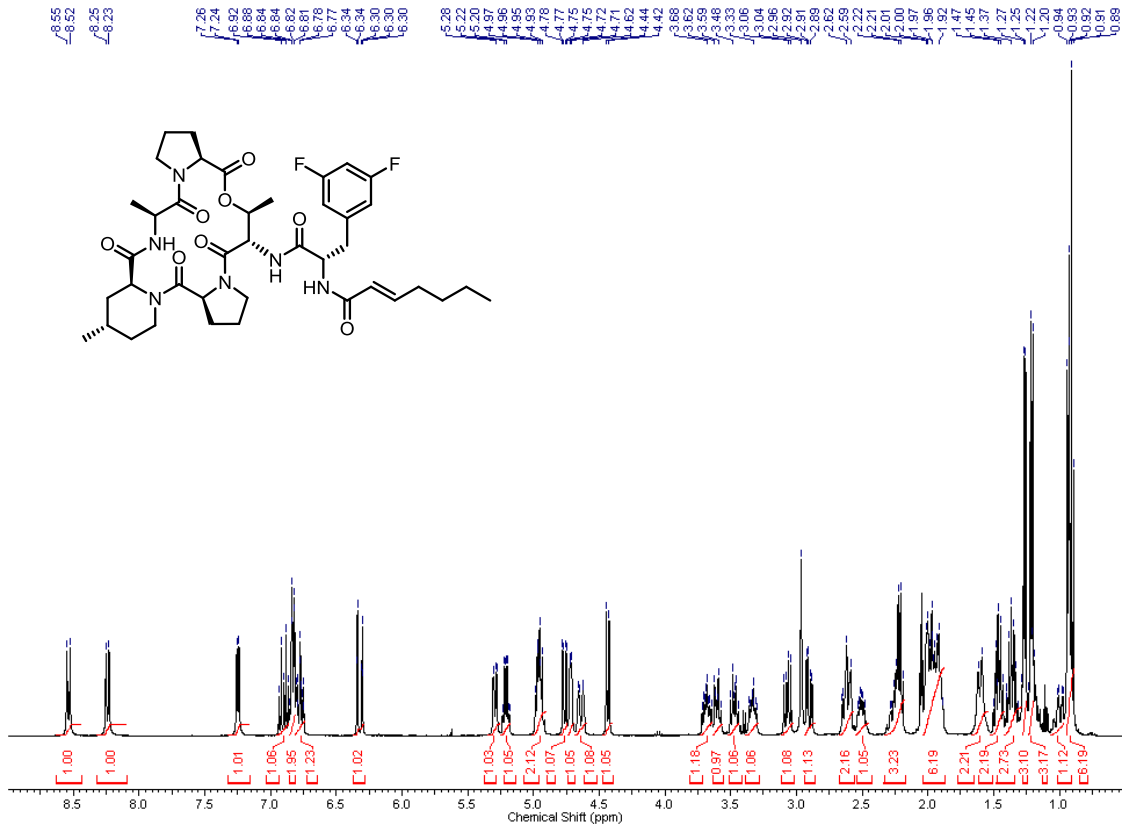






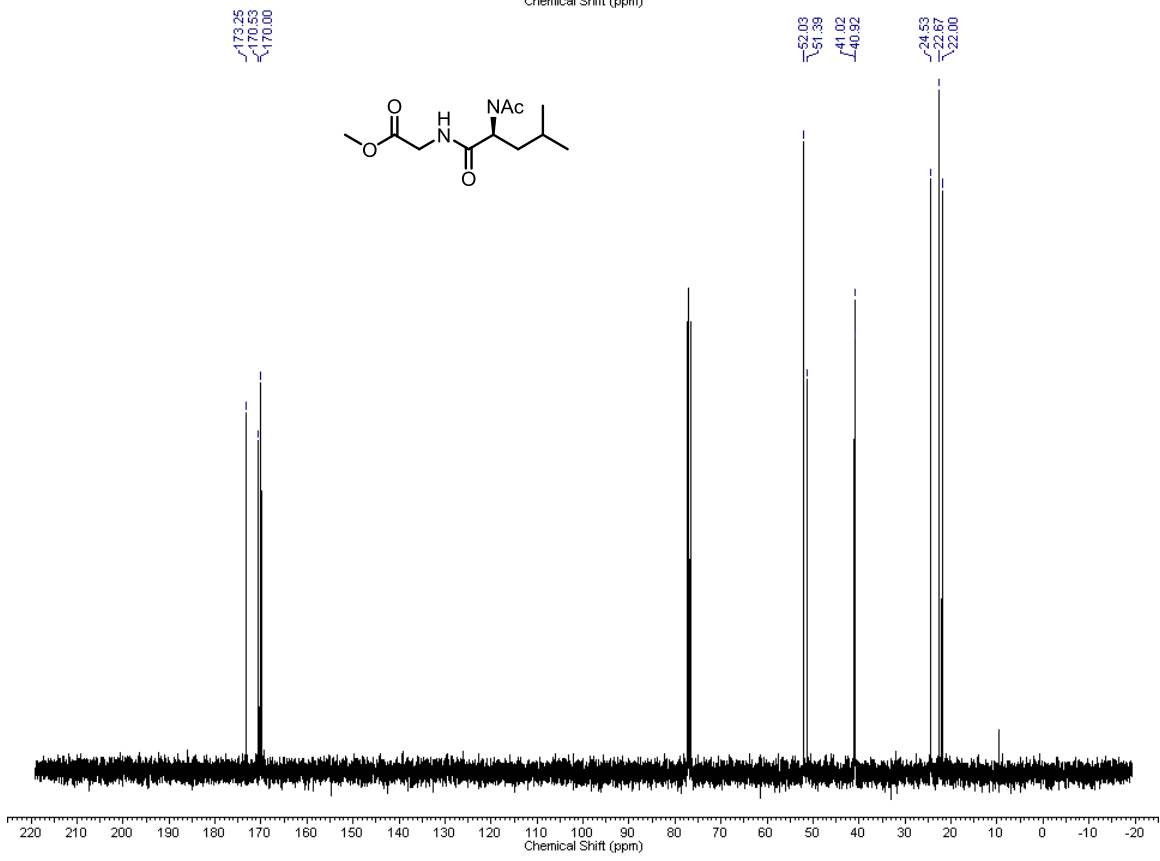
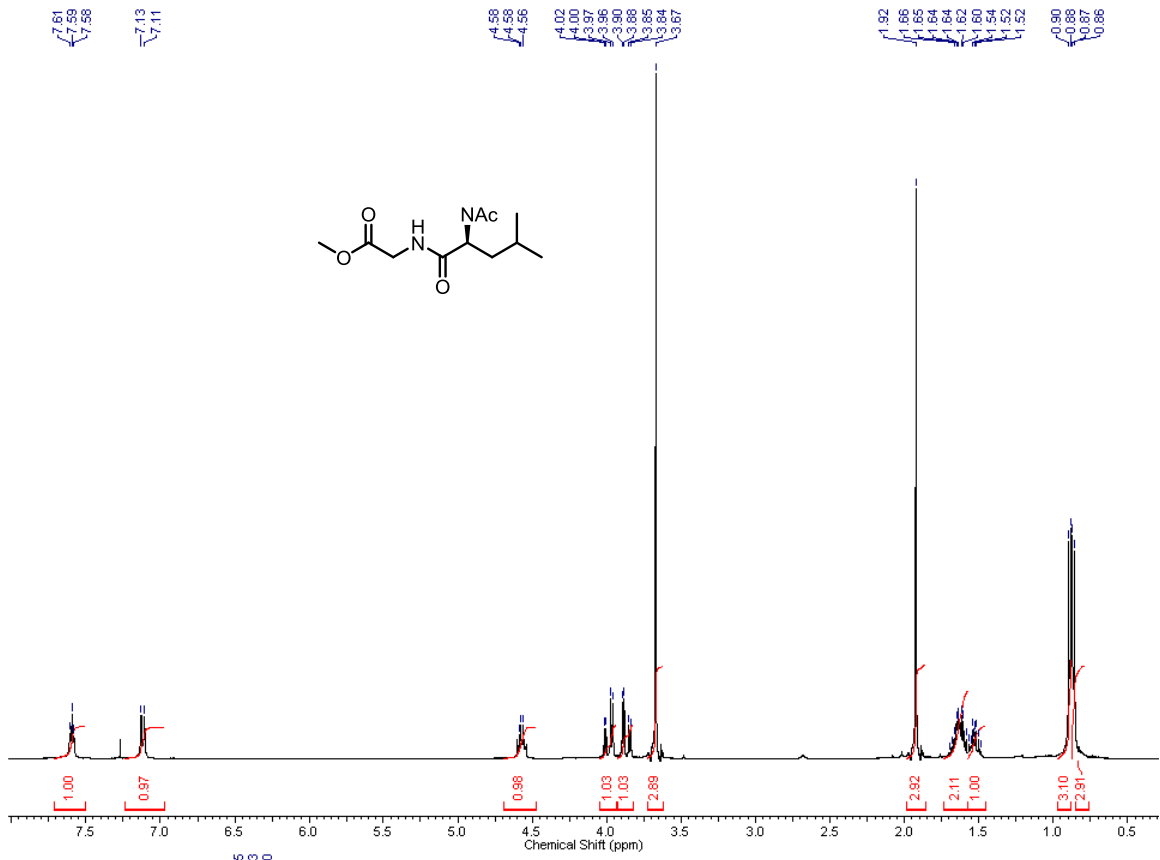


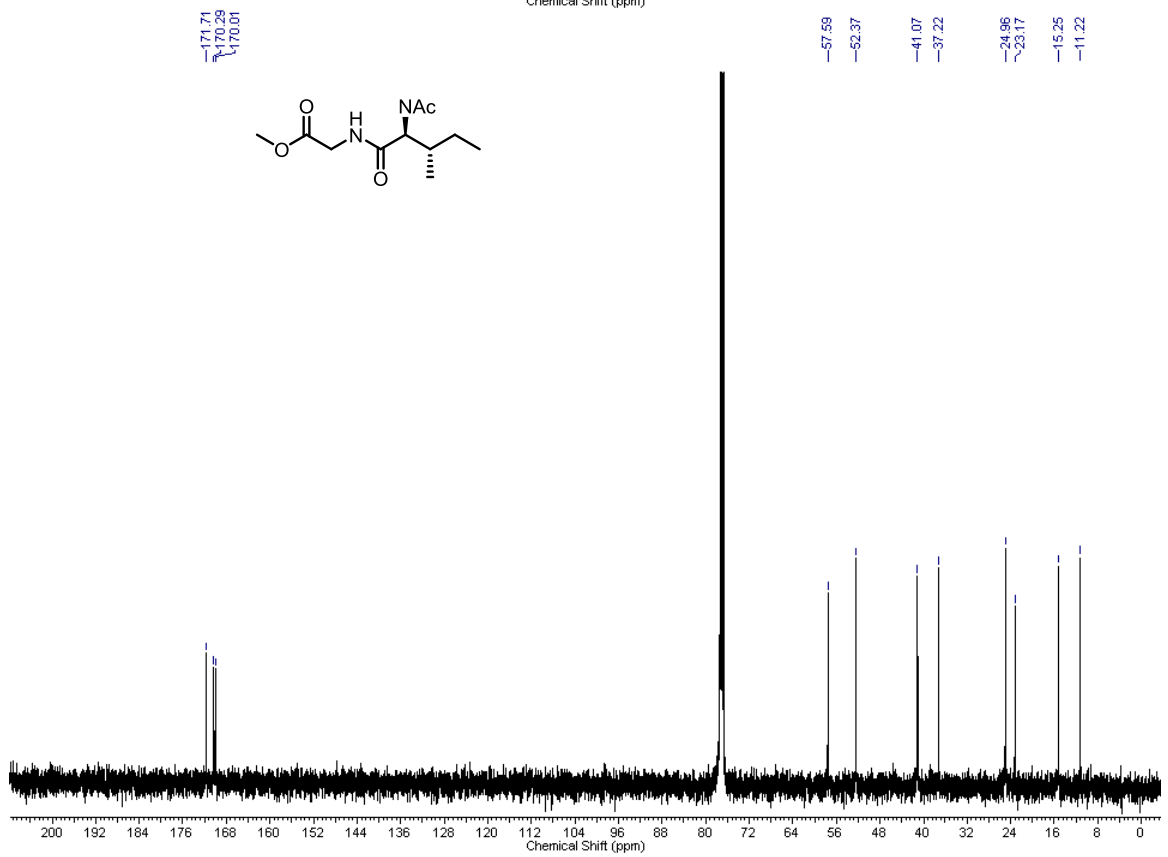
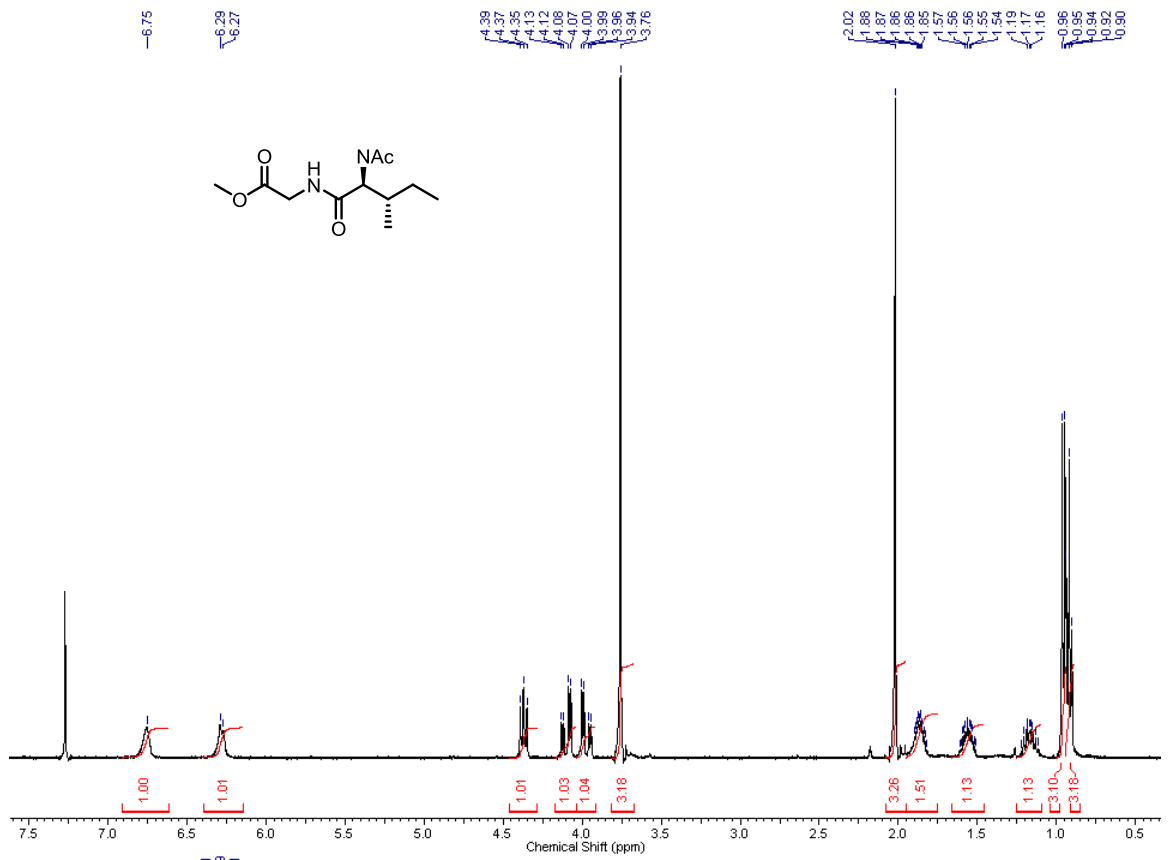


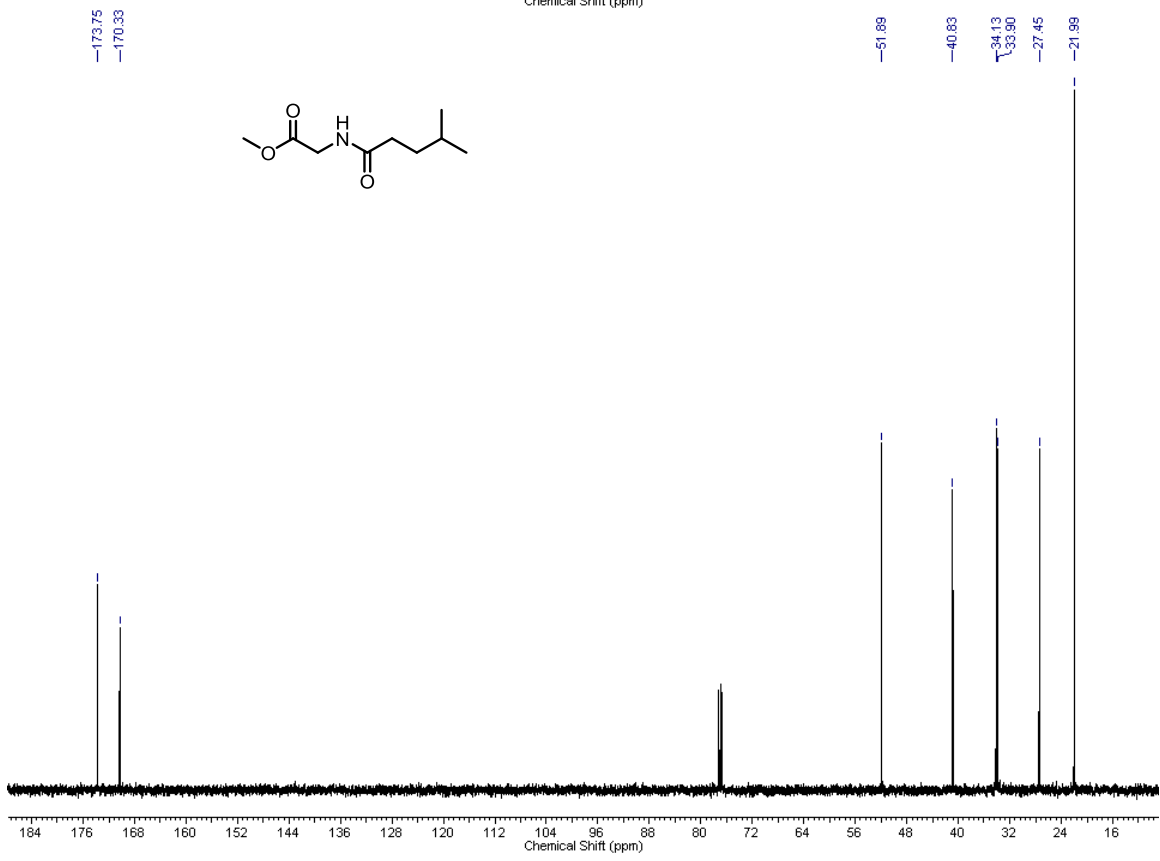
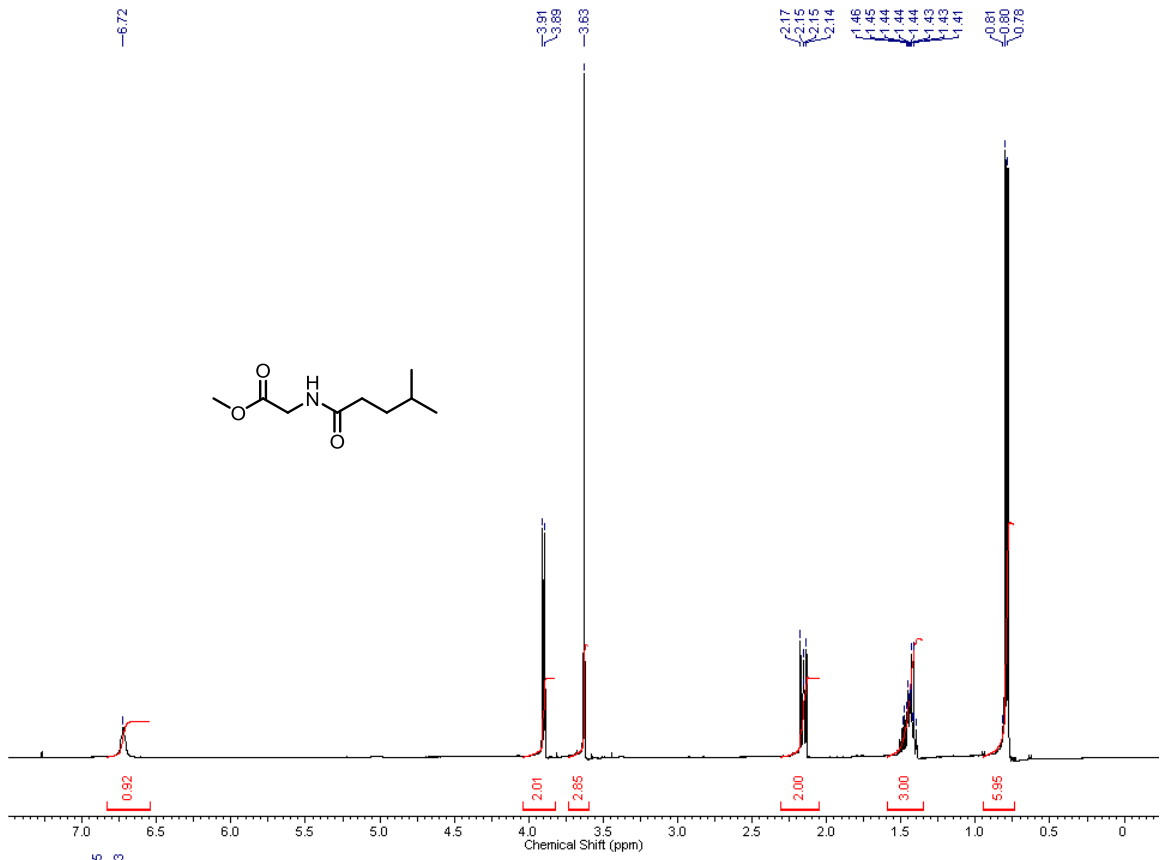


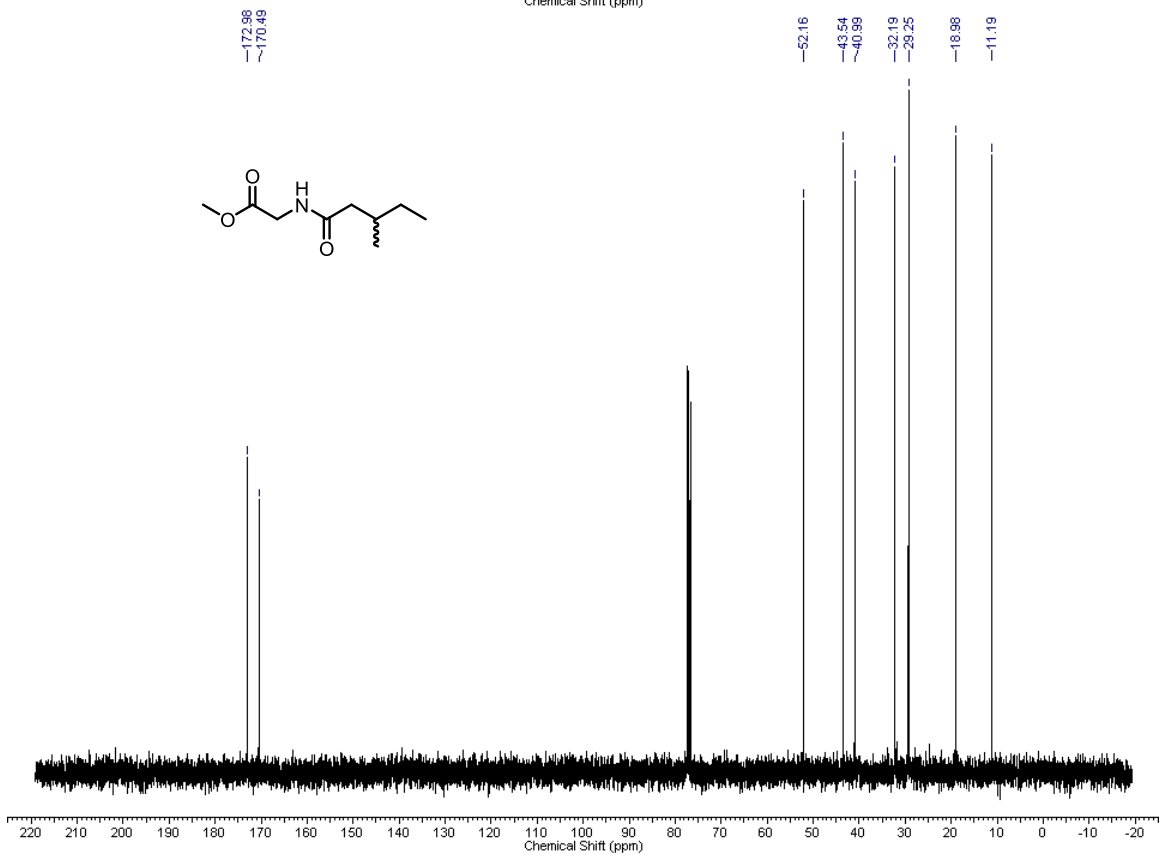
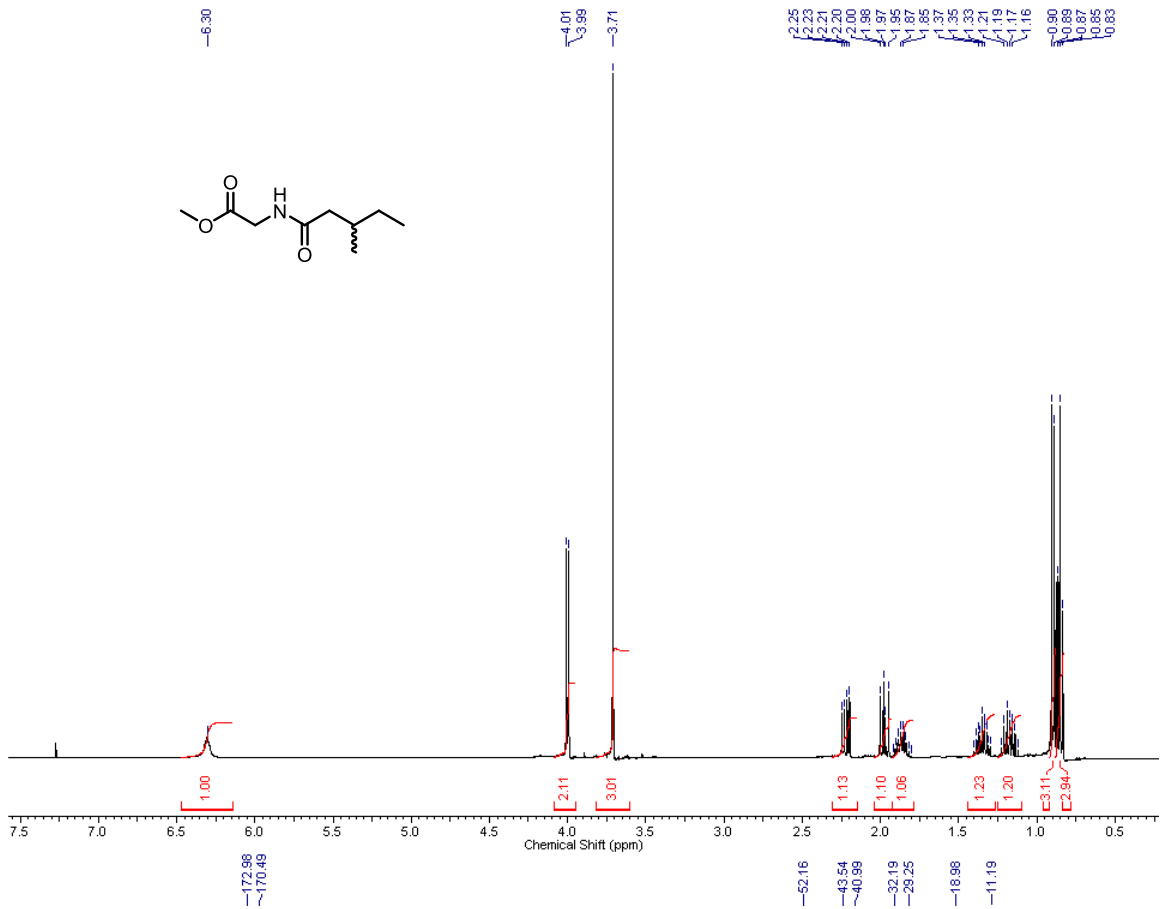


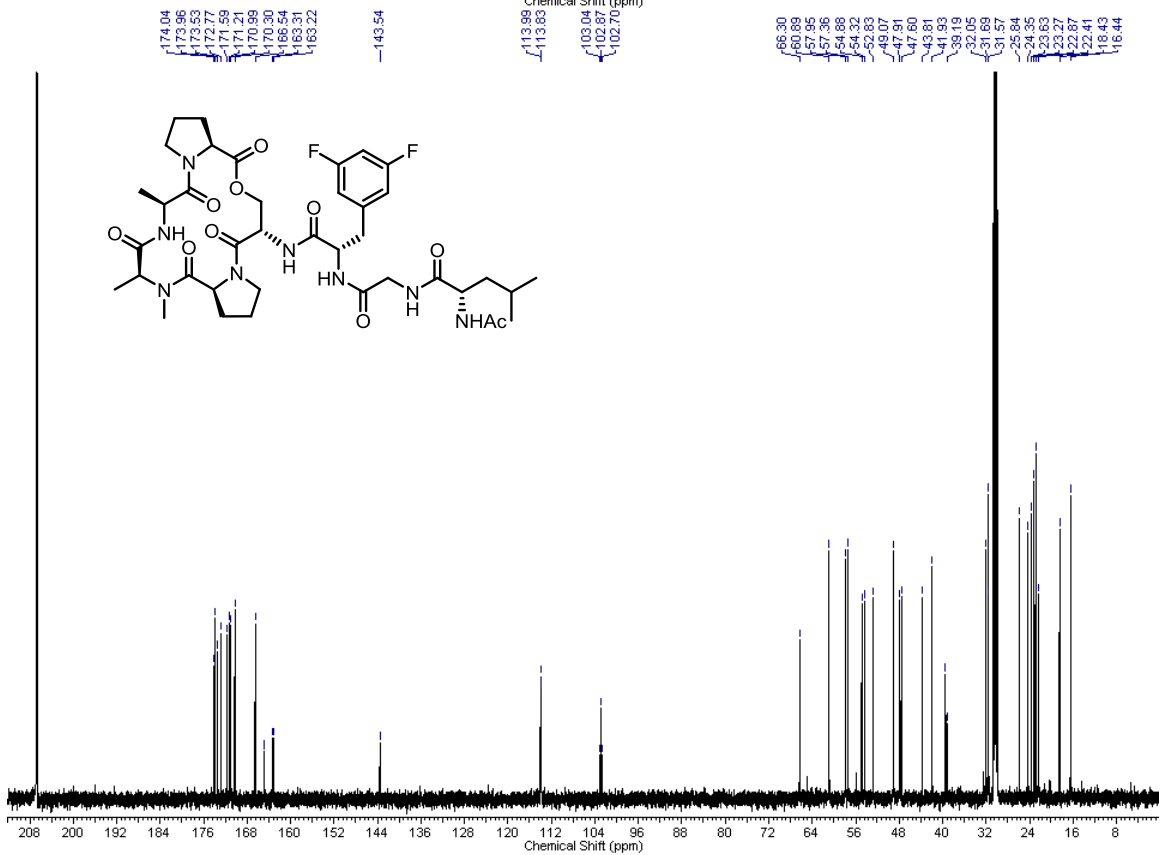
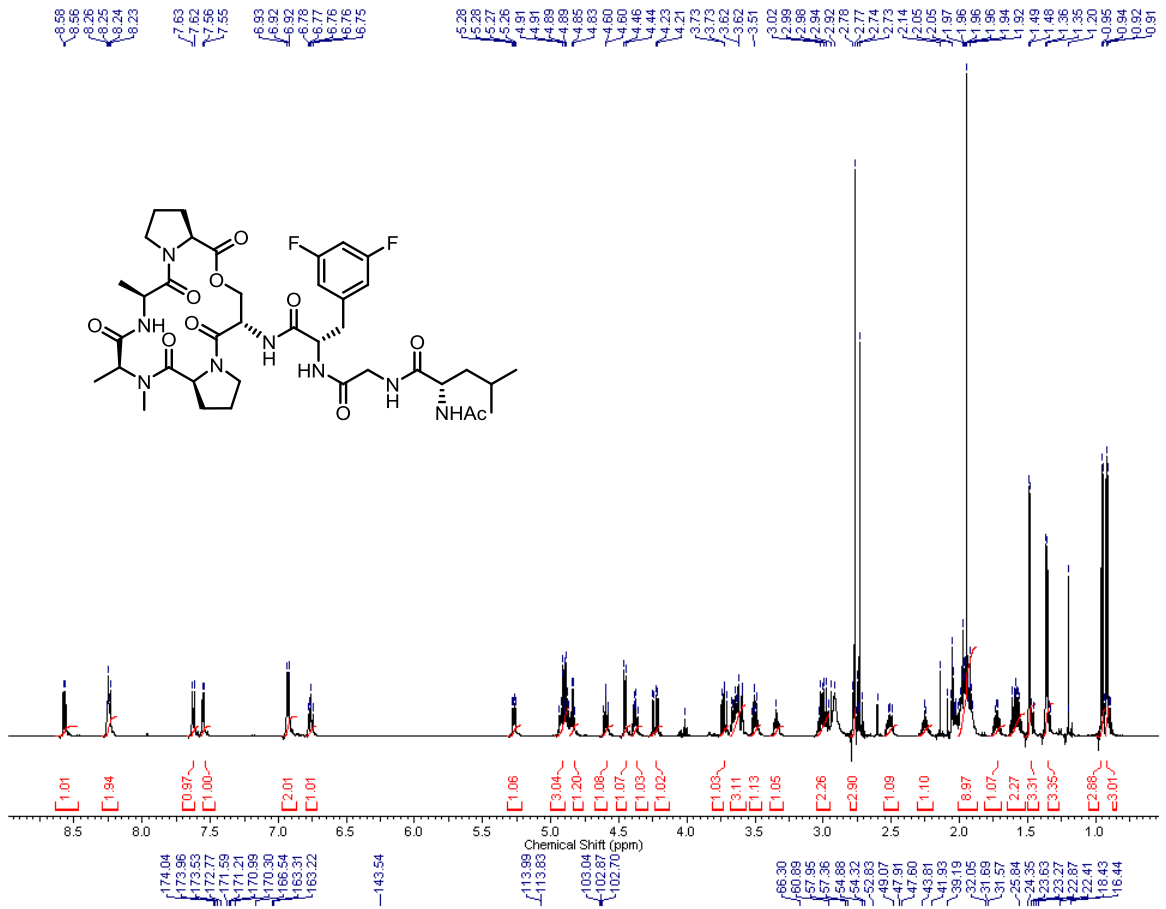
## **Chapter 7 – Synthesis and Evaluation of ADEPs with Modified side Chains**

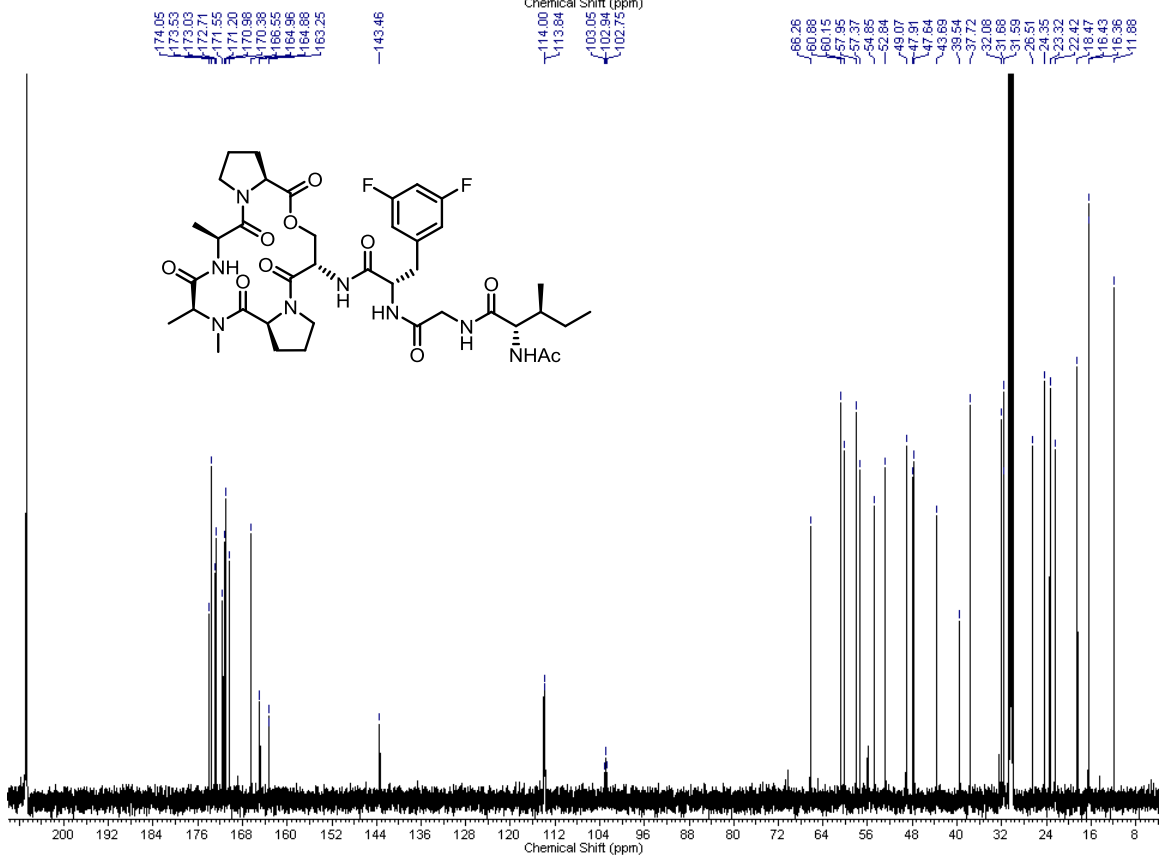
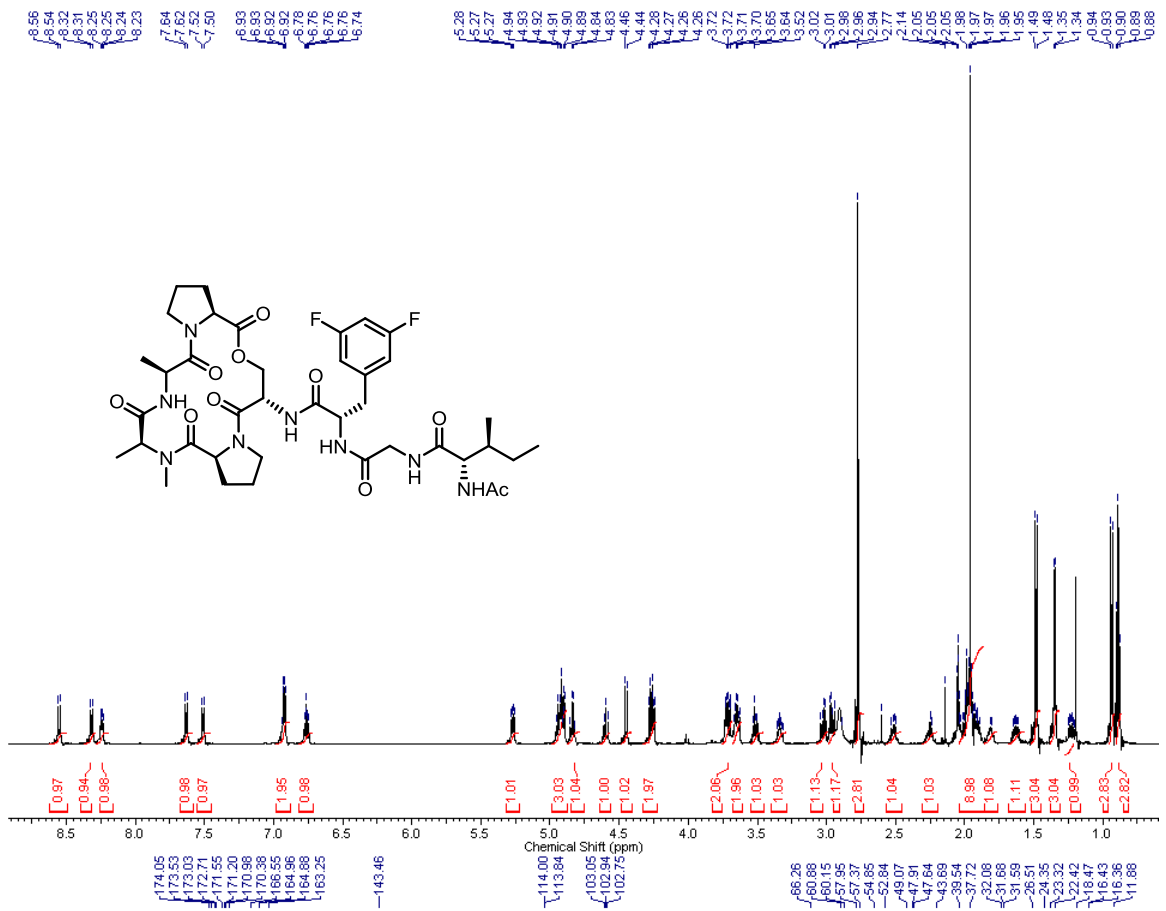


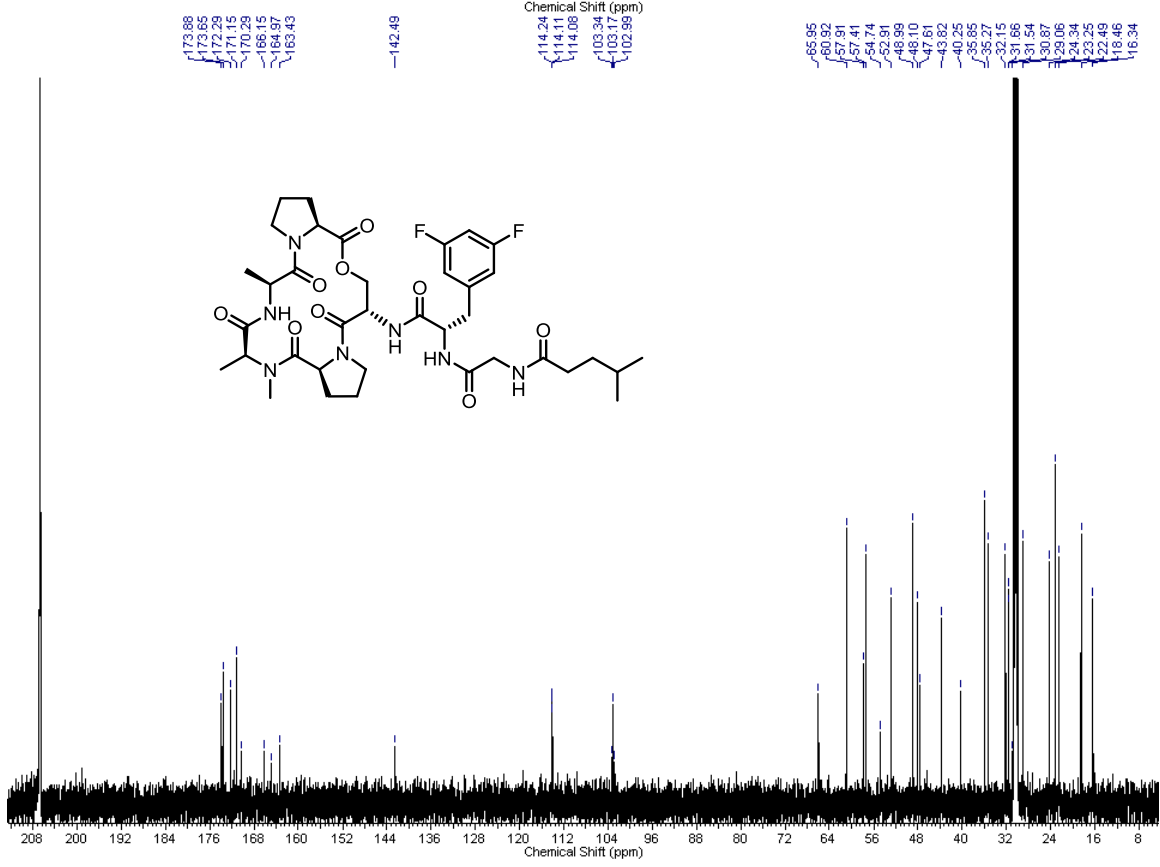
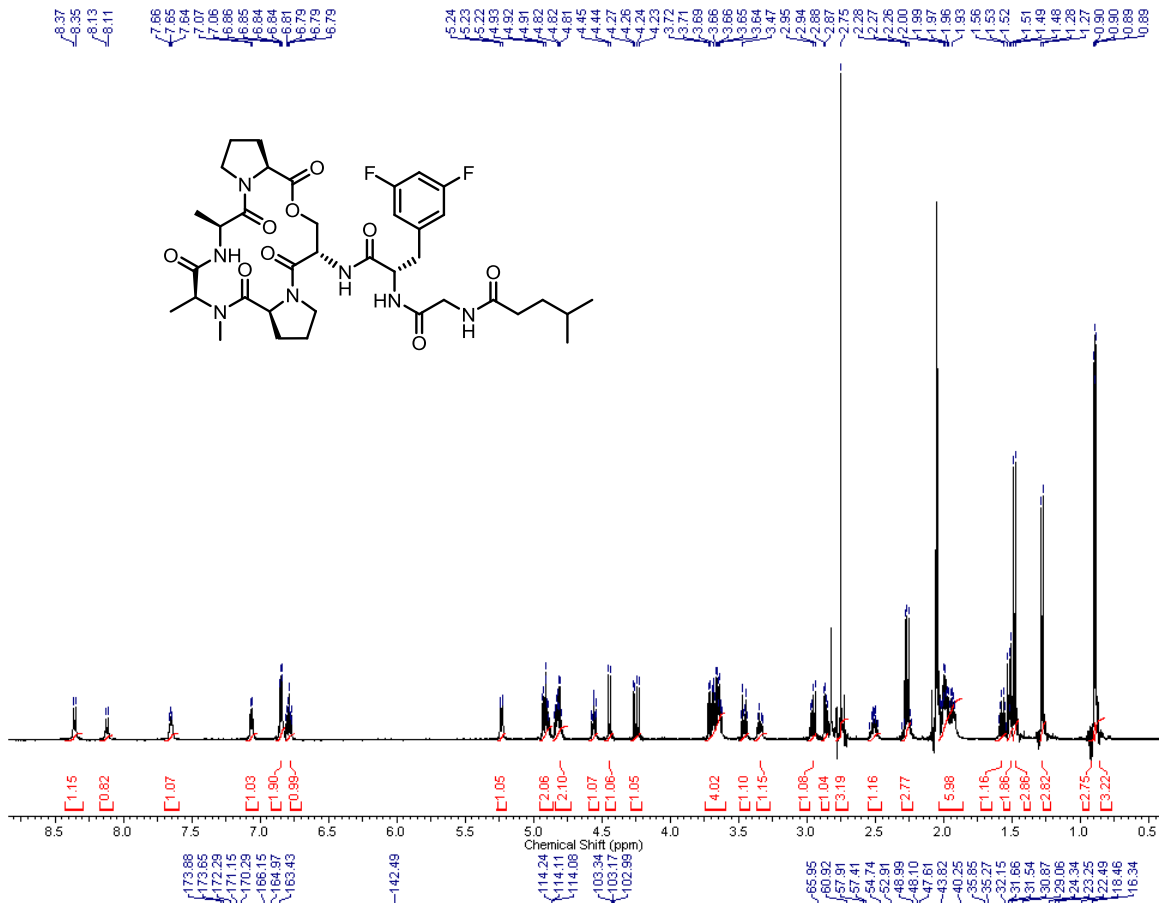






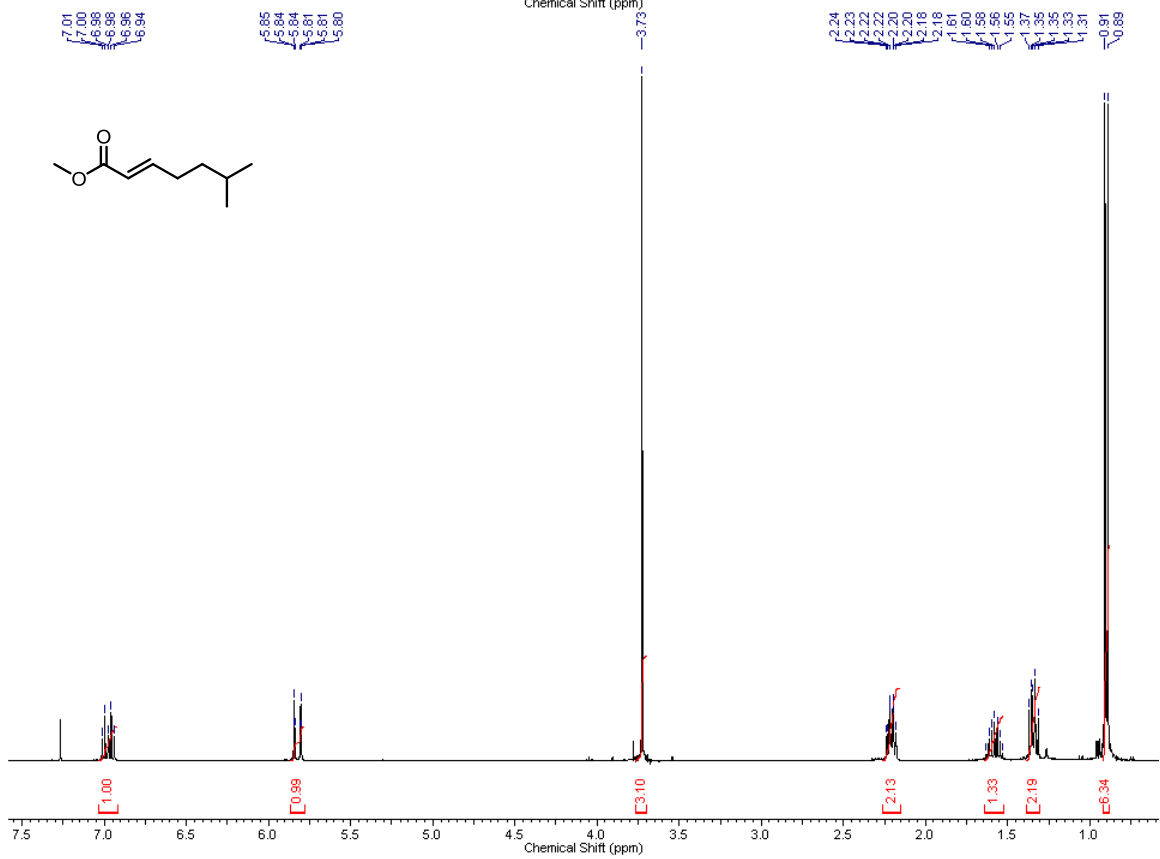
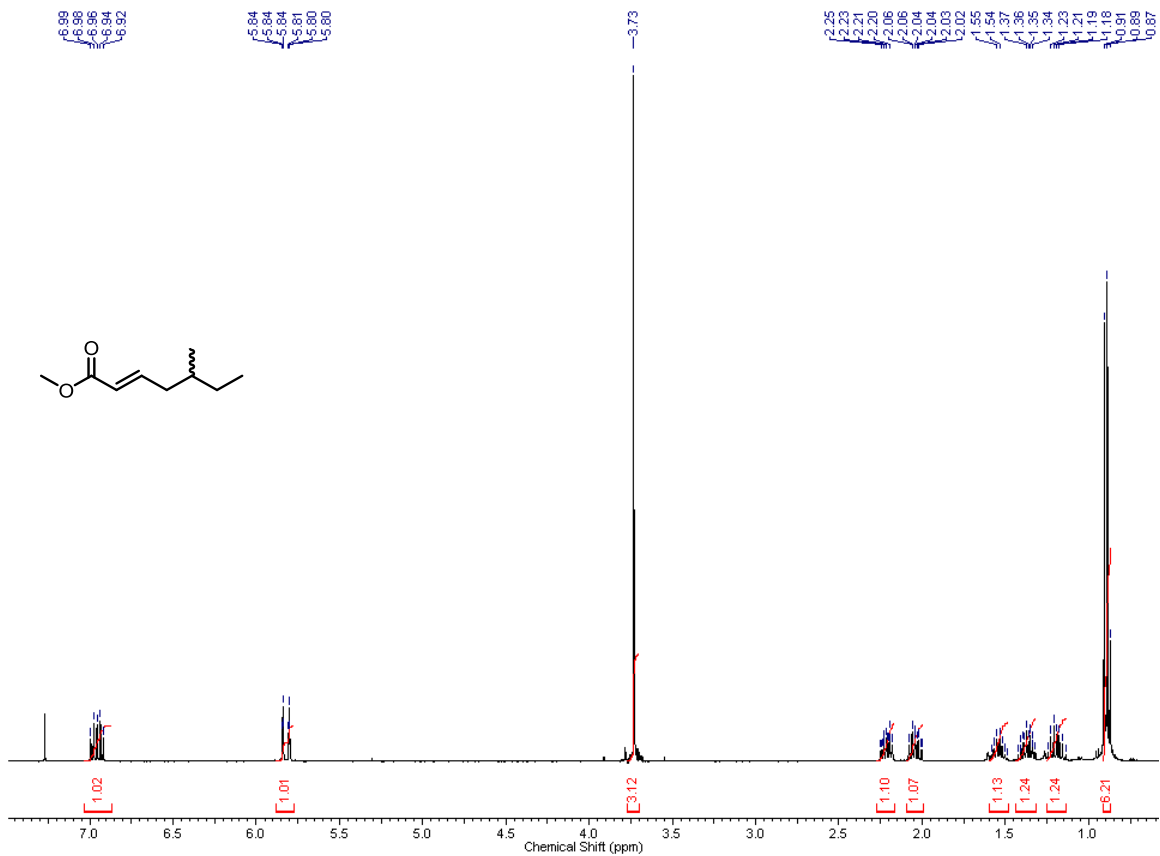


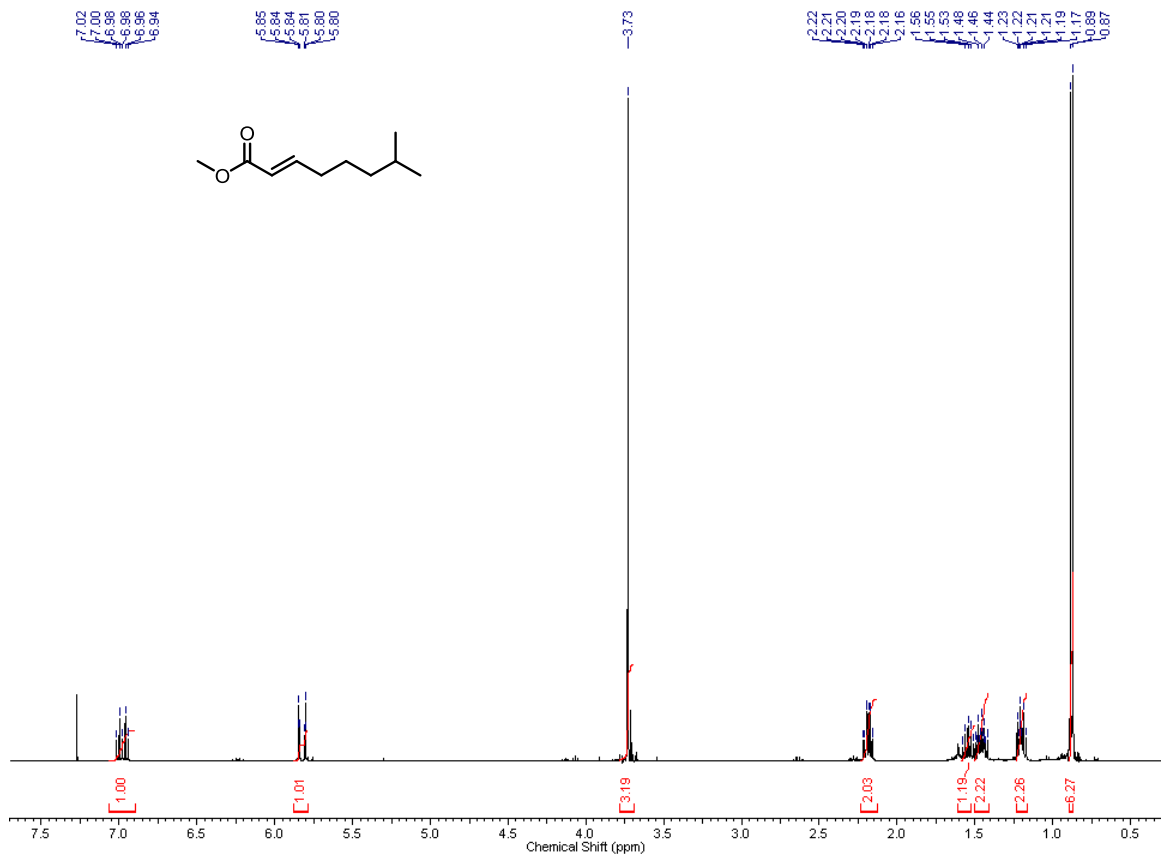


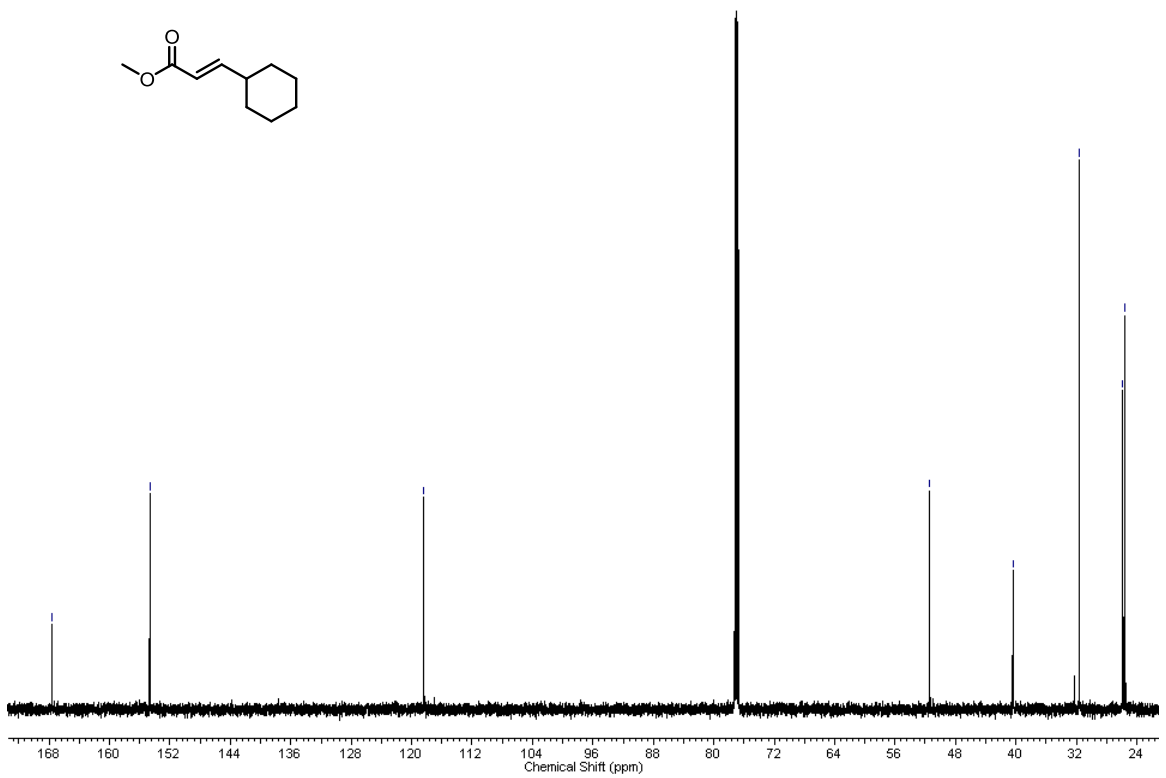
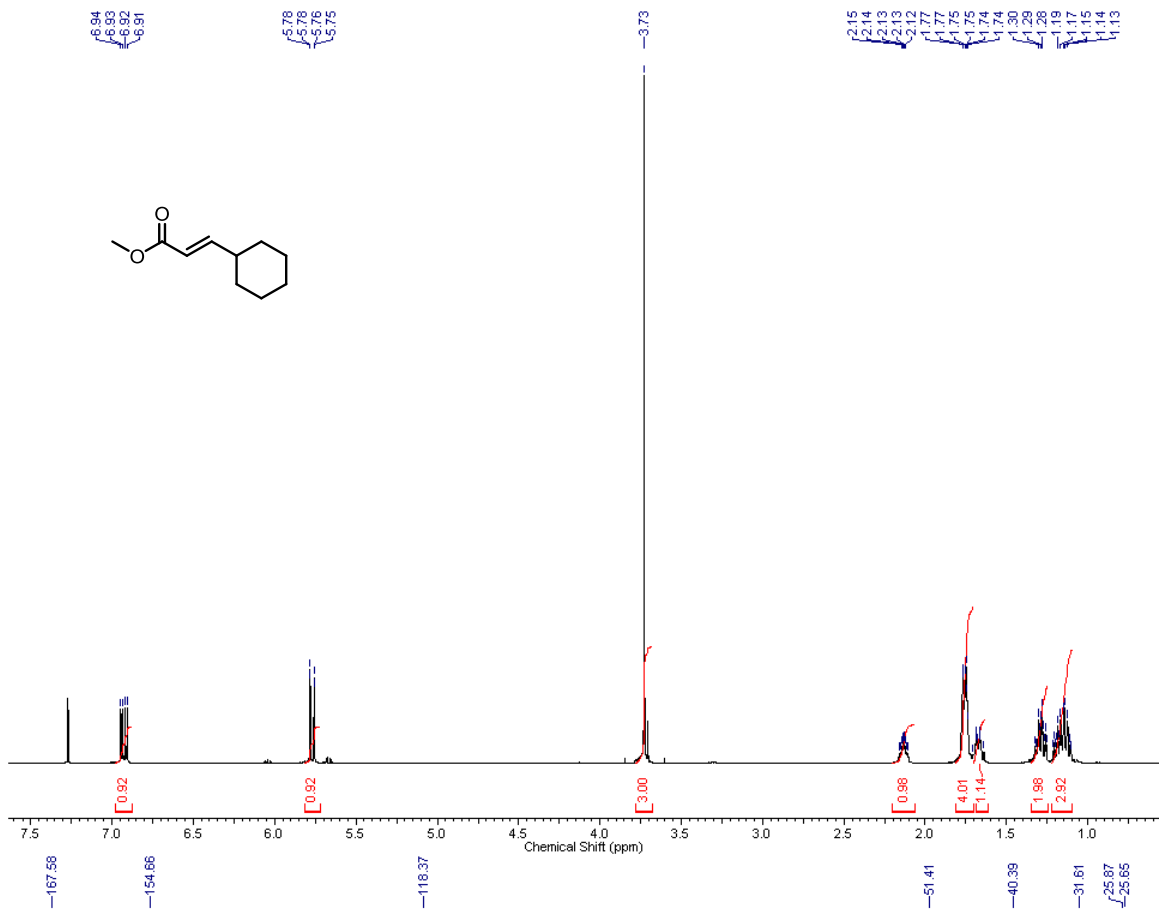


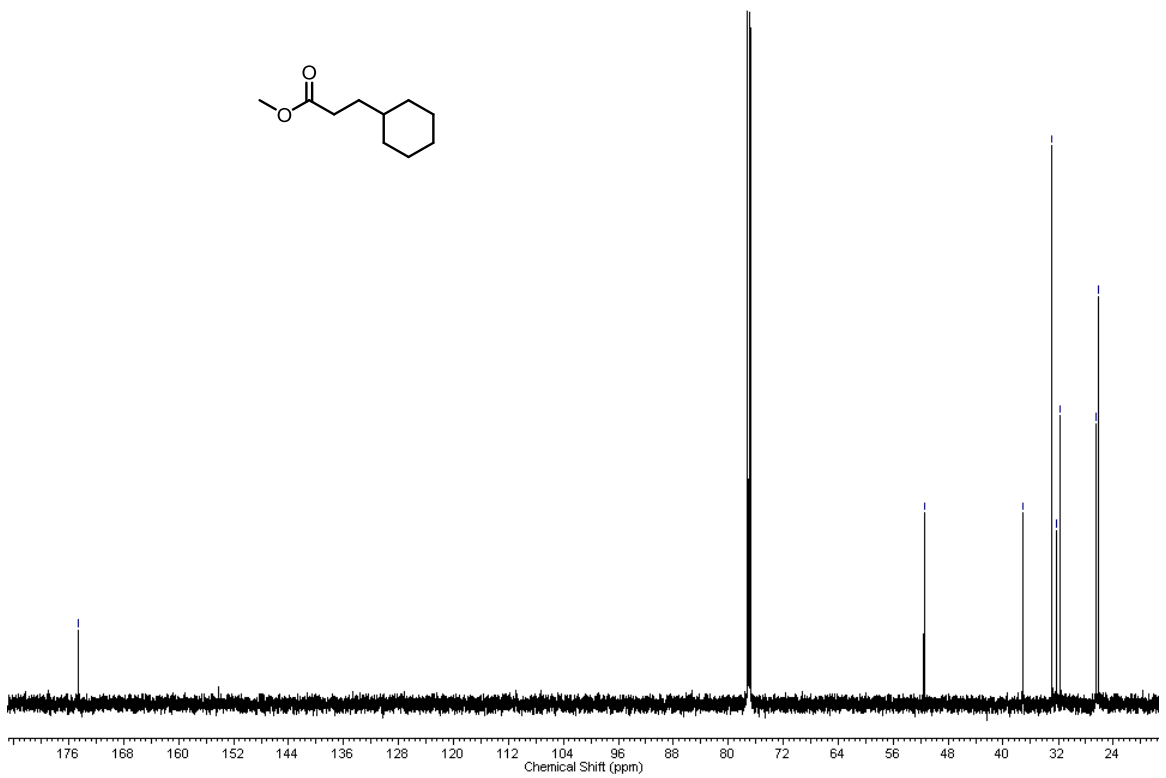
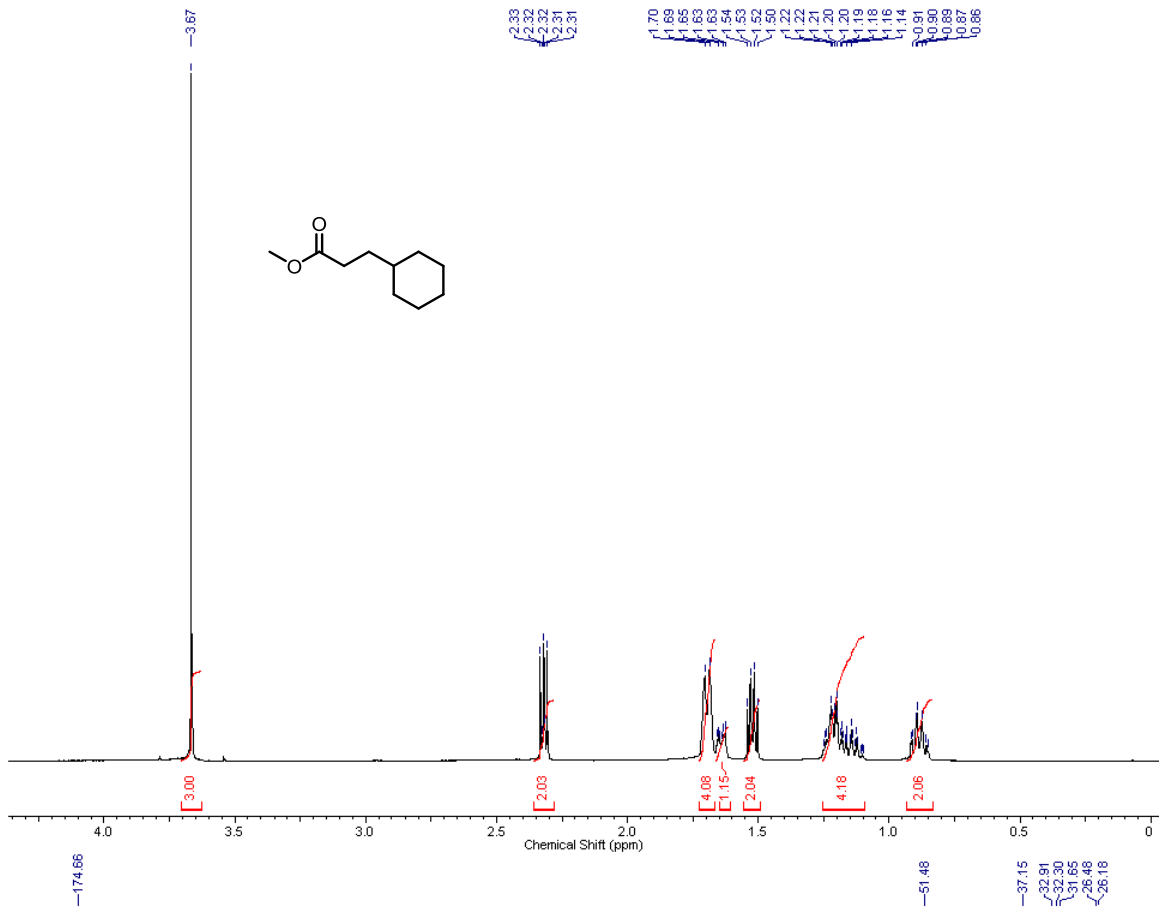


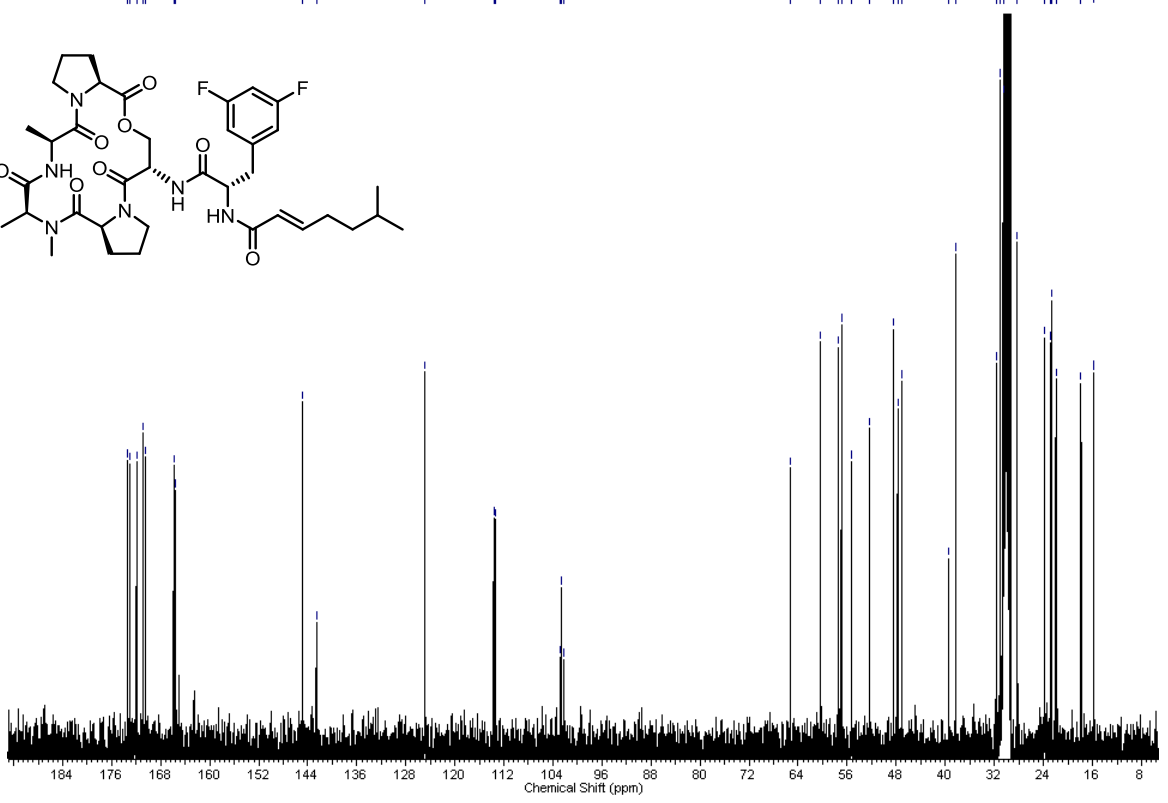
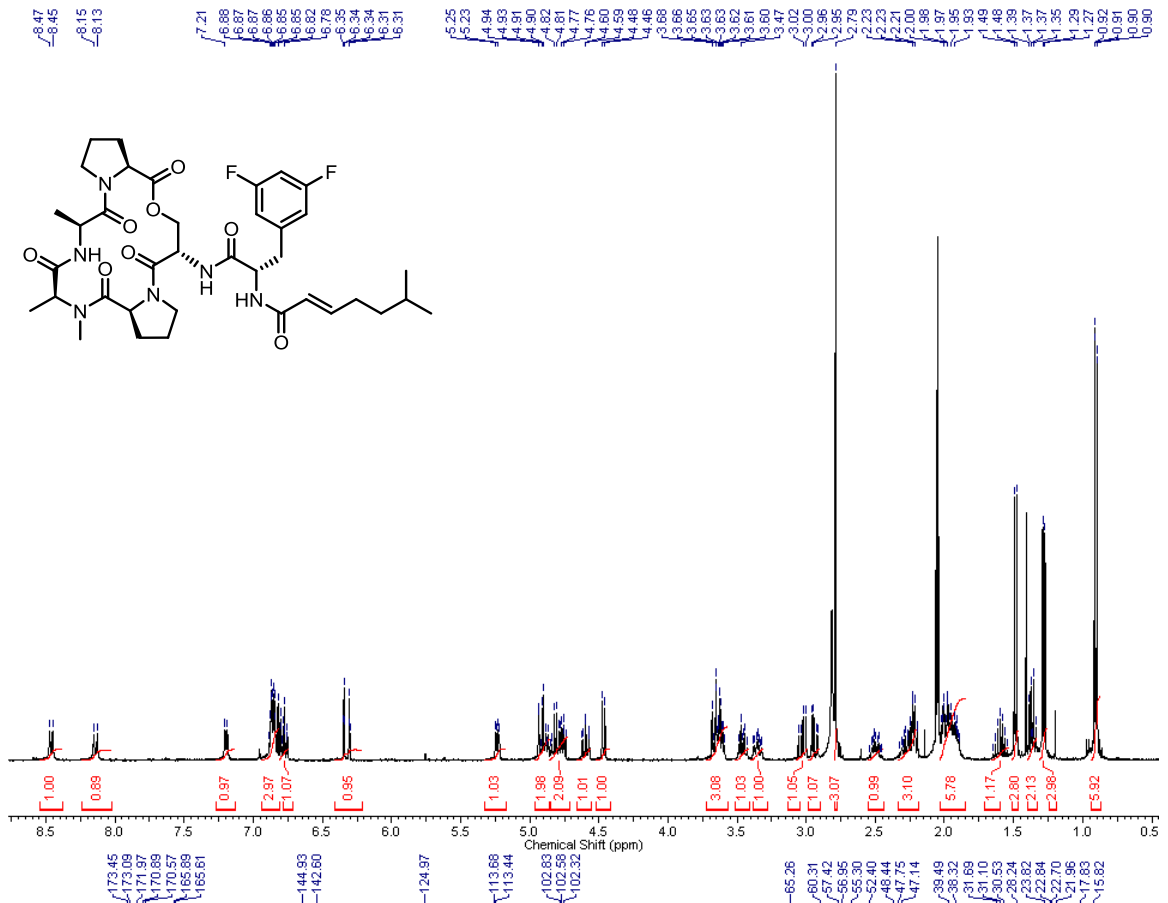


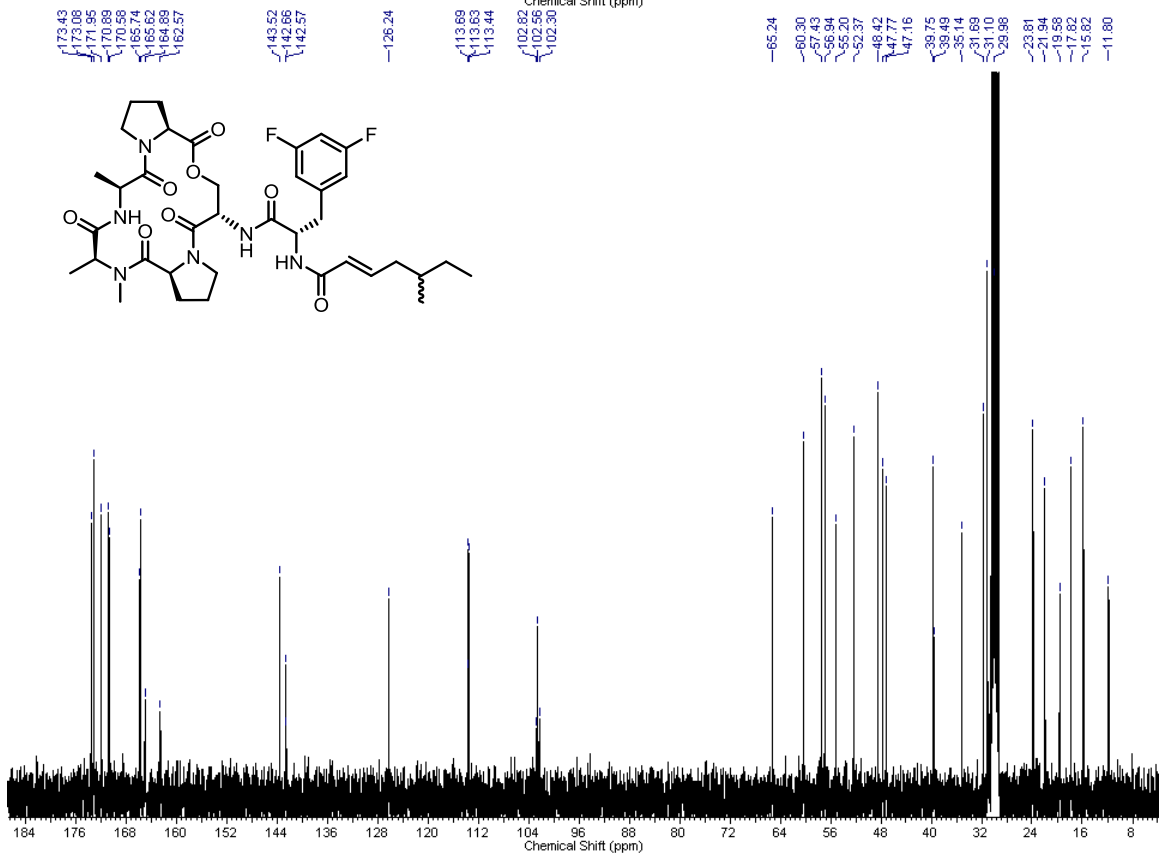
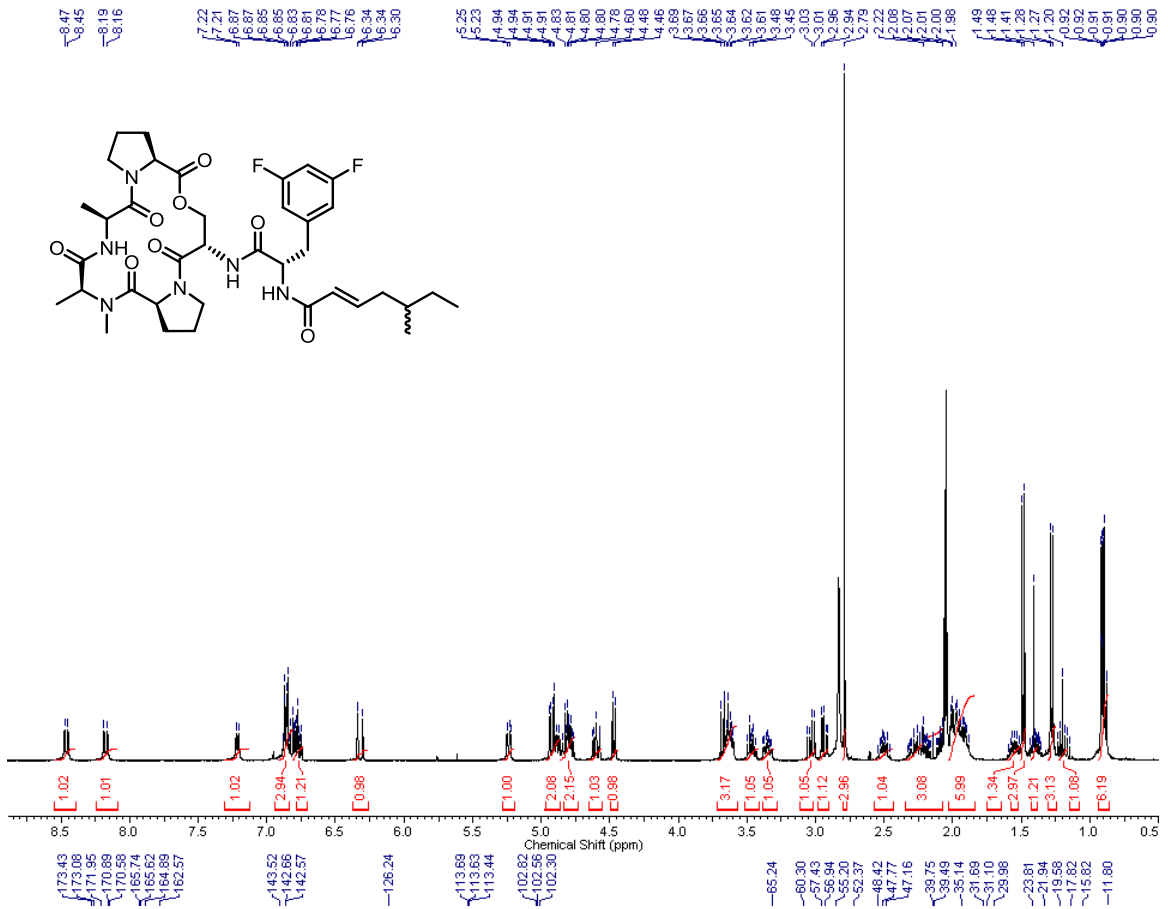


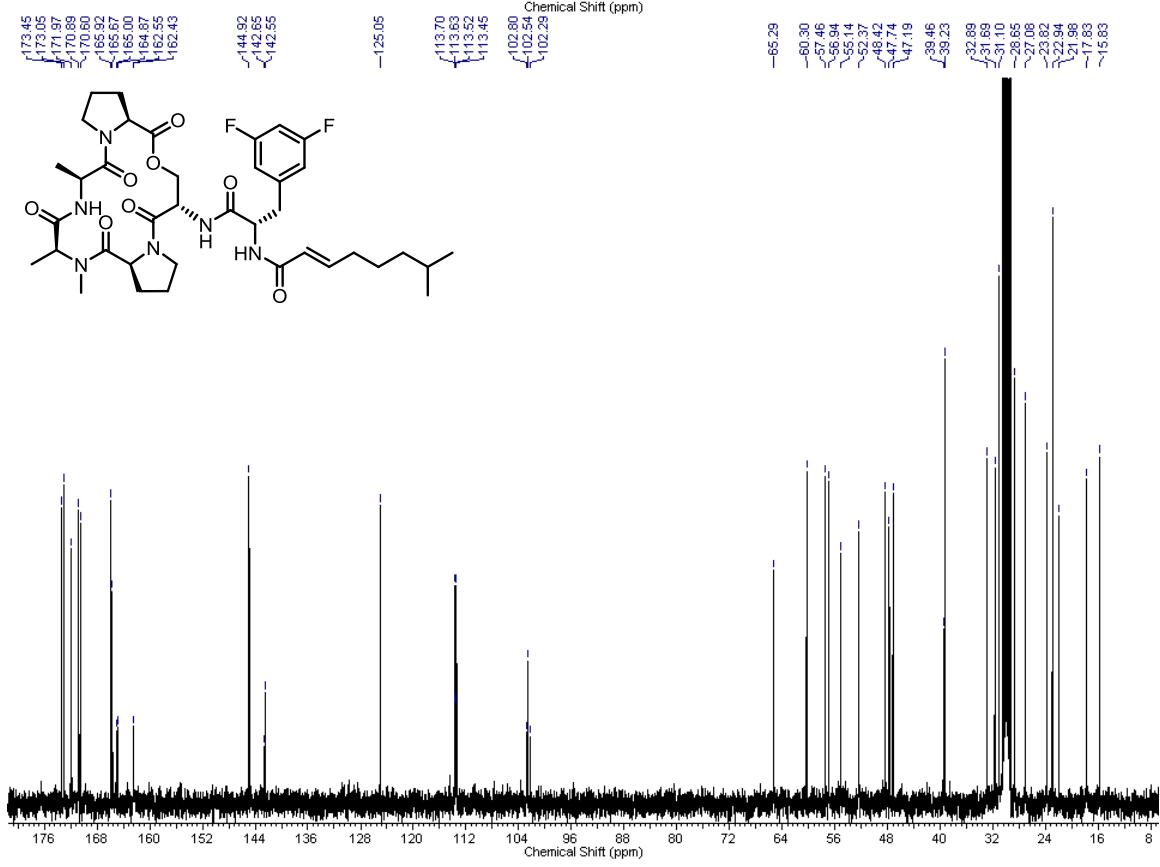
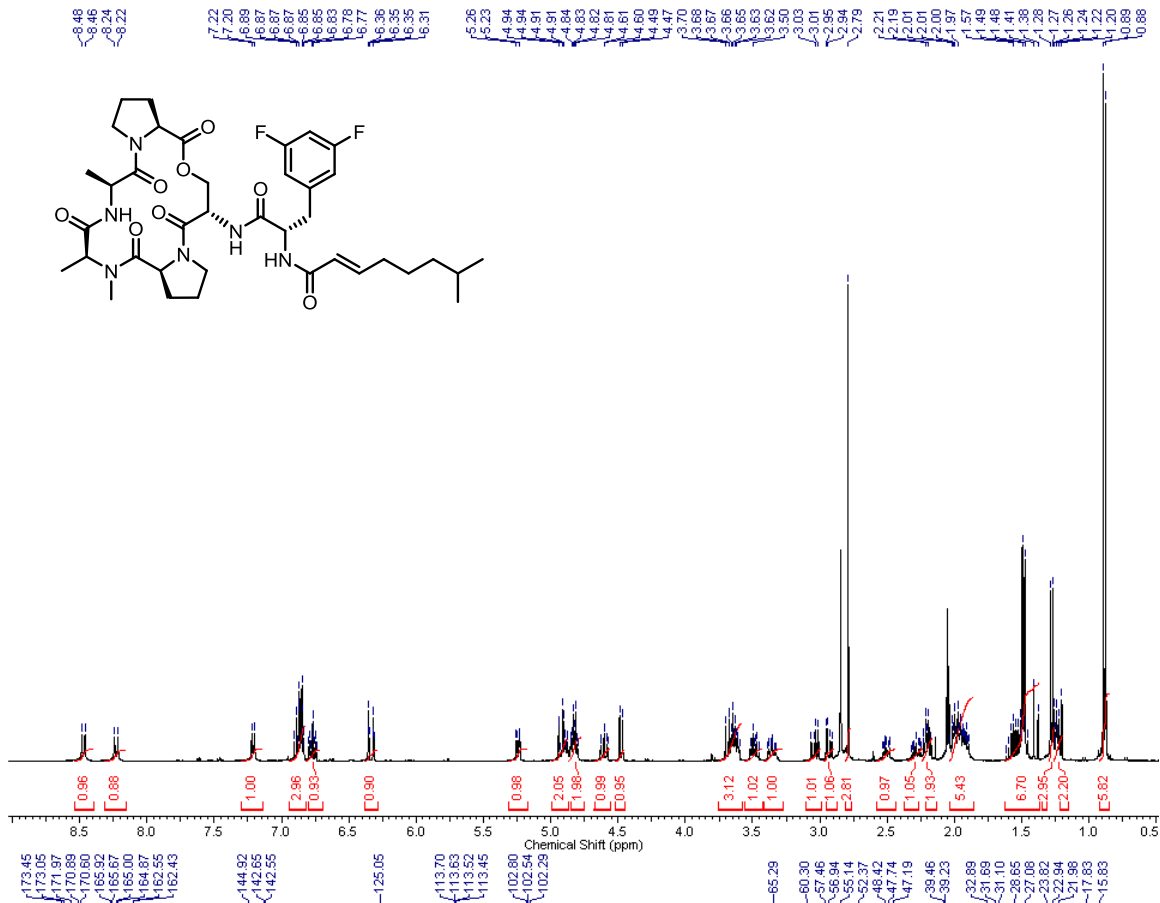




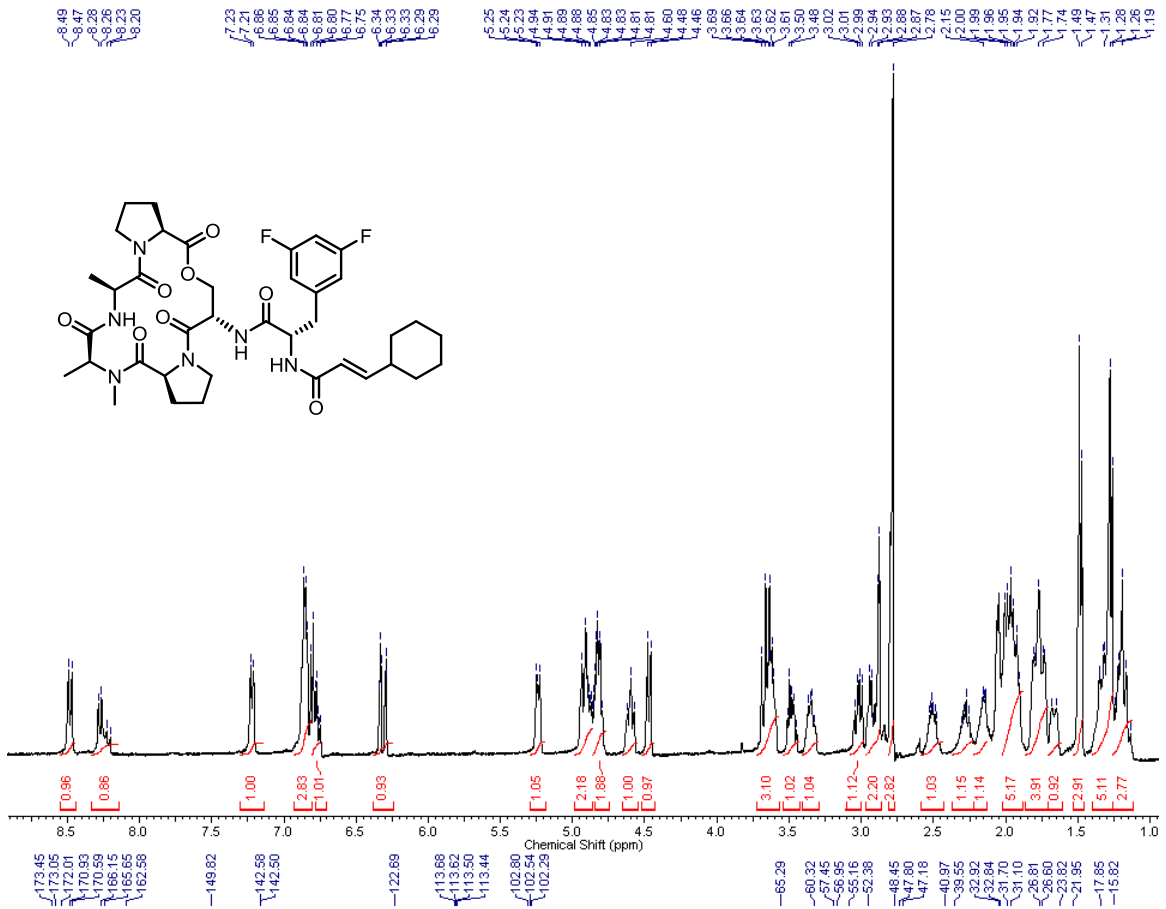


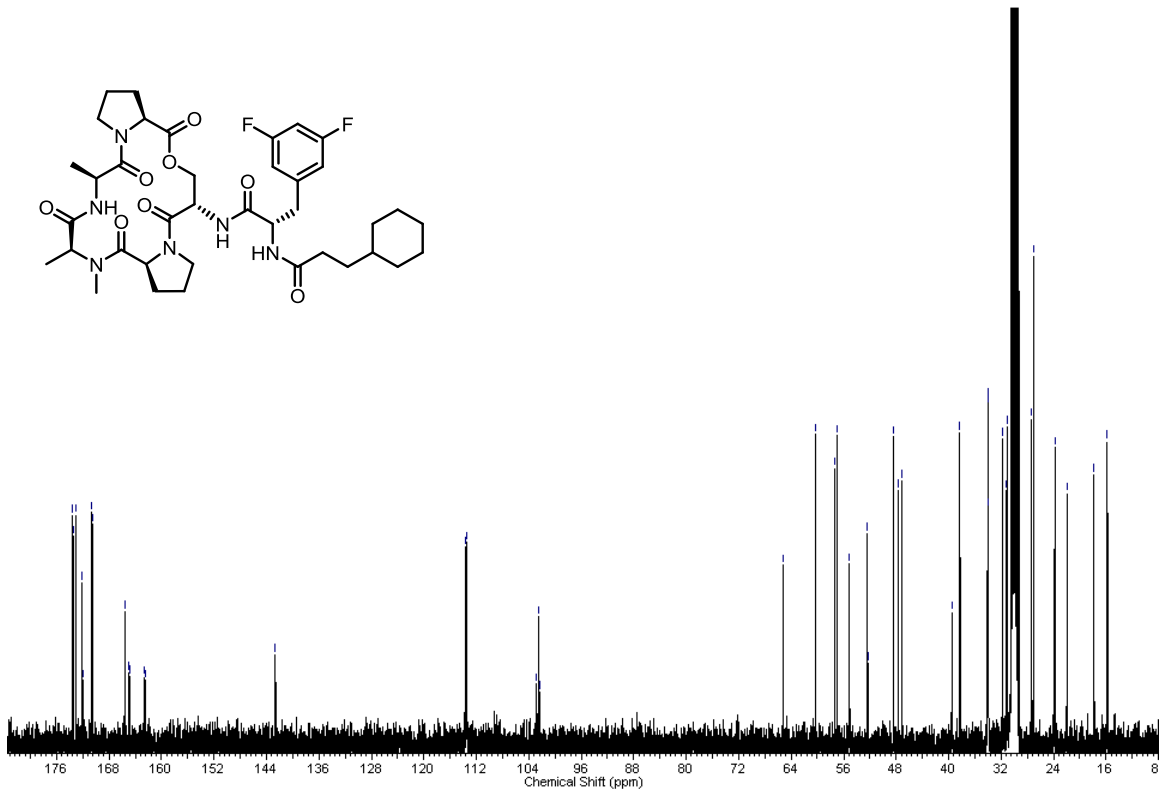
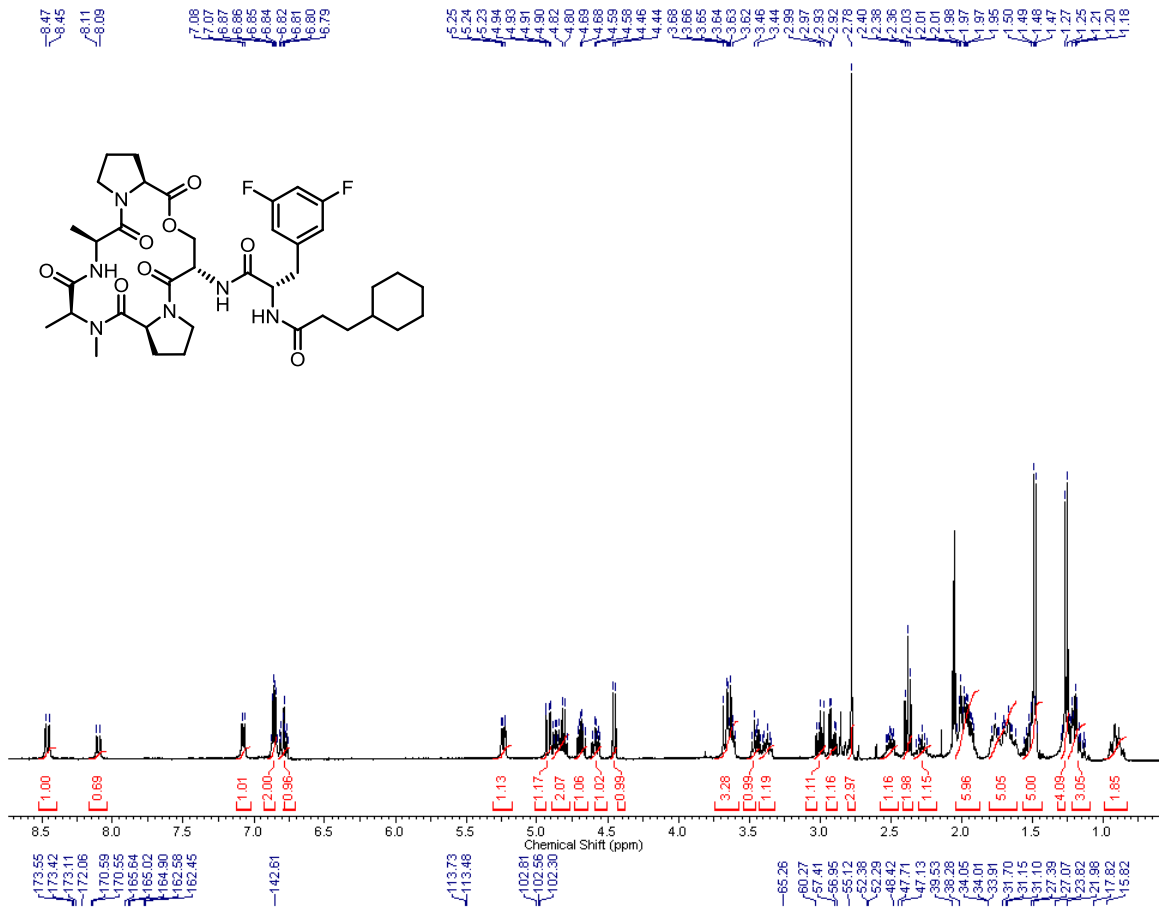


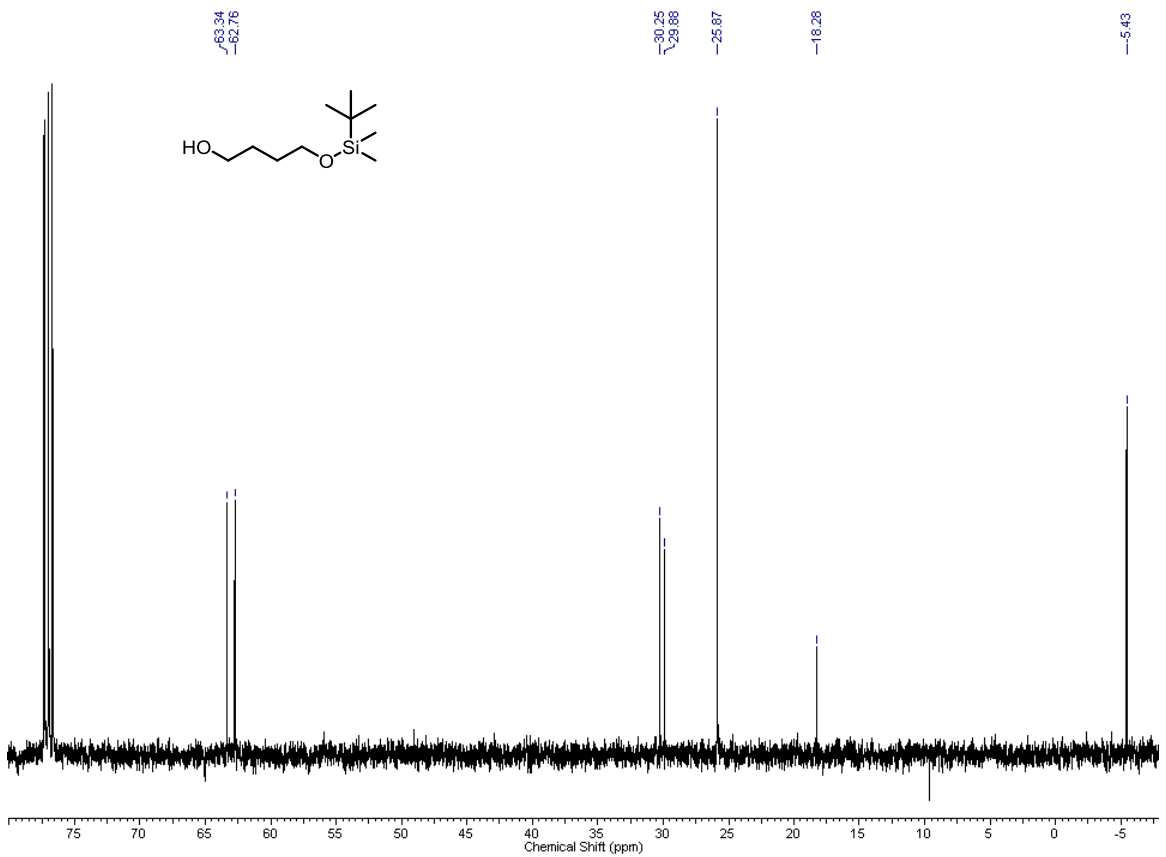
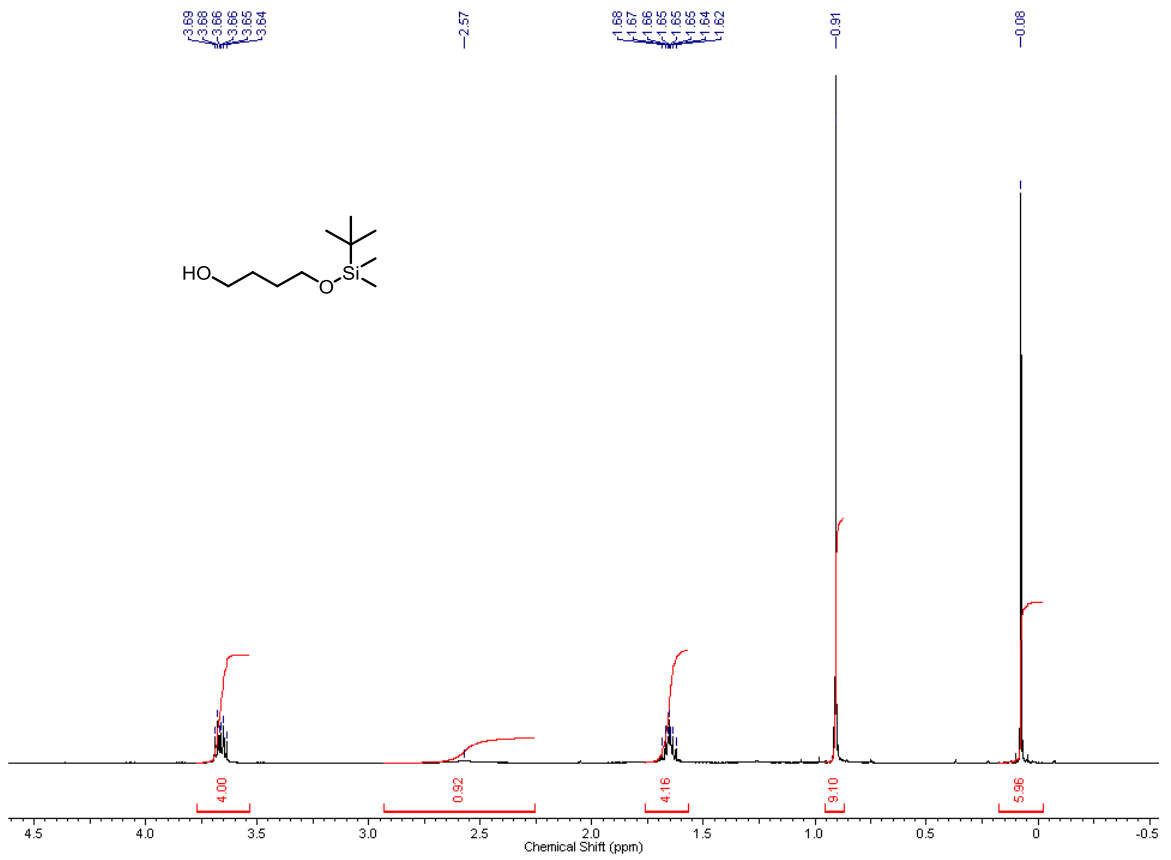


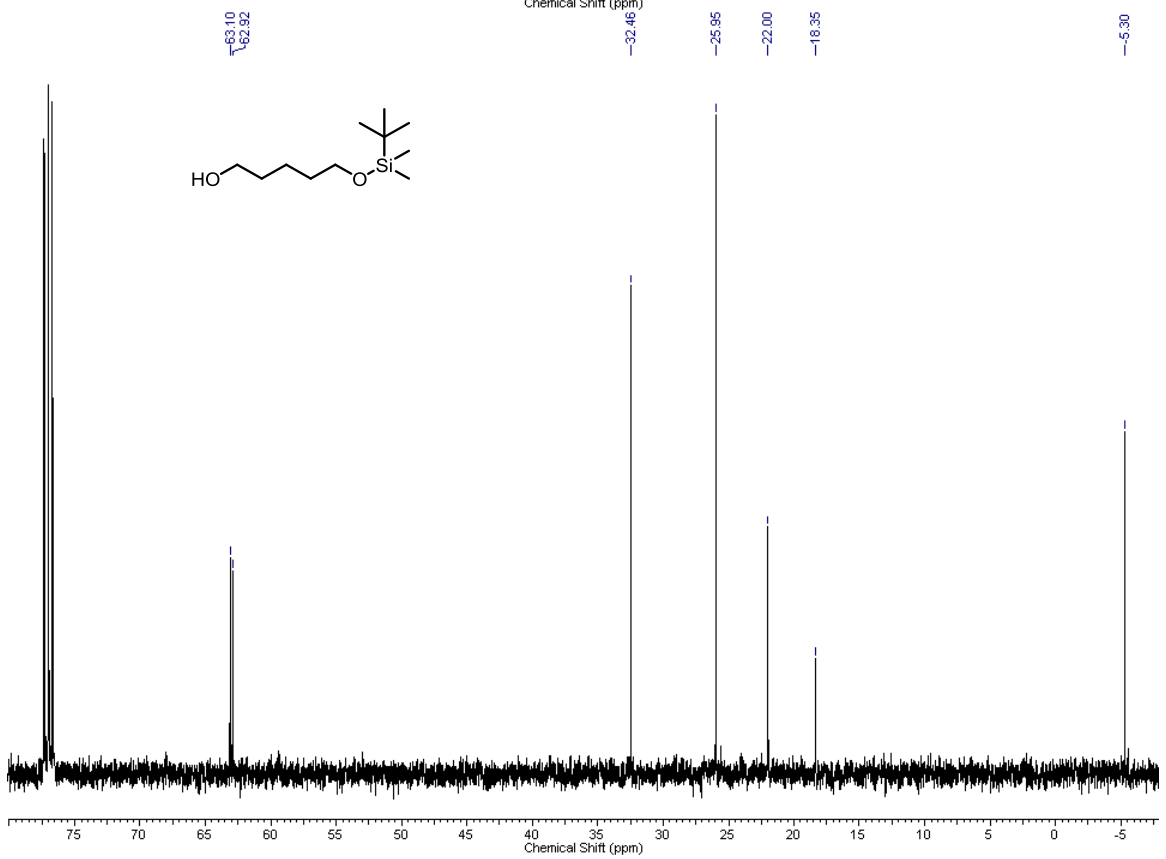
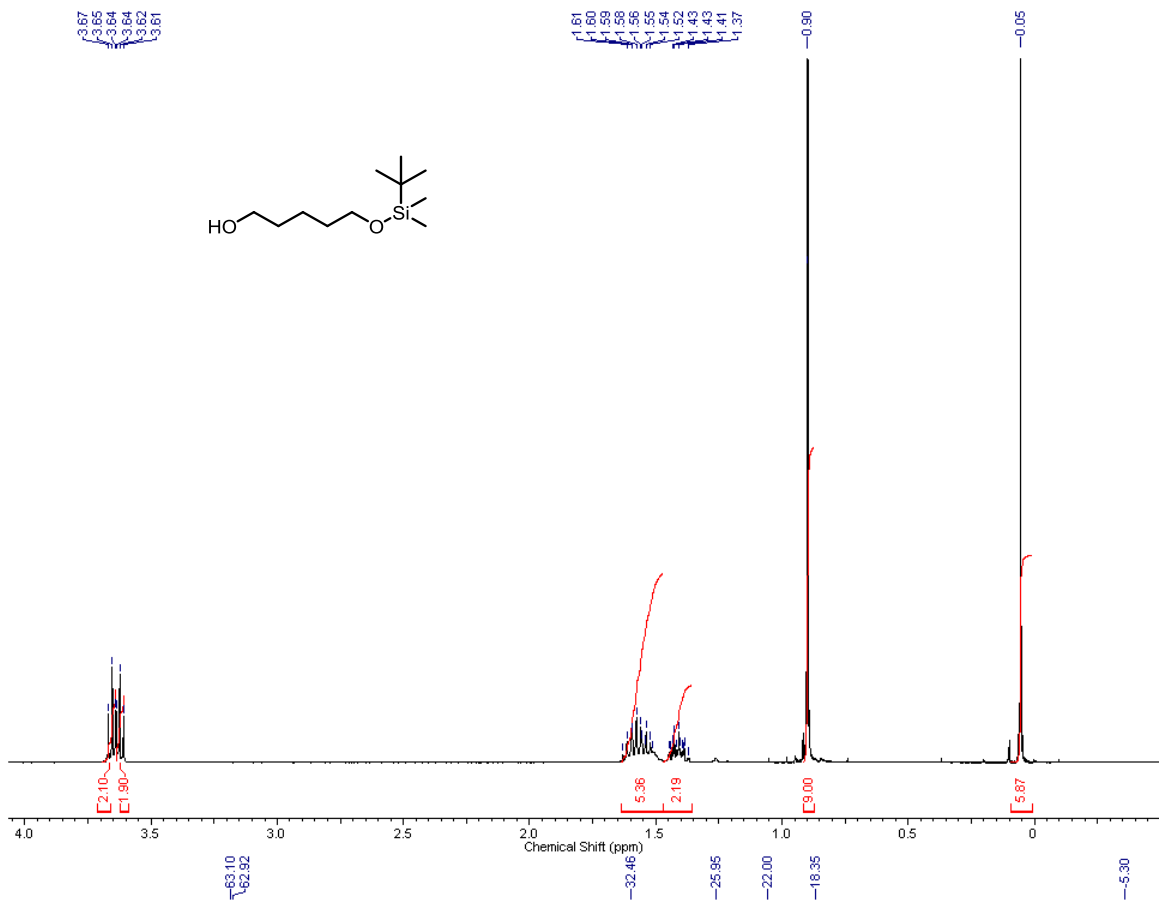


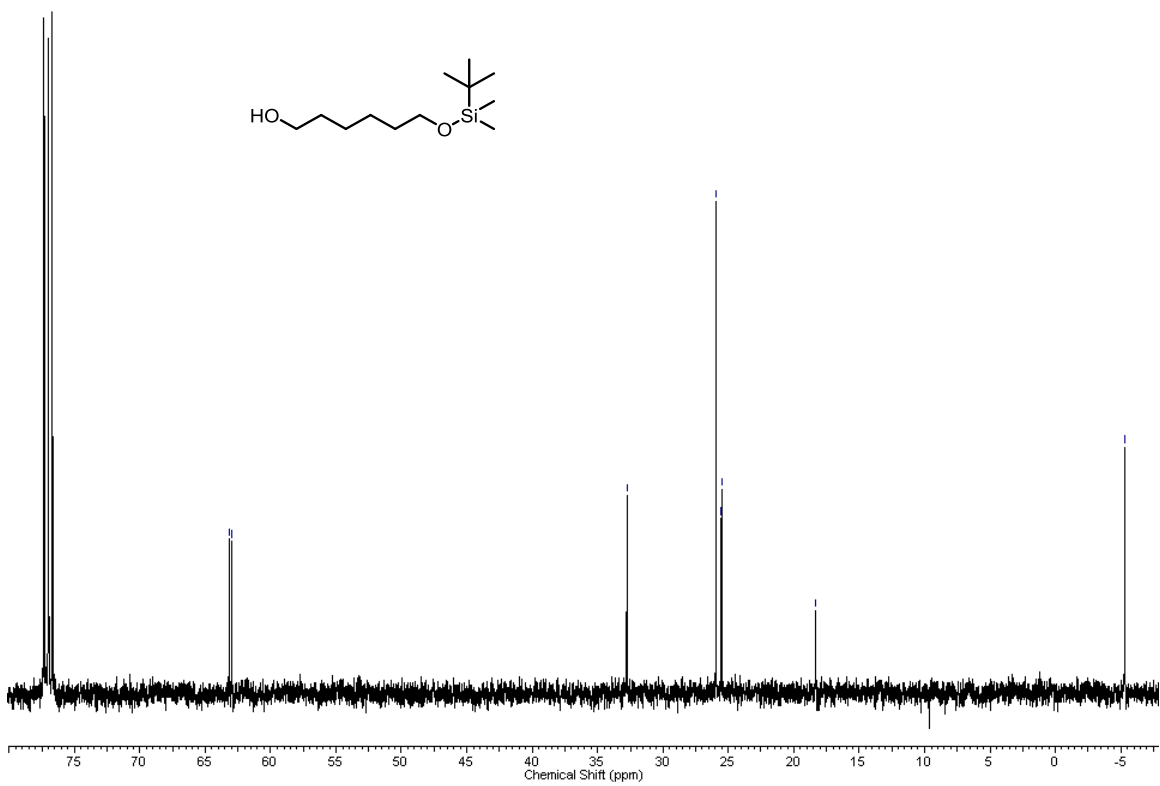
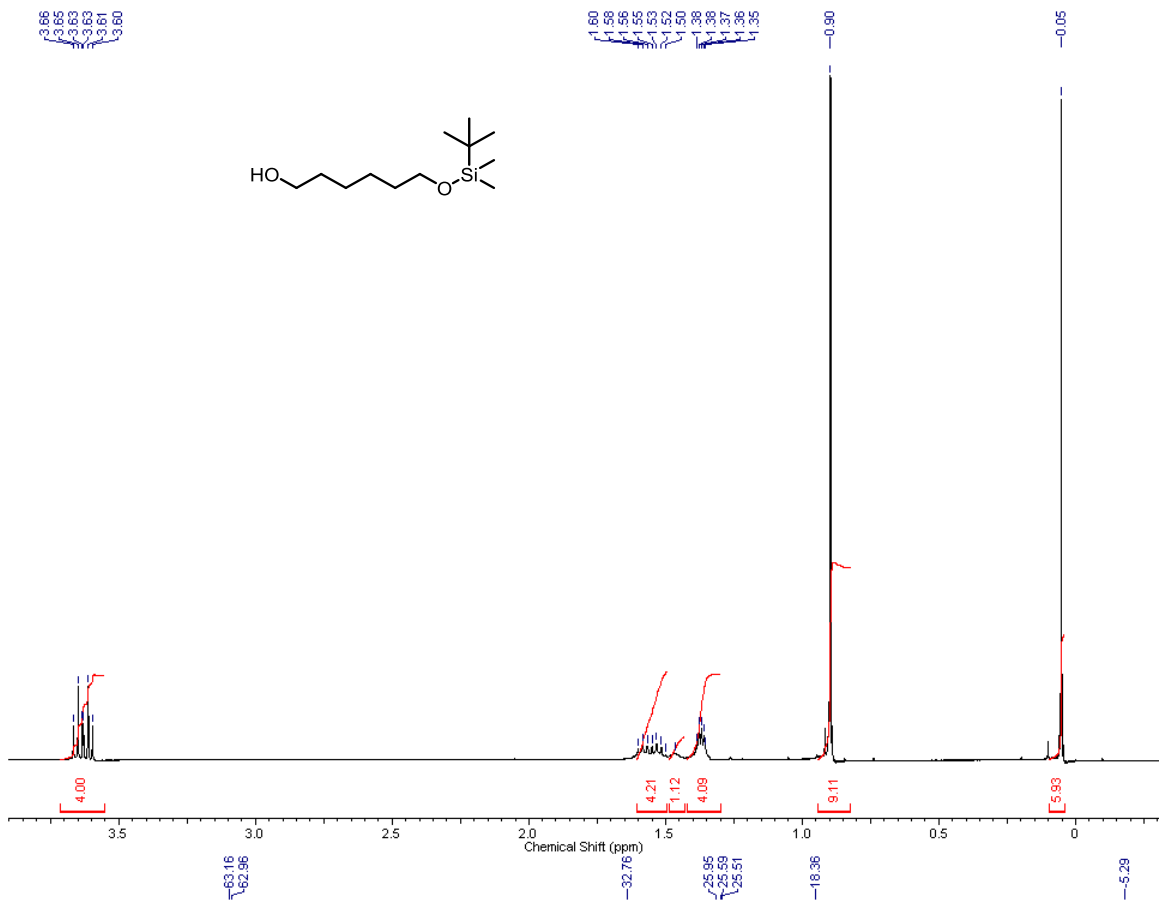


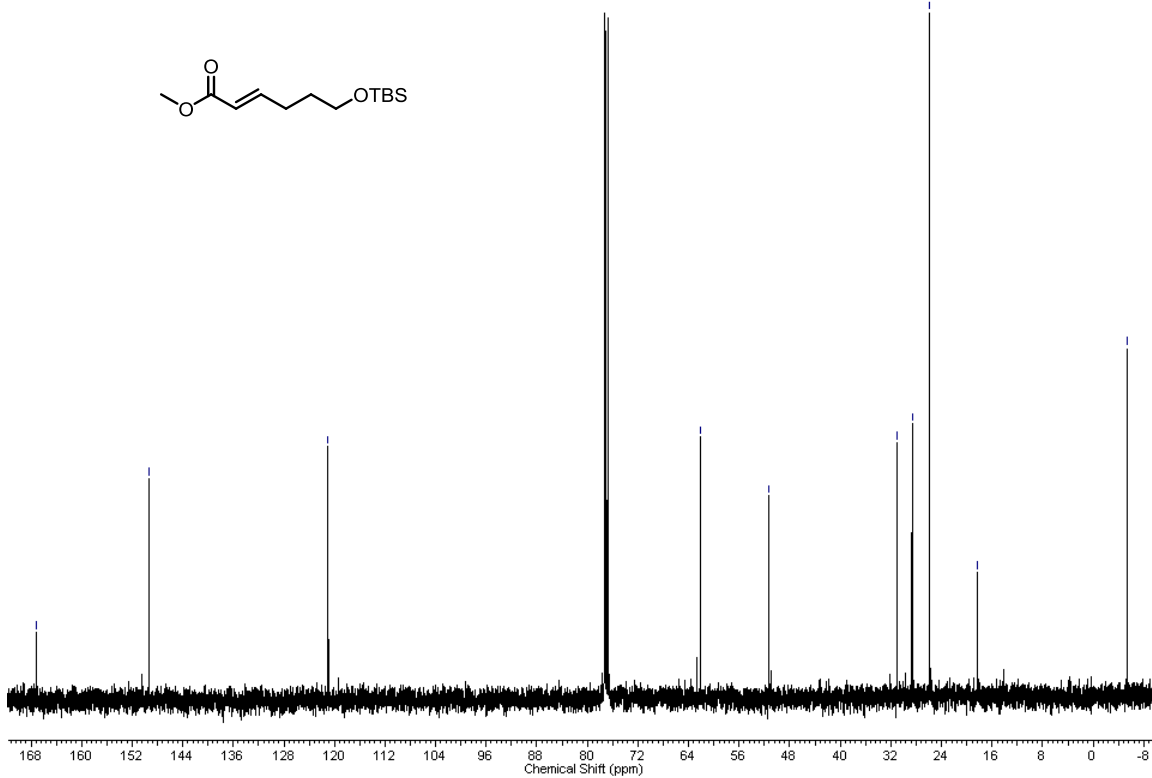
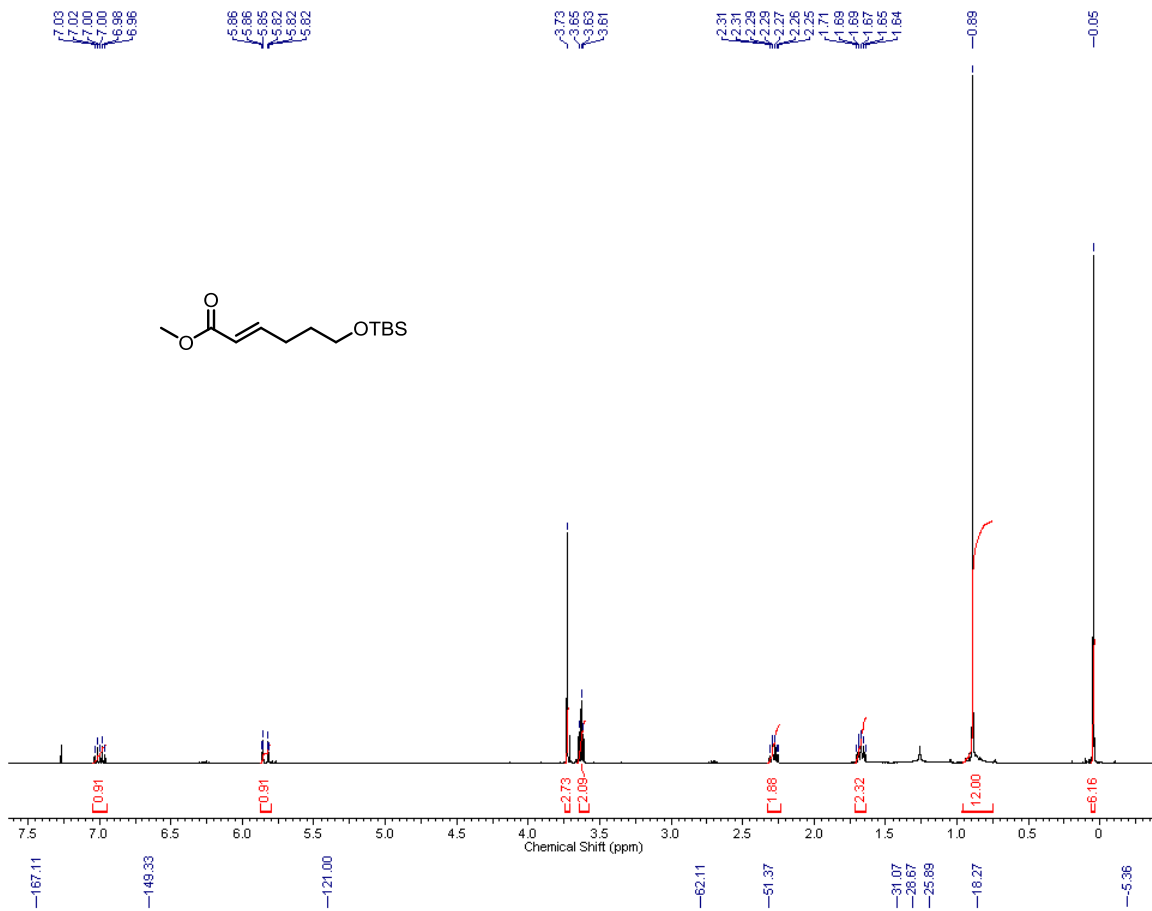


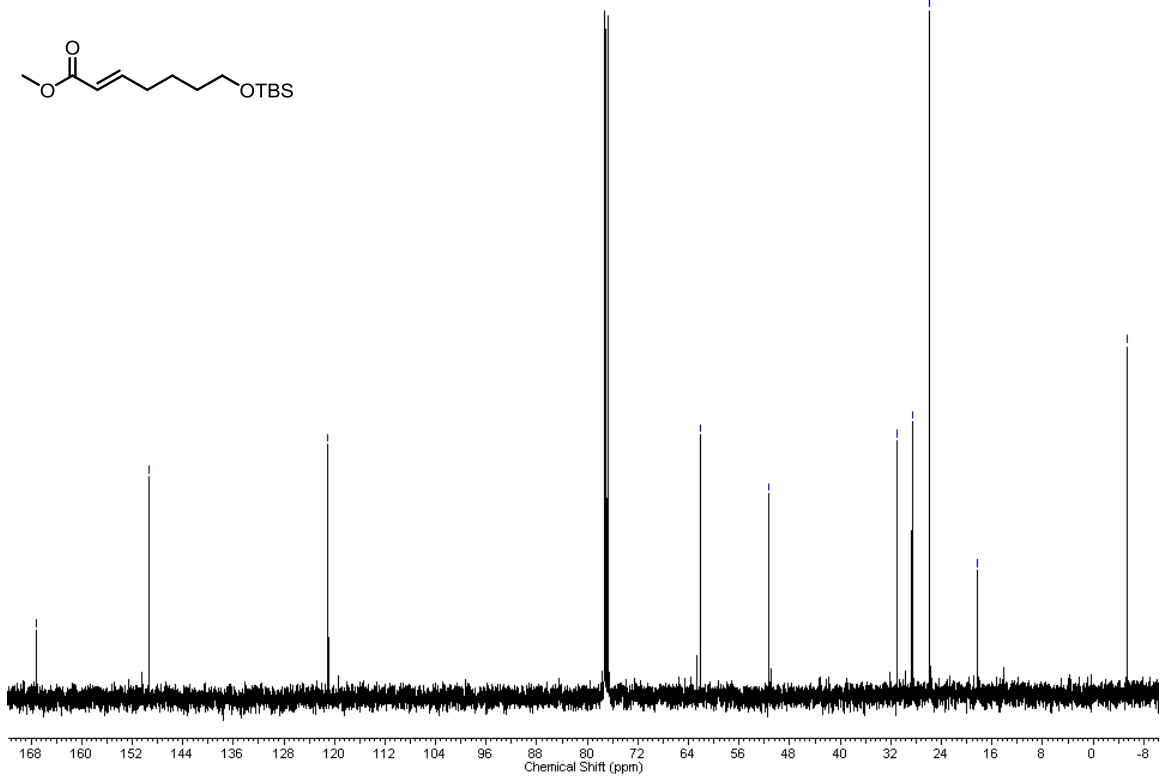
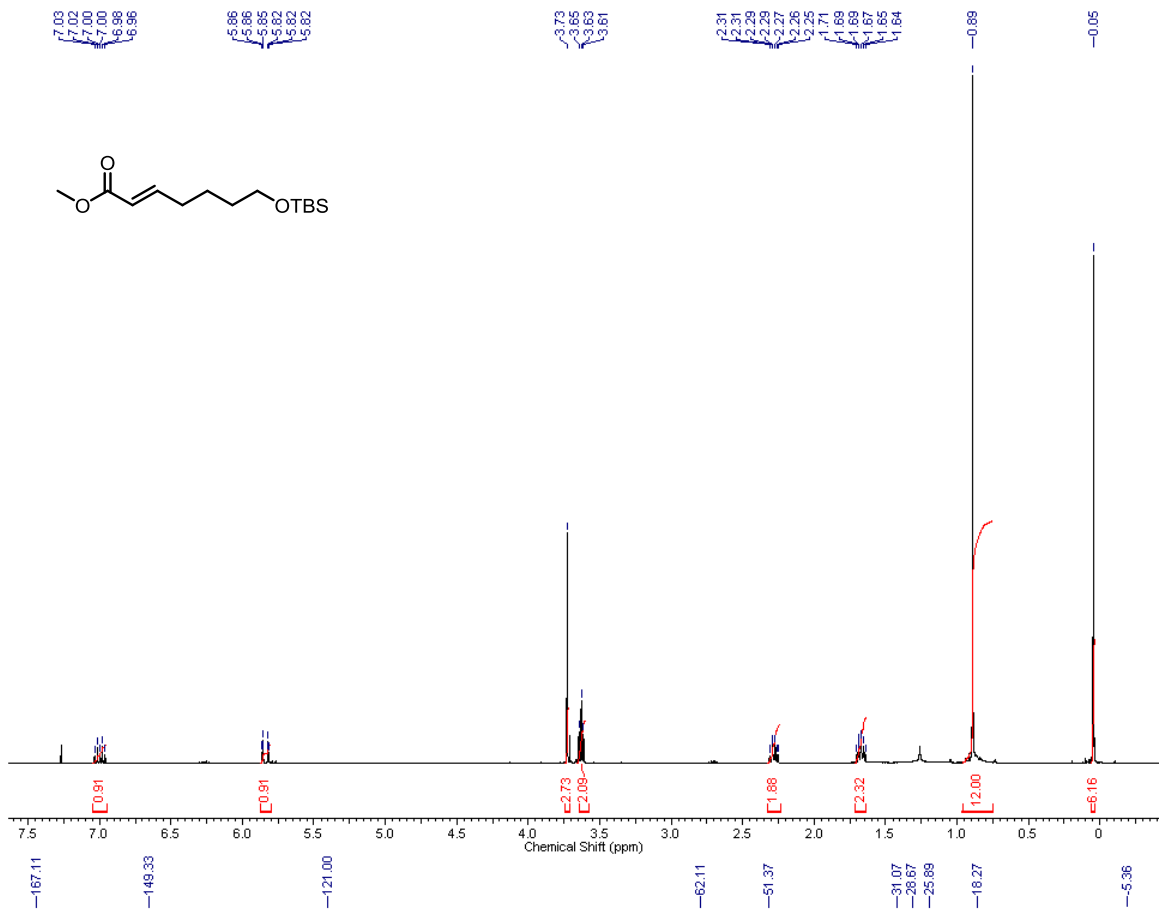


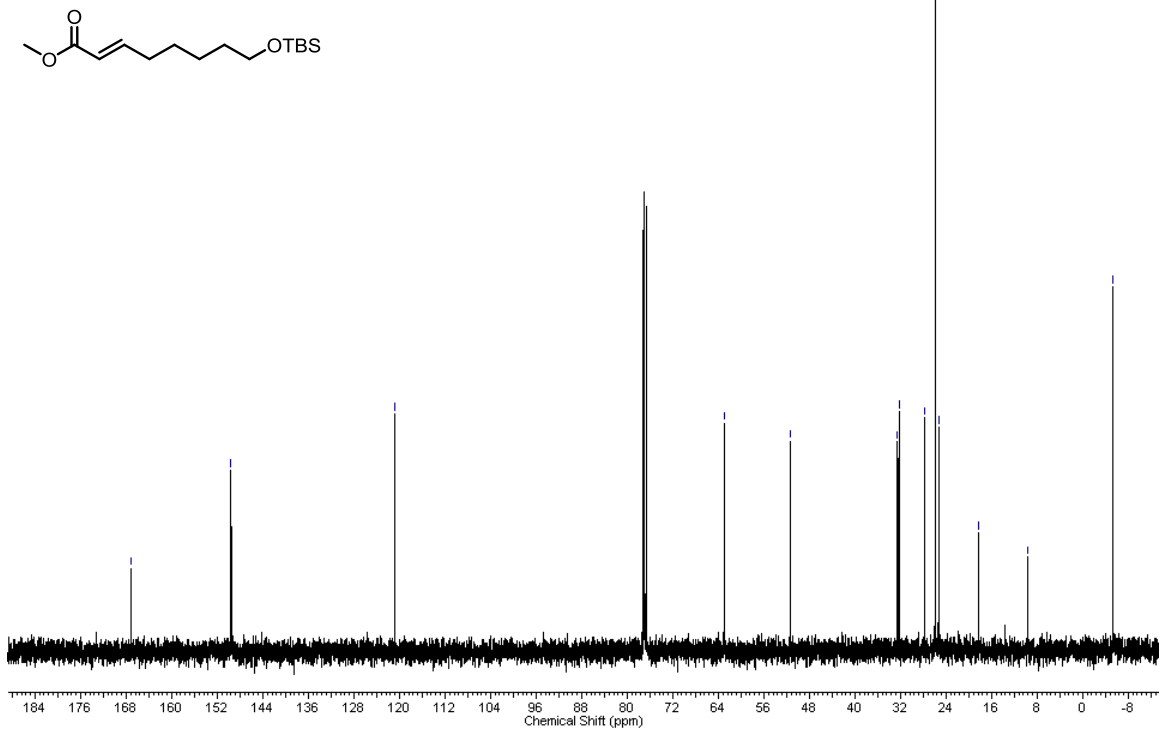
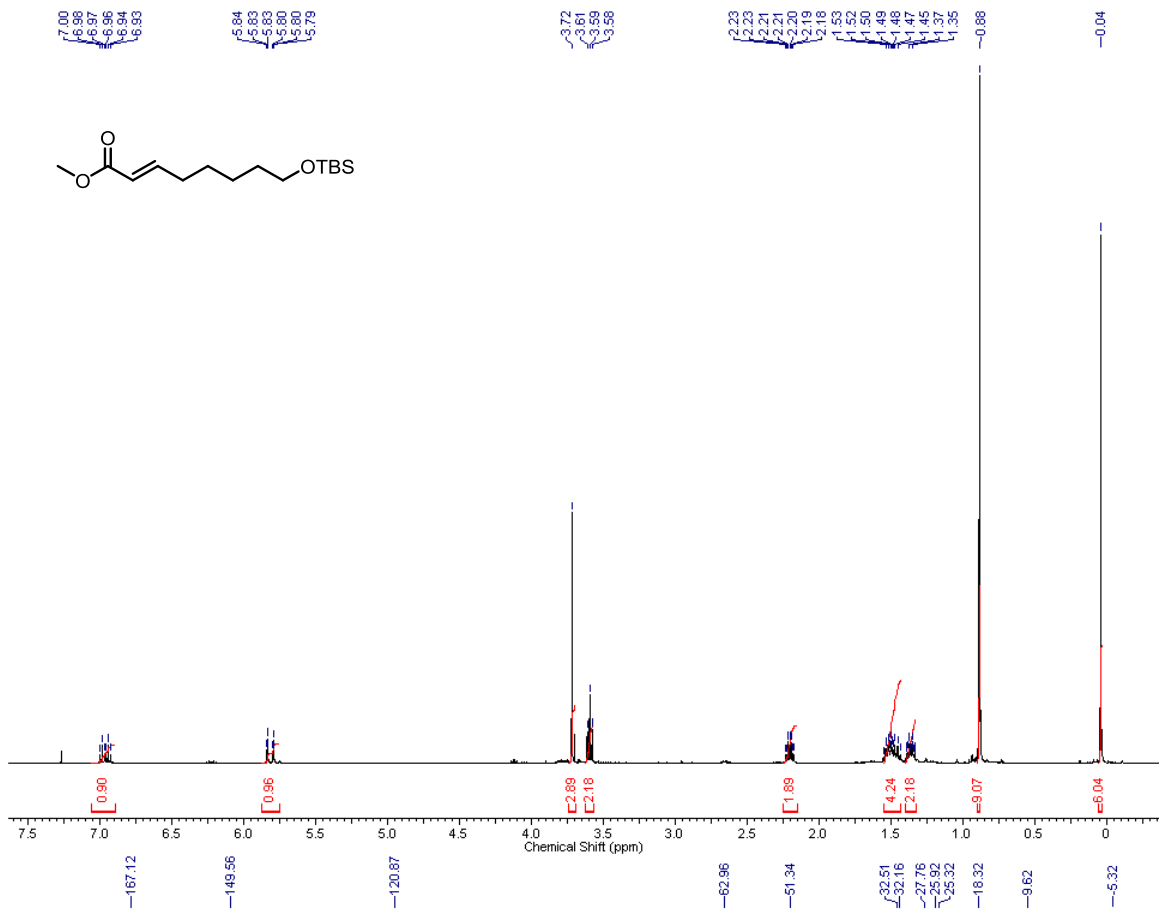




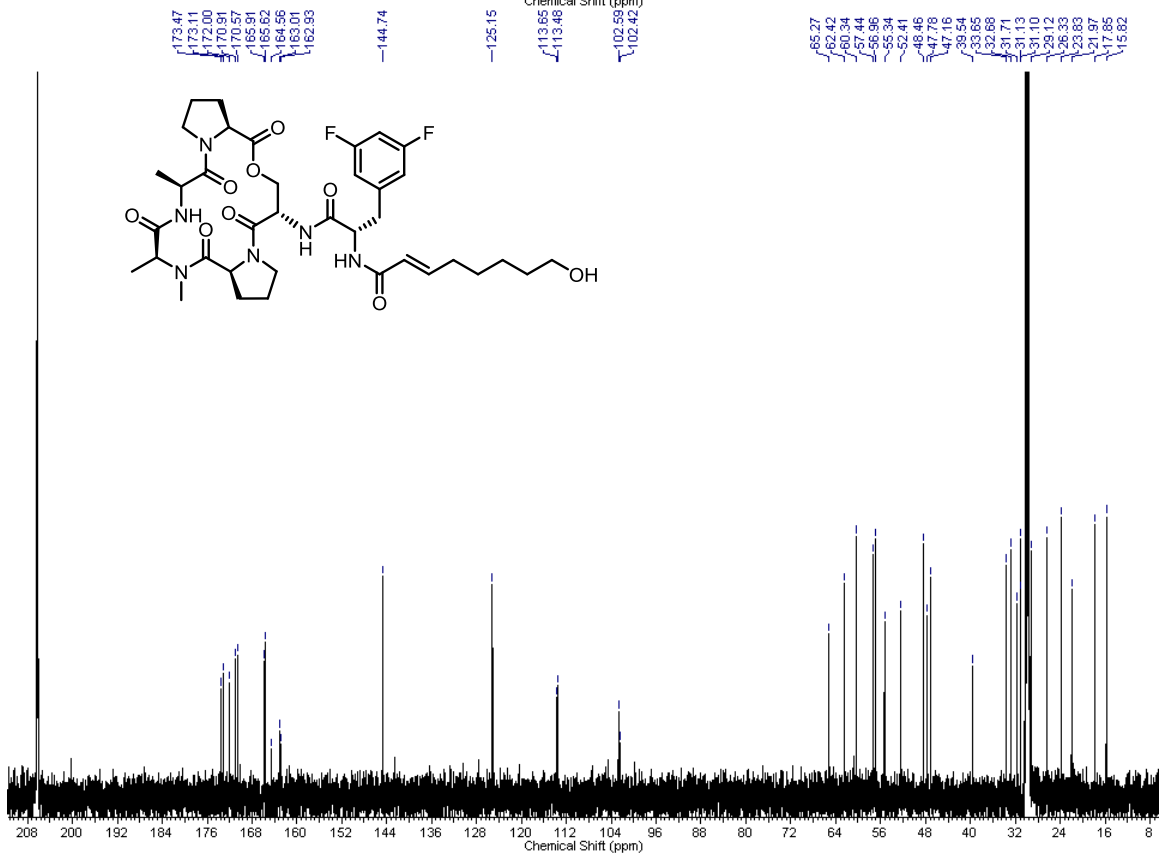
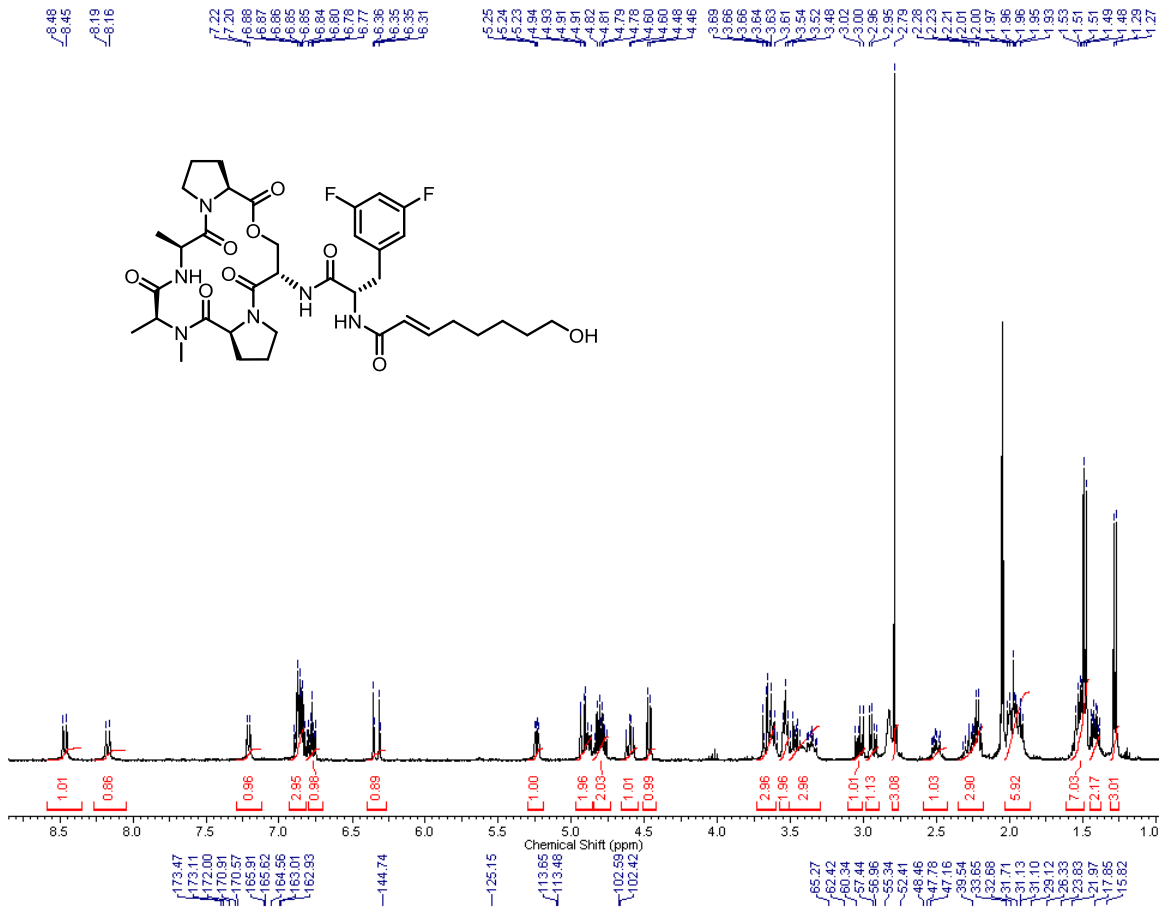


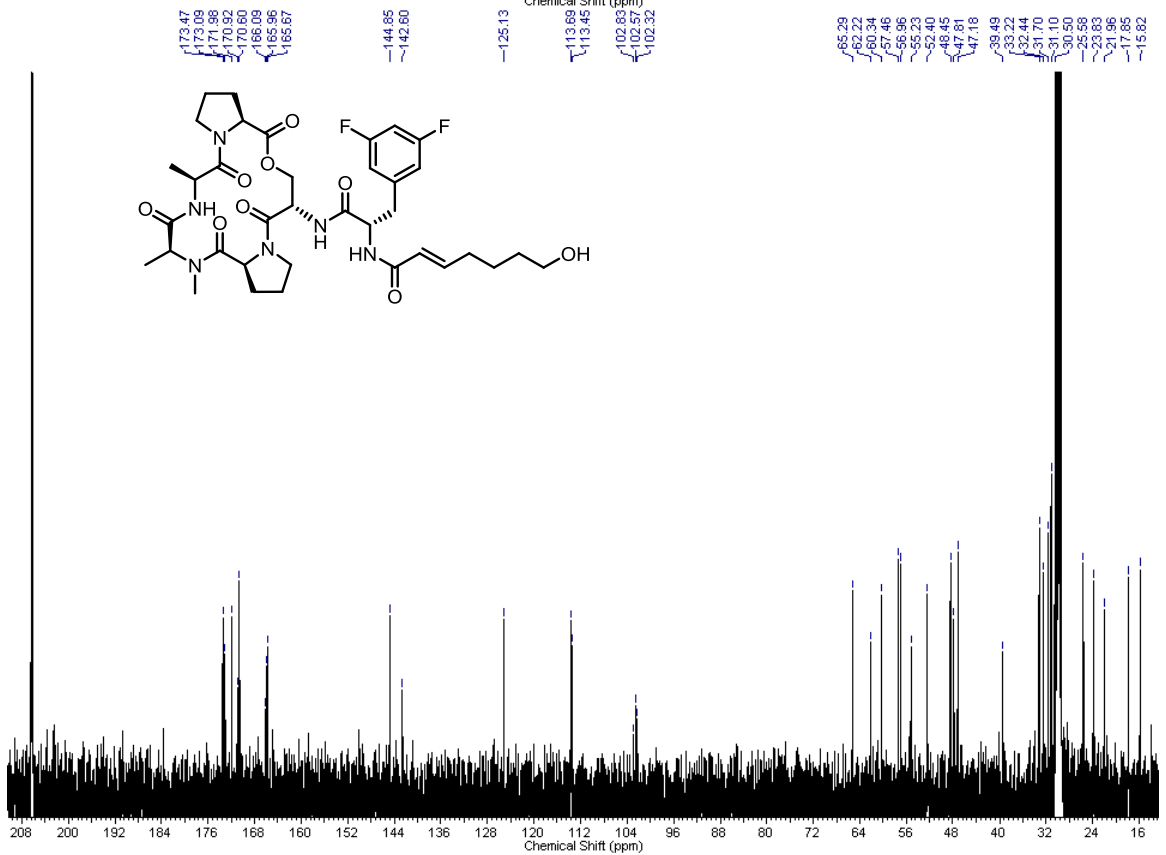
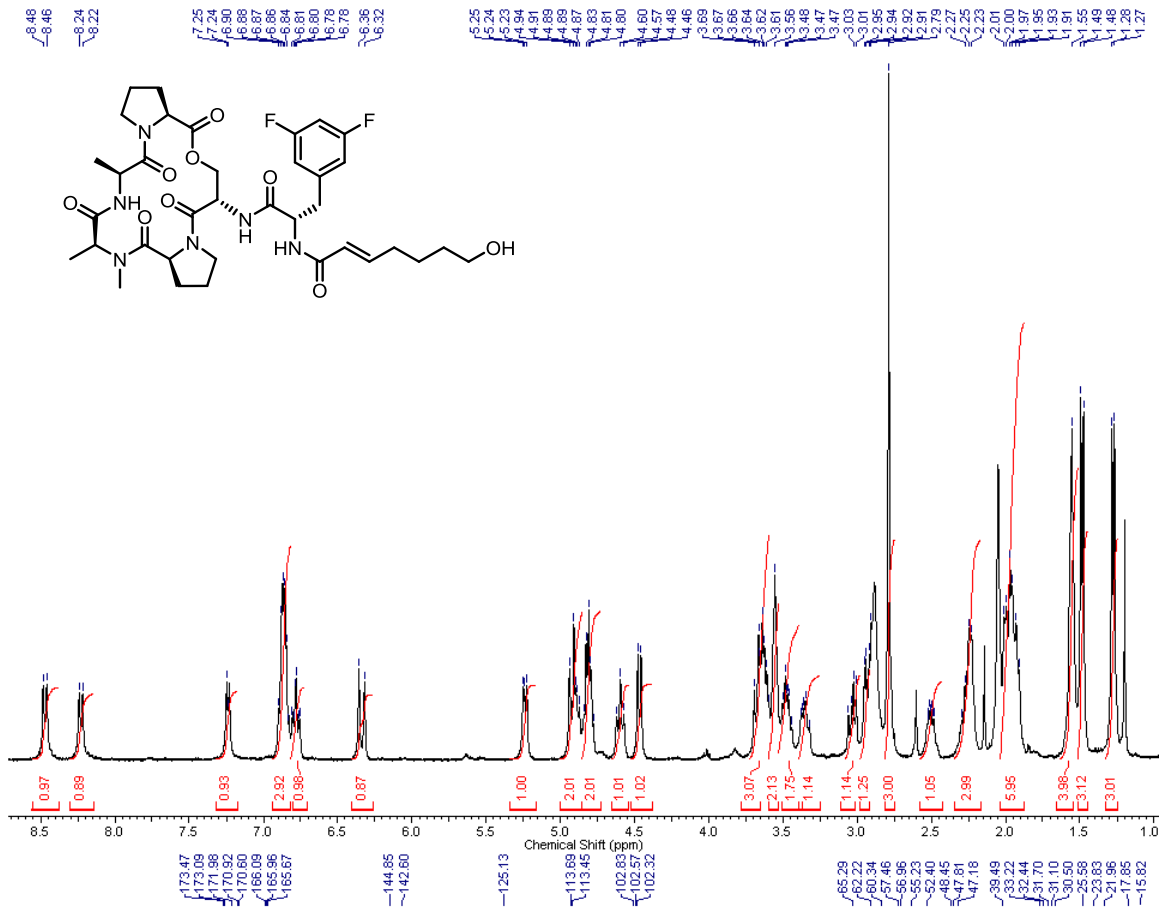




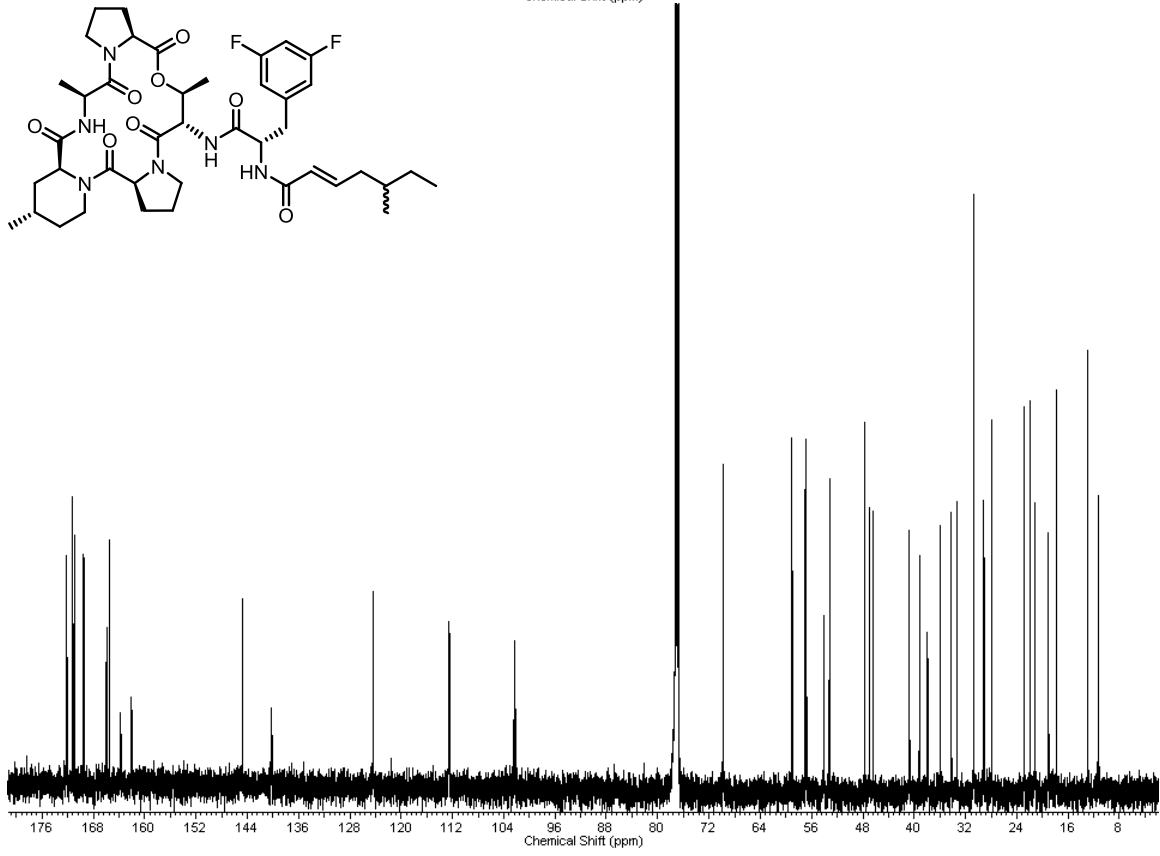
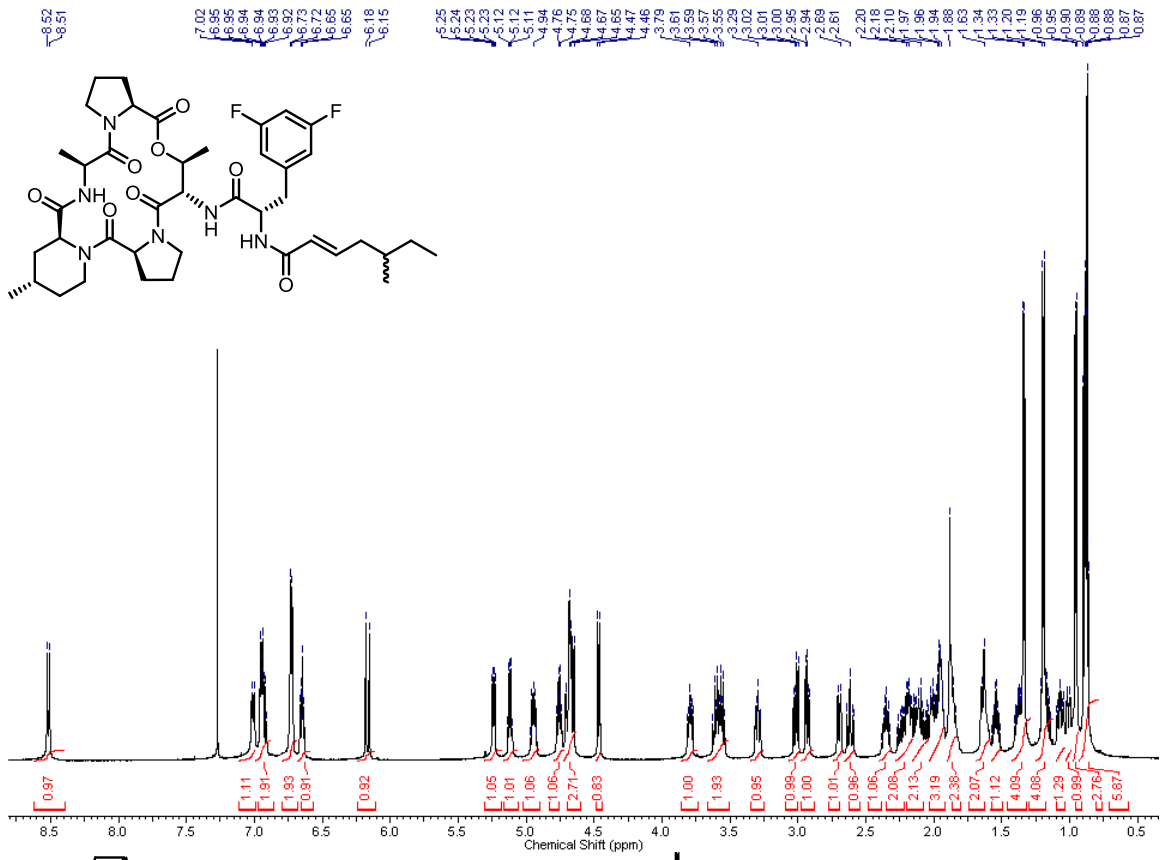




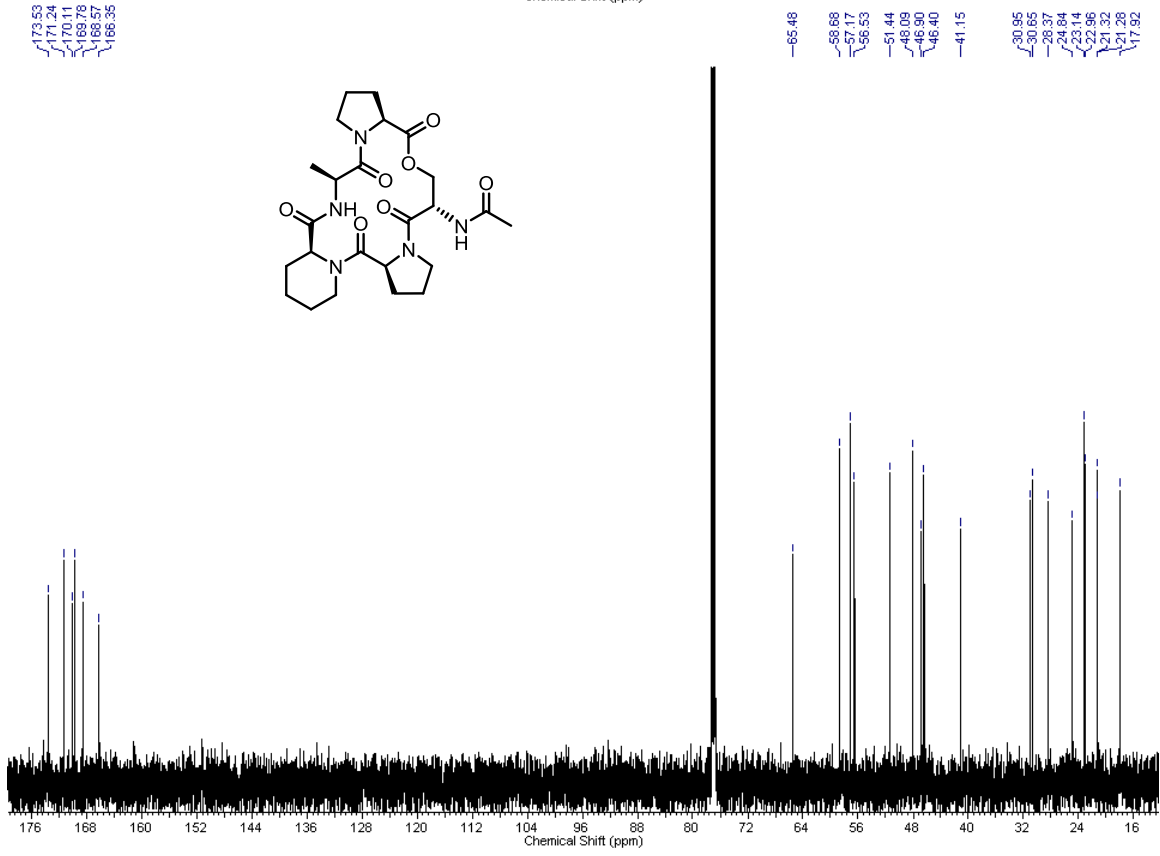
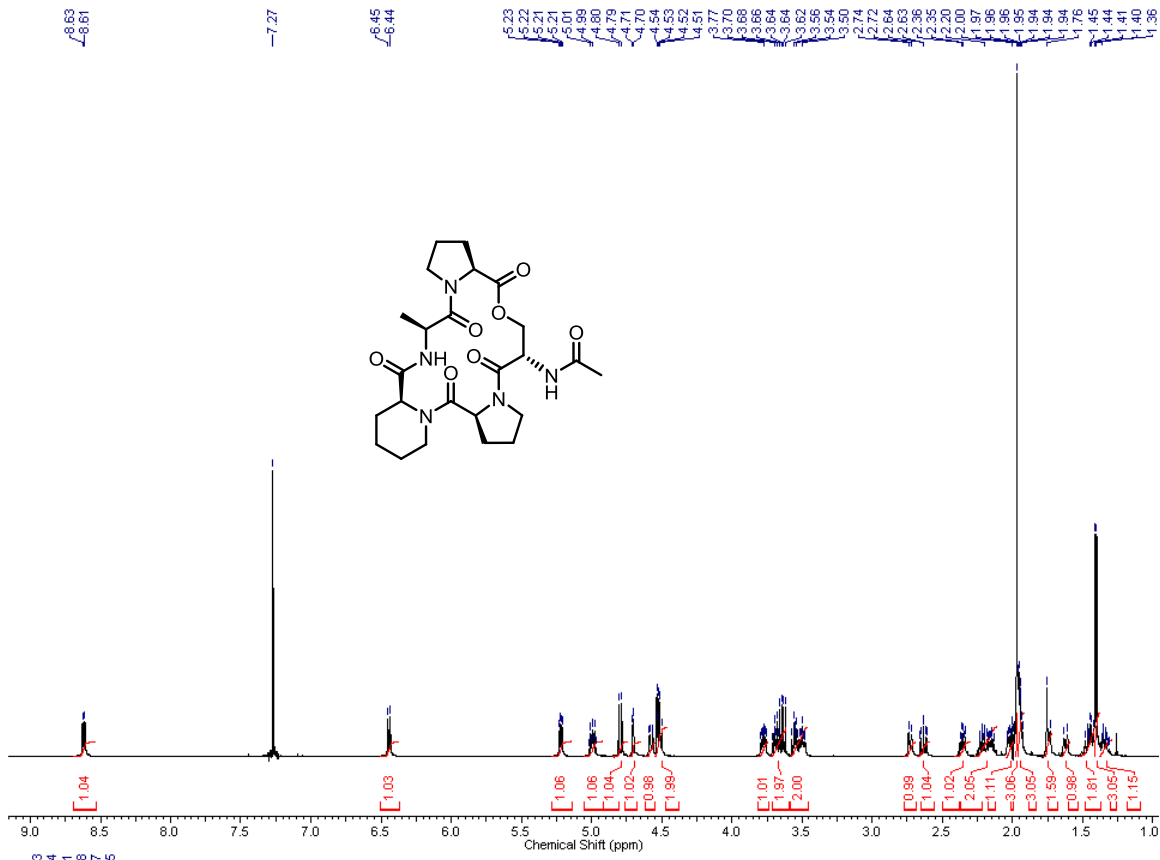


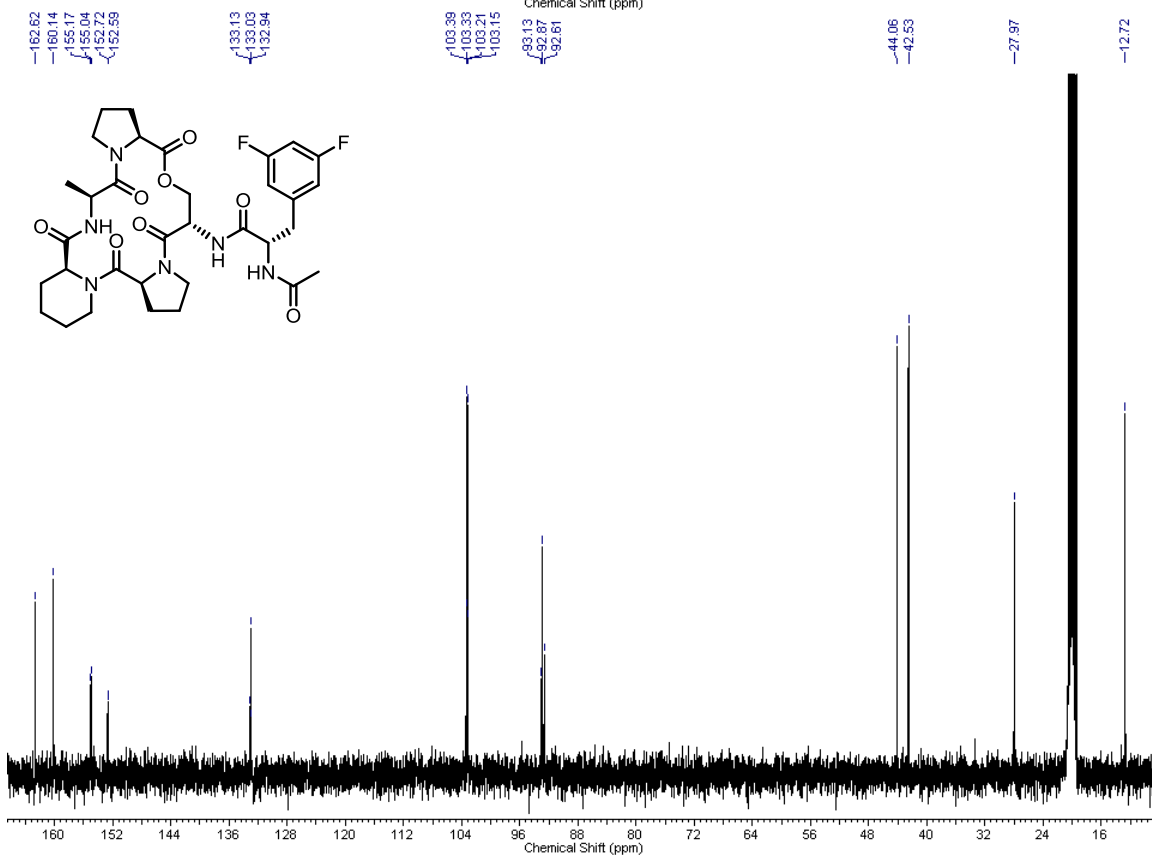
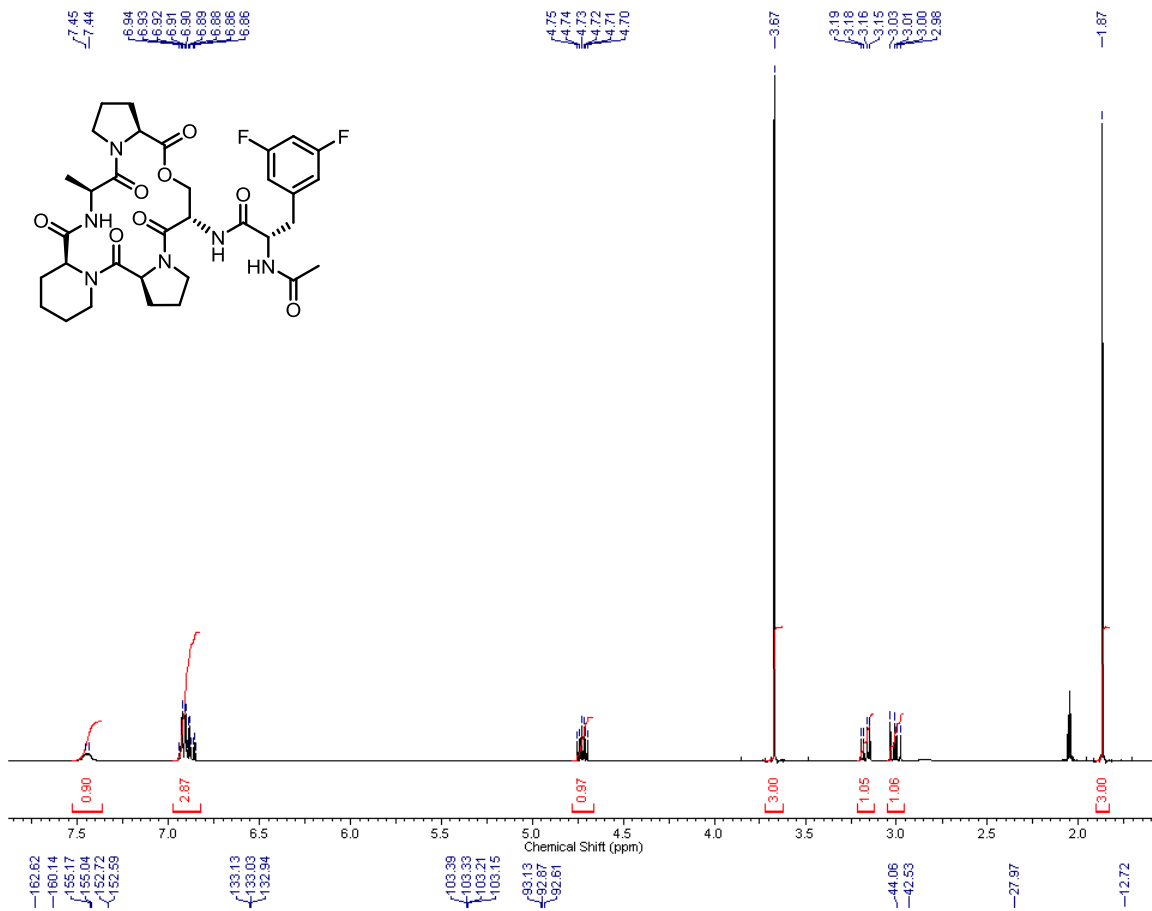


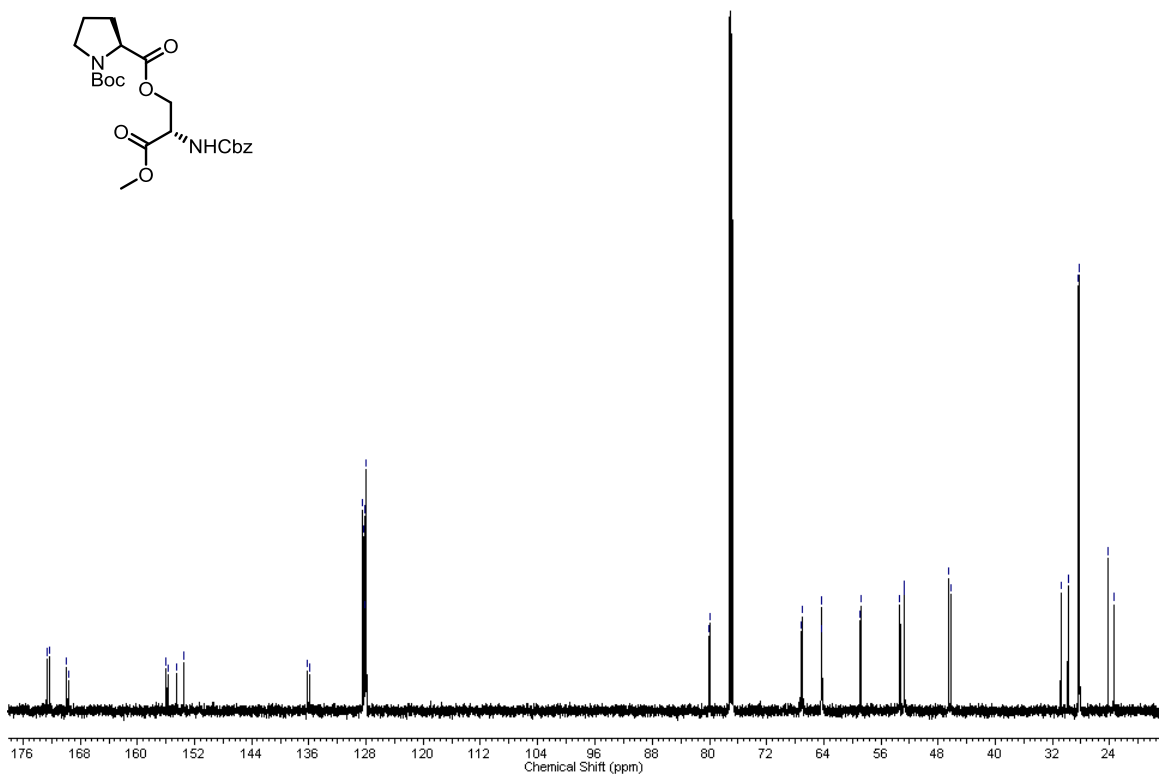
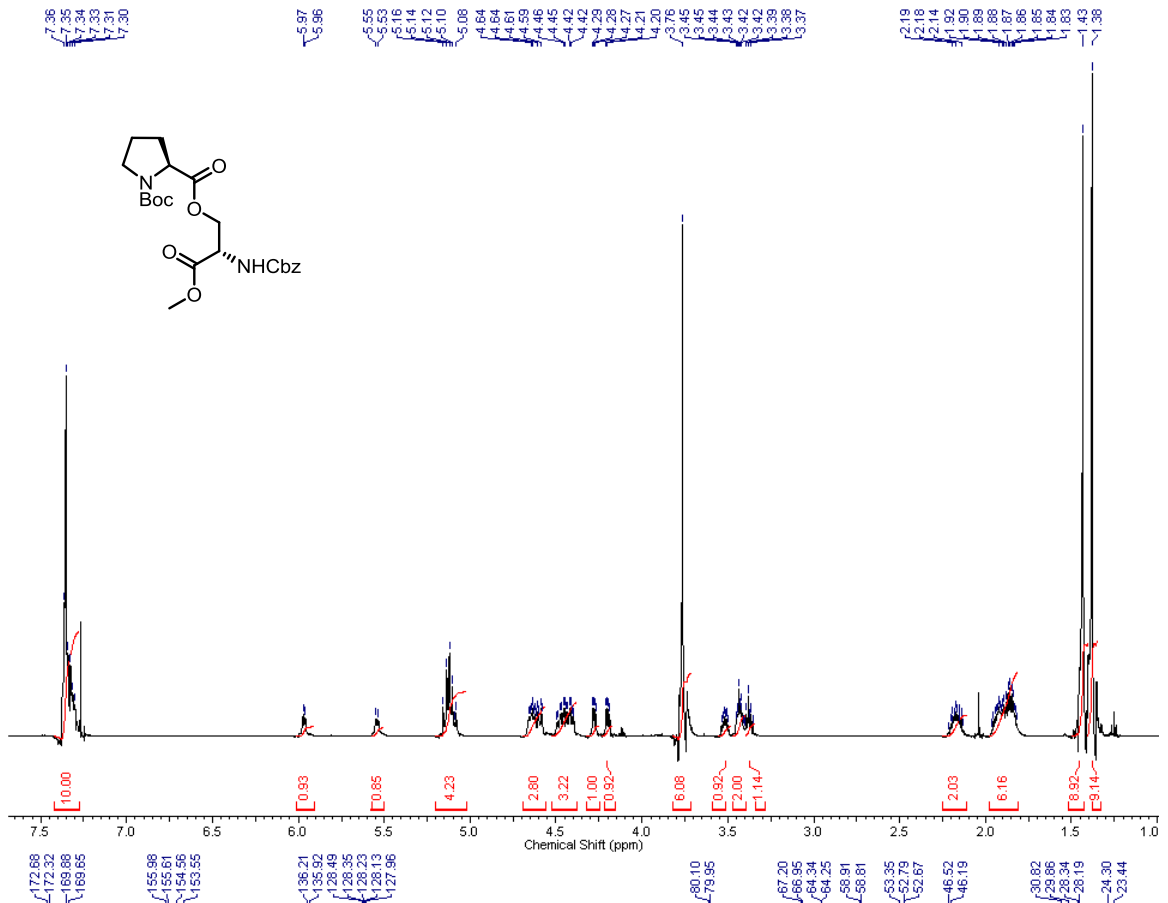




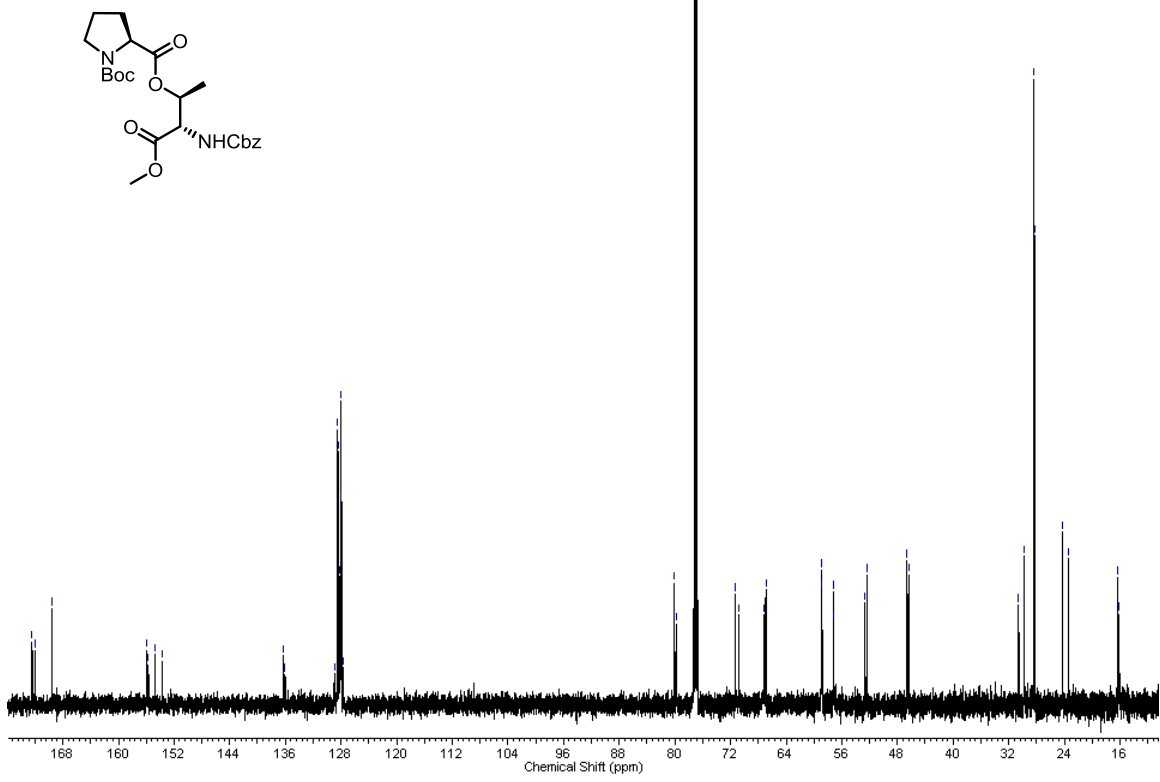
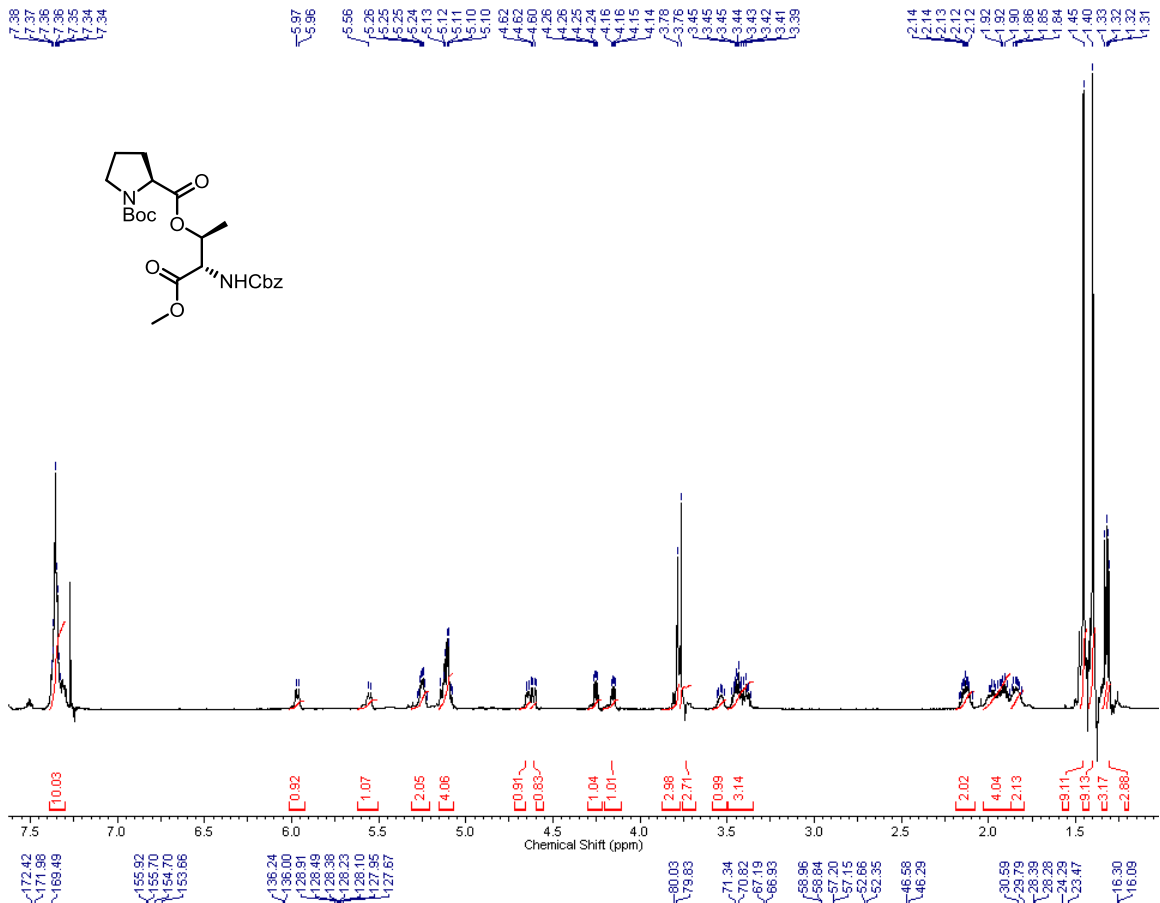
**Chapter 8 – The *N*-Acyldifluorophenyllanine Moiety is Necessary and Sufficient for ClpP Activation.**

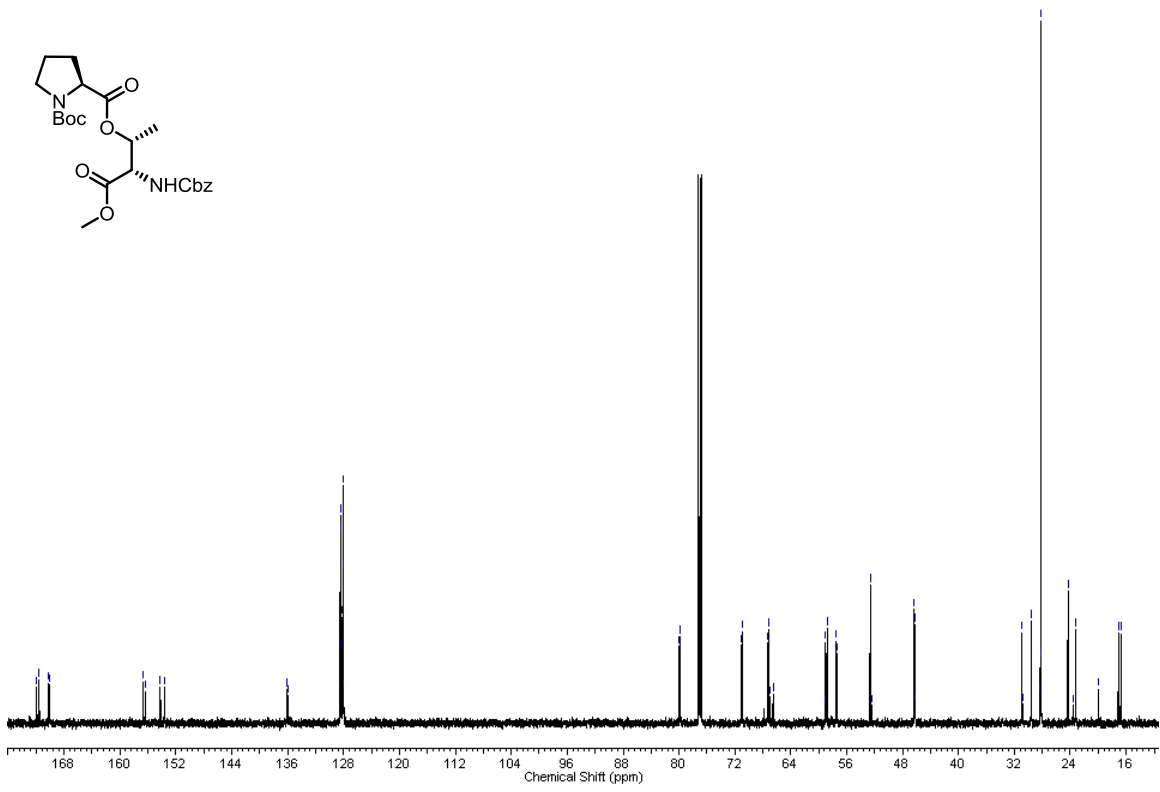
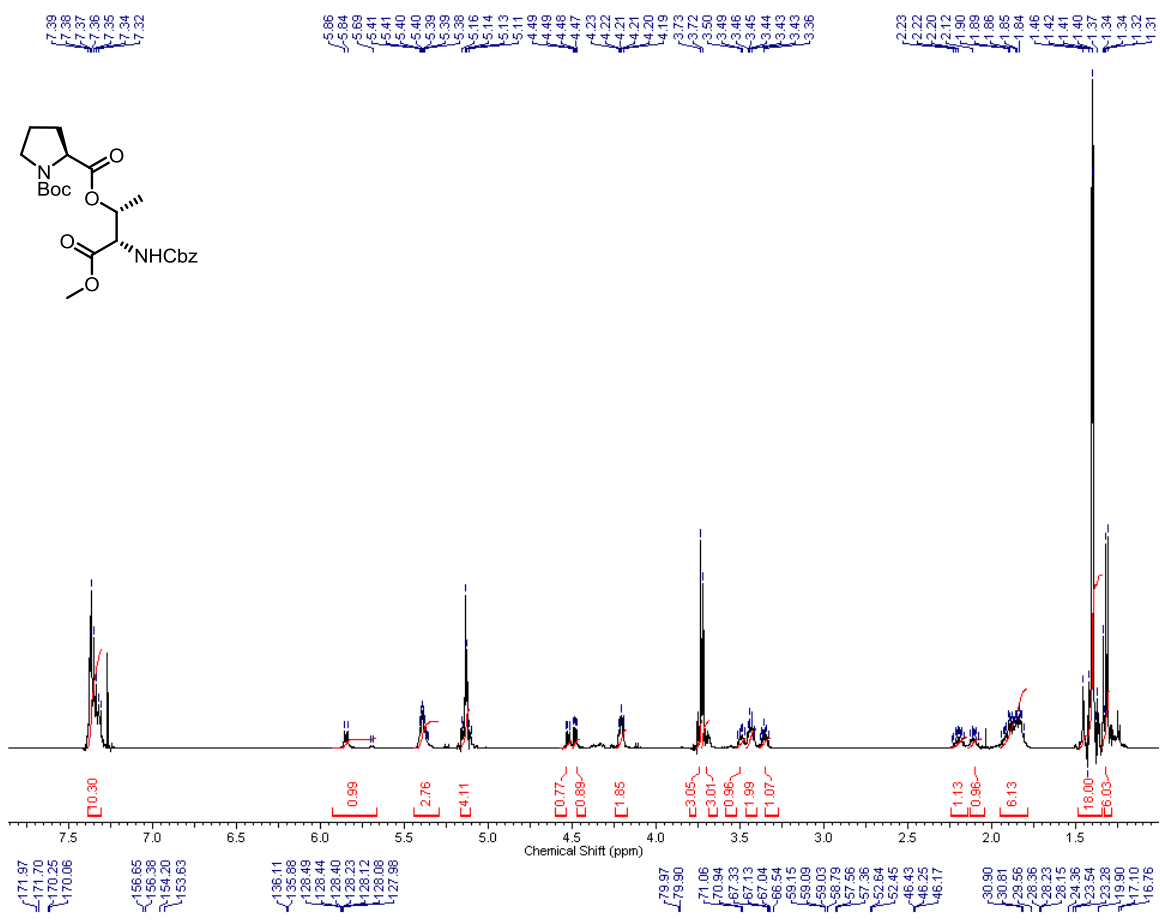


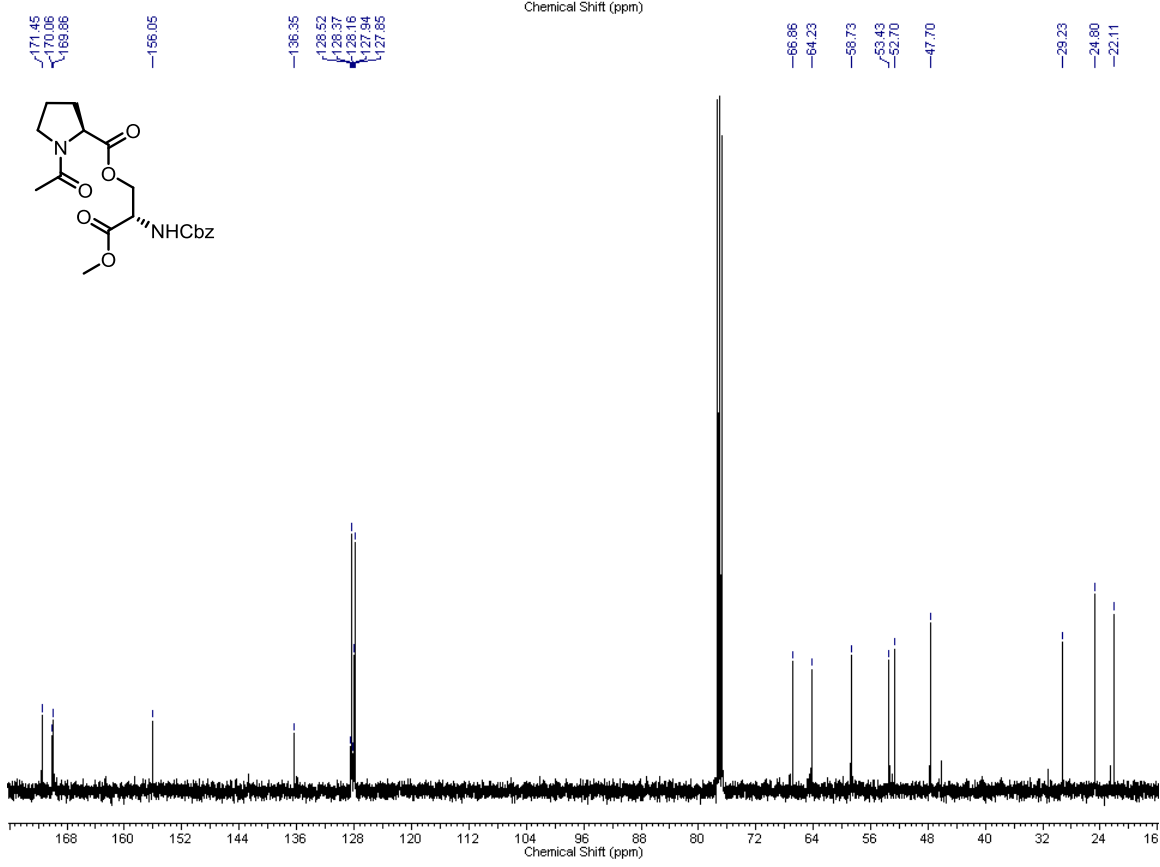
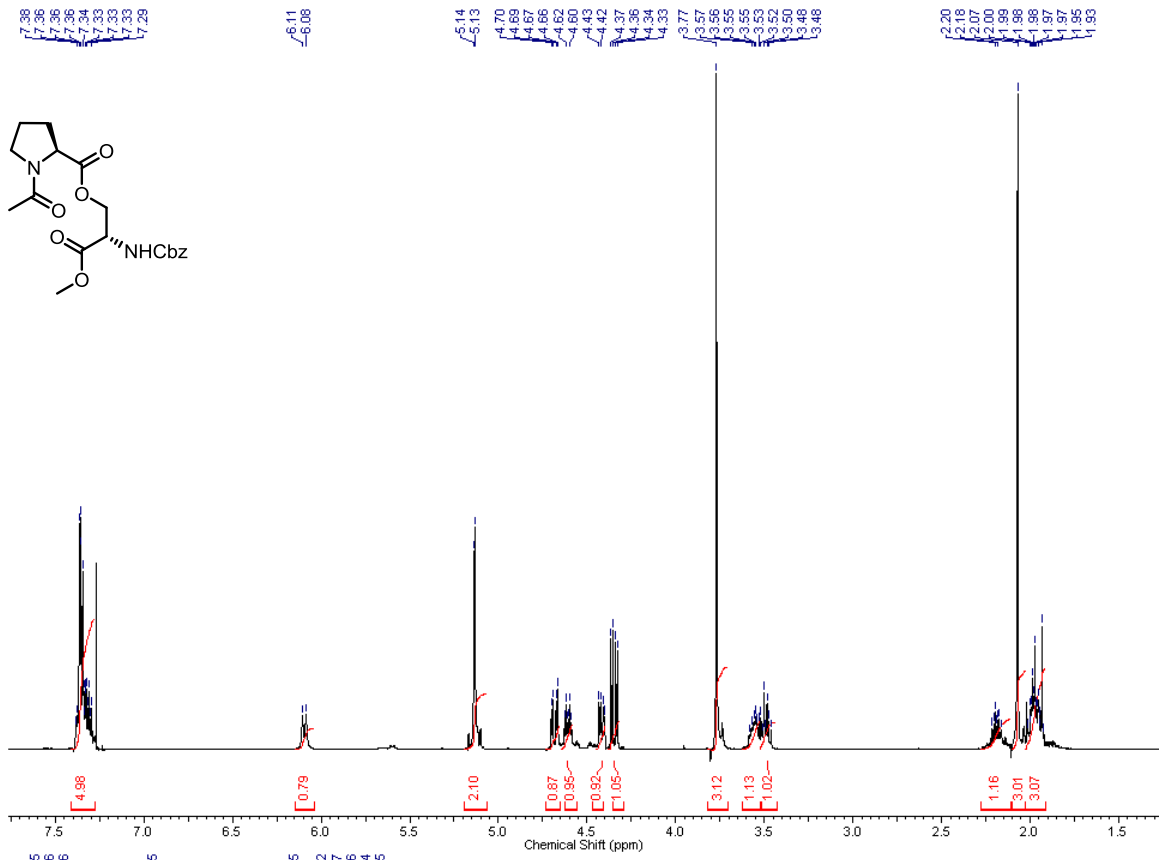


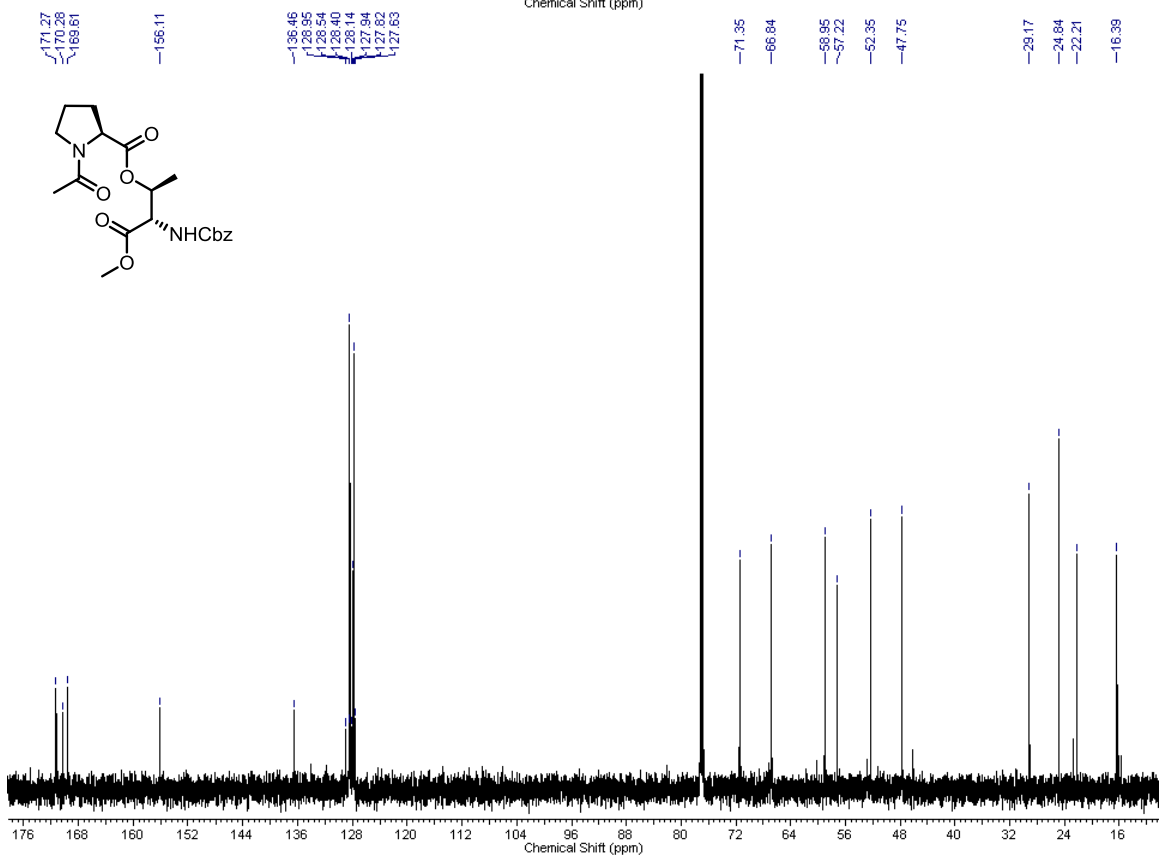
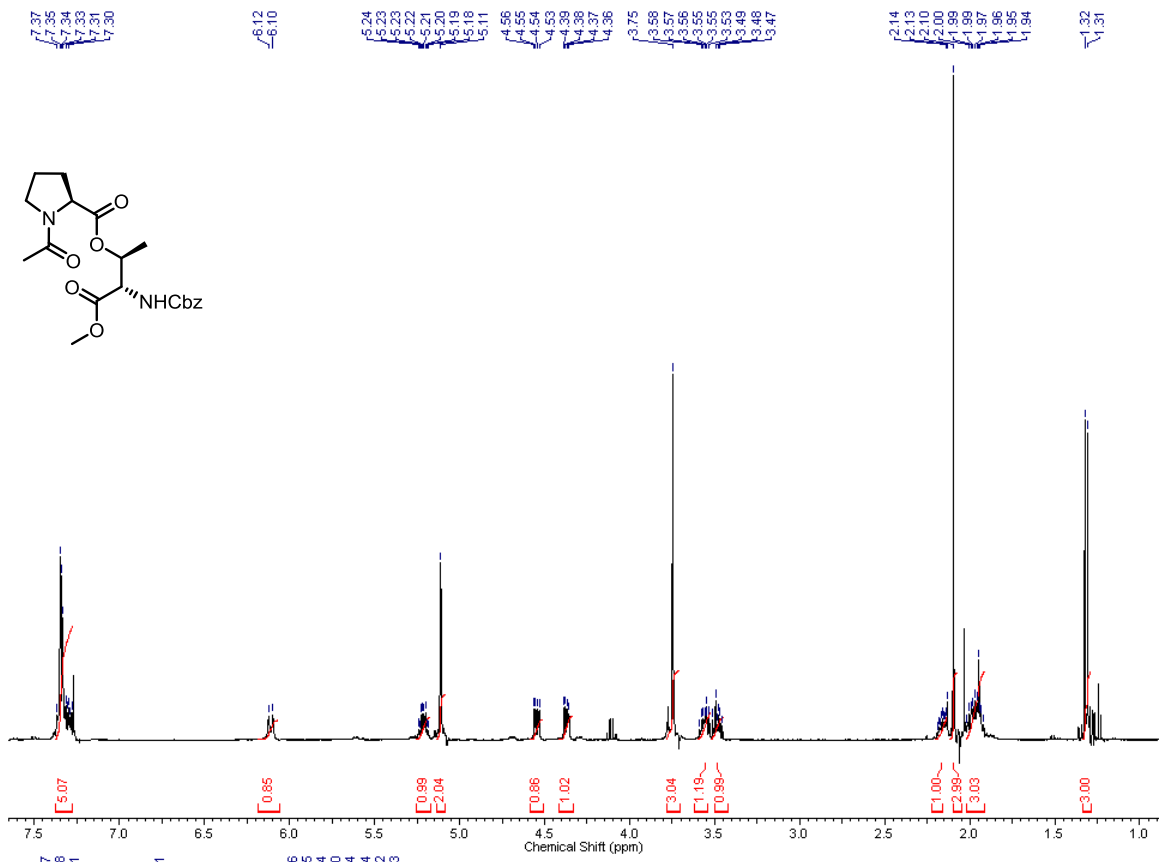


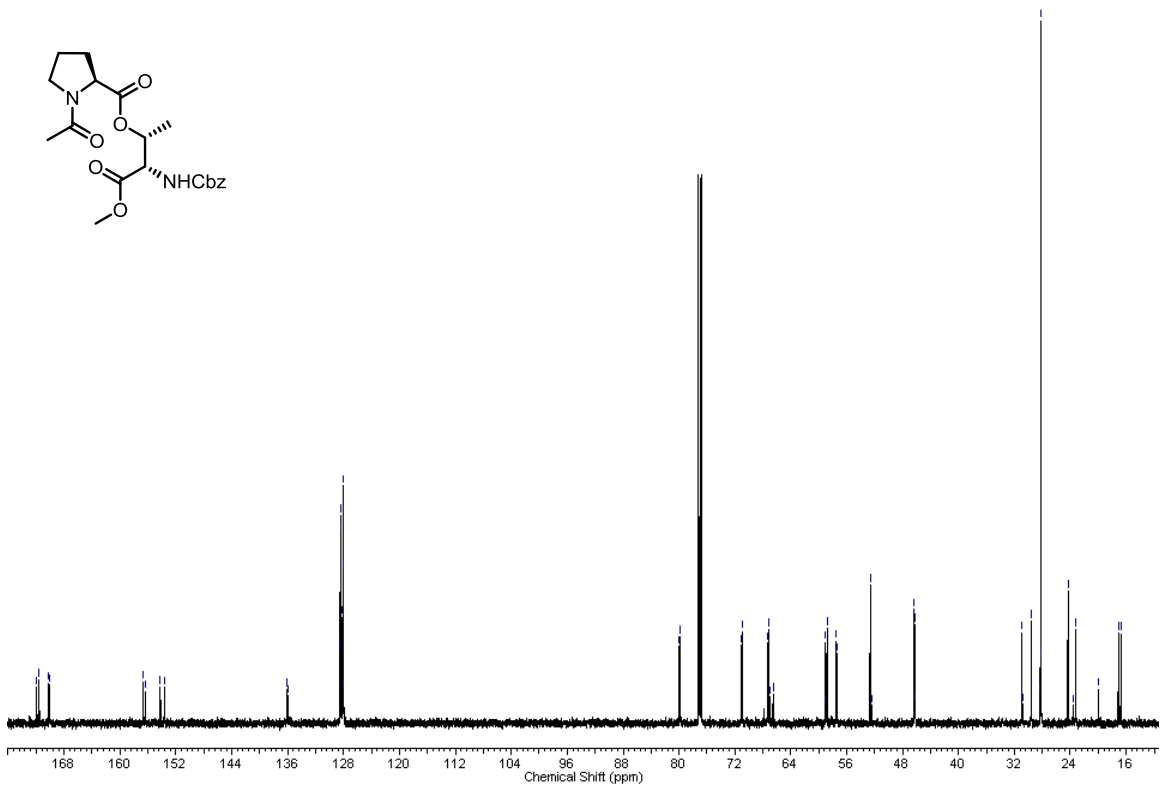
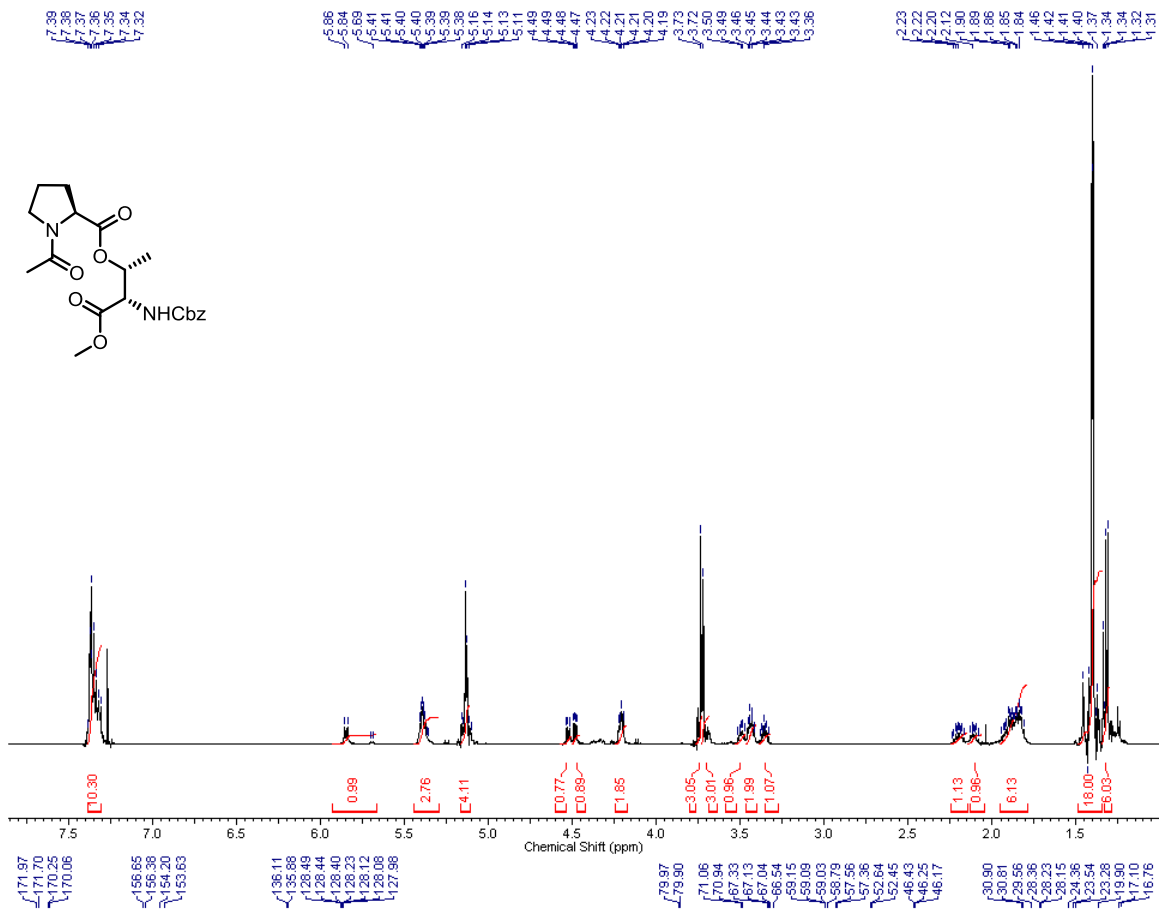


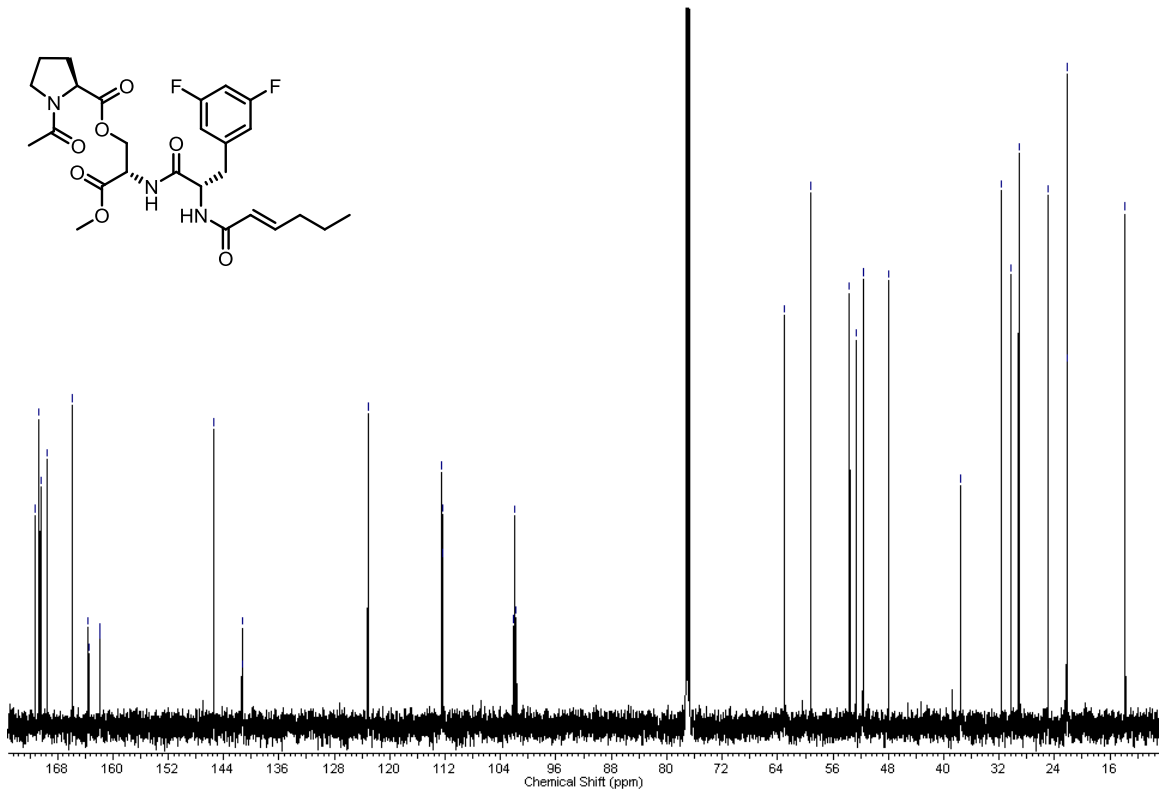
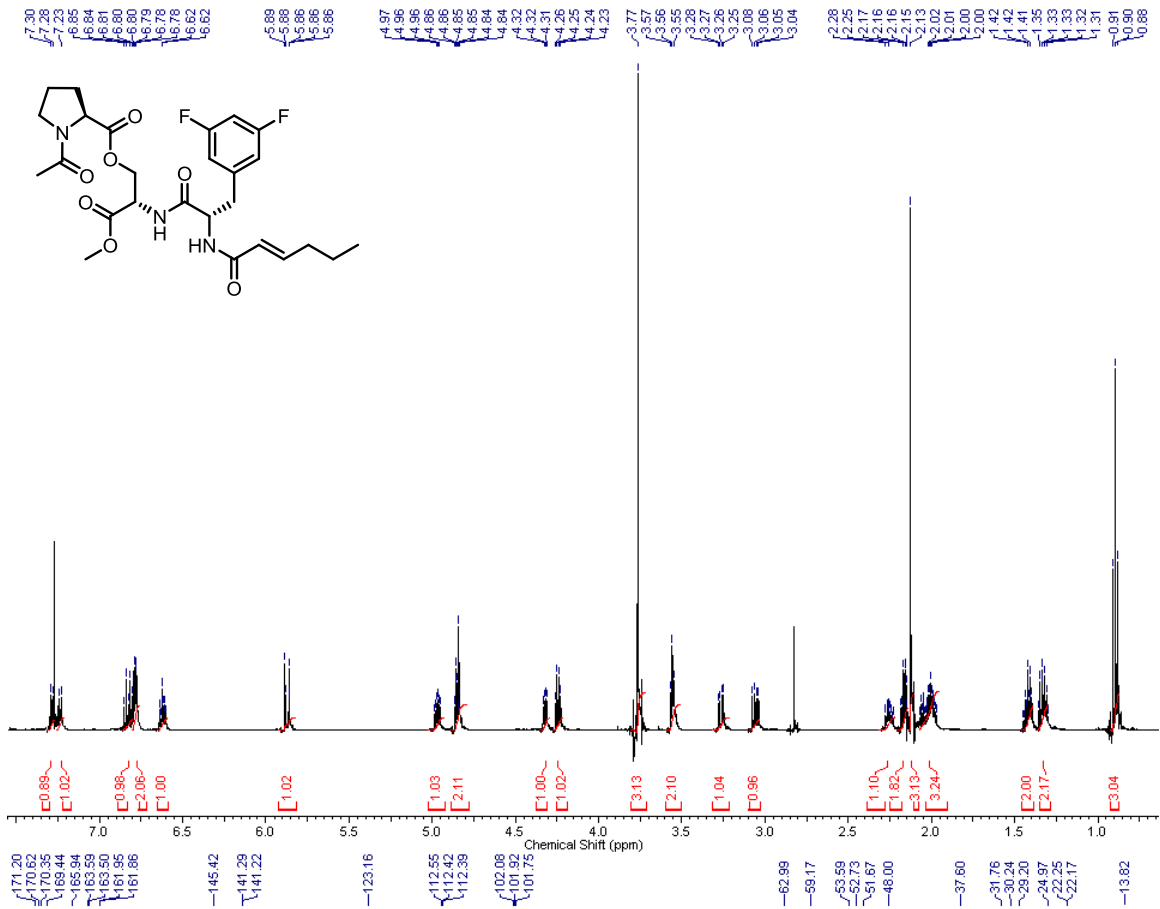


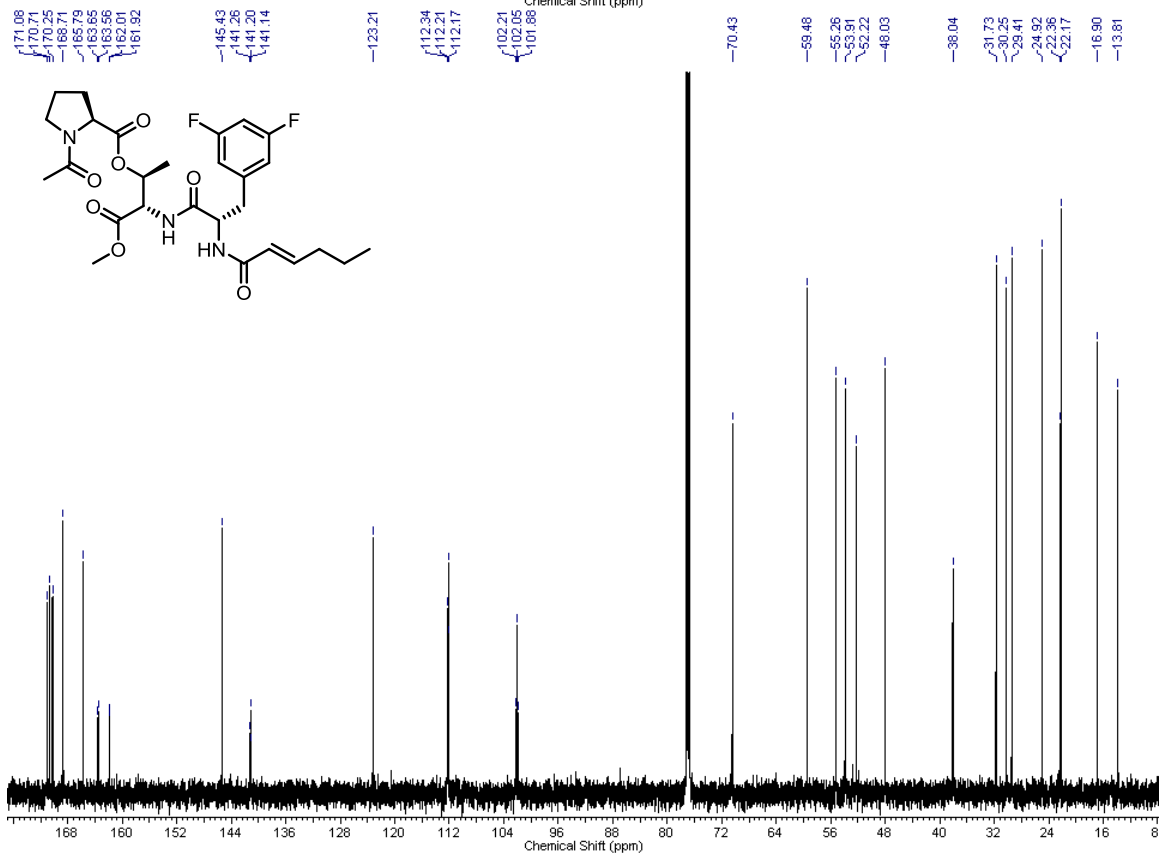
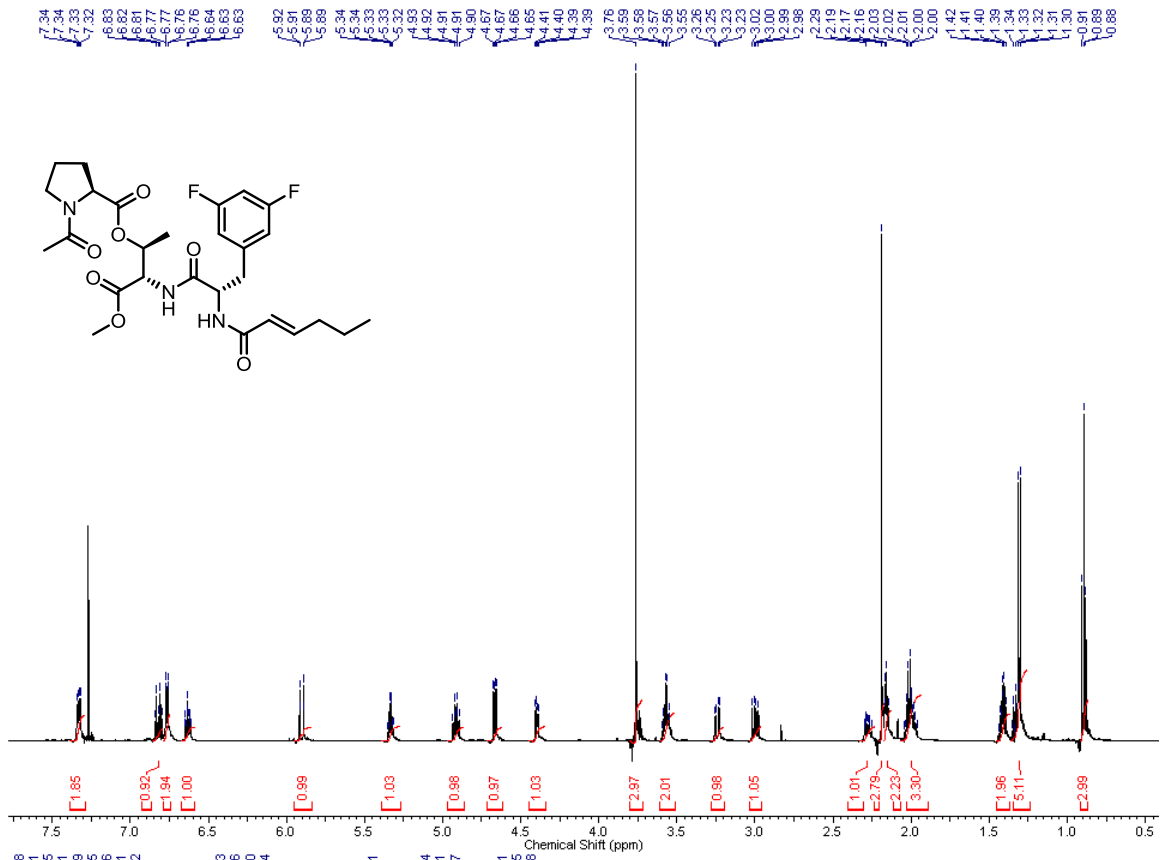


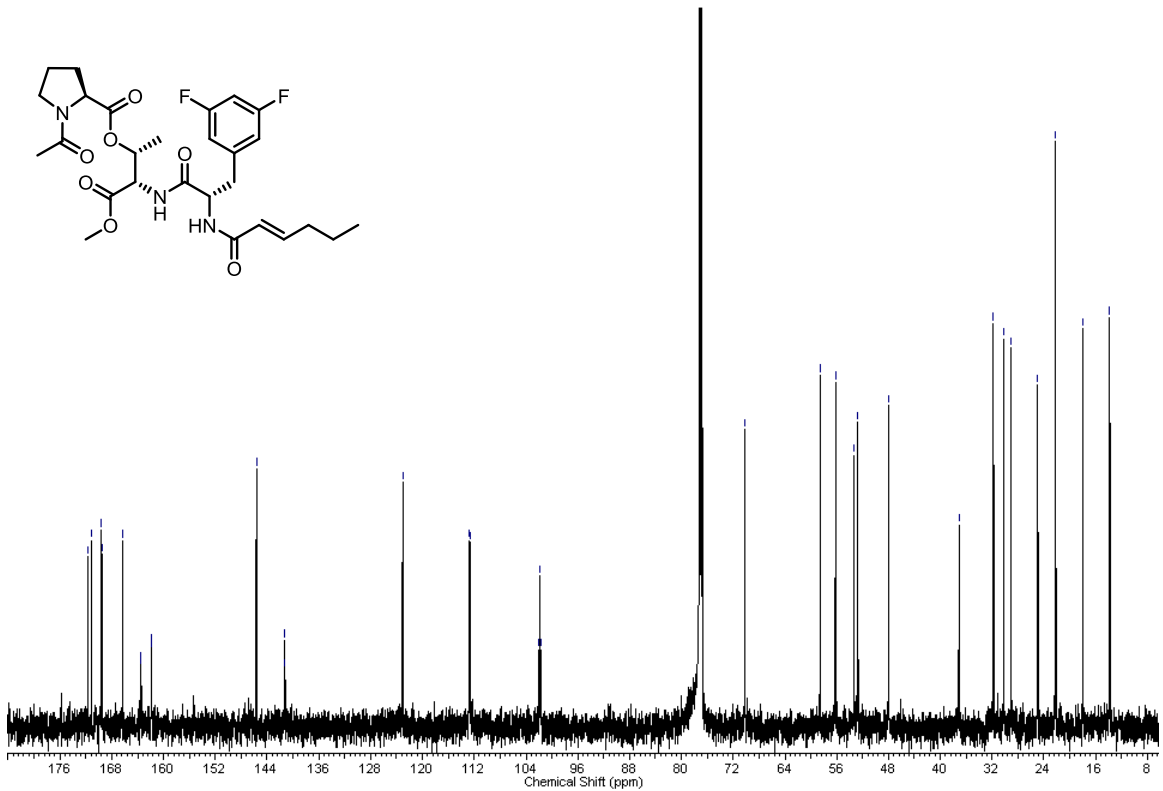
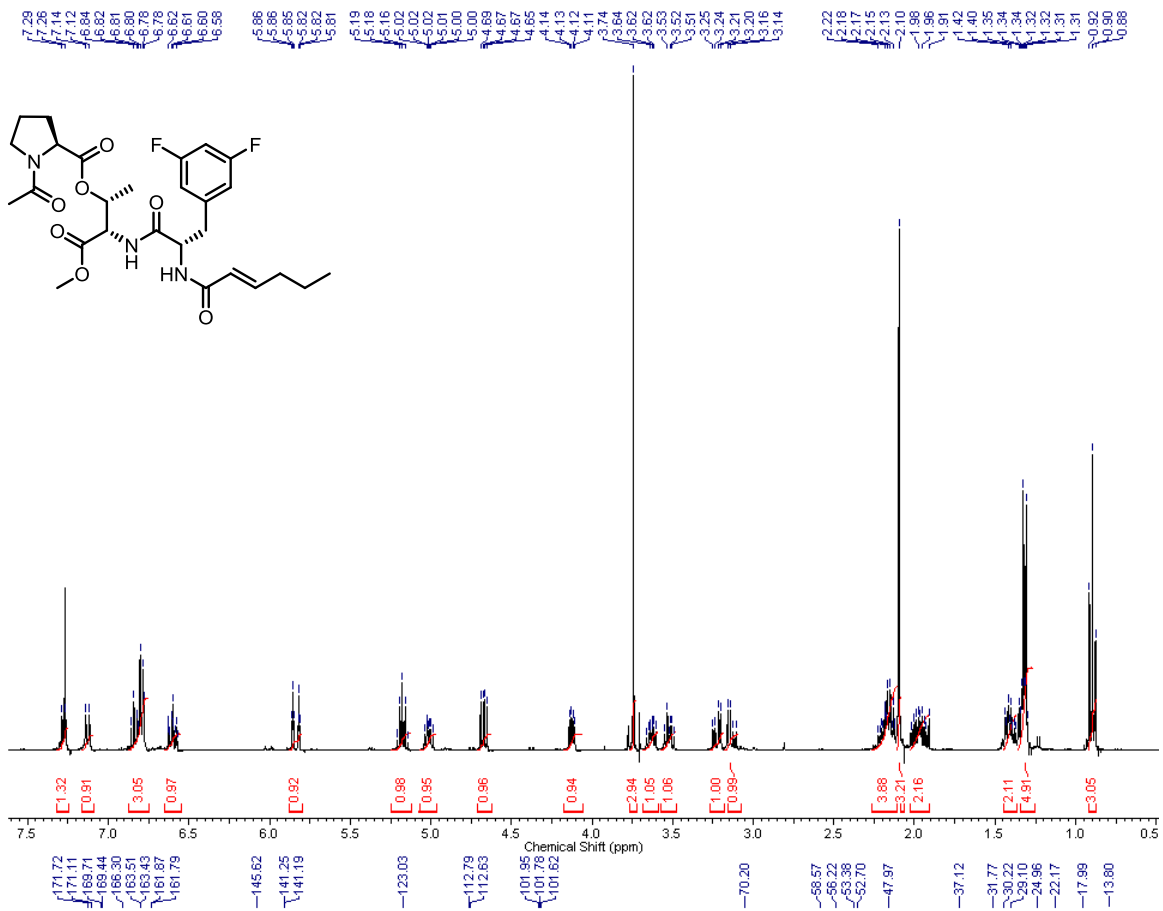




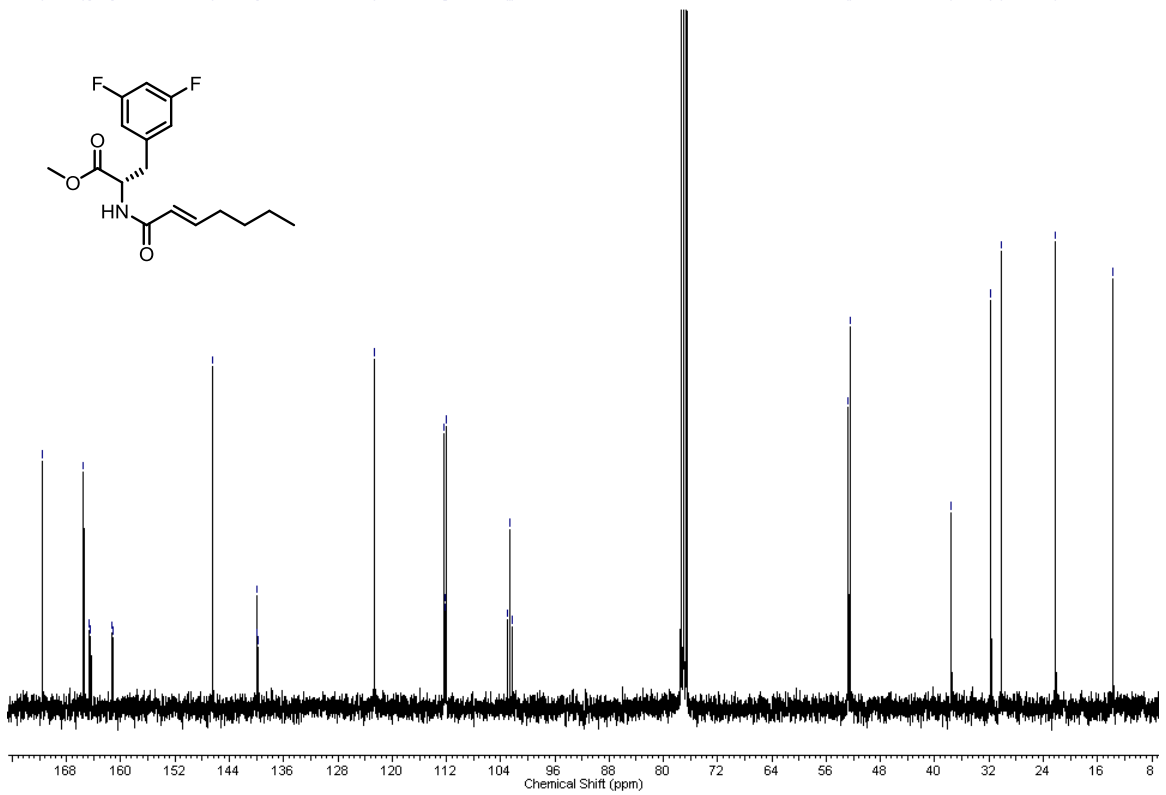
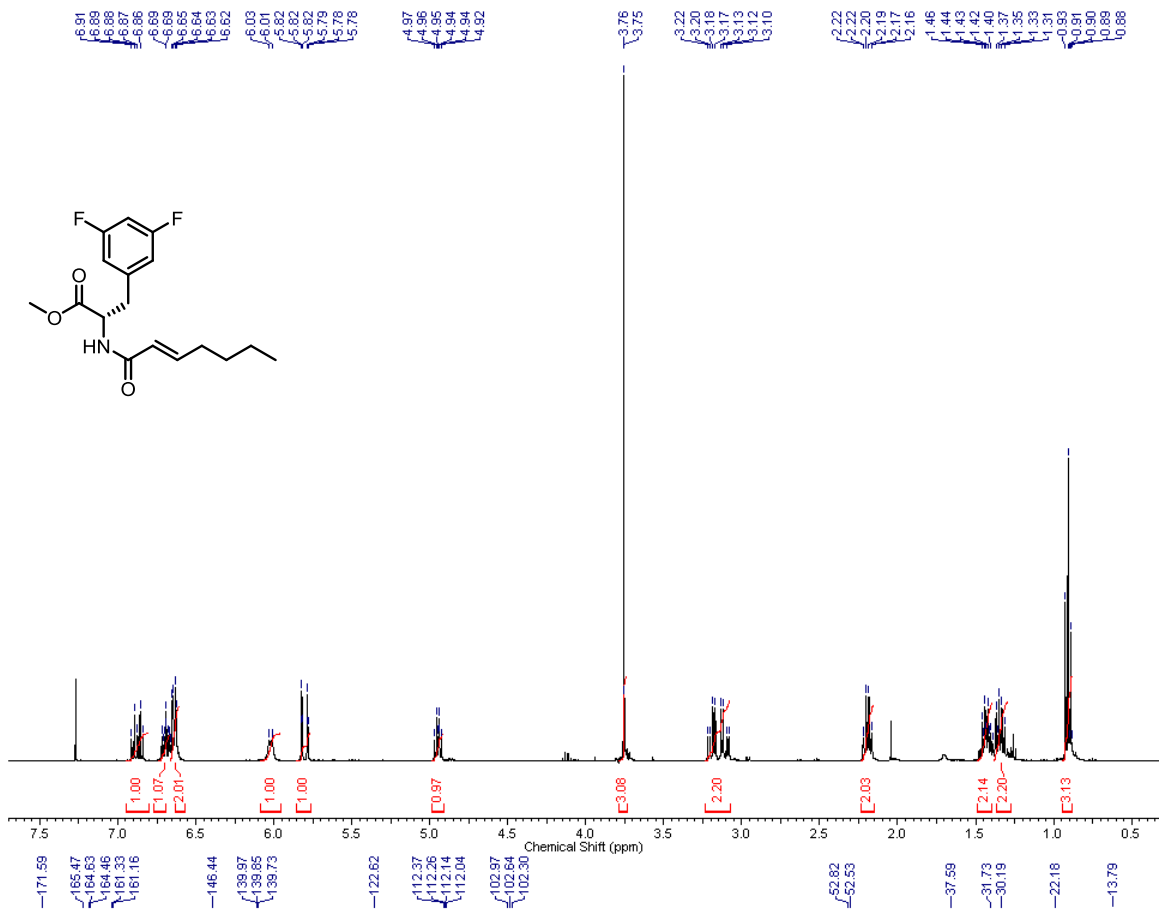


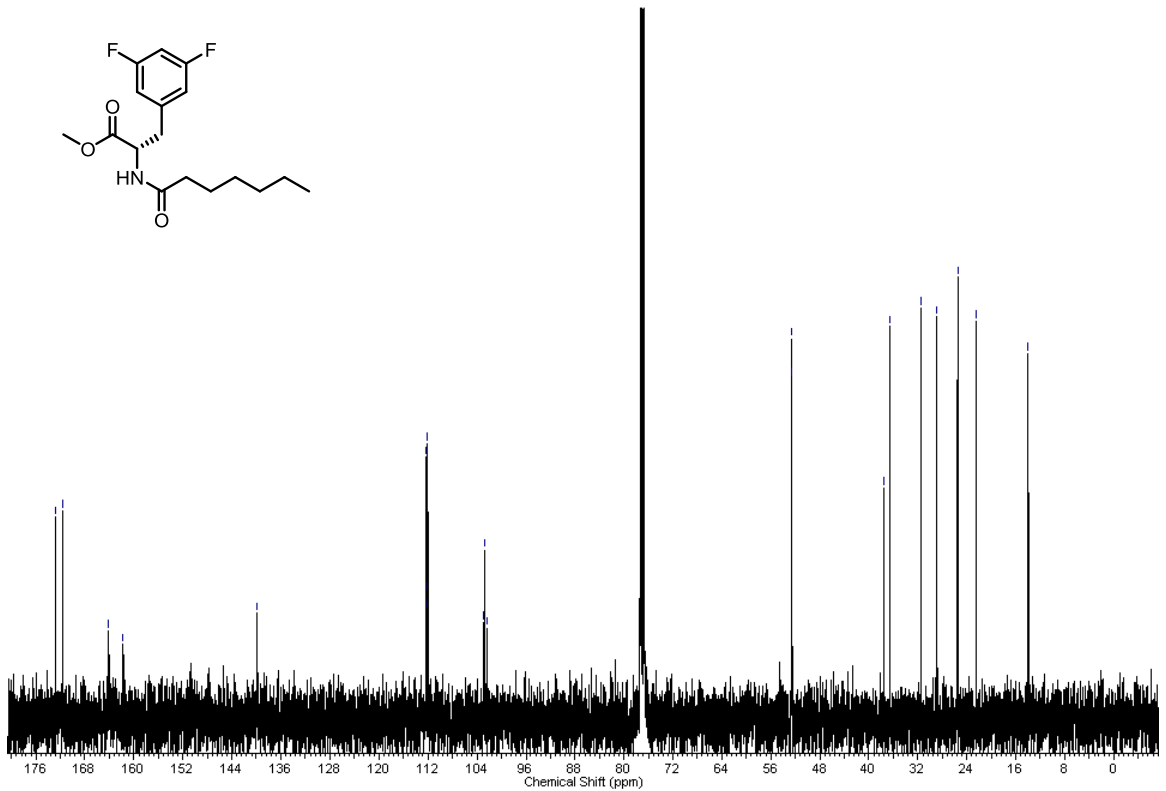
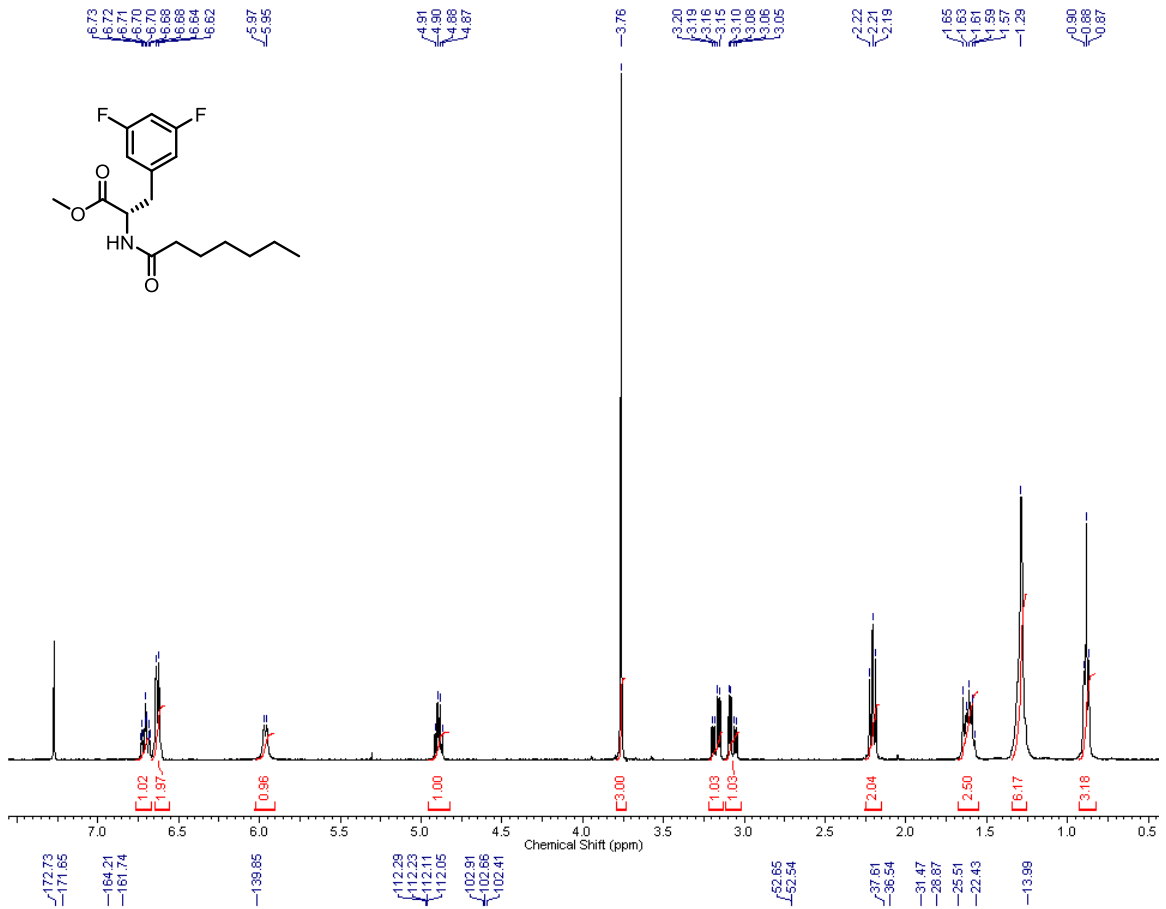


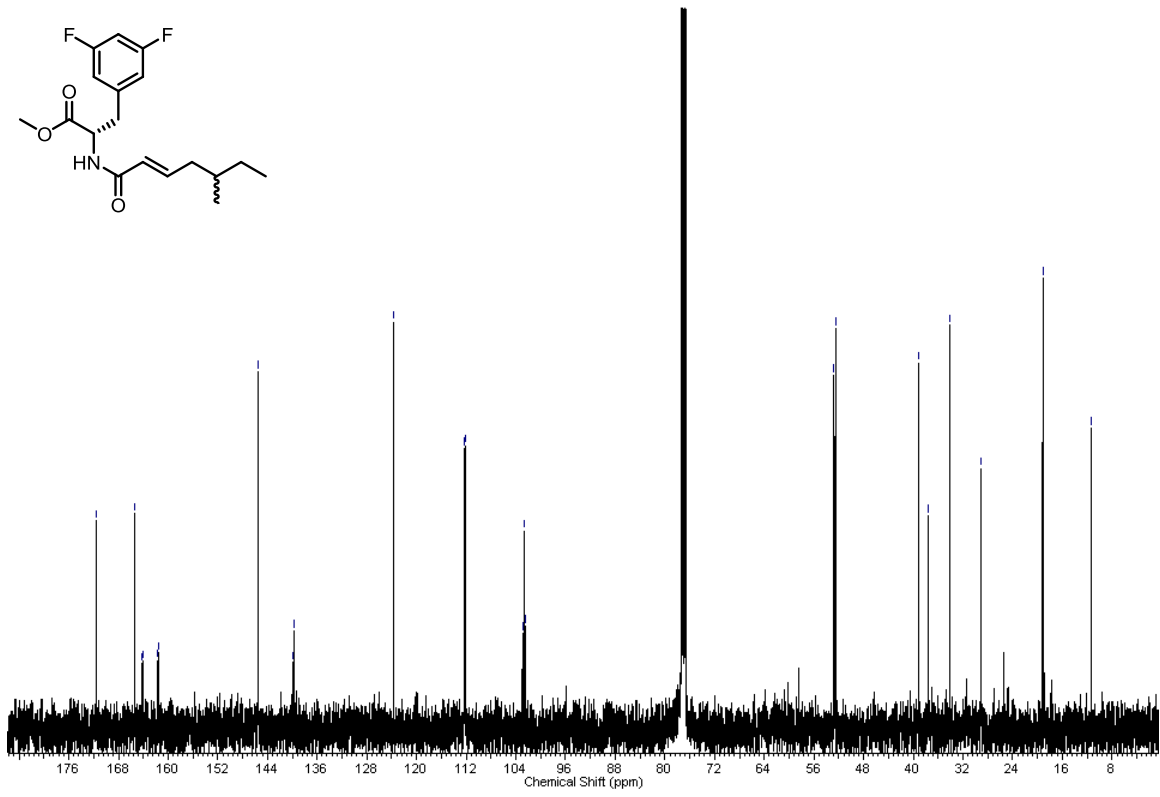
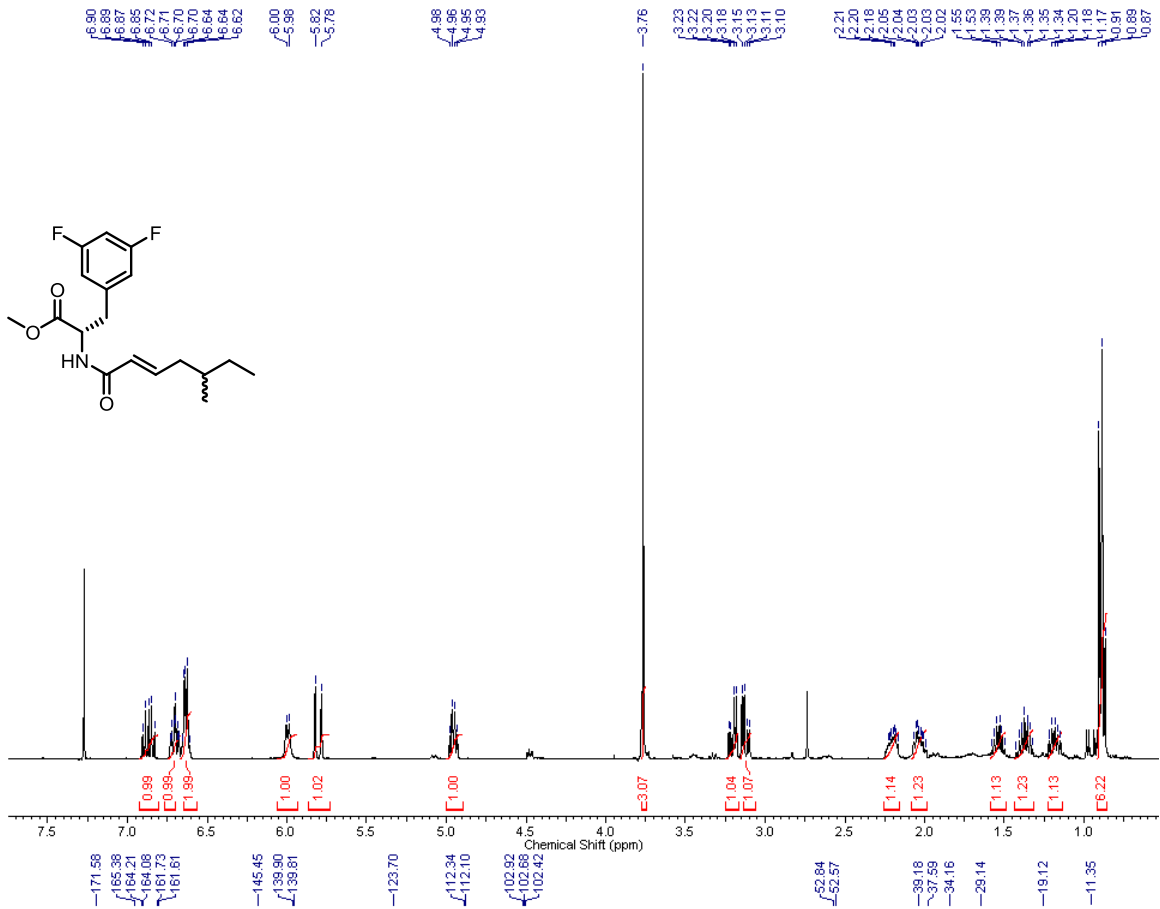


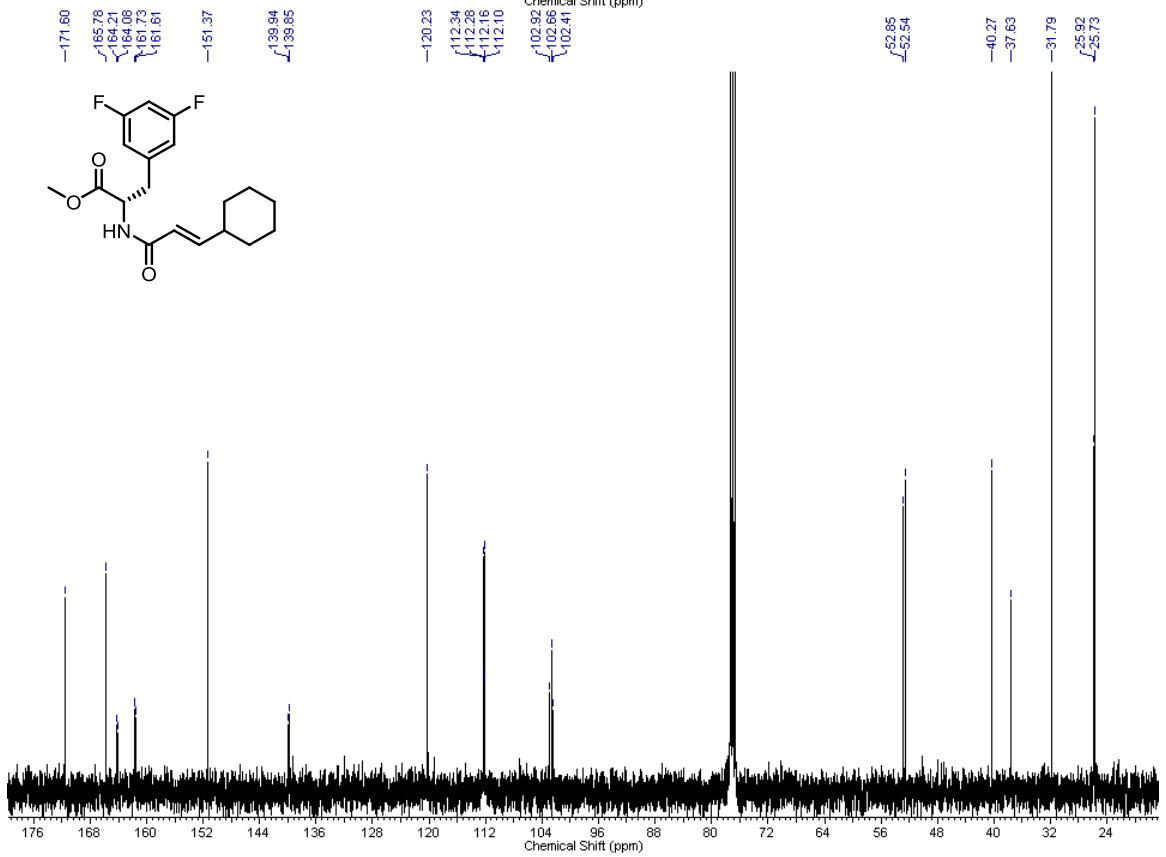
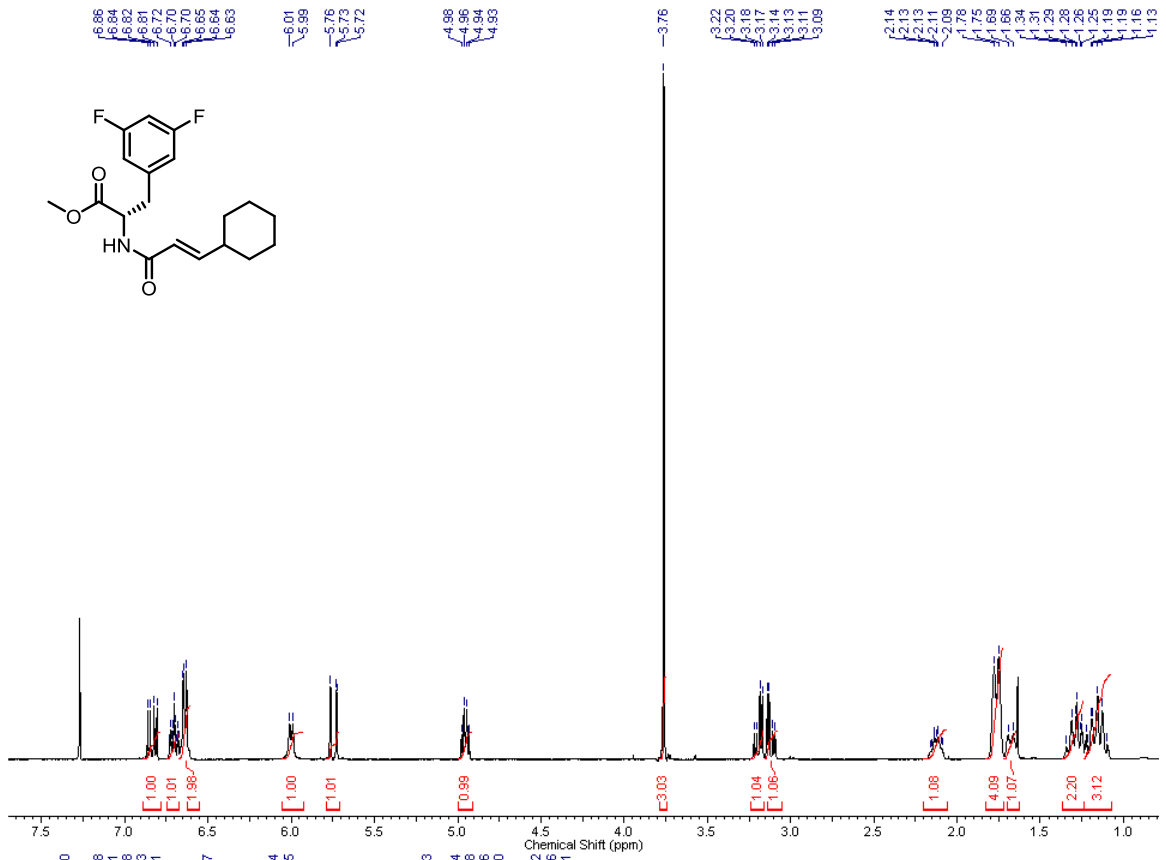


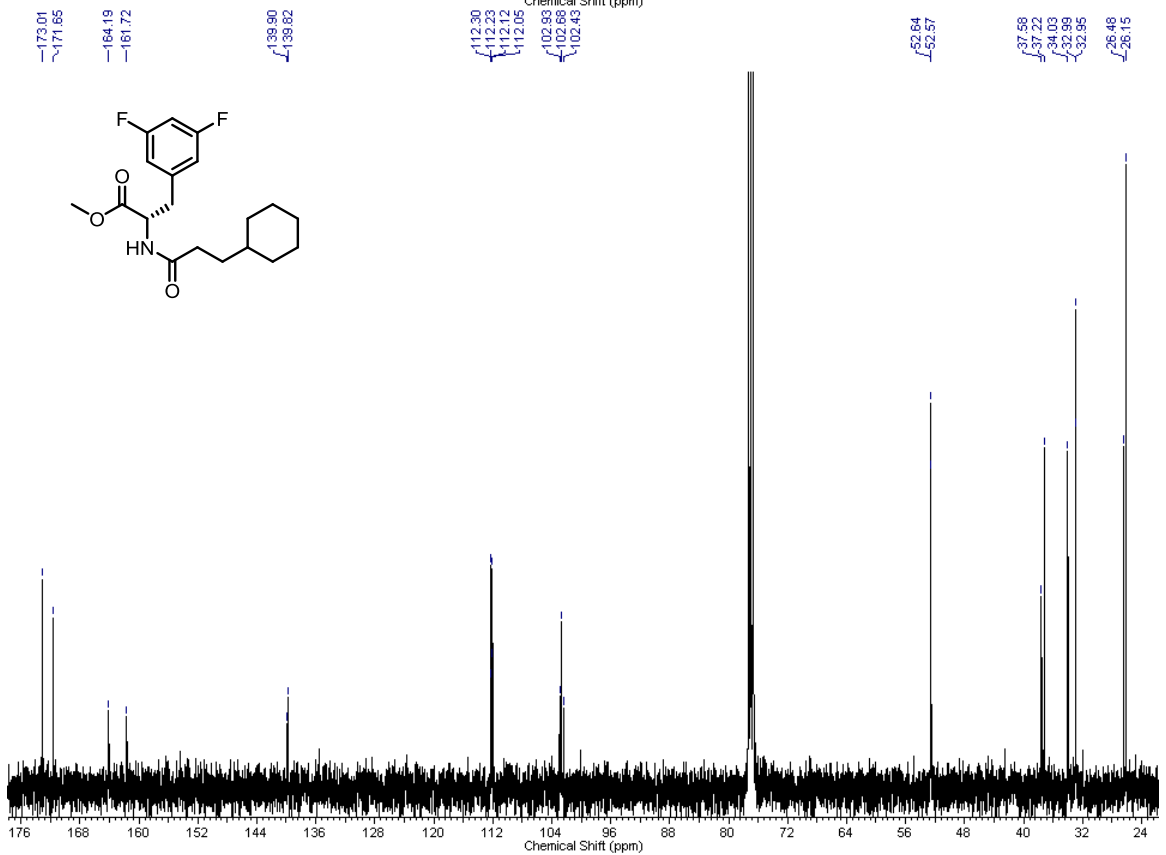
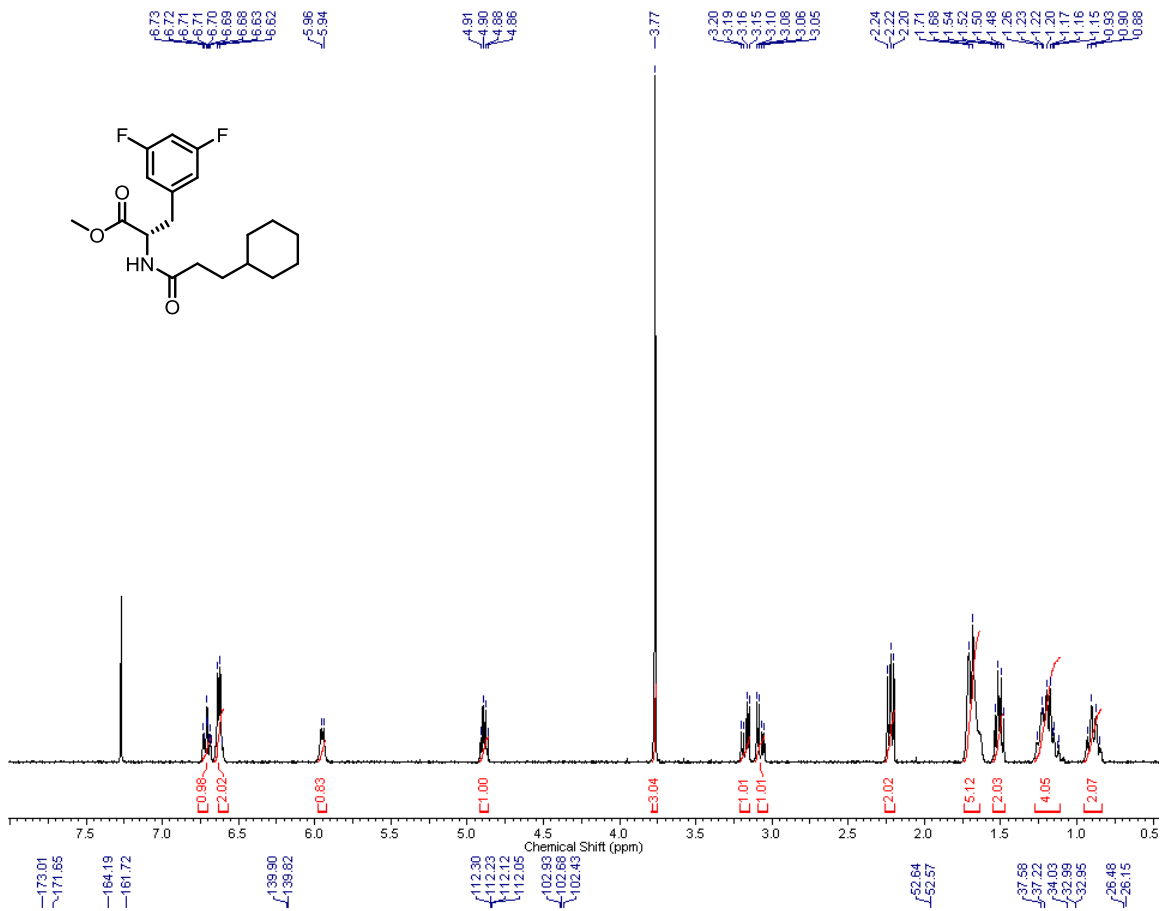


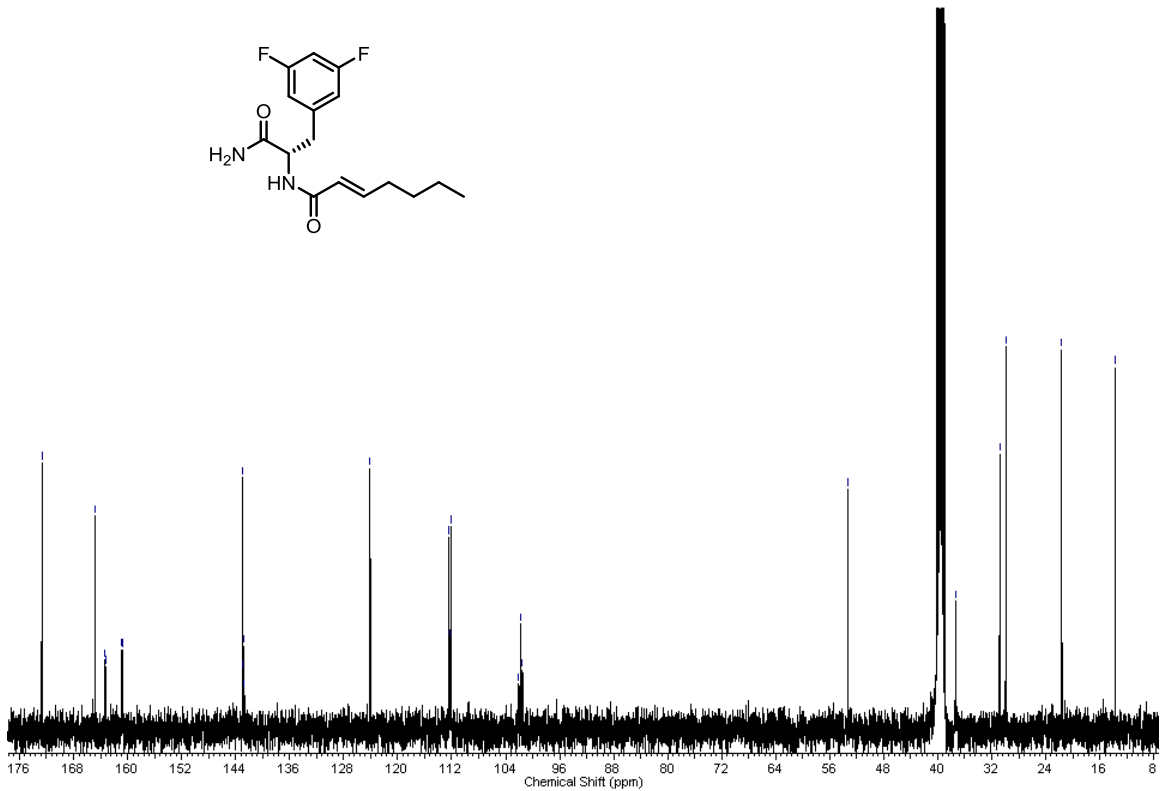
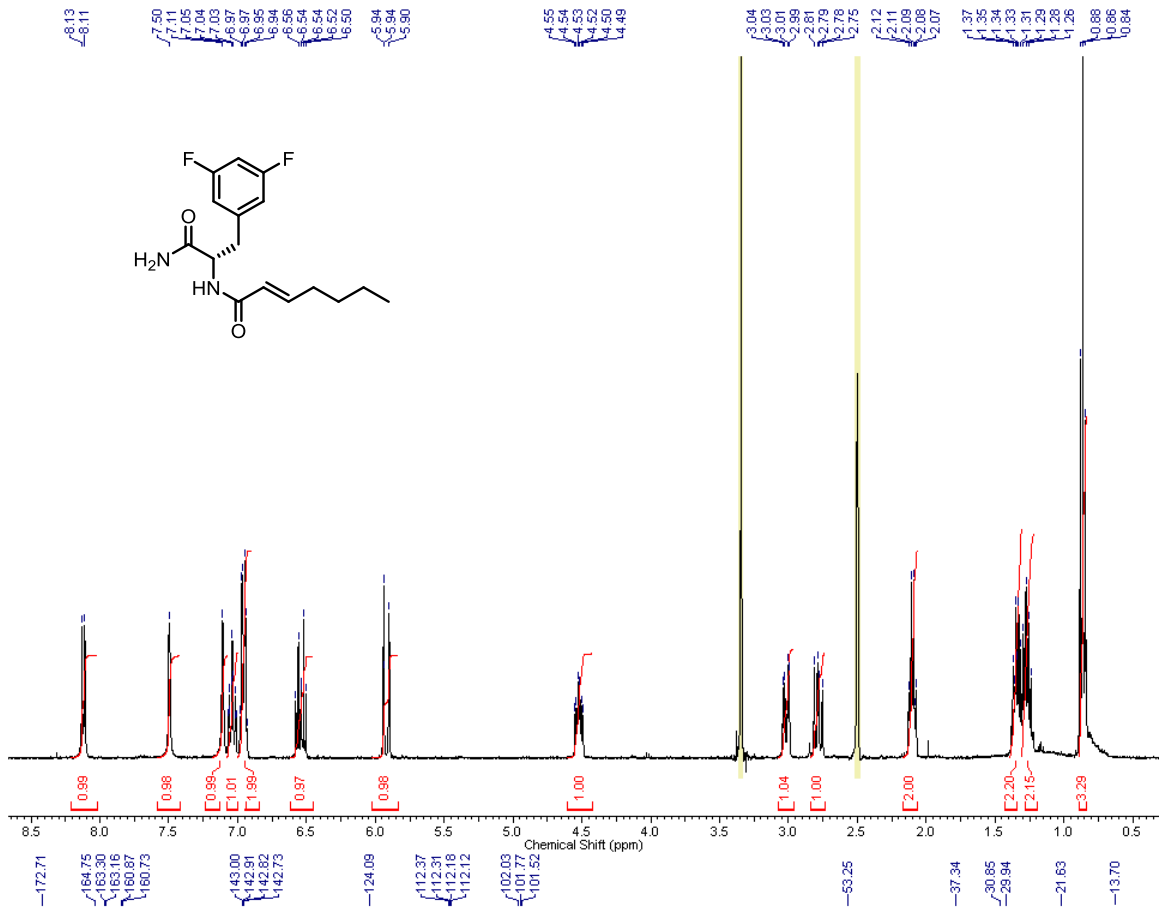


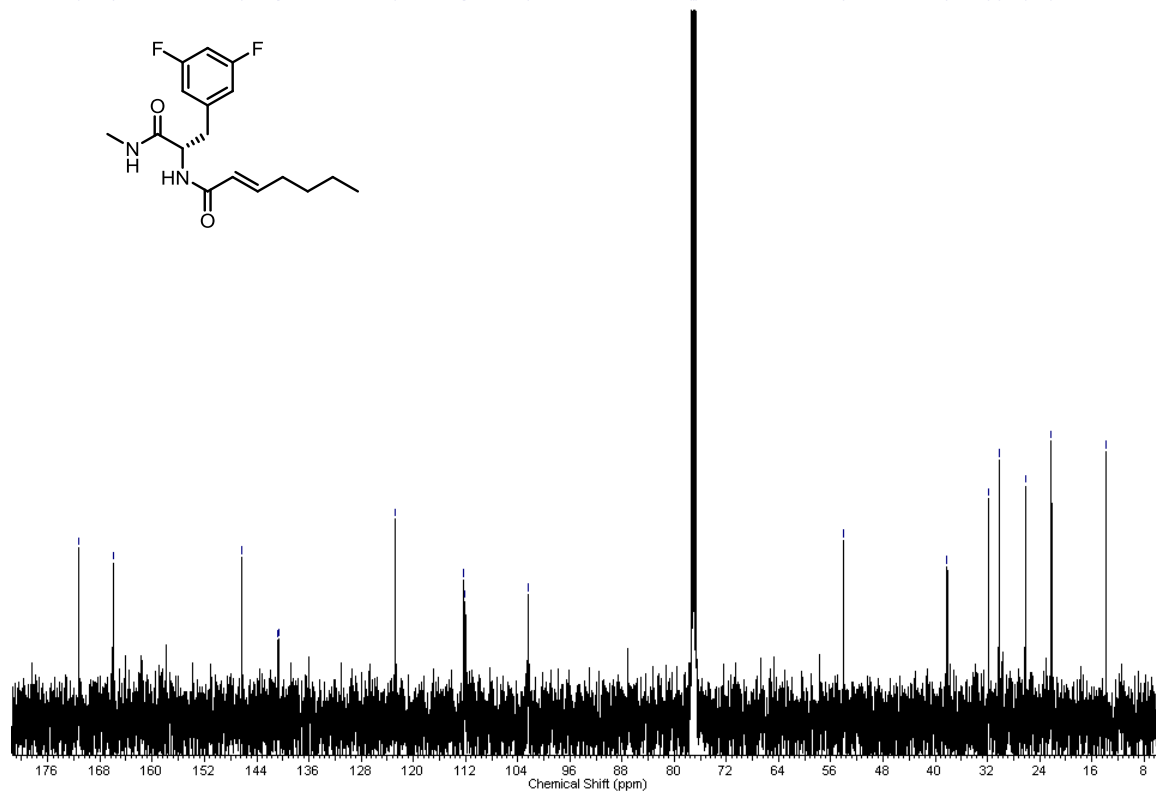
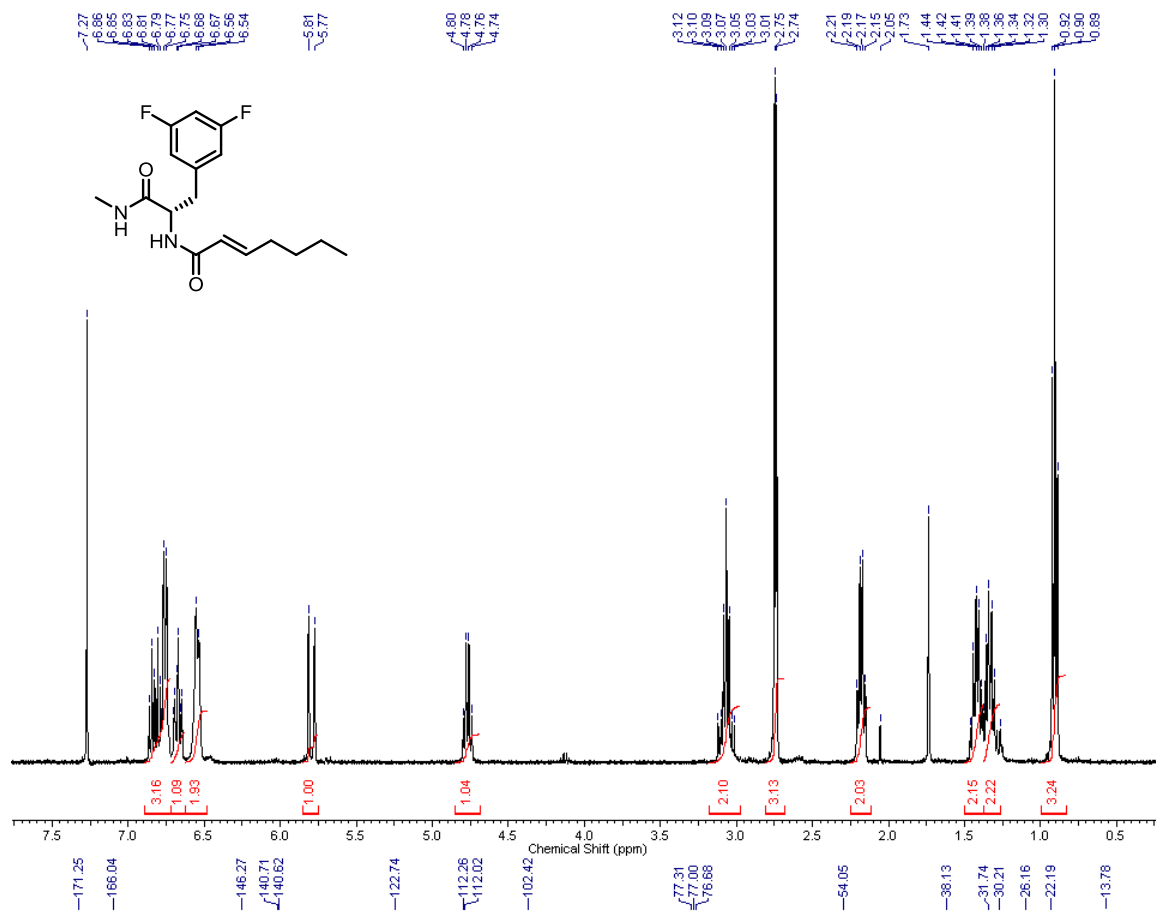


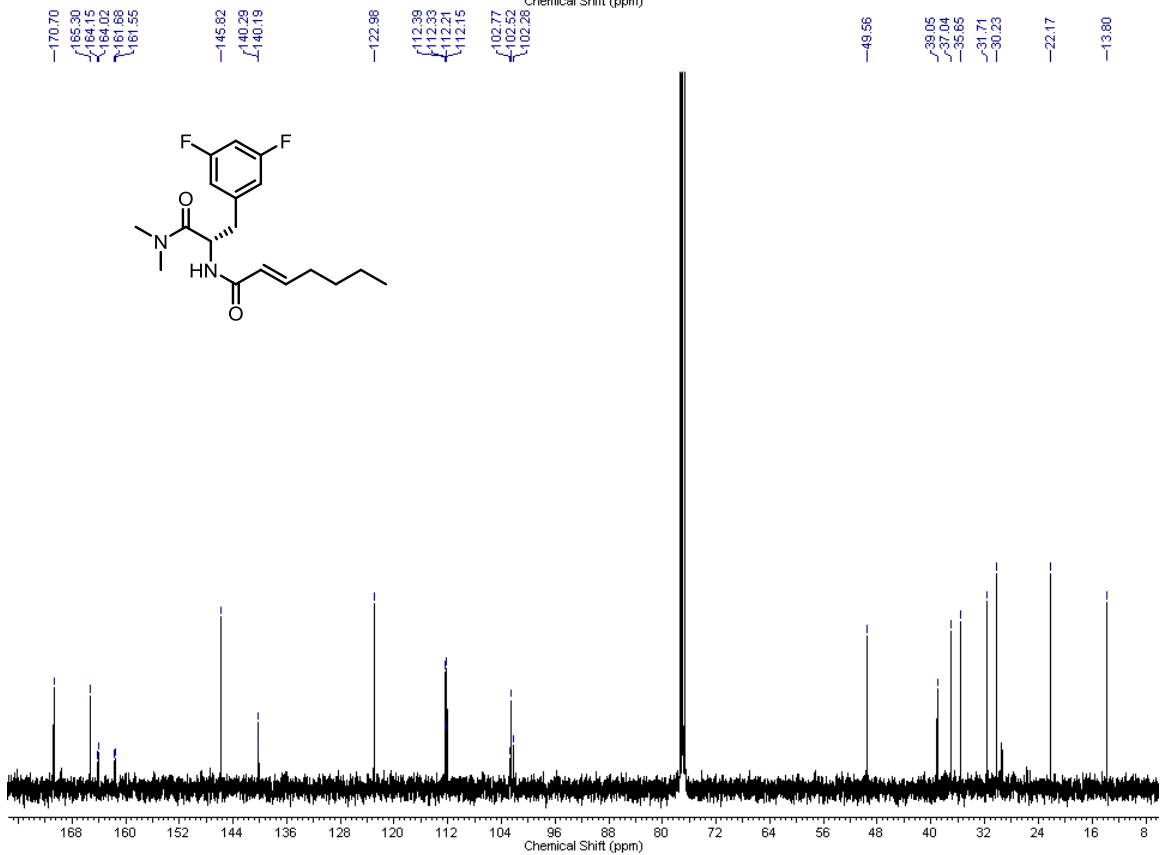
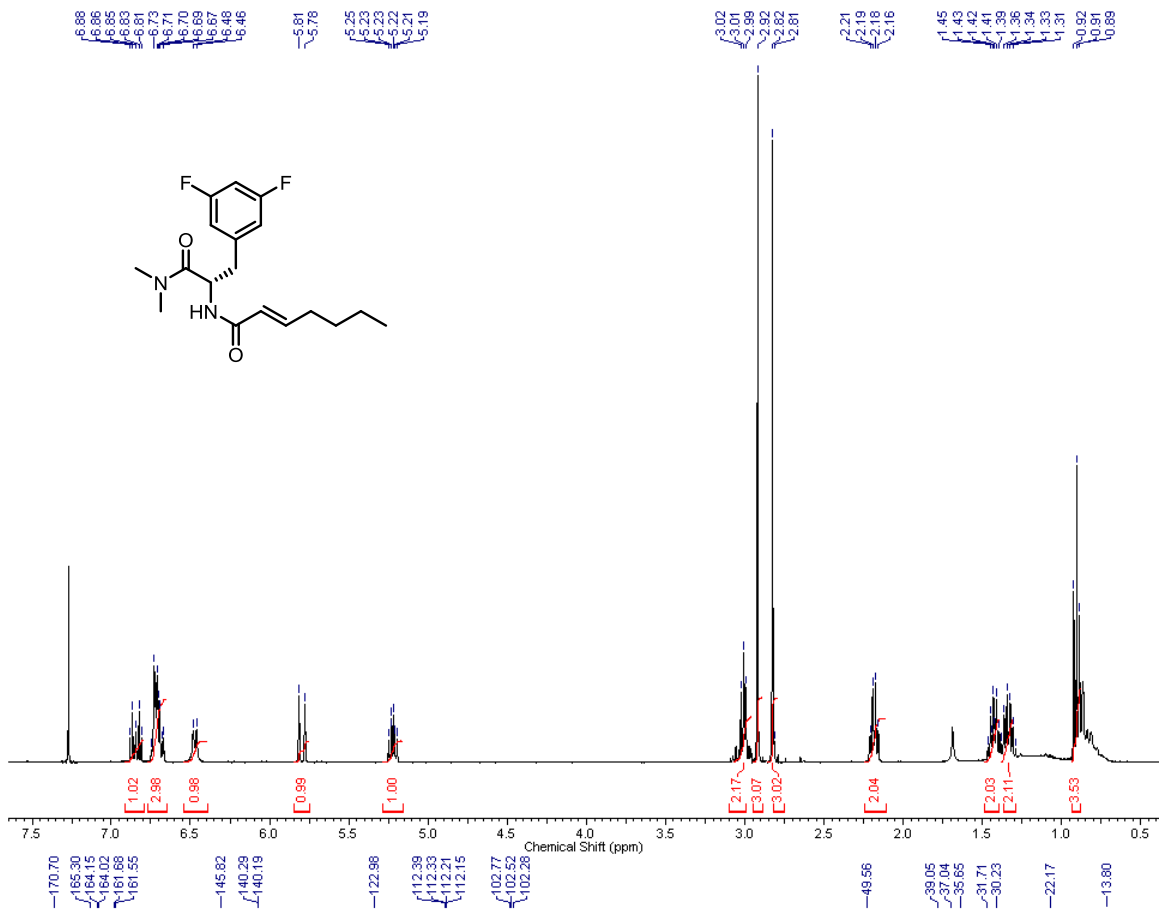




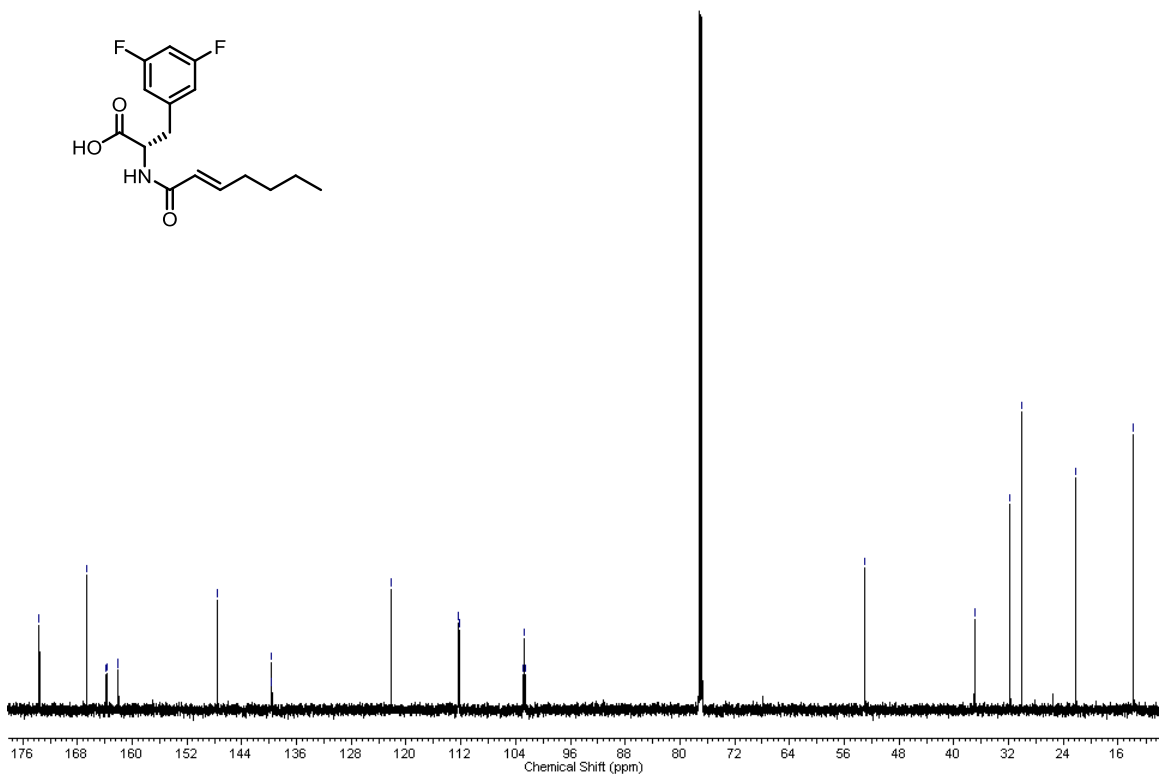
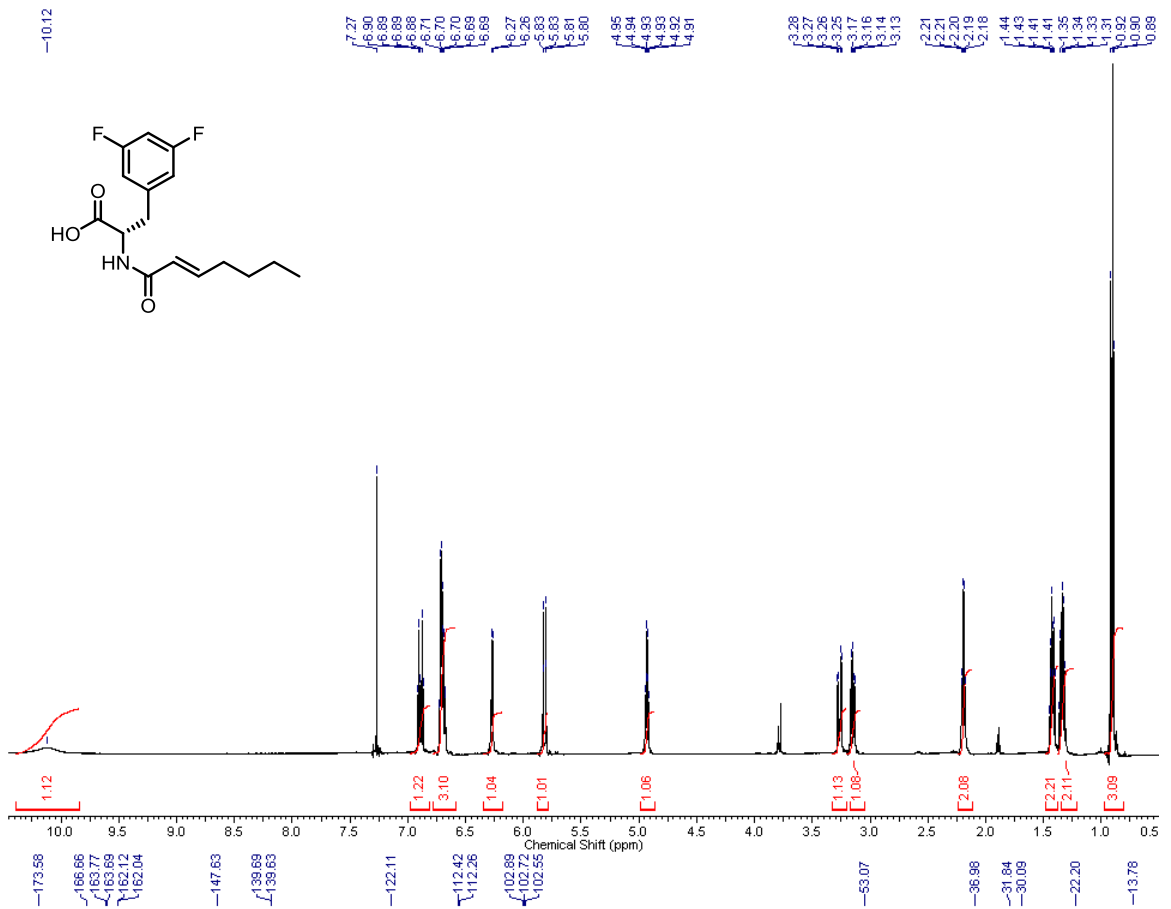


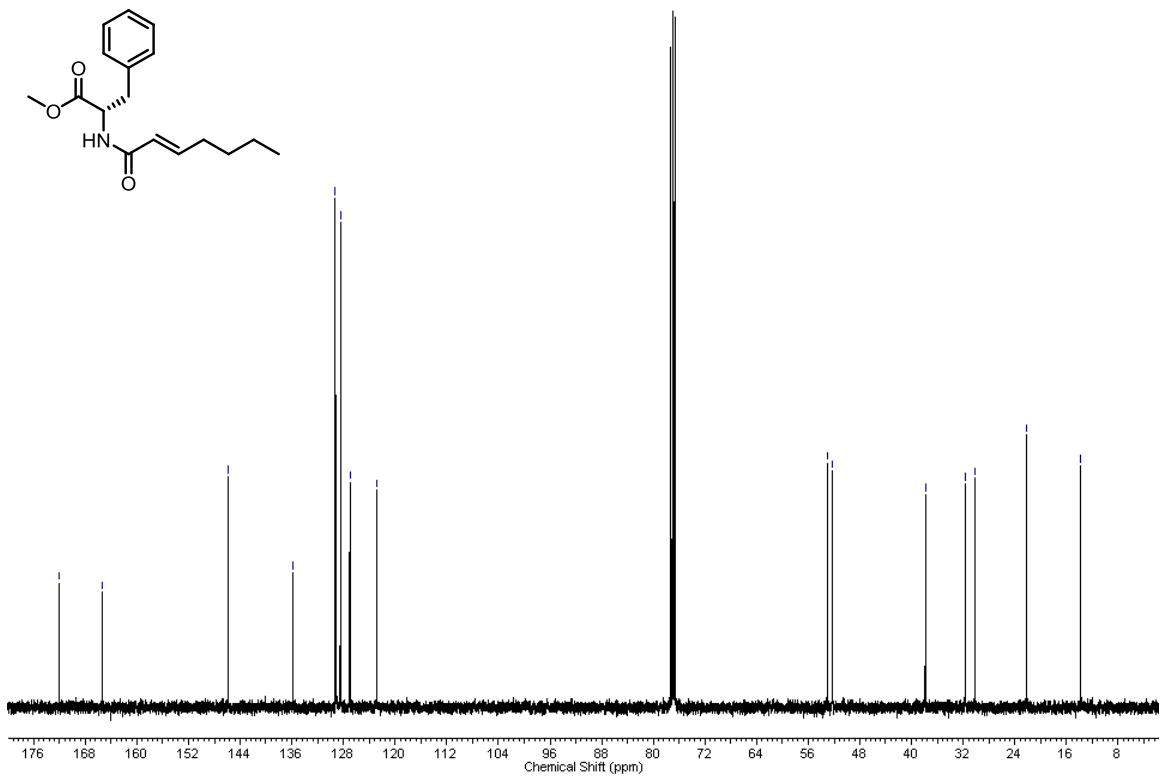
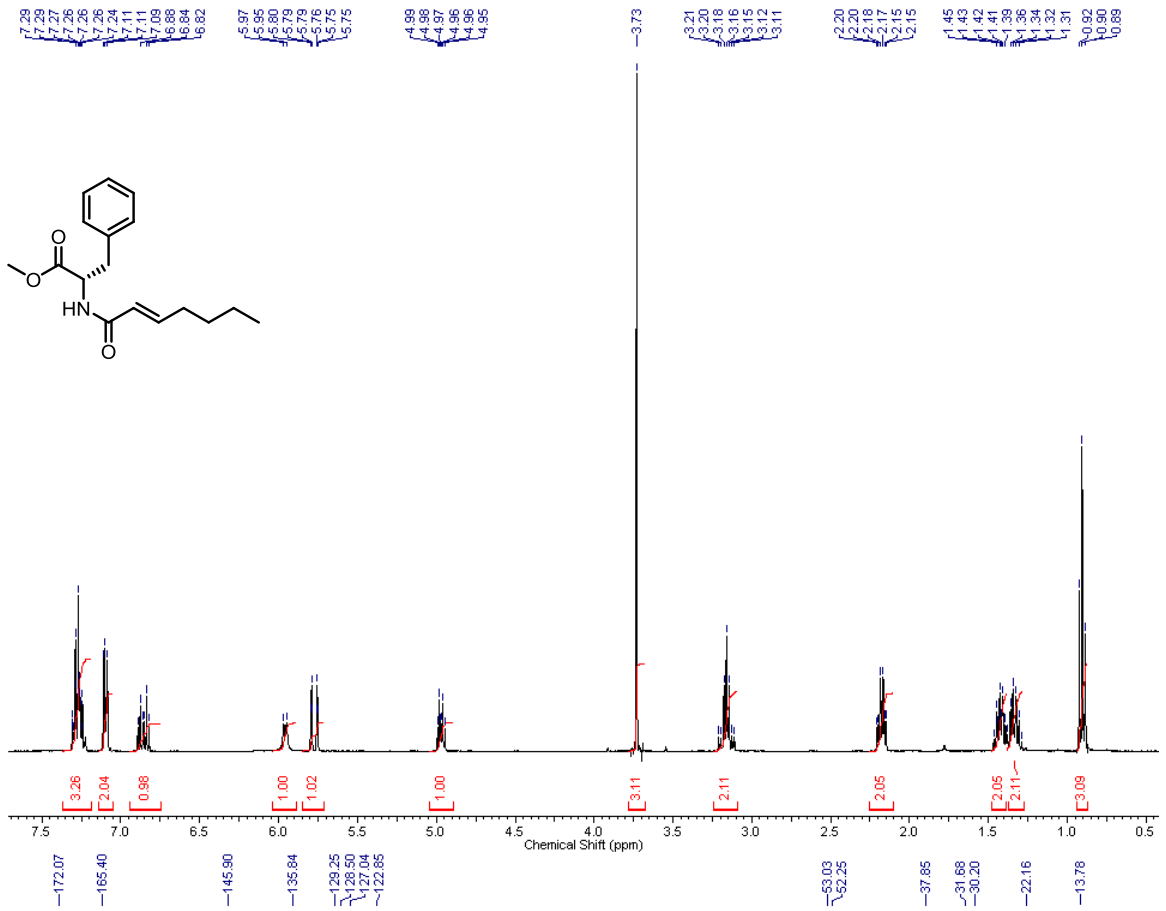


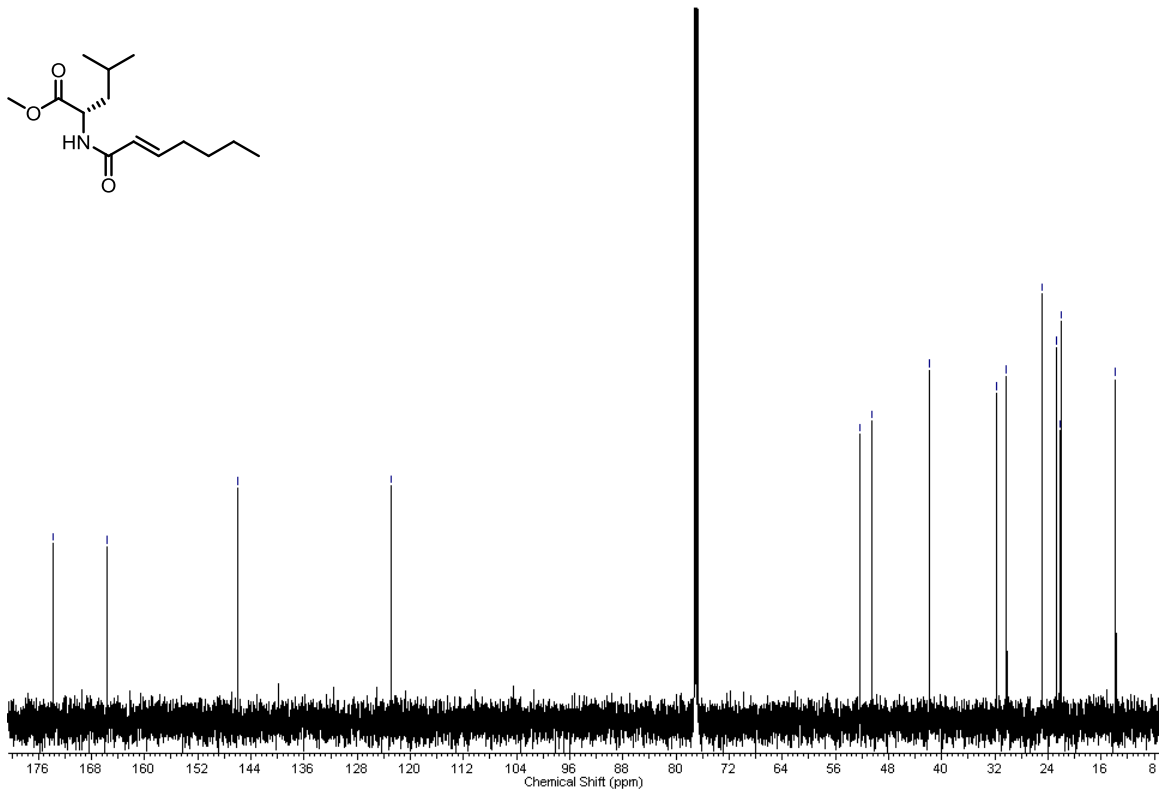
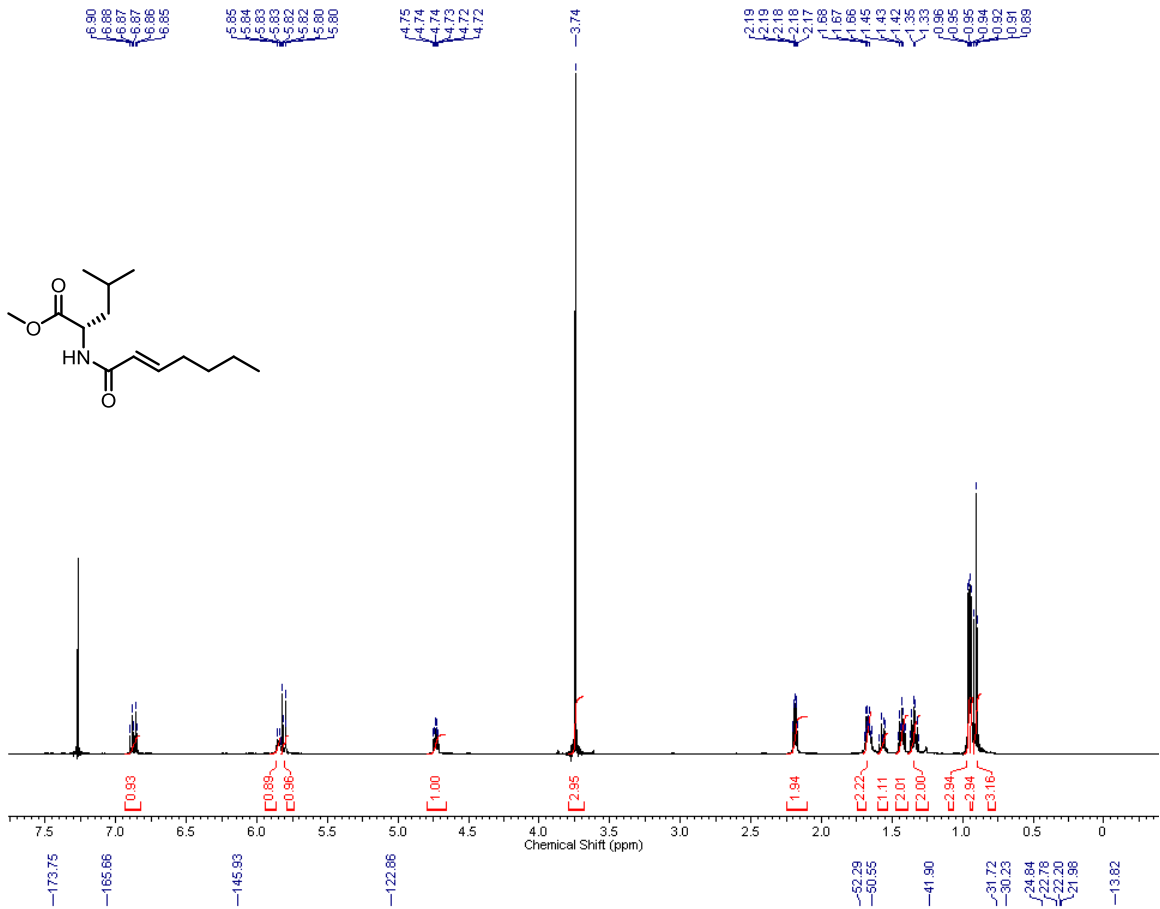


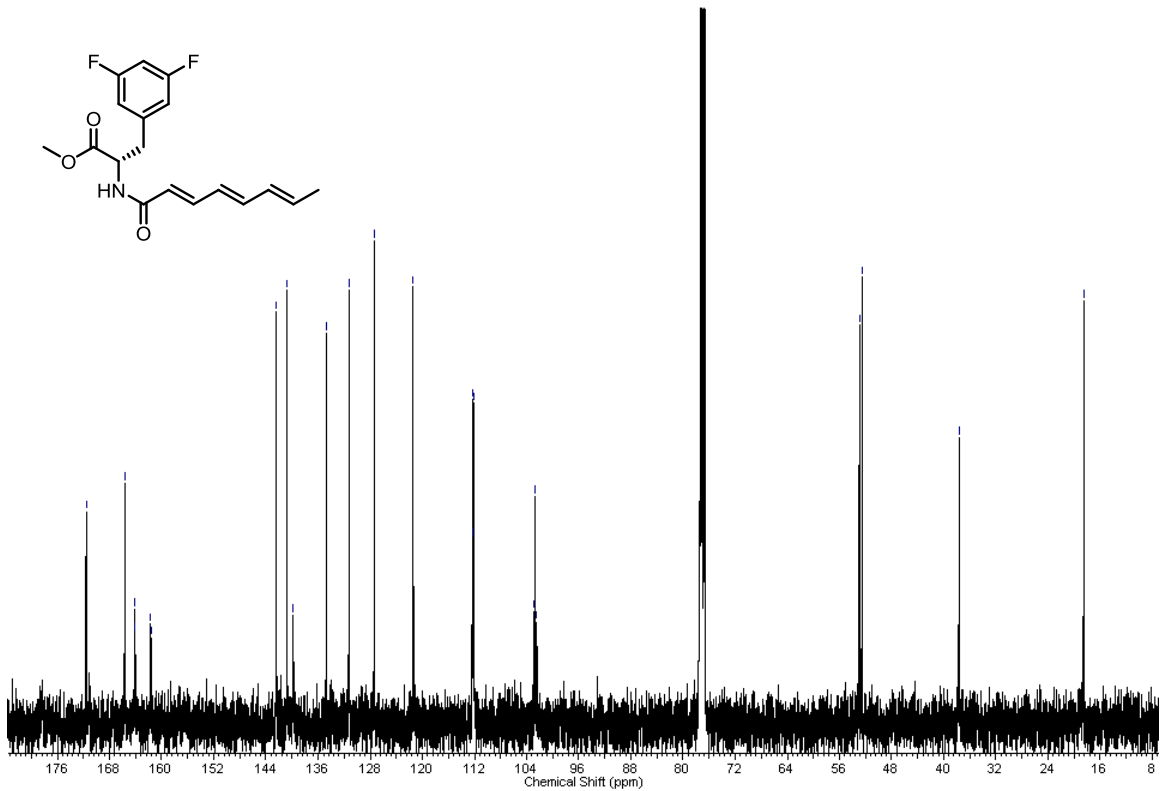
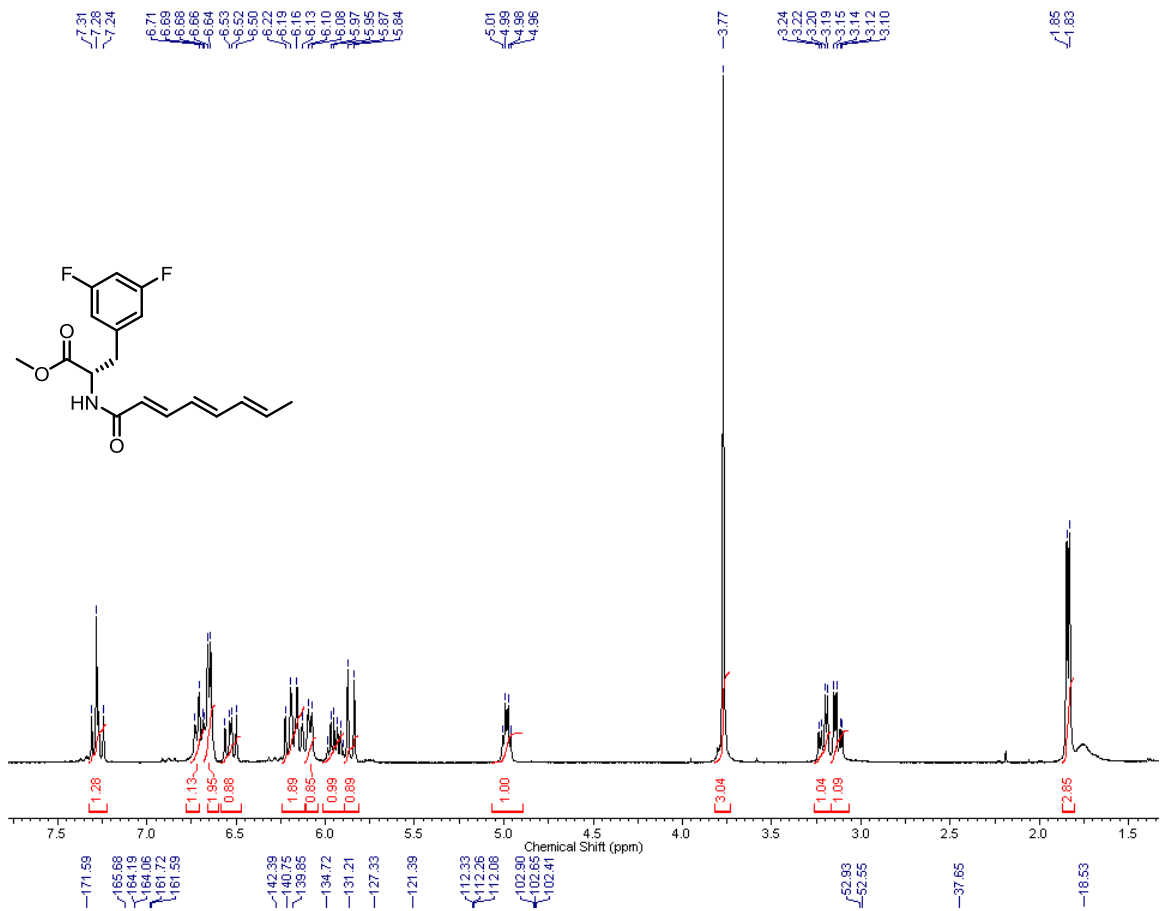


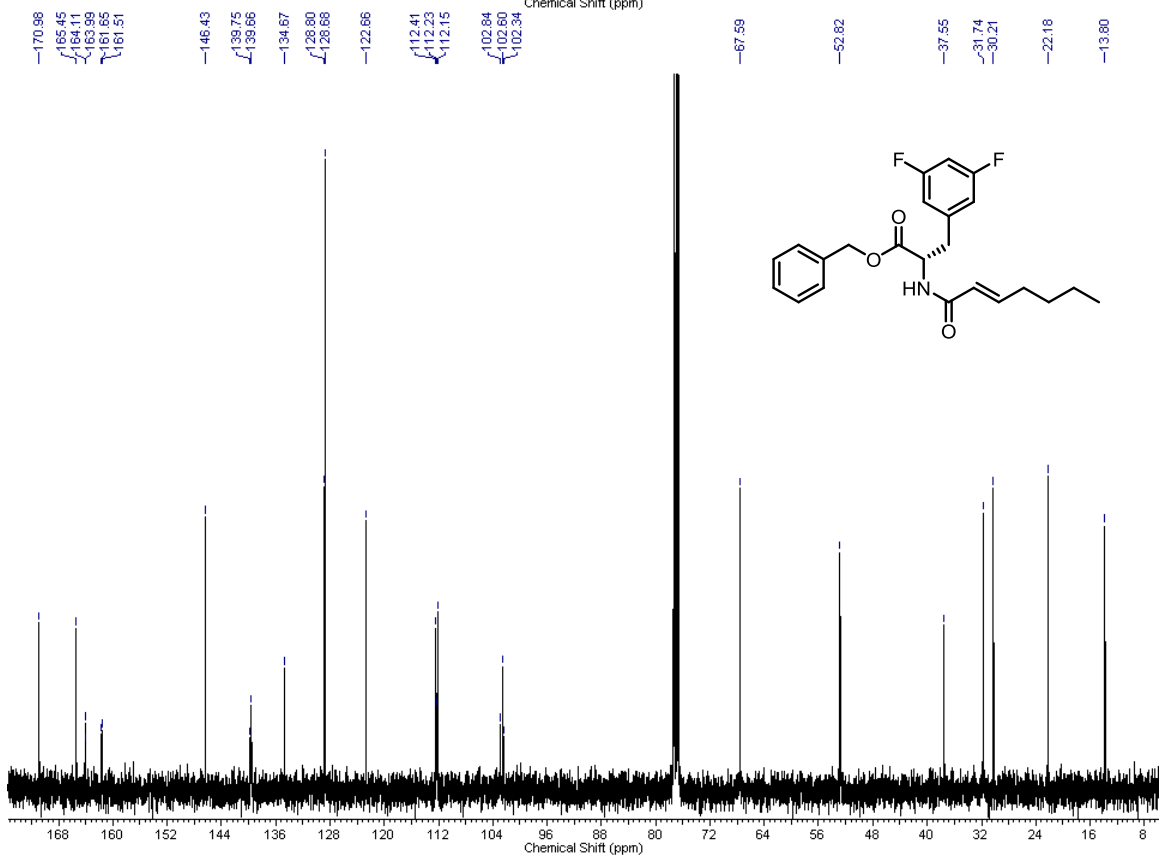
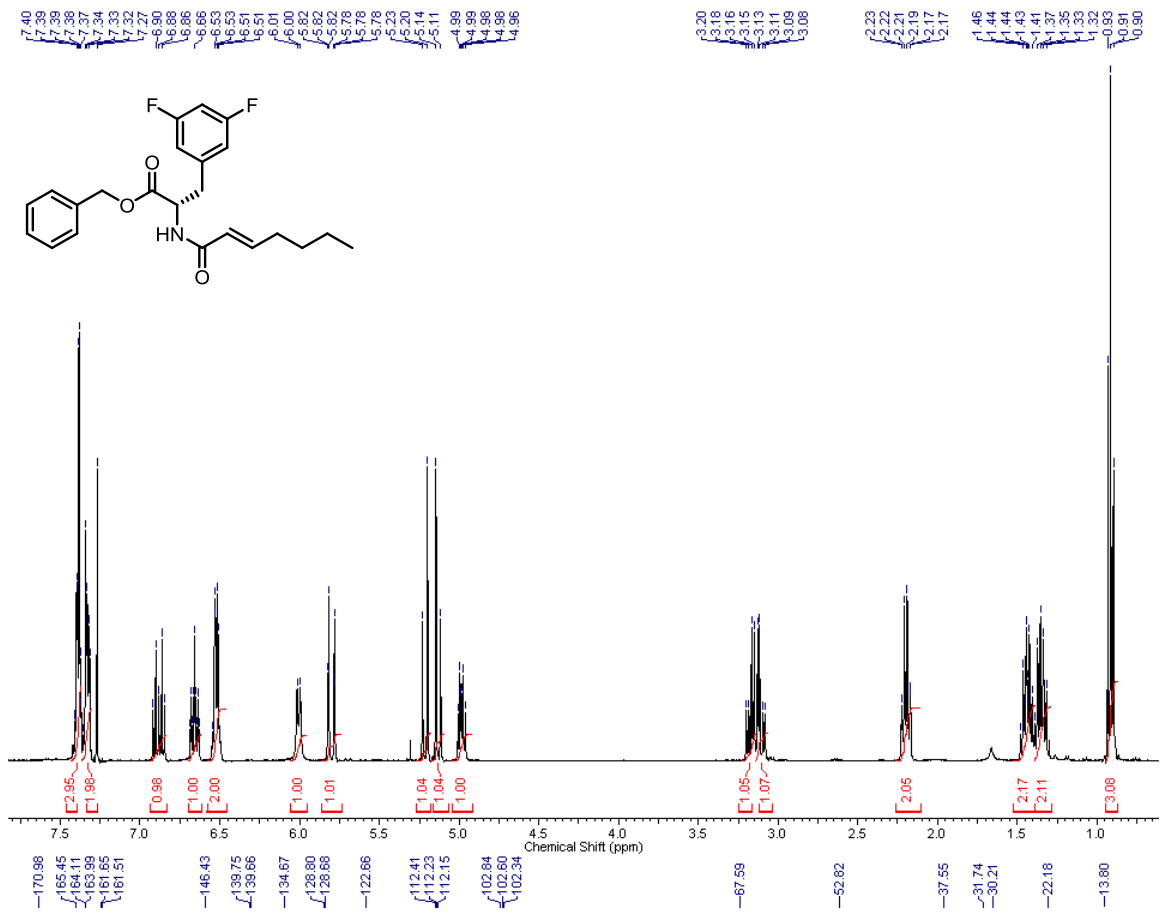


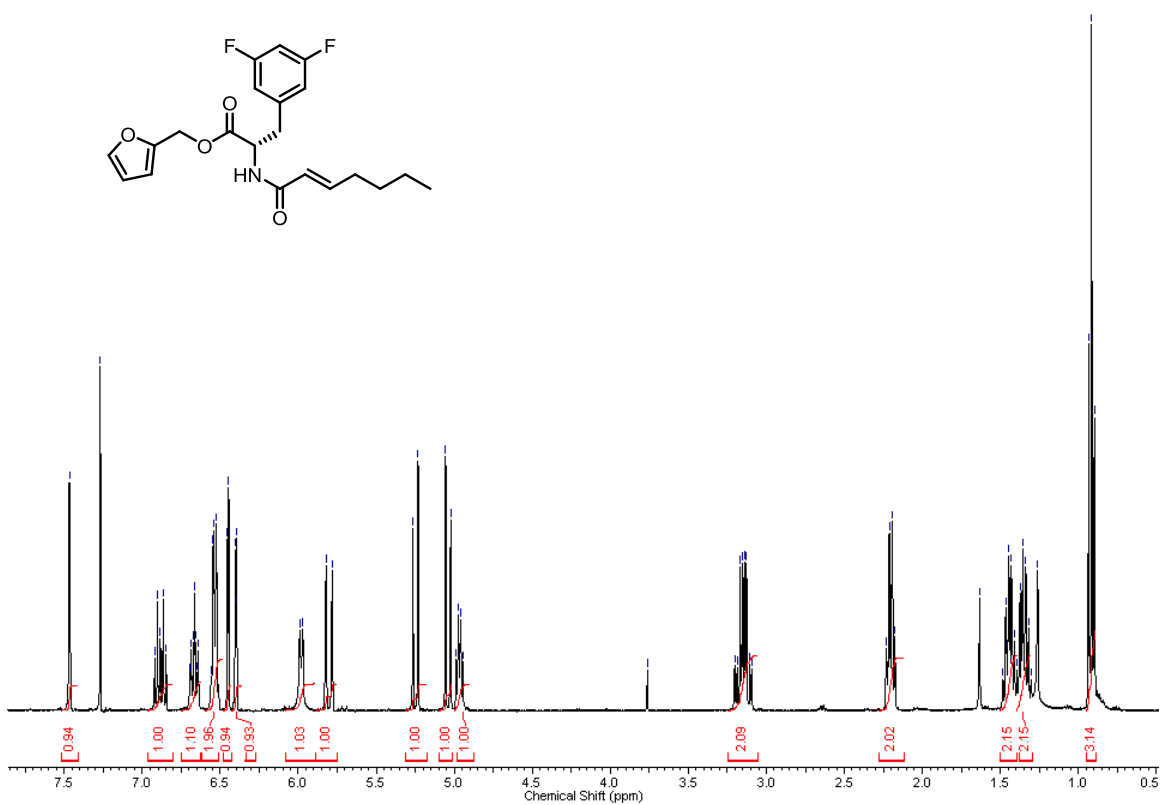
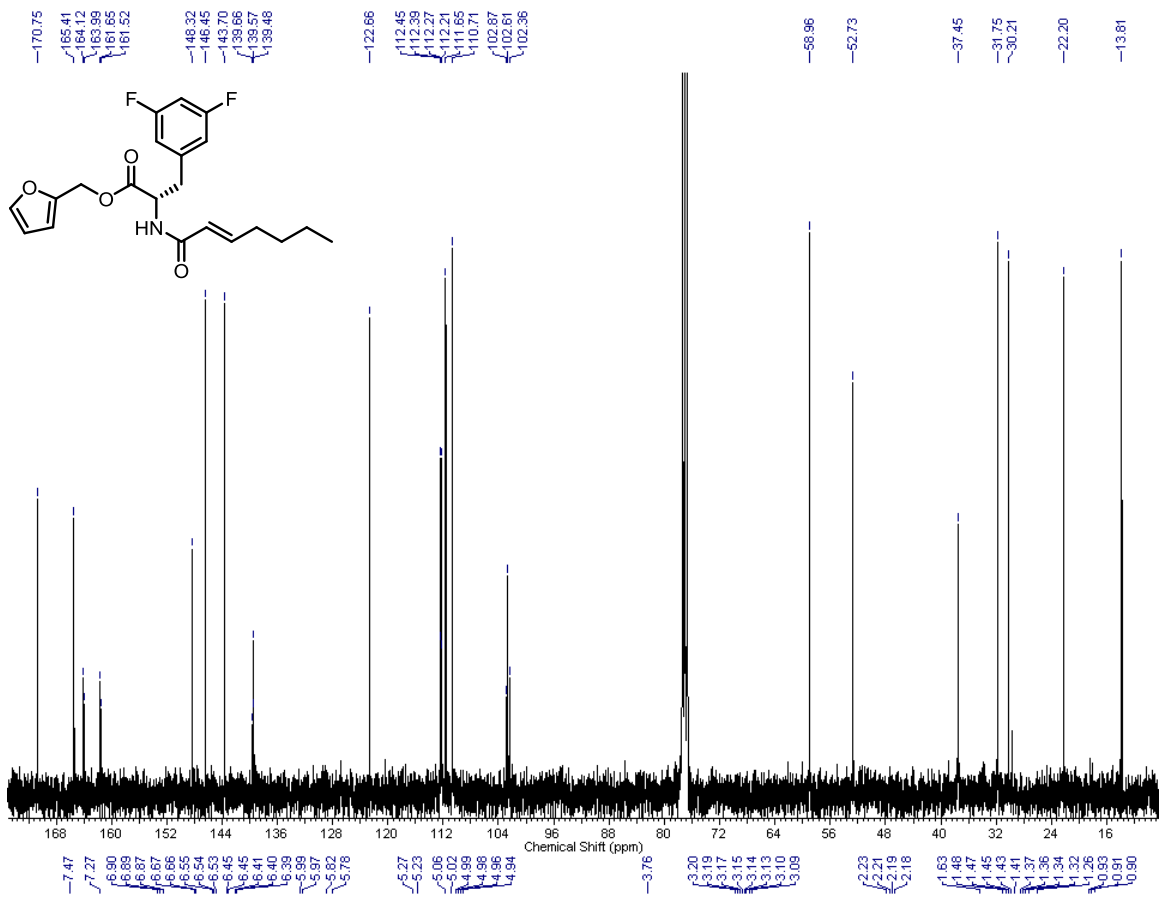


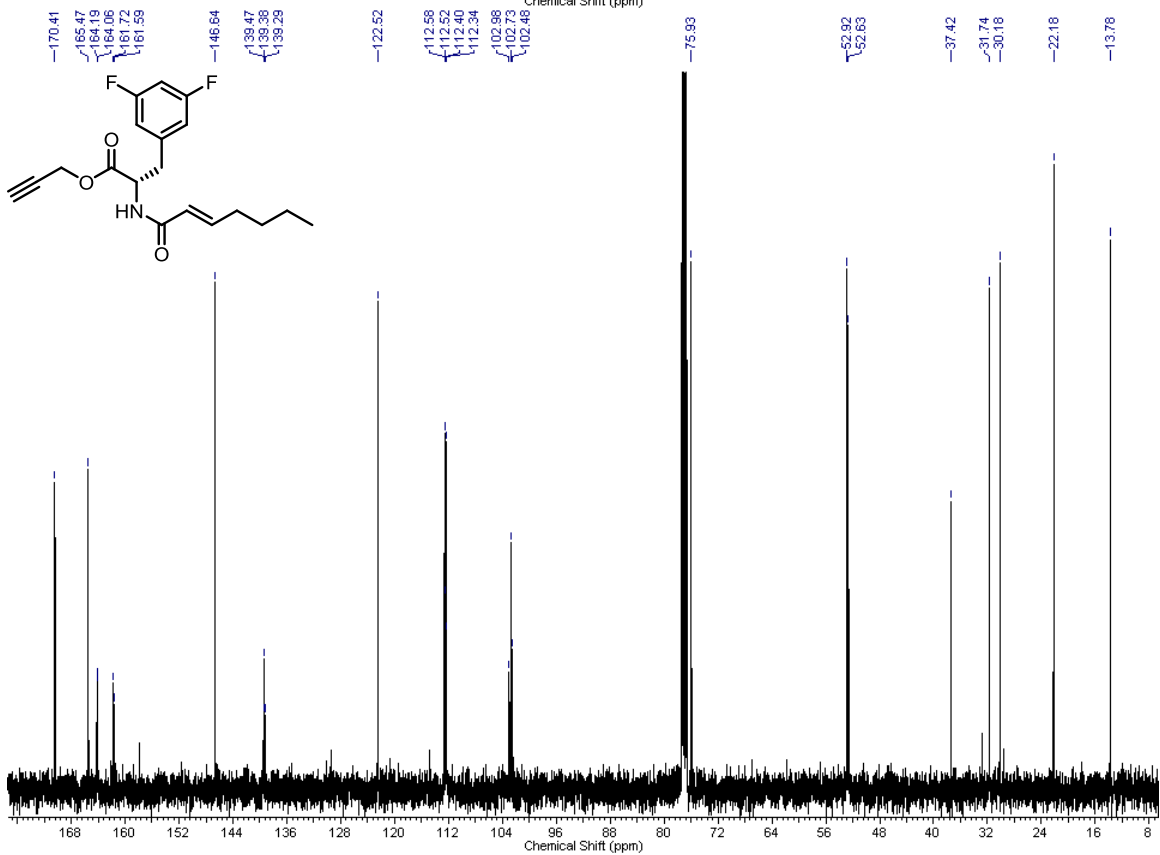
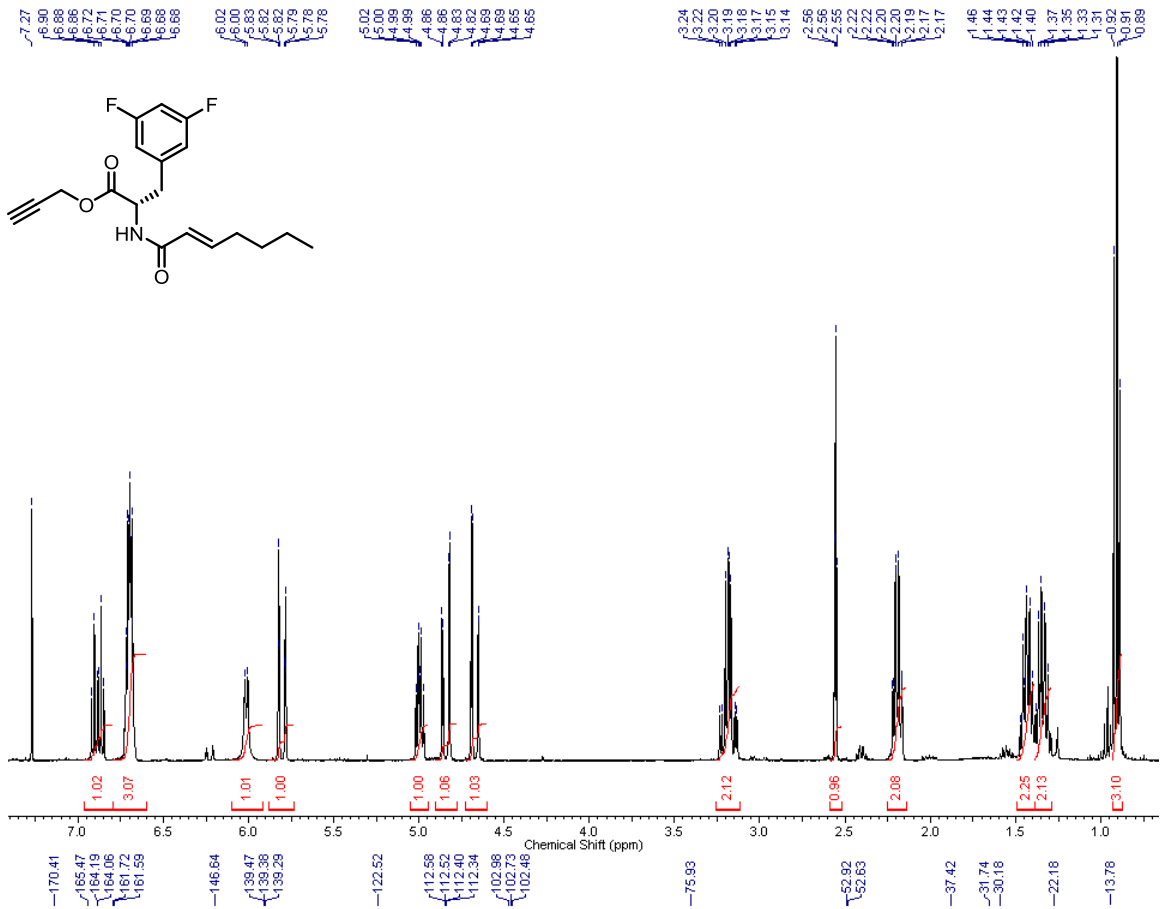






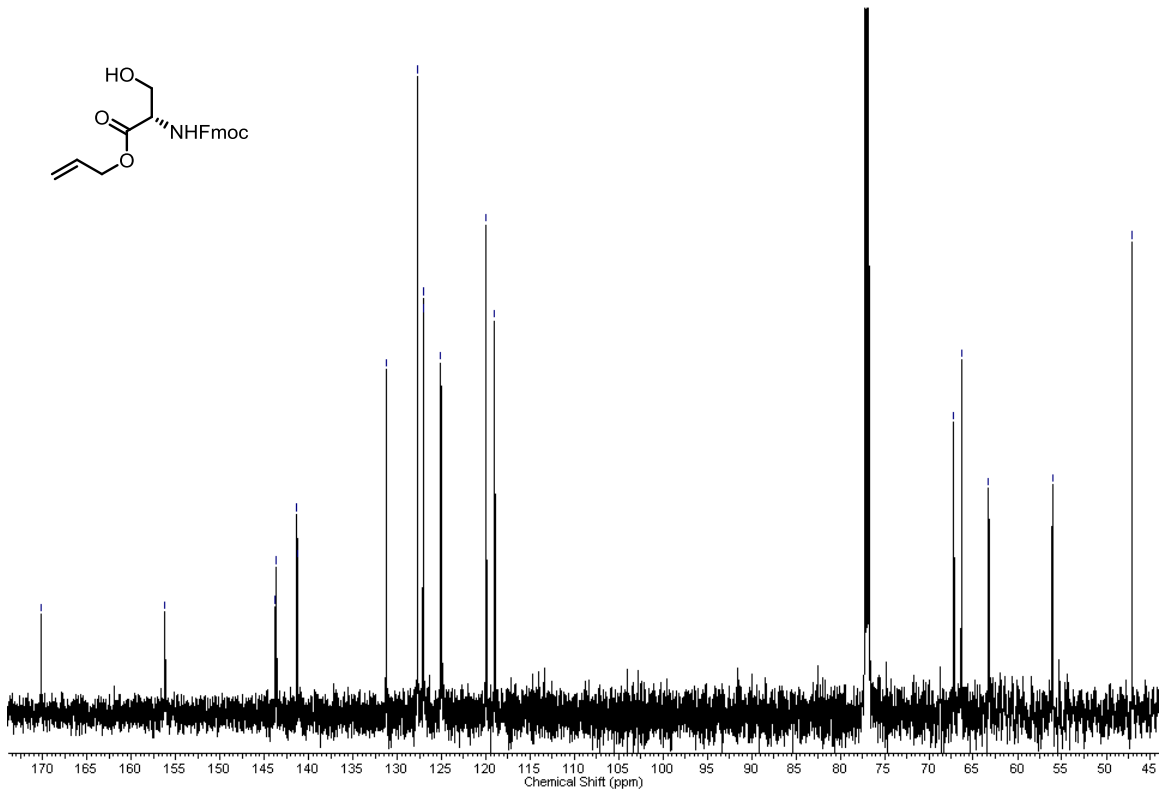
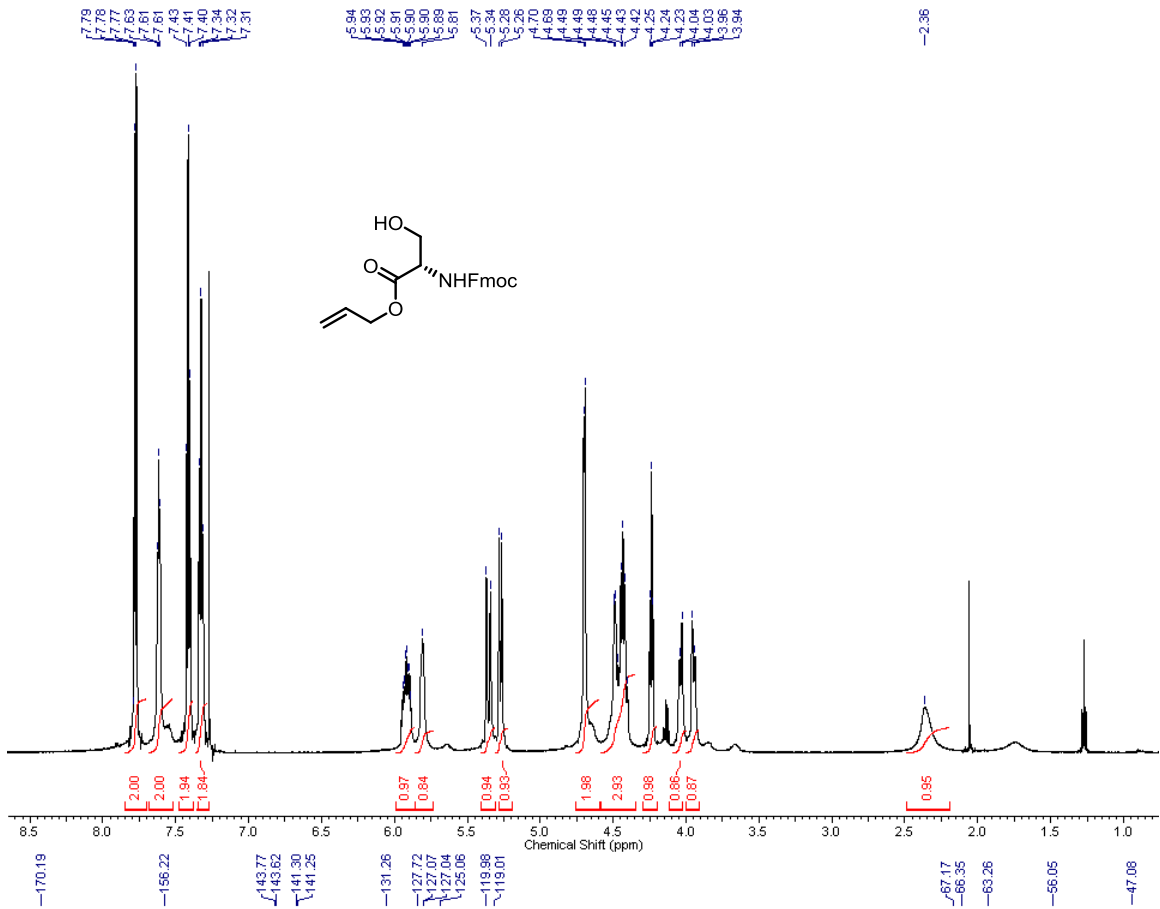


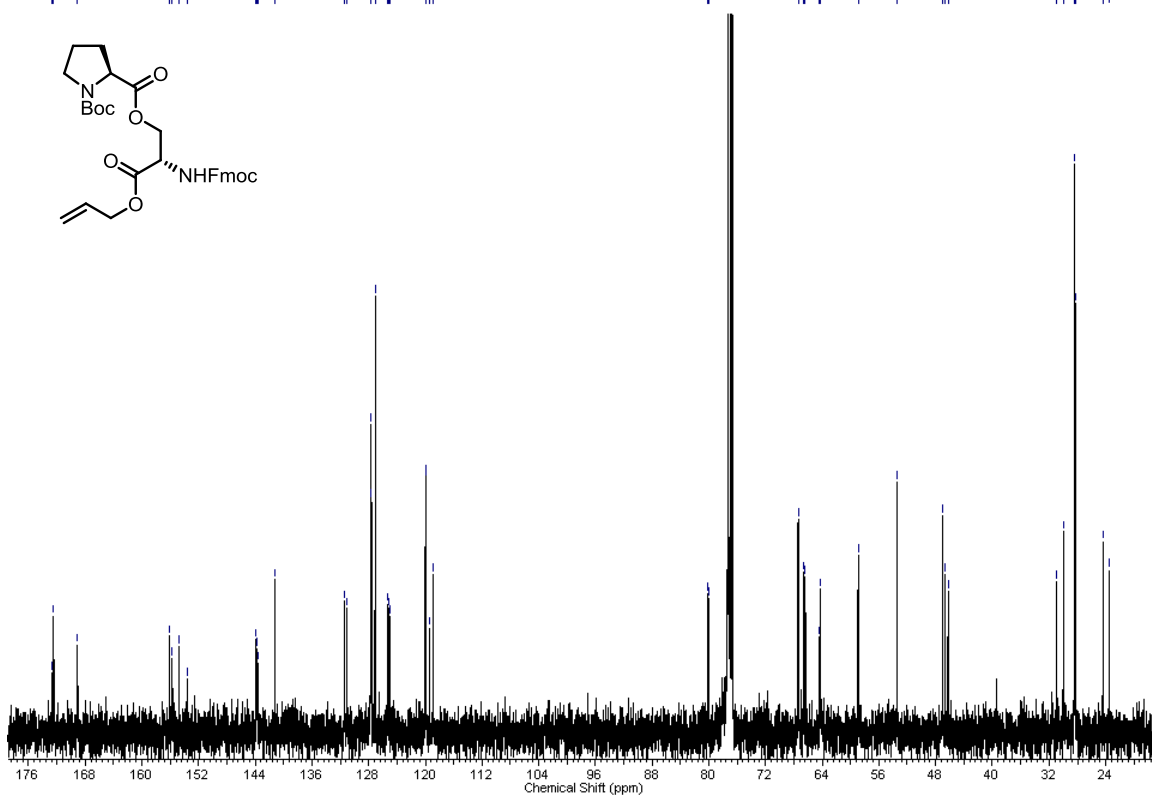
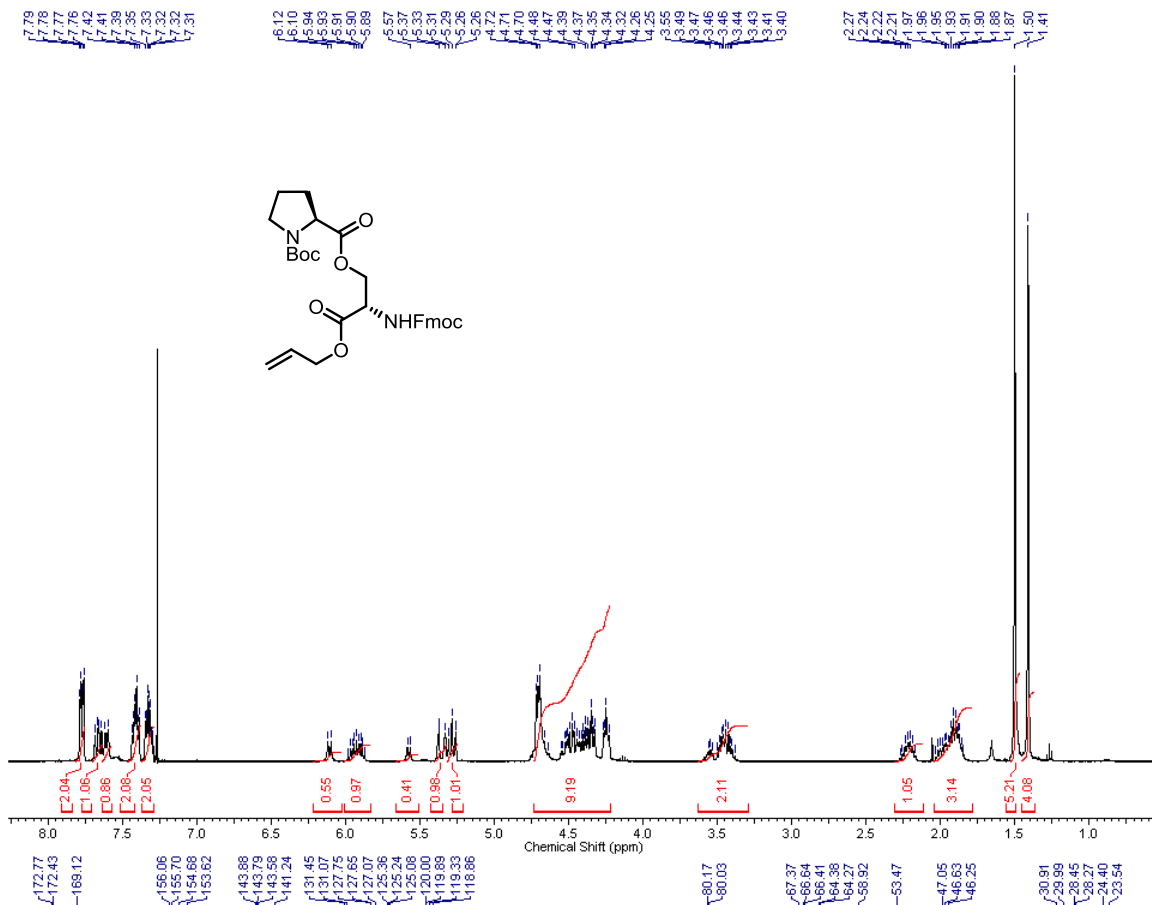




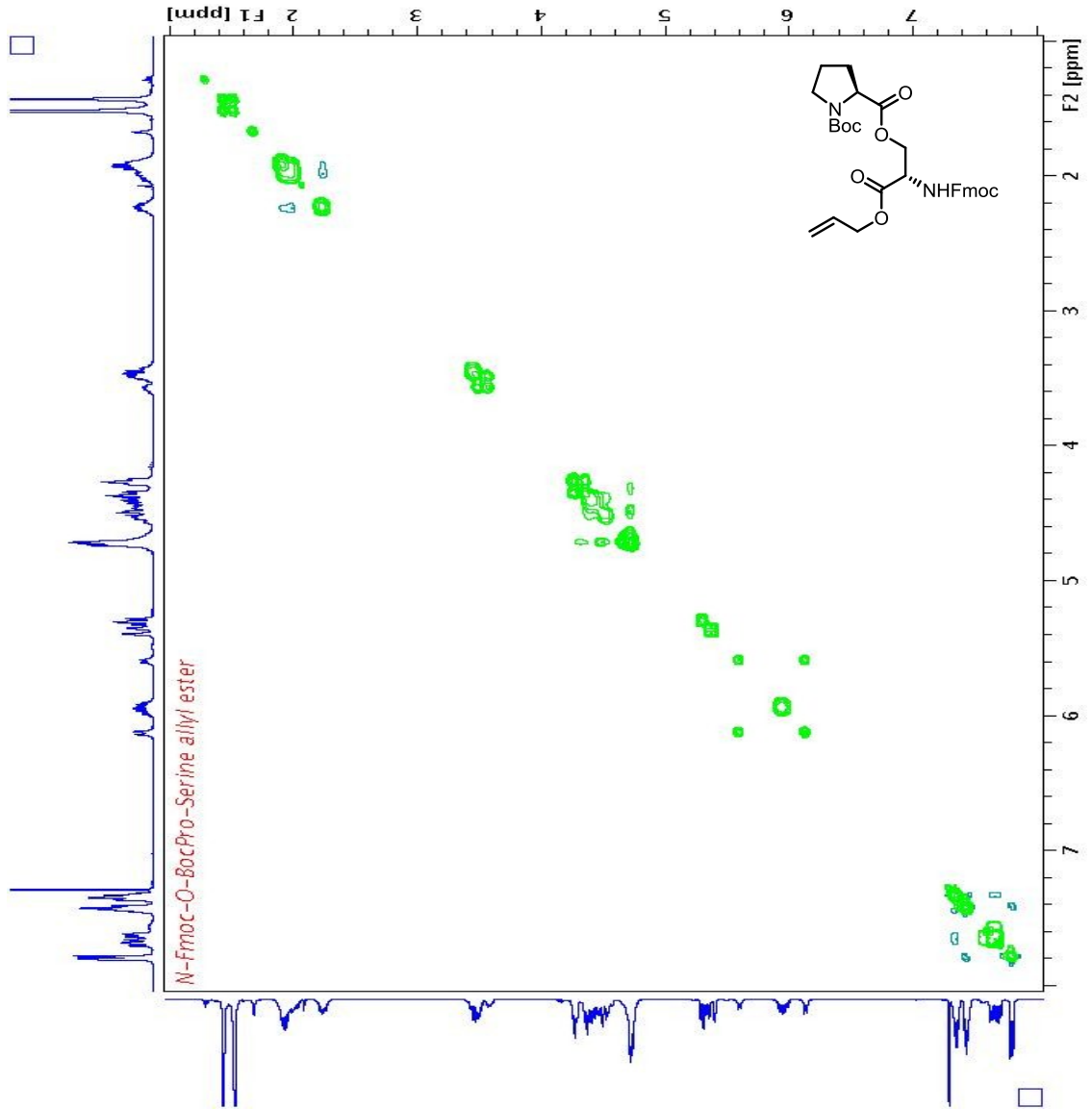
**Chapter 9 – *N*-Acyldifluorophenylalanine Fragment Hit to lead development.**

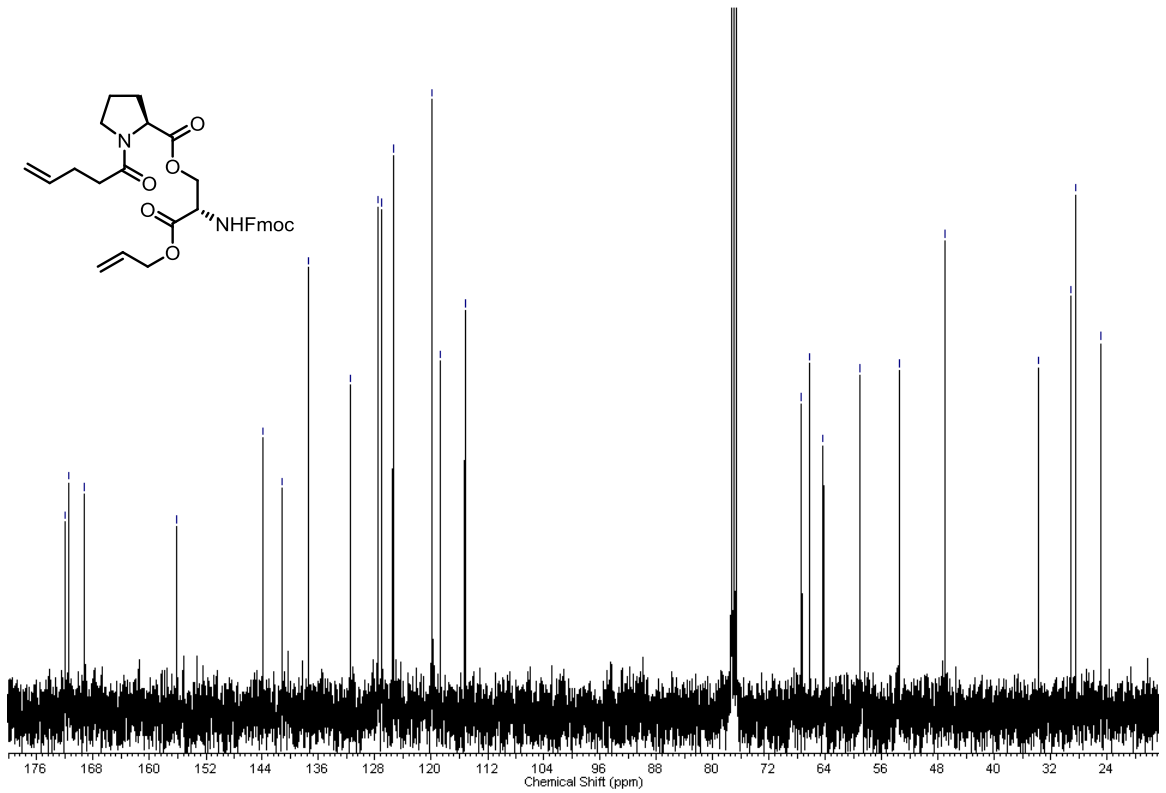
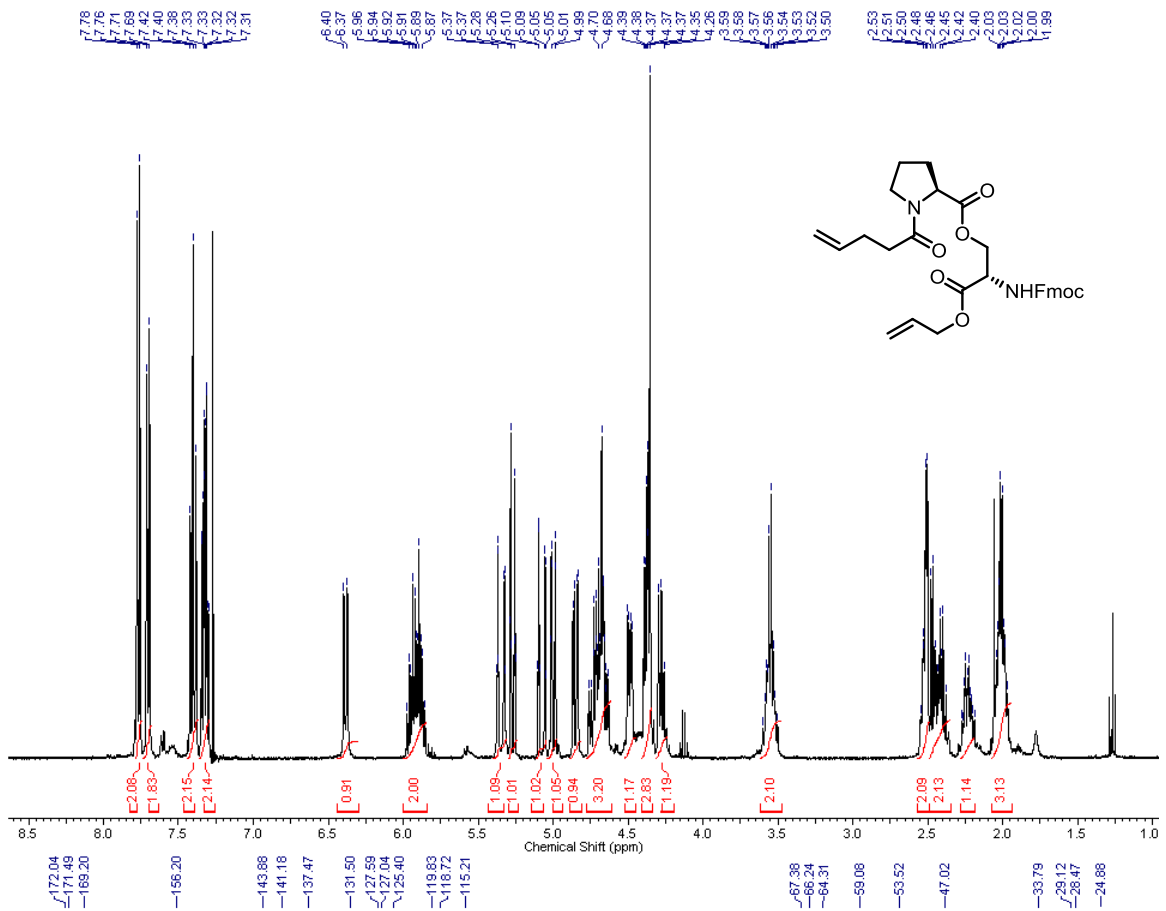


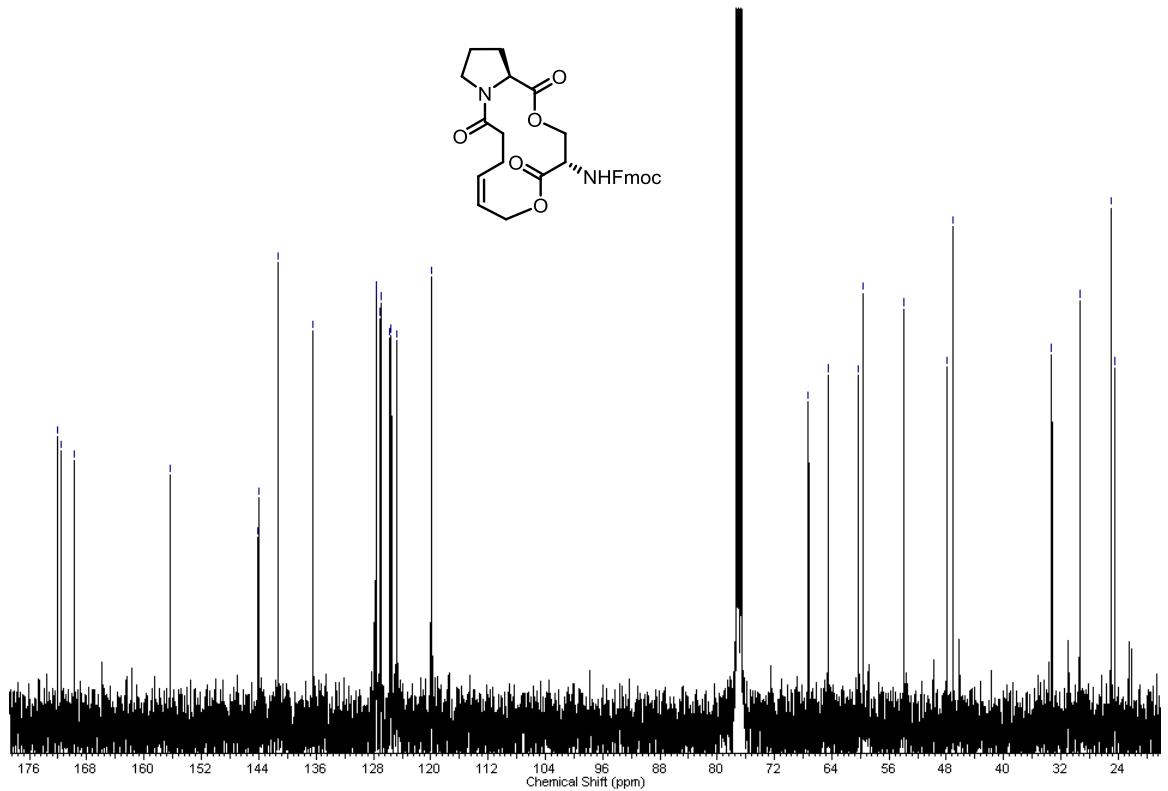
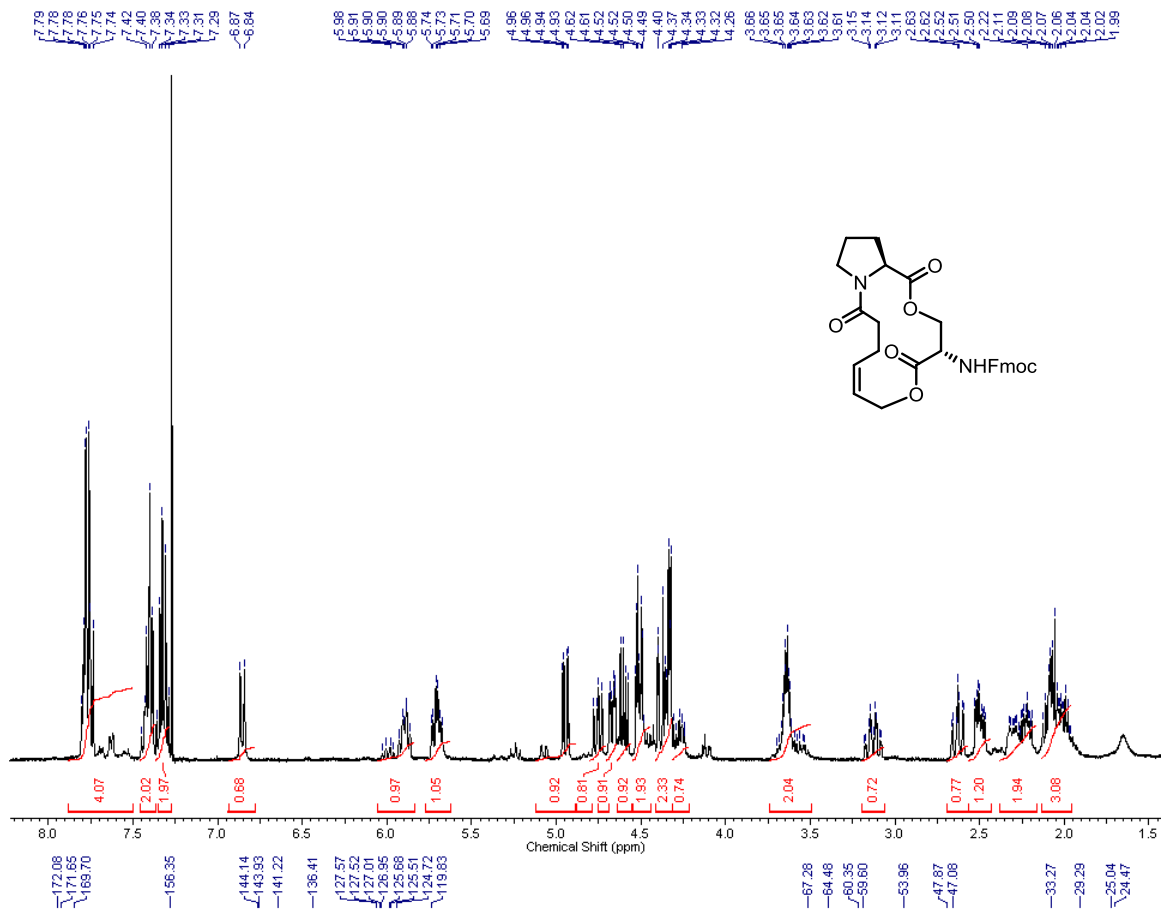


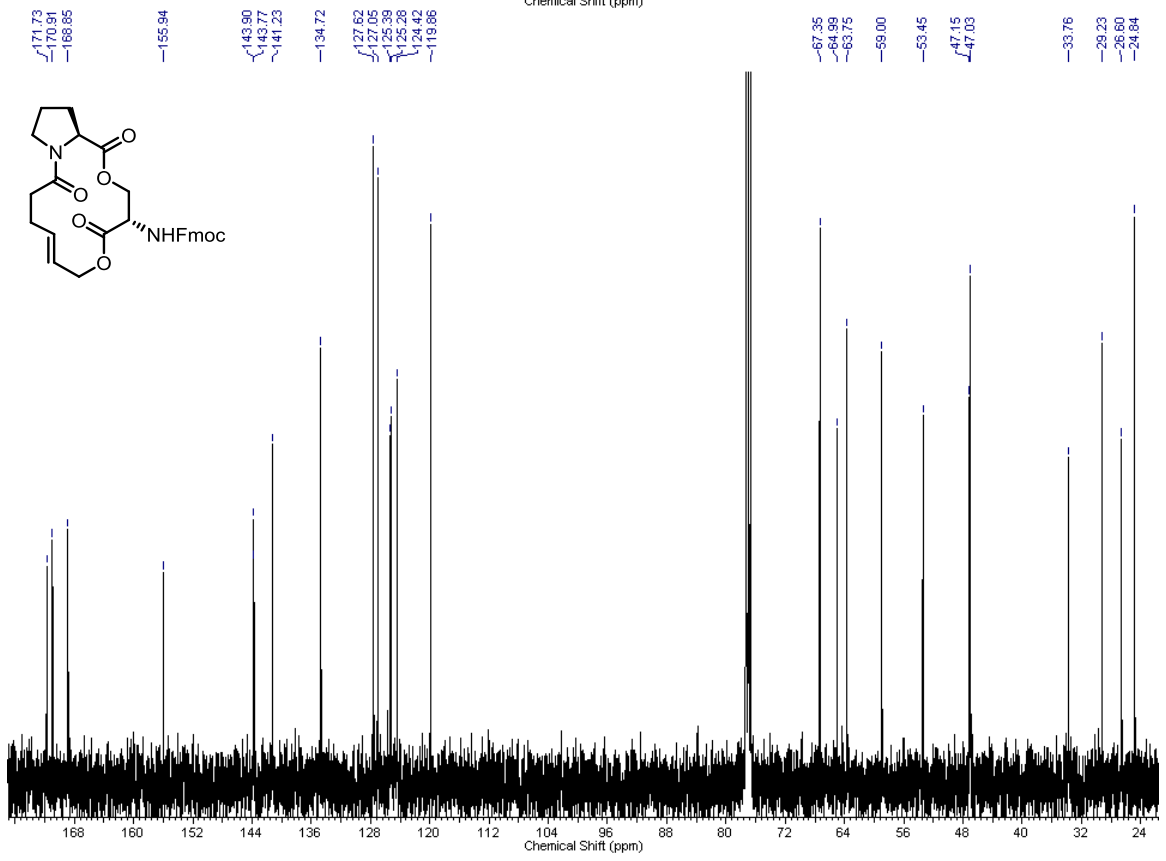
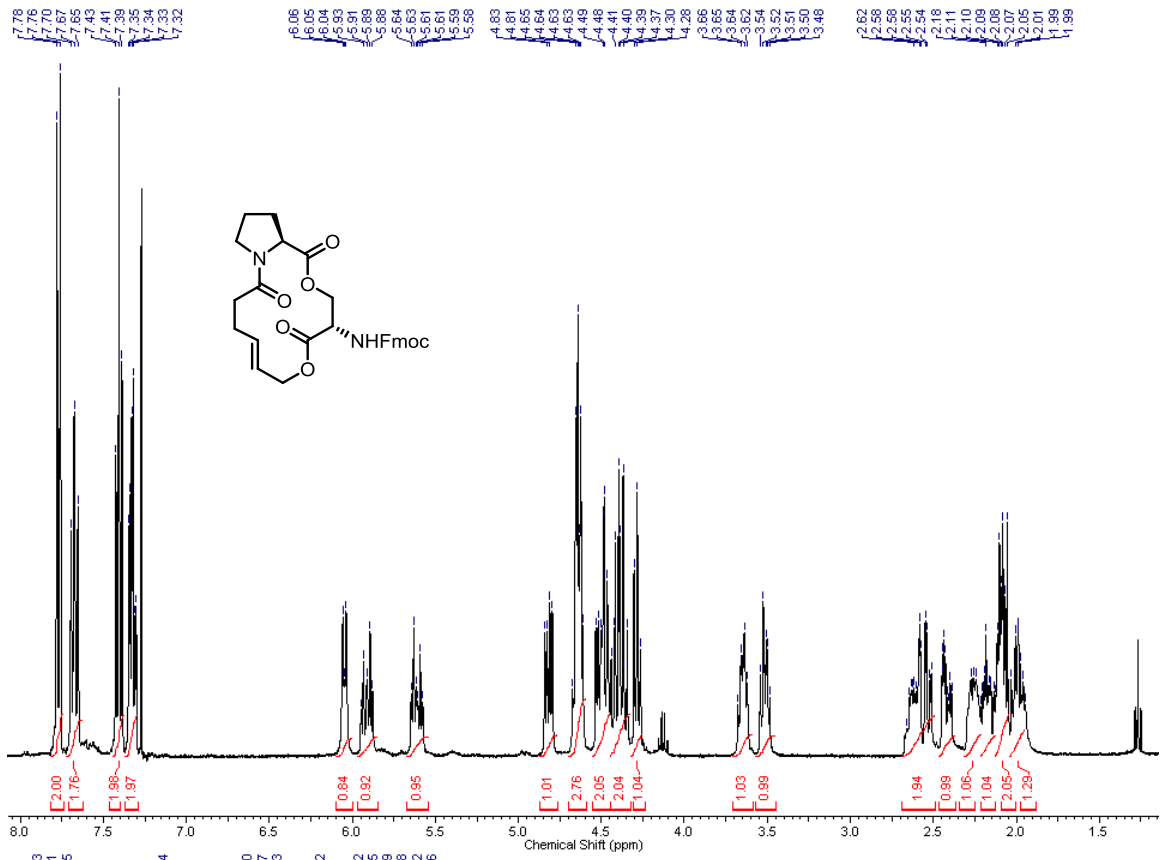


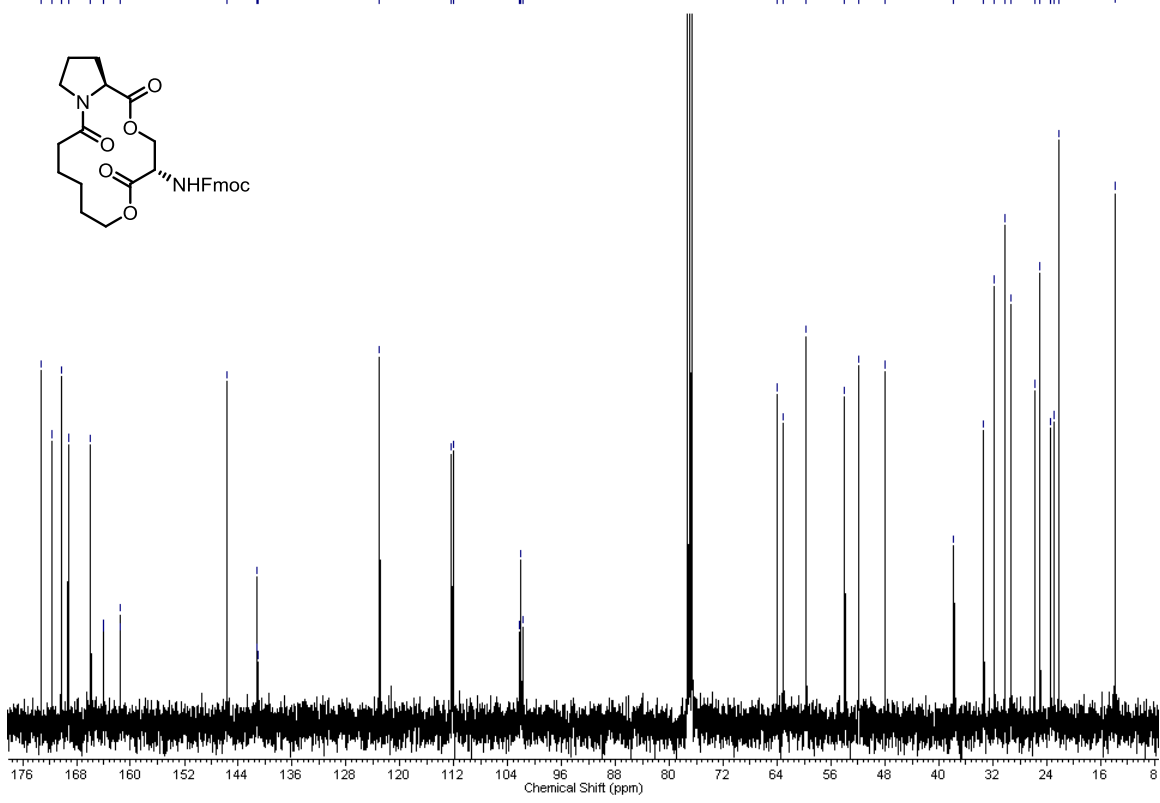
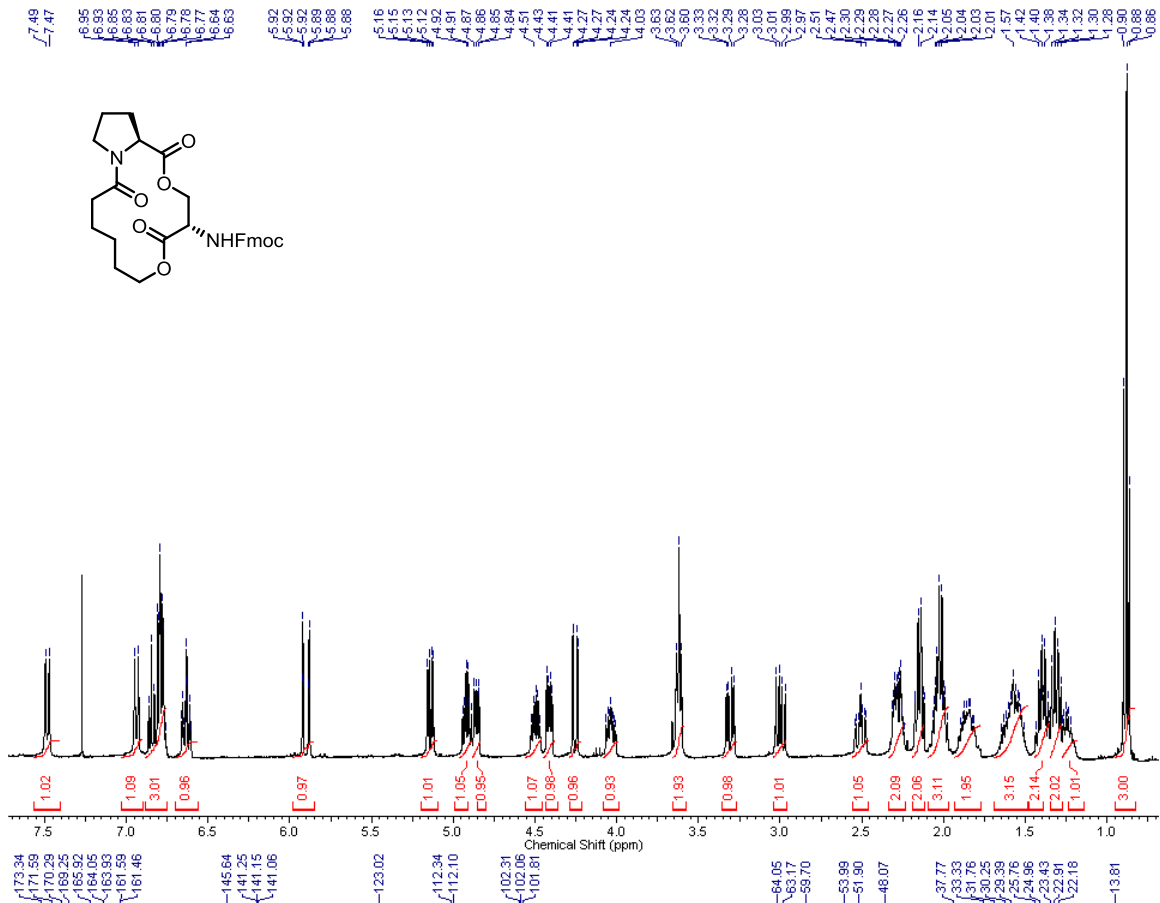
NOSEY Spectrum – Exchange signals shown in green NOE correlations shown in teal.

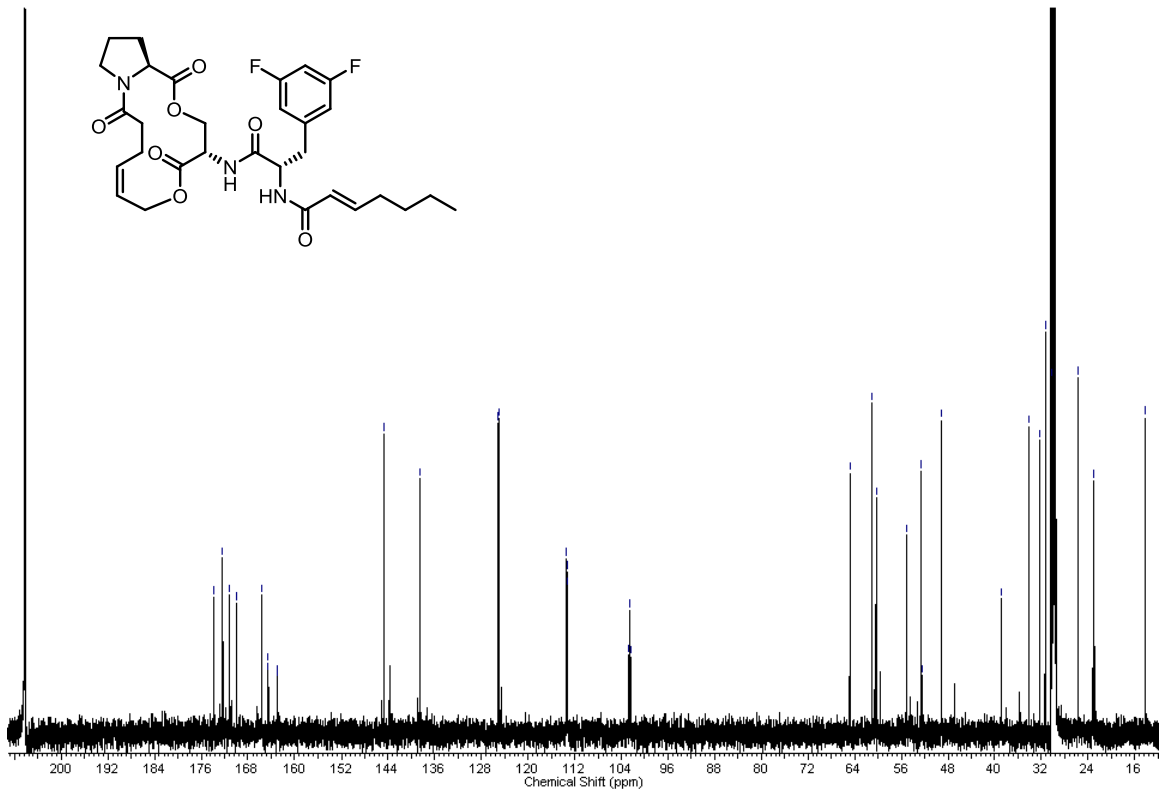
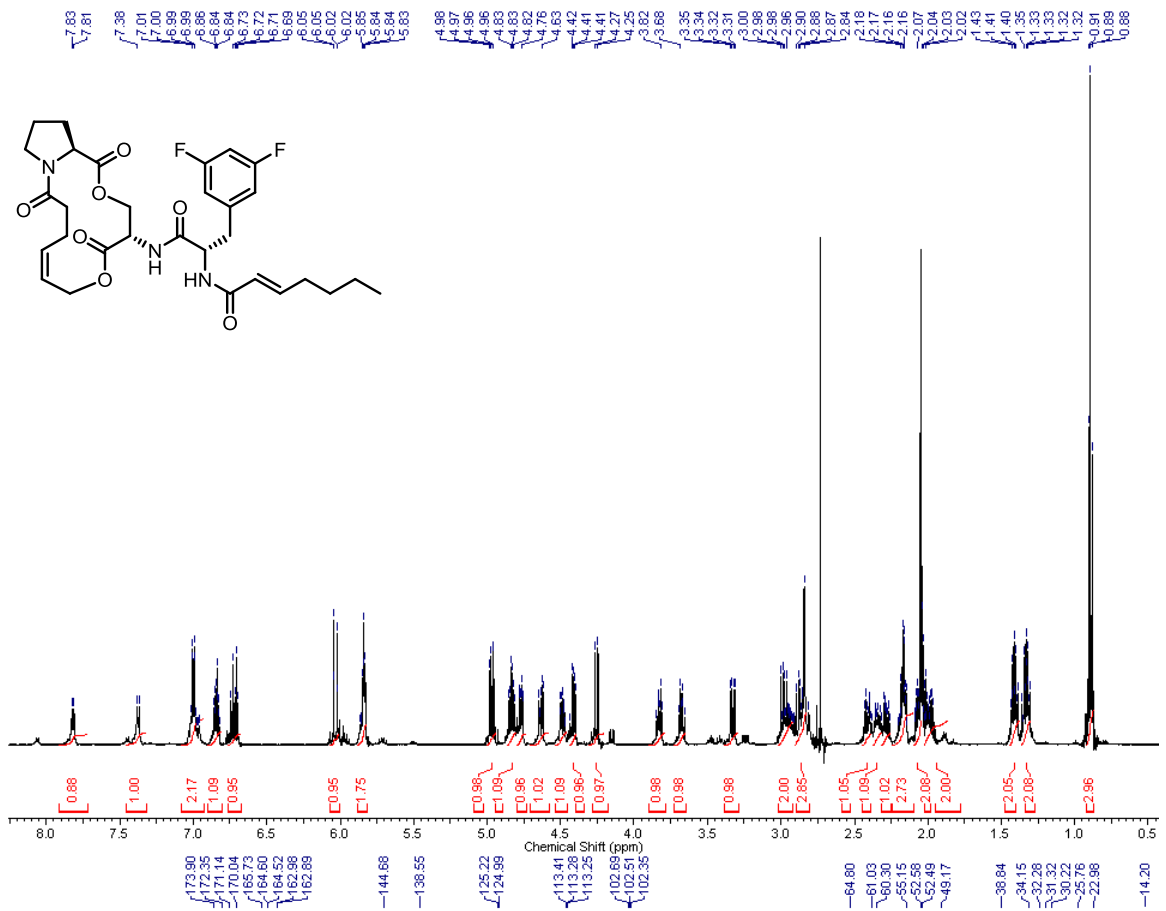




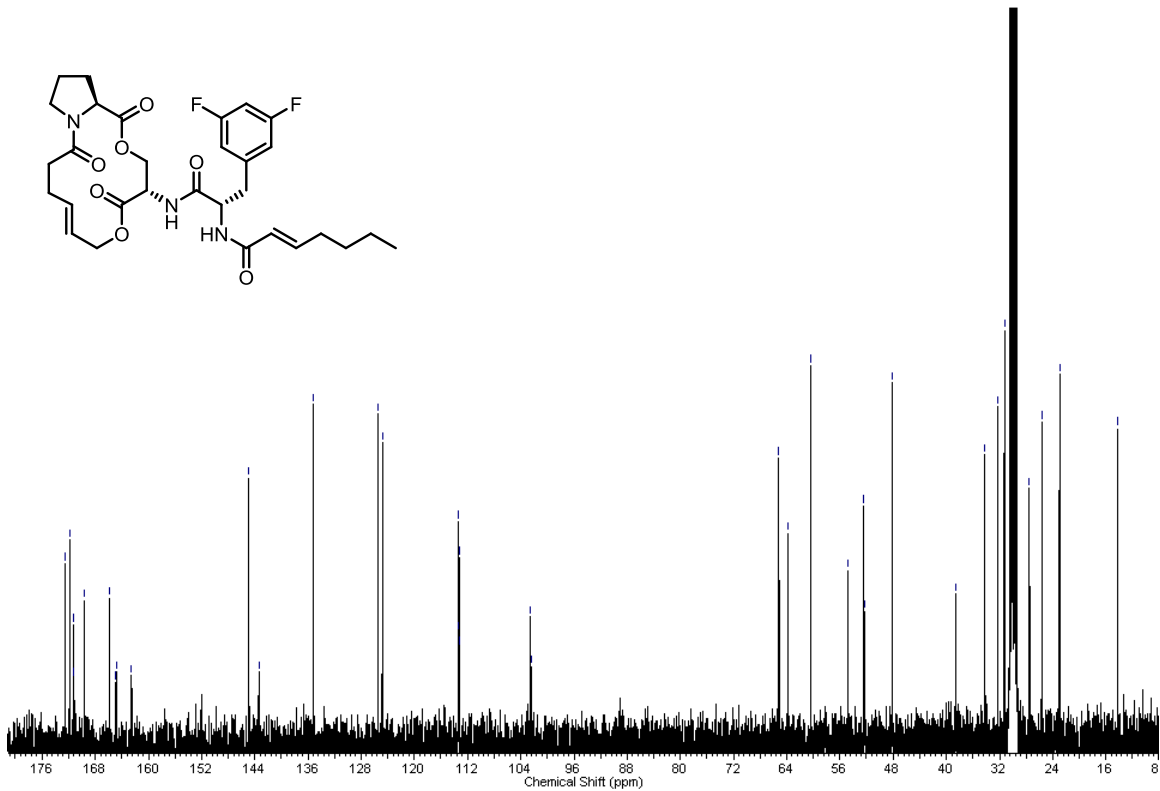
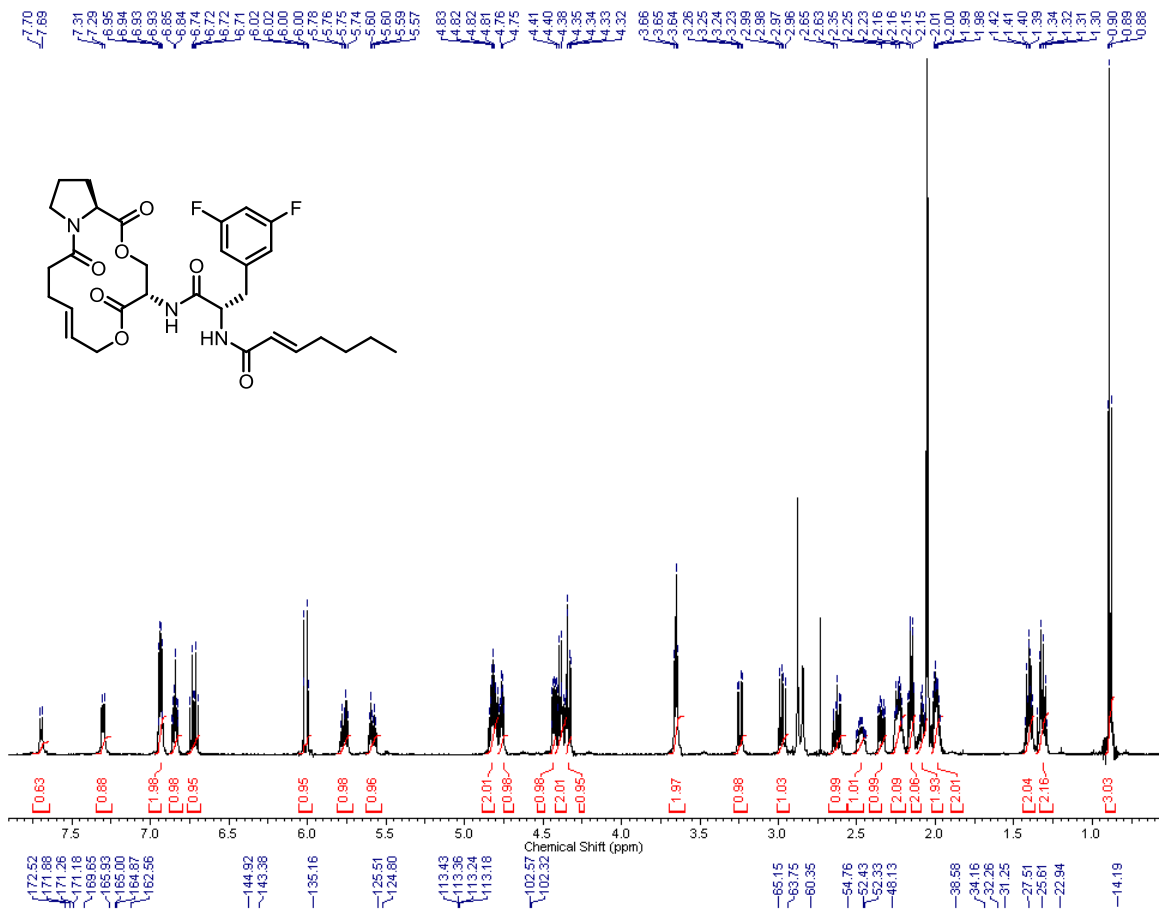


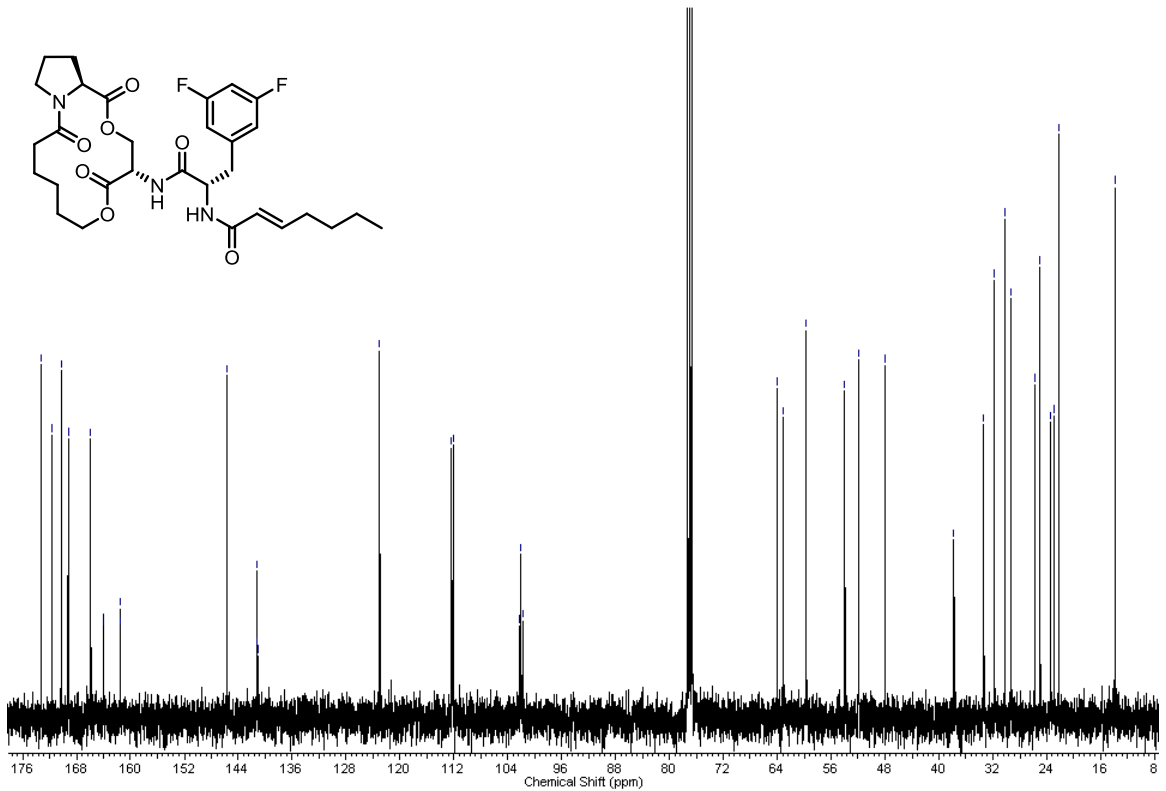
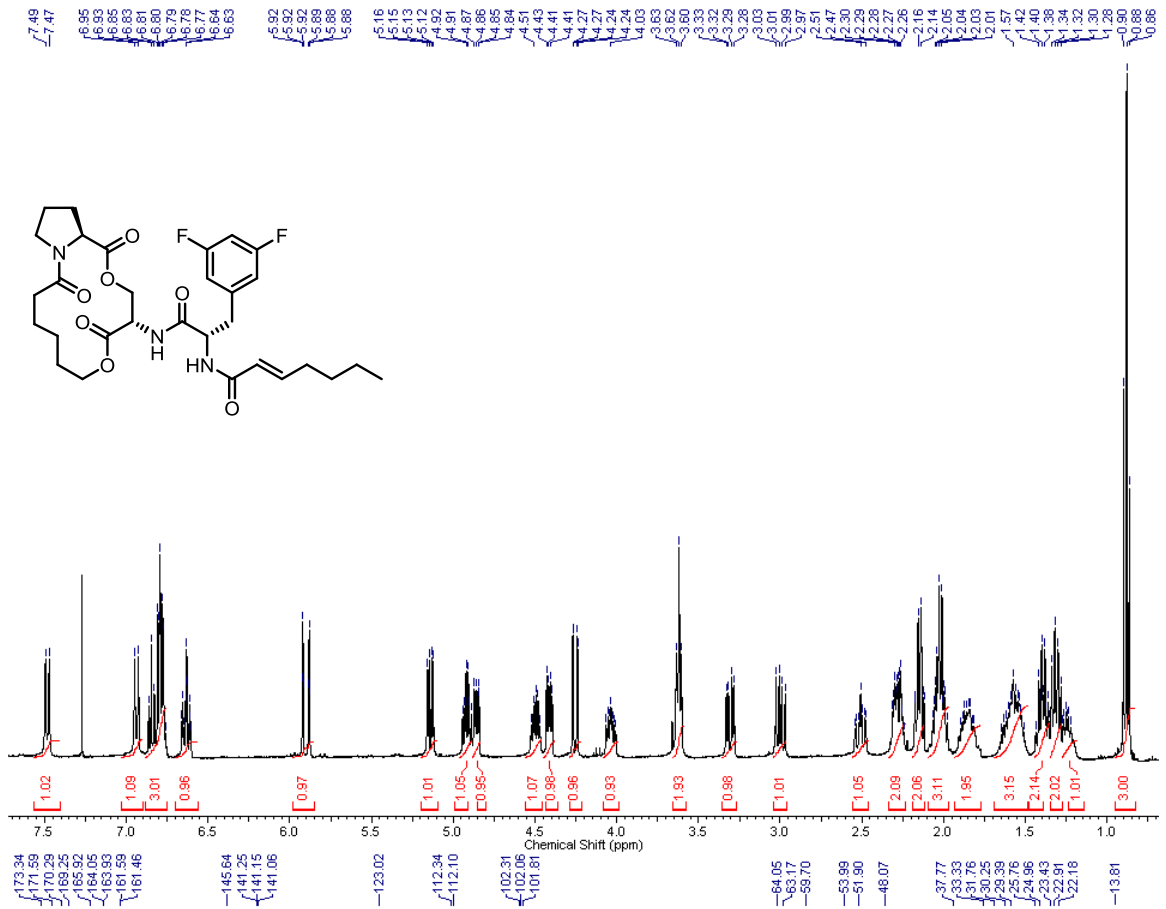




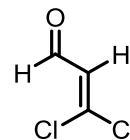
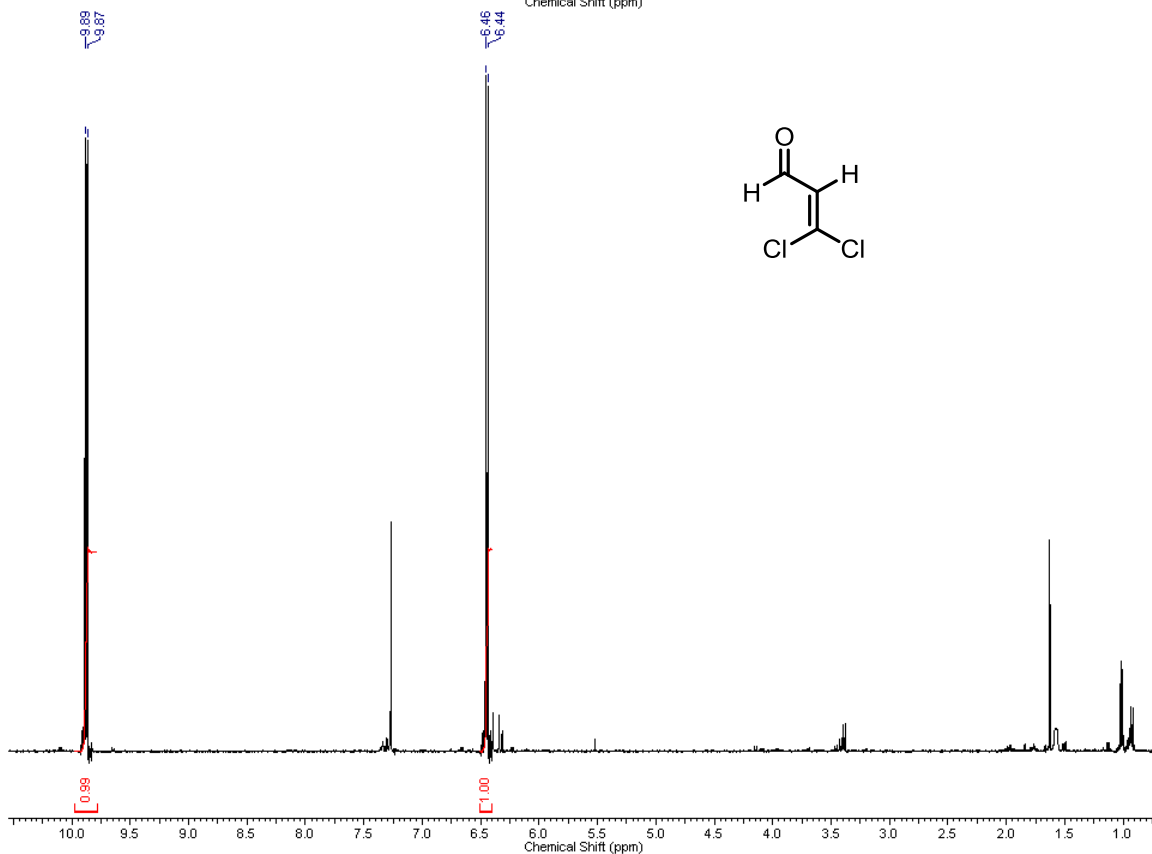
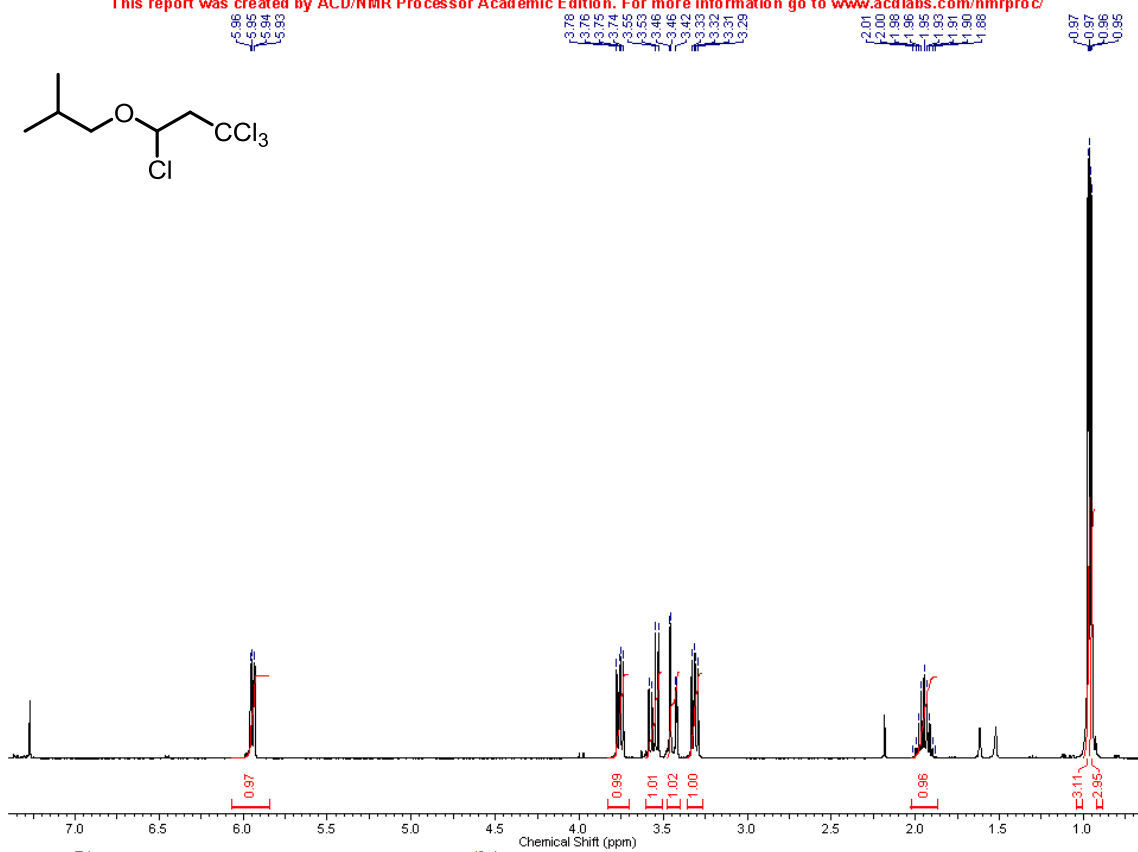
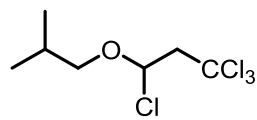


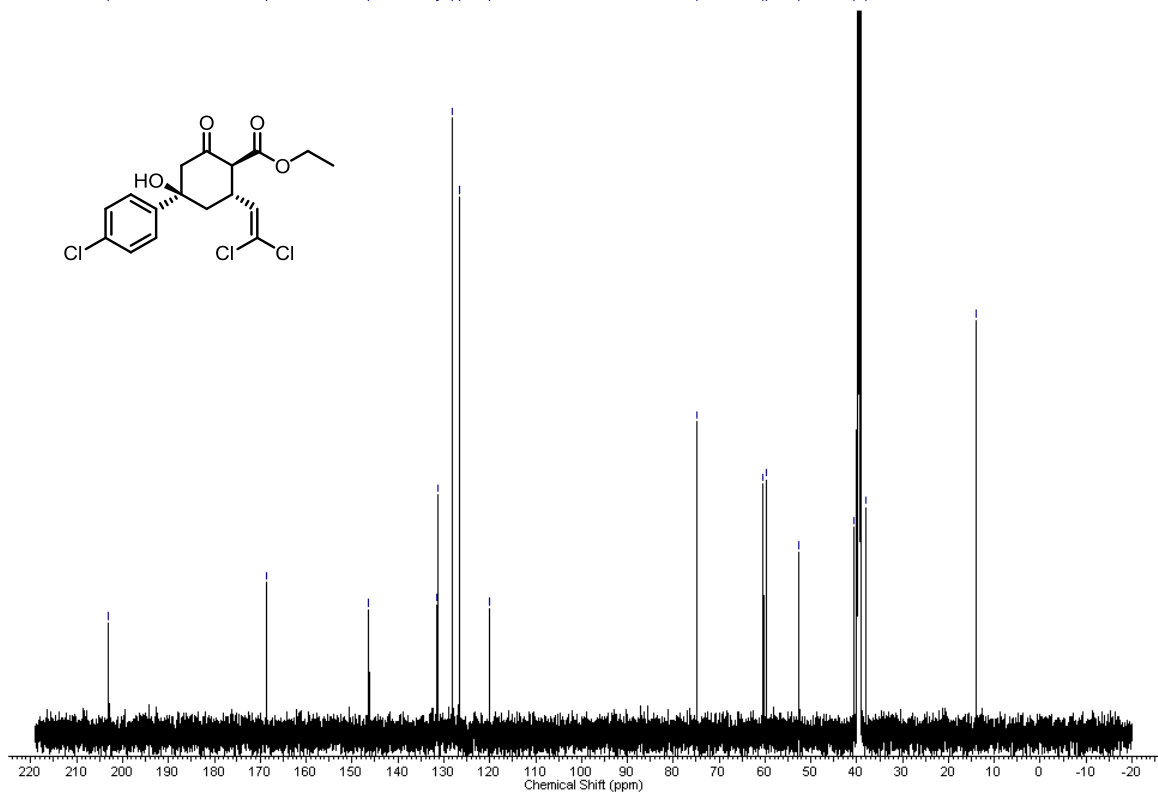
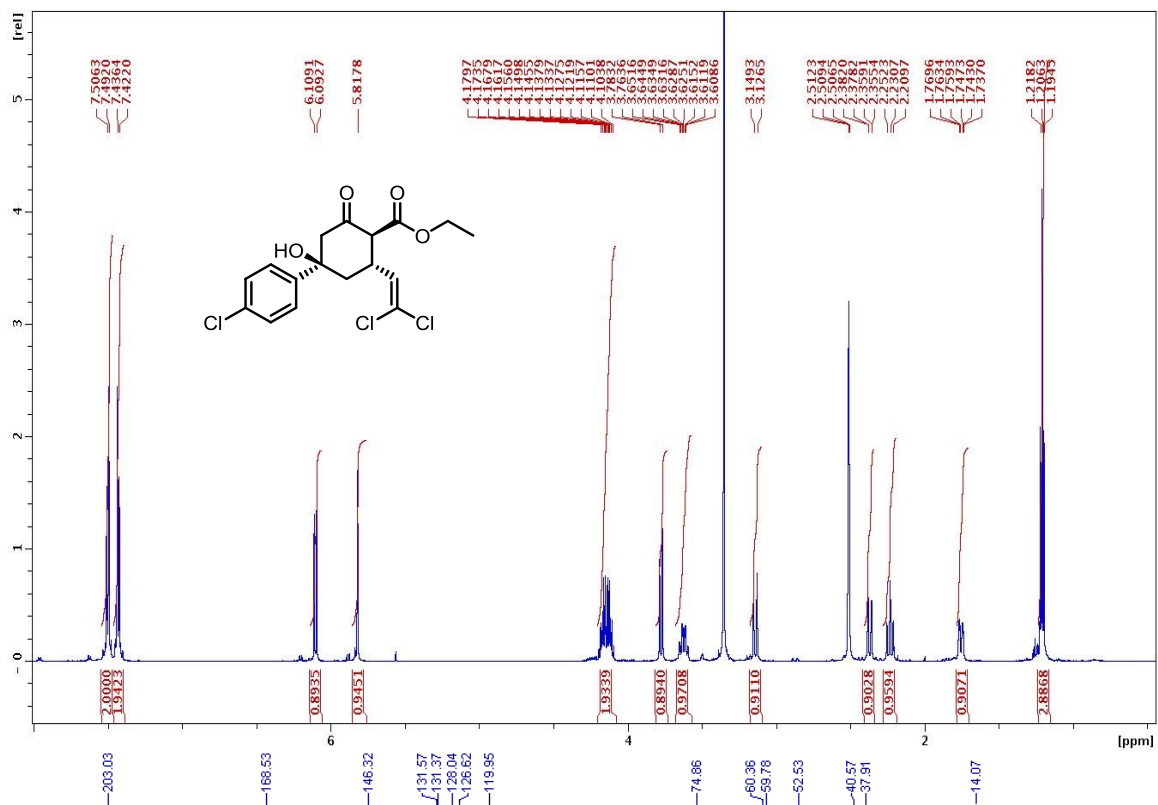




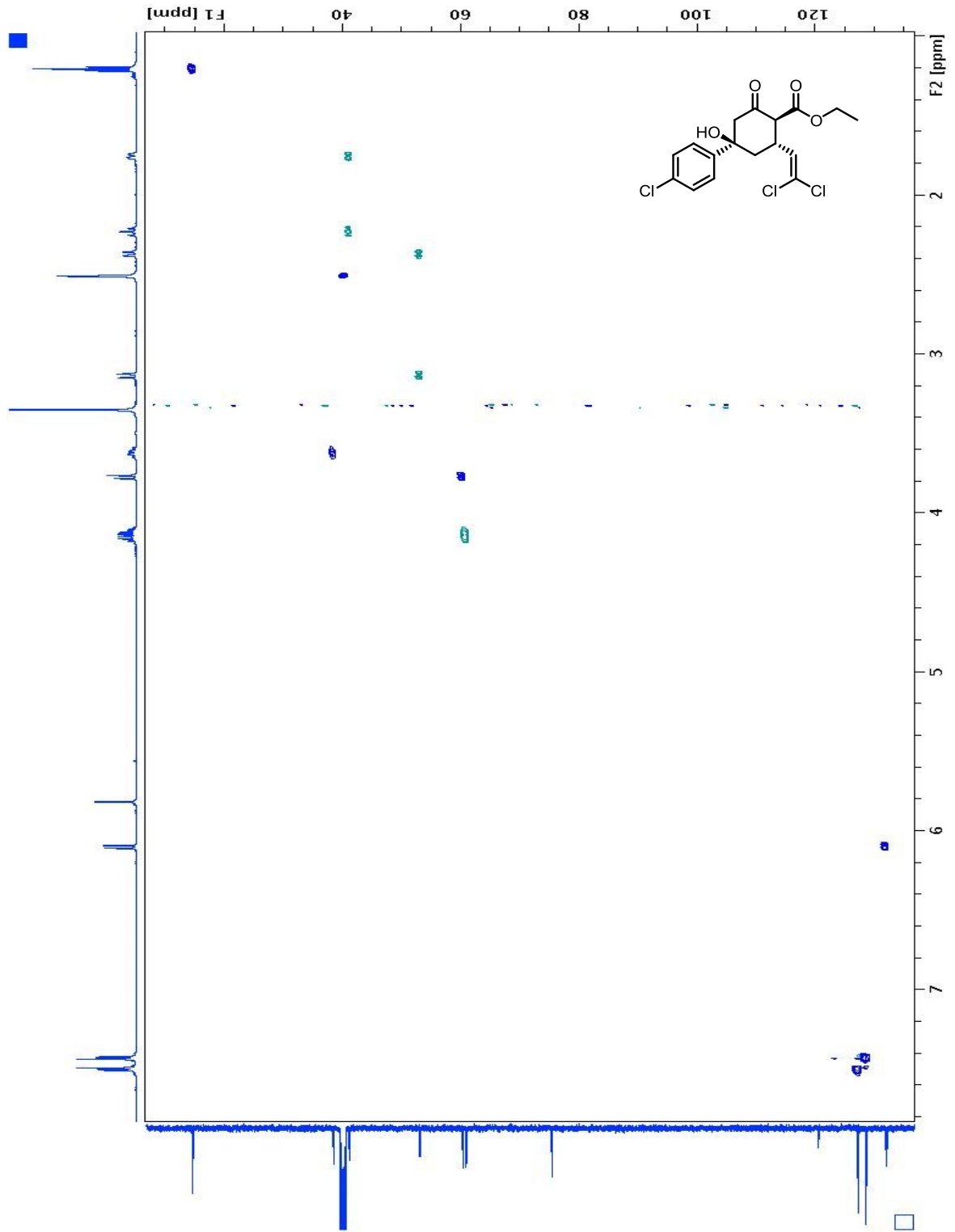


## **Chapter 11 – Antibacterial Phenylcyclohexane Carboxylates (PCHCs)**

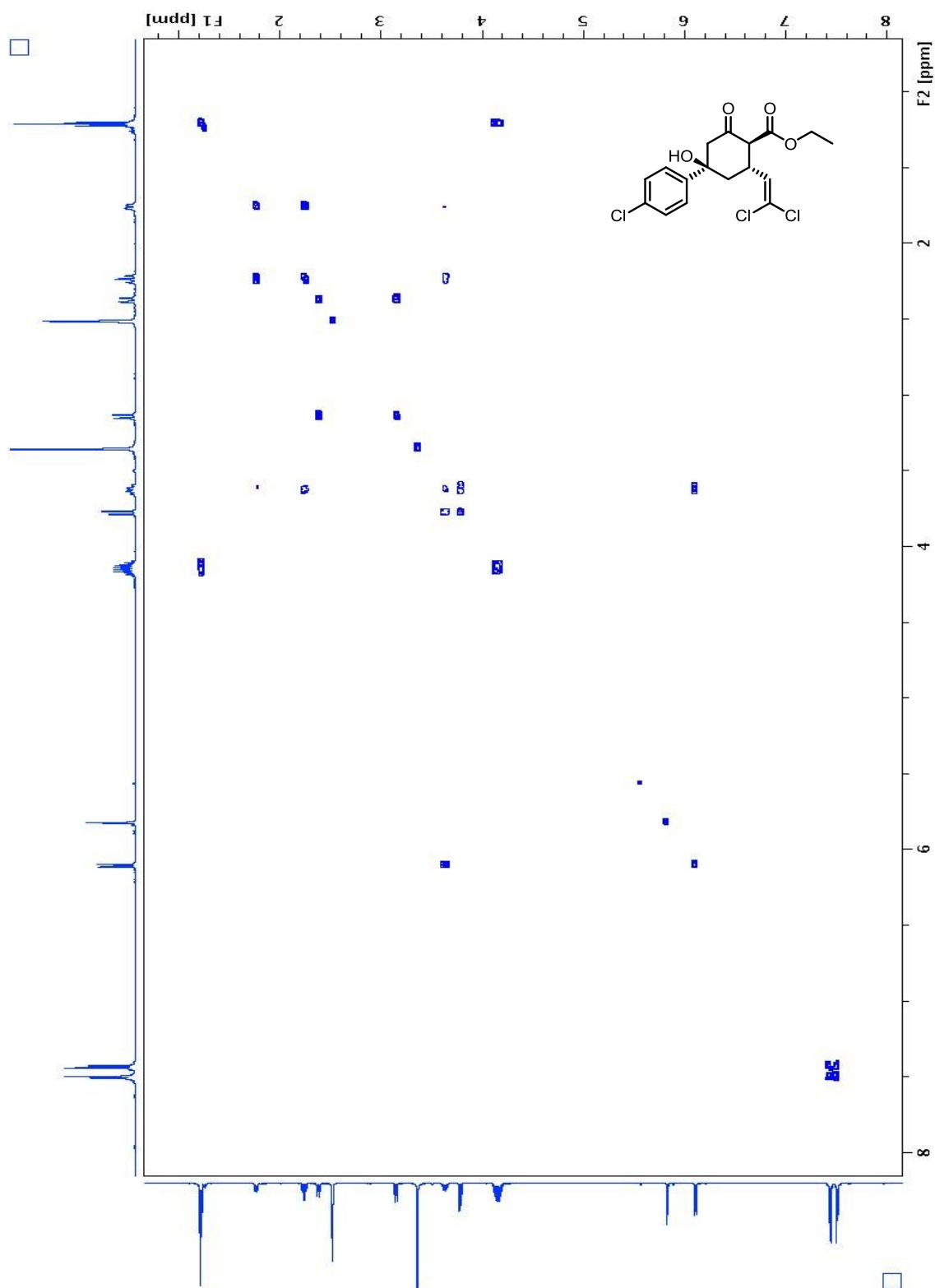




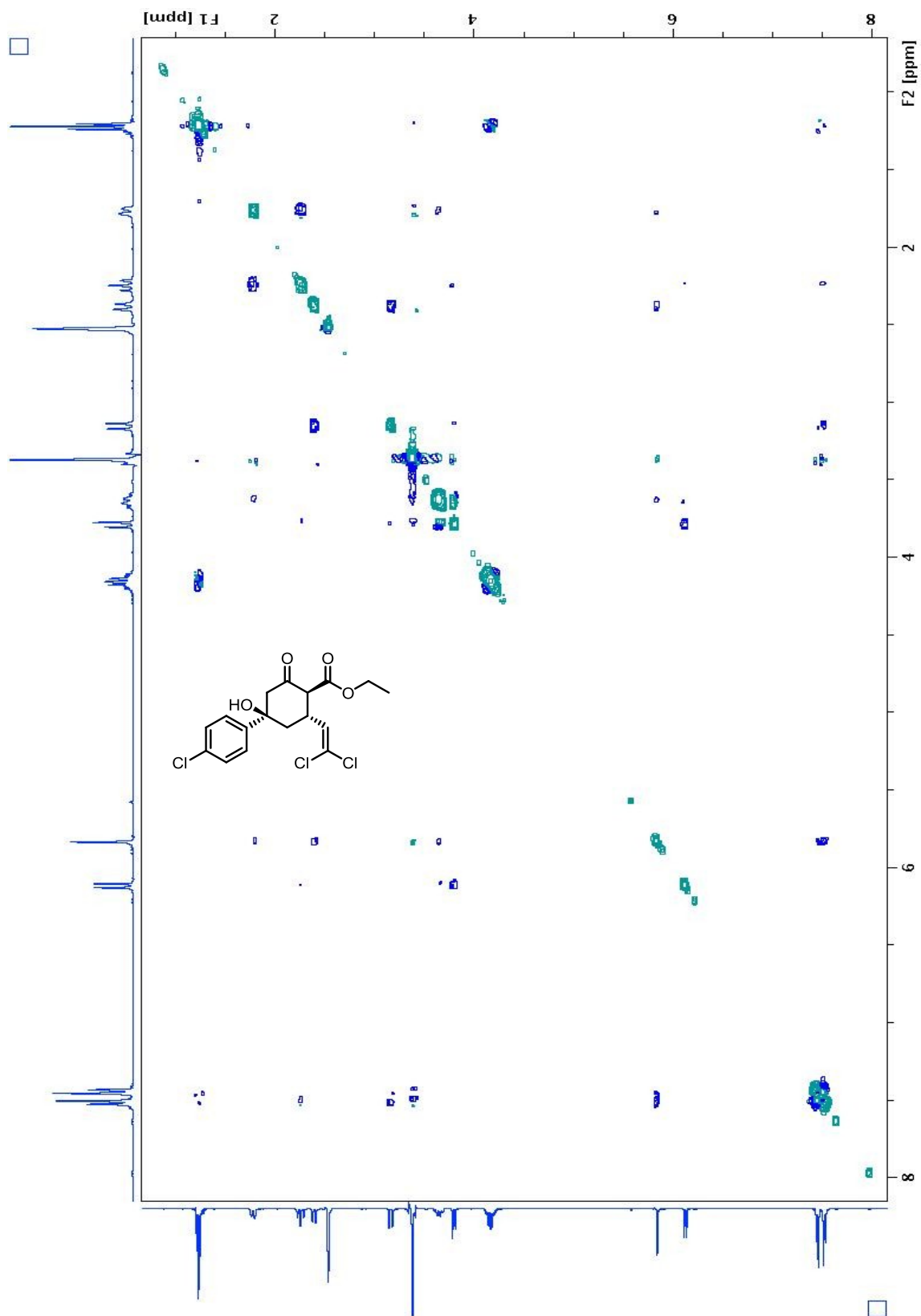
# HSQC Spectrum



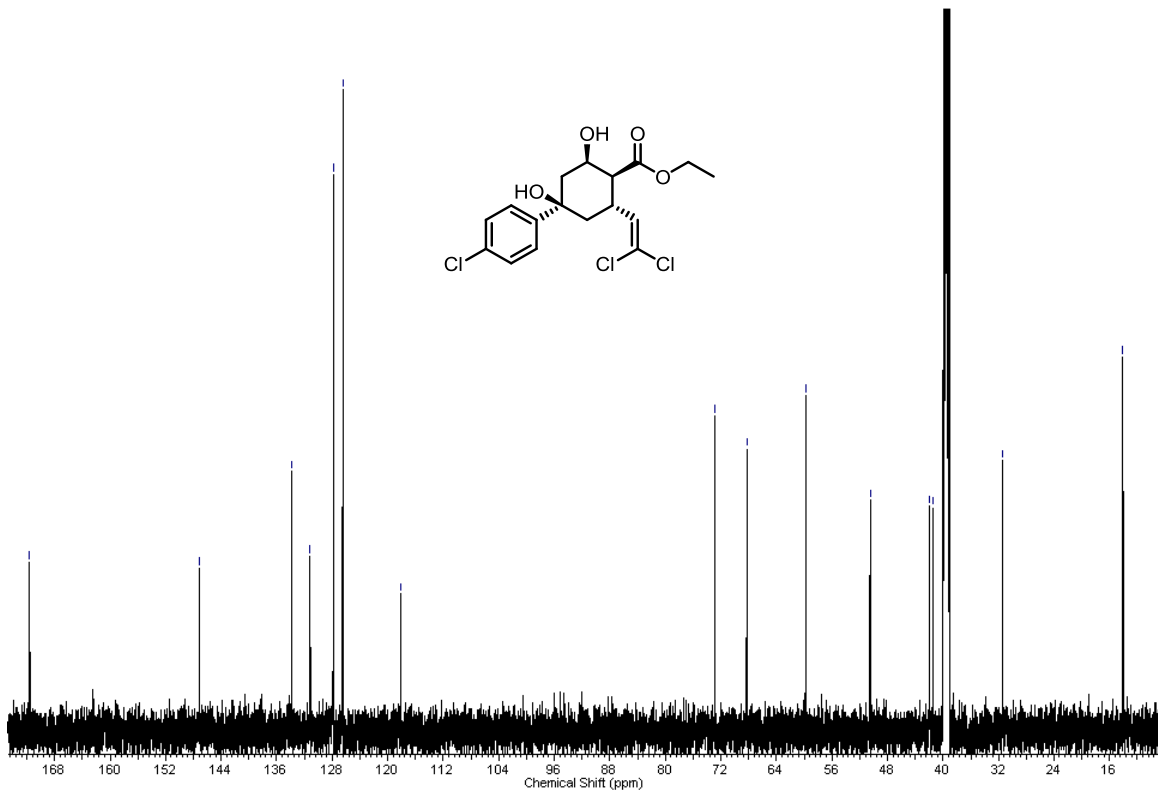
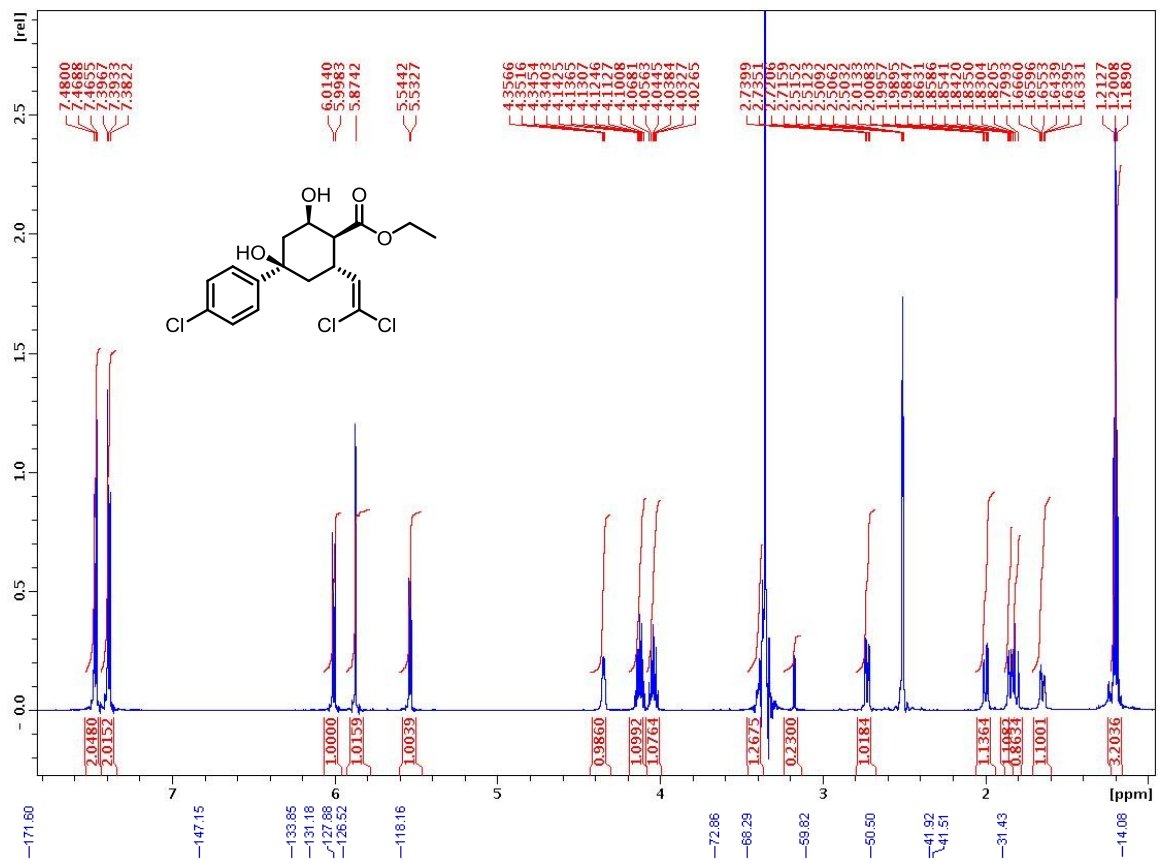
# COSEY Spectrum



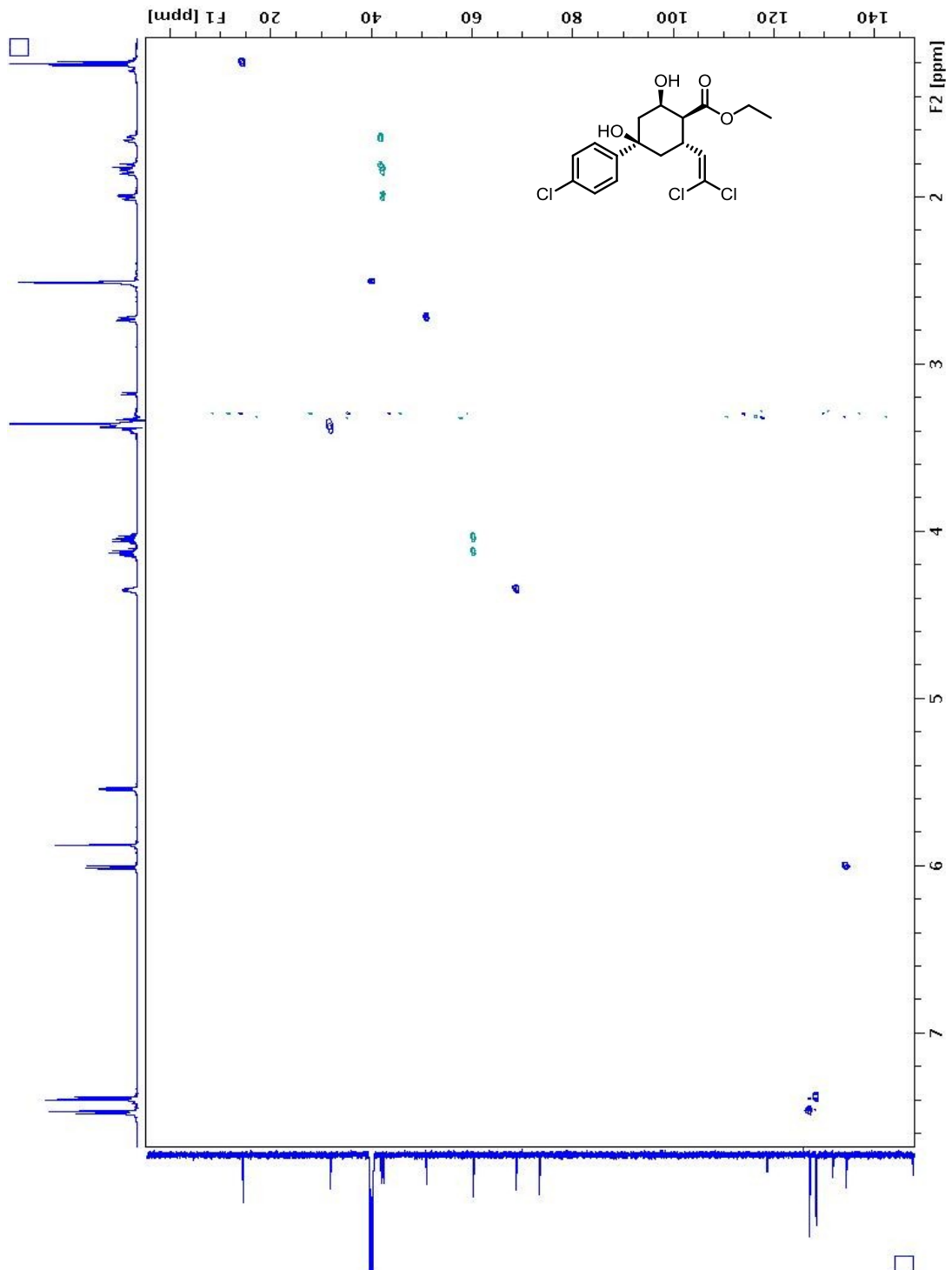
**NOSEY Spectrum – Exchange signals shown in teal NOE correlations shown in teal**



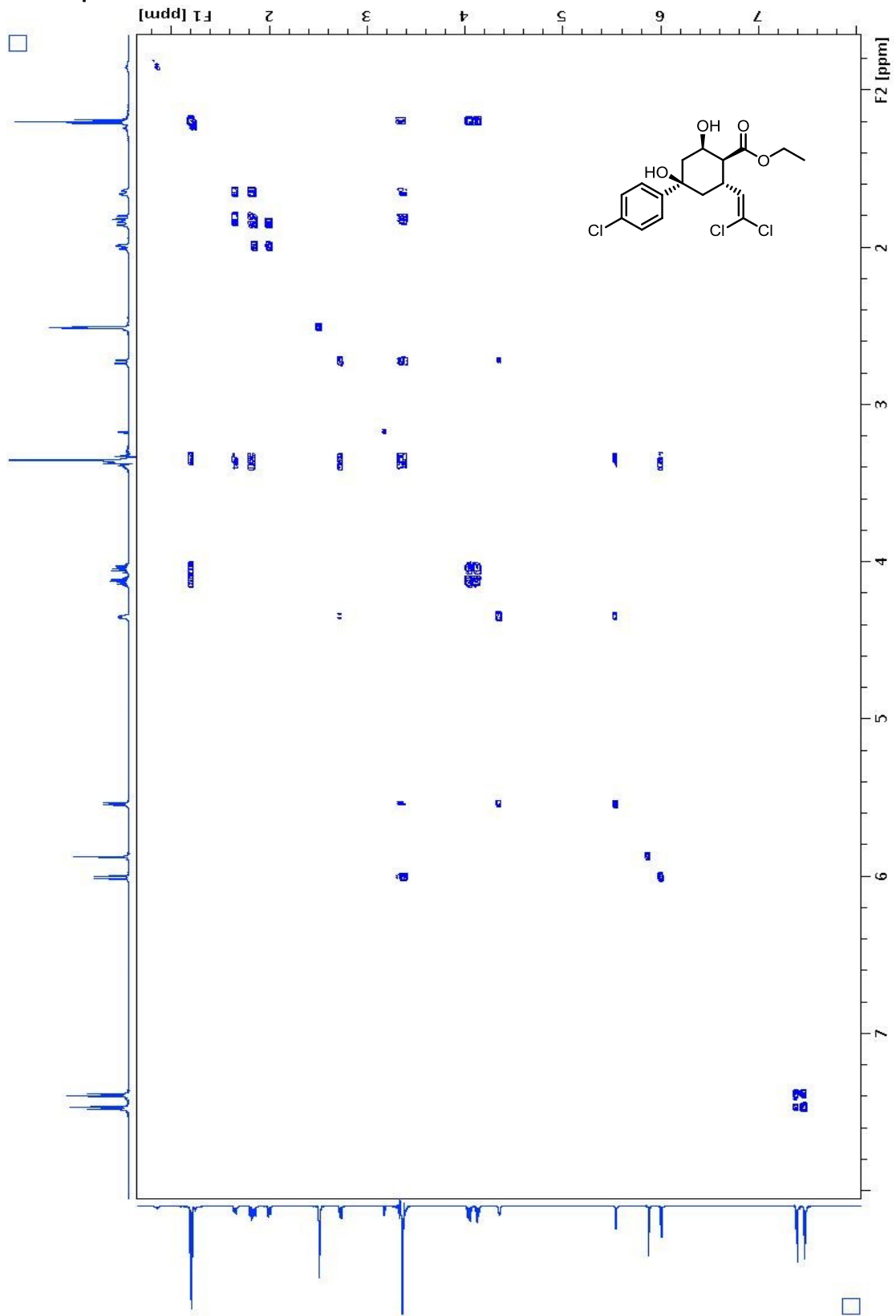




# HSQC Spectrum



COSEY Spectrum



NOSY Spectrum – Exchange signals shown in teal, NOE correlations shown in blue

